VOLUME 27 / NUMBER 14
JULY 23, 1989
ACC. NOS. N89-20920 TO N89-21761

STAR
AN ABSTRACT JOURNAL

Scientific and Technical Aerospace Reports

PRODUCED BY THE
SCIENTIFIC AND TECHNICAL
INFORMATION
DIVISION

NASA

NATIONAL AERONAUTICS AND SPACE ADMINISTRATION

WHAT YOU CAN DO FOR *STAR*

All users of this abstract service are urged to forward reports to be considered for announcement in *STAR*. This will aid NASA in its efforts to provide the fullest possible coverage of all scientific and technical publications that might support aeronautics and space research and development. If you have prepared relevant reports (other than those that you will transmit to NASA, DoD, or DOE through the usual contract- or grant-reporting channels), please send them for consideration to the NASA Scientific and Technical Information Facility, P.O. Box 8757, BWI Airport, Maryland 21240.

Reprints of journal articles, book chapters, and conference papers are also welcome. These will be considered for announcement in *STAR's* companion journal, *International Aerospace Abstracts.*

You may specify a particular source to be included in a report announcement if you wish; otherwise the report will be placed on public sale at the National Technical Information Service. Copyrighted publications will be announced but not distributed or sold.

PURCHASE OF *STAR*

The semimonthly issues are available to registered users on annual subscription for $99.00 from the NASA Scientific and Technical Information Facility, ATTN: Registration Services, P.O. Box 8757, BWI Airport, MD 21240. *STAR* is publically available on annual subscription for $99.00 from the Superintendent of Documents, U.S. Government Printing Office, Washington, DC 20402.

PUBLISHED BY:

UNITED STATES GOVERNMENT
NATIONAL AERONAUTICS AND SPACE ADMINISTRATION
SCIENTIFIC AND TECHNICAL INFORMATION DIVISION
Scientific and Technical Aerospace Reports, Volume 27, is prepared by the NASA Scientific and Technical Information Facility operated for the National Aeronautics and Space Administration by RMS Associates.

The Administrator of the National Aeronautics and Space Administration has determined that the publication of this periodical is necessary in the transaction of the public business required by law of this Agency. Use of funds for printing this periodical has been approved by the Director of the Office of Management and Budget through March 22, 1989.

US ISSN 0036-8741

INTRODUCTION

Scientific and Technical Aerospace Reports (STAR) is a major component of a comprehensive National Aeronautics and Space Administration information system covering aeronautics, space, and supporting disciplines. *STAR* is issued on the 8th and 23rd of each month and announces current publications of the following types:

- NASA, NASA contractor, and NASA grantee reports
- Reports issued by other U.S. Government Agencies, domestic and foreign institutions, universities, and private firms
- Translations in report form
- NASA-owned patents and patent applications
- Other U.S. Government Agency and foreign patents and patent applications
- Domestic and foreign dissertations and theses

Journal, book, and conference literature, cover-to-cover journal translations, and certain foreign dissertations are announced in a companion journal, *International Aerospace Abstracts (IAA),* available on subscription from the American Institute of Aeronautics and Astronautics, Technical Information Service, 555 West 57th Street, 12th Floor, New York, New York 10019.

SUBJECT SCOPE

Subject scope of *STAR,* and *IAA* includes all aspects of aeronautics and space research and development, supporting basic and applied research, and applications. Aerospace aspects of earth resources, energy development, conservation, oceanography, environmental protection, urban transportation, and other topics of high national priority are also covered.

OTHER NASA PUBLICATIONS

Other NASA publications and information services are described in the publication, *The NASA Scientific and Technical Information System ... and How to Use It,* available without charge from the NASA Scientific and Technical Information Facility, P.O. Box 8757, BWI Airport, Maryland 21240.

HOW TO USE *STAR* SUBJECT CATEGORIES

STAR is categorized by 10 major subject divisions divided into 76 specific subject categories and one general category/division. The major subject divisions are listed in the Table of Contents, together with a note for each that defines its scope and provides any cross-references. For example:

AERONAUTICS

Includes aeronautics (general); aerodynamics; air transportation and safety; aircraft communications and navigation; aircraft design, testing and performance; aircraft instrumentation; aircraft propulsion and power; aircraft stability and control; and research and support facilities (air).

For related information see also *Astronautics.*

Each major division is further divided into as many as nine specific categories, which are identified by category numbers.

Abstracts in *STAR* are grouped by specific category, the categories appearing in sequential order. Category breaks in the abstract section are identified by the category number and title, and a scope note. Cross-references to other categories are provided as appropriate. For example:

02 AERODYNAMICS

Includes aerodynamics of bodies, combinations, wings, rotors, and control surfaces; and internal flow in ducts and turbomachinery.

For related information see also *34 Fluid Mechanics and Heat Transfer.*

CROSS-REFERENCES

Individual *STAR* abstracts are not ordinarily cross-referenced, except for certain conference reports or book translations that have had separate abstracts written for their component papers or chapters. Citations and abstracts of the components follow immediately after those of the parent document. When the subject content of a component differs sufficiently from the general content of the parent, a cross-reference citation also is printed at the end of the category to which it normally would have been assigned if it were independent.

DOCUMENTS ON MICROFICHE

Documents on microfiche[1] are designated by a pound sign (#) following the accession number. The pound sign is used without regard to the source or quality of the microfiche.

AVAILABILITIES

One or more sources from which a document announced in *STAR* is available to the public is given in each citation. The most commonly indicated sources and their acronyms or abbreviations are listed below. If the publication is available from a source other than those listed, the publisher and his address will be displayed on the availability line or in combination with the corporate source line.

Avail: NTIS. Sold by the National Technical Information Service. Prices for hard copy (HC) and microfiche (MF) are indicated by a price code following the letters HC or MF in the *STAR* citation. Current values for the price codes are given in the tables on page vii.

Initially distributed microfiche under the NTIS SRIM (Selected Research in Microfiche) is available at greatly reduced unit prices. For this service and for information concerning subscription to NASA printed reports, consult the NTIS Subscription Section, Springfield, Va. 22161.

NOTE ON ORDERING DOCUMENTS: When ordering NASA publications (those followed by the * symbol), use the N accession number. NASA patent applications (only the specifications are offered) should be ordered by the US-Patent-Appl-SN number. Non-NASA publications (no asterisk) should be ordered by the AD, PB, or other *report number* shown on the last line of the citation, not by the N accession number. It is also advisable to cite the title and other bibliographic identification.

Avail: SOD (or GPO). Sold by the Superintendent of Documents, U.S. Government Printing Office, in hard copy. The current price and order number are given following the availability line. (NTIS will fill microfiche requests, as indicated above, for those documents identified by a # symbol.)

(1) A microfiche is a transparent sheet of film, 105 by 148 mm in size, containing as many as 60 to 98 pages of information reduced to micro images (not to exceed 26:1 reduction).

Avail: BLL (formerly NLL): British Library Lending Division, Boston Spa, Wetherby, Yorkshire, England. Photocopies available from this organization at the price shown. (If none is given, inquiry should be addressed to the BLL.)

Avail: DOE Depository Libraries. Organizations in U.S. cities and abroad that maintain collections of Department of Energy reports, usually in microfiche form, are listed in *Energy Research Abstracts.* Services available from the DOE and its depositories are described in a booklet, *DOE Technical Information Center - Its Functions and Services* (TID-4660), which may be obtained without charge from the DOE Technical Information Center.

Avail: ESDU. Pricing information on specific data, computer programs, and details on ESDU topic categories can be obtained from ESDU International Ltd. Requesters in North America should use the Virginia address while all other requesters should use the London address, both of which are on page vi.

Avail: Fachinformationszentrum, Karlsruhe. Sold by the Fachinformationszentrum Energie, Physik, Mathematik GMBH, Eggenstein Leopoldshafen, Federal Republic of Germany, at the price shown in deutschmarks (DM).

Avail: HMSO. Publications of Her Majesty's Stationery Office are sold in the U.S. by Pendragon House, Inc. (PHI), Redwood City, California. The U.S. price (including a service and mailing charge) is given, or a conversion table may be obtained from PHI.

Avail: NASA Public Document Rooms. Documents so indicated may be examined at or purchased from the National Aeronautics and Space Administration, Public Documents Room (Room 126), 600 Independence Ave., S.W., Washington, D.C. 20546, or public document rooms located at each of the NASA research centers, the NASA Space Technology Laboratories, and the NASA Pasadena Office at the Jet Propulsion Laboratory.

Avail: Univ. Microfilms. Documents so indicated are dissertations selected from *Dissertation Abstracts* and are sold by University Microfilms as xerographic copy (HC) and microfilm. All requests should cite the author and the Order Number as they appear in the citation.

Avail: US Patent and Trademark Office. Sold by Commissioner of Patents and Trademarks, U.S. Patent and Trademark Office, at the standard price of $1.50 each, postage free. (See discussion of NASA patents and patent applications below.)

Avail: (US Sales Only). These foreign documents are available to users within the United States from the National Technical Information Service (NTIS). They are available to users outside the United States through the International Nuclear Information Service (INIS) representative in their country, or by applying directly to the issuing organization.

Avail: USGS. Originals of many reports from the U.S. Geological Survey, which may contain color illustrations, or otherwise may not have the quality of illustrations preserved in the microfiche or facsimile reproduction, may be examined by the public at the libraries of the USGS field offices whose addresses are listed in this Introduction. The libraries may be queried concerning the availability of specific documents and the possible utilization of local copying services, such as color reproduction.

Avail: Issuing Activity, or Corporate Author, or no indication of availability. Inquiries as to the availability of these documents should be addressed to the organization shown in the citation as the corporate author of the document.

NASA PATENTS AND PATENT APPLICATIONS

Patents and patent applications owned by NASA are announced in *STAR* under appropriate subject categories and are referenced in the *STAR* indexes. In the Report/Accession Number Index, patents are indexed by the NASA Case Number (which appears in lieu of the report number in other indexes), the U.S. Patent Number, the U.S. Patent Application Serial Number, and the U.S. Patent Class. Patent applications for which patents have not yet been issued are indexed by the NASA Case Number and the U.S. Patent Application Serial Number.

NASA *patent application specifications* are sold in paper copy by the National Technical Information Service at price code A02. Microfiche are sold at price code A01. The US-Patent-Appl-SN- number should be used in ordering either paper copy or microfiche from NTIS. Printed copies of *patents* (which are not microfiched) are available for purchase at $1.50 per copy from:

Commissioner of Patents and Trademarks
U.S. Patent and Trademark Office
Washington, D.C. 20231

When ordering patents, the U.S. Patent Number should be used, and payment must be remitted in advance, preferably by money order or check payable to the Commissioner of Patents and Trademarks. Prepaid purchase coupons for ordering are also available from the Patent and Trademark Office. The patents and patent applications announced in *STAR* are owned by NASA and are available for royalty-free licensing. Requests for licensing terms and further information should be addressed to:

Associate General Counsel for Intellectual Property/Code GP
National Aeronautics and Space Administration
Washington, D.C. 20546

ELIGIBILITY AND REGISTRATION FOR NASA INFORMATION PRODUCTS AND SERVICES

A variety of services is available to organizations of the following types that have registered with NASA to receive specific services or products:

1. NASA offices, research centers, contractors, subcontractors, grantees, and consultants;
2. Other U.S. Government agencies and their contractors;
3. Libraries in the United States that have arrangements with NASA to maintain collections of NASA documents for public reference;
4. Other organizations in the United States having a need for NASA documents in work related to aeronautics and space research;
5. Organizations abroad that have established reciprocal document exchange arrangements with NASA.

Only the central service points or central points of document acquisition and control within qualified organizations are eligible to register for NASA products and services. Domestic organizations that may be eligible to receive various classes of NASA publications and services should address their requests for registration or for further information to:

NASA Scientific and Technical Information Facility
ATTN: Registration Services
Post Office Box 8757
BWI Airport, Maryland 21240

Organizations abroad should direct requests to Manager, International STI Activities, NTT, NASA Headquarters, Washington, D.C. 20546.

AVAILABILITY OF *STAR* ABSTRACTS ON MICROFICHE

Microfiche of the abstract sections of this issue and other issues of *STAR* are available on annual subscription from NTIS as PB89-911300, Attn: Subscriptions, 5285 Port Royal Road, Springfield, Virginia 22161. Annual subscription rates are $70.00 North America; $140.00 foreign. Abstract sections for previous years retroactive to 1964 are available at the current rates. Microfiche for individual *STAR* issue abstract sections are not available.

PUBLIC COLLECTIONS OF NASA DOCUMENTS

DOMESTIC: NASA and NASA-sponsored documents and a large number of aerospace publications are available to the public for reference purposes at the library maintained by the American Institute of Aeronautics and Astronautics, Technical Information Service, 555 West 57th Street, 12th Floor, New York, New York 10019

EUROPEAN: An extensive collection of NASA and NASA-sponsored publications is maintained by the British Library Lending Division, Boston Spa, Wetherby, Yorkshire, England for public access. The British Library Lending Division also has available many of the non-NASA publications cited in *STAR*. European requesters may purchase facsimile copy or microfiche of NASA and NASA-sponsored documents, those identified by both the symbols # and * from ESA - Information Retrieval Service European Space Agency, 8-10 rue Mario-Nikis, 75738 Paris CEDEX 15, France.

FEDERAL DEPOSITORY LIBRARY PROGRAM

In order to provide the general public with greater access to U.S. Government publications, Congress established the Federal Depository Library Program under the Government Printing Office (GPO), with 50 regional depositories responsible for permanent retention of material, inter-library loan, and reference services. At least one copy of nearly every NASA and NASA-sponsored publication, either in printed or microfiche format, is received and retained by the 50 regional depositories. A list of the regional GPO libraries, arranged alphabetically by state, appears on the inside back cover. These libraries are *not* sales outlets. A local library can contact a Regional Depository to help locate specific reports, or direct contact may be made by an individual.

ADDRESSES OF ORGANIZATIONS

American Institute of Aeronautics and Astronautics
Technical Information Service
555 West 57th Street, 12th Floor
New York, New York 10019

British Library Lending Division,
Boston Spa, Wetherby, Yorkshire,
England

Commissioner of Patents and Trademarks
U.S. Patent and Trademark Office
Washington, D.C. 20231

Department of Energy
Technical Information Center
P.O. Box 62
Oak Ridge, Tennessee 37830

ESA-Information Retrieval Service
ESRIN
Via Galileo Galilei
00044 Frascati (Rome) Italy

ESDU International
P.O. Box 1633
Manassas, Virginia 22110

ESDU International, Ltd.
251-259 Regent Street
London, W1R 7AD, England

Fachinformationszentrum Energie, Physik, Mathematik GMBH
7514 Eggenstein Leopoldshafen
Federal Republic of Germany

Her Majesty's Stationery Office
P.O. Box 569, S.E. 1
London, England

NASA Scientific and Technical Information Facility
P.O. Box 8757
B.W.I. Airport, Maryland 21240

National Aeronautics and Space Administration
Scientific and Technical Information Division (NTT)
Washington, D.C. 20546

National Technical Information Service
5285 Port Royal Road
Springfield, Virginia 22161

Pendragon House, Inc.
899 Broadway Avenue
Redwood City, California 94063

Superintendent of Documents
U.S. Government Printing Office
Washington, D.C. 20402

University Microfilms
A Xerox Company
300 North Zeeb Road
Ann Arbor, Michigan 48106

University Microfilms, Ltd.
Tylers Green
London, England

U.S. Geological Survey Library
National Center - MS 950
12201 Sunrise Valley Drive
Reston, Virginia 22092

U.S. Geological Survey Library
2255 North Gemini Drive
Flagstaff, Arizona 86001

U.S. Geological Survey
345 Middlefield Road
Menlo Park, California 94025

U.S. Geological Survey Library
Box 25046
Denver Federal Center, MS914
Denver, Colorado 80225

NTIS PRICE SCHEDULES

(Effective January 1, 1989)

Schedule A
STANDARD PRICE DOCUMENTS AND MICROFICHE

PRICE CODE	NORTH AMERICAN PRICE	FOREIGN PRICE
A01	$ 6.95	$13.90
A02	10.95	21.90
A03	13.95	27.90
A04-A05	15.95	31.90
A06-A09	21.95	43.90
A10-A13	28.95	57.90
A14-A17	36.95	73.90
A18-A21	42.95	85.90
A22-A25	49.95	99.90
A99	*	*
NO1	55.00	70.00
NO2	55.00	80.00

Schedule E
EXCEPTION PRICE DOCUMENTS AND MICROFICHE

PRICE CODE	NORTH AMERICAN PRICE	FOREIGN PRICE
E01	$ 9.00	18.00
E02	11.50	23.00
E03	13.00	26.00
E04	15.50	31.00
E05	17.50	35.00
E06	20.50	41.00
E07	23.00	46.00
E08	25.50	51.00
E09	28.00	56.00
E10	31.00	62.00
E11	33.50	67.00
E12	36.50	73.00
E13	39.00	78.00
E14	42.50	85.00
E15	46.00	92.00
E16	50.50	101.00
E17	54.50	109.00
E18	59.00	118.00
E19	65.50	131.00
E20	76.00	152.00
E99	*	*

*Contact NTIS for price quote.

IMPORTANT NOTICE

NTIS Shipping and Handling Charges
U.S., Canada, Mexico — ADD $3.00 per TOTAL ORDER
All Other Countries — ADD $4.00 per TOTAL ORDER

Exceptions — Does NOT apply to:
ORDERS REQUESTING NTIS RUSH HANDLING
ORDERS FOR SUBSCRIPTION OR STANDING ORDER PRODUCTS *ONLY*

NOTE: Each additional delivery address on an order requires a separate shipping and handling charge.

VOLUME 27 NUMBER 14 / JULY 23, 1989

TABLE OF CONTENTS

AERONAUTICS

Includes aeronautics (general); aerodynamics; air transportation and safety; aircraft communications and navigation; aircraft design, testing and performance; aircraft instrumentation; aircraft propulsion and power; aircraft stability and control; and research and support facilities (air).

For related information see also *Astronautics.*

01 AERONAUTICS (GENERAL) **N.A.**

02 AERODYNAMICS **1905**

Includes aerodynamics of bodies, combinations, wings, rotors, and control surfaces; and internal flow in ducts and turbomachinery.

For related information see also *34 Fluid Mechanics and Heat Transfer*

03 AIR TRANSPORTATION AND SAFETY **1914**

Includes passenger and cargo air transport operations; and aircraft accidents.

For related information see also *16 Space Transportation* and *85 Urban Technology and Transportation.*

04 AIRCRAFT COMMUNICATIONS AND NAVIGATION **1915**

Includes digital and voice communication with aircraft; air navigation systems (satellite and ground based); and air traffic control.

For related information see also *17 Space Communications, Spacecraft Communications, Command and Tracking* and *32 Communications and Radar.*

05 AIRCRAFT DESIGN, TESTING AND PERFORMANCE **1915**

Includes aircraft simulation technology.

For related information see also *18 Spacecraft Design, Testing and Performance* and *39 Structural Mechanics.* For land transportation vehicles see *85 Urban Technology and Transportation.*

06 AIRCRAFT INSTRUMENTATION **1918**

Includes cockpit and cabin display devices; and flight instruments.

For related information see also *19 Spacecraft Instrumentation* and *35 Instrumentation and Photography.*

07 AIRCRAFT PROPULSION AND POWER **1918**

Includes prime propulsion systems and systems components, e.g., gas turbine engines and compressors; and onboard auxiliary power plants for aircraft.

For related information see also *20 Spacecraft Propulsion and Power, 28 Propellants and Fuels,* and *44 Energy Production and Conversion.*

08 AIRCRAFT STABILITY AND CONTROL **1919**

Includes aircraft handling qualities; piloting; flight controls; and autopilots.

For related information see also *05 Aircraft Design, Testing and Performance.*

09 RESEARCH AND SUPPORT FACILITIES (AIR) **1920**

Includes airports, hangars and runways; aircraft repair and overhaul facilities; wind tunnels; shock tubes; and aircraft engine test stands.

For related information see also *14 Ground Support Systems and Facilities (Space).*

ASTRONAUTICS

Includes astronautics (general); astrodynamics; ground support systems and facilities (space); launch vehicles and space vehicles; space transportation; space communications, spacecraft communications, command and tracking; spacecraft design, testing and performance; spacecraft instrumentation; and spacecraft propulsion and power.

For related information see also *Aeronautics*

12 ASTRONAUTICS (GENERAL) **1921**

For extraterrestrial exploration see *91 Lunar and Planetary Exploration.*

13 ASTRODYNAMICS **1921**

Includes powered and free-flight trajectories; and orbital and launching dynamics.

14 GROUND SUPPORT SYSTEMS AND FACILITIES (SPACE) **N.A.**

Includes launch complexes, research and production facilities; ground support equipment, e.g., mobile transporters; and simulators.

For related information see also *09 Research and Support Facilities (Air).*

15 LAUNCH VEHICLES AND SPACE VEHICLES **1922**

Includes boosters; operating problems of launch/space vehicle systems; and reusable vehicles.

For related information see also *20 Spacecraft Propulsion and Power.*

16 SPACE TRANSPORTATION **N.A.**

Includes passenger and cargo space transportation, e.g., shuttle operations; and space rescue techniques.

For related information see also *03 Air Transportation and Safety* and *18 Spacecraft Design, Testing and Performance.* For space suits see *54 Man/System Technology and Life Support.*

17 SPACE COMMUNICATIONS, SPACECRAFT COMMUNICATIONS, COMMAND AND TRACKING **1922**

Includes telemetry; space communications networks; astronavigation and guidance; and radio blackout.

For related information see also *04 Aircraft Communications and Navigation* and *32 Communications and Radar.*

18 SPACECRAFT DESIGN, TESTING AND PERFORMANCE **1922**

Includes satellites; space platforms; space stations; spacecraft systems and components such as thermal and environmental controls; and attitude controls.

For life support systems see *54 Man/System Technology and Life Support.* For related information see also *05 Aircraft Design, Testing and Performance, 39 Structural Mechanics,* and *16 Space Transportation.*

19 SPACECRAFT INSTRUMENTATION **N.A.**

For related information see also *06 Aircraft Instrumentation* and *35 Instrumentation and Photography.*

20 SPACECRAFT PROPULSION AND POWER **1925**

Includes main propulsion systems and components, e.g. rocket engines; and spacecraft auxiliary power sources.

For related information see also *07 Aircraft Propulsion and Power, 28 Propellants and Fuels, 44 Energy Production and Conversion,* and *15 Launch Vehicles and Space Vehicles.*

CHEMISTRY AND MATERIALS

Includes chemistry and materials (general); composite materials; inorganic and physical chemistry; metallic materials; nonmetallic materials; propellants and fuels; and materials processing.

23 CHEMISTRY AND MATERIALS (GENERAL) **1926**

24 COMPOSITE MATERIALS **1926**

Includes physical, chemical, and mechanical properties of laminates and other composite materials.

For ceramic materials see *27 Nonmetallic Materials.*

25 INORGANIC AND PHYSICAL CHEMISTRY **1929**

Includes chemical analysis, e.g., chromatography; combustion theory; electrochemistry; and photochemistry.

For related information see also *77 Thermodynamics and Statistical Physics.*

26 METALLIC MATERIALS **1933**

Includes physical, chemical, and mechanical properties of metals, e.g., corrosion; and metallurgy.

27 NONMETALLIC MATERIALS **1938**

Includes physical, chemical, and mechanical properties of plastics, elastomers, lubricants, polymers, textiles, adhesives, and ceramic materials.

For composite materials see *24 Composite Materials.*

28 PROPELLANTS AND FUELS **1942**

Includes rocket propellants, igniters and oxidizers; their storage and handling procedures; and aircraft fuels.

For related information see also *07 Aircraft Propulsion and Power, 20 Spacecraft Propulsion and Power,* and *44 Energy Production and Conversion.*

29 MATERIALS PROCESSING **1944**

Includes space-based development of products and processes for commercial application.

For biological materials see *55 Space Biology.*

ENGINEERING

Includes engineering (general); communications and radar; electronics and electrical engineering; fluid mechanics and heat transfer; instrumentation and photography; lasers and masers; mechanical engineering; quality assurance and reliability; and structural mechanics.

For related information see also *Physics.*

31 ENGINEERING (GENERAL) **1944**

Includes vacuum technology; control engineering; display engineering; cryogenics; and fire prevention.

32 COMMUNICATIONS AND RADAR **1944**

Includes radar; land and global communications; communications theory; and optical communications.

For related information see also *04 Aircraft Communications and Navigation* and *17 Space Communications, Spacecraft Communications, Command and Tracking.* For search and rescue see *03 Air Transportation and Safety,* and *16 Space Transportation.*

33 ELECTRONICS AND ELECTRICAL ENGINEERING **1950**

Includes test equipment and maintainability; components, e.g., tunnel diodes and transistors; microminiaturization; and integrated circuitry.

For related information see also *60 Computer Operations and Hardware* and *76 Solid-State Physics.*

34 FLUID MECHANICS AND HEAT TRANSFER **1954**

Includes boundary layers; hydrodynamics; fluidics; mass transfer and ablation cooling.

For related information see also *02 Aerodynamics* and *77 Thermodynamics and Statistical Physics.*

35 INSTRUMENTATION AND PHOTOGRAPHY **1958**

Includes remote sensors; measuring instruments and gages; detectors; cameras and photographic supplies; and holography.

For aerial photography see *43 Earth Resources and Remote Sensing.* For related information see also *06 Aircraft Instrumentation* and *19 Spacecraft Instrumentation.*

36 LASERS AND MASERS **1960**

Includes parametric amplifiers.

For related information see also *76 Solid-State Physics.*

37 MECHANICAL ENGINEERING **1962**

Includes auxiliary systems (nonpower); machine elements and processes; and mechanical equipment.

38 QUALITY ASSURANCE AND RELIABILITY **1966**

Includes product sampling procedures and techniques; and quality control.

39 STRUCTURAL MECHANICS **1966**

Includes structural element design and weight analysis; fatigue; and thermal stress.

For applications see *05 Aircraft Design, Testing and Performance* and *18 Spacecraft Design, Testing and Performance.*

GEOSCIENCES

Includes geosciences (general); earth resources and remote sensing; energy production and conversion; environment pollution; geophysics; meteorology and climatology; and oceanography.

For related information see also *Space Sciences.*

42 GEOSCIENCES (GENERAL) **1972**

43 EARTH RESOURCES AND REMOTE SENSING **2002**

Includes remote sensing of earth resources by aircraft and spacecraft; photogrammetry; and aerial photography.

For instrumentation see *35 Instrumentation and Photography.*

44 ENERGY PRODUCTION AND CONVERSION **2003**

Includes specific energy conversion systems, e.g., fuel cells; global sources of energy; geophysical conversion; and windpower.

For related information see also *07 Aircraft Propulsion and Power, 20 Spacecraft Propulsion and Power,* and *28 Propellants and Fuels.*

45 ENVIRONMENT POLLUTION **2005**

Includes atmospheric, noise, thermal, and water pollution.

46 GEOPHYSICS **2007**

Includes aeronomy; upper and lower atmosphere studies; ionospheric and magnetospheric physics; and geomagnetism.

For space radiation see *93 Space Radiation.*

47 METEOROLOGY AND CLIMATOLOGY **2015**

Includes weather forecasting and modification.

48 OCEANOGRAPHY **2017**

Includes biological, dynamic, and physical oceanography; and marine resources.

For related information see also *43 Earth Resources and Remote Sensing.*

LIFE SCIENCES

Includes life sciences (general); aerospace medicine; behavioral sciences; man/system technology and life support; and space biology.

51 LIFE SCIENCES (GENERAL) **2018**

52 AEROSPACE MEDICINE **2020**

Includes physiological factors; biological effects of radiation; and effects of weightlessness on man and animals.

53 BEHAVIORAL SCIENCES **2022**

Includes psychological factors; individual and group behavior; crew training and evaluation; and psychiatric research.

54 MAN/SYSTEM TECHNOLOGY AND LIFE SUPPORT **2023**

Includes human engineering; biotechnology; and space suits and protective clothing.

For related information see also *16 Space Transportation.*

55 SPACE BIOLOGY **N.A.**

Includes exobiology; planetary biology; and extraterrestrial life.

MATHEMATICAL AND COMPUTER SCIENCES

Includes mathematical and computer sciences (general); computer operations and hardware; computer programming and software; computer systems; cybernetics; numerical analysis; statistics and probability; systems analysis; and theoretical mathematics.

59 MATHEMATICAL AND COMPUTER SCIENCES (GENERAL) **2025**

60 COMPUTER OPERATIONS AND HARDWARE **2032**

Includes hardware for computer graphics, firmware, and data processing.

For components see *33 Electronics and Electrical Engineering.*

61 COMPUTER PROGRAMMING AND SOFTWARE **2032**

Includes computer programs, routines, algorithms, and specific applications, e.g., CAD/CAM.

62 COMPUTER SYSTEMS **2040**

Includes computer networks and special application computer systems.

63 CYBERNETICS **2042**

Includes feedback and control theory, artificial intelligence, robotics and expert systems.

For related information see also *54 Man/System Technology and Life Support.*

64 NUMERICAL ANALYSIS **2043**

Includes iteration, difference equations, and numerical approximation.

65 STATISTICS AND PROBABILITY **2047**

Includes data sampling and smoothing; Monte Carlo method; and stochastic processes.

66 SYSTEMS ANALYSIS **2047**

Includes mathematical modeling; network analysis; and operations research.

67 THEORETICAL MATHEMATICS **2048**

Includes topology and number theory.

PHYSICS

Includes physics (general); acoustics; atomic and molecular physics; nuclear and high-energy physics; optics; plasma physics; solid-state physics; and thermodynamics and statistical physics.

For related information see also *Engineering.*

70 PHYSICS (GENERAL) **2048**

For precision time and time interval (PTTI) see *35 Instrumentation and Photography;* for geophysics, astrophysics or solar physics see *46 Geophysics, 90 Astrophysics,* or *92 Solar Physics.*

71 ACOUSTICS 2049
Includes sound generation, transmission, and attenuation.
For noise pollution see *45 Environment Pollution.*

72 ATOMIC AND MOLECULAR PHYSICS 2050
Includes atomic structure, electron properties, and molecular spectra.

73 NUCLEAR AND HIGH-ENERGY PHYSICS 2051
Includes elementary and nuclear particles; and reactor theory.
For space radiation see *93 Space Radiation.*

74 OPTICS 2051
Includes light phenomena and optical devices.
For lasers see *36 Lasers and Masers.*

75 PLASMA PHYSICS 2054
Includes magnetohydrodynamics and plasma fusion.
For ionospheric plasmas see *46 Geophysics.* For space plasmas see *90 Astrophysics.*

76 SOLID-STATE PHYSICS 2055
Includes superconductivity.
For related information see also *33 Electronics and Electrical Engineering* and *36 Lasers and Masers.*

77 THERMODYNAMICS AND STATISTICAL PHYSICS 2060
Includes quantum mechanics; theoretical physics; and Bose and Fermi statistics.
For related information see also *25 Inorganic and Physical Chemistry* and *34 Fluid Mechanics and Heat Transfer.*

SOCIAL SCIENCES

Includes social sciences (general); administration and management; documentation and information science; economics and cost analysis; law, political science, and space policy; and urban technology and transportation.

80 SOCIAL SCIENCES (GENERAL) N.A.
Includes educational matters.

81 ADMINISTRATION AND MANAGEMENT 2060
Includes management planning and research.

82 DOCUMENTATION AND INFORMATION SCIENCE 2061
Includes information management; information storage and retrieval technology; technical writing; graphic arts; and micrography.
For computer documentation see *61 Computer Programming and Software.*

83 ECONOMICS AND COST ANALYSIS 2063
Includes cost effectiveness studies.

84 LAW, POLITICAL SCIENCE AND SPACE POLICY 2063
Includes NASA appropriation hearings; aviation law; space law and policy; international law; international cooperation; and patent policy.

85 URBAN TECHNOLOGY AND TRANSPORTATION N.A.
Includes applications of space technology to urban problems; technology transfer; technology assessment; and surface and mass transportation.
For related information see *03 Air Transportation and Safety, 16 Space Transportation,* and *44 Energy Production and Conversion.*

SPACE SCIENCES

Includes space sciences (general); astronomy; astrophysics; lunar and planetary exploration; solar physics; and space radiation.
For related information see also *Geosciences.*

88 SPACE SCIENCES (GENERAL) N.A.

89 ASTRONOMY 2064
Includes radio, gamma-ray, and infrared astronomy; and astrometry.

90 ASTROPHYSICS 2064
Includes cosmology; celestial mechanics; space plasmas; and interstellar and interplanetary gases and dust.
For related information see also *75 Plasma Physics.*

91 LUNAR AND PLANETARY EXPLORATION N.A.
Includes planetology; and manned and unmanned flights.
For spacecraft design or space stations see *18 Spacecraft Design, Testing and Performance.*

92 SOLAR PHYSICS 2066
Includes solar activity, solar flares, solar radiation and sunspots.
For related information see *93 Space Radiation.*

93 SPACE RADIATION 2066
Includes cosmic radiation; and inner and outer earth's radiation belts.
For biological effects of radiation see *52 Aerospace Medicine.* For theory see *73 Nuclear and High-Energy Physics.*

GENERAL

Includes aeronautical, astronautical, and space science related histories, biographies, and pertinent reports too broad for categorization; histories or broad overviews of NASA programs.

99 GENERAL 2067

Note: N.A. means that no abstracts were assigned to this category for this issue.

SUBJECT INDEX I-1
PERSONAL AUTHOR INDEX I-57
CORPORATE SOURCE INDEX I-63
CONTRACT NUMBER INDEX I-75
REPORT/ACCESSION NUMBER INDEX I-77

TYPICAL CITATION AND ABSTRACT

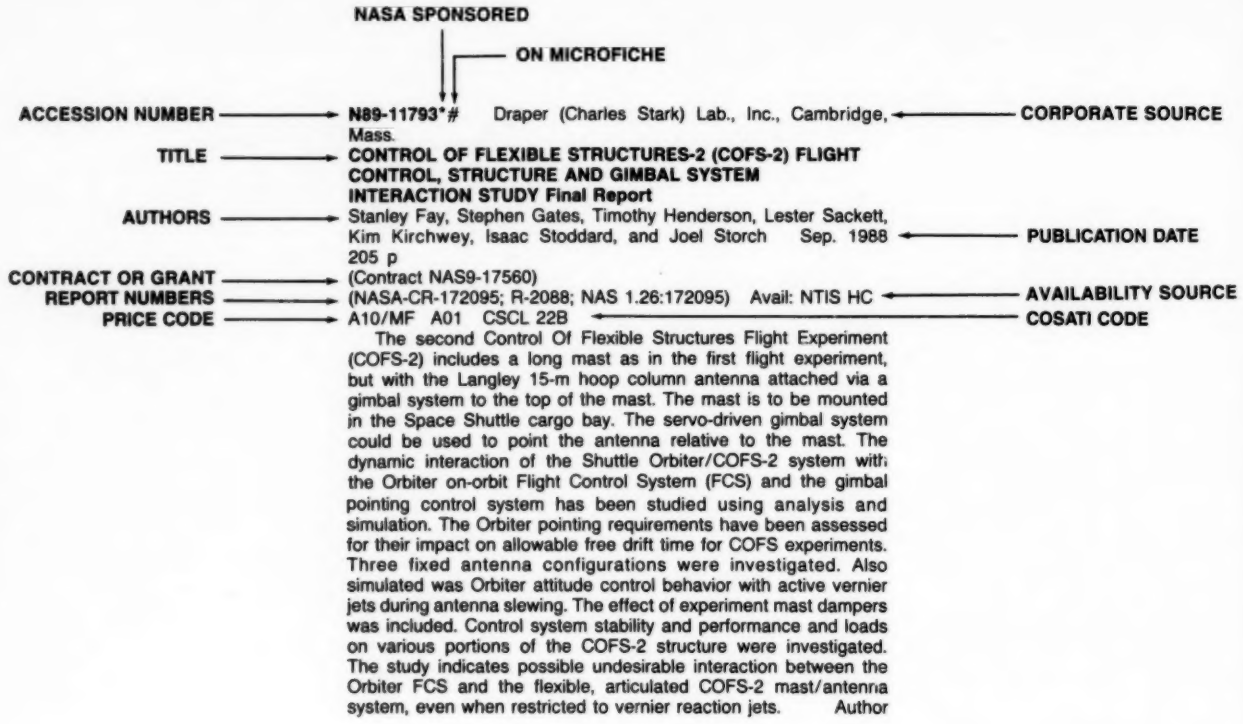
NASA SPONSORED
ON MICROFICHE
ACCESSION NUMBER
N89-11793*# Draper (Charles Stark) Lab., Inc., Cambridge, Mass.
CORPORATE SOURCE
TITLE
CONTROL OF FLEXIBLE STRUCTURES-2 (COFS-2) FLIGHT CONTROL, STRUCTURE AND GIMBAL SYSTEM INTERACTION STUDY Final Report
AUTHORS
Stanley Fay, Stephen Gates, Timothy Henderson, Lester Sackett, Kim Kirchwey, Isaac Stoddard, and Joel Storch Sep. 1988
205 p
PUBLICATION DATE
CONTRACT OR GRANT
(Contract NAS9-17560)
REPORT NUMBERS
(NASA-CR-172095; R-2088; NAS 1.26:172095) Avail: NTIS HC
AVAILABILITY SOURCE
PRICE CODE
A10/MF A01 CSCL 22B
COSATI CODE
The second Control Of Flexible Structures Flight Experiment (COFS-2) includes a long mast as in the first flight experiment, but with the Langley 15-m hoop column antenna attached via a gimbal system to the top of the mast. The mast is to be mounted in the Space Shuttle cargo bay. The servo-driven gimbal system could be used to point the antenna relative to the mast. The dynamic interaction of the Shuttle Orbiter/COFS-2 system with the Orbiter on-orbit Flight Control System (FCS) and the gimbal pointing control system has been studied using analysis and simulation. The Orbiter pointing requirements have been assessed for their impact on allowable free drift time for COFS experiments. Three fixed antenna configurations were investigated. Also simulated was Orbiter attitude control behavior with active vernier jets during antenna slewing. The effect of experiment mast dampers was included. Control system stability and performance and loads on various portions of the COFS-2 structure were investigated. The study indicates possible undesirable interaction between the Orbiter FCS and the flexible, articulated COFS-2 mast/antenna system, even when restricted to vernier reaction jets. Author

VOLUME 27 NUMBER 14 / JULY 23, 1989

Scientific and Technical Aerospace Reports

A Semimonthly Publication of the National Aeronautics and Space Administration

01 AERONAUTICS (GENERAL)

No abstracts in this category.

02 AERODYNAMICS

Includes aerodynamics of bodies, combinations, wings, rotors, and control surfaces; and internal flow in ducts and turbomachinery.

For related information see also *34 Fluid Mechanics and Heat Transfer.*

N89-20920*# Sverdrup Technology, Inc., Cleveland, OH.
SUBHARMONIC AND FUNDAMENTAL HIGH AMPLITUDE EXCITATION OF AN AXISYMMETRIC JET
Ganesh Raman and Edward J. Rice (National Aeronautics and Space Administration. Lewis Research Center, Cleveland, OH.) Mar. 1989 28 p Presented at the 2nd Shear Flow Conference, Tempe, AZ, 13-16 Mar. 1989; sponsored in part by AIAA
(NASA-TM-101946; E-4595; NAS 1.15:101946; AIAA-89-0993)
Avail: NTIS HC A03/MF A01 CSCL 01A

A circular jet was excited simultaneously by two different harmonically related tones. Data for three pairs of Strouhal numbers (St(D) = f*D/U (sub j) = 0.2 and 0.4, 0.3 and 0.6, 0.4 and 0.8). For each case the initial phase difference between the two waves was varied in steps of 45 deg, for one full cycle and the level of the fundamental and subharmonic forcing were varied independently over the range of 0.1 to 7 percent of the jet exit velocity. Our initial findings concurred with published findings, such as a critical level of the fundamental is required for subharmonic augmentation, the initial phase difference is critical in determining whether the subharmonic is augmented or suppressed. The detailed documentation of several aspects of this phenomenon all measured in one and the same experimental facility in a controlled manner, bring out several important points that eluded previous researchers: (1) At high amplitudes of the fundamental and subharmonic forcing levels the subharmonic augmentation is independent of the initial phase difference. (2) Contrary to the earlier belief that stable pairing could be produced only with an initial laminar boundary layer, the present work shows that by the two-frequency excitation method this phenomenon can be induced over a range of conditions for a jet with an initially turbulent boundary layer. (3) It is seen that two-frequency excitation is indeed more effective than single frequency excitation in jet mixing enhancement. Higher spreading rates seem to go along with higher subharmonic levels. Author

N89-20921*# Sverdrup Technology, Inc., Cleveland, OH.
COMPARISON OF 3D COMPUTATION AND EXPERIMENT FOR NON-AXISYMMETRIC NOZZLES Final Report
H. Lai and E. Nelson Feb. 1989 12 p Presented at the 27th Aerospace Sciences Meeting, Reno, NV, 9-12 Jan. 1989; sponsored in part by AIAA
(Contracts NAS3-24105; NAS3-25266)
(NASA-CR-182245; E-4574; NAS 1.26:182245; AIAA-89-0007)
Avail: NTIS HC A03/MF A01 CSCL 01A

Three dimensional solutions of a single expansion ramp nozzle are computed with the existing PARC computer code by solving the full Navier-Stokes equations. The computations are performed to simulate the non-axisymmetric nozzle flowfield in both the internal/external expansion regions and the exhaust plume in a quiescent ambient environment. Two different configurations of the nozzle at a pressure ratio NPR = 10 are examined. Numerical results of laminar flows are presented, and the wall pressure distributions are compared with the experimental data. Author

N89-20922*# Boeing Advanced Systems Co., Seattle, WA.
ADDITIONAL DEVELOPMENT OF THE XTRAN3S COMPUTER PROGRAM Final Report
C. J. Borland Jan. 1989 98 p
(Contract NAS1-17864)
(NASA-CR-181743; NAS 1.26:181743) Avail: NTIS HC A05/MF A01 CSCL 01A

Additional developments and enhancements to the XTRAN3S computer program, a code for calculation of steady and unsteady aerodynamics, and associated aeroelastic solutions, for 3-D wings in the transonic flow regime are described. Algorithm improvements for the XTRAN3S program were provided including an implicit finite difference scheme to enhance the allowable time step and vectorization for improved computational efficiency. The code was modified to treat configurations with a fuselage, multiple stores/nacelles/pylons, and winglets. Computer program changes (updates) for error corrections and updates for version control are provided. Author

N89-20923 California Univ., Los Angeles.
TRANSVERSE JETS IN COMPRESSIBLE CROSSFLOWS Ph.D. Thesis
Stephen Douglas Heister 1988 211 p
Avail: Univ. Microfilms Order No. DA8826010

The deflection and mixing of both gaseous and liquid jets in compressible crossflows are discussed. For gaseous jets, the jet cross-section is modeled as a compressible vortex pair which results from viscous forces at the periphery of the jet. The behavior of the vortex pair is then combined with mass and momentum balances along the axis of the jet to form a model which describes the trajectory and mixing of the injected fluid. In the case of a supersonic crossflow, a numerical technique is used to solve the inviscid outer flow and the position of the bow shock which envelopes the jet. This solution was combined with a liquid jet model developed by T.T. Nguyen to calculate liquid jet trajectories and the location of jet breakup. The solution was also combined with the compressible vortex pair of solution to generate trajectories of gaseous jets in supersonic crossflows. Dissert. Abstr.

N89-20924 Stanford Univ., CA.
NUMERICAL SIMULATION OF THE FLOW FIELD OVER DELTA WINGS WITH LEADING EDGE BLOWING Ph.D. Thesis
David T. Yeh 1988 131 p
Avail: Univ. Microfilms Order No. DA8826271

The vortical flow over a delta wing contributes an important part of the lift - the so-called nonlinear vortex lift. Controlling this vortical flow with its favorable influence would enhance the maneuverability and control of the aircraft. Several experiments have revealed that span-wise and tangential leading edge blowing can be applied as a means of controlling the position and strength

of the leading edge vortices. The present research studies these effects by numerical solution of the three-dimensional Navier-Stokes equations. The leading edge jet is simulated by defining a permeable boundary, corresponding to the jet slot, where suitable boundary conditions are implemented. Numerical results are shown to compare favorably with experimental measurements. It is found that the use of spanwise leading edge blowing at moderate angle of attack magnifies the size and strength of the leading edge vortices, and moves the vortex cores outboard and upward. The increase in lift primarily comes from the greater nonlinear vortex lift. However, spanwise blowing causes earlier vortex breakdown, thus decreasing the stall angle. The effects of tangential blowing at low to moderate angles of attack tend to reduce the pressure peaks associated with leading edge vortices and to increase the suction peak around the leading edge.
Dissert. Abstr.

N89-20925*# National Aeronautics and Space Administration. Langley Research Center, Hampton, VA.
TRANSONIC SYMPOSIUM: THEORY, APPLICATION, AND EXPERIMENT, VOLUME 1, PART 1
Jerome T. Foughner, Jr., comp. Mar. 1989 416 p Symposium held in Hampton, VA, 19-21 Apr. 1988; sponsored by NASA, Washington Original contains color illustrations
(NASA-CP-3020-Vol-1-Pt-1; L-16501-Vol-1-Pt-1; NAS 1.55:3020-Vol-1-Pt-1) Avail: NTIS HC A18/MF A01 CSCL 01A

Topics addressed include: wind tunnel and flight experiments; computational fluid dynamics (CFD) applications, industry overviews; and inviscid methods and grid generations. For individual titles, see N89-20926 through N89-20941.

N89-20926*# National Aeronautics and Space Administration. Langley Research Center, Hampton, VA.
AIRFRAME/PROPULSION INTEGRATION CHARACTERISTICS AT TRANSONIC SPEEDS
William P. Henderson and Bobby L. Berrier *In its* Transonic Symposium: Theory, Application, and Experiment, Volume 1, Part 1 Mar. 1989 p 1-31 (For primary document see N89-20925 14-02)
Avail: NTIS HC A18/MF A01 CSCL 01A

The aerodynamic characteristics for both single and twin-engine high-performance aircraft are significantly affected by shock induced flow interactions as well as other local flow interference effects which usually occur at transonic speeds. These adverse interactions can not only cause high drag, but also cause unusual aerodynamic loadings and/or severe stability and control problems. Many programs are under way to not only develop method for reducing the adverse effects, but also to develop an understanding of the basic flow conditions which are the primary contributors. It is anticipated that these programs will result in technologies which can reduce the aircraft cruise drag through improved integration as well as increase aircraft maneuverability through the application of thrust vectoring. Some of the primary integration problems for twin-engine aircraft at transonic speeds are identified, and several methods are demonstrated for reducing or eliminating the undersirable characteristics, while enhancing configuration effectiveness. Author

N89-20927*# National Aeronautics and Space Administration. Hugh L. Dryden Flight Research Facility, Edwards, CA.
FLIGHT RESEARCH AND TESTING
Terrill W. Putnam and Theodore G. Ayers *In* NASA, Langley Research Center, Transonic Symposium: Theory, Application, and Experiment, Volume 1, Part 1 Mar. 1989 p 33-59 Previously announced as N88-26361 (For primary document see N89-20925 14-02)
Avail: NTIS HC A18/MF A01 CSCL 01A

Flight research and testing form a critical link in the aeronautic research and development chain. Brilliant concepts, elegant theories, and even sophisticated ground tests of flight vehicles are not sufficient to prove beyond a doubt that an unproven aeronautical concept will actually perform as predicted. Flight research and testing provide the ultimate proof that an idea or concept performs as expected. Ever since the Wright brothers, flight research and testing were the crucible in which aeronautical concepts were advanced and proven to the point that engineers and companies are willing to stake their future to produce and design aircraft. This is still true today, as shown by the development of the experimental X-30 aerospace plane. The Dryden Flight Research Center (Ames-Dryden) continues to be involved in a number of flight research programs that require understanding and characterization of the total airplane in all the aeronautical disciplines, for example the X-29. Other programs such as the F-14 variable-sweep transition flight experiment have focused on a single concept or discipline. Ames-Dryden also continues to conduct flight and ground based experiments to improve and expand the ability to test and evaluate advanced aeronautical concepts. A review of significant aeronautical flight research programs and experiments is presented to illustrate both the progress being made and the challenges to come. Author

N89-20928*# High Technology Corp., Hampton, VA.
SHOCK-BOUNDARY-LAYER INTERACTION IN FLIGHT
Arild Bertelrud *In* NASA, Langley Research Center, Transonic Symposium: Theory, Application, and Experiment, Volume 1, Part 1 Mar. 1989 p 61-77 (For primary document see N89-20925 14-02)
Avail: NTIS HC A18/MF A01 CSCL 01A

A brief survey is given on the study of transonic shock/boundary layer effects in flight. Then the possibility of alleviating the adverse shock effects through passive shock control is discussed. A Swedish flight experiment on a swept wing attack aircraft is used to demonstrate how it is possible to reduce the extent of separated flow and increase the drag-rise Mach number significantly using a moderate amount of perforation of the surface. Author

N89-20929*# Boeing Commercial Airplane Co., Seattle, WA. Computational Fluid Dynamics Lab.
TRANSONIC CFD APPLICATIONS AT BOEING
E. N. Tinoco *In* NASA, Langley Research Center, Transonic Symposium: Theory, Application, and Experiment, Volume 1, Part 1 Mar. 1989 p 79-107 (For primary document see N89-20925 14-02)
Avail: NTIS HC A18/MF A01 CSCL 01A

The use of computational methods for three dimensional transonic flow design and analysis at the Boeing Company is presented. A range of computational tools consisting of production tools for every day use by project engineers, expert user tools for special applications by computational researchers, and an emerging tool which may see considerable use in the near future are described. These methods include full potential and Euler solvers, some coupled to three dimensional boundary layer analysis methods, for transonic flow analysis about nacelle, wing-body, wing-body-strut-nacelle, and complete aircraft configurations. As the examples presented show, such a toolbox of codes is necessary for the variety of applications typical of an industrial environment. Such a toolbox of codes makes possible aerodynamic advances not previously achievable in a timely manner, if at all. Author

N89-20930*# General Dynamics Corp., Fort Worth, TX.
THE APPLICATION OF CFD FOR MILITARY AIRCRAFT DESIGN AT TRANSONIC SPEEDS
C. W. Smith, W. W. Braymen, I. C. Bhateley, and W. K. Londenberg *In* NASA, Langley Research Center, Transonic Symposium: Theory, Application, and Experiment, Volume 1, Part 1 Mar. 1989 p 109-132 (For primary document see N89-20925 14-02)
Avail: NTIS HC A18/MF A01 CSCL 01A

Numerous computational fluid dynamics (CFD) codes are available that solve any of several variations of the transonic flow equations from small disturbance to full Navier-Stokes. The design philosophy at General Dynamics Fort Worth Division involves use of all these levels of codes, depending on the stage of configuration development. Throughout this process, drag calculation is a central issue. An overview is provided for several transonic codes and

representative test-to-theory comparisons for fighter-type configurations are presented. Correlations are shown for lift, drag, pitching moment, and pressure distributions. The future of applied CFD is also discussed, including the important task of code validation. With the progress being made in code development and the continued evolution in computer hardware, the routine application of these codes for increasingly more complex geometries and flow conditions seems apparent. Author

N89-20931*# Grumman Aerospace Corp., Bethpage, NY. Aircraft Systems.
APPLIED TRANSONICS AT GRUMMAN
W. H. Davis *In* NASA, Langley Research Center, Transonic Symposium: Theory, Application, and Experiment, Volume 1, Part 1 Mar. 1989 p 133-152 (For primary document see N89-20925 14-02)
Avail: NTIS HC A18/MF A01 CSCL 01A

A review of several applications of Computational Fluid Dynamics (CFD) to various aspects of aerodynamic design recently carried out at Grumman is presented. The emphasis is placed on project-oriented applications where the ease of use of the methods and short start-to-completion times are required. Applications cover transonic wing design/optimization, wing mounted stores load prediction, transonic buffet alleviation, fuselage loads estimation, and compact offset diffuser design for advanced aircraft configurations. Computational methods employed include extended transonic small disturbance (automatic grid embedding) formulation for analysis/design/optimization and a thin layer Navier-Stokes formulation for both external and internal flow analyses. Author

N89-20932*# Lockheed Aeronautical Systems Co., Burbank, CA.
TRANSONICS AND FIGHTER AIRCRAFT: CHALLENGES AND OPPORTUNITIES FOR CFD
Luis R. Miranda *In* NASA, Langley Research Center, Transonic Symposium: Theory, Application, and Experiment, Volume 1, Part 1 Mar. 1989 p 153-173 Original document contains color illustrations (For primary document see N89-20925 14-02)
Avail: NTIS HC A18/MF A01 CSCL 01A

The application of computational fluid dynamics (CFD) to fighter aircraft design and development is discussed. Methodology requirements for the aerodynamic design of fighter aircraft are briefly reviewed. The state-of-the-art of computational methods for transonic flows in the light of these requirements is assessed and the techniques found most adequate for the subject application are identified. Highlights from some proof-of-feasibility Euler and Navier-Stokes computations about a complete fighter aircraft configuration are presented. Finally, critical issues and opportunities for design application of CFD are discussed. Author

N89-20933*# Lockheed Aeronautical Systems Co., Marietta, GA. Advanced Flight Sciences Dept.
COMPUTATION OF AIRCRAFT COMPONENT FLOW FIELDS AT TRANSONIC MACH NUMBERS USING A THREE-DIMENSIONAL NAVIER-STOKES ALGORITHM
George D. Shrewsbury, Joseph Vadyak, David M. Schuster, and Marilyn J. Smith *In* NASA, Langley Research Center, Transonic Symposium: Theory, Application, and Experiment, Volume 1, Part 1 Mar. 1989 p 175-194 Original document contains color illustrations (For primary document see N89-20925 14-02)
Avail: NTIS HC A18/MF A01 CSCL 01A

A computer analysis was developed for calculating steady (or unsteady) three-dimensional aircraft component flow fields. This algorithm, called ENS3D, can compute the flow field for the following configurations: diffuser duct/thrust nozzle, isolated wing, isolated fuselage, wing/fuselage with or without integrated inlet and exhaust, nacelle/inlet, nacelle (fuselage) afterbody/exhaust jet, complete transport engine installation, and multicomponent configurations using zonal grid generation technique. Solutions can be obtained for subsonic, transonic, or hypersonic freestream speeds. The algorithm can solve either the Euler equations for inviscid flow, the thin shear layer Navier-Stokes equations for viscous flow, or the full Navier-Stokes equations for viscous flow. The flow field solution is determined on a body-fitted computational grid. A fully-implicit alternating direction implicit method is employed for the solution of the finite difference equations. For viscous computations, either a two layer eddy-viscosity turbulence model or the k-epsilon two equation transport model can be used to achieve mathematical closure. Author

N89-20934*# Rockwell International Corp., Los Angeles, CA. Aircraft Operations.
TRANSONIC AERODYNAMIC DESIGN EXPERIENCE
E. Bonner *In* NASA, Langley Research Center, Transonic Symposium: Theory, Application, and Experiment, Volume 1, Part 1 Mar. 1989 p 195-216 (For primary document see N89-20925 14-02)
Avail: NTIS HC A18/MF A01 CSCL 01A

Advancements have occurred in transonic numerical simulation that place aerodynamic performance design into a relatively well developed status. Efficient broad band operating characteristics can be reliably developed at the conceptual design level. Recent aeroelastic and separated flow simulation results indicate that systematic consideration of an increased range of design problems appears promising. This emerging capability addresses static and dynamic structural/aerodynamic coupling and nonlinearities associated with viscous dominated flows. Author

N89-20935*# Michigan Univ., Ann Arbor.
EULER SOLVERS FOR TRANSONIC APPLICATIONS
Bram vanLeer *In* NASA, Langley Research Center, Transonic Symposium: Theory, Application, and Experiment, Volume 1, Part 1 Mar. 1989 p 217-230 (For primary document see N89-20925 14-02)
Avail: NTIS HC A18/MF A01 CSCL 01A

The 1980s may well be called the Euler era of applied aerodynamics. Computer codes based on discrete approximations of the Euler equations are now routinely used to obtain solutions of transonic flow problems in which the effects of entropy and vorticity production are significant. Such codes can even predict separation from a sharp edge, owing to the inclusion of artificial dissipation, intended to lend numerical stability to the calculation but at the same time enforcing the Kutta condition. One effect not correctly predictable by Euler codes is the separation from a smooth surface, and neither is viscous drag; for these some form of the Navier-Stokes equation is needed. It, therefore, comes as no surprise to observe that the Navier-Stokes has already begun before Euler solutions were fully exploited. Moreover, most numerical developments for the Euler equations are now constrained by the requirement that the techniques introduced, notably artificial dissipation, must not interfere with the new physics added when going from an Euler to a full Navier-Stokes approximation. In order to appreciate the contributions of Euler solvers to the understanding of transonic aerodynamics, it is useful to review the components of these computational tools. Space discretization, time- or pseudo-time marching and boundary procedures, the essential constituents are discussed. The subject of grid generation and grid adaptation to the solution are touched upon only where relevant. A list of unanswered questions and an outlook for the future are covered. Author

N89-20936*# Michigan Univ., Ann Arbor. Dept. of Aerospace Engineering.
AN EMBEDDED MESH PROCEDURE FOR LEADING-EDGE VORTEX FLOWS
Kenneth G. Powell and Earll M. Murman (Massachusetts Inst. of Tech., Cambridge.) *In* NASA, Langley Research Center, Transonic Symposium: Theory, Application, and Experiment, Volume 1, Part 1 Mar. 1989 p 231-259 (For primary document see N89-20925 14-02)
Avail: NTIS HC A18/MF A01 CSCL 01A

A cell-vertex scheme is outlined for solving the flow about a delta wing with M (sub infinity) is greater than 1. Embedded regions of mesh refinement allow solutions to be obtained which have much higher resolution than those achieved to date. Effects of mesh refinement and artificial viscosity on the solutions are studied,

to determine at what point leading-edge vortex solutions are grid-converged. A macroscale and a microscale for the size of the vortex are defined, and it is shown that the macroscale (which includes the wing surface properties) is converged on a moderately refined grid, while the microscale is very sensitive to grid spacing. The level of numerical diffusion in the core of the vortex is found to be substantial. Comparisons with the experiment are made for two cases which have transonic cross-flow velocities. Author

N89-20937*# Michigan Univ., Ann Arbor.
ASYMPTOTIC METHODS FOR INTERNAL TRANSONIC FLOWS
T. C. Adamson, Jr. and A. F. Messiter *In* NASA, Langley Research Center, Transonic Symposium: Theory, Application, and Experiment, Volume 1, Part 1 Mar. 1989 p 261-291 (For primary document see N89-20925 14-02)
Avail: NTIS HC A18/MF A01 CSCL 01A

For many internal transonic flows of practical interest, some of the relevant nondimensional parameters typically are small enough that a perturbation scheme can be expected to give a useful level of numerical accuracy. A variety of steady and unsteady transonic channel and cascade flows is studied with the help of systematic perturbation methods which take advantage of this fact. Asymptotic representations are constructed for small changes in channel cross-section area, small flow deflection angles, small differences between the flow velocity and the sound speed, small amplitudes of imposed oscillations, and small reduced frequencies. Inside a channel the flow is nearly one-dimensional except in thin regions immediately downstream of a shock wave, at the channel entrance and exit, and near the channel throat. A study of two-dimensional cascade flow is extended to include a description of three-dimensional compressor-rotor flow which leads to analytical results except in thin edge regions which require numerical solution. For unsteady flow the qualitative nature of the shock-wave motion in a channel depends strongly on the orders of magnitude of the frequency and amplitude of impressed wall oscillations or fluctuations in back pressure. One example of supersonic flow is considered, for a channel with length large compared to its width, including the effect of separation bubbles and the possibility of self-sustained oscillations. The effect of viscosity on a weak shock wave in a channel is discussed. Author

N89-20938*# Rensselaer Polytechnic Inst., Troy, NY.
WAVE DRAG DUE TO LIFT FOR TRANSONIC AIRPLANES
Julian D. Cole and Norman D. Malmuth *In* NASA, Langley Research Center, Transonic Symposium: Theory, Application, and Experiment, Volume 1, Part 1 Mar. 1989 p 293-308 Sponsored in part by Rockwell North American Aircraft (For primary document see N89-20925 14-02)
(Grant AF-AFOSR-0037-88)
Avail: NTIS HC A18/MF A01 CSCL 01A

Lift dominated pointed aircraft configurations are considered in the transonic range. These are treated as lifting wings of zero thickness with an aspect ratio of order one. An inner expansion which starts as Jones' theory is matched to a nonlinear outer transonic theory as in Barnwell's earlier work. Expressions for the wave drag due to the equivalent body are derived. Some examples of numerical calculations for different configurations are presented. Author

N89-20939*# California Univ., Davis.
VECTOR POTENTIAL METHODS
M. Hafez *In* NASA, Langley Research Center, Transonic Symposium: Theory, Application, and Experiment, Volume 1, Part 1 Mar. 1989 p 309-339 (For primary document see N89-20925 14-02)
Avail: NTIS HC A18/MF A01 CSCL 01A

Vector potential and related methods, for the simulation of both inviscid and viscous flows over aerodynamic configurations, are briefly reviewed. The advantages and disadvantages of several formulations are discussed and alternate strategies are recommended. Scalar potential, modified potential, alternate formulations of Euler equations, least-squares formulation, variational principles, iterative techniques and related methods, and viscous flow simulation are discussed. Author

N89-20940*# Princeton Univ., NJ.
DEVELOPMENTS AND TRENDS IN THREE-DIMENSIONAL MESH GENERATION
Timothy J. Baker *In* NASA, Langley Research Center, Transonic Symposium: Theory, Application, and Experiment, Volume 1, Part 1 Mar. 1989 p 341-376 Original document contains color illustrations (For primary document see N89-20925 14-02)
Avail: NTIS HC A18/MF A01 CSCL 01A

An intense research effort over the last few years has produced several competing and apparently diverse methods for generating meshes. Recent progress is reviewed and the central themes are emphasized which form a solid foundation for future developments in mesh generation. Author

N89-20941*# National Aeronautics and Space Administration. Langley Research Center, Hampton, VA.
GENERATION OF UNSTRUCTURED GRIDS AND EULER SOLUTIONS FOR COMPLEX GEOMETRIES
Rainald Loehner, Paresh Parikh (Vigyan Research Associates, Inc., Hampton, VA.), and Manuel D. Salas *In its* Transonic Symposium: Theory, Application, and Experiment, Volume 1, Part 1 Mar. 1989 p 377-408 Prepared in cooperation with Naval Research Lab., Washington, DC (For primary document see N89-20925 14-02)
Avail: NTIS HC A18/MF A01 CSCL 01A

Algorithms are described for the generation and adaptation of unstructured grids in two and three dimensions, as well as Euler solvers for unstructured grids. The main purpose is to demonstrate how unstructured grids may be employed advantageously for the economic simulation of both geometrically as well as physically complex flow fields. Author

N89-20942*# National Aeronautics and Space Administration. Langley Research Center, Hampton, VA.
TRANSONIC SYMPOSIUM: THEORY, APPLICATION, AND EXPERIMENT, VOLUME 1, PART 2
Jerome T. Foughner, Jr., comp. Mar. 1989 511 p Symposium held in Hampton, VA, 19-21 Apr.1988; sponsored by NASA, Washington Original contains color illustrations
(NASA-CP-3020-Vol-1-Pt-2; L-16501-Vol-1-Pt-2; NAS 1.55:3020-Vol-1-Pt-2) Avail: NTIS HC A22/MF A01 CSCL 01A

In order to assess the state of the art in transonic flow disciplines and to glimpse at future directions, NASA-Langley held a Transonic Symposium. Emphasis was placed on steady, three dimensional external, transonic flow and its simulation, both numerically and experimentally. The symposium included technical sessions on wind tunnel and flight experiments; computational fluid dynamic applications; inviscid methods and grid generation; viscous methods and boundary layer stability; and wind tunnel techniques and wall interference. This, being volume 1, is unclassified. For individual titles, see N89-20943 through N89-20961.

N89-20943*# McDonnell Aircraft Co., Saint Louis, MO. Computation Fluid Dynamics.
TRANSONIC PROPULSION SYSTEM INTEGRATION ANALYSIS AT MCDONNELL AIRCRAFT COMPANY **c07**
Raymond R. Cosner *In* NASA, Langley Research Center, Transonic Symposium: Theory, Application, and Experiment, Volume 1, Part 2 Mar. 1989 p 409-436 (For primary document see N89-20942 14-02)
Avail: NTIS HC A22/MF A01 CSCL 21E

The technology of Computational Fluid Dynamics (CFD) is becoming an important tool in the development of aircraft propulsion systems. Two of the most valuable features of CFD are: (1) quick acquisition of flow field data; and (2) complete description of flow fields, allowing detailed investigation of interactions. Current analysis methods complement wind tunnel testing in several ways. Herein, the discussion is focused on CFD

methods. However, aircraft design studies need data from both CFD and wind tunnel testing. Each approach complements the other. Author

N89-20944*# National Aeronautics and Space Administration. Ames Research Center, Moffett Field, CA.

AERODYNAMIC ANALYSIS OF THREE ADVANCED CONFIGURATIONS USING THE TRANAIR FULL-POTENTIAL CODE

M. D. Madson, R. L. Carmichael, and J. P. Mendoza *In* NASA, Langley Research Center, Transonic Symposium: Theory, Application, and Experiment, Volume 1, Part 2 Mar. 1989 p 437-452 (For primary document see N89-20942 14-02)
Avail: NTIS HC A22/MF A01 CSCL 21E

Computational results are presented for three advanced configurations: the F-16A with wing tip missiles and under wing fuel tanks, the Oblique Wing Research Aircraft, and an Advanced Turboprop research model. These results were generated by the latest version of the TranAir full potential code, which solves for transonic flow over complex configurations. TranAir embeds a surface paneled geometry definition in a uniform rectangular flow field grid, thus avoiding the use of surface conforming grids, and decoupling the grid generation process from the definition of the configuration. The new version of the code locally refines the uniform grid near the surface of the geometry, based on local panel size and/or user input. This method distributes the flow field grid points much more efficiently than the previous version of the code, which solved for a grid that was uniform everywhere in the flow field. TranAir results are presented for the three configurations and are compared with wind tunnel data. Author

N89-20945*# Grumman Aerospace Corp., Bethpage, NY. Aircraft Systems Div.

METHOD TO PREDICT EXTERNAL STORE CARRIAGE LOADS AT TRANSONIC SPEEDS **c05**

Bruce S. Rosen *In* NASA, Langley Research Center, Transonic Symposium: Theory, Application, and Experiment, Volume 1, Part 2 Mar. 1989 p 453-465 Previously announced in IAA as A88-22003 (For primary document see N89-20942 14-02)
(Contract NAS1-18105)
Avail: NTIS HC A22/MF A01 CSCL 01C

A computational method for prediction of external store carriage loads at transonic speeds is described. The geometric flexibility required for treatment of isolated and underwing, pylon mounted stores is achieved by computing solutions on a five level embedded grid arrangement. A completely automated grid generation procedure facilitates applications. Store modeling capability consists of bodies of revolution with multiple fore and aft fins. A body conforming grid improves the accuracy of the computed store body flow field. A nonlinear finite difference relaxation scheme, developed specifically for modified transonic small disturbance flow equations, enhances numerical stability and accuracy. As a result, more accurate treatment of low aspect ratio, highly swept and tapered wing planforms is possible. A limited supersonic freestream capability is also provided. Pressure, load distribution, force and moment correlation show good agreement for several test cases. Author

N89-20946*# National Aeronautics and Space Administration. Langley Research Center, Hampton, VA.

STEADY AND UNSTEADY TRANSONIC SMALL DISTURBANCE ANALYSIS OF REALISTIC AIRCRAFT CONFIGURATIONS **c05**

John T. Batina, David A. Seidel, Robert M. Bennett, Herbert J. Cunningham, and Samuel R. Bland *In its* Transonic Symposium: Theory, Application, and Experiment, Volume 1, Part 2 Mar. 1989 p 467-496 (For primary document see N89-20942 14-02)
Avail: NTIS HC A22/MF A01 CSCL 01C

A transonic unsteady aerodynamic and aeroelastic code called CAP-TSD (Computational Aeroelasticity Program - Transonic Small Disturbance) was developed for application to realistic aircraft configurations. It permits the calculation of steady and unsteady flows about complete aircraft configurations for aeroelastic analysis of the flutter critical transonic speed range. The CAP-TSD code uses a time accurate approximate factorization algorithm for solution of the unsteady transonic small disturbance potential equation. An overview is given of the CAP-TSD code development effort along with recent algorithm modifications which are listed and discussed. Calculations are presented for several configurations including the General Dynamics 1/9th scale F-16C aircraft model to evaluate the algorithm and hence the reliability of the CAP-TSD code in general. Calculations are also presented for a flutter analysis of a 45 deg sweptback wing which agree well with the experimental data. Descriptions are presented of the CAP-TSD code and algorithm details along with results and comparisons which demonstrate the stability, accuracy, efficiency, and utility of CAP-TSD. Author

N89-20947*# National Aeronautics and Space Administration. Langley Research Center, Hampton, VA.

INVERSE WING DESIGN IN TRANSONIC FLOW INCLUDING VISCOUS INTERACTION **c05**

Leland A. Carlson, Robert R. Ratcliff, Thomas A. Gally (Texas A&M Univ., College Station.), and Richard L. Campbell *In its* Transonic Symposium: Theory, Application, and Experiment, Volume 1, Part 2 Mar. 1989 p 497-519 (For primary document see N89-20942 14-02)
(Grant NsG-1619)
Avail: NTIS HC A22/MF A01 CSCL 01C

Several inverse methods were compared and initial results indicate that differences in results are primarily due to coordinate systems and fuselage representations and not to design procedures. Further, results from a direct-inverse method that includes 3-D wing boundary layer effects, wake curvature, and wake displacement are represented. These results show that boundary layer displacements must be included in the design process for accurate results. Author

N89-20948*# McDonnell-Douglas Research Labs., Saint Louis, MO.

EULER/NAVIER-STOKES CALCULATIONS OF TRANSONIC FLOW PAST FIXED- AND ROTARY-WING AIRCRAFT CONFIGURATIONS

J. E. Deese and R. K. Agarwal *In* NASA, Langley Research Center, Transonic Symposium: Theory, Application, and Experiment, Volume 1, Part 2 Mar. 1989 p 521-545 Original document contains color illustrations (For primary document see N89-20942 14-02)
Avail: NTIS HC A22/MF A01 CSCL 01A

Computational fluid dynamics has an increasingly important role in the design and analysis of aircraft as computer hardware becomes faster and algorithms become more efficient. Progress is being made in two directions: more complex and realistic configurations are being treated and algorithms based on higher approximations to the complete Navier-Stokes equations are being developed. The literature indicates that linear panel methods can model detailed, realistic aircraft geometries in flow regimes where this approximation is valid. As algorithms including higher approximations to the Navier-Stokes equations are developed, computer resource requirements increase rapidly. Generation of suitable grids become more difficult and the number of grid points required to resolve flow features of interest increases. Recently, the development of large vector computers has enabled researchers to attempt more complex geometries with Euler and Navier-Stokes algorithms. The results of calculations for transonic flow about a typical transport and fighter wing-body configuration using thin layer Navier-Stokes equations are described along with flow about helicopter rotor blades using both Euler/Navier-Stokes equations. Author

N89-20949*# National Aeronautics and Space Administration. Ames Research Center, Moffett Field, CA.

NAVIER-STOKES AND VISCOUS-INVISCID INTERACTION **c34**

Joseph L. Steger and William R. VanDalsem *In* NASA, Langley Research Center, Transonic Symposium: Theory, Application, and

Experiment, Volume 1, Part 2 Mar. 1989 p 547-570 (For primary document see N89-20942 14-02)
Avail: NTIS HC A22/MF A01 CSCL 20D

Some considerations toward developing numerical procedures for simulating viscous compressible flows are discussed. Both Navier-Stokes and boundary layer field methods are considered. Because efficient viscous-inviscid interaction methods have been difficult to extend to complex 3-D flow simulations, Navier-Stokes procedures are more frequently being utilized even though they require considerably more work per grid point. It would seem a mistake, however, not to make use of the more efficient approximate methods in those regions in which they are clearly valid. Ideally, a general purpose compressible flow solver that can optionally take advantage of approximate solution methods would suffice, both to improve accuracy and efficiency. Some potentially useful steps toward this goal are described: a generalized 3-D boundary layer formulation and the fortified Navier-Stokes procedure. Author

N89-20950*# National Aeronautics and Space Administration. Langley Research Center, Hampton, VA.
THE 3-D EULER AND NAVIER-STOKES CALCULATIONS FOR AIRCRAFT COMPONENTS c34
Veer N. Vatsa, Bruce W. Wedan, and Eli Turkel (Institute for Computer Applications in Science and Engineering, Hampton, VA.) *In its* Transonic Symposium: Theory, Application, and Experiment, Volume 1, Part 2 Mar. 1989 p 571-579 (For primary document see N89-20942 14-02)
Avail: NTIS HC A22/MF A01 CSCL 20D

An explicit multistage Runge-Kutta type of time-stepping scheme is used for solving transonic flow past a transport type wing/fuselage configuration. Solutions for both Euler and Navier-Stokes equations are obtained for quantitative assessment of boundary layer interaction effects. The viscous solutions are obtained on both a medium resolution grid of approximately 270,000 points and a find grid of 460,000 points to assess the effects of grid density on the solution. Computed pressure distributions are compared with the experimental data. Author

N89-20951*# National Aeronautics and Space Administration. Ames Research Center, Moffett Field, CA.
TURBULENCE AND MODELING IN TRANSONIC FLOW
Morris W. Rubesin and John R. Viegas *In* NASA, Langley Research Center, Transonic Symposium: Theory, Application, and Experiment, Volume 1, Part 2 Mar. 1989 p 581-610 (For primary document see N89-20942 14-02)
Avail: NTIS HC A22/MF A01 CSCL 01A

A review is made of the performance of a variety of turbulence models in the evaluation of a particular well documented transonic flow. This is done to supplement a previous attempt to calibrate and verify transonic airfoil codes by including many more turbulence models than used in the earlier work and applying the calculations to an experiment that did not suffer from uncertainties in angle of attack and was free of wind tunnel interference. It is found from this work, as well as in the earlier study, that the Johnson-King turbulence model is superior for transonic flows over simple aerodynamic surfaces, including moderate separation. It is also shown that some field equation models with wall function boundary conditions can be competitive with it. Author

N89-20952*# Iowa State Univ. of Science and Technology, Ames. Dept. of Aerospace Engineering.
TURBULENT EDDY VISCOSITY MODELING IN TRANSONIC SHOCK/BOUNDARY-LAYER INTERACTIONS
G. R. Inger *In* NASA, Langley Research Center, Transonic Symposium: Theory, Application, and Experiment, Volume 1, Part 2 Mar. 1989 p 611-627 Previously announced in IAA as A88-40758 (For primary document see N89-20942 14-02)
Avail: NTIS HC A22/MF A01 CSCL 01A

The treatment of turbulence effects on transonic shock/turbulent boundary layer interaction is addressed within the context of a triple deck approach valid for arbitrary practical Reynolds numbers between 1000 and 10 billion. The modeling of the eddy viscosity and basic turbulent boundary profile effects in each deck is examined in detail using Law-of-the-Wall/Law-of-the-Wake concepts as the foundation. Results of parametric studies showing how each of these turbulence model aspects influences typical interaction zone property distributions (wall pressure, displacement thickness and local skin friction) are presented and discussed. Author

N89-20953*# Virginia Polytechnic Inst. and State Univ., Blacksburg. Dept. of Engineering Science and Mechanics.
STABILITY OF COMPRESSIBLE BOUNDARY LAYERS
Ali H. Nayfeh *In* NASA, Langley Research Center, Transonic Symposium: Theory, Application, and Experiment, Volume 1, Part 2 Mar. 1989 p 629-689 (For primary document see N89-20942 14-02)
Avail: NTIS HC A22/MF A01 CSCL 01A

The stability of compressible 2-D and 3-D boundary layers is reviewed. The stability of 2-D compressible flows differs from that of incompressible flows in two important features: There is more than one mode of instability contributing to the growth of disturbances in supersonic laminar boundary layers and the most unstable first mode wave is 3-D. Whereas viscosity has a destabilizing effect on incompressible flows, it is stabilizing for high supersonic Mach numbers. Whereas cooling stabilizes first mode waves, it destabilizes second mode waves. However, second order waves can be stabilized by suction and favorable pressure gradients. The influence of the nonparallelism on the spatial growth rate of disturbances is evaluated. The growth rate depends on the flow variable as well as the distance from the body. Floquet theory is used to investigate the subharmonic secondary instability. Author

N89-20954*# Old Dominion Univ., Norfolk, VA. Dept. of Mechanical Engineering and Mechanics.
SECONDARY THREE-DIMENSIONAL INSTABILITY IN COMPRESSIBLE BOUNDARY LAYERS
Nabil M. El-Hady *In* NASA, Langley Research Center, Transonic Symposium: Theory, Application, and Experiment, Volume 1, Part 2 Mar. 1989 p 691-704 (For primary document see N89-20942 14-02)
Avail: NTIS HC A22/MF A01 CSCL 01A

Three dimensional linear secondary instability theory is extended for compressible boundary layers on a flat plate in the presence of finite amplitude Tollmien-Schlichting waves. The focus is on principal parametric resonance responsible for strong growth of subharmonics in low disturbance environment. Author

N89-20955*# National Aeronautics and Space Administration. Langley Research Center, Hampton, VA.
TEST TECHNIQUES: A SURVEY PAPER ON CRYOGENIC TUNNELS, ADAPTIVE WALL TEST SECTIONS, AND MAGNETIC SUSPENSION AND BALANCE SYSTEMS c09
Robert A. Kilgore, David A. Dress, Stephen W. D. Wolf, and Colin P. Britcher (Old Dominion Univ., Norfolk, VA.) *In its* Transonic Symposium: Theory, Application, and Experiment, Volume 1, Part 2 Mar. 1989 p 705-740 (For primary document see N89-20942 14-02)
Avail: NTIS HC A22/MF A01 CSCL 14B

The ability to get good experimental data in wind tunnels is often compromised by things seemingly beyond our control. Inadequate Reynolds number, wall interference, and support interference are three of the major problems in wind tunnel testing. Techniques for solving these problems are available. Cryogenic wind tunnels solve the problem of low Reynolds number. Adaptive wall test sections can go a long way toward eliminating wall interference. A magnetic suspension and balance system (MSBS) completely eliminates support interference. Cryogenic tunnels, adaptive wall test sections, and MSBS are surveyed. A brief historical overview is given and the present state of development and application in each area is described. Author

N89-20956*# National Aeronautics and Space Administration. Lewis Research Center, Cleveland, OH.
AN LDA (LASER-DOPPLER ANEMOMETRY) INVESTIGATION OF THREE-DIMENSIONAL NORMAL SHOCK WAVE BOUNDARY-LAYER INTERACTIONS
R. M. Chriss, W. R. Hingst, A. J. Strazisar, and T. G. Keith, Jr. (Toledo Univ., OH.) *In* NASA, Langley Research Center, Transonic Symposium: Theory, Application, and Experiment, Volume 1, Part 2 Mar. 1989 p 741-764 (For primary document see N89-20942 14-02)
Avail: NTIS HC A22/MF A01 CSCL 01A

Nonintrusive measurements were made of a normal shock wave/boundary layer interaction. Two dimensional measurements were made throughout the interaction region while 3-D measurements were made in the vicinity of the shock wave. The measurements were made in the corner of the test section of a continuous supersonic wind tunnel in which a normal shock wave had been stabilized. Laser Doppler Anemometry, surface pressure measurement and flow visualization techniques were employed for two freestream Mach number test cases: 1.6 and 1.3. The former contained separated flow regions and a system of shock waves. The latter was found to be far less complicated. The results define the flow field structure in detail for each case. Author

N89-20957*# National Aeronautics and Space Administration. Langley Research Center, Hampton, VA.
INSTRUMENTATION ADVANCES FOR TRANSONIC TESTING **c09**
Percy J. Bobbitt *In its* Transonic Symposium: Theory, Application, and Experiment, Volume 1, Part 2 Mar. 1989 p 765-816 (For primary document see N89-20942 14-02)
Avail: NTIS HC A22/MF A01 CSCL 14B

New and improved instrumentation, like new and improved wind tunnels, provide capabilities which stimulate innovative research and discovery. During the past few years there have been a number of instrumentation developments which have aided and abetted the acquisition of more accurate aerodynamic data and have led to new physical insights as well. Some of these advances are reviewed, particularly in the area of thin film gages, hot wire anemometry, and laser instrumentation. A description is given of the instruments and/or techniques and some sample results are shown. Author

N89-20958*# National Aeronautics and Space Administration. Langley Research Center, Hampton, VA.
WALL INTERFERENCE ASSESSMENT AND CORRECTIONS
P. A. Newman, W. B. Kemp, Jr., and J. A. Garriz (Vigyan Research Associates, Inc., Hampton, VA.) *In its* Transonic Symposium: Theory, Application, and Experiment, Volume 1, Part 2 Mar. 1989 p 817-851 (For primary document see N89-20942 14-02)
Avail: NTIS HC A22/MF A01 CSCL 01A

Wind tunnel wall interference assessment and correction (WIAC) concepts, applications, and typical results are discussed in terms of several nonlinear transonic codes and one panel method code developed for and being implemented at NASA-Langley. Contrasts between 2-D and 3-D transonic testing factors which affect WIAC procedures are illustrated using airfoil data from the 0.3 m Transonic Cryogenic Tunnel and Pathfinder 1 data from the National Transonic Facility. Initial results from the 3-D WIAC codes are encouraging; research on and implementation of WIAC concepts continue. Author

N89-20959*# Calspan Field Services, Inc., Arnold AFS, TN.
TWO-MEASURED VARIABLE METHOD FOR WALL INTERFERENCE ASSESSMENT/CORRECTION
C. F. Lo and W. L. Sickles *In* NASA, Langley Research Center, Transonic Symposium: Theory, Application, and Experiment, Volume 1, Part 2 Mar. 1989 p 853-866 (For primary document see N89-20942 14-02)
Avail: NTIS HC A22/MF A01 CSCL 01A

An iterative method for wall interference assessment and/or correction is presented for transonic flow conditions in wind tunnels equipped with two component velocity measurements on a single interface. The iterative method does not require modeling of the test article and tunnel wall boundary conditions. Analytical proof for the convergence and stability of the iterative method is shown in the subsonic flow regime. The numerical solutions are given for both 2-D and axisymmetrical cases at transonic speeds with the application of global Mach number correction. Author

N89-20960*# National Aeronautics and Space Administration. Langley Research Center, Hampton, VA.
COMPARISON OF AIRFOIL RESULTS FROM AN ADAPTIVE WALL TEST SECTION AND A POROUS WALL TEST SECTION
Raymond E. Mineck *In its* Transonic Symposium: Theory, Application, and Experiment, Volume 1, Part 2 Mar. 1989 p 867-890 (For primary document see N89-20942 14-02)
Avail: NTIS HC A22/MF A01 CSCL 01A

Two wind tunnel investigations were conducted to assess two different wall interference alleviation/correction techniques: adaptive test section walls and classical analytical corrections. The same airfoil model has been tested in the adaptive wall test section of the NASA-Langley 0.3 m Transonic Cryogenic Tunnel (TCT) and in the National Aeronautical Establishment (NAE) High Reynolds Number 2-D facility. The model has a 9 in. chord and a CAST 10-2/DOA 2 airfoil section. The 0.3 m TCT adaptive wall test section has four solid walls with flexible top and bottom walls. The NAE test section has porous top and bottom walls and solid side walls. The aerodynamic results corrected for top and bottom wall interference at Mach numbers from 0.3 to 0.8 at a Reynolds number of 10 by 1,000,000. Movement of the adaptive walls was used to alleviate the top and bottom wall interference in the test results from the NASA tunnel. Author

N89-20961*# National Aeronautics and Space Administration. Langley Research Center, Hampton, VA.
CAPABILITIES OF WIND TUNNELS WITH TWO-ADAPTIVE WALLS TO MINIMIZE BOUNDARY INTERFERENCE IN 3-D MODEL TESTING **c09**
Rainer Rebstock and Edwin E. Lee, Jr. *In its* Transonic Symposium: Theory, Application, and Experiment, Volume 1, Part 2 Mar. 1989 p 891-910 Sponsored in part by National Research Council (For primary document see N89-20942 14-02)
Avail: NTIS HC A22/MF A01 CSCL 14B

An initial wind tunnel test was made to validate a new wall adaptation method for 3-D models in test sections with two adaptive walls. First part of the adaptation strategy is an on-line assessment of wall interference at the model position. The wall induced blockage was very small at all test conditions. Lift interference occurred at higher angles of attack with the walls set aerodynamically straight. The adaptation of the top and bottom tunnel walls is aimed at achieving a correctable flow condition. The blockage was virtually zero throughout the wing planform after the wall adjustment. The lift curve measured with the walls adapted agreed very well with interference free data for Mach 0.7, regardless of the vertical position of the wing in the test section. The 2-D wall adaptation can significantly improve the correctability of 3-D model data. Nevertheless, residual spanwise variations of wall interference are inevitable. Author

N89-20962# Maryland Univ., College Park. Dept. of Aerospace Engineering.
UNSTEADY FORCE CALCULATIONS ON CIRCULAR CYLINDERS AND ELLIPTICAL AIRFOILS WITH CIRCULATION CONTROL
Venkatraman Raghavan Dec. 1987 182 p
(UMAERO-87-37) Avail: NTIS HC A09/MF A01

A numerical method is developed to study the unsteady circulation control aerodynamics of two-dimensional airfoils. Two cases of unsteadiness in flow are considered. The first case is the unsteadiness arising from an unsteady, periodic freestream and the second is the unsteadiness due to unsteady blowing momentum. A simple solution for the potential flow is obtained using conformal mapping. The changes due to the presence of

the separated wake region behind the airfoil is calculated by distributing a set of source panels in the wake region along the surface. The source strengths are determined by using the condition of constant pressure at the control points and that the velocity at the separation points must be zero. The unsteady potential flow is assumed to be a periodic variation of the steady potential flow, in phase with the periodic freestream. The boundary layer flow is calculated by solving the unsteady boundary layer equations using an implicit finite difference method. The flow due to the wall jet is calculated from quasi one-dimensional flow upto the slot on the surface and further downstream the mixing shear layer is computed numerically as part of the boundary layer solution. The finite difference method uses backward differences whenever reverse flow is encountered. The potential flow and the boundary layer and wall jet calculations are combined in an iterative procedure to get a converged solution for the entire flow field. The solution provides the velocity and pressure fields which is used to determined the lift and drag forces under given freestream and jet momentum conditions. The pressure distribution obtained from the potential flow is used to calcualte the lift and pressure drag forces. The wall shear data obtained from the boundary layer flow gives the skin friction drag.Satisfactory correlation of predicted results with experimental data is achieved for steady lift over circular cylinders as well as elliptic airfoils. Author

N89-20963*# Kansas Univ. Center for Research, Inc., Lawrence.

INVESTIGATION OF A FREE-TIP ROTOR CONFIGURATION FOR RESEARCH ON SPANWISE LIFE DISTRIBUTIONS AND WAKE VELOCITY SURVEYS OF A SEMI-SPAN WING WITH A DISCONTINUOUS TWIST Final Report

Paul Fortin and Hiroyuki Kumagai Apr. 1989 209 p (Contract NCC2-175)

(NASA-CR-184948; NAS 1.26:184948) Avail: NTIS HC A10/MF A01 CSCL 01A

A wind tunnel test was conducted in the NASA Ames 7 x 10 Foot Wind Tunnel to investigate the lift distribution on a semi-span wing with a discontinuous change in spanwise twist. The semi-span wing had a tip with an adjustable pitch angle independent on the inboard section pitch angle simulating the free-tip rotor blade when its free-tip is at a deflected position. The spanwise lift distribution over the wing and the tip were measured and three component velocity surveys behind the wing were obtained with a three dimensional laser Doppler velocimeter (LV) with the wing at one angle of attack and the tip deflected at different pitch angles. A six component internal strain gage balance was also used to measure total forces and moments on the tip. The three dimensional lift was computed from the two dimensional life distributions obtained from the LV and from the strain gage balance. The results from both experimental methods are shown to be in agreement with predictions made by a steady, three dimensional panel code, VSAERO. Author

N89-20964*# National Aeronautics and Space Administration. Ames Research Center, Moffett Field, CA.

THREE-DIMENSIONAL SINGULAR POINTS IN AERODYNAMICS

Aynur Unal Jan. 1988 19 p Prepared in cooperation with Army Aviation System s Command, Saint Louis, MO Submitted for publication

(NASA-TM-100045; A-88029; NAS 1.15:100045; AD-A197978; USAAVSCOM-TR-87-A-14) Avail: NTIS HC A03/MF A01 CSCL 01A

When three-dimensional separation occurs on a body immersed in a flow governed by the incompressible Navier-Stokes equations, the geometrical surfaces formed by the three vector fields (velocity, vorticity and the skin-friction) and a scalar field (pressure) become interrelated through topological maps containing their respective singular points and extremal points. A mathematically consistent description of these singular points becomes inevitable when we want to study the geometry of the separation. A separated stream surface requires, for example, the existence of a saddle-type singular point on the skin-friction surface. This singular point is actually, in the proper language of mathematics, a saddle of index two. The index is a measure of the dimension of the outset (set leaving the singular point). Hence, when a saddle of index two is specified, a two dimensional surface that becomes separated from the osculating plane of the saddle is implied. The three-dimensional singular point is interpreted mathematically and the most common aerodynamical singular points are discussed through this perspective. Author

N89-20965# Air Force Armament Lab., Eglin AFB, FL. Aerodynamics Branch.

A STUDY OF TRANSONIC DRAG REDUCTION OF A BLUNT CYLINDER BY A CYLINDER PROBE Final Report, 18 Oct. 1985 - 1 Jul. 1988 M.S. Thesis - Mississippi State Univ., MS - Aug.1987

David H. Bridges Aug. 1988 69 p

(AD-A202557; AFATL-TR-88-95) Avail: NTIS HC A04/MF A01 CSCL 20D

This thesis examines the reduction of the drag of a blunt cylinder by a cylindrical probe in the transonic regime, and determines characteristics of the flowfield from the experimental drag coefficient data. The experiment was conducted in the NASA-Ames Research Center 6 x 6 ft supersonic wind tunnel. The model consisted of a blunt cylinder with diameter d2 and several extendable cylindrical probes, yielding probe-to-cylinder diameter ratios d1/d2 of 0.248, 0.368, an 0.45, an probe length-to-cylinder diameter ratios 1/d2 up to 2.0 (3.0 for the smallest probe). These configurations were tested at Mach numbers between 0.8 and 1.5. C sub D decreased as both 1/d2 and d1/d2 increased, due to the fact that the cylinder face was immersed in a wake of reduced stagnation pressure created by the probe. After reaching a minimum, C sub D increased as 1/d2 increased, indicating a transition of the flow over the probe from a lower-drag open cavity mode to a higher-drag open cavity mode to a higher-drag closed cavity mode. This change was rather abrupt, and there was also hysteresis in the supersonic tests in agreement with previous experiments. C sub D also reached a minimum and increased as d1/d2 approached 1. C sub D usually increased with Mach number due to the increase in stagnation pressure with M. For a particular range of length and diameter ratios, C sub D decreased with increasing M for 0.8 is less than M is less than 0.95. This was attributed to the transition of the flow over the probe from the high-drag closed mode to the low-drag open mode as M increased. GRA

N89-20966# Calspan Field Services, Inc., Arnold AFS, TN.

INVESTIGATION OF THE DEVELOPMENT OF LAMINAR BOUNDARY-LAYER INSTABILITIES ALONG A COOLED-WALL CONE IN HYPERSONIC FLOWS Final Report, 20 - 24 Jun. 1988

J. C. Donaldson and M. G. Hatcher Dec. 1988 51 p Prepared in cooperation with Arnold Engineering D evelopment Center, Arnold AFS, TN

(AD-A202587; AEDC-TSR-88-V32) Avail: NTIS HC A04/MF A01 CSCL 01A

Measurements of fluctuating flow and mean flow parameters were made in the boundary layer on a cooled wall, sharp 7-deg (half-angle) cone in an investigation of wall temperature effects on the stability of laminar boundary layers in hypersonic flow. The flow fluctuation measurements were made using constant-current hot-wire anemometry techniques. Boundary-layer profiles and cone surface conditions were measured to supplement the hot-wire data. Testing was done at Mach numbers 8 and 6 with a free-stream unit Reynolds number of 1.0-million per foot. The test equipment, test techniques, and the data acquisition and reduction procedures are described. Analysis of the hot wire anemometer data is beyond the scope of this report. GRA

N89-20967# Air Force Inst. of Tech., Wright-Patterson AFB, OH. School of Engineering.

EFFECT OF RIBLETS UPON FLOW SEPARATION IN A SUBSONIC DIFFUSER M.S. Thesis

Nathan W. Martens Dec. 1988 102 p
(AD-A203178; AFIT/GAE/AA/88D-23) Avail: NTIS HC A06/MF A01 CSCL 20D

This thesis investigates the effect of riblets upon flow separation in a two-dimensional straight-walled subsonic diffuser. Riblets are small flow-aligned grooves which can be attached to an aerodynamic body. Studies involving the application of riblets to turbulent flow over a flat plate have consistently shown a decrease in viscous drag as compared to the same surface without riblets. The purpose of this investigation was to determine the effect applying riblets to the walls of a subsonic diffuser would have upon flow separation in the fluid handling device. For this investigation, it was found separation was indeed delayed in a diffuser employing riblets as compared to a geometrically identical plain diffuser. For the smaller throat widths, this delay was significant, being as high as 250 percent due to riblets. As the diffuser throat width increased, the delay in flow separation due to riblets decreased. Also evident in the investigation was the strong dependence of flow separation upon throat velocity for the diffuser with riblets. GRA

N89-20968# National Aeronautical Establishment, Ottawa (Ontario).
AN EXPERIMENTAL STUDY OF TRANSONIC BUFFET OF A SUPERCRITICAL AIRFOIL WITH TRAILING EDGE FLAP
B. H. Lee and F. C. Tang Sep. 1988 85 p
(AD-A203189; NAE-AN-54) Avail: NTIS HC A05/MF A01 CSCL 01A

A supercritical airfoil with a trailing edge flap has been the subject of aerodynamic investigation in the National Aeronautical Establishment's High Reynolds Number 2-D Test Facility. The effects of flap deflection on buffet intensities and delay of buffet onset at transonic speeds were studied. Buffet boundaries for various flap angles were determined from the divergence of the fluctuating balance normal force measurements (C prime sub N). The onset of buffet was obtained from plots of C prime sub N versus C sub L at values of C sub L where the slope was 0.1. This value for the slope was arbitrarily chosen, but was found to give consistent results which agreed well with values computed from the criterion using the trailing edge pressure divergence for those cases where buffet onset is primarily due to trailing edge separation. For given flow conditions the deflection of the trailing edge flap altered the circulation and hence the position of the shock wave and its strength. The variations of these two quantities with flap angles were determined from pressure measurements carried out on the airfoil surface. The test was performed quite deep inside the buffet regime and shock wave oscillations were investigated from spectral analyses of the balance outputs. Fluctuations in the shock motion of approximately 70 Hz were detected. The drag of the airfoil was computed from the wake stagnation pressure deficit and the drag penalties for large flap angles were quite significant. GRA

N89-20969# Air Force Inst. of Tech., Wright-Patterson AFB, OH. School of Engineering.
NUMERICAL SIMULATION OF FLOW OVER ICED AIRFOILS M.S. Thesis
Larry A. Coleman Dec. 1988 145 p
(AD-A203291; AFIT/GAE/AA/88D-4) Avail: NTIS HC A07/MF A01 CSCL 01A

This thesis evaluates the performance of an iced NACA 0012 airfoil numerically. The full Navier-Stokes equations are solved using the Beam-Warming algorithm. Steady-state solutions are obtained at a Mach number of 0.12 and a Reynolds number based on chord of 1.41 million, for angles of attack from 2 to 8 deg. Lift and drag curves obtained from the numerical solutions were compared to experimental data and other numerical results. This comparison showed that the Beam-Warming algorithm provides a good estimate of the lift and drag at angles of attack below stall. Computed lift coefficients were within 11.5 percent of experimental data. These results were in excellent agreement with other numerical solutions. After stall, however, the code did not predict the expected decrease in lift and the calculated drag coefficient was much lower than the experimental data. Comparison of two local flowfield characteristics with the experimental data was less encouraging. A computed velocity profile was compared to the experimental profile for a station in the separated region on the upper surface. This comparison showed that the computed separation bubble is approximately one half the thickness of the bubble measured experimentally. Flow reattachment location is another measure of the predictive accuracy of the numerical scheme. GRA

N89-20970# Air Force Inst. of Tech., Wright-Patterson AFB, OH. School of Engineering.
THIN-LAYER NAVIER-STOKES SOLUTIONS FOR A CRANKED DELTA WING M.S. Thesis
Francis R. Smith Dec. 1988 100 p
(AD-A203292; AFIT/GAE/AA/88D-34) Avail: NTIS HC A05/MF A01 CSCL 20D

For thin, highly swept wings operating at moderate to high angles of attack, flow over the wing is dominated by formation of leading edge vortices. These vortices produce a minimum pressure which results in an additional lift increment. The lift increment is nonlinear with angle of attack and cannot be accurately predicted using present design methods. Thin-layer Navier-Stokes equations were used to calculate flow over a straight delta wing and a cranked delta wing. The straight delta wing was used as the test case due to the availability of both experimental and numerical procedure. The computer code uses an implicit, time marching algorithm developed by Beam and Warming. The solution is marched in time until a steady state is achieved. The code is approximately factored and diagonalized in order to reduce computational work. A solid state disk is used to allow for the large grid needed for a 3-D solution. Thin-layer Navier-Stokes equations are capable of accurately calculating vortical flows. The cranked delta wing exhibited flow similar to a straight delta wing upstream of the crank. The vortex generated at the crank quickly became paired with the vortex from the front of the wing. Vortex location aft of the crank changes with streamwise location. GRA

N89-20971# Air Force Inst. of Tech., Wright-Patterson AFB, OH. Aerodynamics and Airframe Branch.
TWO-DIMENSIONAL NAVIER-STOKES SOLUTION OF THE FLOW OVER A THICK SUPERCRITICAL AIRFOIL WITH STRONG SHOCK-INDUCED SEPARATION Interim Report, Jan. 1987 - Jan. 1988
Don W. Kinsey Nov. 1988 73 p
(AD-A203331; AFWAL-TR-88-3085) Avail: NTIS HC A04/MF A01 CSCL 20D

This report describes a numerical solution of the Navier-Stokes equations for transonic flow over a thick supercritical airfoil with strong shock-induced separation on both the upper and lower surfaces. The separated flow region extends from the shock (approximately 50 percent chord) to the trailing edge on both surfaces. The report first reviews the processes involved in producing a computational solution of the Navier-Stokes equations for a two-dimensional airfoil in a perfect gas. A brief development of the Navier-Stokes equations is provided. The solution algorithm used (an explicit predictor-corrector method) is developed and described. An algebraic turbulence model used to model the turbulent Reynolds stresses is described and the need for such a model is discussed. A hyperbolic, two-dimensional procedure for producing a computational grid (mesh) is also described. The boundary conditions imposed at the outer regions of the computational domain (farfield) and at the airfoil surface are discussed and described. The second part of the report discusses the treatment of the eddy viscosity development through the shock, in the separated regions over the airfoil and in the near wake. This work was critical for obtaining a successful solution on the very difficult test case chosen. GRA

N89-20972# George Washington Univ., Washington, DC.
METHODOLOGY FOR USING STEADY EXPERIMENTAL AERODYNAMIC DATA TO IMPROVE STEADY AND

UNSTEADY AERODYNAMIC ANALYSIS M.S. Thesis
Carol Danielle Wieseman Feb. 1989 110 p
Avail: NTIS HC A06/MF A01

Correction factor methodologies were developed which use steady experimental or accurate analytical pressure or force data to correct steady and unsteady aerodynamic calculations obtained by simpler methods. Three methods of calculating these factors were developed to match steady lifting pressure distributions, airfoil section properties (lift and moment derivatives) and total force and moment derivaties with respect to angle of attack and control surface deflection. A rectangular supercritical wing previously tested in the NASA-Langley Transonic Dynamics Tunnel was used as a test case for tne methodology. The reasons for choosing this wing as a test case were that an abundance of pressure data were available, both steady and unsteady, at Mach numbers ranging from subsonic and transonic, for a range of reduced frequencies. This test case was a severe test for the methodology. Correction factors were calculated to match distributions of lifting pressure derivatives or to match section lift and moment derivatives obtained by the doublet lattice method to the corresponding steady state experimental values. These factors were then applied to steady and unsteady aerodynamic calculations. Author

N89-20973*# Continuum Dynamics, Inc., Princeton, NJ.
PERFORMANCE OPTIMIZATION FOR ROTORS IN HOVER AND AXIAL FLIGHT
T. R. Quackenbush, D. A. Wachspress, A. E. Kaufman, and D. B. Bliss (Duke Univ., Durham, NC.) Apr. 1989 41 p
(Contract NAS2-12789)
(NASA-CR-177524; NAS 1.26:177524) Avail: NTIS HC A03/MF A01 CSCL 01A

Performance optimization for rotors in hover and axial flight is a topic of continuing importance to rotorcraft designers. The aim of this Phase 1 effort has been to demonstrate that a linear optimization algorithm could be coupled to an existing influence coefficient hover performance code. This code, dubbed EHPIC (Evaluation of Hover Performance using Influence Coefficients), uses a quasi-linear wake relaxation to solve for the rotor performance. The coupling was accomplished by expanding of the matrix of linearized influence coefficients in EHPIC to accommodate design variables and deriving new coefficients for linearized equations governing perturbations in power and thrust. These coefficients formed the input to a linear optimization analysis, which used the flow tangency conditions on the blade and in the wake to impose equality constraints on the expanded system of equations; user-specified inequality contraints were also employed to bound the changes in the design. It was found that this locally linearized analysis could be invoked to predict a design change that would produce a reduction in the power required by the rotor at constant thrust. Thus, an efficient search for improved versions of the baseline design can be carried out while retaining the accuracy inherent in a free wake/lifting surface performance analysis. Author

N89-21522# Ballistic Research Labs., Aberdeen Proving Ground, MD.
INFLUENCE OF REFLECTED SHOCK WAVES ON A HYPERSONIC SHAPED CHARGE JET
H. W. Meyer and J. E. Danberg *In* Army Research Office, Transactions of the Fifth Army Conference on Applied Mathematics and Computing Mar. 1988 p 617-630 (For primary document see N89-21490 14-59)
Avail: NTIS HC A99/MF E03 CSCL 01B

03 AIR TRANSPORTATION AND SAFETY

Includes passenger and cargo air transport operations; and aircraft accidents.

For related information see also *16 Space Transportation* and *85 Urban Technology and Transportation.*

N89-20974# General Accounting Office, Washington, DC.
AVIATION SAFETY: MEASURING HOW SAFELY INDIVIDUAL AIRLINES OPERATE
Mar. 1988 40 p
(GAO/RCED-88-61) Avail: NTIS HC A03/MF A01

The deregulation of airline fares and schedules in 1978 led to rapid growth and change in the airline industry, placing increased burdens on FAA'S airline inspection program. Because of growing concern that airlines may be operating less safely under deregulation, improved ways to measure how safely individual airlines operate are sought. Information was provided on the feasibility of developing and publishing for air travelers indicators that compare how safely individual airlines operate. The focus was on identifying: areas of airline performance recognized as important to airline safety, the availability and quality of data in these areas, and ongoing research on measuring individual airline safety. Author

N89-20975# Naval Environmental Prediction Research Facility, Monterey, CA.
ICING CONSIDERATIONS FOR HALE (HIGH ALTITUDE, LONG ENDURANCE) AIRCRAFT Final Technical Report
Gerard N. Vogel Nov. 1988 54 p
(AD-A202584; NEPRF-TR-88-11) Avail: NTIS HC A04/MF A01 CSCL 04B

Although a low probability event, ice accretion does present a major obstacle to safe aircraft operations. In this report, the character of the aircraft icing environment is explored in terms of key meteorological and aerodynamic factors as related to the HALE (High Altitude, Long Endurance) aircraft. The distribution of icing in the atmosphere, mainly a function of temperature and cloud structure, is presented. Ice forecasting techniques and icing instrumentation are discussed as viable approaches for minimizing potential aircraft icing hazards. It is concluded that an onboard ice accumulation detector in combination with ground-based remote sensing instrumentation would provide the best capability icing forecasting program, which is often both effort- and time-efficient, is recommended. GRA

N89-20976# Air Force Flight Dynamics Lab., Wright-Patterson AFB, OH.
IN-FLIGHT LIGHTNING CHARACTERIZATION PROGRAM ON A CV-580 AIRCRAFT Final Report, Oct. 1983 - Sep. 1987
Harold D. Burket, Lawrence C. Walko, Jean S. Reazer, and Arturo V. Serrano Jun. 1988 185 p
(AD-A203954; AFWAL-TR-88-3024) Avail: NTIS HC A09/MF A01 CSCL 04B

A CV-580 aircraft was instrumented with external displacement current density sensors, surface current density sensors, current shunts, and static electric field mill sensors and was flown in active thunderstorms in central Florida during the summer of 1984 and 1985. Electromagnetic data were collected and analyzed for 52 direct lightning strikes to the aircraft flying at altitudes between 2,000 and 18,000 ft. The data consisted of analog records with dc to 2-MHz bandwidth and 10-us windows of digital samples taken at 5-ns intervals. The data show the physical mechanism of lightning attachment to aircraft and suggest comparison of aircraft responses to lightning and simulated NEMP is also provided. GRA

04 AIRCRAFT COMMUNICATIONS AND NAVIGATION

Includes digital and voice communication with aircraft; air navigation systems (satellite and ground based); and air traffic control.

For related information see also *17 Space Communications, Spacecraft Communications, Command and Tracking* and *Communications and Radar.*

N89-20977# General Accounting Office, Washington, DC.
MICROWAVE LANDING SYSTEMS: ADDITIONAL SYSTEMS SHOULD NOT BE PROCURED UNLESS BENEFITS PROVEN
May 1988 74 p
(GAO/RCED-88-118) Avail: NTIS HC A04/MF A01

Important parts of the national airspace system (NAS) are the precision landing systems which allow aircraft equipped with the necessary electronic hardware (avionics) to land in conditions of limited visibility, thereby increasing the time an airport can operate during poor weather. The current precision landing system, the instrument landing system (ILS), is scheduled to be replaced with the microwave landing system (MLS) as part of the Federal Aviation Administration's (FAA) effort to modernize the nation's air traffic control system-known as the NAS plan. The MLS program was reviewed, addressing the following objectives: assess the justification and requirements for a new precision landing system to replace ILS and determine and analyze ILS improvements since MLS was justified, determine whether FAA has adequately demonstrated MLS' potential operational and economic benefits, and determine the reasonableness of FAA'S MLS siting strategy. Author

N89-20978*# National Aeronautics and Space Administration. Ames Research Center, Moffett Field, CA.
AH-1S COMMUNICATION SWITCH INTEGRATION PROGRAM
Loran Haworth, Zoltan Szoboszlay, Robert Shively, and Frank J. Bick (Army Aviation Systems Command, Saint Louis, MO.) Mar. 1989 62 p
(NASA-TM-101053; A-89005; NAS 1.15:101053; USAAVSCOM-TR-88-A-009) Avail: NTIS HC A04/MF A01 CSCL 17G

The C-6533/ARC communication system as installed on the test AH-1E Cobra helicopter was modified to allow discrete radio selection of all aircraft radios at the cyclic radio/intercommunication system switch. The current Cobra-fleet use of the C-6533 system is cumbersome, particularly during low-altitude operations. Operationally, the current system C-6533 configuration and design requires the pilot to estimate when he can safely remove his hand from an active flight control to select radios during low-altitude flight. The pilot must then physically remove his hand from the flight control, look inside the cockpit to select and verify the radio selection and then effect the selected radio transmission by activating the radio/ICS switch on the cyclic. This condition is potentially hazardous, especially during low-level flight at night in degraded weather. To improve pilot performance, communications effectiveness, and safety, manprint principles were utilized in the selection of a design modification. The modified C-6533 design was kept as basic as possible for potential Cobra-fleet modification. The communications system was modified and the design was subsequently flight-tested by the U.S. Army Aeroflightdynamics Directorate and NASA at the NASA Ames Research Center, Mountain View, California. The design modification enables the Cobra pilot to maintain hands-on flight controls while selecting radios during nap-of-the-Earth (NOE) flight without looking inside the cockpit which resulted in reduced pilot workload ratings, better pilot handling quality ratings and increased flight safety for the NOE flight environment. Author

N89-20979# Air Force Inst. of Tech., Wright-Patterson AFB, OH. School of Engineering.
A DIAGNOSTIC SYSTEM BLENDING DEEP AND SHALLOW REASONING M.S. Thesis
James M. Skinner Dec. 1988 188 p
(AD-A202547; AFIT/GCE/ENG/88D-5) Avail: NTIS HC A09/MF A01 CSCL 12I

Repair of the Dual Miniature Inertial Navigation System (DMINS), a navigation system used on fast attack submarines, is the responsibility of the Aerospace Guidance and Metrology Center (AGMC) located at Newark AFB, OH. Currently, diagnostics of the system are conducted by automatic test equipment (ATE). Recent plans for upgrades of the computer that drives the ATE have made possible the integration of an expert system with the ATE, thereby increasing system reliability, decreasing test times, and improving retention of site knowledge. The traditional approach to developing an expert system is to use shallow reasoning. Shallow reasoning, which encodes knowledge into a set of IF-THEN rules, is useful for incorporating diagnostic experience accumulated with a unit under test (UUT). Recent research in expert systems has emphasized the use of deep reasoning for diagnostics. A deep reasoning system diagnoses faults by constructing a model of the UUT, relying on the principle of locality and causal reasoning. Deep reasoning is suitable for a new system; if applied to an older system however, it fails to take advantage of the lessons learned by repair technicians. The focus of the thesis is the development of BDS (Blended Diagnostic System), a diagnostic system which emulates a human technician by combining shallow and deep reasoning. GRA

N89-20980# Air Force Inst. of Tech., Wright-Patterson AFB, OH. School of Engineering.
AIRCRAFT TRACKING WITH DUAL TACAN M.S. Thesis
Christopher J. McCormack Dec. 1988 71 p
(AD-A202647; AD-E900870; AFIT/GE/ENG/88D-28) Avail: NTIS HC A04/MF A01 CSCL 17G

This thesis addresses the problem of determining aircraft position during flight given noisy and biased measurements from a barometric altimeter and two tactical air navigation (TACAN) transceivers. A Kalman smoother is developed to perform post-flight data processing on the measurement data. The smoother estimates aircraft position, velocity, and acceleration as well as biases in the measurements. Since actual flight test data is not available, computer simulations examine the performance of this tracking technique. The simulated flight includes low and high-speed turns, constant rate ascents, descents, and accelerations. The tracking algorithm tracked the aircraft inertial navigation system used by the 4950th Test Wing in another flight test program that showed a position error growth rate of 2000 meters per hour. GRA

05 AIRCRAFT DESIGN, TESTING AND PERFORMANCE

Includes aircraft simulation technology.

For related information see also *18 Spacecraft Design, Testing and Performance* and *39 Structural Mechanics.* For land transportation vehicles see *85 Urban Technology and Transportation.*

N89-20981*# California Univ., Los Angeles. School of Engineering and Applied Science.
HYPERSONIC DRONE DESIGN: A MULTIDISCIPLINARY EXPERIENCE
Jun. 1988 302 p
(Grant NGT-21-002-080)
(NASA-CR-184740; NAS 1.26:184740) Avail: NTIS HC A14/MF A01 CSCL 01C

Efforts were focused on design problems of an unmanned hypersonic vehicle. It is felt that a scaled hypersonic drone is necessary to bridge the gap between present theory on hypersonics and the future reality of the National Aerospace Plane (NASP) for two reasons: to fulfill a need for experimental data in the hypersonic regime, and to provide a testbed for the scramjet engine which is to be the primary mode of propulsion for the NASP. Three areas of great concern to NASP design were examined: propulsion, thermal management, and flight systems. Problem solving in these

areas was directed towards design of the drone with the idea that the same design techniques could be applied to the NASP. A seventy degree swept double delta wing configuration, developed in the 70's at NASA Langley, was chosen as the aerodynamic and geometric model for the drone. This vehicle would be air-launched from a B-1 at Mach 0.8 and 48,000 feet, rocket boosted by two internal engines to Mach 10 and 100,000 feet, and allowed to cruise under power of the scramjet engine until burnout. It would then return to base for an unpowered landing. Preliminary energy calculations based upon the flight requirements give the drone a gross launch weight of 134,000 lb. and an overall length of 85 feet. Author

N89-20982*# National Aeronautics and Space Administration. Langley Research Center, Hampton, VA.
INTEGRATED AERODYNAMIC/DYNAMIC OPTIMIZATION OF HELICOPTER ROTOR BLADES
Aditi Chattopadhyay, Joanne L. Walsh, and Michael F. Riley (Planning Research Corp., Hampton, VA.) Feb. 1989 15 p Presented at the 30th AIAA/ASME/ASCE/AHS/ASC Structures, Structural Dynamics and Materials Conference, Mobile, AL, 3-5 Apr. 1989
(NASA-TM-101553; NAS 1.15:101553; AIAA-89-1269) Avail: NTIS HC A03/MF A01 CSCL 01C

An integrated aerodynamic/dynamic optimization procedure is used to minimize blade weight and 4 per rev vertical hub shear for a rotor blade in forward flight. The coupling of aerodynamics and dynamics is accomplished through the inclusion of airloads which vary with the design variables during the optimization process. Both single and multiple objective functions are used in the optimization formulation. The Global Criteria Approach is used to formulate the multiple objective optimization and results are compared with those obtained by using single objective function formulations. Constraints are imposed on natural frequencies, autorotational inertia, and centrifugal stress. The program CAMRAD is used for the blade aerodynamic and dynamic analyses, and the program CONMIN is used for the optimization. Since the spanwise and the azimuthal variations of loading are responsible for most rotor vibration and noise, the vertical airload distributions on the blade, before and after optimization, are compared. The total power required by the rotor to produce the same amount of thrust for a given area is also calculated before and after optimization. Results indicate that integrated optimization can significantly reduce the blade weight, the hub shear and the amplitude of the vertical airload distributions on the blade and the total power required by the rotor. Author

N89-20983*# National Aeronautics and Space Administration. Ames Research Center, Moffett Field, CA.
SIMULATION AT DRYDEN FLIGHT RESEARCH FACILITY FROM 1957 TO 1982
John P. Smith, Lawrence J. Schilling, and Charles A. Wagner Feb. 1989 14 p Presented at the SES/SFTE Simulation-Aircraft Test and Evaluation Symposium, Patuxent River, MD, 16-17 Mar. 1982
(NASA-TM-101695; H-1530; NAS 1.15:101695) Avail: NTIS HC A03/MF A01 CSCL 01C

The Dryden Flight Research Facility has been a leader in developing simulation as an integral part of flight test research. The history of that effort is reviewed, starting in 1957 and continuing to the present time. The contributions of the major program activities conducted at Dryden during this 25-year period to the development of a simulation philosophy and capability is explained. Author

N89-20984# Air Force Occupational and Environmental Health Lab., Brooks AFB, TX.
CONTAMINATION OF THE EXTERIOR OF A C-130E AIRCRAFT USED FOR AERIAL SPRAY, 907 TAG, RICKENBACKER ANGB, OH Final Report
Thomas H. Lillie Sep. 1988 14 p
(AD-A202430; USAFOEHL-88-137EQ0110JEF) Avail: NTIS HC A03/MF A01 CSCL 15F

Contamination of the exterior of a C-130E aircraft was evaluated during flight tests of a new modular aerial spray system at Dobbins AFB, GA and Avon Park AFR, FL. Oil sensitive cards and paper index cards were taped to 50 sites on the exterior of the aircraft to monitor deposition of Dibrom, Malathion, soybean oil, and water during aerial spray operations. Light contamination of the aileron occurred when the wing booms were used and heavy contamination of the cargo door and horizontal stabilizer occurred when the fuselage booms were used. GRA

N89-20985# Air Force Inst. of Tech., Wright-Patterson AFB, OH. School of Engineering.
PERFORMANCE ANALYSIS OF THE FIBER DISTRIBUTED DATA INTERFACE IN THE SUPER COCKPIT AUDIO WORLD M.S. Thesis
Juancho E. Forlanda Dec. 1988 288 p
(AD-A202535; AFIT/GCS/ENG/88D-6) Avail: NTIS HC A13/MF A01 CSCL 12G

The purpose of this thesis was to determine if the Fiber Distributed Data Interface (FDDI) network, a 100 Mbps fiber optic ring network, could satisfy the networking requirement (to support up to 130 terminals) of the Super Cockpit Audio World. To help make this determination a computer simulation was created to model the FDDI network and the load that may be created by several audio world terminals on that network. The simulation model used the mean token rotation time (TRT) in combination with a specified target TRT (TTRT) as the performance parameter of interest. The TRT responses of FDDI were observed for cases where all terminals used 16-bit PCM, 5-bit ADPCM, CVSD, or LPC (packetized to 4096, 16384, or 35904 bits; for 50, 100, 130, and 150 stations) with or without silence suppression to the audio signals begin transmitted. The simulation results (the TRT responses) revealed that FDDI can support 130 audio terminals using 16-bit PCM; however, it cannot support 150 audio terminals. When silence suppression is applied, FDDI is able to support the same 150 terminals with less than a 2 percent probability that an audio packet would be late for play out on a receiving audio terminal. The simulation results also showed that at least 150 terminals using 5-bit ADPCM, CVSD, or LPC with or without silence suppression could be accommodated by FDDI. GRA

N89-20986# Air War Coll., Maxwell AFB, AL.
INCORPORATING FIVE NATIONS' OPERATIONAL REQUIREMENTS INTO A SINGLE AIRCRAFT: THE F-16 MULTINATIONAL FIGHTER PROGRAM VIEWED FROM THE OPERATIONAL SIDE
Einar Smedsvig Apr. 1988 62 p
(AD-A202552) Avail: NTIS HC A04/MF A01 CSCL 05A

Remarks on the background for the F-16 multinational program introduce a detailed discussion of the operational facets of the total program. A description of the operational organizations follows to complete the background for the author's views on the importance of the international participation in the F-16 program. After a discussion of how the international participation improved the F-16 operational dialogue has improved interoperability and cooperation beyond the original F-16 program. Lessons learned and potential future applications are discussed. GRA

N89-20987# Air Force Inst. of Tech., Wright-Patterson AFB, OH. School of Engineering.
PRELIMINARY DESIGN OF A MODULAR UNMANNED RESEARCH VEHICLE. VOLUME 1: SYSTEM DESIGN DOCUMENT M.S. Thesis
Christopher D. Hall, Richard L. Johnson, Peter J. Lamatsch, Douglas A. McCabe, Paul J. Mueller, III, Michael E. Paul, and Letitia M. Pohl Dec. 1988 215 p
(AD-A202765; AFIT/GSE/AA/88D-2-Vol-1) Avail: NTIS HC A10/MF A01 CSCL 01C

This thesis presents the analysis and development of a modular unmanned research vehicle (MURV) to support aeronautical research for AFIT. The MURV is proposed as a test vehicle to permit experimental efforts beyond the restrictions of pure analytical and wind tunnel research, yet less costly and more accessible

than full-scale flight tests. A classical systems approach was applied in concert with a conventional aircraft design process which emphasized system level needs and objectives in the design of MURV subsystems. The primary design drivers were the need for adequate data acquisition for anticipated experiments, structural and functional modularity to permit simple reconfiguration, and focus on a set of unique experiments relating to fighter-like supermaneuverability. The supermaneuverability experiments dictated that the general arrangement of the MURV baseline design would resemble a typical modern fighter aircraft configuration, the recommended baseline being a turbojet-powered delta wing design with canards, single vertical tail, and control-configured ventral fins. Modularity implications resulted in the design of a flexible, digital flight control system with primary functions distributed between the vehicle and a remote pilot/control ground station, and a fuselage design which allows for relocation and replacement of wings and tails or canards. The data acquisition system is fully integrated with the flight control system and the remote ground station. The MURV is capable of flight speeds approaching 260 knots for altitudes up to 20,000 feet, and has fuel to fly for well over 30 minutes. GRA

N89-20988# Air Force Inst. of Tech., Wright-Patterson AFB, OH. School of Engineering.

A WIND TUNNEL AND COMPUTER INVESTIGATION OF THE LOW SPEED AERODYNAMIC CHARACTERISTICS OF THE PRONE ESCAPE SYSTEM (PRESS) M.S. Thesis

Lonnie R. Dillon Dec. 1988 104 p

(AD-A202768; AFIT/GAE/AA/88D-09) Avail: NTIS HC A06/MF A01 CSCL 01A

Due to new design technology, future jet fighters will fly at higher g levels than before. A previous preliminary design study was conducted to develop an ejection seat providing higher g-tolerance for the crewmember during maneuvering as well as improved windblast protection during ejection. This seat used the crewmember in a prone, or leaning forward, position. The Prone Ejection System was computer simulated at supersonic conditions in the earlier report and found satisfactory. It was the purpose of this present research to perform an experimental low speed study of the aerodynamic characteristics of the PRESS. Wind tunnel testing was performed to determine the static stability of the PRESS and measure pressures over the seat. It was determined that static pitch stability did not occur at the desired angle of attack, but could be easily corrected with aerodynamic fins and/or a shift in the center of gravity. Directional stability was also confirmed. An analytical experiment was also performed to determine whether a potential paneling code could be modified to predict flow conditions about the PRESS. An apparent body was constructed by including the regions of flow separation as part of the seat itself. Water tunnel flow visualization was used to determine the shape of the apparent body. The computer analysis showed that a paneling code could accurately predict the pressure coefficients on the cowling. GRA

N89-20989# Air Force Inst. of Tech., Wright-Patterson AFB, OH. School of Engineering.

RESPONSE EQUIVOCATION ANALYSIS FOR THE SMART STICK CONTROLLER M.S. Thesis

John M. Pracher Nov. 1988 148 p

(AD-A203146; AFIT/GE/ENG/88D-38) Avail: NTIS HC A07/MF A01 CSCL 01D

This thesis provides an analysis of response equivocation (lost information) for subjects who use the smart stick controller -- an aircraft stick controller designed by the Armstrong Aerospace Medical Research Laboratory (AAMRL) to improve a pilot's tracking performance. First, a control theory model of a compensatory tracking task is developed and analyzed. Then, using an information theory model of the pilot, the results are used to develop expressions for information theory parameters (input entropy, transinformation, and equivocation). Six subjects were tested using the smart stick controller and experimental an apparatus developed by the AAMRL. Each subject was tested twice: first in the passive stick mode (normal stick operation), and again in the active stick mode. In the active stick mode, the smart stick actively exerts a force in the direction opposite to the desired stick motion. Power spectral densities of the display error and the operator response were used to calculate the information theory parameters. GRA

N89-20990# Georgia Inst. of Tech., Atlanta. School of Mechanical Engineering.

NONLINEAR ROTORCRAFT ANALYSIS-EXPERIMENTAL AND ANALYTICAL Final Report, 15 Sep. 1985 - 14 Jan. 1989

Benson H. Tongue 13 Nov. 1988 8 p

(Contract DAAG29-85-K-0207)

(AD-A203967; ARO-22557.5-EG) Avail: NTIS HC A02/MF A01 CSCL 01C

A parallel effort involving both analytical and experimental work was performed to allow a deeper understanding of the limit cycle behavior of rotorcraft and of the implication of this behavior for the safe operation of such rotorcraft. The theoretical development encompassed articulated and hingeless rotors with a great enough number of included degrees of freedom to allow accurate predictions of a simplified rotorcraft's responses. The experimental model allowed the simulation of both hingeless and articulated rotors in ground resonance. The purpose of the above work was to identify the regimes of helicopters operation that can support limit cycling and the range of excitations the system can withstand before entering a limit cycle. GRA

N89-20991*# National Aeronautics and Space Administration. Langley Research Center, Hampton, VA.

AEROELASTIC MODELING FOR THE FIT TEAM F/A-18 SIMULATION

Thomas A. Zeiler and Carol D. Wieseman Mar. 1989 19 p Presented at the 2nd NASA/AF Symposium on Recent Advances in Multidisciplinary Analysis and Optimization, Hampton, VA, Sep. 1988

(NASA-TM-101569; NAS 1.15:101569) Avail: NTIS HC A03/MF A01 CSCL 01C

Some details of the aeroelastic modeling of the F/A-18 aircraft done for the Functional Integration Technology (FIT) team's research in integrated dynamics modeling and how these are combined with the FIT team's integrated dynamics model are described. Also described are mean axis corrections to elastic modes, the addition of nonlinear inertial coupling terms into the equations of motion, and the calculation of internal loads time histories using the integrated dynamics model in a batch simulation program. A video tape made of a loads time history animation was included as a part of the oral presentation. Also discussed is work done in one of the areas of unsteady aerodynamic modeling identified as needing improvement, specifically, in correction factor methodologies for improving the accuracy of stability derivatives calculated with a doublet lattice code. Author

N89-20945*# Grumman Aerospace Corp., Bethpage, NY. Aircraft Systems Div.

METHOD TO PREDICT EXTERNAL STORE CARRIAGE LOADS AT TRANSONIC SPEEDS

Bruce S. Rosen *In* NASA, Langley Research Center, Transonic Symposium: Theory, Application, and Experiment, Volume 1, Part 2 Mar. 1989 p 453-465 Previously announced in IAA as A88-22003 (For primary document see N89-20942 14-02)

(Contract NAS1-18105)

Avail: NTIS HC A22/MF A01 CSCL 01C

N89-20946*# National Aeronautics and Space Administration. Langley Research Center, Hampton, VA.

STEADY AND UNSTEADY TRANSONIC SMALL DISTURBANCE ANALYSIS OF REALISTIC AIRCRAFT CONFIGURATIONS

John T. Batina, David A. Seidel, Robert M. Bennett, Herbert J. Cunningham, and Samuel R. Bland *In its* Transonic Symposium: Theory, Application, and Experiment, Volume 1, Part 2 Mar. 1989 p 467-496 (For primary document see N89-20942 14-02)

Avail: NTIS HC A22/MF A01 CSCL 01C

N89-20947*# National Aeronautics and Space Administration. Langley Research Center, Hampton, VA.
INVERSE WING DESIGN IN TRANSONIC FLOW INCLUDING VISCOUS INTERACTION
Leland A. Carlson, Robert R. Ratcliff, Thomas A. Gally (Texas A&M Univ., College Station.), and Richard L. Campbell *In its* Transonic Symposium: Theory, Application, and Experiment, Volume 1, Part 2 Mar. 1989 p 497-519 (For primary document see N89-20942 14-02)
(Grant NsG-1619)
Avail: NTIS HC A22/MF A01 CSCL 01C

06 AIRCRAFT INSTRUMENTATION

Includes cockpit and cabin display devices; and flight instruments.

For related information see also *19 Spacecraft Instrumentation* and *35 Instrumentation and Photography.*

N89-20992# Air Force Inst. of Tech., Wright-Patterson AFB, OH. School of Engineering.
A SOURCE CODE ANALYZER TO PREDICT COMPILATION TIME FOR AVIONICS SOFTWARE USING SOFTWARE SCIENCE MEASURES. VOLUME 1: MAIN REPORT M.S. Thesis
Eric R. Geopper Dec. 1988 154 p
(AD-A202737; AFIT/GCS/ENG/88D-7) Avail: NTIS HC A08/MF A01 CSCL 12E

This thesis describes the construction of an Ada source code analyzer (SCA) which produces values for the Software Science measures 1c1, 1c2, N1, and N2. The measures are used to evaluate a mathematical model designed to predict the compile time of Ada modules. The primary goal of this effort was to provide a software tool to metrics researchers which could automatically compute Software Science measures for Ada modules. A secondary goal was to produce a convenient method for Ada compiler researchers to predict the amount of time consumed during compilation of given avionics software modules. As the SCA was built, we incorporated the rules of a new Ada token counting strategy designed to yield meaningful results for entire Ada programs, not just executable code. Once satisfied the SCA implemented the rules correctly and produced accurate counts for the Software Science measures, we added the compile time model to the SCA. To test the validity of the compile time model, over 200 modules were selected at random from among the Common Ada Missile Packages (CAMP) software library. For each module chosen, both the compile time as predicted by the SCA and the actual compile time using the Verdix Ada compiler were recorded. Finally, the prediction error values (predicted compile time minus actual compile time) were recorded and analyzed. GRA

N89-20993# Air Force Inst. of Tech., Wright-Patterson AFB, OH. School of Engineering.
REAL-TIME DISPLAY OF TIME DEPENDENT DATA USING A HEAD-MOUNTED DISPLAY M.S. Thesis
Gary K. Lorimor Dec. 1988 64 p
(AD-A203051; AFIT/GE/ENG/88D-22) Avail: NTIS HC A04/MF A01 CSCL 25C

The purpose of this investigation was the development of a software system to integrate time-dependent data with a three-dimensional virtual environment. Red Flag data tapes were used as a source of time-dependent data. To project this into a virtual environment a head-mounted display was used. The software development was done on a Silicon Graphics Iris 3130 workstation. The design of the software system allows the user to be free of the keyboard for most situations. The position of the user's head was determined using a Polhemus 3-space tracker. The user could exercise basic control of the system with input from mouse buttons. The user was allowed to move to any position in the environment by looking in the direction of desired travel. The user was also given the option to ride in any cockpit which was in the environment. This allowed the user to see the environment from a pilots perspective at a specific point and time in the display sequence. Minimal machine dependent routines were used in the development of the software system. The software system was developed using the C programming language. The results of this effort were encouraging. There appears to be further possibilities of use for a system of this type in the training arena. The update rate of this system is about 10 frames per second. There appears to be several open questions concerning the benefits of such a system in the training environment. GRA

N89-20994# Air Force Inst. of Tech., Wright-Patterson AFB, OH. School of Engineering.
A HELMET-MOUNTED VIRTUAL ENVIRONMENT DISPLAY SYSTEM M.S. Thesis
Robert Keith Rebo Dec. 1988 87 p
(AD-A203055; AFIT/GCS/ENG/88D-17) Avail: NTIS HC A05/MF A01 CSCL 25C

This effort researches existing Helmet Mounted Display (HMD) systems and presents a prototype design of a color Helmet-Mounted Virtual Environment Display System. Many existing systems are discussed, including systems currently in use by the U.S. Navy, Air Force, and Army. Several differing designs are presented and evaluated. The Air Force Institute of Technology Helmet Mounted Virtual Environment Display System places the user in a visual situation that is generated by a computer. This HMD system could easily be adapted for use with a video camera. This paper presents an inexpensive system design that incorporates the benefits of other efforts. The cost trade offs are evaluated and the best design for the lowest cost is presented. The optics, three dimensional considerations, the mounting platform and display technologies are also discussed. The final HMD system design is described in detail and presented so that any reader could build a similar system for minimal cost. This system uses color Liquid Crystal Displays (LCD) mounted directly before the eyes of the user. Specially designed optics were developed to enable the user to focus on the image only inches away. The positional information of the user is determined by a sensitive electro-magnetic device developed by Polhemus Navigational Sciences. This system is very accurate but has a limited effective range. Predictive tracking is discussed and implemented using a simple Kalman filter equation. GRA

07 AIRCRAFT PROPULSION AND POWER

Includes prime propulsion systems and systems components, e.g., gas turbine engines and compressors; and onboard auxilliary power plants for aircraft.

For related information see also *20 Spacecraft Propulsion and Power, 28 Propellants and Fuels,* and *44 Energy Production and Conversion.*

N89-20995*# National Aeronautics and Space Administration. Lewis Research Center, Cleveland, OH.
A REAL-TIME SIMULATOR OF A TURBOFAN ENGINE
Jonathan S. Litt (Army Aviation Research and Development Command, Cleveland, OH.), John C. DeLaat, and Walter C. Merrill Mar. 1989 32 p
(NASA-TM-100869; E-4578; NAS 1.15:100869; AVSCOM-TR-89-C-001) Avail: NTIS HC A03/MF A01 CSCL 21E

A real-time digital simulator of a Pratt and Whitney F100 engine has been developed for real-time code verification and for actuator diagnosis during full-scale engine testing. This self-contained unit can operate in an open-loop stand-alone mode or as part of closed-loop control system. It can also be used for control system design and development. Tests conducted in conjunction with the NASA Advanced Detection, Isolation, and Accommodation program show that the simulator is a valuable tool for real-time code verification and as a real-time actuator simulator for actuator fault diagnosis. Although currently a small perturbation model, advances in microprocessor hardware should allow the simulator to evolve into a real-time, full-envelope, full engine simulation. Author

N89-20996*# National Aeronautics and Space Administration. Lewis Research Center, Cleveland, OH.
A COMPENDIUM OF CONTROLLED DIFFUSION BLADES GENERATED BY AN AUTOMATED INVERSE DESIGN PROCEDURE
Jose M. Sanz Mar. 1989 204 p
(NASA-TM-101968; E-4665; NAS 1.15:101968) Avail: NTIS HC A10/MF A01 CSCL 21E

A set of sample cases was produced to test an automated design procedure developed at the NASA Lewis Research Center for the design of controlled diffusion blades. The range of application of the automated design procedure is documented. The results presented include characteristic compressor and turbine blade sections produced with the automated design code as well as various other airfoils produced with the base design method prior to the incorporation of the automated procedure. Author

N89-20997# Naval Postgraduate School, Monterey, CA.
HOLOGRAPHIC PARTICLE SIZING IN SOLID FUEL RAMJETS M.S. Thesis
Robert P. Paty Sep. 1988 49 p
(AD-A202699) Avail: NTIS HC A03/MF A01 CSCL 21D

An investigation was conducted to determine the suitability of a holographic technique as a diagnostic tool for metallized fuel combustion in a two-dimensional solid fuel ramjet. The highly metallized fuels were burned under conditions similar to actual flight conditions. If found suitable, the objective was to produce a three-dimensional image of a volume in the boundary layer above the fuel surface, and to determine the particle size distribution in that volume. This distribution could be used to validate current models which must assume particle size, and could lead to better estimates of fuel regression rates and combustion efficiencies. Once the conditions for sustained combustion were determined, the technique was successfully demonstrated, even in the presence of large amounts of smoke. Holograms were obtained at two different chamber pressures for each of the fuels. However, current resolution limits of the technique are not sufficient to reveal the vast majority of the particles in the combustor. GRA

N89-20943*# McDonnell Aircraft Co., Saint Louis, MO. Computation Fluid Dynamics.
TRANSONIC PROPULSION SYSTEM INTEGRATION ANALYSIS AT MCDONNELL AIRCRAFT COMPANY
Raymond R. Cosner *In* NASA, Langley Research Center, Transonic Symposium: Theory, Application, and Experiment, Volume 1, Part 2 Mar. 1989 p 409-436 (For primary document see N89-20942 14-02)
Avail: NTIS HC A22/MF A01 CSCL 21E

08 AIRCRAFT STABILITY AND CONTROL

Includes aircraft handling qualities; piloting; flight controls; and autopilots.

For related information see also *05 Aircraft Design, Testing and Performance.*

N89-20998 Purdue Univ., West Lafayette, IN.
ACTUATION CONSTRAINTS IN MULTIVARIABLE FLIGHT CONTROL SYSTEMS Ph.D. Thesis
Mark Ronald Anderson 1988 202 p
Avail: Univ. Microfilm Oder No. DA8825502

This research deals with stability and performance robustness of non-linear multivariable feedback control systems. The systems considered include linear as well as non-linear idealizations, where non-linear models are used to represent practical limitations (limiting) in the physical devices. A robustness analysis methodology, intended for use early in the control-law synthesis, is developed to evaluate stability and performance with respect to control surface deflection and rate limits specifically. The methodology consists of three steps. First, a linear actuator signal approximation is chosen based on a priori bounds, developed herein, between the time response of the linear signal approximation and the actual actuator signal. Second, the peak magnitude of the linear signal approximation is used to define a quasi-linear representation of the deflection and rate limit saturation elements using either describing function or sector methods. Third, stability and performance robustness with respect to the quasi-linear saturation models may then be evaluated using matrix-singular-value or eigenvalue techniques. The analysis methodology is used to evaluate the stability robustness of two high-authority, multivariable flight control laws for two different pilot stick force inputs to a generic foward-swept-wing aircraft. Dissert. Abstr.

N89-20999*# Systems Technology, Inc., Hawthorne, CA.
TAILLESS AIRCRAFT PERFORMANCE IMPROVEMENTS WITH RELAXED STATIC STABILITY
Irving L. Ashkenas and David H. Klyde Mar. 1989 145 p
(Contract NAS1-18524)
(NASA-CR-181806; NAS 1.26:181806; STI-TR-1252-1) Avail: NTIS HC A07/MF A01 CSCL 01C

The purpose is to determine the tailless aircraft performance improvements gained from relaxed static stability, to quantify this potential in terms of range-payload improvements, and to identify other possible operational and handling benefits or problems. Two configurations were chosen for the study: a modern high aspect ratio, short-chord wing proposed as a high-altitude long endurance (HALE) remotely piloted vehicle; a wider, lower aspect ratio, high volume wing suitable for internal stowage of all fuel and payload required for a manned long-range reconnaissance mission. Flying at best cruise altitude, both unstable configurations were found to have a 14 percent improvement in range and a 7 to 9 percent improvement in maximum endurance compared to the stable configurations. The unstable manned configuration also shows a 15 percent improvement in the 50 ft takeoff obstacle distance and an improved height response to elevator control. However, it is generally more deficient in control power due to its larger adverse aileron yaw and its higher takeoff and landing lift coefficient C(sub L), both due to the downward trimmed (vs. upward trimmed for stable configurations) trailing edge surfaces. Author

N89-21000# Air Force Inst. of Tech., Wright-Patterson AFB, OH. School of Engineering.
FLIGHT CONTROLLER DESIGN WITH NONLINEAR AERODYNAMICS, LARGE PARAMETER UNCERTAINTY AND PILOT COMPENSATION M.S. Thesis
Thomas J. Kobylarz Dec. 1988 115 p
(AD-A202727; AFIT/GE/ENG/88D-19) Avail: NTIS HC A06/MF A01 CSCL 01D

Nonlinear Quantitative Feedback Theory (QFT), developed by Dr. Isaac Horowitz, is used to design a flight control system for the YF-16 aircraft. Upon completing this stability augmentation system (SAS) additional compensation is added to reduce pilot workload while improving handling qualities. The YF-16 uncertain plant is simulated with C (a blend of normal acceleration at pilot station and pitch rate) as the controlled output. The simulation includes the full six degree of freedom nonlinear dynamic equations of motion and aerodynamic data throughout the entire subsonic flight envelope. A technique is presented which enables the uncertain nonlinear YF-16 to be represented as a set of linear timer invariant plants which is equivalent to the nonlinear plant with respect to the set of acceptable outputs. Once this set of plants is obtained, a linear QFT controller is synthesized yielding fixed compensation which is extremely insensitive to varying flight conditions. Simulations in the time and frequency domains demonstrate that the desired performance is attained. Further work with real-time man-in-the-loop simulations should be accomplished to expand the area of pilot compensation. GRA

N89-21001# Air Force Inst. of Tech., Wright-Patterson AFB, OH. School of Engineering.
A DIGITAL RATE CONTROLLER FOR THE CONTROL RECONFIGURABLE COMBAT AIRCRAFT DESIGNED USING QUANTITATIVE FEEDBACK THEORY M.S. Thesis

Kurt Nyle Neumann Dec. 1988 149 p
(AD-A203050; AFIT/GE/ENG/88D-33) Avail: NTIS HC A07/MF A01 CSCL 01D

The objective of this thesis is to develop a digital controller using Quantitative Feedback Theory for a fighter aircraft with unstable, nonminimum phase dynamics that meets performance specifications despite surface failures. Aircraft design trends for highly maneuverable fighter aircraft are relaxing stability requirements in order to increase performance in the transonic and supersonic regions. However, as a result, the aircraft is statically unstable in the subsonic region which makes the flight control system critical to flight safety. The conventional approach to the flight safety problem is to provide multiple redundancy throughout the fight control system. However, QFT provides an alternative to excessive hardware. The three controlled states are the pitch, roll, and yaw rates. A weighting matrix is derived which linearly combines the nine control surfaces into three control inputs. The plant is converted to a certain plane using the Hoffman algorithm. Three constant gain controllers and three prefilters are designed for a single flight condition of 0.9 Mach and 30000 ft altitude. The controllers and prefilters are transformed to the z plane for simulation purposes. The design is simulated with healthy plant and 24 combinations of surface failures. GRA

09 RESEARCH AND SUPPORT FACILITIES (AIR)

Includes airports, hangars and runways; aircraft repair and overhaul facilities; wind tunnels; shock tubes; and aircraft engine test stands.

For related information see also *14 Ground Support Systems and Facilities (Space).*

N89-21002*# National Aeronautics and Space Administration. Lewis Research Center, Cleveland, OH.
FLOWFIELD MEASUREMENTS IN THE NASA LEWIS RESEARCH CENTER 9- BY 15-FOOT LOW-SPEED WIND TUNNEL
Christopher E. Hughes Mar. 1989 78 p
(NASA-TM-100883; E-4116; NAS 1.15:100883) Avail: NTIS HC A05/MF A01 CSCL 14B

An experimental investigation was conducted in the NASA Lewis 9- by 15-Foot Low-Speed Wind Tunnel to determine the flow characteristics in the test section during wind tunnel operation. In the investigation, a 20-probe horizontally-mounted Pitot-static flow survey rake was used to obtain cross-sectional total and static pressure surveys at four axial locations in the test section. At each axial location, the cross-sectional flowfield surveys were made by repositioning the Pitot-static flow survey rake vertically. In addition, a calibration of the new wind tunnel rake instrumentation, used to determine the wind tunnel operating conditions, was performed. Boundary laser surveys were made at three axial locations in the test section. The investigation was conducted at tunnel Mach numbers 0.20, 0.15, 0.10, and 0.05. The test section profile results from the investigation indicate that fairly uniform total pressure profiles (outside the test section boundary layer) and fairly uniform static pressure and Mach number profiles (away from the test section walls and downstream of the test section entrance) exist throughout in the wind tunnel test section. Author

N89-21003# Systems Control Technology, Inc., Arlington, VA.
HELIPORT SYSTEM PLANNING GUIDELINES
Deborah Peisen Apr. 1988 113 p
(Contract DTFA01-87-C-00014)
(AD-A199081; DOT/FAA/PM-87/33; DOT/FAA/PP-88/3) Avail: NTIS HC A06/MF A01 CSCL 01E

State and city governments generally realize that continued vitality depends on a steady expansion of industry and services as a function of planned growth. The helicopter is a proven catalyst for enhancement of those desired growth patterns. However, without the necessary support infrastructure, this positive contribution of the helicopter cannot be realized. Determining the need for such a support system can be achieved through an understanding of local helicopter activities and the metropolitan or state-wide socioeconomic dynamics in which they occur. This allows for data base development, including a fleet inventory, and analysis to provide a foundation for determining current, and forecasting future, helicopter activity and support facility requirements. Heliport planning is a relatively new field. Previous efforts, although based on proven fixed-wing airport methods, have produced a series of uncoordinated and nonstandardized products from many various individual planners and organizations. Consequently, the data collected and the analytical processes used have not been consistent or directly comparable. Fundamental planning criteria by which urban area heliport requirements may be assessed at any jurisdictional level are given Author

N89-21004*# Vigyan Research Associates, Inc., Hampton, VA.
PERFORMANCE OF THE ACTIVE SIDEWALL BOUNDARY-LAYER REMOVAL SYSTEM FOR THE LANGLEY 0.3-METER TRANSONIC CRYOGENIC TUNNEL
S. Balakrishna, W. Allen Kilgore, and A. V. Murthy Feb. 1989 26 p
(Contract NAS1-17919)
(NASA-CR-181793; NAS 1.26:181793) Avail: NTIS HC A03/MF A01 CSCL 14B

A performance evaluation of an active sidewall boundary-layer removal system for the Langley 0.3-m Transonic Cryogenic Tunnel (TCT) was evaluated in 1988. This system uses a compressor and two throttling digital valves to control the boundary-layer mass flow removal from the tunnel. The compressor operates near the maximum pressure ratio for all conditions. The system uses a surge prevention and flow recirculation scheme. A microprocessor based controller is used to provide the necessary mass flow and compressor pressure ratio control. Initial tests on the system indicated problems in realizing smooth mass flow control while running the compressor at high speed and high pressure ratios. An alternate method has been conceived to realize boundary-layer mass flow control which avoids the recirculation of the compressor mass flow and operation near the compressor surge point. This scheme is based on varying the speed of the compressor for a sufficient pressure ratio to provide needed mass flow removal. The system has a mass flow removal capability of about 10 percent of test section flow at M = 0.3 and 4 percent at M = 0.8. The system performance has been evaluated in the form of the compressor map, and compressor tunnel interface characteristics covering most of the 0.3-m TCT operational envelope. Author

N89-21005# Naval Civil Engineering Lab., Port Hueneme, CA.
EXPERIMENTAL EXAMINATION OF THE AEROTHERMAL PERFORMANCE OF THE T-10 TEST CELL AT NAS (NAVAL AIR STATION), CUBI POINT Report, Oct. 1986 - Sep. 1987
C. A. Kodres, E. E. Cooper, and P. L. Stone Sep. 1988 140 p
(AD-A203887; NCEL-TN-1788) Avail: NTIS HC A07/MF A01 CSCL 14B

This report presents results of aerodynamic and thermodynamic tests conducted on the first standard Navy air-cooled T-10 test cell. Objectives of the tests were to: (1) Determine if aerodynamic and thermodynamic design objectives for the standard T-10 test cells were met; (2) Obtain data for comparing analytical predictions and validating analytical modeling techniques, and (3) Obtain baseline data of cell performance for use in case of future changes in design or operations. GRA

N89-20955*# National Aeronautics and Space Administration. Langley Research Center, Hampton, VA.
TEST TECHNIQUES: A SURVEY PAPER ON CRYOGENIC TUNNELS, ADAPTIVE WALL TEST SECTIONS, AND MAGNETIC SUSPENSION AND BALANCE SYSTEMS
Robert A. Kilgore, David A. Dress, Stephen W. D. Wolf, and Colin P. Britcher (Old Dominion Univ., Norfolk, VA.) *In its* Transonic Symposium: Theory, Application, and Experiment, Volume 1, Part 2 Mar. 1989 p 705-740 (For primary document see N89-20942

14-02)
Avail: NTIS HC A22/MF A01 CSCL 14B

N89-20957*# National Aeronautics and Space Administration. Langley Research Center, Hampton, VA.
INSTRUMENTATION ADVANCES FOR TRANSONIC TESTING
Percy J. Bobbitt *In its* Transonic Symposium: Theory, Application, and Experiment, Volume 1, Part 2 Mar. 1989 p 765-816 (For primary document see N89-20942 14-02)
Avail: NTIS HC A22/MF A01 CSCL 14B

N89-20961*# National Aeronautics and Space Administration. Langley Research Center, Hampton, VA.
CAPABILITIES OF WIND TUNNELS WITH TWO-ADAPTIVE WALLS TO MINIMIZE BOUNDARY INTERFERENCE IN 3-D MODEL TESTING
Rainer Rebstock and Edwin E. Lee, Jr. *In its* Transonic Symposium: Theory, Application, and Experiment, Volume 1, Part 2 Mar. 1989 p 891-910 Sponsored in part by National Research Council (For primary document see N89-20942 14-02)
Avail: NTIS HC A22/MF A01 CSCL 14B

12 ASTRONAUTICS (GENERAL)

For extraterrestrial exploration see *91 Lunar and Planetary Exploration.*

N89-21006# Air War Coll., Maxwell AFB, AL.
SPACE TECHNOLOGY AND THE SOVIET/US STRATEGIC COMPETITION: A PERSPECTIVE AND FORECAST USING 12-YEAR CYCLES
George W. Criss, III May 1988 92 p
(AD-A202538) Avail: NTIS HC A05/MF A01 CSCL 22A

This report contends that exploiting space technology for national power has been the dominant theme of the U.S./Soviet strategic competition since World War II. Furthermore, markedly different approaches to realizing this potential have evolved on both sides. To support this thesis, the author develops a paradigm of 12-year cycles marked by major space spectaculars. The all-important political and strategic conditions which surround and shape these major events are explored, compared, and linked. A second thesis, that this 40-year competition has led to swift retaliatory nuclear forces far in excess of desirable levels, is then presented and supported. Finally, conclusions distilled from the foregoing historical perspective and the current space-strategic situation, plus a forecast, are offered. GRA

13 ASTRODYNAMICS

Includes powered and free-flight trajectories; and orbital and launching dynamics.

N89-21007# Air Force Inst. of Tech., Wright-Patterson AFB, OH. School of Engineering.
OPTIMAL LAUNCH TIME FOR A DISCONTINUOUS LOW THRUST ORBIT TRANSFER M.S. Thesis
Jeffrey M. McCann Dec. 1988 66 p
(AD-A202693; AFIT/GA/AA/88D-7) Avail: NTIS HC A04/MF A01 CSCL 22C

This thesis searches for the optimal launch time of a discontinuous, low thrust transfer between non-coplanar, circular orbits. The spacecraft is assumed to be solar-powered rocket that cannot provide thrust in the earth's shadow. Two time scales are used to calculate a minimum time trajectory. The fast timescale produces a control law which maximizes a change in orbital elements for a single orbit. The slow timescale incorporates the control law so that the final boundary conditions are met in minimum time. Minimum transfer times are determined between winter and summer. GRA

N89-21008# Air Force Inst. of Tech., Wright-Patterson AFB, OH. School of Engineering.
CONTROL SYSTEM FOR MAINTAINING STABLE ORBITS AROUND PHOBOS M.S. Thesis
Mary K. Solomon Dec. 1988 88 p
(AD-A202776; AFIT/GA/AA/88D-10) Avail: NTIS HC A05/MF A01 CSCL 03C

Phobos can be modeled as a triaxial ellipsoid in a circular orbit around Mars. The orbital dynamics of a satellite in orbit around Phobos are derived using Hamilton's canonical equations. An algorithm is then developed to find closed orbits for a specified period. Periodic orbits in Phobos' orbital plane have been found to be unstable. A control system is developed using scalar modal control to stabilize the orbit by shifting the unstable Poincar exponent to the left-half plane. GRA

N89-21009# Air Force Inst. of Tech., Wright-Patterson AFB, OH. School of Engineering.
HYPERSURFACE INSERTION WINDOW FOR LONG TERM ORBITAL STABILITY OF ARTIFICIAL SATELLITES ABOUT THE PLANET VENUS M.S. Thesis
Robert L. Dudley, Jr. Dec. 1988 173 p
(AD-A202808; AFIT/GA/AA/88D-03) Avail: NTIS HC A08/MF A01 CSCL 12C

This study develops an analytic function for the six dimensional surface (or hypersurface) above the planet Venus for a five earth year survivability for an artificial satellite. Current U.S. policy concerning the exploration of other planets, via artificial satellites, requires the satellites be sterilized (5:61). This is a very time intensive and costly practice. Developing the ability to estimate the life time of an artificial satellite that can no longer perform its station keeping duties may allow the sterilization procedures before launch to be waived. The objective is to develop a five year survivability function in the orbital parameter space above which a satellite has at least five years to survive before it impacts the planet's surface. Perturbations effects which would cause the satellite's orbit to deteriorate are modeled and include: (1) the geopotential of the planet, (2) the effects of solar wind, and (3) the drag on the satellite due to the atmosphere of the planet. The model was then interpolated to provide an analytic function for five year survivability. GRA

N89-21010# Air Force Inst. of Tech., Wright-Patterson AFB, OH. School of Engineering.
STABILITY SOLUTION TO LINEARIZED EQUATIONS OF MOTION FOR A SYMMETRIC SPINNING SATELLITE IN AN ELLIPTICAL ORBIT APPLIED TO THE NON-LINEAR EQUATIONS M.S. Thesis
Dale E. Shell Dec. 1988 91 p
(AD-A202934; AFIT/GA/AA/88D-09) Avail: NTIS HC A05/MF A01 CSCL 22C

The attitude of a spinning symmetrical satellite in an elliptical orbit is analyzed. The perturbed motion of the satellite is described by linear equations with periodic coefficients. Stability is determined by Floquet theory. Active control is added to the system and results lead to a linear periodic control law. Scalar control from the linearized system is implemented to evaluate the performance of the control law on the non-linear equations of motion. For small disturbances, it is illustrated that the controlled non-linear response duplicates the linear case. For larger disturbances, phase portraits show the resulting behavior of the coupled modes. As the perturbed motion increases in magnitude, stability regions appear. Initial motion results either a return to the initial equilibrium, an oscillation around the equilibrium point or divergence from the initial equilibrium. GRA

N89-21011# Air Force Inst. of Tech., Wright-Patterson AFB, OH. School of Engineering.
ESTIMATED SATELLITE CLUSTER ELEMENTS IN NEAR CIRCULAR ORBIT M.S. Thesis
Michael L. Ward Dec. 1988 50 p
(AD-A202938; AFIT/GA/AA/88D-13) Avail: NTIS HC A03/MF A01 CSCL 22C

Arraying satellites into clusters has been under consideration for commercial communications applications. Stationing these satellites in a restricted section of an orbit allows for in-orbit spares to replace satellites as they fail. An additional benefit to military planners increased wartime system survivability. A proposed use of such a satellite cluster would be a space based radar. In order to form a cohesive image of the radar return, the relative positions of the satellites need to be known to within one quarter of the radar wavelength. For the purposes of this thesis, 25 meters is considered sufficiently accurate. This thesis investigated the performance of an on-board filter algorithm in estimating the relative positions of each element in a ten satellite orbital cluster. The on-board estimator is the U-D covariance factorization version of the Kalman filter with dynamics based on the Clohessy-Wiltshire equations. Performance is measured by comparing the square root of the position covariance eigenvalues to the magnitude of true position errors. True errors are also compared to minimum accuracy requirements. Filter tuning is limited to adjusting the diagonal entries of the dynamics noise matrix. Test cases include: perfect initial conditions with perfect range data; and perfect initial conditions with noise corrupted measurements. The position errors were well within the accuracy requirements for all test cases. GRA

14 GROUND SUPPORT SYSTEMS AND FACILITIES (SPACE)

Includes launch complexes, research and production facilities; ground support equipment, e.g., mobile transporters; and simulators.

For related information see also *09 Research and Support Facilities (Air).*

No abstracts in this category.

15 LAUNCH VEHICLES AND SPACE VEHICLES

Includes boosters; operating problems of launch/space vehicle systems; and reusable vehicles.

For related information see also *20 Spacecraft Propulsion and Power.*

N89-21012# Air Force Inst. of Tech., Wright-Patterson AFB, OH. School of Engineering.

AN ANALYTICAL FRAMEWORK FOR DETERMINING LIFE CYCLE COST IMPLICATIONS OF THE ADVANCED LAUNCH SYSTEM M.S. Thesis

William K. Stockman Dec. 1988 153 p (AD-A202873; AFIT/GOR/ENS/88D-19) Avail: NTIS HC A08/MF A01 CSCL 05C

The product of this research effort was a simplified cost analysis tool that can be used to determine life cycle costs for the Advanced Launch System. The major objective was to develop a tool that would allow quick analysis of proposals and provide data input in a timely fashion. This effort produced a core program that can be used to determine life cycle costs as a function of system components, production infrastructures, reliability assumptions and flexible mission models. The life cycle cost model can operate in either a deterministic or stochastic mode depending on user inputs. An additional effort modeled the production infrastructure using a network flow system. This system modeled the flow of the basic vehicle components from initial production through final launch. The analysis tool uses a commercially available spreadsheet package available for most personal computers. The analyst using this program operates in a user-friendly environment that simplifies data input and problem formulation. The user has a wide variety of output formats and graphics options that simplify report generation. GRA

16 SPACE TRANSPORTATION

Includes passenger and cargo space transportation, e.g., shuttle operations; and space rescue techniques.

For related information see also *03 Air Transportation and Safety* and *18 Spacecraft Design, Testing and Performance.* For space suits see *54 Man/System Technology and Life Support.*

No abstracts in this category.

17 SPACE COMM., SPACECRAFT COMM., COMMAND & TRACKING

Includes telemetry; space communications networks; astronavigation and guidance; and radio blackout.

For related information see also *04 Aircraft Communications and Navigation* and *32 Communications and Radar.*

N89-21013# Fish and Wildlife Service, Fairbanks, AK.

SATELLITE TELEMETRY: A NEW TOOL FOR WILDLIFE RESEARCH AND MANAGEMENT

Steve G. Fancy, Larry F. Pank, David C. Douglas, Catherine H. Curby, Gerald W. Garner, Steven E. Amstrup, and Wayne L. Regelin (Alaska Dept. of Fish and Game, Fairbanks.) 1988 61 p (PB88-249255; RESOURCE-Pub-172; LC-88-600161) Avail: NTIS HC A04/MF A01 CSCL 08B

The Argos Data Collection and Location System can be used to systematically acquire detailed locational and behavioral data from animals via satellite. System components, applications of satellite technology to wildlife research and management, and use of geographic information systems are described. A computer software package for analyzing satellite telemetry data is presented. GRA

18 SPACECRAFT DESIGN, TESTING AND PERFORMANCE

Includes satellites; space platforms; space stations; spacecraft systems and components such as thermal and environmental controls; and attitude controls.

For life support systems see *54 Man/System Technology and Life Support.* For related information see also *05 Aircraft Design, Testing and Performance, 39 Structural Mechanics,* and *16 Space Transportation.*

N89-21014 Virginia Polytechnic Inst. and State Univ., Blacksburg.

TIME OPTIMAL SLEWING OF FLEXIBLE SPACECRAFT Ph.D. Thesis

Joseph Zalman Ben-Asher 1988 148 p Avail: Univ. Microfilms Order No. DA8824964

The time optimal slewing problem for flexible spacecraft is considered. We study single-axis rotational maneuvers for a simple flexible system, consisting of a rigid hub with an elastic appendage. The equations of motions are derived by Hamilton's Principle, and a discrete nonlinear model is obtained by the assumed modes method. The problem is first solved in a discrete linearized space by parameter optimization. Optimality is verified by Pontryagin's Maximum Principle. The linear solutions are then used to obtain the time optimal solutions for the nonlinear problem by a multiple-shooting algorithm. Although this approach is applicable to arbitrary boundary conditions, this work is confined, almost exclusively, to rest-to-rest maneuvers. These maneuvers are shown to possess some interesting symmetric and asymptotic properties. The problem is further analyzed in infinite-dimensional space, and the convergence of the finite-dimensional approximations is studied. Finally, a soft version of the time optimal slewing problem is

considered, where the control is bounded only by a penalty term in the cost functional. A perturbation technique is applied to further simplify this problem. Dissert. Abstr.

N89-21015# Photometrics, Inc., Woburn, MA.
EXCITATION AND DIAGNOSTICS OF OPTICAL CONTAMINATION IN THE SPACECRAFT ENVIRONMENT Final Report, 13 Aug. 1985 - 30 Jun. 1988
I. L. Kofsky, J. L. Barrett, T. E. Brownrigg, P. N. McNicholl, and N. H. Tran 1 Jul. 1988 158 p
(Contract F19628-85-C-0148)
(AD-A202429; PHM-88-06; AFGL-TR-88-0293) Avail: NTIS HC A08/MF A01 CSCL 22E

The ultraviolet and infrared contaminant glows produced by spacecraft traversing the thermosphere are identified and their spatial extents and brightnesses estimated from laboratory reaction-rate data, in support of planning of systematic spectroradiometric measurements from space shuttle. A formalism is developed for calculating radiances and irradiances of the emissions from metastable molecules formed at vehicle surfaces exposed to the atmosphere, which serves in selecting the view projections and angular fields of optical sensors. GRA

N89-21016# Control Dynamics Co., Huntsville, AL.
ACTIVE CONTROL TECHNIQUE EVALUATION FOR SPACECRAFT (ACES) Final Report, 15 Aug. 1986 - 30 Jul. 1987
R. D. Irwin, Victoria Jones, Sally C. Rice, Sherman M. Seltzer, and Danny K. Tollison 16 Jun. 1988 242 p
(Contract F33615-86-C-3225)
(AD-A202475; AFWAL-TR-88-3038) Avail: NTIS HC A11/MF A01 CSCL 22B

This report describes the Active Control Technique Evaluation for Spacecraft (ACES) Program. Three Large Space Structures control system design techniques, developed under the Active Control of Space Structures (ACOSS) Program, were compared. The three techniques included Filter Accommodated Model Error Sensitivity Suppression (FAMESS), High Authority Control/Low Authority Control (HAC/LAC), and Positivity. The comparison was accomplished both analytically and experimentally. Each controller was implemented and tested at the NASA/MSFC Large Space Structure Ground Test Facility on the ACES test article. The design and implementation of each controller were performed under identical conditions. The identical control model, sensor/actuator complement, computer, disturbances, and performance criteria were applied to each control design/evaluation. GRA

N89-21017# Air Force Inst. of Tech., Wright-Patterson AFB, OH. School of Engineering.
LIGHT SATELLITES: A DILEMMA FOR THE US ARMY M.S. Thesis
James R. Pierson Dec. 1988 95 p
(AD-A202648; AD-E900870; AFIT/GSO/MA/88D-2) Avail: NTIS HC A05/MF A01 CSCL 12D

This thesis seeks to assist senior Army leaders in determining whether light satellite (LIGHTSAT) should be procured to meet current and future reconnaissance, surveillance and target acquisition (RSTA) needs on the battlefield. Two methods were developed: the decision analysis approach and the analytical hierarchy process. For each method, LIGHTSAT was evaluated against the Joint Surveillance Target Attack Radar System alternative. Sample data was used in place of actual values (unless otherwise noted). The decision analysis method required an influence diagram of the overall decision, a value model that elicited outcomes for each alternative, a model that would help determine the level of reconnaissance, surveillance and target acquisition achieved by each alternative and an assessment of probabilities of certain events occurring. Use of decision analysis lends considerable insight into the decision through the expected value of perfect information (EVPI). EVPI illustrates how much additional money should be invested into reducing the uncertainty within the decision. The analytical hierarchy process analyzed the decision through a hierarchy of objectives approach. Subjective judgments based upon experience were combined with quantifiable measurements to apply weightings to the various criteria within a level of the hierarchy. Synthesis of preferences between alternatives and weightings yielded an overall preference for the decision. GRA

N89-21018# Air Force Inst. of Tech., Wright-Patterson AFB, OH. School of Engineering.
REMOTE ORBITAL CAPTURE USING AN ORBITAL MANEUVERING VEHICLE EQUIPPED WITH A MULTIBODY GRAPPLING ARM ASSEMBLY M.S. Thesis
F. Joseph Bishop Dec. 1988 165 p
(AD-A202760; AFIT/GA/AA/88D-02) Avail: NTIS HC A08/MF A01 CSCL 22A

The problem of detumbling and despinning a freely spinning and precessing axisymmetric target satellite using an orbital maneuvering vehicle is considered. The axisymmetric orbital maneuvering vehicle is equipped with a multibody grappling arm assembly to capture the target. Counter-masses are used to maintain dynamic balancing and stability throughout the deployment of the arm and the subsequent spin-up of the grappling device prior to docking. The five-body system is modeled using Eulerian-based equations of motion developed by Hooker and Margulies. Open-loop control laws are formulated to deploy the grappling arm assembly and spin-up the grappling device using internal motor torques. A Liapunov technique is applied to derive a nonlinear feedback control law that drives the docked system to a final spin-stabilized state of equilibrium. External thrusters are used to maintain the absolute motion of the system during this process. Variations in grappling length, target coning angle, and response times are examined for design purposes. State and control histories are presented and the results from this five-body model are compared with the Widhalm and Conway two-body study. The simulation indicates that the required control magnitudes are higher for the five-body model but are still quite reasonable. The addition of the grappling arm assembly adds both realism and flexibility to the capture process. GRA

N89-21019# Lowell Univ., MA. Dept. of Mathematics.
DERIVATION AND TESTING OF COMPUTER ALGORITHMS FOR AUTOMATIC REAL-TIME DETERMINATION OF SPACE VEHICLE POTENTIALS IN VARIOUS PLASMA ENVIRONMENTS Final Report, 1 Jan. 1985 - 31 Mar. 1988
Stanley L. Spiegel 31 May 1988 66 p
(Grant AF-AFOSR-0015-85; AF Proj. 2311)
(AD-A203019; AFOSR-88-1254TR) Avail: NTIS HC A04/MF A01 CSCL 22B

A new algorithm for spacecraft charge detection based on a drop in electrostatic analyzer ion count spectra at energy levels higher than the level of vehicle potential has been derived. This so-called Count Drop algorithm was found to be effective in cases where, owing either to rapidly fluctuating potentials or significant secondary ion production, there were substantial ion counts in channels below the level of peak charging. In such cases, the Count Ratio (renamed Count Rise) and Distribution Function algorithms, both based on a sharp increase in counts at the level of charging, were able to detect maximum vehicle potential. A corresponding algorithm based on a sharp decrease in ion distribution function, called the Distribution-function Drop Algorithm has also been tested using SCATHA data. The ion count spectra associated with 11 instances of low earth orbit spacecraft charging in polar latitudes have been examined. GRA

N89-21020# Air Force Inst. of Tech., Wright-Patterson AFB, OH. School of Engineering.
ACTIVE CONTROL OF A LARGE SPACE STRUCTURE AS APPLIED TO THE PHASE 1 CETF (CRITICAL EVALUATION TASK FORCE) SPACE STATION M.S. Thesis
Dale A. Cope Dec. 1988 117 p
(AD-A203293; AFIT/GAE/AA/88D-5) Avail: NTIS HC A06/MF A01 CSCL 22E

The major objective of this thesis is to apply a decoupled control technique to a specific space station model. The model is

a finite element model of the Phase 1 Critical Evaluation Task Force (CETF) Space Station. The control technique allows for the active control of a large number of modes by using several decoupled controllers. The space station attitude control system provides attitude stabilization and disturbance rejection. Its performance is evaluated by the station's response to two disturbances - crew motion and shuttle docking. GRA

N89-21021# Systems Science and Software, La Jolla, CA.
CHARGING POTENTIALS FOR TWO SAMPLE SETS OF SPECTRA FROM DMSP SATELLITES Scientific Report No. 8, Jan. - Feb. 1988
T. G. Barker Feb. 1988 17 p
(Contract F19628-86-C-0056)
(AD-A203694; SSS-R-88-9339; W/O-11304; AFGL-TR-88-0057)
Avail: NTIS HC A03/MF A01 CSCL 22A

The importance has been discussed of accurately including the emission of secondary and backscattered electrons in the calculations of flux balances that are used to predict the equilibrium potential of satellites during intense electron precipitation. This concept is applied to a sequence of electron and ion flux spectra observed by DMSP satellites to determine the levels of negative charging, if any, experienced by the satellites. The net electron current incident minus backscattered and secondary electrons is a diagnostic quantity that can be used to determine whether charging has occurred. Using simple models of the satellite and ion collection, along with secondary and backscatter yields for the appropriate covering, one can quickly scan large amounts of data for charging events and estimate the equilibrium potential. GRA

N89-21022# Air Force Geophysics Lab., Hanscom AFB, MA.
PRECIPITATING ION AND ELECTRON DETECTORS (SSJ/4) FOR THE BLOCK 5D/FLIGHT 8 DMSP (DEFENSE METEOROLOGICAL SATELLITE PROGRAM) SATELLITE Interim Report
T. L. Schumaker, D. A. Hardy, S. Moran, A. Huber, J. McGarity, and J. Pantazis 4 Feb. 1988 61 p
(AD-A203999; AFGL-TR-88-0030; AFGL-IP-335) Avail: NTIS HC A04/MF A01 CSCL 04A

The satellites of the Defense Meteorological Satellite Program are flown operationally to provide data for the specification of terrestrial weather and near-Earth space environment. In support of space environment specifications, the satellites, starting with Flight 6 (F6), carry an improved set of electrostatic analyzers (SSJ/4). These instruments are designed to measure the flux of precipitating electrons and ions with energies between 30 eV and 30 KeV. The data from these analyzers are routinely processed at the Air Force Geophysics Laboratory (AFGL) and are available to the scientific community. A description of the SSJ/4 electrostatic analyzers for the DMSP satellite, results of the extensive calibration of the instruments, and examples of data use are given in this report. The report was prepared to facilitate the widespread use of the SSJ/4 data. Both by itself, and in combination with other sensors on the satellite, the SSJ/4 detectors provide important data for the study of auroral processes. GRA

N89-21023*# Lockheed Missiles and Space Co., Huntsville, AL. Engineering Center.
CONJUGATING BINARY SYSTEMS FOR SPACECRAFT THERMAL CONTROL Final Report
Philomena G. Grodzka, William G. Dean, Lori A. Sisk, and Zain S. Karu Jan. 1989 112 p
(Contract NAS8-36199)
(NASA-CR-183608; NAS 1.26:183608; LMSC-HEC-TR-F226066)
Avail: NTIS HC A06/MF A01 CSCL 22B

The materials search was directed to liquid pairs which can form hydrogen bonds of just the right strength, i.e., strong enough to give a high heat of mixing, but weak enough to enable phase change to occur. The cursory studies performed in the area of additive effects indicate that Conjugating Binary (CB) performance can probably be fine-tuned by this means. The Fluid Loop Test Systems (FLTS) tests of candidate CBs indicate that the systems Triethylamine (TEA)/water and propionaldehyde/water show close to the ideal, reversible behavior, at least initially. The Quick Screening Tests QSTs and FLTS tests, however, both suffer from rather severe static due either to inadequate stirring or temperature control. Thus it is not possible to adequately evaluate less than ideal CB performers. Less than ideal performers, it should be noted, may have features that make them better practical CBs than ideal performers. Improvement of the evaluation instrumentation is thus indicated. Author

N89-21024# Johns Hopkins Univ., Laurel, MD. Applied Physics Lab.
REENTRY RESPONSE OF THE LIGHT WEIGHT RADIOISOTOPE HEATER UNIT RESULTING FROM A VENUS-EARTH-EARTH GRAVITY ASSIST MANEUVER ACCIDENT
James C. Hagan Oct. 1988 141 p
(Contract DE-AI01-88NE-32140)
(DE89-005359; ANSP-M-19; DOE/OSA-32087-19) Avail: NTIS HC A07/MF A01

Reentry analyses consisting of ablation response, thermal response and thermal stress response have been conducted on the Light Weight Radioisotope Heater Unit for Galileo/VEEGA reentry conditions. Sequential ablation analyses of the LWRHU aeroshell, the fuel clad, and the fuel pellet have been conducted in reentry regimes where the aeroshell has been deemed to fail. The failure criterion for ablation is assumed to be recession corresponding to 50 percent of the wall thickness (the design criterion recommended in the DOE Overall Safety Manual). Although the analyses have been carried far beyond this limit (as presented and discussed herein), JHU/APL endorses the position that failure may occur at the time that this recession is achieved or at lower altitudes within the heat pulse considering the uncertainties in the aerodynamic, thermodynamic, and thermo-structural analyses and modeling. These uncertainties result mainly because of the high energies involved in the VEEGA reentries compared to orbital decay reentries. Risk evaluations should consider the fact that for shallow flight paths the unit may disassemble at high-altitude as a result of ablation or may remain intact until it impacts with a clad that had been molten. DOE

N89-21731*# South Carolina Univ., Columbia. Dept. of Mechanical Engineering.
SMALL EXPENDABLE DEPLOYER SYSTEM MEASUREMENT ANALYSIS
Connie K. Carrington *In* Alabama Univ., Research Reports: 1988 NASA/ASEE Summer Faculty Fellowship Program Dec. 1988 16 p (For primary document see N89-21726 14-99)
Avail: NTIS HC A99/MF E03 CSCL 22B

N89-21740*# Mississippi State Univ., Mississippi State. Dept of Aerospace Engineering.
GUIDANCE FOR AN AEROASSISTED ORBITAL TRANSFER VEHICLE
Kenneth R. Hall *In* Alabama Univ., Research Reports: 1988 NASA/ASEE Summer Faculty Fellowship Program Dec. 1988 11 p (For primary document see N89-21726 14-99)
Avail: NTIS HC A99/MF E03 CSCL 22B

N89-21743*# Ohio Univ., Athens. Dept. of Electrical and Computer Engineering.
INVESTIGATION OF PRACTICAL APPLICATIONS OF H INFINITY CONTROL THEORY TO THE DESIGN OF CONTROL SYSTEMS FOR LARGE SPACE STRUCTURES
R. Dennis Irwin *In* Alabama Univ., Research Reports: 1988 NASA/ASEE Summer Faculty Fellowship Program Dec. 1988 26 p (For primary document see N89-21726 14-99)
Avail: NTIS HC A99/MF E03 CSCL 22B

19 SPACECRAFT INSTRUMENTATION

For related information see also *06 Aircraft Instrumentation* and *35 Instrumentation and Photography.*

No abstracts in this category.

20 SPACECRAFT PROPULSION AND POWER

Includes main propulsion systems and components, e.g., rocket engines; and spacecraft auxilliary power sources.

For related information see also *07 Aircraft Propulsion and Power, 28 Propellants and Fuels, 44 Energy Production and Conversion,* and *15 Launch Vehicles and Space Vehicles.*

N89-21025*# National Aeronautics and Space Administration. Lewis Research Center, Cleveland, OH.
THREE DIMENSIONAL THERMAL ANALYSIS OF ROCKET THRUST CHAMBERS
M. H. N. Naraghi (Manhattan Coll., New York.) and E. S. Armstrong Jun. 1988 33 p Presented at the Thermophysics, Plasmadynamics and Lasers Conference, San Antonio, TX, 27-29 Jun. 1988; sponsored in part by AIAA Previously announced in IAA as A88-43721
(NASA-TM-101973; E-4673; NAS 1.15:101973) Avail: NTIS HC A03/MF A01 CSCL 21H

A numerical model for the three dimensional thermal analysis of rocket thrust chambers and nozzles has been developed. The input to the model consists of the composition of the fuel/oxidant mixture and flow rates, chamber pressure, coolant entrance temperature and pressure, dimensions of the engine, materials and the number of nodes in different parts of the engine. The model allows for temperature variation in three dimensions: axial, radial and circumferential directions and by implementing an iterative scheme, it provides nodal temperature distribution, rates of heat transfer, hot gas and coolant thermal and transport properties. Author

N89-21026*# National Aeronautics and Space Administration, Washington, DC.
NASA DIRECTIONS IN SPACE PROPULSION FOR 2000 AND BEYOND
Gregory M. Reck 1989 12 p Presented at the Symposium on Space Commercialization: Roles of Developing Countries, Nashville, TN, 5-10 Mar. 1989
(NASA-TM-102281; NAS 1.15:102281) Avail: NTIS HC A03/MF A01 CSCL 21H

In his National Space Policy of 1988, President Reagan committed to a goal of expanding human presence and activity in the solar system. This goal has provided the impetus for a resurgence of activity in a broad range of space technology efforts in general and for a number of propulsion technology programs in particular. Building on recommendations from several detailed studies of the U.S. space program, NASA has increased the level of investment in propulsion technology development. The Civil Space Technology Initiative is developing propulsion technology in support of near-Earth operations. These efforts are focused on both main and booster engines and seek to provide design methods and databases to support future developments of low cost, reliable transportation systems. Program elements include turbomachinery, combustion systems, and condition monitoring and diagnostics, and the design methodology developed at component levels will be verified in large scale systems. The Pathfinder program is developing a suite of technologies to enable a broad range of manned and unmanned missions beyond Earth's orbit. These include both chemical and electric propulsion technologies to support potential missions to the moon and Mars. Author

N89-21027# Air Force Inst. of Tech., Wright-Patterson AFB, OH. School of Engineering.
GEOMAGNETIC FIELD ENERGY AS A SOURCE OF THRUST M.S. Thesis
Stephen R. Hildenbrandt Dec. 1988 97 p
(AD-A202567; AFIT/GSO/ENP/88D-3) Avail: NTIS HC A05/MF A01 CSCL 22A

This study determines analytic solutions to the interactive net force between the dipole created by a current loop and a non-uniform expanse of the geomagnetic field. A simple dipole approximation is used for the geomagnetic field and it is assumed that the current loop can be maintained in any desired orientation. Analytic solutions are found for four different orientations: the current loop parallel to the earth's surface, the current loop perpendicular to the earth's surface, the current loop dipole parallel to the instantaneous geomagnetic field, and an inertial orientation. A hypothetical satellite current loop system is discussed and the action-at-a-distance magnetic interaction force is compared to aerodynamic drag and solar radiation pressure. The magnetic force is also compared to the force that some space thrusters produce. In terms of lifetime impulse or total impulse deliverable over one orbit, the magnetic force compares favorably to many thrusters in use today or under consideration. GRA

N89-21028# Draper (Charles Stark) Lab., Inc., Cambridge, MA.
RCS/LINEAR DISCRETE ACTUATOR STUDY Final Report, Aug. 1985 - Jan. 1988
Thomas Bailey, Alexander Gruzen, and Paul Madden Aug. 1988 299 p
(Contract F04611-85-K-0051)
(AD-A202822; CSDL-R-2075; AFAL-TR-88-039) Avail: NTIS HC A13/MF A01 CSCL 22B

The objective of the program was to develop the technology and demonstrate the use of linear discrete actuators combined with a rocket control system (RCS) to control the large angle slew and fine pointing/tracking of a simulated large flexible space structure. The linear actuators included proof-mass actuators, and a hub torquer to simulate a control moment gyro or reaction wheel actuator. The demonstration used the CSDL/AFAL ground test facility located at CSDL, Inc. The facility comprises the flexible test structure and actuators which are mounted on a low-friction, air-bearing table, and associated test instrumentation. The combined linear discrete and RCS actuators demonstrated significantly improved fine pointing/tracking a vibration suppression capability relative to the uses of the RCS alone. GRA

N89-21029# Martin Marietta Aerospace, Denver, CO. Astronautics Group.
SPACE PROPULSION HAZARDS ANALYSIS MANUAL (SPHAM), VOLUME 1 Final Report, Dec. 1983 - Jun. 1986
David C. Erdahl, Douglas W. Banning, and Elvis D. Simon Oct. 1988 501 p
(Contract F04611-84-C-0003)
(AD-A203204; MCR-88-590-Vol-1; AFAL-TR-88-096-Vol-1) Avail: NTIS HC A22/MF A01 CSCL 21H

SPHAM is a compilation of methods and data directed at hazards analysis and safety for space propulsion and associated vehicles, but broadly applicable to other environments and systems. It includes methods for compiling imposed requirements and deriving design requirements. It describes in detail the steps to constructing accident scenarios for formal risk assessment. It discusses the approaches the developing probabilities for events in scenarios, and probabilities for scenarios. It illustrates data anlaysis from experience data for the purpose of probability modeling. The SPHAM provides methods for predicting blast, fragmentation, thermal, acoustic and toxicity post-accident environments. SPHAM describes in overview fashion a large number of qualitative and quantitative analytical methods available to perform hazards analysis complete with guidelines for application. Examples are FMEA, Fault-tree and Energy Analysis. It describes methods to organize analysis by type, phase, or subsystem. Examples are interface hazards analysis, preliminary hazards analysis, and ordnance hazards analysis. Qualitative and

quantitative risk assessments are described. The formal processes for hazards analysis and safety for various agencies and departments of the government and DOD are described. The appendices to SPHAM contain voluminous data on available references in the form of an annotated bibliography, summary of the hazardous nature of 27 commodities common the space propulsion, and system descriptions for a variety of space vehicles, upper stage vehicles, and spacecraft. GRA

N89-21030# Naval Postgraduate School, Monterey, CA.
AUTOMATIC MEASUREMENT OF PARTICLES FROM HOLOGRAMS TAKEN IN THE COMBUSTION CHAMBER OF A ROCKET MOTOR M.S. Thesis
Denis Joseph Gaston Carrier Dec. 1988 85 p
(AD-A203955) Avail: NTIS HC A05/MF A01 CSCL 21H

Performance of solid propellants in rocket motors is increased by the addition of aluminum and additives (aluminum oxide, zirconium, and so on). Some of the original metal and metal oxides are found in the combustion chamber (from the surface of the propellant to the nozzle exit). The increased propellant performance is related to its particle size distribution. This thesis describes the procedure used for the automatic measurement of particles from holograms taken in the combustion chamber of a rocket motor while firing. It describes the investigation done on two averaging techniques used to reduce speckle noise, capturing the image focused on a spinning mylar disk and software averaging of several image frames. The spinning disk and software averaging of several image frames. The spinning disk technique proved superior for this application. The Kolmogorov-Smirnov two-sample test is applied to different particle samples in order to find an estimate of the number of particles required to obtain a stable distribution function. The number of particles is calculated and given. The last part of this study shows real particle distributions in the form of frequency histograms. GRA

N89-21031# Lawrence Livermore National Lab., CA.
INITIATIVE FOR THE 21ST CENTURY: ADVANCED SPACE POWER AND PROPULSION BASED ON LASERS
B. G. Logan 1 Feb. 1989 25 p Presented at the Initiative for the 21st Century: Advanced Space Power and Propulsion Based on Lasers, Cleveland, OH, 25 Apr. 1988
(Contract W-7405-eng-48)
(DE89-008034; UCRL-98520; CONF-8804249-1) Avail: NTIS HC A03/MF A01

This paper discusses the use of lasers in spacecraft propulsion systems. Cost, efficiencies and comparisons with other propulsion systems are discussed. DOE

N89-21733*# North Carolina Agricultural and Technical State Univ., Greensboro. Dept. of Mechanical Engineering.
COMPUTER CODES FOR THERMAL ANALYSIS OF A SOLID ROCKET MOTOR NOZZLE
Rajinder Singh Chauhan *In* Alabama Univ., Research Reports: 1988 NASA/ASEE Summer Faculty Fellowship Program Dec. 1988 11 p (For primary document see N89-21726 14-99)
Avail: NTIS HC A99/MF E03 CSCL 21H

N89-21734*# Illinois Univ., Chicago. Dept. of Mechanical Engineering.
RADIATION EFFECT ON ROCKET ENGINE PERFORMANCE
Huei-huang Chiu *In* Alabama Univ., Research Reports: 1988 NASA/ASEE Summer Faculty Fellowship Program Dec. 1988 41 p (For primary document see N89-21726 14-99)
Avail: NTIS HC A99/MF E03 CSCL 21H

N89-21752*# Alabama A & M Univ., Huntsville. Dept. of Mathematics.
SSME PROPULSION PERFORMANCE RECONSTRUCTION TECHNIQUES
Enoch C. Temple *In* Alabama Univ., Research Reports: 1988 NASA/ASEE Summer Faculty Fellowship Program Dec. 1988 11 p (For primary document see N89-21726 14-99)
Avail: NTIS HC A99/MF E03 CSCL 21H

N89-21760*# Alabama Univ., Huntsville. Dept. of Computer Science.
SPACE SHUTTLE MAIN ENGINE NUMERICAL MODELING CODE MODIFICATIONS AND ANALYSIS
John P. Ziebarth *In* Alabama Univ., Research Reports: 1988 NASA/ASEE Summer Faculty Fellowship Program Dec. 1988 21 p (For primary document see N89-21726 14-99)
Avail: NTIS HC A99/MF E03 CSCL 21H

23 CHEMISTRY AND MATERIALS (GENERAL)

N89-21032*# National Aeronautics and Space Administration. Lewis Research Center, Cleveland, OH.
CONVECTION AND CHEMISTRY EFFECTS IN CVD: A 3-D ANALYSIS FOR SILICON DEPOSITION
S. A. Gokoglu, M. A. Kuczmarski, P. Tsui (Sverdrup Technology, Inc., Cleveland, OH.), and A. Chait 1989 20 p Prepared for presentation at the Euro CVD 7 Conference, Perpignan, France, 19-23 Jun. 1989; sponsored in part by Institut de Science et de Genie des Materiaux et Precedes
(NASA-TM-102001; E-4702; NAS 1.15:102001) Avail: NTIS HC A03/MF A01 CSCL 07D

The computational fluid dynamics code FLUENT has been adopted to simulate the entire rectangular-channel-like (3-D) geometry of an experimental CVD reactor designed for Si deposition. The code incorporated the effects of both homogeneous (gas phase) and heterogeneous (surface) chemistry with finite reaction rates of important species existing in silane dissociation. The experiments were designed to elucidate the effects of gravitationally-induced buoyancy-driven convection flows on the quality of the grown Si films. This goal is accomplished by contrasting the results obtained from a carrier gas mixture of H2/Ar with the ones obtained from the same molar mixture ratio of H2/He, without any accompanying change in the chemistry. Computationally, these cases are simulated in the terrestrial gravitational field and in the absence of gravity. The numerical results compare favorably with experiments. Powerful computational tools provide invaluable insights into the complex physicochemical phenomena taking place in CVD reactors. Such information is essential for the improved design and optimization of future CVD reactors. Author

N89-21033# California Univ., Berkeley. Lawrence Berkeley Lab. Center for Advanced Materials.
CENTER FOR ADVANCED MATERIALS Annual Report, 1987
Apr. 1988 123 p
(Contract DE-AC03-76SF-00098)
(DE89-008854; LBL-25912) Avail: NTIS HC A06/MF A01

Research programs from Lawrence Berkeley Laboratory in materials research are described. Program headings include: polymers and composites; instrumentation for surface science; structural materials; ceramic and metal interfaces; electronic materials; surface science and catalysis; enzymatic synthesis of materials; and industry participation. A list of publications resulting from research staffing and awards follow each section. DOE

24 COMPOSITE MATERIALS

Includes physical, chemical, and mechanical properties of laminates and other composite materials.

For ceramic materials see *27 Nonmetallic Materials*.

N89-21034# Atomic Energy Research Establishment, Harwell (England). National NDT Centre.
NONDESTRUCTIVE TESTING TECHNIQUES FOR METAL MATRIX COMPOSITES
W. N. Reynolds Jun. 1988 17 p
(AERE-R-13040; HL88/1250) Avail: NTIS HC A03/MF A01

The emergence of practical composite materials consisting of a metal matrix (commonly aluminum or titanium) reinforced with ceramic particles, whiskers or fibers, either short or continuous, raises many problems of inspection in the nondestructive test (NDT) field. The existing literature is surveyed and comments are made on current understanding. Author

N89-21035# Atomic Energy Research Establishment, Harwell (England). Materials Physics and Metallurgy Div.
ACOUSTIC EMISSION SOURCE LOCATION IN FIBRE REINFORCED PLASTIC COMPOSITES
D. J. Buttle and C. B. Scruby Jun. 1988 40 p
(AERE-R-13039; HL88/1238) Avail: NTIS HC A03/MF A01

Acoustic emission (AE) source location in fiber reinforced composite materials is difficult due to the variation of ultrasonic velocity with respect to fiber axes. In general, the location accuracy will depend upon the accuracy with which the AE arrival time is measured, ultrasonic attenuation, anisotropy of the test material, and the size and geometry of the transducer array. A 2-D location algorithm was developed and results are presented for uniaxial and biaxial glass and uniaxial carbon fiber reinforced plastics where the ratio of maximum and minimum velocities were 1.6, 1.2, and 3.9 respectively. The algorithm incorporates the velocity dependence and requires AE event arrival times to calculate the source location using an iterative process. Author

N89-21036*# Sverdrup Technology, Inc., Cleveland, OH.
THERMODYNAMIC ANALYSIS OF CHEMICAL COMPATIBILITY OF SEVERAL REINFORCEMENT MATERIALS WITH NIOBIUM ALUMINIDES Final Contractor Report
Ajay K. Misra Mar. 1989 46 p
(Contract NAS3-25266)
(NASA-CR-182260; E-4648; NAS 1.26:182260) Avail: NTIS HC A03/MF A01 CSCL 11D

Chemical compatibility of several reinforcement materials with three niobium aluminides, Nb3Al, Nb2Al, and NbAl3, were examined from thermodynamic considerations. The reinforcement materials considered in this study include carbides, borides, nitrides, oxides, silicides, and Engel-Brewer compounds. Thermodynamics of the Nb-Al system were reviewed and activities of Nb and Al were derived at desired calculation temperatures. Criteria for chemical compatibility between the reinforcement material and Nb-Al compounds have been defined and several chemically compatible reinforcement materials have been identified. Author

N89-21037# Virginia Polytechnic Inst. and State Univ., Blacksburg. Materials Response Group.
INVESTIGATION OF MODELING OF DAMAGE GROWTH IN COMPOSITE LAMINATES Final Report, 1 Jan. - 31 Dec. 1988
K. Reifsnider, W. W. Stinchcomb, C. E. Bakis, H. R. Yih, and Doron Shalev 25 Sep. 1988 496 p
(Grant AF-AFOSR-0087-85; AF Proj. 2302)
(AD-A202433; AFOSR-88-1253TR) Avail: NTIS HC A21/MF A01 CSCL 20K

Damage initiation and growth has been studied in several material systems and two notched geometries, revealing generic characteristics of damage development and its relationship to microstructure. Stress redistribution has been studied with photoelastic methods and simulated analytically. Adiabatic thermoelastic methods for strain field analysis under dynamic loading have been developed and the first micromechanical formulation of that problem has been achieved. A formulation of the singular stress problem in the boundary layer near a hole in composite laminates has been completed. And a brief study of the applicability of chaos theory to damage development representation was conducted. A critical element model of remaining strength and life of notched composite laminates has been constructed and validated. GRA

N89-21038# Atomic Energy Research Establishment, Harwell (England). Materials Development Div.
THE BEHAVIOR OF CERAMIC MATRIX, FIBER COMPOSITES UNDER COMBINED IMPACT AND TENSILE STRESSES Final Report, Sep. 1986 - Sep. 1987
D. Clive Phillips, Nicholas Park, Richard J. Lee, Roy F. Preston, and David M. Dawson May 1988 94 p
(Contract F33615-86-C-5144)
(AD-A202518; AERE-R-12941; AFWAL-TR-88-4016) Avail: NTIS HC A05/MF A01 CSCL 11D

An investigation has been carried out of the impact behavior of fiber composites with glass and glass-ceramic matrices. The materials, which were selected as model systems for high temperature ceramic composites, consisted of graphite fibers in borosilicate glass and lithium aluminosilicate (LAS) glass-ceramic matrices. Impact testing was carried out on crossplied material of lay-up (0, 90) 2S. Several different types of impact experiments were carried out. In one, specimens were impacted at room temperature by an instrumental falling weight impactor while subjected to a superimposed tensile stress. The amount of damage caused in this test depends on the level of stress and impact energy. The concept of an impact map has been developed: taking total fracture as the failure criterion, an impact map can be constructed in which impact energy is plotted against applied stress. GRA

N89-21039# Royal Aircraft Establishment, Farnborough (England).
THE USE OF PRIMERS IN THE ADHESIVE BONDING OF CARBON-FIBRE REINFORCED COMPOSITES
B. M. Parker Jul. 1988 22 p
(AD-A202542; RAE-TR-88048; DRIC-BR-108255) Avail: NTIS HC A03/MF A01 CSCL 11D

The effect of priming carbon-fibre reinforced composite on adhesive-bonded joints has been studied by comparing joint strengths, bondline void contents and modes of failure for primed and unprimed composite. Six epoxy film adhesives were used with their recommended primers. In general, the use of a primer had very little effect on bonded joints. From the changes in mode of failure, it was possible that primers had improved adhesion between composite and adhesive. In one case, the use of primer resulted in increased bondline void contents, reduced strengths and plasticization of the adhesive. GRA

N89-21040# Air Force Inst. of Tech., Wright-Patterson AFB, OH. School of Engineering.
A STUDY OF FAILURE CHARACTERISTICS IN A THERMOPLASTIC COMPOSITE MATERIAL AT HIGH TEMPERATURE M.S. Thesis
James M. Fisher Dec. 1988 216 p
(AD-A203015; AFIT/GAE/AA/88D-15) Avail: NTIS HC A10/MF A01 CSCL 11D

The purpose of this thesis was to study the failure characteristics of the thermoplastic composite Graphite/Polyetheretherketone (Gr/PEEK) at 250 F. Specimens of Gr/PEEK containing a hole (1/3 diameter to width ratio) were tested at 250 F to determine stress-strain response near the hole, the progression of failure, and ultimate tensile strength. Testing of the specimens containing 45 degree fibers was complicated when the high temperature coupled with the high strains caused the strain gages to become unglued prematurely. Optical techniques of measuring strains were used on both the basic property specimens with a hole to determine the feasibility of these techniques and to provide an experimental basis for comparison for the analysis. A high speed video camera was used to record failure of the specimens with holes. Data on approximately how rapidly the different ply lay-ups fail is valuable in modeling the progression of failure analytically. GRA

N89-21041# Air Force Inst. of Tech., Wright-Patterson AFB, OH. School of Engineering.
EFFECTS OF BATTLE DAMAGE REPAIR ON THE NATURAL FREQUENCIES AND MODE SHAPES OF CURVED RECTANGULAR COMPOSITE PANELS M.S. Thesis

William P. Goodwin Dec. 1988 194 p
(AD-A203179; AFIT/GAE/AA/88D-18) Avail: NTIS HC A09/MF A01 CSCL 19D

Interferometric holography and a finite element computer code, NISA, were used to experimentally and numerically determine the effects of battle damage repairs on the free vibrational behavior of thin, cylindrical composite panels. The primary objective was to experimentally determine how mass and stiffness changes introduced by mechanically fastened aluminum patches altered the natural frequencies and mode shapes of the panels. The secondary objective was to investigate the accuracy of the PC version of NISA in predicting the free vibrational behavior of the same panels. GRA

N89-21042# Army Armament Research, Development and Engineering Center, Watervliet, NY. Weapons Lab.
MICROSCOPIC ASPECTS OF FAILURE AND FRACTURE IN CROSS-PLY FIBER-REINFORCED COMPOSITE LAMINATES Final Report
S. Bandyopadhyay, E. P. Gellert, V. M. Silva, and J. H. Underwood Nov. 1988 28 p
(AD-A203202; ARCCB-TR-88040) Avail: NTIS HC A03/MF A01 CSCL 11D

Tensile fracture and interlaminar mode I delamination failure may be considered as the upper and lower bounds of performance for fracture of fiber composite laminates. While these failures have been studied extensively in the literature, little progress has been made towards developing an understanding of the micromechanisms of the failure processes which, in fact, govern the macroscopic performance. GRA

N89-21043# Naval Air Development Center, Warminster, PA. Air Vehicle and Crew Systems Technology Dept.
HIGH TEMPERATURE COMPOSITES USING SCHIFF'S BASE PYROPOLYMER MATRICES Final Report
Steven J. Thoman and Leonardi J. Buckley 15 Jul. 1988 43 p
(AD-A203311; NADC-88096-60) Avail: NTIS HC A03/MF A01 CSCL 11D

Two acetylene functional Schiff's base pyropolymers have been evaluated as matrix materials for fiber reinforced composite materials. Autoclave processing techniques were developed to produce high quality laminated composites. These matrix resins can be made conductive through post-cure heat treatments and were studied in a conductivity range from 10-10 to 10 S/cm. The insulating resin composites have very stable mechanical properties up to 300 C; however, these properties are significantly lower than state-of-the-art polyimides. The post-processing heat treatments required to make the pyropolymers conductive, also caused extensive transverse matrix cracking in the laminates. GRA

N89-21044# Georgia Inst. of Tech., Atlanta. School of Civil Engineering
INELASTIC DEFORMATION AND FAILURE ANALYSIS OF FILAMENT-WOUND COMPOSITE STRUCTURES Final Technical Report, 1 May - 31 Oct. 1988
Gerald Wempner and Wan-Lee Yin Dec. 1988 18 p
(Contract DAAL03-88-K-0071)
(AD-A203382; ARO-25400.1-EG) Avail: NTIS HC A03/MF A01 CSCL 11D

This report summarizes the results of investigation during the initial phase of the project. Much of the effort in this period was expended in two areas. First, the existing literature on theoretical and experimental studies of the response, strength and failure behavior of filament-wound tubes was examined and studied. Secondly, a tentative analytical approach was conceived on the basis of available experimental results. The immediate objective of this analytical approach is to describe, in a qualitative manner, the dominant effects associated with the occurrence of the expansion mode and the shear mode of failure, and to provide a mathematical model for the small-strain inelastic deformation accompanying the initiation of such failures. GRA

N89-21045# Air Force Materials Lab., Wright-Patterson AFB, OH. Structural Materials Branch.
PHYSICAL AND MECHANICAL PROPERTIES OF AMERICAN CYANAMID'S ACETYLENE-TERMINATED PREPREG SYSTEM: T-300/CATB-44 Final Report, Jan. - Jul. 1988
D. B. Curliss Oct. 1988 56 p
(AD-A203737; AFWAL-TR-88-4243) Avail: NTIS HC A04/MF A01 CSCL 11D

A carbon-fiber-reinforced modified acetylene-terminated (AT) resin carbon-fiber composite, designated T-300/CATB-44, was evaluated for its potential as a 4000 F to 450 F structural material with a good balance of properties. Such a composite is needed for advanced Air Force Aircraft and weapons systems. AT resins have demonstrated good high-temperature capability, but lack the toughness of State-of-the-Art Bismaleimide (BMI) resins. Composite test panels were fabricated from prepreg provided by American Cyanamid. These panels were machined into test specimens for the standard AFWAL/MLBC material characterization. Thermophysical characteristics of the prepreg were measured. Physical and mechanical properties of the cured composite were also determined. The results from these tests are compared to the first-generation T-300/V378A carbon-fiber-reinforced bismaleimide composite. The RT mechanical properties of the T-300/CATB-44 were generally comparable to the T-300/V378A composite. GRA

N89-21046*# Wyoming Univ., Laramie. Composite Materials Research Group.
STATIC TENSILE AND TENSILE CREEP TESTING OF FIVE CERAMIC FIBERS AT ELEVATED TEMPERATURES
Richard S. Zimmerman and Donald F. Adams Apr. 1989 130 p
(NASA Order A-39603-C)
(NASA-CR-177525; NAS 1.26:177525) Avail: NTIS HC A07/MF A01 CSCL 11D

Static tensile and tensile creep testing of five ceramic fibers at elevated temperature was performed. J.P. Stevens, Co., Astroquartz 9288 glass fiber; Nippon Carbon, Ltd., (Dow Corning) nicalon NLM-102 silicon carbide fiber; and 3M Company Nextel 312, 380, and 480 alumina/silica/boria fibers were supplied in unsized tows. Single fibers were separated from the tows and tested in static tension and tensile creep. Elevated test temperatures ranged from 400 C to 1300 C and varied for each fiber. Room temperature static tension was also performed. Computer software was written to reduce all single fiber test data into engineering constants using ASTM Standard Test Method D3379-75 as a reference. A high temperature furnace was designed and built to perform the single fiber elevated temperature testing up to 1300 C. A computerized single fiber creep apparatus was designed and constructed to perform four fiber creep tests simultaneously at temperatures up to 1300 C. Computer software was written to acquire and reduce all creep data. Author

N89-21047*# National Aeronautics and Space Administration. Langley Research Center, Hampton, VA.
EFFECT OF GEOMETRY ON THERMAL AGING BEHAVIOR OF CELION/LARC-160 COMPOSITES
James B. Nelson Dec. 1987 23 p
(NASA-TM-100496; NAS 1.15:100496) Avail: NTIS HC A03/MF A01 CSCL 11D

Laminates of Celion/LARC-160, fabricated in thicknesses from 4 to 16 ply and in unidirectional, x-ply and fabric ply configurations, were isothermally aged at temperatures of 204, 260 and 316 C for periods up to 15,000 hours. Weight-loss of the test panels was measured at selected intervals during aging. At the lower aging temperatures, it was observed that panel thickness and ply arrangement influenced the apparent stability: i.e., thicker panels degraded less than thin panels and unidirectional panels degraded less than x-ply or fabric reinforced panels. At higher aging temperatures, all panel configurations and thicknesses converged toward the same behavior. Author

N89-21495# Cornell Univ., Ithaca, NY. Mathematical Sciences Inst.
THE SHEAR-LAG MODEL FOR A UNIDIRECTIONAL COMPOSITE WITH VISCOELASTIC MATRIX
Dimitris C. Lagoudas, Chung-Yuen Hui, and S. Leigh Phoenix *In* Army Research Office, Transactions of the Fifth Army Conference on Applied Mathematics and Computing Mar. 1988 p 87-109 (For primary document see N89-21490 14-59)
Avail: NTIS HC A99/MF E03 CSCL 11D

N89-21500# Virginia Polytechnic Inst. and State Univ., Blacksburg. Dept. of Engineering Science and Mechanics.
ON A REFINED NONLINEAR THEORY OF LAMINATED COMPOSITE PLATES
J. N. Reddy *In* Army Research Office, Transactions of the Fifth Army Conference on Applied Mathematics and Computing Mar. 1988 p 183-206 (For primary document see N89-21490 14-59)
(Contract DAAG29-85-K-00017)
Avail: NTIS HC A99/MF E03 CSCL 11D

25 INORGANIC AND PHYSICAL CHEMISTRY

Includes chemical analysis, e.g., chromatography; combustion theory; electrochemistry; and photochemistry.

For related information see also *77 Thermodynamics and Statistical Physics.*.

N89-21048# California Univ., Berkeley. Lawrence Berkeley Lab. Materials and Chemical Sciences Div.
FLUIDS, BOTH IONIC AND NONIONIC, OVER WIDE RANGES OF TEMPERATURE AND COMPOSITION
Kenneth S. Pitzer Aug. 1988 12 p Presented at the 10th Conference on Chemical Thermodynamics, Prague, Czechoslovakia, 29 Aug. 1988
(Contract DE-AC03-76SF-00098)
(DE89-001265; LBL-25859; CONF-880810-1) Avail: NTIS HC A03/MF A01

After a brief historical review of the determination of standard state properties of hydrocarbons, the present status of nonideal gas and liquid state properties is considered. The accuracy to which various fluids follow the acentric factor system is examined. The shapes of vapor-liquid and liquid-liquid coexistence curves are considered with comparisons of theory and experiment for both short-range and long-range attractive forces. The effective critical exponent Beta (sub e) is a sensitive measure of the shapes of these curves. Systems with short-range forces have low Beta (sub e) throughout the entire range of temperature and never approach the high values of mean-field theories. Ionic systems show Beta (sub e) congruent to 0.5 over wide ranges of temperature. The apparent conflict between the theoretical value 0.325 and a reasonable extrapolation of the experimental Beta (sub e) to 0.35-0.36 for Ar and Xe at the critical temperature is discussed in relation to the model used in current theory and the desirability is expressed for a better model for the vapor-liquid system. An equation of state is described for NaCl-H2O which is valid at the critical point of H2O and over the coexistence surface to 873 K. Equations are considered for mixed aqueous electrolytes of unlimited complexity valid for liquid-like densities. Recent results for Na2SO4 (aq) to 573 K are described, together with their use in predictions of solubilities in both Na2SO4-H2O and in Na2SO4-NaCl-NaOH-H2O. DOE

N89-21049# National Inst. of Standards and Technology, Gaithersburg, MD. Center for Fire Research.
STUDY OF THE IGNITION INHIBITING PROPERTIES OF COMPRESSED AIR FOAM
Daniel Madrzykowski Oct. 1988 27 p Sponsored by Fire Administration, Emmitsburg, MD
(PB89-127559; NISTIR-88/3880) Avail: NTIS HC A03/MF A01 CSCL 21B

The report describes an initial step to quantify the effectiveness of water-based compressed air foam (CAF) generated with a synthetic hydrocarbon-based surfactant. Two series of tests were conducted with the synthetic hydrocarbon surfactant based CAF: ignition retardation tests and mass retention tests. The ignition delaying capability of the foam was twice that of water when protectina a T1-11 plywood surface irradiated from an external source in the range of 15 kW/sq m to 60 kW/sq m. The mass retention test, conducted on T1-11 plywood siding, exhibited an initial retention efficiency for the foam of approximately 20 times the efficiency of water. This type of foam may have potential for improving performance of fixed fire suppression systems, such as residential sprinkler systems. Further study is recommended to generalize the results of these tests and to quantify the extinguishing capabilities of the CAF relative to water. Author

N89-21050# National Inst. of Standards and Technology, Gaithersburg, MD. Ceramics Div.
XRAYL: A POWDER DIFFRACTION PROFILE REFINEMENT PROGRAM
C. R. Hubbard, J. M. Stewart, Y. Zhang, B. Morosin, and E. L. Venturini (Sandia National Labs., Albuquerque, NM.) Oct. 1988 37 p
(PB89-127567; NISTIR-88/3850) Avail: NTIS HC A03/MF A01 CSCL 07D

In many applications of X-ray powder diffraction in material studies, when overlap occurs it is necessary to separate the total (or composite) profile into its components. A computer program, XRAYL, has been developed to fit analytical functions to powder diffraction lines. After fitting, the powder diffraction data, given as counts at steps in 2 theta, is represented diffraction line by diffraction line, by parameters of a profile function. The resulting profile parameters may then be used to generate idealized powder diffraction lines, effectively free of statistical noise and contributions from overlapping lines, extending to background intensity on each side. Because of this capability XRAYL may be employed in X-ray powder diffraction profile analysis as a preprocessor program, that is, separating peaks and feeding the resolved data to subsequent analysis programs. The NBS-IR contains: (1) profile functions and the nonlinear least-squares algorithm utilized in XRAYL: (2) user options and execution of the program; and (3) several examples. Author

N89-21051*# National Aeronautics and Space Administration. Lewis Research Center, Cleveland, OH.
FUEL-RICH CATALYTIC COMBUSTION OF JET-A FUEL-EQUIVALENCE RATIOS 5.0 TO 8.0
Theodore A. Brabbs and Carmen M. Gracia-Salcedo (Army Aviation Research and Development Command, Cleveland, OH.) May 1989 10 p Prepared for presentation at the Central States Meeting of the Combustion Inst., Dearborn, MI, 30 Apr. - 3 May 1989
(NASA-TM-101975; E-4675; AVSCOM-TR-89-C-001; NAS 1.15:101975) Avail: NTIS HC A02/MF A01 CSCL 21B

Fuel-rich catalytic combustion (E.R. greater than 5.0) is a unique technique for preheating a hydrocarbon fuel to temperatures much higher than those obtained by conventional heat exchangers. In addition to producing very reactive molecules, the process upgrades the structure of the fuel by the formation of hydrogen and smaller hydrocarbons and produces a cleaner burning fuel by removing some of the fuel carbon from the soot formation chain. With fuel-rich catalytic combustion as the first stage of a two stage combustion system, enhanced fuel properties can be utilized by both high speed engines, where time for ignition and complete combustion is limited, and engines where emission of thermal NO sub x is critical. Two-stage combustion (rich-lean) has been shown to be effective for NO sub x reduction in stationary burners where residence times are long enough to burn-up the soot formed in the first stage. Such residence times are not available in aircraft engines. Thus, the soot-free nature of the present process is critical for high speed engines. The successful application of fuel-rich catalytic combustion to Jet-A, a multicomponent fuel used in gas turbine combustors, is discusssed. Author

N89-21052# Argonne National Lab., IL. Mathematics and Computer Science Div.
SPECTRAL ANALYSIS OF A FOURTH-ORDER SINGULAR DIFFERENTIAL OPERATOR ARISING IN COMBUSTION
Hans G. Kaper and Bernd Schultze (Essen Univ., Germany, F.R.) 1988 8 p Presented at the International Conference on Theory and Applications of Differential Equations, Columbus, OH, 21 Mar. 1988
(Contract W-31-109-eng-38)
(DE89-005841; CONF-8803184-1) Avail: NTIS HC A02/MF A01

Sivashinsky, Law, and Joulin (SLJ) present a mathematical model of stagnation-point flow combustion, where a premixed flame is stabilized in a combustible gas mixture flowing towards a flat plate. The configuration is two-dimensional Cartesian, the relevant coordinates being x and y. The plate is located in the plane y = 0. The flow, which is symmetric around x = 0, is coming in from the positive y-direction. At any point (x,y) element of (- infinity, infinity) x (0, infinity), the flow velocity is given by the vector v = alpha (x, - y), where alpha is greater than 0; alpha may be interpreted as a measure of the Reynolds number. Thus, as the flow approaches the plate, the streamlines bend outward away from the y-axis to become tangential at the plate. Under appropriate circumstances, a flame is stabilized parallel to the plate at some finite distance away from it. The flame is not necessarily planar; it may develop a spatial structure, which may evolve with time. Assuming that the position of the flame above the plate is described by a function y = phi(x,t), SLJ derived the following nonlinear fourth-order differential equation for phi: phi (sub t) + 4 phi (sub xxxx) + phi (sub xx) - 1/2 (phi sub x) squared + aplha (x phi)(sub x) = 0, - infinity is less than x is less than infinity, t is greater than 0. Our intention is to study the bifurcation of solutions for this equation from the trivial solution, using 0 as the bifurcation parameter. In this article we take the first step towards this goal and investigate the linearized equation phi (sub t) + 4 phi (sub xxxx) + phi (sub xx) + alpha (x phi)(sub x) = 0, - infinity is less than x is less than infinity, t is greater than 0. DOE

N89-21053# Ames Lab., IA. Dept. of Physical Chemistry.
TOPICS IN CHEMICAL PHYSICS. 1: SEMICLASSICAL REACTIVE SCATTERING THEORY. 2: CORRECTED EFFECTIVE MEDIUM THEORY Ph.D. Thesis
Joel David Kress Jul. 1988 245 p
(Contract W-7405-eng-82)
(DE89-007606; IS-T-1385) Avail: NTIS HC A12/MF A01

Two distinct areas within theoretical chemical physics are investigated in this dissertation. First, the dynamics of collinear exchange reactions is treated within a semiclassical Gaussian wavepacket (GWP) description. Second, a corrected effective medium (CEM) theory is derived which yields: a one-active-body description of the binding energy between an atom and an inhomogeneous host; and an N-active-body description of the interaction energy for an N atom system. To properly treat the dynamics of collinear exchange reactions, two extensions to the previous methodology of GWP dynamics are presented: evaluation of the interaction picture wavefunction propagators directly via the GWP solution to the time-dependent Schrodinger equation; and use of an expansion of GWPs to represent the initial translational plane wave. This extended GWP dynamical approach is applied to the H + H sub 2 collinear exchange reaction using the Porter-Karplus II potential energy surface. DOE

N89-21054# Utah Univ., Salt Lake City. Dept. of Chemistry.
SPECTROSCOPIC STUDIES OF FLUID/SOLID INTERFACES
Joel M. Harris 1988 6 p
(Contract N00014-85-K-0712)
(AD-A202436) Avail: NTIS HC A02/MF A01 CSCL 20D

This program of research has been to develop spectroscopic methods for exploring chemical structure and molecular dynamics at interfaces between dielectric solids and liquids or supercritical fluids. The research was carried out using fluorescence and vibrational spectroscopy from probe molecules where spectral and temporal differences in emission, absorption, or scattering provide information about the surface onto which they are absorbed or bound. Studies focused on the interfacial chemistry of silica and derivatized silica surfaces in contact with liquids and dense gases. The spectral response of probe molecules was used to observe differences in the chemical environment at the liquid-solid interface due to the presence of bound or adsorbed molecules. GRA

N89-21055# MSNW, Inc., San Marcos, CA.
CHEMICAL VAPOR SYNTHESIS OF NIOBIUM ALUMINIDES Final Technical Report, Aug. 1987 - Apr. 1988
J. H. Norman and G. H. Reynolds Oct. 1988 56 p
(Contract F33615-87-C-5274)
(AD-A202591; AFWAL-TR-88-4166) Avail: NTIS HC A04/MF A01 CSCL 07B

Phase 1 experiments to produce thin films of various niobium aluminide compositions by chemical vapor deposition and supporting process models are described. GRA

N89-21056# Aerospace Corp., El Segundo, CA. Chemistry and Physics Lab.
ELECTRON PARAMAGNETIC RESONANCE AND PHOTOLUMINESCENCE STUDIES OF IMPURITIES IN CdTe
R. C. Bowman, Jr. and D. E. Cooper 31 Oct. 1988 16 p Prepared in cooperation with Rockwell International Science Center, Thousands Oaks, CA
(Contract F04701-85-C-0086)
(AD-A202841; TR-0088(3945-07)-4; SD-TR-88-100) Avail: NTIS HC A03/MF A01 CSCL 07B

CdTe single crystals from different sources have been examined to detect the presence of impurities which may be detrimental to applications in the fabrication of infrared detectors. Distinctive EPR signals from various donor impurities, including substitutional paramagnetic Fe, were found in several samples. A photoluminescence transition at 1.1 eV was also seen in these crystals and the amplitudes of the photoluminescence signals and the Fe EPR signals are strongly correlated. Elemental analysis of the samples indicates that EPR and PL are able to detect Fe concentrations of less than 0.1 ppm. GRA

N89-21057# Oklahoma State Univ., Stillwater. Dept. of Chemistry.
THEORETICAL STUDIES OF HETEROGENEOUS REACTIONS IN SILICON CVD (SILICON VAPOR DEPOSITION) CATALYSIS Final Report, 1 Nov. 1985 - 31 Oct. 1986
Lionel M. Raff and Donald L. Thompson 25 Oct. 1988 33 p
(Grant AF-AFOSR-0043-86; AF Proj. 2303)
(AD-A202905; AFOSR-88-1269TR) Avail: NTIS HC A03/MF A01 CSCL 11C

The results of a theoretical/computational research program to develop new methods and to investigate the chemical dynamics of various elementary homogeneous and heterogeneous processes occurring in the chemical vapor deposition of silicon form silane are described. The types of elementary processes we have studied include: Unimolecular dissociation of isolated gas-phase molecules and radicals, silicon clustering, gas-surface scattering, chemisorption, processes, diffusion on silicon surfaces, bimolecular gas-phase reactions, and tunneling in H-atom diffusion on silicon surfaces. Much of the research was done using standard classical trajectory methods. Monte Carlo variational phase-space and transition-state theories, which were developed in this research program were used to study processes that occur on long timescales. GRA

N89-21058# Chemical Research and Development Center, Aberdeen Proving Ground, MD.
SURFACE ACOUSTIC WAVE DETECTION OF ORGANOPHOSPHORUS COMPOUNDS Technical Report, May - Oct. 1987
Dennis M. Davis, Raymond E. Miller, and John A. Parsons Oct. 1988 28 p Prepared in cooperation with Geo-Centers, Inc., F ort Washington, MD
(AD-A202909; CRDEC-TR-88101) Avail: NTIS HC A03/MF A01 CSCL 07C

Surface Acoustic Wave (SAW) devices are potentially useful as small, sensitive chemical vapor sensors. The operating principles of these devices have been described in detail. Their use in detecting dimethyl methylphosphonate vapor has been reported previously. The basic operating principle for the SAW devices is the reversible adsorption of chemical vapors by adsorbent coatings that are sensitive and selective to the vapors that one is trying to detect. That is, SAW devices act as mass sensitive detectors. The SAW device used in this study consists of an array of four coated sensor elements with each coating giving a characteristic response to each of the vapors to be detected. GRA

N89-21059# Emory Univ., Atlanta, GA. Dept. of Chemistry.
THE SPECTROSCOPY AND ENERGY TRANSFER KINETICS OF THE INTERHALOGENS Final Report, 1 Jun. 1987 - 1 Jul. 1988
Michael C. Heaven, Wafaa M. Fawzy, and Michel Macler 20 Oct. 1988 45 p
(Grant AF-AFOSR-0197-87; AF Proj. 2303)
(AD-A202954; AFOSR-88-1255TR) Avail: NTIS HC A03/MF A01 CSCL 07B

The objective of this program has been the determination of spectroscopic and radiative lifetime data for the low energy, metastable states of the halogens and interhalogens. This information was obtained by recording wavelength and time resolved laser excitation spectra for molecules isolated in rare gas matrices. GRA

N89-21060# Pennsylvania State Univ., University Park.
THE EFFECT OF PLATINUM CATALYSTS ON PROPANE OXIDATION AT ELEVATED PRESSURE
Wannam Lee, Thomas A. Litzinger, and Domenic A. Santavicca 1988 11 p Presented at the International Fuels and Lubricants Meeting and Exposition, Portland, OR, 10-13 Oct. 1988
(Contract DAAG29-85-K-0043)
(AD-A202999; ARO-21763.2-EG; ISSN-0148-7191) Avail: NTIS HC A03/MF A01 CSCL 07C

The potential for catalytically enhanced ignition in low-heat rejection Diesel engines has been experimentally studied under engine simulated conditions in a high pressure chemical flow reactor. Results are presented for propane oxidation on platinum at 6 and 10 atmospheres, at temperatures from 800K to 1050K, and at equivalence ratios from 0.5 to 4.0. For turbulent transport rates which are typical of those in an engine, as much as 20 percent of the fuel was found to react on the catalyst before the onset of the gas-phase ignition reactions. Depending on the adiabaticity of the combustion chamber walls, this could lead to significant thermal enhancement of the gas-phase ignition process. Evidence of chemical enhancement was also observed, at 10 atm under very fuel rich conditions, in terms of a change in the concentration and distribution of the hydrocarbon intermediate species. Possible mechanisms for the observed chemical enhancement due to surface generated species are discussed. GRA

N89-21061# State Univ. of New York, Buffalo. Dept. of Chemistry.
PHOTOCHEMISTRY AT CORRUGATED THIN METAL FILMS: A PHENOMENOLOGICAL APPROACH
P. T. Leung, Y. S. Kim, and Thomas F. George Dec. 1988 15 p Submitted for publication
(Contract N00014-86-K-0043)
(AD-A203070; UBUFFALO/DC/88/TR-89) Avail: NTIS HC A03/MF A01 CSCL 07E

A phenomenological model is adopted to explore possible novel photochemical phenomena for molecules in the vicinity of a corrugated thin metal film, with detailed results worked out for the photoabsorption cross section for molecules in the vicinity of a grating film. A mechanism is proposed by which enhanced selective photoabsorption may be achieved based on the different nature of the coupling of the molecular dipole and the incident laser light to the surface plasmon modes of the thin films. GRA

N89-21062# Pittsburgh Univ., PA. Dept. of Chemistry.
FLOW REACTOR STUDIES OF ELEMENTARY RADICAL REACTION RATES Final Report, 14 Feb. 1985 - 13 Aug. 1988
Michael F. Golde 5 Dec. 1988 30 p
(Contract DAAG29-85-K-0041)
(AD-A203126; ARO-22413.5-CH) Avail: NTIS HC A03/MF A01 CSCL 07D

The kinetic behavior of several elementary gas-phase reactions has been studied using the discharge-flow technique. Detection techniques include resonance fluorescence, laser-induced fluorescence and mass spectrometry. The rate of the reaction of H atoms with O2 to form HO2 has been determined over the temperature range 298 to 639K, with He, N2, and H2) as third bodies. The efficiency of CH30 formation in the reactions of F and OH radicals with CH3OH has been probed via product studies of the former reaction and via rate constant measurements of several isotopic variants of the latter reaction. Rate constants of the CH30 + NO reaction have been measured over a range of pressure and temperature. The products of both channels have been detected, establishing that atom transfer is the major channel at low pressure. Initial measurements suggest that the reaction of CH30 with H atoms is extremely fast, the reaction of CH30 with O atoms is significantly slower. GRA

N89-21063# State Univ. of New York, Albany. Research Foundation.
THEORETICAL STUDIES OF THE CHEMISTRY AND PHYSICS OF OXYGEN IN SILICON Final Report, 15 Apr. 1985 - 14 Apr. 1988
Lawrence C. Snyder and James W. Corbett 18 Nov. 1988 10 p
(Contract DAAG29-85-K-0097)
(AD-A203168; ARO-21623.26-PH) Avail: NTIS HC A02/MF A01 CSCL 09A

We have developed a cyclic-cluster program to compute the structure and properties of defects in crystalline solids. We have found the semi-empirical electronic structure method MINDO/3 to give the best account of the structure, stability and states near the gap for defects in silicon. We have applied the cyclic cluster program to describe the chemistry and physics of hydrogen and oxygen in a silicon crystal. We have concluded that a di-ylid is a promising candidate for the core of the 450 oxygen thermal donor in silicon. We have discovered that a four-member ring containing two oxygen atoms is likely to diffuse much faster than interstitial oxygen in silicon. We have applied perturbation theory to give a qualitative explanation of the ladder of effective mass states associated with oxygen clusters in silicon and germanium. GRA

N89-21064# IBM Research Lab., San Jose, CA. Almaden Research Center.
AN IN-SITU GRAZING INCIDENCE X-RAY SCATTERING STUDY OF THE INITIAL STAGES OF ELECTROCHEMICAL GROWTH OF LEAD ON SILVER (III) Interim Technical Report
O. R. Melroy, M. F. Toney, G. L. Borges, M. G. Samant, J. B. Kortright, P. Ross, and Lesser Blum (Puerto Rico Univ., Rio Piedras.) 5 Nov. 1988 24 p Prepared in cooperation with IBM Almaden Research Center, San Jose, CA and Lawrence Berkeley Lab., CA
(Contract N00014-81-C-0776)
(AD-A203385; TR-35) Avail: NTIS HC A03/MF A01 CSCL 07D

The potential dependent structure of under-potentially deposited lead on silver (III) and the initial stages of bulk lead deposition on the ad-layer have been studied using grazing incidence X-ray scattering. Measurements were made in-situ and under potential control. The closed packed triangular lattice of lead formed by the underpotential deposition (at full monolayer coverage) is compressed 1.4 percent relative to bulk lead. This compressive strain increases linearly with applied potential until the onset of bulk deposition where the ad-layer is compressed 2.8 percent. Bulk lead is not deposited epitaxially on this template because of the large compressive strain. Instead, it grows as islands that have (III) texture but are randomly oriented in the plane of the

substrate. After the deposition of approximately five equivalent monolayers of bulk lead, the initial ad-layer appears to reconstruct. GRA

N89-21065# Tel-Aviv Univ. (Israel). School of Chemistry.
EXCITED STATE ENERGETICS AND DYNAMICS OF LARGE MOLECULES, COMPLEXES AND CLUSTERS Final Report, May 1985 - Jul. 1988
Joshua Jortner and Uzi Even Jul. 1988 112 p
(Contract DAJA45-85-C-0008; DA Proj. 1L1-61103-BH-57)
(AD-A203514; R/D-4759-CH-01) Avail: NTIS HC A06/MF A01 CSCL 07D

New techniques for spectroscopy in supersonic expansions and in the development of specific supersonic sources were developed, including vacuum ultraviolet absorption spectroscopy in supersonic expansions, development of conical nozzles for supersonic jets and pulse extraction mass spectrometer. Research included studies of energetics of rydberg states of jet-cooled molecules, rydberg states of anthracene, intramolecular relaxation of rydberg states and interference effects between extravalence and intravalence molecular excitations. The rotational state dependence of intramolecular dynamics was investigated as well as the coupling between intrastate vibrational energy redistribution and interstate electronic relaxation and the coriolis rotation-vibration coupling and intramolecular dynamics. Mediated intersystem crossing phenomenology, inverse isotope effects and microscopic level shifts were explored. Studies of fluorescence quantum yields for highly-excited states of large molecules and photoisomerization dynamics of selected molecules were conducted, including an examination of energy-resolved photoisomerization rates and excited state energetics of van der Waals complexes and porphyrins. Large van der Waals complexes consisting of rare-gas (R) an atom(s) bound to a large aromatic molecule were studied by fluorescence excitation and by two-photon, two-color spectroscopy in conjunction with mass-resolved detection. GRA

N89-21066# Texas A&M Univ., College Station. Dept. of Chemistry.
A FRESH LOOK AT TRANSPORT IN PERFLUOROSULFONATE IONOMERS: ULTRAMICROELECTRODE INVESTIGATIONS OF NAFION AND DOW IONOMERS Technical Report No. 31
Lisa D. Whitely and Charles R. Martin 11 Jan. 1989 56 p
(Contract N00014-82-K-0612; NR Proj. 627838)
(AD-A203855; TR-31) Avail: NTIS HC A04/MF A01 CSCL 07B

Chronoamperometry at ultramicroelectrodes is a powerful and convenient technique for the determination of apparent diffusion coefficients and concentrations of electroactive cations ion-exchanged into Nafion and Dow perfluorosulfonate films. This technique offers tremendous advantages over the conventional electrochemical methods which employ film coated macro sized electrodes. These advantages stem from the elimination of IR distortion at the ultramicroelectrode and from the ability to determine both the concentration and apparent diffusion coefficient of the electroactive cation from a single experiment. Further improvements over the conventional approach were achieved by eliminating coupled diffusion and migration contributions to the measured current response. Under these conditions, charge is transported via ionic diffusion rather than through electron hopping. Furthermore, the apparent diffusion coefficients decrease with increasing concentration of the electroactive cation in the film. GRA

N89-21067# Naval Postgraduate School, Monterey, CA.
HOLOGRAPHIC INVESTIGATION OF SOLID PROPELLANT COMBUSTION M.S. Thesis
Albert George Butler Dec. 1988 56 p
(AD-A203928; AD-E951302) Avail: NTIS HC A04/MF A01 CSCL 21H

An investigation into the behavior of aluminized solid propellant combustion in a two-dimensional windowed rocket motor was conducted using holographic techniques. Holograms were recorded in the motor port, aft of the propellant grain and at the entrance to the exhaust nozzle for two different propellant compositions at varying operating pressures. Quantitative particle size data for particles larger than 20 microns were obtained from the holograms. From these data, the mean diameters (D32) of the larger particles were calculated and utilized to compare what effects pressure, location in the motor and aluminum content had on the behavior of the aluminum/aluminum oxide particles. D32 was found to decrease with increasing pressure, but was unaffected by variations in low values of propellant aluminum loading. D32 at the grain exit was found to be significantly less than within the grain port. GRA

N89-21068# Dayton Univ., OH.
THEORETICAL STUDIES OF RARE GAS HALIDE SYSTEMS Final Report, Aug. 1987 - Apr. 1984
Marcy Rosenkrantz Nov. 1988 19 p
(Contract F04611-83-C-0046)
(AD-A203985; UDR-TR-88-56; AFAL-TR-88-013) Avail: NTIS HC A03/MF A01 CSCL 20E

The purpose of this task is to determine viable high energy density (HED) materials for use as energy storage media in rockets. The approach is to use theoretical and computational chemistry techniques to determine what materials will have the best chance of success in meeting these goals. Calculations on the potential energy surfaces of the ground electronic state of ArH and several of its excited states, as well as the potential energy curve of ArH(+) are discussed. The need for a basis set that is both small enough to be tractable and large enough to include adequate polarizing functions to describe the long-range interaction in ground state ArH is also presented. These calculations were performed to aid in understanding the mechanisms by which energy can be stored by stabilizing a proton in a rare gas matrix. Plans for expansion of this work are discussed as is the effort expended in getting state-of-the-art-molecular electronic structure algorithms to work on the Cray-2 computer. GRA

N89-21069# Air Force Academy, CO.
MOPAC MANUAL, 5TH EDITION: A GENERAL MOLECULAR ORBITAL PACKAGE Technical Report, Oct. 1987 - Nov. 1988
James J. P. Stewart Dec. 1988 183 p
(AD-A204003; FJSRL-TR-88-0007) Avail: NTIS HC A09/MF A01 CSCL 07D

MOPAC is a general purpose, semi empirical molecular orbital program for the study of chemical reactions involving molecules, ions, and linear polymers. It implements the semi-empirical Hamiltonians MNDO, AMI, PM3, and MINDO/3 and combines the calculations of vibrational spectra, thermodynamic quantities, isotopic substitution effects, time dependent effects, and force constants in a fully integrated program. Elements parametrized at the MNDO level include Hydrogen, Lithium, Beryllium, Boron, Carbon, Nitrogen, Oxygen, Fluorine, Aluminum, Silicon, Phosphorus, Sulfur, Chlorine, Chromium, Germanium, Tin, Mercury, Lead, Iodine. Within the electronic part of the calculation, molecular and localized orbitals excited states up to sextets, chemical bond indices, charges, etc., are computed. Both intrinsic and dynamic reaction coordinates can be calculated. A transition-state location routine and two transition-state optimizing routines are available for studying chemical reactions. GRA

N89-21070# Argonne National Lab., IL. Theoretical and Computational Chemistry Group.
CALCULATION OF THE ENERGETICS OF CHEMICAL REACTIONS
T. H. Dunning, Jr., L. B. Harding, R. L. Shepard, and R. J. Harrison 1988 20 p Presented at the 2nd International Symposium on Computational Chemistry on Cray Supercomputers, Chicago, IL, 11 Sep. 1988
(Contract W-31-109-eng-38)
(DE89-007262; CONF-8809117-2) Avail: NTIS HC A03/MF A01

To calculate the energetics of chemical reactions we must solve the electronic Schroedinger equation for the molecular conformations of importance for the reactive encounter. Substantial

changes occur in the electronic structure of a molecular system as the reaction progresses from reactants through the transition state to products. To describe these changes, our approach includes the following three elements: the use of multiconfiguration self-consistent field wave functions to provide a consistent zero-order description of the electronic structure of the reactants, transition state, and products; the use of configuration interaction techniques to describe electron correlation effects needed to provide quantitative predictions of the reaction energetics; and the use of large, optimized basis sets to provide the flexibility needed to describe the variations in the electronic distributions. With this approach we are able to study reactions involving as many as 5 to 6 atoms with errors of just a few kcal/mol in the predicted reaction energetics. Predictions to chemical accuracy, i.e., to 1 kcal/mol or less, are not yet feasible, although continuing improvements in both the theoretical methodology and computer technology suggest that this will soon be possible, at least for reactions involving small polyatomic species. DOE

N89-21071# Princeton Univ., NJ. Dept. of Mechanical and Aerospace Engineering.
FUELS COMBUSTION RESEARCH Final Technical Report, 1 Oct. 1985 - 30 Sep. 1988
Irvin Glassman, Frederick L. Dryer, and Forman A. Williams 30 Nov. 1988 47 p
(Contract F49620-86-C-0006)
(AD-A204161; AFOSR-89-0087TR) Avail: NTIS HC A03/MF A01 CSCL 21D

Studies of near and slightly sooting inverse and normal co-flow diffusion flames determined aromatics as the key intermediates to soot formation. The extent of aromatic formation was correlated with the earlier Princeton smoke height test results. The effect of oxygen addition to tightly bound fuels (ethene, ethyne and benzene) in diffusion flames was found to accelerate the pyrolysis and thus the soothing tendency, but not to affect other fuels in the temperature range of soot formation. Flow reactor experiments determined oxidation kinetic results for the mono and dialkylated aromatic components of jet fuels. Succinctly, it was found that the alkyl chains are attached initially and in the case of dialkylated compounds not simultaneously. Mechanisms have been presented. Results on boron slurry droplet combustion were obtained and provided a basis for calculating when droplet disruption would occur. Questions with respect to boron cloud combustion addressed mechanisms of ignition and combustion in the regime of chemical kinetic control. GRA

N89-21527# Purdue Univ., Indianapolis, IN. Dept. of Mathematical Sciences.
MODELLING OF THE LEAN FLAMMABILITY LIMIT IN FLAME THEORY
Richard Y. Tam and G. S. S. Ludford (Cornell Univ., Ithaca, NY.) *In* Army Research Office, Transactions of the Fifth Army Conference on Applied Mathematics and Computing Mar. 1988 p 735-743 (For primary document see N89-21490 14-59)
Avail: NTIS HC A99/MF E03 CSCL 21B

N89-21736*# University of Central Arkansas, Conway. Dept. of Physics.
X-RAY FLUORESCENCE SURFACE CONTAMINANT ANALYZER: A FEASIBILITY STUDY
Hudson B. Eldridge *In* Alabama Univ., Research Reports: 1988 NASA/ASEE Summer Faculty Fellowship Program Dec. 1988 34 p (For primary document see N89-21726 14-99)
Avail: NTIS HC A99/MF E03 CSCL 07D

N89-21749*# Georgia Inst. of Tech., Atlanta. School of Aerospace.
SIMULATION OF WATER VAPOR CONDENSATION ON LOX DROPLET SURFACE USING LIQUID NITROGEN
Eugene A. Powell *In* Alabama Univ., Research Reports: 1988 NASA/ASEE Summer Faculty Fellowship Program Dec. 1988 26 p (For primary document see N89-21726 14-99)
Avail: NTIS HC A99/MF E03 CSCL 07D

26 METALLIC MATERIALS

Includes physical, chemical, and mechanical properties of metals, e.g., corrosion; and metallurgy.

N89-21072*# Rockwell International Corp., Canoga Park, CA. Rocketdyne Div.
ADVANCED SINGLE CRYSTAL FOR SSME TURBOPUMPS
L. G. Fritzemeier Mar. 1989 51 p
(Contract NAS3-24646)
(NASA-CR-182244; NAS 1.26:182244; RI/RD-88-273) Avail: NTIS HC A04/MF A01 CSCL 11F

The objective of this program was to evaluate the influence of high thermal gradient casting, hot isostatic pressing (HIP) and alternate heat treatments on the microstructure and mechanical properties of a single crystal nickel base superalloy. The alloy chosen for the study was PWA 1480, a well characterized, commercial alloy which had previously been chosen as a candidate for the Space Shuttle Main Engine high pressure turbopump turbine blades. Microstructural characterization evaluated the influence of casting thermal gradient on dendrite arm spacing, casting porosity distribution and alloy homogeneity. Hot isostatic pressing was evaluated as a means of eliminating porosity as a preferred fatigue crack initiation site. The alternate heat treatment was chosen to improve hydrogen environment embrittlement resistance and for potential fatigue life improvement. Mechanical property evaluation was aimed primarily at determining improvements in low cycle and high cycle fatigue life due to the advanced processing methods. Statistically significant numbers of tests were conducted to quantitatively demonstrate life differences. High thermal gradient casting improves as-cast homogeneity, which facilitates solution heat treatment of PWA 1480 and provides a decrease in internal pore size, leading to increases in low cycle and high cycle fatigue lives. Author

N89-21073# Atomic Energy Research Establishment, Harwell (England). Materials Physics and Metallurgy Div.
THE EFFECT OF MIXED-MODE LOADING ON STRESS-DRIVEN SOLUTE SEGREGATION DURING HIGH-TEMPERATURE BRITTLE INTERGRANULAR FRACTURE
H. Rauh (Oxford Univ., England), C. A. Hippsley, and R. Bullough Feb. 1988 28 p
(AERE-R-12897; HL88/1097) Avail: NTIS HC A03/MF A01

A model of stress-driven solute segregation to the vicinity of growing crack-tips during high-temperature brittle intergranular fracture of low alloys steels was previously presented. This model is extended to account for the mixed-mode loading prevailing as the crack propagates, and for the unfractured grain boundary ahead of the crack as an additional point-defect sink. Under these conditions, solute enrichment on both the crack surfaces and the grain boundary is predicted, in accordance with recent experimental observations. The agreement between calculated and measured values of sulphur coverage on the fracture surfaces of 2.25 Cr1Mo steel established previously is maintained. Author

N89-21074 Aston Univ., Birmingham (England).
THE PROPERTIES OF ADVANCED ALUMINIUM ALLOY SYSTEMS Ph.D. Thesis
Frank Leslie Haddleton 1987 273 p
Avail: Univ. Microfilms Order No. BRDX83352

Possible alternatives for the existing conventional aluminum alloy 2014 were evaluated for aircraft wheel applications. Three technologies in alloy development were considered: a metal matrix composite, an aluminum-lithium alloy, and a powder metallurgical alloy. The basic mechanical properties of these advanced materials have already been established to an extent, but their fatigue behavior has yet to be fully understood. The fatigue properties of the materials concerned were investigated in both air and an aerated 3.5 percent NaCl solution, and compared to 2014-T6 properties. As well as the basic mechanical properties, fatigue crack initiation data is presented for the aluminum-lithium alloy and 2014. The D.C. electrical potential method was used to monitor crack growth. Of the materials investigated, the most promising was the aluminum-lithium alloy. However, short transverse

properties need to be increased, and the commercial cost of the material needs to be decreased before it can be considered as a direct replacement for 2014 for aircraft structural applications. It was considered that the cost of the powder metallurgical alloy would limit its further use. The metal matrix composite material proved to be unsuitable for most ambient temperature applications. Dissert. Abstr.

N89-21075# Ames Lab., IA. Dept. of Physics.
NUCLEAR MAGNETIC RESONANCE STUDY OF HYDROGEN IN NIOBIUM-VANADIUM ALLOYS Ph.D. Thesis
Lyle Raymond Lichty Feb. 1989 192 p
(Contract W-7405-eng-82)
(DE89-007578; IS-T-1345) Avail: NTIS HC A09/MF A01

Proton spin relaxation rates have been measured across the random alloy system NbyV(1-y)Hx at temperatures from 10 to 800 K and various frequencies from 4.45 to 127.5 MHz. Enhanced spin-lattice relaxation rates found below 100 K in all samples with Nb, including NbH0.2, at frequencies of 40 MHz and below have been explained by a process of dipolar cross relaxation between proton Zeeman energy levels and the combined Zeeman-quadrupole levels of Nb-93. A semi-quantitative model, applicable in metal-hydrogen as well as other multi-spin systems, has been developed to describe the cross relaxation mechanism. Unusual features found experimentally and interpreted via this model include: (1) cross relaxation in unrotated polycrystalline samples, (2) cross relaxation to spins with pure quadrupole frequencies substantially less than the proton Larmor frequency, and (3) both temperature-dependent and temperature-independent contributions which can vary with frequency. Effects of Zeeman-quadrupole splittings on motional relaxation rates at higher temperatures were also estimated. DOE

N89-21076# Ames Lab., IA.
EFFECT OF Te ON THE MICROSTRUCTURAL CHANGES DURING THE GRAY-TO-WHITE AND WHITE-TO-GRAY TRANSITION IN DIRECTIONAL SOLIDIFICATION OF Fe-C-Si ALLOYS Ph.D. Thesis
Jang-Sik Park Jul. 1988 125 p
(Contract W-7405-eng-82)
(DE89-007607; IS-T-1387) Avail: NTIS HC A06/MF A01

The purpose of the present study is to understand the nature of the solidification of cast irons using the directional solidification technique. Cast irons can solidify directly by either the graphite-austenite or the iron carbide-austenite eutectic reactions. The existence of two eutectic systems is probably the most important fact to be considered in the study of the solidification of cast irons. Normally, the graphite eutectic, called a gray iron, is the more stable form and solidifies at a higher temperature than the carbide eutectic, called a white iron. Based on the fact that the addition of low levels of tellurium to a cast iron melt very strongly promotes the white iron structure at slower solidification rates, addition of tellurium to Fe-C-Si system was attempted in order to study the transition phenomenon within an acceptable range of the experimental solidification rates. The advantages of the directional solidification technique are that the temperature gradient, solidification rate, and the alloy composition can be varied independently. Varying the solidification rate with the temperature gradient and composition held constant will allow both the determination of the transition rates and the investigation of the continuous changes in structure, such as graphite morphology, accompanying the transition within a single sample. DOE

N89-21077# Ames Lab., IA. Dept. of Physics.
STUDIES OF THE INITIAL OXIDATION OF Fe-Si ALLOYS BY AES, XPS, EELS AND LEED Ph.D. Thesis
Young Pak Lee Jul. 1988 137 p
(Contract W-7405-eng-82)
(DE89-007610; IS-T-1343) Avail: NTIS HC A07/MF A01

Polycrystalline Fe-8.75at. percent Si alloys were investigated at room temperature by various surface spectroscopies, i.e., Auger electron spectroscopy (AES) (including Ar(+) depth profiling), electron energy loss spectroscopy (EELS), and X-ray induced photoelectron spectroscopy (XPS), during the initial oxidation stages under very low oxygen pressure. Experiments performed include: (1) scraping to see if the surface concentration of Si on the alloy is inherently different from that of the bulk, (2) AES, EELS, and XPS monitoring during both initial oxidation of pure Fe and Fe-Si, and Ar(+) or Xe(+) etching back to the clean surfaces to determine the relative distribution of Si in the oxide and alloy, and (3) various comparative experiments to identify oxidation states across a thin oxide layer. Fe-6.85at. percent Si (110) and (111) single crystal surfaces, and a (110) surface of pure Fe were investigated at room temperature by AES and LEED during the initial oxidation stages under very low oxygen pressures, and by Ar(+) AES depth profiling the oxidized surfaces back to the clean surface. performed include: (1) determination of the best annealing condition for each crystal to provide the cleanest single plane surface, (2) AES monitoring during both initial oxidation of pure Fe and Fe-Si (110), the close-packed plane of bcc crystals, and Ar(+) etching back to the clean surfaces to determine the relative distribution of Si in the oxide and alloy, and (3) repetition on Fe-Si (111) to see the effects of different crystallographic orientations on the initial oxidation behavior. DOE

N89-21078# Ames Lab., IA. Dept. of Materials Science and Engineering.
HYDROGEN AND DEUTERIUM INTERNAL FRICTION BEHAVIOR IN VANADIUM-NIOBIUM ALLOYS Ph.D. Thesis
Seon Jin Kim Jul. 1988 88 p
(Contract W-7405-eng-82)
(DE89-007616; IS-T-1296) Avail: NTIS HC A05/MF A01

Internal friction behavior of hydrogen in vanadium-niobium alloys containing from 40 at. pct. niobium to 100 at. pct. niobium as a function of hydrogen concentrations was investigated. The internal friction measurements were performed in an electrostatic drive and detection apparatus for rods in flexural vibration in the temperature range from 30 K to 290 K. An internal friction peak due to hydrogen was found in all the vanadium-niobium alloys. The peak was considered to be due to the jumps of hydrogen atoms in solid solution. The peak moved toward lower temperatures with increasing hydrogen concentration. In other words, the activation energies of the hydrogen motion responsible for the internal friction peaks decreased with increasing hydrogen concentration. The activation energies and tau(0) values for the hydrogen internal friction processes obtained from the present study were compared to those obtained from long range diffusion experiments. In order to examine the isotope effect, internal friction of deuterium in the same alloys were measured and compared to those of hydrogen. Effects of oxygen on the internal friction behavior of hydrogen and deuterium were also investigated.
DOE

N89-21079# Air Force Environmental Technical Applications Center, Scott AFB, IL.
CORROSION CONTROL CLIMATOLOGY
Debra L. Stoner Oct. 1988 42 p
(AD-A202477; USAFETAC/PR-88/002) Avail: NTIS HC A03/MF A01 CSCL 11F

Tabular climatological data for 183 locations worldwide prepared in response to a request by an Air Force corrosion prevention and control contractor is presented. Tables give mean number of days with temperature less than or equal to 40F at noon LST, precipitation greater than a trace, temperature greater than 85F for 5 hours or more, thunderstorms, relative humidity greater than 60 percent at noon LST, wind greater than 15 knots between 06 and 18 LST, and wind greater than 15 knots for all hours. GRA

N89-21080# Brown Univ., Providence, RI. Materials Research Lab.
MICROSCOPIC OBSERVATIONS OF ADIABATIC SHEAR BANDS IN THREE DIFFERENT STEELS
K. Cho, Y. C. Chi, and J. Duffy Sep. 1988 50 p
(Contract DAAL03-88-K-0015)
(AD-A202522; Rept-3; ARO-25544.4-EG) Avail: NTIS HC A03/MF A01 CSCL 11F

Microscopic observations are made of the shear band material in three different steels: (1) an AISI 1018 cold rolled steel, (2) a high strength low alloy structural steel, and (3) an AISI 4340 VAR steel tempered to either of two hardnesses, RHC 44 or 55. Dynamic deformation in shear was imposed to produce shear bands in all the steels tested. It was found that whenever the shear band led to fracture of the specimen, the fracture occurred by a process of void nucleation and coalescence; no cleavage was observed on any fracture surface, including the most brittle of the steels tested (RHC = 55). This is presumably due to the softening of the shear band material that results from the local temperature rise occurring during dynamic deformation. Differences in shear band behavior between the various microstructures are also described. GRA

N89-21081# Air Force Inst. of Tech., Wright-Patterson AFB, OH. School of Engineering.
INVESTIGATION OF CRACK GROWTH IN TITANIUM-ALUMINIDE AT ELEVATED TEMPERATURES M.S. Thesis
Ernest A. Staubs Dec. 1988 130 p
(AD-A202570; AFIT/GAE/AA/88D-36) Avail: NTIS HC A07/MF A01 CSCL 11F

This study investigates crack growth at elevated temperatures in a titanium-aluminide alloy (Ti3Al). The objectives are to determine the creep crack growth characteristics and the applicability of linear cumulative damage modeling to Ti3Al alloy. All tests were conducted on compact tension specimens of Ti3Al under isothermal conditions. Sustained load tests were used to characterize creep crack growth behavior. A fatigue test and several hold-time tests were used to test the applicability of linear cumulative damage modeling. The linear elastic stress intensity factor, K, was used as a correlating parameter for all the tests. A model was generated using baseline data from the sustained load and fatigue tests and compared with the hold-time tests. The test results showed that sustained load crack growth is insensitive to temperature. Crack growth rates for all tested temperatures were only a factor of five apart between the slowest and fastest growth rates. GRA

N89-21082# Air Force Inst. of Tech., Wright-Patterson AFB, OH. School of Engineering.
THE EFFECTS OF LOADING HISTORY AND CLOSURE OF THE FATIGUE CHARACTERISTICS OF HEAT TREATED Ti-6Al-2Sn-4Zr-6Mo M.S. Thesis
Jerardo A. Perez Dec. 1988 144 p
(AD-A202652; AD-E900870; AFIT/GAE/AA/88D-30) Avail: NTIS HC A07/MF A01 CSCL 11F

The purpose of this study was to investigate the effects of loading history and crack closure on the fatigue threshold properties of additionally heat treated Ti-6Al-2Sn-4Zr-6Mo. The crack closure measurements taken by a clip gage, strain gage mounted on the back face (BFS), and laser interferometric displacement gage (IDG) were compared. Also, the effects of heat treatment on the fatigue behavior of Ti 6246 were discussed. Three tests were run using compact test specimens at a test frequency of 30 Hz. The results from these tests indicated that additionally heat treating Ti 6246 did improve its fatigue threshold characteristics. GRA

N89-21083# Air Force Inst. of Tech., Wright-Patterson AFB, OH. School of Engineering.
CRACK GROWTH OF A TITANIUM-ALUMINIDE ALLOY UNDER THERMAL-MECHANICAL FATIGUE M.S. Thesis
David G. Burgess Dec. 1988 111 p
(AD-A202767; AFIT/GAE/AA/88D-3) Avail: NTIS HC A06/MF A01 CSCL 11F

New materials must be developed in order to increase the operating temperature of Air Force gas turbines. One of the materials under consideration is a titanium-aluminide alloy, Ti3Al. Before this material can be used, its behavior under combined thermal-mechanical fatigue (TMF) conditions must be understood. To understand this behavior, three 315 to 649 C TMF test and one 649 C isothermal fatigue test with load hold time were conducted. Crack growth data from these tests were compared with each other as well as with crack growth data from four previous TMF and isothermal fatigue tests of the same material. GRA

N89-21084# Illinois Univ., Urbana. Materials Research Lab.
HYDROGEN SEGREGATION TO GRAIN BOUNDARIES AND EXTERNAL SURFACES
H. K. Birnbaum, E. Sirois, and B. Ladna Oct. 1988 10 p
(Contract N00014-83-K-0968)
(AD-A202892) Avail: NTIS HC A02/MF A01 CSCL 11F

Segregation of hydrogen to grain boundaries, surfaces and defects has been studied in Nb, Nb - V alloys, and Ni using Secondary Ion Mass Spectrometry. This technique has been shown capable of determining the distribution of hydrogen at interfaces under suitable experimental conditions. Very large segregation enhancements are shown for surfaces and grain boundaries. The enhanced concentrations extend for significant distances from the surfaces. Secondary Ion Mass Spectrometry (SIMS) is one of the very few techniques capable of determining the distribution of hydrogen and its isotopes on a microscopic scale (1,2,3,4). Due to the complexity of the instrumentation and the experimental variables care must be taken to ensure that measurement artifacts do not interfere with the determinations. Generally, only qualitative analysis can be carried out unless internal standards are available; as is the case in many hydride forming systems. In the present paper a review of some of the necessary experimental conditions will be presented (1) and the results of applying the technique to hydrogen distributions in Nb - V alloys and Ni will be presented. GRA

N89-21085# Pennsylvania State Univ., University Park. Dept. of Materials Science and Engineering.
HIGH TEMPERATURE OXIDATION AND ELECTROCHEMICAL STUDIES RELATED TO HOT CORROSION Annual Technical Report
D-H. Kim, R. F. Reidy, and G. Simkovich Dec. 1988 41 p
(Contract N00014-86-K-0133)
(AD-A203038) Avail: NTIS HC A03/MF A01 CSCL 07D

To aid in understanding hot corrosion processes, investigations of the electrical behavior of molten sodium sulfate have been undertaken. Wagner-Hebb type polarization experiments and total electrical conductivity measurements by an ac impedance technique were carried out on melts of Na_2SO_4, both pure and those containing .001 m/o, .18 m/o, and supersaturated (10 m/o) Nickel oxide, as a function of sodium monoxide activity at 1173 K. The relative contributions of cation versus anion transport in the molten sodium sulfate was investigated by employing a potentiostatic polarization technique. It was observed that the total electrical conductivity of pure Na_2SO_4 was of the order of .257 (ohm/cm) and varied only slightly with changes in the activity of Na_2O. From the Wagner-Hebb type dc polarization experiments on pure Na_2SO_4, the electron conductivity was shown to be much greater than the electron hole conductivity over the entire range of Na_2O activities. The partial conductivity of electrons in Na_2SO_4 was about three orders of magnitude less than the total electrical conductivity. The introduction of NiO into Na_2SO_4 melts at 1173 K did not produce massive changes in the total electrical conductivities of these melts as compared to those of a pure Na_2SO_4 melt. The addition of NiO in the melt decreases the electronic conductivities as well as the transport numbers of electronic species, regardless of the concentrations of NiO in the melt at 1173 K. GRA

N89-21086# Pittsburgh Univ., PA. Surface Science Center.
ORGANIC FUNCTIONAL GROUP REACTIVITIES AT METAL SURFACES Final Report, 15 Oct. 1985 - 14 Oct. 1988
John T. Yates, Jr. Dec. 1988 6 p
(Contract DAAL03-86-K-0005)
(AD-A203094; ARO-22997.24-CH) Avail: NTIS HC A02/MF A01 CSCL 11F

This report is a summary of the results of an effort to understand the details of chemical bond activation on atomically clean transition metal single crystal surfaces. Modern experimental methods of

surface science were employed and developed in this work. The following general classes of chemical bond activation (elementary reaction steps) have been studied on close packed planes of Ni, Pt, Pd, and Mo: O-H; HC-H; C-C; H(3)C-OH; H(3)-CN; H(3)CN-H(2); HC=N; O-O; and certain of the bonds in a phosphonic ester.
GRA

N89-21087# Army Armament Research, Development and Engineering Center, Watervliet, NY. Weapons Lab.
STRESS-CORROSION CRACKING OF LIQUID-PHASE SINTERED TUNGSTEN ALLOYS Final Report
M. Z. Shah Khan, J. H. Underwood, and I. A. Burch Oct. 1988 35 p
(AD-A203201; ARCCB-TR-88039) Avail: NTIS HC A03/MF A01 CSCL 11F

This study addresses the stress-corrosion cracking susceptibility of liquid-phase sintered tungsten alloys during long-term storage. These alloys are used for kinetic energy penetrators in military applications and it is essential that the structural integrity of the penetrator is not diminished due to the combined action of the chemical environment and the residual manufacturing stresses.
GRA

N89-21088# Virginia Univ., Charlottesville.
SYNTHESIS PROCESSING OF HIGH-LITHIUM Al-Li ALLOYS Progress Report, 8 Jul. 1986 - 30 Apr. 1988
John Wert 27 Jun. 1988 75 p
(AD-A203401; NADC-88078-60; PR-62234N/RS34A57-1-ZP180) Avail: NTIS HC A04/MF A01 CSCL 11F

The goal of this research project is to determine the feasibility of producing Al-Li-base alloys suitable for structural applications with densities in the range 2.2 to 2.4 Mg/m3. Alloys belonging to two broad categories have been studied thus far: Al-Li-Mg alloys and Al-Li-(Y,Sb) alloys. The alloy compositions were selected to avoid formation of the AlLi phase which has deleterious effects on mechanical and electrochemical properties when a substantial volume fraction is present. Rapid solidification has been used to retain a fine microstructure, since all of the alloys exceeded the solubility limit. Splat-quenched flakes of several compositions within each category have been studied, both as-quenched and after an annealing treatment designed to simulate hot vacuum degassing. After annealing, the Al-Li-Mg alloys contained the Al2LiMg phase in equilibrium with an Al matrix.
GRA

N89-21089# State Univ. of New York, Buffalo. Dept. of Chemistry.
LASER-INDUCED METAL DEPOSITION ON SEMICONDUCTORS FROM LIQUID ELECTROLYTES
L. Nanai, I. Hevesi, F. V. Bunkin, B. S. Lukyanchuk, M. R. Brook, G. A. Shafeev, Daniel A. Jelski (State Univ. of New York, Fredonia.), Z. C. Wu, and Thomas F. George Dec. 1988 21 p
(Contract N00014-86-K-0043)
(AD-A203612; TR-90) Avail: NTIS HC A03/MF A01 CSCL 07B

Maskless deposition of gold and copper from electrolyte solutions onto n-doped semiconductors (GaAs, Si) is investigated. The metal deposits are found to have lateral dimensions of about 1 micro and are in barrier contact with the semiconductor. The proposed deposition mechanism is governed by the electric fields resulting from the Dember effect, the p-n junction and the thermal emf.
GRA

N89-21090# Saarland Univ., Saarbrucken (Germany, F.R.). Inst. fuer Werkstoffphysik.
MARTENSITIC PHASE TRANSITIONS IN NANOCRYSTALLINE MATERIALS Interim Report No. 4, 2 Dec. 1987 - 2 Jun. 1989
H. Gleiter 2 Jun. 1988 3 p
(Contract DAJA45-87-C-0008)
(AD-A203636; R/D-5647-MS-01.4) Avail: NTIS HC A02/MF A01 CSCL 07B

As indicated in our third interim report, we have carried out Mossbauer spectroscopy on isolated nanometer-sized crystals cooled to 4.2 K under ultra-high vacuum conditions in order to decide whether or not nucleation of martensite is possible in nanometer-sized, unconstrained crystals. The spectrometer necessary to carry out those experiments was developed in January 1988. It consists of a quartz tube which has locally a section of two thin walls which are transparent to the Mossbauer gamma-rays. The loose powder of isolated small crystals is filled under UHV conditions into the tube and is subsequently cooled to 4.2 K. However, when we recorded the Mossbauer spectra, they turned out not to be conclusive for two reasons: (1) The isolated 5 nm Fe-Ni crystals are superparamagnetic at 4.2 k. (2) The resolution of the spectra is not as high as required to distinguish between bcc and fcc FeNI due to the small amount of material in the tube.
GRA

N89-21091# Virginia Commonwealth Univ., Richmond.
ELECTRONIC STRUCTURE AND PROPERTIES OF DEFECT COMPLEXES IN METALS Final Report, 25 Sep. 1985 - 24 Sep. 1988
Purusottam Jena Nov. 1988 25 p
(Contract DAAG29-85-K-0244)
(AD-A203657; ARO-22655.19-PH) Avail: NTIS HC A03/MF A01 CSCL 07B

Work has been confined to three different areas. These include: (1) Defect complexes - Interaction of hydrogen with vacancies, substitutional impurities, impurity-vacancy complexes, and lattice strain. Also studied are the interaction of He with metals, electric field gradient produced by impurities at host sites in cubic metals, positron annihilation in clean voids, as well as those containing rare-gas atoms and impurities, and the effect of lattice relaxation on the positron lifetime. (2) Disordered Systems - Electronic states, magnetic behavior and the electrical transport in metal-metalloid glasses; role of metalloids in affecting the electronic spectrum. (3) Clusters - Equilibrium geometries, stability, electronic structure, and properties of neutral and charged micro-clusters consisting of up to ten atoms.
GRA

N89-21092# Naval Air Development Center, Warminster, PA. Air Vehicle and Crew Systems Technology Dept.
THE MICROSTRUCTURAL AND PHASE CHARACTERIZATION OF RST Al-Ti-X ALLOYS Final Report, 1 Oct. 1987 - 1 Jul. 1988
William E. Frazier and James J. Thompson 1 Jul. 1988 19 p
(AD-A203734; NADC-88007-60) Avail: NTIS HC A03/MF A01 CSCL 11F

Powder Metallurgy Al-4 wt. percent Ti and Al-6 wt. percent Ti alloys have demonstrated potential for elevated temperature (200 to 300 C) aircraft applications. These materials derive their excellent strength, ductility, and creep resistance from their fine grain structure, oxide dispersion, and Al Ti intermetallics. Inert gas atomization and mechanical alloying have been used to produce the binary alloy powders. However, because of the large solidification range (1200 to 665 C) large quantities of primary Al3 Ti were produced. In this study Al-Ti, Al-TiCe, and Al-Ti-V alloy powders were produced by melt spinning. The alloys were fully characterized in order to assess the effect of composition and processing conditions on microstructure and phase stability. Optical and electron microscopy was used to study the morphology and distribution of second phase disperoids. X-ray diffraction, differential scanning calorimetry (DSC), and selected area electron diffraction (SAD) techniques were used to establish the crystallography of the phases present. The microstructure of the melt spun Al-Ti-X alloys have a higher volume fraction of finely dispersed submicron aluminides than did the previously studied inert gas atomized alloy powders. The major phases identified included Al (fcc), Al3 Ti(14/mmm), and Al3 Ti (14/mmm).
GRA

N89-21093# Lawrence Livermore National Lab., CA.
MEASUREMENT OF GROUND STATE COPPER DENSITY USING HOOK SPECTROSCOPY
William A. Molander Jan. 1989 10 p Presented at the SPIE Conference on Optics, Electro-optics and Laser Applications in Science and Engineering, Los Angeles, CA, 15-20 Jan. 1989

(Contract W-7405-eng-48)
(DE89-005098; UCRL-99003; CONF-890145-17) Avail: NTIS HC A02/MF A01

The density of ground state copper atoms has been measured in an operating large-bore copper laser using hook spectroscopy. In this method, dispersion, due to the copper resonance lines at 327.4 nm and 324.7 nm, is measured by placing the copper laser tube in one arm of a Mach-Zehnder interferometer illuminated by a broad bandwidth UV source. The light source was a Nd:YAG-laser-pumped dye laser which was modified to have a 15 nm bandwidth and then frequency doubled in a 3 mm thick KDP crystal, resulting in a UV beam with an 8 nm bandwidth. The Nd:YAG laser was synchronized with the copper laser, allowing a time resolution of 8 ns. Copper density was measured both as a function of time and as a function of radial position across the bore of the tube. The radial resolution was about 2mm. The space-dependent data gives information about the gas temperature distribution since the density is inversely proportional to the temperature. The gas temperature distribution found in this way agrees well with the predictions of a simple heat-conduction model which assumes uniform power deposition. The power deposition found in this way was compared to that found by calorimetry. DOE

N89-21094# Los Alamos National Lab., NM.
SHEAR BANDING IN TITANIUM WITH CONTROLLED ELONGATIONS AT 1 MILLION/SEC
Karl P. Staudhammer and Alton J. Gray 1989 9 p Presented at the 4th International Conference on Mechanical Properties of Materials at High Rates of Strain, Oxford, England, 20-22 Mar. 1989
(Contract W-7405-eng-36)
(DE89-006555; LA-UR-89-249; CONF-890324-3) Avail: NTIS HC A02/MF A01

Adiabatic shear bands were obtained in titanium with controlled strains to 10.8 percent. Two types of shear bands were observed and characterized. In general the quantity and shear band width increased with increasing elongation. At elongations below approximately 5 percent the shear bands were typically characteristic of shear bands observed at lower strain rates. Above 5 percent elongations many of the shear bands contained a boundary regime adjacent to the shear band and increased in width with increasing total elongation. This effect was attributed to the strain heat. DOE

N89-21095# Sandia National Labs., Albuquerque, NM.
SHOCK-INDUCED CHEMICAL SYNTHESIS OF INTERMETALLIC COMPOUNDS
Steve J. Work, Li-Hsing Yu, Naresh N. Thadhani, Marc A. Meyers (California Univ., San Diego, La Jolla.), Robert A. Graham, and William F. Hammetter 1988 30 p Presented at the International Symposium on Combustion and Plasma Synthesis of High Temperature Materials, San Francisco, CA, 23-26 Oct. 1988
(Contract DE-AC04-76DP-00789)
(DE89-007035; SAND-88-1558C; CONF-8810203-2) Avail: NTIS HC A03/MF A01

Shock synthesis experiments were performed on elemental powder mixtures of Ni-Al and Nb-Al, to study the effect of material parameters on solid-state chemical synthesis. Elemental powders of different morphologies were pre-mixed in a proportion of approximately 65 wt percent Ni, or Nb, and 35 wt percent Al. Shock-compression loading experiments were conducted on Ni-Al mixtures at 19 to 22 GPa pressures using the Sandia Bear fixtures, and on Nb-Al mixtures at 30 to 40 GPa pressures using a 12-capsule Sawaoka recovery fixture. In the case of Ni-Al mixtures, the starting powder morphology plays a significant role in determining the extent of reaction. The Nb-Al powder mixtures shock processed at higher pressures underwent complete reaction. Preliminary results of the shock synthesis experiments on the nickel and niobium aluminide systems are presented, with particular emphasis on the characteristics of the reaction products. DOE

N89-21096# Oak Ridge National Lab., TN.
STRUCTURAL ENERGY DIFFERENCES IN Al3Ti: THE ROLE OF TETRAGONAL DISTORTION IN APB AND TWIN ENERGIES
D. M. Nicholson, G. M. Stocks, W. M. Temmerman, P. Sterne, and D. G. Pettifor (Imperial Coll. of Science and Technology, London, England) 1988 7 p Presented at the Fall Meeting of the Materials Research Society, Boston, MA, 28 Nov. 1988
(Contract DE-AC05-84OR-21400)
(DE89-007210; CONF-881155-47) Avail: NTIS HC A02/MF A01

At stoichiometry, DO (sub 22) is the observed ground state of Al3Ti and has a C/A ratio of 2.23, but as a function of both concentration and temperature other ordered arrangements of APB's are observed. These phase transitions have sparked many studies in which the energy has been treated as that of chemical rearrangement on an fcc lattice. We have found that at the ideal C/A ratio, the L1 (sub 2) structure is lower in energy, but as the tetragonal distortion increases the DO (sub 22) energy drops below that of L1 (sub 2). The critical role played by the tetragonal distortion in the balance between L1 (sub 2) and DO (sub 22) energies precludes the use of any model based on the undistorted lattice. The major impediment to the development of Al3Ti as a high-temperature material is its lack of ductility. The standard approach is to make alloy additions which transform the structure to L1 (sub 2). The Al3Ti can be stabilized in L1 (sub 2) by the addition of Fe, Ni, or Cu, however, it remains brittle. An alternate approach is to work toward the enhancement of ductility in the DO (sub 22) phase. As a first step in a search for alloy additions which will reduce the twinning energy and improve twin related ductility, we have calculated the twinning energy in Al3Ti. DOE

N89-21097# California Univ., Berkeley. Lawrence Berkeley Lab.
Nb MODIFICATION OF MICROCOMPOSITE Fe/C/Cr/Mn STEEL Ph.D. Thesis
Jongkeun Kim Dec. 1988 99 p
(Contract DE-AC03-76SF-00098)
(DE89-008297; LBL-26145) Avail: NTIS HC A05/MF A01

A microcomposite steel which is desired to be attained in this investigation, is a composite microstructure consisting of fine packets of heavily dislocated martensite laths surrounded by continuous thin films of interlath retained austenite. Heavily dislocated lath martensite gives ultrahigh strength; a softer, tough austenite phase provides high fracture toughness. This composite microstructure has been achieved in the Fe/Cr/Mn/C system containing more than a total of four percent of alloying elements in previous work. The present work is concerned with obtaining superior combinations of mechanical properties by adding the microalloy element of niobium to the basic quaternary alloy of Fe/2.0 wt percent Cr/1.2 wt percent Mn/0.25 wt percent C and by applying controlled rolling practice to processing of the experimental alloys to attain fine austenite grains, giving rise to high Charpy V-notch impact toughness. The basis is to have sufficient hardenability after retrenching the chromium content, so that processing will not destroy the microcomposite structure of heavily dislocated martensite laths and thin films of interlath retained austenite after the martensite phase transformation, following rolling and quenching. DOE

N89-21098# California Univ., Berkeley. Lawrence Berkeley Lab.
MECHANISMS OF FATIGUE CRACK PROPAGATION AND FRACTURE TOUGHNESS BEHAVIOR IN ADVANCED ALUMINUM-LITHIUM ALLOYS Ph.D. Thesis
Kondapavuluru Tiruma VenkateswaraRao Jun. 1988 196 p
(Contract DE-AC03-76SF-00098)
(DE89-008300; LBL-26449) Avail: NTIS HC A09/MF A01

Mechanisms and mechanics influencing the fatigue crack propagation and plain-stain fracture toughness behavior commercial aluminum-lithium alloys are investigated as a function of the microstructure and plate orientation, both at ambient and liquid nitrogen temperatures. With ultra-low density, improved elastic modulus and high strength, in comparison to existing 7XXX and

2XXX alloys, the alloys additionally exhibit superior long (approximately or greater than 10 mm) fatigue crack properties, even after prolonged exposures at high temperatures, excel under tension-dominated spectrum loading and in some instances show superior fracture toughness values at ambient and liquid nitrogen temperatures. However, the properties are strongly dependent on plate orientation; moreover, the benefits of lithium additions are not realized for small (2 to 1000 micrometers) fatigue cracks.
DOE

N89-21738*# Auburn Univ., AL. Dept. of Physics.
EXPERIMENTAL RESULTS ON ATOMIC OXYGEN CORROSION OF SILVER
Albert T. Fromhold *In* Alabama Univ., Research Reports: 1988 NASA/ASEE Summer Faculty Fellowship Program Dec. 1988 24 p (For primary document see N89-21726 14-99)
Avail: NTIS HC A99/MF E03 CSCL 11F

27 NONMETALLIC MATERIALS

Includes physical, chemical, and mechanical properties of plastics, elastomers, lubricants, polymers, textiles, adhesives, and ceramic materials.

For composite materials see *24 Composite Materials*.

N89-21099*# PRC Kentron, Inc., Hampton, VA.
FRACTURE CHARACTERISTICS OF BALLOON FILMS
Marc A. Portanova Jan. 1989 36 p
(Contract NAS1-18000)
(NASA-CR-181686; NAS 1.26:181686) Avail: NTIS HC A03/MF A01 CSCL 11C

An attempt was made to determine the failure modes of high altitude scientific balloons through an investigation of the fracture characteristics of the thin polyethylene films. Two films were the subject of the evaluation, Winzen Int.'s Stratafilm SF-85 and Raven Industries' Astro-E. Research began with an investigation of the film's cold brittleness point and it's effect on the ultimate strength and elasticity of the polyethylene film. A series of preliminary investigations were conducted to develop an understanding of the material characteristics. The primary focus of this investigation was on the notch sensitivity of the films. Simple stress strain tests were also conducted to enable analysis employing fracture toughness parameters. Studies were conducted on both film types at 23 C (room temperature), -60 C, -90 C, and -120 C. Author

N89-21100*# National Aeronautics and Space Administration. Lewis Research Center, Cleveland, OH.
EVALUATION OF ATOMIC OXYGEN RESISTANT PROTECTIVE COATINGS FOR FIBERGLASS-EPOXY COMPOSITES IN LEO
Sharon K. Rutledge, Phillip E. Paulsen, and Joyce A. Brady (Sverdrup Technology, Inc., Cleveland, OH.) 1989 13 p Presented at the 34th SAMPE Technical Conference, Reno, NV, 8-11 May 1989
(NASA-TM-101955; E-4649; NAS 1.15:101955) Avail: NTIS HC A03/MF A01 CSCL 11B

Fiberglass-epoxy composite masts are the prime structural members for the Space Station Freedom solar array. At the altitude where Space Station Freedom will operate, atomic oxygen atoms are the most predominant species. Atomic oxygen is highly reactive and has been shown to oxidize organic and some metallic materials. Tests with random and directed atomic oxygen exposure have shown that the epoxy is removed from the composite exposing brittle glass fibers which could be easily removed from the surface where they could contaminate Space Station Freedom Systems. Protection or fiber containment systems; inorganic based paints, aluminum braid, and a metal coating; were evaluated for resistance to atomic oxygen, vacuum ultraviolet radiation, thermal cycling, and mechanical flexing. All appeared to protect well against atomic oxygen and provide fiber containment except for the single aluminum braid covering. UV radiation resistance was acceptable and in general, thermal cycling and flexure had little to no effect on the mass loss rate for most coatings. Author

N89-21101# Atomic Energy Research Establishment, Harwell (England). Materials Physics and Metallurgy Div.
ACOUSTIC MICROSCOPY OF LOW DUCTILITY MATERIALS
D. G. P. Fatkin, C. B. Scruby, and G. A. D. Briggs (Oxford Univ., England) Dec. 1987 59 p
(AERE-R-12848; HL88/1135) Avail: NTIS HC A04/MF A01

Acoustic microscopy offers materials scientists not only high resolution but also the ability to image subsurface and surface features by its elastic contrast mechanisms. It is a particularly powerful tool for detecting discontinuities such as voids and cracks, and for characterizing interfacial boundaries between different phases. The application of acoustic microscopy to two important classes of low ductility materials (engineering ceramics and ceramic fiber composites) is described. Images of a wide range of near-surface defects are presented for the six ceramics studied. An application to crack length determination during indentation tests is also discussed. In the composites, there were systematic variations in contrast from the fiber-matrix interface, which appeared to correlate with changes in interfacial strength. Finally the line-focus microscope was used to demonstrate how the Rayleigh velocity and attenuation can be used to characterize the microstructure of ceramics and ceramic composites. Author

N89-21102 Pennsylvania State Univ., University Park.
SYNTHESIS OF CERAMICS AT LOW TEMPERATURES Ph.D. Thesis
Michael Ray Silsbee 1988 261 p
Avail: Univ. Microfilms Order No. DA8826820

Chemically bonded ceramics were researched. Chemically bonded ceramics is a term coined to describe materials where the energy for binding reaction reactions is derived from internal chemical energy rather than externally supplied thermal energy as is the case for most conventional ceramics. Portland cement represents a chemically bonded material that on a per ton basis is one of the most commonly employed materials in modern society. Small improvements in the understanding of this material can therefore result in substantial benefits. The partial replacement of Portland cement with a ground granulated blast furnace slag, an industrial by-product is discussed. The use of this material offers the potential for significant energy savings and may in many cases result in improved performance of the mixtures. The chemistry and rheological behavior of these mixtures was found to be similar to that of pure Portland cements. A different type of chemically bonded materials is addressed. Materials based on reactions in the system alumina-phosphoric acid were employed for many years. The behavior of materials in this system was found to contain many elements of similarity to hydraulic bonded materials, in spite of differences in the chemical and phase behavior of these materials. The work described forms a foundation for a clearer understanding of these materials and offers the possibility of applying these systems to new and different applications.
Dissert. Abstr.

N89-21103*# National Aeronautics and Space Administration. Lewis Research Center, Cleveland, OH.
DEGRADATION AND CROSSLINKING OF PERFLUOROALKYL POLYETHERS UNDER X-RAY IRRADIATION IN ULTRAHIGH VACUUM
Shigeyuki Mori (National Academy of Sciences - National Research Council, Washington, DC.) and Wilfredo Morales Mar. 1989 15 p Prepared in cooperation with Iwate Univ., Morioka (Japan)
(NASA-TP-2910; E-4500; NAS 1.60:2910) Avail: NTIS HC A03/MF A01 CSCL 11B

Degradation of three types of commercially available perfluoroalkyl polyethers (PFPE)-Demnum S200, Fomblin Z25, and Krytox 16256-by X-ray irradiation was studied by using X-ray photoemission spectroscopy (XPS) and a mass spectrometer under ultra-high-vacuum conditions. The carbons in the polymers were characterized by chemical shifts of Cls binding energies. Gaseous products containing COF2 and low-molecular-weight fluorocarbons were formed. From Fomblin Z25, which has acetal linkages (-OCF2O-), a large quantity of COF2 gas was evolved. Liquid products became tacky after a long irradiation time, and some did

not dissolve in Freon. High-pressure liquid chromatography (HPLC) showed that molecular weight distribution became broader and that higher molecular weight polymers were formed from Demnum and Krytox. We concluded from these results that degradation and cross-linking took place simultaneously. Demnum crosslinked more easily than the other fluids. The time dependence of both XPS spectra of Cls and mass spectra showed that C-O-bonded carbons in PFPE'S were removed faster than other carbons. There was no substrate effect on the degradation reaction because the first-order rate constants calculated from the change of gaseous products were similar when stainless steel (440C) and gold-coated surfaces were used. Metal fluorides were formed on stainless steel during the reaction. A mechanism for the degradation of PFPE'S is discussed on the basis of their molecular structures. Author

N89-21104*# National Aeronautics and Space Administration. Lewis Research Center, Cleveland, OH.

SIMULATION OF THE LOW EARTH ORBITAL ATOMIC OXYGEN INTERACTION WITH MATERIALS BY MEANS OF AN OXYGEN ION BEAM

Bruce A. Banks, Sharon K. Rutledge, Phillip E. Paulsen, and Thomas J. Steuber (Sverdrup Technology, Inc., Cleveland, OH.) 1989 32 p Presented at the 18th Annual Symposium on Applied Vacuum Science and Technology, Clearwater Beach, FL, 6-8 Feb. 1989; sponsored by American Vacuum Society
(NASA-TM-101971; E-4671; NAS 1.15:101971) Avail: NTIS HC A03/MF A01 CSCL 11C

Atomic oxygen is the predominant species in low-Earth orbit between the altitudes of 180 and 650 km. These highly reactive atoms are a result of photodissociation of diatomic oxygen molecules from solar photons having a wavelength less than or equal to 2430A. Spacecraft in low-Earth orbit collide with atomic oxygen in the 3P ground state at impact energies of approximately 4.2 to 4.5 eV. As a consequence, organic materials previously used for high altitude geosynchronous spacecraft are severely oxidized in the low-Earth orbital environment. The evaluation of materials durability to atomic oxygen requires ground simulation of this environment to cost effectively screen materials for durability. Directed broad beam oxygen sources are necessary to evaluate potential spacecraft materials performance before and after exposure to the simulated low-Earth orbital environment. This paper presents a description of a low energy, broad oxygen ion beam source used to simulate the low-Earth orbital atomic oxygen environment. The results of materials interaction with this beam and comparison with actual in-space tests of the same meterials will be discussed. Resulting surface morphologies appear to closely replicate those observed in space tests. Author

N89-21105*# TRW Space Technology Labs., Redondo Beach, CA.

IMPROVED HIGH-TEMPERATURE RESISTANT MATRIX RESINS

H. E. Green, G. E. Chang, W. F. Wright, K. Ueda, and M. K. ORell Apr. 1989 84 p
(Contract NAS3-23933)
(NASA-CR-180826; NAS 1.26:180826) Avail: NTIS HC A05/MF A01 CSCL 11C

A study was performed with the objective of developing matrix resins that exhibit improved thermo-oxidative stability over state-of-the-art high temperature resins for use at temperatures up to 644 K (700 F) and air pressures up to 0.7 MPa (100 psia). The work was based upon a TRW discovered family of polyimides currently licensed to and marketed by Ethyl Corporation as EYMYD(R) resins. The approach investigated to provide improved thermo-oxidative properties was to use halogenated derivatives of the diamine, 2, 2-bis (4-(4-aminophenoxy)phenyl) hexafluoropropane (4-BDAF). Polyimide neat resins and Celion(R) 12,000 composites prepared from fluorine substituted 4-BDAF demonstrated unexpectedly lower glass transition temperatures (Tg) and thermo-oxidative stabilities than the baseline 4-BDAF/PMDA polymer. Author

N89-21106# Cambridge Univ. (England). Dept. of Physics.

INVESTIGATION OF THE IMPACT PERFORMANCE OF VARIOUS GLASS AND CERAMIC SYSTEMS Final Technical Report, 3 Jul. 1985 - 30 Jun. 1988

J. E. Field 31 Aug. 1988 92 p
(Contract DAJA45-85-C-0021; DA Proj. 1L1-61103-BH-57)
(AD-A202443; R/D-5087-MS-01-F) Avail: NTIS HC A05/MF A01 CSCL 11B

This report describes our research on the impact behavior of various glass and ceramic systems. The first section describes the liquid impact technique and experiments in which high velocity liquid jets were fired at specimens over a range of velocities and the post impact (i.e., residual) strength measured. The jet technique velocities and the post impact (i.e., residual) strength are measured. The jet technique is a convenient method for applying an intense stress pulse and studying the dynamic response a material. If impact experiments are made over a range of velocities, it is possible to plot residual strength versus impact velocity. Such curves give the threshold velocity for damage and also show how rapidly the strength decreases for impacts above the threshold condition. GRA

N89-21107# Pennsylvania State Univ., University Park. Dept. of Materials Science and Engineering.

SURFACE CHEMISTRY AND STRUCTURAL EFFECTS IN THE STRESS CORROSION OF GLASS AND CERAMIC MATERIALS Final Report, Mar. 1986 - Mar. 1988

Carlo G. Pantano 15 Sep. 1988 23 p
(Contract F49620-86-K-0005)
(AD-A202452; AFOSR-88-1211TR) Avail: NTIS HC A03/MF A01 CSCL 11B

This report describes a unique instrumental facility where chemically-assisted crack propagation can be studied; i.e., crack-velocity/stress intensity measurements can be made in the presence of specific environments, and the fracture surfaces so created can be analyzed, in-situ, using a neutral beam static secondary ion mass spectrometer (SIMS) technique. The report also summarizes studies of slow crack growth, corrosion and fatigue of fluorozirconate glasses. GRA

N89-21108# Clark Univ., Worcester, MA.

A NMR (NUCLEAR MAGNETIC RESONANCE) STUDY OF THE MOLECULAR INTERACTIONS AND DYNAMIC BEHAVIOR IN POLYMER-DILUENT BLENDS IN THE SOLID STATE Final Report, 1 Jun. 1985 - 30 Jun. 1988

Paul T. Inglefield and Alan A. Jones 25 Jul. 1988 150 p
(Contract DAAG29-85-K-0126)
(AD-A202459; ARO-22533.12-CH) Avail: NTIS HC A07/MF A01 CSCL 07F

A study of the molecules detailing interactions between small molecule diluents and polymers was carried out using a variety of Nuclear Magnetic Resonance methods. The focus of the study was to allow a molecular level comparison with macroscopic properties (thermal and mechanical) in multicomponent polymer blends. The details of plasticization, antiplasticization diluent sorption and blend compatibility were addressed. The polymer systems studied were high impact strength engineering plastics: polycarbonates and poly (2,6-dimethylphenyl oxide) blends with polystyrene and structural analogues of these two fundamental systems. A three fold approach was used, with experiments which probe: (1) the host polymer and changes in its dynamics as a consequence of diluent addition, (2) the dynamics of the diluent itself modified by the host, and (3) experiments which probe directly the intermolecular intimacy in a multicomponent glassy blend. GRA

N89-21109# Crystal Growth and Materials Testing Associates, Lanham, MD.

CERAMICS Final Report No. 219, 29 Aug. 1986 - 29 Feb. 1988

R. J. Arsenault, N. Louat, M. Duesbery, R. Spann, and S. Lawrence 3 Nov. 1988 59 p
(Contract N00014-86-C-2180)
(AD-A202504) Avail: NTIS HC A04/MF A01 CSCL 11B

The intrinsic task of this contract was to perform research to obtain fundamental insights into the mechanical and electrical properties of ceramics. The specific items in the statement of work are necessary steps that had to be completed in order to reach the goal of obtaining fundamental insights. In this final report, five topics will be discussed in detail: Fracture of ceramics, Computer modelling of ceramics containing ordered voids, Interaction of dislocations with planar free surfaces, Application of superconducting ceramics to microwave substrates, High T sub c superconducting ceramic oxides. GRA

N89-21110# United Kingdom Atomic Energy Authority, Risley (England).
ADVANCED TRIBOLOGICAL COATINGS FOR HIGH SPECIFIC STRENGTH ALLOYS Progress Report No. 3, 29 Mar. - 29 Sep. 1988
29 Sep. 1988 3 p
(Contract DAJA45-87-C-0044)
(AD-A202505; R/D-5876-MS-01-3) Avail: NTIS HC A02/MF A01 CSCL 11F

A presentation on the progress of this contract was made at the 12 April 1988 at the SCORE meeting held at the Ministry of Defence, London. The status of the research is as follows: The company was only able to deposit aluminium at below 900C. Plate specimens treated and metallographic sections were prepared. A 25 micron depth of aluminized layer has been formed, of hardness 360 HV 50g, but the high temperature treatment has caused softening of the substrate (from 380 HV to 280 HV 20kg). This a promising result and further plate samples were sent for treatment at differing conditions to ascertain if the hardened layer (of titanium aluminides) can be formed without substrate tempering or whether re-solution treatment will restore substrate properties. GRA

N89-21111# Massachusetts Inst. of Tech., Cambridge. Dept. of Mechanical Engineering.
DILATATIONALLY NONLINEAR ELASTIC MATERIALS. PART 2: AN EXAMPLE ILLUSTRATING STRESS CONCENTRATION REDUCTION Technical Report No. 6
Rohan Abeyaratne and Guo-Hua Jiang Sep. 1988 34 p
(Contract N00014-87-K-0117)
(AD-A202521; TR-6) Avail: NTIS HC A03/MF A01 CSCL 20K

This paper, which is the second in a two part study, uses a specific boundary value problem to illustrate some of the features of the theory discussed in the first part. Here, the spherically symmetric deformation of a hollow sphere which has a traction-free inner wall and a prescribed radial displacement delta at its outer wall is studied. The analysis is carried out within the small-strain theory of nonlinear elasticity and the body is assumed to be composed of an elastic material which is homogeneous and isotropic, and which has a linear response in shear and a tri-linear response in dilatation. For a certain range of values of the applied displacement delta the problem has an infinity of solutions and these describe configurations which involve a phase boundary; the strain field is continuous on either side of the phase boundary but suffers a jump discontinuity across it. A kinetic law, which is a supplementary constitutive law pertaining to particles located on the phase boundary and relating the driving traction on the phase boundary to its velocity, is then imposed, leading to a unique response in all quasi-static motions. GRA

N89-21112# Texas A&M Univ., College Station. Mechanics and Materials Center.
A CONTINUUM DIFFUSION MODEL FOR VISCOELASTIC MATERIALS
Y. Weitsman Nov. 1988 35 p
(Contract N00014-82-K-0562)
(AD-A202588; MM-4762-88-17) Avail: NTIS HC A03/MF A01 CSCL 07F

A model for diffusion in polymers is established from basic principles of irreversible thermodynamics, employing the methodology of continuum mechanics. The polymeric materials are considered to respond viscoelastically, with ageing. It is shown that effects of stress on diffusion and certain anomalies in the moisture sorption process can be explained by the present model. GRA

N89-21113# Air Force Inst. of Tech., Wright-Patterson AFB, OH. School of Engineering.
INVESTIGATION OF FAILURE MODES IN FIBER REINFORCED CERAMIC MATRIX COMPOSITES M.S. Thesis
Joseph W. Moschler, Jr. Dec. 1988 132 p
(AD-A202705; AFIT/GAE/AA/88D-28) Avail: NTIS HC A07/MF A01 CSCL 11B

This experimental study was conducted to investigate the damage progression in fiber reinforced ceramic matrix composites under tensile loading. As part of this study, the effect of the residual stresses at the fiber-matrix interface on damage progression was evaluated. Composite samples were fabricated from silicon carbide fibers and boro-silicate glass matrices. Each glass had a different coefficient of thermal expansion than the fiber and through the variation of this mismatch, the residual stresses at the fiber-matrix interface were varied resulting in different bonding conditions at the fiber-matrix interface. The mechanical properties of the composites were measured using a servo-hydraulic mechanical testing machine. During these tests, transverse strain reversal was observed which is believed to be caused by axial matrix cracks and fiber-matrix debonding. Tensile tests were conducted on the composites using a constant load straining device in which damage progression was observed using an optical microscope. GRA

N89-21114# Air Force Inst. of Tech., Wright-Patterson AFB, OH. School of Engineering.
FRACTURE TOUGHNESS TESTING OF A CERAMIC MATRIX COMPOSITE AT ELEVATED TEMPERATURES M.S. Thesis
John H. Mol Dec. 1988 142 p
(AD-A202738; AFIT/GAE/AA/88D-26) Avail: NTIS HC A07/MF A01 CSCL 11B

The need for a load fixture and technique for determining the fracture toughness in fiber reinforced ceramic composites at elevated temperatures was identified. A three point bend load fixture capable of withstanding temperatures up to 1000 degrees Fahrenheit was designed and constructed. A test procedure for finding compliance and critical load at room and elevated temperatures was developed. Specimens were tested at varying crack lengths at room temperature, 600, and 1000 degrees Fahrenheit. Postmortem examination was done on specimens for each temperature. Specimens tested at 600 F had smoother Mode II fracture surfaces than the room temperature specimens including a more brittle fracture and supporting the experimental results. The specimens tested at 1000 F had a rougher Mode II fracture surface with fiber pull-out and small matrix fragments attached to the fibers indicating a more ductile failure and therefore increasing the fracture toughness. A color change from black to dark gray and the presence of crystals on the Mode I fracture surface of the 1000 F specimens indicated a chemical change in the specimens. The apparent chemical change and significantly higher fracture toughness in the material at elevated temperatures. GRA

N89-21115# San Diego State Univ., CA. Dept. of Chemistry.
PREPOLYMER CHARACTERIZATION Final Report, Jul. 1984 - Mar. 1988
Richard J. Laub Oct. 1988 147 p
(Contract F04611-84-K-0016)
(AD-A202821; AFAL-TR-88-068) Avail: NTIS HC A07/MF A01 CSCL 07C

Some fundamental aspects of the physicochemical characterization of propellant prepolymers were explored for the purpose of developing and optimizing analytical procedures for molecular weight, degree of branching, and functionality distributions. Fractional solution fractionation, vapor phase osmometry, gas, and high-performance column liquid chromatography, and mass spectrometry were employed with model polystyrene polymers as well as bulk and fractionated R-45M and HMDS-treated R-45M. The methodologies and techniques of

analysis ultimately developed make use only of readily available equipment, are applicable to characterization and routine quality control of virtually any prepolymer system, and can be implemented in any vendor or governmental laboratory. GRA

N89-21116# Westinghouse Research and Development Center, Pittsburgh, PA.
RESEARCH ON SILICON, CARBON, AND SILICON CARBIDE HETEROSTRUCTURES Annual Report No. 1, 1 Aug. 1987 - 1 Aug. 1988
W. D. Partlow, W. J. Choyke, John T. Yates, Jr., L. E. Kline, R. R. Mitchell, Juai Ruan, and J. V. R. Heberlein 26 Sep. 1988 57 p
(Contract F49620-87-C-0101)
(AD-A202866; Rept-88-9S31-HETRO-R1; AFOSR-88-1221TR)
Avail: NTIS HC A04/MF A01 CSCL 07B

The progress made during the first year of a three-year program to study heterostructures of Group 4 materials is reported here. The equipment for the three experimental components of the program was assembled and characterized. These facilities include a remote plasma deposition reactor with extensive process diagnostics, an UHV apparatus for quantitative studies of the kinetics of adsorption/desorption of reactive species on atomically clean silicon surfaces, and an UHV, cryogenic cathodoluminescence spectroscopic facility. A model for the production, losses, and transport of metastable species in the remote reactor was completed. Experiments have begun to determine the reactive species present in the deposition process, the reaction of ethylene at silicon surfaces, and the catholuminescence of carbon in the diamond phase. GRA

N89-21117# Air Force Inst. of Tech., Wright-Patterson AFB, OH. School of Engineering.
COMPRESSIVE PROPERTIES OF HIGH PERFORMANCE POLYMERIC FIBERS M.S. Thesis
Scott A. Fawaz Dec. 1988 103 p
(AD-A202947; AFIT/GAE/AA/88D-13) Avail: NTIS HC A06/MF A01 CSCL 07F

In directing the research effort for improving the compressive properties of rigid rod polymeric composite fibers, a reliable testing technique for determining compressive properties is needed. The technique developed used the Tecam Micro-Tensile Testing Machine, MTM-8 and allowed direct tension and compression testing of composite fibers of extremely short gage length. The measured data was analyzed for corrections in machine compliance and possible errors in gage length misreading, fiber slippage, glue deformation, fiber misalignment, and nonuniform stress distribution. A nonpolymeric fiber was tested to determine if any fiber material dependence existed. The data was compared to the compressive properties obtained from the elastica loop, bending beam, recoil, and composite tests. This was the only known research of high performance polymer fibers in direct tension and compression testing which allowed the construction of a full stress-strain curve. GRA

N89-21118# Harvard Univ., Cambridge, MA. Dept. of Chemistry.
ORGANIC CHEMISTRY IN TWO DIMENSIONS: SURFACE-FUNCTIONALIZED POLYMERS AND SELF-ASSEMBLED MONOLAYER FILMS Interim Technical Report No. 9
George M. Whitesides and Gregory S. Ferguson Sep. 1988 23 p
(Contract N00014-85-K-0898; NR Proj. 356856)
(AD-A202955) Avail: NTIS HC A03/MF A01 CSCL 07C

Organic chemistry is largely derived from studies of the reactivity and properties of molecules in homogeneous solution, and much of the intuition of organic chemists is based on the behavior of molecules in solution. Surfaces and interfaces (that is, quasi two-dimensional assemblies of molecules or functional groups) provide environments that can be quite different from those of solutions, and chemical intuition derived from solution is often wrong when applied to processes occurring at surfaces. The central focus of our program in organic surface chemistry is on new science: that is, understanding and controlling the phenomena characteristic of surfaces, interfaces, and thin films. A charm of surface chemistry is, however, its ability to combine new science with relevance to a wide range of technological problems, and we hope to contribute to these applied areas as well. GRA

N89-21119# Connecticut Univ., Storrs. Liquid Crystalline Polymer Research Center.
STRUCTURE DEVELOPMENT DURING CONVERGING FLOW OF A LIQUID CRYSTAL DISPERSED TWO-PHASE FLUID Interim Technical Report
P. J. Yanisko and R. A. Weiss 3 Jan. 1989 10 p Prepared for presentation at ANTEC, New York, NY, May 1989
(Contract N00014-86-K-0772)
(AD-A203062; TR-31) Avail: NTIS HC A02/MF A01 CSCL 07C

The flow dynamics of liquid crystal (LC)-dispersed two phase fluids were studied in order to determine the relationships between the deformation of the dispersed phase (D), the weber number (We) and the viscosity ratio of the two phases (k). A flow visualization apparatus consisting of a glass capillary with aconical converging entrance and a video system was constructed and used to measure droplet deformation in the entrance region (extensional flow) and in the capillary (shear flow). The systems studied included p-ethoxybenzyline p-butylanine (EBBA) dispersed in three Newtonian fluids (50, 80, and 100 percent glycerin (aq)) and three viscoelastic, non Newtonian fluids (0.35, 1.0, and 1.5 percent polyacrylamide (aq)). The data were compared with the theoretical predictions for non-LC containing two phase fluids by Reijden-Stolk and Sara. D increased with increasing We and it appeared that LC droplets may experience more deformation than isotropic fluid dispersions for comparable values of We and K. GRA

N89-21120# Ceramatec, Inc., Salt Lake City, UT.
HIGH TEMPERATURE EVALUATION OF NEW FERROELASTIC TOUGHENED CERAMIC MATERIALS Final Report, 15 Aug. 1987 - 15 Feb. 1988
Roger Matsumoto and Robert J. Mayhew Feb. 1988 40 p
(Contract DAAL04-87-C-0058A)
(AD-A203197) Avail: NTIS HC A03/MF A01 CSCL 11B

The toughness behavior of ceria tetragonal zirconia polycrystalline (TZP) ceramics was investigated relative to the effect of various dopants (coded as dopants A, B and C in this report due to pending patent applications). Additions of dopant A enhanced the toughness of zirconia ceramics, dopant B suppressed the fracture toughness and, dopant C had little effect on toughness. High temperature strength retention in zirconia ceramics containing dopant A suggest that mechanisms other than transformation toughening are operative. Switching of X-ray peak intensities showed that the tetragonal zirconia used in the present study as ferroelastic. GRA

N89-21121# Aerospace Corp., El Segundo, CA. Materials Sciences Lab.
ADHESION IN CHEMICALLY HOSTILE ENVIRONMENTS: THE USE OF FILLED POLYMERS AS DIFFUSION BARRIERS
Robert S. Bretzlaff and Richard Y. Sugihara 1 Nov. 1988 99 p
(Contract F04701-85-C-0086)
(AD-A203333; TR-0088(3935-03)-1; SD-TR-88-98) Avail: NTIS HC A05/MF A01 CSCL 07F

Polymer metal bonding is accomplished, in general, through a combination of chemical bonding and mechanical interlocking. In either case, the metal surface must remain uncorroded in order to preserve adhesion. If material layers that are close to the bonded interface evolve corrosive species, then the metal can be corroded and the adhesive strength reduced. One way to ameliorate this adhesive degradation is to coat the metal substrate with a barrier liner that is relatively impervious to the corrosive species. If subsequently bonded material layers evolve corrosive species, then relatively fewer of these molecules would be able to penetrate the barrier liner and corrode the substrate. The experiments reported here were performed on a polyurethane (Uralane 5753)

with or without filler particles (alumina, strontium chromate, magnesium silicate, or carbon black) and subjected to gaseous hydrogen fluoride at ambient temperature. GRA

N89-21122# Royal Aircraft Establishment, Farnborough (England).
CALCULATION OF THE GLASS TRANSITION TEMPERATURES OF LINEAR POLYMERS. PART 3: EVALUATION OF CALCULATION RELATIONSHIPS
W. A. Lee Jun. 1988 108 p
(AD-A203357; RAE-TR-88044; DRIC-BR-108121) Avail: NTIS HC A06/MF A01 CSCL 07F

Four equations, relating the structure of polymers in numerical form to their glass transition temperatures (Tg)s, are evaluated using a large data set of 1179 polymers. Additive temperature parameters, for the relationship giving the best fit to the data, are tabulated which enable predictions to be made of many polymer Tgs outside the data set. These parameters also provide a measure of the relative effectiveness of groups in internally plasticizing polymers. GRA

N89-21123# Institute for Defense Analyses, Alexandria, VA.
ELECTROLYTIC PROTECTION AGAINST HIGH-TEMPERATURE OXIDATION Final Report, Feb. 1987 - Feb. 1988
Thomas F. Kearns Nov. 1988 45 p
(Contract MDA903-84-C-0031)
(AD-A203890; AD-E501064; IDA-P-2093; IDA/HQ-88-33190)
Avail: NTIS HC A03/MF A01 CSCL 11C

This paper describes and discusses protection of materials against high-temperature oxidation achieved by coating their surfaces with a solid electrolyte and making the substrate cathodic in an electrolytic cell created by a potential applied across the electrolyte. This approach, similar in nature to the widely followed practice of cathodic protection against aqueous corrosion, is shown to be theoretically sound and potentially advantageous for protection of materials such as refractory metals and carbon-carbon composites. Current status of activity in the field is described and suggestions are made for future work. GRA

N89-21124# Ford Motor Co., Dearborn, MI.
PRE-PILOT SYNTHESIS OF LOW CARBON Si3N4
G. M. Crosbie, J. M. Nicholson, R. L. Predmesky, and E. D. Stiles 1988 6 p Presented at the 2nd International Conference on Ceramic Powder Processing Science, Berchtesgaden, (Germany F. R.), 1 Oct. 1988
(Contract DE-AC05-84OR-21400)
(DE89-007202; CONF-8810292-1) Avail: NTIS HC A02/MF A01

Of interest to present powder needs is a silicon nitride powder of high cation and anion purity without carbon residues. As part of the U.S. Ceramic Technology for Advanced Heat Engines (CTAHE) program, this process study is directed toward pressurized reactions of SiCl sub 4 (vapor and liquid) with liquid NH sub 3 without organics. In the vapor chloride process, we observed that the cooling from latent heat of vaporization of NH sub 3 more than offsets the heat of reaction at 0 C and 0.6 MPa. Crystallites of 0.2 to 0.3 micron size and of primarily equi-axed shapes were found. In the present phase, our goal is to test for unique properties of the ceramics sintered from larger quantities of the low carbon powders. For this, we have installed a pre-pilot plant at 4 L scale and have shown rapid chloride by-product removal. DOE

N89-21753*# Georgia Inst. of Tech., Atlanta.
DYNAMIC FATIGUE TESTING OF ZERODUR GLASS-CERAMIC
Dennis S. Tucker *In* Alabama Univ., Research Reports: 1988 NASA/ASEE Summer Faculty Fellowship Program Dec. 1988 22 p (For primary document see N89-21726 14-99)
Avail: NTIS HC A99/MF E03 CSCL 11B

28 PROPELLANTS AND FUELS

Includes rocket propellants, igniters, and oxidizers; their storage and handling procedures; and aircraft fuels.

For related information see also *07 Aircraft Propulsion and Power, 20 Spacecraft Propulsion and Power,* and *44 Energy Production and Conversion.*

N89-21125# Detroit Diesel Allison, Indianapolis, IN.
HIGH DENSITY FUEL EFFECTS Final Report, Sep. 1985 - Apr. 1988
N. K. Rizk, V. L. Oechsie, P. T. Ross, and H. C. Mongia 18 Aug. 1988 174 p
(Contract F33615-86-C-2604)
(AD-A202426; DDA-EDR-13471; AFWAL-TR-88-2046) Avail: NTIS HC A08/MF A01 CSCL 21D

The purpose of this program was to determine, by combustor rig tests and data evaluation, the effects of the high density fuel properties on the performance and durability of the Allison T56-A-15 combustion system. Four high density fuels in addition to baseline JP4 were evaluated in the effort. The rig test program included: nozzle flow bench testing, aerothermal performance and wall temperature, flame stability and ignition, injector coking and plugging, and flow transient effect. The data evaluation effort involved the utilization of empirical correlations in addition to analytical multidimensional tools to analyze the performance of the combustor. The modifications required to optimize the performance with high density fuels were suggested and the expected improvement in performance was evaluated. GRA

N89-21126# Coordinating Research Council, Inc., Atlanta, GA.
CRC (COORDINATING RESEARCH COUNCIL) HOT-START AND DRIVEAWAY DRIVEABILITY PROGRAM AT HIGH AND INTERMEDIATE TEMPERATURES USING GASOLINE-ALCOHOL BLENDS
Aug. 1988 222 p
(Contract DAAK70-86-C-0011)
(AD-A202471; CRC-555) Avail: NTIS HC A10/MF A01 CSCL 21D

A cooperative CRC test program was conducted at Failure Analysis Associates Test Track in Phoenix, Arizona, from September 4 through October 4, 1985. The program investigated the hot-start driveability of thirteen 1985 model vehicles with eight hydrocarbon-alcohol blends and two hydrocarbon-only gasolines at nominal ambient temperatures of 90 and 70 F. The driveability procedure was modified to emphasize conditions which may cause fuel foaming. Carburetted, throttle-body-injected (TBI), port-fuel-injected (PFI), and port-fuel-injected turbocharged fuel systems were represented in the vehicle fleet. Ambient temperature effects were highly significant for carburetted and throttle-body-injected vehicle fuel-metering systems and for the total fleet. Carburetted vehicles were more sensitive to fuel properties and ambient conditions than fuel-injected vehicles. GRA

N89-21127# Aerojet Solid Propulsion Co., Sacramento, CA. Chemical Research and Development Dept.
SYNTHESIS OF ENERGETIC BINDERS Quarterly Report No. 7, 1 Jul. - 31 Oct. 1988
G. E. Manser 19 Dec. 1988 3 p
(Contract N00014-86-C-0164)
(AD-A203060) Avail: NTIS HC A02/MF A01 CSCL 07C

Large scale synthesis of the cubane oxetane monomer, CUBOX, was developed during the last reporting period. The key intermediate from commercially available cubane dicarboxylic acid is cubane monocarboxylic acid. Several routes to its synthesis were outlined in the Fifth Quarterly Summary. The original method supplied by Dr. Eaton was abandoned when scale-up gave poor yields. In this method, the n-hydroxypyridine-2-thion ester undergoes free radical decarboxylation in ter-butylmercaptan. Also the odor (natural gas) of ter-butylmercaptan could not be contained and this was a concern in our laboratory. GRA

N89-21128# Cambridge Univ. (England). Physics and Chemistry of Solids.
DEFORMATION, FRACTURE AND EXPLOSIVE PROPERTIES OF REACTIVE MATERIALS Final Technical Report, 12 Nov. 1985 - 12 Aug. 1988
J. E. Field, M. M. Chaudhri, J. N. Huntley, M. P. Parry, and C. M. Pereira 22 Aug. 1988 113 p
(Contract DAJA45-85-C-0052; DA Proj. 1L1-61103-BH-57)
(AD-A203083; R/D-4380A-R-AN) Avail: NTIS HC A06/MF A01 CSCL 19A

A range of techniques have been developed for studies of the behavior of explosives when impacted and for recording their strength, failure and ignition properties; these are described in Section 2. They include a drop-weight facility with transparent anvil, an instrumented drop-weight machine, a miniaturized Hopkins bar system for high rate of strain property measurement, laser speckle for studies of deformation and fracture of PBX's, an automated system for analyzing speckle and moire' records, and a heat sensitive film technique for recording the position and temperatures of hot spots. The report gives data on the behavior of polymer layers, binder materials, a range of PBX's, a range of HMX's of different particle sizes, and PETN when impacted in the drop-weight test. GRA

N89-21129# Ballistic Research Labs., Aberdeen Proving Ground, MD.
EFFECTIVE IGNITION KINETICS FOR LOVA PROPELLANT Final Report, Dec. 1984 - Sep. 1986
M. S. Miller, A. J. Kotlar, A. Cohen, D. L. Puckett, H. E. Holmes, and K. Troung Dec. 1988 24 p
(AD-A203149; BRL-MR-3724) Avail: NTIS HC A03/MF A01 CSCL 19A

Reactions leading to the ignition of nitramine propellants by hot metal fragments have been idealized as a sequence of two global reactions, the first endothermic and the second exothermic. The effective kinetics parameters were obtained by a nonlinear least squares fit of the theoretical expression for heat released (or absorbed) from an overall reaction to the endotherms and exotherms measured for the propellant in a DSC. Good representations of the data are found for a wild range in heating rates and inert gas purge flow rates. The simplified descriptions of the reactive heat release are proposed for use in a theoretical conductive ignition model being developed by K. K. Kuo. GRA

N89-21130# Utah Univ., Salt Lake City. Dept. of Chemistry.
MODERN MULTIPLE-PULSE, HIGH FIELD NMR STUDIES OF HIGH DENSITY JET FUELS Final Report
Donald W. Alderman, Janet C. Curtis, David M. Grant, Charles L. Mayne, and Ronald J. Pugmire Aug. 1988 54 p
(Contract F33615-86-C-2643)
(AD-A203320; AFWAL-TR-88-2049) Avail: NTIS HC A04/MF A01 CSCL 21D

Modern high field nuclear magnetic resonance (NMR) spectroscopic techniques have been evaluated in order to assess the capabilities of such techniques for the study of jet fuels and related materials. The utility and quantitative aspects of spectral editing techniques were evaluated. The field of 2-dimensional NMR spectroscopy is growing rapidly and several existing 2-D techniques are quite attractive for jet fuel studies. The protonhomonuclear correlation experiment is shown to provide useful information even in complex fuels. The heteronuclear correlation (1H-13C) experiment permits one to sort out overlapping lines in both the proton and carbon frequency domains. The J-coupled 2-D experiment is very useful for characterizing the nature of the carbon resonances as C, CH, CH2 and CH3 groups in jet fuels. A combination of heteronuclear correlation and J-coupled 2-D experiments allow one to sort and identify the hundreds of resonance lines in jet fuels. The 2-D inadequate method was shown to be a particularly useful experiment for determining carbon-carbon connectivities. A combination of the heteronuclear correlation, J-coupled, and INADEQUATE 2-D experiments proved to be a very powerful combination of techniques for identifying all of the major structural types of fragments in the JP-4, JP5, and MIG-25 fuels. GRA

N89-21131# Ballistic Research Labs., Aberdeen Proving Ground, MD.
DENSITY OF TRIETHANOLAMMONIUM NITRATE AND LIQUID PROPELLANT Final Report, Mar. - Sep. 1988
Ronald A. Sasse Dec. 1988 20 p
(AD-A203767; BRL-MR-3728) Avail: NTIS HC A03/MF A01 CSCL 19A

The density of hydroxylammonium nitrate based liquid propellants has been evaluated with particular attention given to the system 1845 containing triethanolammonium nitrate as fuel. It was found that density relationships of such systems could be correlated to the molten density of ingredients as opposed to crystalline density values. Equations are presented relating densities to concentrations and satisfactory comparisons are made to experimental measurements. GRA

N89-21132# Army Armament Research, Development and Engineering Center, Picatinny Arsenal, NJ. Armament Engineering Directorate.
EFFECT OF TNT MISCIBLE ADDITIVES ON THE MECHANICAL BEHAVIOR AND SHOCK SENSITIVITY OF COMPOSITION B
Rodolf W. Velicky Jan. 1989 68 p
(AD-A203968; ARAED-TR-88031) Avail: NTIS HC A04/MF A01 CSCL 19A

TNT miscible additives are expected to desensitize Composition B to thermal and shock initiation by filling the microvoids (porosity) developed during casting by TNT's liquid or solid volume differential. Evaluation of this concept pointed out that the effect these additives have on the explosive's mechanical response to stress may increase its vulnerability to ignition through adiabatic compression. The wax in regular Composition B appears to develop a mechanical behavior in its crushed material similar to that caused by substituting TNT miscible additives and, therefore, is suspected of being responsible for inbore explosions through the adiabatic compression mechanism. Experimental procedures are described which should be able to test the validity of these suspicions. In addition, an approach is described which would improve safety of RDX and TNT castings by controlling reaction rate during simple burning, and reducing its sensitivity to initiation by shock without the use of additives. GRA

N89-21133# Pennsylvania State Univ., University Park. Dept. of Aerospace Engineering.
MAGNETIC FLOWMETER MEASUREMENT OF SOLID PROPELLANT PRESSURE-COUPLED AND VELOCITY-COUPLED RESPONSES Final Report, 20 Sep. 1982 - 31 May 1988
M. M. Micci, R. D. Taylor, I. Chung, and A. Colozza Nov. 1988 87 p
(Contract F04611-82-X-0063)
(AD-A203988; AFAL-TR-88-075) Avail: NTIS HC A05/MF A01 CSCL 21I

This report documents a continuation of previous work with the pressure-coupled magnetic flowmeter burner to extend its measurements capacity to include a wider frequency spectrum and variety of propellants. The results obtained in this experimental program extend the operable frequency range of a magnetic flowmeter burner to a lower limit of 200 Hz, well into the range where intermediate frequency instabilities occur. Six formulations of AP-HTPB composite propellant (including one moderately aluminized composition) were successfully tested, and their pressure-coupled response functions measured over the burner's operating frequency range. This research also attempted to directly measure a high-frequency solid propellant velocity-coupled admittance. The velocity-coupled admittance was defined in this research as the complex ratio of the oscillatory mass-flow velocity generated from the surface of a burning propellant to the oscillatory cross-flow velocity above the surface. These oscillatory velocities were measured simultaneously inside a rectangular slab-burning

combustion chamber with a magnetic flowmeter. The admittance results show similar trends under the same burning conditions, and approximate values could be estimated. GRA

29 MATERIALS PROCESSING

Includes space-based development of products and processes for commercial applications.

For biological materials see *55 Space Biology.*

N89-21134*# Arizona Univ., Tucson. Dept. of Materials Science and Engineering.
COMPUTER SIMULATION OF MACROSEGREGATION IN DIRECTIONALLY SOLIDIFIED CIRCULAR INGOTS
K. S. Yeum and D. R. Poirier 7 Jan. 1988 65 p
(Grant NAG3-723)
(NASA-CR-182838; NAS 1.26:182838) Avail: NTIS HC A04/MF A01 CSCL 22A

The formulation and employment of a computer code designed to simulate the directional solidification of lead-rich Pb-Sn alloys in the form of an ingot with a uniform and circular cross-section are described. The formulation is for steady-state solidification in which convection in the all-liquid zone is ignored. Particular attention was given to designing a code to simulate the effect of a subtle variation of temperature in the radial direction. This is important because a very small temperature difference between the center and the surface of the ingot (e.g., less than 0.5 C) is enough to cause substantial convection within the mushy-zone when the solidification rate is approximately 0.001 to 0.0001 cm/s. Author

N89-21758*# Alabama Univ., Huntsville. Dept. of Biological Sciences.
TECHNIQUES FOR STUDYING THE EFFECTS OF MICROGRAVITY ON MODEL PARTICLE/CELL SYSTEMS
Ronald B. Young *In* Alabama Univ., Research Reports: 1988 NASA/ASEE Summer Faculty Fellowship Program Dec. 1988 17 p (For primary document see N89-21726 14-99)
Avail: NTIS HC A99/MF E03 CSCL 22A

31 ENGINEERING (GENERAL)

Includes vacuum technology; control engineering; display engineering; cryogenics; and fire prevention.

N89-21135*# National Aeronautics and Space Administration. Langley Research Center, Hampton, VA.
A MAGNETIC BEARING CONTROL APPROACH USING FLUX FEEDBACK
Nelson J. Groom Mar. 1989 28 p
(NASA-TM-100672; NAS 1.15:100672) Avail: NTIS HC A03/MF A01 CSCL 13I

A magnetic bearing control approach using flux feedback is described and test results for a laboratory model magnetic bearing actuator are presented. Test results were obtained using a magnetic bearing test fixture, which is also described. The magnetic bearing actuator consists of elements similar to those used in a laboratory test model Annular Momentum Control Device (AMCD). Author

N89-21136*# National Aeronautics and Space Administration. Langley Research Center, Hampton, VA.
ANALYTICAL MODEL OF A FIVE DEGREE OF FREEDOM MAGNETIC SUSPENSION AND POSITIONING SYSTEM
Nelson J. Groom Mar. 1989 18 p
(NASA-TM-100671; NAS 1.15:100671) Avail: NTIS HC A03/MF A01 CSCL 13H

An analytical model of a five degree of freedom magnetic suspension and positioning system is presented. The suspended element is a cylinder which is composed of permanent magnet material and the magnetic actuators are air core electromagnets mounted in a planar array. The analytical model consists of an open loop representation of the suspension and positioning system with electromagnet currents as inputs and displacements and rates in inertial coordinates as outputs. The uncontrolled degree of freedom is rotation about the long axis of the suspended cylinder. Author

N89-21137# Alabama Cryogenic Engineering, Inc., Huntsville.
A CRYOCOOLER FOR HIGH ACCELERATION APPLICATIONS Quarterly Report No. 1, 15 Sep. - 14 Dec. 1988
Michael L. Dingus 23 Dec. 1988 4 p
(Contract N00014-88-C-0571)
(AD-A203063) Avail: NTIS HC A02/MF A01 CSCL 20M

The design of the gas handling and gas panel system are finished. Baseline designs for the dewar support mount top plate have been completed. A commercially manufactured Gifford-McMahan (GM) cryocooler owned by ACE, Inc. has been identified for use as a heat sink for the heat exchanger during initial performance tests. This cryccooler would take the place of the liquid nitrogen vessel that was identified in the original proposal. Using the GM cryocooler for preliminary testing would simplify the experiments and improve reliability without adding any additional cost to the program. After preliminary testing is completed a separate unit containing the original cryostat design and the finalized Linde-Hampson cryocooler will be constructed. GRA

N89-21727*# Tennessee Univ., Tullahoma. Space Inst.
CRYOGENIC FLUID MANAGEMENT IN SPACE
Basil N. Antar *In* Alabama Univ., Research Reports: 1988 NASA/ASEE Summer Faculty Fellowship Program Dec. 1988 16 p (For primary document see N89-21726 14-99)
Avail: NTIS HC A99/MF E03 CSCL 13B

32 COMMUNICATIONS AND RADAR

Includes radar; land and global communications; communications theory; and optical communications.

For related information see also *04 Aircraft Communications and Navigation* and *17 Space Communications, Spacecraft Communications, Command and Tracking.* For search and rescue see *03 Air Transportation and Safety,* and *16 Space Transportation.*

N89-21138*# Illinois Univ., Urbana-Champaign.
A COMPARISON OF REFLECTOR ANTENNA DESIGNS FOR WIDE-ANGLE SCANNING
M. Zimmerman, S. W. Lee, B. Houshmand, Y. Rahmat-Samii, and R. Acosta Feb. 1989 30 p Presented at the NASA Technology Workshop for Earth Science Geostationary Platforms, 21-22 Sep. 1988, Hampton, VA Prepared in cooperation with Jet Propulsion Lab., California Inst. of Tech., Pasadena, and NASA, Lewis Research Center, Cleveland, OH
(NASA-TM-101459; E-4569; NAS 1.15:101459) Avail: NTIS HC A03/MF A01 CSCL 20N

Conventional reflector antennas are typically designed for up to + or - 20 beamwidths scan. An attempt was made to stretch this scan range to some + or - 300 beamwidths. Six single and dual reflector antennas were compared. It is found that a symmetrical parabolic reflector with f/D = 2 and a single circular waveguide feed has the minimum scan loss (only 0.6 dB at Theta sub 0 = 8 deg, or a 114 beamwidths scan). The scan is achieved by tilting the parabolic reflector by an angle equal to the half-scan angle. The f/D may be shortened if a cluster 7 to 19 elements instead of one element is used for the feed. The cluster excitation is adjusted for each new beam scan direction to compensate for the imperfect field distribution over the reflector aperture. The antenna can be folded into a Cassegrain configuration except that, due to spillover and blockage considerations, the amount of folding achievable is small. Author

N89-21139# Atomic Energy Research Establishment, Harwell (England). Theoretical Physics Div.
FREQUENCY DEPENDENT ULTRASONIC RAY TRACING: A PRELIMINARY STUDY

J. A. Ogilvy Jan. 1988 35 p
(AERE-R-13119; HL88/1219) Avail: NTIS HC A03/MF A01

Ray tracing theory is valid in the limit of high frequencies and gives predictions which are independent of frequency. In practice many ultrasonic inspections are carried out at low frequencies for which the predictions of ray tracing theory may not be sufficiently accurate. To help overcome the problem a modified ray tracing model was developed, whereby the material properties used in the ray tracing depend on the ray frequency. This is intended to represent the dependence on ultrasonic wavelength of the sensitivity of a ray to material inhomogeneities. The modified model was applied to three austenitic welds, for beams of frequencies between 1 and 10 MHz. The predictions show the expected trends, with lower frequencies appearing less sensitive to weld structure. There are, however, uncertainties in the model which are discussed and it is emphasized that comparison with other models and with experiments is necessary to validate the model. Author

N89-21140# Lowell Univ., MA.
RESEARCH ON ACOUSTIC COUPLING TO ELECTROMAGNETIC PULSES IN TISSUE Final Report, 15 Feb. 1987 - 29 Apr. 1988
Harry E. Moses 29 Apr. 1988 2 p
(Grant AF-AFOSR-0151-87; AF Proj. 2304)
(AD-A195644; AFOSR-88-0635TR) Avail: NTIS HC A02/MF A01 CSCL 20N

Six papers were written and submitted for publications. Topics include: A Refinement of the Radon Transform and its Inverse; Exact Solutions of the Three-Dimensional Scalar Wave Equation from the Approximate Solutions in the Wave Zone Through the Use of the Radon Transform; Exact Solutions of Maxwell's Equations from the Approximate Solutions in the Wave Zone Through the Use of the Radon Transform; Propagation of an Electromagnetic Field through a Planar Slab; and Generation of acoustic pulses in liquids by electromagnetic pulses. GRA

N89-21141*# Johns Hopkins Univ., Baltimore, MD. Dept. of Electrical and Computer Engineering.
OPTICAL COMMUNICATION WITH SEMICONDUCTOR LASER DIODE Interim Progress Report. Ph.D. Thesis
Frederic Davidson and Xiaoli Sun Mar. 1989 154 p
(Grant NAG5-356)
(NASA-CR-184817; NAS 1.26:184817) Avail: NTIS HC A08/MF A01 CSCL 17B

Theoretical and experimental performance limits of a free-space direct detection optical communication system were studied using a semiconductor laser diode as the optical transmitter and a silicon avalanche photodiode (APD) as the receiver photodetector. Optical systems using these components are under consideration as replacements for microwave satellite communication links. Optical pulse position modulation (PPM) was chosen as the signal format. An experimental system was constructed that used an aluminum gallium arsenide semiconductor laser diode as the transmitter and a silicon avalanche photodiode photodetector. The system used Q=4 PPM signaling at a source data rate of 25 megabits per second. The PPM signal format requires regeneration of PPM slot clock and word clock waveforms in the receiver. A nearly exact computational procedure was developed to compute receiver bit error rate without using the Gaussion approximation. A transition detector slot clock recovery system using a phase lock loop was developed and implemented. A novel word clock recovery system was also developed. It was found that the results of the nearly exact computational procedure agreed well with actual measurements of receiver performance. The receiver sensitivity achieved was the closest to the quantum limit yet reported for an optical communication system of this type. Author

N89-21142*# National Aeronautics and Space Administration. Lewis Research Center, Cleveland, OH.
EXTERNAL ELECTRO-OPTIC PROBING OF MILLIMETER-WAVE INTEGRATED CIRCUITS
J. F. Whitaker, J. A. Valdmanis, T. A. Jackson, K. B. Bhasin, Robert R. Romanofsky, and G. A. Mourou (Michigan Univ., Ann Arbor.) 1989 6 p Prepared for presentation at the IEEE MTT-S International Microwave Symposium, Long Beach, CA, 13-15 Jun. 1989
(NASA-TM-101990; E-4693; NAS 1.15:101990) Avail: NTIS HC A02/MF A01 CSCL 20N

An external, noncontact electro-optic measurement system, designed to operate at the wafer level with conventional wafer probing equipment and without any special circuit preparation, has been developed. Measurements have demonstrated the system's ability to probe continuous and pulsed signals on microwave integrated circuits on arbitrary substrates with excellent spatial resolution. Experimental measurements on a variety of digital and analog circuits, including a GaAs selectively-doped heterostructure transistor prescaler, an NMOS silicon multiplexer, and a GaAs power amplifier MMIC are reported. Author

N89-21143# California Univ., Berkeley. Electronics Research Lab.
CONFORMAL TIME DOMAIN FINITE DIFFERENCE METHOD OF SOLVING ELECTROMAGNETIC WAVE SCATTERING Final Report, 1 Feb. 1984 - 30 Sep. 1987
Kenneth K. Mei 28 Nov. 1988 9 p
(Contract N00014-84-K-0272)
(AD-A202434) Avail: NTIS HC A02/MF A01 CSCL 20N

The objective of this research project is to develop simple solution techniques for time domain differential equations, with conforming boundaries, air-ground interfaces and proper absorbing boundary conditions. The accomplishments in that effort is represented by numerous dissertations and journal publications. GRA

N89-21144# Air Force Inst. of Tech., Wright-Patterson AFB, OH. School of Engineering.
SPEECH RECOGNITION USING NEURAL NETS AND DYNAMIC TIME WARPING M.S. Thesis
Gary Dean Barmore Dec. 1988 291 p
(AD-A202528; AFIT/GEO/ENG/88D-1) Avail: NTIS HC A13/MF A01 CSCL 25D

The purpose of this study is to demonstrate the feasibility of using Kohonen neural nets in speech recognition. This is done by combining a first level Kohonen net with a work recognition algorithm which is either dynamic time warping (DTW) or a second Kohonen net. A digitized utterance is sliced and processed to obtain a sequence of 15 component vectors. Each component corresponds to the energy in a selected frequency range. An utterance of the digits zero through nine is used to train the first Kohonen net. After training, an utterance input to the net produces a trajectory through the net. Each point on the trajectory corresponds to a node and a particular sound. These trajectories are input to a work recognition algorithm. The first of these, DTW, compares unknown utterances to template utterances. It is a computationally intense, mathematical algorithm, and it was used primarily to test the preprocessing and neural net training procedures. The second algorithm is a second Kohonen neural net. Digits are assigned to each node so that when an unknown trajectory is input to the second net, the node that lights up identifies the utterance. Using DTW, 99 percent isolated and 93 percent connected speech recognition rates are achieved. With the second Kohonen net, isolated speech is recognized at up to 96 percent, depending upon the net format. GRA

N89-21145# Air Force Inst. of Tech., Wright-Patterson AFB, OH. School of Engineering.
A MODELING PERSPECTIVE FOR METEOR BURST COMMUNICATION M.S. Thesis
Brian C. Healy Dec. 1988 208 p
(AD-A202562; AFIT/GCS/ENG/88D-8) Avail: NTIS HC A10/MF A01 CSCL 15B

Meteor burst communication (MBC) is well suited for military applications. MBC offers better security compared to other long range communication systems because of its low probability of intercept and antijamming characteristics. MBC, however, has two major drawbacks: low throughout and long message waiting time.

In order for MBC to be used effectively, methods need to be developed to predict and optimize system performance. The result of this research is the design and development of a methodology to analyze MBC networks. A decision support system was developed that provides a simulation model for any single or multiple-link MBC network. This model runs on an IBM XT/AT compatible computer and consists of two distinct components. The first component uses engineering parameters to compute intermediate queueing characteristics used by a discrete event simulation component. The simulation component provides point estimates for throughput, message delay, and resource utilization in tabular and graphical form. The MBC process is shown to be a M/G/1 queue with server vacations. Applicable analytical equations are presented and their limitations are discussed. Analytical equations and empirical data were both used to validate the MBC performance model. GRA

N89-21146# Air Force Inst. of Tech., Wright-Patterson AFB, OH. School of Engineering.
THE USE OF CHAFF IN SPACE AS A JAMMING DEVICE BETWEEN GROUND STATIONS AND SATELLITES M.S. Thesis
Alan R. Sterns Dec. 1988 183 p
(AD-A202577; AFIT/GSO/ENP/88D-6) Avail: NTIS HC A09/MF A01 CSCL 17D

This study predicts the time evolution of the attenuation characteristics of a chaff cloud deployed in orbit around the earth. The study consists of three parts: applying the statistical mechanics solution of a satellite breakup model by William Heard of the Naval Research Laboratory, solving for particle density at any time after dispensing, and calculating the attenuation of an 8 GHz signal through the cloud. The study shows that significant levels of signal attenuation can be achieved, with attenuations of greater than -50 db lasting for several hours. GRA

N89-21147# Air Force Inst. of Tech., Wright-Patterson AFB, OH. School of Engineering.
PERFORMANCE OF AN ADAPTIVE MATCHED FILTER USING THE GRIFFITHS ALGORITHM M.S. Thesis
Peter D. Pasko Dec. 1988 146 p
(AD-A202578; AFIT/GE/ENG/88D-35) Avail: NTIS HC A07/MF A01 CSCL 17D

This thesis presents a CW and noise jamming analysis of an adaptive matched filter that: (1) uses the Griffiths algorithm, and (2) has a pseudonoise sequence as an input. The analysis is conducted over several jamming powers, frequencies, and phases. The Griffiths adaptive matched filter is shown to converge for raised cosine pulses that experience no distortion, quadratic delay distortion, and cubic delay distortion. The Griffiths adaptive matched filter diverges for pulses that experience linear delay distortion even though the convergence rate constant is within limits. Throughout the analysis the P-vector is determined apriori and held constant. The Griffiths filter is shown to converge for CW jamming and noise jamming. Noise jamming is shown to be more effective in the higher power ranges. A comparison is made between the Griffiths adaptive matched filter and an adaptive matched filter that uses the LMS algorithm. The degradation is performance of the Griffiths filter compared to an LMS filter that uses a stored reference is calculated for several selected runs. The actual computer programs used are presented in the Appendix. GRA

N89-21148# Air Force Inst. of Tech., Wright-Patterson AFB, OH. School of Engineering.
MULTIPLE MODEL ADAPTIVE TRACKING OF AIRBORNE TARGETS M.S. Thesis
John E. Norton Dec. 1988 375 p
(AD-A202696; AFIT/GA/ENG/88D-2) Avail: NTIS HC A16/MF A01 CSCL 17E

Over the past ten years considerable work has been accomplished at the Air Force Institute of Technology (AFIT) towards improving the ability of tracking airborne targets. Motivated by the performance advantages in using established models of tracking environment variables within a Kalman filter, an advanced tracking algorithm has been developed based on adaptive estimation filter structures. A multiple model bank of filters that have been designed for various target dynamics, which each accounting for atmospheric disturbance of the Forward Looking Infrared (FLIR) sensor data and mechanical vibrations of the sensor platform, outperforms a correlator tracker. The bank of filters provides the estimation capability to guide the pointing mechanisms of a shared aperture laser/sensor system. The data is provided to the tracking algorithm via an (8 x 8)-pixel tracking Field of View (FOV) from the FLIR image plane. Data at each sample period is compared by an enhanced correlator to a target template. These offsets are measurements to a bank of linear Kalman filters which provide estimates of the target's location in azimuth and elevation coordinates based on a Gauss-Markov acceleration model, and a reduced form of the atmospheric jitter model for the disturbance in the IR wavefront carrying future measurements. GRA

N89-21149# Air Force Inst. of Tech., Wright-Patterson AFB, OH. School of Engineering.
ANALYSIS AND SIMULATION OF A PSEUDONOISE SYNCHRONIZATION SYSTEM M.S. Thesis
Fernando A. Morgan Dec. 1988 130 p
(AD-A202779; AFIT/GE/ENG/88D-31) Avail: NTIS HC A07/MF A01 CSCL 17D

The purpose of this study was to investigate the performance characteristics of a synchronization system that uses an auxiliary matched filter channel to speed acquisition time. The study entailed a quantitative analysis and simulation of the matched filter channel. Following a presentation on computer simulation of communication systems, the investigation took the following approach: (1) Perform a quantitative analysis to characterize mean acquisition time under varying conditions of matched filter length, noise levels, and number of users in the system. (2) Build and validate a simulation model of the synchronization system using the Block Oriented Systems Simulator (BOSS); and (3) Test the matched filter channel against the analytic expectations for false alarm performance via the simulation model. The quantitative results indicate that the matched filter channel improves acquisition time. For signal-to-noise ratios above OdB and a particular matched filter length, the mean acquisition time was directly a function of the number of users in the system. GRA

N89-21150# Air Force Inst. of Tech., Wright-Patterson AFB, OH. School of Engineering.
IMPROVING THE SURVIVABILITY OF A STOCHASTIC COMMUNICATION NETWORK M.S. Thesis
Eugene Yim Dec. 1988 208 p
(AD-A202872; AFIT/GOR/ENS/88D-25) Avail: NTIS HC A10/MF A01 CSCL 12C

This research examined the performance of communication networks with stochastically failing components; it also investigated investment strategies to improve network performance. The performance of the network was measured in terms of the amount of information that could be handled. Since the exact calculation of expected maximum flow, which measures the performance of a stochastic network, is mathematically intractable, the bounds of expected maximum flow were investigated. The network performance, both under normal and adverse conditions, was measured analytically by formulating the problem as a linear programming model. The improvement of network performance was made by increasing the capability of the components to handle the information. Mixed integer programming models were developed to determine the investment strategy which maximized the lower bound of expected maximum flow. Because of the complexity involved in developing these models for a large network, a Prolog program was written to generate formulations for all performance and investment strategy models based on the arc-path incidence matrix. Such formulations serve as a direct input file to off-the-shelf mathematical programming packages such as the LP/MIP-83 linear and mixed integer programming system. In this research, three realistic communication networks of various sizes and topologies were analyzed. GRA

N89-21151# Applied Technology Associates, Inc., Albuquerque, NM.
LOW-COST POINTING-AND-TRACKING SYSTEM FOR OPTICAL COMMUNICATIONS (PATSOC) Final Report, Oct. 1987 - May 1988
K. A. Joyce Jun. 1988 129 p
(Contract N66001-88-C-0004)
(AD-A202921; ATA-M-SBIR-025; NOSC/TD-1287) Avail: NTIS HC A07/MF A01 CSCL 25C

This report briefly describes the development of a low-cost, ship-to ship optical communications system (OCS) under a six-month Phase 1 Small Business Innovative Research (SBIR) contract. Laser communication systems have been developed for use at fixed ground stations, aircraft, and satellites. However, they have not been successfully used in ship-to-ship applications. The difficulty is that ships have large, random linear and angular motion, which interferes with holding a narrow-beam laser on an optical receiver. This study prepared a conceptual design of a relatively short range, low-power ship-to-ship system that would operate under severe sea conditions. The emphasis of the study was on the design of a low-cost gimbal set and its associated tracking system. GRA

N89-21152# Air Force Inst. of Tech., Wright-Patterson AFB, OH. School of Engineering.
THE RADAR CROSS SECTION OF A TWO DIMENSIONAL DIELECTRIC COATED CYLINDER USING ON-SURFACE RADIATION CONDITIONS M.S. Thesis
William D. Oetting Dec. 1988 114 p
(AD-A202935; AFIT/MA/GE/88D-2) Avail: NTIS HC A06/MF A01 CSCL 17I

The purpose of this study was to use On-Surface Radiation Conditions (OSRC) to approximate the RCS of a two dimensional dielectric coated circular cylinder and compare the results to an exact solution. The comparisons were made to determine a lower and/or upper bound on the frequency, radius of curvature of the cylinder or any other pertinent parameters for a valid approximation. The problem was formulated for a circular cylinder of radius a coated by a lossy dielectric of radius b and a unit magnitude plane wave incident from the theta = 180 degrees direction with wave number k. The OSRC solution and the eigenfunction solution were nearly identical; however, the overall accuracy of the OSRC technique was shown to be governed by a complicated expression which was dependent on the dielectric material parameters as well as the kb product. The solutions were compared for three different circumstances: fixed frequency and varying dielectric layer thickness; fixed geometry and bistatic RCS. The OSRC solution was said to be good if the error was less than 2db. GRA

N89-21153# Air Force Inst. of Tech., Wright-Patterson AFB, OH. School of Engineering.
ON THE IMPULSE RESPONSE OF MONOPULSE RADARS M.S. Thesis
Dennis L. Tackett Dec. 1988 69 p
(AD-A202936; AFIT/GE/ENG/88D-52) Avail: NTIS HC A04/MF A01 CSCL 17I

The purpose of this study was to develop an analytical model to determine the response of an amplitude-amplitude monopulse radar to an impulsive input signal. This study was sponsored by the Air Force Electronic Warfare Center at Kelly AFB and represents a first step for determining if impulsive jamming has any merit against monopulse radar systems. From a literature review, it was determined that the receiver components most affected by an impulsive signal were filters in the receiver channel. Inverse Laplace transform techniques were used to determine the impulse response of a three-pole and a five-pole filter. A model of a logarithmic amplifier was also used. A FORTRAN computer program was written to simulate imbalances between the receiving channels of the radar. The results of the analyses showed that an impulsive signal would not cause a substantial tracking error until four to six seconds after the pulse arrive at the input of the filter, which is well out of the range gate. This signal may produce angle errors in the angle circuits of the radar without being detected by the range circuitry or the operator. It is recommended that experimental results using an impulsive electronic countermeasures signal against a monopulse radar be obtained. GRA

N89-21154# Air Force Inst. of Tech., Wright-Patterson AFB, OH. School of Engineering.
EFFECT OF TWO-BODY MOTION ON RADAR BEAM QUALITY FOR VARIOUS DISTRIBUTED SPARSE ARRAY CONFIGURATIONS M.S. Thesis
Michael G. Spencer Dec. 1988 88 p
(AD-A202937; AFIT/GA/AA/88D-11) Avail: NTIS HC A05/MF A01 CSCL 17I

The purpose of this thesis was to develop a computer program to model the motion and rather beam characteristics of different configurations for the distributed sparse array. The effect of the two-body motion on the beam quality of the array was analyzed. Two groups of arrays, planar and three-dimensional were considered. The planar phased arrays were rectangles and disks, and the other arrays included cones and spheres. The number of emitters in the configurations ranged from five to two hundred. The beam quality parameter was the half-power beamwidth as determined in discrete directions throughout the hemisphere below the array. An array was considered feasible if the beamwidths degraded only slightly during and orbit. The most useful configuration was found to be a sphere of randomly spaced emitters because it provided narrow beamwidths in all directions below the array. Because of the motion of the array, the beamwidths changed in a predictable, periodic manner. The half-power beamwidths actually improved in certain directions and only slightly degraded in others. The sphere also required the least number of emitters and could be used at any altitude. GRA

N89-21155# Yale Univ., New Haven, CT. Dept. of Chemistry.
A RAPID NUMERICAL PROCEDURE FOR DETERMINING AXISYMMETRIC TRANSVERSE ELECTRIC ELECTROMAGNETIC FIELDS VIA BOUNDARY INTEGRALS
Ira B. Bernstein and V. Rokhlin Sep. 1988 43 p
(Contracts N00014-83-K-0610; N00014-86-K-0310)
(AD-A202959; YALEU/DCS/RR-652) Avail: NTIS HC A03/MF A01 CSCL 20N

An important engineering problem is the determination of the electromagnetic fields in microwave systems, for example tapered waveguides, horns, scatterers, close cavities, and open resonators. Consider the case of axisymmetric transverse electric modes. Such problems for monochromatic radiation can be reduced to consideration of an elliptic partial differential equation similar to the Helmholtz equation. Methods have been developed for the direct numerical solution of the partial differential equation. Variational principles have been used to optimally determine approximate values of object of interest like reflection and transmission coefficients. An alternative approach is the reduction of the problem to consideration of an integral equation defined on the metallic walls defining the object (the boundary integral method). These have been solved for the case of scalar fields described by the Helmholtz equation. The boundary integral equation method is feasible when the Green's function is known in a computationally convenient form, and is very often much more computationally efficient than its competitors, particularly when the geometry is complex. The theory and effective numerical implementation are described of such a boundary integral equation approach for the case of an axisymmetric transverse electric electromagnetic field. GRA

N89-21156# Johns Hopkins Univ., Laurel, MD. Applied Physics Lab.
SPECTRAL CHARACTERISTICS OF HIGH FREQUENCY (HF) BACKSCATTER FOR HIGH LATITUDE IONOSPHERIC IRREGULARITIES: PRELIMINARY ANALYSIS OF STATISTICAL PROPERTIES Interim Report, Jul. 1984 - Aug. 1986
K. B. Baker, R. A. Greenwald, J. P. Villian, and S. Wing Jul. 1988 99 p
(Contract MIPR-00039-87-C-5301; AF Proj. 4600)

(AD-A202998; RADC-TR-87-284) Avail: NTIS HC A05/MF A01 CSCL 20N

OTH-B radar signals backscattered from ionospheric irregularities can be very intense, and any effort to mitigate against their influence requires knowledge of at least the Doppler shift and spread that they introduce in the backscattered signals. This report presents the Doppler spectral characteristics of HF signals backscattered from F-region ionospheric irregularities at high latitudes. The report will show that the variability in spread of the Doppler returns make it difficult to discriminate against ionospheric clutter by Doppler techniques alone. The data presented have been obtained with the Johns Hopkins University/Applied Physics Laboratory (APL) HF radar located at Goose Bay, Labrador. This is an auroral site and signals from the radar are subjected to ionospheric clutter from magnetic-field-aligned irregularities at high latitudes. The report discusses the various procedures that may be used for spectral and/or autocorrelation analysis of backscattered radar signals, the method by which these autocorrelation functions are obtained to remove contributions from ground backscatter and unwanted signal sources. The autocorrelation functions are analyzed to determine their decorrelation time and finally, the parameters are converted to Doppler velocity width and shift. GRA

N89-21157# Air Force Inst. of Tech., Wright-Patterson AFB, OH. School of Engineering.

RESPONSE SURFACE METHODOLOGY APPLIED TO THE RADAR RANGE EQUATION M.S. Thesis

Wesley D. True, Jr. Dec. 1988 144 p

(AD-A203044; AFIT/GOR/ENS/88D-23) Avail: NTIS HC A07/MF A01 CSCL 17D

The purpose of this thesis is to analyze the Electronic Warfare Integrated Reprogramming (EWIR) database elements. The integration time for continuous wave radars is illustrated. The effects of the confidence factors on data within the database is analyzed. These confidence factors affect certain parameters more than others and they also affect the radar range. Response surface methodology is used to identify the significant effects on the radar range equation, using EWIR database parameters. Linear equations are created for several radars and are compared to the actual ranges. GRA

N89-21158# Air Force Inst. of Tech., Wright-Patterson AFB, OH. School of Engineering.

PROBLEM SPECIFIC APPLICATIONS FOR NEURAL NETWORKS M.S. Thesis

Mark K. Lutey Dec. 1988 112 p

(AD-A203052; AFIT/GE/ENG/88D-23) Avail: NTIS HC A06/MF A01 CSCL 12I

This thesis examines several topics relating to neural networks. First, the investigation of the error output for a multi-layer perceptron is examined to determine if the error calculation can be modified to decrease the training time. The sigmoid function usually used by multi-layer perceptrons is investigated to determine if modifying terms within the sigmoid function will decrease training time. An improvement is found in the performance by as much as an order of magnitude. The subject of adding an additional class to the problem space is examined. Regardless of the data class added or the network size, there is no advantage to using a previously trained multi-layer perceptron as a starting state to be trained additionally to include the new data class. An investigation to determine whether a multi-layer perceptron can be used to reduce noise added to a signal. Results show that the multi-layer perception, when trained with three specific frequencies, reduced noise but would resonate at these frequencies only. The combination of using a Kohonen self-organizing feature map and a multi-layer perceptron to perform isolated word recognition is tested. An 80 percent accuracy is achieved for speaker dependent, isolated word recognition. GRA

N89-21159# Air Force Inst. of Tech., Wright-Patterson AFB, OH. School of Engineering.

AN ANALYSIS OF NOISE REDUCTION USING BACK-PROPAGATION NEURAL NETWORKS M.S. Thesis

Kevin S. Cox Dec. 1988 90 p

(AD-A203057; AFIT/GCE/ENG/88D-3) Avail: NTIS HC A05/MF A01 CSCL 12I

This thesis explored a new approach to filtering noise from digitized signals. A back-propagation neural network was trained to become a filter; and experiments were conducted using single sine wave inputs, multiple sine wave inputs, and human speech inputs. The network's output were then compared to the original signals, and the frequency spectrum was examined to determine the networks' performance. Results indicated that the networks were indeed able to filter noise. However, the network's filtering ability was strictly limited to signals from the training set. The networks were not able to generalize enough to filter signals whose frequencies had never been encountered. The ability of a back-propagation network to filter noise from actual human speech was particularly interesting, since network performance was not significantly impacted as larger amounts of noise were used to corrupt the input signals significantly impacted as larger amounts of noise were used to corrupt the input signals. The conclusion was that back-propagation neural networks can indeed be trained to become digital filters. GRA

N89-21160# Massachusetts Inst. of Tech., Cambridge. Research Lab. of Electronics.

SPEECH RECOGNITION: ACOUSTIC-PHONETIC KNOWLEDGE ACQUISITION AND REPRESENTATION Fiscal Report, 1 Oct. 1987 - 30 Sep. 1988

Victor W. Zue 30 Sep. 1988 10 p

(Contract N00014-82-K-0727)

(AD-A203081) Avail: NTIS HC A02/MF A01 CSCL 25D

The long-term research goal is to develop and implement speaker-independent continuous speech recognition systems. It is believed that the proper utilization of speech-specific knowledge is essential for such advanced systems. This research is thus directed toward the acquisition, quantification, and representation, of acoustic-phonetic and lexical knowledge, and the application of this knowledge to speech recognition algorithms. In addition, we are exploring new speech recognition alternatives based on artificial intelligence and connectionist techniques. We developed a statistical model for predicting the acoustic realization of stop consonants in various positions in the syllable template. A unification-based grammatical formalism was developed for incorporating this model into the lexical access algorithm. We provided an information-theoretic justification for the hierarchical structure of the syllable template. We analyzed segmented duration for vowels and fricatives in continuous speech. Based on contextual information, we developed durational models for vowels and fricatives that account for over 70 percent of the variance, using data from multiple, unknown speakers. We rigorously evaluated the ability of human spectrogram readers to identify stop consonants spoken by many talkers and in a variety of phonetic contexts. Incorporating the declarative knowledge used by the readers, we developed a knowledge-based system for stop identification. We achieved comparable system performance to that to the readers. GRA

N89-21161# Teledyne Geotechnical, Alexandria, VA.

FINITE-DIFFERENCE MODELING OF RAYLEIGH WAVE SCATTERING AND P-SV(Lg) COUPLING PROBLEMS Final Report, Feb. 1986 - Feb. 1988

Rong-Song Jih and Keith L. McLaughlin Mar. 1988 66 p

(Contract F19628-86-C-0054)

(AD-A203221; TGAL-88-02; AFGL-TR-88-0093) Avail: NTIS HC A04/MF A01 CSCL 08K

The work has focused on the effects of near-source heterogeneity upon seismic wave scattering and phase conversions. The basic tool was a developing 2-dimensional explicit linear finite-difference code. By use of various initial conditions and/or the principle of reciprocity, one can generate the teleseismic

response of the Earth model to a general seismic source. The propagation of Pn/Sn/Rg phases with some Arctic paths are also modeled without using the principle of reciprocity. This FORTRAN-77 code has been run under the UNIX operating system on VAX, SUN, Convex, and Celerity computers. Rayleigh waves normally incident upon 2-D shallow heterogeneity are simulated by the linear finite-difference method to study attenuation, transmission, and reflection of Rayleigh waves and and to measure the Rayleigh-to-P and -SV body wave conversion. Transmission, reflection, and scattering depend on the depth, average scale size of the heterogeneity, and the amplitude of the spatial fluctuation of velocity. Linear finite-difference (FD) method was used to compare the excitation of far-field P-and SV-waves generated by shallow dilatational sources in a suite of heterogeneous 2-D crustal models. GRA

N89-21162# Army Engineer Topographic Labs., Fort Belvoir, VA. Research Inst.
COMPUTER STRATEGY FOR DETECTING LINE FEATURES ON SIMULATED BINARY ARRAYS IN SUPPORT OF RADAR FEATURE EXTRACTION Technical Report, May - Nov. 1988
Frederick W. Rohde Nov. 1988 27 p
(AD-A203257; ETL-0478) Avail: NTIS HC A03/MF A01
CSCL 17I

Line search techniques for linear features in digital radar images are developed and described. It is shown that the search techniques can be represented by codes. The codes determine the major directions of search and removal of side branches. The testbed that is necessary to investigate and test the search techniques is described. GRA

N89-21163# Harry Diamond Labs., Adelphi, MD.
RAPID BACKSCATTER SIMULATION TECHNIQUES FOR DETAILED B-SPLINE TARGET MODELS Final Report, Oct. 1985 - Jul. 1987
Karl D. Reinig Dec. 1988 57 p
(AD-A203260; HDL-TR-2139) Avail: NTIS HC A04/MF A01
CSCL 17I

The report describes a method for rapidly evaluating the simulated radar backscatter signatures of B-spline target models moving relative to a source/receiver. A geometric optics approach is used to estimate the radar return from a complex target surface described by a bicubic B-spline mesh. The method exploits the second-order continuity of bicubic B-spline surfaces to reduce the problem of finding all the specular points associated with each new trajectory position to that of tracking the motion of existing points. In particular, it is shown that the locations of the annihilations and creations of specular paths may be predicted for an entire trajectory, eliminating the need to search the whole surface for specular points as the target moves in relation to the source/receiver. The method is shown to work for the multiple-bounce case as well. The report contains several recommendations for further exploitation of the properties of B-spline surfaces for the tracking of specular points. GRA

N89-21164# Mitre Corp., Bedford, MA.
SURVNET USER'S MANUAL Final Report
Kirsten Y. Kissmeyer Aug. 1988 48 p
(Contract F19628-86-C-0001)
(AD-A203372; MTR-10295; ESD-TR-88-268) Avail: NTIS HC
A03/MF A01 CSCL 12G

SURVNET is a connection-oriented survivable local-area communication network, allowing users at different locations on the network to communicate with each other. A connection-oriented network allows a user to communicate with only one other network user at a time. A connection is the term for a communication line between two users on a network, established by request of the users. SURVNET provides a virtual circuit of connections, enabling any user of SURVNET to connect to any other user of SURVNET. This manual provides information for using SURVNET, from assembling the system to invoking the user-level capabilities provided by SURVNET. GRA

N89-21165# La Jolla Inst., CA. Center for the Study of Nonlinear Dynamics.
IMAGING OF OCEAN WAVES BY SAR
R. L. Schult, F. S. Henyey, and J. A. Wright 1988 42 p
(Contract N00014-87-C-0687)
(AD-A203604; LJI-87-P-467) Avail: NTIS HC A03/MF A01
CSCL 17I

A model is presented for Synthetic Aperture Radar imaging of the ocean surface. The model attempts to avoid making assumptions about the relative importance of various imaging mechanisms. The model is applied to three issues, the focus setting, the asymmetry in the images obtained with obtained with opposite airplane flight directions, and the azimuthal image shift of features on range directed waves. The focus setting depends on a combination of the velocity of the pattern being imaged and on the velocity of the Bragg scatterers. The focus setting does not depend significantly on the imaging mechanism, that is velocity bunching, modulation of Bragg waves, and so on. Comparisons of our model predictions are made with the TOWARD results. A simple analytic prediction is obtained for the complete curve of the observed energy in swell versus the focus setting. The maximum of this curve is predicted to occur at one-half of the phase speed of the swell for azimuthally traveling swell and a simple explanation is provided for this result. The asymmetry in the visibility of the swell obtained by flying with or against the long waves is estimated. The asymmetry arises from competition between velocity bunching and hydrodynamic modulations. GRA

N89-21166# Naval Postgraduate School, Monterey, CA.
IMPLEMENTATION AND TESTING OF A NEW 16-PSK TRANSMITTER M.S. Thesis
George S. Brock Dec. 1988 58 p
(AD-A203936) Avail: NTIS HC A04/MF A01 CSCL 12I

The work reported herein deals with the design, implementation, and testing the performance of a specific 16-PSK transmitter for use in conjunction (in future tests) with a specific direct bit detection receiver. A specific design procedure is utilized for generating sets of 2(n) phase shifted sinusoids with constant phase difference, each of which represents an n bit symbol. The design of the 16-PSK transmitter is extendable to the implementation of higher order M-PSK transmitter, i.e., M = 32, 64, etc. The procedure utilizes a shift register and associated digital devices to produce a set of square waveforms each of which is equally and successively delayed by a fixed time increment. Frequency selective filtering is then employed to convert this collection of square waves to a set of sinusoids while maintaining the time and therefore the desired phase relationship amongst members of the set. This implementation made it possible to produce an offset 16-PSK signal constellation whose members were all of equal amplitude and possessed the desired phase relationship to within one tenth of a degree. The signal constellation was highly stable and displayed an average phase drift amongst its members of less than three tenths of a degree after five and one half hours of operation. Photographs of signals in the time domain and displays of signals in the frequency domain are presented in order to highlight the important features of the system's performance. (RH) GRA

N89-21167# Princeton Univ., NJ. Information Sciences and Systems Lab.
A ROBUST ADAPTIVE ARRAY STRUCTURE USING THE SOFT CONSTRAINED LMS ALGORITHM
Gary F. Hatke and Stuart C. Schwartz Jul. 1988 6 p
(Contract N00014-88-K-0162)
(AD-A203959) Avail: NTIS HC A02/MF A01 CSCL 12E

This paper presents a new algorithm for adaptive beamforming which is robust to both desired signal misalignment and array geometry imperfections. It extends the work done by Jablon and Widrow by utilizing a priori knowledge of the desired signal direction to generate new soft constraints on the pattern of the array. GRA

N89-21168*# Eastman Kodak Co., Rochester, NY. Advanced Technology Products.
APPLICATION OF A SINGLE AREA ARRAY DETECTOR FOR ACQUISTION, TRACKING AND POINT-AHEAD IN SPACE OPTICAL COMMUNICATIONS
D. L. Clark, M. Cosgrove, R. VanVranken, H. Park, and M. Fitzmaurice (National Aeronautics and Space Administration. Goddard Space Flight Center, Greenbelt, MD.) 1989 22 p Submitted for publication
(Contract NAS5-30158)
(NASA-CR-183423; NAS 1.26:183423) Avail: NTIS HC A03/MF A01 CSCL 17B

Functions of acquisition, tracking, and point-ahead in space optical communications are being combined into a single system utilizing an area array detector. An analysis is presented of the feasibility concept. The key parameters are: optical power less than 1 pW at 0.86 micrometer, acquisition in less than 30 seconds in an acquisition field of view (FOV) of 1 mrad, tracking with 0.5 microrad rms noise at 1000 Hz update rate, and point ahead transfer function precision of 0.25 microrad over a region of 150 microrad. Currently available array detectors were examined. The most demanding specifications are low output noise, a high detection efficiency, a large number of pixels, and frame rates over 1kHz. A proof of concept (POC) demonstration system is currently being built utilizing the Kodak HS-40 detector (a 128 x 128 photodiode array with a 64 channel CCD readout architecture which can be operated at frame rates as high as 40,000/sec). The POC system implements a windowing scheme and special purpose digital signal processing electronic for matched filter acquisition and tracking algorithms. Author

N89-21505# Harry Diamond Labs., Adelphi, MD. Advanced Electronics Systems Lab.
A RAPID-BACKSCATTER SIMULATION TECHNIQUE FOR COMPLEX B-SPLINE TARGET MODELS
Karl D. Reinig *In* Army Research Office, Transactions of the Fifth Army Conference on Applied Mathematics and Computing Mar. 1988 p 331-344 (For primary document see N89-21490 14-59)
Avail: NTIS HC A99/MF E03 CSCL 20N

N89-21515# Defence Research Establishment Valcartier (Quebec).
PROPAGATOR MATRICES IN THE SOLUTION OF EMP PROBLEMS
K. C. Heaton *In* Army Research Office, Transactions of the Fifth Army Conference on Applied Mathematics and Computing Mar. 1988 p 475-514 (For primary document see N89-21490 14-59)
Avail: NTIS HC A99/MF E03 CSCL 20N

33 ELECTRONICS AND ELECTRICAL ENGINEERING

Includes test equipment and maintainability; components, e.g., tunnel diodes and transistors; microminiaturization; and integrated circuitry.

For related information see also *60 Computer Operations and Hardware* and *76 Solid-State Physics*.

N89-21169*# National Aeronautics and Space Administration. Lewis Research Center, Cleveland, OH.
ANALYTICAL AND EXPERIMENTAL PROCEDURES FOR DETERMINING PROPAGATION CHARACTERISTICS OF MILLIMETER-WAVE GALLIUM ARSENIDE MICROSTRIP LINES
Robert R. Romanofsky Mar. 1989 21 p
(NASA-TP-2899; E-4273; NAS 1.60:2899) Avail: NTIS HC A03/MF A01 CSCL 20N

In this report, a thorough analytical procedure is developed for evaluating the frequency-dependent loss characteristics and effective permittivity of microstrip lines. The technique is based on the measured reflection coefficient of microstrip resonator pairs. Experimental data, including quality factor Q, effective relative permittivity, and fringing for 50-omega lines on gallium arsenide (GaAs) from 26.5 to 40.0 GHz are presented. The effects of an imperfect open circuit, coupling losses, and loading of the resonant frequency are considered. A cosine-tapered ridge-guide text fixture is described. It was found to be well suited to the device characterization. Author

N89-21170# National Inst. of Standards and Technology, Gaithersburg, MD.
CENTER FOR ELECTRONICS AND ELECTRICAL ENGINEERING TECHNICAL PROGRESS BULLETIN COVERING CENTER PROGRAMS, APRIL TO JUNE 1988 WITH 1988 CEEE EVENTS CALENDAR
E. Jane Walters, comp. Oct. 1988 28 p
(PB89-123137; NISTIR-88/3866) Avail: NTIS HC A03/MF A01 CSCL 09C

The twenty-third issue of the quarterly publication provides information on the technical work of the National Institute of Standards and Technology (formerly National Bureau of Standards) Center for Electronics and Electrical Engineering. This issue of the CEEE Technical Progress Bulletin covers the second quarter of calendar year 1988. Abstracts are provided by technical area for both published papers and papers approved by NIST for publication. GRA

N89-21171*# National Aeronautics and Space Administration. Lewis Research Center, Cleveland, OH.
DESIGN, FABRICATION, AND PERFORMANCE OF BRAZED, GRAPHITE ELECTRODE, MULTISTAGE DEPRESSED COLLECTORS WITH 500-W, CONTINUOUS WAVE, 4.8- TO 9.6-GHz TRAVELING-WAVE TUBES
Peter Ramins and Ben Ebihara Mar. 1989 18 p
(NASA-TP-2904; E-4361; NAS 1.60:2904) Avail: NTIS HC A03/MF A01 CSCL 09A

A small, isotropic graphite electrode, multistage depressed collector (MDC) was designed, fabricated, and evaluated in conjunction with a 500-W, continuous wave (CW), 4.8- to 9.6-GHz traveling-wave tube (TWT). The carbon electrode surfaces were used to improve the TWT overall efficiency by minimizing the secondary electron emission losses in the MDC. The design and fabrication of the brazed graphite MDC assembly are described. The brazing technique, which used copper braze filler metal, is compatible with both vacuum and the more commonly available hydrogen atmosphere brazing furnaces. The TWT and graphite electrode MCC bakeout, processing, and outgassing characteristics were evaluated and found to be comparable to TWT's equipped with copper electrode MDC's. The TWT and MDC performance was optimized for broadband CW operation at saturation. The average radiofrequency (RF), overall, and MDC efficiencies were 14.9, 46.4, and 83.6 percent, respectively, across the octave operating band. A 1500-hr CW test, conducted without the use of an appendage ion pump, showed no gas buildup and excellent stability of the electrode surfaces. Author

N89-21172*# National Aeronautics and Space Administration. Lewis Research Center, Cleveland, OH.
CHANNELIZED COPLANAR WAVEGUIDE: DISCONTINUITIES, JUNCTIONS, AND PROPAGATION CHARACTERISTICS
Rainee N. Simons (Case Western Reserve Univ., Cleveland, OH.), George E. Ponchak, Konstantinos S. Martzaklis, and Robert R. Romanofsky 1989 7 p Proposed for presentation at the 1989 IEEE MTT-S International Microwave Symposium, Long Beach, CA, 13-15 Jun. 1989
(NASA-TM-101483; E-4616; NAS 1.15:101483) Avail: NTIS HC A02/MF A01 CSCL 09A

A new variant of CPW which has been termed channelized CPW, CCPW, is presented. Measured and computed propagation characteristics are presented. Lumped equivalent circuit element values for a CCPW open circuit and right angle bend have been obtained. CCPW power divider junctions and a coax-to-CCPW in-phase, radial power divider are also presented. Author

N89-21173*# Honeywell, Inc., Bloomington, MN. Sensors and Signal Processing Lab.
DEVELOPMENT OF GALLIUM ARSENIDE HIGH-SPEED, LOW-POWER SERIAL PARALLEL INTERFACE MODULES: EXECUTIVE SUMMARY Final Report
31 May 1988 38 p
(Contract NAS3-24676)
(NASA-CR-182272; NAS 1.26:182272) Avail: NTIS HC A03/MF A01 CSCL 09A

Final report to NASA LeRC on the development of gallium arsenide (GaAS) high-speed, low power serial/parallel interface modules. The report discusses the development and test of a family of 16, 32 and 64 bit parallel to serial and serial to parallel integrated circuits using a self aligned gate MESFET technology developed at the Honeywell Sensors and Signal Processing Laboratory. Lab testing demonstrated 1.3 GHz clock rates at a power of 300 mW. This work was accomplished under contract number NAS3-24676. Author

N89-21174*# National Aeronautics and Space Administration. Lewis Research Center, Cleveland, OH.
RESTRICTIVE LOADS POWERED BY SEPARATE OR BY COMMON ELECTRICAL SOURCES
J. Appelbaum Mar. 1989 20 p
(NASA-TM-102008; E-4594; NAS 1.15:102008) Avail: NTIS HC A03/MF A01 CSCL 09C

In designing a multiple load electrical system, the designer may wish to compare the performance of two setups: a common electrical source powering all loads, or separate electrical sources powering individual loads. Three types of electrical sources: an ideal voltage source, an ideal current source, and solar cell source powering resistive loads were analyzed for their performances in separate and common source systems. A mathematical proof is given, for each case, indicating the merit of the separate or common source system. The main conclusions are: (1) identical resistive loads powered by ideal voltage sources perform the same in both system setups, (2) nonidentical resistive loads powered by ideal voltage sources perform the same in both system setups, (3) nonidentical resistive loads powered by ideal current sources have higher performance in separate source systems, and (4) nonidentical resistive loads powered by solar cells have higher performance in a common source system for a wide range of load resistances. Author

N89-21175# Massachusetts Inst. of Tech., Cambridge. Lab. of Electronics.
TIME DOMAIN WAVE PROPAGATION IN MULTILAYERED INTEGRATED CIRCUITS Final Report, 1 Aug. 1986 - 30 Sep. 1988
Jin A. Kong 1 Nov. 1988 87 p
(Contract N00014-86-K-0533)
(AD-A202427) Avail: NTIS HC A05/MF A01 CSCL 20N

Under the sponsorship of the ONR Contract N00014-86-K-0533 we have published 15 referenced journal and conference papers on time domain electromagnetic waves in multilayer media. A rigorous dyadic Green's function formulation in the spectral domain is used to study to dispersion characteristics of signal strip lines in the presence of metallic crossing strips. A set of coupled vector integral equations for the current distribution on the conductors is derived. Galerkin's method is then applied to derive the matrix eigenvalue equation for the propagation constant. The dispersion properties of the signal lines are studied for both cases of finite and infinite length crossing strips. The effects of the structure dimensions on the passband and stopband characteristics are investigated. For crossing strips of finite length, the stopband is mainly and affected by the period, the crossing strip length, and the separation between the signal and the crossing strips. For crossing strips of infinite length carrying traveling waves, attenuation along the signal line exists over the whole frequency range of operation. In order to provide shorter interconnects between chips, modern multilayer integrated circuit packages for high-performance mainframe computers employ not only conventional striplines but vertical transmission lines or so-called vias as well. GRA

N89-21176# North Carolina State Univ., Raleigh. Dept. of Materials Science and Engineering.
CONTINUED DEVELOPMENT AND CHARACTERIZATION OF DOPED LAYERS, CONTACTS AND ASSOCIATED ELECTRONIC DEVICES IN SILICON CARBIDE Annual Letter Report, 1 Apr. - 30 Sep. 1988
R. F. Davis 31 Oct. 1988 31 p
(Contract N00014-88-K-0341)
(AD-A202450; NCS-MAT/E-001) Avail: NTIS HC A03/MF A01 CSCL 20L

The primary thrust of research of this period has been to deposit and characterize the contact materials of TaSi2 and Al on n- and p-type material, respectively. Auger electron spectroscopy detected some oxygen throughout the thickness of these films. Current voltage characteristics were non-linear and highly resistive due to oxygen contamination in the films. A new ultra-high vacuum deposition chamber is being constructed to deposit pure contacts. Rectifying contacts of Au, Pt, and PtSix were also studied. Pt surpassed Au in its rectifying properties. Ion implantation into alpha and beta SiC at room temperature and 550 C were also conducted. A new capacitance voltage system was purchased and commissioned. GRA

N89-21177# Air Force Inst. of Tech., Wright-Patterson AFB, OH. School of Engineering.
A MULTIPLE-VALUED LOGIC SYSTEM FOR CIRCUIT EXTRACTION TO VHDL 1076-1987 M.S. Thesis
Michael A. Dukes Sep. 1988 167 p
(AD-A202646; AD-E900870; AFIT/GE/ENG/88S-1) Avail: NTIS HC A08/MF A01 CSCL 09A

Multiple-valued logic is a topic of concern for modeling standards in the VHSIC Hardware Description Language, VHDL 1076-1987. With the various forms of layout styles in MOS device there exist different strengths of electrical signals propagated throughout a circuit. Additionally, logic extraction to VHDL of VLSI layout designs may contain left over transistors that must be modeled correctly in VHDL. A multiple-valued logic system can adequately model signals with different strengths as well as conflicts between signal values. Once a multiple-valued logic system is defined, a logic extraction system may then produce VHDL for hardware component representations down to the transistor level. The goal of this thesis is to present a ten-level multiple-valued logic system and provide a Prolog-based logic extraction tool for generation of VHDL from a transistor net list. The Prolog-based logic extraction system will also provide groundwork for further research in the area of formal verification with VHDL. Various tools using symbolic representations and multiple-valued logic are essential in a CAD environment where logic extraction from layout to VHDL is incorporated into validation and verification. GRA

N89-21178# Air Force Inst. of Tech., Wright-Patterson AFB, OH. School of Engineering.
THE 8755 EMULATOR DESIGN M.S. Thesis
John L. Woods Dec. 1988 207 p
(AD-A202649; AD-E900870; AFIT/GE/ENG/88D-63) Avail: NTIS HC A10/MF A01 CSCL 12F

The purpose of this design project was to design and build a device which could replace the INTEL 8755 microchip in experimental circuit designs. The 8755 emulator provides the standard input/output ports and 2048 bytes of memory. It also provides the ability to load this memory from the z-100, to single-step a target circuit, break on a specified address, and control the I/O ports from the Z-100. The design had 5 basic objectives: (1) Allow the user to download 8755 emulation memory; (2) Allow control of the target program from the z-100 microcomputer; (3) Provide a single step capability; (4) Provide breaking at a specified address; and (5) Allow the user to set or change the emulated 8755 input/output ports. This thesis describes the standard memory and input/output capabilities of the 8755. It describes in detail the emulator enhancement features to the standard 8755. The hardware circuits used to implement the

emulator are discussed at the block diagram, component, and signal levels. It concludes with a detail description of the emulator software used to control the hardware. GRA

N89-21179# Lockheed Electronics Co., Plainfield, NJ.
RELIABILITY/MAINTAINABILITY/TESTABILITY DESIGN FOR DORMANCY Final Report, Mar. 1985 - Feb. 1988
Robert M. Seman, Julius M. Etzl, and Arthur W. Purnell May 1988 418 p
(Contract F30602-85-C-0040)
(AD-A202704; RADC-TR-88-110) Avail: NTIS HC A18/MF A01 CSCL 09A

This document has been prepared as a tool for designers of dormant military equipment and systems. The purpose of this handbook is to provide design engineers with Reliability/Maintainability/Testability design guidelines for systems which spend significant portions of their life cycle in a dormant state. The dormant state is defined as a nonoperating mode where a system experiences very little or no electrical stress. The guidelines in this report present design criteria in the following categories: (1) Part Selection and Control; (2) Derating Practices; (3) Equipment/System Packaging; (4) Transportation and Handling; (5) Maintainability Design; (6) Testability Design; (7) Evaluation Methods for In-Plant and Field Evaluation; and (8) Product Performance Agreements. Whereever applicable, design guidelines for operating systems were included with the dormant design guidelines. This was done in an effort to produce design guidelines for a more complete life cycle. Although dormant systems spend significant portions of their life cycle in a nonoperating mode, the designer must design the system for the complete life cycle, including nonoperating as well as operating modes. The guidelines are primarily intended for use in the design of equipment composed of electronic parts and components. However, they can also be used for the design of systems which encompass both electronic and nonelectronic parts, as well as for the modification of existing systems. GRA

N89-21180# Air Force Inst. of Tech., Wright-Patterson AFB, OH. School of Engineering.
INVESTIGATION OF THE IMPEDANCE MODULATION OF THIN FILMS WITH A CHEMICALLY-SENSITIVE FIELD-EFFECT TRANSISTOR M.S. Thesis
John M. Wiseman 5 Dec. 1988 252 p
(AD-A202766; AFIT/GE/ENG/88D-61) Avail: NTIS HC A12/MF A01 CSCL 09A

This study resulted in the design and fabrication of a Chemically-Sensitive Field-Effect Transistor (CHEMFET) with an interdigitated gate electrode structure. The electrical performance of the CHEMFET, both in the time-domain and frequency domain, was evaluated for detecting changes in the molecular structure and chemical composition in three thin films: an epoxy, copper phthalocyanine (CuPc), and acetylcholinesterase (ACHE). The change in the chemical state of a film was manifested as a change in the electrical impedance of the interdigitated gate electrode structure. For the epoxy, its molecular structure changed as a result of the curing reaction. To induce a change in the chemical state of the CuPc and ACHE films they were exposed to part-per billion concentrations of a challenge gas, either nitrogen dioxide (NO2) or the the organophosphorus compound, diisopropyl methylphosphonate (DIMP). The results clearly show that the CHEMFET can detect chemical and structural changes in an epoxy and CuPc film. The sensitivity of the ACHE film was not unequivocally determined due to long term drift in the ACHE film's electrical properties. The most remarkable result of this effort was the demonstration of a unique selectivity feature in the CHEMFET's frequency dependent response to a challenge gas. The examination of the relative changes in the electrical properties of the CHEMFET at different frequencies showed that the CHEMFET can be used to distinguish between NO2 and Dimp EXPOSURE. GRA

N89-21181# Giner, Inc., Waltham, MA.
ADVANCED DOUBLE LAYER CAPACITOR Quarterly Report No. 2, 1 Aug. - 31 Oct. 1988
Anthony B. LaConti and Philip Lessner Dec. 1988 9 p
(Contract N00014-88-C-0391; ARPA Order 9526)
(AD-A203059; C87A-25-2) Avail: NTIS HC A02/MF A01 CSCL 09A

The overall goal of this project is to develop electrochemical capacitors utilizing an electrode-solid ionomer electrolyte composite. An advantage of these devices over conventional double layer capacitors would be the absence of free liquid electrolyte and thus greater safety and reliability. In the second quarter, we have continued our efforts on Task IA of the Work Plan. Specifically we have: (1) fabricated noble metal oxides of the RuOx type into electrodes, (2) formed metal oxide-Nafion electrode composites, (3) integrally bonded Nafion membranes to composite electrode structures, (4) constructed electrode holders for properly gasketing these electrodes during testing, and (5) begun to set up an ac impedance test system for characterizing the response of these electrodes. GRA

N89-21182# Massachusetts Inst. of Tech., Lexington. Lincoln Lab.
MICROWAVE POWER AMPLIFIER ANALYSIS AND DESIGN
L. J. Kushner 16 Dec. 1988 54 p
(Contract F19628-85-C-0002)
(AD-A203170; TR-812; ESD-TR-88-181) Avail: NTIS HC A04/MF A01 CSCL 09A

Output power, efficiency, power dissipation, and optimum load-resistance expressions for idealized microwave Class A and B power amplifiers are derived based on a waveform analysis. The effects of device transconductance variation with bias and circuit harmonic termination are examined. Large-signal gain is determined by calculating the input power needed to produce a given output power. Both closed-form and CAD-based solutions are presented, all based on device dc I-V characteristics and small-signal models. A practical power amplifier design procedure is given and used to design a 22-GHz permeable-based transistor (PBT) power amplifier. Although the analysis and design results presented here are useful by themselves, they are also intended to be used in conjunction with other CAD and measurement techniques (such as harmonic balance and load pull) to arrive at a starting point. Device designers also should find these results useful, allowing them to predict how changes in device parameters will affect microwave power amplifier performance. GRA

N89-21183# TRW Space Technology Labs., Redondo Beach, CA. Applied Technology Div.
DEMONSTRATION OF SQUID PARAMETRIC AMPLIFIER Final Report, 1 Oct. 1983 - 30 Jun. 1988
25 Oct. 1988 71 p
(Contract N00014-81-C-2495)
(AD-A203252) Avail: NTIS HC A04/MF A01 CSCL 20L

Superconductive electronics incorporating Josephson junctions and SQUIDs (Superconducting Quantum Interference Devices) offers electronic systems of unrivaled sensitivity, speed, and efficiency which are important for the Navy and other DoD agencies. Under this contract, TRW has developed microwave parametric amplifiers based upon Josephson junction SQUIDs operating at X-band and K-band with noise levels approaching the quantum limit. This development makes possible microwave and millimeter-wave heterodyne receivers with noise temperatures below 10 k beyond 100 GHz. The amplifiers demonstrated here can serve as RF preamplifiers which set the noise figure in advance of the mixer in receiver systems. As the front-end RF amplifier, this device will have much greater electromagnetic survivability than conventional mixer diodes. The amplifier developed under this contract served as the model for an integrated receiver under development for SDIO/IST. This research has demonstrated 10 dB gain amplifier operated at X-band with measured noise temperature equal to 6 K. GRA

N89-21184# Massachusetts Inst. of Tech., Cambridge. Research Lab. of Electronics.
FOCUSED ION BEAM FABRICATION OF GRADED CHANNEL FIELD EFFECT TRANSISTORS (FETs) IN GaAs AND Si Final Report, 1 Jul. 1985 - 30 Sep. 1988
John Melngailis 21 Nov. 1988 74 p
(Contract MDA903-85-C-0215)
(AD-A203365) Avail: NTIS HC A04/MF A01 CSCL 09A

The aim of our focused ion beam research program at M.I.T. is to exploit the unique capabilities of this novel technology in fabricating devices which have a lateral gradient of doping. (This program of research will be continued so that this final report will be exhaustive.) Using internal institute funds, M.I.T. purchased a focused ion beam system capable of producing beams of the common dopants of Si and GaAs (i.e., B, Si, and Be) at energies up to 300 KeV. In order to carry out the proposed implantations the system needed to be upgraded in several ways. Pattern writing software was developed, as well as software for translating patterns written in MAGIC, a layout system in use at M.I.T., into the FIB format. To achieve the minimum beam diameter the ion column had to be realigned mechanically and electrical noise needed to be reduced in the circuits which deflect the beam. With the upgraded system we have written patterns in PMMA with 50 nm line width, and achieved metal lift-off of 50 nm width lines. GRA

N89-21185# Texas Univ., Austin. Microwave Lab.
THE BOUNDARY-INTEGRAL METHOD FOR PLANAR MICROSTRIP CIRCUITS
Sanchi S. Chang and Tatsuo Itoh Dec. 1988 45 p
(Contract DAAL03-88-K-0005)
(AD-A203715; MW-88-P-5; ARO-25045.11-EL) Avail: NTIS HC A03/MF A01 CSCL 09A

The main subject of this thesis is to develop a general purpose computer program for the analysis containing a planar microstrip circuit arbitrarily shaped. Based on the boundary-integral method (also called the contour-integral method), the analyses of circuits containing right - angled microstrip bend with or without a miter cut and circuits of a T-junctions with or without a V-shaped cut are presented in this thesis. Scattering parameters and other related data of the circuits are calculated and presented. They agree well with the published data. It is shown that the boundary-integral method is an applicable and effective computer-aided design tool for microstrip circuits of more complicated geometries. GRA

N89-21186# Syracuse Univ., NY. Dept. of Electrical and Computer Engineering.
A GENERALIZED APPROACH TO DIRECTION FINDING Final Technical Report, May 1986 - May 1987
Hamza Ouibrahim and Donald Weiner Aug. 1988 127 p
(Contract F30602-81-C-0169)
(AD-A203768; RADC-TR-88-176) Avail: NTIS HC A07/MF A01 CSCL 17K

The problem of direction finding with a sensor array in a multiple source environment is addressed. In this research a generalized formulation to the problem is developed. In the generalized formulation a matrix pencil is constructed. The rank reducing values are shown to contain the information needed to estimate the angles of arrival. It is also shown that several different nonsearch procedures are special cases of the generalized approach. The attractiveness of these techniques is their computational efficiency. The techniques differ depending upon the manner in which either the measured data is processed, or the angular information is extracted from the resulting equations. The pencil theorem establishes the relationship between the rank reducing values and the functional form generated by the operators applied to the measurements. This generalized approach allows for the inclusion of prefiltering before applying an operator to the measurements. Based on the generalized approach a new nonsearch direction of arrival estimation procedure is presented which is shown to be valid for the case of coherent sources. GRA

N89-21187# Princeton Univ., NJ. Information Sciences and Systems Lab.
SOFT CONSTRAINED LMS ALGORITHMS: A ROBUST PROCEDURE FOR SIGNAL MISALIGNMENT
Gary F. Hatke and Stuart C. Schwartz Nov. 1988 6 p Prepared for presentation at the 22nd Asilomar Conference on Signals, Systems and Computers, 1989
(Contract N00014-88-K-0162)
(AD-A203880) Avail: NTIS HC A02/MF A01 CSCL 09A

This paper presents a new algorithm for both broadband and narrowband adaptive beamforming which is robust to both desired signal misalignment and array imperfections. By utilizing available a priori information, the new algorithm minimizes desired signal cancellation by introducing new soft constraints which are incorporated into the LMS adaptation algorithm. GRA

N89-21188# Imatran Voima Oy, Helsinki (Finland).
ON-LINE LOCATION OF PARTIAL DISCHARGES IN POWER TRANSFORMER THROUGH ACOUSTIC EMISSION
Heikki Eronen Jun. 1988 31 p In FINNISH; ENGLISH summary
(DE88-757043; IVO-A-04/88; ISBN-951-9100-89-X; ISSN-0782-7415) Avail: NTIS (US Sales Only) HC A03/MF A01

The detection and location of partial discharge faults in power transformers make it possible to minimize the repairing costs and time out of use. This report deals with a movable equipment, which was designed for on-line locating of partial discharges. A partial discharge generates oscillations at the ultrasonic frequency range, which propagate through the surrounding insulation materials to the walls of a transformer tank. These signals are possible to be indicated by acoustic emission transducers and measuring of differences in propagation times at different points makes it possible to calculate the location of a discharge. The measuring equipment consists of four acoustic emission transducers with their amplifiers, a signal memory recorder and a microcomputer. When the transducers detect a signal, the recorder reads it in its memory, where it can be manipulated and averaged for damping of noise. The microcomputer reads the signals coming from different transducers from the memory of the recorder and calculates the propagation times at different channels by which it locates the discharge. Tests results are given. DOE

N89-21189# Oak Ridge National Lab., TN.
EVALUATION OF TIME DELAY REQUIREMENTS FOR CLOSED-LOOP STABILITY USING CLASSICAL AND MODERN METHODS
G. V. Murphy and J. M. Bailey 1989 4 p Presented at the 21st Southeastern Symposium on System Theory, Tallahassee, FL, 26 Mar. 1989 Prepared in cooperation with Tennessee Univ., Knoxville
(Contract DE-AC05-84OR-21400)
(DE89-006417; CONF-890361-1) Avail: NTIS HC A02/MF A01

This paper uses classical and modern methods for computing the maximum allowable time delay a closed-loop system can tolerate before destabilizing. Maximum allowable time delays are computed using both methods for three control systems previously designed for a simple process. The three control systems are proportional plus integral (PI), linear quadratic Gaussian (LQG), and linear quadratic Gaussian with loop transfer recovery (LQG/LTR). The allowable time delays obtained from the modern method are compared with the results of the well established classical method for single input-single output (SISO) systems. DOE

N89-21499# Massachusetts Inst. of Tech., Cambridge. Dept. of Mathematics.
OPTIMAL DESIGN OF A TWO-WAY CONDUCTOR
Gilbert Strang and Robert Kohn (New York Univ., New York.) *In* Army Research Office, Transactions of the Fifth Army Conference on Applied Mathematics and Computing Mar. 1988 p 161-182 Submitted for publication Sponsored in part by NSF, Washington,

D.C. (For primary document see N89-21490 14-59)
(Contracts DAAL03-86-K-0171; N00014-83-K-0536)
Avail: NTIS HC A99/MF E03 CSCL 09K

N89-21730*# Tennessee Univ., Chattanooga. Center of Excellence for Computer Applications.
SIRE: A SIMPLE INTERACTIVE RULE EDITOR FOR NICBES
Alex Bykat *In* Alabama Univ., Research Reports: 1988 NASA/ASEE Summer Faculty Fellowship Program Dec. 1988 22 p (For primary document see N89-21726 14-99)
Avail: NTIS HC A99/MF E03 CSCL 09A

34 FLUID MECHANICS AND HEAT TRANSFER

Includes boundary layers; hydrodynamics; fluidics; mass transfer; and ablation cooling.

For related information see also *02 Aerodynamics* and *77 Thermodynamics and Statistical Physics.*

N89-21190*# National Aeronautics and Space Administration. Ames Research Center, Moffett Field, CA.
COMPUTATIONAL STUDIES OF AN IMPULSIVELY STARTED VISCOUS FLOW
Sanford S. Davis Dec. 1988 7 p Proposed for presentation at the 4th Asian Congress of Fluid Mechanics, Hong Kong, 19-23 Aug. 1989
(NASA-TM-101037; A-88295; NAS 1.15:101037) Avail: NTIS HC A02/MF A01 CSCL 20D

Progress in validating incompressible Navier-Stokes codes is described using a predictor/corrector scheme. The flow field under study is the impulsive start of a circular cylinder and the unsteady evolution of the separation bubble. In the current code, a uniform asymptotic expansion is used as an initial condition in order to correctly capture the initial growth of the vortex sheet. Volocity fields at selected instants of time are decomposed into vectorial representations of Navier-Stokes equations which are then used to analyze dominant contributions in the boundary-layer region.
Author

N89-21191*# Hughes Aircraft Co., Torrance, CA. Electron Dynamics Div.
HIGH CAPACITY DEMONSTRATION OF HONEYCOMB PANEL HEAT PIPES Final Technical Report
H. J. Tanzer Feb. 1989 73 p
(Contract NAS1-17674; NASA Order W-30851)
(NASA-CR-181776; NAS 1.26:181776) Avail: NTIS HC A04/MF A01 CSCL 20D

The feasibility of performance enhancing the sandwich panel heat pipe was investigated for moderate temperature range heat rejection radiators on future-high-power spacecraft. The hardware development program consisted of performance prediction modeling, fabrication, ground test, and data correlation. Using available sandwich panel materials, a series of subscale test panels were augumented with high-capacity sideflow and temperature control variable conductance features, and test evaluated for correlation with performance prediction codes. Using the correlated prediction model, a 50-kW full size radiator was defined using methanol working fluid and closely spaced sideflows. A new concept called the hybrid radiator individually optimizes heat pipe components. A 2.44-m long hybrid test vehicle demonstrated proof-of-principle performance.
Author

N89-21192*# National Aeronautics and Space Administration. Lewis Research Center, Cleveland, OH.
NUMERICAL COMPUTATION OF SHOCK WAVE-TURBULENT BOUNDARY LAYER INTERACTION IN TRANSONIC FLOW OVER AN AXISYMMETRIC CURVED HILL
S.-W. Kim Feb. 1989 31 p
(NASA Order C-99066-G)
(NASA-TM-101473; E-4589; ICOMP-89-3; NAS 1.15:101473)
Avail: NTIS HC A03/MF A01 CSCL 20D

A control-volume based finite difference computation of a turbulent transonic flow over an axisymmetric curved hill is presented. The numerical method is based on the SIMPLE algorithm, and hence the conservation of mass equation is replaced by a pressure correction equation for compressible flows. The turbulence is described by a k-epsilon turbulence model supplemented by a near-wall turbulence model. In the method, the dissipation rate in the region very close to the wall is obtained from an algebraic equation and that for the rest of the flow domain is obtained by solving a partial differential equation for the dissipation rate. The other flow equations are integrated up to the wall. It is shown that the present turbulence model yields the correct location of the compression shock. The other computational results are also in good agreement with experimental data.
Author

N89-21193*# National Aeronautics and Space Administration. Langley Research Center, Hampton, VA.
A REVIEW OF REACTION RATES AND THERMODYNAMIC AND TRANSPORT PROPERTIES FOR THE 11-SPECIES AIR MODEL FOR CHEMICAL AND THERMAL NONEQUILIBRIUM CALCULATIONS TO 30000 K
Roop N. Gupta, Jerrold M. Yos (Avco Systems Div., Wilmington, MA.), and Richard A. Thompson Feb. 1989 69 p
(NASA-TM-101528; NAS 1.15:101528) Avail: NTIS HC A04/MF A01 CSCL 20D

Reaction rate coefficients and thermodynamic and transport properties are provided for the 11-species air model which can be used for analyzing flows in chemical and thermal nonequilibrium. Such flows will likely occur around currently planned and future hypersonic vehicles. Guidelines for determining the state of the surrounding environment are provided. Approximate and more exact formulas are provided for computing the properties of partially ionized air mixtures in such environments.
Author

N89-21194 Washington Univ., Seattle.
A NUMERICAL STUDY OF THE TURBULENT FREE CONVECTION IN RECTANGULAR CAVITIES Ph.D. Thesis
Abdelouahab Abrous 1988 240 p
Avail: Univ. Microfilms Order No. DA8826359

The steady two-dimensional, laminar, and turbulant free convection in rectangular enclosures has been studied numerically. The physical model used was a 2-D model of a rectangular cavity with the vertical walls maintained at different, but constant temperatures and the horizontal walls either adiabatic or perfectly conductive. The turbulent shear stresses and heat fluxes appearing in the momentum and energy equations are modeled using a two-equation (kappa minus epsilon) turbulence model involving the solution of the differential equations for kappa, the kinetic energy of turbulence, and epsilon, its rate of dissipation. The continuity, two momentum, and energy equations, coupled with the two transport equations for kappa and epsilon constitute a closed system of six equations in six unknowns describing a turbulent, bouyancy-driven, two-dimensional flow. These equations are normalized and then solved for the mean values of the dependent variables (U,V,T,P, kappa, epsilon) using a numerical method based on a control volume finite difference approach. With this numerical technique, solutions for the two-dimensional buoyancy-induced flows inside rectangular cavities characterized by wide range of Rayleigh numbers (1000 is less than Ra is less than 10 to the 12th power) have been obtained. The effects of adiabatic and perfectly conductive horizontal boundary conditions on the mean flow parameters and turbulence fields inside the cavity are examined. Moreover, the effects of turbulence model constants were studied. The predictions of velocities, temperatures, and the Nusselt numbers are in good comparison with the numerical and experimental data. Applciations of the mumerical technique, simulate the effect of plumes, infiltration, and horizontal partitions on the basic flow pattern in occupied rooms.
Dissert. Abstr.

N89-21195 Illinois Univ., Urbana-Champaign.
COHERENT STRUCTURES IN FULLY DEVELOPED TURBULENT PIPE FLOW Ph.D. Thesis
Ioannis Constantinos Lekakis 1988 267 p
Avail: Univ. Microfilms Order No. DA8823182

The structure of large scale organized motions in the turbulent flow of air through a 12.5 cm diameter pipe at 50,000 Reynolds number was studied using time delayed measurements of the three-dimensional velocity vector. A triple hot-film probe was used to measure: (1) the complete time-delayed Reynolds stress tensor R sub ij(tau) = (u sub i(x,t)u sub j(x,t + tau)), (2) the conditionally averaged velocity (u sub i (x,t + tau) / E(x,t)), where E consisted of various velocity events at (x,t), and (3) the linear stochastic estimates of the conditional averages. A new methodology was developed for the interpretation of non-orthogonal triple-sensor probe signals. This interpretation takes into consideration the uniqueness of the solution from a multiple set of possible velocity vectors corresponding to a measured set of anemometry voltages. Optimum probe geometries are shown to be a compromise between the size of the domain in which the true velocity vector can be singled out unambiguously and the overall sensitivity of the probe. A physically consistant method for the calibration of multiple sensor probes has also been developed. Triple sensor probes, together with smoke-wire flow visualization techniques, were used to study the turbulent structure in fully developed pipe flow.
Dissert. Abstr.

N89-21196*# National Aeronautics and Space Administration. Lewis Research Center, Cleveland, OH.
ON THE CONDITIONS FOR RESONANCE INTERACTIONS OF INSTABILITY WAVES IN THE AXISYMMETRIC JET
Reda R. Mankbadi, Ganesh Raman, and Edward J. Rice (Sverdrup Technology, Inc., Cleveland, OH.) Mar. 1989 13 p Prepared in cooperation with Cairo Univ. (Egypt)
(NASA Order C-99066-G)
(NASA-TM-101477; E-4598; ICOMP-89-4; NAS 1.15:101477)
Avail: NTIS HC A03/MF A01 CSCL 20D

The conditions for resonance interaction between two instability waves in an axisymmetric jet were investigated. Considerations of the energy equation of the wave resulting from the interaction indicate that the phase angle between the wave-induced stresses and the wave-induced strains plays a crucial role in the resonance interaction. This fact is demonstrated experimentally by exciting a jet at fundamental and subharmonic frequencies. The phase angle between the waves stresses and strains was varied by varying the initial phase-difference between the two excitation waves. The subharmonic resonance was found to be highly dependent on this angle. Favorable agreement was found between the phase angles predicted by a nonlinear theory and the measured ones. The theory is used to explain the subharmonic's resonance in terms of the phase-angles.
Author

N89-21197*# National Aeronautics and Space Administration. Lewis Research Center, Cleveland, OH.
THE RESPONSE OF A LAMINAR BOUNDARY LAYER IN SUPERSONIC FLOW TO SMALL AMPLITUDE PROGRESSIVE WAVES
Peter W. Duck Mar. 1989 39 p
(NASA Order C-99066-G)
(NASA-TM-101965; E-4663; NAS 1.15:101965; ICOMP-89-6)
Avail: NTIS HC A03/MF A01 CSCL 20D

The effect of a small amplitude progressive wave on the laminar boundary layer on a semi-infinite flat plate, due to a uniform supersonic freestream flow, is considered. The perturbation to the flow divides into two streamwise zones. In the first, relatively close to the leading edge of the plate, on a transverse scale comparable to the boundary layer thickness, the perturbation flow is described by a form of the unsteady linearized compressible boundary layer equations. In the freestream, this component of flow is governed by the wave equation, the solution of which provides the outer velocity conditions for the boundary layer. This system is solved numerically, and also the asymptotic structure in the far downstream limit is studied. This reveals a breakdown and a subsequent second streamwise zone, where the flow disturbance is predominantly inviscid. The two zones are shown to match in a proper asymptotic sense.
Author

N89-21198*# Hampton Inst., VA. Dept. of Mathematics.
IMPLICATIONS OF PRESSURE DIFFUSION FOR SHOCK WAVES Progress Report, 1 Aug. 1988 - 31 Jan. 1989
Ram Bachan Ram 3 Apr. 1989 10 p
(Grant NAG1-904)
(NASA-CR-184858; NAS 1.26:184858) Avail: NTIS HC A02/MF A01 CSCL 20D

The report deals with the possible implications of pressure diffusion for shocks in one dimensional traveling waves in an ideal gas. From this new hypothesis all aspects of such shocks can be calculated except shock thickness. Unlike conventional shock theory, the concept of entropy is not needed or used. Our analysis shows that temperature rises near a shock, which is of course an experimental fact; however, it also predicts that very close to a shock, density increases faster than pressure. In other words, a shock itself is cold.
Author

N89-21199# Naval Ship Research and Development Center, Bethesda, MD. Ship Hydromechanics Dept.
POTENTIAL FLOW EVALUATION OF THE INTERFERENCE EFFECT OF STRUT-THROUGH-APPENDAGE-TIP MODEL MOUNTING TECHNIQUE AND REDUCTION OF THE EFFECT USING BLOWING AND SUCTION
Robert W. Mellish and David W. Coder Nov. 1988 76 p
(AD-A202424; DTRC-SHD-1229-01) Avail: NTIS HC A05/MF A01 CSCL 13J

A parametric study based on incompressible, irrotational flow theory was conducted to evaluate the effect of strut support interference on the flow field about a model. The use of suction and blowing to correct the support interference is also investigated. Two struts were considered for numerical analysis, a small chord strut of constant cross section and a large chord strut of varying cross section, both attached to the tip of a model submarine sail. For the present study the SS N21 class and SSN 688 class sail geometries are utilized. To assess the level of strut interference, the presence fields on the surface of the sail and a flat representation of the hull were evaluated as follows. The flow field was computed for the model geometry without a strut attached (baseline configuration) and the results are compared with identical calculations for the model-strut combination. The calculated results are presented graphically as contour plots of the pressure coefficient (Cp). Contour plots of delta p (the difference between baseline ad sail-strut results) are utilized to identify regions of principal strut interference. Finally, suction and blowing was applied to minimize strut interference in areas considered important to hull boundary layer and sail flow that would affect wake measurements.
GRA

N89-21200# Calspan Field Services, Inc., Arnold AFS, TN.
INVESTIGATION OF THE DEVELOPMENT OF LAMINAR BOUNDARY-LAYER INSTABILITIES ALONG A BLUNTED CONE Final Report, 16 Jul. - 21 Jul. 1986
J. C. Donaldson and S. A. Simons Dec. 1988 56 p Prepared in cooperation with Arnold Engineering Development Center, Arnold AFS, TN
(AD-A202425; AEDC-TSR-86-V46) Avail: NTIS HC A04/MF A01 CSCL 20D

Measurements of mean-flow and fluctuating-flow parameters were made in the boundary layer of a spherically blunted (0.7-in. radius), 7-deg (half-angle) cone in an investigation of the stability of laminar boundary layers. The flow-fluctuation measurements were made using hot-wire anemometry techniques. Flow-field profiles and model surface pressures were also measured. The testing was performed at free-stream Mach number 8 with a free-stream unit Reynolds number of 1.6-million per foot. The test equipment and techniques, and the data acquisition and reduction procedures are described. Analysis of the hot-wire anemometer data is beyond the scope of this report.
GRA

N89-21201# Michigan Univ., Ann Arbor. Gas Dynamics Labs.
TURBULENCE MODULATION AND DENSE-SPRAY STRUCTURE Annual Report, 15 Jul. 1987 - 14 Jul. 1988
R. N. Parthasarathy, G. A. Ruff, and G. M. Faeth Aug. 1988 92 p
(Grant AF-AFOSR-0244-85; AF Proj. 2308)
(AD-A202449; AFOSR-88-1217TR) Avail: NTIS HC A05/MF A01 CSCL 20D

A theoretical and experimental study of phenomena related to dense sprays is described. Two aspects of dense sprays are being considered: effects of turbulence modulation, which is the direct effect of particle (drop) motion on the turbulence properties of multiphase flows; and the structure and mixing properties of the dense-spray region of pressure atomized sprays. Turbulence modulation is being studied by considering spherical monodisperse glass particles falling in a stagnant water bath, where effects of turbulence modulation are responsible for the entire turbulence field. Measurements involve phase velocities and temporal and spatial correlations and spectra of the continuous phase velocities using a two-point phase-discriminating laser Doppler anemometer. Flow properties are being analyzed using stochastic methods: assuming linear superposition of randomly arriving particle wakes (Poisson statistics) for liquid phase properties; and random-walk calculations based on statistical time-series methods for particle properties. GRA

N89-21202# Stanford Univ., CA.
ADVANCED DIAGNOSTICS FOR REACTING FLOWS Final Report, 1 Oct. 1987 - 30 Sep. 1988
R. K. Hanson 1 Oct. 1988 39 p
(Grant AF-AFOSR-0057-87; AF Proj. 2308)
(AD-A202451; AFOSR-88-1218TR) Avail: NTIS HC A03/MF A01 CSCL 21B

Progress is reported for the past year of an interdisciplinary program aimed at establishing advanced optical diagnostic techniques applicable to combustion and plasma flows. The primary effort is on digital flowfield imaging techniques, which offer significant potential for a wide range of spatially resolved 2-d and 3-d measurements. The imaging is accomplished by recording light scattered from a planar laser-illuminated region using a modern solid-state camera. The scattering process is generally laser-induced fluorescence, though Mie scattering is also used in connection with sizing particles. Activities reported herein include: (1) basic spectroscopy and fluorescence imaging of O2 and NO; (2) molecular velocity imaging; (3) imaging diagnostics for supersonic combustion; (4) imaging diagnostics for hypersonic flows; (5) plasma diagnostics; (6) laser photolysis shock tube for fundamental studies of reaction kinetics and spectroscopy; and (7) development of flow imaging hardware and software. GRA

N89-21203# Air Force Inst. of Tech., Wright-Patterson AFB, OH. School of Engineering.
NUMERICAL STUDY OF THREE VISCOUS/INVISCID INTERACTION METHODS M.S. Thesis
Jeffrey C. Tromp Sep. 1988 120 p
(AD-A202575; AFIT/GA/AA/88S-1) Avail: NTIS HC A06/MF A01 CSCL 20D

The study of flows with viscous/inviscid interaction has attracted many researchers over the last decade. These flows occur whenever the adverse gradient is large enough to cause flow separation. The current emphasis is to find efficient ways of solving these types of flows without solving the full Navier-Stokes equations. Three methods for solving the viscous/inviscid problem were studied. The first method uses finite difference equations to model both the viscous and inviscid regions. A coupling scheme is developed to match the two solutions. The second method solves the integral boundary layer equations in the viscous region and finite difference equations in the inviscid region. The third method solves the Hilbert integral to generate a correction to the inviscid velocity using the boundary layer equations as the viscous model. The model problem used in this work is Howarth flow over a flat plate. The three methods were evaluated in terms of solution accuracy, memory requirements, and computation times. GRA

N89-21204# Air Force Inst. of Tech., Wright-Patterson AFB, OH. School of Engineering.
VOLUMETRIC RENDERING TECHNIQUES FOR THE DISPLAY OF THREE-DIMENSIONAL AERODYNAMIC FLOW FIELD DATA M.S. Thesis
David J. Bridges Dec. 1988 74 p Original contains color illustrations
(AD-A202661; AFIT/GCS/ENG/88D-2) Avail: NTIS HC A04/MF A01 CSCL 20D

Navier-Stokes equations are so complex that their use by engineers was impractical until the advent of the modern computer but a new problem was created: Data saturation. The solution to the Navier-Stokes equations is comprised of thousands of numbers which makes it virtually impossible to conceptualize the situation within the flow field. To alleviate this problem, various computer graphics techniques have been used to provide images of flow fields. This thesis applies a relatively new graphics technique known as volumetric rendering to generate three-dimensional images of aerodynamic flow fields. Advantage of this technique are that it doesn't rely on geometric primitives to approximate a surface; and no a priori knowledge of the flow field's form is required to produce the final flow visualization image. To assess the utility of volumetric rendering in the field of computational fluid dynamics (CFD), a program known as VIPER is developed. This thesis outlines the requirements and specific algorithms for this program. Images of flow fields are presented and discussed along with program enhancements. VIPER's design also permits its use in applications other than CFD. GRA

N89-21205# Air Force Inst. of Tech., Wright-Patterson AFB, OH. School of Engineering.
AN EXPERIMENTAL INVESTIGATION OF FLOW MIXING ON THRUST EJECTION EFFICIENCY M.S. Thesis
Donald J. Morfitt, Jr. Dec. 1988 88 p
(AD-A202707; AFIT/GAE/AA/88D-27) Avail: NTIS HC A05/MF A01 CSCL 01A

The purpose of this study was to determine the effect flow mixing has on the thrust augmentation of an ejector. The experimental studies were divided into four phases. The four phases were baseline verification, a nozzle tip inclination study, a primary flow pulsing study, and a study of the quality of the ejector. The baseline verification study showed that thrust augmentation is dependent upon the injection angle and height of the primary nozzles. The nozzle tip inclination study investigated the effects of having the tips inclined from the inlet surface of the ejector. The nozzle tips were inclined in four different configurations. The different configurations established a baseline or attempted to promote flow mixing and swirling. GRA

N89-21206# Naval Research Lab., Washington, DC. Lab. for Computational Physics and Fluid Dynamics.
A CANCELLATION TECHNIQUE FOR REDUCING BACKGROUND NOISE WITHIN TURBULENT FLOW ENVIRONMENTS CHARACTERIZED BY PIPES AND ANNULI Interim Report, Jun. 1985 - Jul. 1988
M. P. Horne, E. W. Hendricks, and R. A. Handler 30 Dec. 1988 19 p
(AD-A202924; NRL-MR-6384) Avail: NTIS HC A03/MF A01 CSCL 20A

Experimental studies of turbulent boundary layer wall pressure fluctuations are typically complicated by flow generated acoustic pressure levels which are superimposed on the turbulent fluctuations of interest. This problem can be particularly acute when the test fluid is water or similar liquid with a high bulk wave propagation velocity. The present paper describes a method for addressing this problem which permits wall pressure fluctuation experiments of high quality to be conducted within internal flow geometries over a bandwidth of 1 kHz. The method improves on a technique of using 3 flush mounted transducers located within a coaxial plane, thereby providing up to 20 dB reduction over previous measurements for the bandwidth investigated. Experimental results show that using the improved technique allows measurements of both the nearfield and farfield pressure

components. Excellent agreement with previously reported wall pressure fluctuation measurements is demonstrated for the geometries evaluated. GRA

N89-21207# Air Force Inst. of Tech., Wright-Patterson AFB, OH. School of Engineering.

INCOMPRESSIBLE FLOW FRICTION COEFFICIENTS IN A SIMULATED HEAT PIPE M.S. Thesis

David A. Manley Dec. 1988 96 p

(AD-A203176; AFIT/GAE/AA/88D-22) Avail: NTIS HC A05/MF A01 CSCL 20M

This thesis examines the combined effects of pressure gradients and blowing and suction on frictional forces in a heat pipe with relatively low radial Reynolds numbers. A porous tube is used to simulate the heat pipe and a vacuum pump is used to generate the air flow. By measuring the static pressure variation along the pipe wall and using a one-dimensional, incompressible, numerical model, the frictional forces are obtained and compared to laminar fully-developed theoretical values. GRA

N89-21208# Arizona Univ., Tucson. Dept. of Aerospace and Mechanical Engineering.

STUDIES IN THE COMPUTATION OF COMPRESSIBLE AND VISCOUS FLOW Final Scientific Report, 15 Feb. 1983 - 15 Aug. 1988

K-Y. Fung 13 Oct. 1988 39 p

(Grant AF-AFOSR-0071-83; AF Proj. 2307)

(AD-A203334; AFOSR-88-1291TR) Avail: NTIS HC A03/MF A01 CSCL 20D

The theme has been adaptive solution refinement. A novel approach called Truncation Error Injection (TEI) was introduced during the course of research. The idea behind TEI is very simple, i.e., the exact nodal value of the solution to a differential equation could be obtained on any grid and from solving a difference equation that models the differential equation if the truncation error were known. Although the TE is not known in general, it can be approximated on a local grid patch. This approach of approximating tne local error due to discretization in effect decouples a problem of multiple disparate length scales into problems of single length scale so that they can be solved more efficiently on a computer than the original problem. Three types of applications have been demonstrated. In addition to solution refinement by TEI, we have shown that the decoupling of the unsteady computation from the steady one by TEI could significantly reduce the computing time and storage for flutter prediction, and that viscous effects can be computed separately and injected into the solution of an inviscid solver for viscous flow computation. Some of the advantages of this approach are: it requires very little modification to the base solver; no compatibility problems in using different grids and different solvers; readily suited for multi processors. GRA

N89-21209# Michigan State Univ., East Lansing. Turbulence Structure Lab.

WHOLE FIELD MEASUREMENTS OF VORTICITY IN TURBULENT AND UNSTEADY FLOWS Final Report, 1 Aug. 1986 - 31 Jul. 1988

R. E. Falco, C. P. Gendrich, and C. C. Chu 11 Oct. 1988 91 p

(Grant AF-AFOSR-0242-86; AF Proj. 2307)

(AD-A203349; TSL-88-5; AFOSR-88-1320TR) Avail: NTIS HC A05/MF A01 CSCL 20D

Measurements of cross-stream and streamwise vorticity have been made over important regions of an experimental simulation of the bursting process of turbulent boundary layers. Vorticity measurements have also been made of the starting vortex of an airfoil, in a vortex ring, and in a Stokes' layer. Using a new technique developed under this contract, these measurements have been made at approximately fifty simultaneous positions over the flow structures of interest. The technique can accurately measure vorticity and strain rate, as well as instantaneous Reynolds stress and velocities over a field. It requires only a clock and ruler for calibration. It also directly measures these quantities, avoiding indirect interpretations. It uses long time persistence of irradiation of a photochemical to mark fluid particles. The technique has been named LIPA, (Laser Induced Photochemical Anemometry). Its accuracy has been measured by comparing it to an exact solution of the Navier-Stokes equations. This indicated an absolute accuracy of cross-stream vorticity of + or - 1 sec. Data reduction procedures have been developed which use high resolution digitization and image processing. Algorithms have been written and tested which allow almost complete automation of the data reduction procedure. GRA

N89-21210# New York Univ., New York. Inst. of Mathematical Sciences.

COMPUTATIONAL TECHNIQUES FOR SHOCK WAVE DIFFRACTION PROBLEMS Final Report, 1 Oct. 1985 - 30 Sep. 1988

James Glimm and John Grove 30 Nov. 1988 13 p

(Contract DAAG29-83-K-0188)

(AD-A203439; ARO-22770.15-MA) Avail: NTIS HC A03/MF A01 CSCL 12B

This document discusses results concerning mathematical theory, computational methods, and statistical modeling of chaotic mixing processes. In mathematical theory, the authors have proposed a new paradigm from uniqueness and regularization of discontinuous solutions of hyperbolic conservation laws. Contrary to common opinion, there is no requirement from physics for uniqueness of solutions for these systems. Nonuniqueness, if it occurs, must be resolved as in bifurcation theory by an unfolding of critical bifurcation parameters. Similarly regularization does not have to be accomplished by higher order terms in an equation, but may be based on enlarging the system. Many common mathematically based entropy conditions have been shown to be inadequate in specific examples. Work is in progress on two dimensional nonlinear wave interactions, from a theoretical point of view. Computationally, several difficult phenomena were encountered in the study of shock waves interacting with a liquid-gas interface. Chaotic mixing due to a Rayleigh-Taylor or Richtmyer-Meshkov unstable interface has been studied. Front tracking has provided a unique computational tool, and has produced a unique data set of computational results which are presently being analyzed. High quality models for single-mode growth in the large amplitude regime have been proposed, and validated. GRA

N89-21211# Wisconsin Univ., Madison. Dept. of Computer Sciences.

INSTABILITIES IN SHEAR FLOW OF VISCOELASTIC FLUIDS WITH FADING MEMORY Technical Summary Report

Bradley J. Plohr Sep. 1988 17 p

(Contract DAAL03-87-K-0036; NSF DMS-87-112058)

(AD-A203735; CMS-TSR-89-13) Avail: NTIS HC A03/MF A01 CSCL 20D

For certain models of viscoelastic fluids with fading memory, classical steady channel flow does not exist beyond a maximal wall shear stress. This occurs when the shear stress for steady flow decreases with strain. For generalized Newtonian models of viscoelastic flow, such a decrease implies that the flow is unstable. Because of this example, a constitutive relation that exhibits a maximal wall shear stress in regarded as defective. The author reports on work showing that, contrary to this intuition, such models correctly describe the experimentally observed spurt phenomenon: exceeding this critical stress results in large increase in volumetric flow rate. The transition to spurt flow is analogous to a dynamically generated phase transition. To analyze this phenomenon, we derive a system of conservation laws that govern the flow; these equations take the form of gas dynamics with relaxation terms. We solve the Riemann problem for this non-strictly-hyperbolic system, and incorporate this solution into the random choice method. Numerical simulation of channel flow, with the maximal wall shear stress exceeded, shows that a discontinuity forms at the wall, allowing the fluid to slip; no steady state exists. However, when a small Newtonian viscosity is included in the model, a slip layer forms and the flow approaches a discontinuous steady state. GRA

N89-21212# Colorado State Univ., Fort Collins. Dept. of Chemistry
MOLECULAR JET STUDIES OF vdW (VAN DER WAALS) CLUSTERS AND SOLVATION Final Report, Sep. 1984 - Aug. 1988
Mark Schauer, K. S. Law, Elliot R. Bernstein, J. Wanna, and J. A. Menapace 16 Dec. 1988 28 p
(Contract N00014-79-C-0647)
(AD-A203766) Avail: NTIS HC A03/MF A01 CSCL 20D

This report includes abstracts on the following topics: Molecular jet study of aniline-helium van der Waals molecules and aniline radiationless relaxation in the B excited electronic state, Molecular supersonic jet studies of aniline solvation by helium and methane, Brillouin scattering studies of the successive phase transitions in (CH3NH3)2FeCl4, Supersonic molecular jet studies of toluene-helium and toluenemethane clusters, Molecular jet study of the solvation of benzene by methane, ethane, and propane, Molecular jet study of the solvation of toluene by methane, ethane, and propane, Dimers of aromatic molecules: (Benzene)2, (toluene)2, and benzene-toluene, Calculations of the geometry and binding energy of aromatic dimers: Benzene, toluene, and toluene-benzene. GRA

N89-21213# Texas Univ., Austin. Dept. of Physics.
SYMMETRY BREAKING BIFURCATIONS AND THE GROWTH OF CHAOS IN A ROTATING FLUID Annual Report, 1 Oct. 1987 - 30 Sep. 1988
Harry L. Swinney 10 Nov. 1988 5 p
(Contract N00014-86-K-0385)
(AD-A204010; Rept-88-1) Avail: NTIS HC A02/MF A01 CSCL 20D

Laboratory experiments and numerical simulations on flow between concentric independently rotating cylinders (the Couette-Taylor system) reveal a primary bifurcation to a new state, ribbons, which are traveling waves in the azimuthal direction but standing waves in the axial direction. Other experiments, conducted on a rigid rapidly rotating annulus, are designed to explore parameter regimes characteristic of planetary scale flows. Eastward jets are found to exhibit Rossby waves for a wide range of control parameters, and these jets (or, more precisely, the potential vorticity gradients in the core of the jets) act as a strong barrier to tracer transport: these observations have important implication for the transport of pollutants in oceans and the atmosphere. The behavior of westward jets is found to be markedly different from that of eastward jets: persistent vortices (like the Great Red Spot of Jupiter) are found to form spontaneously in a turbulent shear flow formed by westward jets. GRA

N89-21214# Sandia National Labs., Albuquerque, NM. Fluid and Thermal Sciences Dept.
A MODEL FOR INTERFACE TEMPERATURES INDUCED BY CONVECTION HEAT TRANSFER IN POROUS MATERIALS
M. R. Baer Feb. 1989 22 p
(Contract DE-AC04-76DP-00789)
(DE89-008202; SAND-88-1073) Avail: NTIS HC A03/MF A01

An evolutionary relationship for granular interface temperature is developed for use in multiphase heat transfer models. Temperature at particle surfaces within a packed bed are represented by the thermal fields of isolated spheres. An integral method is used for the solution of thermal conduction within individual grains and approximations are employed for the limits of large and small Biot number. A composite of these solutions is formulated which treats a broad range of transient heat transfer. The resulting model is a differential equation which easily adapts to Eulerian or Lagrangian multiphase models. To test this simplified model, several comparisons to exact and model solutions were conducted investigating the transient thermal response of a convectively heated isolated sphere. DOE

N89-20949*# National Aeronautics and Space Administration. Ames Research Center, Moffett Field, CA.
NAVIER-STOKES AND VISCOUS-INVISCID INTERACTION
Joseph L. Steger and William R. VanDalsem *In* NASA, Langley Research Center, Transonic Symposium: Theory, Application, and Experiment, Volume 1, Part 2 Mar. 1989 p 547-570 (For primary document see N89-20942 14-02)
Avail: NTIS HC A22/MF A01 CSCL 20D

N89-20950*# National Aeronautics and Space Administration. Langley Research Center, Hampton, VA.
THE 3-D EULER AND NAVIER-STOKES CALCULATIONS FOR AIRCRAFT COMPONENTS
Veer N. Vatsa, Bruce W. Wedan, and Eli Turkel (Institute for Computer Applications in Science and Engineering, Hampton, VA.) *In its* Transonic Symposium: Theory, Application, and Experiment, Volume 1, Part 2 Mar. 1989 p 571-579 (For primary document see N89-20942 14-02)
Avail: NTIS HC A22/MF A01 CSCL 20D

N89-21512# New York Univ., New York. Inst. of Mathematical Sciences.
THE NUMERICAL SIMULATION OF RICHTMYER-MESHKOV UNSTABLE INTERFACES: A CONFERENCE REPORT
John Grove *In* Army Research Office, Transactions of the Fifth Army Conference on Applied Mathematics and Computing Mar. 1988 p 423-436 (For primary document see N89-21490 14-59)
(Contract DAAG29-84-K-0130)
Avail: NTIS HC A99/MF E03 CSCL 20D

N89-21523# Army Engineer Waterways Experiment Station, Vicksburg, MS. Hydraulics Lab.
SKEW GRIDS AND IRROTATIONAL FLOW
Robert S. Bernard *In* Army Research Office, Transactions of the Fifth Army Conference on Applied Mathematics and Computing Mar. 1988 p 631-642 (For primary document see N89-21490 14-59)
Avail: NTIS HC A99/MF E03 CSCL 20D

N89-21756*# Alabama Univ., Huntsville. Dept. of Aerospace Engineering.
THE ROLE OF THE TURBULENT PRANDTL NUMBER IN TURBINE BLADE HEAT TRANSFER PREDICTION
Kevin W. Whitaker *In* Alabama Univ., Research Reports: 1988 NASA/ASEE Summer Faculty Fellowship Program Dec. 1988 20 p (For primary document see N89-21726 14-99)
Avail: NTIS HC A99/MF E03 CSCL 20D

35 INSTRUMENTATION AND PHOTOGRAPHY

Includes remote sensors; measuring instruments and gages; detectors; cameras and photographic supplies; and holography.

For aerial photography see *43 Earth Resources and Remote Sensing.* For related information see also *06 Aircraft Instrumentation,* and *19 Spacecraft Instrumentation.*

N89-21215# National Center for Atmospheric Research, Boulder, CO.
THERMOPILE TEMPERATURE SENSITIVITY CALIBRATION PROCEDURE FOR EPPLEY BROADBAND RADIOMETERS
W. L. Smith, Jr., Stephen K. Cox (Colorado State Univ., Fort Collins.), and Vince Glover Jul. 1988 24 p Sponsored in part by Colorado State Univ., Fort Collins
(Grant NSF ATM-87-09659)
(PB89-104129; NCAR/TN-320-STR) Avail: NTIS HC A03/MF A01 CSCL 14B

Eppley Laboratory, Inc. pyranometers and pyrgeometers have built-in temperature compensation circuitory designed to limit relative errors in the measurement of radiation of plus or minus 2 percent for a temperature range of -20 to +40 C. A procedure developed to verify the specification and to determine the relative sensitivity to temperatures below -20 C is described. Results of

the calibration and application to data correction are also presented. GRA

N89-21216# Ames Lab., IA. Dept. of Physics.
PERFORMANCE OF A PROTOTYPE ELECTROMAGNETIC CALORIMETER Ph.D. Thesis
Randall Robert Holmes Jul. 1988 69 p
(Contract W-7405-eng-82)
(DE89-007608; IS-T-1350) Avail: NTIS HC A04/MF A01

In this thesis, we study the performance of a prototype High Density Projection Chamber (HPC) The HPC will serve as the electromagnetic calorimeter for the barrel region of the DELPHI detector at LEP. By placing the HPC in a beam of electrons with well defined momentum, the response and energy resolution of the detector are determined. If the readout chamber high voltage is suitably chosen, the output signal is directly proportional to the incident energy of the particle for energies up to 35 GeV. We also find evidence that at high energies the energy resolution deviates from its expected behavior. DOE

N89-21217# Scripps Institution of Oceanography, La Jolla, CA. Marine Physical Lab.
LOCALIZING AND BEAMFORMING FREELY-DRIFTING VLF (VERY LOW FREQUENCY) ACOUSTIC SENSORS Ph.D. Thesis
Richard L. Culver Sep. 1988 153 p
(Contracts N00014-82-K-0147; N00014-87-K-0010)
(AD-A202638; AD-E900870; MPL-U-23/88; SIO-REF-88-16)
Avail: NTIS HC A08/MF A01 CSCL 20A

Self contained, freely-drifting Swallow floats capable of recording ambient ocean noise in the 1 to 25 Hz band have been designed, built and deployed by the Marine Physical Laboratory, Scripps Institution of Oceanography, University of California, San Diego, California. The buoys are ballasted to neutral buoyancy at midwater depth where they record the components of particle velocity from which sound pressure levels may be derived. Float positions are estimated using an 8 kHz acoustic ranging system and a Kalman tracking filter. Individual float times series are then combined to obtain passive, directional acoustic measurements from 1 to 25 Hz which are not contaminated by flow noise or tether strumming. The float localization and beamforming techniques are illustrated using measurements from a September 1986 Swallow float experiments conducted approximately 50 miles west of San Diego, california. A distant target of opportunity (apparently a surface ship) provides six spectral lines between 9 and 22,5 Hz which are tracked for about 90 minutes. The complex bathymetry of the experiment site complicates signal propagation, but the signal level in the beam-former output indicates that the element time series are being properly combined. GRA

N89-21218# Air Force Inst. of Tech., Wright-Patterson AFB, OH. School of Engineering.
AN ANALYSIS OF PLATINUM SILICIDE AND INDIUM ANTIMONIDE FOR REMOTE SENSORS IN THE 3 TO 5 MICROMETER WAVELENGTH BAND M.S. Thesis
Neil F. Schoon Dec. 1988 126 p
(AD-A202663; AFIT/GSO/ENP/88D-4) Avail: NTIS HC A07/MF A01 CSCL 17E

Platinum Silicide and Indium Antimonide are compared as detector materials in a space based remote sensor using the 3 to 5 micrometer wavelength band. The comparison is based on a scaled count rate involving the material's quantum efficiency, a target's reflected solar and thermal emittances, the atmospheric transmission, and the wavelength. The comparison is made using a baseline scenario and seven sensitivity analysis scenarios. The baseline scenario uses a target at 298K and a vertical line-of-sight from the target to the remote sensor in space. The atmospheric transmission is calculated using the 1962 U.S. Standard atmospheric model resident in LOWTRAN 6, with a 23 kilometer rural visibility and no cloud cover. A sensitivity analysis was performed by varying the target temperature, target reflectance, and finally the atmospheric properties. GRA

N89-21219# Utah State Univ., Bedford, MA. Radiance Lab.
ADAPTING SCHOTTKY DIODE DETECTOR TECHNOLOGY TO A SPACE PLATFORM Final Report, Jul. 1986 - Jul. 1987
Joseph Kristl and Ronald Huppi 10 Feb. 1988 281 p
(Contract F19628-86-K-0035)
(AD-A202825; AFGL-TR-87-0234) Avail: NTIS HC A13/MF A01 CSCL 17E

Schottky barrier focal plane arrays have demonstrated superior performance in imagery and sensitivity in cameras deployed on the ground and on airborne platforms. This study determines the feasibility of placing a camera using one of these arrays in space in the space shuttle cargo bay or on the Shuttle Pallet Satellite. The basic operation and performance of platinum silicide Schottky barrier detectors is first discussed. Then a detailed analysis of all of the technical issues involved in constructing a space based Schottky camera are examined at length. Optical performance, cryogenic cooling, image compensation, data recording, system control, host platform restraints, and relevant MIL-SPECs are covered. A preliminary design that meets all of the design criteria is then described. It is concluded that this application is feasible and would be an extremely valuable research tool to investigate infrared properties of objects in space. GRA

N89-21220# Vanderbilt Univ., Nashville, TN. Dept. of Physics and Astronomy.
MAGNETIC MAPPING OF CURRENT DISTRIBUTIONS IN TWO-DIMENSIONAL ELECTRONIC DEVICES Annual Report, 1 Sep. 1987 - 1 Sep. 1988
John P. Wikswo, Jr. Sep. 1988 4 p
(Grant AF-AFOSR-0337-87; AF Proj. 2306)
(AD-A203035; AFOSR-88-1279TR) Avail: NTIS HC A02/MF A01 CSCL 14B

The 4-channel, high-resolution SQUID magnetometer system has been ordered. This system will have a spatial resolution of approximately 1 mm. The motors for the three-axis, non-magnetic positioning system have been obtained after lengthy discussions to eliminate magnetic components from their motors. Assembly of the equipment required for the prototype sub-millimeter SQUID system progresses. The temperature controller for the existing Janis continuous flow cryostat, and a Cooke 3-inch vacuum system was obtained. Obtained were all of the analog and digital hardware and presently being completed are the software for the microcomputer controls of the temperature controller, the pumping system, and the data acquisition system. Developed is the analytic models required to interpret two-dimensional magnetic field maps in terms of the current distributions that produce them were developed. The detailed mechanical design was completed for a 6-foot by 5-foot by 3-foot, four-layer, magnetically shielded enclosure. GRA

N89-21221# Air Force Inst. of Tech., Wright-Patterson AFB, OH. School of Engineering.
A POSITION, SCALE AND ROTATION INVARIANT HOLOGRAPHIC ASSOCIATIVE MEMORY M.S. Thesis
Kenneth H. Fielding Dec. 1988 77 p
(AD-A203289; AFIT/GEO/ENG/88D-2) Avail: NTIS HC A05/MF A01 CSCL 14C

This thesis investigates an all-optical position, scale, and rotation invariant (PSRI) holographic associative memory employing phase conjugation. The PSRI feature space is the ln-polar representation of the magnitude of the Fourier transform of the objects. This representation is generated using a coordinate transform computer generated hologram. Diffuse Fourier transform holograms of the PSRI feature space and the use of angularly multiplexed references allow access to the correlation domain where the nonlinear properties of the phase conjugate mirror, self-pumped BaTiO3, reduces cross-correlation noise and provides object discrimination. The self-pumped phase conjugate mirror is characterized and a procedure for consistent production of high diffraction efficiency holograms is developed. The holographic associative memory is constructed and its operational parameters are defined. One object is stored in the memory because of limitations on the size of the Fourier transforming optic and the

properties of the ground glass diffuser. Fast optics and a custom designed phase diffuser are recommended to alleviate this system characteristic. GRA

N89-21222# Indiana Univ., Bloomington. Dept. of Chemistry.
CORRECTION OF GAIN AND OPTICAL THROUGHPUT VARIATIONS IN A TWO-DIMENSIONAL IMAGING SPECTROMETER
C. A. Monning, B. D. Gebhart, and Gary M. Hieftje 28 Oct. 1988 9 p
(Contract N00014-86-K-0366)
(AD-A203495; INDU/DC/GMH-TR-47) Avail: NTIS HC A02/MF A01 CSCL 07D

Whenever an imaging spectrometer is employed, pixel to pixel variations and changes in sensitivity, gain, or noise can distort a recorded image. As a result, some form of normalization is required if faithful images are to be recorded. Although a number of alternative approaches have been explored for such normalization, the method described in this paper is novel in its effectiveness and simplicity. In this approach, a chemiluminescence substance is introduced into a flat sample cell whose dimensions are large enough to ensure uniform coverage of the photodetector array of interest. Because the chemiluminescence solution is homogeneous, it can be used to uniformly irradiate the imaging detector; recording of the resulting image then indicates any variations that exist across the detector face. In turn, the array of data so produced serves nicely as a normalization vehicle for later images to be taken. GRA

N89-21223# Naval Ship Research and Development Center, Bethesda, MD. Ship Hydromechanics Dept.
RADIO-CONTROLLED MODEL GYRO MEASUREMENT STUDY Final Report
Richard Nigon and Faria Abedin Aug. 1988 19 p
(AD-A204002; DTRC-88/024) Avail: NTIS HC A03/MF A01 CSCL 17G

The radio-controlled model (RCM) has been used extensively for mode I tests since 1970. An assumption that has been made is that the angles measured by the RCM gyros are the Euler angles for Euler coordinate transformation. A recent study of the gyros indicates that this assumption is incorrect not only for the RCM but for most model testing instrumentation packages used at DTRC. (The Euler angle assumption can be a good assumption as long as the combination of pitch and roll angles are small). This report present a set of transformation equations that can be used to convert RCM data to the desired Euler angles. GRA

N89-21224*# National Aeronautics and Space Administration. Lewis Research Center, Cleveland, OH.
INFRARED SURFACE TEMPERATURE MEASUREMENTS FOR THE SURFACE TENSION DRIVEN CONVECTION EXPERIMENT M.S. Thesis - Case Western Reserve Univ., Aug. 1988
Alexander D. Pline Mar. 1989 29 p
(NASA-TM-101353; E-4383; NAS 1.15:101353) Avail: NTIS HC A03/MF A01 CSCL 14B

In support of the Surface Tension Driven Convection Experiment (STDCE), a planned space transportation system (STS) flight experiment, a commercially available infrared thermal imaging system is used to quantify the imposed thermal signature along the free surface. The system was tested and calibrated for the STDCE with ground-based equivalents of the STDCE hardware. Before using the system, consideration was given to the radiation characteristics of the target (silicone oil). Absorption coefficients were calculated to understand the surface depth as seen by the imager and the penetration depth of the surface heater (CO2 laser). The performance and operational specifications for the imager and image processing system are described in detail to provide an understanding of the equipment. Measurements made with the system were compared to thermocouple measurements and a calculated surface temperature distribution. This comparison showed that in certain regions the IR imager measurements were within 5 percent of the overall temperature difference across the free surface. In other regions the measurements were within + or - 10 percent of the overall temperature gradient across the free surface. The effective emissivity of silicone oil for these experimental conditions was also determined. Measurement errors and their possible solutions are discussed. Author

N89-21225# Lawrence Livermore National Lab., CA. Biomedical Sciences Div.
DEVELOPMENT AND CHARACTERIZATION OF A FIBER OPTIC IMMUNO BIOSENSOR
M. Allen Northrup, Larry H. Stanker, Martin Vanderlaan, and Bruce E. Watkins Dec. 1988 15 p Presented at the NATO Advance Study Institute on Spectroscopy of Inorganic Bioactivators, Loutraki, Greece, 1 Nov. 1988
(Contract W-7405-eng-48)
(DE89-005062; UCRL-100110; CONF-8811163-1) Avail: NTIS HC A03/MF A01

In this paper we describe preliminary results from the development and characterization of a fiber optic biosensor that utilizes a fluorescently-labeled monoclonal antibody to pyrethroid pesticides. A synthetic pyrethroid-like antigen was coupled to bovine serum albumin and immobilized on the surface of a stripped portion of the distal end of an optical fiber. Each fiber was individually calibrated for its optical response using standard solutions of fluoresceinamine. Binding of the antibody was detected via the evanescent wave of the fiber by use of a portable fiber optic fluorimeter. Initial binding rate and equilibrium levels of bound antibody showed a linear relationship with antibody concentrations between 7 nM and 25 uM. To test the reversibility of the biosensor, bound antibody was removed with protein denaturing agents and the same fibers were re-tested with similar concentrations of antibody. When re-immersed in antibody solution, binding of the antibodies was again observed. The results provide encouraging evidence that such a biosensor may be useful for the determination of small organic molecules in situ. DOE

N89-21506# Army Missile Test and Evaluation Directorate, White Sands Missile Range, NM. Directed Energy Directorate.
AN ALGORITHM FOR PROCESSING SCANNING SPECTROMETER DATA
Joseph E. Zurlinden *In* Army Research Office, Transactions of the Fifth Army Conference on Applied Mathematics and Computing Mar. 1988 p 345-354 (For primary document see N89-21490 14-59)
Avail: NTIS HC A99/MF E03 CSCL 14B

N89-21739*# Memphis State Univ., TN. Dept. of Physics.
CONSTRUCTION OF AN ALTERNATING GRADIENT MAGNETOMETER
Michael M. Garland *In* Alabama Univ., Research Reports: 1988 NASA/ASEE Summer Faculty Fellowship Program Dec. 1988 26 p (For primary document see N89-21726 14-99)
Avail: NTIS HC A99/MF E03 CSCL 14B

36 LASERS AND MASERS

Includes parametric amplifiers.
For related information see also *76 Solid-State Physics.*

N89-21226*# Texas Christian Univ., Fort Worth. Dept. of Physics.
SOLAR-POWERED ALKALI METAL VAPOR LASERS Final Report, 1 Aug. 1986 - 31 Oct. 1988
Charles E. Blount 28 Feb. 1989 16 p
(Grant NAG1-691)
(NASA-CR-180480; NAS 1.26:180480) Avail: NTIS HC A03/MF A01 CSCL 20E

The emission spectrum of the A(1 Sigma u +) - X(1 Sigma g +) band of Na2 has been recorded following excitation by monochromatic radiation in the region of X-A and X-B absorption. The spectral profile has been investigated as a function of excitation wavelength, sodium vapor temperature and buffer gas pressure.

Additionally, gain measurements were made for the satellite of the A-X band as a function of the sodium vapor temperature and buffer gas pressure. Author

N89-21227# Naval Research Lab., Washington, DC. Plasma Physics Div.
TRANSFORMATIONS OF GAUSSIAN LIGHT BEAMS CAUSED BY REFLECTION IN FEL (FREE ELECTRON LASERS) RESONATORS Interim Report
S. Riyopoulos (Science Applications International Corp., McLean, VA.), C. M. Tang, and P. Sprangle 27 Oct. 1988 73 p
(AD-A202472; NRL-MR-6347) Avail: NTIS HC A04/MF A01 CSCL 09C

The transformation of Gaussian radiation beams caused by reflection off mirrors is an important issue for FELs operating as oscillators. The reflected radiation from a single incident Gaussian mode will contain other modes due to the finite mirror size, the deflection of the beam and mismatches in the curvature. A method for analytic computation of the reflection matrix is developed by taking the convolution of the source function at the surface of the mirror with the paraxial propagator. The mirror surface that reflects spherical incoming wavefronts into spherical outgoing is determined analytically. Integral expressions for the reflection coefficients R(mn) sub pq for any incoming mode u sub mn into the outgoing u sub pq are obtained as functions of the deflection angle phi, the reflected beam waist sub 0 and the mirror size. Analytic expansions of the reflection matrix in powers of the diffraction angle theta sub d much less than 1 are then obtained in both Hermite and Laguerre representations. The cross-coupling among vector components of the radiation field, caused by the curvature of the mirror surface, is included. It is shown that the lowest order contribution to the off-diagonal matrix elements is caused by the finite mirror size. The effects of the mirror curvature and the deflection of the light beam enter the reflection matrix as first order corrections in theta sub d. GRA

N89-21228# Rochester Univ., NY. Inst. of Optics.
OPTOELECTRONIC WORKSHOPS. PART 4: LIQUID CRYSTALS FOR LASER APPLICATIONS Interim Report
Stephen Jacobs and Juergen Pohlmann 11 May 1988 94 p
Workshop held in Rochester, NY, 11 May 1988
(Contract DAAL03-86-K-0173)
(AD-A202526; ARO-24626.52-PH-UIR) Avail: NTIS HC A05/MF A01 CSCL 09E

This optoelectronic workshop represents the fourth of a series of intensive academic/government interactions in the field of advanced electro-optics as part of the Army sponsored University Research Initiative. The workshops are a collaboration between the Center of Opto-Electronic Systems Research at the University of Rochester, Rochester, New York and the U.S. Army Center for Night Vision and Electro-Optics, Ft. Belvoir, Virginia. By documenting the associated technology status and dialogue it is hoped that this baseline will serve all interested parties towards providing a solution to high priority Army requirements. Responsible for program and program execution are Dr. Nicholas George, University of Rochester (ARO-URI) and Dr. Rudy Buser, NVEOC. GRA

N89-21229# Iowa Univ., Iowa City.
A LASER TRAP FOR NEUTRAL ATOMS Final Project Report, 15 Nov. 1985 - 14 Nov. 1987
William C. Stwalley 22 Nov. 1988 13 p
(Contract N00014-83-K-0646; RR01103)
(AD-A202581; IATRAP-88-1) Avail: NTIS HC A03/MF A01 CSCL 09C

The purpose of this project is to construct and study a laser trap for neutral atoms, initially potassium (K). At low densities, such a trap could be used to address a number of fundamental questions, e.g., the interaction of an individual atom with an electromagnetic field, collision dynamics and recombination. We have studied the feasibility and imitations of a purely laser trap concept, a corner cube trap, for trapping neutral K atoms. The confinement of the atoms in the two dimensions perpendicular to the laser is provided in the cavity of a newly constructed high power alexandrite laser operating in the CW TEM asterisk 01 mode (doughnut mode) tuned slightly to the blue side of the resonance line of the K atom. By reflecting the TEM askerisk 01 laser back on itself with two mirrors, one caps the ends of the cylindrical trap, resulting in a slightly weaker end plug. GRA

N89-21230# Air Force Inst. of Tech., Wright-Patterson AFB, OH. School of Engineering.
ANALYSIS OF SPACE-BASED LIDAR FOR AIRCRAFT TRACKING M.S. Thesis
Scott P. Simmonsa Nov. 1988 135 p
(AD-A202665; AFIT/GSO/ENP/88D-5) Avail: NTIS HC A07/MF A01 CSCL 17E

This study is a general analysis of the feasibility of tracking aircraft from space using a laser radar or lidar. The basis for the analysis is the lidar range equation. Specific hardware is not discussed. A computer program was written to model the different parameters involved with the analysis. Atmospheric attenuation equations, which were developed from FASCODE data, define the atmospheric losses for two type of atmospheres (clear and haze). Other lidar range equation variables are either computed from input data or are directly inserted into the program for analysis. Four different types of lasers were investigated. The output data from the model was plotted to show the relationship of various input parameters with the power available at the receiver. The results indicate that lidar systems carried on low-earth orbiting satellites may have the potential to track aircraft. Further analysis is required to develop complete feasibility windows over a wider range of conditions. GRA

N89-21231# Air Force Inst. of Tech., Wright-Patterson AFB, OH. School of Engineering.
LASER BEAM COUPLING VIA OPTICAL PHASE CONJUGATION IN BaTiO3 M.S. Thesis
Karen A. Wink Dec. 1988 55 p
(AD-A202874; AFIT/GEP/ENP/88D-7) Avail: NTIS HC A04/MF A01 CSCL 09C

The nonlinear crystal barium titanate was used to couple mutually incoherent argon-ion laser beams using a co-pumped four-wave mixing mechanism which transfers photons from each beam into the phase-conjugate outputs of the others. The four-wave mixing geometry which was used has been described in the literature as the mutually incoherent beam coupler. The beams, all incident on the same crystal a face, form coupling loops as they internally reflect into each other at the opposite crystal corner. Coupling between two and three beams was investigated. Coupling between two beams resulted in phase-conjugate returns which were both self-pumped and co-pumped. Reflectivities of 9 to 42 percent were obtained for all angles of incidence greater than 50 degrees. (The angle between beams was less than 7 degrees). GRA

N89-21232# Defense Intelligence Agency, Washington, DC. Directorate for Scientific and Technical Intelligence.
BIBLIOGRAPHY OF SOVIET LASER DEVELOPMENTS, SEPTEMBER-OCTOBER 1987
Oct. 1988 130 p
(AD-A203366; DST-2700Z-005-88) Avail: NTIS HC A07/MF A01 CSCL 09C

This is the Soviet Laser Bibliography for September to October 1987, and is No. 91 in a continuing series on Soviet laser developments. The coverage includes basic research on solid state, liquid, gas, and chemical lasers; components; nonlinear optics; spectroscopy of laser materials; ultrashort pulse generation; crystal growing; theoretical aspects of advanced lasers; and general laser theory. Laser applications are listed under biological effects; communications systems; beam propagation; adaptive optics; computer technology; holography; laser induced chemical reactions; measurement of laser parameters; laser measurement applications; laser excited optical effects; laser spectroscopy; beam target interaction; and plasma generation and diagnostics. GRA

N89-21233# Air Force Systems Command, Wright-Patterson AFB, OH. Foreign Technology Div.
PEOPLE'S REPUBLIC OF CHINA LASER RADIATION SAFETY STANDARD
Yigao Jian 10 Jan. 1989 25 p Transl. into ENGLISH of Jiguang Fushe Anquan Biaojun (People's Republic of China), v. 6, no. 3, 1985 p 1-6
(AD-A203777; FTD-ID(RS)T-0604-88) Avail: NTIS HC A03/MF A01 CSCL 13L

The recommended draft of Safety Standard of Laser Radiation is compiled by the National Colloborated Group of Laser Safety and Protection Research, organized by the National Scientific and Technical Commission. GRA

N89-21234# University of Central Florida, Orlando. Center for Research in Electro-Optics and Lasers.
OPTICAL POWER LIMITER Final Report
M. J. Soileau and Eric W. VanStryland 21 Oct. 1988 41 p
(Contract DAAK20-83-C-0164)
(AD-A203964) Avail: NTIS HC A03/MF A01 CSCL 20F

We have performed a fundamental study of optical/materials interactions which can be used for a passive control of the spatial energy (or power) distribution of optical beams. The study included materials for use in various spectral bands within the spectral range of the UV to 11 microns and the temporal range from CW to picoseconds. We concentrated on materials and concepts with broadband response. Materials studied under DARPA/CNVEO program include aromatic liquids, liquid crystals, semiconductors, and liquid suspensions. We have demonstrated optical limiting using nonlinear absorption in liquid crystals, optical self-action (self-focusing) in liquids and solids, and multiphoton absorption plus sub-sequent self-defocusing in semiconductors. We have theoretically modeled the nonlinearities in these materials and understand the limiting mechanisms although in the organic materials the magnitudes of the nonlinearities are not well understood. In the semiconductors we have developed a predictive capability that allows us to calculate the nonlinearity knowing only a few fundamental material parameters. In addition, we have developed a preliminary model that explains the very low limiting thresholds observed in a liquid suspension of carbon particles as due to nonlinear scattering from rapidly expanding microplasmas initiated by thermionic emission. GRA

N89-21235# Los Alamos National Lab., NM.
NUCLEAR-PUMPED LASERS FOR LARGE-SCALE APPLICATIONS
R. E. Anderson, E. M. Leonard, R. E. Shea, and R. R. Berggren 1988 10 p Presented at the LASERS '88, Lake Tahoe, NV, 5-9 Dec. 1988
(Contract W-7405-eng-36)
(DE89-006532; LA-UR-89-151; CONF-881244-7) Avail: NTIS HC A02/MF A01

Efficient initiation of large-volume chemical lasers may be achieved by neutron induced reactions which produce charged particles in the final state. When a burst mode nuclear reactor is used as the neutron source, both a sufficiently intense neutron flux and a sufficient short initiation pulse may be possible. Proof-of-principle experiments are planned to demonstrate lasing in a direct nuclear-pumped large-volume system: to study the effects of various neutron absorbing materials on laser performance; to study the effects of long initiation pulse lengths; to determine the performance of large-scale optics and the beam quality that may be obtained; and to assess the performance of alternative designs of burst systems that increase the neutron output and burst repetition rate. DOE

N89-21236# Columbia Univ., New York, NY.
LASER ENHANCED CHEMICAL REACTIONS Progress Report
G. W. Flynn 1989 10 p
(Contract DE-FG02-88ER-13937)
(DE89-008084; DOE/ER-13937/1) Avail: NTIS HC A02/MF A01

This report contains information on the following topics: the diode laser probe techniques; hot atoms excitation of vibrational states of polyatomic molecules, and biomolecular quenching and reactions of O(1D). DOE

N89-21237# Lawrence Livermore National Lab., CA.
ATMOSPHERIC EFFECTS ON LASER PROPAGATION
T. J. Karr 22 Nov. 1988 20 p
(Contract W-7405-eng-48)
(DE89-008646; UCID-21578) Avail: NTIS HC A03/MF A01

The linearized theory of thermal blooming instabilities is reviewed. The dispersion relation is derived for unstable modes with and without correction. Perfect phase-only correction is unstable at all spatial scales, while perfect field conjugation is stable at all scales. Various atmospheric phenomena, such as turbulence, diffusion and wind shear may mitigate or dampen the instabilities. Full nonlinear time-dependent computer simulations of laser atmospheric propagation agree with the dispersion relation for small perturbations, and show saturation and nonlinear mode beating at long times. DOE

37 MECHANICAL ENGINEERING

Includes auxiliary systems (nonpower); machine elements and processes; and mechanical equipment.

N89-21238# National Inst. of Standards and Technology, Gaithersburg, MD. Intelligent Controls Group.
MANIPULATOR PRIMITIVE LEVEL TASK DECOMPOSITION Final Report
Albert J. Wavering Oct. 1988 56 p
(PB89-133532; NIST/TN-1256) Avail: NTIS HC A04/MF A01; also available SOD HC $2.75 as 003-003-02907-6 CSCL 13I

The structure, function, and interfaces of a trajectory generation task decomposition module in a hierarchical manipulator control system are described. The module generates dynamic motion and force commands from a static description of the desired behavior, and is called the Primitive (Prim) level of task decomposition, since it generates primitive motion segments. For instance, Prim can generate dynamic position and force trajectories from parametrically-defined static position and force paths. The Prim task decomposition module consists of three subcomponents; the Job Assignment module, the Planning module, and the Execution module. The operation of these modules and the internal Prim interfaces between them are discussed, showing how various trajectory planning techniques are accommodated by the task decomposition module. The discussion in the document is limited to single-arm manipulators and does not include interfaces for end effectors to active wrist devices. GRA

N89-21239*# Mechanical Technology, Inc., Latham, NY.
ADVANCED HELIUM PURGE SEALS FOR LIQUID OXYGEN (LOX) TURBOPUMPS Final Report, Sep. 1985 - Aug. 1987
Wilbur Shapiro and Chester C. Lee Mar. 1989 175 p
(Contract NAS3-24645)
(NASA-CR-182105; NAS 1.26:182105; MTI-87TR72) Avail: NTIS HC A08/MF A01 CSCL 13I

Program objectives were to determine three advanced configurations of helium buffer seals capable of providing improved performance in a space shuttle main engine (SSME), high-pressure liquid oxygen (LOX) turbopump environment, and to provide NASA with the analytical tools to determine performance of a variety of seal configurations. The three seal designs included solid-ring fluid-film seals often referred to as floating ring seals, back-to-back fluid-film face seals, and a circumferential sectored seal that incorporated inherent clearance adjustment capabilities. Of the three seals designed, the sectored seal is favored because the self-adjusting clearance features accommodate the variations in clearance that will occur because of thermal and centrifugal distortions without compromising performance. Moreover, leakage can be contained well below the maximum target values; minimizing leakage is important on the SSME since helium is provided by an external tank. A reduction in tank size translates to an increase in

payload that can be carried on board the shuttle. The computer codes supplied under this program included a code for analyzing a variety of gas-lubricated, floating ring, and sector seals; a code for analyzing gas-lubricated face seals; a code for optimizing and analyzing gas-lubricated spiral-groove face seals; and a code for determining fluid-film face seal response to runner excitations in as many as five degrees of freedom. These codes proved invaluable for optimizing designs and estimating final performance of the seals described. Author

N89-21240 Stanford Univ., CA.
EXPERIMENTS IN END-POINT CONTROL OF MANIPULATORS WITH ELASTIC DRIVES Ph.D. Thesis
Michael Grant Hollars 1988 283 p
Avail: Univ. Microfilms Order No. DA8826150

Excitation of lightly-damped drive system resonances severely limits the performance of most present-day robotic manipulators. Discussed here is the development of practical high-performance control strategies for manipulators in which the flexibility resides primarily in the drive system. To test the control strategies, an experimental two-link planar manipulator was constructed that exhibits very lightly damped drive system resonances, highly nonlinear dynamics, and large variations in payload mass. Baseline performance of standard proportional integral derivative (PID) controllers is demonstrated. Linear quadratic Gaussian control techniques improve by a factor of four many shortcomings of PID designs when the system is at or near the design configuration. To reduce sensitivity to the change in geometry, a constant-gain extended Kalman filter (CGEKF) coupled with a linear-quadratic regulator (LQR) is developed in which the state estimates are propagated by integrating the full nonlinear equations of motion. Extensive benefits of the CGEKF/LQR controller are detailed. Dissert. Abstr.

N89-21241 Ohio State Univ., Columbus.
DIFFUSION WELDING OF AN RS/PM ALUMINUM ALLOY Ph.D. Thesis
V. Ananthanarayanan 1988 212 p
Avail: Univ. Microfilms Order No. DA8820244

A methodology was devised for optimizing diffusion welding parameters for an RS/PM Al-9Fe-4Ce alloy. Temperature-time and temperature-pressure bonding parameter zones developed for the alloy using short-term coarsening studies showed that it was possible to perform diffusion welding operations on the alloy at temperatures up to 600 C (1112 F) without structural support. The bonding parameter zones were useful in limiting microstructural coarsening and consequent softening of the alloy during diffusion welding operations with silver electroplated interlayers. Joint efficiencies up to 70percent were obtained with increased specimen deformation (i.e., combined deformation and diffustion welding). Bonds consisted of Ag2Al type binary intermetallic layers surrounded by complex quarternary intermetallic layers. Kirkendall porosity was found to limit joint-strengths in all specimens. In specimens that experienced no deformation during bonding, the porosity promoted separation at the interface between the base material and the intermetallic layers. Bond-strengths increased with increasing deformation during bonding. Specimen geometries that permitted higher bonding pressures without increasing specimen deformation during bonding were not found to suppress or heal the porosity. Non-wetting of the base material surfaces by eutectic liquid formed with an electroplated silver layer resulted in poor transient-liquid phase bonds between the Al-Fe-Ce alloy specimens. Dissert. Abstr.

N89-21242 Aston Univ., Birmingham (England).
MILD WEAR IN DRY AND LUBRICATED SLIDING SYSTEMS Ph.D. Thesis
Stuart Gregory Hodgson 1988 300 p
Avail: Univ. Microfilms Order No. BRDX83343

A vertical pin on horizontal disc machine was used to conduct a series of experiments in air under dry and lubricating sliding conditions. For dry sliding low load and speed combinations were chosen to correspond to the mild wear region below the Welsh T sub 1 transition. Lubricated tests were conducted under flooded conditions using Esso Technical White Oil alone and with a 0.1 percent stearic acid additive, for load and speed ranges that produced substantial amounts of asperity contact and thus a boundary lubricated regime of wear. The test material in all cases was AISI 52100 steel, for unlubricated sliding subjected to loads from 5 to 50 N and a range of speeds from 0.001 to 1.0/ms, and for lubricated sliding loads of 50 to 123 N and for speeds of 0.01 to 1.0/ms. Unlubricated wear debris was found to be a mixture of alpha-Fe2O3 and alpha-Fe. Unlubricated wear was found to occur via a thin film logarithmic oxide growth followed by agglomeration into thicker oxide plateaux 2 to 10 micrometer thickness. Lubricated wear occurred via a thick film diffusion controlled oxide growth producing homogeneous oxide plateaux 0.1 to 0.2 micrometer in thickness. X-ray photoelectron spectroscopy identified the presence of a surface film on pins worn in White Oil with stearic acid, which is thought to be iron stearate. A model was developed for unlubricated wear based upon the postulated growth of thin film oxides by a logarithmic rate law. The importance of sliding geometry and environment to the dominant wear mechanism was illustrated. Dissert. Abstr.

N89-21243*# National Aeronautics and Space Administration. Lewis Research Center, Cleveland, OH.
COMPARISON STUDY OF GEAR DYNAMIC COMPUTER PROGRAMS AT NASA LEWIS RESEARCH CENTER
James J. Zakrajesek Mar. 1989 31 p Prepared in cooperation with Army Aviation Research and Development Command, Cleveland, OH
(DA Proj. 1L1-62209-AH-76)
(NASA-TP-2901; E-4144; NAS 1.60:2901; AVSCOM-TR-88-C-010)
Avail: NTIS HC A03/MF A01 CSCL 13I

A comparison study was performed on four gear dynamic analysis computer programs developed under NASA/Army sponsorship. These programs are GRDYNMULT (a multimesh program applicable to a number of epicyclic systems), TELSGE (a single mesh program), PGT (a multimesh program applicable to a planetary system with three planets), and DANST (a single mesh program). The capabilities and features, input and output options, and technical aspects of the programs were reviewed and compared. Results are presented in a concise tabular form. Parametric studies of the program models were performed to investigate the predicted results of the programs as input parameters such as speed, torque, and mesh damping were varied. In general, the program models predicted similar dynamic load and stress levels as operating conditions were varied. Flash temperature predictions from programs GRDYNMULT and TELSGE indicated similar trends; however, actual values were not in close agreement. The program GRDYNMULT was found to be the most versatile in system size, type, and analysis capabilities. The programs DANST, TELSGE, and PGT are more specialized for specific systems; however, in specific areas they provide a more detailed treatment than GRDYNMULT. Author

N89-21244*# National Aeronautics and Space Administration. Lewis Research Center, Cleveland, OH.
MODAL ANALYSIS OF GEAR HOUSING AND MOUNTS
Teik C. Lim, Raj. Singh (Ohio State Univ., Columbus.), and James J. Zakrajsek Feb. 1989 14 p Presented at the 7th International Modal Analysis Conference, Las Vegas, NV, 30 Jan. - 2 Feb. 1989; sponsored in part by Union College and the Society for Experimental Mechanics, Inc. Prepared in cooperation with Army Aviation Systems Command, Cleveland, OH
(DA Proj. 1L1-62209-A-47-A)
(NASA-TM-101445; E-4551; NAS 1.15:101445;
AVSCOM-TR-88-C-041) Avail: NTIS HC A03/MF A01 CSCL 13I

Dynamic finite element analysis of a real gear housing is presented. The analysis was conducted for the housing without the rotating components (gears, shafts, and bearings). Both rigid and flexible mounting conditions for the gear housing are considered in this analysis. The flexible support simulates the realistic mounting condition on a rotorcraft, and the rigid one is

analyzed for comparison purposes. The effect of gear housing stiffeners is also evaluated. The results indicate that the first six natural modes of the flexibly mounted gear housing in the 0 to 200 Hz range correspond to the translational and rotational rigid body vibration modes of the housing. Above this range, the housing plate elastic modes begin to occur. In the case of the rigid mount, only the housing plate elastic modes are observed which are verified by modal analysis experiments. Parametric studies show that the housing plate stiffeners and rigid mounts tend to increase most of the natural frequencies, the lower ones being affected the most. Author

N89-21245*# National Aeronautics and Space Administration. Lewis Research Center, Cleveland, OH.
INVESTIGATION OF WEIBULL STATISTICS IN FRACTURE ANALYSIS OF CAST ALUMINUM
Frederic A. Holland, Jr. and Erwin V. Zaretsky 1989 18 p Prepared for presentation at the Failure Prevention and Reliability Conference, Montreal, Quebec, 17-20 Sep. 1989
(NASA-TM-102000; E-4452; NAS 1.15:102000) Avail: NTIS HC A03/MF A01 CSCL 20K

The fracture strengths of two large batches of A357-T6 cast aluminum coupon specimens were compared by using two-parameter Weibull analysis. The minimum number of these specimens necessary to find the fracture strength of the material was determined. The applicability of three-parameter Weibull analysis was also investigated. A design methodology based on the combination of elementary stress analysis and Weibull statistical analysis is advanced and applied to the design of a spherical pressure vessel shell. The results from this design methodology are compared with results from the applicable ASME pressure vessel code. Author

N89-21246*# National Aeronautics and Space Administration. Marshall Space Flight Center, Huntsville, AL.
OBLIQUE HYPERVELOCITY IMPACT RESPONSE OF DUAL-SHEET STRUCTURES
William P. Schonberg (Alabama Univ., Huntsville.) and Roy A. Taylor Jan. 1989 44 p
(NASA-TM-100358; NAS 1.15:100358) Avail: NTIS HC A03/MF A01 CSCL 20K

The results of a continuing investigation of the phenomena associated with the oblique hypervelocity impact of spherical projectiles onto multi-sheet aluminum structures are given. A series of equations that quantitatively describes these phenomena is obtained through a regression of experimental data. These equations characterize observed ricochet and penetration damage phenomena in a multi-sheet structure as functions of geometric parameters of the structure and the diameter, obliquity, and velocity of the impacting projectile. Crater damage observed on the ricochet witness plates is used to determine the sizes and speeds of the ricochet debris particles that caused the damage. It is observed that the diameter of the most damaging ricochet debris particle can be as large as 40 percent of the original particle diameter and can travel at speeds between 24 percent and 36 percent of the original projectile impact velocity. The equations necessary for the design of shielding panels that will protect external systems from such ricochet debris damage are also developed. The dimensions of these shielding panels are shown to be strongly dependent on their inclination and on their circumferential distribution around the spacecraft. Author

N89-21247# Rochester Univ., NY. Dept. of Computer Science.
THE ROCHESTER ROBOT
Christopher M. Brown Aug. 1988 68 p
(Contract DACA76-85-C-0001)
(AD-A202633; AD-E900870; TR-257) Avail: NTIS HC A04/MF A01 CSCL 12I

The Rochester Robot is a unique design that was built to study the use of real-time vision in cognition and movement. The major feature of the robot is the robot head. The head consists of binocular cameras that can be moved at over 400 degrees per second. During rapid movements visual data can be analyzed with a pipeline processor and used to control the motion of a body. The body is a PUMA 761 six degree-of-freedom arm which has a two meter radius workspace and a top speed of about 100 cm/second. These features combine to give the robot the capability of reacting to features in its environment in complicated ways in real time. GRA

N89-21248# Air Force Inst. of Tech., Wright-Patterson AFB, OH. School of Engineering.
DEVELOPMENT OF A SHOCK CAPTURING CODE FOR USE AS A TOOL IN DESIGNING HIGH-WORK LOW ASPECT RATIO TURBINES M.S. Thesis
Mark A. Driver Dec. 1988 76 p
(AD-A202706; AFIT/GAE/AA/88D-10) Avail: NTIS HC A05/MF A01 CSCL 01A

A numerical algorithm is developed with the capability of capturing shocks in the internal blade passages of a modern gas turbine. The algorithm uses MacCormack's explicit finite difference scheme to solve the two-dimensional form of the Euler equations. Inlet and exit boundary conditions are developed that allow disturbances to propagate out of the computational domain without reflection. Periodic boundary conditions are applied such that an infinite cascade is modeled. The computed steady state solution is compared with experimental data for a high-work low aspect ratio turbine. The ability to obtain a reasonably accurate blade loading diagram within a practical execution time is demonstrated. Two oblique shocks, typical of those formed at the trailing edge of a transonic rotor blade, are captured. These shocks are smeared over several grid points, as expected with a shock capturing scheme, but their influence on the blade loading diagram is evident. GRA

N89-21249# Air Force Inst. of Tech., Wright-Patterson AFB, OH. School of Engineering.
ROBOTIC COMPLIANT MOTION CONTROL FOR AIRCRAFT REFUELING APPLICATIONS M.S. Thesis
David J. Duvall Dec. 1988 219 p
(AD-A202710; AFIT/GA/ENG/88D-1) Avail: NTIS HC A10/MF A01 CSCL 12I

A promising Air Force application of robotics technology is the refueling of aircraft or spacecraft with a robotic manipulator. The refueling task is fundamentally a component assembly task, and like many other assembly tasks, successful completion requires compliance between the manipulator and the environment for success. Compliant motion control techniques, such as impedance control, use force feedback to generate active compliance in the robot manipulator. In this thesis a compliant motion control environment was established, and a simplified, preliminary version of an impedance control law was implemented. The compliant motion environment employs three digital processors in a hierarchial control structure to command a PUMA 560 robot arm. Applied force and moment information are provided by a wrist mounted, three axis force sensor. An original method was developed to transform forces and moments acting on the tool, measured in the sensor frame, to the cartesian world coordinate frame. This method eliminates the forces and moments caused by the tool weight from the measured values. The concept of impedance control law is presented. The simplified impedance is explained, and motivated as the basis for compliant motion control. The theoretical development leading to the simplified impedance control law was used to provide active compliance for links 2 and 3 of the PUMA arm. The remaining four links of the PUMA were not actively used in the impedance control experiment. GRA

N89-21250# Air Force Inst. of Tech., Wright-Patterson AFB, OH. School of Engineering.
ROBOTIC TACTILE SENSOR FABRICATED FROM PIEZOELECTRIC POLYVINYLIDENE FLUORIDE FILMS M.S. Thesis
Rocky R. Reston Dec. 1988 127 p
(AD-A202724; AFIT/GE/ENG/88D-41) Avail: NTIS HC A07/MF A01 CSCL 07B

The purpose of this research effort was to design, fabricate

and test a robotic tactile sensor fabricated from polyvinylidend fluoride (PVDF) films coupled to a silicon substrate containing active amplification circuitry. The integrated circuit incorporated 25 sensor electrode pads (0.6mmx0.6mm each) arrayed in a 5x5 grid with a spacing of 0.6mm between electrodes (this corresponds to a spatial resolution four times greater than the human fingertip). The on-board amplification circuitry consisted of a dual MOSFET amplifier (with a gain of 5) for each sensor electrode. Four different sensor configurations were fabricated and tested. The configurations varied only in the thickness of the PVDF film used (25 microns, 40 microns, 52 microns, and 110 microns). The individual elements of each of the sensor configurations were tested and the sensor based on the 25 micron thick film was considered the optimal sensor of the four. GRA

N89-21251# Massachusetts Inst. of Tech., Cambridge. Artificial Intelligence Lab.

MODELING ROBOT DYNAMIC PERFORMANCE FOR ENDPOINT FORCE CONTROL Ph.D. Thesis

Steven D. Eppinger Aug. 1988 140 p

(Contracts N00014-86-K-0685; N00014-85-K-0124)

(AD-A202881; AI-TR-1072) Avail: NTIS HC A07/MF A01 CSCL 12I

This thesis aims to understand the fundamental dynamic behavior of servo-controlled machinery in response to various types of sensory feedback. As an example of such a system, the author studies robot force control, a scheme which promises to greatly expand the capabilities of industrial robots by allowing manipulators to interact with uncertain and dynamic tasks. Implementations of compliant motion control strategies typically display extremely limited performance. Furthermore, the instabilities observed in these systems are generally not predicted by robot performance models. In this research, dynamic models are developed which allow the effects of actuator dynamics, structural flexibility, and workpiece interaction to be explored in the frequency and time domains. The models are used first to explain the causes of robot force control instability, and then to find methods of improving this performance. Emphasis is placed on the use of both laboratory testing and mathematical modeling to gain a fundamental understanding of machine dynamic behavior. The insights developed will help the designers of the next generation of automated manufacturing equipment to build more capable systems. GRA

N89-21252# North Staffordshire Polytechnic, Stafford (England). Dept. of Mechanical and Computer-Aided Engineering.

VIBRATION CONTROL IN ROTATING MACHINERY USING VARIABLE DYNAMIC STIFFNESS SQUEEZE-FILMS Final Report, Sep. 1984 - Mar. 1988

M. J. Goodwin and M. P. Roach Jun. 1988 22 p

(Grant AF-AFOSR-0368-84; AF Proj. 2302)

(AD-A202902; AFOSR-88-1290TR) Avail: NTIS HC A03/MF A01 CSCL 13I

This report describes work carried out with the aim of developing a combined hydrostatic and squeeze-film bearing, for rotating machinery, whose dynamic characteristics may be tuned during operation of the machine. The purpose of this is to enable the operator to exercise control over machine critical speeds and vibrations. A computer program has been written to predict the characteristics of the bearing type. The program allows for the presence of accumulators linked to the bearing oil film whose purpose is to modify the bearing dynamic characteristics. A test rig has been designed and built, based on a General Electric TF34 turbofan engine, and both theoretical and experimental results confirm that a substantial shift in critical speed is effected by using the bearing, and that system vibration and force transmissibility may be reduced substantially when compared with the performance of conventional squeeze film bearings and journal bearings. GRA

N89-21253# Southwest Research Inst., San Antonio, TX. Fuels and Lubricants Research Facility.

FOULING TESTS OF AGT-1500 GAS TURBINE FUEL NOZZLES Interim Report, Sep. 1986 - Sep. 1988

Lee G. Dodge, Leo L. Stavinoha, and Howard W. Marbach, Jr. Sep. 1988 42 p

(Contracts DAAK70-85-C-0007; DAAK70-87-C-0043; DA Proj. 1L7-62786-AH-20)

(AD-A203360; BFLRF-258) Avail: NTIS HC A03/MF A01 CSCL 21D

AGT-1500 gas turbine engines have experienced significant starting problems due to fuel nozzle fouling. The first objective of these tests was to evaluate the effects of fuel additives on deposit formation in fuel injectors for combustors in AGT-1500 gas-turbine engines. A second objective was to determine what other standard ASTM or bench-type tests could be used to predict the full-scale fouling results without the expense of the full-scale tests. A third objective was to evaluate solvents and cleaners of removing the deposits. A 125-cycle start-up, run, and shutdown test was used in full-scale tests to evaluate fuel nozzle fouling during the shutdown heatsoak period. Two standard Cat 1-H reference fuels with different thermal stability characteristics were tested. GRA

N89-21254# Army Lab. Command, Watertown, MA. Materials Producibility Branch.

REDUCTION OF M1 WELD FABRICATION COSTS: THE EFFECT OF WELD SHIELDING GAS COMPOSITION Final Report

Steven A. Gedeon and James E. Catalano Dec. 1988 36 p

(AD-A204001; MTL-TR-88-49) Avail: NTIS HC A03/MF A01 CSCL 11F

This project was initiated in October, 1986, to find a lower cost alternative to the weld shielding gas used for M1 fabrication at the U.S. Army Lima Tank Plant. The shielding gas in use was a newly patented mixture termed Transferred Ionized Molten Energy (TIME) gas. This gas was manufactured in Canada (and for a short time in Chicago, and now Columbus), and is much more expensive than other gas mixtures. The objective of this project is to evaluate a wide variety of weld shielding gas mixtures for welding the armor steel used in the U.S. Army M1 Abram's main battle tank. It is greatly desired to find an inexpensive gas mixture to replace the TIME gas used in 1986 at the Lima Army Tank Plant without decreasing weld performance. The gas mixtures were evaluated on gas cost, deposition rate, amount of weld hydrogen, beak profile, and amount of spatter. The effects of gas composition, weld voltage, electrode stickout, base metal composition, and nozzle geometry on welding characteristics were also evaluated. GRA

N89-21255# Technical Research Centre of Finland, Espoo.

OPERATION OF VEHICLE ENGINES IN COLD CONDITIONS: START UP, LUBRICATION AND FUEL CONSUMPTION

Nils-Olof Nylund, Matti Kytoe, and Juhani Laurikko Nov. 1988 54 p In FINNISH; ENGLISH summary

(DE88-757111; VTT-TIED-907) Avail: NTIS (US Sales Only) HC A04/MF A01

Studied were the fuel consumption and wear of engines in cold conditions. The type of lubricant (mineral, semisynthetic or synthetic oil) affects start-up and start of lubrication. The fuel consumption depends mainly on temperature, type of engine, driving manner and viscosity of lubricant. Test were carried out with three gasoline engines and two diesel engines in a special cold research room. The test engines were put under load by an engine dynamometer. On one of the gasoline engines, tests were also made with a manual transaxle. The start of lubrication and the fuel consumption were determined by 30-minute engine tests with different lubricants at the temperature range of +20 to -30 C. The engines were run both under constant load and cyclic load. The effect of electric preheaters (block and oil heaters) was also studied. Although the viscosity class of all the test oils was SAE 10W30 or SAE 10W40, the time required for the rise of the oil pressure on the most remote bearing of the camshaft decreased even by 50 percent at low temperatures when using synthetic oil

instead of mineral oil. Compared to the mineral oil the synthetic oil gave easier startability, although the rotating speed in start-up was the same with both oils. The compression pressure was higher and the friction lower when using synthetic oil. The start-up was considerably easier when an electric block heater was used. As the block heater does not warm up the oil in the oil sump, the cold viscosity of the oil must be sufficiently low. The fuel consumption in a 30-minute test increased by 4 to 9 percent in diesel engines and by 5 to 22 percent in gasoline engines, when the test temperature was lowered from +20 to -25 C. The type of the oil did not affect significantly the fuel consumption, though compared to the mineral oil the synthetic oil clearly decreased friction loss in the gearbox. DOE

N89-21735*# Carnegie-Mellon Univ., Pittsburgh, PA. Dept. of Mechanical Engineering.
A PERFORMANCE/LOSS EVALUATION OF SSME HPFTP TURBINE
Mingking K. Chyu *In* Alabama Univ., Research Reports: 1988 NASA/ASEE Summer Faculty Fellowship Program Dec. 1988 20 p (For primary document see N89-21726 14-99)
Avail: NTIS HC A99/MF E03 CSCL 13I

N89-21746*# Tennessee Univ., Chattanooga. Dept. of Mechanical Engineering-Mechanics.
THE SIMULATION OF THE ALTERNATE TURBOPUMP DEVELOPMENT HIGH PRESSURE OXYGEN AND FUEL TURBOPUMPS FOR THE SPACE SHUTTLE MAIN ENGINE USING THE SHABERTH COMPUTER PROGRAM
Gary H. McDonald *In* Alabama Univ., Research Reports: 1988 NASA/ASEE Summer Faculty Fellowship Program Dec. 1988 32 p (For primary document see N89-21726 14-99)
Avail: NTIS HC A99/MF E03 CSCL 13I

N89-21750*# Alabama Univ., Huntsville. Dept. of Mechanical Engineering.
FURTHER INVESTIGATIONS OF OBLIQUE HYPERVELOCITY IMPACT PHENOMENA
William P. Schonberg *In* Alabama Univ., Research Reports: 1988 NASA/ASEE Summer Faculty Fellowship Program Dec. 1988 45 p (For primary document see N89-21726 14-99)
Avail: NTIS HC A99/MF E03 CSCL 13I

N89-21755*# California Polytechnic State Univ., San Luis Obispo. Dept. of Metallurgy and Materials Engineering.
THE KEYHOLE REGION IN VPPA WELDS
Daniel W. Walsh *In* Alabama Univ., Research Reports: 1988 NASA/ASEE Summer Faculty Fellowship Program Dec. 1988 27 p (For primary document see N89-21726 14-99)
Avail: NTIS HC A99/MF E03 CSCL 13I

N89-21759*# Auburn Univ., AL. Dept. of Algebra, Combinatorics and Analysis.
ROTORDYNAMIC ANALYSIS OF A BEARING TESTER
Richard A. Zalik *In* Alabama Univ., Research Reports: 1988 NASA/ASEE Summer Faculty Fellowship Program Dec. 1988 25 p (For primary document see N89-21726 14-99)
Avail: NTIS HC A99/MF E03 CSCL 13I

38 QUALITY ASSURANCE AND RELIABILITY

Includes product sampling procedures and techniques; and quality control.

N89-21256*# Virginia Polytechnic Inst. and State Univ., Blacksburg. Dept. of Engineering Science and Mechanics.
A STUDY OF THE STRESS WAVE FACTOR TECHNIQUE FOR EVALUATION OF COMPOSITE MATERIALS Final Report
J. C. Duke, Jr., E. G. Henneke, II, M. T. Kiernan, and P. P. Grosskopf Washington NASA Jan. 1989 61 p
(Grant NAG3-172)
(NASA-CR-4195; E-4385; NAS 1.26:4195) Avail: NTIS HC A04/MF A01 CSCL 14D

The acousto-ultrasonic approach for nondestructive evaluation provides a measurement procedure for quantifying the integrated effect of globally distributed damage characteristic of fiber reinforced composite materials. The evaluation procedure provides a stress wave factor that correlates closely with several material performance parameters. The procedure was investigated for a variety of materials including advanced composites, hybrid structure bonds, adhesive bonds, wood products, and wire rope. The research program focused primarily on development of fundamental understanding and applications advancements of acousto-ultrasonics for materials characterization. This involves characterization of materials for which detection, location, and identification of imperfections cannot at present be analyzed satisfactorily with mechanical performance prediction models. In addition to presenting definitive studies on application potentials, the understanding of the acousto-ultrasonic method as applied to advanced composites is reviewed. Author

39 STRUCTURAL MECHANICS

Includes structural element design and weight analysis; fatigue; and thermal stress.

For applications see *05 Aircraft Design, Testing and Performance* and *18 Spacecraft Design, Testing and Performance.*

N89-21257# Delaware Univ., Newark. Sea Grant Coll. Program.
FUNCTION THEORY FOR THIN ELASTIC SHELLS
Robert P. Gilbert and Yongzghi Xu Aug. 1988 18 p Sponsored in part by NOAA, Rockville, MD
(Grant NSF DNS-86-01318)
(PB89-101943; DEL-SG-16-88) Avail: NTIS HC A03/MF A01 CSCL 20K

It is well known in the thoery of elastic shells that a first order approximation using the shell thickness as an expansion parameter leads to the membrane theory of shells. The membrane equations have as solutions the generalized analytic functions. Gilbert and Hile introduced an extension of these systems to include elliptic systems of 2n equations in the plane and named the solutions of these systems generalized hyperanalytic functions. It is shown that the next order approximation to the shell, which permits, moreover, the introduction of bending, may be described in terms of the generalized hyperanalytic functions. It is strongly suspected that the higher order approximations may also be described in terms of corresponding hypercomplex systems. Author

N89-21258*# Georgia Inst. of Tech., Atlanta. School of Materials Engineering.
DEFORMATION MODELING AND CONSTITUTIVE MODELING FOR ANISOTROPIC SUPERALLOYS Final Contractor Report
Walter W. Milligan and Stephen D. Antolovich Washington NASA Feb. 1989 294 p
(Grant NAG3-503)
(NASA-CR-4215; E-4543; NAS 1.26:4215) Avail: NTIS HC A13/MF A01 CSCL 20K

A study of deformation mechanisms in the single crystal superalloy PWA 1480 was conducted. Monotonic and cyclic tests were conducted from 20 to 1093 C. Both (001) and near-(123) crystals were tested, at strain rates of 0.5 and 50 percent/minute. The deformation behavior could be grouped into two temperature regimes: low temperatures, below 760 C; and high temperatures, above 820 to 950 C depending on the strain rate. At low temperatures, the mechanical behavior was very anisotropic. An orientation dependent CRSS, a tension-compression asymmetry, and anisotropic strain hardening were all observed. The material was deformed by planar octahedral slip. The anisotropic properties were correlated with the ease of cube cross-slip, as well as the number of active slip systems. At high temperatures, the material

was isotropic, and deformed by homogeneous gamma by-pass. It was found that the temperature dependence of the formation of superlattice-intrinsic stacking faults was responsible for the local minimum in the CRSS of this alloy at 400 C. It was proposed that the cube cross-slip process must be reversible. This was used to explain the reversible tension-compression asymmetry, and was used to study models of cross-slip. As a result, the cross-slip model proposed by Paidar, Pope and Vitek was found to be consistent with the proposed slip reversibility. The results were related to anisotropic viscoplastic constitutive models. The model proposed by Walter and Jordan was found to be capable of modeling all aspects of the material anisotropy. Temperature and strain rate boundaries for the model were proposed, and guidelines for numerical experiments were proposed. Author

N89-21259# Northwestern Polytechnical Univ., Xian (China).
DYNAMIC STRUCTURAL OPTIMIZATION AND EXPERIMENT
Jifeng Chen 1987 10 p
(PB89-111462; ISTIC-TR-C-000195) Avail: NTIS HC A02/MF A01 CSCL 20K

An optimal method with the frequency constraints, the nodal position constraints of the mode shape, and upper and lower bounds on the design variables are presented. The design algorithm is essentially an iterative solution of the Kuhn-Tucker optimality criterion, and the experimental results are given. GRA

N89-21260*# National Aeronautics and Space Administration. Langley Research Center, Hampton, VA.
NONLINEAR SHELL ANALYSES OF THE SPACE SHUTTLE SOLID ROCKET BOOSTERS
Norman F. Knight, Jr., Ronnie E. Gillian, and Michael P. Nemeth Jan. 1989 26 p Submitted for publication
(NASA-TM-101546; NAS 1.15:101546) Avail: NTIS HC A03/MF A01 CSCL 20K

A variety of structural analyses have been performed on the Solid Rocket Boosters (SRB's) to provide information that would contribute to the understanding of the failure which destroyed the Space Shuttle Challenger. This paper describes nonlinear shell analyses that were performed to characterize the behavior of an overall SRB structure and a segment of the SRB in the vicinity of the External Tank Attachment (ETA) ring. Shell finite element models were used that would accurately reflect the global load transfer in an SRB in a manner such that nonlinear shell collapse and ovalization could be assessed. The purpose of these analyses was to calculate the overall deflection and stress distributions for these SRB models when subjected to mechanical loads corresponding to critical times during the launch sequence. Static analyses of these SRB models were performed using a snapshot picture of the loads. Analytical results obtained using these models show no evidence of nonlinear shell collapse for the pre-liftoff loading cases considered. Author

N89-21261# Instituut TNO voor Bouwmaterialen en Bouwconstructies, Delft (Netherlands).
NUMERICAL AND EXPERIMENTAL DETERMINATION OF STRAIN (STRESS) CONCENTRATION FACTORS OF WELDED JOINTS BETWEEN SQUARE HOLLOW SECTIONS
R. S. Puthli, J. Wardenier, C. H. M. deKoning, A. M. vanWingerde, and F. J. vanDooren 1988 55 p Submitted for publicatoin
Prepared in cooperation with Technische Hogeschool, Delft, Netherlands
(PB89-131734) Avail: NTIS HC A04/MF A01 CSCL 20K

Methods of approach are presented for finite element modeling of joints made of rectangular hollow steel sections where the brace members are welded to the face of the chord, to obtain strain (stress) concentration factors, SNCF (SCF). X, T and K type joints are considered. Simple modeling method are applied for practical reasons, so that straight forward use in large scale parametric studies is possible. Details that influence the results due to modeling are discussed. In the range of parameters considered for subsequent parametric studies, a few selected representative joints are considered for experimental comparison. The comparisons between experimental and finite element analyses give confidence in the results. SNCF values at critical locations are determined for a range of preselected geometrical parameters and used in regression analyses to provide parametric SNCF formulae. The SNCF values from these formulae have a good correlation with the values determined from the finite element analyses. The SNCF formulae are also shown graphically to give a visual impression of the influence of the various geometrical parameters on the magnitudes. GRA

N89-21262 Akron Univ., OH.
GLOBAL-LOCAL METHODOLOGY FOR FRACTURE ANALYSIS OF ENGINEERING STRUCTURES Ph.D. Thesis
Daniel P. Dougherty 1989 325 p
Avail: Univ. Microfilms Order No. DA8825204

The design of engineering structures and components is dependent upon many parameters which are used to optimize the structure or component for cost, performance and durability. Many of these structures and components are subjected to an environment of cyclic loads and eventually fail from fatigue fracture. Therefore, the design phase must incorporate the effects of linear elastic fracture mechanics and local high stress states. The objective is to develop a methodology for a global-local finite element design tool which will be capable of modelling crack growth, local high stress states and the onset of sudden unstable fracture. The initial global stress field determines the zones of the structure which require refinement. At this point, a multi-level substructuring scheme is employed in order to better define local stress states and crack behavior. The global solution passes displacement parameters to the local levels where crack propagation is simulated. Locally modified stiffness parameters are returned to the global level where an iterative procedure continues the cyclic analysis. Dissert. Abstr.

N89-21263 Maryland Univ., College Park.
STRESS INTENSITY FACTORS FOR BODIES CONTAINING INITIAL STRESS Ph.D. Thesis
Stephen Murphy Graham 1988 195 p
Avail: Univ. Microfilms Order No. DA8827075

Prediction of fracture response of a body containing initial stress requires determining the stress intensity factor for the initial field. Currently accepted design practice utilizes the principle of linear superposition to transfer internal loading to the crack faces. Established analytical methods are then used to determine the stress intensity for that crack face loading. Careful examination of the fundamental principles of mechanics used to derive the linear superposition principle reveals that superposition can not be used to transfer internal load. Consequently, the currently accepted design practice is in error. An alternative means for calculating stress intensity factor based on the total strain energy release rate of a cracked body is presented. Numerical calculations of stress intensity for a typical initial stress field problem using the total strain energy release rate method are compared with analytical predictions using linear superposition. The results obtained using the strain energy method are in agreement with physical reasoning, while the predictions based on linear superposition are not. Experimental measurements of initial displacement field resistribution during crack extension confirm the numerical predictions. Dissert. Abstr.

N89-21264 Arizona State Univ., Tempe.
BENDING AND VIBRATION OF VARIABLE THICKNESS ORTHOTROPIC PLATES Ph.D. Thesis
Wei-Cheun Liu 1988 108 p
Avail: Univ. Microfilms Order No. DA8825693

The problems of bending and free vibration of arbitrarily shaped orthotropic plates with variable thickness and mixed boundary conditions are solved by a modified energy method. A general expression is written for the deflection of the plate without aiming at any particular combination of boundary conditions. Boundary conditions are satisfied approximately by adjusting a set of so-called fixity factors. Computer programs were developed to compute the static deflection and natural frequencies, respectively. Numerical results are compared with those cases for which solutions are

known. In most cases agreements are excellent. Results were generated on variable thickness orthotropic annular plates, hexagonal plates with a circular hole at the center and on many other combinations of shapes and boundary conditions.
Dissert. Abstr.

N89-21265*# Case Western Reserve Univ., Cleveland, OH. Dept. of Civil Engineering.
ANALYSIS OF INTERFACE CRACK BRANCHING
R. Ballarini, D. J. Mukai, and G. R. Miller (Washington Univ., Seattle.) Mar. 1989 23 p
(Grant NAG3-856)
(NASA-CR-182273; NAS 1.26:182273) Avail: NTIS HC A03/MF A01 CSCL 20K

A solution is presented for the problem of a finite length crack branching off the interface between two bonded dissimilar isotropic materials. Results are presented in terms of the ratio of the energy release rate of a branched interface crack to the energy release rate of a straight interface crack with the same total length. It is found that this ratio reaches a maximum when the interface crack branches into the softer material. Longer branches tend to have smaller maximum energy release rate ratio angles indicating that all else being equal, a branch crack will tend to turn back parallel to the interface as it grows. Author

N89-21266*# National Aeronautics and Space Administration. Lewis Research Center, Cleveland, OH.
CHARACTERIZATION OF STRUCTURAL CONNECTIONS USING FREE AND FORCED RESPONSE TEST DATA
Charles Lawrence and Arthur A. Huckelbridge (Case Western Reserve Univ., Cleveland, OH.) 1989 14 p Proposed for presentation at the 12th Biennial Conference on Mechanical Vibration and Noise, Montreal, Quebec, 17-20 Sep. 1989; sponsored by ASME
(NASA-TM-101991; E-4695; NAS 1.15:101991) Avail: NTIS HC A03/MF A01 CSCL 20K

The accurate prediction of system dynamic response often has been limited by deficiencies in existing capabilities to characterize connections adequately. Connections between structural components often are complex mechanically, and difficult to accurately model analytically. Improved analytical models for connections are needed to improve system dynamic preditions. A procedure for identifying physical connection properties from free and forced response test data is developed, then verified utilizing a system having both a linear and nonlinear connection. Connection properties are computed in terms of physical parameters so that the physical characteristics of the connections can better be understood, in addition to providing improved input for the system model. The identification procedure is applicable to multi-degree of freedom systems, and does not require that the test data be measured directly at the connection locations. Author

N89-21267*# Analytical Services and Materials, Inc., Hampton, VA.
IMPLEMENTATION OF EQUIVALENT DOMAIN INTEGRAL METHOD IN THE TWO-DIMENSIONAL ANALYSIS OF MIXED MODE PROBLEMS
I. S. Raju and K. N. Shivakumar Apr. 1989 57 p
(Contract NAS1-18599)
(NASA-CR-181813; NAS 1.26:181813) Avail: NTIS HC A04/MF A01 CSCL 20K

An equivalent domain integral (EDI) method for calculating J-intergrals for two-dimensional cracked elastic bodies is presented. The details of the method and its implementation are presented for isoparametric elements. The total and product integrals consist of the sum of an area of domain integral and line integrals on the crack faces. The line integrals vanish only when the crack faces are traction free and the loading is either pure mode 1 or pure mode 2 or a combination of both with only the square-root singular term in the stress field. The EDI method gave accurate values of the J-integrals for two mode I and two mixed mode problems. Numerical studies showed that domains consisting of one layer of elements are sufficient to obtain accurate J-integral values. Two procedures for separating the individual modes from the domain integrals are presented. The procedure that uses the symmetric and antisymmetric components of the stress and displacement fields to calculate the individual modes gave accurate values of the integrals for all problems analyzed. The EDI method when applied to a problem of an interface crack in two different materials showed that the mode 1 and mode 2 components are domain dependent while the total integral is not. This behavior is caused by the presence of the oscillatory part of the singularity in bimaterial crack problems. The EDI method, thus, shows behavior similar to the virtual crack closure method for bimaterial problems. Author

N89-21268# Brown Univ., Providence, RI. Div. of Engineering.
LARGE DEFORMATIONS NEAR A PAIR OF CLOSELY-SPACED SPHERICAL VOIDS IN A RATE-DEPENDENT SOLID Interim Technical Report, May - Sep. 1988
Janet A. Blume Sep. 1988 25 p
(Contract DAAL03-88-K-0015)
(AD-A202465; ARO-25544.5-EG) Avail: NTIS HC A03/MF A01 CSCL 20K

The deformation in a rate-dependent solid containing a pair of closely-spaced spherical voids is analytically determined. Results are obtained which are valid in the material that separates the cavities. The solid is assumed to be infinite in its extent, and is remotely subjected to a uniform stress field which is axially symmetric about the axes of the two voids; the cavities themselves remain traction free. GRA

N89-21269# Rockwell International Science Center, Thousand Oaks, CA.
FURTHER STUDIES OF THE HRR FIELD OF A MOVING CRACK. AN EXPERIMENTAL ANALYSIS
Mahyar S. Dadkhah and Albert S. Kobayashi (Washington Univ., Seattle.) Dec. 1988 25 p
(Contract N00014-85-K-0187)
(AD-A202545; UWA/DME/TR-88/61) Avail: NTIS HC A03/MF A01 CSCL 11F

An improved moire interferometry was used to record simultaneously both the vertical and horizontal displacements associated with stable crack growth in an uniaxially loaded 5052-H32 aluminum, single edge notched specimens. For stable crack growth up to 2 mm, the vertical displacement field showed the dominance of the crack tip region (HRR) field. HRR field was detected in the horizontal displacement only at the initial stage of loading. The far and near field J-integrals were path independent during this incremental crack extension. These results and previous results involving 2024-0 and 2024-T3 aluminum specimens indicate that J-characterization of a crack, is not valid for such ductile materials in this specimen configuration. GRA

N89-21270# Air Force Inst. of Tech., Wright-Patterson AFB, OH. School of Engineering.
APPLICATION OF THE BOUNDARY ELEMENT METHOD TO FATIGUE CRACK GROWTH ANALYSIS M.S. Thesis
Timothy C. Kelley Sep. 1988 142 p
(AD-A202565; AFIT/GAE/AA/88S-1) Avail: NTIS HC A07/MF A01 CSCL 20K

This investigation analyzes a crack emanating from one hole, and approaching a second hole, in a two hole tension strip with finite boundaries using the Boundary Element Method. The study included the effects of varying the hole diameter, hole separation and the length of the geometric correction factor beta, which can be presented as a family of curves. An example damage tolerance analysis is presented with the beta curves being incorporated into a beta look-up table as used in the NASA/FLAGRO fatigue crack growth program. This technique is acceptable in most fatigue crack growth programs now used in the aircraft industry to ensure aircraft structural integrity. Several classic fracture mechanics problems are analyzed, and computational efficiency as compared to conventional finite element techniques is investigated. Agreement with analytic solutions as well as other numerical methods (finite

element) is excellent. The computation efficiency was shown to an improvement over existing methods. GRA

N89-21271# Air Force Inst. of Tech., Wright-Patterson AFB, OH. School of Engineering.
NONLINEAR FINITE ELEMENT ANALYSIS OF A GENERAL COMPOSITE SHELL M.S. Thesis
Gregory S. Egan Dec. 1988 194 p
(AD-A202572; AFIT/GAE/AA/88D-12) Avail: NTIS HC A09/MF A01 CSCL 12A

An analytical study, using the STAGSC-1 computer code, was conducted on a Kevlar/Polyester composite shell of general shape with internal asymmetrical pressure loading. Experimentation was conducted on the shell to find displacements in the shell due to this internal pressure loading. Modeling of the composite structure was done in increments whereby each change in the finite element model better approximated the actual shell. Nonlinear computer runs were done at each model increment to compare against experimental results. Linear computer runs were also completed for comparison purposes. It was found that accurate modeling of the shell to include thickness variations, boundary conditions, and materials is essential to obtain reasonable results. Also, the incorporation of the nonlinear analysis leads to displacement results that are within 15 percent of experimentation. Linear results from the same model are in error by over 75 percent due to large displacements in the shell. GRA

N89-21272# California Inst. of Tech., Pasadena. Graduate Aeronautical Labs.
THREE DIMENSIONAL EFFECTS NEAR A CRACK TIP IN A DUCTILE THREE POINT BEND SPECIMEN. PART 2: AN EXPERIMENTAL INVESTIGATION USING INTERFEROMETRY AND CAUSTICS
Alan T. Zehnder and Ares J. Rosakis Mar. 1988 43 p
(Contract N00014-85-K-0596)
(AD-A202637; AD-E900870; GALCIT-SM-88-7-Pt-2) Avail: NTIS HC A03/MF A01 CSCL 20K

An experimental investigation is undertaken to assess three-dimensional effects near a crack front in a ductile three-point bend specimen. The possibility of using the optical method of caustics for the measurement of the J integral in the presence of large scale yielding and three dimensional fields is also investigated. Experiments using the optical methods of caustics by reflection and Twyman-Green interferometry are performed simultaneously on either side of the test specimen. The load and load-point displacement are also measured. The experimental results are compared with very good agreement to the results of a finite element simulation of the experiment. The caustics experiments are used to obtain a calibration relation between the value of the J integral and the caustic diameter for load levels up to fracture initiation. It is proposed that such a calibration be used in dynamic fracture initiation experiments for the measurement of the time history of the dynamic J integral. GRA

N89-21273# Naval Postgraduate School, Monterey, CA.
ANALYTICAL AND EXPERIMENTAL INVESTIGATION OF CONSTRAINED VISCOELASTIC LAYER DAMPING FOR A PLATE AND SHELL MODEL M.S. Thesis
James R. Nault Sep. 1988 96 p
(AD-A202698) Avail: NTIS HC A05/MF A01 CSCL 20K

The use of constrained viscoelastic layer damping treatments has recently been found to be effective in reducing unwanted resonant vibrations in structures. The proper design of such damping treatments has been difficult, however, since closed form equations to describe system behavior can only be used for simple beams and plates. In addition, finite element analysis has been difficult since the material properties of viscoelastic materials show a marked dependence on frequency and temperature, resulting in the need to run an excessive number of finite element analyses for each design a proper constrained viscoelastic layer damping treatment for a test structure consisting of two concentric cylinders connected by four vanes. GRA

N89-21274# Army Armament Research, Development and Engineering Center, Watervliet, NY.
FRACTOGRAPHIC ANALYSIS OF A FAILED CRANE BOLT Final Report
A. A. Kapusta Nov. 1988 22 p
(AD-A202703; ARCCB-TR-88041) Avail: NTIS HC A03/MF A01 CSCL 11F

A failed crane bolt was examined by scanning electron microscopy to determine its failure mode. Failure occurred by fatigue crack initiation at the root of a thread with subsequent propagation by fatigue through essentially the entire approx. 0.7-inch diameter cross section of the bolt. GRA

N89-21275# Air Force Inst. of Tech., Wright-Patterson AFB, OH. School of Engineering.
A NEW MODEL FOR THE FORCED RESPONSE OF A MISTUNED DISK M.S. Thesis
Jeffrey S. Turcotte Dec. 1988 100 p
(AD-A202769; AFIT/GAE/AA/88D-38) Avail: NTIS HC A05/MF A01 CSCL 20K

A simple model is developed for the forced response of a mistuned, center-clamped disk to predict experimental observations. The response near a resonance can take the form of rotating node lines. A simple model of a mistuned stationary disk was developed and the transverse responses to both rotating point loads and stationary point loads oscillating in time were determined. The disk model uses torsional springs applied at points on the outer edge of an annular disk to mistune a given transverse vibration mode such that the two resulting mistuned mode shapes are each described by only four terms. The response of all modes other than the two mistuned modes being examined was neglected, as only the behavior near a resonance was considered. The responses to both types did indeed have rotating node lines near a resonance. The node lines were predicted to be slightly distorted and rotating at a varying but average angular speed identical to the circular frequency of excitation. The results also indicate that the node lines will normally rotate forward due to a stationary load and backward due to a forward rotating load. GRA

N89-21276# Massachusetts Inst. of Tech., Cambridge. Dept. of Mechanical Engineering.
DILATATIONALLY NONLINEAR ELASTIC MATERIALS. (1): SOME THEORY
Rohan Abeyaratne and Guo-Hua Jiang Sep. 1988 34 p
(Contract N00014-87-K-0117)
(AD-A202824; TR-5) Avail: NTIS HC A03/MF A01 CSCL 20K

This paper, which is the first in a two part study, addresses certain issues concerning the small strain theory of nonlinear elasticity. It considers isotropic materials which possess a linear response in shear and a nonlinear response in dilatation, and (1) establishes an explicit necessary and sufficient condition for the existence of piecewise homogeneous deformations, (2) obtains a characterization of the set of all such deformations, (3) derives an expression for the driving traction on a surface of discontinuity in the strain, and finally (4) discusses the notion of a kinetic law. While the analysis is carried out within a three-dimensional setting, the results are shown to have a particularly simple form when expressed in terms of a certain constitutive function sigma. In Part 2 of this study we examine a specific boundary value problem. GRA

N89-21277# Naval Postgraduate School, Monterey, CA.
A TRIANGULAR THIN SHELL ELEMENT FOR THE LINEAR ANALYSIS OF STIFFENED COMPOSITE STRUCTURES Final Report, Jan. - Jun. 1987
Edward Wilson and Gilles Cantin Apr. 1988 30 p
(AD-A202864; NPS69-88-003) Avail: NTIS HC A03/MF A01 CSCL 13M

A three node flat shell element with six engineering displacement degree-of-freedom at each node is developed. The basic formulation allows for the arbitrary location of the reference surface in which the membrane forces and bending moments are

fully coupled. The well-known, highly accurate, DKT bending element is combined with a higher order membrane element in order to obtain a consistent formulation. The higher order membrane behavior is obtained by the introduction of three additional normal rotational degree-of-freedom. This report presents a summary of the theoretical steps involved in the development of the element. The accuracy of the element is illustrated by the solution of several standard problems and a comparison of results with other thin shell elements. GRA

N89-21278# Air Force Inst. of Tech., Wright-Patterson AFB, OH. School of Engineering.
VIBRATION AND BUCKLING CHARACTERISTICS OF COMPOSITE CYLINDRICAL PANELS INCORPORATING THE EFFECTS OF A HIGHER ORDER SHEAR THEORY M.S. Thesis
Peter E. Linnemann Dec. 1988 181 p
(AD-A202939; AFIT/GA/AA/88D-06) Avail: NTIS HC A09/MF A01 CSCL 20K

An analytical study is conducted to determine the fundamental frequencies and critical buckling loads for laminated anisotropic circular cylindrical shell panels, including the effects of transverse shear deformation and rotary inertia, by using the Galerkin Technique. A linearized form of Sander's shell strain-displacement relations are derived, which include a parabolic distribution of transverse shear strains. The theory is valid for laminate thickness to radius ratios, h/R, of 1/5. Higher order constitutive relations are derived for the laminate. A set of five coupled partial differential equations of motion and boundary conditions are derived and then solved using the Galerkin Technique. Simply supported and clamped boundary conditions are investigated. It is found that the Galerkin Technique converges for all panel configurations investigated; additionally, it is found that buckling problems need more terms in the approximation than vibration problems to obtain proper convergence. Theory compares exactly with the Donnel solutions, which are valid up to h/R = 1/50. As expected, as length to thickness ratios are reduced shear deformation effects significantly lower the natural frequencies and buckling loads. Analysis also shows that rotary inertia effects are very small. Finally, as h/R is varied from 0 (flat plate) to 1/5 (maximum limit), the frequencies and buckling loads increase due to membrane and bending coupling. GRA

N89-21279# Air Force Inst. of Tech., Wright-Patterson AFB, OH. School of Engineering.
FINITE ELEMENT ANALYSIS OF COMPOSITE PLATES INCLUDING SHEAR DEFORMATION M.S. Thesis
Michael E. Owens Dec. 1988 154 p
(AD-A202941; AFIT/GAE/AA/88D-29) Avail: NTIS HC A08/MF A01 CSCL 20K

This thesis will study the effects of material properties, thickness ratio, aspect ratio, boundary conditions, and ply layup on the reactions of a transversely loaded rectangular composite plate. Geometric nonlinearities, i.e., the Von Karman nonlinear plate equations, and through the thickness shear effects were included. Both geometrically linear and nonlinear solutions were done. This research was done using an existing finite element code with a four-noded, 28 DOF rectangular element. All plates were 48 plies thick to be representative of a real world application. Material properties had the largest effect when the plate was thick. The linear solution approaches the classical laminated plate theory solution as the plate gets thin. The nonlinear solution deflects much less than the stiffen the plate. For a clamped plate the linear and nonlinear solutions are comparable until the plate is quite thin. Aspect ratio has a large effect on the plate for an isotropic material. However, in the ply layups investigated, aspect ratio had much less effect because half the fibers were oriented in the direction of the short dimension of the plate. Ply layup did not have a great effect on the deflections of the plate. This occurred because all the layups chosen had at least half the plies oriented in the same direction. GRA

N89-21280# Texas A&M Univ., College Station. Mechanics and Materials Research Center.
ON THE ENERGY RELEASE RATE FOR DYNAMIC TRANSIENT ANTI-PLANE SHEAR CRACK PROPAGATION IN A GENERAL LINEAR VISCOELASTIC BODY
J. M. Herrmann and J. R. Walton Sep. 1988 44 p
(Contract N00014-86-K-0298; GR/E/40538)
(AD-A202942; MM-5488-88-14) Avail: NTIS HC A03/MF A01 CSCL 20K

The problem of a semi-infinite mode III crack that suddenly begins to propagate at a constant speed is considered for a general linear viscoelastic body. Simple closed form expressions are derived for the Laplace transform of the stress, displacement, and stress intensity factor. A Barenblatt type failure zone is assumed to exist at the crack tip and an expression for the total energy flux into the failure zone per unit crack advance, G(t), is derived. The short time asymptotic form of G is constructed and the rate at which it converges to its steady-state limit is studied. It is shown that the rate of convergence to steady-state is dependent upon crack speed and material properties. GRA

N89-21281# Army Armament Research, Development and Engineering Center, Watervliet, NY. Weapons Lab.
AN INVESTIGATION OF STRESSES AND STRAINS IN AN INTERNALLY PRESSURIZED, COMPOSITE-JACKETED, STEEL CYLINDER Final Report
M. D. Witherell and M. A. Scavullo Nov. 1988 33 p
(AD-A202969; ARCCB-TR-88042) Avail: NTIS HC A03/MF A01 CSCL 11D

This report presents the results of a theoretical and experimental investigation of the effects on bore strain when a portion of the wall thickness of a steel cylinder is replaced with organic composite material. The pressure vessel is pressurized internally and the bore strain is theoretically predicted and experimentally measured as a function of wall ratio. Theoretical results for various ratios of steel to composite, from all-steel to all-composite, are given. The theoretical solution was obtained by equating the hoop strain of the steel with the hoop strain of the composite at the material interface. Lame's stress solution was used as input for the steel hoop strain, whereas Lekhnitskii's stress solution obtained for orthotropic cylinders was used as input to the composite hoop strain equation. GRA

N89-21282# Air Force Inst. of Tech., Wright-Patterson AFB, OH. School of Engineering.
MACROCRACK-MULTIPLE DEFECT INTERACTION CONSIDERING ELASTIC, PLASTIC AND VISCOPLASTIC EFFECTS M.S. Thesis
LeRoy K. Smith Dec. 1988 129 p
(AD-A203186; AFIT/GAE/AA/88D-35) Avail: NTIS HC A07/MF A01 CSCL 20K

A finite element investigation was conducted to analyze an axial tension specimen with collinear defects placed symmetrically about a center crack. The material modeled was IN-718, a nickel-based superalloy used in jet engines. The effects of crack/defect interaction were compared using elastic, elastic plastic, and viscoplastic constitutive models. A 2-D nonlinear finite element code called SNAP was used. This program has the capability to simulate crack growth and closure by releasing or closing nodes along the crack plane. Elastic stress intensity solutions were developed for two different finite width specimens. The stress intensity versus crack length plots compared well with infinite theory. Results show that the defect can partially shield the crack from finite width effects. A critical spacing was also noted where the stress intensity of the crack exceeded the stress intensity for the combined length of the crack and defect. The defect has a prominent influence range equal to approximately one defect length for all constitutive models. The presence of a defect increases the magnitude of the crack opening and stress/strain fields in front of the crack tip. GRA

N89-21283# Air Force Inst. of Tech., Wright-Patterson AFB, OH. School of Engineering.
TRANSVERSE SHEAR CONSIDERATIONS IN ANISOTROPIC PLATES M.S. Thesis
Richard H. Reams Dec. 1988 210 p
(AD-A203187; AFIT/GAE/AA/88D-32) Avail: NTIS HC A10/MF A01 CSCL 11D

This work was initiated by a need for solutions to a higher order shear deformation plate theory, which better approximates the through-the-thickness deformation and interlaminar shear stresses, using plates other than simply support. The non-simply support boundary conditions necessitated the Galerkin approximate technique. Solutions desired were natural frequencies and buckling loads for the following boundary conditions: simply supported, clamped, and clamped-simply support. Two graphite/epoxy laminates of different construction were investigated for effects of varying span-to-depth ratios. Comparisons of the higher order theory with linear and classical theory were made along with convergence characteristics of the Galerkin technique. GRA

N89-21284# Washington State Univ., Pullman. Dept. of Civil and Environmental Engineering.
THE IMPLEMENTATION OF A NONREFLECTING BOUNDARY INTO THE SAMSON2 CODE Final Report, 17 Feb. - 31 Dec. 1987
B. L. Haverson and H. C. Sorensen Nov. 1988 180 p
(Contract F29601-85-K-0050)
(AD-A203394; AFWL-TR-88-102) Avail: NTIS HC A09/MF A01 CSCL 20K

A nonreflecting boundary has been implemented into a dynamic explicit finite element code called SAMSON2. The nonreflecting boundary is a practical application of a viscous boundary developed by Lysmer and Kuhlemeyer. The basic principle involves an introduction of a set of dissipative stresses applied normal to and tangentially along the boundary which match the impedances of the interior of the mesh. The original viscous boundary scheme is limited to a plane elastic isotropic medium. This study expanded the versatility of the viscous boundary by including a medium that is axisymmetric, inelastic and/or anisotropic. A series of tests were conducted to determine the effectiveness of the nonreflecting boundary under a variety of circumstances. The implemented nonreflecting boundary performed very well for normal values of Poisson's ratio and for axisymmetric problems. A decrease in the effectiveness was noticed for materials with high values of Poisson's ratio and when the nonreflecting boundary is placed too close to the axis of symmetry. GRA

N89-21285# California Inst. of Tech., Pasadena.
AN INVESTIGATION OF VISCOELASTIC FRACTURE NEAR AND AT INTERFACES Final Report, 27 Sep. 1985 - 30 Jun. 1988
Wolfgang G. Knauss Nov. 1988 48 p
(Contract F04611-85-K-0106)
(AD-A203760; AFAL-TR-88-083) Avail: NTIS HC A03/MF A01 CSCL 20K

This report summarizes research on the effect of interfaces between two materials on the crack propagation process in its vicinity. The program contained both experimental as well as analytical components. The aim was to examine the applicability of optical caustics to crack propagation near interfaces. The main result of the work to date is the assurance that caustics can be employed to characterize interfacial cohesion and decohesion problems when crack tips are involved. On the experimental side of the program the method to generate bimaterial specimens with a plane interface has been developed and caustics involving large deformations have been studied and related to analysis. Examples of caustics in monolithic sheets of Solithane 113 of two different compositions (different material stiffness) are presented as well as caustics derived from crack tips at interfaces. GRA

N89-21286*# Wyoming Univ., Laramie. Composite Materials Research Group.
STRAIN ENERGY RELEASE RATE AS A FUNCTION OF TEMPERATURE AND PRELOADING HISTORY UTILIZING THE EDGE DELAMINATION FATIQUE TEST METHOD Contractor Resepor, Jul. 1986 - Oct. 1988
Richard S. Zimmerman and Donald F. Adams Feb. 1989 270 p
(Grant NAG1-674)
(NASA-CR-184966; NAS 1.26:184966; UW-CMRG-R-89-106)
Avail: NTIS HC A12/MF A01 CSCL 20K

Static laminate and tension-tension fatigue tests of IM7/8551-7 composite materials was performed. The Edge Delamination Test (EDT) was utilized to evaluate the temperature and preloading history effect on the critical strain energy release rate. Static and fatigue testing was performed at room temperature and 180 F (82 C). Three preloading schemes were used to precondition fatigue test specimens prior to performing the normal tension-tension fatigue EDT testing. Computer software was written to perform all fatigue testing while monitoring the dynamic modulus to detect the onset of delamination and record the test information for later retrieval and reduction. Author

N89-21496# Army Materials Technology Lab., Watertown, MA. Mechanics and Structures Div.
ELEMENT LEVEL ELIMINATION OF NONLINEAR CONSTRAINTS IN TOTAL LAGRANGIAN FINITE ELEMENT FORMULATIONS
A. R. Johnson and C. J. Quigley *In* Army Research Office, Transactions of the Fifth Army Conference on Applied Mathematics and Computing Mar. 1988 p 111-138 (For primary document see N89-21490 14-59)
Avail: NTIS HC A99/MF E03 CSCL 20K

N89-21498# Army Armament Research, Development and Engineering Center, Watervliet, NY. Close Combat Armaments Center.
A SIMPLE ANALYSIS OF SWAGE AUTOFRETTAGE PROCESS
Peter C. T. Chen *In* Army Research Office, Transactions of the Fifth Army Conference on Applied Mathematics and Computing Mar. 1988 p 149-160 (For primary document see N89-21490 14-59)
Avail: NTIS HC A99/MF E03 CSCL 20K

N89-21504# Military Academy, West Point, NY. Dept. of Mathematics.
KNOT SELECTION FOR LEAST SQUARES APPROXIMATION USING THIN PLATE SPLINES
John R. McMahon and Richard Franke (Naval Postgraduate School, Monterey, CA.) *In* Army Research Office, Transactions of the Fifth Army Conference on Applied Mathematics and Computing Mar. 1988 p 311-330 (For primary document see N89-21490 14-59)
(Proj. BR033-02-WH)
Avail: NTIS HC A99/MF E03 CSCL 20K

N89-21517# Brunel Univ., Uxbridge (England). Inst. of Computational Mathematics.
ON SOME FINITE ELEMENT ERROR ESTIMATES FOR STRESS INTENSITY FACTORS IN MODE 1 LINEAR ELASTIC FRACTURE PROBLEMS
J. R. Whiteman and G. Goodsell *In* Army Research Office, Transactions of the Fifth Army Conference on Applied Mathematics and Computing Mar. 1988 p 541-548 (For primary document see N89-21490 14-59)
Avail: NTIS HC A99/MF E03 CSCL 20K

N89-21518# Army Materials Technology Lab., Watertown, MA. Mechanics and Structures Div.
SOME ISSUES OF NUMERICAL INTEGRATION AND PENALTY RELAXATION IN ANISOPARAMETRIC SHELL ELEMENT FORMULATION
Alexander Tessler and Luciano Spiridigliozzi *In* Army Research

Office, Transactions of the Fifth Army Conference on Applied Mathematics and Computing Mar. 1988 p 549-566 (For primary document see N89-21490 14-59)
Avail: NTIS HC A99/MF E03 CSCL 20K

N89-21751*# Arkansas Univ., Fayetteville. Dept. of Mechanical Engineering.
EVALUATE THE APPLICATION OF MODAL TEST AND ANALYSIS PROCESSES TO STRUCTURAL FAULT DETECTION IN MSFC-STS PROJECT ELEMENTS
William T. Springer *In* Alabama Univ., Research Reports: 1988 NASA/ASEE Summer Faculty Fellowship Program Dec. 1988 23 p (For primary document see N89-21726 14-99)
Avail: NTIS HC A99/MF E03 CSCL 20K

42 GEOSCIENCES (GENERAL)

N89-21287*# Lunar and Planetary Inst., Houston, TX.
GLOBAL CATASTROPHES IN EARTH HISTORY: AN INTERDISCIPLINARY CONFERENCE ON IMPACTS, VOLCANISM, AND MASS MORTALITY Abstracts Only
1988 238 p Conference held in Snowbird, UT, 20-23 Oct. 1988; sponsored by LPI and NAS-NRC
(Contract NASw-4066)
(NASA-CR-183329; NAS 1.26:183329; LPI-Contrib-673) Avail: NTIS HC A11/MF A01 CSCL 08G

Topics addressed include: Cretaceous-Tertiary . mass extinctions; geologial indicators for meteorite collisions; carbon dioxide catastrophes; volcanism; climatic changes; geochemistry; mineralogy; fossil records; biospheric traumas; stratigraphy; mathematical models; and ocean dynamics. For individual titles, see N89-21288 through N89-21414.

N89-21288*# California Univ., Berkeley. Dept. of Geology and Geophysics.
THE DEBATE OVER THE CRETACEOUS-TERTIARY BOUNDARY Abstract Only **c46**
W. Alvarez, F. Asaro, L. W. Alvarez, and H. V. Michel *In* Lunar and Planetary Inst., Global Catastrophes in Earth History: An Interdisciplinary Conference on Impacts, Volcanism, and Mass Mortality 1988 p 1 Prepared in cooperation with California Univ., Berkeley. Lawrence Berkeley Lab. (For primary document see N89-21287 14-42)
Avail: NTIS HC A11/MF A01 CSCL 08G

Large-body impact on the Earth is a rare but indisputable geologic process. The impact rate is approximately known from objects discovered in Earth-crossing orbits and from the statistics of craters on the Earth's surface. Tektite and microtektite strewn fields constitute unmistakable ejecta deposits that can be due only to large-body impacts. The Cretaceous-Tertiary (K-T) boundary coincides with an unusually severe biological trauma, and this stratigraphic horizon is marked on a worldwide basis by anomalous concentrations of noble metals in chondritic proportions, mineral spherules with relict quench-crystallization textures, and mineral and rock grains showing shock deformation. These features are precisely compatible with an impact origin. Although only impact explains all the types of K-T boundary evidence, the story may not be as simple as once thought. The original hypothesis envisioned one large impact, triggering one great extinction. Newer evidence hints at various complications. Different challenges are faced by the occupants of each apex of a three-cornered argument over the K-T event. Proponents of a non-impact explanation must show that the evidence fits their preferred model better than it fits the impact scenario. Proponents of the single impact-single extinction view must explain away the complications. Proponents of a more complex impact crisis must develop a reasonable scenario which honors the new evidence. Author

N89-21289*# Witwatersrand Univ., Johannesburg (South Africa). Dept. of Geophysics
GEOLOGICAL INDICATORS FOR IMPACT: THE ANOMALOUS CASE OF THE VREDEFORT STRUCTURE, SOUTH AFRICA **c46**
L. A. G. Antoine and W. U. Reimold *In* Lunar and Planetary Inst., Global Catastrophes in Earth History: An Interdisciplinary Conference on Impacts, Volcanism, and Mass Mortality 1988 p 2-3 (For primary document see N89-21287 14-42)
Avail: NTIS HC A11/MF A01 CSCL 08G

The Vredefort Dome is located within and almost central to the Witwatersrand basin in its presently known extent. It exposes a central Archean granite core which is surrounded by a collar of supracrustal rocks. These collar rocks outline a strong polygonal geometry. The Archean core is comprised of two concentric zones, the Outer Granite Gneiss (OGG), and the core central Inlandsee Leucogranofels (ILG). The rocks of the inner core display granulite facies metamorphism, while the OGG is in amphibolite facies. The inner core is believed from recent drill hole information to be underlain by mafic and ultramafic gneisses, the extent of which cannot be assessed at present. A fairly broad zone of charnockites separates the OGG and ILG domains. This zone is characterized by a high concentration of pseudotachylite and ductile shearing. Whereas a number of other domical structures are located within or surrounding the Witwatersrand basin, the Vredefort structure is anomalous, in that it has: a partly polygonal geometry; extensive alkali intrusives in the northwestern sector; granophyre dykes (ring-dykes peripheral to the contact collar-basement and NW-SE or NE-SW trending dykes within the Archean basement); contact metamorphism of the collar supracrustal rocks; the overturning of collar supracrustals in the northern sectors; deformation phenomena widely regarded as representing shock metamorphism (pseudotachylite, (sub)planar microdeformation features in quartz, shatter cones and occurrences of high-P quartz polymorphs); a positive 30 mgal gravity anomaly; and high amplitude magnetic anomalies. Recent geophysical, structural and petrological evidence pertinent for the identification of the processes that led to the formation of the Vredefort structure are summarized. Author

N89-21290*# California Univ., San Diego. Dept. of Biology.
LIMITATIONS ON K-T MASS EXTINCTION THEORIES BASED UPON THE VERTEBRATE RECORD **c51**
J. David Archibald and Laurie J. Bryant *In* Lunar and Planetary Inst., Global Catastrophes in Earth History: An Interdisciplinary Conference on Impacts, Volcanism, and Mass Mortality 1988 p 4-5 Prepared in cooperation with California Univ., Berkeley (For primary document see N89-21287 14-42)
Avail: NTIS HC A11/MF A01 CSCL 06B

Theories of extinction are only as good as the patterns of extinction that they purport to explain. Often such patterns are ignored. For the terminal Cretaceous events, different groups of organisms in different environments show different patterns of extinction that to date cannot be explained by a single causal mechanism. Several patterns of extinction (and/or preservational bias) can be observed for the various groups of vertebrates from the uppermost Cretaceous Hell Creek Formation and lower Paleocene Tullock Formation in eastern Montana. The taxonomic level at which the percentage of survivals (or extinctions) is calculated will have an effect upon the perception of faunal turnover. In addition to the better known mammals and better publicized dinosaurs, there are almost 60 additional species of reptiles, birds, amphibians, and fish in the HELL Creek Formation. Simple arithmetic suggests only 33 percent survival of these vertebrates from the Hell Creek Fm. into the Tullock Fm. A more critical examination of the data shows that almost all Hell Creek species not found in the Tullock are represented in one of the following categories; extremely rare forms, elasmobranch fish that underwent rapid speciation taxa that although not known or rare in the Tullock, are found elsewhere. Each of the categories is largely the result of the following biases: taphonomy, ecological differences, taxonomic artifact paleogeography. The two most important factors appear to be the possible taphonomic biases

and the taxonomic artifacts. The extinction patterns among the vertebrates do not appear to be attributable to any single cause, catastrophic or otherwise. Author

N89-21291*# California Univ., Berkeley. Lawrence Berkeley Lab.
POSSIBLE WORLD-WIDE MIDDLE MIOCENE IRIDIUM ANOMALY AND ITS RELATIONSHIP TO PERIODICITY OF IMPACTS AND EXTINCTIONS **c46**
F. Asaro, W. Alvarez, H. V. Michel, L. W. Alvarez, Mark H. Anders, A. Montanari, and James P. Kennett *In* Lunar and Planetary Inst., Global Catastrophes in Earth History: An Interdisciplinary Conference on Impacts, Volcanism, and Mass Mortality 1988 p 6-7 Prepared in cooperation with California Univ., Berkeley; and California Univ., Santa Barbara (For primary document see N89-21287 14-42)
Avail: NTIS HC A11/MF A01 CSCL 08G

In a study of one million years of Middle Miocene sediment deposition in ODP Hole 689B in the Weddell Sea near Antarctica, a single iridium (Ir) anomaly of 44 (+ or - 10) x 10 to the 12th gram Ir per gram rock (ppt) was observed in core 6H, section 3, 50 to 60 cm, after background contributions associated with manganese precipitates and clay are subtracted. The ODP Hole 689B is 10,000 km away from another site, DSDP Hole 588B in the Tasman Sea north of New Zealand, where a single Ir anomaly of 144 + or - 7 ppt over a background of 11 ppt was found in an earlier study of 3 million years of deposition. From chemical measurements the latter deposition was thought to be impact-related. Ir measurements were made, following neutron activation, with the Iridium Coincidence Spectrometer. The age vs depth calibration curves given in the DSDP and ODP preliminary reports indicate the ages of the Iranomalies are identical, 11.7 million years, but the absolute and relative uncertainties in the curves are not known. Based on the newest age data the age estimate is 10 million years. As the Ir was deposited at the two sites at about the same time and they are one quarter of the way around the world from each other it seems likely that the deposition was world-wide. The impact of a large asteroid or comet could produce the wide distribution, and this data is supportive of the impact relationship deduced for Deep Sea Drilling Project (DSDP) 588B from the chemical evidence. If the surface densities of Ir at the two sites are representative of the world-wide average, the diameter of a CI type asteroid containing the necessary Ir would be 3 + or - 1 km, which is large enough to cause world-wide darkness and hence extinctions although the latter point is disputed. Author

N89-21292*# Lunar and Planetary Inst., Houston, TX.
THE CRATERING RECORD IN THE INNER SOLAR SYSTEM: IMPLICATIONS FOR EARTH **c46**
N. G. Barlow *In its* Global Catastrophes in Earth History: An Interdisciplinary Conference on Impacts, Volcanism, and Mass Mortality 1988 p 8-9 (For primary document see N89-21287 14-42)
Avail: NTIS HC A11/MF A01 CSCL 08G

Internal and external processes have reworked the Earth's surface throughout its history. In particular, the effect of meteorite impacts on the early history of the earth is lost due to fluvial, aeolian, volcanic and plate tectonic action. The cratering record on other inner solar system bodies often provides the only clue to the relative cratering rates and intensities that the earth has experienced throughout its history. Of the five major bodies within the inner solar system, Mercury, Mars, and the Moon retain scars of an early episode of high impact rates. The heavily cratered regions on Mercury, Mars, and the Moon show crater size-frequency distribution curves similar in shape and crater density, whereas the lightly cratered plains on the Moon and Mars show distribution curves which, although similar to each other, are statistically different in shape and density from the more heavily cratered units. The similarities among crater size-frequency distribution curves for the Moon, Mercury, and Mars suggest that the entire inner solar system was subjected to the two populations of impacting objects but Earth and Venus have lost their record of heavy bombardment impactors. Thus, based on the cratering record on the Moon, Mercury, and Mars, it can be inferred that the Earth experienced a period of high crater rates and basin formation prior to about 3.8 BY ago. Recent studies have linked mass extinctions to large terrestrial impacts, so life forms were unable to establish themselves until impact rates decreased substantially and terrestrial conditions became more benign. The possible periodicity of mass extinctions has led to the theory of fluctuating impact rates due to comet showers in the post heavy bombardment period. The active erosional environment on the Earth complicates attempts to verify these showers by erasing geological evidence of older impact craters. The estimated size of the impactor purportedly responsible for the Cretaceous-Tertiary mass extinctions is 10 km in diameter. Thus impactors greater than or equal to the size postulated for K-T impactor are rare within the inner solar system since the end of heavy bombardment. Author

N89-21293*# University of Southern California, Los Angeles. Dept. of Chemistry.
CARBON DIOXIDE CATASTROPHES: PAST AND FUTURE MENACE **c45**
Mario E. Baur *In* Lunar and Planetary Inst., Global Catastrophes in Earth History: An Interdisciplinary Conference on Impacts, Volcanism, and Mass Mortality 1988 p 10-11 (For primary document see N89-21287 14-42)
Avail: NTIS HC A11/MF A01 CSCL 04A

Carbon dioxide is important in its role as coupler of the terrestrial biosphere to inorganic chemical processes and as the principal greenhouse gas controlling Earth's surface temperature. The hypothesis that atmospheric CO2 levels have diminished with time, with the resulting cooling effect offsetting an increase in the solar constant, seems firmly established, and it is shown that feedback mechanisms exist which can maintain the terrestrial surface in a relatively narrow temperature range over geological time. Of the factors involved in such CO2 variation, the oceanic reservoir appears the most important. Surface waters are probably in approximate equilibrium with regard to CO2 exchange with the ambient atmosphere in most regions, but data from deep-ocean water sampling indicates that such waters are somewhat undersaturated in the sense that they would tend to absorb CO2 from the atmosphere if brought to the surface without change in composition or temperature. If major impacts into the ocean can result in loss of a substantial portion of the atmospheric CO2 reservoir, then any such future event could imperil the continuation of most higher forms of life on Earth. The most likely candidate for an inverse Nyos global event in previous Earth history is the Cretaceous-Tertiary terminal extinction event. The Cretaceous was characterized by warm, equable temperatures presumably indicative of relatively high CO2 levels and an intense greenhouse heating. Cooling of the oceans in absence of massive transfer of CO2 to the oceanic reservoir in itself would promote a condition of CO2 undersaturation in abyssal waters, and this is made even more extreme by the pattern of ocean water circulation. It is possible to envision a situation in which deep ocean waters were at least occasionally profoundly undersaturated with regard to CO2. Turnover of a major fraction of such an ocean would then remove, on a very short time scale, as much as 90 percent of the atmospheric CO2 inventory. Author

N89-21294*# Hawaii Univ., Honolulu. Inst. of Geophysics.
IMPLICATIONS OF ASTEROID COMPOSITION FOR THE GEOCHEMISTRY OF THE ANCIENT TERRESTRIAL PROJECTILE FLUX Abstract Only **c46**
Jeffrey F. Bell *In* Lunar and Planetary Inst., Global Catastrophes in Earth History: An Interdisciplinary Conference on Impacts, Volcanism, and Mass Mortality 1988 p 12 (For primary document see N89-21287 14-42)
Avail: NTIS HC A11/MF A01 CSCL 08G

The discovery of enhanced siderophile abundances at the Cretaceous/Tertiary boundary has provoked many searches for geochemical signatures which could reveal other catastrophic impacts in Earth's history. These searches implicitly assume that most large impactors are of chondritic, iron, or stony-iron

composition, with a greatly enhanced abundance of siderophile elements. Impactors composed of asteroidal crust or mantle rocks analogous to the achondritic meteorites would not leave a distinct geochemical trace since their siderophile abundances are grossly similar to those of the Earth's crust. In recent years studies of the mineralogical composition of the current asteroid belt have suggested that the composition of impacting projectiles may be highly variable with both projectile size and time. In particular it seems possible that in the distant past projectiles derived from asteroid mantle material may have caused a large fraction of the cratering events on Earth. Such impacts would be missed by any geochemical search relying on iridium or any other siderophile element. The questions of the effect of size and time variations on projectile composition and the significance of hidden impacts missing in current geochemical searches are examined. Author

N89-21295*# California Univ., Berkeley. Marine Sciences Group.

LATE WENLOCK (MIDDLE SILURIAN) BIO-EVENTS: CAUSED BY VOLATILE BOLOID IMPACT/S **c51**

W. B. N. Berry and P. Wilde *In* Lunar and Planetary Inst., Global Catastrophes in Earth History: An Interdisciplinary Conference on Impacts, Volcanism, and Mass Mortality 1988 p 13-14 (For primary document see N89-21287 14-42)

Avail: NTIS HC A11/MF A01 CSCL 06B

Late Wenlockian (late mid-Silurian) life is characterized by three significant changes or bioevents: sudden development of massive carbonate reefs after a long interval of limited reef growth; sudden mass mortality among colonial zooplankton, graptolites; and origination of land plants with vascular tissue (Cooksonia). Both marine bioevents are short in duration and occur essentially simultaneously at the end of the Wenlock without any recorded major climatic change from the general global warm climate. These three disparate biologic events may be linked to sudden environmental change that could have resulted from sudden infusion of a massive amount of ammonia into the tropical ocean. Impact of a boloid or swarm of extraterrestrial bodies containing substantial quantities of a volatile (ammonia) component could provide such an infusion. Major carbonate precipitation (formation), as seen in the reefs as well as, to a more limited extent, in certain brachiopods, would be favored by increased pH resulting from addition of a massive quantity of ammonia into the upper ocean. Because of the buffer capacity of the ocean and dilution effects, the pH would have returned soon to equilibrium. Major proliferation of massive reefs ceased at the same time. Addition of ammonia as fertilizer to terrestrial environments in the tropics would have created optimum environmental conditions for development of land plants with vascular, nutrient-conductive tissue. Fertilization of terrestrial environments thus seemingly preceded development of vascular tissue by a short time interval. Although no direct evidence of impact of a volatile boloid may be found, the bioevent evidence is suggestive that such an impact in the oceans could have taken place. Indeed, in the case of an ammonia boloid, evidence, such as that of the Late Wenlockian bioevents may be the only available data for impact of such a boloid. Author

N89-21296*# Physical Research Lab., Ahmedabad (India).

GEOCHEMISTRY OF K/T BOUNDARIES IN INDIA AND CONTRIBUTIONS OF DECCAN VOLCANISM **c46**

N. Bhandari, M. Gupta, J. Pandey (Malviya, K. D. Inst. for Petroleum Exploration, Dehradun, India), and P. N. Shukla *In* Lunar and Planetary Inst., Global Catastrophes in Earth History: An Interdisciplinary Conference on Impacts, Volcanism, and Mass Mortality 1988 p 15-16 (For primary document see N89-21287 14-42)

Avail: NTIS HC A11/MF A01 CSCL 08G

Three possible Cretaceous/Tertiary (K/T) boundary sections in the Indian subcontinent were studied for their geochemical and fossil characteristics. These include two marine sections of Meghalaya and Zanskar and one continental section of Nagpur. The Um Sohryngkew river section of Meghalaya shows a high iridium, osmium, iron, cobalt, nickel and chromium concentration in a 1.5 cm thick limonitic layer about 30 cm below the planktonic Cretaceous-Palaeocene boundary identified by the characteristic fossils. The Bottaccione and Contessa sections at Gubbio were also analyzed for these elements. The geochemical pattern at the boundary at the Um Sohryngkew river and Gubbio sections are similar but the peak concentrations and the enrichment factors are different. The biological boundary is not as sharp as the geochemical boundary and the extinction appears to be a prolonged process. The Zanskar section shows, in general, similar concentration of the siderophile, lithophile and rare earth elements but no evidence of enrichment of siderophiles has so far been observed. The Takli section is a shallow inter-trappean deposit within the Deccan province, sandwiched between flow 1 and flow 2. The geochemical stratigraphy of the inter-trappeans is presented. The various horizons of ash, clay and marl show concentration of Fe and Co, generally lower than the adjacent basalts. Two horizons of slight enrichment of iridium are found within the ash layers, one near the contact of flow 1 and other near the contact of flow 2, where iridium occurs at 170 and 260 pg/g. These levels are lower by a factor of 30 compared to Ir concentration in the K/T boundary in Meghalaya section. If the enhanced level of some elements in a few horizons of the ash layer are considered as volcanic contribution by some fractionation processes than the only elements for which it occurs are REE, Ir and possibly Cr.

Author

N89-21297*# Geological Survey, Denver, CO.

SHOCKED QUARTZ AND MORE: IMPACT SIGNATURES IN K-T BOUNDARY CLAYS AND CLAYSTONES **c46**

Bruce F. Bohor *In* Lunar and Planetary Inst., Global Catastrophes in Earth History: An Interdisciplinary Conference on Impacts, Volcanism, and Mass Mortality 1988 p 17-18 (For primary document see N89-21287 14-42)

Avail: NTIS HC A11/MF A01 CSCL 08G

Quartz grains displaying multiple sets of planar features are described from numerous Cretaceous-Tertiary (K-T) boundary clays and claystones at both marine and nonmarine depositional sites around the world. All these sites also show anomalously high amounts of iridium and enrichments of other siderophile elements in cosmic ratios within these boundary units. This combination of mineralogical and geochemical features are used in support of an impact hypothesis for the end-Cretaceous event. Recently, it was suggested that some combination of explosive and nonexplosive volcanism associated with the formation of the Deccan traps in India could be responsible for the mineralogy and geochemistry seen in the K-T boundary units. Besides the obvious contradition of simultaneous explosive and nonexplosive volcanism from one locality during an instant of geologic time, there remains the difficulty of spreading both iridium (and trace elements in cosmic proportions) and quartz grains around the world by volcanic (atmospheric) transport. In addition, the ability of volcanism to produce the type of shock metamorphism seen in minerals at the K-T boundary was not demonstrated. Multiple sets of shock lamellae in quartz are considered characteristic of shock metamorphism in rocks at the sites of known impact craters and are the type of deformation seen in quartz from K-T boundary clays and claystones. Single sets of poorly defined lamellae described from rare quartz grains in certain volcanic deposits are characteristic of tectonic deformation and do not correspond to the shock lamellae in quartz from K-T sediments and impact structures. So-called shock mosaicism in quartz and feldspar grains described from volcanic deposits can result from many processes other than shock metamorphism, and therefore is not considered to be an effect characteristic solely of shock. The mineralogy of shock-metamorphosed grains at the K-T boundary also argues against a volcanic origin. Author

N89-21298*# National Center for Atmospheric Research, Boulder, CO.

RESPONSE OF MARINE AND FRESHWATER ALGAE TO NITRIC ACID AND ELEVATED CARBON DIOXIDE LEVELS SIMULATING ENVIRONMENTAL EFFECTS OF BOLIDE IMPACT **c45**

P. J. Boston *In* Lunar and Planetary Inst., Global Catastrophes in Earth History: An Interdisciplinary Conference on Impacts, Volcanism, and Mass Mortality 1988 p 19-20 Prepared in cooperation with Colorado Univ., Boulder (For primary document see N89-21287 14-42)
Avail: NTIS HC A11/MF A01 CSCL 13B

One of the intriguing facets of the Cretaceous-Tertiary extinction is the apparently selective pattern of mortality amongst taxa. Some groups of organisms were severely affected and some remained relatively unscathed as they went through the K/T boundary. While there is argument concerning the exact interpretation of the fossil record, one of the best documented extinctions at the Cretaceous-Tertiary boundary is that of the calcareous nannoplankton. These organisms include coccolithic algae and foraminiferans. Attempts to explain their decline at the K/T boundary center around chemistry which could affect their calcium carbonate shells while leaving their silica-shelled cousins less affected or unaffected. Two environmental consequences of an extraterrestrial body impact which were suggested are the production of large quantities of nitrogen oxides generated by the shock heating of the atmosphere and the possible rise in CO2 from the dissolution of CaCO3 shells. Both of these phenomena would acidify the upper layers of the oceans and bodies of freshwater not otherwise buffered. The effects of nitric acid, carbon dioxide, or both factors on the growth and reproduction of calcareous marine coccoliths and non-calcareous marine and freshwater species of algae were considered. These experiments demonstrate that nitric acid and carbon dioxide have significant effects on important aspects of the physiology and reproduction of modern algae representative of extinct taxa thought to have suffered significant declines at the Cretaceous-Tertiary boundary. Furthermore, calcareous species showed more marked effects than siliceous species and marine species tested were more sensitive than freshwater species. Author

N89-21299*# Washington Univ., Seattle. Dept. of Geological Sciences.
SEDIMENTOLOGICAL EFFECTS OF TSUNAMIS, WITH PARTICULAR REFERENCE TO IMPACT-GENERATED AND VOLCANOGENIC WAVES **c46**
Joanne Bourgeois and Patricia L. Wiberg *In* Lunar and Planetary Inst., Global Catastrophes in Earth History: An Interdisciplinary Conference on Impacts, Volcanism, and Mass Mortality 1988 p 21-22 Prepared in cooperation with University of Western Washington, Bellingham (For primary document see N89-21287 14-42)
Avail: NTIS HC A11/MF A01 CSCL 08G

Impulse-generated waves (tsunamis) may be produced, at varying scales and global recurrence intervals (RI), by several processes. Meteorite-water impacts will produce tsunamis, and asteroid-scale impacts with associated mega-tsunamis may occur. A bolide-water impact would undoubtedly produce a major tsunami, whose sedimentological effects should be recognizable. Even a bolide-land impact might trigger major submarine landslides and thus tsunamis. In all posulated scenarios for the K/T boundary event, then, tsunamis are expected, and where to look for them must be determined, and how to distinguish deposits from different tsunamis. Also, because tsunamis decrease in height as they move away from their source, the proximal effects will differ by perhaps orders of magnitude from distal effects. Data on the characteristics of tsunamis at their origin are scarce. Some observations exist for tsunamis generated by thermonuclear explosions and for seismogenic tsunamis, and experimental work was conducted on impact-generated tsunamis. All tsunamis of interest have wave-lengths of 0(100) km and thus behave as shallow-water waves in all ocean depths. Typical wave periods are 0(10 to 100) minutes. The effect of these tsunamis can be estimated in the marine and coastal realm by calculating boundary shear stresses (expressed as U*, the shear velocity). An event layer at the K/T boundary in Texas occurs in mid-shelf muds. Only a large, long-period wave with a wave height of 0(50) m, is deemed sufficient to have produced this layer. Such wave heights imply a nearby volcanic explosion on the scale of Krakatau or larger, or a nearby submarine landslide also of great size, or a bolide-water impact in the ocean. Author

N89-21300*# New York Univ., New York. Earth Systems Group.
OCEAN ALKALINITY AND THE CRETACEOUS/TERTIARY BOUNDARY Abstract Only **c48**
K. G. Caldeira and Michael R. Rampino *In* Lunar and Planetary Inst., Global Catastrophes in Earth History: An Interdisciplinary Conference on Impacts, Volcanism, and Mass Mortality 1988 p 23 (For primary document see N89-21287 14-42)
Avail: NTIS HC A11/MF A01 CSCL 08C

A biogeochemical cycle model resolving ocean carbon and alkalinity content is applied to the Maestrichtian and Danian. The model computes oceanic concentrations and distributions of Ca(2+), Mg(2+), and Sigma-CO2. From these values an atmospheric pCO2 value is calculated, which is used to estimate rates of terrestrial weathering of calcite, dolomite, and calcium and magnesium silicates. Metamorphism of carbonate rocks and the subsequent outgassing of CO2 to the atmosphere are parameterized in terms of carbonate rock reservoir sizes, total land area, and a measure of overall tectonic activity, the sea-floor generation rate. The ocean carbon reservoir computed by the model is used with Deep Sea Drilling Project (DSDP) C-13 data to estimate organic detrital fluxes under a variety of ocean mixing rate assumptions. Using Redfield ratios, the biogenic detrital flux estimate is used to partition the ocean carbon and alkalinity reservoirs between the mixed layer and deep ocean. The calcite flux estimate and carbonate ion concentrations are used to determine the rate of biologically mediated CaCO3 titration. Oceanic productivity was severely limited for approximately 500 kyr following the K/T boundary resulting in significant increases in total ocean alkalinity. As productivity returned to the ocean, excess carbon and alkalinity was removed from the ocean as CaCO3. Model runs indicate that this resulted in a transient imbalance in the other direction. Ocean chemistry returned to near-equilibrium by about 64 mybp. Author

N89-21301*# Carpenter (Kenneth), Philadelphia, PA.
DINOSAUR BONE BEDS AND MASS MORTALITY: IMPLICATIONS FOR THE K-T EXTINCTION **c51**
Kenneth Carpenter *In* Lunar and Planetary Inst., Global Catastrophes in Earth History: An Interdisciplinary Conference on Impacts, Volcanism, and Mass Mortality 1988 p 24-25 (For primary document see N89-21287 14-42)
Avail: NTIS HC A11/MF A01 CSCL 06B

Mass accumulations of fossilized large terrestrial vertebrate skeletons (bone beds: BB) provide a test for K-T catastrophic extinction hypotheses. The two major factors contributing to BB formation are mode of death and sedimentation rate. Catastrophic mass mortality (CMM) is the sudden death of numerous individuals where species, age, health, gender, or social ranking offer no survivorship advantage. Noncatastrophic mass mortality (NCMM) occurs over time and is strongly influenced by species, age, or gender. In addition to cause of death, sedimentation rate is also important in BB formation. Models of BBs can be made. The CMM drops all individuals in their tracks, therefore, the BB should reflect the living population with respect to species, age, or gender. The NCMM results in monospecific BBs skewed in the direction of the less fit, usually the very young or very old, or towards a specific gender. The NCMM and AM BBs may become more similar the more spread out over time NCMM deaths occur because carcasses are widely scattered requiring hydraulic accumulation, and the greater time allows for more disarticulation and weathering. The CMM and NCMM BB appear to be dominated by social animals. Applying this and the characteristics of mortality patterns to the uppermost Cretaceous Hell Creek Formation indicates that only NCMM and AM BB occur. Furthermore, NCMM BB are rare in the upper third of the Hell Creek. Near the K-T boundary, only AM BB are known. The absence of CMM and NCMM BB appears to be real reflecting a decrease in population levels of some dinosaurs prior to the K-T event. The absence of CMM suggests that the

K-T event did not lead to an instantaneous extinction of dinosaurs. Nor was there a protracted die-off due to an asteroid impact winter, because no NCMM BB are known at or near the K-T boundary.
Author

N89-21302*# Arizona Univ., Tucson. Planetary Science Inst.
RISK TO CIVILIZATION: A PLANETARY SCIENCE PERSPECTIVE **c90**
Clark R. Chapman and David Morrison *In* Lunar and Planetary Inst., Global Catastrophes in Earth History: An Interdisciplinary Conference on Impacts, Volcanism, and Mass Mortality 1988 p 26-27 Prepared in cooperation with Hawaii Univ., Honolulu (For primary document see N89-21287 14-42)
Avail: NTIS HC A11/MF A01 CSCL 03B

One of the most profound changes in our perspective of the solar system resulting from the first quarter century of planetary exploration by spacecraft is the recognition that planets, including Earth, were bombarded by cosmic projectiles for 4.5 aeons and continue to be bombarded today. Although the planetary cratering rate is much lower now than it was during the first 0.5 aeons, sizeable Earth-approaching asteroids and comets continue to hit the Earth at a rate that poses a finite risk to civilization. The evolution of this planetary perspective on impact cratering is gradual over the last two decades. It took explorations of Mars and Mercury by early Mariner spacecraft and of the outer solar system by the Voyagers to reveal the significance of asteroidal and cometary impacts in shaping the morphologies and even chemical compositions of the planets. An unsettling implication of the new perspective is addressed: the risk to human civilization. Serious scientific attention was given to this issue in July 1981 at a NASA-sponsored Spacewatch Workshop in Snowmass, Colorado. The basic conclusion of the 1981 NASA sponsored workshop still stands: the risk that civilization might be destroyed by impact with an as-yet-undiscovered asteroid or comet exceeds risk levels that are sometimes deemed unacceptable by modern societies in other contexts. Yet these impact risks have gone almost undiscussed and undebated. The tentative quantitative assessment by some members of the 1981 workshop was that each year, civilization is threatened with destruction with a probability of about 1 in 100,000. The enormous spread in risk levels deemed by the public to be at the threshold of acceptability derives from a host of psychological factors that were widely discussed in the risk assessment literature. Slovic shows that public fears of hazards are greatest for hazards that are uncontrollable, involuntary, fatal, dreadful, globally catastrophic, and which have consequences that seem inequitable, especially if they affect future generations. Author

N89-21303*# California Univ., Santa Barbara.
MAGNETIC MICROSPHERULES ASSOCIATED WITH THE K/T AND UPPER EOCENE EXTINCTION EVENTS **c46**
Stanley M. Cisowski *In* Lunar and Planetary Inst., Global Catastrophes in Earth History: An Interdisciplinary Conference on Impacts, Volcanism, and Mass Mortality 1988 p 28-29 (For primary document see N89-21287 14-42)
Avail: NTIS HC A11/MF A01 CSCL 08G

Magnetic microspherules were identified in over 20 K/T boundary sites, and in numerous Deep Sea Drilling Project (DSDP) cores from the Caribbean and Pacific, synchronous with the extinction of several radiolarian species near the end of the Eocene. The K/T magnetic spherules are of particular interest as carriers of Ir and other siderophiles generally found in abundance in K/T boundary clay. Furthermore the textures and unusual chemistry of their component magnetic phases indicate an origin at high temperature, possibly related to (an) unusual event(s) marking the end of the Cretaceous and Eocene periods. Their origin, along with the non-magnetic (sanidine) spheules, is generally ascribed directly to megaimpact events hypothesized to have periodically disrupted life on Earth. A survey of microspherical forms associated with known meteorite and impact derived materials reveals fundamental differences from the extinction related spherules. Low temperature magnetic experiments on the K/T and Upper Eocene spheroids indicate that, unlike tektites, extremely small superparamagnetic carriers are not present in abundance. The extensive subaerial exposure of Cretaceous combustible black shale during sea level regression in the latest Cretaceous represents a potential source for the magnetic spheroids found in certain K/T boundary clays. The recent discovery of high Ir abundances distributed above and below the K/T boundary within shallow water sediments in Israel, which also contain the most extensive known zones of combustion metamorphism, the so called Mottled Zone, adds a further dramatic footnote to the proposed association between the magnetic spheroids and combustion of organic shales. Interestingly, the Mottled Zone also contains the rare mineral magnesioferrite, which was identified both within the K/T magnetic spheroids and as discrete crystals in boundary clay from marine and continental sites. Author

N89-21304*# Colorado Univ., Boulder. Dept. of Geology.
ORIGINATION, DIVERSITY, AND EXTINCTION METRICS ESSENTIAL FOR ANALYSIS OF MASS BIOTIC CRISIS EVENTS: AN EXAMPLE FROM CRETACEOUS AMMONOIDEA Abstract Only **c51**
Christopher J. Collom *In* Lunar and Planetary Inst., Global Catastrophes in Earth History: An Interdisciplinary Conference on Impacts, Volcanism, and Mass Mortality 1988 p 30 (For primary document see N89-21287 14-42)
Avail: NTIS HC A11/MF A01 CSCL 06B

Traditional mass extinction research has predominently concentrated on statistically demonstrating that mass extinction intervals are significantly above background levels of familial and generic extinction in terms of extinction percentage, extinction rate, and per-taxon extinction rate; mass extinction intervals occur on a set periodicity throughout geologic time, which is estimated to be some 30 MYR in duration. The published literature has given little emphasis to equally important considerations and metrics such as origination rate, standing diversity, and rate of generation of new taxa DURING mass extinction intervals. The extent to which a mass extinction affects the regional or global biota, must ultimately be gauged by taking into consideration both the number of taxa which become extinct at or near the event (stage) boundary, and the number of taxa which are either not affected at all by the extinction or actually evolved during or shortly before/after the extinction interval. These effects can be seen in Cretaceous Ammonoidea (at the genus level), and their combined usage allow better insight into paleobiological dynamics and responses to mass extinction and its affect on this dominant Molluscan organism.
Author

N89-21305*# Paris VI Univ. (France). Lab. de Paleomagnetisme et Geodynamique.
DECCAN VOLCANISM AT THE CRETACEOUS-TERTIARY BOUNDARY **c46**
V. Courtillot, D. Vandamme, and J. Besse *In* Lunar and Planetary Inst., Global Catastrophes in Earth History: An Interdisciplinary Conference on Impacts, Volcanism, and Mass Mortality 1988 p 31-32 (For primary document see N89-21287 14-42)
Avail: NTIS HC A11/MF A01 CSCL 08K

The accuracy with which one can claim that Deccan trap volcanism occurred at the Cretaceous-Tertiary boundary (KTB) over a very short time interval is of key importance in deciding whether a volcanic origin of the KTB events should be taken seriously. In the two years since paleomagnetic, paleontological and geodynamic evidence was published, further data have become available and the case now appears to be well constrained. The Ar-40/Ar-39 results from six labs have yielded some 24 reliable plateau ages that narrow the age range to 65 to 69 Ma. Moreover, it appears that a significant part of this range results from inter-lab spread and possible minor alteration. Paleontology demonstrates that volcanism started in the Maestrichtian, more precisely in the A. mayaroensis zone. Paleomagnetism shows that volcanism spanned only 3 chrons and only one correlation remains possible, that of the main central reversed chron with 29R. Therefore, whereas Ar-40/Ar-39 is able only to restrict the duration of volcanism to some 4 Ma, paleomagnetism restricts it to 0.5 Ma. Using some geochemical indicators such as C-13 as proxy, it is suggested that volcanism actually consists of a few shorter events

of unequal magnitude. Extrusion rates may be as high as 100 cu km/yr and fissure lengths as long as several 100 km. Such a scenario appears to be at least as successful as others in accounting for most anomalies observed at the KTB. Particularly important are Iridium and other platinum group elements (PGE) profiles, Sr-87/Sr-86, C-13, 0-18, other exotic geochemical signatures, spherules, soot, shocked minerals, selective and stepwise extinctions. The environmental impact of CO2 possibly released during explosive phases of volcanism, and SO2 released during effusive phases, and the ability of volcanism to ensure worldwide distribution of KTB products are now all addressed. In conclusion, the case for a causal link between internal hotspot activity, birth of the Reunion hotspot itself as the Deccan and KTB events appears to rest on an increasingly stronger basis.

Author

N89-21306*# Lawrence Livermore National Lab., CA.

GLOBAL ENVIRONMENTAL EFFECTS OF IMPACT-GENERATED AEROSOLS: RESULTS FROM A GENERAL CIRCULATION MODEL Abstract Only **c45**

C. Covey, S. J. Ghan, and Paul R. Weissman *In* Lunar and Planetary Inst., Global Catastrophes in Earth History: An Interdisciplinary Conference on Impacts, Volcanism, and Mass Mortality 1988 p 33 Prepared in cooperation with Jet Propulsion Lab., California Inst. of Tech., Pasadena (For primary document see N89-21287 14-42)

Avail: NTIS HC A11/MF A01 CSCL 13B

Cooling and darkening at Earth's surface are expected to result from the interception of sunlight by the high altitude worldwide dust cloud generated by impact of a large asteroid or comet, according to the one-dimensional radioactive-convective atmospheric model (RCM) of Pollack et al. An analogous three-dimensional general circulation model (GCM) simulation obtains the same basic result as the RCM but there are important differences in detail. In the GCM simulation the heat capacity of the oceans, not included in the RCM, substantially mitigates land surface cooling. On the other hand, the GCM's low heat capacity surface allows surface temperatures to drop much more rapidly than reported by Pollack et al. These two differences between RCM and GCM simulations were noted previously in studies of nuclear winter; GCM results for comet/asteroid winter, however, are much more severe than for nuclear winter because the assumed aerosol amount is large enough to intercept all sunlight falling on Earth. In the simulation the global average of land surface temperature drops to the freezing point in just 4.5 days, one-tenth the time required in the Pollack et al. simulation. In addition to the standard case of Pollack et al., which represents the collision of a 10-km diameter asteroid with Earth, additional scenarios are considered ranging from the statistically more frequent impacts of smaller asteroids to the collision of Halley's comet with Earth. In the latter case the kinetic energy of impact is extremely large due to the head-on collision resulting from Halley's retrograde orbit.

Author

N89-21307*# McMaster Univ., Hamilton (Ontario). Dept. of Geology.

NOBLE METALS IN MID-OCEAN RIDGE VOLCANISM: A SIGNIFICANT FRACTIONATION OF GOLD WITH RESPECT TO PLATINUM GROUP METALS **c48**

James H. Crocket *In* Lunar and Planetary Inst., Global Catastrophes in Earth History: An Interdisciplinary Conference on Impacts, Volcanism, and Mass Mortality 1988 p 34-35 (For primary document see N89-21287 14-42)

Avail: NTIS HC A11/MF A01 CSCL 08C

Hydrothermal precipitates, black smoker particulate, and massive sulphide dredge samples from the Explorer Ridge on the Juan de Fuca Plate and the TAG hydrothermal area on the Mid-Atlantic Ridge were analyzed for selected noble metals including Au, Ir and Pd by radiochemical neutron activation analysis. The preliminary results indicate that gold contents may reach the ppm range although values in the neighborhood of 100 to 200 ppb are more typical. The platinum group elements (PGE) represented by Ir and Pd are typically less than 0.02 ppb and less than 2 ppb respectively. These abundances represent a significant enrichment of gold relative to the PGE in comparison with average noble metal abundances in mid-ocean ridge basalts (MORB). A partial explanation of this distinctive fractionation can be found in the concepts of sulfur-saturation of basic magma in mid-ocean ridge (MOR) settings, and the origin of MOR hydrothermal fluids. Experimental and petrological data suggest that MORBs are sulfur-saturated at the time of magma generation and that an immiscible sulfide component remains in the mantle residue. Hence, MORBs are noble metal-poor, particularly with respect to PGE. Consequently, black smoker fluids can be expected to reflect the low Ir and Pd contents of the rock column. The average Au content of MORB is 1.3 ppb, and so the rock column is not significantly enriched in Au. The generation of fluids which precipitate solids with 200 ppb Au is apparently dependent on highly efficient fluid chemistry to mobilize Au from the rock column, high Au solubility in seawater hydrothermal fluids and efficient precipitation mechanisms to coprecipitate Au on Fe, Zn and Cu sulfides. Significant differences in these parameters appear to be the ultimate cause of the strong Au-PGE fractionation in the MOR setting. It does not appear from the current data base that MOR hydrothermal fluids are significant contributors to the Ir enrichment seen in Cretaceous-Tertiary boundary sediments.

Author

N89-21308*# Applied Research Corp., College Station, TX.

ABRUPT CLIMATE CHANGE AND EXTINCTION EVENTS **c45**

Thomas J. Crowley *In* Lunar and Planetary Inst., Global Catastrophes in Earth History: An Interdisciplinary Conference on Impacts, Volcanism, and Mass Mortality 1988 p 36-37 (For primary document see N89-21287 14-42)

Avail: NTIS HC A11/MF A01 CSCL 13B

There is a growing body of theoretical and empirical support for the concept of instabilities in the climate system, and indications that abrupt climate change may in some cases contribute to abrupt extinctions. Theoretical indications of instabilities can be found in a broad spectrum of climate models (energy balance models, a thermohaline model of deep-water circulation, atmospheric general circulation models, and coupled ocean-atmosphere models). Abrupt transitions can be of several types and affect the environment in different ways. There is increasing evidence for abrupt climate change in the geologic record and involves both interglacial-glacial scale transitions and the longer-term evolution of climate over the last 100 million years. Records from the Cenozoic clearly show that the long-term trend is characterized by numerous abrupt steps where the system appears to be rapidly moving to a new equilibrium state. The long-term trend probably is due to changes associated with plate tectonic processes, but the abrupt steps most likely reflect instabilities in the climate system as the slowly changing boundary conditions caused the climate to reach some threshold critical point. A more detailed analysis of abrupt steps comes from high-resolution studies of glacial-interglacial fluctuations in the Pleistocene. Comparison of climate transitions with the extinction record indicates that many climate and biotic transitions coincide. The Cretaceous-Tertiary extinction is not a candidate for an extinction event due to instabilities in the climate system. It is quite possible that more detailed comparisons and analysis will indicate some flaws in the climate instability-extinction hypothesis, but at present it appears to be a viable candidate as an alternate mechanism for causing abrupt environmental changes and extinctions.

Author

N89-21309*# Lunar and Planetary Inst., Houston, TX.

EXPLOSIVE VOLCANISM, SHOCK METAMORPHISM AND THE K-T BOUNDARY **c46**

S. L. deSilva and V. L. Sharpton *In its* Global Catastrophes in Earth History: An Interdisciplinary Conference on Impacts, Volcanism, and Mass Mortality 1988 p 38-39 (For primary document see N89-21287 14-42)

Avail: NTIS HC A11/MF A01 CSCL 08G

The issue of whether shocked quartz can be produced by explosive volcanic events is important in understanding the origin of the K-T boundary constituents. Proponents of a volcanic origin for the shocked quartz at the K-T boundary cite the suggestion of

Rice, that peak overpressures of 1000 kbars can be generated during explosive volcanic eruptions, and may have occurred during the May, 1980 eruption of Mt. St. Helens. Attention was previously drawn to the fact that peak overpressures during explosive eruptions are limited by the strength of the rock confining the magma chamber to less than 8 kbars even under ideal conditions. The proposed volcanic mechanisms for generating pressures sufficient to shock quartz are further examined. Theoretical arguments, field evidence and petrographic data are presented showing that explosive volcanic eruptions cannot generate shock metamorphic features of the kind seen in minerals at the K-T boundary. Author

N89-21310*# Princeton Univ., NJ. Dept. of Geological and Geophysical Sciences.

AN EXTENDED CRETACEOUS-TERTIARY (K/T) STABLE ISOTOPE RECORD. IMPLICATIONS FOR PALEOCLIMATE AND THE NATURE OF THE K/T BOUNDARY EVENT **c45**

Steven DHondt *In* Lunar and Planetary Inst., Global Catastrophes in Earth History: An Interdisciplinary Conference on Impacts, Volcanism, and Mass Mortality 1988 p 40-41 (For primary document see N89-21287 14-42)

Avail: NTIS HC A11/MF A01 CSCL 13B

In order to obtain a detailed single site record of marine productivity and temperature across the Cretaceous-Tertiary (K/T) boundary, both delta C-13 and delta O-18 values were measured in paired surface and deep water microfossil and nannofossil samples of mid-latitude South Atlantic Deep Sea Drilling Project (DSDP) Site 528. Additionally, the percent sedimentary carbonate content of the rock samples from which the analyzed fossil samples were taken, were determined. The analyzed interval spanned the last approximately 1 million years of the Cretaceous (the Abathomphalus mayaroensis foraminiferal zone) and the first approximately 9 million years of the Tertiary (the Paleocene). Paired samples were analyzed every 150 cm of the entire 165 m sampled interval (1 sample per recovered DSDP section), every 20 cm for 2.0 m below and 2.5 m above the K/T boundary, and every 0.25 cm immediately below, at, and above the K/T boundary clay. The Cretaceous-Tertiary boundary and earliest Paleocene record of DSDP Site 528 is marked by at least two strong decreases in the surface-to-deep delta C-13 gradient (one at the K/T boundary (66.4 mybp1) and one approximately 150,000 to 200,000 years later). Both of these decreases co-occur with radical decreases in percent carbonate content and appear to indicate not one, but two, strong decreases in marine primary productivity during the analyzed interval. Author

N89-21311*# Geological Survey of Canada, Toronto (Ontario).

THE SUDBURY STRUCTURE (ONTARIO, CANADA) AND VREDEFORT STRUCTURE (SOUTH AFRICA): A COMPARISON **c46**

B. O. Dressler and W. U. Reimold *In* Lunar and Planetary Inst., Global Catastrophes in Earth History: An Interdisciplinary Conference on Impacts, Volcanism, and Mass Mortality 1988 p 42-43 Prepared in cooperation with Witwatersrand Univ., Johannesburg (South Africa) (For primary document see N89-21287 14-42)

Avail: NTIS HC A11/MF A01 CSCL 08G

Both the Sudbury Structure (SS) and the Witwatersrand Basin surrounding the Vredefort Structure (VS) host some of the most important base and precious metal deposits on earth. In both structures Precambrian igneous, sedimentary and volcanic rocks were affected by the structure forming process, either meteorite impact or endogenic explosion, or as some VS workers propose, by high strain tectonics. Besides these general features there are some geological and geophysical characteristics that are strikingly similar in both structures. There are, however, some obvious differences. Directly related to the structure forming processes are breccias in the footwall rocks of both structures. Pseudotachylite breccias occurring in both structures display great similarities. Chemical and physical characteristics of the pseudotachylites are similar in both structures. Both structures are characterized by overturned collar rocks, not evident everywhere around the SS. The VS is rimmed by an up or overturned collar of sediments and volcanics of the Witwatersrand, Ventersdorp and Transvaal Supergroups. Drilling information proved that the strata of the Witwatersrand Supergroup in the south of the VS are lying horizontally. Shockmetamorphic features such as planar microdeformations in rock forming minerals and shatter cones are present in both structures in the footwall rocks and in the SS also in the breccias of the OF. Both structures have large geophysical anomalies associated with them. In both structures the anomalies were interpreted as being caused by mafic-ultramafic complexes underlying the structures. Author

N89-21312*# New Mexico Univ., Albuquerque. Dept. of Geology.

PROTEROZOIC BUSHVELD-VREDEFORT CATASTROPHE: POSSIBLE CAUSES AND CONSEQUENCES **c46**

W. E. Elston and D. Twist *In* Lunar and Planetary Inst., Global Catastrophes in Earth History: An Interdisciplinary Conference on Impacts, Volcanism, and Mass Mortality 1988 p 44-45 Prepared in cooperation with Pretoria Univ. (South Africa) (For primary document see N89-21287 14-42)

Avail: NTIS HC A11/MF A01 CSCL 08G

Bushveld Complex and Vredefort Dome are unique features, formed in close proximity during the same time interval, approximately 2 Ga. Both show evidence of catastrophic events in the shallow marine environment of the otherwise stable Kaapvaal Craton. Explanation by multiple impacts of an asteroid, brecciated by an inter-asteroidal collision and disintegrating in Earth's gravity field is supported by pseudotachylite, shatter cones, coesite, and stishovite at Vredefort but these shock phenomena were not found in the Bushveld Complex. The Bushveld Complex was formerly interpreted as a lopolith, a view incompatible with gravity, electrical resistivity, magnetic, and seismic-reflection data. It is outlined by five inward-dipping lobes of layered ultramafic-mafic plutonic rocks that partly coalesce to form a basin-like feature 400 km in diameter and 65,000 sq. km. in area, equivalent to a small lunar mare. The Bushveld Complex is orders of magnitudes larger than other proposed terrestrial impact structures and differs from them in important ways. Its principal members, in order of age, are Rooiberg Felsite, RLS, and Lebowa Granite. The Bushveld-Vredefort events occurred during the interval from neutral or reducing atmosphere to oxidizing atmosphere. This transition is usually related to the evolution of photosynthesizing organisms. If the impact hypothesis for Bushveld-Vredefort can be confirmed, it may represent a global catastrophe sufficient to contribute to environmental changes favoring aerobic photosynthesizing eukaryotes over anaerobic prokaryotes. Author

N89-21313*# Rhode Island Univ., Kingston. Dept. of Geology.

ROCKS, RESOLUTION, AND THE RECORD AT THE TERRESTRIAL K/T BOUNDARY, EASTERN MONTANA AND WESTERN NORTH DAKOTA **c46**

D. E. Fastovsky *In* Lunar and Planetary Inst., Global Catastrophes in Earth History: An Interdisciplinary Conference on Impacts, Volcanism, and Mass Mortality 1988 p 46-47 (For primary document see N89-21287 14-42)

Avail: NTIS HC A11/MF A01 CSCL 08G

Reconstructions of mass extinction events are based upon faunal patterns, reconstructed from numerical and diversity data ultimately derived from rocks. It follows that geological complexity must not be subsumed in the desire to establish patterns. This is exemplified at the Terrestrial Cretaceous-Tertiary (K/T) boundary in eastern Montana and western North Dakota, where there are represented all of the major indicators of the terrestrial K/T transition: dinosaurian and non-dinosaurian vertebrate faunas, pollen, a megaflora, iridium, and shocked quartz. It is the patterns of these indicators that shape ideas about the terrestrial K/T transition. In eastern Montana and western North Dakota, the K/T transition is represented lithostratigraphically by the Cretaceous Hell Creek Formation, and the Tertiary Tullock Formation. Both of these are the result of aggrading, meandering, fluvial systems, a fact that has important consequences for interpretations of fossils they contain. Direct consequences of the fluvial depositional

environments are: facies are lenticular, interfingering, and laterally discontinuous; the occurrence of fossils in the Hell Creek and Tullock formations is facies-dependent; and the K/T sequence in eastern Montana and western North Dakota is incomplete, as indicated by repetitive erosional contacts and soil successions. The significance for faunal patterns of lenticular facies, facies-dependent preservation, and incompleteness is discussed. A project attempting to reconstruct vertebrate evolution in a reproducible manner in Hell Creek-type sediments must be based upon a reliable scale of correlations, given the lenticular nature of the deposits, and a recognition of the fact that disparate facies are not comparable in terms of either numbers of preserved vertebrates or depositional rates. Author

N89-21314*# Los Alamos National Lab., NM.
IRIDIUM EMISSIONS FROM HAWAIIAN VOLCANOES Abstract Only **c46**
D. L. Finnegan, W. H. Zoller, and T. M. Miller *In* Lunar and Planetary Inst., Global Catastrophes in Earth History: An Interdisciplinary Conference on Impacts, Volcanism, and Mass Mortality 1988 p 48 (For primary document see N89-21287 14-42)
Avail: NTIS HC A11/MF A01 CSCL 08G

Particle and gas samples were collected at Mauna Loa volcano during and after its eruption in March and April, 1984 and at Kilauea volcano in 1983, 1984, and 1985 during various phases of its ongoing activity. In the last two Kilauea sampling missions, samples were collected during eruptive activity. The samples were collected using a filterpack system consisting of a Teflon particle filter followed by a series of 4 base-treated Whatman filters. The samples were analyzed by INAA for over 40 elements. As previously reported in the literature, Ir was first detected on particle filters at the Mauna Loa Observatory and later from non-erupting high temperature vents at Kilauea. Since that time Ir was found in samples collected at Kilauea and Mauna Loa during fountaining activity as well as after eruptive activity. Enrichment factors for Ir in the volcanic fumes range from 10,000 to 100,000 relative to BHVO. Charcoal impregnated filters following a particle filter were collected to see if a significant amount of the Ir was in the gas phase during sample collection. Iridium was found on charcoal filters collected close to the vent, no Ir was found on the charcoal filters. This indicates that all of the Ir is in particulate form very soon after its release. Ratios of Ir to F and Cl were calculated for the samples from Mauna Loa and Kilauea collected during fountaining activity. The implications for the KT Ir anomaly are still unclear though as Ir was not found at volcanoes other than those at Hawaii. Further investigations are needed at other volcanoes to ascertain if basaltic volcanoes other than hot spots have Ir enrichments in their fumes. Author

N89-21315*# Arizona Univ., Tucson. Dept. of Geosciences.
THE IMPACT OF MASS EXTINCTIONS **c45**
Karl W. Flessa *In* Lunar and Planetary Inst., Global Catastrophes in Earth History: An Interdisciplinary Conference on Impacts, Volcanism, and Mass Mortality 1988 p 49 Prepared in cooperation with National Science Foundation, Washington, DC (For primary document see N89-21287 14-42)
Avail: NTIS HC A11/MF A01 CSCL 13B

In the years since Snowbird an explosive growth of research on the patterns, causes, and consequences of extinction was seen. The fossil record of extinction is better known, stratigraphic sections were scrutinized in great detail, and additional markers of environmental change were discovered in the rock record. However flawed, the fossil record is the only record that exists of natural extinction. Compilations from the primary literature contain a faint periodic signal: the extinctions of the past 250 my may be regulary spaced. The reality of the periodicity remains a subject for debate. The implications of periodicity are so profound that the debate is sure to continue. The greater precision from stratigraphic sections spanning extinction events has yet to resolve controversies concerning the rates at which extinctions occurred. Some sections seem to record sudden terminations, while others suggest gradual or steplike environmental deterioration. Unfortunately, the manner in which the strata record extinctions and compile stratigraphic ranges makes a strictly literal reading of the fossil record inadvisable. Much progress was made in the study of mass extinctions. The issues are more sharply defined but they are not fully resolved. Scenarios should look back to the phenomena they purport to explain - not just an iridium-rich layer, but the complex fabric of a mass extinction. Author

N89-21316*# Lunar and Planetary Inst., Houston, TX.
VOLCANISM, GLOBAL CATASTROPHE AND MASS MORTALITY **c46**
P. W. Francis and K. Burke *In its* Global Catastrophes in Earth History: An Interdisciplinary Conference on Impacts, Volcanism, and Mass Mortality 1988 p 50-51 (For primary document see N89-21287 14-42)
Avail: NTIS HC A11/MF A01 CSCL 08G

The effects of very large volcanic eruptions are well documented in many studies, mostly based on observations made on three historic eruptions, Laki 1783; Tambora 1815 and Krakatau 1883. Such eruptions have effects that are catastrophic locally and measurable globally, but it is not clear that even the largest volcanic eruptions have had global catastrophic effects, nor caused mass extinctions. Two different types of volcanic eruption were considered as likely to have the most serious widespread effects: large silicic explosive eruptions producing hundreds or thousands of cubic kilometers of pyroclastic materials, and effusive basaltic eruptions producing of approximately 100 cubic kilometers of lava. In both cases, the global effects are climatic, and attributable to production of stratospheric aerosols. Other possibilities need to be explored. Recent research on global change has emphasized the extreme sensitivity of the links between oceanic circulation, atmospheric circulation and climate. In particular, it was argued that the pattern of ocean current circulation (which strongly influences climate) is unstable; it may rapidly flip from one pattern to a different one, with global climatic consequences. If volcanism has been a factor in global environmental change and a cause of mass extinctions, it seems most likely that it has done so by providing a trigger to other processes, for example by driving oceanic circulation from one mode to another. Author

N89-21317*# National Aeronautics and Space Administration. Goddard Space Flight Center, Greenbelt, MD.
GEOLOGICAL REMOTE SENSING SIGNATURES OF TERRESTRIAL IMPACT CRATERS **c43**
J. B. Garvin, C. Schnetzler, and R. A. F. Grieve *In* Lunar and Planetary Inst., Global Catastrophes in Earth History: An Interdisciplinary Conference on Impacts, Volcanism, and Mass Mortality 1988 p 52-53 Prepared in cooperation with Geological Survey of Canada, Toronto (Ontario) (For primary document see N89-21287 14-42)
Avail: NTIS HC A11/MF A01 CSCL 08B

Geological remote sensing techniques can be used to investigate structural, depositional, and shock metamorphic effects associated with hypervelocity impact structures, some of which may be linked to global Earth system catastrophies. Although detailed laboratory and field investigations are necessary to establish conclusive evidence of an impact origin for suspected crater landforms, the synoptic perspective provided by various remote sensing systems can often serve as a pathfinder to key deposits which can then be targetted for intensive field study. In addition, remote sensing imagery can be used as a tool in the search for impact and other catastrophic explosion landforms on the basis of localized disruption and anomaly patterns. In order to reconstruct original dimensions of large, complex impact features in isolated, inaccessible regions, remote sensing imagery can be used to make preliminary estimates in the absence of field geophysical surveys. The experienced gained from two decades of planetary remote sensing of impact craters on the terrestrial planets, as well as the techniques developed for recognizing stages of degradation and initial crater morphology, can now be applied to the problem of discovering and studying eroded impact landforms on Earth. Preliminary results of remote sensing analyses of a set of terrestrial impact features in various states of degradation,

geologic settings, and for a broad range of diameters and hence energies of formation are summarized. The intention is to develop a database of remote sensing signatures for catastrophic impact landforms which can then be used in EOS-era global surveys as the basis for locating the possibly hundreds of missing impact structures. In addition, refinement of initial dimensions of extremely recent structures such as Zhamanshin and Bosumtwi is an important objective in order to permit re-evaluation of global Earth system responses associated with these types of events. Author

N89-21318*# Geological Survey of Canada, Toronto (Ontario).
THE FRASNIAN-FAMENNIAN MASS KILLING EVENT(S), METHODS OF IDENTIFICATION AND EVALUATION **c45**
H. H. J. Geldsetzer *In* Lunar and Planetary Inst., Global Catastrophes in Earth History: An Interdisciplinary Conference on Impacts, Volcanism, and Mass Mortality 1988 p 54-55 (For primary document see N89-21287 14-42)
Avail: NTIS HC A11/MF A01 CSCL 13B

The absence of an abnormally high number of earlier Devonian taxa from Famennian sediments was repeatedly documented and can hardly be questioned. Primary recognition of the event(s) was based on paleontological data, especially common macrofossils. Most paleontologists place the disappearance of these common forms at the gigas/triangularis contact and this boundary was recently proposed as the Frasnian-Famennian (F-F) boundary. Not unexpectedly, alternate F-F positions were suggested caused by temporary Frasnian survivors or sudden post-event radiations of new forms. Secondary supporting evidence for mass killing event(s) is supplied by trace element and stable isotope geochemistry but not with the same success as for the K/T boundary, probably due to additional 300 ma of tectonic and diagenetic overprinting. Another tool is microfacies analysis which is surprisingly rarely used even though it can explain geochemical anomalies or paleontological overlap not detectable by conventional macrofacies analysis. The combination of microfacies analysis and geochemistry was applied at two F-F sections in western Canada and showed how interdependent the two methods are. Additional F-F sections from western Canada, western United States, France, Germany and Australia were sampled or re-sampled and await geochemical/microfacies evaluation. Author

N89-21319*# Chicago Univ., IL.
EVIDENCE FOR A SINGLE IMPACT AT THE CRETACEOUS-TERTIARY BOUNDARY FROM TRACE ELEMENTS **c46**
Iain Gilmour and Edward Anders *In* Lunar and Planetary Inst., Global Catastrophes in Earth History: An Interdisciplinary Conference on Impacts, Volcanism, and Mass Mortality 1988 p 56-57 (For primary document see N89-21287 14-42)
(Grants NAG9-52; NSF EAR-86-09218)
Avail: NTIS HC A11/MF A01 CSCL 08G

Not only meteoritic elements (Ir, Ni, Au, Pt metals), but also some patently non-meteoritic elements (As, Sb) are enriched at the K-T boundary. Eight enriched elements at 7 K-T sites were compared and it was found that: All have fairly constant proportions to Ir and Kilauea (invoked as an example of a volcanic source of Ir by opponents of the impact theory) has too little of 7 of these 8 elements to account for the boundary enrichments. The distribution of trace elements at the K-T boundary was reexamined using data from 11 sites for which comprehensive are available. The meteoritic component can be assessed by first normalizing the data to Ir, the most obviously extraterrestrial element, and then to CI chondrites. The double normalization reduces the concentration range from 11 decades to 5 and also facilitates the identification of meteoritic elements. At sites where trace elements were analyzed in sub-divided samples of boundary clay, namely, Caravaca (SP), Stevns Klint (DK), Flaxbourne River (NZ) and Woodside Creek (NZ), Sb, As and Zn are well correlated with Ir across the boundary implying a common deposition mechanism. Elemental carbon is also enriched by up to 10,000 x in boundary clay from 5 K-T sides and is correlated with Ir across the boundary at Woodside Creek. While biomass would appear to be the primary fuel source for this carbon a contribution from a fossil fuel source may be necessary in order to account for the observed C abundance. Author

N89-21320*# Chicago Univ., IL.
NITROGEN GEOCHEMISTRY OF A CRETACEOUS-TERTIARY BOUNDARY SITE IN NEW ZEALAND **c46**
Iain Gilmour and Stuart R. Boyd *In* Lunar and Planetary Inst., Global Catastrophes in Earth History: An Interdisciplinary Conference on Impacts, Volcanism, and Mass Mortality 1988 p 58-59 Prepared in cooperation with Open Univ., Milton (England) (For primary document see N89-21287 14-42)
Avail: NTIS HC A11/MF A01 CSCL 08G

Nitrogen in the basal layer of the K-T boundary clay at Woodside Creek, New Zealand, has an abundance of 1100 ppm, a 20-fold enrichment over Cretaceous and Tertiary values. The enrichment parallels that for Ir and elemental carbon (soot); all decrease over the next 6 mm of the boundary clay. The C/N ratio, assuming the nitrogen to be associated with organic rather than elemental carbon, is approximately 5 for the basal layer compared to 20 to 30 for the remainder of the boundary clay. The correlation between N and Ir abundances appears to persist above the boundary, implying that the N is intimately associated with the primary fallout and remained with it during the secondary redeposition processes that kept the Ir abundance relatively high into the lowermost Tertiary. Apparently the basal layer of the boundary clay represents the accumulation of a substantial quantity of N with an isotopic composition approximately 10 percent heavier than background delta value of N-15 values. If the boundary clay represents an altered impact glass from a meteorite impact than it probably denotes a time period of less than 1 year. Therefore, the changes in nitrogen geochemistry apparently occurred over a very short period of time. The high abundance of N and the correspondingly low C/N ratio may reflect enhanced preservation of organic material as a result of the rapid sweepout and burial of plankton by impact ejecta, with little or no bacterial degradation. It is conceivable that the shift in delta value of N-15 may represent an influx of nitrogen from a different source deposited contemporaneously with the impact ejecta. An interesting possibility is that it may be derived from nitrate, produced from the combustion of atmospheric nitrogen. Author

N89-21321*# Chicago Univ., IL.
THE GLOBAL CRETACEOUS-TERTIARY FIRE: BIOMASS OR FOSSIL CARBON **c46**
Iain Gilmour and Frank Guenther *In* Lunar and Planetary Inst., Global Catastrophes in Earth History: An Interdisciplinary Conference on Impacts, Volcanism, and Mass Mortality 1988 p 60-62 Prepared in cooperation with National Bureau of Standards, Gaithersburg, MD (For primary document see N89-21287 14-42)
Avail: NTIS HC A11/MF A01 CSCL 08G

The global soot layer at the K-T boundary indicates a major fire triggered by meteorite impact. However, it is not clear whether the principal fuel was biomass or fossil carbon. Forests are favored by delta value of C-13, which is close to the average for trees, but the total amount of elemental C is approximately 10 percent of the present living carbon, and thus requires very efficient conversion to soot. The PAH was analyzed at Woodside Creek, in the hope of finding a diagnostic molecular marker. A promising candidate is 1-methyl-7-isopropyl phenanthrene (retene,), which is probably derived by low temperature degradation of abietic acid. Unlike other PAH that form by pyrosynthesis at higher temperatures, retene has retained the characteristic side chains of its parent molecule. A total of 11 PAH compounds were identified in the boundary clay. Retene is present in substantial abundance. The identification was confirmed by analysis of a retene standard. Retene is characteristic of the combustion of resinous higher plants. Its formation depends on both temperature and oxygen access, and is apparently highest in oxygen-poor fires. Such fires would also produce soot more efficiently which may explain the high soot abundance. The relatively high level of coronene is not typical of a wood combustion source, however, though it can be produced

during high temperature pyrolysis of methane, and presumably other H, C-containing materials. This would require large, hot, low O2 zones, which may occur only in very large fires. The presence of retene indicates that biomass was a significant fuel source for the soot at the Cretaceous-Tertiary boundary. The total amount of elemental C produced requires a greater than 3 percent soot yield, which is higher than typically observed for wildfires. However, retene and presumably coronene imply limited access of O2 and hence high soot yield. Author

N89-21322*# Delaware Univ., Newark. Dept. of Geology.
LATE EOCENE IMPACT EVENTS RECORDED IN DEEP-SEA SEDIMENTS **c48**
B. P. Glass *In* Lunar and Planetary Inst., Global Catastrophes in Earth History: An Interdisciplinary Conference on Impacts, Volcanism, and Mass Mortality 1988 p 63-64 (For primary document see N89-21287 14-42)
Avail: NTIS HC A11/MF A01 CSCL 08C

Raup and Sepkoski proposed that mass extinctions have occurred every 26 Myr during the last 250 Myr. In order to explain this 26 Myr periodicity, it was proposed that the mass extinctions were caused by periodic increases in cometary impacts. One method to test this hypothesis is to determine if there were periodic increases in impact events (based on crater ages) that correlate with mass extinctions. A way to test the hypothesis that mass extinctions were caused by periodic increases in impact cratering is to look for evidence of impact events in deep-sea deposits. This method allows direct observation of the temporal relationship between impact events and extinctions as recorded in the sedimentary record. There is evidence in the deep-sea record for two (possibly three) impact events in the late Eocene. The younger event, represented by the North American microtektite layer, is not associated with an Ir anomaly. The older event, defined by the cpx spherule layer, is associated with an Ir anomaly. However, neither of the two impact events recorded in late Eocene deposits appears to be associated with an unusual number of extinctions. Thus there is little evidence in the deep-sea record for an impact-related mass extinction in the late Eocene. Author

N89-21323*# Max-Planck-Inst. fuer Chemie, Mainz (Germany, F.R.).
MINERALOGY AND PHASE-CHEMISTRY OF THE CRETACEOUS/TERTIARY SECTION IN THE LATTENGEBIRGE, BAVARIAN ALPS **c46**
G. Graup *In* Lunar and Planetary Inst., Global Catastrophes in Earth History: An Interdisciplinary Conference on Impacts, Volcanism, and Mass Mortality 1988 p 65 (For primary document see N89-21287 14-42)
Avail: NTIS HC A11/MF A01 CSCL 08G

The Lattengebirge K/T section reveals three distinct Ir spikes. Two of them are contained in the K/T transition zone sensu-strictu termed clayey interval, with 4.4 ppb Ir at the actual K/T boundary, and 2.8 ppb Ir 10 cm above the boundary. The highest Ir enrichment of 9 ppb, however, was detected in semi-cleaned organic material from a thin sandstone layer of Upper Maastrichtian age at 16 cm below the boundary. In this layer various discernible phases are preserved, contrasting with the worldwide observed K/T transition zones which are generally entirely composed of diagenetically altered materials. Given that, important clues to understanding the Cretaceous terminal events may be provided. The phases of the Cretaceous Ir bearing layer at Lattengebirge consist of: sandstone fragmental minerals in a carbonate matrix, coal which is partly burnt, melt glasses presumably of combustion-metamorphic origin, and sulfides, mainly chalcopyrite, contained in the coal. Like many known K/T sections and the Lattengebirge boundary sensu-strictu, the Cretaceous horizon is enriched in Ir and chalcophile elements as well. Although the Lattengebirge section offers the freshest materials, including melt glasses, of all K/T localities investigated, no unequivocal evidence of formation by impact has been found there. Author

N89-21324*# Birmingham Univ. (England). Dept. of Geological Sciences.
THE END-TRIASSIC MASS EXTINCTION EVENT **c51**
A. Hallam *In* Lunar and Planetary Inst., Global Catastrophes in Earth History: An Interdisciplinary Conference on Impacts, Volcanism, and Mass Mortality 1988 p 66-67 (For primary document see N89-21287 14-42)
Avail: NTIS HC A11/MF A01 CSCL 06B

The end-Triassic is the least studied of the five major episodes of mass extinction recognized in the Phanerozoic, and the Triassic-Jurassic boundary is not precisely defined in most parts of the world, with a paucity of good marine sections and an insufficiency of biostratigraphically valuable fossils. Despite these limitations it is clear that there was a significant episode of mass extinction, affecting many groups, in the Late Norian and the existing facts are consistent with it having taken place at the very end of the period. The best record globally comes from marine strata. There was an almost complete turnover of ammonites across the T-J boundary, with perhaps no more than one genus surviving. About half the bivalve genera and most of the species went extinct, as did many archaeogastropods. Many Paleozoic-dominant brachiopods also disappeared, as did the last of the conodonts. There was a major collapse and disappearance of the Alpine calcareous sponge. Among terrestrial biota, a significant extinction event involving tetrapods was recognized. With regard to possible environmental events that may be postulated to account for the extinctions, there is no evidence of any significant global change of climate at this time. The existence of the large Manicouagan crater in Quebec, dated as about late or end-Triassic, has led to the suggestion that an impact event might be implicated, but so far despite intensive search no unequivocal iridium anomaly or shocked quartz was discovered. On the other hand there is strong evidence for significant marine regression in many parts of the world. It is proposed therefore that the likeliest cause of the marine extinctions is severe reduction in habitat area caused either by regression of epicontinental seas, subsequent widespread anoxia during the succeeding transgression, or a combination of the two. Author

N89-21325*# Geological Inst., Oster Voldgade (Denmark).
DIACHRONISM BETWEEN EXTINCTION TIME OF TERRESTRIAL AND MARINE DINOSAURS **c51**
H. J. Hansen *In* Lunar and Planetary Inst., Global Catastrophes in Earth History: An Interdisciplinary Conference on Impacts, Volcanism, and Mass Mortality 1988 p 2 (For primary document see N89-21287 14-42)
Avail: NTIS HC A11/MF A01 CSCL 06B

The dinosaur eggs of southern France occur in continental, fine-grained red-beds, rich in carbonate. The last eggs in the region occur in the magnetic polarity interval 30 normal. Estimates of the accumulation rate of these sediments on the basis of the magneto-stratigraphy leads to placement of the time of disappearance of the dinosaurs in this region of 200,000 to 400,000 years earlier than the Cretaceous-Tertiary boundary. In the Red Deer Valley, Canada, estimates of average accumulation rate lead to a time of disappearance of the dinosaurs of 135,000 to 157,000 years earlier than the Cretaceous-Tertiary boundary. In the central part of Poland, in the Nasilow Quarry, the paleomagnetic pattern shows 7 m of chalk of reversed polarity containing in its upper part the marine Cretaceous-Tertiary biostratigraphic boundary. A greensand deposit contains numerous re-deposited Maastrichtian fossils. The fossils show no signs of wear and are of very different sizes including 1 mm thick juvenile belemnites. The deposit was described as a lag-sediment. Among the various fossils are teeth of mosasaurs. Thus there is coincidence in time between the extinction of mosasaurs and other Cretaceous organisms. This leads to the conclusion, that extinction of terrestrial dinosaurs took place earlier than extinction of marine dinosaurs at the Cretaceous-Tertiary boundary. Author

N89-21326*# Solar System Associates, Des Moines, IA.
THE MANSON IMPACT STRUCTURE, A POSSIBLE SITE FOR A CRETACEOUS-TERTIARY (K-T) BOUNDARY IMPACT **c46**

J. B. Hartung, M. J. Kunk, and R. R. Anderson (Geological Survey, Iowa City, IA.) *In* Lunar and Planetary Inst., Global Catastrophes in Earth History: An Interdisciplinary Conference on Impacts, Volcanism, and Mass Mortality 1988 p 70-71 (For primary document see N89-21287 14-42)
Avail: NTIS HC A11/MF A01 CSCL 08G

The Manson impact structure, about 35 km in diameter, is the largest impact crater recognized in the United States. Its center is located near the town of Manson, 29 km west of Fort Dodge, Iowa. The structure is not well known geologically because it is covered by tens of meters of glacial deposits. What is known about the structure was learned mostly from the study of water well cuttings. At Manson the normal Phanerozoic and Proterozoic sedimentary rocks were replaced by centrally uplifted Proterozoic crystalline rocks that are representative of the normal basement: This central uplift is surrounded by completely disrupted rocks which are roughly encircled by peripherally faulted and slumped sequences of normal sedimentary strata. Radially outward normal sedimentary strata are uplifted slightly. Manson, once interpreted as a cryptovolcanic structure, is now considered an impact structure based on its circular shape, its central uplift and the presence of multiple intersecting sets of shock lamellae in quartz grains from the central uplift. The Ar-40/Ar-39 age spectrum dating results for a microcline separate from the Manson 2-A core in the central uplift is shown. This spectrum is interpreted to indicate a nearly complete degassing of the microcline at the time of the Manson impact. The remainder of the gas released climbs in age with increasing temperature of release. This pattern of the age spectrum is interpreted to represent diffusional loss due to reheating at the time of the impact and during subsequent cooling. Shocked quartz grains, present in the iridium-bearing layer at the K-T boundary throughout the world, have a significantly larger size and are more abundant in the western interior of North America than elsewhere in the world. Furthermore, shocked feldspar and granitic fragments are found at the K-T boundary in North America. These observations indicate the K-T boundary impact must have penetrated continental crust in North America. Author

N89-21327*# Louisiana State Univ., Baton Rouge. Dept. of Geology and Geophysics.
HOW MANY UPPER EOCENE MICROSPHERULE LAYERS: MORE THAN WE THOUGHT c46
Joseph E. Hazel *In* Lunar and Planetary Inst., Global Catastrophes in Earth History: An Interdisciplinary Conference on Impacts, Volcanism, and Mass Mortality 1988 p 72-73 (For primary document see N89-21287 14-42)
(Grant NSF EAR-88-95268)
Avail: NTIS HC A11/MF A01 CSCL 08G

The scientific controversy over the origin of upper Eocene tektites, microtektites and other microspherules cannot be logically resolved until it is determined just how many events are involved. The microspherule-bearing beds in marine sediments have been dated using standard biozonal techniques. Although a powerful stratigraphic tool, zonal biostratigraph has its limitations. One is that if an event, such as a microspherule occurrence, is observed to occur in a zone at one locality and then a similar event observed in the same zone at another locality, it still may be unwarranted to conclude that these events exactly correlate. To be in a zone a sample only need be between the fossil events that define the zone boundaries. It is often very difficult to accurately determine where within a zone one might be. Further, the zone defining events do not everywhere occur at the same points in time. That is, the ranges of the defining taxa are not always filled. Thus, the length of time represented by a zone (but not, of course, its chronozone) can vary from place to place. These problems can be offset by use of chronostratigraphic modelling techniques such as Graphic Correlation. This technique was used to build a Cretaceous and Cenozoic model containing fossil, magnetopolarity, and other events. The scale of the model can be demonstrated to be linear with time. This model was used to determine the chronostratigraphic position of upper Eocene microspherule layers. Author

N89-21328*# Princeton Univ., NJ. Dept. of Geological and Geophysical Sciences.
HIGH RESOLUTION CHRONOLOGY OF LATE CRETACEOUS-EARLY TERTIARY EVENTS DETERMINED FROM 21,000 YR ORBITAL-CLIMATIC CYCLES IN MARINE SEDIMENTS Abstract Only c48
Timothy D. Herbert and Steven DHondt *In* Lunar and Planetary Inst., Global Catastrophes in Earth History: An Interdisciplinary Conference on Impacts, Volcanism, and Mass Mortality 1988 p 74 (For primary document see N89-21287 14-42)
Avail: NTIS HC A11/MF A01 CSCL 08C

A number of South Atlantic sites cored by the Deep Sea Drilling Project (DSDP) recovered late Cretaceous and early Tertiary sediments with alternating light-dark, high-low carbonate content. The sedimentary oscillations were turned into time series by digitizing color photographs of core segments at a resolution of about 5 points/cm. Spectral analysis of these records indicates prominent periodicity at 25 to 35 cm in the Cretaceous intervals, and about 15 cm in the early Tertiary sediments. The absolute period of the cycles that is determined from paleomagnetic calibration at two sites is 20,000 to 25,000 yr, and almost certainly corresponds to the period of the earth's precessional cycle. These sequences therefore contain an internal chronometer to measure events across the K/T extinction boundary at this scale of resolution. The orbital metronome was used to address several related questions: the position of the K/T boundary within magnetic chron 29R, the fluxes of biogenic and detrital material to the deep sea immediately before and after the K/T event, the duration of the Sr anomaly, and the level of background climatic variability in the latest Cretaceous time. The carbonate/color cycles that were analyzed contain primary records of ocean carbonate productivity and chemistry, as evidenced by bioturbational mixing of adjacent beds and the weak lithification of the rhythmic sequences. It was concluded that sedimentary sequences that contain orbital cyclicity are capable of providing resolution of dramatic events in earth history with much greater precision than obtainable through radiometric methods. The data show no evidence for a gradual climatic deterioration prior to the K/T extinction event, and argue for a geologically rapid revolution at this horizon. Author

N89-21329*# Washington State Univ., Pullman. Dept. of Geology.
SELECTIVE EXTINCTION OF MARINE PLANKTON AT THE END OF THE MESOZOIC ERA: THE FOSSIL AND STABLE ISOTOPE RECORD Abstract Only c51
Y. Herman and S. K. Bhattacharya *In* Lunar and Planetary Inst., Global Catastrophes in Earth History: An Interdisciplinary Conference on Impacts, Volcanism, and Mass Mortality 1988 p 75 Prepared in cooperation with Physical Research Lab., Ahmedabad (India) (For primary document see N89-21287 14-42)
Avail: NTIS HC A11/MF A01 CSCL 06B

Floral, faunal and stable isotope evidence in a continuous sequence of latest Cretaceous and earliest Tertiary shallow water marine deposits in the Mangyshlak Peninsula, USSR suggest severe environmental changes at the Cretaceous/Tertiary (K/T) boundary. Time frame is provided by nanno, micro and macrofossils as well as by magnetic stratigraphy and an iridium spike. Oxygen isotopic analyses of the bulk sediments, composed of nanno and microplankton skeletal remains, show a sharp positive spike at the K/T boundary. This shift is primarily attributed to severe cooling possibly accompanied by increased salinities of the surface mixed layer. Floral and faunal extinctions were selective, affecting approximately 90 percent of the warm water calcareous phyto and zooplankton genera in the Tethyan-Paratethyan regions. These highly diverse taxa with many endemic representatives were at the peak of their evolutionary development. Geologic evidence indicates that the terminal Cretaceous temperature decline was coeval with widespread and intense volcanic activity which reached a peak at the close of the Mesozoic Era. Increased acidity temporarily prohibited calcite nucleation of the surface dwelling warm-water plankton. Superimposed upon decreased alkalinity,

severe and rapid climatic changes caused the extinction of calcareous phyto and zooplankton. Author

N89-21330*# Arizona Univ., Tucson. Lunar and Planetary Lab.
IMPACT WAVE DEPOSITS PROVIDE NEW CONSTRAINTS ON THE LOCATION OF THE K/T BOUNDARY IMPACT c48
A. R. Hildebrand and W. V. Boynton *In* Lunar and Planetary Inst., Global Catastrophes in Earth History: An Interdisciplinary Conference on Impacts, Volcanism, and Mass Mortality 1988 p 76-77 (For primary document see N89-21287 14-42)
Avail: NTIS HC A11/MF A01 CSCL 08C

All available evidence is consistent with an impact into oceanic crust terminating the Cretaceous Period. Although much of this evidence is incompatible with an endogenic origin, some investigators still feel that a volcanic origin is possible for the Cretaceous/Tertiary (K/T) boundary clay layers. The commonly cited evidence for a large impact stems from delicate clay layers and their components and the impact site has not yet been found. Impact sites have been suggested all over the globe. The impact is felt to have occurred near North America by: the occurrence of a 2 cm thick ejecta layer only at North American locales, the global variation of shocked quartz grain sizes peaking in North America, the global variation of spinel compositions with most refractory compositions occurring in samples from the Pacific region and possibly uniquely severe plant extinctions in the North American region. The K/T boundary interval was investigated as preserved on the banks of the Brazos River, Texas. The K/T fireball and ejecta layers with associated geochemical anomalies were found interbedded with this sequence which apparently allows a temporal resolution 4 orders of magnitude greater than typical K/T boundary sections. A literature search reveals that such coarse deposits are widely preserved at the K/T boundary. Impact wave deposits have not been found elsewhere on the globe, suggesting the impact occurred between North and South America. The coarse deposits preserved in Deep Sea Drilling Project (DSDP) holes 151-3 suggest the impact occurred nearby. Subsequent tectonism has complicated the picture. Author

N89-21331*# Arizona Univ., Tucson. Lunar and Planetary Lab.
PROVENANCE OF THE K/T BOUNDARY LAYERS c48
A. R. Hildebrand and W. V. Boynton *In* Lunar and Planetary Inst., Global Catastrophes in Earth History: An Interdisciplinary Conference on Impacts, Volcanism, and Mass Mortality 1988 p 78-79 (For primary document see N89-21287 14-42)
Avail: NTIS HC A11/MF A01 CSCL 08C

An array of chemical, physical and isotopic evidence indicates that an impact into oceanic crust terminated the Cretaceous Period. Approximately 1500 cu km of debris, dispersed by the impact fireball, fell out globally in marine and nonmarine environments producing a 2 to 4 mm thick layer (fireball layer). In North American locales, the fireball layer overlies a 15 to 25 mm thick layer of similar but distinct composition. This 15 to 25 mm layer (ejecta layer) may represent approximately 1000 cu km of lower energy ejecta from a nearby impact site. Isotopic and chemical evidence supports a mantle provenance for the bulk of the layers. The extraordinary REE pattern of the boundary clays was modelled as a mixture of oceanic crust, mantle, and approximately 10 percent continental material. The results are presented. If the siderophiles of the ejecta layer were derived solely from the mantle, a test may be available to see if the siderophile element anomaly of the fireball layer had an extraterrestrial origin. Radiogenic Os-187 is depleted in the mantle relative to an undifferentiated chondritic source. Os-187/Os-186 ratios of 1.049 and 1.108 were calculated for the ejecta and fireball layers, respectively. Author

N89-21332*# Eidgenoessische Technische Hochschule, Zurich (Switzerland).
STRANGELOVE OCEAN AT ERA BOUNDARIES, TERRESTRIAL OR EXTRATERRESTRIAL CAUSE Abstract Only c46
Kenneth J. Hsue *In* Lunar and Planetary Inst., Global Catastrophes in Earth History: An Interdisciplinary Conference on Impacts, Volcanism, and Mass Mortality 1988 p 80 (For primary document see N89-21287 14-42)
Avail: NTIS HC A11/MF A01 CSCL 08G

Negative perturbations in carbon-isotope value of calcite in pelagic sediments were found at times of biotic crisis, marking horizons which are, or were proposed as era boundaries: Cretaceous/Tertiary (K/T), Permian/Triassic (P/T), and Precambrian/Cambrian (PreC/C). The anomaly was also found at several other mass-extinction horizons, such as terminal Ordovician, Frasnian-Famenian, etc. Studies of K/T boundary indicate that only the planktic fraction of the sediments has the negative isotope anomaly, whereas the benthic fraction has the same value across the boundary. This geochemical signal is thus considered a record of strangelove ocean, or an ocean where isotope fractionation of dissolved carbonate ions in surface waters (by biotic function of planktic organisms) has been significantly reduced because of the drastic reduction of the biomass in the oceans. The reduction of marine biomass at each of the era boundaries was related to chemical pollution of the oceans as a consequence of a catastrophic event; a pH decrease of 0.5 could inhibit the fertility of planktons. Studies of earthquakes, volcanic eruptions, and meteorite-impact occurrences have indicated a linearly inverse log/log relationship between the magnitude and frequency of events. The frequency of era boundaries in geologic history supports the postulate that the rare events causing those biotic crises were large bolide-impacts. Author

N89-21333*# Texas A&M Univ., College Station. Center for Tectonophysics.
IRIDIUM, SHOCKED MINERALS, AND TRACE ELEMENTS ACROSS THE CRETACEOUS/TERTIARY BOUNDARY AT MAUD RISE, WEDELL SEA, AND WALVIS RIDGE, SOUTH ATLANTIC OCEAN c48
Alan R. Huffman, James H. Crocket, and Neville L. Carter *In* Lunar and Planetary Inst., Global Catastrophes in Earth History: An Interdisciplinary Conference on Impacts, Volcanism, and Mass Mortality 1988 p 82-82 Prepared in cooperation with McMaster Univ., Hamilton (Ontario) (For primary document see N89-21287 14-42)
Avail: NTIS HC A11/MF A01 CSCL 08C

Sediments spanning a 5 meter section across the Cretaceous-Tertiary boundary at ODP holes 689B and 690D, Maud Rise, Wedell Sea and hole 527, Walvis Ridge, are being analyzed for shock deformation, PGE's and other trace elements (including REE's). Mineral separates from each sample were studied with optical microscopy to determine the distribution and microstructural state of quartz and feldspar present in the sediments. Samples from Maud Rise were taken of the K/T transition and at about 50 cm intervals above and below it. These samples consist of carbonate-rich sediments, with the K/T transition marked by a change from white Maastrichtian oozes to a greenish ooze with higher concentrations of altered volcanic clay and vitric ash. The Walvis Ridge site is characterized by more clay-rich sediments with average carbonate content about 60 to 70 percent. Initial results from RNAA studies indicate that iridium is present in all the Maud Rise samples in concentrations equal to or greater than 0.01 ppb (whole-rock basis). Preliminary results from optical microscopy indicate the occurrence of shock mosaicism in quartz and feldspar in all of the samples studied. The pervasiveness of shock mosaicism and presence of planar features to 2 meters from the K/T boundary indicates that a single impact or volcanic explosion 66 ma may be ruled out as responsible for the K/T event. A similar conclusion may be drawn independently from the distribution of iridium and other trace elements. Regardless of the source of the shock waves and sediment contamination, multiple events are required over a ca.0.5 my timespan; currently we favor endogenous sources. Author

N89-21334*# Geological Survey, Denver, CO.
THE WESTERN NORTH AMERICAN CRETACEOUS-TERTIARY (K-T) BOUNDARY INTERVAL AND ITS CONTENT OF SHOCK-METAMORPHOSED MINERALS: IMPLICATIONS CONCERNING THE K-T BOUNDARY IMPACT-EXTINCTION THEORY **c46**
G. A. Izett *In* Lunar and Planetary Inst., Global Catastrophes in Earth History: An Interdisciplinary Conference on Impacts, Volcanism, and Mass Mortality 1988 p 83-84 (For primary document see N89-21287 14-42)
Avail: NTIS HC A11/MF A01 CSCL 08G

At 20 sites in the Raton Basin of Colorado and New Mexico, and at several other sites in Wyoming, Montana, and Canada, a pair of claystone units, an Ir abundance anomaly, and a concentration of shock-metamorphosed minerals mark the palynological K-T boundary. The K-T boundary claystone, which is composed of kaolinite and small amounts of illite/smectite mixed-layer clay, is similar in most respects to kaolinite tonstein layers in coal beds. At some, but not all, K-T boundary localities, the boundary claystone contains solid kaolinite and hollow and solid goyazite spherules, 0.05 to 1.2 mm in diameter. The upper unit, the K-T boundary impact layer, consists chiefly of kaolinite and various amounts of illite/smectite mixed-layer clay. The impact layer and boundary claystone are similar chemically, except that the former has slightly more Fe, K, Ba, Cr, Cu, Li, V, and Zn than the latter. The facts that the boundary claystone and impact layer contain anomalous amounts of Ir, comprise a stratigraphic couplet at Western North American sites, and form thin, discrete layers, similar to air-fall units (volcanic or impact), suggest that the claystone units are of impact origin. Significantly, the impact layer contains as much as 2 percent clastic mineral grains, about 30 percent of which contain multiple sets of shock lamellae. Only one such concentration of shocked minerals has been found near the K-T boundary. The type of K-T boundary shock-metamorphosed materials (quartzite and metaquartzite) in the impact layer and the lack of shock lamellae in quartz and feldspar of pumice lapilli and granitic xenoliths in air-fall pumice units of silicic tuffs, such as the Bishop Tuff, eliminate the possibility that the shock-metamorphosed minerals in the K-T impact layer are of volcanic origin. The global size distribution and abundance of shock-metamorphosed mineral grains suggest that the K-T impact occurred in North America. Author

N89-21335*# Bedford Inst. of Oceanography, Dartmouth (Nova Scotia). Atlantic Geoscience Centre.
MASS MORTALITY AND EXTRATERRESTRIAL IMPACTS **c45**
L. F. Jansa, F. M. Gradstein, and M. Pierre-Aubry *In* Lunar and Planetary Inst., Global Catastrophes in Earth History: An Interdisciplinary Conference on Impacts, Volcanism, and Mass Mortality 1988 p 85-86 (For primary document see N89-21287 14-42)
Avail: NTIS HC A11/MF A01 CSCL 13B

The discovery of iridium enrichment at the Cretaceous/Tertiary boundary resulted in formulation of hypothesis of a cometary or asteroid impact as the cause of the biological extinctions at this boundary. Subsequent discoveries of geochemical anomalies at major stratigraphic boundaries like the Precambrian/Cambrian, Permian/Triassic, Middle/Late Jurassic, resulted in the application of similar extraterrestrial impact theories to explain biological changes at these boundaries. Until recently the major physical evidence, as is the location of the impact crater site, to test the impact induced biological extinction was lacking. The diameter of such a crater would be in the range of 60 to 100 km. The recent discovery of the first impact crater in the ocean provide the first opportunity to test the above theory. The crater, named Montagnais and located on the outer shelf off Nova Scotia, Canada, has a minimum diameter of 42 km, with some evidence to a diameter of more than 60 km. At the Montagnais impact site, micropaleontological analysis of the uppermost 80 m of the fall-back breccia represented by a mixture of pre-impact sediments and basement rocks which fills the crater and of the basal 50 m of post-impact marine sediments which overly the impact deposits, revealed presence of diversified foraminiferal and nannoplankton assemblages. The sediments which are intercalated within the uppermost part of the fall-back breccia, had to be deposited before the meteorite impact. The post-impact deposits were laid down almost immediately after the impact as also supported by the micropaleontological data. In conclusion, micropaleontological studies of sediments from the first submarine impact crater site identified in the ocean did not reveal any mass extinction or significant biological changes at the impact site or in the proximal deep ocean basin. Author

N89-21336*# Yale Univ., New Haven, CT. Dept. of Geology and Geophysics.
PATTERNS OF MEGAFLORAL CHANGE ACROSS THE CRETACEOUS-TERTIARY BOUNDARY IN THE NORTHERN GREAT PLAINS AND ROCKY MOUNTAINS Abstract Only **c46**
Kirk R. Johnson and Leo J. Hickey *In* Lunar and Planetary Inst., Global Catastrophes in Earth History: An Interdisciplinary Conference on Impacts, Volcanism, and Mass Mortality 1988 p 87 (For primary document see N89-21287 14-42)
Avail: NTIS HC A11/MF A01 CSCL 08G

The spatial and temporal distribution of vegetation in the terminal Cretaceous of Western Interior North America was a complex mosaic resulting from the interaction of factors including a shifting coastline, tectonic activity, a mild, possibly deteriorating climate, dinosaur herbivory, local facies effects, and a hypothesized bolide impact. In order to achieve sufficient resolution to analyze this vegetational pattern, over 100 megafloral collecting sites were established, yielding approximately 15,000 specimens, in Upper Cretaceous and lower Paleocene strata in the Williston, Powder River, and Bighorn basins in North Dakota, Montana, and Wyoming. These localities were integrated into a lithostratigraphic framework that is based on detailed local reference sections and constrained by vertebrate and palynomorph biostratigraphy, magnetostratigraphy, and sedimentary facies analysis. A regional biostratigraphy based on well located and identified plant megafossils that can be used to address patterns of floral evolution, ecology, and extinction is the goal of this research. Results of the analyses are discussed. Author

N89-21337*# Princeton Univ., NJ. Dept. of Geological and Geophysical Sciences.
EXTENDED PERIOD OF K/T BOUNDARY MASS EXTINCTION IN THE MARINE REALM **c46**
G. Keller *In* Lunar and Planetary Inst., Global Catastrophes in Earth History: An Interdisciplinary Conference on Impacts, Volcanism, and Mass Mortality 1988 p 88-89 (For primary document see N89-21287 14-42)
Avail: NTIS HC A11/MF A01 CSCL 08G

The Cretaceous/Tertiary (K/T) boundary mass extinction has been widely recognized as a nearly instantaneous catastrophy among marine plankton such as foraminifera. However, the suddenness of this extinction event may have been overemphasized because most pelagic K/T boundary sequences are stratigraphically incomplete and generally lack the earliest Tertiary (Zones P0 and P1a) either due to carbonate dissolution and/or non-deposition. Stratigraphically complete sections appear to be restricted to continental shelf regions with high sedimentation rates and deposition well above the CCD. Such sections have been recovered from El Kef, Tunisia (1) and Brazos River, Texas. Quantitative foraminiferal analysis of these sections indicate an extinction pattern beginning below the K/T boundary and ending above the boundary. These data imply that the mass extinction event was not geologically instantaneous, but occurred over an extended period of time. Evidence supporting this conclusion is discussed. Author

N89-21338*# Princeton Univ., NJ. Dept. of Geological and Geophysical Sciences.
FAUNAL AND EROSIONAL EVENTS IN THE EASTERN TETHYAN SEA ACROSS THE K/T BOUNDARY **c46**
G. Keller and C. Benjamini *In* Lunar and Planetary Inst., Global Catastrophes in Earth History: An Interdisciplinary Conference on

Impacts, Volcanism, and Mass Mortality 1988 p 90-91 Prepared in cooperation with Ben Gurion Univ. of the Negev, Beer Sheva (Israel) (For primary document see N89-21287 14-42)
Avail: NTIS HC A11/MF A01 CSCL 08G

A regional pattern of three closely spaced erosional events at and above the K/T boundary was determined from six Cretaceous/Tertiary boundary sections in the Negev of Israel. The sections were collected from locations throughout the central and northern Negev. All sections are lithologically similar. The Maastrichtian consists of a sequence of limestone beds intercalated with thin marly beds. In some sections, the last limestone bed is followed by 1 to 2 m of calcareous marls grading upwards into several meters of grey shale. In other sections the limestone bed is followed directly by grey shale with the contact containing particles of limestone and marl. A 5 to 20 cm thick dark grey organic-rich clay layer is present about 1.5 to 2.5 m above the base of the grey shale. The grey shale grades upwards into increasingly carbonate rich marls. No unconformities are apparent in field outcrops. During field collection the dark grey clay layer was believed to represent the K/T boundary clay. Microfossil analysis however identified the boundary at the base of the grey shale. The black shale represents a low productivity anoxic event similar to, but younger than, the K/T boundary clay in other K/T boundary sections. High resolution planktic foraminiferal and carbonate analysis of these sections (at 5 to 10 cm intervals) yield surprising results. The K/T boundary is marked by an erosional event which removed part or all of the uppermost Maastrichtian marls above the last limestone bed. Percent carbonate data for four Negev sections are illustrated and show the regional similarities in carbonate sedimentation. Faunal and carbonate data from the Negev sections thus show three closely spaced short erosional events at the K/T boundary and within the first 50,000 to 100,000 years of the Danian. These K/T boundary erosional events may represent global climatic or paleoceanographic events. Author

N89-21339*# National Center for Atmospheric Research, Boulder, CO.
WIDESPREAD HABITAT CHANGE THROUGH PALUDIFICATION AS AN INTERACTIVE MECHANISM IN MASS EXTINCTION EVENTS Abstract Only **c45**
L. F. Klinger *In* Lunar and Planetary Inst., Global Catastrophes in Earth History: An Interdisciplinary Conference on Impacts, Volcanism, and Mass Mortality 1988 p 92 (For primary document see N89-21287 14-42)
Avail: NTIS HC A11/MF A01 CSCL 13B

The study of mass extinction events has largely focused on defining an environmental factor or factors that might account for specific patterns of faunal demise. Several hypotheses elaborate on how a given environmental factor might affect fauna directly, but differentially, causing extinction in certain taxa but not others. Yet few studies have considered specific habitat changes that might result from natural vegetation processes or from perturbations of vegetation. The role of large-scale habitat change induced by natural successional change from forest to bog (paludification) is examined and how large perturbations (e.g., volcanism, bolide impacts) might favor increased rates of paludification and consequent mass extinctions is considered. This hypothesis has an advantage over other hypotheses for mass extinctions in that modern day analogs of paludification are common throughout the world, thus allowing for considerable testing. Author

N89-21340*# Lunar and Planetary Inst., Houston, TX.
VOLCANIC ASH LAYERS IN BLUE ICE FIELDS (BEARDMORE GLACIER AREA, ANTARCTICA): IRIDIUM ENRICHMENTS **c46**
Christian Koeberl *In its* Global Catastrophes in Earth History: An Interdisciplinary Conference on Impacts, Volcanism, and Mass Mortality 1988 p 93-94 Prepared in cooperation with Technische Univ., Vienna (Austria) (For primary document see N89-21287 14-42)
Avail: NTIS HC A11/MF A01 CSCL 08G

Dust bands on blue ice fields in Antarctica have been studied and have been identified to originate from two main sources: bedrock debris scraped up from the ground by the glacial movement (these bands are found predominantly at fractures and shear zones in the ice near moraines), and volcanic debris deposited on and incorporated in the ice by large-scale eruptions of Antarctic (or sub-Antractic) volcanoes. Ice core studies have revealed that most of the dust layers in the ice cores are volcanic (tephra) deposits which may be related to some specific volcanic eruptions. These eruptions have to be related to some specific volcanic eruptions. These eruptions have to be relatively recent (a few thousand years old) since ice cores usually incorporate younger ice. In contrast, dust bands on bare blue ice fields are much older, up to a few hundred thousand years, which may be inferred from the rather high terrestrial age of meteorites found on the ice and from dating the ice using the uranium series method. Also for the volcanic ash layers found on blue ice fields correlations between some specific volcanoes (late Cenozoic) and the volcanic debris have been inferred, mainly using chemical arguments. During a recent field expedition samples of several dust bands found on blue ice fields at the Lewis Cliff Ice Tongue were taken. These dust band samples were divided for age determination using the uranium series method, and chemical investigations to determine the source and origin of the dust bands. The investigations have shown that most of the dust bands found at the Ice Tongue are of volcanic origin and, for chemical and petrological reasons, may be correlated with Cenozoic volcanoes in the Melbourne volcanic province, Northern Victoria Land, which is at least 1500 km away. Major and trace element data have been obtained and have been used for identification and correlation purposes. Recently, some additional trace elements were determined in some of the dust band samples, including Ir. Iridium determinations were made using INAA, with synthetical and natural (meteorite) standards. These findings are discussed. Author

N89-21341*# Lunar and Planetary Inst., Houston, TX.
THE KARA AND UST-KARA IMPACT STRUCTURES (USSR) AND THEIR RELEVANCE TO THE K/T BOUNDARY EVENT **c46**
Christian Koeberl, M. A. Nazarov, T. M. Harrison, V. L. Sharpton, A. V. Murali, and K. Burke *In its* Global Catastrophes in Earth History: An Interdisciplinary Conference on Impacts, Volcanism, and Mass Mortality 1988 p 95-96 Prepared in cooperation with Technische Univ., Vienna (Austria; Academy of Sciences (USSR), Moscow; and State Univ. of New York, Albany (For primary document see N89-21287 14-42)
Avail: NTIS HC A11/MF A01 CSCL 08G

The Kara and Ust-Kara craters are twin impact structures situated at about 69 deg 10 min N; 65 deg 00 min E at the Kara Sea. For Kara a diameter of about 55 km would be a very conservative estimate, and field observations indicate a maximum current diameter of about 60 km. The diameter of Ust-Kara has to be larger than 16 km. A better estimate might be 25 km but in all likelihood it is even larger. Suevites and impactites from the Kara area have been known since the beginning of the century, but had been misidentified as glacial deposits. Only about 15 years ago the impact origin of the two structures was demonstrated, following the recognition of shock metamorphism in the area. The composition of the target rocks is mirrored by the composition of the clasts within the suevites. In the southern part of Kara, Permian shales and limestones are sometimes accompanied by diabasic dykes, similar to in the central uplift. Due to the high degree of shock metamorphism the shocked magmatic rocks are not easily identified, although most of them seem to be of diabasic or dioritic composition. The impact melts (tagamites) are grey to dark grey fine grained crystallized rocks showing very fine mineral components and are the product of shock-melting with later recrystallization. The impact glasses show a layered structure, inclusions, and vesicles, and have colors ranging from translucent white over brown and grey to black. A complete geochemical characterization of the Kara and Ust-Kara impact craters was attempted by analyzing more than 40 samples of target rocks, shocked rocks, suevites, impact melts, and impact glasses for major and trace elements. Author

N89-21342*# Moscow State Univ. (USSR). Geology Faculty.
ISOTOPIC INVESTIGATIONS IN THE AREA OF THE TUNGUSKA CATASTROPHE IN 1908 YEAR **c46**
E. M. Kolesnikov *In* Lunar and Planetary Inst., Global Catastrophes in Earth History: An Interdisciplinary Conference on Impacts, Volcanism, and Mass Mortality 1988 p 97-98 (For primary document see N89-21287 14-42)
Avail: NTIS HC A11/MF A01 CSCL 08G

The hypotheses of the annihilation and thermonuclear character of the Tunguska explosion have been tested by measuring inductive Ar-39 radioactivity from K and Ca in rocks and soil under the explosion epicentrum. Ar-39 was not detected though its estimated radioactivity was expected to be 100 times higher than the radio-metrical plant sensitivity. These results testify against the nuclear nature of the Tunguska explosion. The contents of 11 elements in the ultrasmall quantity of matter of the silicate microspherules isolated from catastrophe peat layer at the explosion site were measured by method of neutron activation analysis. It was demonstrated that the enrichment of microspherules by light and volatile elements (Al, Na, Zn, Cs) and the impoverishment by more heavy and hard volatile ones (Fe, Co, Sc). It was shown that the microspherules were not the product of differentiation of the terrestrial soil or of an ordinary meteorite material. It was demonstrated that Pb isotopic content in catastrophe peat layer had more Pb-204, Pb-207, Pb-208 than Pb-206 as compared with Pb isotopic content of other peat layers and common Pb in this area. In the peat column taken at the Ostraya hill area in three nearcatastrophe layers, small increases of isotopic C-13 was determined. Isotopic C effect in the peat layer is confirmed also for the North peatbog. Observed isotopic changes are not accounted for by climatic changes or other physico-chemical reasons. They seem to be related to preservation in the peat of matter resembling carbonaceous chrondrites of the CI type or more probably of cometary matter enriched much more in volatile elements. Author

N89-21343*# Moscow State Univ. (USSR).
THE KARSKIY CRATERS ARE THE PROBABLE RECORDS OF CATASTROPHE AT THE CRETACEOUS-TERTIARY BOUNDARY **c46**
E. M. Kolesnikov, M. A. Nazarov, D. D. Badjukov, and Yu. A. Shukolyukov *In* Lunar and Planetary Inst., Global Catastrophes in Earth History: An Interdisciplinary Conference on Impacts, Volcanism, and Mass Mortality 1988 p 99-10 Prepared in cooperation with Academy of Sciences (USSR), Moscow (For primary document see N89-21287 14-42)
Avail: NTIS HC A11/MF A01 CSCL 08G

In order to corroborate the hypothesis of Alvarez and others about the connection of mass mortality and meteorite or cometary impact at the Cretaceous-Tertiary boundary, it is necessary to find a meteorite crater which was formed at the same time. Masaitiss suggested that the Karskiy craters (USSR) are suitable, but previous K/Ar data from other laboratories are very different (from 47 to 82 million years). Impact glasses were gathered from the Karskiy and Ust-Karskiy craters K/Ar age analyses were performed. The glasses cooled very rapidly and had the youngest model ages from 65.8 to 67.6 million years. The slower cooling crypto-crystalline aggregates had more ancient model ages, from 70.5 to 73.9 my as had tagamite because they captured excess argon during crystallization. Least squares analysis showed that with probability of 99 percent the findings on crypto-crystalline aggregates, tagamite and quartz glasses from the Karskiy and Ust-Karskiy craters lie on an isochron which has an age of 65.8 + or - 1.1 million years and a content of excess argon. For the two glasses with identical composition which have different quantities of secondary non-potassium minerals, an independent method determined the content of excess argon. Taking into account these data a more exact slope of the first isochron of 66.4 + or - 1.0 million years was observed and the second glass isochron with age 66.5 + or - 1.1 million years was constructed. Author

N89-21344*# California Univ., Los Angeles. Inst. of Geophysics and Planetary Physics.
ACCRETION RATE OF EXTRATERRESTRIAL MATTER: IRIDIUM DEPOSITED OVER THE LAST 70 MILLION YEARS **c46**
Frank T. Kyte *In* Lunar and Planetary Inst., Global Catastrophes in Earth History: An Interdisciplinary Conference on Impacts, Volcanism, and Mass Mortality 1988 p 101 (For primary document see N89-21287 14-42)
Avail: NTIS HC A11/MF A01 CSCL 08G

In order to quantify the accretion rate of extraterrestrial matter during the Cenozoic, Ir concentrations were measured in a continuous series of 450 samples across most of the length of piston core LL44-GPC3. LL44-GPC3 is a 25-meter-long, large-diameter piston core of abyssal clay from the central North Pacific. This core contains a nearly continuous record of sedimentation over the last 70 Ma, as this site migrated from a region near the Equator in the late Cretaceous to its present position north of Hawaii. The first-cut survey across the core is nearing completion, and all of the conclusions of the earlier study, in which was reported the concentrations of Ir, Co, and Sb across 9 meters of this core, remain unchanged. The only strongly enhanced Ir concentrations occur at the Cretaceous-Tertiary (K-T) boundary and outside the K-T boundary Ir correlates well with Co, a terrestrial element which is largely present in hydrogenous ferromanganese oxide precipitates from seawater. Concentrations of both elements appear to be inversely correlated with the sedimentation rate. Although the K-T Ir anomaly is unique in magnitude in this core, there are several small bumps in the Ir profile which may reflect smaller accretionary events. The most promising Ir enhancement was observed in a 30 cm section approximately 1 m below the K-T boundary. Preliminary data suggest deposition of an excess across this interval at a time estimate to be approximate 1 Ma before the K-T impact event, but there is insufficient evidence at present to prove that this reflects enhanced accretion of extraterrestrial matter. A detailed model is being prepared of the chemical record of sedimentation in this core using a combined database of 39 elements in approximately 450 samples across the Cenozoic. Preliminary working model indicates that the only sedimentary sources which contribute significantly to the Ir budget in this core are the hydrogenous precipitates and extraterrestrial particulates. Author

N89-21345*# Basque Univ., Lejona (Spain).
THE CRETACEOUS-TERTIARY BOUNDARY BIOTIC CRISIS IN THE BASQUE COUNTRY **c46**
M. A. Lamolda *In* Lunar and Planetary Inst., Global Catastrophes in Earth History: An Interdisciplinary Conference on Impacts, Volcanism, and Mass Mortality 1988 p 102-103 (For primary document see N89-21287 14-42)
Avail: NTIS HC A11/MF A01 CSCL 08G

The Zumaya section has been selected as a classic locality for the study of the Cretaceous-Tertiary (K-T) boundary due to its richness in microfaune, macrofaune, and nannoflora. The sections present similar good conditions for the study of the K-T boundary. The sedimentary rocks of the Uppermost Maastrichtian from the Basque Country are purple or pink marls and marls-tones. Above it is found a clayed bed, 40 to 29 cm thick, grey or dark grey in its basal part, of Lowermost Danian age. Above there is alternation of micritic grey-pink limestones and thin clay beds of Dano-Montian age. The average sedimentation is 7 to 8 times higher during the Upper Maastrichtian than in the Dano-Montian. The macrofauna underwent a decrease since the Campanian and was not found in the last 11 m of the Zumaya section; it was associated with changes in paleoceanographic conditions and primary productivity of the oceans. The microfossil assemblages in the K-T transition allows the recognition of several phases of a complex crisis between two well established planktonic ecosystems. In the Mayaroensis Zone there is a stable ecosystem with 45 to 47 planktonic foraminifera species. The disappearance of A. mayaroensis starts a degradation of the ecosystem. The number of planktonic foraminiera species decreases between 20 and 45 percent. The next phase of the crisis was the result of main

extinction events in the planktonic calcareous ecosystem. There are several cretaceous planktonic foraminifera species, probably reworked, whose numbers decrease upward. The next and last phase of the biotic crisis shows a diversification of the ecosystem; the number of planktonic foraminifera is 2 to 3 times higher than before and it is noted the first appearance of Tertiary nannoflora species, while Cretaceous species decrease and persisting species are still the main ones. Author

N89-21346*# Geological Survey, Denver, CO.
CATASTROPHIC VOLCANISM c46
Peter W. Lipman *In* Lunar and Planetary Inst., Global Catastrophes in Earth History: An Interdisciplinary Conference on Impacts, Volcanism, and Mass Mortality 1988 p 104-105 (For primary document see N89-21287 14-42)
Avail: NTIS HC A11/MF A01 CSCL 08G

Since primitive times, catastrophes due to volcanic activity have been vivid in the mind of man, who knew that his activities in many parts of the world were threatened by lava flows, mudflows, and ash falls. Within the present century, increasingly complex interactions between volcanism and the environment, on scales not previously experienced historically, have been detected or suspected from geologic observations. These include enormous hot pyroclastic flows associated with collapse at source calderas and fed by eruption columns that reached the stratosphere, relations between huge flood basalt eruptions at hotspots and the rifting of continents, devastating laterally-directed volcanic blasts and pyroclastic surges, great volcanic-generated tsunamis, climate modification from volcanic release of ash and sulfur aerosols into the upper atmosphere, modification of ocean circulation by volcanic constructs and attendent climatic implications, global pulsations in intensity of volcanic activity, and perhaps triggering of some intense terrestrial volcanism by planetary impacts. Complex feedback between volcanic activity and additional seemingly unrelated terrestrial processes likely remains unrecognized. Only recently has it become possible to begin to evaluate the degree to which such large-scale volcanic processes may have been important in triggering or modulating the tempo of faunal extinctions and other evolutionary events. In this overview, such processes are examined from the viewpoint of a field volcanologist, rather than as a previous participant in controversies concerning the interrelations between extinctions, impacts, and volcanism. Author

N89-21347*# Florida State Univ., Tallahassee. Geophysical Fluid Dynamics Inst.
CATASTROPHIC VOLCANISM AS A CAUSE OF SHOCKED FEATURES FOUND AT THE K/T BOUNDARY AND IN CRYPTOEXPLOSION STRUCTURES c46
D. E. Loper and K. McCartney *In* Lunar and Planetary Inst., Global Catastrophes in Earth History: An Interdisciplinary Conference on Impacts, Volcanism, and Mass Mortality 1988 p 106-107 (For primary document see N89-21287 14-42)
Avail: NTIS HC A11/MF A01 CSCL 08G

The presence of quartz grains containing shock lamellae at the Cretaceous/Tertiary (K/T) boundary is viewed by many as the single most compelling evidence of meteoritic or cometary impact because there is no known endogenous mechanism for producing these features. Similarly the presence of shocked quartz, shatter cones, coesite and stishovite at cryptoexplosion structures is comonly taken as conclusive evidence of impact. However, several recent studies have cast doubt on this interpretation. It is argued that basaltic volcanism, although not normally explosive, can under exceptional circumstances produce overpressures sufficiently high to produce shock features. The exceptional circumstances include a high content of volatiles, usually CO_2, and no preestablished pathway to the surface. Rapid cooling of the saturated basaltic magma can occur if it underlies a cooler more evolved magma in a chamber. Initial slow cooling and partial exsolution of the volatiles will cause the density of the basaltic magma to become less than that of the overlying magma, leading to overturning and mixing. Gas will escape the magma chamber along planar cracks once the pressure becomes sufficiently high. In the vicinity of the crack tip there is a smallscale deviatoric stress pattern which is thought to be sufficiently high to produce transient cracks along secondary axes in the quartz crystals, causing the planar features. The CO_2-rich fluid inclusions which have been found along planar elements of quartz in basement rocks of the Vredefort Dome were likely to have been emplaced by such a process. If the mechanism described is capable of producing shocked features as above, it would require a reassessment of the origin of many cryptoexplosion structures as well as seriously weakening the case for an impact origin of the K/T event. Author

N89-21348*# Stanford Univ., CA.
EVIDENCE FOR AND IMPLICATIONS OF AN EARLY ARCHEAN TERRESTRIAL IMPACT RECORD c46
Donald R. Lowe and Gary R. Byerly *In* Lunar and Planetary Inst., Global Catastrophes in Earth History: An Interdisciplinary Conference on Impacts, Volcanism, and Mass Mortality 1988 p 108 Prepared in cooperation with Louisiana State Univ., Baton Rouge (For primary document see N89-21287 14-42)
Avail: NTIS HC A11/MF A01 CSCL 08G

Early Archean, 3.5 to 3.2 Ga, greenstone sequences in South Africa and Western Australia contain a well-preserved record of early terrestrial meteorite impacts. The main impact-produced deposits are layers, 10 cm to over 1 m thick, composed largely of sand-sized spherules, 0.1 to 4 mm in diameter. The beds studied to date show an assemblage of features indicating formation by the fall of debris from impact-generated ejecta clouds. Some presented data effectively rule out normal magmatic or sedimentary processes in the origin of these units and provide substantial support for an origin by large impacts on the early earth. The presence of at least four, remarkably thick, nearly pure spherule layers suggests that smaller-scale impact deposits may be even more abundant in these sequences. The existence of a well-preserved Archean terrestrial impact record suggests that a direct source of evidence is available regarding a number of important aspects of early earth history. Author

N89-21349*# Pennsylvania Univ., Philadelphia. Dept. of Geology.
MAGNETIC REVERSAL SPURTS: RAIN GAUGES FOR COMET SHOWERS c46
T. M. Lutz *In* Lunar and Planetary Inst., Global Catastrophes in Earth History: An Interdisciplinary Conference on Impacts, Volcanism, and Mass Mortality 1988 p 109-110 (For primary document see N89-21287 14-42)
Avail: NTIS HC A11/MF A01 CSCL 08G

Abrupt increases in the rate of magnetic reversals (magnetic reversal spurts) were first studied by many others. They hypothesized that spurts result from increased turbulence in the earth's core dynamo during episodes of intense bolide bombardment of the earth. Mechanisms for creating episodes of intense bombardment of the earth involve gravitational perturbation of the Oort cloud of comets, either by a hidden planet, a solar companion, or massive matter in the galactic plane. Herein, the time variation in reversal rate is analyzed using methods of statistical density estimation. A smooth, continuous estimate of reversal rate is obtained using an adaptive kernel method, in which the kernel width is adjusted as a function of reversal rate. The estimates near the ends of the data series (at 165 my ago and the present) are obtained by extending the data by reflection. The results show that the reversal spurts are not associated demonstrably with extinctions or well-dated impacts. If the spurts do record episodes of intense bombardment of the earth, then the mass extinctions do not, in general, occur at times of impacts. Furthermore, the large impact craters seen are not obviously related to the spurts, suggesting that the craters may have been caused by bolides of a different nature and with a different temporal pattern. However, the most simple explanation seems to be that the spurts do not record comet showers, either because the recording mechanism suggested by Muller and Morris is not effective or because comet showers are not triggered in the ways considered by Hut et al. Author

N89-21350*# Scripps Institution of Oceanography, La Jolla, CA.
SEAWATER STRONTIUM ISOTOPES AT THE CRETACEOUS-TERTIARY BOUNDARY **c48**
J. D. Macdougall and E. Martin *In* Lunar and Planetary Inst., Global Catastrophes in Earth History: An Interdisciplinary Conference on Impacts, Volcanism, and Mass Mortality 1988 p 111 (For primary document see N89-21287 14-42)
Avail: NTIS HC A11/MF A01 CSCL 08C

Anomalously high values of Seawater Sr-87/Sr-86 near the Cretaceous-Tertiary (K-T) boundary have been reported. However, few of the data from the literature are from a single continuous section, and perhaps the most complete study of the boundary region, from a shallow marine limestone sequence in Alabama, showed elevated Sr-87/Sr-86 but no pronounced spike. Thus, in order to investigate the cause of the change in strontium isotopic composition, it is important to determine the exact nature and magnitude of the increase by studying in detail continuous sections through the boundary. If there is indeed a Sr isotope spike at the K-T boundary, it requires the addition of a large amount of radiogenic Sr to the oceans over a short time period, a phenomenon that may be linked to other large-scale environmental disturbances which occurred at that time. In order to address this question, a high-resolution strontium isotope study of foraminifera from three Deep Sea Drilling Project (DSDP) cores which recovered the K-T boundary section: Site 356 in the South Atlantic, Site 384 in the North Atlantic and Site 577 from the Shatsky Rise in the Pacific was initiated. The isotope measurements are being made on either single or small numbers of forams carefully picked and identified and in most cases examined by SEM before analysis. Because this work is not yet complete, conclusions drawn here must be viewed as tentative. They are briefly discussed. Author

N89-21351*# Michigan Univ., Ann Arbor. Dept. of Geological Sciences and Museum of Paleontology.
INDUCEMENT OF HETEROCHRONIC VARIATION IN A SPECIES OF PLANKTIC FORAMINIFERA BY A LATE EOCENE IMPACT EVENT **c46**
N. MacLeod and J. A. Kitchell *In* Lunar and Planetary Inst., Global Catastrophes in Earth History: An Interdisciplinary Conference on Impacts, Volcanism, and Mass Mortality 1988 p 112 (For primary document see N89-21287 14-42)
Avail: NTIS HC A11/MF A01 CSCL 08G

While it is well known that the cosmic impact event at or near the Cretaceous-Tertiary boundary coincides with an interval of mass extinction, a similar impact (or series of impacts) near the Eocene-Oligocene boundary presents a more complex picture, in terms of associated fluctuations in marine biotic diversity. Tektites, microtektites, and mineral grains exhibiting features of shock metamorphism found in Eocene sediments of the western N. Atlantic, Caribbean, and Gulf of Mexico (comprising the North American microtektite strewn field) offer compelling evidence for a catastrophic impact event. Despite the magnitude of this event, however, few extinctions in the planktic marine fauna are known to have occurred coincident with this event. Instead, changes in relative abundance, morphology, and development occurred. Cosmic impacts generally have been interpreted as influencing the course of evolution through the wholesale elimination of significant portions of standing biotic diversity. Indeed, extinction traditionally has been viewed as the negative side of evolution. In some instances, it is suggested such impact events can serve instead to increase, rather than decrease, morphological and ecological diversity, by altering the developmental programs within species at the level of the local population. Author

N89-21352*# California Univ., Davis. Dept. of Geology.
TRACE ELEMENT AND ISOTOPE GEOCHEMISTRY OF CRETACEOUS-TERTIARY BOUNDARY SEDIMENTS: IDENTIFICATION OF EXTRA-TERRESTRIAL AND VOLCANIC COMPONENTS **c46**
S. V. Margolis and E. F. Doehne *In* Lunar and Planetary Inst., Global Catastrophes in Earth History: An Interdisciplinary Conference on Impacts, Volcanism, and Mass Mortality 1988 p 113-114 (For primary document see N89-21287 14-42)
Avail: NTIS HC A11/MF A01 CSCL 08G

Trace element and stable isotope analyses were performed on a series of sediment samples crossing the Cretaceous-Tertiary (K-T) boundary from critical sections at Aumaya and Sopelano, Spain. The aim is to possibly distinguish extraterrestrial vs. volcanic or authigenic concentration of platinum group and other elements in K-T boundary transitional sediments. These sediments also have been shown to contain evidence for step-wise extinction of several groups of marine invertebrates, associated with negative oxygen and carbon isotope excursions occurring during the last million years of the Cretaceous. These isotope excursions have been interpreted to indicate major changes in ocean thermal regime, circulation, and ecosystems that may be related to multiple events during latest Cretaceous time. Results to date on the petrographic and geochemical analyses of the Late Cretaceous and Early Paleocene sediments indicate that diagenesis has obviously affected the trace element geochemistry and stable isotope compositions at Zumaya. Mineralogical and geochemical analysis of K-T boundary sediments at Zumaya suggest that a substantial fraction of anomalous trace elements in the boundary marl are present in specific mineral phases. Platinum and nickel grains perhaps represent the first direct evidence of siderophile-rich minerals at the boundary. The presence of spinels and Ni-rich particles as inclusions in aluminosilicate spherules from Zumaya suggests an original, non-diagenetic origin for the spherules. Similar spherules from southern Spain (Caravaca), show a strong marine authigenic overprint. This research represents a new approach in trying to directly identify the sedimentary mineral components that are responsible for the trace element concentrations associated with the K-T boundary. Author

N89-21353*# Harvard-Smithsonian Center for Astrophysics, Cambridge, MA.
IMPACT, AND ITS IMPLICATIONS FOR GEOLOGY **c46**
Ursula B. Marvin *In* Lunar and Planetary Inst., Global Catastrophes in Earth History: An Interdisciplinary Conference on Impacts, Volcanism, and Mass Mortality 1988 p 115-116 (For primary document see N89-21287 14-42)
Avail: NTIS HC A11/MF A01 CSCL 08G

The publication of seminal texts on geology and on meteoritics in the 1790s, laid the groundwork for the emergence of each discipline as a modern branch of science. Within the past three decades, impact cratering has become universally accepted as a process that sculptures the surfaces of planets and satellites throughout the solar system. Nevertheless, one finds in-depth discussions of impact processes mainly in books on the Moon or in surveys of the Solar System. The historical source of the separation between meteoritics and geology is easy to identify. It began with Hutton. Meteorite impact is an extraordinary event acting instantaneously from outside the Earth. It violates Hutton's principles, which were enlarged upon and firmly established as fundamental to the geological sciences by Lyell. The split between meteoritics and geology surely would have healed as early as 1892 if the investigations conducted by Gilbert (1843-1918) at the crater in northern Arizona had yielded convincing evidence of meteorite impact. The 1950s and 1960s saw a burgeoning of interest in impact processes. The same period witnessed the so-called revolution in the Earth Sciences, when geologists yielded up the idea of fixed continents and began to view the Earth's lithosphere as a dynamic array of horizontally moving plates. Plate tectonics, however, is fully consistent with the geological concepts inherited from Hutton: the plates slowly split, slide, and suture, driven by forces intrinsic to the globe. Author

N89-21354*# Florida International Univ., Miami. Dept. of Geology.
STEP-WISE EXTINCTIONS AT THE CRETACEOUS-TERTIARY BOUNDARY AND THEIR CLIMATIC IMPLICATIONS **c51**
Florentin J-M. R. Maurrasse *In* Lunar and Planetary Inst., Global Catastrophes in Earth History: An Interdisciplinary Conference on Impacts, Volcanism, and Mass Mortality 1988 p 117 (For

primary document see N89-21287 14-42)
Avail: NTIS HC A11/MF A01 CSCL 06B

A comparative study of planktonic foraminifera and radiolarian assemblages from the Cretaceous-Tertiary (K-T) boundary section of the Beloc Formation in the southern Peninsula of Haiti, and the lowermost Danian sequence of the Micara Formation in southern Cuba reveals a remarkable pattern of step-wise extinctions. This pattern is consistent in both places despite the widely different lithologies of the two formations. Because of a step-wise extinction and the delayed disappearance of taxa known to be more representative of cooler water realms, it is inferred that a cooling trend which characterized the close of the Maastrichtian and the onset of the Tertiary had the major adverse effect on the existing biota. Although repetitive lithologic and faunal fluctuations throughout the Maastrichtian sediments found at Deep Sea Drilling Project (DSDP) site 146/149 in the Caribbean Sea indicate variations reminiscent of known climatically induced cycles in the Cenozoic, rapid biotic succession appears to have taken place during a crisis period of a duration greater than 2 mission years. Widespread and abundant volcanic activities recorded in the Caribbean area during the crisis period gives further credence to earlier contention that intense volcanism may have played a major role in exhacerbating pre-existing climatic conditions during that time. Author

N89-21355*# Arizona State Univ., Tempe. Dept. of Geology.
SHATTER CONES: DIAGNOSTIC IMPACT SIGNATURES c46
J. F. McHone and R. S. Dietz *In* Lunar and Planetary Inst., Global Catastrophes in Earth History: An Interdisciplinary Conference on Impacts, Volcanism, and Mass Mortality 1988 p 118-119 (For primary document see N89-21287 14-42)
Avail: NTIS HC A11/MF A01 CSCL 08G

Uniquely fractured target rocks known as shatter cones are associated with more than one half the world's 120 or so presently known impact structures. Shatter cones are a form of tensile rock failure in which a positive conical plug separates from a negative outer cup or mold and delicate ornaments radiating from an apex are preserved on surfaces of both portions. Although distinct, shatter cones are sometimes confused with other striated geologic features such as ventifacts, stylolites, cone-in-cone, slickensides, and artificial blast plumes. Complete cones or solitary cones are rare, occurrences are usually as swarms in thoroughly fractured rock. Shatter cones may form in a zone where an expanding shock wave propagating through a target decays to form an elastic wave. Near this transition zone, the expanding primary wave may strike a pebble or other inhomogeneity whose contrasting transmission properties produce a scattered secondary wave. Interference between primary and secondary scattered waves produce conical stress fields with axes perpendicular to the plane of an advancing shock front. This model supports mechanism capable of producing such shatter cone properties as orientation, apical clasts, lithic dependence, and shock pressure zonation. Although formational mechanics are still poorly understood, shatter cones have become the simplest geologic field criterion for recognizing astroblemes (ancient terrestrial impact structures).
Author

N89-21356*# Ottawa Univ. (Ontario). Dept. of Geology.
MASS KILLINGS AND DETECTION OF IMPACTS Abstract Only c46
Digby J. McLaren *In* Lunar and Planetary Inst., Global Catastrophes in Earth History: An Interdisciplinary Conference on Impacts, Volcanism, and Mass Mortality 1988 p 120 (For primary document see N89-21287 14-42)
Avail: NTIS HC A11/MF A01 CSCL 08G

Highly energetic bolide impacts occur and their flux is known. For larger bodies the energy release is greater than for any other short-term global phenomenon. Such impacts produce or release a large variety of shock induced changes including major atmospheric, sedimentologic, seismic and volcanic events. These events must necessarily leave a variety of records in the stratigraphic column, including mass killings resulting in major changes in population density and reduction or extinction of many taxonomic groups, followed by characteristic patterns of faunal and flora replacement. Of these effects, mass killings, marked by large-scale loss of biomass, are the most easily detected evidence in the field but must be manifest on a near-global scale. Such mass killings that appear to be approximately synchronous and involve disappearance of biomass at a bedding plane in many sedimentologically independent sections globally suggest a common cause and probable synchroneity. Mass killings identify an horizon which may be examined for evidence of cause. Geochemical markers may be ephemeral and absence may not be significant. There appears to be no reason why ongoing phenomena such as climate and sea-level changes are primary causes of anomolous episodic events. Author

N89-21357*# Virginia Polytechnic Inst. and State Univ., Blacksburg. Dept. of Geological Sciences.
EARTH ORBITAL VARIATIONS AND VERTEBRATE BIOEVOLUTION c51
Dewey M. McLean *In* Lunar and Planetary Inst., Global Catastrophes in Earth History: An Interdisciplinary Conference on Impacts, Volcanism, and Mass Mortality 1988 p 121 (For primary document see N89-21287 14-42)
Avail: NTIS HC A11/MF A01 CSCL 06B

Cause of the Pleistocene-Holocene transition mammalian extinctions at the end of the last age is the subject of debate between those advocating human predation and climate change. Identification of an ambient air temperature (AAT)-uterine blood flow (UBF) coupling phenomenon supports climate change as a factor in the extinctions, and couples the extinctions to earth orbital variations that drive ice age climatology. The AAT-UBF phenomenon couples mammalian bioevolution directly to climate change via effects of environmental heat upon blood flow to the female uterus and damage to developing embryos. Extinctions were in progress during climatic warming before the Younger Dryas event, and after, at times when the AAT-UBF couple would have been operative; however, impact of a sudden short-term cooling on mammals in the process of adapting to smaller size and relatively larger S/V would have been severe. Variations in earth's orbit, and orbital forcing of atmospheric CO_2 concentrations, were causes of the succession of Pleistocene ice ages. Coincidence of mammalian extinctions with terminations of the more intense cold stages links mammalian bioevolution to variations in earth's orbit. Earth orbital variations are a driving source of vertebrate bioevolution. Author

N89-21358*# Geological Survey, Lansing, MI.
THE CALVIN 28 CRYPTOEXPLOSIVE DISTURBANCE, CASS COUNTY, MICHIGAN: EVIDENCE FOR IMPACT ORIGIN c46
Randall L. Milstein *In* Lunar and Planetary Inst., Global Catastrophes in Earth History: An Interdisciplinary Conference on Impacts, Volcanism, and Mass Mortality 1988 p 122-123 (For primary document see N89-21287 14-42)
Avail: NTIS HC A11/MF A01 CSCL 08G

The Calvin 28 cryptoexplosive disturbance is an isolated, nearly circular subsurface structure of Late Ordovician age in southwestern Michigan. The structure is defined by 107 wells, is about 7.24 km in diameter and consists of a central dome, an annular depression and an encircling anticlinal rim. Seismic and geophysical well log data confirm that an intricate system of faults and structural derangement exists within the structure. Deformation decreases with depth and distance from the structure. U.S.G.S. topographic maps and aerial imagery show the structure is reflected as a subtle surface topographic rise controlling local drainage. Igneous or diapiric intrusion and solution collapse are rejected as possible origins for Calvin 28 on the basis of stratigraphic, structural and geophysical evidence. A volcanic origin is inconsistent with calculated energy requirements and an absence of igneous material. Although shock-metamorphic features are unidentified, microbreccias occur in deep wells that penetrate the structure. Morphology and structural parameters support an impact origin.
Author

N89-21359*# Yamaguchi Univ. (Japan). Dept. of Earth Sciences.
MINERALOGICAL AND GEOCHEMICAL ANOMALOUS DATA OF THE K-T BOUNDARY SAMPLES **c46**
Y. Miura, G. Shibya, M. Imai, N. Takaoka, and S. Saito *In* Lunar and Planetary Inst., Global Catastrophes in Earth History: An Interdisciplinary Conference on Impacts, Volcanism, and Mass Mortality 1988 p 124-125 Prepared in cooperation with Yamagata Univ. (Japan). (For primary document see N89-21287 14-42)
Avail: NTIS HC A11/MF A01 CSCL 08G

Cretaceous-Tertiary boundary problem has been discussed previously from the geological research, mainly by fossil changes. Although geochemical bulk data of Ir anomaly suggest the extraterrestrial origin of the K-T boundary, the exact formation process discussed mainly by mineralogical and geochemical study has been started recently, together with noble gas contents. The K-T boundary sample at Kawaruppu River, Hokkaido was collected, in order to compare with the typical K-T boundary samples of Bubbio, Italy, Stevns Klint, Denmark, and El Kef, Tunisia. The experimental data of the silicas and calcites in these K-T boundary samples were obtained from the X-ray unit-cell dimension (i.e., density), ESR signal and total linear absorption coefficient, as well as He and Ne contents. The K-T boundary samples are usually complex mixture of the terrestrial activities after the K-T boundary event. The mineralogical and geochemical anomalous data indicate special terrestrial atmosphere at the K-T boundary formation probably induced by asteroid impact, followed the many various terrestrial activities (especially the strong role of sea-water mixture, compared with terrestrial highland impact and impact craters in the other earth-type planetary bodies). Author

N89-21360*# Princeton Univ., NJ. Dept. of Geological and Geophysical Sciences.
FLOOD BASALTS AND MASS EXTINCTIONS Abstract Only **c46**
W. Jason Morgan *In* Lunar and Planetary Inst., Global Catastrophes in Earth History: An Interdisciplinary Conference on Impacts, Volcanism, and Mass Mortality 1988 p 126 (For primary document see N89-21287 14-42)
Avail: NTIS HC A11/MF A01 CSCL 08G

There appears to be a correlation between the times of flood basalts and mass-extinction events. There is a correlation of flood basalts and hotspot tracks--flood basalts appear to mark the beginning of a new hotspot. Perhaps there is an initial instability in the mantle that bursts forth as a flood basalt but then becomes a steady trickle that persists for many tens of millions of years. Suppose that flood basalts and not impacts cause the environmental changes that lead to mass-extinctions. This is a very testable hypothesis: it predicts that the ages of the flows should agree exactly with the times of extinctions. The Deccan and K-T ages agree with this hypothesis; An iridium anomaly at extinction boundaries apparently can be explained by a scaled-up eruption of the Hawaiian type; the occurrence of shocked-quartz is more of a problem. However if the flood basalts are all well dated and their ages indeed agree with extinction times, then surely some mechanism to appropriately produce shocked-quartz will be found. Author

N89-21361*# California Univ., Berkeley. Dept. of Physics
ASTROPHYSICAL IMPLICATIONS OF PERIODICITY Abstract Only **c46**
Richard A. Muller *In* Lunar and Planetary Inst., Global Catastrophes in Earth History: An Interdisciplinary Conference on Impacts, Volcanism, and Mass Mortality 1988 p 127 Prepared in cooperation with California Univ., Berkeley, Lawrence Berkeley Laboratory (For primary document see N89-21287 14-42)
Avail: NTIS HC A11/MF A01 CSCL 08G

Two remarkable discoveries of the last decade have profound implications for astrophysics and for geophysics. These are the discovery by Alvarez et al., that certain mass extinctions are caused by the impact on the earth of a large asteroid or comet, and the discovery by Raup and Sepkoski that such extinctions are periodic, with a cycle time of 26 to 30 million years. The validity of both of these discoveries is assumed and the implications are examined. Most of the phenomena described depend not on periodicity, but just on the weaker assumption that the impacts on the earth take place primarily in showers. Proposed explanations for the periodicity include galactic oscillations, the Planet X model, and the possibility of Nemesis, a solar companion star. These hypotheses are critically examined. Results of the search for the solar companion are reported. The Deccan flood basalts of India have been proposed as the impact site for the Cretaceous impact, but this hypotheisis is in contradiction with the conclusion of Courtillot et al., that the magma flow began during a period of normal magnetic field. A possible resolution of this contradiction is proposed. Author

N89-21362*# Lunar and Planetary Inst., Houston, TX.
DECCAN VOLCANISM AND K-T BOUNDARY SIGNATURES **c46**
A. V. Murali, B. C. Schuraytz, and P. P. Parekh *In its* Global Catastrophes in Earth History: An Interdisciplinary Conference on Impacts, Volcanism, and Mass Mortality 1988 p 128-129 Prepared in cooperation with New York State Dept. of Health, Albany (For primary document see N89-21287 14-42)
Avail: NTIS HC A11/MF A01 CSCL 08G

The Deccan Traps in the Indian subcontinent represent one of the most extensive flood basalt provinces in the world. These basalts occur mainly as flat-lying, subaerially erupted tholeiitic lava flows, some of which are traceable for distances of more than 100 km. Offshore drilling and geophysical surveys indicate that a part of the Deccan subsided or was downfaulted to the west beneath the Arabian Sea. The presence of 1 to 5 m thick intertrappean sediments deposited by lakes and rivers indicates periods of quiescence between eruptions. The occurrence of numerous red bole beds among the flows suggests intense weathering of flow tops between eruptive intervals. Although the causative relationship of the Cretaceous-Tertiary (K-T) biotic extinctions to Deccan volcanism is debatable, the fact that the main Deccan eruptions straddle the K-T event appears beyond doubt from the recent Ar-40/Ar-39 ages of various Deccan flows. This temporal relationship of the K-T event with Deccan volcanism makes the petrochemical signatures of the entire Deccan sequence (basalt flows, intercalated intertrappean sediments, infratrappean Lameta beds (with dinosaur fossils), and the bole beds) pertinent to studies of the K-T event. The results of ongoing study is presented. Author

N89-21363*# Geological Survey, Denver, CO.
PLANT MICROFOSSIL RECORD OF THE TERMINAL CRETACEOUS EVENT IN THE WESTERN UNITED STATES AND CANADA **c51**
D. J. Nichols and R. F. Fleming *In* Lunar and Planetary Inst., Global Catastrophes in Earth History: An Interdisciplinary Conference on Impacts, Volcanism, and Mass Mortality 1988 p 130-131 (For primary document see N89-21287 14-42)
Avail: NTIS HC A11/MF A01 CSCL 06B

Plant microfossils, principally pollen grains and spores produced by land plants, provide an excellent record of the terminal Cretaceous event in nonmarine environments. The record indicates regional devastation of the latest Cretaceous vegetation with the extinction of many groups, followed by a recolonization of the earliest Tertiary land surface, and development of a permanently changed land flora. The regional variations in depositional environments, plant communities, and paleoclimates provide insight into the nature and effects of the event, which were short-lived but profound. The plant microfossil data support the hypothesis that an abruptly initiated, major ecological crisis occurred at the end of the Cretaceous. Disruption of the Late Cretaceous flora ultimately contributed to the rise of modern vegetation. The plant microfossils together with geochemical and mineralogical data are consistent with an extraterrestrial impact having been the cause of the terminal Cretaceous event. Author

N89-21364*# Dartmouth Coll., Hanover, NH. Dept. of Earth Sciences.

CRETACEOUS-TERTIARY FINDINGS, PARADIGMS AND PROBLEMS Abstract Only **c46**

C. B. Officer and C. L. Drake *In* Lunar and Planetary Inst., Global Catastrophes in Earth History: An Interdisciplinary Conference on Impacts, Volcanism, and Mass Mortality 1988 p 132 (For primary document see N89-21287 14-42)

Avail: NTIS HC A11/MF A01 CSCL 08G

The asteroid hypothesis has stimulated numerous studies of the paleontological record at Cretaceous/Tertiary time as well as of geological indicators of environmental crisis preserved in the rock record. Both extinctions and geological anomalies often occur at times that do not appear to be synchronous or instantaneous. The record includes paleontological indicators of dinosaurs, terrestrial flora, marine planktonic organisms, and shallow water marine macrofauna and geological phenomena include occurrences of iridium and other platinum metals, trace elements, clay mineralogy, shocked minerals, soot, microspherules, and isotopes of osmium, strontium and carbon. These findings are reviewed in the context of the alternate hypotheses of an exogenic cause, involving either a single asteroid impact or multiple commentary impacts, and an endogenic cause, involving intense global volcanism and major sea level regression. Author

N89-21365*# California Inst. of Tech., Pasadena. Seismological Lab.

ENVIRONMENTAL EFFECTS OF LARGE IMPACTS ON THE EARTH; RELATION TO EXTINCTION MECHANISMS **c45**

John D. OKeefe, Thomas J. Ahrens, and Detlef Koschny *In* Lunar and Planetary Inst., Global Catastrophes in Earth History: An Interdisciplinary Conference on Impacts, Volcanism, and Mass Mortality 1988 p 133-134 (For primary document see N89-21287 14-42)

Avail: NTIS HC A11/MF A01 CSCL 13B

Since Alvarez et al., discovered a worldwide approx. cm-thick layer of fine sediments laden with platinum group elements in approximately chondritic proportions exactly at the Cretaceous-Tertiary (C-T) boundary, and proposed bolide-impact as triggering mass extinctions, many have studied this hypothesis and the layer itself with its associated spherules and shocked quartz. At issue is whether the mass extinctions, and this horizon has an impact versus volcanic origin. A critical feature of the Alvarez hypothesis is the suggestion that the bolide or possibly a shower of objects delivered to the earth approx. 0.6 x 10 to the 18th power g of material which resulted in aerosol-sized ejecta such that global insolation was drastically reduced for significant periods. Such an event would lower temperatures on continents and halt photosynthesis in the upper 200 m of th eocean. The latter would strangle the marine food chain and thus produce the major marine faunal extinctions which mark the C-T boundary. Crucial issues examined include: What are the dynamics of atmospheric flow occurring upon impact of a large bolide with the earth; What is the size distributions of the very fine impact ejecta and how do these compare to the models of ejecta which are used to model the earth's radiative thermal balance. The flow field due to passage of a 10 km diameter bolide through an exponential atmosphere and the interaction of the gas flow and bolide with the solid ear was calculated. The CO2 released upon impact onto shallow marine carbonate sections was modeled and found that the mass of CO2 released exceeds the present 10 to the 18th power g CO2 budget of the earth's atmosphere by several times. Using the calculations of Kasting and Toon it was found that to compute the temperature rise of the earth's surface as a function of CO2 content, it was found that sudden and prolonged global increases are induced from impact of 20 to 50 km radius projectiles and propose that sudden terrestrial greenhouse-induced heating, not cooling, produced the highly variable extinctions seen at the C-T boundary. Author

N89-21366*# Lamont-Doherty Geological Observatory, Palisades, NY.

THE TRIASSIC-JURASSIC BOUNDARY IN EASTERN NORTH AMERICA **c46**

P. E. Olsen and B. Comet *In* Lunar and Planetary Inst., Global Catastrophes in Earth History: An Interdisciplinary Conference on Impacts, Volcanism, and Mass Mortality 1988 p 135-136 (For primary document see N89-21287 14-42)

Avail: NTIS HC A11/MF A01 CSCL 08G

Rift basins of the Atlantic passive margin in eastern North America are filled with thousands of meters of continental rocks termed the Newark Supergroup which provide an unprecedented opportunity to examine the fine scale structure of the Triassic-Jurassic mass extinction in continental environments. Time control, vital to the understanding of the mechanisms behind mass extinctions, is provided by lake-level cycles apparently controlled by orbitally induced climate change allowing resolution at the less than 21,000 year level. Correlation with other provinces is provided by a developing high resolution magnetostratigraphy and palynologically-based biostratigraphy. A large number of at least local vertebrate and palynomorph extinctions are concentrated around the boundary with survivors constituting the earliest Jurassic assemblages, apparently without the introduction of new taxa. The palynofloral transition is marked by the dramatic elimination of a relatively high diversity Triassic pollen assemblage with the survivors making up a Jurassic assemblage of very low diversity overwhelmingly dominated by Corollina. Based principally on palynological correlations, the hypothesis that these continental taxonomic transitions were synchronous with the massive Triassic-Jurassic marine extinctions is strongly corroborated. An extremely rapid, perhaps catastrophic, taxonomic turnover at the Triassic-Jurassic boundary, synchronous in continental and marine realms is hypothesized and discussed. Author

N89-21367*# California Univ., Los Angeles.

PERMO-TRIASSIC VERTEBRATE EXTINCTIONS: A PROGRAM **c51**

E. C. Olson *In* Lunar and Planetary Inst., Global Catastrophes in Earth History: An Interdisciplinary Conference on Impacts, Volcanism, and Mass Mortality 1988 p 137-138 (For primary document see N89-21287 14-42)

Avail: NTIS HC A11/MF A01 CSCL 06B

Since the time of the Authors' study on this subject, a great deal of new information has become available. Concepts of the nature of extinctions have changed materially. The Authors' conclusion that a catastrophic event was not responsible for the extinction of vertebrates has modified to the extent that hypotheses involving either the impact of a massive extra-terrestrial body or volcanism provide plausible but not currently fully testable hypotheses. Stated changes resulted in a rapid decrease in organic diversity, as the ratio of origins of taxa to extinctions shifted from strongly positive to negative, with momentary equilibrium being reached at about the Permo-Triassic boundary. The proximate causes of the changes in the terrestrial biota appear to lie in two primary factors: (1) strong climatic changes (global mean temperatures, temperature ranges, humidity) and (2) susceptibility of the dominant vertebrates (large dicynodonts) and the glossopteris flora to disruption of the equlibrium of the world ecosystem. The following proximate causes have been proposed: (1) rhythmic fluctuations in solar radiation, (2) tectonic events as Pangea assembled, altering land-ocean relationships, patterns of wind and water circulation and continental physiography, (3) volcanism, and (4) changes subsequent to impacts of one or more massive extra terrestrial objects, bodies or comets. These hypotheses are discussed. Author

N89-21368*# Los Alamos National Lab., NM. Isotope and Nuclear Chemistry Div.

IRIDIUM ABUNDANCE MEASUREMENTS ACROSS BIO-EVENT HORIZONS IN THE GEOLOGICAL RECORD **c46**

C. J. Orth and M. Attrep, Jr. *In* Lunar and Planetary Inst., Global Catastrophes in Earth History: An Interdisciplinary

Conference on Impacts, Volcanism, and Mass Mortality 1988 p 139-140 (For primary document see N89-21287 14-42)
Avail: NTIS HC A11/MF A01 CSCL 08G

Geochemical studies have been performed on thousands of rock samples collected across bio-event horizons in the fossil record using INAA for about 40 common and trace elements and radiochemical isolation procedures for Os, Ir, Pt, and Au on selected samples. These studies were begun soon after the Alvarez team announced their discovery of the Cretaceous-Tertiary (K-T) Ir anomaly in marine rock sequences in Europe. With their encouragement the Authors searched for the anomaly in nearby continental (freshwater coal swamp) deposits. In collaboration with scientists from the U.S.G.S. in Denver, the anomaly was located and it was observed that a floral crisis occurred at the same stratigraphic position as the Ir spike. Further work in the Raton Basin has turned up numerous well-preserved K-T boundary sections. Although the Authors have continued to study the K-T boundary and provide geochemical measurements for other groups trying to precisely locate it, the primary effort was turned to examining the other bio-events in the Phanerozoic, especially to those that are older than the terminal Cretaceous. A list of horizons that were examined in collaboration with paleontologists and geologists is given. Results are also given and discussed.
Author

N89-21369*# Saint Lawrence Univ., Canton, NY. Dept. of Geology.
CATHODOLUMINESCENCE OF SHOCKED QUARTZ AT THE CRETACEOUS-TERTIARY BOUNDARY c46
Michael R. Owen and Mark H. Anders *In* Lunar and Planetary Inst., Global Catastrophes in Earth History: An Interdisciplinary Conference on Impacts, Volcanism, and Mass Mortality 1988 p 141-142 Prepared in cooperation with California Univ., Berleley (For primary document see N89-21287 14-42)
Avail: NTIS HC A11/MF A01 CSCL 08G

Empirical studies have documented an association between rock type and the cathodoluminescence color of constituent quartz grains. Quartz from extrusive igneous sources luminesces uniform pale blue. Quartz from intrusive igneous and high-grade metamorphic rocks generally luminesces darker purple-blue, whereas quartz recrystallized under low-grade metamorphic conditions luminesces reddish-brown. Quartz grains in most sandstones luminesce a heterogeneous mixture of these colors because the grains were derived from a variety of ultimate source rocks. If shocked quartz found at the Cretaceous-Tertiary (K-T) boundary is volcanic in origin, its cathodoluminescence should be predominantly pale blue. Alternatively, quartz grains derived from bolide impact upon, and ejection of, mixed igneous, metamorphic, and sedimentary rocks should luminesce a variety of colors. Grain mounts of sand collected at the K-T boundary horizon from the Clear Creek North site in the Raton Basin, Colorado were examined. Shocked quartz luminesced a variety of colors and very few grains luminesced the pale blue color that is typical of volcanic quartz. It was concluded that the shocked quartz was derived from a petrologically diverse source region without substantial volcanic contribution. Most shocked grains apparently were derived from low-grade metamorphic rocks, with a slightly smaller contribution from high-grade metamorphic and intrusive igneous rocks. Rare quartz grains with brown-luminescing rims reflect a minor addition from detrital sedimentary sources. The apparent relative abundances of intrusive (and rare extrusive) igneous, metamorphic, and sedimentary ultimate source rocks suggested by CL colors of shock-deformed quartz at the K-T boundary is consistent with a crustal/supracrustal origin for the grains.
Author

N89-21370*# Technische Univ., Vienna (Austria).
BIO-, MAGNETO- AND EVENT-STRATIGRAPHY ACROSS THE K-T BOUNDARY c46
A. Preisinger, H. Stradner, and H. J. Mauritsch (Montanuniversitat Leoben, Austria) *In* Lunar and Planetary Inst., Global Catastrophes in Earth History: An Interdisciplinary Conference on Impacts, Volcansim, and Mass Mortality 1988 p 143-144 (For primary document see N89-21287 14-42)
Avail: NTIS HC A11/MF A01 CSCL 08G

Determining the time and the time structure of rare events in geology can be accomplished by applying three different and independent stratigraphic methods: Biostratigraphy, magneto-stratigraphy and event-stratigraphy. The optimal time resolution of the two former methods is about 1000 years, while by means of event-stratigraphy a resolution of approximately one year can be achieved. For biostratigraphy across the Cretaceous-Tertiary (K-T) boundary micro- and nannofossils have been found best suited. The qualitative and quantitative analyses of minerals and trace elements across the K-T boundary show anomalies on a millimeter scale and permit conclusions regarding the time structure of the K-T event itself. The results of the analyses find a most consistent explanation by the assumption of an extraterrestrial impact. The main portion of the material rain from the atmosphere evidently was deposited within a short time. The long-time components consist of the finest portion of the material rain from the atmosphere and the transported and redeposited fall-out.
Author

N89-21371*# Massachusetts Inst. of Tech., Cambridge. Dept. of Earth, Atmospheric and Planetary Sciences.
BIOSPHERIC TRAUMAS CAUSED BY LARGE IMPACTS AND PREDICTED RELICS IN THE SEDIMENTARY RECORD c46
R. G. Prinn and B. Fegley, Jr. *In* Lunar and Planetary Inst., Global Catastrophes in Earth History: An Interdisciplinary Conference on Impacts, Volcanism, and Mass Mortality 1988 p 145 (For primary document see N89-21287 14-42)
(Grants NAG9-108; NSF ATM-87-10102)
Avail: NTIS HC A11/MF A01 CSCL 08G

When a large asteroid or comet impacts the Earth the supersonic plume ejected on impact causes severe shock heating and chemical reprocessing of the proximal atmosphere. The resultant NO is converted rapidly to NO2, foliage damage due to exposure to NO2 and HNO3, toxicosis resulting from massive mobilization of soil trace metals, and faunal asphyxiation due to exposure to NO2. One class of relic evidence for the above effects arises because extinction of species caused by these chemically induced traumas would be selective. A second class of relic evidence arises because the acid rain will cause massive weathering of continental rocks and soils characterized by large ratios of the relatively insoluble metals, to the more soluble metals. This weathering would be best recorded in fossils in unperturbed deltaic, neritic, or limnetic sediments and for metals with very long oceanic residence times in deep ocean sediments as well. This evidence is discussed.
Author

N89-21372*# New York Univ., New York. Earth Systems Group.
FLOOD BASALT ERUPTIONS, COMET SHOWERS, AND MASS EXTINCTION EVENTS Abstract Only c46
Michael R. Rampino and Richard B. Stothers (National Aeronautics and Space Administration. Goddard Space Flight Center, Greenbelt, MD.) *In* Lunar and Planetary Inst., Global Catastrophes in Earth History: An Interdisciplinary Conference on Impacts, Volcanism, and Mass Mortality 1988 p 146 Prepared in cooperation with NASA Goddard Space Flight Center, Greenbelt, MD (For primary document see N89-21287 14-42)
Avail: NTIS HC A11/MF A01 CSCL 08G

A chronology of initiation dates of the major continental flood basalt episodes has been established from compilation of published K-Ar and Ar-Ar ages of basaltic flows and related basic intrusions. The dating is therefore independent of the biostratigraphic and paleomagnetic time scales, and the estimated errors of the inititation dates are approximately + or - 4 pct. There are 11 distinct episodes of continental flood basalts known during the past 250 Myr. The data show that flood basalt episodes are generally relatively brief geologic events, with intermittent eruptions during peak output periods lasting ony 2 to 3 Myr or less. Statistical analyses suggest that these episodes may have occurred quasi-periodically with a mean cycle time of 32 + or - 1 Myr. The initiation dates of the flood basalts are close to the estimated

dates of marine mass extinctions and impact-crater clusters. Although a purely internal forcing might be argued for the flood basalt volcanism, quasi-periodic comet impacts may be the trigger for both the flood basalts and the extinctions. Impact cratering models suggest that large-body impactors lead to deep initial cratering, and therefore may cause mantle disturbances and initiate mantle plume activity. The flood basalt episodes commonly mark the initiation or jump of a mantle hotspot, and are often followed by continental rifting and separation. Evidence from dynamical studies of impacts, occurrences of craters and hotspots, and the geochemistry of boundary layers is synthesized to provide a possible model of impact-generated volcanism. Flood basalt eruptions may themselves have severe effects on climate, and possibly on life. Impacts might, as a result, have led to mass extinctions through direct atmospheric disturbances, and/or indirectly through prolonged flood basalt volcanism. Author

N89-21373*# New York Univ., New York. Earth Systems Group.

CLIMATIC CHANGES RESULTING FROM MASS EXTINCTIONS AT THE K-T BOUNDARY (AND OTHER BIO-EVENTS) Abstract Only **c46**

Michael R. Rampino and Tyler Volk *In* Lunar and Planetary Inst., Global Catastrophes in Earth History: An Interdisciplinary Conference on Impacts, Volcanism, and Mass Mortality 1988 p 147 (For primary document see N89-21287 14-42)
Avail: NTIS HC A11/MF A01 CSCL 08G

The mass extinctions at the Cretaceous-Tertiary (K-T) boundary include about 90 percent of marine calcareous nannoplankton (coccoliths), and carbon-isotope data show that marine primary productivity was drastically reduced for about 500,000 years after the boundary event, the so-called Strangelove Ocean effect. One result of the elimination of most marine phytoplankton would have been a severe reduction in production of dimethyl sulfide (DMS), a biogenic gas that is believed to be the major precursor of cloud condensation nuclei (CCN) over the oceans. A drastic reduction in marine CCN should lead to a cloud canopy with significantly lower reflectivity, and hence cause a significant warming at the earth's surface. Calculations suggest that, all other things being held constant, a reduction in CCN of more than 80 percent (a reasonable value for the K-T extinctions) could have produced a rapid global warming of 6 C or more. Oxygen-isotope analyses of marine sediments, and other kinds of paleoclimatic data, have provided for a marked warming, and a general instability of climate coincident with the killoff of marine plankton at the K-T boundary. Similar reductions in phytoplankton abundance at other boundaries, as indicated by marked shifts in carbon-isotope curves, suggest that severe temperature changes may have accompanied other mass extinctions, and raises the intriguing possibility that the extinction events themselves could have contributed to the climatic instabilities at critical bio-events in the geologic record. Author

N89-21374*# Chicago Univ., IL.

IMPACT AS A GENERAL CAUSE OF EXTINCTION: A FEASIBILITY TEST **c46**

David M. Raup *In* Lunar and Planetary Inst., Global Catastrophes in Earth History: An Interdisciplinary Conference on Impacts, Volcanism, and Mass Mortality 1988 p 148-149 (For primary document see N89-21287 14-42)
Avail: NTIS HC A11/MF A01 CSCL 08G

Large body impact has been implicated as the possible cause of several extinction events. This is entirely plausible if one accepts two propositions: (1) that impacts of large comets and asteroids produce environmental effects severe enough to cause significant species extinctions and (2) that the estimates of comet and asteroid flux for the Phanerozoic are approximately correct. A resonable next step is to investigate the possibility that impact could be a significant factor in the broader Phanerozoic extinction record, not limited merely to a few events of mass extinction. Monte Carlo simulation experiments based on existing flux estimates and reasonable predictions of the relationship between bolide diameter and extinction are discussed. The simulation results raise the serious possibility that large body impact may be a more pervasive factor in extinction than has been assumed heretofore. At the very least, the experiments show that the comet and asteroid flux estimates combined with a reasonable kill curve produces a reasonable extinction record, complete with occasional mass extinctions and the irregular, lower intensity extinctions commonly called background extinction. Author

N89-21375*# Witwatersrand Univ., Johannesburg (South Africa). Centre for Nuclear Sciences.

REPORT ON AN INTERNATIONAL WORKSHOP ON CRYPTOEXPLOSIONS AND CATASTROPHES IN THE GEOLOGICAL RECORD, WITH A SPECIAL FOCUS ON THE VREDEFORT STRUCTURE **c46**

W. U. Reimold *In* Lunar and Planetary Inst., Global Catastrophes in Earth History: An Interdisciplinary Conference on Impacts, Volcanism, and Mass Mortality 1988 p 150-151 Workshop held in Parys, Republic of South Africa, 6-10 Jul. 1987 (For primary document see N89-21287 14-42)
Avail: NTIS HC A11/MF A01 CSCL 08G

Eighty-five geoscientists gathered in the heart of the Vredefort Cryptoexplosion structure to discuss and evaluate the current knowledge about mass extinctions, impact and volcanic cratering and to obtain first-hand information on the Vredefort structure and its origin. Presentations were made within 8 topical sessions: (1) the regional setting of the Vredefort structure; (2) the Vredefort structure itself; (3) deformations and microdeformations; (4) large cryptoexplosion structures; (5) the Ries Crater; (6) tektites; (7) the K-T boundary, and (8) tectonophysics of cratering. The program was rounded up by working group and plenum discussions culminating in a Workshop report emphasizing problem areas, gaps in the data base and recommendations for future research. Author

N89-21376*# Witwatersrand Univ., Johannesburg (South Africa). Centre for Nuclear Sciences.

MICRODEFORMATION IN VREDEFORT ROCKS; EVIDENCE FOR SHOCK METAMORPHISM **c46**

W. U. Reimold, M. A. G. Andreoli, and R. J. Hart *In* Lunar and Planetary Inst., Global Catastrophes in Earth History: An Interdisciplinary Conference on Impacts, Volcanism, and Mass Mortality 1988 p 152-153 (For primary document see N89-21287 14-42)
Avail: NTIS HC A11/MF A01 CSCL 08G

Planar microdeformations in quartz from basement or collar rocks of the Vredefort Dome have been cited for years as the main microtextural evidence for shock metamorphism in this structure. In addition, Schreyer describes feldspar recrystallization in rocks from the center of the Dome as the result of transformation of diaplectic glass, and Lilly reported the sighting of mosaicism in quartz. These textural observations are widely believed to indicate either an impact or an internally produced shock origin for the Vredefort Dome. Two types of (mostly sub) planar microdeformations are displayed in quartz grains from Vredefort rocks: (1) fluid inclusion trails, and (2) straight optical discontinuities that sometimes resemble lamellae. Both types occur as single features or as single or multiple sets in quartz grains. Besides qualitative descriptions of cleavage and recrystallization in feldspar and kinkbands in mica, no further microtextural evidence for shock metamorphism at Vredefort has been reported to date. Some 150 thin sections of Vredefort basement rocks were re-examined for potential shock and other deformation effects in all rock-forming minerals. This included petrographic study of two drill cores from the immediate vicinity of the center of the Dome. Observations recorded throughout the granitic core are given along with conclusions. Author

N89-21377*# Colorado Univ., Boulder. Dept. of Physics.

DYNAMICS OF EXPLODING MAGMA CHAMBERS: IMPLICATIONS FOR K-T VOLCANISM AND MASS EXTINCTIONS **c46**

A. R. Rice *In* Lunar and Planetary Inst., Global Catastrophes in Earth History: An Interdisciplinary Conference on Impacts,

Volcanism, and Mass Mortality 1988 p 154-155 (For primary document see N89-21287 14-42)
Avail: NTIS HC A11/MF A01 CSCL 08G

Although it is well known that unconfined chemical explosives may yield pressures to several megabars on detonation in air, the explosive literature has yet to be accessed by some contributors to the volcanological literature who've indicated that pressures in excess of the overburden and/or tensile cannot be obtained. Idealized ballistic assessments of pressures internal to volcanoes yield pressures in the hundreds of kilobar range upon correction by addition of friction, etc. Previous assessments of exploding magma chamber pressure have been made from the characteristics of the Mt. St. Helens explosion. A variety of methods yield pressures of similar value: at least hundreds of kilobars. Such results are consistent with free energy requirements for quench supersaturation explosion, a process occurring in solidifying industrial melts. Several reviews of geochemical literature emphasize the carbon event at the Cretaceous-Tertiary (K-T) boundary as being an indicator of a massive dump of CO2 derived from the mantle and entering the atmosphere by extensive global volcanism. Oxygen isotope data indicates extreme warming at the end of the Cretaceous which is consistent with a greenhouse effect attending the CO2 event. Reaction rate equations for the quench supersaturation explosion mechanism indicated, are consistent with the rise in pressure to 30 kbar on solidification of magmatic melts, these pressures limited by the strength of the experimental apparatus. Author

N89-21378*# Centre National de la Recherche Scientifique, Gif-sur-Yvette (France). Centre des Faibles Radioactivites.
SEARCH FOR THE TUNGUSKA EVENT IN THE ANTARCTIC SNOW **c46**
R. Rocchia, M. deAngelis, D. Doclet, Ph. Bonte, C. Jehanno, and E. Robin *In* Lunar and Planetary Inst., Global Catastrophes in Earth History: An Interdisciplinary Conference on Impacts, Volcanism, and Mass Mortality 1988 p 156-157 Prepared in cooperation with Commissariat a l'Energie Atomique, Saclay (France) (For primary document see N89-21287 14-42)
Avail: NTIS HC A11/MF A01 CSCL 08G

The Tunguska explosion in 1908 is supposed to have been produced by the impact of a small celestial body. The absence of any identifiable crater together with the huge energy released by the event suggest that the impactor exploded in midair and that its material was widely spread over the Earth. The short term contribution of such exceptional events to the total accretion rate of extraterrestrial material by the Earth could be significant. Samples were chosen in a core electromechanically drilled in 1984 near South Pole Station. There, the low temperatures, preventing melting all year long, and the nearly regular snow fall rate provide good conditions for a reliable continuous record of any infalling material. In many samples Ir was below the detection limit of the instrumentation. The iridium infall averaged over 45 samples is given. In a few samples the iridium content is significantly higher than the average: the frequency and amplitude of such fluctuations can be explained by the presence on some filters of finite size cosmic particles. No significant systematic increase above the average level is observed in the part of the core corresponding to the Tunguska event. The two major results of this study are: (1) The presence of Tunguska explosion debris in the Antarctic snow is not confirmed; and (2) The estimate of the average iridium infall, is an order of magnitude lower than the Ganapathy's background but is close to the values measured in Antarctic snow and atmospheric samples by Takahashi et al. The results are also consistent with the flux of micrometeoroids deduced from optical and radar observations or derived from the study of Greenland cosmic dust collection but are lower than the flux at mid-latitude measured in paleocene-oligocene sediments from the central part of the Pacific Ocean. Author

N89-21379*# Geological Survey, Flagstaff, AZ.
COMPUTER MODELING OF LARGE ASTEROID IMPACTS INTO CONTINENTAL AND OCEANIC SITES: ATMOSPHERIC, CRATERING, AND EJECTA DYNAMICS **c46**
D. J. Roddy, S. H. Schuster, M. Rosenblatt, L. B. Grant, P. J. Hassig, and K. N. Kreyenhagen *In* Lunar and Planetary Inst., Global Catastrophes in Earth History: An Interdisciplinary Conference on Impacts, Volcanism, and Mass Mortality 1988 p 158-159 Prepared in cooperation with California Research and Technology, Inc., Chatsworth (For primary document see N89-21287 14-42)
Avail: NTIS HC A11/MF A01 CSCL 08G

Numerous impact cratering events have occurred on the Earth during the last several billion years that have seriously affected our planet and its atmosphere. The largest cratering events, which were caused by asteroids and comets with kinetic energies equivalent to tens of millions of megatons of TNT, have distributed substantial quantities of terrestrial and extraterrestrial material over much or all of the Earth. In order to study a large-scale impact event in detail, computer simulations were completed that model the passage of a 10 km-diameter asteroid through the Earth's atmosphere and the subsequent cratering and ejecta dynamics associated with impact of the asteroid into two different targets, i.e., an oceanic site and a continental site. The calcuations were designed to broadly represent giant impact events that have occurred on the Earth since its formation and specifically represent an impact cratering event proposed to have occurred at the end of Cretaceous time. Calculation of the passage of the asteroid through a U.S. Standard Atmosphere showed development of a strong bow shock that expanded radially outward. Behind the shock front was a region of highly shock compressed and intensely heated air. Behind the asteroid, rapid expansion of this shocked air created a large region of very low density that also expanded away from the impact area. Calculations of the cratering events in both the continental and oceanic targets were carried to 120 s. Despite geologic differences, impacts in both targets developed comparable dynamic flow fields, and by approx. 29 s similar-sized transient craters approx. 39 km deep and approx. 62 km across had formed. For all practical purposes, the atmosphere was nearly completely removed from the impact area for tens of seconds, i.e., air pressures were less than fractions of a bar out to ranges of over 50 km. Consequently, much of the asteroid and target materials were ejected upward into a near vacuum. Effects of secondary volcanism and return of the ocean over hot oceanic crater floor could also be expected to add substantial solid and vaporized material to the atmosphere, but these conditions were not studied. Author

N89-21380*# Geological Survey, Denver, CO.
LATE FRASNIAN MASS EXTINCTION: CONODONT EVENT STRATIGRAPHY, GLOBAL CHANGES, AND POSSIBLE CAUSES **c51**
Charles A. Sandberg, Willi Ziegler, Roland Dreesen (INIEX, Liege, Belgium), and Jamie L. Butler *In* Lunar and Planetary Inst., Global Catastrophes in Earth History: An Interdisciplinary Conference on Impacts, Volcanism, and Mass Mortality 1988 p 160-161 (For primary document see N89-21287 14-42)
Avail: NTIS HC A11/MF A01 CSCL 06B

Several abrupt changes in conodont biofacies are documented to occur synchronously at six primary control sections across the Frasnian-Famennian boundary in Euramerica. These changes occurred within a time-span of only about 100,000 years near the end of the latest Frasnian linguiformis Zone, which is formally named to replace the Uppermost gigas Zone. The conodont-biofacies changes are interpreted to reflect a eustatic rise followed by an abrupt eustatic fall immediately preceding the late Frasnian mass extinction. Two new conodont species are named and described. Ancyrognathus ubiquitus n.sp. is recorded only just below and above the level of late Frasnian extinction and hence is a global marker for that event. Palmatolepispraetriangularis n.sp. is the long-sought Frasnian ancestor of the formerly cryptogenic species, Pa. triangularis, indicator of the earliest Famennian Lower triangularis Zone. The actual extinction event occurred entirely within the Frasnian and is interpreted to have been of brief duration-from as long as 20,000 years to as short as several days. The eustatic rise-and-fall couplet associated with the late Frasnian mass extinction is similar to eustatic couplets associated with the demise of most Frasnian

(F2h) reefs worldwide about 1 m.y. earlier and with a latest Famennian mass extinction about 9.5 m.y. later. All these events may be directly or indirectly attributable to extraterrestrial triggering mechanisms. An impact of a small bolide or a near miss of a larger bolide may have caused the earlier demise of Frasnian reefs. An impact of possibly the same larger bolide in the Southern Hemisphere would explain the late Frasnian mass extinction. Global regression during the Famennian probably resulted from Southern-Hemisphere glaciation triggered by the latest Frasnian impact. Glaciation probably was the indirect cause of the latest Famennian mass extinction. Author

N89-21381*# Boeing Aerospace Co., Seattle, WA.
CRATER SIZE ESTIMATES FOR LARGE-BODY TERRESTRIAL IMPACT **c46**
Robert M. Schmidt and Kevin R. Housen *In* Lunar and Planetary Inst., Global Catastrophes in Earth History: An Interdisciplinary Conference on Impacts, Volcanism, and Mass Mortality 1988 p 162-163 (For primary document see N89-21287 14-42)
Avail: NTIS HC A11/MF A01 CSCL 08G

Calculating the effects of impacts leading to global catastrophes requires knowledge of the impact process at very large size scales. This information cannot be obtained directly but must be inferred from subscale physical simulations, numerical simulations, and scaling laws. Schmidt and Holsapple presented scaling laws based upon laboratory-scale impact experiments performed on a centrifuge (Schmidt, 1980 and Schmidt and Holsapple, 1980). These experiments were used to develop scaling laws which were among the first to include gravity dependence associated with increasing event size. At that time using the results of experiments in dry sand and in water to provide bounds on crater size, they recognized that more precise bounds on large-body impact crater formation could be obtained with additional centrifuge experiments conducted in other geological media. In that previous work, simple power-law formulae were developed to relate final crater diameter to impactor size and velocity. In addition, Schmidt (1980) and Holsapple and Schmidt (1982) recognized that the energy scaling exponent is not a universal constant but depends upon the target media. Recently, Holsapple and Schmidt (1987) includes results for non-porous materials and provides a basis for estimating crater formation kinematics and final crater size. A revised set of scaling relationships for all crater parameters of interest are presented. These include results for various target media and include the kinematics of formation. Particular attention is given to possible limits brought about by very large impactors. Author

N89-21382*# California Univ., Berkeley. Lawrence Berkeley Lab.
MARINE AND CONTINENTAL K-T BOUNDARY CLAYS COMPARED **c46**
B. Schmitz *In* Lunar and Planetary Inst., Global Catastrophes in Earth History: An Interdisciplinary Conference on Impacts, Volcanism, and Mass Mortality 1988 p 164-165 (For primary document see N89-21287 14-42)
Avail: NTIS HC A11/MF A01 CSCL 08G

Detailed geochemical and mineralogical studies (1 to 5) of sediments across the Cretaceous-Tertiary (K-T) boundary at Stevns Klint, Karlstrup, Nye Klov, Dania, and Kjolby Gaard in Denmark, at Limhamn in Sweden, at Caravaca in Spain, at Waipara and Woodside Creek in New Zealand, at Trinidad in Colorado, and at various sites in Montana, have induced conclusions and reflections which are given and briefly discussed. Author

N89-21383*# Brown Univ., Providence, RI. Dept. of Geological Sciences.
OBLIQUE IMPACTS: CATASTROPHIC VS. PROTRACTED EFFECTS **c46**
P. H. Schultz *In* Lunar and Planetary Inst., Global Catastrophes in Earth History: An Interdisciplinary Conference on Impacts, Volcanism, and Mass Mortality 1988 p 166-167 Prepared in cooperation with Murphys Center of Planetology, CA (For primary document see N89-21287 14-42)
Avail: NTIS HC A11/MF A01 CSCL 08G

Proposed impacts as the cause of biologic catastrophes at the end of the Cretaceous and Eocene face several enigmas: protracted extinctions, even prior to the stratigraphic cosmogenic signature; widespread but non-uniform dispersal of the meteoritic component; absence of a crater of sufficient size; and evidence for massive intensive fires. Various hypotheses provide reasonable mechanisms for mass mortalities: global cooling by continental impact sites; global warming by oceanic impact sites; contrasting effects of asteroidal, cometary, and even multiple impacts; and stress on an already fragile global environment. Yet not every known large impact is associated with a major biologic catastrophe. An alternative is expanded: the consequences of an oblique impact. The most probable angle of impact is 45 deg with the probability for an impact at smaller angles decreasing: A vertical impact is as rare as a tangential impact with a 5 deg impact angle or less occurring only 8 percent of the time. Consequently a low-angle impact is a rare but probable event. Laboratory experiments at the NASA-Ames Vertical Gun Range reveal important information about cratering efficiency, impact vaporization, projectile dispersal, and phenomenology, thereby providing perspective for possible consequences of such an impact on both the Earth and Moon. Oblique impacts are rare but certain events through geologic time: A 5 deg impact by a 2 km-diameter impactor on the Earth would occur only once in about 18 my with a 10 km-diameter once in about 450 my. Major life extinctions beginning prior to the stratigraphic cosmogenic signature or protracted extinctions seemingly too long after the proposed event may not be evidence against an impact as a cause but evidence for a more complex but probable sequence of events. Author

N89-21384*# Brown Univ., Providence, RI. Dept. of Geological Sciences.
NON-RANDOM CRATERING FLUX IN RECENT TIME **c46**
P. H. Schultz *In* Lunar and Planetary Inst., Global Catastrophes in Earth History: An Interdisciplinary Conference on Impacts, Volcanism, and Mass Mortality 1988 p 168-169 Prepared in cooperation with Arizona State Univ., Tempe (For primary document see N89-21287 14-42)
Avail: NTIS HC A11/MF A01 CSCL 08G

Proposed periodic cycles of mass mortality have been linked to periodic changes in the impact flux on Earth. Such changes in the impact flux, however, also should be recorded on the Moon. Previous studies have concluded that the impact flux on the Moon over the last 1 to 2 billion years has been reasonably constant, but sudden changes in the impact flux over time intervals as short as 30 my could not be detected in these studies unless the added crater population greatly exceeded the cumulative cratering record. Consequently this study focuses only on bright-rayed craters larger than 1 km thereby not only limiting the study to recent craters but also largely eliminating contamination by secondary craters. Preservation of ray patterns and other fine-scale surface textures in the ejecta provides first-order culling of craters younger than Tycho, i.e., about 100 my. Although a periodic change in the impact flux in the Earth-Moon system cannot yet be confirmed from the data, a non-random component appears to exist with an increased flux around 7 and 15 my. The concentrations in different quadrants of the lunar hemisphere would be consistent with a shower of debris generally smaller than 0.5 km. Author

N89-21385*# Chicago Univ., IL. Dept. of the Geophysical Sciences.
PERIODICITY OF EXTINCTION: A 1988 UPDATE **c51**
J. John Sepkowski, Jr. *In* Lunar and Planetary Inst., Global Catastrophes in Earth History: An Interdisciplinary Conference on Impacts, Volcanism, and Mass Mortality 1988 p 170-171 (For primary document see N89-21287 14-42)
Avail: NTIS HC A11/MF A01 CSCL 06B

The hypothesis that events of mass extinction recur periodically at approximately 26 my intervals is an empirical claim based on analysis of data from the fossil record. The hypothesis has become closely linked with catastrophism because several events in the periodic series are associated with evidence of extraterrestrial impacts, and terrestrial forcing mechanisms with long, periodic

recurrences are not easily conceived. Astronomical mechanisms that have been hypothesized include undetected solar companions and solar oscillation about the galactic plane, which induce comet showers and result in impacts on Earth at regular intervals. Because these mechanisms are speculative, they have been the subject of considerable controversy, as has the hypothesis of periodicity of extinction. In response to criticisms and uncertainties, a data base was developed on times of extinction of marine animal genera. A time series is given and analyzed with 49 sample points for the per-genus extinction rate from the Late Permian to the Recent. An unexpected pattern in the data is the uniformity of magnitude of many of the periodic extinction events. Observations suggest that the sequence of extinction events might be the result of two sets of mechanisms: a periodic forcing that normally induces only moderate amounts of extinction, and independent incidents or catastrophes that, when coincident with the periodic forcing, amplify its signal and produce major-mass extinctions. Author

N89-21386*# Lunar and Planetary Inst., Houston, TX.
K-T IMPACT(S): CONTINENTAL, OCEANIC OR BOTH **c46**
V. L. Sharpton, B. C. Schuraytz, A. V. Murali, G. Ryder, and K. Burke *In its* Global Catastrophes in Earth History: An Interdisciplinary Conference on Impacts, Volcanism, and Mass Mortality 1988 p 172-173 (For primary document see N89-21287 14-42)
Avail: NTIS HC A11/MF A01 CSCL 08G

Although geochemical and mineralogical evidence indicate that a major accretionary event occurred at the K-T boundary, no impact crater of suitable size and age was recognized. The 35 km Manson Structure, Iowa, was suggested recently as a possibility and Ar-40/Ar-39 determinations indicate that its formation age is indistinguishable from that of the K-T boundary. In order to test a possible association between Manson and the K-T boundary clay, the geochemistry and mineralogy of the K-T boundary clays at the Scollard Canyon section, Alberta and the Starkville South section, Colorado are compared with three dominant lithologies affected by the Manson impact: Proterozoic red clastics, underlying late-state granites, and gneisses. The chemical and mineralogical makeup of the Scollard Canyon boundary clay and its clastic constituents are presented, commenting on the implications for impact models. An impact into crystalline material of continental affinity appears to be required to explain the mineralogy and chemistry of the Scollard Canyon (and other Western N. American K-T sections). The low REE abundances of some K-T boundary layers are unusual but perhaps attempts should be made to understand the contributions of individual crustal components (e.g., carbonates, arkoses) as well as the potential for alteration involving these and other elements during and after impact-induced vaporization, before mantle excavation is invoked. If further studies confirm the results of published studies of marine boundary clays that indicate an oceanic target, attention must be paid to the possibility that multiple impacts occurred at the K-T boundary - one or more on the continents and one or more in the ocean. Author

N89-21387*# Geological Survey, Flagstaff, AZ.
ASTEROID AND COMET FLUX IN THE NEIGHBORHOOD OF THE EARTH **c90**
Eugene M. Shoemaker, Carolyn S. Shoemaker, and Ruth F. Wolfe *In* Lunar and Planetary Inst., Global Catastrophes in Earth History: An Interdisciplinary Conference on Impacts, Volcanism, and Mass Mortality 1988 p 174-176 (For primary document see N89-21287 14-42)
Avail: NTIS HC A11/MF A01 CSCL 03B

Significant advances in the knowledge and understanding of the flux of large solid objects in the neighborhood of Earth have occurred. The best estimates of the collision rates with Earth of asteroids and comets and the corresponding production of impact craters are presented. Approximately 80 Earth-crossing asteroids were discovered through May 1988. Among 42 new Earth-crossing asteroids found in the last decade, two-thirds were discovered from observations at Palomar Observatory and 15 were discovered or independently detected in dedicated surveys with the Palomar Observatory and 15 were discovered or independently detected in dedicated surveys with the Palomar 46 cm Schmidt. Probabilities of collision with Earth have been calculated for about two-thirds of the known Earth-crossing asteroids. When multiplied by the estimated population of Earth-crossers, this yields an estimated present rate of collision about 65 pct higher than that previously reported. Spectrophotometric data obtained chiefly in the last decade show that the large majority of obvserved Earth-crossers are similar to asteroids found in the inner part of the main belt. The number of discovered Earth-crossing comets is more than 4 times greater than the number of known Earth-crossing asteroids, but reliable data on the sizes of comet nuclei are sparse. The flux of comets almost certainly was highly variable over late geologic time, owing to the random perturbation of the Oort comet cloud by stars in the solar neighborhood. Author

N89-21388*# Rhode Island Univ., Kingston. Graduate School of Oceanography.
ASSESSMENT OF THE ATMOSPHERIC IMPACT OF VOLCANIC ERUPTIONS **c45**
H. Sigurdsson *In* Lunar and Planetary Inst., Global Catastrophes in Earth History: An Interdisciplinary Conference on Impacts, Volcanism, and Mass Mortality 1988 p 177-178 (For primary document see N89-21287 14-42)
Avail: NTIS HC A11/MF A01 CSCL 13B

The dominant global impact of volcanic activity is likely to be related to the effects of volcanic gases on the Earth's atmosphere. Volcanic gas emissions from individual volcanic arc eruptions are likely to cause increases in the stratospheric optical depth that result in surface landmass temperature decline of 2 to 3 K for less than a decade. Trachytic and intermediate magmas are much more effective in this regard than high-silica magmas, and may also lead to extensive ozone depletion due to effect of halogens and magmatic water. Given the assumed relationship between arc volcanism and subduction rate, and the relatively small variation in global spreading rates in the geologic record, it is unlikely that the rates of arc volcanism have varied greatly during the Cenozoic. Hotspot related basaltic fissure eruptions in the subaerial environment have a higher mass yield of sulfur, but lofting of the valcanic aerosol to levels above the tropopause is required for a climate impact. High-latitude events, such as the Laki 1783 eruption can easily penetrate the tropopause and enter the stratosphere, but formation of a stratospheric volcanic aerosol form low-latitude effusive basaltic eruptions is problematical, due to the elevated low-latitude tropopause. Due to the high sulfur content of hotspot-derived basaltic magmas, their very high mass eruption rates and the episodic behavior, hotspots must be regarded as potentially major modifiers of Earth's climate through the action of their volcanic volatiles on the chemistry and physics of the atmosphere. Author

N89-21389*# Smithsonian Institution, Washington, DC.
VOLCANOES AND GLOBAL CATASTROPHES **c46**
Tom Simkin *In* Lunar and Planetary Inst., Global Catastrophes in Earth History: An Interdisciplinary Conference on Impacts, Volcanism, and Mass Mortality 1988 p 179 (For primary document see N89-21287 14-42)
Avail: NTIS HC A11/MF A01 CSCL 08G

The search for a single explanation for global mass extinctions has let to polarization and the controversies that are often fueled by widespread media attention. The historic record shows a roughly linear log-log relation between the frequency of explosive volcanic eruptions and the volume of their products. Eruptions such as Mt. St. Helens 1980 produce on the order of 1 cu km of tephra, destroying life over areas in the 10 to 100 sq km range, and take place, on the average, once or twice a decade. Eruptions producing 10 cu km take place several times a century and, like Krakatau 1883, destroy life over 100 to 1000 sq km areas while producing clear global atmospheric effects. Eruptions producting 10,000 cu km are known from the Quaternary record, and extrapolation from the historic record suggests that they occur perhaps once in 20,000 years, but none has occurred in historic time and little is known of their biologic effects. Even larger eruptions must also exist in

the geologic record, but documentation of their volume becomes increasingly difficult as their age increases. The conclusion is inescapable that prehistoric eruptions have produced catastrophes on a global scale: only the magnitude of the associated mortality is in question. Differentiation of large magma chambers is on a time scale of thousands to millions of years, and explosive volcanoes are clearly concentrated in narrow belts near converging plate margins. Volcanism cannot be dismissed as a producer of global catastrophes. Its role in major extinctions is likely to be at least contributory and may well be large. More attention should be paid to global effects of the many huge eruptions in the geologic record that dwarf those known in historic time. Author

N89-21390*# Minnesota Univ., Minneapolis. Dept. of Geology and Geophysics.

BIOSTRATIGRAPHIC CASE STUDIES OF SIX MAJOR EXTINCTIONS **c51**

R. E. Sloan *In* Lunar and Planetary Inst., Global Catastrophes in Earth History: An Interdisciplinary Conference on Impacts, Volcanism, and Mass Mortality 1988 p 180-181 (For primary document see N89-21287 14-42)

Avail: NTIS HC A11/MF A01 CSCL 06B

Biostratigraphic case studies of six major extinctions show all are gradual save one, which is a catastrophic extinction of terrestrial origin. These extinctions show a continuum of environmental insults from major to minor. The major causes of these extinctions are positive and negative eustatic sea level changes, temperature, or ecological competition. Extraterrestrial causes should not be posited without positive association with a stratigraphically sharp extinction. The Cretaceous-Tertiary terrestrial extinction is considerably smaller in percentage of extinction than the marine extinction and is spread over 10 my of the Cretaceous and 1 my of the Tertiary. Sixty percent of the 30 dinosaurs in the northern Great Plains of the U.S. and Canada had become extinct in the 9 my before the late Maastrichtian sea level drop. The best data on the Permo-Triassic terrestrial extinction are from the Karoo basin of South Africa. This is a series of 6 extinctions in some 8 my, recorded in some 2800 meters of sediment. Precision of dating is enhanced by the high rate of accumulation of these sediments. Few data are readily available on the timing of the marine Permo-Triassic extinction, due to the very restricted number of sequences of Tatarian marine rocks. The terminal Ordovician extinction at 438 my is relatively rapid, taking place over about 0.5 my. The most significant aspect of this extinction is a eustatic sea level lowering associated with a major episode of glaciation. New data on this extinction is the reduction from 61 genera of trilobites in North America to 14, for a 77 percent extinction. Another Ordovician extinction present over 10 percent of the North American craton occurs at 454 my in the form of a catastrophic extinction due to a volcanic eruption which blanketed the U.S. east of the Transcontinental Arch. This is the only other sizeable extinction in the Ordovician. Author

N89-21391*# Vrije Univ., Amsterdam (Netherlands). Geomarine Center.

IMPACT AND EXTINCTION SIGNATURES IN COMPLETE CRETACEOUS-TERTIARY (K-T) BOUNDARY SECTIONS **c46**

J. Smit, H. Groot, R. deJonge, and P. Smit *In* Lunar and Planetary Inst., Global Catastrophes in Earth History: An Interdisciplinary Conference on Impacts, Volcanism, and Mass Mortality 1988 p 182-183 (For primary document see N89-21287 14-42)

Avail: NTIS HC A11/MF A01 CSCL 08G

The Zumaya, Caravaca and Agost sections in Spain, the El Kef section in Tunisia and the Negev (Nahal Avdat) sections in Israel are among the most continuous, expanded and complete K-T boundary sections. The distribution patterns of the planktic faunas were quantitatively analyzed in closely spaced samples across the K-T boundary in these sections, in conjuction with the geochemistry, stable isotopes, mineralogy and magnetostratigraphy. Three hundred foraminiferal specimens were randomly selected and determined. Reliable estimates for the foraminiferal productivity changes across the K-T boundary and for the 1 to 2 Ma interval preceding the K-T boundary were made from the numbers of individuals/gram of sediment corrected for the sedimentation rates (calculated from magnetic reversals and lithology). No gradual or stepwise extinction is seen below the K-T boundary nor any productivity decrease. Stable isotope analyses show a warming just after deposition of the ejecta layer, not cooling as predicted by nuclear winter scenarios, although the duration of such cooling may be too short to be observed even in these complete sections. Low REE values and cpx spherules with quench textures idential to quench-textures in diagenetically altered spherules, strongly indicate an oceanic site of (one of) the impactor(s). Author

N89-21392*# California Univ., Santa Barbara. Marine Science Inst.

CRETACEOUS-TERTIARY BOUNDARY IN THE ANTARCTIC: CLIMATIC COOLING PRECEDES BIOTIC CRISIS **c45**

Lowell D. Stott and James P. Kennett *In* Lunar and Planetary Inst., Global Catastrophes in Earth History: An Interdisciplinary Conference on Impacts, Volcanism, and Mass Mortality 1988 p 184-185 (For primary document see N89-21287 14-42)

Avail: NTIS HC A11/MF A01 CSCL 13B

Stable isotopic investigations were conducted on calcareous microfossils across two deep sea Cretaceous-Tertiary boundary sequences on Maud Rise, Weddell Sea, Antarctica. The boundary is taken at the level of massive extinctions in calcareous planktonic microfossils, and coincides with a sharp lithologic change from pure calcareous ooze to calcareous ooze with a large volcanic clay component. The uppermost Maestrichtian is marked by a long-term decrease in delta value of 0 to 18 which spans most of the lower and middle A. mayaroensis Zone and represents a warming trend which culminated in surface water temperatures of about 16 C. At approximately 3 meters below the K-T boundary this warming trend terminates abruptly and benthic and planktonic isotopic records exhibit a rapid increase in delta value of 0 to 18 that continues up to the K-T boundary. The trend towards cooler surface water temperatures stops abruptly at the K-T boundary and delta value of 0 to 18 values remain relatively stable through the Paleocene. Comparison of the Antarctic sequence with the previously documented deep sea records in the South Atlantic reveal shifts of similar magnitude in the latest Maestrichtian. It is indicated that the Southern Ocean underwent the most significant, and apparently permanent, climatic change. The latest Cretaceous oxygen isotopic shift recorded at Maud Rise and other deep sea sites is similar in magnitude to large positive delta valve of 0 to 18 shifts in the middle Eocene, at the Eocene/Oligocene boundary and in the middle Miocene that marked large scale climatic transitions which ultimately lead to cryospheric development of the Antarctic. The climatic shift at the end of the Cretaceous represents one of the most significant climatic transitions recorded in the latest Phanerozoic and had a profound effect on global climate as well as oceanic circulation. Author

N89-21393*# Geological Survey, Vancouver, WA. Cascades Volcano Observatory.

SOME VOLCANOLOGIC ASPECTS OF COLUMBIA RIVER BASALT VOLCANISM RELEVANT TO THE EXTINCTION CONTROVERSY **c46**

Donald A. Swanson *In* Lunar and Planetary Inst., Global Catastrophes in Earth History: An Interdisciplinary Conference on Impacts, Volcanism, and Mass Mortality 1988 p 186-187 (For primary document see N89-21287 14-42)

Avail: NTIS HC A11/MF A01 CSCL 08G

The Columbia River Basalt Group is the youngest and most thoroughly studied flood-basalt province known; information about it should be relevant to questions about the possible relation of flood-basalt volcanism to mass extinctions. The group has a total volume of about 174,000 cu km and covers an area of about 164,000 sq km. It was erupted between 17.5 and 6 Ma, as measured by K-Ar and Ar-40/Ar-39 dates. Early eruptions formed the Imnaha Basalt. More than 85 percent of the group was produced during a 1.5 my period between 17 and 15.5 Ma, forming the Grande Ronde and greatly subordinate Picture Gorge Basalts.

Later flows formed the Wanapum Basalt, which includes the well-known Roza Member, and the Saddle Mountains Basalt. Linear vent systems for many of the flows are known and are located only in the eastern third of the Columbia Plateau. No systematic migration of vents occurred throughout the 11.5 my period of activity; this and other considerations make it unlikely that the province is related to a hot spot. Model calculations based on observations that little cooling occurred during flow of hundreds of kilometers suggest eruption and emplacement durations of a few days. Some voluminous flows occur in all formations, but most such flows apparently were erupted during Grande Ronde time. The eruption and emplacement of more than 1,000 cu km of 1100 C basaltic lava on the surface within several days doubtless had at least local meteorologic effects. Whether the effects were broader can at present only be hypothesized. Grande Ronde Basalt and Picture Gorge Basalts contain moderately common but thin sedimentary interbeds between flows, whereas earlier and later formations contain numerous, locally thick sediment accumulations. Volcaniclastic debris derived from extra-plateau sources commonly occurs in the testbeds. Author

N89-21394*# Forest Service, Corvallis, OR.
PROXIMAL ECOLOGICAL EFFECTS OF THE 1980 ERUPTIONS OF MOUNT ST. HELENS **c45**
F. J. Swanson *In* Lunar and Planetary Inst., Global Catastrophes in Earth History: An Interdisciplinary Conference on Impacts, Volcanism, and Mass Mortality 1988 p 188-189 (For primary document see N89-21287 14-42)
Avail: NTIS HC A11/MF A01 CSCL 13B

The diversity of ecosystems and volcanic processes involved in the 1980 eruptions of Mount St. Helens, southwest Washington, provide an excellent setting for examining effects of volcanic events on ecosystems. These eruptions included a lateral blast, debris avalanche, mudflows, pyroclastic flows, and airfall tephra. Affected ecosystems within 30 km of the vent were lakes, streams, upland and riparian forest, and meadows. Ecological disturbances imposed by the Mount St. Helens events were predominantly physical, rather than climatic or chemical which are the dominant classes of disturbances considered in analysis of global catastrophes. Analysis of ecosystem response to disturbance should be based on consideration of composition and structure of the predisturbance system in terms that represent potential survivability of organisms, mechanisms in the primary disturbance, initial survivors, secondary disturbances arising from the primary disturbance and the biological responses to secondary disturbances, invasion of the site by new propagules, interactions among secondary disturbance processes and surviving and invading organisms. Predicting ecosystem response to disturbance is enchanced by considering the mechanisms of disturbance rather than type of disturbance. In the 1980 Mount St. Helens events, the disturbance types, involved primarily the mechanisms of sedimentation, heating, and shear stress. Each disturbance type involved one or more mechanisms. Ecosystem response varied greatly across the landscape. Analysis of ecosystem response to disturbance, regardless of type, should include detailed consideration of the properties of individual species, primary and secondary disturbance mechanisms, and their distributions across landscapes. Author

N89-21395*# Geological Survey of Canada, Calgary (Alberta).
A REGIONAL PERSPECTIVE ON THE PALYNOFLORAL RESPONSE TO K-T BOUNDARY EVENT(S) WITH EMPHASIS ON VARIATIONS IMPOSED BY THE EFFECTS OF SEDIMENTARY FACIES AND LATITUDE **c46**
A. R. Sweet *In* Lunar and Planetary Inst., Global Catastrophes in Earth History: An Interdisciplinary Conference on Impacts, Volcanism, and Mass Mortality 1988 p 190-191 (For primary document see N89-21287 14-42)
Avail: NTIS HC A11/MF A01 CSCL 08G

Palynological studies deal with fossil reproductive bodies that were produced by fully functioning plants, whereas most faunal studies are based on death assemblages. Therefore, changes in pollen and spore assemblages cannot be used directly as evidence of catastrophic mass killings but only to indicate changes in ecological conditions. The impact of the Cretaceous-Tertiary boundary event on terrestrial plant communities is illustrated by the degree, rate and selectivity of change. As in most classical palynological studies, the degree of change is expressed in terms of relative abundance and changes in species diversity. It is recognized that sampling interval and continuity of the rock record within individual sections can affect the percieved rate of change. Even taking these factors into account, a gradual change in relative abundance and multiple levels of apparent extinctions, associated with the interval bounding the K-T boundary, can be demonstrated. Climatic change, which locally exceeds the tolerance of individual species, and the possible loss of a group of pollinating agents are examined as possible explanations for the selectivity of apparent extinctions and/or locally truncated occurrences. The aspects of change are demonstrated with data from four different K-T boundary localities in Western Canada between paleolatitudes 60 and 75 deg north. Together, the four localities discussed allow changes imposed by latitude and differences in the depositional environment be isolated from the boundary event itself which is reflected by the truncated ranges of several species throughout the region of study. What must be recognized is that variations in the response of vegetation to the K-T boundary event(s) occurred throughout the Western Interior basin. Author

N89-21396*# Wesleyan Univ., Middletown, CT. Dept. of Earth and Environmental Sciences.
MASS EXTINCTIONS IN THE DEEP SEA **c51**
E. Thomas *In* Lunar and Planetary Inst., Global Catastrophes in Earth History: An Interdisciplinary Conference on Impacts, Volcanism, and Mass Mortality 1988 p 192-193 (For primary document see N89-21287 14-42)
Avail: NTIS HC A11/MF A01 CSCL 06B

The character of mass extinctions can be assessed by studying extinction patterns of organisms, the fabric of the extinction, and assessing the environmental niche and mode of life of survivors. Deep-sea benthic foraminifera have been listed as little affected by the Cretaceous-Tertiary (K-T) mass extinction, but very few quantitative data are available. New data on deep-sea Late Maestrichtian-Eocene benthic foraminifera from Maud Rise (Antractica) indicate that about 10 percent of the species living at depths of 2000 to 2500 m had last appearances within 1 my of the Cretaceous-Tertiary (K-T) boundary, versus about 25 percent of species at 1000 to 1500 m. Many survivors from the Cretaceous became extinct in a period of global deep-sea benthic foraminiferal extinction at the end of the Paleocene, a time otherwise marked by very few extinctions. Preliminary conclusions suggest that the deep oceanic environment is essentially decoupled from the shallow marine and terrestrial environment, and that even major disturbances of one of these will not greatly affect the other. This gives deep-sea benthic faunas a good opportunity to recolonize shallow environments from greater depths and vice versa after massive extinctions. The decoupling means that data on deep-sea benthic boundary was caused by the environmental effects of asteriod impact or excessive volcanism. The benthic foraminiferal data strongly suggest, however, that the environmental results were strongest at the Earth's surface, and that there was no major disturbance of the deep ocean; this pattern might result both from excessive volcanism and from an impact on land. Author

N89-21397*# National Center for Atmospheric Research, Boulder, CO.
MULTI-YEAR GLOBAL CLIMATIC EFFECTS OF ATMOSPHERIC DUST FROM LARGE BOLIDE IMPACTS
Abstract Only **c45**
Starley L. Thompson *In* Lunar and Planetary Inst., Global Catastrophes in Earth History: An Interdisciplinary Conference on Impacts, Volcanism, and Mass Mortality 1988 p 194 (For primary document see N89-21287 14-42)
Avail: NTIS HC A11/MF A01 CSCL 13B

The global climatic effects of dust generated by the impact of a 10 km-diameter bolide was simulated using a one-dimensional (vertical only) globally-averaged climate model by Pollack et al. The goal of the simulation is to examine the regional climate

effects, including the possibility of coastal refugia, generated by a global dust cloud in a model having realistic geographic resolution. The climate model assumes the instantaneous appearance of a global stratospheric dust cloud with initial optical depth of 10,000. The time history of optical depth decreases according to the detailed calculations of Pollack et al., reaching an optical depth of unity at day 160, and subsequently decreasing with an e-folding time of 1 year. The simulation is carried out for three years in order to examine the atmospheric effects and recovery over several seasons. The simulation does not include any effects of NOx, CO2, or wildfire smoke injections that may accompany the creation of the dust cloud. The global distribution of surface temperature changes, freezing events, precipitation and soil moisture effects and sea ice increases will be discussed. Author

N89-21398*# National Center for Atmospheric Research, Boulder, CO.

ACUTE EFFECTS OF A LARGE BOLIDE IMPACT SIMULATED BY A GLOBAL ATMOSPHERIC CIRCULATION MODEL
Abstract Only **c45**

Starley L. Thompson and P. J. Crutzen *In* Lunar and Planetary Inst., Global Catastrophes in Earth History: An Interdisciplinary Conference on Impacts, Volcanism, and Mass Mortality 1988 p 195 Prepared in cooperation with Max-Planck-Inst. fuer Chemie, Mainz (Federal Republic of Germany) (For primary document see N89-21287 14-42)
Avail: NTIS HC A11/MF A01 CSCL 13B

The goal is to use a global three-dimensional atmospheric circulation model developed for studies of atmospheric effects of nuclear war to examine the time evolution of atmospheric effects from a large bolide impact. The model allows for dust and NOx injection, atmospheric transport by winds, removal by precipitation, radiative transfer effects, stratospheric ozone chemistry, and nitric acid formation and deposition on a simulated Earth having realistic geography. Researchers assume a modest 2 km-diameter impactor of the type that could have formed the 32 km-diameter impact structure found near Manson, Iowa and dated at roughly 66 Ma. Such an impact would have created on the order of 5 x 10 to the 10th power metric tons of atmospheric dust (about 0.01 g cm(-2) if spread globally) and 1 x 10 to the 37th power molecules of NO, or two orders of magnitude more stratospheric NO than might be produced in a large nuclear war. Researchers ignore potential injections of CO2 and wildfire smoke, and assume the direct heating of the atmosphere by impact ejecta on a regional scale is not large compared to absorption of solar energy by dust. Researchers assume an impact site at 45 N in the interior of present day North America. Author

N89-21399*# Forest Service, Flagstaff, AZ.

EFFECTS OF GLOBAL ATMOSPHERIC PERTURBATIONS ON FOREST ECOSYSTEMS: PREDICTIONS OF SEASONAL AND CUMULATIVE EFFECTS **c45**

R. W. Tinus and D. J. Roddy (Geological Survey, Flagstaff, AZ.) *In* Lunar and Planetary Inst., Global Catastrophes in Earth History: An Interdisciplinary Conference on Impacts, Volcanism, and Mass Mortality 1988 p 196-197 (For primary document see N89-21287 14-42)
Avail: NTIS HC A11/MF A01 CSCL 13B

The physical effects of certain large events, such as giant impacts, explosive volcanism, or combined nuclear explosions, have the potential of inducing global catastrophes in our terrestrial environment. Such highly energetic events can inject substantial quantities of material into the atmosphere. In turn, this changes the amount of sunlight reaching the Earth's surface and modifies atmospheric temperatures to produce a wide range of global effects. One consequence is the introduction of serious stresses in both plants and animals throughout the Earth's biosphere. For example, recent studies predict that forest lands, crop lands, and range lands would suffer specific physical and biological degradations if major physical and chemical disruptions occurred in our atmosphere. Forests, which cover over 4 times 10 to the 9th power hectares (4 times 10 to the 7th power sq km) of our planet, or about 3 times the area now cultivated for crops, are critical to many processes in the biosphere. Forests contribute heavily to the production of atmospheric oxygen, supply the major volume of biomass, and provide a significant percentage of plant and animal habitats. Author

N89-21400*# Witwatersrand Univ., Johannesburg (South Africa). Centre for Nuclear Sciences.

GEOCHEMICAL COMPARISON OF K-T BOUNDARIES FROM THE NORTHERN AND SOUTHERN HEMISPHERES **c46**

M. Tredous, B. Th. Verhagen, R. J. Hart, C. B. DeWit, C. B. Smith, K. Perch-Nielsen, and J. P. F. Sellschop *In* Lunar and Planetary Inst., Global Catastrophes in Earth History: An Interdisciplinary Conference on Impacts, Volcanism, and Mass Mortality 1988 p 198-199 (For primary document see N89-21287 14-42)
Avail: NTIS HC A11/MF A01 CSCL 08G

Closely spaced (cm-scale) traverses through the K-T boundary at Stevns Klint (Denmark), Woodside Creek (New Zealand) and a new Southern Hemisphere site at Richards Bay (South Africa) were subjected to trace element and isotopic (C, O, Sr) investigation. Intercomparison between these data-sets, and correlation with the broad K-T database available in the literature, indicate that the chemistry of the boundary clays is not globally constant. Variations are more common than similarities, both of absolute concentrations, and interelement ratios. For example, the chondrite normalized platinum-group elements (PGE) patterns of Stevns Klint are not like those of Woodside Creek, with the Pt/Os ratios showing the biggest variation. These differences in PGE patterns are difficult to explain by secondary alteration of a layer that was originally chemically homogeneous, especially for elements of such dubious crustal mobility as Os and Ir. The data also show that enhanced PGE concentrations, with similar trends to those of the boundary layers, occur in the Cretaceous sediments below the actual boundary at Stevns Klint and all three the New Zealand localities. This confirms the observations of others that the geochemistry of the boundary layers apparently does not record a unique component. It is suggested that terrestrial processes, eg. an extended period of Late Cretaceous volcanism can offer a satisfactory explanation for the features of the K-T geochemical anomaly. Such models would probably be more consistent with the observed stepwise, or gradual, palaeontological changes across this boundary, than the instant catastrophe predicated by the impact theory. Author

N89-21401*# Wisconsin Univ., Madison. Dept. of Meteorology.

A 3-DIMENSIONAL NUMERICAL SIMULATION OF THE ATMOSPHERIC INJECTION OF AEROSOLS BY A HYPOTHETICAL BASALTIC FISSURE ERUPTION **c45**

Gregory J. Tripoli and Starley L. Thompson *In* Lunar and Planetary Inst., Global Catastrophes in Earth History: An Interdisciplinary Conference on Impacts, Volcanism, and Mass Mortality 1988 p 200-201 Prepared in cooperation with National Center for Atmospheric Research Boulder, CO (For primary document see N89-21287 14-42)
Avail: NTIS HC A11/MF A01 CSCL 13B

Researchers simulated the atmospheric response to a hypothetical basaltic fissure eruption using heating rates based on the Roza flow eruption. The simulation employs the Colorado State University Regional Atmospheric Model (RAMS) with scavenging effects. The numerical model is a three-dimensional non-hydrostatic time-split compressible cloud/mesoscale model. Explicit microphysics include prediction of cloud, rain, crystal, and hail precipitation types. Nucleation and phoretic scavenging are predicted assuming that the pollutant makes an effective cloud droplet nucleus. Smoke is carried as a passive tracer. Long and short wave radiation heating tendencies, including the effects of the smoke, are parameterized. The longwave emission by the lava surface is neglected in the parameterization and included as an explicit heating term instead. A regional scale domain of 100 x 100 km in the horizontal and 22 km high is used. The horizontal grid spacing is taken to be 2 km and the vertical spacing is taken to be 0.75 km. The initial atmospheric state is taken to be horizontally homogenous and based on the standard atmospheric

sounding. The fissure is assumed to be 90 km long and oriented in a zig/zag pattern. Author

N89-21402*# Yale Univ., New Haven, CT. Dept. of Geology and Geophysics.
THE CAUSES FOR GEOGRAPHICAL VARIATIONS IN OS187/OS186 AT THE CRETACEOUS-TERTIARY BOUNDARY Abstract Only **c46**
K. K. Turekian, B. K. Esser, and G. E. Ravizza *In* Lunar and Planetary Inst., Global Catastrophes in Earth History: An Interdisciplinary Conference on Impacts, Volcanism, and Mass Mortality 1988 p 202-203 (For primary document see N89-21287 14-42)
Avail: NTIS HC A11/MF A01 CSCL 08G

Researchers at Yale has approached the problem of the osmium isotopic composition of marine deposits formed in contact with both oxidized and reduced bottom waters. The measured (187) Os/(186) Os ratios of modern bulk sediment can be explained using mixing equations involving continental detrital, volcaniclastic, cosmogenic and hydrogeneous components. These studies show that sediments deposited under reducing marine conditions contain a hydrogenous component which is enriched in Re and has a radiogenic (187) Os/(186) Os ratio. The presence of such a hydrogenous component in the marine fish clay at Stevns Klint can account for the elevation of its (187) Os/(186) Os ration above the expected meteoritic value. Mass balance considerations require the Re/Os ratio of the phase precipitated from the terminal Cretaceous sea at Stevns Klint to have been about one tenth the value observed in contemporary deposits in the Black Sea, assuming Re has not been lost (or Os gained) subsequent to precipitation. In continental sections, the elevation of the (187) Os/(186) Os ratio in boundary layers may be due to precipitation from continental waters of crustally-derived radiogenic osmium either contemporaneous with the meteoritic (or mantle) osmium deposition or later during diagenesis. Author

N89-21403*# Arizona Univ., Tucson. Lunar and Planetary Lab.
ATMOSPHERIC EROSION BY IMPACTS: AN ANALYTIC INVESTIGATION **c45**
A. M. Vickery and H. J. Melosh *In* Lunar and Planetary Inst., Global Catastrophes in Earth History: An Interdisciplinary Conference on Impacts, Volcanism, and Mass Mortality 1988 p 204-205 (For primary document see N89-21287 14-42)
Avail: NTIS HC A11/MF A01 CSCL 13B

Until recently, models for the origin and evolution of the atmospheres of terrestrial planets ignored the effects of accretionary impacts. In the 1970's, however, it was suggested that heating and/or vaporization of accreting carbonaceous-chondrite-type planetesimals could result in the release of their volatile components. Modeling of this process strongly suggests that substantial atmospheres/hydrospheres could develop this way. During most of the accretionary process, impact velocities generally differed little from the escape velocity of the growing proto-planet because most of the collisions were between bodies in nearly matching orbits. Toward the end of accretion, however, collisions were rarer but much more energetic, involving large planetesimals and higher impact velocities. It has been postulated that such impacts result in a net loss of atmosphere from a planet, and that the cumulative effect impacts during the period of heavy bombardment might have dramatically depleted the original atmospheres. Author

N89-21404*# Washington Univ., Seattle. Dept. of Geological Sciences.
MACROFOSSIL EXTINCTION PATTERNS AT BAY OF BISCAY CRETACEOUS-TERTIARY BOUNDARY SECTIONS **c51**
Peter D. Ward and Kenneth MacLeod *In* Lunar and Planetary Inst., Global Catastrophes in Earth History: An Interdisciplinary Conference on Impacts, Volcanism, and Mass Mortality 1988 p 206-207 (For primary document see N89-21287 14-42)
Avail: NTIS HC A11/MF A01 CSCL 06B

Researchers examined several K-T boundary cores at Deep Sea Drilling Project (DSDP) core repositories to document biostratigraphic ranges of inoceramid shell fragments and prisms. As in land-based sections, prisms in the deep sea cores disappear well before the K-T boundary. Ammonites show a very different extinction pattern than do the inoceramids. A minimum of seven ammonite species have been collected from the last meter of Cretaceous strata in the Bay of Biscay basin. In three of the sections there is no marked drop in either species numbers or abundance prior to the K-T boundary Cretaceous strata; at the Zumaya section, however, both species richness and abundance drop in the last 20 m of the Cretaceous, with only a single ammonite specimen recovered to date from the uppermost 12 m of Cretaceous strata in this section. Researchers conclude that inoceramid bivalves and ammonites showed two different times and patterns of extinction, at least in the Bay of Biscay region. The inoceramids disappeared gradually during the Early Maestrichtian, and survived only into the earliest Late Maestrichtian. Ammonites, on the other hand, maintained relatively high species richness throughout the Maestrichtian, and then disappeared suddenly, either coincident with, or immediately before the microfossil extinction event marking the very end of the Cretaceous. Author

N89-21405*# California Univ., Los Angeles.
TEKTITES: ORIGIN AS MELTS PRODUCED BY THE IMPACT OF SMALL PROJECTILES ONTO DRY TARGETS Abstract Only **c46**
John T. Wasson *In* Lunar and Planetary Inst., Global Catastrophes in Earth History: An Interdisciplinary Conference on Impacts, Volcanism, and Mass Mortality 1988 p 208 (For primary document see N89-21287 14-42)
Avail: NTIS HC A11/MF A01 CSCL 08G

The formation of tektites in general and layered tektites in particular seems to require a very special kind of cratering event. Evidence for the formation of pools of melt free of unmelted clasts has not been reported for the well-studied terrestrial craters such as Manicouagan or Ries. It is suggested that large amounts of relict-free melt were produced only when a sizeable fraction of the cratered target consisted of dry, high-porosity materials such as aeolian sediments. Since dry, high-porosity target materials are always confined to the outer 100 to 200 m of the Earth, the fraction of melt produced melt is probably higher in small (radius 50 to 500 m) craters than in large (r greater than 1 km) craters. Another reason to infer that the Southeast Asian tektites were produced in a multitude of small craters is the wide distribution of layered tektites. The file spans at least 1200 km, which would require ballistic ejection at velocities greater than 2 km s(-1) if all melt was generated in a single crater. It seems impossible to devise a scenario that would lead to the deposition of primary melt as a crystal-free pool at a distance of 600 km from the crater. Author

N89-21406*# Alabama Univ., Birmingham. Dept. of Physics.
HEAVY METAL TOXICITY AS A KILL MECHANISM IN IMPACT CAUSED MASS EXTINCTIONS **c51**
T. J. Wdowiak, S. A. Davenport, D. D. Jones, and P. Wdowiak (Wdowiak, P., Birmingham, AL) *In* Lunar and Planetary Inst., Global Catastrophes in Earth History: An Interdisciplinary Conference on Impacts, Volcanism, and Mass Mortality 1988 p 209-210 (For primary document see N89-21287 14-42)
Avail: NTIS HC A11/MF A01 CSCL 06B

Heavy metals that are known to be toxic exist in carbonaceous chrondrites at abundances considerably in excess to that of the terrestrial crust. An impactor of relatively undifferentiated cosmic matter would inject into the terrestrial environment large quantities of toxic elements. The abundances of toxic metals found in the Allende CV carbonaceous chondrite and the ratio of meteoritic abundance to crustal abundance are: Cr, 3630 PPM, 30X; Co, 662 PPM, 23X; ni, 13300 PPm, 134X; se, 8.2 PPM, 164X; Os, 0.828 PPM, 166X. The resulting areal density for global dispersal of impactor derived heavy metals and their dilution with terrestrial ejecta are important factors in the determination of the significance of impactor heavy metal toxicity as a kill mechanism in impact caused mass extinctions. A 10 km-diameter asteroid having a

density of 3 gram per cu cm would yield a global areal density of impact dispersed chondritic material of 3 kg per square meter. The present areal density of living matter on the terrestrial land surface is 1 kg per square meter. Dilution of impactor material with terrestrial ejecta is determined by energetics, with the mass of ejecta estimated to be in the range of 10 to 100 times that of the mass of the impactor. Because a pelagic impact would be the most likely case, the result would be a heavy metal rainout.
Author

N89-21407*# Jet Propulsion Lab., California Inst. of Tech., Pasadena.
THE COMETARY AND ASTEROIDAL IMPACTOR FLUX AT THE EARTH **c90**
Paul R. Weissman *In* Lunar and Planetary Inst., Global Catastrophes in Earth History: An Interdisciplinary Conference on Impacts, Volcanism, and Mass Mortality 1988 p 211-212 (For primary document see N89-21287 14-42)
Avail: NTIS HC A11/MF A01 CSCL 03B

The cratering records on the Earth and the lunar maria provide upper limits on the total impactor flux at the Earth's orbit over the past 600 Myr and the past 3.3 Gyr, respectively. These limits can be compared with estimates of the expected cratering rate from observed comets and asteroids in Earth-crossing orbits, corrected for observational selection effects and incompleteness, and including expected temporal variations in the impactor flux. Both estimates can also be used to calculate the probability of large impacts which may result in biological extinction events on the Earth. The estimated cratering rate on the Earth for craters greater than 10 km-diameter, based on counted craters on dated surfaces is 2.2 + or - 1.1 x 10 to the minus 14th power km(-2) yr(-1) (Shoemaker et al., 1979). Using a revised mass distribution for cometary nuclei based on the results of the spacecraft flybys of Comet Halley in 1986, and other refinements in the estimate of the cometary flux in the terrestrial planets zone, it is now estimated that long-period comets account for 11 percent of the cratering on the Earth (scaled to the estimate above), and short-period comets account for 4 pct (Weissman, 1987). However, the greatest contribution is from large but infrequent, random cometary showers, accounting for 22 pct of the terrestrial cratering. Author

N89-21408*# University of Southwestern Louisiana, Lafayette. Dept. of Physics.
DISRUPTION OF GIANT COMETS IN THE SOLAR SYSTEM AND AROUND OTHER STARS **c90**
D. P. Whitmire and J. J. Matese *In* Lunar and Planetary Inst., Global Catastrophes in Earth History: An Interdisciplinary Conference on Impacts, Volcanism, and Mass Mortality 1988 p 213-214 (For primary document see N89-21287 14-42)
Avail: NTIS HC A11/MF A01 CSCL 03B

In a standard cometary mass distribution (dN/dM) alpha M(-a), a = 1.5 to 2.0) most of the mass resides in the largest comets. The maximum mass M sub max for which this distribution holds uncertain but there are theoretical and observational indications that M sub max is at least approx. 10(23)g. Chiron, although formally classified as an asteroid, is most likely a giant comet in this mass range. Its present orbit is unstable and it is expected to evolve into a more typical short period comet orbit on a timescale of approx. 10(6) to 10(7)yr. The breakup of a chiron-like comet of mass approx. 10(23)g could in principle produce approx. 10(5) Halley-size comets, or a distribution with an even larger number. If a giant comet was in a typical short period comet orbit, such a breakup could result in a relatively brief comet shower (duration approx. less than 10(6)yr) with some associated terrestrial impacts. However, the most significant climatic effects may not in general be due to the impacts themselves but to the greatly enhanced zodiacal dust cloud in the inner Solar System. (Although this is probably not the case for the unique K-T impact). Researchers used a least Chi square program with error analysis to confirm that the 2 to 5 micrometer excess spectrum of Giclas 29 to 38 can be adequately fitted with either a disk of small inefficient (or efficient) grains or a single temperature black body. Further monitoring of this star may allow discrimination between these two models.
Author

N89-21409*# California Univ., Berkeley. Marine Science Group.
COLLISIONS WITH ICE-VOLATILE OBJECTS: GEOLOGICAL IMPLICATIONS **c46**
P. Wilde, M. S. Quinby-Hunt, and W. B. N. Berry *In* Lunar and Planetary Inst., Global Catastrophes in Earth History: An Interdisciplinary Conference on Impacts, Volcanism, and Mass Mortality 1988 p 215-216 (For primary document see N89-21287 14-42)
Avail: NTIS HC A11/MF A01 CSCL 08G

The collision of the Earth with extra-terrestrial ice-volatile bodies is proposed as a mechanism to produce rapid changes in the geologic record. These bodies would be analogs of the ice satellites found for the Jovian planets and suspected for comets and certain low density bodies in the Asteroid belt. Five generic end-members are postulated: (1) water ice; (2) dry ice: carbon-carbon dioxide rich, (3) oceanic (chloride) ice; (4) sulfur-rich ice; (5) ammonia hydrate-rich ice; and (6) clathrate: methane-rich ice. Due to the volatile nature of these bodies, evidence for their impact with the Earth would be subtle and probably best reflected geochemically or in the fossil record. Actual boloids impacting the Earth may have a variable composition, generally some admixture with water ice. However for discussion purposes, only the effects of a dominant component will be treated. The general geological effects of such collisions, as a function of the dominant component would be: (1) rapid sea level rise unrelated to deglaciation, (2) decreased oceanic pH and rapid climatic warming or deglaciation; (3) increased paleosalinities; (4) increased acid rain; (5) increased oceanic pH and rapid carbonate deposition; and (6) rapid climatic warming or deglaciation.
Author

N89-21410*# Florida State Univ., Tallahassee. Dept. of Geology.
EVIDENCE OF VOLCANIC ASH AT A K-T BOUNDARY SECTION: OCEAN DRILLING PROGRAM HOLE 690 C, MAUD RISE, WEDDELL SEA OFF EAST ANTARCTICA **c48**
S. W. Wise, N. Hamilton, J. Pospichal, P. F. Barker, James P. Kennett, S. OConnell, W. R. Bryant, L. H. Burckle, P. K. Egeberg, and D. K. Futterer et al *In* Lunar and Planetary Inst., Global Catastrophes in Earth History: An Interdisciplinary Conference on Impacts, Volcanism, and Mass Mortality 1988 p 217-218 Prepared in cooperation with Southampton Univ. (England) (For primary document see N89-21287 14-42)
Avail: NTIS HC A11/MF A01 CSCL 08C

Rare vitric volcanogenic ash but more abundant clay minerals considered volcanogenic in origin are associated with an expanded and essentially complete K-T boundary sequence from Ocean Drilling Project (ODP) Hole 690 C on Maud Rise in the Weddell Sea off East Antarctica. Results at this writing are preliminary and are still based to some extent on shipboard descriptions. Further shore-based studies are in progress. It would appear, however, that the presence of volcanic ash and altered ash in the Danian section beginning at the biostratigraphically and paleomagnetically determined K-T boundary on Maud Rise can be cited as evidence of significant volcanic activity within the South Atlantic-Indian Ocean sector of the Southern Ocean coincident with the time of biotic crises at the end of the Maestrichtian. This is a postulated time of tectonic and volcanic activity within this Southern Hemisphere region, including possible initiation of the Reunion hot spot and a peak in explosive volcanism on Walvis Ridge (1) among other events. A causal relationship with the biotic crisis is possible and volcanism should be given serious consideration as a testable working hypothesis to explain these extinctions.
Author

N89-21411*# Chicago Univ., IL. Dept. of Chemistry.
DARKNESS AFTER THE K-T IMPACT: EFFECTS OF SOOT **c45**
Wendy S. Wolbach, Edward Anders, and Charles J. Orth *In* Lunar and Planetary Inst., Global Catastrophes in Earth History: An Interdisciplinary Conference on Impacts, Volcanism, and Mass Mortality 1988 p 219-220 Prepared in cooperation with Los

Alamos National Lab., NM (For primary document see N89-21287 14-42)
Avail: NTIS HC A11/MF A01 CSCL 13B

Dust from the K-T impact apparently settled from the atmosphere in less than 6 months, restoring sunlight to minimum photosynthesis levels in about 4 months. However, the discovery of a global soot component in the boundary clay makes it necessary to reconsider the problem, as soot particles not only are smaller (0.1 vs. about 0.5 micrometer) and thus settle more slowly, but also are better light absorbers (optical depth of 13 mg soot cm(-2) about 1800; and are more resistant to rainout. Still, the darkness cannot have lasted very much longer than 6 months, else no larger animals would have survived. Perhaps the soot coagulated with the rock dust and fell out with it. Evidence on this point may be sought at a relatively undisturbed K-T boundary site, such as Woodside Creek, N.Z. There the boundary clay and lowermost Tertiary strata are finely laminated and show large chemical and isotopic differences on a millimeter scale, apparently representing a detailed time sequence. Researchers studied a 3 m section across the boundary at this site, analyzing the principal forms of carbon (soot, elemental C, kerogen, and carbonate) as well as 33 elements. Correlations among the elements were sought. Apparently soot came early and coagulated with the ejecta, staying with them for the primary fallout and in the next 5 cm, but then parting company, perhaps due to size sorting. Author

N89-21412*# Rhode Island Univ., Narragansett. Graduate School of Oceanography.
THE CRETACEOUS-TERTIARY BOUNDARY MARINE EXTINCTION AND GLOBAL PRIMARY PRODUCTIVITY COLLAPSE **c51**
J. C. Zachos, M. A. Arthus, and W. E. Dean *In* Lunar and Planetary Inst., Global Catastrophes in Earth History: An Interdisciplinary Conference on Impacts, Volcanism, and Mass Mortality 1988 p 221-222 Prepared in cooperation with Geological Survey, Denver, CO (For primary document see N89-21287 14-42)
Avail: NTIS HC A11/MF A01 CSCL 06B

The extinction of marine phyto-and zoo-plankton across the K-T boundary has been well documented. Such an event may have resulted in decreased photosynthetic fixation of carbon in surface waters and a collapse of the food chain in the marine biosphere. Because the vertical and horizontal distribution of the carbon isotopic composition of total dissolved carton (TDC) in the modern ocean is controlled by the transfer of organic carbon from the surface to deep reservoirs, it follows that a major disruption of the marine biosphere would have had a major effect on the distribution of carbon isotopes in the ocean. Negative carbon isotope excursions have been identified at many marine K-T boundary sequences worldwide and are interpreted as a signal of decreased oceanic primary productivity. However, the magnitude, duration and consequences of this productivity crisis have been poorly constrained. On the basis of planktonic and benthic calcareous microfossil carbon isotope and other geochemical data from DSDP Site 577 located on the Shatsky Rise in the north-central Pacific, as well as other sites, researchers have been able to provide a reasonable estimate of the duration and magnitude of this event. Author

N89-21413*# National Aeronautics and Space Administration. Ames Research Center, Moffett Field, CA.
IMPACT PRODUCTION OF NO AND REDUCED SPECIES **c45**
K. Zahnle, J. Kasting, and N. Sleep *In* Lunar and Planetary Inst., Global Catastrophes in Earth History: An Interdisciplinary Conference on Impacts, Volcanism, and Mass Mortality 1988 p 223-224 Prepared in cooperation with Stanford Univ., CA (For primary document see N89-21287 14-42)
Avail: NTIS HC A11/MF A01 CSCL 13B

It has recently been suggested that a reported spike in seawater (87)Sr/(86)Sr at the K-T boundary is the signature of an impact-generated acid deluge. However, the amount of acid required is implausibly large. Some about 3 x 10 to the 15th power moles of Sr must be weathered from silicates to produce the inferred Sr spike. The amount of acid required is at least 100 and probably 1000 times greater. Production of 3 x 10 to the 18th power moles of NO is clearly untenable. The atmosphere presently contains only 1.4 x 10 to the 20th power moles of N-sub 2 and 3.8 x 10 to the 19th power moles of O sub 2 If the entire atmosphere were shocked to 2000 K and cooled within a second, the total NO produced would be about 3 x 10 to the 18th power moles. This is obviously unrealistic. A (still to short) cooling time of 10th to the 3rd power sec reduces NO production by an order of magnitude. In passing, we note that if the entire atmosphere had in fact been shocked to 2000 K, acid rain would have been the least of a dinosaur's problems. Acid rain as a mechanism poses poses other difficulties. Recently deposited carbonates would have been most susceptable to acid attack. The researchers' preferred explanation is simply increased continental erosion following ecological trauma, coupled with enchanced levels of CO-sub 2. Author

N89-21414*# Academia Sinica, Beijing (China). Inst. of Geology.
NEW APPROACH TO THE ORIGIN OF THE TEKTITE IN CHINA **c90**
Zhang Qin-Wen, Xu Dao-Yi, and Yan Zheng *In* Lunar and Planetary Inst., Global Catastrophes in Earth History: An Interdisciplinary Conference on Impacts, Volcanism, and Mass Mortality 1988 p 225-226 Prepared in cooperation with State Seismological Bureau of China, Beijing (For primary document see N89-21287 14-42)
Avail: NTIS HC A11/MF A01 CSCL 03B

The tektites in China are distributed on the north part of Australia - Southeastern Asia strewfield of tektite: Leizhou Peninsula of Guangdong Province and Hainan Island, and located exactly at the boundary between Zanjiang Formation and Beihai Formation. A new hypothesis is suggested: During the end of Lower Pleistocene, a comet of special components from the outer part of the Solar System approached the Earth, and then it was captured by the Earth, when it came approximately to the Roche's limet. It was crushed into countless fragments, detritus and dusts, which rotated around the Earth, probably far above the Earth's atmosphere, as a cloud ring. Under the action of crushing energy they could be in the situation of liquid-melt drop in the almost vacuum circumstances and the flow and bubble structure were formed. During their rotation the climate became anomalous and the violet Fe-Si concentration were formed on the surface of sediments. After a rather short time of rotation the unstable ring was broken and the fragments impacted on the hard ground instantaneously. Author

43 EARTH RESOURCES AND REMOTE SENSING

Includes remote sensing of earth resources by aircraft and spacecraft; photogrammetry; and aerial photography.

For instrumentation see *35 Instrumentation and Photography.*

N89-21415# National Oceanic and Atmospheric Administration, Washington, DC. Assessment and Information Services Center.
ICE COVER ON CHESAPEAKE BAY FROM AVHRR (ADVANCED VERY HIGH RESOLUTION RADIOMETER) AND LANDSAT IMAGERY, WINTER OF 1987-88
Michael J. Dowgiallo, Martin C. Predoehl, and Richard P. Stumpf Jun. 1988 36 p
(PB89-117261; NOAA-TM-NESDIS-AISC-14) Avail: NTIS HC A03/MF A01 CSCL 08L

Ice cover on Chesapeake Bay during winter 1987-88 was analyzed using two types of satellite imagery and ice reconnaissance data from the U.S. Coast Guard. Multispectral Scanner (MSS) data from LANDSAT and Advanced Very High Resolution Radiometer (AVHRR) data from the NOAA TIROS-N polar-orbiting satellites were compared for usefullness in detection and evaluation of ice on Chesapeake Bay. Decreases in air

temperatures and surface water temperatures in the upper Bay are quantitatively linked to ice formation. Ice conditions during 1987-88, a near-normal winter in the Bay area, were compared to conditions in winter 1981-82, a much colder winter with more ice. Maximum ice cover was 14 percent during winter 1987-88 and 34 percent during winter 1981-82. GRA

N89-21416* Miami Univ., FL. Dept. of Marine Geology and Geophysics.
NEOTECTONICS IN CENTRAL MEXICO FROM LANDSAT TM DATA Final Report
Christopher G. A. Harrison and Christopher A. Johnson 15 Dec. 1988 136 p Original document contains color illustrations
(Contract NAS5-28745)
(NASA-CR-183416; NAS 1.26:183416) Avail: Issuing Activity CSCL 08B

A summary is presented of results from a Thematic Mapper survey of neotectonics in central Mexico, dealing specifically with faulting and its relationship to volcanism there. The Mexican Volcanic Belt (MVB) is the dominant physiographic province in the study area. Late Miocene to Quaternary calc-alkaline volcanics of the MVB have been generated by active subduction of the Cocos plate beneath Mexico along the Middle America (Acapulco) Trench. The results firmly establish a link between deformation in the overriding plate (expressed as neotectonic activity) and the distribution and character of volcanism in the MVB. Volcanism appears to be controlled by tectonics at all scales from local to regional. The large variation in eruption styles along the MVB may be explained as the result of the influence of various tectonic domains created by differential movement of crustal blocks above a zone of magma production. In addition to the neotectonic synthesis, problems and questions regarding much older deformation may be addressed in unusual ways using the TM images. Examples are given. Author

N89-21317*# National Aeronautics and Space Administration. Goddard Space Flight Center, Greenbelt, MD.
GEOLOGICAL REMOTE SENSING SIGNATURES OF TERRESTRIAL IMPACT CRATERS
J. B. Garvin, C. Schnetzler, and R. A. F. Grieve *In* Lunar and Planetary Inst., Global Catastrophes in Earth History: An Interdisciplinary Conference on Impacts, Volcanism, and Mass Mortality 1988 p 52-53 Prepared in cooperation with Geological Survey of Canada, Toronto (Ontario) (For primary document see N89-21287 14-42)
Avail: NTIS HC A11/MF A01 CSCL 08B

N89-21507# Army Engineer Waterways Experiment Station, Vicksburg, MS. Coastal Engineering Research Center.
THE KP EQUATION: A COMPARISON TO LABORATORY GENERATED BIPERIODIC WAVES
Norman W. Scheffner *In* Army Research Office, Transactions of the Fifth Army Conference on Applied Mathematics and Computing Mar. 1988 p 355-368 Presented at the 20th International Conference on Coastal Engineering, Taipei, Taiwan, 9-14 Nov. 1986 Submitted for publication (For primary document see N89-21490 14-59)
Avail: NTIS HC A99/MF E03 CSCL 08C

N89-21521# Army Engineer Waterways Experiment Station, Vicksburg, MS. Geotechnical Lab.
COLUMN MOVEMENT MODEL USED TO SUPPORT AMM
George B. McKinley *In* Army Research Office, Transactions of the Fifth Army Conference on Applied Mathematics and Computing Mar. 1988 p 601-616 (For primary document see N89-21490 14-59)
Avail: NTIS HC A99/MF E03 CSCL 08B

44 ENERGY PRODUCTION AND CONVERSION

Includes specific energy conversion systems, e.g., fuel cells; global sources of energy; geophysical conversion; and windpower.

For related information see also *07 Aircraft Propulsion and Power, 20 Spacecraft Propulsion and Power,* and *28 Propellants and Fuels.*

N89-21417*# National Aeronautics and Space Administration. Lewis Research Center, Cleveland, OH.
GAS TURBINE ALTERNATIVE FUELS COMBUSTION CHARACTERISTICS Final Report
R. James Rollbuhler Feb. 1989 27 p
(Contract DE-AI01-85CE-50111)
(NASA-TM-101470; E-4584; DOE/NASA/50111-3; NAS 1.15:101470) Avail: NTIS HC A03/MF A01 CSCL 21D

An experimental investigation was conducted to obtain combustion performance and exhaust pollutant concentrations for specific synthetic hydrocarbon fuels. Baseline comparison fuels used were gasoline and diesel fuel number two. Testing was done over a range of fuel to air mass ratios, total mass flow rates, and input combustion air temperatures in a flame-tube-type gas turbine combustor. Test results were obtained in terms of released heat and combustion gas emission values. The results were comparable to those obtained with the base fuels with variations being obtained with changing operating conditions. The release of carbon particles during the tests was minimal. Author

N89-21418# Department of Energy, Washington, DC. Office of Energy Storage and Distribution.
ELECTRIC ENERGY SYSTEMS ENERGY STORAGE
Feb. 1988 303 p
(DE88-007217; DOE/CE-30844/T1) Avail: NTIS HC A14/MF A01

The mission of the Office of Energy Storage and Distribution (OESD) is to lead a national research and development (R and D) effort to provide the basis for a range of technological options in energy storage, control, and delivery. These technology options will find application throughout the nation's electric utility, industrial, commercial, residential, and transportation sectors. Further, these technologies have strong ties to both renewable and conservation options which will play important roles in the future energy profile of the nation. The OESD research and technology development efforts are organized into programs in Electric Energy Systems and Energy Storage. The first two sections introduce the objectives of these two programs followed by project summaries for each program. Each of the two major programs is further organized into four major research areas. Each area is introduced separately and has a table of contents listing each project. Additionally, a section on Research Support and Integration lists and discusses projects necessary for overall support of program activities. Each project or task is presented as a separate entity. The project title is given first in the heading, followed by the name and location of the performing institution, the name(s) of the principal investigator(s), and the project or contract number. The text associated with each entry gives the formal objectives of the project, its current status with respect to those objectives, and relevant publications or sources of additional information. Author

N89-21419*# National Aeronautics and Space Administration. Lewis Research Center, Cleveland, OH.
CRYOGENIC REACTANT STORAGE FOR LUNAR BASE REGENERATIVE FUEL CELLS
Lisa L. Kohout 1989 30 p Presented at the International Conference on Space Power, Cleveland, OH, 5-7 Jun. 1989; sponsored by the International Astronautical Federation
(NASA-TM-101980; E-4679; NAS 1.15:101980) Avail: NTIS HC A03/MF A01 CSCL 10B

There are major advantages to be gained by integrating a cryogenic reactant storage system with a hydrogen-oxygen regenerative fuel cell (RFC) to provide on-site electrical power

during the lunar night. Although applicable to any power system using hydrogen-oxygen RFC's for energy storage, cryogenic reactant storage offers a significant benefit whenever the sun/shade cycle and energy storage period approach hundreds of hours. For solar power installations on the moon, cryogenic reactant storage reduces overall specific mass and meteoroid vulnerability of the system. In addition, it offers synergistic benefits to on-site users, such as availability of primary fuel cell reactants for surface rover vehicles and cryogenic propellants for OTV's. The integration involves processing and storing the RFC reactant streams as cryogenic liquids rather than pressurized gases, so that reactant containment (tankage per unit mass of reactants) can be greatly reduced. Hydrogen-oxygen alkaline RFC's, GaAs photovoltaic (PV) arrays, and space cryogenic processing/refrigeration technologies are assumed to be available for the conceptual system design. Advantages are demonstrated by comparing the characteristics of two power system concepts: a conventional lunar surface PV/RFC power system using pressurized gas storage in SOA filament wound pressure vessels and, that same system with gas liquefaction and storage replacing the pressurized storage. Comparisons are made at 20 and 250 kWe. Although cryogenic storage adds a processing plant (drying and liquefaction) to the system plus 30 percent more solar array to provide processing power, the approximate order of magnitude reduction in tankage mass, confirmed by this analysis, results in a reduction in overall total system mass of approximately 50 percent. Author

N89-21420# Midwest Research Inst., Golden, CO. Solar Energy Research Inst.
WIND ENERGY PROGRAM SUMMARY. VOLUME 1, OVERVIEW: FISCAL YEAR 1988
Feb. 1989 13 p
(Contract DE-AC02-83CH-10093)
(DE89-000856; DOE/CH-10093/41) Avail: NTIS HC A03/MF A01

The goal of the Federal Wind Energy Program is to establish, by supporting appropriate research, an advanced technology base that will assist industry in designing and producing wind turbines that can serve as an alternative energy supply. The Federal effort complements efforts in the private sector to develop wind systems that are safe, reliable, and cost effective. The wind program undertakes research in two general areas: the basic science of wind turbine dynamics, and research on advanced components and systems. Research on wind turbine dynamics includes atmospheric fluid dynamics, aerodynamics, and structural dynamics. The overall goal of these activities is to improve the understanding of the basic physical processes created by the wind turbine's interaction with the incoming wind, with particular emphasis on processes that affect energy capture and structural loading. Research in the advanced components and system areas includes improvements for rotors, such as advanced airfoils, and for generators, such as variable speed operation. The goal of these activities is to develop the technology base necessary for industry to achieve major improvements in wind turbine performance, lifetime, and capital cost. DOE

N89-21421# Department of Energy, Washington, DC. Geothermal Technology Div.
OCEAN ENERGY PROGRAM SUMMARY. VOLUME 1, OVERVIEW: FISCAL YEAR 1988
Feb. 1989 16 p
(Contract DE-AC02-83CH-10093)
(DE89-000858; DOE/CH-10093/43) Avail: NTIS HC A03/MF A01

Past studies conducted by the U.S. Department of Energy (DOE) have identified ocean thermal energy conversion (OTEC) as the largest potential contributor to U.S. energy supplies from the ocean resource. As a result, the OET Program concentrates on research to advance OTEC technology. The program also continues to monitor and study developments in wave energy, ocean current and salinity gradient concepts, but it is not actively developing these technologies at the present time. DOE

N89-21422# Department of Energy, Washington, DC. Geothermal Technology Div.
GEOTHERMAL ENERGY PROGRAM SUMMARY: VOLUME 1: OVERVIEW FISCAL YEAR 1988
Feb. 1989 27 p
(Contract DE-AC02-83CH-10093)
(DE89-000864; DOE/CH-10093/49) Avail: NTIS HC A03/MF A01

Geothermal energy is a here-and-now technology for use with dry steam resources and high-quality hydrothermal liquids. These resources are supplying about 6 percent of all electricity used in California. However, the competitiveness of power generation using lower quality hydrothermal fluids, geopressured brines, hot dry rock, and magma still depends on the technology improvements sought by the DOE Geothermal Energy R and D Program. The successful outcome of the R and D initiatives will serve to benefit the U.S. public in a number of ways. First, if a substantial portion of our geothermal resources can be used economically, they will add a very large source of secure, indigenous energy to the nation's energy supply. In addition, geothermal plants can be brought on line quickly in case of a national energy emergency. Geothermal energy is also a highly reliable resource, with very high plant availability. For example, new dry steam plants at The Geysers are operable over 99 percent of the time, and the small flash plant in Hawaii, only the second in the United States, has an availability factor of 98 percent. Geothermal plants also offer a viable baseload alternative to fossil and nuclear plants -- they are on line 24 hours a day, unaffected by diurnal or seasonal variations. The hydrothermal power plants with modern emission control technology have proved to have minimal environmental impact. The results to date with geopressured and hot dry rock resources suggest that they, too, can be operated so as to reduce environmental effects to well within the limits of acceptability. Preliminary studies on magma are also encouraging. In summary, the character and potential of geothermal energy, together with the accomplishments of DOE's Geothermal R and D Program, ensure that this huge energy resource will play a major role in future U.S. energy markets. DOE

N89-21423# Sandia National Labs., Albuquerque, NM.
THE POTENTIAL OF GaAs-BASED MECHANICALLY STACKED MULTIJUNCTION SOLAR CONCENTRATOR CELLS
J. M. Gee, C. J. Chiang, and D. L. King 1989 7 p Presented at the 4th International Photovoltaic Science and Engineering Conference, Sydney, Australia, 14 Feb. 1989
(Contract DE-AC04-76DP-00789)
(DE89-007975; SAND-88-2577C; CONF-890211-5) Avail: NTIS HC A02/MF A01

The potential performance of GaAs-based mechanically stacked, multijunction (MSMJ) solar concentrator cells in 500X and 1000X concentrator modules are analyzed. The module operating temperature of MSMJ cells is higher than that of single-junction cells due to the stacked cell construction, which reduces the expected performance advantages of MSMJ versus single-junction cells. DOE

N89-21424# Sandia National Labs., Albuquerque, NM. Photovoltaic Cell Research Div.
ESSENTIAL ELEMENTS IN THE NUMERICAL MODELING OF SOLAR CELLS
Paul A. Basore 1989 9 p Presented at the 4th International Photovoltaic Science and Engineering Conference, Sydney, Australia, 14 Feb. 1989
(Contract DE-AC04-76DP-00789)
(DE89-008113; SAND-88-3109C; CONF-890211-4) Avail: NTIS HC A02/MF A01

The use of computer-based numerical device simulators to model high-performance solar cells is reviewed. The approximations necessary to convert the fundamental equations into a form that can be solved numerically are presented, with techniques for including multidimensional effects in a one-dimensional model. DOE

45 ENVIRONMENT POLLUTION

Includes atmospheric, noise, thermal, and water pollution.

N89-21425*# ST Systems Corp., Hampton, VA.
OPERATIONAL IMPLICATIONS OF A CLOUD MODEL SIMULATION OF SPACE SHUTTLE EXHAUST CLOUDS IN DIFFERENT ATMOSPHERIC CONDITIONS Final Report
J. A. Zak Washington NASA Mar. 1989 78 p Prepared in cooperation with Mesoscale Environmen tal Simulations, Inc., Hampton, VA
(Contract NAS8-36715)
(NASA-CR-4222; NAS 1.26:4222) Avail: NTIS HC A05/MF A01 CSCL 13B

A three-dimensional cloud model was used to characterize the dominant influence of the environment on the Space Shuttle exhaust cloud. The model was modified to accept the actual heat and moisture from rocket exhausts and deluge water as initial conditions. An upper-air sounding determined the ambient atmosphere in which the cloud would grow. The model was validated by comparing simulated clouds with observed clouds from four actual Shuttle launches. Results are discussed with operational weather forecasters in mind. The model successfully produced clouds with dimensions, rise, decay, liquid water contents, and vertical motion fields very similar to observed clouds whose dimensions were calculated from 16 mm film frames. Once validated, the model was used in a number of different atmospheric conditions ranging from very unstable to very stable. Wind shear strongly affected the appearance of both the ground cloud and vertical column cloud. The ambient low-level atmospheric moisture governed the amount of cloud water in model clouds. Some dry atmospheres produced little or no cloud water. An empirical forecast technique for Shuttle cloud rise is presented and differences between natural atmospheric convection and exhaust clouds are discussed. Author

N89-21426*# ST Systems Corp., Hampton, VA.
A CLOUD MODEL SIMULATION OF SPACE SHUTTLE EXHAUST CLOUDS IN DIFFERENT ATMOSPHERIC CONDITIONS
C. Chen and J. A. Zak Washington NASA Mar. 1989 135 p Prepared in cooperation with Mesoscale Environmental Simulations, Inc., Hampton, VA
(Contract NAS8-36715)
(NASA-CR-4223; NAS 1.26:4223) Avail: NTIS HC A07/MF A01 CSCL 13B

A three-dimensional cloud model was used to characterize the dominant influence of the environment on the Space Shuttle exhaust cloud. The model was modified to accept the actual heat and moisture from rocket exhausts and deluge water as initial conditions. An upper-air sounding determined the ambient atmosphere in which the cloud could grow. The model was validated by comparing simulated clouds with observed clouds from four actual Shuttle launches. The model successfully produced clouds with dimensions, rise, decay, liquid water contents and vertical motion fields very similar to observed clouds whose dimensions were calculated from 16 mm film frames. Once validated, the model was used in a number of different atmospheric conditions ranging from very unstable to very stable. In moist, unstable atmospheres simulated clouds rose to about 3.5 km in the first 4 to 8 minutes then decayed. Liquid water contents ranged from 0.3 to 1.0 g kg-1 mixing ratios and vertical motions were from 2 to 10 ms-1. An inversion served both to reduce entrainment (and erosion) at the top and to prevent continued cloud rise. Even in the most unstable atmospheres, the ground cloud did not rise beyond 4 km and in stable atmospheres with strong low level inversions the cloud could be trapped below 500 m. Wind shear strongly affected the appearance of both the ground cloud and vertical column cloud. The ambient low-level atmospheric moisture governed the amount of cloud water in model clouds. Some dry atmospheres produced little or no cloud water. One case of a simulated TITAN rocket explosion is also discussed. Author

N89-21427# Battelle Memorial Inst., Richland, WA.
AIR QUALITY AND FOREST HEALTH ISSUES IN THE 1990s
W. Ted Hinds Oct. 1988 4 p Presented at the Northeastern Regional Meeting of the Pulp and Paper Manufacturers' National Council for Air and Stream Improvement, Boston, MA, 27 Oct. 1988
(Contract DE-AC06-76RL-01830)
(DE89-006941; PNL-SA-16628; CONF-8810301-1) Avail: NTIS HC A02/MF A01

Interactions of trace gases such as ozone, with forests and with climate stress forests, alter the earth's radiation budget, are increasing in concentration, and can affect the earth's climate. In such cases, three research questions arise regarding air quality: (1) What will change, and by how much, if global air quality induces a climatic change; (2) Where is the climate likely to change; and (3) How might man-made stresses or causative factors be altered to ameliorate or prevent such change. Environmental causes and consequences of human activities are linked together, and linked with natural processes. In this case, the linked concerns are fairly clear: industry, energy generation, and natural processes produce trace gas omissions; these emissions affect both stratospheric and tropospheric ozone concentrations and the earth's radiation budget; reductions in stratospheric ozone allow increases in surface UV-B flux, which is detrimental to both agricultural and forest productivity. Tropospheric ozone increases affect both acidic deposition and forest productivity, and the global effect of any climatic change will affect forest ecosystems and agroecosystems by likely alterations in temperature or rainfall patterns. DOE

N89-21428# Oak Ridge National Lab., TN. Environmental Sciences Div.
AN INDIVIDUAL-BASED FOREST ECOSYSTEMS MODEL FOR PROJECTING FOREST RESPONSE TO NUTRIENT CYCLING AND CLIMATE CHANGES
Wilfred M. Post and John Pastor (Minnesota Univ., Duluth.) 1988 21 p Presented at the IUFRO Forest Simulation Systems Conference, Berkeley, CA, 2 Nov. 1988
(Contract DE-AC05-84OR-21400)
(DE89-007212; CONF-8811173-1) Avail: NTIS HC A03/MF A01

Forest ecosystem control over nutrient cycling and response to climate change is explored using a model that simulates the annual establishment, growth, and death of individual trees. The aboveground populations dynamics are extended into the soil environment by tracking changes in carbon and nitrogen content of annual cohorts of litter. In this model, carbon and nitrogen cycles form a positive feedback loop because nitrogen cycling partially limits production and also depends on the amount and chemistry of carbon compounds produced. Temperature and soil water availability are constraints to population dynamics directly and through their feedbacks with soil nitrogen availability and light extinction. Embedding ecosystem feedbacks within a geological and climatological framework, we can expand our view of ecosystems from the stand level to the landscape and regional level. Our model, incorporating these feedbacks and constraints, can predict regional and global ecosystems responses to perturbations such as climate change. Species composition and population dynamics can have a large impact on forest productivity. Simulations of a boreal forest indicate that spruce declines observed for many North American forests can be caused by biotically induced changes in nutrient availability that result from an inverse relationship between litter quality and shade-tolerance of the dominant species. DOE

N89-21293*# University of Southern California, Los Angeles. Dept. of Chemistry.
CARBON DIOXIDE CATASTROPHES: PAST AND FUTURE MENACE
Mario E. Baur *In* Lunar and Planetary Inst., Global Catastrophes in Earth History: An Interdisciplinary Conference on Impacts, Volcanism, and Mass Mortality 1988 p 10-11 (For primary document see N89-21287 14-42)
Avail: NTIS HC A11/MF A01 CSCL 04A

N89-21298*# National Center for Atmospheric Research, Boulder, CO.
RESPONSE OF MARINE AND FRESHWATER ALGAE TO NITRIC ACID AND ELEVATED CARBON DIOXIDE LEVELS SIMULATING ENVIRONMENTAL EFFECTS OF BOLIDE IMPACT
P. J. Boston *In* Lunar and Planetary Inst., Global Catastrophes in Earth History: An Interdisciplinary Conference on Impacts, Volcanism, and Mass Mortality 1988 p 19-20 Prepared in cooperation with Colorado Univ., Boulder (For primary document see N89-21287 14-42)
Avail: NTIS HC A11/MF A01 CSCL 13B

N89-21306*# Lawrence Livermore National Lab., CA.
GLOBAL ENVIRONMENTAL EFFECTS OF IMPACT-GENERATED AEROSOLS: RESULTS FROM A GENERAL CIRCULATION MODEL Abstract Only
C. Covey, S. J. Ghan, and Paul R. Weissman *In* Lunar and Planetary Inst., Global Catastrophes in Earth History: An Interdisciplinary Conference on Impacts, Volcanism, and Mass Mortality 1988 p 33 Prepared in cooperation with Jet Propulsion Lab., California Inst. of Tech., Pasadena (For primary document see N89-21287 14-42)
Avail: NTIS HC A11/MF A01 CSCL 13B

N89-21308*# Applied Research Corp., College Station, TX.
ABRUPT CLIMATE CHANGE AND EXTINCTION EVENTS
Thomas J. Crowley *In* Lunar and Planetary Inst., Global Catastrophes in Earth History: An Interdisciplinary Conference on Impacts, Volcanism, and Mass Mortality 1988 p 36-37 (For primary document see N89-21287 14-42)
Avail: NTIS HC A11/MF A01 CSCL 13B

N89-21310*# Princeton Univ., NJ. Dept. of Geological and Geophysical Sciences.
AN EXTENDED CRETACEOUS-TERTIARY (K/T) STABLE ISOTOPE RECORD. IMPLICATIONS FOR PALEOCLIMATE AND THE NATURE OF THE K/T BOUNDARY EVENT
Steven DHondt *In* Lunar and Planetary Inst., Global Catastrophes in Earth History: An Interdisciplinary Conference on Impacts, Volcanism, and Mass Mortality 1988 p 40-41 (For primary document see N89-21287 14-42)
Avail: NTIS HC A11/MF A01 CSCL 13B

N89-21315*# Arizona Univ., Tucson. Dept. of Geosciences.
THE IMPACT OF MASS EXTINCTIONS
Karl W. Flessa *In* Lunar and Planetary Inst., Global Catastrophes in Earth History: An Interdisciplinary Conference on Impacts, Volcanism, and Mass Mortality 1988 p 49 Prepared in cooperation with National Science Foundation, Washington, DC (For primary document see N89-21287 14-42)
Avail: NTIS HC A11/MF A01 CSCL 13B

N89-21318*# Geological Survey of Canada, Toronto (Ontario).
THE FRASNIAN-FAMENNIAN MASS KILLING EVENT(S), METHODS OF IDENTIFICATION AND EVALUATION
H. H. J. Geldsetzer *In* Lunar and Planetary Inst., Global Catastrophes in Earth History: An Interdisciplinary Conference on Impacts, Volcanism, and Mass Mortality 1988 p 54-55 (For primary document see N89-21287 14-42)
Avail: NTIS HC A11/MF A01 CSCL 13B

N89-21335*# Bedford Inst. of Oceanography, Dartmouth (Nova Scotia). Atlantic Geoscience Centre.
MASS MORTALITY AND EXTRATERRESTRIAL IMPACTS
L. F. Jansa, F. M. Gradstein, and M. Pierre-Aubry *In* Lunar and Planetary Inst., Global Catastrophes in Earth History: An Interdisciplinary Conference on Impacts, Volcanism, and Mass Mortality 1988 p 85-86 (For primary document see N89-21287 14-42)
Avail: NTIS HC A11/MF A01 CSCL 13B

N89-21339*# National Center for Atmospheric Research, Boulder, CO.
WIDESPREAD HABITAT CHANGE THROUGH PALUDIFICATION AS AN INTERACTIVE MECHANISM IN MASS EXTINCTION EVENTS Abstract Only
L. F. Klinger *In* Lunar and Planetary Inst., Global Catastrophes in Earth History: An Interdisciplinary Conference on Impacts, Volcanism, and Mass Mortality 1988 p 92 (For primary document see N89-21287 14-42)
Avail: NTIS HC A11/MF A01 CSCL 13B

N89-21365*# California Inst. of Tech., Pasadena. Seismological Lab.
ENVIRONMENTAL EFFECTS OF LARGE IMPACTS ON THE EARTH; RELATION TO EXTINCTION MECHANISMS
John D. OKeefe, Thomas J. Ahrens, and Detlef Koschny *In* Lunar and Planetary Inst., Global Catastrophes in Earth History: An Interdisciplinary Conference on Impacts, Volcanism, and Mass Mortality 1988 p 133-134 (For primary document see N89-21287 14-42)
Avail: NTIS HC A11/MF A01 CSCL 13B

N89-21388*# Rhode Island Univ., Kingston. Graduate School of Oceanography.
ASSESSMENT OF THE ATMOSPHERIC IMPACT OF VOLCANIC ERUPTIONS
H. Sigurdsson *In* Lunar and Planetary Inst., Global Catastrophes in Earth History: An Interdisciplinary Conference on Impacts, Volcanism, and Mass Mortality 1988 p 177-178 (For primary document see N89-21287 14-42)
Avail: NTIS HC A11/MF A01 CSCL 13B

N89-21392*# California Univ., Santa Barbara. Marine Science Inst.
CRETACEOUS-TERTIARY BOUNDARY IN THE ANTARCTIC: CLIMATIC COOLING PRECEDES BIOTIC CRISIS
Lowell D. Stott and James P. Kennett *In* Lunar and Planetary Inst., Global Catastrophes in Earth History: An Interdisciplinary Conference on Impacts, Volcanism, and Mass Mortality 1988 p 184-185 (For primary document see N89-21287 14-42)
Avail: NTIS HC A11/MF A01 CSCL 13B

N89-21394*# Forest Service, Corvallis, OR.
PROXIMAL ECOLOGICAL EFFECTS OF THE 1980 ERUPTIONS OF MOUNT ST. HELENS
F. J. Swanson *In* Lunar and Planetary Inst., Global Catastrophes in Earth History: An Interdisciplinary Conference on Impacts, Volcanism, and Mass Mortality 1988 p 188-189 (For primary document see N89-21287 14-42)
Avail: NTIS HC A11/MF A01 CSCL 13B

N89-21397*# National Center for Atmospheric Research, Boulder, CO.
MULTI-YEAR GLOBAL CLIMATIC EFFECTS OF ATMOSPHERIC DUST FROM LARGE BOLIDE IMPACTS Abstract Only
Starley L. Thompson *In* Lunar and Planetary Inst., Global Catastrophes in Earth History: An Interdisciplinary Conference on Impacts, Volcanism, and Mass Mortality 1988 p 194 (For primary document see N89-21287 14-42)
Avail: NTIS HC A11/MF A01 CSCL 13B

N89-21398*# National Center for Atmospheric Research, Boulder, CO.
ACUTE EFFECTS OF A LARGE BOLIDE IMPACT SIMULATED BY A GLOBAL ATMOSPHERIC CIRCULATION MODEL Abstract Only
Starley L. Thompson and P. J. Crutzen *In* Lunar and Planetary Inst., Global Catastrophes in Earth History: An Interdisciplinary Conference on Impacts, Volcanism, and Mass Mortality 1988 p 195 Prepared in cooperation with Max-Planck-Inst. fuer Chemie, Mainz (Federal Republic of Germany) (For primary document see N89-21287 14-42)
Avail: NTIS HC A11/MF A01 CSCL 13B

N89-21399*# Forest Service, Flagstaff, AZ.
EFFECTS OF GLOBAL ATMOSPHERIC PERTURBATIONS ON FOREST ECOSYSTEMS: PREDICTIONS OF SEASONAL AND CUMULATIVE EFFECTS
R. W. Tinus and D. J. Roddy (Geological Survey, Flagstaff, AZ.) *In* Lunar and Planetary Inst., Global Catastrophes in Earth History: An Interdisciplinary Conference on Impacts, Volcanism, and Mass Mortality 1988 p 196-197 (For primary document see N89-21287 14-42)
Avail: NTIS HC A11/MF A01 CSCL 13B

N89-21401*# Wisconsin Univ., Madison. Dept. of Meteorology.
A 3-DIMENSIONAL NUMERICAL SIMULATION OF THE ATMOSPHERIC INJECTION OF AEROSOLS BY A HYPOTHETICAL BASALTIC FISSURE ERUPTION
Gregory J. Tripoli and Starley L. Thompson *In* Lunar and Planetary Inst., Global Catastrophes in Earth History: An Interdisciplinary Conference on Impacts, Volcanism, and Mass Mortality 1988 p 200-201 Prepared in cooperation with National Center for Atmospheric Research Boulder, CO (For primary document see N89-21287 14-42)
Avail: NTIS HC A11/MF A01 CSCL 13B

N89-21403*# Arizona Univ., Tucson. Lunar and Planetary Lab.
ATMOSPHERIC EROSION BY IMPACTS: AN ANALYTIC INVESTIGATION
A. M. Vickery and H. J. Melosh *In* Lunar and Planetary Inst., Global Catastrophes in Earth History: An Interdisciplinary Conference on Impacts, Volcanism, and Mass Mortality 1988 p 204-205 (For primary document see N89-21287 14-42)
Avail: NTIS HC A11/MF A01 CSCL 13B

N89-21411*# Chicago Univ., IL. Dept. of Chemistry.
DARKNESS AFTER THE K-T IMPACT: EFFECTS OF SOOT
Wendy S. Wolbach, Edward Anders, and Charles J. Orth *In* Lunar and Planetary Inst., Global Catastrophes in Earth History: An Interdisciplinary Conference on Impacts, Volcanism, and Mass Mortality 1988 p 219-220 Prepared in cooperation with Los Alamos National Lab., NM (For primary document see N89-21287 14-42)
Avail: NTIS HC A11/MF A01 CSCL 13B

N89-21413*# National Aeronautics and Space Administration. Ames Research Center, Moffett Field, CA.
IMPACT PRODUCTION OF NO AND REDUCED SPECIES
K. Zahnle, J. Kasting, and N. Sleep *In* Lunar and Planetary Inst., Global Catastrophes in Earth History: An Interdisciplinary Conference on Impacts, Volcanism, and Mass Mortality 1988 p 223-224 Prepared in cooperation with Stanford Univ., CA (For primary document see N89-21287 14-42)
Avail: NTIS HC A11/MF A01 CSCL 13B

46 GEOPHYSICS

Includes aeronomy; upper and lower atmosphere studies; ionospheric and magnetospheric physics; and geomagnetism.

For space radiation see *93 Space Radiation.*

N89-21429*# Northeast Radio Observatory Corp., Westford, Mass. Haystack Observatory. Haystack Observatory.
OBSERVATIONS OF NEUTRAL CIRCULATION AT MID-LATITUDES DURING THE EQUINOX TRANSITION STUDY
M. J. Buonsanto, J. E. Salah, K. L. Miller, W. L. Oliver, R. G. Burnside, and P. G. Richards (Alabama Univ., Huntsville.) [1988] 34 p
(Grants NAGw-996; NSF ATM-88-08137; NSF ATM-87-15367; NSF ATM-87-16036)
(NASA-CR-184792; NAS 1.26:184792) Avail: NTIS HC A03/MF A01 CSCL 04A

Measurements of ion drift velocity made by the Millstone Hill incoherent scatter radar have been used to calculate the meridional neutral wind velocity during the Sept. 17 to 24, 1984 period. Strong daytime southward neutral surges were observed during the magnetically disturbed days of September 19 and 23, in contrast to the small daytime winds obtained as expected during the magnetically quiet days. The surge on September 19 was also seen at Arecibo. In addition, two approaches have been used to calculate the meridional wind component from the radar-derived height of the F-layer electron density peak. Results confirm the wind surge, particularly when the strong electric fields measured during the disturbed days are included in the calculations. The two approaches for the F-layer peak wind calculations are applied to the radar-derived electron density peak height as a function of latitude to study the variation of the southward daytime surges with latitude. Author

N89-21430*# National Aeronautics and Space Administration. Goddard Space Flight Center, Greenbelt, MD.
RELATIONSHIPS OF EARTHQUAKES (AND EARTHQUAKE-ASSOCIATED MASS MOVEMENTS) AND POLAR MOTION AS DETERMINED BY KALMAN FILTERED, VERY-LONG-BASELINE-INTERFEROMETRY
Joseph Richard Mark Preisig Oct. 1988 254 p
(NASA-TM-100711; Rept-88B0254; NAS 1.15:100711) Avail: NTIS HC A12/MF A01 CSCL 08K

A Kalman filter was designed to yield optimal estimates of geophysical parameters from Very Long Baseline Interferometry (VLBI) group delay data. The geophysical parameters are the polar motion components, adjustments to nutation in obliquity and longitude, and a change in the length of day parameter. The VLBI clock (and clock rate) parameters and atmospheric zenith delay parameters are estimated simultaneously. Filter background is explained. The IRIS (International Radio Interferometric Surveying) VLBI data are Kalman filtered. The resulting polar motion estimates are examined. There are polar motion signatures at the times of three large earthquakes occurring in 1984 to 1986: Mexico, 19 September, 1985 (Magnitude M sub s = 8.1); Chile, 3 March, 1985 (M sub s = 7.8); and Taiwan, 14 November, 1986 (M sub s = 7.8). Breaks in polar motion occurring about 20 days after the earthquakes appear to correlate well with the onset of increased regional seismic activity and a return to more normal seismicity (respectively). While the contribution of these three earthquakes to polar motion excitations is small, the cumulative excitation due to earthquakes, or seismic phenomena over a Chandler wobble damping period may be significant. Mechanisms for polar motion excitation due to solid earth phenomena are examined. Excitation functions are computed, but the data spans are too short to draw conclusions based on these data. Author

N89-21431# National Geophysical Data Center, Boulder, CO.
SOLAR-GEOPHYSICAL DATA NUMBER 529, SEPTEMBER 1988. PART 1: (PROMPT REPORTS). DATA FOR AUGUST, JULY 1988 AND LATE DATA
Helen E. Coffey, ed. and John A. McKinnon, ed. Sep. 1988 139 p
(Contract N00014-86-F-0049)
(PB89-121305; SGD-529-Pt-1; ISSN-0038-0911; LC-79-640375)
Avail: NTIS HC A07/MF A01 CSCL 04A

Solar-geophysical information is presented in tabular and graphic form. Categories include data for July and August 1988; IUWDS alert periods (advance and worldwide); solar activity indices; solar flares: solar radio emission; solar interferometric charts; and Standford mean solar magnetic field. B.G.

N89-21432# National Geophysical Data Center, Boulder, CO.
SOLAR-GEOPHYSICAL DATA NUMBER 529, SEPTEMBER 1988. PART 2: (COMPREHENSIVE REPORTS). DATA FOR MARCH 1988
Helen E. Coffey, ed. and John A. McKinnon, ed. Sep. 1988 79 p
(Contract N00014-86-F-0049)
(PB89-121313; SGD-529-Pt-2; ISSN-0038-0911; LC-79-640374)
Avail: NTIS HC A05/MF A01 CSCL 04A

Solar-geophysical information is presented in tabular and graphic form. Categories include data for March 1988; Meudon

carte synoptique; solar flares; solar radio bursts at fixed frequencies; solar X-ray radiation from GOES satellite; mass ejections from the Sun; and active prominences and filaments. B.G.

N89-21433# National Center for Atmospheric Research, Boulder, CO. Atmospheric Technology Div.
FLUX AND SOUNDING DATA FROM THE NCAR (NATIONAL CENTER FOR ATMOSPHERIC RESEARCH) KING AIR AIRCRAFT DURING HAPEX (HYDROLOGIC ATMOSPHERIC PILOT EXPERIMENT)
Peter H. Hildebrand Sep. 1988 386 p
(Grant NSF ATM-87-09659)
(PB89-124481; NCAR/TN-319-STR) Avail: NTIS HC A17/MF A01 CSCL 04A

The technical Note presents the flux and sounding data collected by the NCAR King Air aircraft during the Hydrologic, Atmospheric Pilot Experiment (HAPEX). The major goal of HAPEX was measuring the hydrological budget and evaporation flux at the scale of a general circulation model grid square, i.e., 10(sup 4) km(sup 2). The NCAR King Air aircraft was operated in support of a two and one half month intensive observing period for the purpose of making detailed measurements of atmospheric fluxes. The Technical Note describes the operation of the NCAR King Air aircraft during HAPEX, the methods of processing the data, and presents a large portion of the data from the aircraft. Author

N89-21434*# National Aeronautics and Space Administration. Goddard Space Flight Center, Greenbelt, MD.
ON PRINCIPLES, METHODS AND RECENT ADVANCES IN STUDIES TOWARDS A GPS-BASED CONTROL SYSTEM FOR GEODESY AND GEODYNAMICS
Demitris Delikaraoglou Feb. 1989 114 p
(NASA-TM-100716; Rept-89B00058; NAS 1.15:100716) Avail: NTIS HC A06/MF A01 CSCL 08G

Although Very Long Baseline Interferometry (VLBI) and Satellite Laser Ranging (SLR) are becoming increasingly important tools for geodynamic studies, their future role may well be fulfilled by using alternative techniques such as those utilizing the signals from the Global Positioning System (GPS). GPS, without the full implementation of the system, already offers a favorable combination of cost and accuracy and has consistently demonstrated the capability to provide high precision densification control in the regional and local areas of the VLBI and SLR networks. This report reviews VLBI and SLR vis-a-vis GPS and outlines the capabilities and limitations of each technique and how their complementary application can be of benefit to geodetic and geodynamic operations. It demonstrates, albeit with a limited data set, that dual-frequency GPS observations and interferometric type analysis techniques make possible the modelling of the GPS orbits for several days with an accuracy of a few meters. The use of VLBI or SLR sites as fiducial stations together with refinements in the orbit determination procedures can greatly reduce the systematic errors in the GPS satellite orbits used to compute the positions of non-fiducial locations. In general, repeatability and comparison with VLBI of the GPS determined locations are of the order of between 2 parts in 10 to the 7th power and 5 parts in 10 to the 8th power for baseline lengths less than 2000 km. This report is mainly a synthesis of problems, assumptions, methods and recent advances in the studies towards the establishment of a GPS-based system for geodesy and geodynamics and is one phase in the continuing effort for the development of such a system. To some, including the author, it seems reasonable to expect within the next few years that more evidence will show GPS to be as a powerful and reliable a tool as mobile VLBI and SLR are today, but largely more economical. Author

N89-21435*# Scripps Institution of Oceanography, San Diego, CA. Inst. of Geophysics and Planetary Physics.
CONFIDENCE SET INFERENCE WITH A PRIOR QUADRATIC BOUND
George E. Backus 1989 102 p
(Grant NAG5-818)
(NASA-CR-184839; NAS 1.26:184839) Avail: NTIS HC A06/MF A01 CSCL 08G

In the uniqueness part of a geophysical inverse problem, the observer wants to predict all likely values of P unknown numerical properties z=(z sub 1,...,z sub p) of the earth from measurement of D other numerical properties y (sup 0) = (y (sub 1) (sup 0), ..., y (sub D (sup 0)), using full or partial knowledge of the statistical distribution of the random errors in y (sup 0). The data space Y containing y(sup 0) is D-dimensional, so when the model space X is infinite-dimensional the linear uniqueness problem usually is insoluble without prior information about the correct earth model x. If that information is a quadratic bound on x, Bayesian inference (BI) and stochastic inversion (SI) inject spurious structure into x, implied by neither the data nor the quadratic bound. Confidence set inference (CSI) provides an alternative inversion technique free of this objection. Confidence set inference is illustrated in the problem of estimating the geomagnetic field B at the core-mantle boundary (CMB) from components of B measured on or above the earth's surface. Author

N89-21436*# Massachusetts Inst. of Tech., Cambridge. Dept. of Earth, Atmospheric, and Planetary Sciences.
THE INTERPRETATION OF CRUSTAL DYNAMICS DATA IN TERMS OF PLATE MOTIONS AND REGIONAL DEFORMATION NEAR PLATE BOUNDARIES Semiannual Status Report No. 5, 22 Sep. 1988 - 21 Mar. 1989
Sean C. Solomon 6 Apr. 1989 91 p
(Grant NAG5-814)
(NASA-CR-180077; NAS 1.26:180077) Avail: NTIS HC A05/MF A01 CSCL 08G

A particularly detailed set of observations in the vicinity of an intraplate, thrust earthquake (M 7.4) in Argentina, indicate a cyclic pattern of deformation very similar to that reported previously for interplate earthquakes. This deformation cycle, which may be characteristic of many seismically active areas, consists of: (1) steady strain accumulation, possibly punctuated by strain reversals; (2) coseismic strain release; (3) a period of continued strain release due to afterslip (persisting for perhaps a year or so); and (4) rapid postseismic strain accumulation which decreases exponentially and grades into steady strain accumulation. Deformation associated with three earthquakes in the U.S. (1940, M7.1 Imperial Valley California; 1964, M8.4 Alaska; 1959, M7.5 Hebgen Lake, Montana) are interpreted in light of this general earthquake cycle and are used to investigate the mechanics of strain release for these events. These examples indicate that large postseismic movements can occur for strike-slip, thrust, and normal fault events, and both viscoelastic relaxation and postseismic after-slip must be incorporated in models of earthquake related deformation. The mechanics of the strain release process revealed by these examples has implications for estimating earthquake repeat times from geodetic observations near active faults. Author

N89-21437# Polytechnic Univ., Farmingdale, NY.
THE ROLE OF HYDROMAGNETIC WAVES IN THE MAGNETOSPHERE AND THE IONOSPHERE Final Report, 1 Feb. 1985 - 31 Jan. 1988
S. P. Kuo May 1988 121 p
(Grant AF-AFOSR-0133-85; AF Proj. 2311)
(AD-A202800; POLY-WRI-1537-88; AFOSR-88-1251TR) Avail: NTIS HC A06/MF A01 CSCL 04A

The topics of investigation are divided into four general categories: (1) cavity modes of the magnetosphere resulting in the discrete spectrum of the resonant ultralow frequency waves; (2) a hydromagnetic code for the numerical study of the coupling of hydromagnetic waves in the dipole model of the magnetosphere; (3) a theoretical model developed for explaining the phenomenon of plasma line over shoot observed in the ionospheric HF heating experiments; and (4) thermal flamentation instability as the mechanism for generation of large scale field aligned ionospheric irregularities. For the first two topics, the hydromagnetic wave equations are analyzed analytically in cylindrical model of the magnetosphere and numerically in dipole model of the

magnetosphere, respectively. While the steady state eigenvalue problem is studied in the first topic, the second topic is generalized to the boundary value problem considering the coupling between hydromagnetic waves in the realistic geometry of the magnetosphere. For the third topic, a nonlinear turbulent theory (resonance instability excited by a powerful high frequency in the ionosphere. For the last topic, the thermal nonlinearity gives rise to the mode-mode coupling; threshold field and the growth rate of the instability are derived. GRA

N89-21438# Lockheed Missiles and Space Co., Palo Alto, CA.
MECHANISMS FOR THE SOURCE AND LOSS OF ELECTRONS Progress Report, period ending 30 Nov. 1988
W. L. Imhof, D. W. Datlowe, H. D. Voss, and J. Mobilia 1988 21 p
(Contract N00014-88-C-0033)
(AD-A203066; LMSC/F247028) Avail: NTIS HC A03/MF A01 CSCL 04A

The objectives are to use available satellite particle and bremsstrahlung X-ray data as well as ground based measurements to evaluate the source and loss mechanisms for electrons trapped throughout the radiation belts. Effort has concentrated on compiling the existing electron precipitation data over a wide range of latitudes and comparing the electron data with available wave data. At midlatitudes extensive effort has been devoted to comparing the short duration bursts observed in the SEEP payload on the S81-1 satellite with narrow bursts in the wave data recorded. In several daytime cases general agreement was obtained between chorus wave emission and electron precipitation bursts, but one-to-one coincidences were not observed. The association of electron precipitation at nighttime with lightning generated whistlers is much better in several recently uncovered examples as well as earlier ones. A major contribution to the total electron precipitation rate is associated with those injected into the drift loss cone. Much of the flux observed in the drift loss cone is associated with the nearly monochromatic waves emitted from VLF transmitters, as indicated by narrow peaks in the energy spectra. Study of electron precipitation at high latitudes has benefited from use of bremsstrahlung X-ray data acquired on the SEEP payload as well as the P78-1 satellite. The X-ray spectrometers on P78-1 have been very useful for studying the electron precipitation that regularly occurs near the trapping boundary. GRA

N89-21439# Naval Ocean Systems Center, San Diego, CA.
UTILITY OF A DUAL-LIDAR METHOD TO MEASURE INTEGRATED EXTINCTION Final Report
M. R. Paulson Nov. 1988 17 p
(AD-A203145; NOSC/TD-1375) Avail: NTIS HC A03/MF A01 CSCL 04A

This report considers a proposal for a dual-lidar method to directly measure atmospheric extinction and backscatter coefficient profiles without the need to make the usual assumptions of horizontal homogeneity or constant backscatter-to-extinction ratio. A complete mathematical derivation for both techniques is presented. A dual-lidar method for measuring optical depths is demonstrated, but while the theory is valid, evaluating the accuracy of the results is difficult. GRA

N89-21440# Aerospace Corp., El Segundo, CA. Space Sciences Lab.
COMMENTARY ON FAST ATMOSPHERIC PULSATIONS
A. L. Vampola 22 Nov. 1988 19 p
(Contract F04701-85-C-0086)
(AD-A203172; TR-0088(3940-05)-6; SD-TR-88-106) Avail: NTIS HC A03/MF A01 CSCL 04A

A recent paper proposed that Fast Atmospheric Light Pulsations (FAPs), which have been observed at L = 1.5 to 2.2 in the Northern Hemisphere, are optical signatures of greater than 2 MeV electrons associated with Lightning induced Electron Precipitation (LEP) events produced by lightning strokes in the Southern Hemisphere. FAPs cannot be produced by greater than 2 MeV electrons in the inner radiation belt because the upper limit for fluxes of such particles is only about 0.2 percent of the value that was used in the analysis and would lead to an unrealistically short electron lifetime. The discrepancy comes from using an electron model, AE-2, which included the Starfish fission electrons. Later inner zone electron environment models, show the inner-zone to have negligible fluxes of electrons in excess of 2 MeV. The use of a model in which Southern Hemisphere lightning strokes result in Northern Hemisphere FAPs via a cyclotron mode interaction between magnetospheric electrons and lightning generated waves is also untenable because it would result in FAP intensities two orders of magnitude greater in the Southern Hemisphere than in the Northern Hemisphere, leading to a further two orders of magnitude reduction in estimated inner zone electron lifetimes. GRA

N89-21441# Lockheed Missiles and Space Co., Palo Alto, CA.
AURORAL PHOTOGRAPHY EXPERIMENT Scientific Report No. 1, Jun. 1987 - Mar. 1988
Stephen B. Mende 15 Feb. 1988 18 p
(Contract F19628-87-C-0097)
(AD-A203623; AFGL-TR-88-0027) Avail: NTIS HC A03/MF A01 CSCL 04A

Lockheed Palo Alto Research Laboratories is performing a joint experiment with AFGL to make observations of the aurora; airglow; and shuttle induced emission effects such as surface discharge, shuttle glow, and thruster induced effects. In this program, the Air Force will be flying Lockheed instrumentation as a secondary payload on the shuttle, and will make observations through the orbiter windows with the specialized equipment. The hardware is essentially a re-flight of the Auroral Photography Experiment (APE) which was flown on mission 41-G. Current status of the program is: (1) All the Lockheed hardware was delivered to Johnson Space Center; (2) Most of the hardware has been qualified for flight; (3) Experiment Operation definition is in progress; and (4) Data Analysis and scientific publication program is progressing with two papers submitted for publication. GRA

N89-21442# Ohio State Univ., Columbus. Dept. of Geodetic Science and Surveying.
DOWNWARD CONTINUATION OF THE FREE-AIR GRAVITY ANOMALIES TO THE ELLIPSOID USING THE GRADIENT SOLUTION, POISSON'S INTEGRAL AND TERRAIN CORRECTION-NUMERICAL COMPARISON AND COMPUTATIONS Scientific Report No. 4
Yan Ming Wang Jun. 1988 42 p
(Contract F19628-86-K-0016)
(AD-A203739; OSU/DGSS-393; AFGL-TR-88-0199; SR-4) Avail: NTIS HC A03/MF A01 CSCL 08E

The formulas for the determination of the coefficients of the spherical harmonic expansion of the disturbing potential of the earth are defined for data given on a sphere. In order to determine the spherical harmonic coefficients, the gravity anomalies have to be analytically downward continued from the earth's surface to a sphere - at least to the ellipsoid. The goal of this work is to continue the gravity anomalies from the earth's surface downward to the ellipsoid using recent elevation models. The basic method for the downward continuation is the gradient solution (the g1 term). The terrain correction has also been computed because of the role it can play as a correction term when calculating harmonic coefficients from surface gravity data. Because there is no global, dense gravity anomaly data, 5 minute x 5 minute mean elevation data has been used for the computations of the g1 term and the terrain correction on a global basis. The fast Fourier transformation has been applied to the computations. GRA

N89-21443# Lamont-Doherty Geological Observatory, Palisades, NY.
A COMPREHENSIVE STUDY OF THE SEISMOTECTONICS OF THE EASTERN ALEUTIAN ARC AND ASSOCIATED VOLCANIC SYSTEMS Summary Report, 1987 - 1988
J. Taber, K. H. Jacob, T. Boyd, and C. Estabrook Nov. 1988 37 p
(Contract DE-FG02-84ER-13221)

(DE89-007357; DOE/ER-13221/T4) Avail: NTIS HC A03/MF A01

We have made significant progress in the past two years towards our goal of understanding fundamental processes of subduction. The results range in spatial dimensions from small scale details of the plate interface within the Shumagin seismic gap to updated probabilities of the occurrence of great earthquakes along the entire Aleutian arc, and in time from the earliest instrumentally recorded earthquakes to automatic processing of the most recent events. It is necessary to study the entire range of scale lengths because of the interaction between different tectonic elements. A simple kinematic model describing flow of material down the Aleutian subduction zone shows that arc geometry and current convergent directions and rates can explain the distribution of seismicity and volcanism along the arc. Studies of the seismic source have begun to expand the frequency band over which seismic rupture can be analyzed. A comparison of short and long-period data from the Andreanoff Island earthquake raises fundamental questions about how decoupled in space and time can the radiation of high frequency energy be from the release of moment-rate producing slip during a dynamic rupture. The basic source parameters were modeled by inverting long-period P and SH waves while the high frequency characteristics were approximated by the superposition of many small earthquakes used as empirical Green's functions. Modeling of the earthquake source has also added insight into the mechanics of the transition from subduction zone to transform fault in the Gulf of Alaska region.

DOE

N89-21288*# California Univ., Berkeley. Dept. of Geology and Geophysics.

THE DEBATE OVER THE CRETACEOUS-TERTIARY BOUNDARY Abstract Only

W. Alvarez, F. Asaro, L. W. Alvarez, and H. V. Michel *In* Lunar and Planetary Inst., Global Catastrophes in Earth History: An Interdisciplinary Conference on Impacts, Volcanism, and Mass Mortality 1988 p 1 Prepared in cooperation with California Univ., Berkeley. Lawrence Berkeley Lab. (For primary document see N89-21287 14-42)

Avail: NTIS HC A11/MF A01 CSCL 08G

N89-21289*# Witwatersrand Univ., Johannesburg (South Africa). Dept. of Geophysics

GEOLOGICAL INDICATORS FOR IMPACT: THE ANOMALOUS CASE OF THE VREDEFORT STRUCTURE, SOUTH AFRICA

L. A. G. Antoine and W. U. Reimold *In* Lunar and Planetary Inst., Global Catastrophes in Earth History: An Interdisciplinary Conference on Impacts, Volcanism, and Mass Mortality 1988 p 2-3 (For primary document see N89-21287 14-42)

Avail: NTIS HC A11/MF A01 CSCL 08G

N89-21291*# California Univ., Berkeley. Lawrence Berkeley Lab.

POSSIBLE WORLD-WIDE MIDDLE MIOCENE IRIDIUM ANOMALY AND ITS RELATIONSHIP TO PERIODICITY OF IMPACTS AND EXTINCTIONS

F. Asaro, W. Alvarez, H. V. Michel, L. W. Alvarez, Mark H. Anders, A. Montanari, and James P. Kennett *In* Lunar and Planetary Inst., Global Catastrophes in Earth History: An Interdisciplinary Conference on Impacts, Volcanism, and Mass Mortality 1988 p 6-7 Prepared in cooperation with California Univ., Berkeley; and California Univ., Santa Barbara (For primary document see N89-21287 14-42)

Avail: NTIS HC A11/MF A01 CSCL 08G

N89-21292*# Lunar and Planetary Inst., Houston, TX.

THE CRATERING RECORD IN THE INNER SOLAR SYSTEM: IMPLICATIONS FOR EARTH

N. G. Barlow *In its* Globa! Catastrophes in Earth History: An Interdisciplinary Conference on Impacts, Volcanism, and Mass Mortality 1988 p 8-9 (For primary document see N89-21287 14-42)

Avail: NTIS HC A11/MF A01 CSCL 08G

N89-21294*# Hawaii Univ., Honolulu. Inst. of Geophysics.

IMPLICATIONS OF ASTEROID COMPOSITION FOR THE GEOCHEMISTRY OF THE ANCIENT TERRESTRIAL PROJECTILE FLUX Abstract Only

Jeffrey F. Bell *In* Lunar and Planetary Inst., Global Catastrophes in Earth History: An Interdisciplinary Conference on Impacts, Volcanism, and Mass Mortality 1988 p 12 (For primary document see N89-21287 14-42)

Avail: NTIS HC A11/MF A01 CSCL 08G

N89-21296*# Physical Research Lab., Ahmedabad (India).

GEOCHEMISTRY OF K/T BOUNDARIES IN INDIA AND CONTRIBUTIONS OF DECCAN VOLCANISM

N. Bhandari, M. Gupta, J. Pandey (Malviya, K. D. Inst. for Petroleum Exploration, Dehradun, India), and P. N. Shukla *In* Lunar and Planetary Inst., Global Catastrophes in Earth History: An Interdisciplinary Conference on Impacts, Volcanism, and Mass Mortality 1988 p 15-16 (For primary document see N89-21287 14-42)

Avail: NTIS HC A11/MF A01 CSCL 08G

N89-21297*# Geological Survey, Denver, CO.

SHOCKED QUARTZ AND MORE: IMPACT SIGNATURES IN K-T BOUNDARY CLAYS AND CLAYSTONES

Bruce F. Bohor *In* Lunar and Planetary Inst., Global Catastrophes in Earth History: An Interdisciplinary Conference on Impacts, Volcanism, and Mass Mortality 1988 p 17-18 (For primary document see N89-21287 14-42)

Avail: NTIS HC A11/MF A01 CSCL 08G

N89-21299*# Washington Univ., Seattle. Dept. of Geological Sciences.

SEDIMENTOLOGICAL EFFECTS OF TSUNAMIS, WITH PARTICULAR REFERENCE TO IMPACT-GENERATED AND VOLCANOGENIC WAVES

Joanne Bourgeois and Patricia L. Wiberg *In* Lunar and Planetary Inst., Global Catastrophes in Earth History: An Interdisciplinary Conference on Impacts, Volcanism, and Mass Mortality 1988 p 21-22 Prepared in cooperation with University of Western Washington, Bellingham (For primary document see N89-21287 14-42)

Avail: NTIS HC A11/MF A01 CSCL 08G

N89-21303*# California Univ., Santa Barbara.

MAGNETIC MICROSPHERULES ASSOCIATED WITH THE K/T AND UPPER EOCENE EXTINCTION EVENTS

Stanley M. Cisowski *In* Lunar and Planetary Inst., Global Catastrophes in Earth History: An Interdisciplinary Conference on Impacts, Volcanism, and Mass Mortality 1988 p 28-29 (For primary document see N89-21287 14-42)

Avail: NTIS HC A11/MF A01 CSCL 08G

N89-21305*# Paris VI Univ. (France). Lab. de Paleomagnetisme et Geodynamique.

DECCAN VOLCANISM AT THE CRETACEOUS-TERTIARY BOUNDARY

V. Courtillot, D. Vandamme, and J. Besse *In* Lunar and Planetary Inst., Global Catastrophes in Earth History: An Interdisciplinary Conference on Impacts, Volcanism, and Mass Mortality 1988 p 31-32 (For primary document see N89-21287 14-42)

Avail: NTIS HC A11/MF A01 CSCL 08K

N89-21309*# Lunar and Planetary Inst., Houston, TX.

EXPLOSIVE VOLCANISM, SHOCK METAMORPHISM AND THE K-T BOUNDARY

S. L. deSilva and V. L. Sharpton *In its* Global Catastrophes in Earth History: An Interdisciplinary Conference on Impacts, Volcanism, and Mass Mortality 1988 p 38-39 (For primary document see N89-21287 14-42)

Avail: NTIS HC A11/MF A01 CSCL 08G

N89-21311*# Geological Survey of Canada, Toronto (Ontario).

THE SUDBURY STRUCTURE (ONTARIO, CANADA) AND VREDEFORT STRUCTURE (SOUTH AFRICA): A COMPARISON

B. O. Dressler and W. U. Reimold *In* Lunar and Planetary Inst., Global Catastrophes in Earth History: An Interdisciplinary Conference on Impacts, Volcanism, and Mass Mortality 1988 p 42-43 Prepared in cooperation with Witwatersrand Univ., Johannesburg (South Africa) (For primary document see N89-21287 14-42)
Avail: NTIS HC A11/MF A01 CSCL 08G

N89-21312*# New Mexico Univ., Albuquerque. Dept. of Geology.
PROTEROZOIC BUSHVELD-VREDEFORT CATASTROPHE: POSSIBLE CAUSES AND CONSEQUENCES
W. E. Elston and D. Twist *In* Lunar and Planetary Inst., Global Catastrophes in Earth History: An Interdisciplinary Conference on Impacts, Volcanism, and Mass Mortality 1988 p 44-45 Prepared in cooperation with Pretoria Univ. (South Africa) (For primary document see N89-21287 14-42)
Avail: NTIS HC A11/MF A01 CSCL 08G

N89-21313*# Rhode Island Univ., Kingston. Dept. of Geology.
ROCKS, RESOLUTION, AND THE RECORD AT THE TERRESTRIAL K/T BOUNDARY, EASTERN MONTANA AND WESTERN NORTH DAKOTA
D. E. Fastovsky *In* Lunar and Planetary Inst., Global Catastrophes in Earth History: An Interdisciplinary Conference on Impacts, Volcanism, and Mass Mortality 1988 p 46-47 (For primary document see N89-21287 14-42)
Avail: NTIS HC A11/MF A01 CSCL 08G

N89-21314*# Los Alamos National Lab., NM.
IRIDIUM EMISSIONS FROM HAWAIIAN VOLCANOES Abstract Only
D. L. Finnegan, W. H. Zoller, and T. M. Miller *In* Lunar and Planetary Inst., Global Catastrophes in Earth History: An Interdisciplinary Conference on Impacts, Volcanism, and Mass Mortality 1988 p 48 (For primary document see N89-21287 14-42)
Avail: NTIS HC A11/MF A01 CSCL 08G

N89-21316*# Lunar and Planetary Inst., Houston, TX.
VOLCANISM, GLOBAL CATASTROPHE AND MASS MORTALITY
P. W. Francis and K. Burke *In its* Global Catastrophes in Earth History: An Interdisciplinary Conference on Impacts, Volcanism, and Mass Mortality 1988 p 50-51 (For primary document see N89-21287 14-42)
Avail: NTIS HC A11/MF A01 CSCL 08G

N89-21319*# Chicago Univ., IL.
EVIDENCE FOR A SINGLE IMPACT AT THE CRETACEOUS-TERTIARY BOUNDARY FROM TRACE ELEMENTS
Iain Gilmour and Edward Anders *In* Lunar and Planetary Inst., Global Catastrophes in Earth History: An Interdisciplinary Conference on Impacts, Volcanism, and Mass Mortality 1988 p 56-57 (For primary document see N89-21287 14-42)
(Grants NAG9-52; NSF EAR-86-09218)
Avail: NTIS HC A11/MF A01 CSCL 08G

N89-21320*# Chicago Univ., IL.
NITROGEN GEOCHEMISTRY OF A CRETACEOUS-TERTIARY BOUNDARY SITE IN NEW ZEALAND
Iain Gilmour and Stuart R. Boyd *In* Lunar and Planetary Inst., Global Catastrophes in Earth History: An Interdisciplinary Conference on Impacts, Volcanism, and Mass Mortality 1988 p 58-59 Prepared in cooperation with Open Univ., Milton (England) (For primary document see N89-21287 14-42)
Avail: NTIS HC A11/MF A01 CSCL 08G

N89-21321*# Chicago Univ., IL.
THE GLOBAL CRETACEOUS-TERTIARY FIRE: BIOMASS OR FOSSIL CARBON
Iain Gilmour and Frank Guenther *In* Lunar and Planetary Inst., Global Catastrophes in Earth History: An Interdisciplinary Conference on Impacts, Volcanism, and Mass Mortality 1988 p 60-62 Prepared in cooperation with National Bureau of Standards, Gaithersburg, MD (For primary document see N89-21287 14-42)
Avail: NTIS HC A11/MF A01 CSCL 08G

N89-21323*# Max-Planck-Inst. fuer Chemie, Mainz (Germany, F.R.).
MINERALOGY AND PHASE-CHEMISTRY OF THE CRETACEOUS/TERTIARY SECTION IN THE LATTENGEBIRGE, BAVARIAN ALPS
G. Graup *In* Lunar and Planetary Inst., Global Catastrophes in Earth History: An Interdisciplinary Conference on Impacts, Volcanism, and Mass Mortality 1988 p 65 (For primary document see N89-21287 14-42)
Avail: NTIS HC A11/MF A01 CSCL 08G

N89-21326*# Solar System Associates, Des Moines, IA.
THE MANSON IMPACT STRUCTURE, A POSSIBLE SITE FOR A CRETACEOUS-TERTIARY (K-T) BOUNDARY IMPACT
J. B. Hartung, M. J. Kunk, and R. R. Anderson (Geological Survey, Iowa City, IA.) *In* Lunar and Planetary Inst., Global Catastrophes in Earth History: An Interdisciplinary Conference on Impacts, Volcanism, and Mass Mortality 1988 p 70-71 (For primary document see N89-21287 14-42)
Avail: NTIS HC A11/MF A01 CSCL 08G

N89-21327*# Louisiana State Univ., Baton Rouge. Dept. of Geology and Geophysics.
HOW MANY UPPER EOCENE MICROSPHERULE LAYERS: MORE THAN WE THOUGHT
Joseph E. Hazel *In* Lunar and Planetary Inst., Global Catastrophes in Earth History: An Interdisciplinary Conference on Impacts, Volcanism, and Mass Mortality 1988 p 72-73 (For primary document see N89-21287 14-42)
(Grant NSF EAR-88-95268)
Avail: NTIS HC A11/MF A01 CSCL 08G

N89-21332*# Eidgenoessische Technische Hochschule, Zurich (Switzerland).
STRANGELOVE OCEAN AT ERA BOUNDARIES, TERRESTRIAL OR EXTRATERRESTRIAL CAUSE Abstract Only
Kenneth J. Hsue *In* Lunar and Planetary Inst., Global Catastrophes in Earth History: An Interdisciplinary Conference on Impacts, Volcanism, and Mass Mortality 1988 p 80 (For primary document see N89-21287 14-42)
Avail: NTIS HC A11/MF A01 CSCL 08G

N89-21334*# Geological Survey, Denver, CO.
THE WESTERN NORTH AMERICAN CRETACEOUS-TERTIARY (K-T) BOUNDARY INTERVAL AND ITS CONTENT OF SHOCK-METAMORPHOSED MINERALS: IMPLICATIONS CONCERNING THE K-T BOUNDARY IMPACT-EXTINCTION THEORY
G. A. Izett *In* Lunar and Planetary Inst., Global Catastrophes in Earth History: An Interdisciplinary Conference on Impacts, Volcanism, and Mass Mortality 1988 p 83-84 (For primary document see N89-21287 14-42)
Avail: NTIS HC A11/MF A01 CSCL 08G

N89-21336*# Yale Univ., New Haven, CT. Dept. of Geology and Geophysics.
PATTERNS OF MEGAFLORAL CHANGE ACROSS THE CRETACEOUS-TERTIARY BOUNDARY IN THE NORTHERN GREAT PLAINS AND ROCKY MOUNTAINS Abstract Only
Kirk R. Johnson and Leo J. Hickey *In* Lunar and Planetary Inst., Global Catastrophes in Earth History: An Interdisciplinary Conference on Impacts, Volcanism, and Mass Mortality 1988 p 87 (For primary document see N89-21287 14-42)
Avail: NTIS HC A11/MF A01 CSCL 08G

N89-21337*# Princeton Univ., NJ. Dept. of Geological and Geophysical Sciences.
EXTENDED PERIOD OF K/T BOUNDARY MASS EXTINCTION IN THE MARINE REALM
G. Keller *In* Lunar and Planetary Inst., Global Catastrophes in Earth History: An Interdisciplinary Conference on Impacts, Volcanism, and Mass Mortality 1988 p 88-89 (For primary document see N89-21287 14-42)
Avail: NTIS HC A11/MF A01 CSCL 08G

N89-21338*# Princeton Univ., NJ. Dept. of Geological and Geophysical Sciences.
FAUNAL AND EROSIONAL EVENTS IN THE EASTERN TETHYAN SEA ACROSS THE K/T BOUNDARY
G. Keller and C. Benjamini *In* Lunar and Planetary Inst., Global Catastrophes in Earth History: An Interdisciplinary Conference on Impacts, Volcanism, and Mass Mortality 1988 p 90-91 Prepared in cooperation with Ben Gurion Univ. of the Negev, Beer Sheva (Israel) (For primary document see N89-21287 14-42)
Avail: NTIS HC A11/MF A01 CSCL 08G

N89-21340*# Lunar and Planetary Inst., Houston, TX.
VOLCANIC ASH LAYERS IN BLUE ICE FIELDS (BEARDMORE GLACIER AREA, ANTARCTICA): IRIDIUM ENRICHMENTS
Christian Koeberl *In its* Global Catastrophes in Earth History: An Interdisciplinary Conference on Impacts, Volcanism, and Mass Mortality 1988 p 93-94 Prepared in cooperation with Technische Univ., Vienna (Austria) (For primary document see N89-21287 14-42)
Avail: NTIS HC A11/MF A01 CSCL 08G

N89-21341*# Lunar and Planetary Inst., Houston, TX.
THE KARA AND UST-KARA IMPACT STRUCTURES (USSR) AND THEIR RELEVANCE TO THE K/T BOUNDARY EVENT
Christian Koeberl, M. A. Nazarov, T. M. Harrison, V. L. Sharpton, A. V. Murali, and K. Burke *In its* Global Catastrophes in Earth History: An Interdisciplinary Conference on Impacts, Volcanism, and Mass Mortality 1988 p 95-96 Prepared in cooperation with Technische Univ., Vienna (Austria; Academy of Sciences (USSR), Moscow; and State Univ. of New York, Albany (For primary document see N89-21287 14-42)
Avail: NTIS HC A11/MF A01 CSCL 08G

N89-21342*# Moscow State Univ. (USSR). Geology Faculty.
ISOTOPIC INVESTIGATIONS IN THE AREA OF THE TUNGUSKA CATASTROPHE IN 1908 YEAR
E. M. Kolesnikov *In* Lunar and Planetary Inst., Global Catastrophes in Earth History: An Interdisciplinary Conference on Impacts, Volcanism, and Mass Mortality 1988 p 97-98 (For primary document see N89-21287 14-42)
Avail: NTIS HC A11/MF A01 CSCL 08G

N89-21343*# Moscow State Univ. (USSR).
THE KARSKIY CRATERS ARE THE PROBABLE RECORDS OF CATASTROPHE AT THE CRETACEOUS-TERTIARY BOUNDARY
E. M. Kolesnikov, M. A. Nazarov, D. D. Badjukov, and Yu. A. Shukolyukov *In* Lunar and Planetary Inst., Global Catastrophes in Earth History: An Interdisciplinary Conference on Impacts, Volcanism, and Mass Mortality 1988 p 99-10 Prepared in cooperation with Academy of Sciences (USSR), Moscow (For primary document see N89-21287 14-42)
Avail: NTIS HC A11/MF A01 CSCL 08G

N89-21344*# California Univ., Los Angeles. Inst. of Geophysics and Planetary Physics.
ACCRETION RATE OF EXTRATERRESTRIAL MATTER: IRIDIUM DEPOSITED OVER THE LAST 70 MILLION YEARS
Frank T. Kyte *In* Lunar and Planetary Inst., Global Catastrophes in Earth History: An Interdisciplinary Conference on Impacts, Volcanism, and Mass Mortality 1988 p 101 (For primary document see N89-21287 14-42)
Avail: NTIS HC A11/MF A01 CSCL 08G

N89-21345*# Basque Univ., Lejona (Spain).
THE CRETACEOUS-TERTIARY BOUNDARY BIOTIC CRISIS IN THE BASQUE COUNTRY
M. A. Lamolda *In* Lunar and Planetary Inst., Global Catastrophes in Earth History: An Interdisciplinary Conference on Impacts, Volcanism, and Mass Mortality 1988 p 102-103 (For primary document see N89-21287 14-42)
Avail: NTIS HC A11/MF A01 CSCL 08G

N89-21346*# Geological Survey, Denver, CO.
CATASTROPHIC VOLCANISM
Peter W. Lipman *In* Lunar and Planetary Inst., Global Catastrophes in Earth History: An Interdisciplinary Conference on Impacts, Volcanism, and Mass Mortality 1988 p 104-105 (For primary document see N89-21287 14-42)
Avail: NTIS HC A11/MF A01 CSCL 08G

N89-21347*# Florida State Univ., Tallahassee. Geophysical Fluid Dynamics Inst.
CATASTROPHIC VOLCANISM AS A CAUSE OF SHOCKED FEATURES FOUND AT THE K/T BOUNDARY AND IN CRYPTOEXPLOSION STRUCTURES
D. E. Loper and K. McCartney *In* Lunar and Planetary Inst., Global Catastrophes in Earth History: An Interdisciplinary Conference on Impacts, Volcanism, and Mass Mortality 1988 p 106-107 (For primary document see N89-21287 14-42)
Avail: NTIS HC A11/MF A01 CSCL 08G

N89-21348*# Stanford Univ., CA.
EVIDENCE FOR AND IMPLICATIONS OF AN EARLY ARCHEAN TERRESTRIAL IMPACT RECORD
Donald R. Lowe and Gary R. Byerly *In* Lunar and Planetary Inst., Global Catastrophes in Earth History: An Interdisciplinary Conference on Impacts, Volcanism, and Mass Mortality 1988 p 108 Prepared in cooperation with Louisiana State Univ., Baton Rouge (For primary document see N89-21287 14-42)
Avail: NTIS HC A11/MF A01 CSCL 08G

N89-21349*# Pennsylvania Univ., Philadelphia. Dept. of Geology.
MAGNETIC REVERSAL SPURTS: RAIN GAUGES FOR COMET SHOWERS
T. M. Lutz *In* Lunar and Planetary Inst., Global Catastrophes in Earth History: An Interdisciplinary Conference on Impacts, Volcanism, and Mass Mortality 1988 p 109-110 (For primary document see N89-21287 14-42)
Avail: NTIS HC A11/MF A01 CSCL 08G

N89-21351*# Michigan Univ., Ann Arbor. Dept. of Geological Sciences and Museum of Paleontology.
INDUCEMENT OF HETEROCHRONIC VARIATION IN A SPECIES OF PLANKTIC FORAMINIFERA BY A LATE EOCENE IMPACT EVENT
N. MacLeod and J. A. Kitchell *In* Lunar and Planetary Inst., Global Catastrophes in Earth History: An Interdisciplinary Conference on Impacts, Volcanism, and Mass Mortality 1988 p 112 (For primary document see N89-21287 14-42)
Avail: NTIS HC A11/MF A01 CSCL 08G

N89-21352*# California Univ., Davis. Dept. of Geology.
TRACE ELEMENT AND ISOTOPE GEOCHEMISTRY OF CRETACEOUS-TERTIARY BOUNDARY SEDIMENTS: IDENTIFICATION OF EXTRA-TERRESTRIAL AND VOLCANIC COMPONENTS
S. V. Margolis and E. F. Doehne *In* Lunar and Planetary Inst., Global Catastrophes in Earth History: An Interdisciplinary Conference on Impacts, Volcanism, and Mass Mortality 1988 p 113-114 (For primary document see N89-21287 14-42)
Avail: NTIS HC A11/MF A01 CSCL 08G

N89-21353*# Harvard-Smithsonian Center for Astrophysics, Cambridge, MA.
IMPACT, AND ITS IMPLICATIONS FOR GEOLOGY
Ursula B. Marvin *In* Lunar and Planetary Inst., Global Catastrophes

in Earth History: An Interdisciplinary Conference on Impacts, Volcanism, and Mass Mortality 1988 p 115-116 (For primary document see N89-21287 14-42)
Avail: NTIS HC A11/MF A01 CSCL 08G

N89-21355*# Arizona State Univ., Tempe. Dept. of Geology.
SHATTER CONES: DIAGNOSTIC IMPACT SIGNATURES
J. F. McHone and R. S. Dietz *In* Lunar and Planetary Inst., Global Catastrophes in Earth History: An Interdisciplinary Conference on Impacts, Volcanism, and Mass Mortality 1988 p 118-119 (For primary document see N89-21287 14-42)
Avail: NTIS HC A11/MF A01 CSCL 08G

N89-21356*# Ottawa Univ. (Ontario). Dept. of Geology.
MASS KILLINGS AND DETECTION OF IMPACTS Abstract Only
Digby J. McLaren *In* Lunar and Planetary Inst., Global Catastrophes in Earth History: An Interdisciplinary Conference on Impacts, Volcanism, and Mass Mortality 1988 p 120 (For primary document see N89-21287 14-42)
Avail: NTIS HC A11/MF A01 CSCL 08G

N89-21358*# Geological Survey, Lansing, MI.
THE CALVIN 28 CRYPTOEXPLOSIVE DISTURBANCE, CASS COUNTY, MICHIGAN: EVIDENCE FOR IMPACT ORIGIN
Randall L. Milstein *In* Lunar and Planetary Inst., Global Catastrophes in Earth History: An Interdisciplinary Conference on Impacts, Volcanism, and Mass Mortality 1988 p 122-123 (For primary document see N89-21287 14-42)
Avail: NTIS HC A11/MF A01 CSCL 08G

N89-21359*# Yamaguchi Univ. (Japan). Dept. of Earth Sciences.
MINERALOGICAL AND GEOCHEMICAL ANOMALOUS DATA OF THE K-T BOUNDARY SAMPLES
Y. Miura, G. Shibya, M. Imai, N. Takaoka, and S. Saito *In* Lunar and Planetary Inst., Global Catastrophes in Earth History: An Interdisciplinary Conference on Impacts, Volcanism, and Mass Mortality 1988 p 124-125 Prepared in cooperation with Yamagata Univ. (Japan). (For primary document see N89-21287 14-42)
Avail: NTIS HC A11/MF A01 CSCL 08G

N89-21360*# Princeton Univ., NJ. Dept. of Geological and Geophysical Sciences.
FLOOD BASALTS AND MASS EXTINCTIONS Abstract Only
W. Jason Morgan *In* Lunar and Planetary Inst., Global Catastrophes in Earth History: An Interdisciplinary Conference on Impacts, Volcanism, and Mass Mortality 1988 p 126 (For primary document see N89-21287 14-42)
Avail: NTIS HC A11/MF A01 CSCL 08G

N89-21361*# California Univ., Berkeley. Dept. of Physics
ASTROPHYSICAL IMPLICATIONS OF PERIODICITY Abstract Only
Richard A. Muller *In* Lunar and Planetary Inst., Global Catastrophes in Earth History: An Interdisciplinary Conference on Impacts, Volcanism, and Mass Mortality 1988 p 127 Prepared in cooperation with California Univ., Berkeley, Lawrence Berkeley Laboratory (For primary document see N89-21287 14-42)
Avail: NTIS HC A11/MF A01 CSCL 08G

N89-21362*# Lunar and Planetary Inst., Houston, TX.
DECCAN VOLCANISM AND K-T BOUNDARY SIGNATURES
A. V. Murali, B. C. Schuraytz, and P. P. Parekh *In its* Global Catastrophes in Earth History: An Interdisciplinary Conference on Impacts, Volcanism, and Mass Mortality 1988 p 128-129 Prepared in cooperation with New York State Dept. of Health, Albany (For primary document see N89-21287 14-42)
Avail: NTIS HC A11/MF A01 CSCL 08G

N89-21364*# Dartmouth Coll., Hanover, NH. Dept. of Earth Sciences.
CRETACEOUS-TERTIARY FINDINGS, PARADIGMS AND PROBLEMS Abstract Only
C. B. Officer and C. L. Drake *In* Lunar and Planetary Inst., Global Catastrophes in Earth History: An Interdisciplinary Conference on Impacts, Volcanism, and Mass Mortality 1988 p 132 (For primary document see N89-21287 14-42)
Avail: NTIS HC A11/MF A01 CSCL 08G

N89-21366*# Lamont-Doherty Geological Observatory, Palisades, NY.
THE TRIASSIC-JURASSIC BOUNDARY IN EASTERN NORTH AMERICA
P. E. Olsen and B. Comet *In* Lunar and Planetary Inst., Global Catastrophes in Earth History: An Interdisciplinary Conference on Impacts, Volcanism, and Mass Mortality 1988 p 135-136 (For primary document see N89-21287 14-42)
Avail: NTIS HC A11/MF A01 CSCL 08G

N89-21368*# Los Alamos National Lab., NM. Isotope and Nuclear Chemistry Div.
IRIDIUM ABUNDANCE MEASUREMENTS ACROSS BIO-EVENT HORIZONS IN THE GEOLOGICAL RECORD
C. J. Orth and M. Attrep, Jr. *In* Lunar and Planetary Inst., Global Catastrophes in Earth History: An Interdisciplinary Conference on Impacts, Volcanism, and Mass Mortality 1988 p 139-140 (For primary document see N89-21287 14-42)
Avail: NTIS HC A11/MF A01 CSCL 08G

N89-21369*# Saint Lawrence Univ., Canton, NY. Dept. of Geology.
CATHODOLUMINESCENCE OF SHOCKED QUARTZ AT THE CRETACEOUS-TERTIARY BOUNDARY
Michael R. Owen and Mark H. Anders *In* Lunar and Planetary Inst., Global Catastrophes in Earth History: An Interdisciplinary Conference on Impacts, Volcanism, and Mass Mortality 1988 p 141-142 Prepared in cooperation with California Univ., Berleley (For primary document see N89-21287 14-42)
Avail: NTIS HC A11/MF A01 CSCL 08G

N89-21370*# Technische Univ., Vienna (Austria).
BIO-, MAGNETO- AND EVENT-STRATIGRAPHY ACROSS THE K-T BOUNDARY
A. Preisinger, H. Stradner, and H. J. Mauritsch (Montanuniversitat Leoben, Austria) *In* Lunar and Planetary Inst., Global Catastrophes in Earth History: An Interdisciplinary Conference on Impacts, Volcansim, and Mass Mortality 1988 p 143-144 (For primary document see N89-21287 14-42)
Avail: NTIS HC A11/MF A01 CSCL 08G

N89-21371*# Massachusetts Inst. of Tech., Cambridge. Dept. of Earth, Atmospheric and Planetary Sciences.
BIOSPHERIC TRAUMAS CAUSED BY LARGE IMPACTS AND PREDICTED RELICS IN THE SEDIMENTARY RECORD
R. G. Prinn and B. Fegley, Jr. *In* Lunar and Planetary Inst., Global Catastrophes in Earth History: An Interdisciplinary Conference on Impacts, Volcanism, and Mass Mortality 1988 p 145 (For primary document see N89-21287 14-42)
(Grants NAG9-108; NSF ATM-87-10102)
Avail: NTIS HC A11/MF A01 CSCL 08G

N89-21372*# New York Univ., New York. Earth Systems Group.
FLOOD BASALT ERUPTIONS, COMET SHOWERS, AND MASS EXTINCTION EVENTS Abstract Only
Michael R. Rampino and Richard B. Stothers (National Aeronautics and Space Administration. Goddard Space Flight Center, Greenbelt, MD.) *In* Lunar and Planetary Inst., Global Catastrophes in Earth History: An Interdisciplinary Conference on Impacts, Volcanism, and Mass Mortality 1988 p 146 Prepared in cooperation with NASA Goddard Space Flight Center, Greenbelt, MD (For primary document see N89-21287 14-42)
Avail: NTIS HC A11/MF A01 CSCL 08G

N89-21373*# New York Univ., New York. Earth Systems Group.
CLIMATIC CHANGES RESULTING FROM MASS EXTINCTIONS AT THE K-T BOUNDARY (AND OTHER BIO-EVENTS) Abstract Only
Michael R. Rampino and Tyler Volk *In* Lunar and Planetary Inst., Global Catastrophes in Earth History: An Interdisciplinary Conference on Impacts, Volcanism, and Mass Mortality 1988 p 147 (For primary document see N89-21287 14-42)
Avail: NTIS HC A11/MF A01 CSCL 08G

N89-21374*# Chicago Univ., IL.
IMPACT AS A GENERAL CAUSE OF EXTINCTION: A FEASIBILITY TEST
David M. Raup *In* Lunar and Planetary Inst., Global Catastrophes in Earth History: An Interdisciplinary Conference on Impacts, Volcanism, and Mass Mortality 1988 p 148-149 (For primary document see N89-21287 14-42)
Avail: NTIS HC A11/MF A01 CSCL 08G

N89-21375*# Witwatersrand Univ., Johannesburg (South Africa). Centre for Nuclear Sciences.
REPORT ON AN INTERNATIONAL WORKSHOP ON CRYPTOEXPLOSIONS AND CATASTROPHES IN THE GEOLOGICAL RECORD, WITH A SPECIAL FOCUS ON THE VREDEFORT STRUCTURE
W. U. Reimold *In* Lunar and Planetary Inst., Global Catastrophes in Earth History: An Interdisciplinary Conference on Impacts, Volcanism, and Mass Mortality 1988 p 150-151 Workshop held in Parys, Republic of South Africa, 6-10 Jul. 1987 (For primary document see N89-21287 14-42)
Avail: NTIS HC A11/MF A01 CSCL 08G

N89-21376*# Witwatersrand Univ., Johannesburg (South Africa). Centre for Nuclear Sciences.
MICRODEFORMATION IN VREDEFORT ROCKS; EVIDENCE FOR SHOCK METAMORPHISM
W. U. Reimold, M. A. G. Andreoli, and R. J. Hart *In* Lunar and Planetary Inst., Global Catastrophes in Earth History: An Interdisciplinary Conference on Impacts, Volcanism, and Mass Mortality 1988 p 152-153 (For primary document see N89-21287 14-42)
Avail: NTIS HC A11/MF A01 CSCL 08G

N89-21377*# Colorado Univ., Boulder. Dept. of Physics.
DYNAMICS OF EXPLODING MAGMA CHAMBERS: IMPLICATIONS FOR K-T VOLCANISM AND MASS EXTINCTIONS
A. R. Rice *In* Lunar and Planetary Inst., Global Catastrophes in Earth History: An Interdisciplinary Conference on Impacts, Volcanism, and Mass Mortality 1988 p 154-155 (For primary document see N89-21287 14-42)
Avail: NTIS HC A11/MF A01 CSCL 08G

N89-21378*# Centre National de la Recherche Scientifique, Gif-sur-Yvette (France). Centre des Faibles Radioactivites.
SEARCH FOR THE TUNGUSKA EVENT IN THE ANTARCTIC SNOW
R. Rocchia, M. deAngelis, D. Doclet, Ph. Bonte, C. Jehanno, and E. Robin *In* Lunar and Planetary Inst., Global Catastrophes in Earth History: An Interdisciplinary Conference on Impacts, Volcanism, and Mass Mortality 1988 p 156-157 Prepared in cooperation with Commissariat a l'Energie Atomique, Saclay (France) (For primary document see N89-21287 14-42)
Avail: NTIS HC A11/MF A01 CSCL 08G

N89-21379*# Geological Survey, Flagstaff, AZ.
COMPUTER MODELING OF LARGE ASTEROID IMPACTS INTO CONTINENTAL AND OCEANIC SITES: ATMOSPHERIC, CRATERING, AND EJECTA DYNAMICS
D. J. Roddy, S. H. Schuster, M. Rosenblatt, L. B. Grant, P. J. Hassig, and K. N. Kreyenhagen *In* Lunar and Planetary Inst., Global Catastrophes in Earth History: An Interdisciplinary Conference on Impacts, Volcanism, and Mass Mortality 1988 p 158-159 Prepared in cooperation with California Research and Technology, Inc., Chatsworth (For primary document see N89-21287 14-42)
Avail: NTIS HC A11/MF A01 CSCL 08G

N89-21381*# Boeing Aerospace Co., Seattle, WA.
CRATER SIZE ESTIMATES FOR LARGE-BODY TERRESTRIAL IMPACT
Robert M. Schmidt and Kevin R. Housen *In* Lunar and Planetary Inst., Global Catastrophes in Earth History: An Interdisciplinary Conference on Impacts, Volcanism, and Mass Mortality 1988 p 162-163 (For primary document see N89-21287 14-42)
Avail: NTIS HC A11/MF A01 CSCL 08G

N89-21382*# California Univ., Berkeley. Lawrence Berkeley Lab.
MARINE AND CONTINENTAL K-T BOUNDARY CLAYS COMPARED
B. Schmitz *In* Lunar and Planetary Inst., Global Catastrophes in Earth History: An Interdisciplinary Conference on Impacts, Volcanism, and Mass Mortality 1988 p 164-165 (For primary document see N89-21287 14-42)
Avail: NTIS HC A11/MF A01 CSCL 08G

N89-21383*# Brown Univ., Providence, RI. Dept. of Geological Sciences.
OBLIQUE IMPACTS: CATASTROPHIC VS. PROTRACTED EFFECTS
P. H. Schultz *In* Lunar and Planetary Inst., Global Catastrophes in Earth History: An Interdisciplinary Conference on Impacts, Volcanism, and Mass Mortality 1988 p 166-167 Prepared in cooperation with Murphys Center of Planetology, CA (For primary document see N89-21287 14-42)
Avail: NTIS HC A11/MF A01 CSCL 08G

N89-21384*# Brown Univ., Providence, RI. Dept. of Geological Sciences.
NON-RANDOM CRATERING FLUX IN RECENT TIME
P. H. Schultz *In* Lunar and Planetary Inst., Global Catastrophes in Earth History: An Interdisciplinary Conference on Impacts, Volcanism, and Mass Mortality 1988 p 168-169 Prepared in cooperation with Arizona State Univ., Tempe (For primary document see N89-21287 14-42)
Avail: NTIS HC A11/MF A01 CSCL 08G

N89-21386*# Lunar and Planetary Inst., Houston, TX.
K-T IMPACT(S): CONTINENTAL, OCEANIC OR BOTH
V. L. Sharpton, B. C. Schuraytz, A. V. Murali, G. Ryder, and K. Burke *In its* Global Catastrophes in Earth History: An Interdisciplinary Conference on Impacts, Volcanism, and Mass Mortality 1988 p 172-173 (For primary document see N89-21287 14-42)
Avail: NTIS HC A11/MF A01 CSCL 08G

N89-21389*# Smithsonian Institution, Washington, DC.
VOLCANOES AND GLOBAL CATASTROPHES
Tom Simkin *In* Lunar and Planetary Inst., Global Catastrophes in Earth History: An Interdisciplinary Conference on Impacts, Volcanism, and Mass Mortality 1988 p 179 (For primary document see N89-21287 14-42)
Avail: NTIS HC A11/MF A01 CSCL 08G

N89-21391*# Vrije Univ., Amsterdam (Netherlands). Geomarine Center.
IMPACT AND EXTINCTION SIGNATURES IN COMPLETE CRETACEOUS-TERTIARY (K-T) BOUNDARY SECTIONS
J. Smit, H. Groot, R. deJonge, and P. Smit *In* Lunar and Planetary Inst., Global Catastrophes in Earth History: An Interdisciplinary Conference on Impacts, Volcanism, and Mass Mortality 1988 p 182-183 (For primary document see N89-21287 14-42)
Avail: NTIS HC A11/MF A01 CSCL 08G

N89-21393*# Geological Survey, Vancouver, WA. Cascades Volcano Observatory.
SOME VOLCANOLOGIC ASPECTS OF COLUMBIA RIVER BASALT VOLCANISM RELEVANT TO THE EXTINCTION CONTROVERSY
Donald A. Swanson *In* Lunar and Planetary Inst., Global Catastrophes in Earth History: An Interdisciplinary Conference on Impacts, Volcanism, and Mass Mortality 1988 p 186-187 (For primary document see N89-21287 14-42)
Avail: NTIS HC A11/MF A01 CSCL 08G

N89-21395*# Geological Survey of Canada, Calgary (Alberta).
A REGIONAL PERSPECTIVE ON THE PALYNOFLORAL RESPONSE TO K-T BOUNDARY EVENT(S) WITH EMPHASIS ON VARIATIONS IMPOSED BY THE EFFECTS OF SEDIMENTARY FACIES AND LATITUDE
A. R. Sweet *In* Lunar and Planetary Inst., Global Catastrophes in Earth History: An Interdisciplinary Conference on Impacts, Volcanism, and Mass Mortality 1988 p 190-191 (For primary document see N89-21287 14-42)
Avail: NTIS HC A11/MF A01 CSCL 08G

N89-21400*# Witwatersrand Univ., Johannesburg (South Africa). Centre for Nuclear Sciences.
GEOCHEMICAL COMPARISON OF K-T BOUNDARIES FROM THE NORTHERN AND SOUTHERN HEMISPHERES
M. Tredous, B. Th. Verhagen, R. J. Hart, C. B. DeWit, C. B. Smith, K. Perch-Nielsen, and J. P. F. Sellschop *In* Lunar and Planetary Inst., Global Catastrophes in Earth History: An Interdisciplinary Conference on Impacts, Volcanism, and Mass Mortality 1988 p 198-199 (For primary document see N89-21287 14-42)
Avail: NTIS HC A11/MF A01 CSCL 08G

N89-21402*# Yale Univ., New Haven, CT. Dept. of Geology and Geophysics.
THE CAUSES FOR GEOGRAPHICAL VARIATIONS IN OS187/OS186 AT THE CRETACEOUS-TERTIARY BOUNDARY Abstract Only
K. K. Turekian, B. K. Esser, and G. E. Ravizza *In* Lunar and Planetary Inst., Global Catastrophes in Earth History: An Interdisciplinary Conference on Impacts, Volcanism, and Mass Mortality 1988 p 202-203 (For primary document see N89-21287 14-42)
Avail: NTIS HC A11/MF A01 CSCL 08G

N89-21405*# California Univ., Los Angeles.
TEKTITES: ORIGIN AS MELTS PRODUCED BY THE IMPACT OF SMALL PROJECTILES ONTO DRY TARGETS Abstract Only
John T. Wasson *In* Lunar and Planetary Inst., Global Catastrophes in Earth History: An Interdisciplinary Conference on Impacts, Volcanism, and Mass Mortality 1988 p 208 (For primary document see N89-21287 14-42)
Avail: NTIS HC A11/MF A01 CSCL 08G

N89-21409*# California Univ., Berkeley. Marine Science Group.
COLLISIONS WITH ICE-VOLATILE OBJECTS: GEOLOGICAL IMPLICATIONS
P. Wilde, M. S. Quinby-Hunt, and W. B. N. Berry *In* Lunar and Planetary Inst., Global Catastrophes in Earth History: An Interdisciplinary Conference on Impacts, Volcanism, and Mass Mortality 1988 p 215-216 (For primary document see N89-21287 14-42)
Avail: NTIS HC A11/MF A01 CSCL 08G

47 METEOROLOGY AND CLIMATOLOGY

Includes weather forecasting and modification.

N89-21444*# National Aeronautics and Space Administration. Goddard Space Flight Center, Greenbelt, MD.
ER-2 LIDAR OBSERVATIONS FROM THE OCTOBER 1986 FIRE CIRRUS EXPERIMENT
J. D. Spinhirne, D. L. Hlavka, and W. D. Hart (Science Systems and Applications, Inc., Seabrook, MD.) Jun. 1988 53 p
(NASA-TM-100704; NAS 1.15:100704) Avail: NTIS HC A04/MF A01 CSCL 04B

A description of the ER-2 lidar data characteristics and available products, plus flight times and locations is presented for the FIRE cirrus experiment of October 13 through November 2, 1986. The CALS airborne lidar was flown for this experiment on the NASA ER-2 high altitude aircraft. The primary objectives of the CALS observations were to intensively measure cirrus cloud top height and structure for basic cirrus studies and for validation of satellite cloud retrievals. Author

N89-21445# National Climate Program Office, Rockville, MD.
NATIONAL CLIMATE PROGRAM Annual Report, 1986
Jan. 1988 57 p
(PB89-118608) Avail: NTIS HC A04/MF A01 CSCL 04B

Potential climatic effects of increased concentrations of atmospheric carbon dioxide and other greenhouse gases, a possible El Nino-Southern Oscillation event, ozone depletion, and drought in the southeastern United States were major scientific issues in the National Climate Program in 1986. The report summarizes these events and includes climate data, international activities and budget details for 1980 to 1987. Author

N89-21446# National Center for Atmospheric Research, Boulder, CO.
CCM (COMMUNITY CLIMATE MODEL) Progress Report
David L. Williamson, ed. Oct. 1988 95 p
(Grant NSF ATM-87-09659)
(PB89-120927; NCAR/TN-324-PPR) Avail: NTIS HC A05/MF A01 CSCL 04B

The advantages of the Community Climate Model (CCM) concept, in which many scientists use the same basic model for a variety of scientific studies, were demonstrated in the CCM workshops held at NCAR in July 1985 and 1987. At these workshops many diverse experiments were seen to relate to each other when performed with the same model, and much constructive dialogue took place between experts in different disciplines. Unfortunately, not all users of the CCM were able to participate in these workshops. To augment these workshops and foster interchange between all users of the NCAR CCM, the CCM Advisory Committee recommended that a CCM Progress Report be required of all CCM users both inside and outside of NCAR. These individual reports are assembled in section 4 of the report as submitted by the users with no additional editing. GRA

N89-21447# National Center for Atmospheric Research, Boulder, CO.
COUPLED DYNAMICAL-RADIATIONAL MODEL OF STRATOCUMULUS AND ITS APPLICATIONS Ph.D. Thesis
Weizuo Ye 1988 109 p
(Grant NSF ATM-87-09659)
(PB89-104137; NCAR/CT-115) Avail: NTIS HC A06/MF A01 CSCL 04B

A model dealing with interactions between radiation and low stratiform clouds is presented (hereafter referred to as the DRS model), based on the mixed-layer model Lilly (1968) pioneered and on Deardorff's three-dimensional numerical model results. Its main new aspects lie in: (1) consideration of the natures of both atmosphere and cloud; (2) a new entrainment velocity scheme with few arbitrary assumptions; (3) transition from a one-mixed layer to a two-mixed layer model; and (4) parameterization of radiation and precipitation calculations. The model results for radiation, moisture, and heat turbulent fluxes are agreement with those calculated or observed. Author

N89-21448*# National Aeronautics and Space Administration. Goddard Space Flight Center, Greenbelt, MD.
THE SEASONAL CYCLE OF ENERGETICS FROM THE GLAS/UMD CLIMATE GCM
David M. Straus and J. Shukla (Maryland Univ., College Park.)

Dec. 1988 39 p
(NASA-TM-100714; Rept-89B00067; NAS 1.15:100714) Avail: NTIS HC A03/MF A01 CSCL 04B

The annual cycle of atmospheric energetics from a 2-year integration of the GLAS/UMD Climate GCM is computed and compared to results from the European Centre analyses of the GWE year, and to previously published results on a global basis. All calculations are done in the mixed space-time domain. The main conclusions are: (1) the seasonal cycle of today's eddy kinetic energy (in both hemispheres), and of the transient eddy available potential energy and the potential-to-kinetic energy conversions (mean and eddy) in the Northern Hemisphere are well simulated by the GCM; (2) the GCM's tendency to have anomalously large mean u-winds at upper levels in high latitudes leads to excessive wintertime values of mean kinetic and available potential energies, and causes distortions in the GCM latitude-height distribution of kinetic energy and of many of the conversions; (3) the eddy conversion of available potential-to-kinetic energy obtained from the ageostrophic wind in these analyses; and (4) the conversions in the Southern Hemisphere are not well simulated by the GCM, although the observations are somewhat questionable. Author

N89-21449*# Pennsylvania State Univ., University Park. Dept. of Meteorology.
COMBINED VHF DOPPLAR RADAR AND AIRBORNE (CV-990) MEASUREMENTS OF ATMOSPHERIC WINDS ON THE MESOSCALE Final Technical Report
Christopher W. Fairall and Dennis W. Thomson Apr. 1989 149 p
(Grant NAG8-050)
(NASA-CR-184953; NAS 1.26:184953) Avail: NTIS HC A07/MF A01 CSCL 04B

Hourly measurements of wind speed and direction obtained using two wind profiling Doppler radars during two prolonged jet stream occurrences over western Pennsylvania were analyzed. In particular, the time-variant characteristics of derived shear profiles were examined. To prevent a potential loss of structural detail and retain statistical significance, data from both radars were stratified into categories based on the location data from the Penn State radar were also compared to data from Pittsburgh radiosondes. Profiler data dropouts were studied in an attempt to determine possible reasons for the apparently reduced performance of profiling radars operating beneath a jet stream. Temperature profiles for the radar site were obtained using an interpolated temperature and dewpoint temperature sounding procedure developed at Penn State. The combination of measured wind and interpolated temperature profiles allowed Richardson number profiles to be generated for the profiler sounding volume. Both Richardson number and wind shear statistics were then examined along with pilot reports of turbulence in the vicinity of the profiler. Author

N89-21450# Atmospheric and Environmental Research, Inc., Cambridge, MA.
ENHANCEMENTS TO THE AFGL (AIR FORCE GEOPHYSICS LABORATORY) STATISTICAL ANALYSIS PROGRAM (ASAP) FOR THE GLOBAL MULTIVARIATE ANALYSIS OF HEIGHTS AND WINDS Scientific Report No. 4
Ross N. Hoffman, Mark Mickelson, and Thomas Nehrkorn 17 Sep. 1988 107 p
(Contract F19628-86-C-0141)
(AD-A202912; AFGL-TR-88-0279) Avail: NTIS HC A06/MF A01 CSCL 04B

This report documents changes to and experiments designed to test the impact of these changes on the AFGL Statistical Analysis Program (ASAP) of heights and winds on the model sigma surfaces. Key enhancements include a new, simpler and more efficient method of converting pressure layer temperatures into sigma level heights, a corrected and improved handling of the least squares equations and a new solver for these systems of equations based on standard LINPACK routines. We conducted several offline tests of the new versions of procedures SATLTMP and ASAP2 which embody these enhancements to verify their correctness, to compare their results to results of the earlier versions and to tune certain control constants. We then conducted a one week data assimilation experiment, using simulated data to examine the impact of the enhanced ASAP. The changes made to ASAP have enhanced its consistency and operation. Separate studies of the satellite profile data preprocessing and the specification and solution of the normal equations demonstrated that the changes made are desirable. The overall positive impact of the enhancements is small as measured by a one week data assimilation experiment based on simulated data. GRA

N89-21451# Naval Oceanography Command Detachment, Asheville, NC.
SUMMARY OF METEOROLOGICAL OBSERVATIONS, SURFACE (SMOS) FOR MOFFETT FIELD, CALIFORNIA Reference Report, 1955 - 1986
Dec. 1988 670 p
(AD-A203628) Avail: NTIS HC A99/MF A01 CSCL 04B

This data report consists of a six part statistical summary of surface weather observations. The six parts are: Part A - Weather Conditions/Atmospheric Phenomena, Part B - Precipitation/Snow Depth, Part C - Surface Winds, Part D - Ceiling versus Visibility/Sky Cover, Part E - Psychrometric Summaries, Part F - Station Pressure/Sea Level Pressure. GRA

N89-21452# Naval Postgraduate School, Monterey, CA.
SATELLITE SIGNATURES OF RAPID CYCLOGENESIS M.S. Thesis
Jose F. H. Atangan Dec. 1988 58 p
(AD-A203934) Avail: NTIS HC A04/MF A01 CSCL 04B

Animation of satellite visual and infrared imagery indicates that rapid cloud growth is a characteristic of explosively deepening cyclones. The working hypothesis in this thesis is that the intense vertical motions responsible for the low-level spin-up will produce rapid cloud expansion in the upper troposphere that can be detected using digital satellite data. Using digital IR data from GOES-West, the cloud growth of three explosive storms that developed over the eastern North Pacific Ocean were measured quantitatively and compared with the cyclone deepening rate. The results indicate that the growth in areal coverage of clouds colder than -45 C is most closely related to the explosive development period while the growth of the warmer cloud tops is related to the open wave stage. This relationship is dependent on the cloud pattern of the maturing cyclone. Correlations between cloud growth and pressure deepening were calculated but provide only a general estimate of the relationship between the two parameters. This study demonstrates the feasibility of using digitized satellite data to quantitatively analyze the cloud growth and structure of explosively developing cyclones. GRA

N89-21453# Air Force Environmental Technical Applications Center, Scott AFB, IL.
UPPER-WIND CLIMATOLOGY FOR CONUS
Susan Reyes-Sauter Nov. 1988 115 p
(AD-A203961; USAFETAC/PR-88/003) Avail: NTIS HC A06/MF A01 CSCL 04B

Report consists of 12 sets (one set for each month) of CONUS maps with upper-wind speed/direction plots at every 5 degrees of latitude and longitude. Winds are plotted at nine levels, starting at 5,000 feet MSL and ending at 45,000 feet MSL. Database used was the Air Force Global Weather Central's SADS (Summarized Analysis Data Set), period of record 1977 to 1982. GRA

N89-21454# Air Force Environmental Technical Applications Center, Scott AFB, IL.
SEASONAL SNOWFALL STATISTICS FOR SELECTED STATIONS
Oct. 1988 38 p
(AD-A203965; USAFETAC/TN-88/005) Avail: NTIS HC A03/MF A01 CSCL 04B

This pamphlet provides a convenient reference to seasonal snowfall statistics at 64 selected locations worldwide. Data is for the 10-year period from 1976 to 1986. Total snowfall amounts for

each season (defined as July of one year to June of the next) is provided, along with 24-hour snowfall extremes, and dates. Seasonal means and standard deviations are also given. All values are in inches. GRA

N89-21455# Air Force Environmental Technical Applications Center, Scott AFB, IL.
GLOBAL SNOW DEPTH CLIMATOLOGY
Dudley F. Foster, Jr. and Robert D. Davy Dec. 1988 56 p
(AD-A203969; USAFETAC/TN-88/006) Avail: NTIS HC A04/MF A01 CSCL 04B

This report describes the USAF Environmental Technical Applications Center's Global Snow Depth Climatic Database; tells how the database was created and how it can be updated. It also tells potential users of the Snow Depth Database how to order data. Contoured charts that show mean mid-month snow depths for September through June in North America, Europe, and Asia are included in an appendix. GRA

N89-21456# Air Force Geophysics Lab., Hanscom AFB, MA.
BLENDING OF SURFACE AND RAWINSONDE DATA IN MESOSCALE OBJECTIVE ANALYSIS Final Report
Samuel Y. K. Yee and Arthur J. Jackson 14 Jun. 1988 37 p
(AD-A203984; AFGL-TR-88-0144; AFGL-ERP-1005) Avail: NTIS HC A03/MF A01 CSCL 04A

This report describes a simple technique to blend surface and rawinsonde observations in the planetary boundary layer (PBL) using a Barnes-type objective analysis. This goal is to improve the mesoscale detail of boundary layer input fields for a mesoscale numerical weather prediction model. The technique uses both surface and rawinsonde data in the boundary layer, where it is known that mesoscale details are inadequately resolved by the rawinsonde network and where the influence of the ground surface is strongest. Our challenge is to blend the signals contained in the denser surface observations that capture at least some mesoscale detail with those contained in the denser surface observations that capture at least some mesoscale detail with those contained in the boundary layer rawinsonde data. This is accomplished simply by comparing two analyses at the ground, one containing both rawinsonde data-resolvable and surface-data-resolvable information and the other, only the rawinsonde scale information. Differences between these two fields are assumed to be the signals undetected by the rawinsonde network. These mesoscale signals are then incorporated into the PBL analyses as a function of the distance from the ground. Results show a positive impact on boundary layer analyses due to the blending of surface and rawinsonde data. GRA

N89-21457# Pacific Northwest Labs., Richland, WA.
A SIMPLE MODEL FOR WIND FIELD ESTIMATION IN COMPLEX TERRAIN
E. D. Skyllingstad and G. L. Andrews Jan. 1989 15 p Presented at the 6th Joint Conference on Applications of Air Pollution Meteorology, Anaheim, CA, 29 Jan. 1989
(Contract DE-AC06-76RL-01830)
(DE89-007240; PNL-SA-16315; CONF-890133-6) Avail: NTIS HC A03/MF A01

A prognostic mixed-layer model is presented that provides a time-dependent wind field for use in situations where data are sparse or limited to only one observing site. Such a model could provide improved estimates of atmospheric transport for dispersion modeling. The model is based on a form of the Navier-Stokes equations integrated over the depth of the atmospheric boundary layer. This type of model has been used in many applications including the simulation of terrain drag, development of a climatological wind field, and modeling drainage winds. To provide a more realistic approximation of boundary layer growth, a one-dimensional boundary-layer model is used for obtaining entrainment rates at the top of the mixed layer. DOE

N89-21458# Pacific Northwest Labs., Richland, WA.
ROTATIONALLY SAMPLED WIND CHARACTERISTICS FOR SEVERAL ROTOR SIZES USING LASER ANEMOMETER MEASUREMENTS
J. R. Connell and V. R. Morris Feb. 1989 60 p
(Contract DE-AC06-76RL-01830)
(DE89-007942; PNL-6811) Avail: NTIS HC A04/MF A01

The concept of measuring the wind velocity rotationally around crosswind circles using a circle-scanning Doppler laser anemometer is investigated to determine the technique's suitability as an effective, simple, economical, and nonintrusive method for estimation turbulence at a wind turbine rotor. Estimates of wind features obtained using the lidar technique are compared to actual wind measurements obtained using a vertical plane array of anemometers, and to other estimates generated using a single-tower technique. Although the lack of a common data set precludes a firm conclusion regarding the lidar method's accuracy, it appears that the rotationally scanning lidar has the potential of becoming an excellent tool for measuring turbulent wind around the disk of rotation of a turbine blade. DOE

N89-21728*# Auburn Univ., AL. Dept. of Electrical Engineering.
FINITE ELEMENT SIMULATION OF THUNDERSTORM ELECTRODYNAMICS IN THE PROXIMITY OF THE STORM
Michael Edward Baginski *In* Alabama Univ., Research Reports: 1988 NASA/ASEE Summer Faculty Fellowship Program Dec. 1988 22 p (For primary document see N89-21726 14-99)
Avail: NTIS HC A99/MF E03 CSCL 04B

N89-21732*# Texas Technological Univ., Lubbock. Atmospheric Science Group.
THE ROLE OF RADIATION-DYNAMICS INTERACTION IN REGIONAL NUMERICAL WEATHER PREDICTION
Chia-Bo Chang *In* Alabama Univ., Research Reports: 1988 NASA/ASEE Summer Faculty Fellowship Program Dec. 1988 18 p (For primary document see N89-21726 14-99)
Avail: NTIS HC A99/MF E03 CSCL 04B

48 OCEANOGRAPHY

Includes biological, dynamic, and physical oceanography; and marine resources.

For related information see also *43 Earth Resources and Remote Sensing.*

N89-21459# Woods Hole Oceanographic Institution, MA.
COMPUTER PROGRAM FOR CALCULATING FREQUENCIES AND MODAL STRUCTURES OF FREE COASTAL-TRAPPED WAVES
John L. Wilkin Dec. 1987 54 p
(Grant NSF OCE-85-21837)
(PB88-243928; WHOI-87-53) Avail: NTIS HC A04/MF A01 CSCL 08C

A listing and full documentation is presented for a FORTRAN computer program which computes the dispersion curves and across-shelf modal structures of free coastal trapped waves in a coastal channel. The three velocity components, mass transport stream function, and density and pressure perturbation fields are computed. The solution procedure used (horizontal finite differences on a staggered grid and an expansion in the vertical in terms of modified Chebyshev polynomials) makes the solution compatible (without interpolation) with the numerical scheme employed in the Haidvogel et al., primitive equation ocean circulation model. Author

N89-21460# Defence Research Establishment Pacific, Victoria (British Columbia).
OSRMS (OCEAN SURFACE ROUGHNESS MEASUREMENT SYSTEM): THE DREP (DEFENCE RESEARCH ESTABLISHMENT PACIFIC) NEAR-NADIR SCATTEROMETER
L. C. Pempel, B. A. Hughes, and S. J. Hughes Aug. 1988

45 p
(AD-A202983; DREP-TM-88-15) Avail: NTIS HC A03/MF A01 CSCL 17E

The ocean surface roughness measurement system (OSRMS) is a near-nadir-directed infrared (IR) scatterometer. It has been used to measure ocean-surface parameters and particularly for the examination from an aircraft of internal waves. This paper gives a description of the configuration and operation of the OSRMS including the mechanical, electrical, electronic, optical, and software components. A brief overview of the trial, SCATTMOD III and the data obtained in that trail are also described. The discussion of the data from this trial contains examples of internal waves, ship wakes, and aircraft attitude compensation, and a description of wind velocity effects on the speckle noise. GRA

N89-21300*# New York Univ., New York. Earth Systems Group.
OCEAN ALKALINITY AND THE CRETACEOUS/TERTIARY BOUNDARY Abstract Only
K. G. Caldeira and Michael R. Rampino *In* Lunar and Planetary Inst., Global Catastrophes in Earth History: An Interdisciplinary Conference on Impacts, Volcanism, and Mass Mortality 1988 p 23 (For primary document see N89-21287 14-42)
Avail: NTIS HC A11/MF A01 CSCL 08C

N89-21307*# McMaster Univ., Hamilton (Ontario). Dept. of Geology.
NOBLE METALS IN MID-OCEAN RIDGE VOLCANISM: A SIGNIFICANT FRACTIONATION OF GOLD WITH RESPECT TO PLATINUM GROUP METALS
James H. Crocket *In* Lunar and Planetary Inst., Global Catastrophes in Earth History: An Interdisciplinary Conference on Impacts, Volcanism, and Mass Mortality 1988 p 34-35 (For primary document see N89-21287 14-42)
Avail: NTIS HC A11/MF A01 CSCL 08C

N89-21322*# Delaware Univ., Newark. Dept. of Geology.
LATE EOCENE IMPACT EVENTS RECORDED IN DEEP-SEA SEDIMENTS
B. P. Glass *In* Lunar and Planetary Inst., Global Catastrophes in Earth History: An Interdisciplinary Conference on Impacts, Volcanism, and Mass Mortality 1988 p 63-64 (For primary document see N89-21287 14-42)
Avail: NTIS HC A11/MF A01 CSCL 08C

N89-21328*# Princeton Univ., NJ. Dept. of Geological and Geophysical Sciences.
HIGH RESOLUTION CHRONOLOGY OF LATE CRETACEOUS-EARLY TERTIARY EVENTS DETERMINED FROM 21,000 YR ORBITAL-CLIMATIC CYCLES IN MARINE SEDIMENTS Abstract Only
Timothy D. Herbert and Steven DHondt *In* Lunar and Planetary Inst., Global Catastrophes in Earth History: An Interdisciplinary Conference on Impacts, Volcanism, and Mass Mortality 1988 p 74 (For primary document see N89-21287 14-42)
Avail: NTIS HC A11/MF A01 CSCL 08C

N89-21330*# Arizona Univ., Tucson. Lunar and Planetary Lab.
IMPACT WAVE DEPOSITS PROVIDE NEW CONSTRAINTS ON THE LOCATION OF THE K/T BOUNDARY IMPACT
A. R. Hildebrand and W. V. Boynton *In* Lunar and Planetary Inst., Global Catastrophes in Earth History: An Interdisciplinary Conference on Impacts, Volcanism, and Mass Mortality 1988 p 76-77 (For primary document see N89-21287 14-42)
Avail: NTIS HC A11/MF A01 CSCL 08C

N89-21331*# Arizona Univ., Tucson. Lunar and Planetary Lab.
PROVENANCE OF THE K/T BOUNDARY LAYERS
A. R. Hildebrand and W. V. Boynton *In* Lunar and Planetary Inst., Global Catastrophes in Earth History: An Interdisciplinary Conference on Impacts, Volcanism, and Mass Mortality 1988 p 78-79 (For primary document see N89-21287 14-42)
Avail: NTIS HC A11/MF A01 CSCL 08C

N89-21333*# Texas A&M Univ., College Station. Center for Tectonophysics.
IRIDIUM, SHOCKED MINERALS, AND TRACE ELEMENTS ACROSS THE CRETACEOUS/TERTIARY BOUNDARY AT MAUD RISE, WEDELL SEA, AND WALVIS RIDGE, SOUTH ATLANTIC OCEAN
Alan R. Huffman, James H. Crocket, and Neville L. Carter *In* Lunar and Planetary Inst., Global Catastrophes in Earth History: An Interdisciplinary Conference on Impacts, Volcanism, and Mass Mortality 1988 p 82-82 Prepared in cooperation with McMaster Univ., Hamilton (Ontario) (For primary document see N89-21287 14-42)
Avail: NTIS HC A11/MF A01 CSCL 08C

N89-21350*# Scripps Institution of Oceanography, La Jolla, CA.
SEAWATER STRONTIUM ISOTOPES AT THE CRETACEOUS-TERTIARY BOUNDARY
J. D. Macdougall and E. Martin *In* Lunar and Planetary Inst., Global Catastrophes in Earth History: An Interdisciplinary Conference on Impacts, Volcanism, and Mass Mortality 1988 p 111 (For primary document see N89-21287 14-42)
Avail: NTIS HC A11/MF A01 CSCL 08C

N89-21410*# Florida State Univ., Tallahassee. Dept. of Geology.
EVIDENCE OF VOLCANIC ASH AT A K-T BOUNDARY SECTION: OCEAN DRILLING PROGRAM HOLE 690 C, MAUD RISE, WEDDELL SEA OFF EAST ANTARCTICA
S. W. Wise, N. Hamilton, J. Pospichal, P. F. Barker, James P. Kennett, S. OConnell, W. R. Bryant, L. H. Burckle, P. K. Egeberg, and D. K. Futterer et al *In* Lunar and Planetary Inst., Global Catastrophes in Earth History: An Interdisciplinary Conference on Impacts, Volcanism, and Mass Mortality 1988 p 217-218 Prepared in cooperation with Southampton Univ. (England) (For primary document see N89-21287 14-42)
Avail: NTIS HC A11/MF A01 CSCL 08C

51 LIFE SCIENCES (GENERAL)

N89-21461# Health Effects Research Lab., Research Triangle Park, NC.
PULMONARY FUNCTION STUDIES IN THE RAT ADDRESSING CONCENTRATION VERSUS TIME RELATIONSHIPS OF OZONE (O3)
D. L. Costa, G. E. Hatch, J. Highfill, M. A. Stevens, and J. S. Tepper Nov. 1988 13 p Prepared in cooperation with Northrop Services, Inc., Research Triangle Park, NC
(PB89-129050; EPA/600/D-88/256) Avail: NTIS HC A03/MF A01 CSCL 06C

Recent data from human studies suggest that the current 1 hr National Ambient Air Quality Standard (NAAQS) for O3 may not be appropriate for exposures of several hours. Animal studies are being used to further investigate this issue. A polynomial model has been developed to depict lung injury from the interaction of O3 concentration (C) and exposure duration (T). The model was derived from lung fluid protein values in rats exposed in a matrix design to 0.1 to 0.8 ppm O3 for 2, 4, or 8 hrs. Airway dysfunction was correlated only at the highest CxT products. Rats, exposed to 0.5 or 0.8 ppm O3 for 2 or 7 hours with intermittent 8 percent CO2 to augment ventilation, were evaluated with static and dynamic lung function tests. Protein leakage into the airspace was also assessed. Although, the impact of T on O3 for 2 or 7 hours with intermittent 8 percent CO2 to augment ventilation, were evaluated with static and dynamic lung function tests. Protein leakage into the airspace was also assessed. Although, the impact of T on O3 toxicity appeared to be C-dependent, loss of function was not necessarily linear. Collectively, studies provide a preliminary basis for the evaluation of duration of exposure on the pulmonary response to O3. Author

N89-21290*# California Univ., San Diego. Dept. of Biology.
LIMITATIONS ON K-T MASS EXTINCTION THEORIES BASED UPON THE VERTEBRATE RECORD
J. David Archibald and Laurie J. Bryant *In* Lunar and Planetary Inst., Global Catastrophes in Earth History: An Interdisciplinary Conference on Impacts, Volcanism, and Mass Mortality 1988 p 4-5 Prepared in cooperation with California Univ., Berkeley (For primary document see N89-21287 14-42)
Avail: NTIS HC A11/MF A01 CSCL 06B

N89-21295*# California Univ., Berkeley. Marine Sciences Group.
LATE WENLOCK (MIDDLE SILURIAN) BIO-EVENTS: CAUSED BY VOLATILE BOLOID IMPACT/S
W. B. N. Berry and P. Wilde *In* Lunar and Planetary Inst., Global Catastrophes in Earth History: An Interdisciplinary Conference on Impacts, Volcanism, and Mass Mortality 1988 p 13-14 (For primary document see N89-21287 14-42)
Avail: NTIS HC A11/MF A01 CSCL 06B

N89-21301*# Carpenter (Kenneth), Philadelphia, PA.
DINOSAUR BONE BEDS AND MASS MORTALITY: IMPLICATIONS FOR THE K-T EXTINCTION
Kenneth Carpenter *In* Lunar and Planetary Inst., Global Catastrophes in Earth History: An Interdisciplinary Conference on Impacts, Volcanism, and Mass Mortality 1988 p 24-25 (For primary document see N89-21287 14-42)
Avail: NTIS HC A11/MF A01 CSCL 06B

N89-21304*# Colorado Univ., Boulder. Dept. of Geology.
ORIGINATION, DIVERSITY, AND EXTINCTION METRICS ESSENTIAL FOR ANALYSIS OF MASS BIOTIC CRISIS EVENTS: AN EXAMPLE FROM CRETACEOUS AMMONOIDEA Abstract Only
Christopher J. Collom *In* Lunar and Planetary Inst., Global Catastrophes in Earth History: An Interdisciplinary Conference on Impacts, Volcanism, and Mass Mortality 1988 p 30 (For primary document see N89-21287 14-42)
Avail: NTIS HC A11/MF A01 CSCL 06B

N89-21324*# Birmingham Univ. (England). Dept. of Geological Sciences.
THE END-TRIASSIC MASS EXTINCTION EVENT
A. Hallam *In* Lunar and Planetary Inst., Global Catastrophes in Earth History: An Interdisciplinary Conference on Impacts, Volcanism, and Mass Mortality 1988 p 66-67 (For primary document see N89-21287 14-42)
Avail: NTIS HC A11/MF A01 CSCL 06B

N89-21325*# Geological Inst., Oster Voldgade (Denmark).
DIACHRONISM BETWEEN EXTINCTION TIME OF TERRESTRIAL AND MARINE DINOSAURS
H. J. Hansen *In* Lunar and Planetary Inst., Global Catastrophes in Earth History: An Interdisciplinary Conference on Impacts, Volcanism, and Mass Mortality 1988 p 2 (For primary document see N89-21287 14-42)
Avail: NTIS HC A11/MF A01 CSCL 06B

N89-21329*# Washington State Univ., Pullman. Dept. of Geology.
SELECTIVE EXTINCTION OF MARINE PLANKTON AT THE END OF THE MESOZOIC ERA: THE FOSSIL AND STABLE ISOTOPE RECORD Abstract Only
Y. Herman and S. K. Bhattacharya *In* Lunar and Planetary Inst., Global Catastrophes in Earth History: An Interdisciplinary Conference on Impacts, Volcanism, and Mass Mortality 1988 p 75 Prepared in cooperation with Physical Research Lab., Ahmedabad (India) (For primary document see N89-21287 14-42)
Avail: NTIS HC A11/MF A01 CSCL 06B

N89-21354*# Florida International Univ., Miami. Dept. of Geology.
STEP-WISE EXTINCTIONS AT THE CRETACEOUS-TERTIARY BOUNDARY AND THEIR CLIMATIC IMPLICATIONS
Florentin J-M. R. Maurrasse *In* Lunar and Planetary Inst., Global Catastrophes in Earth History: An Interdisciplinary Conference on Impacts, Volcanism, and Mass Mortality 1988 p 117 (For primary document see N89-21287 14-42)
Avail: NTIS HC A11/MF A01 CSCL 06B

N89-21357*# Virginia Polytechnic Inst. and State Univ., Blacksburg. Dept. of Geological Sciences.
EARTH ORBITAL VARIATIONS AND VERTEBRATE BIOEVOLUTION
Dewey M. McLean *In* Lunar and Planetary Inst., Global Catastrophes in Earth History: An Interdisciplinary Conference on Impacts, Volcanism, and Mass Mortality 1988 p 121 (For primary document see N89-21287 14-42)
Avail: NTIS HC A11/MF A01 CSCL 06B

N89-21363*# Geological Survey, Denver, CO.
PLANT MICROFOSSIL RECORD OF THE TERMINAL CRETACEOUS EVENT IN THE WESTERN UNITED STATES AND CANADA
D. J. Nichols and R. F. Fleming *In* Lunar and Planetary Inst., Global Catastrophes in Earth History: An Interdisciplinary Conference on Impacts, Volcanism, and Mass Mortality 1988 p 130-131 (For primary document see N89-21287 14-42)
Avail: NTIS HC A11/MF A01 CSCL 06B

N89-21367*# California Univ., Los Angeles.
PERMO-TRIASSIC VERTEBRATE EXTINCTIONS: A PROGRAM
E. C. Olson *In* Lunar and Planetary Inst., Global Catastrophes in Earth History: An Interdisciplinary Conference on Impacts, Volcanism, and Mass Mortality 1988 p 137-138 (For primary document see N89-21287 14-42)
Avail: NTIS HC A11/MF A01 CSCL 06B

N89-21380*# Geological Survey, Denver, CO.
LATE FRASNIAN MASS EXTINCTION: CONODONT EVENT STRATIGRAPHY, GLOBAL CHANGES, AND POSSIBLE CAUSES
Charles A. Sandberg, Willi Ziegler, Roland Dreesen (INIEX, Liege, Belgium), and Jamie L. Butler *In* Lunar and Planetary Inst., Global Catastrophes in Earth History: An Interdisciplinary Conference on Impacts, Volcanism, and Mass Mortality 1988 p 160-161 (For primary document see N89-21287 14-42)
Avail: NTIS HC A11/MF A01 CSCL 06B

N89-21385*# Chicago Univ., IL. Dept. of the Geophysical Sciences.
PERIODICITY OF EXTINCTION: A 1988 UPDATE
J. John Sepkowski, Jr. *In* Lunar and Planetary Inst., Global Catastrophes in Earth History: An Interdisciplinary Conference on Impacts, Volcanism, and Mass Mortality 1988 p 170-171 (For primary document see N89-21287 14-42)
Avail: NTIS HC A11/MF A01 CSCL 06B

N89-21390*# Minnesota Univ., Minneapolis. Dept. of Geology and Geophysics.
BIOSTRATIGRAPHIC CASE STUDIES OF SIX MAJOR EXTINCTIONS
R. E. Sloan *In* Lunar and Planetary Inst., Global Catastrophes in Earth History: An Interdisciplinary Conference on Impacts, Volcanism, and Mass Mortality 1988 p 180-181 (For primary document see N89-21287 14-42)
Avail: NTIS HC A11/MF A01 CSCL 06B

N89-21396*# Wesleyan Univ., Middletown, CT. Dept. of Earth and Environmental Sciences.
MASS EXTINCTIONS IN THE DEEP SEA
E. Thomas *In* Lunar and Planetary Inst., Global Catastrophes in Earth History: An Interdisciplinary Conference on Impacts,

Volcanism, and Mass Mortality 1988 p 192-193 (For primary document see N89-21287 14-42)
Avail: NTIS HC A11/MF A01 CSCL 06B

N89-21404*# Washington Univ., Seattle. Dept. of Geological Sciences.
MACROFOSSIL EXTINCTION PATTERNS AT BAY OF BISCAY CRETACEOUS-TERTIARY BOUNDARY SECTIONS
Peter D. Ward and Kenneth MacLeod *In* Lunar and Planetary Inst., Global Catastrophes in Earth History: An Interdisciplinary Conference on Impacts, Volcanism, and Mass Mortality 1988 p 206-207 (For primary document see N89-21287 14-42)
Avail: NTIS HC A11/MF A01 CSCL 06B

N89-21406*# Alabama Univ., Birmingham. Dept. of Physics.
HEAVY METAL TOXICITY AS A KILL MECHANISM IN IMPACT CAUSED MASS EXTINCTIONS
T. J. Wdowiak, S. A. Davenport, D. D. Jones, and P. Wdowiak (Wdowiak, P., Birmingham, AL) *In* Lunar and Planetary Inst., Global Catastrophes in Earth History: An Interdisciplinary Conference on Impacts, Volcanism, and Mass Mortality 1988 p 209-210 (For primary document see N89-21287 14-42)
Avail: NTIS HC A11/MF A01 CSCL 06B

N89-21412*# Rhode Island Univ., Narragansett. Graduate School of Oceanography.
THE CRETACEOUS-TERTIARY BOUNDARY MARINE EXTINCTION AND GLOBAL PRIMARY PRODUCTIVITY COLLAPSE
J. C. Zachos, M. A. Arthus, and W. E. Dean *In* Lunar and Planetary Inst., Global Catastrophes in Earth History: An Interdisciplinary Conference on Impacts, Volcanism, and Mass Mortality 1988 p 221-222 Prepared in cooperation with Geological Survey, Denver, CO (For primary document see N89-21287 14-42)
Avail: NTIS HC A11/MF A01 CSCL 06B

52 AEROSPACE MEDICINE

Includes physiological factors; biological effects of radiation; and effects of weightlessness on man and animals.

N89-21462# Tulsa Univ., OK. Dept. of Psychology.
BEHAVIORAL EFFECTS OF MICROWAVES: RELATIONSHIP OF TOTAL DOSE AND DOSE RATE
Mary Ellen OConnor and Robert Strattan Oct. 1988 67 p
(Contract EPA-68-02-4120)
(PB89-118640; EPA/600/1-88/005) Avail: NTIS HC A04/MF A01 CSCL 06R

The goal of the research was to compare the realtionship of whole body averaged specific absorption rate (SAR) and specific absorption (SA) to determine whether close rate or dose was the better predictor of biological effects. Sperm positive Long-Evans female rats were exposed to 2450 MHz CW microwave radiation for 1 to 3 hours at approximately 10 W/kg. The maternal subjects were then observed for natural delivery of their litters. Sensitivity to thermally induced seizures and huddling were studied in the offspring. Analyses revealed that there were no statistically significant differences between exposed and control offspring on the behavioral indices. The behavior did not appear to be affected by prenatal exposure to microwave radiation at this level. The huddle sizes became smaller as the pups aged both in exposed and control offspring. GRA

N89-21463*# National Aeronautics and Space Administration. Lyndon B. Johnson Space Center, Houston, TX.
SACCADIC EYE MOVEMENT DURING SPACEFLIGHT
John J. Uri, Barry J. Linder, Thomas P. Moore (Methodist Hospital, Indianapolis, IN.), Sam L. Pool, and William E. Thornton Apr. 1989 13 p
(NASA-TM-100475; S-592; NAS 1.15:100475) Avail: NTIS HC A03/MF A01 CSCL 06P

Saccadic eye movements were studied in six subjects during two Space Shuttle missions. Reaction time, peak velocity and accuracy of horizontal, visually-guided saccades were examined preflight, inflight and postflight. Conventional electro-oculography was used to record eye position, with the subjects responding to pseudo-randomly illuminated targets at 0 deg and + or - 10 deg and 20 deg visual angles. In all subjects, preflight measurements were within normal limits. Reaction time was significantly increased inflight, while peak velocity was significantly decreased. A tendency toward a greater proportion of hypometric saccades inflight was also noted. Possible explanations for these changes and possible correlations with space motion sickness are discussed. Author

N89-21464# Texas Univ., Galveston. Dept. of Physiology and Biophysics.
GATING KINETICS AND ION TRANSFER IN CHANNELS OF NERVE MEMBRANE Annual Report, Nov. 1987 - Nov. 1988
Harvey M. Fishman 9 Nov. 1988 13 p
(Contract N00014-87-K-0055; RR04108)
(AD-A202509) Avail: NTIS HC A03/MF A01 CSCL 06D

Whether the kinetics and thermodynamics of electric-field initiated alteration of nerve membrane to the conduction of specific ions through ion channels (gating) can be validly described by linear, equilibrium models will be determined by examining the time reversal properties of ion channel current fluctuations. The kinetics of gated channels derived from analysis of stochastic current fluctuations and those derived from linear macroscopic determinations (membrane complex admittance determinations) will be compared to ascertain whether the assumed relationship exists. GRA

N89-21465# Air Force Inst. of Tech., Wright-Patterson AFB, OH. School of Engineering.
LMS ADAPTIVE FILTERING APPLIED TO A MICROWAVE ARTERIAL PULSE MONITOR M.S. Thesis
Brian J. Simes Dec. 1988 118 p
(AD-A202732; AFIT/GE/ENG/88D-45) Avail: NTIS HC A06/MF A01 CSCL 06L

A prototype microwave arterial pulse monitor was evaluated and modified. Evaluation test data was collected from the temporal region of human volunteers using the microwave arterial pulse monitor. Three sets of test signals were developed using this test data. These test signals were used to evaluate the feasibility of using a LMS adaptive noise cancellation filter for reduction of noise artifacts observed in the output of the microwave arterial pulse monitor. A computer program using the LMS algorithm was written and the performance of the LMS filter was evaluated for its effectiveness in removing the unwanted noise. A system model describing the performance characteristics of the test subject-monitor-filter interface is presented. GRA

N89-21466# Air Force Inst. of Tech., Wright-Patterson AFB, OH. School of Engineering.
A STUDY OF MOTION SICKNESS: MATHEMATICAL MODELING AND DATA ANALYSIS M.S. Thesis
Mark F. Scott Dec. 1988 106 p
(AD-A202770; AFIT/GEO/ENG/88D-4) Avail: NTIS HC A06/MF A01 CSCL 06J

Male test subjects were given the drug phenytoin in a double blind, placebo controlled crossover experiment. They were then rotated in a motion chair while eleven of their physiological parameters were measured. The drug appeared to delay or even prevent the evolution of motion sickness, depending on the test subject. Barron Associates' Abductive Reasoning Mechanism software was used to develop new motion sickness models. The biophysiological data collected in 1988 were analyzed for trends; several were found. GRA

N89-21467# Texas Univ. Health Science Center, San Antonio. Dept. of Radiology.
EFFECTS OF SIMULTANEOUS RADIOFREQUENCY RADIATION AND CHEMICAL EXPOSURE OF MAMMALIAN CELLS, VOLUME 2 Final Report, 2 Jan. 1984 - 31 Dec. 1986
Martin L. Meltz, Victor Ciaravino, James J. Kerbacher, and Phyllis

Eagan Jul. 1988 84 p
(Contract F33615-84-C-0604)
(AD-A202780; USAFSAM-TR-87-32-Vol-2) Avail: NTIS HC A05/MF A01 CSCL 06G

A circulating water-bath exposure system has been designed for in vitro radiofrequency radiation (RFR) exposure studies in the 915 to 2450 MHz range. A continuously rotating Styrofoam float, holding ten T-25 tissue culture flasks, averages out field heterogeneity and allows mixing in the medium in the flasks. The presence of cells in the exposure flask (as attached monolayer or cell suspension) did not result in an SAR different from that measured in the medium without cells present. We have posed two hypotheses relative to the mutagenic activity of RFR: (1) that RFR by itself is genotoxic to mammalian cells in vitro; and (2) that a simultaneous exposure of mammalian cells to RFR during treatment with a genotoxic chemical will result in an alteration of the genotoxic activity of the chemical alone. RFR exposure alone (at moderate power levels which resulted in a temperature increase in the cell culture medium of no more than 3 C) is not mutagenic. During simultaneous treatment, the RFR does not affect either the inhibition of cell growth or the extent of mutagenesis resulting from the chemical treatment alone. The same two hypotheses were explored for induction of sister chromatid exchanges (SCEs) and chromosome aberrations in Chinese hamster ovary cells which were similarly exposed to RFR and chemicals. The chemicals studied for SCE induction were mitomycin C (MMC) and Adriamycin. GRA

N89-21468# Smith-Kettlewell Inst. of Visual Sciences, San Francisco, CA.
PSYCHOPHYSICAL STUDIES OF VISUAL CORTICAL FUNCTIONS Final Technical Report, 1 Sep. 1985 - 31 Aug. 1988
Ken Nakayama 20 Oct. 1988 6 p
(Grant AF-AFOSR-0320-83; AF Proj. 2313)
(AD-A202814; AFOSR-88-1226TR) Avail: NTIS HC A02/MF A01 CSCL 05H

Our research continues to study two primary areas. First is the area of visual attention where we have shown that there are both transient and sustained components. In contrast to the sustained component, we find that the transient component is much more powerful, is short lasting, is relatively independent of volition and finally, is also independent of the stimulus that elicits it. Thus, it is a genuine attentional effect not tied directly to the sensory stimulus but is probably operative relatively early in visual cortical processing, particularly in relation to the sustained component. We have also shown that the latency of this transient component is reduced by the prior removal of a stimulus fixation mark. Such a finding provides strong support for the view that express saccadic eye movements (seen under similar conditions) are mediated by rapid shifts of attention. Second, we have been studying issues related to partial visibility. In particular, we examine how the visual system deals with occlusion. Our results indicate that the occlusive relations of surfaces have widespread effects in vision, influencing color, motion, transparency and depth. GRA

N89-21469# Oregon Univ., Eugene. Dept. of Computer and Information Science.
RECONSTRUCTION OF BINOCULAR DEPTH ACROSS CONTINUOUS SURFACES
Kent A. Stevens and Allen Brookes 14 Dec. 1988 55 p
(Contract N00014-87-K-0321; RR042)
(AD-A202827) Avail: NTIS HC A04/MF A01 CSCL 06D

This technical report consists of two publications. The first will appear in the Journal of Experimental Psychology: Human Perception and Performance in 1989. This article examines the perception of depth in random dot surface versus volume stimuli, and shows that depth associated with a continuous surface is subject to reconstruction artifacts, where equivalent random-dot volume stimuli are used as a control. The second article has been submitted for publication. This article explores the analogy between the reconstruction of stereoscopic depth and the reconstruction of brightness. The analogy holds for a number of classical simultaneous contrast effects. Dissimilarities are found, however, in terms of the lateral inhibition effects traditionally attributed to underlying spatial-differention operators. GRA

N89-21470# Kings Coll., London (England). Dept. of Physics.
ACCURATE DETERMINATION OF THE COMPLEX PERMITTIVITY OF BIOLOGICAL TISSUE AROUND 35 GHz Final Report, 15 Mar. 1984 - 14 Mar. 1986
Rodney J. Sheppard Sep. 1988 53 p
(Grant AF-AFOSR-0097-84; AF Proj. 2312)
(AD-A202907; USAFSAM-TR-87-13) Avail: NTIS HC A04/MF A01 CSCL 06G

Apparatus is described which enables the complex permittivity of liquids and solid tissue to be measured at a frequency of 35 GHz. The results are presented on various rabbit tissues, including muscle, fat, skin, brain tissues, and eye lens; and some phantom tissue equivalent materials have been devised. Various liquids have been measured, including rabbit blood, water, and saline. The results have been examined for any evidence of an anomalous/resonant behavior, but none was found. GRA

N89-21471# Mayo Clinic, Rochester, MN.
G-INDUCED LOSS OF CONSCIOUSNESS AND ITS PREVENTION Final Report, Jan. 1942 - Jan. 1988
Earl H. Wood Sep. 1988 54 p
(Contract N66001-87-C-0079; AF Proj. 7930)
(AD-A202960; USAFSAM-TR-87-41) Avail: NTIS HC A04/MF A01 CSCL 06J

The current capabilities of trained individuals to maintain clear vision during sustained exposures to 9 Gz, an increase in protected G tolerance of about 4 G over World War II fighter pilots, is a result of combined use of a G suit and very effective self-protective straining maneuvers such as the M-1, L-1 and pressure breathing, all of which are variants of the Valsalva maneuver developed in the 1940s. However, more than ten fatal crashes attributed to acceleration induced loss of consciousness (GLOC) have occurred in recent years. The most plausible causes are: (1) increased capability of jet-powered fighters to sustain, with minimal pilot effort, accelerations in the 7 to 10 Gz range for periods longer than the symptom-free 3 to 8 second cerebral ischemic anoxic period which precedes GLOC, (2) an improperly performed Valsalva-type straining maneuver, and (3) development of a hypotensive vasovagal type reaction. A foolproof GLOC warning system such as detection of zero arterial pulsations at ear level to activate an automatic plane control takeover system could avoid most GLOC crashes. However, an omni-directional surveillance fighter plane cockpit for a fully horizontal position, preferable prone, is the only certain way to eliminate GLOC and to achieve the probable tactical advantages of sustained combat maneuvering in the 9 to 15 Gz range. GRA

N89-21472# Rochester Univ., NY. Center for Visual Science.
PERIPHERAL LIMITATIONS ON SPATIAL VISION Final Report, 1 Dec. 1984 - 31 May 1988
David R. Williams 6 Oct. 1988 16 p
(Grant AF-AFOSR-0019-85; AF Proj. 2313)
(AD-A203388; AFOSR-88-1335TR) Avail: NTIS HC A02/MF A01 CSCL 06D

This project employed psychophysical techniques to examine the limitation on spatial vision imposed by the first stages in the visual pathway. All the experiments capitalized on the use of laser interferometry, which allows sinusoidal gratings to be formed on an observer's retina that are immune to optical blurring. Comparisons of contrast sensitivity to such gratings with contrast sensitivity to gratings viewed under normal conditions provides an estimate of the modulation transfer function of the eye's optics. In addition, the appearance of very high frequency gratings is distorted, or aliased, by the cone mosaic. Such moire patterns provide the basis for a number of psychophysical techniques to assess the topography of the cone mosaic in the living eye. These measurements, accompanied by measurements of visual acuity for interference fringes clarify the relationship between cone

spacing and resolution. Resolution was also measured under conditions in which only the M or L cones could detect the interference fringe. Visual acuity was little different than it was when both cone types detected the grating, showing that resolution is immune to photoreceptor loss under these circumstances. GRA

N89-21473# Massachusetts Inst. of Tech., Cambridge. Artificial Intelligence Lab.
SEEING GHOST SOLUTIONS IN STEREO VISION
Daphna Weinshall Sep. 1988 14 p Prepared in cooperation with Whitaker Coll., MA
(Contracts N00014-85-K-0124; DACA76-85-C-0010)
(AD-A203581; AI-M-1073; CBIP-33) Avail: NTIS HC A03/MF A01 CSCL 06D

A unique matching is a stated objective of most computational theories of stereo vision. This report describes situations where humans perceive a small number of surfaces carried by non-unique matching of random dot patterns, although a unique solution exists and is observed unambiguously in the perception of isolated features. We find both cases where non-unique matchings compete and suppress each other and cases where they are all perceived as transparent surfaces. The circumstances under which each behavior occurs are discussed and a possible explanation is sketched. It appears that matching reduces many false targets to a few, but may still yield multiple solutions in some cases through a (possibly different) process of surface interpolation. GRA

N89-21474# Navy Personnel Research and Development Center, San Diego, CA.
BRAIN ACTIVITY DURING TACTICAL DECISION-MAKING. PART 5: A CROSS-STUDY VALIDATION OF EVOKED POTENTIALS AS INDICES OF WORKLOAD
Leonard J. Trejo, Gregory W. Lewis, and Mark H. Blankenship Oct. 1988 17 p
(AD-A203763; NPRDC-TN-89-7) Avail: NTIS HC A03/MF A01 CSCL 05H

The results of such tests can predict academic performance reasonably well but are less effective in predicting on-job performance. In an attempt to better understand the human as a integrator and decision maker in operating systems, event-related potentials (ERPs) have been employed to assess individual brain processes and their relationship to differences in on-job performance and decision making. The purpose of this report is to demonstrate a cross-study validation of the use of ERPs as indices of cognitive workload. The first study found that certain ERP amplitude measures decreased by about 40 percent as workload increased from baseline to active participation in an anti-air warfare situation (AIRDEF). The study was conducted in the summer of 1985 with group of 30 U.S. Marines stationed at the Naval Air Station, North Island, San Diego. The basic design of the experiment consisted of a single-task condition in which subjects performed an anti-air warfare simulation (AIRDEF) task under three progressively higher levels of difficulty. ERPs were recorded to a visual stimulus that was presented on the same monitor as the higher levels of difficulty. ERPs were recorded to a visual stimulus that was presented on the same monitor as the simulation, but this stimulus had no task relevance. GRA

N89-21475* National Aeronautics and Space Administration, Washington, DC.
AEROSPACE MEDICINE AND BIOLOGY: A CONTINUING BIBLIOGRAPHY WITH INDEXES (SUPPLEMENT 321)
Mar. 1989 54 p
(NASA-SP-7011(321); NAS 1.21:7011(321)) Avail: NTIS HC A04; NTIS standing order as PB89-912300, $10.50 domestic, $21.00 foreign CSCL 06E

This bibliography lists 137 reports, articles, and other documents introduced into the NASA scientific and technical information system in February 1989. Author

N89-21476* National Aeronautics and Space Administration, Washington, DC.
AEROSPACE MEDICINE AND BIOLOGY: A CONTINUING BIBLIOGRAPHY WITH INDEXES (SUPPLEMENT 322)
Apr. 1989 62 p
(NASA-SP-7011(322); NAS 1.21:7011(322)) Avail: NTIS HC A04; NTIS standing order as PB89-912300, $10.50 domestic, $21.00 foreign CSCL 06E

This bibliography lists 163 reports, articles, and other documents introduced into the NASA scientific and technical information system in March 1989. Author

53 BEHAVIORAL SCIENCES

Includes psychological factors; individual and group behavior; crew training and evaluation; and psychiatric research.

N89-21477*# National Aeronautics and Space Administration. Ames Research Center, Moffett Field, CA.
HELICOPTER FLIGHTS WITH NIGHT-VISION GOGGLES: HUMAN FACTORS ASPECTS
Michael S. Brickner Mar. 1989 38 p
(NASA-TM-101039; A-88305; NAS 1.15:101039) Avail: NTIS HC A03/MF A01 CSCL 05I

Night-vision goggles (NVGs) and, in particular, the advanced, helmet-mounted Aviators Night-Vision-Imaging System (ANVIS) allows helicopter pilots to perform low-level flight at night. It consists of light intensifier tubes which amplify low-intensity ambient illumination (star and moon light) and an optical system which together produce a bright image of the scene. However, these NVGs do not turn night into day, and, while they may often provide significant advantages over unaided night flight, they may also result in visual fatigue, high workload, and safety hazards. These problems reflect both system limitations and human-factors issues. A brief description of the technical characteristics of NVGs and of human night-vision capabilities is followed by a description and analysis of specific perceptual problems which occur with the use of NVGs in flight. Some of the issues addressed include: limitations imposed by a restricted field of view; problems related to binocular rivalry; the consequences of inappropriate focusing of the eye; the effects of ambient illumination levels and of various types of terrain on image quality; difficulties in distance and slope estimation; effects of dazzling; and visual fatigue and superimposed symbology. These issues are described and analyzed in terms of their possible consequences on helicopter pilot performance. The additional influence of individual differences among pilots is emphasized. Thermal imaging systems (forward looking infrared (FLIR)) are described briefly and compared to light intensifier systems (NVGs). Many of the phenomena which are described are not readily understood. More research is required to better understand the human-factors problems created by the use of NVGs and other night-vision aids, to enhance system design, and to improve training methods and simulation techniques. Author

N89-21478# Yale Univ., New Haven, CT.
COPING WITH NOVELTY AND HUMAN INTELLIGENCE: THE ROLE OF COUNTERFACTUAL REASONING Final Report
Robert J. Sternberg 1988 123 p
(Contract N00014-85-K-0589)
(AD-A203624) Avail: NTIS HC A06/MF A01 CSCL 05H

This Final Report is divided into four main sections. In the first section, a subset of the empirical research done with my collaborators under the contract is described in detail. Rather than attempt to describe every study, selected studies are described in detail. These studies show some of the range of work accomplished during the contract. In the second section, a list of the publications is presented that have ensued from 1985 to 1988, as well as publications that are in press. These are the years during which the contract was held. In the third section, presentations are listed which were given during the years of the contract. And in the

fourth and final section, the final budgetary accounting for the contract is given. GRA

54 MAN/SYSTEM TECHNOLOGY AND LIFE SUPPORT

Includes human engineering; biotechnology; and space suits and protective clothing.

For related information see also *16 Space Transportation.*

N89-21479*# Pittsburgh Univ., PA. Dept. of Electrical Engineering.

COMPUTER SIMULATION OF A PILOT IN V/STOL AIRCRAFT CONTROL LOOPS Final Report

William G. Vogt, Marlin H. Mickle, Mark E. Zipf, and Senol Kucuk 31 Jan. 1989 447 p

(Grant NAG3-729)

(NASA-CR-184815; NAS 1.26:184815) Avail: NTIS HC A19/MF A01 CSCL 05H

The objective was to develop a computerized adaptive pilot model for the computer model of the research aircraft, the Harrier II AV-8B V/STOL with special emphasis on propulsion control. In fact, two versions of the adaptive pilot are given. The first, simply called the Adaptive Control Model (ACM) of a pilot includes a parameter estimation algorithm for the parameters of the aircraft and an adaption scheme based on the root locus of the poles of the pilot controlled aircraft. The second, called the Optimal Control Model of the pilot (OCM), includes an adaption algorithm and an optimal control algorithm. These computer simulations were developed as a part of the ongoing research program in pilot model simulation supported by NASA Lewis from April 1, 1985 to August 30, 1986 under NASA Grant NAG 3-606 and from September 1, 1986 through November 30, 1988 under NASA Grant NAG 3-729. Once installed, these pilot models permitted the computer simulation of the pilot model to close all of the control loops normally closed by a pilot actually manipulating the control variables. The current version of this has permitted a baseline comparison of various qualitative and quantitative performance indices for propulsion control, the control loops and the work load on the pilot. Actual data for an aircraft flown by a human pilot furnished by NASA was compared to the outputs furnished by the computerized pilot and found to be favorable. Author

N89-21480# Lawrence Livermore National Lab., CA.

REVIEW AND ANALYSIS OF THE LITERATURE IN THE AREA OF HUMAN PERFORMANCE MODELING

Hilary D. Burton, Janice Butler, William W. Banks, and Thomas E. Berghage (RMC International, San Diego, CA.) Nov. 1988 141 p

(Contract W-7405-eng-48)

(DE89-006800; UCID-21558) Avail: NTIS HC A07/MF A01

The following review of the literature in the area of human performance modeling was compiled in conjunction with work sponsored by the U.S. Naval Health Research Center, San Diego, California, on the application of human performance data in wargaming models and simulation. The results were obtained by searching a number of on-line retrieval systems, downloading the data, and processing it using software developed by the Technology Information Systems Program. Databases which were searched included PsycINFO (American Psychological Association), Compendex (Engineering Index), Inspec (Institute of Electrical Engineers), NTIS (National Technical Information Service), DROLS (Department of Defense), NASA-Recon (National Aeronautics and Space Administration), Science Citation Index (Institute for Scientific Information), Conference Papers Index (Cambridge Scientific Abstracts), and a number of other databases which produced no retrieval results. Those citations identified as part of the PsycINFO databases are reprinted with permission of the American Psychological Association, publisher of Psychological abstracts and the PsycINFO database (Copyright c 1967 to 1988 by the American Psychological Association), and may not be reproduced without its prior permission. DOE

N89-21481# Aerospace Medical Research Labs., Wright-Patterson AFB, OH.

LCP-10 INTELLIGIBILITY OF OXYGEN MASKS AND MICROPHONES IN AIRCRAFT NOISE Summary Report, Oct. 1986 - Oct. 1988

Charles W. Nixon and Richard L. McKinley 24 Oct. 1988 37 p

(AD-A202474; AAMRL-TR-88-048) Avail: NTIS HC A03/MF A01 CSCL 25D

A series of studies was conducted to examine the effectiveness and limitations of the Joint Tactical Information Distribution System (JTIDS) voice channel in noisy environments. Initial efforts to improve performance focused on the input to JTIDS, specifically modifications to the oxygen mask and the use of prototype noise cancelling microphones. No improvements in voice communications were observed with the modified masks, prototype microphones or the various mask-microphone combinations. These and other measurement data demonstrated that the limit to voice communications performance with this system in noise was imposed at the listener instead of at the talker (oxygen mask input). The sound attenuation properties of the helmets and headsets were not adequate to provide the required speech-to-noise ratios at the ear in the highest noise levels. Among the conclusions were: (1) speech processed by the JTIDS voice channel may be more vulnerable to noise or easier to mask than regular speech, (2) efforts to improve voice communications effectiveness in noise in the near term should focus on improvements in the signal at the listener, and (3) active noise reduction technology in headsets has been proven, it offers a high potential for enhanced voice communications with the basic JTIDS voice channel and its utility should be pursued. GRA

N89-21482# Army Aeromedical Research Unit, Fort Rucker, AL.

SPH-4 US ARMY FLIGHT HELMET PERFORMANCE 1983-1987 Final Report

Peter Vymwy-Jones, Bernard Lanoue, and Douglas Pritts Aug. 1988 64 p

(AD-A202589; USAARL-88-15) Avail: NTIS HC A04/MF A01 CSCL 05H

Injury data was obtained from the U.S. Safety Center for the occupants of U.S. Army aircraft who were wearing aviator helmets when involved in duty-related aircraft accidents from the period beginning in June 1982 and ending in October 1987. The injury data was correlated with the physical condition of the helmets involved which had been obtained by the U.S. Army Aeromedical Research Laboratory under the Aviation Life Support Equipment Retrieval Program. The helmet performance was evaluated with regard to current injury prevention capabilities and potential improvements for future helmet designs. All helmets involved were involved in aircraft accidents except one SPH-4 which had been damaged by small arms fire. GRA

N89-21483# Air Force Inst. of Tech., Wright-Patterson AFB, OH. School of Engineering.

CAPACITY OF HUMAN OPERATOR USING SMART STICK CONTROLLER M.S. Thesis

Adolpho Cozzone Dec. 1988 138 p

(AD-A202712; AFIT/GE/ENG/88D-7) Avail: NTIS HC A07/MF A01 CSCL 23B

This thesis provides an analysis of transformation rate and capacity for six subjects using the smart stick controller. The subjects were tested in both a passive and active stick mode using three different forcing functions. The smart stick controller is an aircraft stick actively controlled by an algorithm developed by the Armstrong Aerospace Medical Research Laboratory (AAMRL) at Wright-Patterson AFB, OH to improve pilot tracking performance. In the passive mode, the stick behaves as any other stick used to control aircraft. However, in the active mode, the stick exerts a force in the direction opposite to the desired motion. This thesis reviews the literature, develops and analyzes a compensatory tracking task using classical control theory, and

applies information theory results to the human quasilinear model to determine the transinformation rate and capacity of the human operator. Finally, the results for both the active and passive mode are compared. Power spectral densities of the forcing functions, display error, and human response are used to calculate the human transfer function, noise remnant, transinformation rate and capacity. GRA

N89-21484# Anthropology Research Project, Yellow Springs, OH.
MEASURER'S HANDBOOK: US ARMY ANTHROPOMETRIC SURVEY, 1987-1988 Final Technical Report, Oct. 1986 - May 1987
Charles Clauser, Ilse Tebbetts, Bruce Bradtmiller, John McConville, and Claire Gordon 4 May 1988 330 p
(Contract DAAK60-86-C-0128)
(AD-A202721; NATICK-TR-88/043) Avail: NTIS HC A15/MF A01 CSCL 05I

The purpose of this manual is to describe and explain the tools and procedures required for the precise and accurate measurement of U.S. Army men and women. The handbook contains instructions for the measurement of 132 directly measured dimensions of the body, and for obtaining additional head and hand data collected with the use of two pieces fo custom-designed equipment: an electronic headboard and a hand photometric system. Also included in this generously illustrated measurer's guide are instructions for locating and drawing the landmarks required to define and standardize the dimensions, suggestions for handling subjects, and a guide to the operations and care of the personal computers to be used to record and edit the data in the field. The measurements obtained in this anthropometric survey will form the basis for ensuring that Army clothing, equipment, and systems properly accommodate Army personnel who run the body-size gamut from small women to large men. GRA

N89-21485# Navy Clothing and Textile Research Facility, Natick, MA.
THERMAL PROTECTION AFFORDED BY TWO ANTI-EXPOSURE COVERALLS WHEN WORN IN COLD WATER Final Technical Report, Dec. 1987 - Jul. 1988
Nancy A. Pimental and Barbara A. Avellini Oct. 1988 19 p
(AD-A202865; NCTRF-172) Avail: NTIS HC A03/MF A01 CSCL 05H

The Navy Clothing and Textile Research Facility (NCTRF) was contracted by U.S. Coast Guard Headquarters to evaluate the thermal protection afforded by two prototype aircrew anti exposure coveralls when worn in cold water. The coveralls were developed by two different manufacturers to meet U.S. Coast Guard specification G-OAV-3-1401/A of 15 July 1986. The coveralls were evaluated on seven male subjects immersed in 10 C (50 F) water for 2 hours (with air temperature 13 C, minimal wind). When either of the two anti-exposure coveralls was worn, all subjects were able to complete the 2-hour water immersion. There were no differences in the thermal protection afforded by the two coveralls, as measured by rectal temperature, skin temperature, heart rate, and oxygen uptake responses (P greater than 0.05). The decrease in rectal temperature after 2 hours of cold water immersion averaged 1.0 C; mean weighted skin temperature averaged 2.3 C. Final heart rate averaged 77 b/min. Oxygen consumption, which was used as a measure of shivering, was the same when either coverall was worn. Both coveralls met the Coast Guard requirement of preventing rectal temperature from dropping more than 1 C per hour. GRA

N89-21486# Army Aeromedical Research Lab., Fort Rucker, AL.
THE IMPACT OF THE US ARMY'S AH-64 HELMET MOUNTED DISPLAY ON FUTURE AVIATION HELMET DESIGN Final Report
Clarence E. Rash and John S. Martin Aug. 1988 21 p
(AD-A202984; USAARL-88-13) Avail: NTIS HC A03/MF A01 CSCL 05H

Historically, the goal of aviation helmet design has been to primarily provide impact and noise protection to the user. In 1984, the U.S. Army fielded an advanced attack helicopter which required a new helmet concept in which the role of the helmet was expanded to provided a visually coupled interface between the aviator and the aircraft. This new helmet system, the Integrated Helmet and Display Sighting System (IHADSS), uses a helmet fitted with infrared (IR) emitters and a monocular display. The IR emitters allow a slewable IR imaging sensor, mounted on the nose of the aircraft, to be slaved to the aviators head movements. Imagery from this sensor is presented to the aviator through the helmet mounted display. This type system generates several concerns, recognized early on, but still unresolved. These areas include questions of monocular vs. binocular imagery, eye dominance, and binocular rivalry. Additionally, the task of interfacing the aviator's head to the aircraft has introduced previously unrecognized problems relating to head anthropometry and facial anatomy. The fitting process has become a crucial factor in the aviator's ability to interface with the aircraft systems. The development and fielding of the IHADSS helmet mounted display have expanded the role and importance of the helmet. GRA

N89-21487# Air Force Inst. of Tech., Wright-Patterson AFB, OH. School of Engineering.
GRAPHICAL MAN-MACHINE INTERFACE FOR AN INTEGRATED EVALUATION ENVIRONMENT M.S. Thesis
Jerry J. Kanski Dec. 1988 160 p
(AD-A203054; AFIT/GE/ENG/88D-17) Avail: NTIS HC A08/MF A01 CSCL 12E

The purpose of this thesis was to create an effective color graphical man-machine interface prototype for the various software resources used by AFIT researchers. The research was completed in four steps: (1) The general user requirements and specific interface requirements for the interface were determined; (2) An interface design which met all of the requirements determined in step 1 was created; (3) The design created in step 2 was implemented; and (4) The man-machine interface was evaluated by a group of representative users. The design effort resulted in a general purpose interface design that was highly adaptable and expandable. The design met all of the requirements determined in step 1, yet included the flexibility to meet future, as yet undetermined, requirements. The implementation of the interface design also featured adaptability and flexibility. The implementation combined a variety of graphical techniques to create a very powerful system. In addition, the resulting man-machine interface was evaluated by a group of AFIT engineering students and staff. The results of the evaluation indicated that the graphical man machine interface prototype was a success. GRA

N89-21488# Army Aeromedical Research Unit, Fort Rucker, AL.
POLYCARBONATE OPHTHALMIC LENSES FOR AMETROPIC ARMY AVIATORS USING NIGHT VISION GOGGLES Final Report
John K. Crosley Aug. 1988 38 p
(AD-A203100; USAARL-88-12) Avail: NTIS HC A03/MF A01 CSCL 05H

U.S. Army aviators use the AN/PVS-5 Night Vision Goggles (NVG) with a modified faceplate which enables wearing of corrective spectacles, when required. The next generation NVGs, the Aviator Night Vision Imaging System (ANVIS), permit spectacle wear by design. With only glass lenses available to the aviator requiring optical correction, there is a potential for eye injury from broken glass should the goggles accidentally be displaced. This report documents studies to: (1) compare the impact resistance of glass, CR-39 (plastic), and polycarbonate lenses to simulated NVG tubes, (2) establish the approximate forces necessary to cause glass lens breakage by displaced NVG tubes, and (3) determine the performance of polycarbonate lenses in the aviation environment. GRA

N89-21489# Air Force Inst. of Tech., Wright-Patterson AFB, OH. School of Engineering.
F-16 SPEAKER-INDEPENDENT SPEECH RECOGNITION SYSTEM USING COCKPIT COMMANDS (70 WORDS) M.S. Thesis
Peter Y. Kim Dec. 1988 138 p
(AD-A203177; AFIT/GE/ENG/88D-18) Avail: NTIS HC A07/MF A01 CSCL 25D

A system is developed to achieve speaker independent isolated speech recognition. The system uses LPC Spectrum, Formants, and Frication Frequency as a feature set. Dynamic programming is applied for distance calculations. The fundamental design concept is to create a universal template for multiple speakers. A new algorithm, which combines the vocabularies of several speakers to produce one optimal template, is incorporated into the system. An advanced speech analysis tool called SPIRE provides the computational functions required to extract appropriate features. Seventy words, from the list of F-16 cockpit commands, are selected as a vocabulary of the system. The use of a merged template based on three of the feature sets achieves an accuracy of 99 percent. The system is implemented in list programming on Symbolics 3600 series computer. GRA

55 SPACE BIOLOGY

Includes exobiology; planetary biology; and extraterrestrial life.

No abstracts in this category.

59 MATHEMATICAL AND COMPUTER SCIENCES (GENERAL)

N89-21490# Army Research Office, Research Triangle Park, NC.
TRANSACTIONS OF THE FIFTH ARMY CONFERENCE ON APPLIED MATHEMATICS AND COMPUTING
Mar. 1988 849 p Conference held at West Point, N.Y., 15-18 Jun. 1987; sponsored by the Army Mathematics Steering Committee
(AD-A193384; ARO-88-1) Avail: NTIS HC A99/MF E03 CSCL 12E

This is a technical report resulting from the Fifth Army Conference on Applied Mathematics and Computing. It contains most of the papers in the agenda of this meeting. These papers treat various Army applied mathematical problems. For individual titles, see N89-21491 through N89-21531.

N89-21491# Cornell Univ., Ithaca, NY. Center for Applied Mathematics.
LIE TRANSFORMS APPLIED TO A NONLINEAR PARAMETRIC EXCITATION PROBLEM **c64**
Jonathan L. Len and Richard H. Rand *In* Army Research Office, Transactions of the Fifth Army Conference on Applied Mathematics and Computing Mar. 1988 p 1-27 Sponsored in part by NSF, Washington, D.C. (For primary document see N89-21490 14-59)
Avail: NTIS HC A99/MF E03 CSCL 12E

Researchers use Lie transforms to approximate the Poincare map of a weakly non-linear periodic perturbation of the simple harmonic oscillator in order to study the stability of the trivial solution. Resonant frequencies, corresponding to nonremovable terms in the differential equation, are identified through O (epsilon squared). Researchers show that detuning from resonance stabilizes the trivial solution when the perturbation contains no linear periodic terms. Finally, they study a typical bifurcation between two lowest-order resonant frequencies. A MACSYMA program which performs the Lie transform algorithm to arbitrary order is presented in the appendix with a sample run. Author

N89-21492# Columbia Univ., New York, NY. Lab. for Intelligent Design.
KNOWLEDGE REPRESENTATION AND PLANNING CONTROL IN AN EXPERT SYSTEM FOR THE CREATIVE DESIGN OF MECHANISMS **c63**
David A. Hoeltzel, Wei-Hua Chieng, and John Zissimides *In* Army Research Office, Transactions of the Fifth Army Conference on Applied Mathematics and Computing Mar. 1988 p 29-63 (For primary document see N89-21490 14-59)
Avail: NTIS HC A99/MF E03 CSCL 12E

An interactive system, referred to as MECXPERT (Mechanism Expert), has been designed with the expressed purpose of assisting nonexpert design engineers in creating mechanisms for fulfilling specific motion-conversion and/or power-transmission requirements. The particular knowledge representation chosen for this application comprises a hybrid formulation of a rule-based production system with a frame-based approach. The underlying control strategy is based on a series of special-purpose, domain-specific operators whose function is to move from one problem space to another through various stages or states that comprise the mechanism design process. The primary focus here centers on the representation of knowledge and its control within an expert system for creative mechanism design. An overview summarizing the reasons for developing such an expert system is provided, and the formulation of a problem is discussed through an example taken from the design of a variable-stroke internal-combustion engine. Author

N89-21493# Columbia Univ., New York, NY. Dept. of Mechanical Engineering.
STATISTICAL MACHINE LEARNING FOR THE COGNITIVE SELECTION OF NONLINEAR PROGRAMMING ALGORITHMS IN ENGINEERING DESIGN OPTIMIZATION **c61**
David A. Hoeltzel and Wei-Hua Chieng *In* Army Research Office, Transactions of the Fifth Army Conference on Applied Mathematics and Computing Mar. 1988 p 65-78 (For primary document see N89-21490 14-59)
(Contract DAAL03-86-6-0116)
Avail: NTIS HC A99/MF E03 CSCL 12E

In order to overcome the problem of lack of generality in nonlinear programming (NLP) test problem formulation and to introduce the concept of cognitive NLP method switching, statistical machine learning has been applied to a sample data base of nonlinear programming problems. Reasonable conclusions have been drawn about an optimization problem type and a corresponding sequence of NLP solution algorithms, using statistical pattern recognition applied to local (vs. global) design information. A program, referred to as OPTDEX-OLDM, with the capability of learning from statistical pattern recognition is discussed. The statistical aspects and algorithmic optimization of the nonlinear programming problem are emphasized in this discussion. A clustering process has been performed on attributes assigned to the NLP problem sample data base, and an example which describes this statistical clustering process is discussed. Author

N89-21494# Carnegie-Mellon Univ., Pittsburgh, PA. Dept. of Mathematics.
TOWARD A NONEQUILIBRIUM THERMODYNAMICS OF TWO PHASE MATERIALS WITH SHARP INTERFACE **c77**
Morton E. Gurtin *In* Army Research Office, Transactions of the Fifth Army Conference on Applied Mathematics and Computing Mar. 1988 p 79-85 Sponsored in part by NSF, Washington, D.C. (For primary document see N89-21490 14-59)
Avail: NTIS HC A99/MF E03 CSCL 20M

This is a review of recent work of the author toward the development of a nonequilibrium thermodynamics of two-phase continua based on the first two laws in forms which contain interfacial contributions for energy and entropy. Topics discussed

are: thermodynamic restrictions on constitutive equations: interface conditions: free-boundary problems for solidification and melting.
Author

N89-21495# Cornell Univ., Ithaca, NY. Mathematical Sciences Inst.
THE SHEAR-LAG MODEL FOR A UNIDIRECTIONAL COMPOSITE WITH VISCOELASTIC MATRIX **c24**
Dimitris C. Lagoudas, Chung-Yuen Hui, and S. Leigh Phoenix *In* Army Research Office, Transactions of the Fifth Army Conference on Applied Mathematics and Computing Mar. 1988 p 87-109 (For primary document see N89-21490 14-59)
Avail: NTIS HC A99/MF E03 CSCL 11D

The shear-lag model is applied to a monolayer, unidirectional, fiber-reinforced composite loaded in tension. The monolayer contains an infinite number of parallel fibers, with an arbitrary number of them broken simultaneously. While the fibers are modelled as linearly elastic, a linear viscoelastic constitutive law is assumed for the matrix material. The time evolution of the overstress profiles in the fibers and matrix near breaks is determined. The time dependence of the effective load transfer length is also calculated. Explicit evaluations of the above quantities are given for a power-law creep compliance mode suitable for most epoxy thermosetting resins as matrix materials. Author

N89-21496# Army Materials Technology Lab., Watertown, MA. Mechanics and Structures Div.
ELEMENT LEVEL ELIMINATION OF NONLINEAR CONSTRAINTS IN TOTAL LAGRANGIAN FINITE ELEMENT FORMULATIONS **c39**
A. R. Johnson and C. J. Quigley *In* Army Research Office, Transactions of the Fifth Army Conference on Applied Mathematics and Computing Mar. 1988 p 111-138 (For primary document see N89-21490 14-59)
Avail: NTIS HC A99/MF E03 CSCL 20K

Nonlinear constraints in elastic finite deformation theory can be enforced by an iterative element level variable elimination method which takes advantage of the finite element discretization. A Lagrangian potential energy method is used and load steps are taken small enough so that the potential energy is nearly quadratic when expanded as a function of displacement increments. The Newton - Raphson method is used to find minimal locations. Element gradient and tangent matricies are computed and modified to be consistent with an incremental representation of the nonlinear constraint. This iterative variable elimination method is used to determine the solutions to the bending of an elastica around an ellipse for aspect ratios of 0.75, 1.00 and 1.50. Two exterior methods are also used to solve these problems for comparison. The Lagrange multiplier method (ABAQUS code) and a penalty method are used. The results obtained using the element level elimination method are compared to the results obtained using ABAQUS and the penalty method. Author

N89-21497# Boston Univ., MA. Dept. of Mathematics.
CONDITION OF THE FINITE ELEMENT STIFFNESS MATRIX OF HIGHLY IRREGULAR TRIANGULAR GRIDS **c64**
I. Fried and A. R. Johnson (Army Materials Technology Lab., Watertown, MA.) *In* Army Research Office, Transactions of the Fifth Army Conference on Applied Mathematics and Computing Mar. 1988 p 139-148 (For primary document see N89-21490 14-59)
Avail: NTIS HC A99/MF E03 CSCL 12E

Penetration of a sharp object causes large concentrated deformations in an elastomer solid. The nonlinear nearly incompressible elastic stress analysis of the solid is done with quadratic triangular elements and displacements referring to an immovable grid. A lower order triangular mesh for a linear thermal analysis is conveniently layed with vertices at the displaced nodes. This gives rise to highly irregular grids of slender elements near the point of maximum penetration. The condition of the global thermal (stiffness) matrix is estimated in terms of the element geometry. It is concluded that no significant decline in the condition of the matrix takes place in spite of the high deformation.
Author

N89-21498# Army Armament Research, Development and Engineering Center, Watervliet, NY. Close Combat Armaments Center.
A SIMPLE ANALYSIS OF SWAGE AUTOFRETTAGE PROCESS **c39**
Peter C. T. Chen *In* Army Research Office, Transactions of the Fifth Army Conference on Applied Mathematics and Computing Mar. 1988 p 149-160 (For primary document see N89-21490 14-59)
Avail: NTIS HC A99/MF E03 CSCL 20K

Many solutions have been reported for the hydraulic autofrettage process. Here, a simple analysis of the swage autofrettage process is presented. The contact pressure at different locations is determined as a function of interference. The deformation and stress distribution during autofrettage is obtained. At the end of the autofrettage process, the permanent bore enlargement and residual stresses are calculated. Numerical results are presented in graphical forms. Author

N89-21499# Massachusetts Inst. of Tech., Cambridge. Dept. of Mathematics.
OPTIMAL DESIGN OF A TWO-WAY CONDUCTOR **c33**
Gilbert Strang and Robert Kohn (New York Univ., New York.) *In* Army Research Office, Transactions of the Fifth Army Conference on Applied Mathematics and Computing Mar. 1988 p 161-182 Submitted for publication Sponsored in part by NSF, Washington, D.C. (For primary document see N89-21490 14-59)
(Contracts DAAL03-86-K-0171; N00014-83-K-0536)
Avail: NTIS HC A99/MF E03 CSCL 09K

Optimal design presents an extreme case of non-smooth mechanics. The unknown becomes the density of material, and in an ordinary design the density takes the value 0 or 1. It describes a shape which has least weight subject to the constraints. However the optimal design is frequently not at all ordinary. It is given by the weak limit of a sequence of designs in which the density oscillates more and more rapidly between 0 and 1. In other words the average density can take fractional values, and no ordinary shape achieves the minimum weight. Mathematically this is an instance of the relaxation of a nonconvex problem. That is a special topic in the calculus of variations, to widen the class of admissible functions so that the problem becomes correctly posed and its minimum is achieved. To the given nonconvex problem we associate a relaxed problem with the same minimum. The solutions of the relaxed problem are the weak limits of minimizing sequences in the original problem. The application of this technique is to a question of optimal bounds for composite materials.
Author

N89-21500# Virginia Polytechnic Inst. and State Univ., Blacksburg. Dept. of Engineering Science and Mechanics.
ON A REFINED NONLINEAR THEORY OF LAMINATED COMPOSITE PLATES **c24**
J. N. Reddy *In* Army Research Office, Transactions of the Fifth Army Conference on Applied Mathematics and Computing Mar. 1988 p 183-206 (For primary document see N89-21490 14-59)
(Contract DAAG29-85-K-00017)
Avail: NTIS HC A99/MF E03 CSCL 11D

The results of research on the development of a refined shear deformation theory of plates and its analytical solutions in the linear case are summarized. The detailed results are reported in two technical papers, which will appear elsewhere. A third-order, nonlinear shear deformation plate theory that accounts for parabolic distribution of transverse shear stresses through thickness and moderate rotation terms is presented. The Levy type analytical solutions are developed for the linear case. Author

N89-21501# Houston Univ., TX. Dept. of Mathematics.
NUMERICAL SOLUTION OF PARABOLIC PROBLEMS IN HIGH DIMENSIONS **c64**

Edward Dean, Roland Glowinski, and Chin-Hsien Li *In* Army Research Office, Transactions of the Fifth Army Conference on Applied Mathematics and Computing Mar. 1988 p 207-286 (For primary document see N89-21490 14-59)
(Contract DAAL03-86-K-0138)
Avail: NTIS HC A99/MF E03 CSCL 12E

The main goal is to discuss the numerical solution of mathematical problems of parabolic type when the space dimension is high and/or the number of discretization points is quite large. In such cases, we can take advantage of the evolution nature of the problem under consideration to derive numerical methods quite easy to implement and well suited to vector and/or parallel computers. Operator splitting methods are one of the key ingredients of such a methodology. Researchers illustrate the methods described here by solving the time dependent Navier-Stokes equations for incompressible viscous fluids, a variational problem originating from the physics of liquid crystals, and finally advection-diffusion problems in very high dimension associated to the solution of the Zakai equation in stochastic optimal control. Author

N89-21502# Wisconsin Univ., Madison. Dept. of Computer Sciences.
ALGORITHMS FOR RATIONAL SPLINE CURVES c61
Klaus Hollig *In* Army Research Office, Transactions of the Fifth Army Conference on Applied Mathematics and Computing Mar. 1988 p 287-300 (For primary document see N89-21490 14-59)
(Contract DAAG29-80-C-0041; NSF DMS-83-51187)
Avail: NTIS HC A99/MF E03 CSCL 09B

The theory of univariate splines is well understood. However, applying the standard techniques for spline functions does not make use of some important features of piecewise polynomial curves. Since curves are invariant under reparametrization, the smoothness conditions for splines are less restrictive and standard approximation methods can be improved. This note discusses rational cubic spline curves and describes in particular two basic algorithms: the construction of smooth splines from control points and Hermite interpolation. Author

N89-21503# Texas A&M Univ., College Station. Dept. of Mathematics.
CONVEXITY-PRESERVING QUASI-INTERPOLATION AND INTERPOLATION BY BOX SPLINE SURFACES c64
Charles K. Chui, Harvey Diamond, and Louise A. Raphael (Howard Univ., Washington, DC.) *In* Army Research Office, Transactions of the Fifth Army Conference on Applied Mathematics and Computing Mar. 1988 p 301-310 (For primary document see N89-21490 14-59)
Avail: NTIS HC A99/MF E03 CSCL 12E

Given a strictly convex function of two variables f(x,y), a C(1) box spline series approximant of this function, based on data (f(ih,jh)) given at points uniformly spaced by h in the x and y directions, will also be convex if h is sufficiently small. Explicit numerical bounds on h are provided in this paper which guarantee convexity of these box spline series approximants. The bounds are of the form h = c epsilon/L where epsilon is greater than 0 is the minimum value of D(2)(sub u)f, L is a Lipschitz constant associated with the continuity of the second derivatives of f, and the constant c depends on the particular box spline approximant being used. Author

N89-21504# Military Academy, West Point, NY. Dept. of Mathematics.
KNOT SELECTION FOR LEAST SQUARES APPROXIMATION USING THIN PLATE SPLINES c39
John R. McMahon and Richard Franke (Naval Postgraduate School, Monterey, CA.) *In* Army Research Office, Transactions of the Fifth Army Conference on Applied Mathematics and Computing Mar. 1988 p 311-330 (For primary document see N89-21490 14-59)
(Proj. BR033-02-WH)
Avail: NTIS HC A99/MF E03 CSCL 20K

Given a large set of scattered data (x sub i, y sub i, f sub i), a method for selecting a significantly smaller set of knot points which will represent the larger set is described. The algorithm for selection of the knot point locations is based on the minimization of the sum of the squares of the difference between the average number of points per Dirichlet tile and the actual number of points in each tile, subject to the constraint that each knot is located at the centroid of its tile. Using the least squares Thin Plate Spline approximation method for constructing surfaces, various test surfaces are examined and compared to surfaces obtained using the smoothing spline and the bicubic Hermite approximation methods. Author

N89-21505# Harry Diamond Labs., Adelphi, MD. Advanced Electronics Systems Lab.
A RAPID-BACKSCATTER SIMULATION TECHNIQUE FOR COMPLEX B-SPLINE TARGET MODELS c32
Karl D. Reinig *In* Army Research Office, Transactions of the Fifth Army Conference on Applied Mathematics and Computing Mar. 1988 p 331-344 (For primary document see N89-21490 14-59)
Avail: NTIS HC A99/MF E03 CSCL 20N

A method for rapidly evaluating the simulated radar backscatter signatures of B-spline target models moving relative to a source/receiver is described. A geometric optics approach is used to estimate the radar return from a complex target surface described by a bi-cubic B-spline mesh. The method exploits the second-order continuity of bi-cubic B-spline surfaces to reduce the problem of finding all the specular points associated with each new trajectory position to that of tracking the motion of existing points. In particular, it is shown that the locations of the annihilations and creations of specular paths may be predicted for an entire trajectory, eliminating the need to search the whole surface for specular points as the target moves relative to the source/receiver. The method is shown to work for the multiple-bounce case as well. Author

N89-21506# Army Missile Test and Evaluation Directorate, White Sands Missile Range, NM. Directed Energy Directorate.
AN ALGORITHM FOR PROCESSING SCANNING SPECTROMETER DATA c35
Joseph E. Zurlinden *In* Army Research Office, Transactions of the Fifth Army Conference on Applied Mathematics and Computing Mar. 1988 p 345-354 (For primary document see N89-21490 14-59)
Avail: NTIS HC A99/MF E03 CSCL 14B

A method of processing data acquired from a scanning spectrometer is described. The method employs an algorithm designed to find the spectral data from a continuous stream of data from the spectrometer and to provide the experimentor with the relative peak intensities and relative powers of the known spectral lines. This algorithm does not require the use of outside reference sources, such as an electronic pulse synchronized with the output of the spectral data, to find each frame of spectral data. This can save thirty-three percent of the memory storage otherwise required for all the data from the spectrometer, and approximately twenty-five percent of the processing time on the computer. Author

N89-21507# Army Engineer Waterways Experiment Station, Vicksburg, MS. Coastal Engineering Research Center.
THE KP EQUATION: A COMPARISON TO LABORATORY GENERATED BIPERIODIC WAVES c43
Norman W. Scheffner *In* Army Research Office, Transactions of the Fifth Army Conference on Applied Mathematics and Computing Mar. 1988 p 355-368 Presented at the 20th International Conference on Coastal Engineering, Taipei, Taiwan, 9-14 Nov. 1986 Submitted for publication (For primary document see N89-21490 14-59)
Avail: NTIS HC A99/MF E03 CSCL 08C

The propagation of waves in shallow water is a phenomenon of significant practical importance. The ability to realistically predict the complex wave characteristics occurring in shallow water regions

has always been an engineering goal which would make the development of solutions to practical engineering problems a reality. The difficulty in making such predictions stems from the fact that the equations governing the complex three-dimensional flow regime can not be solved without linearizing the problem. The linear equations are solvable; however, their solutions do not reflect the nonlinear features of naturally occurring waves. A recent advance (1984) in nonlinear mathematics has resulted in an explicit solution to a nonlinear equation relevant to water waves in shallow water. The solution posseses features found in observed nonlinear three-dimensional wave fields. Author

N89-21508# Titan Systems, Inc., Princeton, NJ.
ASYMPTOTICS BEYOND ALL ORDERS **c64**
Harvey Segur *In* Army Research Office, Transactions of the Fifth Army Conference on Applied Mathematics and Computing Mar. 1988 p 369-376 Sponsored in part by DOE, Washington Prepared in cooperation with State Univ. of New York, Buffalo (For primary document see N89-21490 14-59)
Avail: NTIS HC A99/MF E03 CSCL 12E

Conventional asymptotic methods often fail to capture effects that are transcendentally small because these effects lie beyond all orders in the asymptotic expansion. New methods have been developed recently to find transcendentally small terms in problems where they control the entire solution. Here, some of these recent developments are surveyed. Author

N89-21509# Army Troop Support Command, Fort Belvoir, VA.
COMPUTATIONAL ISSUES IN GOAL PROGRAMMING RESOURCE ALLOCATION **c61**
Leon Medler *In* Army Research Office, Transactions of the Fifth Army Conference on Applied Mathematics and Computing Mar. 1988 p 377-382 (For primary document see N89-21490 14-59)
Avail: NTIS HC A99/MF E03 CSCL 09B

The U.S. Army Belvoir RD and E Center has been engaged in a program of research aimed at developing an efficient and fair methodology for ranking proposed RD and E programs. A linear goal programming model (LGPM) has been the foundation of this methodology. Problems with this approach have surfaced in two areas: (1) excessive computer time and (2) anomalous results. Reported here is research conducted in order to redress these problems. Analysis of the existing model indicated that time expenditure in sensitivity excursions was the major culprit. Sensitivity analysis was being conducted by decrementing resource constraints and rerunning the LGPM from scratch. Since virtually as much computation was involved in the reruns as in the initital run, significant computation expense was being incurred. Therefore, researchers modified the LGPM to start from the last solution (i.e., the last LGPM simplex tableau). This required the addition of a dual simplex algorithm to supplement the regular simplex algorithm, since the last solution becomes infeasible under certain resource constraint changes. For a 110 project prioritization problem involving ten resource levels the improved LGPM requires only 10 to 20 percent as many simplex iterations as did the old LGPM. Author

N89-21510# Army Armament Research, Development and Engineering Center, Watervliet, NY.
DESIGN OF A FEELING-THINKING MACHINE **c63**
Ray Scanlon and Mark Johnson *In* Army Research Office, Transactions of the Fifth Army Conference on Applied Mathematics and Computing Mar. 1988 p 383-394 (For primary document see N89-21490 14-59)
Avail: NTIS HC A99/MF E03 CSCL 09B

A feeling-thinking machine has been designed using the mammalian brain as a model and current psychobiology concepts as a guide. The machine has been successfully run as a computer simulation. It mimics a primitive organism with eight functional brain centers. They are the recticular ascending substance (RAS), the amygdala, the cingulate gyrus, and medial forebrain bundle, the hippocampus, thalamus, hypothalamus, and the neocortex. Author

N89-21511# Ballistic Research Labs., Aberdeen Proving Ground, MD. Mechanics and Structures Branch.
POLYNOMINAL DEFINITION OF DISCRETE FIELD POINT OF MAP OF DIFFUSION EQUATION **c64**
William F. Donovan *In* Army Research Office, Transactions of the Fifth Army Conference on Applied Mathematics and Computing Mar. 1988 p 395-422 (For primary document see N89-21490 14-59)
Avail: NTIS HC A99/MF E03 CSCL 12E

An averaging type solution in algebraic format is considered for the one-dimensional diffusion equation. The differential equation is given a finite difference expression which is transposed first to geometric and then to polynomial algebraic form. The polynomials, representing discrete solutions to the differential equation, are analyzed by differencing techniques whereby the numerical coefficients of common diagonal terms are found to be expressible in a generalized matrix. M.G.

N89-21512# New York Univ., New York. Inst. of Mathematical Sciences.
THE NUMERICAL SIMULATION OF RICHTMYER-MESHKOV UNSTABLE INTERFACES: A CONFERENCE REPORT **c34**
John Grove *In* Army Research Office, Transactions of the Fifth Army Conference on Applied Mathematics and Computing Mar. 1988 p 423-436 (For primary document see N89-21490 14-59)
(Contract DAAG29-84-K-0130)
Avail: NTIS HC A99/MF E03 CSCL 20D

The interaction between a planar shock wave and a perturbed contact discontinuity is investigated. The interaction is simulated by a front tracking method that uses a local steady state analysis to model the diffraction patterns produced by the collision. This front tracking method automatically adjusts the topology of the tracked interface to account for the wave interactions. The acceleration of the contact discontinuity by the shock wave excites unstable modes in the gas interface that generate Richtmyer-Meshkov instabilities. Author

N89-21513# Military Academy, West Point, NY. Dept. of Mathematics.
A POSTERIORI ERROR ESTIMATION OF ADAPTIVE FINITE DIFFERENCE SCHEMES FOR HYPERBOLIC SYSTEMS **c64**
David C. Arney, Rupak Biswas, and Joseph E. Flaherty (Rensselaer Polytechnic Inst., Troy, NY.) *In* Army Research Office, Transactions of the Fifth Army Conference on Applied Mathematics and Computing Mar. 1988 p 437-457 Prepared in cooperation with Army Armament Munitions and Chemical Command, Watervliet, N.Y. (For primary document see N89-21490 14-59)
Avail: NTIS HC A99/MF E03 CSCL 12E

Several techniques that are based on Richardson's extrapolation for estimating discretization errors of finite difference solutions of one- and two-dimensional hyperbolic systems are described. These a posteriori error estimates are intended for use with adaptive mesh moving and local refinement procedures. Mesh moving algorithms produce nonuniform grids which necessitate special treatment of solution and error estimation techniques. The required adjustments are discussed using a two step MacCormack method as a model finite difference scheme. Automatic time step selection procedures and the effects of artificial viscosity are discussed. Extrapolation schemes that produce separate estimates of the temporal and spatial discretization errors are presented. It is shown how these may be used to control local mesh refinement. Several examples illustrating these techniques are presented. Author

N89-21514# Rensselaer Polytechnic Inst., Troy, NY. Dept. of Computer Science.
AN ADAPTIVE OVERLAPPING LOCAL GRID REFINEMENT METHOD FOR TWO-DIMENSIONAL PARABOLIC SYSTEMS **c64**
Peter K. Moore and Joseph E. Flaherty *In* Army Research Office, Transactions of the Fifth Army Conference on Applied Mathematics and Computing Mar. 1988 p 459-474 Prepared

in cooperation with Army Armament Munitions and Chemical Command, Watervliet, N.Y. (For primary document see N89-21490 14-59)
(Contract DAAL03-86-K-0112)
Avail: NTIS HC A99/MF E03 CSCL 12E

An adaptive local refinement finite element method for solving vector systems of parabolic partial differential equations in two space dimensions and time is presented. The algorithim uses the finite element-Galerkin method in space and backward Euler temporal integration. At each time step, researchers obtain an estimate of the error on each element, group the elements whose error violates a user prescribed tolerance, form new local grids and solve the problem again on each of the new grids. Several aspects of the algorithm, including the necessary data structures, the error estimation technique, and the determination of initial and boundary conditions at coarse-fine mesh interfaces are discussed. Finally, several examples which demonstrate the viability of this approach are presented. Author

N89-21515# Defence Research Establishment Valcartier (Quebec).
PROPAGATOR MATRICES IN THE SOLUTION OF EMP PROBLEMS **c32**
K. C. Heaton *In* Army Research Office, Transactions of the Fifth Army Conference on Applied Mathematics and Computing Mar. 1988 p 475-514 (For primary document see N89-21490 14-59)
Avail: NTIS HC A99/MF E03 CSCL 20N

In this work, the complete set of boundary conditions for the electric and magnetic fields at infinity, between the air and the Earth's surface, and between the air and the perfectly conducting plasma close to the explosion site are derived. The field equations, source functions and boundary conditions are written in terms of spheroidal and torsional vector fields. It is shown that, in this form, a propagator matrix formalism which automatically guarantees that all boundary conditions are satisfied can be developed to solve the equations for the electric and magnetic fields. The propagator matrix formalism developed in this work is applied to the numerical solution of Maxwell's equations for the electric and magnetic fields for the case of a typical explosion. It is found that the boundary conditions along the surface of the Earth impose consistency conditions which must be satisfied by the individual multipoles of the fields, as well as by the source current densities produced by the original explosion. Values are obtained for the electric and magnetic fields and compared with experimental results. Author

N89-21516# Army Cold Regions Research and Engineering Lab., Hanover, NH.
SPLINE-BASED FINITE-ELEMENT METHOD FOR SOLVING A STEFAN'S PROBLEM IN A FINITE DOMAIN: FORMULATION **c64**
Shunsuka Takagi *In* Army Research Office, Transactions of the Fifth Army Conference on Applied Mathematics and Computing Mar. 1988 p 515-534 (For primary document see N89-21490 14-59)
Avail: NTIS HC A99/MF E03 CSCL 12A

The finite-element method presented here has two features. First, a cubic spline is included in the basis functions; the advantage of the inclusion has not yet been examined. Second, space coordinates only are used to determine the temperature distribution. The time-coordinate increment of the phase front corresponding to the space-coordinate increment can be determined consequently. In our problem, where the final position of the phase front may be determined at the start of the solution, the solution method using a space-coordinate sequence is preferred to the one using a time-coordinate sequence. This numerical method can work smoothly even for an extremely large time. Analytical formulation only is presented here. Author

N89-21517# Brunel Univ., Uxbridge (England). Inst. of Computational Mathematics.
ON SOME FINITE ELEMENT ERROR ESTIMATES FOR STRESS INTENSITY FACTORS IN MODE 1 LINEAR ELASTIC FRACTURE PROBLEMS **c39**
J. R. Whiteman and G. Goodsell *In* Army Research Office, Transactions of the Fifth Army Conference on Applied Mathematics and Computing Mar. 1988 p 541-548 (For primary document see N89-21490 14-59)
Avail: NTIS HC A99/MF E03 CSCL 20K

The use of the superconvergence phenomenon for the retrieved gradients of piecewise linear approximations on triangular meshes to the solutions of problems of planar linear elasticity is discussed. In particular, results for problems involving singularities are presented, with particular reference to the apparent shortcomings for the case of linear elastic fracture. Author

N89-21518# Army Materials Technology Lab., Watertown, MA. Mechanics and Structures Div.
SOME ISSUES OF NUMERICAL INTEGRATION AND PENALTY RELAXATION IN ANISOPARAMETRIC SHELL ELEMENT FORMULATION **c39**
Alexander Tessler and Luciano Spiridigliozzi *In* Army Research Office, Transactions of the Fifth Army Conference on Applied Mathematics and Computing Mar. 1988 p 549-566 (For primary document see N89-21490 14-59)
Avail: NTIS HC A99/MF E03 CSCL 20K

A simple two-node axisymmetric shell element with the shallowly curved meridian, shear deformation, and rotary inertia is developed. The major aspects include: (1) anisoparametric interpolations of the displacement variables to design out excessive stiffening due to membrance and shear locking; (2) consistent shear relaxation to further upgrade the element strain energy; and (3) low-order quadrature evaluation. The resulting element posseses an improved condition of the stiffness matrix, increased efficiency in explicit time integration, and enhanced accuracy in coarse discretizations. Comprehensive vibration examples are carried out to assess the element performance. The numerical results demonstrate a wide applicability range with respect to element slenderness and curvature properties. Author

N89-21519# Cornell Univ., Ithaca, NY. Dept. of Computer Science.
A BLOCK QR FACTORIZATION SCHEME FOR LOOSELY COUPLED SYSTEMS OF ARRAY PROCESSORS **c62**
Charles VanLoan *In* Army Research Office, Transactions of the Fifth Army Conference on Applied Mathematics and Computing Mar. 1988 p 567-588 Sponsored in part by IBM Corp. (For primary document see N89-21490 14-59)
(Contract N00014-83-K-0640; NSF CCR-86-02310)
Avail: NTIS HC A99/MF E03 CSCL 09B

A statically scheduled parallel block QR factorization procedure is described. It is based on block Givens rotations and is modeled after the Gentleman-Kung systolic QR procedure. Independent tasks are associated with each block column. Tallest possible subproblems are always solved. The method has been implemented on the IBM Kingston LCAP-1 system which consists of ten FPS-164/MAX array processors that can communicate through a large shared bulk memory. The implementation revealed much about the tradeoff between block size and load balancing. Large blocks make load balancing more difficult but give better 164/MAX performance and less shared memory traffic. The results obtained indicate that this approach to parallelizing the QR factorization is competitive for very large problems, e.g., of the order 5000-by-1000. Author

N89-21520# Cornell Univ., Ithaca, NY. Mathematical Sciences Inst.
NONPARAMTERIC ESTIMATION FROM QUEUES ARISING IN STAGGERED ENTRY CLINICAL TRIALS **c64**
Michael J. Phelan and N. U. Prabhu *In* Army Research Office, Transactions of the Fifth Army Conference on Applied Mathematics

and Computing Mar. 1988 p 589-596 (For primary document see N89-21490 14-59)
Avail: NTIS HC A99/MF E03 CSCL 12E

In clinical trials with staggered entries and fixed duration of study, patients enter at random epochs and are put on test. The objective is to study survival times from a principal cause A, but factors such as end of study or patient withdrawal make it impossible to observe the survival times (censoring). Researchers consider two different situations, (1) for some patients death may actually be from a cause other than A. It is desired to study the survival times associated with both causes A and B, (2) a certain number (equal to or greater than one) treatments are available and each entering patient is diagnosed and assigned to one of these treatments. The objective is to study the survival times from cause A under these treatments. These problems are formulated in terms of queueing models, for which it is desired to obtain nonparametric estimates of service time distributions. Researchers investigate an infinite server model to study case (1) and an m-station model for case (2). The input in both models is a point process. The system over a finite time-interval (0,t) with t fixed. The data collected consist of the arrival epochs, service times of the customers who arrive during (0,t), with some of the service times partially observed, and (in Model 2) delays experienced by them before service. The estimators are martingale estimators, for which we establish consistency and weak convergence of the normalized difference to a Gaussian process. The results for Model 1, are given. Work on Model 2 is in progress. Author

N89-21521# Army Engineer Waterways Experiment Station, Vicksburg, MS. Geotechnical Lab.
COLUMN MOVEMENT MODEL USED TO SUPPORT AMM c43
George B. McKinley *In* Army Research Office, Transactions of the Fifth Army Conference on Applied Mathematics and Computing Mar. 1988 p 601-616 (For primary document see N89-21490 14-59)
Avail: NTIS HC A99/MF E03 CSCL 08B

For many years mobility maps have been created utilizing the Army Mobility Model (AMM). These maps show the maximum speed which a vehicle can attain in off-road terrain and on-road networks. These maps are useful in comparing the performance of vehicles or as an aid in route selection. Three additional computer models have been developed to support the AMM by predicting the performance of military vehicles over digital terrain units along a specified route. These three models are an Acceleration Model, a Traverse Model, and a Column Movement Model. The Acceleration Model produces a time versus speed curve for a vehicle along a specified route across a terrain unit. The Traverse Model uses the Acceleration Model as a building block and predicts a vehicle's performance along a specified route over a series of terrain units. The Column Movement Model uses the Traverse Model as a building block for predicting performance of a column of vehicles along a specified route. The Column Movement Model maintains vehicle spacing within the column in accordance with military doctrine. Author

N89-21522# Ballistic Research Labs., Aberdeen Proving Ground, MD.
INFLUENCE OF REFLECTED SHOCK WAVES ON A HYPERSONIC SHAPED CHARGE JET c02
H. W. Meyer and J. E. Danberg *In* Army Research Office, Transactions of the Fifth Army Conference on Applied Mathematics and Computing Mar. 1988 p 617-630 (For primary document see N89-21490 14-59)
Avail: NTIS HC A99/MF E03 CSCL 01B

Considerable research has been devoted to shaped charge jet formation and penetration but little work has been reported on the aerodynamic forces on the jet particles, particularly the interference caused by nearby surfaces. The object here was to develop numerical methods and apply them to this problem. A Godunov inviscid technique has been used along with high temperature thermodynamic properties to obtain the flow field in front of a hemisphere. This was used as the initial condition for the computation of the flow field in the annular region between the jet and a surrounding cylindrical tube. Computations were done at Mach number 4 and compared to experimental data. The jet problem (Mach number 20.45) was then solved. Author

N89-21523# Army Engineer Waterways Experiment Station, Vicksburg, MS. Hydraulics Lab.
SKEW GRIDS AND IRROTATIONAL FLOW c34
Robert S. Bernard *In* Army Research Office, Transactions of the Fifth Army Conference on Applied Mathematics and Computing Mar. 1988 p 631-642 (For primary document see N89-21490 14-59)
Avail: NTIS HC A99/MF E03 CSCL 20D

Finite-difference computation of incompressible flow through regions of arbitrary shape often requires the implementation of boundary-fitted coordinates for which the grid lines may be non-orthogonal (skew). When the governing equations are expressed in terms of pressure and velocity, conservation of mass is maintained by the gradient of the pressure. In principle, the gradient is irrotational and should have no effect on the existing circulation in the flow field; but if the grid lines are skew, the discrete representation of the gradient can generate spurious vorticity near the boundaries. In the present work this difficulty is eliminated for uniform skew grids, and markedly reduced for non-uniform skew grids, by adopting a discrete formulation of the pressure gradient that helps maintain irrotationality near boundaries. The procedure is applicable for staggered grids with either Poisson or Chorin equations for pressure. Author

N89-21524# Naval Postgraduate School, Monterey, CA. Dept. of Mathematics.
A RANDOMNESS PROPERTY OF m-SEQUENCES c64
Harold Fredricksen and Gary Krahn (Military Academy, West Point, NY.) *In* Army Research Office, Transactions of the Fifth Army Conference on Applied Mathematics and Computing Mar. 1988 p 643-648 (For primary document see N89-21490 14-59)
Avail: NTIS HC A99/MF E03 CSCL 12E

Maximal length linear shift register sequences (m-sequences) are used in a number of communications applications. Their nearly ideal randomness properties are what make these sequences so employable. An additional randomness property that m-sequences possess is discussed. Author

N89-21525# Army Engineer Waterways Experiment Station, Vicksburg, MS.
THERMODYNAMIC GAUGE THEORY OF SOLIDS AND QUANTUM LIQUIDS WITH INTERNAL PHASE c77
Richard A. Weiss *In* Army Research Office, Transactions of the Fifth Army Conference on Applied Mathematics and Computing Mar. 1988 p 649-695 (For primary document see N89-21490 14-59)
Avail: NTIS HC A99/MF E03 CSCL 20C

The local gauge invariance of relativistic thermodynamics under phase rotations suggests that bulk matter systems have density and temperature dependent internal phase angles associated with the state functions. A procedure for determining the internal phase angles associated with energy, pressure, entropy, thermodynamic potentials, and gauge parameters of solids and quantum liquids is presented in terms of the renormalization group equations of relativistic thermodynamics. The calculated magnitudes of the thermodynamic state functions depend on the values of the internal phase angles. It is suggested that the external angular momentum of systems may be coupled to the angular momenta associated with the internal space of thermodynamic phase angles. Applications to mechanical waves in matter with internal phase are considered. These effects are expected to be found in high density and pressure systems such as atomic nuclei, neutron stars, nuclear explosions, and the interaction of directed energy beams with matter. Author

N89-21526# Army Engineer Waterways Experiment Station, Vicksburg, MS.
LAGRANGIAN FORMULATION OF RELATIVISTIC THERMODYNAMICS c77

Richard A. Weiss *In* Army Research Office, Transactions of the Fifth Army Conference on Applied Mathematics and Computing Mar. 1988 p 697-734 (For primary document see N89-21490 14-59)
Avail: NTIS HC A99/MF E03 CSCL 20C

Matter and radiation Lagrangians are developed from which the renormalization group equations of locally gauge invariant relativistic thermodynamics can be obtained by the Euler-Lagrange equations. The Noether current tensor and conservation equations of relativistic thermodynamics can be derived from these Lagrangians. These Lagrangians exhibit a minimum value when expressed in terms of the fractal dimension of a physical system, and are locally symmetric about this minimum value. This suggests that all matter and radiation in matter is fractal in nature. Gases, liquids, solids, quantum liquids, and the mechanical waves that propagate in these systems, have fractal properties. Equations for calculating the fractal dimensions of matter and radiation in matter are presented, and general expressions for the void ratio of gases, condensed matter, and radiation are derived. These results will have applications to matter and radiation at high densities such as occur in neutron stars, nuclear explosions, and the interaction of directed energy beams with matter. Author

N89-21527# Purdue Univ., Indianapolis, IN. Dept. of Mathematical Sciences.
MODELLING OF THE LEAN FLAMMABILITY LIMIT IN FLAME THEORY **c25**
Richard Y. Tam and G. S. S. Ludford (Cornell Univ., Ithaca, NY.) *In* Army Research Office, Transactions of the Fifth Army Conference on Applied Mathematics and Computing Mar. 1988 p 735-743 (For primary document see N89-21490 14-59)
Avail: NTIS HC A99/MF E03 CSCL 21B

The phenomenon of the lean flammability limit is modelled by a four-step reaction mechanism. Analytical results, namely that a fuel mixture will not burn if it is too lean, are obtained through use of activation-energy asymptotics. Author

N89-21528# Maryland Univ. Baltimore County, Catonsville.
THE SOLUTION OF THE TYPE-PROBLEM FOR N LESS THAN OR EQUAL TO 4 **c64**
Nam P. Bhatia and Walter O. Egerland (Ballistic Research Labs., Aberdeen Proving Ground, MD.) *In* Army Research Office, Transactions of the Fifth Army Conference on Applied Mathematics and Computing Mar. 1988 p 745-749 (For primary document see N89-21490 14-59)
Avail: NTIS HC A99/MF E03 CSCL 12E

The solution of the restricted type-problem for N is less than or equal to 4 is presented. The notion of a separated loop (a direct generalization of a loop) is introduced. It is shown that such loops do not obey a linear order. Accordingly, the various period types that appear in the solution for the restricted type-problem are not linearly ordered. The notion of turbulence as introduced by Block and Coppel is considered. It is shown that the notions of turbulence and that of an infinite loop are equivalent. Author

N89-21529# Army Missile Command, Redstone Arsenal, AL. Research Directorate.
NEURAL NETWORKS AND THE SYMMETRIC GROUP S(SUB N) **c62**
John L. Johnson *In* Army Research Office, Transactions of the Fifth Army Conference on Applied Mathematics and Computing Mar. 1988 p 751-761 (For primary document see N89-21490 14-59)
Avail: NTIS HC A99/MF E03 CSCL 09B

A permutation of N objects can be implemented by a neural net which recognizes the initial arrangement and then replaces it with the final arrangement. This is the same process found in parallel computer architectures using symbolic substitution principles, and in turn is the same function performed by optical correlator devices. Since every group is isomorphic to a subgroup of S(sub N), the symmetric group, these interrelationships provide a powerful mathematical base for optical computers and neural networks. Neural nets for the first few symmetric groups are presented. The number of interconnected nodes is shown to be related to the number of strictly parallel inputs and outputs, and a group categorization for any parallel interconnected network is discussed. Author

N89-21530# New York Univ., New York.
THE INTERACTION OF NONLINEAR HYPERBOLIC WAVES: A CONFERENCE REPORT **c64**
James Glimm *In* Army Research Office, Transactions of the Fifth Army Conference on Applied Mathematics and Computing Mar. 1988 p 763-785 (For primary document see N89-21490 14-59)
(Contracts DE-AC02-76ER-03077; DAAG29-85-K-0188)
Avail: NTIS HC A99/MF E03 CSCL 12E

Nonlinearities in wave equations lead to focusing and defocusing of solutions. Focusing causes sharply defined wavefronts. The interaction of such sharply defined wavefronts and more generally of non-linear hyperbolic waves is of fundamental importance and includes such phenomena as Mach triple point formation, shock wave diffraction patterns and the study of Riemann problems in one and higher dimensions. Recent progress in the study of nonlinear hyperbolic wave interactions has revealed a surprising range of new mathematical phenomena and structures. This mathematical theory should be useful in the design of improved computational algorithms and in part was motivated by such considerations. It is also of considerable interest for its own sake as new mathematical phenomena and is also of interest in terms of the direct insight it provides into physical phenomena. Author

N89-21531# Army Research Office, Research Triangle Park, NC.
STABILIZATION OF ZIEGLER'S PENDULUM BY MEANS OF THE METHOD OF VIBRATIONAL CONTROL **c64**
G. L. Anderson and I. G. Tadjbakhsh (Rensselaer Polytechnic Inst., Troy, NY.) *In its* Transactions of the Fifth Army Conference on Applied Mathematics and Computing Mar. 1988 p 787-843 (For primary document see N89-21490 14-59)
Avail: NTIS HC A99/MF E03 CSCL 12E

In the present investigation, Ziegler's pendulum with elastic hinges was subjected to an externally applied force of magnitude P whose orientation is specified by the tangency coefficient alpha. However, the base upon which one extremity of the pendulum is elastically restrained is made to undergo a sinusoidal oscillation along the undeformed axis of the system. It will be assumed here that the base motion is of small amplitude and high frequency. The goal is to stabilize the system by means of vibrational control, i.e., high frequency, low amplitude base motion. The equations of motion are linearized relative to the undeformed equilibrium configuration of the system, and the method of averaging is applied to the system of equations containing periodic coefficients in order to generate a simpler and more convenient system of equations with constant coefficients. This latter system serves for the purpose of easily computing the critical flutter or divergence loads for the system as a function of the tangency coefficient. Author

N89-21532*# National Aeronautics and Space Administration. Ames Research Center, Moffett Field, CA.
APPLICATION OF THE LAPLACE-BOREL TRANSFORMATION TO THE REPRESENTATION OF ANALYTICAL SOLUTIONS OF DUFFING'S EQUATION
K. V. Truong, Aynur Unal, and M. Tobak Feb. 1989 14 p
(NASA-TM-100058; A-88065; NAS 1.15:100058) Avail: NTIS HC A03/MF A01 CSCL 12A

Various features of the solutions of Duffing's equation are described using a representation of the solutions in the Laplace-Borel transform domain. An application of this technique is illustrated for the symmetry-breaking bifurcation of a hard spring. Author

60 COMPUTER OPERATIONS AND HARDWARE

Includes hardware for computer graphics, firmware, and data processing.

For components see *33 Electronics and Electrical Engineering.*

N89-21533# Utah Univ., Salt Lake City. Dept. of Computer Science.
THE VIRTUAL TIME MACHINE
Richard M. Fujimoto 10 Jan. 1989 34 p
(Contract N00014-87-K-0184; NSF DCR-85-04826)
(AD-A203087; UUCS-88-019) Avail: NTIS HC A03/MF A01 CSCL 12F

Existing multiprocessors and multicomputers require the programmer or compiler to perform data dependence analysis at compile time. The author proposes a parallel computer that performs this task at runtime. In particular, the Virtual Time Machine (VTM) detects violations of data dependence constraints as they occur, and automatically recovers from them. A sophisticated memory system that is addressed using both a spatial and a temporal coordinate is used to efficiently implement this mechanism. Initially targeted for discrete event simulation applications, many of the ideas used in the machine architecture have direct application in the more general realm of parallel computation. The long term goal of this work is to develop a general purpose parallel computer that will support a wide range of parallel programming paradigms. This paper outlines the motivations behind the VTM architecture, the underlying computation model, a proposed implementation, and initial performance results. A recurring theme that pervades the entire paper is our contention that existing shared memory and message-base machines do not pay adequate attention to the dimension of time. We argue that this architectural deficiency is the underlying reason behind many difficult problems in parallel computation today. GRA

N89-21534# Utah Univ., Salt Lake City. Dept. of Computer Science.
TIME WARP ON A SHARED MEMORY MULTIPROCESSOR
Richard M. Fujimoto 10 Jan. 1989 35 p
(Contract N00014-87-K-0184; NSF DCR-85-04826)
(AD-A203088; UUCS-88-021A) Avail: NTIS HC A03/MF A01 CSCL 12F

A variation of the Time Warp parallel discrete event simulation mechanism is presented that is optimized for execution on a shared memory multiprocessor. In particular, the direct cancellation mechanism is proposed that eliminates the need for anti-messages and provides an efficient mechanism for cancelling erroneous computations. The mechanism thereby eliminates many of the overheads associated with conventional, message-based implementations of Time Warp. More importantly, this mechanism effects rapid repairs of the parallel computation when an error is discovered. Initial performance measurements of an implementation of the mechanism executing on a BBN Butterfly multiprocessor are presented. These measurements indicate that the mechanism achieves good performance, particularly for many workloads where conservative clock synchronization algorithms perform poorly. Speedups as high as 56.8 using 64 processors were obtained. However, our studies also indicate that state saving overheads represent a significant stumbling block for many parallel simulations using Time Warp. GRA

N89-21535# Utah Univ., Salt Lake City. Dept. of Computer Science.
HOP (HARDWARE VIEWED AS OBJECTS AND PROCESSES): A PROCESS MODEL FOR SYNCHRONOUS HARDWARE SYSTEMS
Ganesh C. Gopalakrishnan and Richard M. Fujimoto 1988 52 p
(AD-A203090; UUCS-88-003) Avail: NTIS HC A04/MF A01 CSCL 12E

A new Hardware Specification Language (HSL) called HOP is presented. HOP stands for Hardware viewed as Objects and Processes. It can be used for specifying the structure, behavior, and timing of digital systems. HOP was designed for several reasons. It integrates well-tested ideas from past work that was based on an abstract data type view of hardware systems into a new, simple, and deterministic process model that we have invented. Our process model is inspired by the works of Mil82, Mil83, and Hoa85. Secondly it is believed that not only should an HSL be founded in mathematical principles, but it also ought to be simple, intuitive to use, and address practical issues, especially if practicing VLSI designers are to be encouraged to use them. HOP was designed to meet the following design objectives: 1) Be capable of modeling large architectures as well as simple MOS digital circuits; (2) support the writing of a priori as well as a posteriori specifications; (3) possess a simple and rigorous semantics; (4) support static analysis techniques and design verification; (5) match digital designer's intuitions closely; (6) be demonstrably efficient in handling many important practical issues; and 7) act as a common repository of related information falling in various domains (functional behavior, timing, geometry, and user documentation. GRA

N89-21536# University of Southern California, Los Angeles. Dept. of Electrical Engineering.
CENTER FOR THE INTEGRATION OF OPTICAL COMPUTING Annual Technical Report, 1 Oct. 1987 - 30 Sep. 1988
A. A. Sawchuk and W. H. Steier 18 Oct. 1988 36 p
(Contract F49620-87-C-0007)
(AD-A203254; AFOSR-88-1281TR) Avail: NTIS HC A03/MF A01 CSCL 20F

This report summarizes the work in the center for the integration of optical computing. Topics reviewed include dynamic optical interconnection networks, low threshold laser arrays, array receivers, waveguide coupled photodiode arrays, optical processors for computer vision, subtraction in optical neural networks, nonlinear Fabry-Perot arrays, all optical associative memories, opto-optical switching, molecular beam epitaxy (MBE) growth and characterization of multiple quantum well (MQW) structures, volume holograms and spatial light modulators (SLM) using MQW structures. GRA

61 COMPUTER PROGRAMMING AND SOFTWARE

Includes computer programs, routines, alogorithms, and specific applications, e.g., CAD/CAM.

N89-21537*# Institute for Computer Applications in Science and Engineering, Hampton, VA.
A LANGUAGE COMPARISON FOR SCIENTIFIC COMPUTING ON MIMD ARCHITECTURES Final Report
Mark T. Jones, Merrell L. Patrick (Duke Univ., Durham, NC.), and Robert G. Voigt Jan. 1989 41 p
(Contracts NAS1-18107; NAS1-18605; NAG1-466)
(NASA-CR-181779; ICASE-89-6; NAS 1.26:181779) Avail: NTIS HC A03/MF A01 CSCL 09B

Choleski's method for solving banded symmetric, positive definite systems is implemented on a multiprocessor computer using three FORTRAN based parallel programming languages, the Force, PISCES and Concurrent FORTRAN. The capabilities of the language for expressing parallelism and their user friendliness are discussed, including readability of the code, debugging assistance offered, and expressiveness of the languages. The performance of the different implementations is compared. It is argued that PISCES, using the Force for medium-grained parallelism, is the appropriate choice for programming Choleski's method on the multiprocessor computer, Flex/32. Author

N89-21538*# National Aeronautics and Space Administration. Langley Research Center, Hampton, VA.
THE ENVIRONMENT FOR APPLICATION SOFTWARE INTEGRATION AND EXECUTION (EASIE) VERSION 1.0. VOLUME 1: EXECUTIVE OVERVIEW
Lawrence F. Rowell and John S. Davis (Computer Sciences Corp., Hampton, VA.) Mar. 1989 41 p
(NASA-TM-100573; NAS 1.15:100573) Avail: NTIS HC A03/MF A01 CSCL 09B

The Environment for Application Software Integration and Execution (EASIE) provides a methodology and a set of software utility programs to ease the task of coordinating engineering design and analysis codes. EASIE was designed to meet the needs of conceptual design engineers that face the task of integrating many stand-alone engineering analysis programs. Using EASIE, programs are integrated through a relational database management system. Volume 1, Executive Overview, gives an overview of the functions provided by EASIE and describes their use. Three operational design systems based upon the EASIE software are briefly described. Author

N89-21539*# National Aeronautics and Space Administration. Langley Research Center, Hampton, VA.
AN INTELLIGENT ADVISOR FOR THE DESIGN MANAGER
James L. Rogers and Sharon L. Padula Feb. 1989 11 p Prepared for presentation at the 1st International Conference on Computer Aided Optimum Design of Structures, Southampton, England, 20-23 Jun. 1989
(NASA-TM-101558; NAS 1.15:101558) Avail: NTIS HC A03/MF A01 CSCL 09B

A design problem is viewed as a complex system divisible into modules. Before the design of a complex system can begin, much time and money are spent in determining the couplings among modules and the presence of iterative loops. This is important because the design manager must know how to group the modules into substems and how to assign subsystems to design teams so that changes in one subsystem will have predictable effects on other subsystems. Determining these subsystems is not an easy, straightforward process and often important couplings are overlooked. Moreover, the planning task must be repeated as new information becomes available or as the design specifications change. The purchase of this research effort is to develop a knowledge-based tool to act as an intelligent advisor for the design manager. This tool identifies the subsystems of a complex design problem, orders them into a well-structured format, and marks the couplings among the subsystems to facilitate the use of multilevel tools. The tool was tested in the decomposition of the COFS (Control of Flexible Structures) mast design which has about 50 modules. This test indicated that this type of approach could lead to a substantial savings by organizing and displaying a complex problem as a sequence of subsystems easily divisible among design teams. Author

N89-21540*# Illinois Univ., Urbana-Champaign. Dept. of Computer Science.
OBJECTS AS CLOSURES: ABSTRACT SEMANTICS OF OBJECT ORIENTED LANGUAGES
Uday S. Reddy 1989 19 p Submitted for publication
(Grants NAG1-613; NSF CCR-87-00988)
(NASA-CR-184877; NAS 1.26:184877) Avail: NTIS HC A03/MF A01 CSCL 09B

We discuss denotational semantics of object-oriented languages, using the concept of closure widely used in (semi) functional programming to encapsulate side effects. It is shown that this denotational framework is adequate to explain classes, instantiation, and inheritance in the style of Simula as well as SMALLTALK-80. This framework is then compared with that of Kamin, in his recent denotational definition of SMALLTALK-80, and the implications of the differences between the two approaches are discussed. Author

N89-21541*# National Aeronautics and Space Administration. Ames Research Center, Moffett Field, CA.
DATAMAP UPGRADE VERSION 4.0
Michael E. Watts and Shabob R. Dejpour (Sterling Software, Palo Alto, CA.) Mar. 1989 59 p
(NASA-TM-100993; A-88164; NAS 1.15:100993) Avail: NTIS HC A04/MF A01 CSCL 09B

The changes made on the data analysis and management program DATAMAP (Data from Aeromechanics Test and Analytics - Management and Analysis Package) are detailed. These changes are made to Version 3.07 (released February, 1981) and are called Version 4.0. Version 4.0 improvements were performed by Sterling Software under contract to NASA Ames Research Center. The increased capabilities instituted in this version include the breakout of the source code into modules for ease of modification, addition of a more accurate curve fit routine, ability to handle higher frequency data, additional data analysis features, and improvements in the functionality of existing features. These modification will allow DATAMAP to be used on more data sets and will make future modifications and additions easier to implement. Author

N89-21542*# Institute for Computer Applications in Science and Engineering, Hampton, VA.
PARALLEL SOLUTION OF SPARSE ONE-DIMENSIONAL DYNAMIC PROGRAMMING PROBLEMS Final Report
David M. Nicol (College of William and Mary, Williamsburg, VA.) Mar. 1989 23 p
(Contract NAS1-18605)
(NASA-CR-181812; ICASE-89-17; NAS 1.26:181812) Avail: NTIS HC A03/MF A01 CSCL 09B

Parallel computation offers the potential for quickly solving large computational problems. However, it is often a non-trivial task to effectively use parallel computers. Solution methods must sometimes be reformulated to exploit parallelism; the reformulations are often more complex than their slower serial counterparts. We illustrate these points by studying the parallelization of sparse one-dimensional dynamic programming problems, those which do not obviously admit substantial parallelization. We propose a new method for parallelizing such problems, develop analytic models which help us to identify problems which parallelize well, and compare the performance of our algorithm with existing algorithms on a multiprocessor. Author

N89-21543# Center for Mathematics and Computer Science, Amsterdam (Netherlands). Dept. of Mathematical Statistics.
LARGE SAMPLE THEORY FOR STATISTICAL INFERENCE IN SEVERAL SOFTWARE RELIABILITY MODELS M.S. Thesis
W. A. J. Geurts, M. M. A. Hasselaar, and J. H. Verhagen (Utrecht State Univ., Netherlands) Jun. 1988 61 p
(CWI-MS-R8807; B8827734; ETN-89-94189) Copyright Avail: NTIS HC A04/MF A01

The theory of counting processes is applied to error-counting, debugging models from software reliability, to estimate the total number of bugs in the system and other parameters. Large-sample results on the maximum likelihood estimators are obtained as the number of software bugs increases while the observation period remains fixed. Testing goodness-of-fit of the (parametric) models is also considered. ESA

N89-21544# Battelle Memorial Inst., Willowbrook, IL. Office of Waste Technology Development.
DOCUMENTATION OF THE FINITE ELEMENT CODE VISCOT/UX FOR THERMOMECHANICAL ANALYSES: VERSION 0.01
E. N. Lindner and Christopher St.John (Agapito, J. F. T. and Associates, Inc., Rolling Hills Estates, CA) Oct. 1988 151 p Prepared in cooperation with Agapito (J.F.T.) and Associates, Inc., Rolling Hills Estates, CA
(Contract DE-AC02-83CH-10139)
(DE89-004719; BMI/OWTD-1) Avail: NTIS (US Sales Only) HC A01

VISCOT/UX is a general purpose finite element code capable of nonlinear, transient, thermoelastic or thermoviscoplastic analyses

in either two-dimensional or axisymmetric geometries. Plastic deformations can be evaluated using a variety of models, based on Tresca, von Mises, Mohr-Coulomb, or Drucker-Prager yield criteria using an isotropic strain-hardening model. Thermal response can be incorporated in analyses with the input of the temperature field. The time-dependent response of materials can be simulated using an exponential creep law, which is thermoviscoelastic. The present version of the code has been specifically designed to be used in a microcomputer environment. To facilitate the code's portability, the code is written in standard FORTRAN77 as implemented under a UNIX operating system. It also employs the Frontal method (i.e., a direct elimination process) as a solution strategy, which minimizes core storage requirements and permits large problem solutions in this microcomputer environment. Under the present application, VISCOT/UX is to provide a tool for scoping analyses of underground excavations and experiments in conditions where the rock mass can be considered to be a relatively continuous body, and the response of various materials or zones is essentially isotropic. DOE

N89-21545# Essex Corp., Orlando, FL.
EMPIRICAL DEMONSTRATION OF ISOPERFORMANCE METHODOLOGY PREPARATORY OF AN INTERACTIVE EXPERT COMPUTERIZED DECISION AID Final Report, Aug. 1987 - Feb. 1988
Robert S. Kennedy, Marshall B. Jones, and Dennis R. Baltzley Nov. 1988 44 p
(Contract MDA903-87-C-0603; DA Proj. 2Q6-65502-M-770)
(AD-A202439; ARI-RN-88-93) Avail: NTIS HC A03/MF A01 CSCL 23B

This research note reports on the increasing need within the Department of Defense to improve systems performance through better integration of men and women into military systems. This underlying theme of the Research Note is that once the level of operational performance is settled upon, trade-offs among available resources can and should be made. Formal methodologies are proposed which permit mixtures of training, equipment, and individual differences to be traded off to arrive at a prescribed level of systems performance. This approach is called isoperformance. GRA

N89-21546# Stanford Univ., CA. Dept. of Computer Science.
DEDUCTIVE PROGRAMMING Final Technical Report, 18 Jun. 1984 - 17 Jun. 1987
Zohar Manna Nov. 1988 9 p
(Contract N00039-84-C-0211)
(AD-A202489) Avail: NTIS HC A02/MF A01 CSCL 12E

Our research concentrated on the following topics: Special Relations in Automated Deduction; Binary-Search Algorithms; A Theory of Plans; Deductive Synthesis of Dataflow Networks; Logic, The Calculus of Computer Science; Verification of Concurrent Programs; A Resolution Approach to Temporal Proofs; Specification and Verification by Predicate Automata; A Hierarchy of Temporal Properties; and Logic Programming Semantics: Techniques and Applications. GRA

N89-21547# Stanford Univ., CA. Dept. of Computer Science.
TABLOG: THE DEDUCTIVE TABLEAU PROGRAMMING LANGUAGE Final Technical Report, 21 Nov. 1985 - 20 Nov. 1987
Zohar Manna Nov. 1988 7 p
(Contract N00039-84-C-0211)
(AD-A202490) Avail: NTIS HC A02/MF A01 CSCL 12E

Our research concentrated on the following topics: The Deductive-Tableau System, The TABLOG language and its implementation, A Resolution Approach to Temporal Proofs, Temporal Logic Programming, Logic Programming Semantics: Techniques and Applications. GRA

N89-21548# Massachusetts Inst. of Tech., Cambridge. Lab. for Information and Decision Systems.
A VERY SIMPLE POLYNOMIAL-TIME ALGORITHM FOR LINEAR PROGRAMMING
Paul Tseng Sep. 1988 13 p
(Contract DAAL03-86-K-0171; NSF ECS-85-19058)
(AD-A202502; LIDS-P-1818; ARO-24635.96-MA-VIR) Avail: NTIS HC A03/MF A01 CSCL 12D

This document proposes a polynomial-time algorithm for linear programming. This algorithm augments the objective by a logarithmic penalty function and then solves a sequence of quadratic approximations of this program. This algorithm has a complexity of iterations and arithmetic operations, where m is a number of variables and L is the size of the problem encoding in binary. This algorithm does not require knowledge of the optimal value and generates a sequence of primal (Dual) feasible solutions that converges to an optimal primal (dual) solution (the latter property provides a particularly simple stopping criterion). Moreover, this algorithm is simple and intuitive, both in the description and in the analysis - in contrast to existing polynomial-time algorithms. It works exclusively in the original space. GRA

N89-21549# Woods Hole Oceanographic Institution, MA.
TIME DELAY ESTIMATION IN STATIONARY AND NON-STATIONARY ENVIRONMENTS
Mordechai Segal and Ehud Weinstein Jul. 1988 76 p
(Contract N00014-85-K-0272)
(AD-A202507; WHOI-88-29) Avail: NTIS HC A05/MF A01 CSCL 20A

We develop computationally efficient iterative algorithms for finding the Maximum Likelihood estimates of the delay and spectral parameters of noise-like Gaussian signals radiated from a common point source and observed by two or more spatially separated receivers. We first consider the stationary case in which the source is stationary (not moving) and the observed signals are modeled as wide sense stationary processes. We then extend the scope by considering a non-stationary (moving) source radiating a possible non-stationary stochastic signal. In that context, we address the practical problem of estimation given discrete-time observations. We also present efficient methods for calculating the log-likelihood gradient (score), the Hessian, and the Fisher's information matrix under stationary and non-stationary conditions. GRA

N89-21550# Nevada Univ., Las Vegas. Dept. of Computer Science and Electrical Engineering.
GRASP: A GRAPH SPECIFICATION LANGUAGE
Todd A. Gross 13 Oct. 1988 22 p
(Contract DAAL03-87-G-0004)
(AD-A202524; CSR-88-10; ARO-24960.27-MA) Avail: NTIS HC A03/MF A01 CSCL 12E

This paper is an introduction to Grasp, a language for defining and prototyping graph theoretic constructs and properties associated with them. The language is a specification language, which means that one gives only the necessary inputs and desired outputs, and the translator generates the necessary algorithm. Section 2 explains why Grasp was devised. Section 3 gives the syntax of the language. Section 4 gives some examples of Grasp specifications. Finally, section 5 discusses the relative strengths and weaknesses of the language. We are currently developing a translator from Grasp specifications into C functions. GRA

N89-21551# Air Force Inst. of Tech., Wright-Patterson AFB, OH. School of Engineering.
SUPERRESOLVED IMAGING USING THE HARTLEY TRANSFORM AND A HEMISPHERICAL OBJECT SPACE M.S. Thesis
Shawn L. Kelly Dec. 1988 46 p
(AD-A202527; AFIT/GEP/ENP/88D-3) Avail: NTIS HC A03/MF A01 CSCL 12E

Resolution in an image can be increased by an iterative technique (introduced by Gerchberg) which effectively continues the known, partial spectrum beyond the limits imposed by an optical system. This increased resolution is called superresolution. Historically, an important constraint assumed for this technique was the knowledge of the finite dimensions of the object such that the object energy outside these dimensions must be zero. It is shown in this thesis that by a change of object space geometry,

the semicircular field of view of an optical system provides a natural dimensional constraint which can be used instead of the object dimensions to achieve superresolution. A further modification of the iterative technique involves using the Fast Hartley Transform (FHT) instead of the Fast Fourier Transform (FFT). The FHT is inherently faster and requires less computer memory than the FFT. GRA

N89-21552# Massachusetts Inst. of Tech., Lexington. Lincoln Lab.
MODEL-BASED SILHOUETTE RECOGNITION
P. L. VanHove and R. A. Jaenicke 25 Nov. 1988 160 p
(Contract F19628-85-C-0002)
(AD-A202540; TR-817; ESD-TR-88-194) Avail: NTIS HC A08/MF A01 CSCL 12E

The authors present a system for recognizing 3-D objects at unknown orientations from their 2-D silhouettes. The geometric description of an object model is provided in CAD form and is then compiled into a set of geometric constraints for a large set of viewing directions. The silhouette is parsed into a set of straight edges, and these edges are compared to the edges of the model by conceptually structuring all possible interpretations in a tree. This enormous search space is pruned by extending the interpretation tree search of Grimson and Lozano-Perez to work for the 3-D model/2-D data case. This includes a precise analysis of the propagation of errors in the position and orientation of silhouette edges, which then provide adequate constraints for pruning the search tree. Any hypotheses that survive the pairwise constraints of tree search are verified by synthesizing a silhouette of the model for the hypothesized orientation and comparing this synthetic silhouette to the observed silhouette. Based only on silhouette data, the system can find all plausible interpretations of the data, including symmetric viewpoints. The system performs in the presence of unknown viewpoint, moderate scale uncertainties, occluding objects, and degradations in the silhouette shape due to image noise and image processing artifacts. GRA

N89-21553# Air Force Inst. of Tech., Wright-Patterson AFB, OH. School of Engineering.
ARCHITECTURE AND DESIGN FOR A LASER PROGRAMMABLE DOUBLE PRECISION FLOATING POINT APPLICATION SPECIFIC PROCESSOR M.S. Thesis
John Henry Comtois Dec. 1988 165 p
(AD-A202560; AFIT/GE/ENG/88-5) Avail: NTIS HC A08/MF A01 CSCL 12F

Numerous signal processing systems in the Department of Defense and industry would benefit from a microprocessor tailored to their specific applications. This thesis effort describes the architecture and design for a 64 bit application specific processor (ASP) which combines the power of double precision floating point hardware with the flexibility of a laser programmable microcode store. This floating point ASP (FPASP) contains a variety of circuits which efficiently perform digital signal processing and other applications requiring double precision floating point arithmetic. This thesis describes a new rapid prototyping methodology for ASPs. The user provides an algorithm which is translated into microcode, tested on a software model, and then cut into the laser PROM of a blank FPASP chip. With this methodology the prototyping of an ASP can be completed in a matter of days, and no hardware design is involved. The programmed FPASP can then be mounted on a circuit board and placed in a host processor to act as a hardware accelerator for computationally intense programs. The FPASP also supports a macro assembly language which can be partially user-defined. So the FPASP can be tailored to higher level applications such as operating system support. GRA

N89-21554# Air Force Inst. of Tech., Wright-Patterson AFB, OH. School of Engineering.
RESPONSE SURFACE ANALYSIS OF STOCHASTIC NETWORK PERFORMANCE M.S. Thesis
Thomas Glenn Bailey Dec. 1988 173 p
(AD-A202561; AFIT/GOR/ENS/88D-01) Avail: NTIS HC A08/MF A01 CSCL 12D

The objective of this thesis was to analyze stochastic binary networks for the purpose of improving their performance as measured by expected maximum flow and source-to-sink reliability. The capacity and survivability of the networks' nodes and arcs formed the parameters of interest in the experimental design used to develop a response surface model. Estimates of network performance was provided by Monte Carlo simulation using a FORTRAN based program designed for this study called MAXFLO. MAXFLO implemented an original form of maximum flow calculation using minimal cuts instead of paths to improve the simulation's speed. MAXFLO was also compiled and run on a VAX 8650, VAX 11/785, and SUN-3 workstation under UNIX and VMS systems to insure portability and simulation performance. GRA

N89-21555# Air Force Inst. of Tech., Wright-Patterson AFB, OH. School of Engineering.
SIMULATING RULE-BASED SYSTEMS M.S. Thesis
Nizar Mahmoud Mahaba Dec. 1988 170 p
(AD-A202563; AFIT/GOR/ENS/88D-12) Avail: NTIS HC A08/MF A01 CSCL 12D

The purpose of this thesis is to develop a methodology for evaluating the performance of rule-based systems (RBSs) using a simulation approach. A numerical scheme is used for knowledge representation; facts are represented by integer numbers and the rules and data memories are represented by matrices. The numeric representation can be handled by simplified algorithms that simulate the function of different types of inference engines. Six types of forward-chaining inference engines that vary according to the conflict resolution strategy and the implementation of filters are simulated and compared. The number of match-tests of the left-hand side of the rules against the data memory is used as a measure of performance to estimate the relative matching effort for each inference engine. Also, a methodology to reduce the matching effort of RBS by changing the order of the facts in the left-hand side or changing the order of the rules is described. GRA

N89-21556# Air Force Inst. of Tech., Wright-Patterson AFB, OH. School of Engineering.
OPTICAL INFORMATION PROCESSING IN A CONFOCAL FABRY-PEROT RESONATOR M.S. Thesis
Jeffery A. Wilson Dec. 1988 129 p
(AD-A202566; AFIT/GEO/ENG/88D-5) Avail: NTIS HC A07/MF A01 CSCL 20F

Many optical information processing algorithms require feedback to perform iterative processing. An algorithm which exemplifies the requirement for feedback is the optical associative memory. This thesis explores the theoretical design of an optical associative memory in a confocal Fabry-Perot resonator. The components of the optical associative memory-BaTiO3 crystals, confocal resonator, and holographic plates-are characterized individually to determine the feasibility of implementing the associative memory. The BaTiO3 crystals are characterized for processing functions such as image amplification, edge enhancement, linear and nonlinear gain, and linear and nonlinear attenuation. Unique 45 degree-cut BaTiO3 crystals are investigated in two-wave coupling experiments. The 45 degree-cut crystals did not perform as expected, and their performance points to a need to improve the mathematical model of two-wave coupling to include the effects of beam-fanning. The sensitivity of the confocal resonator to mechanical vibrations and air currents were learned along with methods to overcome these problems and align/stabilize the resonator. The BaTiO3 crystals were placed within the resonator to perform qualitative analysis on the crystals. Within the resonator, it was verified that the 45 degree crystal does have more gain potential than the z-cut crystal. GRA

N89-21557# Air Force Inst. of Tech., Wright-Patterson AFB, OH. School of Engineering.
AN EDUCATIONAL EXPERT SYSTEM SHELL INTEGRATING OBJECT-ATTRIBUTE-VALUE TRIPLES AND FRAMES M.S. Thesis

Eddy G. Clark Dec. 1988 252 p
(AD-A202574; AFIT/GCE/ENG/88D-2) Avail: NTIS HC A12/MF A01 CSCL 12E

This thesis project investigates the creation of an expert systems shell which integrates object-attribute-value triples with frames and implements the shell in standard Prolog. Additionally, the implemented expert system shell uses certainty factors, which allow it to perform inexact reasoning. The shell, named the Air Force Institute of Technology Backward Chainer, or ABC, represents its knowledge in facts, rules, and frames. ABC has an explanation facility that can explain how it derives a solution or why it asks particular questions when seeking information from the user. The approach used in this thesis was to study and expand upon an educational expert system shell called BC3. BC3, a rule-based shell developed at AFIT, symbolizes its knowledge with OAV triples. Once the decision to expand upon BC3 was made, the thesis project was divided into four separate but interrelated phases. At the end of each phase, a working expert system shell was implemented, limited to the functions of the current and previous phases. GRA

N89-21558# Air Force Inst. of Tech., Wright-Patterson AFB, OH. School of Engineering.
A DECISION-BASED METHODOLOGY FOR OBJECT ORIENTED-DESIGN M.S. Thesis
Patrick Denis Barnes 16 Dec. 1988 223 p
(AD-A202579; AFIT/GCS/ENG/88D-1) Avail: NTIS HC A10/MF A01 CSCL 12E

The task of object-oriented development raises a new set of design problems: specifically, how to scope a problem based on objects rather than functions; how to select the best objects; how to encapsulate data structures with the right set of operations; and when to stop decomposing a system into objects and begin describing the algorithms that implement those objects' behaviors. The difficulty of making these decisions increased when the requirements documentation was not developed with an object-oriented paradigm in mind. Although several software development environments implement an object-oriented design methodology, they seem concerned primarily with programming in the small activities, or with providing capabilities for capturing, representing, and storing design decisions once they are made. Recognizing the importance of supporting design decision making, this study focused on the application of decision support system concepts to formulating a methodology for object-oriented design. This thesis describes an object-oriented design methodology based on the four problems or decisions stated above. An object model structure is also defined to provide a foundation for organizing design information. The object model is described by a set of database relations, and includes a three view graphic representation providing block, detail and control flow graphs. GRA

N89-21559# Naval Ocean Systems Center, San Diego, CA.
GRAPS (GRAPHICAL PLOTTING SYSTEM) USER'S GUIDE. A GRAPHICAL PLOTTING SYSTEM FOR DISPLAYING SCIENTIFIC AND ENGINEERING DATA Final Report, Sep. 1987 - Sep. 1988
James C. Logan and John Strauch Oct. 1988 31 p
(AD-A202583; NOSC/TD-1326) Avail: NTIS HC A03/MF A01 CSCL 12E

This document provides an introduction and update to the Graphical Plotting System (GRAPS), a plotting utility developed by the Naval Ocean Systems Center for the personal computer. GRAPS provides a convenient, user-friendly tool for the display of engineering and scientific data in a number of conventional plot formats. Linear, semi-log, polar, log-log, Smith, and contour plot formats are among those that can be selected. User-friendly features include auto and user-defined scaling, text editing on graphics screens, and data file management options. Auto and user-defined scaling are new GRAPS features. The polar plots have been significantly improved and the contour plot added. The data file management options have also been expanded. GRAPS will plot any data stored in ASCII files in the GRAPS format. GRAPS is intended to be used as a stand-alone utility for the preparation and display of engineering and scientific data. It is not suitable for inclusion as part of another program, although subroutines could be stripped out for inclusion in other programs. GRAPS is set up to read data from a disk file written (in ASCII) to a simple format. The disk file may be created by using an editor or word processor. Preferably, a subroutine may be included in the applications program to write the raw data directly to a disk file in the GRAPS format. GRA

N89-21560# Air Force Inst. of Tech., Wright-Patterson AFB, OH. School of Engineering.
A VECTORIZED HIDDEN-SURFACE ALGORITHM IMPLEMENTED ON THE CRAY-2 SUPERCOMPUTER M.S. Thesis
Roy Donehower Dec. 1988 102 p
(AD-A202657; AD-E900870; AFIT/GCS/ENG/88D-3) Avail: NTIS HC A06/MF A01 CSCL 12F

Recent developments in scientific computing have prompted the need for supercomputer graphics research. These developments include the requirement to visualize large amounts of data which are processed by the supercomputer, preferably by real-time image generation. Unfortunately, most currently used graphics algorithms are not optimized for vector computers. This thesis involves the design and implementation of a hidden-surface removal algorithm for the Cray-2 vector supercomputer, with the goal of real-time image display. A z-buffer hidden-surface algorithm, written in Pascal, was vectorized and implemented on the Cray-2. Special attention was directed toward the methodology of algorithm and data structure design to exploit the Cray-2 architecture. Timing studies comparing the vector version to the equivalent scalar version showed that while tha Pascal vector code produced localized speedups, the vector code was less efficient than the scalar code. GRA

N89-21561# Air Force Inst. of Tech., Wright-Patterson AFB, OH. School of Engineering.
MAINTENANCE METRICS FOR JOVIAL (J73) SOFTWARE M.S. Thesis
Douglas R. Tindell Dec. 1988 128 p
(AD-A202713; AFIT/GE/ENG/88D-57) Avail: NTIS HC A07/MF A01 CSCL 12E

The expense of maintaining software is greater than any other phase in the life cycle. To help reduce the costs, software which may not be maintainable should be identified before being released for use. Measures of software quality, or metrics, may be able to help do this. The goal of this thesis was to identify measures which could indicate the maintainability of JOVIAL (J73) software, and to implement selected ones. Maintainability cannot be measured directly, so a strong indicator, complexity, was measured instead. Five categories of complexity metrics were reviewed: size, control, data, information, and hybrid. Through an analysis of metrics from each category, the information metric was selected for implementation. Using Ada as the implementation language, an analyzer to compute the information metric was constructed. The design was primarily object-oriented but was influenced by compiler theory. The resulting analyzer can easily incorporate new metrics or new input/output requirements. Testing was performed using both simple code examples and actual F-16 flight software. The analyzer properly computes the information metric with few exceptions. A plan to compare the results of the analyzer with the results of the sponsor's present manual review was described. GRA

N89-21562# Air Force Inst. of Tech., Wright-Patterson AFB, OH. School of Engineering.
DESIGN OF A SYNTAX VALIDATION TOOL FOR REQUIREMENTS ANALYSIS USING STRUCTURED ANALYSIS AND DESIGN TECHNIQUE (SADT) M.S. Thesis
Dong H. Jung Sep. 1988 108 p
(AD-A202725; AFIT/GCS/ENG/88S-1) Avail: NTIS HC A06/MF A01 CSCL 12E

This thesis investigation presents the prototype development

of a validation tool for checking the syntax of Structured Analysis and Design Technique (SADT) method from a structured analysis diagram. The tool provides the requirements analyst and the designer with an environment for checking the SADT syntax of an SADT diagram. The tool is operated through the use of an SADT Editor which was developed by Steven E. Johnson at the Air Force Institute of Technology (AFIT). The validation tool was developed in three phases. During the first phase the formal definition of the SADT graphical language was derived using Predicate Logic representation. During the second phase, the SADT Editor was analyzed and the interface issues with the software were identified. Thus, the graphical features were translated. During the third phase, the syntax rules were identified according to the formal definition of the SADT methodology using Predicate Logic representation. The new tool was implemented into a knowledge-based system to ease the extension of the syntax rules, to add knowledge of the SADT graphical structure and to add domain knowledge of an application system developed by the SADT methodology. GRA

N89-21563# Air Force Inst. of Tech., Wright-Patterson AFB, OH. School of Engineering.

DISTRIBUTED DISCRETE-EVENT SIMULATION USING VARIANTS OF THE CHANDY-MISRA ALGORITHM ON THE INTEL HYPERCUBE M.S. Thesis

David L. Mannix Dec. 1988 153 p

(AD-A202849; AFIT/GCS/ENG/88D-14) Avail: NTIS HC A08/MF A01 CSCL 12E

The goal of distributed simulation is to speed up simulation by distributing a simulation model's execution over multiple processors. This thesis reviews existing methods for distributed simulation, the distributed event list algorithm, based on the Chandy-Misra algorithm, with an event list, similar to that used in sequential simulation, at each logical process. Null messages are used for deadlock avoidance. The algorithm is described, and is shown to require a bounded amount of memory at each logical process. A performance analysis of the distributed event list algorithm is performed. In the analytical portion, a linear event list implementation is shown to be of super-linear time complexity in relation to events simulated. This time complexity implies theoretical speed-up of greater than N for a simulation distributed over N processors. This result contradicts a commonly-held view of the existence of a bound of N on attainable speed-up. Alternate strategies for sending the Null messages used for deadlock avoidance are compared. Results show that for tandem and feed-forward topologies, a certain level of Null messages are beneficial to speed-up. The problem of assigning a given simulation model to a set of logical processes is addressed. It is seen that topology of the logical system plays a critical role in the effectiveness of assignment strategy. GRA

N89-21564# Stanford Univ., CA.

OPTICAL COMPUTING RESEARCH Annual Report, 1 Oct. 1987 - 30 Sep. 1988

Joseph W. Goodman and Jehosua Bruck Oct. 1988 66 p

(Grant AF-AFOSR-0024-88; AF Proj. 2305)

(AD-A202963; AFOSR-88-1282TR) Avail: NTIS HC A04/MF A01 CSCL 12I

The research focused on understanding the global as well as local properties of the neural network model. Global properties are the dynamics of the network, convergency properties, computational power and capacity. Local properties mean the theory of threshold logic elements, the basic building blocks of the network. Investigated is the relation between error-correcting codes and neural networks. The motivation was that a neural network model can be viewed as a decoder. The stable states correspond to codewords, the probe vector corresponds to the received vector, and convergence to the closest stable state corresponds to Maximum Likelihood Decoding (MLD). Several natural ways were found for connecting the concepts of error correcting codes with the concept of neural networks. The MLD problem in a linear block code is equivalent to finding the global maximum of the energy function of a neural network that can be easily constructed knowing the basis set of the code. GRA

N89-21565# Massachusetts Inst. of Tech., Cambridge. Lab. for Computer Science.

SEMANTICAL PARADIGMS: NOTES FOR AN INVITED LECTURE

Albert R. Meyer and Stavros S. Cosmadakis Jul. 1988 23 p Presented at the 3rd IFEE Symposium on Logic in Computer Science, Edinburgh, Scotland, Jul. 1988 Prepared in cooperation with IBM Watson Research Center

(Contract N00014-83-K-0125; NSF DCR-85-11190)

(AD-A202995; NIT/LCS/TM-353) Avail: NTIS HC A03/MF A01 CSCL 12E

It took the author a few years to understand the point of continuity in denotational semantics. He's happy to report below on some recent results which justify his muddle-headedness and help explain the point too. What follows are some global comments on denotational semantics of the kind invited lecturers sometimes indulge themselves in, highlighting goodness of fit criteria between semantic domains and symbolic evaluators. For readers impatient with sketchy overviews, two appendices mostly by Cosmadakis provide the key parts of a long proof that Scott domains give a computationally adequate and fully abstract semantics for lambda calculus with simple recursive types. GRA

N89-21566# University of Southern California, Los Angeles. Optical Materials and Devices Lab.

DEVICES AND SYSTEMS FOR NONLINEAR OPTICAL INFORMATION PROCESSING Final Technical Report, 15 May 1983 - 30 Nov. 1987

Armand R. Tanguay, Jr. Nov. 1988 140 p

(Grant AF-AFOSR-0185-83; AF Proj. 2305)

(AD-A203034; USC/OMDL-1501; AFOSR-88-1250TR) Avail: NTIS HC A07/MF A01 CSCL 09E

The principal thrust of this research effort is the development and evaluation of optical devices and associated systems architectures for the implementation of highly parallel nonlinear optical information processing functions such as thresholding, level slicing, logarithms, and power laws. Such devices include the Variable Grating Mode Liquid Crystal Device (VGM LCD), which is uniquely capable of performing a novel and powerful intensity-to-position encoding function. A related and evolving research thrust is the detailed analysis of both the fundamental and technological limitations that affect the performance of envisioned optical information processing and computing devices and systems, for both linear and nonlinear function implementation. The primary objective here is to compare and contrast electronic and optical (as well as hybrid electro-optical or optoelectronic) devices, circuits, and systems with respect to their current, near term projected, and ultimate computational capabilities. The demonstrable goal of such an effort is to be able (on the basis of the above analyses) to segregate classes of problems most appropriate for solution by electronic, optical, or hybrid processors, subject to specific and pre-defined performance metrics. GRA

N89-21567# Air Force Inst. of Tech., Wright-Patterson AFB, OH. School of Engineering.

INFLUENCE DIAGRAMS: AUTOMATED ANALYSIS WITH DYNAMIC PROGRAMMING M.S. Thesis

Christopher Thomas Baron Dec. 1988 102 p

(AD-A203045; AFIT/GOR/MA/88D-1) Avail: NTIS HC A06/MF A01 CSCL 12D

The major goals of this thesis were to develop a user friendly software package for processing influence diagrams, and to implement in software the extensions necessary for dynamic programming without special action or knowledge on the part of the user. The final goal was to demonstrate the efficiency of the dynamic programming techniques by applying them to several example problems. A software package, AFids (AFIT influence diagram system) was developed. The system is capable of performance equivalent to the current state of the art in commercial influence diagram software. AFids incorporates the basic influence

diagram operations, the separable value function extensions, and an algorithm to automatically solve any properly formed influence diagram. Separation of the value function is automatic and requires no action or special knowledge on the part of the user beyond representing the value function explicitly as a sum or product. The software uses menus, data entry screens, and graphics to provide an effective and friendly user interface. Several extensions to influence diagram theory were implemented in the AFids package including the concepts of value rounding and outcome limiting to control the combinatorial explosion encountered when processing chains of deterministic nodes. The system is cost free and available in either source or compiled form for government users. There are no restrictions on use or distribution except for commercial use. The software runs on MS-DOS compatible microcomputers and was programmed in Turbo Pascal. GRA

N89-21568# Air Force Inst. of Tech., Wright-Patterson AFB, OH. School of Engineering.
A SOFTWARE SYSTEM TO CREATE A HIERARCHICAL, MULTIPLE LEVEL OF DETAIL TERRAIN MODEL M.S. Thesis
LeeAnne Roberts Dec. 1988 55 p
(AD-A203047; AFIT/GCS/ENG/88D-18) Avail: NTIS HC A04/MF A01 CSCL 08B

The purpose of this effort was to design and implement a software system that will generate a hierarchical database composed of more than one level of detail of a terrain model and cultural objects from digital elevation and cultural data files. The software system designed and implemented in this effort was written in the C language and implemented on a Digital Equipment GPX Workstation and on a Silicon Graphics Iris 3130 Workstation. Although the primary source of elevation data used in this effort was the Defense Mapping Agencies' (DMA) Digital Terrain Elevation Data (DTED), a method was developed to build a terrain model from non-gridded elevation data. In addition to allowing the use of non-DMA data, this method also makes it possible to build a terrain model from a non-gridded subset of a DMA DTED data file. Two database formats were designed and implemented in this effort. The first database (which was used to generate the terrain model) contains lists of the vertices, exterior edges, interior edges, and polygons (and their interrelations) that form the terrain model. The second database contains polygons (that form the terrain model) and cultural features (such as radio towers) at one or more levels of detail, and a search tree (so that data in a particular area may be retrieved quickly). The list database may be used to generate contours, or non-real-time images of terrain. The hierarchical database may be used in a simulator environment. GRA

N89-21569# Air Force Inst. of Tech., Wright-Patterson AFB, OH. School of Engineering.
A NEURAL NETWORK IMPLEMENTATION OF CHAOTIC TIME SERIES PREDICTION M.S. Thesis
James R. Stright Dec. 1988 123 p
(AD-A203049; AFIT/GE/ENG/88D-50) Avail: NTIS HC A06/MF A01 CSCL 12D

This thesis provides a description of how a neural network can be trained to learn the order inherent in chaotic time series data and then use that knowledge to predict future time series values. It examines the meaning of chaotic time series data, and explores in detail the Glass-Mackey nonlinear differential delay equation as a typical source of such data. An efficient weight update algorithm is derived, and its two-dimensional performance is examined graphically. A predictor network which incorporates this algorithm is constructed and used to predict chaotic data. The network was able to predict chaotic data. Prediction was more accurate for data having a low fractal dimension than for high-dimensional data. Lengthy computer run times were found essential for adequate network training. GRA

N89-21570# Utah Univ., Salt Lake City. Dept. of Computer Science.
PERFORMANCE DIRECTED SIMULATION Final Report, 15 Feb. 1987 - 31 Dec. 1988
Richard M. Fujimoto 31 Dec. 1988 9 p
(Contract N00014-87-K-0184)
(AD-A203089) Avail: NTIS HC A02/MF A01 CSCL 12E

The overall scientific objective of this research was to develop techniques for speeding up discrete event simulation (DES) programs in applications such as simulation of computer architectures, communication networks, battlefield scenarios, etc. Such simulations often require prohibitive amounts of time on conventional computing hardware. Several major successes and important new results were obtained during the grant period in this problem domain. The most significant results are summarized in the following areas: optimistic and conservative synchronization mechanisms; special purpose hardware for discrete event simulation. GRA

N89-21571# Utah Univ., Salt Lake City. Dept. of Computer Science.
THE DESIGN AND PERFORMANCE OF THE ROLLBACK CHIP: HARDWARE SUPPORT FOR TIME WARP M.S. Thesis
Jya-Jang Tsai Oct. 1988 103 p
(AD-A203160) Avail: NTIS HC A06/MF A01 CSCL 09A

The Time Warp mechanism offers an elegant approach to attacking difficult clock synchronization problems that arise in applications such as parallel discrete event simulation. However, because Time Warp relies on a lookahead and rollback mechanism to achieve widespread exploitation of parallelism, the state of each process must periodically be saved. Existing approaches to implementing state saving and rollback are not appropriate for large Time Warp programs. A component called the Rollback Chip (RBC) is proposed in this thesis to efficiently implement these functions. Such a component could be used in a programmable, special purpose parallel discrete event simulation engine based on Time Warp. The algorithms implemented by the rollback chip are described, as well as mechanisms that allow efficient implementation. Results of simulation studies are presented. These results show that the rollback can virtually eliminate the state saving and rollback overheads that plague current software implementations of Time Warp. GRA

N89-21572# Air Force Avionics Lab., Wright-Patterson AFB, OH.
SOFTWARE DEVELOPMENT GUIDELINES
Denice S. Jacobs 1 Apr. 1988 5 p
(AD-A203332; AFWAL-TR-88-1142) Avail: NTIS HC A02/MF A01 CSCL 12E

Due to the growing complexity of avionic systems, the development cycle for mission critical software has evolved into a collective process of organized tasks. These tasks are distinct levels of effort which are implemented by the developer to ensure the creation of a reliable, operational system. This paper summarizes four principle tasks which have proven to be excellent procedures for developing avionics software. The first and foremost task of the project manager is to establish a Configuration Control Board (CCB) as the central core of technical management. It consists of a group of key hardware and software engineers who mutually govern the status of system development, and incorporate design changes on an agreed-to basis. The second task is to logically separate the software project into well-defined phases of development. This, too, requires the cooperation of both hardware and software teams to work together in accordance with master schedule. The third task is to create an automated data base which contains the latest interface specifications (ICDs) and system message definitions for use by the engineers. Finally, the last task is to procure hardware emulators and stand-alone test stations as an effective means of testing software prior to system integration and test. GRA

N89-21573# Tennessee Univ., Knoxville. Management Science Program.
NONPROCEDURAL IMPLEMENTATION OF MATHEMATICAL PROGRAMMING ALGORITHMS Technical Report, for FY88
James K. Ho Dec. 1988 13 p

(Contract N00014-87-K-0163)
(AD-A203392; MSP-88-1) Avail: NTIS HC A03/MF A01 CSCL 12E

It is shown that the implementation of many mathematical programming algorithms using spreadsheet software can be described as instances of a nonprocedural approach to computer programming. This concept is generalized to an abstract computing environment called HYPERCELLS. Its significance in view of rapid development in parallel computation is discussed. With the widespread use of microcomputers in academia, business, industry and government, spreadsheet software has become the most popular general purpose quantitative tool for numerical computation. It is essentially a two dimensional array of cells. Each cell may contain text for documentation, numerical values from data, or a formula dependent on values in other cells. Whenever the value in a cell is changed, the content of cells with formulas depending on it can be recalculated automatically. GRA

N89-21574# New York Univ., New York. Dept. of Computer Science.
DOMAIN MODELING FOR LANGUAGE ANALYSIS
Ralph Grishman Feb. 1988 9 p
(Contract N00014-85-K-0163; NSF DCR-85-01843)
(AD-A203444; PROTEUS-M-14) Avail: NTIS HC A02/MF A01 CSCL 05G

In section 2 of this paper we briefly characterize our notion of understanding a text. In section 3 we give an overview of the system we have constructed for analyzing equipment failure messages, and indicate the points at which it makes use of domain information. We then turn in section 4 to the domain model itself, and describe how it provides the information needed by language analysis. We close with brief sections relating our work to other work on discourse analysis and discussing how our system's coverage may be broadened. GRA

N89-21575# Applied Technology Associates, Inc., Albuquerque, NM.
VAX TO CRAY NASTRAN USER INTERFACE Final Report, Jul. 1986 - Jul. 1987
M. R. James Oct. 1988 71 p
(Contract F29601-86-C-0252)
(AD-A203447; AFWL-TR-87-93) Avail: NTIS HC A04/MF A01 CSCL 12E

The Air Force Weapons Laboratory has access to both the NASTRAN and PATRAN software systems for structural analysis investigations; however, these two codes are resident on separate computer systems at AFWL. NASTRAN is used to perform the bulk of large structural analysis research and is resident on the CRAY1S. PATRAN is installed on Silicon Graphics and allows depictions and animation of modal analysis results. The two software packages are complementary in function, and communication between them can be achieved through the GATEWAY facility. The GATEWAY links the AFWLO4 VAX, the silicon Graphics IRIS, and the CRAY through a common network protocol. This document describes software residential on the VAX and CRAY computer systems which allows PATRAN animation of NASTRAN calculated modal shapes. This section contains general information which should be reviewed by all potential users. Section 2 outlines the step by step implementation of NASTRAN calculation and PATRAN animation. This approach is designated VAX/CRAY/VAX processing. The VAX/CRAY/VAX approach is appropriate regardless of whether the NASTRAN model was created on the Silicon Graphics using PATRAN or created on the VAX using an editor. GRA

N89-21576# Massachusetts Inst. of Tech., Cambridge. Microsystems Research Center.
COMPUTER-AIDED FABRICATION SYSTEM IMPLEMENTATION Semiannual Technical Report, 1 Oct. 1987 - 31 Mar. 1988
Paul Penfield, Jr. 31 Mar. 1988 31 p
(Contract N00014-85-K-0213)
(AD-A203651) Avail: NTIS HC A03/MF A01 CSCL 12F

The purpose of the work reported on here is to design, develop, implement, and deploy information management systems to aid in the fabrication of integrated circuits, particularly in the context of flexible manufacturing. The work includes the development of a hardware-software system, named CAFE, and the support of this program and its use in the MIT Integrated Circuits Laboratory. CAFE should support both manufacturing of ICs and the design of processes, so part of the effort is directed toward the development of a suitable process-development environment. Other projects are concerned with equipment and mechanical-property models and scheduling. GRA

N89-21577# Singer Co., Wayne, NJ. Electronic Systems Div.
IMAGE PROCESSING LANGUAGE, PHASE 2 Final Technical Report, Aug. 1985 - May 1987
Charles R. Giardina and Edward R. Dougherty Nov. 1988 112 p
(Contract F08635-84-C-0296)
(AD-A203994; AD-E801833; AFATL-TR-88-12) Avail: NTIS HC A06/MF A01 CSCL 12I

An image processing language in the form of an algebra is developed to serve as a framework to express image and signal processing algorithms. The operators in the algebra can be expressed in terms of a set of seven primative, or basis operators which has been induced from the underlying algebraic structures of the domain and range spaces. Whereas, the inducement methodology is rather general and its application is not restricted to image processing, the bulk of the report is concentrated on the development of a digital image algebra. In terms of this algebra, operators such as dilation and convolution, which are often defined pointwise, possess closed-form expressions as strings of the seven basic operations. A structured approach to the development of intelligent weapon systems is presented herein with an emphasis in automated image processing algorithm development. These artificial intelligence concepts are implemented in PASCAL. GRA

N89-21578# Los Alamos National Lab., NM.
TIME-OF-FLIGHT SMALL-ANGLE NEUTRON SCATTERING DATA REDUCTION AND ANALYSIS AT LANSCE WITH PROGRAM SMR
Rex P. Hjelm, Jr. and Philip A. Seeger 1988 39 p Presented at the International Collaboration on Advanced Neutron Sources (ICANS), Los Alamos, NM, 3-7 Oct. 1988
(Contract W-7405-eng-36)
(DE89-006520; LA-UR-89-119; CONF-8810182-13) Avail: NTIS HC A03/MF A01

A user-friendly integrated system, SMR, for the display, reduction and analysis of data from time-of-flight small-angle neutron diffractometers is described. Its purpose is to provide facilities for data display and assessment, and to provide these facilities in near real time. This allows the results of each scattering measurement to be available almost immediately, and enables the user to use the results of a measurement as a basis for other measurements in the same time allocation of the instrument. DOE

N89-21579# Argonne National Lab., IL. Mathmatics and Computer Science Div.
AN ALGEBRAIC THEORY OF PROGRAM CORRECTNESS IN A PROBLEM DOMAIN
J. R. Gabriel 1989 9 p
(Contracts W-31-109-eng-38; P-86112)
(DE89-008450; ANL/PPRNT-89-156) Avail: NTIS HC A02/MF A01

The input equivalence classes of a binary computation - those sets of input values giving rise all to the same output - are defined. It is shown that the input equivalences define a group of input/output mappings commuting with the program, and that the value space of problem domain affords an irreducible representation of this symmetry group. It follows that not only does a program define its input equivalences, but a complete set

of input equivalences and one input/output pair define a program. Thus a program may be defined either by its input/output mapping or by its symmetry group, and a good specification might include both. The determination of input equivalences for a system from knowledge of its parts and their interconnections is shown to be mechanically computable in roughly the same circumstances that an input/output relation is mechanically computable. DOE

N89-21580# Argonne National Lab., IL. Mathematics and Computer Science Div.
A THEORY OF PROBLEM DOMAINS AND PROGRAM CORRECTNESS
J. R. Gabriel and R. O. Chapman 1989 10 p
(Contract W-31-109-eng-38)
(DE89-008451; ANL/PPRNT-89-155) Avail: NTIS HC A02/MF A01

A model of a problem domain is introduced comprising a set of variable names, a language describing computations on these variables, and an abstract machine specifying the semantics of the language. The model allows hierarchical definition of an implementation at a low level of a problem defined at a high level. Several modes of real analysis, including a realistic binary computer, are given in terms of well-defined mathematical constructs. A simple, high-level problem specification is used to describe the process of hierarchical definition and proof. The primary software tool proposed for use in proofs is an existing compiler deriving a system specification from that of its parts and interconnections. DOE

N89-21581# Argonne National Lab., IL. Mathematics and Computer Science Div.
OTTER 1.0 USERS' GUIDE
William W. McCune Jan. 1989 21 p
(Contract W-31-109-eng-38)
(DE89-008656; ANL-88-44) Avail: NTIS HC A03/MF A01

OTTER (Other Techniques for Theorem-proving and Effective Research) is a resolution-style theorem-proving program for first-order logic with equality. OTTER includes the inference rules binary resolution, hyperresolution, UR-resolution, and binary paramodulation. Some of its other abilities are conversion from first-order formulas to clauses, forward and back subsumption, factoring, weighting, answer literals, term ordering, forward and back demodulation, and evaluable functions and predicates. OTTER is coded in C, and it is portable to a wide variety of computers. DOE

N89-21493# Columbia Univ., New York, NY. Dept. of Mechanical Engineering.
STATISTICAL MACHINE LEARNING FOR THE COGNITIVE SELECTION OF NONLINEAR PROGRAMMING ALGORITHMS IN ENGINEERING DESIGN OPTIMIZATION
David A. Hoeltzel and Wei-Hua Chieng *In* Army Research Office, Transactions of the Fifth Army Conference on Applied Mathematics and Computing Mar. 1988 p 65-78 (For primary document see N89-21490 14-59)
(Contract DAAL03-86-6-0116)
Avail: NTIS HC A99/MF E03 CSCL 12E

N89-21502# Wisconsin Univ., Madison. Dept. of Computer Sciences.
ALGORITHMS FOR RATIONAL SPLINE CURVES
Klaus Hollig *In* Army Research Office, Transactions of the Fifth Army Conference on Applied Mathematics and Computing Mar. 1988 p 287-300 (For primary document see N89-21490 14-59)
(Contract DAAG29-80-C-0041; NSF DMS-83-51187)
Avail: NTIS HC A99/MF E03 CSCL 09B

N89-21509# Army Troop Support Command, Fort Belvoir, VA.
COMPUTATIONAL ISSUES IN GOAL PROGRAMMING RESOURCE ALLOCATION
Leon Medler *In* Army Research Office, Transactions of the Fifth Army Conference on Applied Mathematics and Computing Mar. 1988 p 377-382 (For primary document see N89-21490 14-59)
Avail: NTIS HC A99/MF E03 CSCL 09B

N89-21729*# Alabama A & M Univ., Huntsville. Dept. of Mathematics.
REFINING, REVISING, AUGMENTING, COMPILING AND DEVELOPING COMPUTER ASSISTED INSTRUCTION K-12 AEROSPACE MATERIALS FOR IMPLEMENTATION IN NASA SPACELINK ELECTRONIC INFORMATION SYSTEM
Jean A. Blake *In* Alabama Univ., Research Reports: 1988 NASA/ASEE Summer Faculty Fellowship Program Dec. 1988 8 p (For primary document see N89-21726 14-99)
Avail: NTIS HC A99/MF E03 CSCL 09B

N89-21742*# Mississippi State Univ., Mississippi State. Dept. of Electrical Engineering.
OPTIMIZATION OF LARGE MATRIX CALCULATIONS FOR EXECUTION ON THE CRAY X-MP VECTOR SUPERCOMPUTER
William A. Hornfeck *In* Alabama Univ., Research Reports: 1988 NASA/ASEE Summer Faculty Fellowship Program Dec. 1988 25 p (For primary document see N89-21726 14-99)
Avail: NTIS HC A99/MF E03 CSCL 09B

N89-21754*# Alabama Univ., Huntsville. Dept. of Mechanical Engineering.
SOFTWARE SYSTEM SAFETY
James G. Uber *In* Alabama Univ., Research Reports: 1988 NASA/ASEE Summer Faculty Fellowship Program Dec. 1988 28 p (For primary document see N89-21726 14-99)
Avail: NTIS HC A99/MF E03 CSCL 09B

N89-21757*# Alaska Univ., Fairbanks. Dept. of Computer Science.
DEVELOPMENT OF A PROTOTYPE COMMONALITY ANALYSIS TOOL FOR USE IN SPACE PROGRAMS
Dorian P. Yeager *In* Alabama Univ., Research Reports: 1988 NASA/ASEE Summer Faculty Fellowship Program Dec. 1988 28 p (For primary document see N89-21726 14-99)
Avail: NTIS HC A99/MF E03 CSCL 09B

62 COMPUTER SYSTEMS

Includes computer networks and special application computer systems.

N89-21582*# Draper (Charles Stark) Lab., Inc., Cambridge, MA.
ADVANCED INFORMATION PROCESSING SYSTEM: LOCAL SYSTEM SERVICES
Laura Burkhardt, Linda Alger, Roy Whittredge, and Peter Stasiowski Apr. 1989 190 p
(Contract NAS1-18061)
(NASA-CR-181767; NAS 1.26:181767) Avail: NTIS HC A09/MF A01 CSCL 09B

The Advanced Information Processing System (AIPS) is a multi-computer architecture composed of hardware and software building blocks that can be configured to meet a broad range of application requirements. The hardware building blocks are fault-tolerant, general-purpose computers, fault- and damage-tolerant networks (both computer and input/output), and interfaces between the networks and the computers. The software building blocks are the major software functions: local system services, input/output, system services, inter-computer system services, and the system manager. The foundation of the local system services is an operating system with the functions required for a traditional real-time multi-tasking computer, such as task scheduling, inter-task communication, memory management, interrupt handling, and time maintenance. Resting on this foundation are the redundancy management functions necessary in a redundant computer and the status reporting functions required for an operator interface. The functional requirements, functional design and detailed specifications for all the local system services are documented. Author

N89-21583# Utah Univ., Salt Lake City. Dept. of Computer Science.
THE DESIGN AND IMPLEMENTATION OF A SPECIAL PURPOSE CACHE FOR THE ROLL BACK CHIP
Narayana S. Mani and Surya Mantha 17 Oct. 1988 12 p
(AD-A203091) Avail: NTIS HC A03/MF A01 CSCL 09A

The roll-back chip (RBC) is an integral part of a special purpose simulation engine based on the Time-Warp mechanism. The RBC is in the critical path of the system and the roll-back processor should not have to access the memory in performing critical operations. We describe the design and implementation (in VLSI) of a special purpose cache that stores the most recently accessed data and performs certain operations on it. The goal of this project was to implement the Cache in VLSI. This is intended to be a prototype chip. The environment in which it will operate was constantly evolving at the time of writing of this report. In fact, the specifications of the Cache itself changed as we were implementing it. A strong case was made in the introduction for the implementation of rollback capabilities in hardware. As of today, no hardware exists to support rollback capabilities in distributed simulation environments. Further research on this topic is underway at the Computer Science department of the University of Utah. GRA

N89-21584# University of Southern California, Los Angeles.
DESIGN SPECIFICATIONS FOR HARDWARE ASSISTED ROLLBACK COMPUTATION
Richard Thomson Jun. 1988 15 p
(AD-A203092; USC-88-014) Avail: NTIS HC A03/MF A01 CSCL 12E

An overview of rollback computation is given, followed by a series of possible design strategies to implement rollback computations in hardware. Design issues and trade-offs are examined for each of the strategies as an iteration to the chosen strategy. The implementation of the chosen strategy is discussed along with an outline of remaining work. GRA

N89-21585# Massachusetts Inst. of Tech., Cambridge. Lab. for Computer Science.
FX-87 PERFORMANCE MEASUREMENTS: DATAFLOW IMPLEMENTATION
R. T. Hammel and David K. Gifford Nov. 1988 54 p
(Contract N00014-83-K-0125)
(AD-A203150; MIT/LCS/TR-421) Avail: NTIS HC A04/MF A01 CSCL 12E

This report documents a series of experiments performed to explore the thesis that the FX-87 effect system permits a compiler to schedule imperative programs (i.e., programs that may contain side-effects) for execution on a parallel computer. We analyze how much the FX-87 static effect system can improve the execution times of five benchmark programs on a parallel graph interpreter. Three of our benchmark programs do not use side-effects (factorial, fibonacci, and polynomial division) and thus did not have any effect induced constraints. Their FX-87 performance was comparable to their performance in a purely functional language. Two of our benchmark programs use side-effects (DNA sequence matching and Scheme interpretation) and our compiler was able to use effect information to reduce their execution times by factors of 1.7 to 5.4 when compared with sequential execution times. These results support our thesis that a static effect system is a powerful tool for compilation to multiprocessor computers. However, the graph interpreter we used was based on unrealistic assumptions, and thus our results may not accurately reflect the performance of a practical FX-87 implementation. The results also suggest that conventional loop analysis would complement the FX-87 effect system. GRA

N89-21586# Massachusetts Inst. of Tech., Cambridge. Microsystems Research Center.
CRITICAL PROBLEMS IN VERY LARGE SCALE COMPUTER SYSTEMS Semiannual Technical Report, 1 Oct. 1987 - 31 Mar. 1988
Paul Penfield, Jr., Anant Agarwal, William J. Dally, Lance A. Glasser, Thomas F. Knight, Jr., F. Thomson Leighton, Charles E. Leiserson, Jacob K. White, and John L. Wyatt, Jr. 31 Mar. 1988 89 p
(Contract N00014-87-K-0825)
(AD-A203299) Avail: NTIS HC A05/MF A01 CSCL 12F

This is the first semiannual report on this contract. The purpose of the present contract is to investigate limiting technologies for a very large computer system, one which, if built during the mid 1990's, would be so large that the nation could only afford one or two of them. The purpose of this contract is to investigate plausibility, which is defined as the step before feasibility. Once plausibility is demonstrated, then separate efforts at demonstrating feasibility and then design and manufacture would be appropriate. It is estimated that the cost of such a building-size computer would be in excess of $1,000,000,000. Six critical areas were identified, and work is in progress in each of these areas. The six areas, and the MIT faculty members who are working in each of the areas, are listed in the chart. The format of this report is based on this table. The work in circuits is a combination of improved techniques in waveform bounding and new ideas in LU factorization and relaxation methods. It has been found that in the context of highly parallel computation, the Gauss-Jacobi technique is never inferior to the Gauss-Seidel technique. Prototype circuits for a proposed processing element have been fabricated, and are under evaluation. GRA

N89-21587# Massachusetts Univ., Amherst.
SpringNet: A NETWORK OF MULTIPROCESSORS FOR HARD REAL-TIME Final Report
John A. Stankovic and Krithi Ramamritham Oct. 1988 9 p
(Contract N00014-87-G-0260)
(AD-A203348) Avail: NTIS HC A02/MF A01 CSCL 12G

The Spring project has been very active in multiple areas of real-time computing. We have developed significant results in many aspects of real-time scheduling, in real-time operating system design, in real-time transactions, and in time constrained communication protocols. We have also made progress in implementing a software (simulation) testbed, in developing a hardware operating system kernel testbed called SpringNet, and in implementing real-time transactions on a hardware testbed called CARAT. We have also begun a substantial research effort concerning dependable real-time systems. In the following sections we provide a brief overview of the status and plans for the Spring project as a whole. GRA

N89-21588# Utah Univ., Salt Lake City. Dept. of Computer Science.
LOOKAHEAD IN PARALLEL DISCRETE EVENT SIMULATION
Richard M. Fujimoto Aug. 1988 8 p Presented at the International Conference on Parallel Processing, Aug. 1988
(Contract N00014-87-K-0184; NSF DCR-85-04826)
(AD-A203902) Avail: NTIS HC A02/MF A01 CSCL 12G

Empirical performance evaluations of parallel, discrete event simulation algorithms using deadlock avoidance and deadlock detection and recovery techniques developed by Chandy and Misra have been performed using the BBN Butterfly multiprocessor. Experiments using synthetic workloads reveal that the degree to which processes can look ahead in simulated time plays a critical role in the performance of distributed simulators using these algorithms. These results are applied to a queueing network simulation where as much as an order of magnitude improvement in performance is observed if the distributed simulator is programmed to fully exploit the lookahead available in the application. Performance measurements of several hypercube-based communication network simulators provide additional empirical data to support these claims. These results demonstrate that substantial improvements in performance are obtainable if the application can be programmed to have good lookahead characteristics. On the other hand, other applications inherently contain poor lookahead properties, and appear to be ill suited for these simulation algorithms. GRA

N89-21589# Clarkson Univ., Potsdam, NY. Dept. of Electrical and Computer Engineering.
PERFORMANCE EVALUATION OF PARALLEL ALGORITHMS AND ARCHITECTURES IN CONCURRENT MULTIPROCESSOR SYSTEMS Final Report, Jan. - Sep. 1987
H. H. Ammar, Y. S. Fong, R. Mukundan, and C. A. Pomalaza-Raez Sep. 1988 22 p
(Contract F30602-81-C-0169)
(AD-A203982; RADC-TR-88-190) Avail: NTIS HC A03/MF A01 CSCL 12E

This report describes the research effort directed towards the study of issues concerning concurrent systems. Specifically the report concentrates on the design, evaluation, and tuning of application programs on parallel architectures. Issues including mapping algorithms to architectures, and parallel programming support tools are discussed. It is recognized that the currently available concurrent system analysis tools are not adequate for determining the detail performance of the application programs on specific architectures. To remedy this shortcomming, we recommend the development of a multiprocessor trace-driven simulator. This simulator will be beneficial to the evaluation on the performance of the SDI battle management algorithms on specific concurrent systems. GRA

N89-21590# Oak Ridge Gaseous Diffusion Plant, TN.
THE CAUSALITY HORIZON AND PARALLEL PROCESSING FOR SIMULATIONS WITH WIDE GEOGRAPHICAL DISPERSIONS
D. S. Hartley, III Feb. 1989 17 p
(Contract DE-AC05-84OT-21400)
(DE89-008484; K/DSRD-59) Avail: NTIS HC A03/MF A01

In some simulations, events that are not strictly simultaneous can be treated as if they were. Because simultaneity of events allows parallel processing with no problems of interaction or causality, enlarging the subset of the event list that can be freely processed in parallel increases the utility of a parallel architecture. It also eliminates the overhead of the rollback mechanisms of Time Warp or the waiting period required of more conservative time-synchronization methods. Even though the potential processing improvement of the causality horizon technique is less than that of completely parallel techniques, it is complementary to and can be used in conjunction with other techniques. DOE

N89-21519# Cornell Univ., Ithaca, NY. Dept. of Computer Science.
A BLOCK QR FACTORIZATION SCHEME FOR LOOSELY COUPLED SYSTEMS OF ARRAY PROCESSORS
Charles VanLoan *In* Army Research Office, Transactions of the Fifth Army Conference on Applied Mathematics and Computing Mar. 1988 p 567-588 Sponsored in part by IBM Corp. (For primary document see N89-21490 14-59)
(Contract N00014-83-K-0640; NSF CCR-86-02310)
Avail: NTIS HC A99/MF E03 CSCL 09B

N89-21529# Army Missile Command, Redstone Arsenal, AL. Research Directorate.
NEURAL NETWORKS AND THE SYMMETRIC GROUP S(SUB N)
John L. Johnson *In* Army Research Office, Transactions of the Fifth Army Conference on Applied Mathematics and Computing Mar. 1988 p 751-761 (For primary document see N89-21490 14-59)
Avail: NTIS HC A99/MF E03 CSCL 09B

63 CYBERNETICS

Includes feedback and control theory, artificial intelligence, robotics and expert systems.

For related information see also *54 Man/System Technology and Life Support.*

N89-21591# Air Force Inst. of Tech., Wright-Patterson AFB, OH. School of Engineering.
DYNAMIC ANALYSIS OF FEEDFORWARD NEURAL NETWORKS USING SIMULATED AND MEASURED DATA M.S. Thesis
Gregory L. Tarr Dec. 1988 105 p
(AD-A202573; AFIT/GE/ENG/88D-54) Avail: NTIS HC A06/MF A01 CSCL 12I

An environment is developed for the study of dynamic changes in patterns of weight and node values for artificial neural networks. Graphic representations of neural network internal states are displayed using a high resolution video terminal. Patterns of node firings and changes in weight vectors are displayed to provide insight during training. Four pattern recognition problems are applied to four types of artificial neural networks. Using simulated data, a simple disjoint region classification problem is developed and examined using a Kohonen net and a multilayer feedforward back propagation (MFB) network. A MFB neural network is also used to simulate a Fourier filter. Using a Kohonen net, a MFB, a counterpropagation and a hybrid network, data measured from infrared and laser radar imagery of military vehicles is analyzed. The accuracy and training times for a MFB net and a Hybrid net are compared using an ambiguous decision region problem. Each classification problem is examined and compared to classical, nearest neighbor pattern recognition techniques. Using dynamic analysis, neural network is developed using Kohonen training rules for the first hidden layer followed by one or two hidden layers using standard back propagation rules for training. Advantage of the hybrid network is shown for classification problems involving anomalies characteristic of measured data. GRA

N89-21592# Air Force Inst. of Tech., Wright-Patterson AFB, OH. School of Engineering.
SELECTION OF A FREQUENCY SENSITIVE QFT (QUANTITATIVE FEEDBACK THEORY) WEIGHTING MATRIX USING THE METHOD OF SPECIFIED OUTPUTS M.S. Thesis
William D. Phillips Dec. 1988 112 p
(AD-A202692; AFIT/GAE/ENG/88D-01) Avail: NTIS HC A06/MF A01 CSCL 01D

Use of Quantitative Feedback Theory (QFT) on a multiple input multiple output control system requires certain mathematical properties of the plant matrix of transfer functions. In general, the plant matrix P(s) does not possess the necessary or desired mathematical properties for the QFT design to proceed. A frequency sensitive weighting matrix Delta(s) is used to transform the plant matrix P(s) into the equivalent plant matrix Pe(s) that does satisfy QFT requirements. In matrix notation, the relationship between the equivalent plant, plant, and weighting matrix is Pe(s)=P(s) Delta(s). This thesis identifies the necessary and desired characteristics of the equivalent plant Pe(s) for the QFT process, explains the use of the Method of Specified Outputs which generates the frequency sensitive weighting matrix Delta(s), and calculates several weighting matrices for a 3-input 2-output lateral-directional model of the F-16 aircraft. For several control system failures, the mathematical structure of the failed equivalent plant matrices Pef(s) is examined for compliance with QFT requirements. A weighting matrix Delta(s) is found that produces acceptable equivalent plant matrices for failures of down to 0.01 percent of available control surface deflections. GRA

N89-21593# California Univ., San Diego, La Jolla.
ARCHITECTURE STUDIES AND SYSTEM DEMONSTRATIONS OF OPTICAL PARALLEL PROCESSOR FOR AI (ARTIFICIAL INTELLIGENCE) AND NI (NEURAL INTELLIGENCE) Semiannual Report
Sing H. Lee and Sadik C. Essner 1 Oct. 1988 34 p

(Grant AF-AFOSR-0022-88; DARPA Order 6150)
(AD-A203241; AFOSR-88-1288TR) Avail: NTIS HC A03/MF A01 CSCL 12F

During the last six months we have applied the results of our studies on existing parallel computing architectures for AI and NI to develop the Programmable OptoElectronic Multiprocessor (POEM) architecture. Our goal was to design a scalable architecture suitable for AI and ultimately for NI that will take full advantage of the hybrid nature of opto-electronic technologies. In the POEM system this is achieved by implementing all communication using phontonics and all logic their local interconnections using electronics. GRA

N89-21594# Air Force Avionics Lab., Wright-Patterson AFB, OH. Artificial Intelligence Applications Office.
A METHODOLOGY FOR SCREENING POTENTIAL ARTIFICIAL INTELLIGENCE APPLICATIONS
Eric N. Hanson, Stephen E. Cross, and Allen Smith (Teknowledge Federal Systems, Inc., Thousand Oaks, CA.) Jul. 1988 20 p
(AD-A203966; AFWAL-TR-88-1083) Avail: NTIS HC A03/MF A01 CSCL 12I

This paper presents a method to rapidly evaluate a large number of possible opportunities to apply artificial intelligence technology. The domain expert for a potential application is interviewed briefly (for 1 to 3 hours) by a knowledge-engineering team. During this interview, the expert is questioned on a carefully chosen set of topics to help quickly assess the level of AI risk, systems engineering risk, and potential payoff of building the application(s) identified during the session. After conducting a series of these interviews for an organization, a report is written summarizing the results, and prioritizing the potential applications for future assessment and prototyping. GRA

N89-21492# Columbia Univ., New York, NY. Lab. for Intelligent Design.
KNOWLEDGE REPRESENTATION AND PLANNING CONTROL IN AN EXPERT SYSTEM FOR THE CREATIVE DESIGN OF MECHANISMS
David A. Hoeltzel, Wei-Hua Chieng, and John Zissimides *In* Army Research Office, Transactions of the Fifth Army Conference on Applied Mathematics and Computing Mar. 1988 p 29-63 (For primary document see N89-21490 14-59)
Avail: NTIS HC A99/MF E03 CSCL 12E

N89-21510# Army Armament Research, Development and Engineering Center, Watervliet, NY.
DESIGN OF A FEELING-THINKING MACHINE
Ray Scanlon and Mark Johnson *In* Army Research Office, Transactions of the Fifth Army Conference on Applied Mathematics and Computing Mar. 1988 p 383-394 (For primary document see N89-21490 14-59)
Avail: NTIS HC A99/MF E03 CSCL 09B

N89-21737*# Alabama Univ., Huntsville. Dept. of MIS/MSC.
INTELLIGENT DATA REDUCTION FOR AUTONOMOUS POWER SYSTEMS
Stephen A. Floyd *In* Alabama Univ., Research Reports: 1988 NASA/ASEE Summer Faculty Fellowship Program Dec. 1988 24 p (For primary document see N89-21726 14-99)
Avail: NTIS HC A99/MF E03 CSCL 09B

64 NUMERICAL ANALYSIS

Includes iteration, difference equations, and numerical approximation.

N89-21595*# National Aeronautics and Space Administration. Lewis Research Center, Cleveland, OH.
INSTITUTE FOR COMPUTATIONAL MECHANICS IN PROPULSION (ICOMP) Annual Report No. 3, 1988
Mar. 1989 62 p
(NASA Order C-99066-G)
(NASA-TM-101961; E-4656; NAS 1.15:101961; ICOMP-89-1)
Avail: NTIS HC A04/MF A01 CSCL 12A

The Institute for Computational Mechanics in Propulsion (ICOMP) is operated jointly by Case Western Reserve University and the NASA Lewis Research Center in Cleveland, Ohio. The purpose of ICOMP is to develop techniques to improve problem-solving capabilities in all aspects of computational mechanics related to propulsion. This report describes the activities at ICOMP during 1988. Author

N89-21596# International Centre for Theoretical Physics, Trieste (Italy).
CONTRACTION OF Z(SUB 2) GRADED LIE ALGEBRAS
K. C. Tripathy and M. K. Patra (Delhi Univ., India) Aug. 1988 5 p Presented at the 17th International Colloquium on Group Theoretical Methods in Physics, Ste. Adele, Canada, 27 Jun. 1988 Submitted for publication
(DE88-705356; IC-88/234; CONF-8806105) Avail: NTIS (US Sales Only) HC A02/MF A01

The Inoenu-Wigner contraction scheme is extended to Z(sub 2) graded Lie algebras. As an illustration, the contraction of Osp(1,2) Lie algebra is presented. The contraction yields the structure and representations of full BRS algebra. Some observations on the link between contraction (deformation) and cohomology theory are also furnished. DOE

N89-21597# George Mason Univ., Fairfax, VA. Dept. of Operations Research and Applied Statisti cs.
ROOTFINDING FOR MARKOV CHAINS WITH QUASI-TRIANGULAR TRANSITION MATRICES
Carl M. Harris 31 Oct. 1988 14 p
(Contract N00014-86-K-0029)
(AD-A202468; GMU/22472/105) Avail: NTIS HC A03/MF A01 CSCL 12C

Numerical rootfinding problems are quite common in stochastic modeling. However, many solutions stop at the presentation of a probability generating function for the state probabilities. But with increasing easy access to computing power, many problems whose answers were typically left in incomplete form or for which there has been a search for alternative solution methods are currently being reexamined. The class of Markov chains with quasi-triangular layouts (i.e., those having sub- or super-triangular sets of zeros) are good case in point. They have an especially nice structure which leads to a rather concise representation for the generating functions. But the complete solution then requires the finding of roots. Fortunately, these problems can be shown to have special properties that make accurate rootfinding quite feasible. In this paper, we show that the roots of the critical equations for these models are indeed unique and located in known regions in the complex plane. GRA

N89-21598# Texas Univ., Austin. Applied Research Lab.
BISPECTRAL INVERSION: THE CONSTRUCTION OF A TIME SERIES FROM ITS BISPECTRUM M.S. Thesis
Peter S. Allison 13 Apr. 1988 102 p
(AD-A202508; ARL-TR-88-19) Avail: NTIS HC A06/MF A01 CSCL 12C

This report presents a method of producing a stochastic time series that has any desired bispectral characteristic. This was done using a quadratically nonlinear, infinite order, moving average model whose bicovariance was obtainable in terms of a finite linear function of the kernels. This expression was inverted to produce an equation for the kernels in terms of the bicovariance. Knowing the kernels, the time series can easily be computed. Alternately the DFT of the time series can also be computed directly. This is actually easier than the time domain computation, as it only involves one summation as opposed to two. GRA

N89-21599# Air Force Inst. of Tech., Wright-Patterson AFB, OH. School of Engineering.
A COMPARISON OF CONTROL VARIATES FOR QUEUEING NETWORK SIMULATION M.S. Thesis

John J. Tomick Dec. 1988 157 p
(AD-A202576; AFIT/GOR/ENS/88D-22) Avail: NTIS HC A08/MF A01 CSCL 12D

The purpose of this thesis was to compare several control variates for queueing network simulation. The author's goal was to provide the simulation community with some guidance for selecting control variates that will lead to significant reductions in the variance of the estimated responses that do not introduce significant bias. Both internal and external control variates were examined. The measures for comparing them were the variance ratios obtained for each control variate against each of the two response variables and the coverage of their respective 95 percent confidence intervals. The two response variables selected for this research were the average sojourn time in the network and the probability that the number in the fourth queue exceeds twice the mean number in queue at steady-state. The internal controls included standardized routing controls and standardized work variables. The external controls included the average sojourn time in the network and the average number in queue at the fourth node. The external controls were further classified into two groups: analytic Jackson controls and analytic approximations. GRA

N89-21600# Air Force Inst. of Tech., Wright-Patterson AFB, OH. School of Engineering.
HYBRID CALCULATION OF INVARIANT MOMENTS M.S. Thesis
Vicky Lynn Robinson Dec. 1988 77 p
(AD-A202594; AD-E900870; AFIT/GEO/ENG/88D-3) Avail: NTIS HC A05/MF A01 CSCL 12I

This thesis investigated a hybrid system for computing a position, scale, rotation invariant (PSRI) feature set. Specifically, the low order ordinary moments of a set of objects were optically calculated. This process required the production of computer generated holograms with amplitude transmittance. The detour phase hologram, a binary method, was used to produce the appropriate wavefronts of the a certain form. Each wavefront was imaged onto the object plane. The Fourier transform of the product of these two transmittances was taken and the resultant intensity pattern recorded. The center intensity value was found by using a frame grabber and the Image-Pro software. The result was the ordinary moment of the object. The moment values were digitally processed to form a PSRI feature set. The moments, both ordinary and PSRI, were tested for pattern recognition possibilities. The Euclidean distances between the objects were calculated, revealing the separation necessary for pattern recognition. GRA

N89-21601# Air Force Inst. of Tech., Wright-Patterson AFB, OH. School of Engineering.
A COMPARISON OF VARIABLE SELECTION CRITERIA FOR MULTIPLE LINEAR REGRESSION: A SIMULATION STUDY M.S. Thesis
Ross J. Hansen Dec. 1988 136 p
(AD-A202708; AFIT/GOR/MA/88D-3) Avail: NTIS HC A07/MF A01 CSCL 12C

The purpose of this thesis was to identify three promising least squares selection procedures discussed in the literature during the previous decade and then test these using simulation. The three criteria chosen for this study were minimum mean square error (Min MSE), minimum Sp, and minimum Cp. Most of the previous simulations in this area are limited to investigating the usefulness of variable selection criteria when all relevant regressors and some noise variables are available. It is questionable whether all relevant variables will be included. This research has examined the effects of not including a significant variable in the variable pool. In examining each criterion, emphasis was placed on the technique's performance under varying amounts of multicollinearity, variable variation, number of variables, and sample size. Response Surface Methodology was used to determine the effects of varying these factors. A comparison was then made using the results from the Response Surface. To supplement the simulation research, a comprehensive literature review of the most current journal articles dealing with several least squares criteria has been provided. This review includes a discussion of each technique's strengths and weaknesses. GRA

N89-21602# Air Force Inst. of Tech., Wright-Patterson AFB, OH. School of Engineering.
A DIAGNOSTIC SYSTEM USING BOOLEAN REASONING M.S. Thesis
James J. Kainec Dec. 1988 371 p
(AD-A202764; AFIT/GE/ENG/88D-16) Avail: NTIS HC A16/MF A01 CSCL 09A

The goal of this thesis is to design and implement a computer aided diagnostic system for combinational circuits, a type of circuit used in the design of all computers. The diagnostic system is to accept a description of the circuit, supervise an adaptive input-output experiment on a potentially faulty implementation of the circuit, and return the locations of all faults in the circuit. The description of the circuit which will be input to this system can be in one of two forms: Boolean equations, or statements in the VHSIC Hardware Description Language (VHDL). Based on the circuit structure, a fault model is developed which can be used to mathematically model the state of faults in the circuit. The circuit description is processed to derive a single Boolean characteristic equation; information gained from testing is used to update this equation. The characteristic equation is manipulated to generate test vectors which are used as inputs to the actual circuit being diagnosed. After a given test vector has been input to the circuit, the output is observed. The state of the circuit output is then input to the diagnostic system which uses it to derive new knowledge about the actual circuit. GRA

N89-21603# Massachusetts Inst. of Tech., Cambridge. Lincoln Lab.
ON RANDOM CORRELATION MATRICES
Robert B. Holmes 28 Oct. 1988 51 p
(Contract F19628-85-C-0002)
(AD-A202786; TR-803; ESD-TR-88-158) Avail: NTIS HC A04/MF A01 CSCL 12B

This report contains a detailed study of random correlation matrices, including algebraic, statistical, and historical background. Such matrices are of particular interest because they serve to model average signals for simulation testing of signal processing algorithms. The latter half of this report extensively discusses the statistical behavior of spectral functions of the two major types of random correlation matrices from both theoretical and empirical aspects. Our emphasis then, is on eigenvalue distribution and condition number behavior. Actual application to algorithm testing will be described in a subsequent report. GRA

N89-21604# Maryland Univ., College Park. Advanced Techniques Branch.
OPTIMAL AND ROBUST MEMORYLESS DISCRIMINATION FROM DEPENDENT OBSERVATIONS Interim Memo. Report, May 1987 - May 1988
Douglas W. Sauder 9 Nov. 1988 94 p
(Contract N00014-85-G-0213)
(AD-A202806; NRL-MR-6340) Avail: NTIS HC A05/MF A01 CSCL 12C

Memoryless discrimination is a method for binary hypothesis testing in which a test statistic is computed by passing each observation through a memoryless nonlinearity and summing the outputs. Under certain conditions, including a mixing condition on the observed process, such a test statistic becomes asymptotically Gaussian, thus permitting the error probabilities to be approximated. In this thesis, asymptotic performance measures are derived as functionals of the nonlinearities, and in this way memoryless discrimination is well formulated as an optimization problem. Both Neyman-Pearson and minimax problems are considered. In all, four different performance measures are derived under different problem formulations, and in each case, the optimal nonlinearity is shown to be the solution of an integral equation. Results for minimax robustness are presented for three of the performance measures. Performance results from numerical simulations for each

of the nonlinearities derived here as well as the optimal iid nonlinearity are presented and discussed. GRA

N89-21605# Carnegie-Mellon Univ., Pittsburgh, PA.
ADAPTIVE OPTICAL LINEAR ALGEBRA PROCESSORS Final Report, 1 Sep. 1984 - 31 Oct. 1988
David Casasent and B. V. Kumar 15 Nov. 1988 142 p
(Grant AF-AFOSR-0239-84; AF Proj. 2305)
(AD-A202996; AFOSR-88-1248TR) Avail: NTIS HC A07/MF A01 CSCL 20F

The final report on research into adaptive optical linear algebra processors includes 3 processors. These include: a space integrating frequency-multiplexed processor, a hybrid space and time integrating processor, and a heterodyned linear analog processor. We also address number representation work using twos complement and negative base representation, plus fundamental new concepts such as matrix and bit partitioning. The applications addressed for these various systems include: the solution of linear and nonlinear algebraic equations, partial differential equations, computational fluid dynamics, finite element problems, adaptive signal processing (including adaptive phased array radar processing), and the potential for use in various adaptive neural etc. processing. We also include data to demonstrate and quantify that a high-accuracy digital multiplication by analog convolution optical architecture is superior to a digital processor. GRA

N89-21606# Tennessee Univ., Knoxville. Management Science Program.
TRIANGULARITY OF THE BASIS IN LINEAR PROGRAMS FOR MATERIAL REQUIREMENTS PLANNING, REVISION
James K. Ho and William A. McKenny Dec. 1988 16 p
(Contract N00014-87-K-0163)
(AD-A203039; MSP-87-3-Rev) Avail: NTIS HC A03/MF A01 CSCL 12D

It is shown that the basis in a class of linear programs arising from material requirements planning can be triangularized. This allows for efficient adaptation of the Simplex Method similar to those for network problems. It also suggests that for finite-loading (i.e., capacitated) MRP, a decomposition approach exploiting both subproblem structure and parallel processing can be effective for handling complex problems in multiproduct, multistage, multiperiod production systems. GRA

N89-21607# Brunel Univ., Uxbridge (England).
COMPUTER ASSISTED ANALYSIS AND MODELLING OF STRUCTURED PROBLEMS Interim Report No. 5, Sep. - Nov. 1988
Cormac Lucas and Gautam Mitra 22 Nov. 1988 24 p
(Contract DAJA45-87-C-0003; DA Proj. 1L1-61102-BH-57)
(AD-A203040; TR/11/88; R/D-5338-CC-03) Avail: NTIS HC A03/MF A01 CSCL 12D

This document argues the case for open system approach towards modelling and application support. The author discuss how the usability and skill analysis naturally leads to a viable strategy for integrating application construction with modelling tools and optimizers. The role of the implementation environment is also seen to be critical in that it is retained as a building block within the resulting system. Computer based methods for supporting optimization applications are of great interest to operational research workers and management scientists. This paper puts forward an analysis of the scope as well as the goal of such systems set against our understanding of the methodological, technological and organizational issues. A number of workers have indicated the importance of the recent developments which take us beyond the considerations of robust optimization routines, and languages and systems for constructing mathematical programming models. The real life use of mathematical programming optimization models is one of many important examples of applying mathematical modeling. GRA

N89-21608# Illinois Univ., Urbana. Dept. of Psychology.
DIMENSIONALITY OF BINARY ITEMS Final Report, Feb. 1984 - Dec. 1988
Lloyd G. Humphreys, Ledyard R. Tucker, and Mary A. Roznowski 15 Dec. 1988 45 p
(Contract N00014-84-K-0186; RR04204)
(AD-A203238) Avail: NTIS HC A03/MF A01 CSCL 12C

Four different approaches are used to assess the dimensionality of binary items. This is done using a population model to allow sampling of both items and people and provides for variation and control of important parameters. Consider indices of dimensionality based on the pattern of second factor loadings derived from simplex theory are also accurate under many combinations of parameters and are second in accuracy to Local Independence. These indices decrease in accuracy substantially at the highest level of factor correlations and the widest dispersion of item difficulties that we used. The fitting of a simplex R-matrix to observed intercorrelations of binary items provides high accuracy under a wide range of parameters, but becomes highly sensitive to the combination of a high level of factor correlations and a wide distribution of item difficulties. An increase in sample size produces no increase in accuracy in the most unfavorable combination of parameters. A quantitative index of the shape of the curve of successive Eigenvalues was used for matrices of phi coefficients, tetrachoric correlations, and variance-covariance matrices. None of these indices produced satisfactory accuracy except under most favorable combinations of parameters. The Eigenvalues of variance-covariance matrices provide a more accurate basis for a decision concerning dimensionality than tetrachoric correlations, which have been the statistics of choice. GRA

N89-21609# Clarkson Univ., Potsdam, NY.
EIGENVECTORS OF GRAPHS Final Report
David Powers 1988 11 p
(Contract N00014-85-K-0497)
(AD-A203317) Avail: NTIS HC A03/MF A01 CSCL 12B

This grant has supported work in several areas: (1) A study of graph eigenvectors shows connections to graph structure in ways that are reminiscent of eigenfunctions of the Laplacian operator in two or three dimensions. Methods developed in this study have also led to estimates of the maximum possible value for the kth eigenvalue of a graph as function of the number of edges or vertices. (2) The convex hull of the rows of an eigenmatrix of a graph is the polytope of an eigenvalue. We investigated relations between such polytopes and the graph. The graph of such a polytope may be isomorphic to the original graph; this is the case for most regular polytopes. For distance-regular graphs and several kinds of less symmetric graphs, we can show that the polytope of some eigenvalue has the same group of automorphisms as the graph, that proximity of points is equivalent to adjacency of vertices, and that other properties of the polytope carry over the graph. Possible directions for future work include the following. Determine the reducibility of the group of automorphisms of a polytope and the significance in the graph of faces and facets of the polytopes. Investigate the intrinsic eigenvectors of a graph (the list of inner products of vertices of a polytope with the normal to a supporting hyperplane is an intrinsic eigenvector). Seek physical models for the interpretation of graph eigenvalues and eigenvectors. GRA

N89-21610# Naval Postgraduate School, Monterey, CA.
ROOT PLACEMENT WITH TRANSFER FUNCTION METHODS (FULL STATE FEEDBACK) M.S. Thesis
Mehmet Ates Dec. 1988 109 p
(AD-A203877) Avail: NTIS HC A06/MF A01 CSCL 12C

A design technique for root placement with full state feedback using transfer functions for all-pole plant is presented in this thesis. A number of examples are presented to demonstrate the procedure with this design technique when all the system states are available to be measured and fedback. The design procedure presented is applicable for linear, time invariant (LTI) systems in the s-domain for continuous time. In order to get the roots at desired locations by transfer function methods very high gains are required.

Therefore, the design procedure should place the zeros in offset locations. To obtain some guidelines for offsetting the zeros, the root movement as a function of gain, offset zero locations chosen by matrix methods to put the roots at the desired locations, and arbitrerily chosen offset zero locations are observed on numerous system examples. The obtained guidelines are applied to the all-pole plants. GRA

N89-21611# California Univ., Davis.
THE APPLICATION OF MODAL COORDINATE METHODS TO LARGE NONLINEAR TIME-DEPENDENT PROBLEMS Final Report, Jan. - Sep. 1988
Kyran D. Mish and Leonard R. Herrmann Nov. 1988 39 p
(Contract N62583-87-M-T227)
(AD-A203913; NCEL-CR-89.002) Avail: NTIS HC A03/MF A01 CSCL 12D

The research presented in this document demonstrates the application of a modal projection scheme based on inverse Lanczos iteration to a variety of problems in computational mechanics. All the cases considered are nonlinear and time-dependent, and Lanczos vectors are used to achieve coordinate reductions that substantially reduce the sizes of the underlying problems. Varying degrees of success are encountered in these reductions, depending upon numerical characteristics of the original Finite-Element models. A review of the theory of modal projection methods is presented in order to explain the results of the reduced coordinate approximations. GRA

N89-21612# State Univ. of New York, Stony Brook. Dept. of Electrical Engineering.
BEST ORDERING FOR FLOATING-POINT ADDITION
T. G. Robertazzi and Stuart C. Schwartz (Princeton Univ., NJ.) Mar. 1988 10 p
(Contract N00014-81-K-0146)
(AD-A203990) Avail: NTIS HC A02/MF A01 CSCL 12C

This correspondence examines the influence of the summation order on the numerical accuracy of the resulting sum when the addition is performed using floating-point, finite-precision arithmetic. A simple statistical model is used to find the relative performance of various addition procedures. It is shown that phrasing the question in terms of finding a best ordering is overly restrictive since the most natural and accurate procedures for performing the addition utilize the storage of intermediate sums as well as performing orderings. GRA

N89-21613# Utah State Univ., Logan. Dept. of Mathematics and Statistics.
NUMERICAL SOLUTION OF NONLINEAR ALGEBRAIC EQUATIONS IN STIFF ODE SOLVING Technical Progress Report, 1986 - 1989
Homer F. Walker 1989 6 p
(Contract DE-FG02-86ER-25018)
(DE89-008284; DOE/ER-25018/T1) Avail: NTIS HC A02

The original objective of this project was to investigate certain numerical methods for solving systems of nonlinear equations which arise in the implementation of implicit methods for solving stiff ODE initial-value problems. Over the course of the project, two major areas of research have developed in which most of the work has been done, viz., matrix-free methods for solving linear systems and Newton-like methods for underdetermined nonlinear systems. We describe the work in these two areas and in other areas below. DOE

N89-21614# Sandia National Labs., Albuquerque, NM.
TIME-DISCRETIZED MOMENTS OF A RANDOMLY EXCITED UNCERTAIN LINEAR OSCILLATOR Ph.D. Thesis
Linda Jean Branstetter Aug. 1988 416 p
(Contract DE-AC04-76DP-00789)
(DE89-008318; SAND-88-1884) Avail: NTIS HC A18/MF A01

Uncertainty is present in all physical systems to some degree. The effect of uncertainty is to make the analysis of a linear structure nonlinear in nature. In conjunction with this effect, the response of a linear oscillator to Gaussian excitation becomes non-Gaussian when its stiffness is uncertain. For large uncertainties, the response and statistical moments are affected significantly. The objective of this thesis is to investigate the actual (not the approximate) behavior of a simple uncertain system. A single-degree-of-freedom damped linear oscillator having uncertain stiffness, and subjected to stationary mean-zero Gaussian white-noise excitation, is considered. General mathematical relations for a total of twenty-nine different statistical moments involving its response, stiffness, and load are derived, numerically integrated, and verified with simulation. The mathematical relations are based on the law of total probability. The moment equations are derived in both continuous and time-discretized form. The time-discretized versions allow the study of various aspects of step-by-step solution procedures employed by several existing stochastic finite element methods which have been proposed by the author and others. The effect of periodic enforcement of a Gaussian response approximation is isolated. It is shown mathematically that as the integration step size becomes small, the moments computed using such an approximation approach those of a deterministic oscillator having a stiffness equal to the mean of its distribution. DOE

N89-21491# Cornell Univ., Ithaca, NY. Center for Applied Mathematics.
LIE TRANSFORMS APPLIED TO A NONLINEAR PARAMETRIC EXCITATION PROBLEM
Jonathan L. Len and Richard H. Rand *In* Army Research Office, Transactions of the Fifth Army Conference on Applied Mathematics and Computing Mar. 1988 p 1-27 Sponsored in part by NSF, Washington, D.C. (For primary document see N89-21490 14-59)
Avail: NTIS HC A99/MF E03 CSCL 12E

N89-21497# Boston Univ., MA. Dept. of Mathematics.
CONDITION OF THE FINITE ELEMENT STIFFNESS MATRIX OF HIGHLY IRREGULAR TRIANGULAR GRIDS
I. Fried and A. R. Johnson (Army Materials Technology Lab., Watertown, MA.) *In* Army Research Office, Transactions of the Fifth Army Conference on Applied Mathematics and Computing Mar. 1988 p 139-148 (For primary document see N89-21490 14-59)
Avail: NTIS HC A99/MF E03 CSCL 12E

N89-21501# Houston Univ., TX. Dept. of Mathematics.
NUMERICAL SOLUTION OF PARABOLIC PROBLEMS IN HIGH DIMENSIONS
Edward Dean, Roland Glowinski, and Chin-Hsien Li *In* Army Research Office, Transactions of the Fifth Army Conference on Applied Mathematics and Computing Mar. 1988 p 207-286 (For primary document see N89-21490 14-59)
(Contract DAAL03-86-K-0138)
Avail: NTIS HC A99/MF E03 CSCL 12E

N89-21503# Texas A&M Univ., College Station. Dept. of Mathematics.
CONVEXITY-PRESERVING QUASI-INTERPOLATION AND INTERPOLATION BY BOX SPLINE SURFACES
Charles K. Chui, Harvey Diamond, and Louise A. Raphael (Howard Univ., Washington, DC.) *In* Army Research Office, Transactions of the Fifth Army Conference on Applied Mathematics and Computing Mar. 1988 p 301-310 (For primary document see N89-21490 14-59)
Avail: NTIS HC A99/MF E03 CSCL 12E

N89-21508# Titan Systems, Inc., Princeton, NJ.
ASYMPTOTICS BEYOND ALL ORDERS
Harvey Segur *In* Army Research Office, Transactions of the Fifth Army Conference on Applied Mathematics and Computing Mar. 1988 p 369-376 Sponsored in part by DOE, Washington Prepared in cooperation with State Univ. of New York, Buffalo (For primary document see N89-21490 14-59)
Avail: NTIS HC A99/MF E03 CSCL 12E

N89-21511# Ballistic Research Labs., Aberdeen Proving Ground, MD. Mechanics and Structures Branch.
POLYNOMINAL DEFINITION OF DISCRETE FIELD POINT OF MAP OF DIFFUSION EQUATION
William F. Donovan *In* Army Research Office, Transactions of the Fifth Army Conference on Applied Mathematics and Computing Mar. 1988 p 395-422 (For primary document see N89-21490 14-59)
Avail: NTIS HC A99/MF E03 CSCL 12E

N89-21513# Military Academy, West Point, NY. Dept. of Mathematics.
A POSTERIORI ERROR ESTIMATION OF ADAPTIVE FINITE DIFFERENCE SCHEMES FOR HYPERBOLIC SYSTEMS
David C. Arney, Rupak Biswas, and Joseph E. Flaherty (Rensselaer Polytechnic Inst., Troy, NY.) *In* Army Research Office, Transactions of the Fifth Army Conference on Applied Mathematics and Computing Mar. 1988 p 437-457 Prepared in cooperation with Army Armament Munitions and Chemical Command, Watervliet, N.Y. (For primary document see N89-21490 14-59)
Avail: NTIS HC A99/MF E03 CSCL 12E

N89-21514# Rensselaer Polytechnic Inst., Troy, NY. Dept. of Computer Science.
AN ADAPTIVE OVERLAPPING LOCAL GRID REFINEMENT METHOD FOR TWO-DIMENSIONAL PARABOLIC SYSTEMS
Peter K. Moore and Joseph E. Flaherty *In* Army Research Office, Transactions of the Fifth Army Conference on Applied Mathematics and Computing Mar. 1988 p 459-474 Prepared in cooperation with Army Armament Munitions and Chemical Command, Watervliet, N.Y. (For primary document see N89-21490 14-59)
(Contract DAAL03-86-K-0112)
Avail: NTIS HC A99/MF E03 CSCL 12E

N89-21516# Army Cold Regions Research and Engineering Lab., Hanover, NH.
SPLINE-BASED FINITE-ELEMENT METHOD FOR SOLVING A STEFAN'S PROBLEM IN A FINITE DOMAIN: FORMULATION
Shunsuka Takagi *In* Army Research Office, Transactions of the Fifth Army Conference on Applied Mathematics and Computing Mar. 1988 p 515-534 (For primary document see N89-21490 14-59)
Avail: NTIS HC A99/MF E03 CSCL 12A

N89-21520# Cornell Univ., Ithaca, NY. Mathematical Sciences Inst.
NONPARAMTERIC ESTIMATION FROM QUEUES ARISING IN STAGGERED ENTRY CLINICAL TRIALS
Michael J. Phelan and N. U. Prabhu *In* Army Research Office, Transactions of the Fifth Army Conference on Applied Mathematics and Computing Mar. 1988 p 589-596 (For primary document see N89-21490 14-59)
Avail: NTIS HC A99/MF E03 CSCL 12E

N89-21524# Naval Postgraduate School, Monterey, CA. Dept. of Mathematics.
A RANDOMNESS PROPERTY OF m-SEQUENCES
Harold Fredricksen and Gary Krahn (Military Academy, West Point, NY.) *In* Army Research Office, Transactions of the Fifth Army Conference on Applied Mathematics and Computing Mar. 1988 p 643-648 (For primary document see N89-21490 14-59)
Avail: NTIS HC A99/MF E03 CSCL 12E

N89-21528# Maryland Univ. Baltimore County, Catonsville.
THE SOLUTION OF THE TYPE-PROBLEM FOR N LESS THAN OR EQUAL TO 4
Nam P. Bhatia and Walter O. Egerland (Ballistic Research Labs., Aberdeen Proving Ground, MD.) *In* Army Research Office, Transactions of the Fifth Army Conference on Applied Mathematics and Computing Mar. 1988 p 745-749 (For primary document see N89-21490 14-59)
Avail: NTIS HC A99/MF E03 CSCL 12E

N89-21530# New York Univ., New York.
THE INTERACTION OF NONLINEAR HYPERBOLIC WAVES: A CONFERENCE REPORT
James Glimm *In* Army Research Office, Transactions of the Fifth Army Conference on Applied Mathematics and Computing Mar. 1988 p 763-785 (For primary document see N89-21490 14-59)
(Contracts DE-AC02-76ER-03077; DAAG29-85-K-0188)
Avail: NTIS HC A99/MF E03 CSCL 12E

N89-21531# Army Research Office, Research Triangle Park, NC.
STABILIZATION OF ZIEGLER'S PENDULUM BY MEANS OF THE METHOD OF VIBRATIONAL CONTROL
G. L. Anderson and I. G. Tadjbakhsh (Rensselaer Polytechnic Inst., Troy, NY.) *In its* Transactions of the Fifth Army Conference on Applied Mathematics and Computing Mar. 1988 p 787-843 (For primary document see N89-21490 14-59)
Avail: NTIS HC A99/MF E03 CSCL 12E

65 STATISTICS AND PROBABILITY

Includes data sampling and smoothing; Monte Carlo method; and stochastic processes.

N89-21615# Center for Mathematics and Computer Science, Amsterdam (Netherlands). Dept. of Mathematical Statistics.
CONDITIONALLY AND STRICTLY DISTRIBUTION-FREE TESTS FOR RANDOMIZED BLOCK DESIGNS THAT ARE ASYMPTOTICALLY OPTIMAL
S. Tardif (Montreal Univ., Quebec) Mar. 1988 13 p
(Grants CAN-NSEC-A4029; EQ540)
(CWI-MS-R8802; B8827729; ETN-89-94185) Copyright Avail: NTIS HC A03/MF A01
The method of ranking after alignment and the Tukey-Quade method of weighted rankings for the analysis of complete blocks are generalized so as to give rise to classes of tests containing a conditionally distribution-free test and strictly distribution-free tests that are asymptotically optimal in the sense that, when the number of blocks tends to infinity, their asymptotic local power reaches the one of the asymptotically minimax test based on block-location-free statistics. ESA

N89-21616# Iowa State Univ. of Science and Technology, Ames. Statistical Lab.
ORDER STATISTICS AND ROBUST INFERENCE Final Report, 1 Jul. 1985 - 30 Sep. 1988
Robert A. David 30 Nov. 1988 7 p
(Contract DAAG29-85-K-0189)
(AD-A203440; ARO-22604.19-MA) Avail: NTIS HC A02/MF A01 CSCL 12C
This paper falls under two headings: Order Statistics and Nonparametric Statistics. Topics investigated include the following: robustness and estimation in the presence of outliers; inequalities for order statistics and functions of order statistics; moving order statistics. New nonparametric methods of analyzing unbalanced paired-comparison experiments were developed. Other topics include rank statistics and U-statistics, censored data, and extreme-value theory. GRA

66 SYSTEMS ANALYSIS

Includes mathematical modeling; network analysis; and operations research.

N89-21617# Air War Coll., Maxwell AFB, AL.
SDI (STRATEGIC DEFENSE INITIATIVE) AND NATIONAL SECURITY POLICY
Richard W. Davis Apr. 1988 109 p
(AD-A202730) Avail: NTIS HC A06/MF A01 CSCL 15C
The paper attempts to answer the fundamental question of,

Can SDI make a significant contribution to U.S. national security. It uses as its evaluation criteria historical arms control measurements of stability, reduction in the probability of war, reduction in the consequences of war, economic benefits, and political benefits. A historical discussion of U.S. nuclear strategy development along with Soviet thinking is provided as a backdrop to set the stage for an analysis of the reasons for President Reagan's March 1983 speech. The objectives of SDI are discussed along with the major concerns expressed by the program critics. Using the evaluation criteria defined above, the author analyzes SDI potential position in a long-term integrated national strategy that includes arms control and competitive strategies. GRA

N89-21618# Illinois Univ., Urbana. Dept. of Computer Science.
THE INTERDEPENDENCIES OF THEORY FORMATION, REVISION, AND EXPERIMENTATION Technical Report, 1 Sep. 1985 - 30 Aug. 1988
Brian Falkenhainer and Shankar Rajamoney 1 Jun. 1988 25 p
(Contract N00014-85-K-0559; RR04206)
(AD-A202882; UIUCDCS-R-88-1439; UILU-ENG-88-1744) Avail: NTIS HC A03/MF A01 CSCL 12I

This paper depicts theory development as a synergistic cooperation of scientific methodologies, each focusing on different aspects of the problem. It discusses how they may be integrated to provide a more unified and comprehensive treatment of scientific theory discovery. A general protocol is described for interaction between theory formation, theory revision, and experimentation. This protocol enables theory formation to make specific queries about the state of the world to fulfill its hypothesis generation goals. It also enables experimentation-based revision to post tasks for theory formation to supply relevant hypotheses. The utility and generality of this protocol is demonstrated by an implementation which integrates two previously autonomous systems. Its performance is described for discovering and revising models of evaporation and osmosis. GRA

N89-21619# Arms Control and Disarmament Agency, Washington, DC.
STRATEGIC DEFENSE INITIATIVE: A CHRONOLOGY, 1983 - 1988
1988 10 p
(AD-A203576) Avail: NTIS HC A02/MF A01 CSCL 15C

Since President Reagan announced his commitment to explore intensively the promise of new technologies for defense against ballistic missile attack, the Strategic Defense Initiative has evolved into a vigorous Research and Development program involving a number of U.S. allies. The objective of SDI is to strengthen U.S. and allied security and enhance long term strategic stability. SDI is an integral part of U.S. and Soviet nuclear arsenals. It also has important potential benefits for spinoffs to other defense programs and for the development of technologies with potentially far reaching applications in the civilian sector. This report provides a chronology which highlights key points in the evolution of U.S. strategic defense policy since March 1983. GRA

N89-21620# Los Alamos National Lab., NM.
ARTIFICIAL ASTEROID IMPACT ON DEFENSIVE SATELLITES
Gregory H. Canavan Mar. 1989 28 p
(Contract W-7405-eng-36)
(DE89-008407; LA-11418-MS) Avail: NTIS HC A03/MF A01

Given the large projected Soviet space lift capacity, it is useful to ask whether its placing large amounts of mass in near-earth orbits could present a serious impediment to defensive satellites deployed there. This report uses a simple model to show that such artificial asteroid belts are feasible and could directly limit the rate of deployment of defensive satellites in the near term, but are not necessarily an attractive use of that lift capacity in the long term. DOE

67 THEORETICAL MATHEMATICS

Includes topology and number theory.

N89-21621# Groningen Rijksuniversiteit (Netherlands). Dept. of Mathematics and Computing Sciences.
THE GL(2n-1,R) SPHERICAL REPRESENTATIONS OF SL(2n,R)
G. vanDijk (Leiden Univ., Netherlands) and M. Poel 1988 27 p
(ZW-8802; ETN-89-94165) Avail: NTIS HC A03/MF A01

Let G = SL(n,R) and H = S(GL(1,R) x GL(n-1,R)), H is a closed subgroup of G isomorphic to GL(n-1,R) and n is greater than or = 3. The objective is to classify, up to equivalence, the irreducible unitary representations of G which can be realized on a G-invariant Hilbert supspace of D'(X) where X = G/H. Irreducibility results for the H-spherical principal series are deduced. These are certain series of induced representations from a parabolic subgroup of G which is closely related to the symmetric space X. It is determined which of these representations have an H-spherical subquotient or submodule. The related spherical distributions are determined. The spherical dual is given for n even and partial results for n odd. ESA

N89-21622# Texas Univ., Austin. Inst. for Fusion Studies.
DIFFUSION IN SYMPLECTIC MAPS
Hyung-tae Kook and James D. Meiss 16 Feb. 1989 25 p
(Contract DE-FG05-80ET-53088)
(DE89-008083; DOE/ET-53088/363; IFSR-363) Avail: NTIS HC A03/MF A01

The characteristic function is used to obtain the diffusion tensor for symplectic maps. At lowest order the quasilinear result is obtained, and a series in higher order correlations is developed. Comparison of the theory to numerical experiments is given using a four-dimensional example of Froeschle. The experiments agree well with the theory for moderately large parameters. Arnol'd diffusion for the 'thick layer' case is discussed. It is shown that the short time correlations in one canonical plane affect the diffusion in the other plane even in the limit of zero coupling. Accelerator modes exist for the Froeschle example, and cause divergences in the diffusion, but these only appear when the accelerating region is included in the ensemble. DOE

70 PHYSICS (GENERAL)

For precision time and time interval (PTTI) see *35 Instrumentation and Photography;* for geophysics, astrophysics or solar physics see *46 Geophysics, 90 Astrophysics,* or *92 Solar Physics.*

N89-21623# National Inst. of Standards and Technology, Gaithersburg, MD. Center for Atomic, Molecular and Optical Physics.
CENTER FOR ATOMIC, MOLECULAR AND OPTICAL PHYSICS TECHNICAL ACTIVITIES, 1988
Katharine Gebbie Dec. 1988 516 p
(PB89-132302; NISTIR-88/3881) Avail: NTIS HC A22/MF A01 CSCL 20C

The research and technical activities of the Center for Atomic, Molecular and Optical Physics during the Fiscal Year 1988 are summarized. These activities include work in the areas of fundamental constants, radiation physics, surface science, plasma spectroscopy, time and frequency, quantum metrology, and quantum physics. GRA

N89-21624# Colorado State Univ., Fort Collins. Dept. of Electrical Engineering.
STUDY OF THE GENERATION OF INTENSE PULSED ELECTRON BEAMS USING GLOW DISCHARGES Final Report, 1 Mar. 1986 - 29 Feb. 1988
Jorge J. Rocca Feb. 1988 112 p
(Grant AF-AFOSR-0096-86; AF Proj. 2301)
(AD-A202438; AFOSR-88-1006TR) Avail: NTIS HC A06/MF A01 CSCL 20C

The electric field distribution in the cathode sheath of an electron-beam glow discharge has been measured and calculated. The electron yield of various cathode materials under helium ion bombardment has been measured. Current densities in excess of 10 amps per sq-cm have been generated from cold cathode glow discharges. The plasma of a pulsed high current density electron beam glow discharge has been characterized. Negative glow plasmas have been studied as electron sources for the generation of high current density electron beams. GRA

N89-21625# Air Force Inst. of Tech., Wright-Patterson AFB, OH. School of Engineering.

CORONA WIND COOLING COMPARISONS FOR HORIZONTAL CYLINDERS M.S. Thesis

Pamela R. Hodge Sep. 1988 141 p
(AD-A202714; AFIT/GE/AA/86J-1) Avail: NTIS HC A07/MF A01 CSCL 20C

Corona wind refers to the movement of gas induced by the repulsion of ions from the vicinity of high voltage discharge electrode. A typical corona test configuration (13:4) is illustrated in Figure 1. Free charges are produced in the ionized region surrounding the high field active electrode. These charged particles migrate and collide with neutral air particles in the drift. Experiments were conducted to determine the effect of the corona wind on the convective heat transfer rate from each of three horizontally mounted, heated aluminum cylinders. The cylinder was maintained at ground potential and an emitter was connected to a high voltage source. Stretched wire and multipoint emitter devices were used. Emitter-to-cylinder spacing and field voltage were parameters. Blown air was also used to simulate the corona wind generated from the stretched wire emitter. An energy balance method was used for data analysis. Free convection heat transfer rates were used as a baseline. The results of all experiments were compared and contrasted. The multipoint emitter was a more efficient emitter device than the stretched wire emitter. The convection heat transfer rate due to the corona wind with an applied high voltage field of 15kV was as much as 6.5 times the free convection heat transfer rate. GRA

N89-21626# Naval Ship Research and Development Center, Bethesda, MD.

STUDIES OF LIQUID METAL FLOWS AND POWER LOSSES IN DUCTS WITH MOVING CONDUCTING WALL, SLANTED MAGNETIC FIELD, AND APPLIED EXTERNAL ELECTRIC POTENTIAL Final Report

John S. Walker, Samuel H. Brown, and Neal A. Sondergaard Nov. 1988 38 p Prepared in cooperation with Illinois Univ., Urbana
(AD-A203981; DTRC-88/040) Avail: NTIS HC A03/MF A01 CSCL 20C

Advanced homopolar electrical machinery is being considered for many new applications. This applied research requires the development of mechanisms for transporting high current at low voltages between rotating and stationary members of the machines with minimal losses and maximal operational stability. Thus, liquid metals rather than more conventional brush technology are often used in the sliding electric contact region. Generally, these machines have large external magnetic fields in the region of the current collector, which has a definite effect on the liquid metal by Lorentz force interactions. Thus, to obtain current collector design parameters, one is interested in liquid-metal channel flow problems, with applied external magnetic fields and boundary conditions containing combinations of moving and fixed, conducting, or insulating walls. These boundary conditions then roughly correspond to a rotor, stator, or sidewall of the current collector and the liquid metal to the sliding electric contact. While many publications treat theoretical magnetohydrodynamic channel duct flow, only a very small percentage of these investigations have studied problems with moving conducting walls. GRA

N89-21627# Pacific Northwest Labs., Richland, WA. Life Sciences Center.

APPLICATIONS, DOSIMETRY AND BIOLOGICAL INTERACTIONS OF STATIC AND TIME-VARYING MAGNETIC FIELDS

T. S. Tenforde Aug. 1988 9 p Presented at the International Commission of Radiation Units and Measurements, Helsinki, Finland, 15 Aug. 1988
(Contract DE-AC06-76RL-01830)
(DE89-006944; PNL-SA-16146; CONF-8808192-1) Avail: NTIS HC A02/MF A01

The primary topics of this presentation include: (1) the applications of magnetic fields in research, industry, and medical technologies; (2) mechanisms of interaction of static and time-varying magnetic fields with living systems; (3) human health effects of exposure to static and time-varying magnetic fields in occupational, medical, and residential settings; and (4) recent advances in the dosimetry of extremely-low-frequency electromagnetic fields. The discussion of these topics is centered about two issues of considerable contemporary interest: (1) potential health effects of the fields used in magnetic resonance imaging and in vivo spectroscopy, and (2) the controversial issue of whether exposure to extremely-low-frequency (ELF) electromagnetic fields in the home and workplace leads to an elevated risk of cancer. DOE

71 ACOUSTICS

Includes sound generation, transmission and attenuation. For noise pollution see *45 Environmental Pollution.*

N89-21628*# National Aeronautics and Space Administration. Lewis Research Center, Cleveland, OH.

COMPARISON OF PROPELLER CRUISE NOISE DATA TAKEN IN THE NASA LEWIS 8- BY 6-FOOT WIND TUNNEL WITH OTHER TUNNEL AND FLIGHT DATA

James H. Dittmar Apr. 1989 23 p Presented at the 12th Aeroacoustics Conference, San Antonio, TX, 10-12 Apr. 1989; sponsored in part by AIAA
(NASA-TM-101976; E-4676; NAS 1.15:101976; AIAA-89-1059)
Avail: NTIS HC A03/MF A01 CSCL 20A

The noise of advanced high speed propeller models measured in the NASA 8- by 6-foot wind tunnel has been compared with model propeller noise measured in another tunnel and with full-scale propeller noise measured in flight. Good agreement was obtained for the noise of a model counterrotation propeller tested in the 8- by 6-foot wind tunnel and in the acoustically treated test section of the Boeing Transonic Wind Tunnel. This good agreement indicates the relative validity of taking cruise noise data on a plate in the 8- by 6-foot wind tunnel compared with the free-field method in the Boeing tunnel. Good agreement was also obtained for both single rotation and counter-rotation model noise comparisons with full-scale propeller noise in flight. The good scale model to full-scale comparisons indicate both the validity of the 8- by 6-foot wind tunnel data and the ability to scale to full size. Boundary layer refraction on the plate provides a limitation to the measurement of forward arc noise in the 8- by 6-foot wind tunnel at the higher harmonics of the blade passing tone. The use of a validated boundary layer refraction model to adjust the data could remove this limitation. Author

N89-21629# Korea Univ., Seoul (South Korea).

SOUNDS IN ONE-DIMENSIONAL SUPERFLUID HELIUM Technical Report No. 88

C. I. Um, W. H. Kahng, M. H. Whang, S. K. Hong, and H. G. Oh Nov. 1988 32 p Prepared in cooperation with State Univ. of New Y ork, Buffalo
(Contract N00014-86-K-0043)
(AD-A202428; UBUFFALO/DC/88/TR-88) Avail: NTIS HC A03/MF A01 CSCL 07B

The temperature variations of first-, second- and third-sound velocity and attenuation coefficients in one-dimensional superfluid

helium are evaluated explicitly for very low temperatures and frequencies (omega s tau is dominated by 1, where omega s is the sound frequency and tau the characteristic time), by using the collisionless kinetic equation and superfluid hydrodynamic equations with the energy dissipation effect. The leading terms for these sounds vary as T2, and the ratio of second-sound to first-sound becomes unity as the temperature decreases to absolute zero. GRA

N89-21630# Mississippi Univ., University. Physical Acoustics Research Lab.
A CONTINUED STUDY OF OPTICAL SOUND GENERATION AND AMPLIFICATION Annual Summary Report, 1 Nov. 1987 - 31 Oct. 1988
Henry E. Bass and F. Douglas Shields 31 Oct. 1988 49 p
(Contract N00014-84-C-0193)
(AD-A202484; PARGUM-88-02) Avail: NTIS HC A03/MF A01 CSCL 20A

This report discusses research on two projects: (1) the optoacoustic generation in fluids, and (2) the propagation sound through gases with a nonequilibrium distribution of vibrational energy states. The experimental method for the optoacoustic experiment involves observing the pressure pulse created when an 800 ps pulse of UV (337 nm) from an N2 laser is absorbed in a liquid. The pressure pulse created by the absorption of the UV is observed by the deflection produced in a second parallel laser beam transversing the liquid. Measurements are concerned with non linear dependence of the deflection of the detecting beam upon energy deposited in the liquid. The results indicate a change of state in the very small irradiated volume. With the propagation of sound through excited gases, an effort has been made to observe SACER in CO. Difficulty has been encountered in heating the vibrational mode in this gas with an electrical discharge. However, CO has been added to N2 in small amounts to act as a indicator of the vibrational temperature in N2. Due to a relatively fast v-v transfer the vibrational modes of the two gases stay in equilibrium. The I.R. radiation coming from the I.R. active CO is then an indicator of the vibrational temperature of the mixture. The decay of the vibrational temperature previously only inferred from the rise and fall of the translational temperature has been measured directly. GRA

N89-21631# Air Force Inst. of Tech., Wright-Patterson AFB, OH. School of Engineering.
ANALYSIS AND SIMULATION OF AN AUDIO ADAPTIVE EQUALIZER M.S. Thesis
John R. Strasburger Dec. 1988 160 p
(AD-A202569; AFIT/GE/ENG/88D-49) Avail: NTIS HC A08/MF A01 CSCL 09A

The purpose of this thesis was to explore the feasibility of replacing a manual audio equalizer with an adaptive filter that adaptively equalizes the spectral distortion of an audio system. The impulse response of an audio system which includes the response of the speaker crossover network, the power amplifiers, speakers, and the acoustic transfer function between the system's input signal spectrum. The Adaptive Inverse Pre-filter, the Filtered-x algorithm, and the Adaptive Inverse Modeling Control System are investigated which remove the distortion by pre-filtering the audio system's input signal with the audio system's inverse. The audio system examined is the Armstrong Aerospace Medical research Laboratory's Performance and Communication Research and Technology reverberation chamber located at Wright-Patterson Air Force Base. GRA

N89-21632# Army Construction Engineering Research Lab., Champaign, IL.
ATTENUATION OF BLAST WAVES USING FOAM AND OTHER MATERIALS Final Report
Richard Raspet, S. K. Griffiths, Joseph M. Powers, Herman Krier, and Timothy D. Panczak Nov. 1988 72 p
(AD-A203148; CERL-TM-N-89/01) Avail: NTIS HC A04/MF A01 CSCL 19I

Noise is a problem everywhere the Army trains or tests with large weapons or helicopters. Noise and hazardous waste have been listed as the major problems facing the Army into the 21st century. Research at the U.S. Army Construction Engineering Research Laboratory (USA-CERL) is aimed at solving the total noise problem for the Army. This report documents several years of fundamental research into methods to quiet explosive noise and materials used to reduce the noise from explosions. This report reproduces journal articles regarding this USA-CERL research in chronological order. GRA

72 ATOMIC AND MOLECULAR PHYSICS

Includes atomic structure, electron properties, and molecular spectra.

N89-21633*# Eoetvoes Lorand Univ., Budapest (Hungary). Dept. of Atomic Physics.
SURFACE ENERGY FROM ORDER PARAMETER PROFILE: AT THE QCD PHASE TRANSITION
Z. Frei and A. Patkos (Fermi National Accelerator Lab., Batavia, IL.) Jan. 1989 7 p
(Grant NAGw-1340)
(NASA-CR-184890; NAS 1.26:184890; FERMILAB-Pub-89/47-A)
Avail: NTIS HC A02/MF A01 CSCL 20H

The order parameter profile between coexisting confined and plasma regions at the quantum chromodynamic (QCD) phase transition is constructed. The dimensionless combination of the surface energy (Sigma) and the correlation length (Zeta) is estimated to be Sigma Zeta 3 approximately equals 0.8. Author

N89-21634*# Stanford Linear Accelerator Center, CA.
A NEW CLASS OF NON-TOPOLOGICAL SOLITONS
Joshua A. Frieman and Bryan W. Lynn Jan. 1989 21 p Prepared in cooperation with Stanford Univ., CA, California Univ., Santa Barbara, and Fermi National Accelerator Lab., Batavia, IL
(Grant NAGw-1340)
(NASA-CR-184889; NAS 1.26:184889; FERMILAB-Pub-89/31-A)
Avail: NTIS HC A03/MF A01 CSCL 20H

A class of non-topological solitons was constructed in renormalizable scalar field theories with nonlinear self-interactions. For large charge Q, the soliton mass increases linearly with Q, i.e., the soliton mass density is approximately independent of charge. Such objects could be naturally produced in a phase transition in the early universe or in the decay of superconducting cosmic strings. Author

N89-21635*# Fermi National Accelerator Lab., Batavia, IL. Astrophysics Center.
POSITRON LINE RADIATION FROM HALO WIMP ANNIHILATIONS AS A DARK MATTER SIGNATURE
Michael S. Turner and Frank Wilczek (Institute for Advanced Study, Princeton, NJ.) Feb. 1989 12 p Prepared in cooperation with Chicago Univ., IL
(Grant NAGw-1340)
(NASA-CR-182918; NAS 1.26:182918; FERMILAB-Pub-89/44-A)
Avail: NTIS HC A03/MF A01 CSCL 20H

We suggest a new signature for dark matter annihilation in the halo: high energy positron line radiation. Because the cosmic ray positron spectrum falls rapidly with energy, e+'s from halo WIMP annihilations can be a significant, clean signal for very massive WIMP's (approx. greater than 30 GeV). In the case that the e+e- annihilation channel has an appreciable branch, the e+ signal should be above background in a future detector, such as have been proposed for ASTROMAG, and of potential importance as a dark matter signature. A significant e+e- branching ratio can occur for neutralinos or Dirac neutrinos. High-energy, continuum positron radiation may also be an important signature for massive neutralino annihilations, especially near or above the threshold of the W+W- and ZoZo annihilation channels. Author

N89-21636# Wisconsin Univ., Madison.
TIME AND STATE RESOLVED STUDIES OF MOLECULAR DECOMPOSITION Final Report, 1 Aug. 1985 - 31 Jul. 1988
F. Fleming Crim 17 Oct. 1988 24 p
(Contract DAAG29-85-K-0122)
(AD-A202464; ARO-22929.3-CH) Avail: NTIS HC A03/MF A01 CSCL 20E

Molecular decompositions often control complex chemical reactions by producing a highly reactive fragment that determines the subsequent chemistry. Despite the importance of such processes, there is little detailed information available for testing theoretical models and guiding the analysis of practical systems. This report describes experiments that produce, characterize, and dissociate highly energized molecules in order to uncover the details of molecular decompositions. These experiments are able to explore decompositions solely in the ground electronic state by vibrational overtone induced dissociation, to investigate the role of vibrational excitation in electronic photodissociation using vibrationally mediated photodissociation, and to identify primary fragments and determine the kinetic energy release in electronic photodissociation using energy selective ionization. GRA

N89-21637# California Inst. of Tech., Pasadena.
BASIC STUDIES OF ION MIXING Final Report
M.-A. Nicolet 16 Nov. 1988 13 p
(Contract N00014-84-K-0275)
(AD-A203093) Avail: NTIS HC A03/MF A01 CSCL 20E

The objective was to elucidate mechanisms of atomic mixing induced by ions with masses greater than 25 amu and energies between 50 and 500 keV. Specifically, the intent was to identify systematic trends that would reveal the nature of the main parameters that affect atomic rearrangements generated by ion irradiation. In addition, the relationship that might exist between the mechanisms of ion mixing and of thermal processing was to be explored. Metallic systems were to be emphasized. The approach was to choose samples and parameters of irradiation in such a way that the complexity of the results was minimized. The idea was that limiting cases would thereby be established for which one mechanism is dominant. Consequently, experiments at low temperatures have been pursued to investigate processes that are independent of temperature. Irradiations at elevated temperatures were employed to investigate the correlation between ion mixing and thermal processing. GRA

N89-21638# Dayton Univ., OH.
THEORETICAL STUDIES OF POTENTIAL ENERGY STORAGE MOLECULES Final Report, Aug. 1987 - Apr. 1988
Daniel D. Konowalow Nov. 1988 34 p
(Contract F04611-83-C-0046)
(AD-A203986; UDR-TR-88-60; AFAL-TR-88-069) Avail: NTIS HC A03/MF A01 CSCL 20E

Investigations at several levels of theory of the quintet states of the Carbon monoxide molecule, which correspond asymptotically to the interaction of C(3)state) + O(3)state), show the 1 (5)sigma(+) state to be a potentially interesting energy storage candidate. Its binding energy (ca. 750 cm) is sufficiently large compared with those (greater than 100 cm) of the other quintets so that one might be able to produce the 1 (5)sigma(+) state preferentially. The decay pathways of the quintets need to be investigated in order to provide a more definitive assessment of their energy storage potential. GRA

N89-21744*# Toledo Univ., OH. Dept. of Physics and Astronomy.
THE MEASUREMENT OF ANGULAR DIFFERENTIAL CROSS SECTIONS AT THE SSL ATOMIC SCATTERING FACILITY
Thomas J. Kvale *In* Alabama Univ., Research Reports: 1988 NASA/ASEE Summer Faculty Fellowship Program Dec. 1988 23 p (For primary document see N89-21726 14-99)
Avail: NTIS HC A99/MF E03 CSCL 20H

N89-21747*# Alabama A & M Univ., Huntsville. Dept. of Physics.
FLUCTUATION ANALYSIS OF RELATIVISTIC NUCLEUS-NUCLEUS COLLISIONS IN EMULSION CHAMBERS
Stephen C. McGuire *In* Alabama Univ., Research Reports: 1988 NASA/ASEE Summer Faculty Fellowship Program Dec. 1988 16 p (For primary document see N89-21726 14-99)
Avail: NTIS HC A99/MF E03 CSCL 20H

73 NUCLEAR AND HIGH-ENERGY PHYSICS

Includes elementary and nuclear particles; and reactor theory.
For space radiation see *93 Space Radiation.*

N89-21639# Pacific Northwest Labs., Richland, WA.
THERMAL AND DYNAMIC ANALYSIS OF THE RING (RADIATIVELY-COOLED, INERTIALLY-DRIVEN NUCLEAR GENERATOR) POWER SYSTEM RADIATOR
Walter J. Apley and Albert L. Babb (Washington Univ., Seattle.) Jan. 1989 5 p Presented at the 6th Symposium on Space Nuclear Power Systems, Albuquerque, NM, 9 Jan. 1989
(Contract DE-AC06-76RL-01830)
(DE89-007236; PNL-SA-15971; CONF-890103-8) Avail: NTIS HC A02/MF A01

The nuclear option for a space-based power system appears most suitable for missions that require long-term, sustained operation at power levels above 100 kWe. Systems currently available operate at relatively low thermal efficiencies (6 to 10 percent). Thus, a 100 kWe system must discharge nearly 2 MWth of waste heat through the comparatively inefficient process of radiative cooling. The impact of the resultant radiator assembly size on overall power system weight is significant, and has led to proposals for radiators with potentially higher efficiencies. Examples include the liquid droplet radiator, fabric radiator, bubble membrane radiator, rotating film radiator, and dust radiator. DOE

74 OPTICS

Includes light phenomena; and optical devices.
For lasers see *36 Lasers and Masers.*

N89-21640*# National Aeronautics and Space Administration. Langley Research Center, Hampton, VA.
OPTICAL FIBER SENSORS AND SIGNAL PROCESSING FOR INTELLIGENT STRUCTURE MONITORING Semiannual Report
Robert Rogowski, R. O. Claus, D. K. Lindner, Daniel Thomas, and Dave Cox Dec. 1988 50 p Prepared in cooperation with Virginia Polytechnic Inst. and State Univ., Blacksburg
(Grant NAG1-895)
(NASA-CR-184841; NAS 1.26:184841) Avail: NTIS HC A03/MF A01 CSCL 20F

The analytic and experimental performance of optical fiber sensors for the control of vibration of large aerospace and other structures are investigated. In particular, model domain optical fiber sensor systems, are being studied due to their apparent potential as distributed, low mass sensors of vibration over appropriate ranges of both low frequency and low amplitude displacements. Progress during the past three months is outlined. Progress since September is divided into work in the areas of experimental hardware development, analytical analysis, control design and sensor development. During the next six months, tests of a prototype closed-loop control system for a beam are planned which will demonstrate the solution of several optical fiber instrumentation device problems, the performance of the control system theory which incorporates the model of the modal domain sensor, and the potential for distributed control which this sensor approach offers. Author

N89-21641# University of Southern California, Los Angeles. Image Processing Inst.
NONLINEAR REAL-TIME OPTICAL SIGNAL PROCESSING Annual Technical Report, 1 Jul. 1987 - 30 Jun. 1988
A. A. Sawchuk and B. K. Jenkins 1 Jul. 1988 125 p
(Grant AF-AFOSR-0181-84; AF Proj. 2305)
(AD-A202445; AFOSR-88-1283TR) Avail: NTIS HC A06/MF A01 CSCL 20F

During the period 1 July 1987 to 30 June 1988, the research under Grant AFOSR-84-0181 has been concerned with binary parallel optical computing architectures with particular attention to cellular logic and symbolic substitution for pattern recognition and numerical operations. Our approach has been to experimentally implement binary optical cellular logic processors and interconnection arrays; define an instruction set and software suited to optical systems; and to study generalizations of optical cellular logic processors such as the hypercube and pyramid. Recent accomplishments include the experimental implementations of a 54-gate binary optical cellular processor with instruction decoders, input/output, memory and test/branch functions; symbolic operations; and the development of binary image algebra algorithms for scale and shift invariant pattern recognition. GRA

N89-21642# Air Force Inst. of Tech., Wright-Patterson AFB, OH. School of Engineering.
OPTICAL ACTIVITY AND ITS INFLUENCE ON PHOTOREFRACTIVE MATERIALS M.S. Thesis
Richard J. Padden Dec. 1988 79 p
(AD-A202530; AFIT/GEO/ENP/88D-4) Avail: NTIS HC A05/MF A01 CSCL 07B

The purpose of this study was to investigate the combined effects of optical activity and linear birefringence on photorefractive crystals. The relation of input-output intensity was determined. These results were discussed with regard to the operation and optimization of the conducting PRIZ. The study focused on the crystal Bi12SiO20 (BSO) in order to correlate results with current experimental work at AFIT. The combination of optical activity and the photorefractive effect caused the crystal to be elliptically birefringent; this birefringence was modeled using Jones matrices for computer simulation. The simulation results showed that optical activity does have a noticeable effect, but for the application investigated the effect was small enough that it could be ignored. Recommendations were made to improve the quality of the output image of the PRIZ. More work should be performed in this area to investigate other applications of this phenomenon and also different crystal materials. GRA

N89-21643# Naval Ocean Systems Center, San Diego, CA.
INFRARED SEA-RADIANCE MODELING USING LOWTRAN 6 Final Report
F. G. Wollenweber Sep. 1988 23 p
(AD-A202582; NOSC/TD-1355) Avail: NTIS HC A03/MF A01 CSCL 20F

This model, based on the Cox-Monk wave-slope statistic and the LOWTRAN 6 radiation model, describes the behavior of the sea as an infrared background. The model addresses atmospheric refraction, aerosol absorption and scattering, molecular scattering, emission, and absorption. Comparisons with measurements of a calibrated thermal-imaging system showed good agreement. GRA

N89-21644# Air Force Inst. of Tech., Wright-Patterson AFB, OH. School of Engineering.
MODIFIED BACKWARD ERROR PROPAGATION FOR TACTICAL TARGET RECOGNITION M.S. Thesis
Charles C. Piazza Dec. 1988 210 p
(AD-A202666; AFIT/GE/ENG/88D-36) Avail: NTIS HC A10/MF A01 CSCL 12I

This thesis explores a new approach to the classification of tactical targets using a new biologically-based neural network. The targets of interest were generated from Doppler imagery and forward looking infrared imagery, and consisted of tanks, trucks, armored personnel carriers, jeeps and petroleum, oil, and lubricant tankers. Each target was described by feature vectors, such as normalized moment invariants. The features were generated from the imagery using a segmenting process. These feature vectors were used as the input to a neural network classifier for tactical target recognition. The neural network consisted of a multilayer perceptron architecture, employing a backward error propagation learning algorithm. The minimization technique used was an approximation to Newton's method. This second order algorithm is a generalized version of well known first order techniques, i.e., gradient of steepest descent and momentum methods. Classification using both first and second order techniques was performed, with comparisons drawn. GRA

N89-21645# Science Applications International Corp., San Diego, CA.
EVALUATION OF AEROSOL SIZE DISTRIBUTION MODELS Final Report
Sep. 1988 31 p
(Contract N66001-87-C-0170)
(AD-A202736; NOSC/TD-1361) Avail: NTIS HC A03/MF A01 CSCL 17E

The Navy aerosol model is important for prediction of atmospheric optical (visible and infrared) properties over the ocean, and hence for predicting the performance of FLIR systems. The use of satellite measurements to measure the aerosol size distribution in the marine boundary layer has been demonstrated by Science Applications International Corporation (SAIC) and provides the possibility of using satellite measurements to make predictions of FLIR performance. In this study, measurements of the aerosol optical thickness using different techniques were compared, with the objective of investigating the feasibility of using satellite data for FLIR performance prediction. SAIC provided satellite and sunphotometer ground truth measurements, and Naval Ocean Systems Center (NOSC) provided aircraft and infrared sky radiance measurements of aerosol properties. This report describes the SAIC measurements. GRA

N89-21646# Massachusetts Inst. of Tech., Cambridge. Artificial Intelligence Lab.
AN OPTIMAL SCALE FOR EDGE DETECTION
Davi Geiger and Tomaso Poggio Sep. 1988 25 p
(Contract N00014-85-K-0214)
(AD-A202747; AI-M-1078) Avail: NTIS HC A03/MF A01 CSCL 12I

Many problems in early vision are ill posed. Edge detection is a typical example. This paper applies regularization techniques to the problem of edge detection. The authors derive an optimal filter for edge detection with a size controlled by the regularization parameter lambda and compare it to the Gaussian filter. A formula relating the signal-to-noise ratio to the parameter lambda is derived from regularization analysis for the case of small values of lambda. Also discussed is the method of Generalized Cross Validation for obtaining the optimal filter scale. Finally, the authors use their framework to explain two perceptual phenomena: coarsely quantized images becoming recognizable by either blurring or adding noise. GRA

N89-21647# Massachusetts Inst. of Tech., Cambridge. Lincoln Lab.
NEW TECHNIQUES FOR HIGH-RESOLUTION OPTICAL SPACE SURVEILLANCE
Timothy P. Wallace 2 Nov. 1988 82 p
(Contract F19628-85-C-0002)
(AD-A202785; TR-819; ESD-TR-88-221) Avail: NTIS HC A05/MF A01 CSCL 17E

The problem of imaging through atmospheric turbulence has plagued astronomers for centuries. Only in the last 20 years has the lost resolution been restored through innovative hardware and algorithms. This report discusses the new optical imaging technologies of adaptive optics and speckle imaging in the space surveillance context. The techniques are compared and contracted, and new imaging methods are proposed which combine elements

of both. New methods are suggested for optical data evaluation. GRA

N89-21648# University Coll. of North Wales, Bangor. School of Electronic Engineering Sciences.

FAST ACTING OPTICAL BEAM DEFLECTION SYSTEM Interim Report Nos. 1-2

D. K. Das-Gupta 1988 7 p

(Contract DAJA45-88-C-0019)

(AD-A203042; R/D-5821-MS-01-1/2) Avail: NTIS HC A02/MF A01 CSCL 20F

The primary objective of the present investigation is to seek an effective and practical method to detect and suitably deflect a coherent optical radiation from its initial direction of incidence and thus avoid the occurrence of serious biological damages which may be caused by such harmful radiations in the wavelength range of 0.4 to 1 micrometer. In the research proposal a possible effective method of simultaneous detection and deflection method using a blazed diffraction grating has been discussed. A diffraction grating is an optical surface with many straight, parallel and equally spaced grooves which provide an optical diffraction due to the mutual interference of the light beams. The distribution of light into various orders of a grating depends upon the microscopic shape of the grooves of the grating. By ruling the grating with and controlling the angles of the grooves it is possible to concentrate the spectral energy in any desired angular region. This is called BLAZING a grating, and the groove-face angle psi is called the blaze angle. GRA

N89-21649# Naval Research Lab., Washington, DC. Bio/Molecular Engineering Branch.

IMMUNOASSAY PROCEDURES FOR FIBER OPTIC SENSORS Final Report

Frances S. Ligler 30 Apr. 1988 28 p

(AD-A203069) Avail: NTIS HC A03/MF A01 CSCL 20F

There is an increasing need for the development of an ultrasensitive immunoassay for use with fiber optic sensors. These detection systems can be used for such applications as disease diagnosis, detection of chemical and biological warfare agents or drugs of abuse, pollution control, therapeutic monitoring, and explosive detection. This specific program is designed to produce generic chemistries for use with existing fiber optic-based sensors to detect pathogens of particular threat to Army personnel as determined by USAMRIID. The detection system under development involves the attachment of antibodies to an optical fiber at high density. In addition, the immobilization must be achieved in a way which retains the antibody's ability to bind antigen. The functionality of the antibody will be tested through the binding of a labelled antigen. In the future, this assay could incorporate the antibodies developed by the Army for pathogens of particularly military concern. GRA

N89-21650# Royal Signals and Radar Establishment, Malvern (England).

A THEORETICAL AND EXPERIMENTAL INVESTIGATION OF LINEAR AND NONLINEAR FOCUSSING CHIRPED OPTICAL DIFFRACTION GRATINGS

M. F. Lewis and C. L. West Jun. 1988 37 p

(AD-A203396; RSRE-MEMO-4129; DRIC-BR-108037) Avail: NTIS HC A03/MF A01 CSCL 20F

In the past the focussing properties of chirped grating structures have been investigated in various disciplines including optics, acousto-optics and acoustics. In this paper we present the results of a detailed theoretical and experimental study of one such structure, namely the chirped optical diffraction grating, although many of the conclusions are of more general validity. We derive some useful fundamental properties of such focussing gratings, and show that to first order their behavior is similar to that of various other classical components such as focussing lenses, grating spectrometers, and matched filters for chirped waveforms. However we also describe a fascinating range of second-order differences in behavior, for example concerning the physical locations of the multiple foci, and the sidelobe structures within and perpendicular to the focal plane. For devices of large numerical aperture we demonstrate the advantages of using a non-linear chirp grating structure, e.g., for sidelobe suppression in the focal plane, and point out that surface acoustic wave (SAW) techniques can be used to generate the non-linear chirp waveforms necessary to implement such gratings in acousto-optic devices. GRA

N89-21651# Washington Univ., Seattle. Inst. for Study of Atmosphere and Ocean.

A NUMERICAL MODEL FOR THE COMPUTATION OF RADIANCE DISTRIBUTIONS IN NATURAL WATERS WITH WIND-ROUGHENED SURFACES. PART 2: USER'S GUIDE AND CODE LISTING

Curtis D. Mobley Jul. 1988 176 p

(Contract N00014-87-K-0525)

(AD-A203441; CONTRIB-44-Pt-2; NOAA/PMEL-ERL-81-Pt-2; NOAA/PMEL-CONTRIB-1047-Pt-2) Avail: NTIS HC A09/MF A01 CSCL 20A

This report is a users' guide for and listing of the FORTRAN V computer code that implements a numerical procedure for computing radiance distributions in natural waters. The mathematical details of the numerical radiance model are described in a companion report (A Numerical Model for the Computation of Radiance Distributions in Natural Waters with Wind-Roughened Surfaces, by Curtis D. Mobley and Rudolph W. Preisendorfer, NOAA Technical Memorandum ERL PMEL-75). The present report describes how to run the computer model and therefore addresses questions such as which routines perform which calculations, what input is required by the various programs, and what is the file structure of the overall program. GRA

N89-21652# Carnegie-Mellon Univ., Pittsburgh, PA. Robotics Inst.

EXTRACTING SHAPE REFLECTANCE OF LAMBERTIAN, SPECULAR, AND HYBRID SURFACES

Shree K. Nayar, Katsushi Ikeuchi, and Takeo Kanade Aug. 1988 51 p

(Contract F33615-87-C-1499)

(AD-A203772; CMU-RI-TR-88-14) Avail: NTIS HC A04/MF A01 CSCL 14D

All existing shape extraction techniques that are based on photometric measurements rely on assumed surface reflection properties. A method is proposed for determining the shape of surfaces whose reflectance properties may vary from Lambertian to specular without prior knowledge of the relative strengths of the Lambertian and specular components of reflection. The object surface is illuminated using extended light sources and is viewed from a single direction. Surface illumination using extended sources makes it possible to ensure the detection of both Lambertian and specular reflections. Multiple source directions are used to obtain an image sequence of the object. An extraction algorithm uses the set of image intensity values measured at each surface point to compute orientation as well as the relative strengths of the Lambertian and specular reflection components. The proposed methods has been named photometric sampling as it uses samples of a photometric function that relates image intensity to surface orientation, reflectance, and light source characteristics that describes the reflectance model and orientation of a surface point. Experiments were conducted on Lambertian surfaces, specular surfaces, and hybrid surfaces whose reflectance model is composed of both Lambertian and specular components. The results show high accuracy in measured orientations and estimated reflectance parameters. GRA

N89-21653# EG and G Energy Measurements, Inc., Los Alamos, NM.

COMPUTER-AIDED X-RAY IMAGING SYSTEM DESIGN AND EVALUATION

C. A. Ciarcia and T. D. Rupp 1988 6 p Presented at the Electronic Imaging '88 Conference, Boston, MA, 3 Oct. 1988

(Contract DE-AC08-88NV-10617)

(DE89-006599; CONF-8810316-1) Avail: NTIS HC A02/MF A01

The use of X-ray imaging techniques, or radiography, as a diagnostic tool for scientific, industrial, and medical applications has increased appreciably in recent years. This increase is the result of new materials and state-of-the-art engineering techniques that have improved X-ray source design, shielding, and recording media. Radiography is now being used in many new applications where conventional optical photography traditionally has been limited or inappropriate. This new flexibility in X-ray imaging techniques has led to a broad latitude in the choice of radiographic system design that can be controlled to meet specific application needs. In many ways this design versatility is similar to that encountered when creating a specialized optical imaging system. Here image resolution and quality are optimized by undertaking analyses of geometrical parameters, ray-trace information, modulation transfer functions (MTFs), resolution grids, and image display or recording media, etc. This very flexibility in design, however, implies combining multiple components to create a complex system that contains many degrees of freedom. For conventional optical system design, this inherent complexity is overcome by using one of the computer design codes (for example, CODEV by Optical Research Associates). For the similar radiographic imaging problem, this paper discusses the X-ray image computer design code XRAD, which uses these same analysis techniques to optimize and predict the two-dimensional X-ray image of a three-dimensional object. DOE

N89-21654# Lawrence Livermore National Lab., CA.
ACOUSTIC DAMAGE TO LARGE-APERTURE OPTICS: REVISION 1
J. R. Smith, J. F. Murray, D. T. Kyrazis, R. B. Wilcox, T. L. Weiland, R. B. Ehrlich, C. E. Thompson, R. B. Engle, and A. E. Brown 1989 17 p Presented at the SPIE Conference on Optics, Electro-optics and Laser Applications in Science and Engineering: OE/LASE '89, Los Angeles, CA, 15 Jan. 1989
(Contract W-7405-eng-48)
(DE89-008025; UCRL-99316-Rev-1; CONF-890145-18-Rev-1)
Avail: NTIS HC A03/MF A01

We have observed damage to 80-cm-diam fused-silica disks and lenses subjected to high-fluence pulses (up to 2.3 J/sq cm) from an upgraded Nova laser beamline (wavelength 351 nm; pulse duration 2.35 ns; beam diameter 70 cm; energy up to 8 kJ). Damage occurred in the center of each element, where a 6-cm-wide obscuration prevented direct illumination. We believe that light strongly scattered by transverse stimulated Brillouin scattering (SBS) interacts with the surface and with the bulk of the substrate, producing two kinds of acoustic waves that propagate to its center, where they become strong enough to do damage. In the surface interaction, scattered light is absorbed by an O-ring near the perimeter of the optic, creating a Rayleigh wave that propagates along the surface to the center of the optic. The resulting damage takes the form of crater-shaped fractures about 8 mm in diameter and 4 mm deep. In the bulk interaction, transverse SBS strongly compresses the optic in large regions transverse to the direction of beam polarization at the perimeter of the beam. The compression may result from electrostriction: the SBS intensity is several times that of the incident beam. Compressive waves resulting from the relaxation of these regions propagated to the perimeter of the optic, where they are reflected as bulk tensile waves. The focusing of these tensile waves in the center of the optic results in cracks along the direction of polarization. We propose design rules for avoiding acoustic damage in large optics and compare observed thresholds for transverse SBS with predictions in the literature. DOE

75 PLASMA PHYSICS

Includes magnetohydrodynamics and plasma fusion.
For ionospheric plasmas see *46 Geophysics*. For space plasmas see *90 Astrophysics*.

N89-21655# Ames Lab., IA. Dept. of Chemistry.
SAMPLE INTRODUCTION TECHNIQUES FOR INDUCTIVELY COUPLED PLASMA MASS SPECTROMETRY Ph.D. Thesis
Shiuh-Jen Jiang Jul. 1988 137 p
(Contract W-7405-eng-82)
(DE89-005724; IS-T-1357) Avail: NTIS HC A07/MF A01

Arc nebulization is employed as a sample introduction method for elemental and isotopic analysis of conducting solids and non-conducting powdered samples with an inductively coupled plasma mass spectrometer (ICP-MS). Detection limits are in the microg/g range and relative precision and accuracy are approximately 5 percent for elements studied. The precision for isotope ratio measurements of non-conducting powders is approximately 1 percent for major constituents. A simple liquid chromatographic method is described for the removal of some interferences for the ICP-MS determination of Cu, Zn, and Cd. Detection limits are 1 to 2 microg/L. Isotope ratios for Cu, Zn, and Cd have also been determined with reasonable precision (1 to 2.5 percent) on eluting peaks. This observation indicates that it is possible to do quantitative elemental analysis by isotope dilution with liquid chromatography (LC) and/or flow injection (FI) sample introduction. Speciation measurements are demonstrated by LC separation of phosphorous and sulfur containing compounds with ICP-MS detection. The response factors for P and S are independent of the individual compound. Detection limits are 0.4 to 4 ng for P and (approximately) 7 ng for S despite the high background at $m/z = 31$ and $m/z = 34$. DOE

N89-21656# Babcock Hitachi K.K., Tokyo (Japan).
PLASMA REACTION METHOD AND APPARATUS
Kurumaji Ryuji and Yokoyama Koichi 1989 13 p
(Contract DE-AC05-84OT-21400)
(DE89-007360; Y/TR-89/2) Avail: NTIS HC A03/MF A01

The present invention involves a plasma reaction method and the accompanying apparatus; specifically, it is concerned with the plasma reaction method wherein a coating is formed by a plasma reaction, in particular where the outer surfaces are coated with materials such as ceramics, and with the relevant apparatus. DOE

N89-21657# Arizona Univ., Tucson.
NUMERICAL MODELING OF NARROW BAND SOFT X-RAY SOURCES Final Report, 15 Nov. 1983 - 14 Aug. 1987
Robert J. Barker May 1988 81 p
(Grant AF-AFOSR-0041-84; AF Proj. 2301)
(AD-A203368; AFOSR-88-1270TR) Avail: NTIS HC A05/MF A01 CSCL 20I

A model has been developed for calculating X-ray line emission from spherical plasmas. This method has been applied to an aluminum target, and the results are in good agreement with previous experimental work. The total energy, summed over all lines, as well as the line intensity ratios (which are a sensitive measure of agreement with experiment) were predicted with good accuracy. The pictures that would be seen by a pinhole camera are also calculated by the code. GRA

N89-21658*# Colorado State Univ., Fort Collins. Dept. of Mechanical Engineering.
SPACE PLASMA CONTRACTOR RESEARCH, 1988 Annual Report, 1 Jan. 1988 - 1 Jan. 1989
John D. Williams and Paul J. Wilbur Feb. 1989 61 p
(Grant NAG3-776)
(NASA-CR-182283; NAS 1.26:182283) Avail: NTIS HC A04/MF A01 CSCL 20I

Results of experiments conducted on hollow cathode-based plasma contractors are reported. Specific tests in which attempts were made to vary plasma conditions in the simulated ionospheric plasma are described. Experimental results showing the effects of

contractor flowrate and ion collecting surface size on contactor performance and contactor plasma plume geometry are presented. In addition to this work, one-dimensional solutions to spherical and cylindircal space-charge limited double-sheath problems are developed. A technique is proposed that can be used to apply these solutions to the problem of current flow through elongated double-sheaths that separate two cold plasmas. Two conference papers which describe the essential features of the plasma contacting process and present data that should facilitate calibration of comprehensive numerical models of the plasma contacting process are also included. Author

N89-21659# Lawrence Livermore National Lab., CA.
FUSION: A NECESSARY COMPONENT OF US ENERGY POLICY
Donald L. Correll, Jr. 11 Jan. 1989 24 p Presented at the McGraw-Hill Nuclear Publication's Forum on US Energy Policy and Nuclear Option, Washington, DC, 31 Jan. 1989
(Contract W-7405-eng-48)
(DE89-006234; UCRL-100194; CONF-890182-1) Avail: NTIS HC A03/MF A01

U.S. energy policy must ensure that its security, its economy, or its world leadership in technology development are not compromised by failure to meet the nation's electrical energy needs. Increased concerns over the greenhouse effect from fossil-fuel combustion mean that U.S. energy policy must consider how electrical energy dependence on oil and coal can be lessened by conservation, renewable energy sources, and advanced energy options (nuclear fission, solar energy, and thermonuclear fusion). In determining how U.S. energy policy is to respond to these issues, it will be necessary to consider what role each of the three advanced energy options might play, and to determine how these options can complement one another. This paper reviews and comments on the principal U.S. studies and legislation that have addressed fusion since 1980, and then suggests a research, development, and demonstration program that is consistent with the conclusions of those prior authorities and that will allow us to determine how fusion technology can fit into a U.S. energy policy that takes a balanced, long term view of U.S. needs. DOE

N89-21660# Auburn Univ., AL. Dept. of Physics.
THEORETICAL STUDIES OF THE HEATING OF TOROIDAL PLASMAS WITH RADIOFREQUENCY ELECTROMAGNETIC RADIATION Progress Report, 1 Jul. 1988 - 30 Jun. 1989
D. G. Swanson, J. M. Wersinger, and J. D. Hanson Feb. 1989 12 p
(Contract DE-FG05-85ER-53206)
(DE89-008003; DOE/ER-53206/11) Avail: NTIS HC A03/MF A01

This report contains papers of studies made in plasma heating of toroidal plasmas. Some topics discussed are: torsatron design; nonlinear lower hybrid wave effects; physics of ion Bernstein wave heating; plasma waves; and other related topics. DOE

N89-21661# Rochester Univ., NY. Lab. for Laser Energetics.
COMPUTER MODELING AND SIMULATION IN INERTIAL CONFINEMENT FUSION
R. L. McCrory and C. P. Verdon Mar. 1989 44 p
(Contract DE-FC03-85DP-40200)
(DE89-008304; DOE/DP-40200/85; Rept-199) Avail: NTIS HC A03/MF A01

The complex hydrodynamic and transport processes associated with the implosion of an inertial confinement fusion (ICF) pellet place considerable demands on numerical simulation programs. Processes associated with implosion can usually be described using relatively simple models, but their complex interplay requires that programs model most of the relevant physical phenomena accurately. Most hydrodynamic codes used in ICF incorporate a one-fluid, two-temperature model. Electrons and ions are assumed to flow as one fluid (no charge separation). Due to the relatively weak coupling between the ions and electrons, each species is treated separately in terms of its temperature. In this paper we describe some of the major components associated with an ICF hydrodynamics simulation code. To serve as an example we draw heavily on a two-dimensional Lagrangian hydrodynamic code (ORCHID) written at the University of Rochester's Laboratory for Laser Energetics. DOE

N89-21662# Texas Univ., Austin. Inst. for Fusion Studies.
SHORT WAVE ELECTRON TEMPERATURE GRADIENT DRIVEN DRIFT WAVE TURBULENCE
N. Bekki, W. Horton, B. G. Hong, and T. Tajima Feb. 1989 17 p
(Contract DE-FG05-80ET-53088)
(DE89-008465; DOE/ET-53088/364; IFSR-364) Avail: NTIS HC A03/MF A01

A local, hydrodynamic model of the short wavelength electrostatic drift waves driven unstable by the electron temperature gradient in toroidal geometry is used to find the saturation level and the mode coupling to the longer wavelength collisionless skin depth c/omega (sub pe) magnetic turbulence. We show that the k-spectrum is peaked in the c/omega (sub pe) wavelength region at the mixing length amplitude. The level of magnetic turbulence is sufficient to produce the empirical neo-Alcator type of confinement formula. DOE

76 SOLID-STATE PHYSICS

Includes superconductivity.

For related information, see also *33 Electronics and Electrical Engineering* and *36 Lasers and Masers.*

N89-21663# Atomic Energy Research Establishment, Harwell (England). Materials Development Div.
THE DETERMINATION OF CRYSTALLITE ORIENTATION DISTRIBUTION FUNCTIONS (CODF) AND THEIR USE IN SURFACE TEXTURE ANALYSIS USING X-RAY DIFFRACTION
A. M. Jones Feb. 1988 44 p
(AERE-R-12839; HL88/1061) Avail: NTIS HC A03/MF A01

Texture of materials describes the orientation of crystallites produced by physical or chemical processes. Texture becomes important when physical properties of materials vary with the crystallographic directions. Texture analysis of the surfaces of materials using X-ray diffraction is described. The concept of texture is briefly discussed, and the measurement of X-ray pole figures is described. The more advanced treatment of the Crystallite Orientation Distribution Function (CODF) to describe texture is introduced, with mention of the mathematical treatment involved. A further application of the CODF is in the evaluation of complete physical property tensors for polycrystalline samples. An example is given of measured pole figures, subsequent CODF analysis and use of the CODF coefficients to calculate a physical property tensor. Author

N89-21664# Helsinki Univ. of Technology, Espoo (Finland). Low Temperature Lab.
HALF-SOLITONS IN SUPERFLUID (3)He-A: NOVEL PI/2-QUANTA OF PHASE SLIPPAGE
M. M. Salomaa and G. E. Volovik 1988 59 p Prepared in cooperation with Illinois Univ., Urbana-Champaign and Nordisk Inst. for Teoretisk Atomfysik, Copenhagen, Denmark
(PB89-128904; TKK-F-A630; ISBN-951-754-600-9) Avail: NTIS HC A04/MF A01 CSCL 20L

Core structures of non-topological solitons between inequivalent vacua in superfluid (3)He-A are considered. The symmetries of these A-A interfaces are analyzed, and their hard-core structures are computed in the Ginzburg-Landau regime. Both domain walls where the orbital anisotropy l-vector is flipped (l-vector to -l-vector), and those with the same l-vector (x = - infinity) and l-vector(x = + infinity) asymptotics are discussed. In particular, new classes of A-A boundaries are found; these novel pi/2-solutions, which can occur in the absence of a change in the asymptotic l-vector field, constitute the elementary quanta of phase slippage in superfluid (3)He-A. These half-solutions are ascribed to a new

topological scenario for the flaring-out of vorticity in the extended (k-vector, r-vector) space. Edges of such walls serve to provide vortices with one quarter quantum of circulation in (3)He-A. GRA

N89-21665# Massachusetts Inst. of Tech., Cambridge. Dept. of Materials Science and Engineering.
GRAIN BOUNDARY KINETICS. 1: IN-SITU OBSERVATIONS OF COUPLED GRAIN BOUNDARY DISLOCATION MOTION, CRYSTAL TRANSLATION AND BOUNDARY DISPLACEMENT
S. E. Babcock and R. W. Balluffi Jan. 1989 33 p
(Contract DE-FG02-87ER-45310)
(DE89-006790; DOE/ER-45310/15-Pt-1) Avail: NTIS HC A03/MF A01

Extensive stress-induced climb-glide motion of secondary grain boundary dislocations (SGBDs) in near-sigma 5 grain boundaries in gold was directly observed and video recorded by means of hot-stage in-situ transmission electron microscopy. The passage of appreciable numbers of SGBDs along the boundary (N) caused a translation of the abutting crystals with respect to one another (T) and a lateral displacement of the boundary with respect to each crystal (D sub i). Quantitative measurements of N, T, and D sub i for a number of boundaries provided unambiguous evidence that these three processes were coupled. The observed T's and D sub i's were in agreement with a geometrical model involving the N's, the Burgers vectors of the moving SGBDs, and the heights of the steps which the SGBDs were expected to produce in the boundary plane. Most of the SGBDs whose motion produced the measured translations and displacements were intrinsic in nature; a minor fraction appeared to be intrinsic. The deduced SGBD-step configurations tended to be those associated with the smaller step heights possible within the framework of the sigma 5 CSL. Operating sources and sinks for moving SGBDs were directly observed in some of the boundaries. DOE

N89-21666# Ames Lab., IA. Solid State Physics Div.
LOW TEMPERATURE PROPERTIES OF TERNARY MAGNETIC RARE EARTH TRANSITION METAL GERMANIDES WITH THE Sc5Co4Ge10-TYPE STRUCTURE Ph.D. Thesis
Chanson Parengkuan Jul. 1988 140 p
(Contract W-7405-eng-82)
(DE89-007628; IS-T-1386) Avail: NTIS HC A07/MF A01

The dc resistivity, dc magnetization, and specific heat of eight Sc5Co4Ge10-type crystal structure compounds R5T4Ge10 for R = Dy, Ho, Er, Tm, and T = Rh and Ir are presented. The resistivity, single crystal magnetization, and specific heat results show that in all those compounds, the magnetic moments order antiferromagnetically in the c direction at low temperature. However, in the Er and Tm compounds, the magnetizations along x-y hard directions do not show any anomalies above 2.0 K. This suggests that the ordered Er and Tm ions, which have positive quadrupole coefficients alpha (sub j), interact with a crystal field that has an electronic potential valley along the c axis. The fitting of the hard axis magnetizations to Curie-Weiss law suggests that the resulting antiferromagnetic-like theta reflects the strength of the crystal field torque on the magnetic moments rather than the strength of antiferromagnetic exchange. DOE

N89-21667# Cambridge Univ. (England).
MBE OF (Hg,Cd)Te Final Report
T. D. Golding and M. Pepper Oct. 1988 54 p
(Contract DAJA45-87-C-0033; DA Proj. 1L1-61103-BH-57)
(AD-A202448; R/D-5841-EE-01-F) Avail: NTIS HC A04/MF A01 CSCL 07B

The work sponsored under this contract has centered on the molecular beam epitaxial growth of InSb/CdTe heterojunctions and multilayer structures, and on (Zn,Cd)Te/CdTe strained layer superlattices. We have been the first to demonstrate the molecular beam epitaxial growth of InSb/CdTe superlattices at temperatures necessary for the growth of electrical active InSb. An indication of the progress in this III-V/II-VI mixed system is the first observation of the quantum hall effect (QHE) in the InSb/CdTe heterojunction, by Simon Greene at the Cavendish Laboratory. As a result of the demonstration of a 2DEG and the ability to grow InSb/CdTe superlattices, the realization of infrared lasers and detectors in the 3 to 5 micro region has been significantly enhanced. We have reported the growth of a novel semiconducting material In2Te3. Work on the II-IV material compounds has centered on the growth of (Zn, Cd)Te/CdTe strained layer superlattices that have the layer thickness ratios and Zn composition tailored to allow the in-plane lattice parameter match that of Hg(0.8)Cd(0.2)Te. GRA

N89-21668# Air Force Inst. of Tech., Wright-Patterson AFB, OH. School of Engineering.
CALCULATION OF CARRIERS IN DEPLETION REGION OF SEMICONDUCTORS WITH CAPACITANCE-VOLTAGE MEASUREMENTS M.S. Thesis
Kim Hyun Jong Dec. 1988 103 p
(AD-A202529; AFIT/GEO/ENP/88D-8) Avail: NTIS HC A06/MF A01 CSCL 20L

Profiles obtained by the capacitance-voltage (C-V) method cannot give carrier distributions information right from the semiconductor surface. Since the prediction of ultimate device performance depends strongly upon an accurate knowledge of the entire carrier depth profile, it is very important to know this profile for the entire crystal including the surface depletion layer. A method was developed for obtaining the measured C-V data. This method was successfully applied to simulated C-V data created from various known linear, parabolic, and Lindhard, Sharff, and Schiott (LSS) Gaussian distributions, and then finally was demonstrated through experimentally measured C-V profiles obtained from Si-implanted GaAs. In this method, barrier potential was assumed to be 0.8 eV for n-type Si-implanted GaAs. GRA

N89-21669# Cornell Univ., Ithaca, NY.
ANALYTIC DISTRIBUTION FOR CHARGE CARRIERS IN A SEMICONDUCTOR DOMINATED BY EQUIVALENT INTERVALLEY SCATTERING
Gregory K. Schenter and Richard L. Liboff 10 Oct. 1988 36 p
(Contract DAAG29-84-K-0093; DA Proj. 3E1-62777-A-879)
(AD-A202537; ARO-20850.3-EL) Avail: NTIS HC A03/MF A01 CSCL 20L

The transport of charge carriers in silicon immersed in an electric field is studied using the quasiclassical Uehling-Uhlenbeck equation. Strain-acoustic and equivalent intervalley electron-phonon interactions are taken into account. A nonlinear difference-differential equation for the distribution function of this equation is constructed from which an expression for drift velocity is derived. Comparison with values obtained from this expression is found to give very good agreement with experimental measurement for electric fields up to 100,000 V/cm. GRA

N89-21670# Universal Energy Systems, Inc., Dayton, OH.
CONTRIBUTIVE RESEARCH IN COMPOUND SEMICONDUCTOR MATERIAL AND RELATED DEVICES Final Technical Report, Oct. 1981 - Sep. 1987
James R. Twist May 1988 38 p
(Contract F33615-82-C-1716)
(AD-A202586; AFWAL-TR-88-1037) Avail: NTIS HC A03/MF A01 CSCL 09A

The objective of this program was to provide the Electronic Device Branch (AFWAL/AADR) with the support needed to perform state of the art electronic device research. In the process of managing and performing on the project, UES has provided a wide variety of scientific and engineering talent who worked in-house for the Avionics Laboratory. These personnel worked on many different types of research programs from gas phase microwave driven lasers, CVD and MOCVD of electronic materials to Electronic Device Technology for new devices. The fields of research included MBE and theoretical research in this novel growth technique. Much of the work was slanted towards the rapidly developing technology of GaAs and the general thrust of the research that these tasks started has remained constant. This work was started because the Avionics Laboratory saw a chance to advance the knowledge and level of the current device technology by working in the compounds semiconductor field. UES

is pleased to have had the opportunity to perform on this program and is looking forward to future efforts with the Avionics Laboratory. GRA

N89-21671# Air Force Inst. of Tech., Wright-Patterson AFB, OH. School of Engineering.
EVALUATION OF THE SPATIAL AND TEMPORAL CHARACTERISTICS OF THE CONDUCTING PRIZ M.S. Thesis
Patrick J. Gardner Dec. 1988 61 p
(AD-A202593; AD-E900870; AFIT/GEO/ENP/88D-3) Avail: NTIS HC A04/MF A01 CSCL 09E

The imaging properties of the conducting PRIZ were re-evaluated using crystals which were carefully ground and polished to minimize surface layer damage. Resolution was quantified as a function of the energy density of the write-beam for both incoherent and coherent light sources. Maximum resolution from a standardized bar chart was determined using a model derived from a hybrid of luminance ratios used to evaluate image quality and the Rayleigh criteria for two point resolution. In addition, the spatial-temporal frequency dependence of the conducting PRIZ in the dynamic imaging mode was demonstrated and, quantified for coherent illumination over a range of spatial and temporal frequencies. The write-beam-induced damage threshold for these carefully prepared crystals was determined in terms of energy density. Optical memory of the device was found to last for 20 to 60 minutes, depending on the specific spatial frequency, at these peak energy densities when a single pulse of write-beam was applied. When multiple pulses of write-beam energy were applied, the frequency of the pulses (temporal frequency) as well as the energy density of the beam and spatial frequency of the object influenced memory decay. GRA

N89-21672# Air Force Inst. of Tech., Wright-Patterson AFB, OH. School of Engineering.
THE RESPONSE OF SINGLE ELEMENT HgCdTe AND InSb SOLID STATE INFRARED DETECTORS TO MILLIMETER WAVE ELECTROMAGNETIC ENERGY M.S. Thesis
Thomas D. Moore Dec. 1988 153 p
(AD-A202667; AFIT/GE/ENG/ENP/88D-1) Avail: NTIS HC A08/MF A01 CSCL 17E

An experimental determination of the millimeter wave (MMW) response of single element InSb and HgCdTe infrared (IR) detectors is made. The detectors were mounted in standard metal dewars and cooled to 77K. Bias and amplification for the detectors were irradiated with amplitude modulated (AM) electromagnetic energy in the Ka and E microwave bands. MMW transmitter power levels were limited to values of less than 10 mW. Tests were accomplished in the near-field of standard gain pyramidal horns. Response measurements were made on a spectrum analyzer by monitoring the level of the MMW AM rate spectral component. The detector MMW responses were measured for linearity, RF, AM rate, and polarization dependence. The effect of simultaneous IR and MMW sources in the detector field-of-view were also examined. Of the detectors tested, only the HgCdTe detector exhibited a MMW response. The measured HgCdTe MMW response was square law in behavior and displayed dependence on the RF, AM rate, and polarization of the incident MMW. The MMW response was not effected by the presence of IR sources. GRA

N89-21673# Arizona Univ., Tucson. Optical Sciences Center
CENTER FOR THIN FILM STUDIES Annual Report, 1 Oct. 1987 - 1 Oct. 1988
Robert R. Shannon and Ursula J. Gibson 31 Oct. 1988 171 p
(Contract F49620-86-C-0123)
(AD-A202742; AFOSR-88-1273TR) Avail: NTIS HC A08/MF A01 CSCL 07B

This report covers the second year of operation of the URI Thin Film Center. This report contains a summary of the research performed under this umbrella grant; separate sections cover work on growth and characterization of thin films by different methods, modeling of thin film growth, and preparation and characterization of substrates for growth. The task numbers have been reassigned from the previous year. GRA

N89-21674# General Atomic Co., San Diego, CA.
HIGH-TEMPERATURE CERAMIC SUPERCONDUCTORS Quarterly Progress Report No. 1, 24 May - 30 Sep. 1988
K. S. Mazdiyasni and K. C. Chen 10 Oct. 1988 34 p
(Contract N00014-88-C-0714)
(AD-A202867; GA-C19465) Avail: NTIS HC A03/MF A01 CSCL 20C

This is the first quarterly progress report on the work performed in the period from May 24, 1988 through September 30, 1988. The principal objectives of this program are: (1) to demonstrate fabrication of high-temperature ceramic superconductors that can operate at or above 90 K with appropriate current density, Jc, in forms useful for application in resonant cavities, magnets, motors, sensors, computers, and other devices; and (2) to fabricate and demonstrate selected components made of these materials, including microwave cavities and magnetic shields. GRA

N89-21675# Stanford Univ., CA. Electronics Lab.
INVESTIGATION OF SCHOTTKY BARRIER ON GaAs AND InP USING A MULTIDISCIPLINED APPROACH Interim Report, 15 Aug. 1987 - 15 Aug. 1988
Nathan Newman, William E. Spicer, and Al Green 20 Oct. 1988 9 p
(Grant AF-AFOSR-0263-86; AF Proj. 2306)
(AD-A202953; AFOSR-88-1328TR) Avail: NTIS HC A02/MF A01 CSCL 20L

A major development this year was the Advanced Unified Defect Model (AUDM). This focus on the AsGa and the GaAs antisites as the key defect which can govern the electronic properties at GaAs/metal as well as other GaAs interfaces. One importance of this is that it provides a framework through which the interfacial chemistry can be related to changes in Schottky barrier height. Details of the AUDM and its development are given in paper 6 on our list of publications. A copy is attached to this report. The Fermi level position will be set by the relative number of AsGa and GaAs antisites. Because of the excess As and LEC GaAs, the AsGa antisites usually dominate when LEC crystals are used. Thus the Fermi level is pinning near midgap. If an interface reaction produces excess As, the Fermi level, Ef, moves toward the CVM; if excess Ga Ef moves toward the VBM. As can be seen from the Figure, good agreement is obtained with the careful experimental data generated under this contract in annealing experiments. However, it is important that this work be expanded to other metals. Oxides or other foreign layers at the interface complicate matters. However, it appears that the model appears even in these cases. The potential significance of this model goes far beyond the annealing experiments listed above. For example, it suggests that interfacial behavior may depend on the amount of As in the As grown crystals. Thus, we are initiating work on LEC crystals grown less As rich. GRA

N89-21676# Air Force Inst. of Tech., Wright-Patterson AFB, OH. School of Engineering.
INVESTIGATION OF A SELF-ALIGNED, STRAINED-CHANNEL,n SUP(+)-In As/Al 0.5 As/In 0.15 Ga 0.85 As SEMICONDUCTOR INSULATOR SEMICONDUCTOR FET (SISFET) M.S. Thesis
David W. Rapp 30 Nov. 1988 169 p
(AD-A203147; AFIT/GE/ENG/88D-40) Avail: NTIS HC A08/MF A01 CSCL 20L

The idea of a new type of Semiconductor Insulator Semiconductor Field Effect Transistor (SISFET) device has been investigated. The attempted design consists of a heavily doped n-type InAs gate with undoped Al(0.5)Ga(0.5)As as the gate insulator and with undoped In(0.15)Ga(0.85)As as a strained-channel on an undoped GaAs buffer layer. SISFETs provide freedom from the Donor complex (DX) center and have threshold voltages which are independent of the AlGaAs doping and thickness. Calculations predict that the proposed pseudomorphic structure would produce a device with a natural

threshold voltage of approximately 0.6 volts. This would be well suited to digital logic applications. Calculations also predict that this new material structure would provide a barrier to gate leakage of greater than 0.3 volts up to 2.5 volts of positive gate bias. The layers were grown by MBE, and devices were fabricated using a self-aligned process which involved ion implantation and rapid thermal annealing. Some finished samples exhibited transistor action, but problems included inordinately high gate leakage and non-ohmic source and drain contacts. GRA

N89-21677# Aerospace Corp., El Segundo, CA. Chemistry and Physics Lab.
DISTRIBUTION OF BORON ATOMS IN ION IMPLANTED COMPOUND SEMICONDUCTORS
R. C. Bowman, Jr., J. F. Knudsen, R. G. Downing, and R. E. Kremer (Oregon Graduate Center for Study and Research, Beaverton.) 22 Nov. 1988 11 p
(Contract F04701-85-C-0086)
(AD-A203173; TR-0088(3945-07)-5; SD-TR-88-102) Avail: NTIS HC A03/MF A01 CSCL 07B

The nondestructive neutron depth profiling (NDP) technique has been used to measure the boron (10B) distributions in GaAs, CdTe, Hg0.7Cd0.3Te, and Hg0.85Mn0.15Te after multiple energy ion implants. The NDP results are found to be in good agreement with the theoretical ion ranges obtained from Monte Carlo computer simulations. Only minor changes in the boron profiles were seen for the chosen annealing conditions. GRA

N89-21678# North Texas State Univ., Denton. Dept. of Physics.
TWO PHOTON CHARACTERIZATION Interim Report, 28 Feb. - 28 Mar. 1988
David G. Seiler Dec. 1988 23 p
(Contract DAAB07-87-C-F094; DA Proj. 1L1-61102-A-31-B)
(AD-A203355) Avail: NTIS HC A03/MF A01 CSCL 20L

Magneto-Optical studies of HgCdTe have provided a rich new group of spectroscopies for studying defects and impurities in narrow band semiconductors such as HgCdTe. GRA

N89-21679# Royal Holloway and Bedford New Coll., Egham (England).
DIELECTRIC SPECTROSCOPY OF SEMICONDUCTORS Progress Report No. 4
Andrew K. Jonscher and Mohammad A. Bari Dec. 1988 4 p
(Contract DAJA45-87-C-0011)
(AD-A203457; R/D-5119-EE-01-04) Avail: NTIS HC A02/MF A01 CSCL 20L

Work in the reporting period was concerned with gaining an improved understanding of the processes in high-resistivity semiconductors and also with the elucidation of the highly intriguing but not yet clearly understood behaviour of two-dimensional electron gas in a nearly-cut-off FET. We report progress in both these areas. GRA

N89-21680# Texas Univ., Austin. Dept. of Electrical and Computer Engineering.
MAGNETIC PROPERTIES OF NANO-HETEROGENEOUS AMORPHOUS, THIN FILMS Annual Technical Report, 1 Jun. 1987 - 31 May 1988
Rogers M. Walser 20 Dec. 1988 11 p
(Contract F49620-87-C-0067)
(AD-A203727; AFOSR-89-0064TR) Avail: NTIS HC A03/MF A01 CSCL 07B

Substantial progress has been made in processing nano heterogeneous, amorphous thin films with attractive magnetic properties. Work has been concentrated on two categories of sputtered thin films: (1) soft magnetic, CoB and CoNbZr alloy thin films, and (2) magneto-optical, compositionally modulated Gd/Co multilayer thin films. We are attempting to understand and control the nanoscale heterogeneous structures of these films for application to, respectively, thin film magnetic recording heads, and magneto-optical recording. GRA

N89-21681# Institute for Defense Analyses, Alexandria, VA.
CENTRAL RESEARCH PROJECT REPORT ON SUPERCONDUCTIVITY (1988). PART 1: MATERIALS AND IR DETECTORS Final Report, Mar. - Sep. 1988
William S. Hong, John E. Hove, and Mark S. Taylor Dec. 1988 40 p
(AD-A203891; AD-E501065; IDA-M-548-Pt-1; IDA/HQ-88-34008)
Avail: NTIS HC A03/MF A01 CSCL 20C

This report reviews and summarizes available information on the phases and crystal structures of known and predicted high temperature superconductors (HTS). Materials involving thallium have already exhibited critical temperatures up to 125 K, and techniques have been suggested to increase this value. Recent theoretical efforts predict that room-temperature superconducting materials, if possible at all, may require different chemical compositions than those oxides presently under investigation. A second part of this report reviews the possible direct use of HTS as infrared sensor elements. This indicates little or no advantage over semiconductors; however, HTS use in the signal-processing circuitry of detector arrays may be highly beneficial. A second (later) report will describe a quantitative analysis on the feasibility of a self-guided probe weapon using superconducting magnetic field gradient sensors. While additional analysis and calculations are still necessary, the tentative conclusion on this Part 2 report is that an HTS seeker and guidance system may be feasible for the destruction of tanks, ships, submarines, or countermeasures such as flares, camouflage, or smoke screens. GRA

N89-21682# Air Force Wright Aeronautical Labs., Wright-Patterson AFB, OH. Electro-Optics Technology Branch.
SPECTROSCOPY AND LASER PERFORMANCE OF Ti(SUP 3+) DOPED AND Cr(SUP 3+), Nd(SUP 3+) CO-DOPED CRYSTALS Final Report, Nov. 1984 - Dec. 1987
K. L. Schepler 24 Aug. 1988 109 p
(AD-A203911; AFWAL-TR-88-1125) Avail: NTIS HC A06/MF A01 CSCL 07B

Lasers used in airborne applications need to be compact, rugged, versatile, and efficient. The objective of this in house research program was to explore, assess, and demonstrate the performance of new, solid state laser materials which have high efficiency and broadband tunability. The temperature dependent spectroscopy of titanium doped sapphire was investigated in detail. Laser performance of commercially available Ti:sapphire crystals was demonstrated to be near the theoretical quantum slope efficiency limit. Tuning was demonstrated over the 695 to 864 nm region using a single set of mirrors. Mirror damage limited energy per pulse to 8 mJ. Ti3+ ions were introduced into other crystalline hosts. Spectroscopic samples of Ti:YA103, Ti:YAG, and Ti:GSAG (Gd-Sc-Al garnet) were grown. Absorption, fluorescence and fluorescence lifetime were measured for each of these samples. GRA

N89-21683# Naval Research Lab., Washington, DC. Composites and Ceramics Branch.
FILM ELASTIC PROPERTIES DETERMINED BY THE INDENTATION TEST-THEORETICAL CONSIDERATIONS Interim Report
H. Y. Yu (Geo-Centers, Inc., Fort Washington, MD.), S. C. Sanday, and B. B. Rath 12 Jan. 1989 33 p
(AD-A203997; NRL-9168) Avail: NTIS HC A03/MF A01 CSCL 20L

The elastic solutions of axisymmetric mixed boundary value problems are considered. An elastic layer is assumed to be either in smooth contact or perfectly bonded to a semi-infinite elastic half-space. The elastic field caused by the indentation of the elastic layer by a rigid indenter is solved for spherical, conical, and flat-ended-cylindrical indenters. The results are obtained by solving a Fredholm integral equation of the second kind with a continuous symmetrical kernel that depends on the bonding conditions. Numerical results are given for several combinations of film and substrate elastic moduli and film thicknesses. These results provide a guideline for selecting appropriate film thickness and substrates to determine the elastic constants of thin films. GRA

N89-21684# Oak Ridge National Lab., TN.
STRUCTURE MAPS AND PHASE STABILITY IN AlTi3 ALLOYED WITH RARE-EARTH ELEMENTS
C. T. Liu, J. A. Horton, and D. G. Pettifor 1988 6 p Presented at the MRS Symposium on High-Temperature Ordered Intermetallic Alloys, Boston, MA, 28 Nov. 1988
(Contract DE-AC05-84OR-21400)
(DE89-005106; CONF-8811161-2) Avail: NTIS HC A02/MF A01

Rare-earth elements including Y, Er and Sc were added to AlTi3 for stabilizing the L1 sub 2 ordered crystal structure, as predicted by the AB3 structure map. The crystal structure and phase composition in the AlTi3 alloys were studied by electron microprobe analysis, X-ray diffraction and TEM. All the results indicate that rare-earth additions are unable to change the crystal structure of AlTi3 from DO sub 19 to L1 sub 2 . The failure to stabilize the L1 sub 2 structure cannot be simply related to atomic size and solubility limit of the rare-earth elements in AlTi3. DOE

N89-21685# Los Alamos National Lab., NM. Theoretical Div.
ATOMISTIC SIMULATIONS OF INTERFACES IN METALS AND ALLOYS
S. P. Chen 1988 13 p Presented at the Fall Meeting of the Materials Research Society, Boston, MA, 28 Nov. 1988
(Contract W-7405-eng-36)
(DE89-006521; LA-UR-89-115; CONF-881155-45) Avail: NTIS HC A03/MF A01

We have used embedded atom potentials to simulate the surfaces, thin films and grain boundaries in metals (Ni and Al) and alloys (NiAl and Ni3Al). The calculated surface relaxations and ripplings of free surfaces are in good agreement with experiments. A new interference phenomena of interlayer relaxation in thin films are observed in the simulation. The segregation behavior of B and S and their effects on the mechanical properties of Ni3Al are correctly predicted with potentials fitted to data obtained by electronic band structure calculations. DOE

N89-21686# Argonne National Lab., IL. Materials Science Div.
AN IN-SITU, HIGH-TEMPERATURE STUDY OF THE SUPERCONDUCTOR YBa1.67Sr0.33Cu3O(6+x)
John Faber, Jr., H. Shaked, B. W. Veal, R. L. Hitterman, A. P. Paulikas, L. J. Nowicki, and J. W. Downey Nov. 1988 13 p Presented at the 41st Pacific Coast Regional Meeting of American Ceramic Society, San Francisco, CA, 24 Oct. 1988
(Contract W-31-109-eng-38)
(DE89-007375; CONF-8810195-5) Avail: NTIS HC A03/MF A01

Neutron diffraction is a powerful scientific probe for the study of ceramic materials. Perhaps the most interesting structural studies of ceramics involve analyzing property behavior under in-situ conditions. This technique has been used to study the high-T (sub c), Sr-doped 123 material, YBa1.67Sr0.33Cu3O(6+x) at high temperature. An order-disorder transition is observed at T = 650 C. Upon heating, the crystal symmetry changes from orthorhombic (Pmmm) below the transition to tetragonal (P4/mmm) above. The mechanism of the phase transition involves the redistribution of anions on the O(1) and O(5) sites. These sites become equivalent in the high temperature phase. In addition, the anions on these lattice sites do not exhibit temperature-dependent thermal vibration behavior, indicating that this behavior is dominated by static displacements due to nonstoichiometric disorder. DOE

N89-21687# Argonne National Lab., IL.
ORDER IN COLD IONIC SYSTEMS: DYNAMIC EFFECTS
John P. Schiffer 1988 39 p Presented at the Workshop on Crystalline Ion Beams, Wertheim, Germany, F.R., 4 Oct. 1988
(Contract W-31-109-eng-38)
(DE89-007377; CONF-8810321-1) Avail: NTIS HC A03/MF A01

The present state and recent developments in Molecular Dynamics calculations modeling cooled heavy-ion beams are summarized. First, a frame of reference is established, summarizing what has happened in the past; then the properties of model systems of cold ions studied in Molecular Dynamics calculations are reviewed, with static boundary conditions with which an ordered state is revealed; finally, more recent results on such modelling, adding the complications in the (time-dependent) boundary conditions that begin to approach real storage rings (ion traps) are reported. DOE

N89-21688# Los Alamos National Lab., NM.
FERMI LIQUID THEORY FOR HIGH TEMPERATURE SUPERCONDUCTORS
Kevin S. Bedell 1988 12 p Presented at the Interacting Electrons in Reduced Dimensions, Torino, Italy, 3 Oct. 1988
(Contract W-7405-eng-36)
(DE89-007982; LA-UR-89-501; CONF-8810299-3) Avail: NTIS HC A03/MF A01

In this article the Fermi liquid theory of metals is discussed starting from Luttinger's theorem. The content of Luttinger's Theorem and its implications for microscopic theories of high temperature superconductors are discussed. A simple quasi-2d Fermi liquid theory is introduced and some of its properties are calculated. It is argued that a number of experiments on YBa2Cu3O sub 6+x, x is much greater than 0.5, strongly suggest the existence of a Fermi surface and thereby a Fermi liquid normal state. DOE

N89-21689# California Univ., Berkeley. Lawrence Berkeley Lab. National Center for Electron Microscopy.
STUDY OF SEMICONDUCTOR VALENCE PLASMON LINE SHAPES VIA ELECTRON ENERGY-LOSS SPECTROSCOPY IN THE TRANSMISSION ELECTRON MICROSCOPE Ph.D. Thesis
Michael K. Kundmann Nov. 1988 198 p Prepared in cooperation with California Univ., Berkeley
(Contract DE-AC03-76SF-00098)
(DE89-008152; LBL-26617) Avail: NTIS HC A09/MF A01

Electron energy-loss spectra of the semiconductors Si, AlAs, GaAs, InAs, InP, and Ge are examined in detail in the regime of outer-shell and plasmon energy losses (0 to 100eV). Particular emphasis is placed on modeling and analyzing the shapes of the bulk valence plasmon lines. A line shape model based on early work by Froehlich is derived and compared to single-scattering probability distributions extracted from the measured spectra. Model and data are found to be in excellent agreement, thus pointing the way to systematic characterization of the plasmon component of EELS spectra. The model is applied to three separate investigations. DOE

N89-21690# California Univ., Berkeley. Lawrence Berkeley Lab.
CHARACTERIZATION OF Nb-Al SUPERCONDUCTING MATERIAL Ph.D. Thesis
Yoonsoon Im Dec. 1988 126 p
(Contract DE-AC03-76SF-00098)
(DE89-008296; LBL-26381) Avail: NTIS HC A07/MF A01

The superconducting A15 phase formation in the Nb/Al binary system was studied in order to provide a systematic approach toward achieving optimum processing conditions for Nb/Al superconducting wires. A series of Nb/Al multi-layered thin-film samples was made to simulate reactions in powder metallurgy (P/M) processed wires while a Nb-Al bulk sample was made by an arc-welding technique to study reactions in the bulk. It was found that the reactions in P/M wires and multi-layered thin-film samples were governed by kinetics while those in the bulk sample were governed by thermodynamics. The optimum Al/Nb layer configuration to avoid remaining Nb or Nb2Al was qualitatively calculated to be 1100 A to approx. 1260 A for Nb and 290 A to approx. 330 A for Al. The average Nb filament thickness and the critical current densities of various superconducting wires showed good correlation in spite of the differences in processing and the microstructural inhomogeneity. It was shown that the critical current density of a superconducting wire increased by improving its Nb/Al filament distribution. It is concluded that the critical current density of a Nb/Al superconducting wire can be maximized if Nb and Al filaments are reduced to the optimum thickness range and homogeneously distributed. DOE

N89-21741*# Tennessee Technological Univ., Cookeville. Dept. of Mechanical Engineering.
TRANSIENT NATURAL CONVECTION HEAT AND MASS TRANSFER IN CRYSTAL GROWTH
Samuel S. Han *In* Alabama Univ., Research Reports: 1988 NASA/ASEE Summer Faculty Fellowship Program Dec. 1988 24 p (For primary document see N89-21726 14-99)
Avail: NTIS HC A99/MF E03 CSCL 20L

N89-21748*# Florida Inst. of Tech., Melbourne. Dept. of Physics/Space Science.
ELECTRON MOBILITY IN MERCURY CADMIUM TELLURIDE
James D. Patterson *In* Alabama Univ., Research Reports: 1988 NASA/ASEE Summer Faculty Fellowship Program Dec. 1988 30 p (For primary document see N89-21726 14-99)
Avail: NTIS HC A99/MF E03 CSCL 20L

77 THERMODYNAMICS AND STATISTICAL PHYSICS

Includes quantum mechanics; theoretical physics; and Bose and Fermi statistics.

For related information see also *25 Inorganic and Physical Chemistry* and *34 Fluid Mechanics and Heat Transfer.*

N89-21691# Air Force Inst. of Tech., Wright-Patterson AFB, OH. School of Engineering.
VARIABLE WALL TEMPERATURE EFFECTS ON MULTICELLULAR NATURAL CONVECTION IN A HORIZONTAL ANNULUS M.S. Thesis
David L. Bennett Dec. 1988 150 p
(AD-A202762; AFIT/GAE/AA/88D-01) Avail: NTIS HC A07/MF A01 CSCL 20M

The purpose of this study was to examine natural convection within a narrow horizontal annulus subject to variable inner cylinder temperature distributions. Both numerical and analytical approaches were taken in determining the effects of variable temperature conditions imposed on the inner cylinder in triggering or suppressing multicellular flow instabilities. The two-dimensional Navier-Stokes equations are simplified into boundary-layer equations for the assumptions of large Rayleigh number, small annular gap, and small Prandtl number. These 2-D unsteady boundary-layer equations are discretized using finite-differencing techniques. Numerical solutions to these governing equations are then obtained by using a stable second-order, fully-implicit, time-accurate, Gauss-Siedel iterative procedure. In addition, analytical steady-state solutions to these simplified equations are obtained using perturbation methods. GRA

N89-21692# Little (Arthur D.), Inc., Cambridge, MA.
THERMOMECHANICAL ANALYSIS WITH PHASE TRANSFORMATIONS: A UNIFIED APPROACH Final Report, 1 Nov. 1985 - 9 Dec. 1988
Daniel C. Peirce 9 Dec. 1988 28 p
(Contract DAAL03-86-C-0001)
(AD-A203383; ARO-22578.2-EG) Avail: NTIS HC A03/MF A01 CSCL 20M

The technical content of this final report describes numerical methodology for analyzing a broad class of materials processing problems. The method emphasizes a close coupling of heat transfer, plastic deformation, and phase transformation. Implementation of the theoretical developments into a finite element calculation is discussed. GRA

N89-21693 Alabama Univ., Huntsville.
EXPERIMENTALLY VERIFIABLE YANG-MILLS SPIN 2 GAUGE THEORY OF GRAVITY WITH GROUP U(1) x SU(2) Ph.D. Thesis
Huei Peng 1988 115 p
Avail: Univ. Microfilms Order No. DA8827802

A Yang-Mills spin 2 gauge theory of gravity is proposed. Based on both the verification of the helicity 2 property of the SU(2) gauge bosons of the theory and the agreement of the theory with most observational and experimental evidence, it is argued that the theory is truly a gravitational theory. Generation by the 4-momentum P sup mu of a fermion of U(1) x SU(2) internal symmetry group for gravity, but not the transformation group T sup 4 is demonstrated. It is shown that the U(1) x SU(2) group represents the time displacement and rotation in ordinary space. Thereby internal space associated with gravity is identical with Minkowski spacetime, so a gauge potential of gravity carries two spacetime indices. Then it is verified that the SU(2) gravitational boson has helicity 2. This theory predicts experimentally verifiable gravitomagnetic fields 4 times smaller than that of general relativity. Dissert. Abstr.

N89-21494# Carnegie-Mellon Univ., Pittsburgh, PA. Dept. of Mathematics.
TOWARD A NONEQUILIBRIUM THERMODYNAMICS OF TWO PHASE MATERIALS WITH SHARP INTERFACE
Morton E. Gurtin *In* Army Research Office, Transactions of the Fifth Army Conference on Applied Mathematics and Computing Mar. 1988 p 79-85 Sponsored in part by NSF, Washington, D.C. (For primary document see N89-21490 14-59)
Avail: NTIS HC A99/MF E03 CSCL 20M

N89-21525# Army Engineer Waterways Experiment Station, Vicksburg, MS.
THERMODYNAMIC GAUGE THEORY OF SOLIDS AND QUANTUM LIQUIDS WITH INTERNAL PHASE
Richard A. Weiss *In* Army Research Office, Transactions of the Fifth Army Conference on Applied Mathematics and Computing Mar. 1988 p 649-695 (For primary document see N89-21490 14-59)
Avail: NTIS HC A99/MF E03 CSCL 20C

N89-21526# Army Engineer Waterways Experiment Station, Vicksburg, MS.
LAGRANGIAN FORMULATION OF RELATIVISTIC THERMODYNAMICS
Richard A. Weiss *In* Army Research Office, Transactions of the Fifth Army Conference on Applied Mathematics and Computing Mar. 1988 p 697-734 (For primary document see N89-21490 14-59)
Avail: NTIS HC A99/MF E03 CSCL 20C

80 SOCIAL SCIENCES (GENERAL)

Includes educational matters.

No abstracts in this category.

81 ADMINISTRATION AND MANAGEMENT

Includes management planning and research.

N89-21694# General Accounting Office, Washington, DC.
STRATEGIC DEFENSE INITIATIVE PROGRAM: BETTER MANAGEMENT DIRECTION AND CONTROLS NEEDED
Nov. 1987 27 p
(GAO/NSIAD-88-26) Avail: NTIS HC A03/MF A01

The Department of Defense's (DOD) Strategic Defense Initiative (SDI) is a multibillion dollar research program to determine the feasibility of establishing a defense system against nuclear ballistic missiles by the early 1990s. A key element of the system is battle management/command, control, and communications (BM/C3) which includes the systems that tie weapons, sensors, and computers together. The BM/C3 is controversial because of its complexity, and it could be a critical limiting factor to the entire SDI system design. The SDI Organization (SDIO) management of

the Systems Analysis and Battle Management (SABM) program element was assessed, particularly as it related to the BM/C3 component. Author

N89-21695# Air Force Inst. of Tech., Wright-Patterson AFB, OH. School of Systems and Logistics.
ANALYSIS OF THE FEDERAL AVIATION ADMINISTRATION'S HOST COMPUTER ACQUISITION PROCESS AND POTENTIAL APPLICATION IN DEPARTMENT OF DEFENSE ACQUISITIONS M.S. Thesis
Barbara J. Cohen Sep. 1988 239 p
(AD-A202623; AD-E900870; AFIT/GLM/LSY/88S-11) Avail: NTIS HC A11/MF A01 CSCL 05A

The primary purpose of this investigation was to develop an acquisition management strategy applicable to DOD program management that would help program managers achieve acquisition sucess. A hypothesized management strategy was formulated from the exploration of the successful Federal Aviation Administration's Host computer program. This exploration used personal interviews to identify those management elements and organizational procedures perceived by the 28 respondents to contribute to Host success. The hypothesized management strategy was subsequently evaluated by experts in DOD acquisition. Through personal interviews each element in the management strategy was evaluated for necessity to achieve program success and applicability to DOD programs. The conclusions and recommendations of the study were based on the results of the DOD acquisition expert opinion survey of the hypothesized management strategy. The result was a management strategy to guide DOD program managers in achieving acquisition success that can be tailored to all programs. GRA

N89-21696# System Planning Corp., Arlington, VA.
SYSTEMS ENGINEERING AND TECHNICAL ASSISTANCE Final Report, 5 Dec. 1987 - 31 Oct. 1988
Ruth Rosati Nov. 1988 9 p
(Contract MDA972-88-C-0004; ARPA Order 7272)
(AD-A203479; SPC-88-2949) Avail: NTIS HC A02/MF A01 CSCL 05B

This final technical report on the Systems Engineering and Technical Assistance contract to the Materials Sciences Division of the Defense Sciences Office of DARPA depicts those activities SPC performed to support the statement of work task objectives. Specifically, SPC provided: (1) evaluation support, (2) library support, (3) technical documentation, (4) conference support, (5) engineering analysis services, and (6) management support services. GRA

N89-21697# Air Force Systems Command Liason Office, Ottawa (Ontario).
GUIDE TO CANADIAN AEROSPACE RELATED INDUSTRIES
Donald J. Pearson and John R. Niles 1 Aug. 1988 157 p
(AD-A203738; AFSC-TR-88-06) Avail: NTIS HC A08/MF A01 CSCL 01C

This Guide to Canadian Aerospace Related Industries presents a compilation of descriptive data on 236 companies located in Canada that have expressed interest in doing business with the United States Air Force. This Guide has been prepared with three main objectives in mind: to encourage Air Force Systems Command Project Officers to take advantage of industrial capability of Canada; to engender interest within AFSC for participating in the U.S./Canada Defense Production and Development Sharing Programs, and to encourage Canadian aerospace industry to take a more active role in presenting their capabilities to the USAF. Th companies profiled in this Guide represent a cross-section of Canadian industry and research facilities with capabilities that may be of interest to the USAF research and development and logistics communities. GRA

82 DOCUMENTATION AND INFORMATION SCIENCE

Includes information management; information storage and retrieval technology; technical writing; graphic arts; and micrography.

For computer documentation see *61 Computer Programming and Software.*

N89-21698# Space Environment Services Center, Boulder, CO.
SESC (SPACE ENVIRONMENT SERVICES CENTER) GLOSSARY OF SOLAR-TERRESTRIAL TERMS, 2ND EDITION
Aug. 1988 74 p
(PB89-120802) Avail: NTIS HC A04/MF A01 CSCL 05B

A collection of customized definitions and standard terms specifically used by the Space Environment Services Center (SESC) in its products, publications, and user support systems is presented. B.G.

N89-21699# Massachusetts Inst. of Tech., Cambridge. Research Lab. of Electronics.
SPEECH DATABASE DEVELOPMENT Final Technical Report, 27 Jun. 1985 - 26 Jun. 1987
Victor W. Zue 21 Nov. 1988 45 p
(Contract N00039-85-C-0341)
(AD-A202461) Avail: NTIS HC A03/MF A01 CSCL 25D

The development of an acoustic - phonetic database is thought to be crucial to the speech program because the acoustic realization of phonemes depends on complex interactions among a multitude of factors. Therefore, in order to successfully develop a speaker-independent, phonetically-based speech recognition system, a large body of speech data, collected from many speakers, is needed to help us discover and quantify these context-dependent phenomena. In addition, the speech database can serve two other functions. First, it can be used for training certain speech recognition systems. For some algorithms, such as hidden Markov modelling (HMM), a large amount of training data is needed to obtain stable estimates of the parameters of the stochastic models. For rule-based algorithms, substantial amounts of data are also needed in order to set proper thresholds on speech parameters. Second, the database can be used for performance evaluation. Given the many different approaches to the speech recognition problem, it is often difficult to compare their relative merits. Testing specific recognition algorithms or entire speech recognition systems on a common database will provide a means to evaluate their relative performance. GRA

N89-21700# Defense Technical Information Center, Alexandria, VA. Office of Information Systems and Technology.
EVALUATION OF THE HIGH TEMPERATURE MATERIALS INFORMATION ANALYSIS CENTER ONLINE NUMERIC DATABASE
Huddy B. Haller Jun. 1988 245 p
(AD-A202900; DTIC/TR-88/13) Avail: NTIS HC A11/MF A01 CSCL 05B

High Temperature Materials Information Analysis Center (HTMIAC) operated by Purdue Univ. under the direction of Dr. C. Y. Ho, requested funds from the Defense Technical Information Center (DTIC) for fiscal year 1988. HTMIAC wanted to convert their high temperature materials numeric data to an online system. Their intention was for DTIC to fund putting the data online, and for the user community to fund maintaining the data online. DTIC agreed to the arrangement for several reasons. High temperature materials data users are also DTIC users and DTIC had never been involved in a numeric database development effort. GRA

N89-21701# Defense Technical Information Center, Alexandria, VA. Office of Information Systems and Technology.
DEFENSE TECHNICAL INFORMATION CENTER'S ROLE IN NUMERIC DATABASE DEVELOPMENT
Huddy B. Haller Aug. 1988 17 p
(AD-A202901; DTIC/TR-88/14) Avail: NTIS HC A03/MF A01 CSCL 05B

Computers have changed the way we handle and distribute numeric data. Computers provide available information, quickly and with various data manipulations for analyses, calculations and evaluations. DTIC has a role to play in developing numeric databases because these new resources are causing DTIC's users' needs to change. DTIC 2000, the program plan, justifies DTIC's participation in numeric database efforts. Traditional bibliographic resources that DTIC provides will no longer suffice because of the advent of computers. Numeric databases provide end users the data itself, not just pointers. Also, DTIC users will be changing because more end users will do their own searches of numeric databases. Intermediary responsibilities will increase because they will assist end users. GRA

N89-21702# Stanford Univ., CA.
ACQUIRING GENERALIZATIONS TO ORGANIZE HUMAN DATABASES Interim Report, 1 Sep. 1987 - 31 Aug. 1988
Gordon H. Bower and John Clapper 1 Oct. 1988 21 p
(Grant AF-AFOSR-0282-87; AF Proj. 2313)
(AD-A202964; AFOSR-88-1206TR) Avail: NTIS HC A03/MF A01 CSCL 05I

Five experiments are briefly described in this report, and plans for three further experiments are set forth. We are investigating the consequences of people forming concepts or categories after they've been exposed to a collection of instances (stimulus objects, patterns, events) for which certain features are highly inter-correlated. One primary consequence is that once such regularities are discovered, they are exploited to greatly simplify the recording of new instances into memory. In particular, new instances come to be recorded simply in terms of their belonging to a familiar category plus having a few distinctive features. We've found strong evidence for this kind of coding of instances. A second consequence is that once the category (correlated features) of an instance is identified, the person can focus his learning efforts on recording the distinctive features of the instances, resulting in better memory for this information. In a short-term memory experiment, we've found strong evidence for this strategy. A third consequence of people learning consistently-correlated features of stimuli is that it affects the way they judge the similarity of two instances. GRA

N89-21703# General Electric Co., Philadelphia, PA. Space Technology Products.
DEVELOPMENT OF THE DOMAIN NAME SYSTEM
Paul V. Mockapetris and Kevin J. Dunlap Dec. 1988 14 p Repr. from SIGCOMM '88 Symposium Communications, Architectures and Protocols, held in Stanford, CA, 16-19 Aug. 1988
(Contract MDA903-87-C-0719)
(AD-A203901; ISI/RS-88-219) Avail: NTIS HC A03/MF A01 CSCL 12G

The Domain Name System (DNS) provides name service for the DARPA Internet. It is one of the largest name services in operation today, serves as a highly diverse community of hosts, users, and networks, and uses a unique combination of hierarchies, caching, and datagram access. This paper examines the ideas behind the initial design of the DNS in 1983, discusses the evolution of these ideas into current implementations and usages, notes conspicuous surprises, successes, and shortcomings, and attempts to predict its future evolution. GRA

N89-21704# Defense Applied Information Technology Center, Alexandria, VA. Hypermedia Lab.
SCIENTIFIC AND TECHNICAL INFORMATION NETWORK (STINET) AND DOD GATEWAY INFORMATION SYSTEM (DGIS): REFERENCE PUBLICATIONS BIBLIOGRAPHY
Allan D. Kuhn Dec. 1988 16 p
(AD-A203926; DAITC/TR-88/011; DTIC/TR-89/6) Avail: NTIS HC A03/MF A01 CSCL 05B

This bibliography lists publications resulting from the efforts of the Scientific and Technical Information Network (STINET) program of the Defense Technical Information Center (DTIC). STINET is the logical outgrowth of the information networking activities of the DOD Gateway Information System (DGIS). STINET is more comprehensive in that it is the amalgamation and coalescence of many efforts, all reflected in this bibliography. Additional references to publications from outside organizations are included, as having direct bearing or influence on STINET development programs. The bibliography was begun in October 1985, contains about 85 references and goes through to the end of December 1988. GRA

N89-21705 Purdue Univ., West Lafayette, IN.
INFORMATION ACQUISITION FOR MODEL CONSTRUCTION: AN INTEGRATIVE, DECISION-THEORETIC PERSPECTIVE Ph.D. Thesis
Ramakrishnan Pakath 1988 140 p
Avail: Univ. Microfilms Order No. DA8900713

Most mathematical models of decision making assume that either complete and accurate input parameter information is freely and readily available or that one must resort to probabilistic modeling when dealing with uncertain information. Very often, the decision maker has the time and resources needed for acquiring information. Further, practicing decision makers favor easily understood and implemented satisfying (satisfying + sacrificing) solution methods for the decision models constructed, as opposed to complicated optimization techniques. This is a key requirement for decision support system design. The use of meta models that guide the decision model specification process are proposed and appropriate decision strategies are suggested. Such meta models assume the decider can choose from several information completeness levels with the consequential effects on both information costs and decision quality. Examples of the construction and solution of such meta models in the context of static and dynamic decision scenarios are presented. Dissert. Abstr.

N89-21706# Tennessee Univ., Knoxville.
AUTOMATED LIBRARY SYSTEMS AND DOCUMENT TRACKING SYSTEMS: COMMERCIAL SOFTWARE ALTERNATIVES, VOLUME 1
J. T. Phillips and P. M. Tarrant Feb. 1989 138 p Sponsored in part by Pacific Missile Test Center, Point Mugu, CA Prepared for Oak Ridge Gaseous Diffusion Plant, TN
(Contract DE-AC05-84OT-21400)
(DE89-007716; K/DSRD-55-Vol-1) Avail: NTIS HC A07/MF A01

Automated Library Systems (ALS) have become complex and powerful applications, and they are increasingly selected as appropriate solutions to the challenge of tracking reports and other documents within organizations. The present ALS prototype at the Pacific Missile Testing Center (PMTC) at Point Mugu, California, was developed in-house and has been in existence for some time. However, with an expected change in the present computing environment on which the ALS presently resides (UNIVAC 1100), a discussion of the features of potential commercial software alternatives was requested. The purpose of this study was to provide an information base of presently available software systems that are similar in operation or capabilities to the present ALS at PMTC. A future step will entail review of this data and begin a selection process. Various Automated Library Systems and Automated Records Management Systems were profiled to allow comparison of their features to the present system. A bibliography of selected readings was provided to assist the PMTC in its initial effort to assess future needs. DOE

N89-21707# Syscon Corp., San Diego, CA.
LOCKHEED AERONAUTICAL SYSTEMS COMPANY TECHNICAL ORDER TRANSFER TESTS
15 Dec. 1988 67 p Prepared for Lawrence Livermore National Lab., CA and Air Force Logistics Command, Wright-Patterson AFB, OH Prepared in cooperation with Lockheed Aeronautical Systems Co., Marietta, GA
(Contract W-7405-eng-48)
(DE89-008092; UCRL-21177; AITI-88-001; PO-2193303) Avail: NTIS HC A04/MF A01

The AFLC/AITI Standards Project has been testing the Military

Standard for the Automated Interchange of Technical Information, MIL-STD-1840 (the Standard). The objective of these tests has been to demonstrate the validity of the transfer protocol defined in the Standard itself and the viability of standardized formats for the transfer of technical information employed in other specifications used by the Standard. This test is the last in the series based on the original Standard. Future tests will use MIL-STD-1840A as the reference. Lockheed Aeronautical Systems Company (LASC), Georgia Division, used its publications laboratory to prepare text and illustrations representing the data and format of several types of Air Force technical manuals. This cross section of styles and formats was prepared on two different composition systems and three illustration systems. All text was SGML-encoded, and illustrations were prepared as IGES files or as CCITT Group 4 raster files. DOE

N89-21708# Sandia National Labs., Albuquerque, NM.
MIGRATION STRATEGIES ROLES FOR DATA MANAGEMENT IN CIM
Olin H. Bray 1989 8 p Presented at the 5th International Congress on CIM Databases, Boston, MA, 19 Mar. 1989
(Contract DE-AC04-76DP-00789)
(DE89-008112; SAND-89-0532C; CONF-890366-2) Avail: NTIS HC A02/MF A01

This paper describes the migration path a company goes through as it moves up the data management learning curve. This migration path is based on four distinct roles for data management in computer integrated manufacturing (CIM). The first two sections review the justification for CIM and data management. The first section describes the changing competitive environment manufacturers face and how CIM addresses the problems this situation creates. The second section identifies the two key characteristics of a database management system and the benefits provided. The third section identifies and discusses the four roles for data management in CIM. These four roles and their variations provide snapshots of where a company is on the data management learning curve. The fourth section describes the migration path a company goes through as it moves up the learning curve. DOE

N89-21709# Sandia National Labs., Albuquerque, NM. Computer Aided Design and Integration Dept.
WhiteStar PROJECT ENGINEERING COMPONENT SELECTION DATABASE
Suzanne L. K. Rountree Jan. 1989 21 p
(Contract DE-AC04-76DP-00789)
(DE89-008321; SAND-88-3328; CADCAM-067) Avail: NTIS HC A03/MF A01

The WhiteStar project is a cooperative effort among many directorates at Sandia National Laboratories, Albuquerque to provide weapon and space systems design engineers with needed part characterization data. The purpose of WhiteStar is to encourage the use of standard parts through development of a user-convenient standard parts database containing quality design data and technical characteristics for standard electronic parts. WhiteStar is following the WhiteStar Project Requirements Document to guide the project design and implementation. WhiteStar project members are working with the SNLA Standard Parts Division to standardize the data requirements and to reflect those requirements in the WhiteStar database. There will be a phased incorporation of data by type/subtype. Continued discussions with engineering users will address user needs early and will assure users that the application product is user-oriented in its implementation. DOE

83 ECONOMICS AND COST ANALYSIS

Includes cost effectiveness studies.

N89-21710# Air Force Inst. of Tech., Wright-Patterson AFB, OH. School of Systems and Logistics.
AN ANALYSIS OF THE BIENNIAL BUDGET PROCESS M.S. Thesis
Luvenia M. Shuman Sep. 1988 68 p
(AD-A202626; AD-E900870; AFIT/GLM/LSY/88S-66) Avail: NTIS HC A04/MF A01 CSCL 05A

This thesis analyzed a Federal biennial budget process from a congressional viewpoint. The thesis examined the reasons for considering the adoption a biennial budget process and explored possible advantages and disadvantages associated with a biennial budget process. A literature search was performed to outline the budget process prior to consideration of a biennial budget process, to determine the original purpose and support for the requirement of a biennial budget submission, and to describe some of the alleged advantages and disadvantages associated with a biennial budget process. A structured interview questionnaire was developed from the information gathered during the literature review. Experts in the field were identified and interviews arranged with the assistance of the Air Force Legislative Liaison Office. A total of 16 interviews were conducted over a five day period in Washington, DC during May 1988. The informed opinions of the committee staffers and defense analysts involved in the spending portions of the Federal budget process were used to indicate the congressional viewpoints on Federal biennial budgeting. GRA

84 LAW, POLITICAL SCIENCE AND SPACE POLICY

Includes NASA appropriation hearings; aviation law; space law and policy; international law; international cooperation; and patent policy.

N89-21711# Air War Coll., Maxwell AFB, AL.
NATIONAL SPACE POLICY
Ernest B. Sutton May 1988 93 p
(AD-A202644; AD-E900870) Avail: NTIS HC A05/MF A01 CSCL 22A

National space policy forms the foundation for decisions and direction of the United States national space program. This review begins with the Eisenhower era and the launching of Sputnik 1, considered by most as the start of the space race with the Soviet Union for national space preeminence. Succeeding administrations are discussed to provide the historical setting affecting the actions of presidents, leaders within NASA, the DOD, and Congress as well as other players in the national space arena. This review analyzes the latest national space policy, established by President Reagan in February, 1988. Finally, specific space development programs are offered as topics which will demand the attention of future administrations. GRA

85 URBAN TECHNOLOGY AND TRANSPORTATION

Includes applications of space technology to urban problems; technology transfer; technology assessment; and surface and mass transportation.

For related information see also *03 Air Transportation and Safety, 16 Space Transportation,* and *44 Energy Production and Conversion.*

No abstracts in this category.

88 SPACE SCIENCES (GENERAL)

No abstracts in this category.

89 ASTRONOMY

Includes radio, gamma-ray, and infrared astronomy, and astrometry.

N89-21712*# National Aeronautics and Space Administration. Marshall Space Flight Center, Huntsville, AL.
NASA MARSHALL SPACE FLIGHT CENTER SOLAR OBSERVATORY REPORT, JANUARY - DECEMBER 1987
James E. Smith Mar. 1989 74 p
(NASA-TM-100360; NAS 1.15:100360) Avail: NTIS HC A04/MF A01 CSCL 03A

This report provides a description of the NASA Marshall Space Flight Center's Solar Vector Magnetograph Facility and gives a summary of its observations and data reduction during January to December 1987. The systems that make up the facility are a magnetograph telescope, an H-alpha telescope, a Questar telescope, and a computer code. The data are represented by longitudinal contours with azimuth plots. Author

N89-21713# Lowell Observatory, Flagstaff, AZ.
LUMINOSITY VARIATIONS OF STARS SIMILAR TO THE SUN Final Report, 1 Jan. 1984 - 31 Dec. 1987
G. W. Lockwood and B. A. Skiff 1 Sep. 1988 109 p
(Contract F19628-84-K-0013)
(AD-A203864; AFGL-TR-88-0221) Avail: NTIS HC A06/MF A01 CSCL 03A

Using precision differential photoelectric photometry at 472 and 551 nm, the variability characteristics of 36 solar-type stars (spectral types F, G, and K) and their 65 comparison stars were determined from nearly 2000 measurements made on more than 350 nights between March 1984 and December 1987. The principal conclusions are: (1) about one-half the program stars and one-fourth the comparison stars are demonstrably variable on short-time scales at levels typically 0.3 percent and greater, (2) variability is about twice as common among K stars as among F- and G-type stars, (3) rotational modulation was measurable in nine stars, (4) sixteen program stars and eight comparison stars varied by more than 0.5 percent over four seasons, (5) twenty-six pairs of exceptionally stable stars varied by less than 0.3 percent over four years, (6) variability of the program stars is strongly correlated with independently determined chromospheric activity levels, and (7) inter-season variability is more consistent with long-term cyclic variation than with stochastic fluctuations. GRA

N89-21714 Manchester Univ. (England).
THE 408 MHz RADIO OBSERVATIONS OF A QUASAR SAMPLE Ph.D. Thesis
Allison Reid 1987 249 p
Avail: Univ. Microfilms Order No. BRD83937

The results of 408 MHz MERLIN (Multi-Element Radio Link Interferometer Network) observations of a sample of 54 quasars selected from the Jodrell Bank 966 MHz survey are presented. Maps of the 408 MHz sources were used in conjunction with existing observations at 1.4, 1.6, and 5 GHz to obtain flux density cores, lobes, hotspots and jets. Statistical properties of the quasar sample were investigated. The relationship between structural class and spectral index was compared with other radio samples selected at different frequencies. The properties of flat-spectrum, core-dominated quasars were compared with those of the extended, steep-spectrum, lobe-dominated quasars in the sample, and both were tested for orientation effects caused by relativistic beaming. It was found that in general, core-dominated sources have properties that correlate with the orientation of the source axis to the line of sight, and that the cores of lobe-dominated sources also show this effect. However, in the lobe-dominated sources intrinsic asymmetries on a lobe to lobe basis play a more significant role than orientation. Dissert. Abstr.

90 ASTROPHYSICS

Includes cosmology; celestial mechanics; space plasmas; and interstellar and interplanetary gases and dust.
For related information see also *75 Plasma Physics*.

N89-21715*# Chicago Univ., IL.
SUPERNOVA 1987A: 18 MONTHS LATER
David N. Schramm Jan. 1989 20 p Prepared in cooperation with Fermi National Accelerator Lab., Bataiva, IL
(Grant NAGw-1340)
(NASA-CR-184891; NAS 1.26:184891; FERMILAB-Conf-89/27-A)
Avail: NTIS HC A03/MF A01 CSCL 03B

An overview of the significance for physics of the closest visual supernova in almost 400 years is presented. The supernova occurred in the Large Magellanic Cloud (LMC), approx. 50 kpc away. The supernova star was a massive star of approx. 15 to 20 solar mass. Observations now show that it was once a red giant but lost its outer envelope. The lower than standard luminosity and higher observed velocities are a natural consequence of the pre-supernova star being a blue rather than a red (supergiant). Of particular importance to physicsts is the detection of neutrinos from the event by detectors in the United States and Japan. Not only did this establish extra-solar system neutrino astronomy, but it also constrained the properties of neutrino. It is shown that the well established Kamioka-IMB neutrino burst experimentally implies an event with about 2 to 4 x 10 to the 53rd power ergs emitted in neutrinos and a temperature, T sub nu e, of between 4 and 4.5 MeV. This event is in excellent agreement with what one would expect from the gravitational core collapse of a massive star. The anticipated frequency of collapse events in our Galaxy is discussed. Author

N89-21716*# Fermi National Accelerator Lab., Batavia, IL. Astrophysics Center.
EVOLUTION OF COSMIC STRING NETWORKS
Andreas Albrecht and Neil Turok (Princeton Univ., NJ.) Mar. 1989 80 p
(Grant NAGw-1340)
(NASA-CR-182836; NAS 1.26:182836; FERMILAB-Pub-89/42-A; PUPT-89-1119) Avail: NTIS HC A05/MF A01 CSCL 03B

A discussion of the evolution and observable consequences of a network of cosmic strings is given. A simple model for the evolution of the string network is presented, and related to the statistical mechanics of string networks. The model predicts the long string density throughout the history of the universe from a single parameter, which researchers calculate in radiation era simulations. The statistical mechanics arguments indicate a particular thermal form for the spectrum of loops chopped off the network. Detailed numerical simulations of string networks in expanding backgrounds are performed to test the model. Consequences for large scale structure, the microwave and gravity wave backgrounds, nucleosynthesis and gravitational lensing are calculated. Author

N89-21717# Stanford Univ., CA. Center for Space Science and Astrophysics.
FORCE-FREE MAGNETIC FIELDS: IS THERE A LOSS OF EQUILIBRIUM
James A. Klimchuk and Peter A. Sturrock 6 Dec. 1988 31 p
(Contract N00014-85-K-0111)
(AD-A203030) Avail: NTIS HC A03/MF A01 CSCL 03B

This paper examines concept in solar physics that is known as loss of equilibrium in which a sequence of force-free magnetic fields, said to represent a possible quasi-static evolution of solar magnetic fields, reaches a critical configuration beyond which no acceptable solution of the prescribed form exists. This concept is used to explain eruptive phenomena ranging from solar flares to coronal mass ejections. Certain sequences of force-free configurations are discussed that exhibit a loss of equilibrium, and it is argued that the concept is devoid of physical significance since each sequence is defined a way that does not represent an acceptable thought experiment. For example, the sequence may be defined in terms of a global constraint on the boundary

conditions, or the evolution of the sequence may require the creation of magnetic flux that is not connected to the photosphere and is not present in the original configuration. The global constraints typically occur in using the so-called generating function method. An acceptable thought experiment is proposed to specify the field configuration in terms of photospheric boundary conditions comprising the normal component of the field and the field-line connectivity. Consider a magnetic-field sequence that, when described in terms of a generating function, exhibits a loss of equilibrium and show that, when one instead defines the sequence in terms of the corresponding boundary conditions, the sequence is well behaved. GRA

N89-21718 Minnesota Univ., Minneapolis.
NUMERICAL STUDIES OF GAS FLOW IN SPIRAL GALAXIES Ph.D. Thesis
Bruce Kevin Edgar 1988 176 p
Avail: Univ. Microfilms Order No. DA8900530

A numerical method is described which is designed to treat the dynamics of an infinitesimally thin, differentially rotating gaseous disk. The method is based on the Piecewise Parabolic Method (PPM), a higher-order extension of Godunov's method which allows the accurate computation of small perturbations. The method is suited to the study of the gaseous response to a spiral density wave in a disk galaxy. A series of two-dimensional hydrodynamical models is computed to test the gravitational response of a uniform, isothermal, massless gaseous disk to an imposed spiral gravitational perturbation. Galaxy parameters are based on the galaxy NGC 628. The solutions have shocks inside and outside corotation, depleting the region around corotation. Implied rapid evolution shown by this model suggests that if galaxies exist with such large perturbations, either gas must be replenished from outside the galaxy or the perturbations must be transitory. Inside corotation with the spiral pattern, the loss of angular momentum by the gas increases the angular momentum of the stars, reducing the wave amplitude. Dissert. Abstr.

N89-21719 Washington Univ., Saint Louis, MO.
ION MICROPROBE OF Mg, Ca, Ti AND Fe ISOTOPIC RATIOS AND TRACE ELEMENT ABUNDANCES IN HIBONITE-BEARING INCLUSIONS FROM PRIMITIVE METEORITES Ph.D Thesis
Albert Joseph Fahey 1988 230 p
Avail: Univ. Microfilms Order No. DA8826911

Isotopic abundances of Mg, Ca, and Ti and rare earth elements in 19 hibonite-bearing inclusions from primative meteorites are reported. Measurements were made by means of secondary ion mass spectrometry (CAMECA IMS-3f). The novel hardware and software developments are described in detail. Samples were studied in thin section in order to investigate the relationship between the inclusions and their mineralogical environments. The isotopes of Ca and Ti show large and correlated abundance anomalies in their most neutron-rich isotopes, Ca-48 and Ti-50. Correlation of isotopic anomalies in two different elements is clear evidence for a nucleosynthetic origin of these effects. Various possibilities for the origin of these isotopic anomalies are discussed and it is shown that a 'Cosmic Chemical Memory'-like model of the incomplete mixing of dust grains from one or several supernovae is sufficient to explain the data. Excesses of Mg-26 in these inclusions are not correlated with Ca and Ti isotopic anomalies and appear to show an anti-correlation with effects in Ca and Ti. Dissert. Abstr.

N89-21720 Indiana Univ., Bloomington.
THE EVOLUTION OF ACTIVE GALACTIC NUCLEI AND GLOBULAR CLUSTERS: MULTI-COMPONENT MODELS Ph.D. Thesis
Brian William Murphy 1988 160 p
Avail: Univ. Microfilms Order No. DA8902584

The direct multi-mass Fokker-Planck method is used to follow the evolution of active galactic nuclei (AGN) and globular clusters. These objects are dense stellar systems in which gravitational interactions between individual stars are important. The stellar system contains stars with a realistic range of masses and a seed black hole at the center for AGN models. Stars lose mass or are depleted by tidal disruptions, star-star collisions, and stellar evolution. Conclusions are given and briefly discussed. Dissert. Abstr.

N89-21721 California Inst. of Tech., Pasadena.
A SEARCH FOR GRAVITATIONAL WAVES FROM COALESING BINARY STARS USING THE CALTECH 40 METER GRAVITY WAVE DETECTOR Ph.D. Thesis
Sheryl Leigh Smith 1988 183 p
Avail: Univ. Microfilms Order No. DA8901786

A search for gravitational radiation from coalescing compact binary stars was conducted. This is the first time the Caltech gravity wave detector has been used to search for burst sources. This detector is made of two 40 meter Fabry-Perot interferometers. The mirrors of the Fabry-Perot cavities are suspended, so that they are free to move in response to a gravity wave. The Caltech detector is a prototype for a set of larger detectors (4 km long cavities). The purpose of this search was to develop techniques applicable to the larger detectors. An algorithm was developed which searches for the distinctive wave-form of a coalescing binary, regardless of the masses of the stars in that binary. Thirty-six minutes of data were analyzed. These data spanned one hour and were collected when the Glasgow detector was also operating, (the Glasgow and Caltech detectors had comparable sensitivity at the time of this experiment). The limit this search sets varies with the mass parameter, eta, which is a function of the stars' masses. For two 1.4 solar mass stars no coalescences were observed with h greater than 5 x 10 to the minus 17th power this corresponds to a binary approximately 25 parsecs away. Dissert. Abstr.

N89-21302*# Arizona Univ., Tucson. Planetary Science Inst.
RISK TO CIVILIZATION: A PLANETARY SCIENCE PERSPECTIVE
Clark R. Chapman and David Morrison *In* Lunar and Planetary Inst., Global Catastrophes in Earth History: An Interdisciplinary Conference on Impacts, Volcanism, and Mass Mortality 1988 p 26-27 Prepared in cooperation with Hawaii Univ., Honolulu (For primary document see N89-21287 14-42)
Avail: NTIS HC A11/MF A01 CSCL 03B

N89-21387*# Geological Survey, Flagstaff, AZ.
ASTEROID AND COMET FLUX IN THE NEIGHBORHOOD OF THE EARTH
Eugene M. Shoemaker, Carolyn S. Shoemaker, and Ruth F. Wolfe *In* Lunar and Planetary Inst., Global Catastrophes in Earth History: An Interdisciplinary Conference on Impacts, Volcanism, and Mass Mortality 1988 p 174-176 (For primary document see N89-21287 14-42)
Avail: NTIS HC A11/MF A01 CSCL 03B

N89-21407*# Jet Propulsion Lab., California Inst. of Tech., Pasadena.
THE COMETARY AND ASTEROIDAL IMPACTOR FLUX AT THE EARTH
Paul R. Weissman *In* Lunar and Planetary Inst., Global Catastrophes in Earth History: An Interdisciplinary Conference on Impacts, Volcanism, and Mass Mortality 1988 p 211-212 (For primary document see N89-21287 14-42)
Avail: NTIS HC A11/MF A01 CSCL 03B

N89-21408*# University of Southwestern Louisiana, Lafayette. Dept. of Physics.
DISRUPTION OF GIANT COMETS IN THE SOLAR SYSTEM AND AROUND OTHER STARS
D. P. Whitmire and J. J. Matese *In* Lunar and Planetary Inst., Global Catastrophes in Earth History: An Interdisciplinary Conference on Impacts, Volcanism, and Mass Mortality 1988 p 213-214 (For primary document see N89-21287 14-42)
Avail: NTIS HC A11/MF A01 CSCL 03B

N89-21414*# Academia Sinica, Beijing (China). Inst. of Geology.
NEW APPROACH TO THE ORIGIN OF THE TEKTITE IN CHINA
Zhang Qin-Wen, Xu Dao-Yi, and Yan Zheng *In* Lunar and Planetary Inst., Global Catastrophes in Earth History: An Interdisciplinary Conference on Impacts, Volcanism, and Mass Mortality 1988 p 225-226 Prepared in cooperation with State Seismological Bureau of China, Beijing (For primary document see N89-21287 14-42)
Avail: NTIS HC A11/MF A01 CSCL 03B

91 LUNAR AND PLANETARY EXPLORATION

Includes planetology; and manned and unmanned flights.
For spacecraft design or space stations see *18 Spacecraft Design, Testing and Performance.*

No abstracts in this category.

92 SOLAR PHYSICS

Includes solar activity, solar flares, solar radiation and sunspots.
For related information see *93 Space Radiation.*

N89-21722# National Geophysical Data Center, Boulder, CO.
SOLAR-GEOPHYSICAL DATA NUMBER 528, AUGUST 1988. PART 2: (COMPREHENSIVE REPORTS). DATA FOR FEBRUARY 1988
Helen E. Coffey, ed. and John A. McKinnon, ed. Aug. 1988 41 p
(Contract N00014-86-F-0049)
(PB89-109912; SGD-528-Pt-2; ISSN-0038-0911; LC-79-640375)
Avail: NTIS HC A03/MF A01 CSCL 03B
Solar-geophysical information is presented in tabular and graphic form. Categories include data for February 1988; Meudon carte synoptique; solar flares; solar radio bursts; bursts at fixed frequencies; solar X-ray radiation from GOES satellite; mass ejections from the sun; and active prominences and filaments.
B.G.

N89-21723# National Center for Atmospheric Research, Boulder, CO.
NEW PICTURE FOR THE INTERNAL ROTATION OF THE SUN
Cherilynn Ann Morrow 1988 321 p
(Grant NSF ATM-87-09659)
(PB89-113377; NCAR/CT-116) Avail: NTIS HC A14/MF A01 CSCL 03B
For the last decade, solar acoustic oscillations have been used to probe the physical properties of the solar interior. The endeavor is called helioseismology and is based on the fact that shifts in the frequency of an oscillation mode, as observed at the surface, contain information about the physical environment in those regions of the interior where the oscillation has energy. A helioseismic quest is described to determine the angular velocity inside the Sun as a function of depth and latitude. Rotational frequency splittings extracted from 15 days of full-disk observations of the solar acoustic oscillations (l=15-99) obtained with the Fourier Tachometer (a Doppler analyzing instrument designed by Tim Brown) were analyzed. The observed frequency splittings are compared to those generated by several different physically-motivated models for the solar internal angular velocity.
GRA

93 SPACE RADIATION

Includes cosmic radiation; and inner and outer earth's radiation belts.
For biological effects of radiation see *52 Aerospace Medicine.* For theory see *73 Nuclear and High-Energy Physics.*

N89-21724 Oxford Univ. (England).
AN OPTICAL STUDY OF THREE TRANSIENT X-RAY SOURCES Ph.D. Thesis
L. Booth 1987 231 p
Avail: Univ. Microfilms Order No. BRD83726
Photometric and spectroscopic studies were performed over extended periods of three stellar X-ray transient sources. It is proposed that 3A1431-409 is a highly active RS CVn with an envelope of matter surrounding the two stars. X-ray source 4U1258-61 displays properties generally associated with Be star/X-ray sources, but in addition has been seen to lose both the optical emission lines and X-ray activity, suggesting that the surrounding shell of matter has dissipated over a period of years. The extreme X-ray and optical behavior of periodic, recurrent X-ray transient A0538-66 is explained by a B star/neutron star binary system with a highly eccentric orbit (e greater than or equal to .7). Observations were made of A0538-66 during a particularly active epoch in 1982.
Dissert. Abstr.

N89-21725# Los Alamos National Lab., NM.
A NOVEL APPROACH TO GAMMA-RAY AND NEUTRINO ASTRO-PARTICLE PHYSICS: THE GRANDE EXPERIMENT
T. Haines (Maryland Univ., College Park.), A. Adams, R. Bond, C. B. Bratton, V. Chaloupka, M. Cherry, L. Coleman, R. Ellsworth, J. Gaidos, and J. Goodman et al 1988 10 p Presented at the 14th Texas Symposium on Relativistic Astrophysics, Dallas, TX, 11-16 Dec. 1988; sponsored by Maryland Univ., College Park Prepared in cooperation with California Univ., Irvine; Hawaii Univ., Honolulu; Purdue Univ., Arkansas Univ., Little Rock; Louisiana State Univ., Baton Rouge; Warsaw Univ., Poland; George Mason Univ., VA; Columbia Univ., NY; Wisconsin Univ., Madison
(Contract W-7405-eng-36)
(DE89-006515; LA-UR-89-280; CONF-881268-1) Avail: NTIS HC A02/MF A01
The GRANDE experiment is a unique next-generation detector capable of making significant contributions to the fields of neutrino and gamma ray astrophysics as well as performing important conventional high-energy physics investigations. The detector, which covers an area of 250 m by 250 m, is based on the well proven water Cerenkov technique. It will have excellent coverage for potential sources of neutrino emission in the Southern Hemisphere and of VHE and UHE sources in the Northern Hemisphere. For VHE and UHE showers, the low threshold (less than or equal to 10 TeV) and complete coverage for all three shower components (electromagnetic, muonic, and hadronic), are unique. Excellent angular resolution, less than 1 deg for neutrinos and less than 0.3 deg for gamma rays, large acceptance, good energy resolution, and wide energy sensitivity will permit detailed studies of the observed signals enabling a quantitative confrontation with theoretical predictions. The detector and some of its physics capabilities will be described.
DOE

N89-21745*# Mississippi State Univ., Mississippi State. Dept. of Physics and Astronomy.
ANGULAR RESPONSE CALIBRATION OF THE BURST AND TRANSIENT SOURCE EXPERIMENT
John Patrick Lestrade *In* Alabama Univ., Research Reports: 1988 NASA/ASEE Summer Faculty Fellowship Program Dec. 1988 34 p (For primary document see N89-21726 14-99)
Avail: NTIS HC A99/MF E03 CSCL 03B

99 GENERAL

N89-21726*# Alabama Univ., Tuscaloosa.
RESEARCH REPORTS: 1988 NASA/ASEE SUMMER FACULTY FELLOWSHIP PROGRAM Final Report
L. Michael Freeman, ed., Charles R. Chappell, ed., Ernestine K. Cothran, ed., and Gerald R. Karr, ed. Dec. 1988 804 p Program held in Huntsville, AL, 6 Jun. - 12 Aug. 1988
(Grant NGT-01-002-099)
(NASA-CR-183553; NAS 1.26:183553) Avail: NTIS HC A99/MF E03 CSCL 05I

The basic objectives are to further the professional knowledge of qualified engineering and science faculty members; to stimulate an exchange of ideas between participants and NASA: to enrich and refresh the research and teaching activities of the participants' institutions; and to contribute to the research objectives of the NASA centers. Topics addressed include: cryogenics; thunderstorm simulation; computer techniques; computer assisted instruction; system analysis weather forecasting; rocket engine design; crystal growth; control systems design; turbine pumps for the Space Shuttle Main engine; electron mobility; heat transfer predictions; rotor dynamics; mathematical models; computational fluid dynamics; and structural analysis. For individual titles, see N89-21727 through N89-21760.

N89-21727*# Tennessee Univ., Tullahoma. Space Inst.
CRYOGENIC FLUID MANAGEMENT IN SPACE **c31**
Basil N. Antar *In* Alabama Univ., Research Reports: 1988 NASA/ASEE Summer Faculty Fellowship Program Dec. 1988 16 p (For primary document see N89-21726 14-99)
Avail: NTIS HC A99/MF E03 CSCL 13B

Many future space based vehicles and satellites will require on orbit refuelling procedures. Cryogenic fluid management technology is being developed to assess the requirements of such procedures as well as to aid in the design and development of these vehicles. Cryogenic fluid management technology for this application could be divided into two areas of study, one is concerned with fluid transfer process and the other with cryogenic liquid storage. This division is based upon the needed technology for the development of each area. In the first, the interaction of fluid dynamics with thermodynamics is essential, while in the second only thermodynamic analyses are sufficient to define the problem. The following specific process related to the liquid transfer area are discussed: tank chilldown and fill; tank pressurization; liquid positioning; and slosh dynamics and control. These specific issues are discussed in relation with the required technology for their development in the low gravity application area. In each process the relevant physics controlling the technology is identified and methods for resolving some of the basic questions are discussed. Author

N89-21728*# Auburn Univ., AL. Dept. of Electrical Engineering.
FINITE ELEMENT SIMULATION OF THUNDERSTORM ELECTRODYNAMICS IN THE PROXIMITY OF THE STORM **c47**
Michael Edward Baginski *In* Alabama Univ., Research Reports: 1988 NASA/ASEE Summer Faculty Fellowship Program Dec. 1988 22 p (For primary document see N89-21726 14-99)
Avail: NTIS HC A99/MF E03 CSCL 04B

Observations of electric fields, Maxwell current density, and air conductivity over thunderstorms were presented. The measurements were obtained using electric field mils and conductivity probes installed on a U2 aircraft as the aircraft passed approximately directly over an active thunderstorm at an altitude of 18 to 20 km. Accurate electrical observations of this type are rare and provide important information to those involved in numerically modeling a thunderstorm. A preliminary set of computer simulations based on this data were conducted and are described. The simulations show good agreement with measurements and are used to infer the thundercloud's charging current and amount of charge exchanged per flash. Author

N89-21729*# Alabama A & M Univ., Huntsville. Dept. of Mathematics.
REFINING, REVISING, AUGMENTING, COMPILING AND DEVELOPING COMPUTER ASSISTED INSTRUCTION K-12 AEROSPACE MATERIALS FOR IMPLEMENTATION IN NASA SPACELINK ELECTRONIC INFORMATION SYSTEM **c61**
Jean A. Blake *In* Alabama Univ., Research Reports: 1988 NASA/ASEE Summer Faculty Fellowship Program Dec. 1988 8 p (For primary document see N89-21726 14-99)
Avail: NTIS HC A99/MF E03 CSCL 09B

The NASA Spacelink is an electronic information service operated by the Marshall Space Flight Center. The Spacelink contains extensive NASA news and educational resources that can be accessed by a computer and modem. Updates and information are provided on: current NASA news; aeronautics; space exploration: before the Shuttle; space exploration: the Shuttle and beyond; NASA installations; NASA educational services; materials for classroom use; and space program spinoffs. Author

N89-21730*# Tennessee Univ., Chattanooga. Center of Excellence for Computer Applications.
SIRE: A SIMPLE INTERACTIVE RULE EDITOR FOR NICBES **c33**
Alex Bykat *In* Alabama Univ., Research Reports: 1988 NASA/ASEE Summer Faculty Fellowship Program Dec. 1988 22 p (For primary document see N89-21726 14-99)
Avail: NTIS HC A99/MF E03 CSCL 09A

To support evolution of domain expertise, and its representation in an expert system knowledge base, a user-friendly rule base editor is mandatory. The Nickel Cadmium Battery Expert System (NICBES), a prototype of an expert system for the Hubble Space Telescope power storage management system, does not provide such an editor. In the following, a description of a Simple Interactive Rule Base Editor (SIRE) for NICBES is described. The SIRE provides a consistent internal representation of the NICBES knowledge base. It supports knowledge presentation and provides a user-friendly and code language independent medium for rule addition and modification. The SIRE is integrated with NICBES via an interface module. This module provides translation of the internal representation to Prolog-type rules (Horn clauses), latter rule assertion, and a simple mechanism for rule selection for its Prolog inference engine. Author

N89-21731*# South Carolina Univ., Columbia. Dept. of Mechanical Engineering.
SMALL EXPENDABLE DEPLOYER SYSTEM MEASUREMENT ANALYSIS **c18**
Connie K. Carrington *In* Alabama Univ., Research Reports: 1988 NASA/ASEE Summer Faculty Fellowship Program Dec. 1988 16 p (For primary document see N89-21726 14-99)
Avail: NTIS HC A99/MF E03 CSCL 22B

The first on-orbit experiment of the Small Expendable Deployer System (SEDS) for tethered satellites will collect telemetry data for tether length, rate of deployment, and tether tension. The post-flight analysis will use this data to reconstruct the deployment history and determine dynamic characteristics such as tether shape and payload position. Linearized observability analysis has determined that these measurements are adequate to define states for a two-mass tether model, and two state estimators were written. Author

N89-21732*# Texas Technological Univ., Lubbock. Atmospheric Science Group.
THE ROLE OF RADIATION-DYNAMICS INTERACTION IN REGIONAL NUMERICAL WEATHER PREDICTION **c47**
Chia-Bo Chang *In* Alabama Univ., Research Reports: 1988 NASA/ASEE Summer Faculty Fellowship Program Dec. 1988 18 p (For primary document see N89-21726 14-99)
Avail: NTIS HC A99/MF E03 CSCL 04B

The role of radiation-dynamics interaction in regional numerical weather prediction of severe storm environment and mesoscale convective systems over the United States is researched. Based

upon the earlier numerical model simulation experiments, it is believed that such interaction can have a profound impact on the dynamics and thermodynamics of regional weather systems. The research will be carried out using real-data model forecast experiments performed on the Cray-X/MP computer. The forecasting system to be used is a comprehensive mesoscale prediction system which includes analysis and initialization, the dynamic model, and the post-forecast diagnosis codes. The model physics are currently undergoing many improvements in parameterizing radiation processes in the model atmosphere. The forecast experiments in conjunction with in-depth model verification and diagnosis are aimed at a quantitative understanding of the interaction between atmospheric radiation and regional dynamical processes in mesoscale models as well as in nature. Thus, significant advances in regional numerical weather prediction can be made. Results shall also provide valuable information for observational designs in the area of remote sensing techniques to study the characteristics of air-land thermal interaction and moist processes under various atmospheric conditions. Author

N89-21733*# North Carolina Agricultural and Technical State Univ., Greensboro. Dept. of Mechanical Engineering.

COMPUTER CODES FOR THERMAL ANALYSIS OF A SOLID ROCKET MOTOR NOZZLE **c20**

Rajinder Singh Chauhan *In* Alabama Univ., Research Reports: 1988 NASA/ASEE Summer Faculty Fellowship Program Dec. 1988 11 p (For primary document see N89-21726 14-99)
Avail: NTIS HC A99/MF E03 CSCL 21H

A number of computer codes are available for performing thermal analysis of solid rocket motor nozzles. Aerotherm Chemical Equilibrium (ACE) computer program can be used to perform one-dimensional gas expansion to determine the state of the gas at each location of a nozzle. The ACE outputs can be used as input to a computer program called Momentum/Energy Integral Technique (MEIT) for predicting boundary layer development development, shear, and heating on the surface of the nozzle. The output from MEIT can be used as input to another computer program called Aerotherm Charring Material Thermal Response and Ablation Program (CMA). This program is used to calculate oblation or decomposition response of the nozzle material. A code called Failure Analysis Nonlinear Thermal and Structural Integrated Code (FANTASTIC) is also likely to be used for performing thermal analysis of solid rocket motor nozzles after the program is duly verified. A part of the verification work on FANTASTIC was done by using one and two dimension heat transfer examples with known answers. An attempt was made to prepare input for performing thermal analysis of the CCT nozzle using the FANTASTIC computer code. The CCT nozzle problem will first be solved by using ACE, MEIT, and CMA. The same problem will then be solved using FANTASTIC. These results will then be compared for verification of FANTASTIC. Author

N89-21734*# Illinois Univ., Chicago. Dept. of Mechanical Engineering.

RADIATION EFFECT ON ROCKET ENGINE PERFORMANCE **c20**

Huei-huang Chiu *In* Alabama Univ., Research Reports: 1988 NASA/ASEE Summer Faculty Fellowship Program Dec. 1988 41 p (For primary document see N89-21726 14-99)
Avail: NTIS HC A99/MF E03 CSCL 21H

The effects of radiation on the performance of modern rocket propulsion systems operating at high pressure and temperature were recognized as a key issue in the design and operation of various liquid rocket engines of the current and future generations. Critical problem areas of radiation coupled with combustion of bipropellants are assessed and accounted for in the formulation of a universal scaling law incorporated with a radiation-enhanced vaporization combustion model. Numerical algorithms are developed and the pertaining data of the Variable Thrust Engine (VTE) and Space Shuttle Main Engine (SSME) are used to conduct parametric sensitivity studies to predict the principal intercoupling effects of radiation. The analysis reveals that low enthalpy engines, such as the VTE, are vulnerable to a substantial performance set back by the radiative loss, whereas the performance of high enthalpy engines such as the SSME, are hardly affected over a broad range of engine operation. Additionally, combustion enhancement by the radiative heating of the propellant has a significant impact in those propellants with high absorptivity. Finally, the areas of research related with radiation phenomena in bipropellant engines are identified. Author

N89-21735*# Carnegie-Mellon Univ., Pittsburgh, PA. Dept. of Mechanical Engineering.

A PERFORMANCE/LOSS EVALUATION OF SSME HPFTP TURBINE **c37**

Mingking K. Chyu *In* Alabama Univ., Research Reports: 1988 NASA/ASEE Summer Faculty Fellowship Program Dec. 1988 20 p (For primary document see N89-21726 14-99)
Avail: NTIS HC A99/MF E03 CSCL 13I

An evaluation of component losses of the High Pressure Fuel Turbopump (HPFTP) in the Space Shuttle Main Engine (SSME) is performed using a mean-line prediction method. This is accompanied with an extensive review of loss correlations in the literature. The present prediction uses an existing gas path velocity triangle, real LH2 and H2O gas properties and loss correlations selected from the literature. The significant losses incurred in the HPFTP turbine include profile loss, secondary loss, and tip clearance loss. Results obtained from the present prediction are compared to those calculated from a quasi-three dimensional numerical analysis. Except for the clearance loss, the present loss coefficients are in general higher than their counterparts from the quasi-three dimensional analysis. The fact that the mean-line velocity data being unable to represent actual flow fields near the hub and the tip regions is largely responsible for the uncertainty involved in the present method. On the other hand, due mainly to the ad-hoc nature of the studies involved, the correlations currently available in the literature may not be suitable for accurate loss prediction of the particular rocket turbine in the SSME HPFTP. Further studies particularly in the areas of tip clearance loff, coolant loss, secondary loss, and their interactions are desirable. Fundamental phenomena concerning flow unsteadiness in wake shedding and turbulence are also important. Author

N89-21736*# University of Central Arkansas, Conway. Dept. of Physics.

X-RAY FLUORESCENCE SURFACE CONTAMINANT ANALYZER: A FEASIBILITY STUDY **c25**

Hudson B. Eldridge *In* Alabama Univ., Research Reports: 1988 NASA/ASEE Summer Faculty Fellowship Program Dec. 1988 34 p (For primary document see N89-21726 14-99)
Avail: NTIS HC A99/MF E03 CSCL 07D

The bonding of liner material to the inner metal surfaces of solid rocket booster cases is adversely affected by minute amounts of impurities on the metal surface. Suitable non-destructive methods currently used for detecting these surface contaminants do not provide the means of identifying their elemental composition. The feasibility of using isotopic source excited energy dispersive X-ray fluorescence as a possible technique for elemental analysis of such contaminants is investigated. A survey is made of the elemental compositions of both D-6ac steel, a common construction material for the booster cases, and Conoco HD-2 grease, a common surface contamination. Source and detector choices that maximize signal to noise ratio in a Recessed Source Geometry are made. A Monte Carlo simulation is then made of the optimized device incorporating the latest available X-ray constants at the energy of the chosen source to determine the device's response to a D-6ac steel surface contained with Conoco HD-2 grease. Author

N89-21737*# Alabama Univ., Huntsville. Dept. of MIS/MSC.

INTELLIGENT DATA REDUCTION FOR AUTONOMOUS POWER SYSTEMS **c63**

Stephen A. Floyd *In* Alabama Univ., Research Reports: 1988 NASA/ASEE Summer Faculty Fellowship Program Dec. 1988 24 p (For primary document see N89-21726 14-99)
Avail: NTIS HC A99/MF E03 CSCL 09B

Since 1984 Marshall Space Flight Center was actively engaged in research and development concerning autonomous power systems. Much of the work in this domain has dealt with the development and application of knowledge-based or expert systems to perform tasks previously accomplished only through intensive human involvement. One such task is the health status monitoring of electrical power systems. Such monitoring is a manpower intensive task which is vital to mission success. The Hubble Space Telescope testbed and its associated Nickel Cadmium Battery Expert System (NICBES) were designated as the system on which the initial proof of concept for intelligent power system monitoing will be established. The key function performed by an engineer engaged in system monitoring is to analyze the raw telemetry data and identify from the whole only those elements which can be considered significant. This function requires engineering expertise on the functionality of the system, the mode of operation and the efficient and effective reading of the telemetry data. Application of this expertise to extract the significant components of the data is referred to as data reduction. Such a function possesses characteristics which make it a prime candidate for the application of knowledge-based systems' technologies. Such applications are investigated and recommendations are offered for the development of intelligent data reduction systems. Author

N89-21738*# Auburn Univ., AL. Dept. of Physics.
EXPERIMENTAL RESULTS ON ATOMIC OXYGEN CORROSION OF SILVER **c26**
Albert T. Fromhold *In* Alabama Univ., Research Reports: 1988 NASA/ASEE Summer Faculty Fellowship Program Dec. 1988 24 p (For primary document see N89-21726 14-99)
Avail: NTIS HC A99/MF E03 CSCL 11F

The results of an experimental study of the reaction kinetics of silver with atomic oxygen in 10 degree increments over the temperature range of 0 to 70 C is reported. The silver specimens, of the order of 10,000 A in thickness, were prepared by thermal evaporation onto 3 inch diameter polished silicon wafers. There were later sliced into pieces having surface areas of the order of 1/4 to 1/2 square inch. Atomic oxygen was generated by a gas discharge in a commercial plasmod asher operating in the megahertz frequency range. The sample temperature within the chamber was controlled by means of a thermoelectric unit. Exposure of the silver specimens to atomic oxygen was incremental, with oxide film thickness measurements being carried out between exposures by means of an automated ellipsometer. For the early growth phase, the data can be described satisfactorily by a logarithmic growth law: the oxide film thickness increases as the logarithm of the exposure time. Furthermore, the oxidation process is thermally activated, the rate increasing with increasing temperature. However, the empirical activation energy parameter deduced from Arrhenius plots is quite low, being of the order of 0.1 eV. Author

N89-21739*# Memphis State Univ., TN. Dept. of Physics.
CONSTRUCTION OF AN ALTERNATING GRADIENT MAGNETOMETER **c35**
Michael M. Garland *In* Alabama Univ., Research Reports: 1988 NASA/ASEE Summer Faculty Fellowship Program Dec. 1988 26 p (For primary document see N89-21726 14-99)
Avail: NTIS HC A99/MF E03 CSCL 14B

A magnetometer is described which was constructed to facilitate the study and characterization of the magnetic properties of high transition temperature superconductors. This instrument was used to measure the dc magnetic susceptibility of several superconducting compounds as a function of temperature. The construction of the magnetometer and the operating parameters are discussed in detail. Author

N89-21740*# Mississippi State Univ., Mississippi State. Dept of Aerospace Engineering.
GUIDANCE FOR AN AEROASSISTED ORBITAL TRANSFER VEHICLE **c18**
Kenneth R. Hall *In* Alabama Univ., Research Reports: 1988 NASA/ASEE Summer Faculty Fellowship Program Dec. 1988 11 p (For primary document see N89-21726 14-99)
Avail: NTIS HC A99/MF E03 CSCL 22B

The use of atmospheric drag for slowing satellite in high energy, high apogee orbits to a lower energy, lower apogee orbit about the Earth is investigated. The high energy orbit is assumed to intercept the Earth's atmosphere. Guidance for the atmospheric phase of the trajectory may be done using the aerodynamic forces generated by the passage through the atmosphere. This research was concerned with the investigation of several methods of guidance during the atmospheric phase to cause a significant reduction in the final velocity as the vehicle leaves the atmosphere. In addition, the velocity direction was controlled to exit to a desired target orbit. Lastly excess aerodynamic lift was used to effect a plane change between the entry orbit plane and the exit orbit plane to achieve a desired orbit plane. The guidance methods were applied to a 3 degree-of-freedom simulation which included an oblate Earth gravity model and a rotating atmosphere. Simulation results were compared on the basis of speed of computation of the guidance parameters and amount of added velocity necessary to achieve the desired orbit. Author

N89-21741*# Tennessee Technological Univ., Cookeville. Dept. of Mechanical Engineering.
TRANSIENT NATURAL CONVECTION HEAT AND MASS TRANSFER IN CRYSTAL GROWTH **c76**
Samuel S. Han *In* Alabama Univ., Research Reports: 1988 NASA/ASEE Summer Faculty Fellowship Program Dec. 1988 24 p (For primary document see N89-21726 14-99)
Avail: NTIS HC A99/MF E03 CSCL 20L

A numerical analysis of transient combined heat and mass transfer across a rectangular cavity is performed by a numerical method based on the SIMPLE algorithm. The physical parameters are selected to represent a range of possible crystal growth in solutions. Numerical results are compared with available experimental data to confirm the accuracy of the results. Good qualitative agreements are obtained for the average mass transfer rate across the cavity. Also, qualitative agreements are observed for the global development of thermal and solute fields. It is found that the thermal and solute fields become highly oscillatory when the thermal and solute Grashof numbers are large. Oscillations are probably caused by a number of different instability mechanisms. By reducing the gravity some of these instabilities were made to disappear at the lower Grashof numbers. Transient temperature and solute distribution near the crystal growing surface are highly non-uniform at the higher Grashof numbers. These non-uniformities are less severe in the reduced gravity environments but still exist. The effects of convection on the rate of average mass transfer are more than one order of magnitude higher than those of conduction in the range of Grashof numbers studied. Dependency of mass transfer rate on the Grashof number indicates that the convection effects many not be negligible even in the microgravity environments for the range of parameters investigated. Author

N89-21742*# Mississippi State Univ., Mississippi State. Dept. of Electrical Engineering.
OPTIMIZATION OF LARGE MATRIX CALCULATIONS FOR EXECUTION ON THE CRAY X-MP VECTOR SUPERCOMPUTER **c61**
William A. Hornfeck *In* Alabama Univ., Research Reports: 1988 NASA/ASEE Summer Faculty Fellowship Program Dec. 1988 25 p (For primary document see N89-21726 14-99)
Avail: NTIS HC A99/MF E03 CSCL 09B

A considerable volume of large computational computer codes were developed for NASA over the past twenty-five years. This code represents algorithms developed for machines of earlier generation. With the emergence of the vector supercomputer as a viable, commercially available machine, an opportunity exists to evaluate optimization strategies to improve the efficiency of existing software. This result is primarily due to architectural differences in the latest generation of large-scale machines and the earlier, mostly uniprocessor, machines. A sofware package being used by NASA

to perform computations on large matrices is described, and a strategy for conversion to the Cray X-MP vector supercomputer is also described. Author

N89-21743*# Ohio Univ., Athens. Dept. of Electrical and Computer Engineering.

INVESTIGATION OF PRACTICAL APPLICATIONS OF H INFINITY CONTROL THEORY TO THE DESIGN OF CONTROL SYSTEMS FOR LARGE SPACE STRUCTURES **c18**

R. Dennis Irwin *In* Alabama Univ., Research Reports: 1988 NASA/ASEE Summer Faculty Fellowship Program Dec. 1988 26 p (For primary document see N89-21726 14-99)
Avail: NTIS HC A99/MF E03 CSCL 22B

The applicability of H infinity control theory to the problems of large space structures (LSS) control was investigated. A complete evaluation to any technique as a candidate for large space structure control involves analytical evaluation, algorithmic evaluation, evaluation via simulation studies, and experimental evaluation. The results of analytical and algorithmic evaluations are documented. The analytical evaluation involves the determination of the appropriateness of the underlying assumptions inherent in the H infinity theory, the determination of the capability of the H infinity theory to achieve the design goals likely to be imposed on an LSS control design, and the identification of any LSS specific simplifications or complications of the theory. The resuls of the analytical evaluation are presented in the form of a tutorial on the subject of H infinity control theory with the LSS control designer in mind. The algorthmic evaluation of H infinity for LSS control pertains to the identification of general, high level algorithms for effecting the application of H infinity to LSS control problems, the identification of specific, numerically reliable algorithms necessary for a computer implementation of the general algorithms, the recommendation of a flexible software system for implementing the H infinity design steps, and ultimately the actual development of the necessary computer codes. Finally, the state of the art in H infinity applications is summarized with a brief outline of the most promising areas of current research. Author

N89-21744*# Toledo Univ., OH. Dept. of Physics and Astronomy.

THE MEASUREMENT OF ANGULAR DIFFERENTIAL CROSS SECTIONS AT THE SSL ATOMIC SCATTERING FACILITY **c72**

Thomas J. Kvale *In* Alabama Univ., Research Reports: 1988 NASA/ASEE Summer Faculty Fellowship Program Dec. 1988 23 p (For primary document see N89-21726 14-99)
Avail: NTIS HC A99/MF E03 CSCL 20H

The design of the SSL Atomic Scattering Facility (ASF) located at the NASA/Marshall Space Flight Center as well as some of the initial experiments to be performed with it, are covered. The goal is to develop an apparatus capable of measuring angular differential cross sections (ADCS) for the scattering of 2 to 14 eV atomic oxygen from various gaseous targets. At present little is known about atomic oxygen scattering with kinetic energies of a few eV. This apparatus is designed to increase the understanding of collisions in this energy region. Atomic oxygen scattering processes are of vital interest to NASA because the space shuttle as well as other low earth orbit satellites will be subjected to a flux of 5 eV atomic oxygen on the ram surfaces while in orbit. The primary experiments will involve the measurements of ADCS for atomic oxygen scattering from gaseous targets (in particular, molecular nitrogen). These, as well as the related initial experiments involving thermal He scattering from N2 and O2 targets will be described. Author

N89-21745*# Mississippi State Univ., Mississippi State. Dept. of Physics and Astronomy.

ANGULAR RESPONSE CALIBRATION OF THE BURST AND TRANSIENT SOURCE EXPERIMENT **c93**

John Patrick Lestrade *In* Alabama Univ., Research Reports: 1988 NASA/ASEE Summer Faculty Fellowship Program Dec. 1988 34 p (For primary document see N89-21726 14-99)
Avail: NTIS HC A99/MF E03 CSCL 03B

The Gamma Ray Observatory includes four experiments designed to observe the gamma-ray universe. Laboratory measurements to test the response the Burst and Transient Source Experiment (BATSE) modules to gamma-ray sources that are non-axial were recently completed. The results of these observations are necessary for the correct interpretation of BATSE data obtained after it is put in Earth orbit. The launch is planned for March, 1900. Preliminary analyses of these test data show the presence of a radial dependence to the detector's light collection efficiency. It is proposed to evaluate the importance of this radial response, analyze future experimental data to derive the actual functional dependence on radius, and calculate the net effect on the output spectrum as a function of the angle of incidence. Author

N89-21746*# Tennessee Univ., Chattanooga. Dept. of Mechanical Engineering-Mechanics.

THE SIMULATION OF THE ALTERNATE TURBOPUMP DEVELOPMENT HIGH PRESSURE OXYGEN AND FUEL TURBOPUMPS FOR THE SPACE SHUTTLE MAIN ENGINE USING THE SHABERTH COMPUTER PROGRAM **c37**

Gary H. McDonald *In* Alabama Univ., Research Reports: 1988 NASA/ASEE Summer Faculty Fellowship Program Dec. 1988 32 p (For primary document see N89-21726 14-99)
Avail: NTIS HC A99/MF E03 CSCL 13I

The Space Shuttle Main Engine (SSME) is basically comprised of a combustion chamber and nozzle, high and low pressure oxygen turbopumps and high and low pressure fuel turbopumps. In the current configuration, the high pressure fuel (HPTFP) and high pressure oxygen turbopumps (HPOTP) have experienced a history of ball bearing wear. The wear problem can be attributed to numerous factors including the hydrodynamic axial and radial loads caused by the flow of liquid oxygen and liquid hydrogen through the turbopump impellers and turbine. Also, friction effects between the rolling elements, races, and cage can create thermally induced bearing geometry changes. To alleviate some of the current configuration problems, an alternate turbopump development (ATD) was proposed. However, the ATD HPOTP and HPTFP are constrained to operate interchangeably with the current turbopumps, thus, the operation conditions must be similar. The ATD configuration features a major change in bearings used to support the integrated shaft, impeller, and turbine system. A single ball and single roller will replace the pump-end and turbine and duplex ball bearings. The Shaft-Bearing-Thermal (SHABERTH) computer code was used to model the ATD HPOTP and ATD HPFTP configurations. A two bearing model was used to simulate the HPOTP and HPFTP bearings and shaft geometry. From SHABERTH, a comparison of bearing reaction loads, frictional heat generation rates, and Hertz contact stresses will be attempted with analysis at the 109 percent and 65 percent power levels. Author

N89-21747*# Alabama A & M Univ., Huntsville. Dept. of Physics.

FLUCTUATION ANALYSIS OF RELATIVISTIC NUCLEUS-NUCLEUS COLLISIONS IN EMULSION CHAMBERS **c72**

Stephen C. McGuire *In* Alabama Univ., Research Reports: 1988 NASA/ASEE Summer Faculty Fellowship Program Dec. 1988 16 p (For primary document see N89-21726 14-99)
Avail: NTIS HC A99/MF E03 CSCL 20H

An analytical technique was developed for identifying enhanced fluctuations in the angular distributions of secondary particles produced from relativistic nucleus-nucleus collisions. The method is applied under the assumption that the masses of the produced particles are small compared to their linear momenta. The importance of particles rests in the fact that enhanced fluctuations in the rapidity distributions is considered to be an experimental signal for the creation of the quark-gluon-plasma (QGP), a state of nuclear matter predicted from the quantum chromodynamics theory (QCD). In the approach, Monte Carlo simulations are employed that make use of a portable random member generator that allow the calculations to be performed on a desk-top computer.

The method is illustrated with data taken from high altitude emulsion exposures and is immediately applicable to similar data from accelerator-based emulsion exposures. Author

N89-21748*# Florida Inst. of Tech., Melbourne. Dept. of Physics/Space Science.
ELECTRON MOBILITY IN MERCURY CADMIUM TELLURIDE **c76**
James D. Patterson *In* Alabama Univ., Research Reports: 1988 NASA/ASEE Summer Faculty Fellowship Program Dec. 1988 30 p (For primary document see N89-21726 14-99)
Avail: NTIS HC A99/MF E03 CSCL 20L

A previously developed program, which includes all electronic interactions thought to be important, does not correctly predict the value of electron mobility in mercury cadmium telluride particularly near room temperature. Part of the reason for this discrepancy is thought to be the way screening is handled. It seems likely that there are a number of contributors to errors in the calculation. The objective is to survey the calculation, locate reasons for differences between experiment and calculation, and suggest improvements. Author

N89-21749*# Georgia Inst. of Tech., Atlanta. School of Aerospace.
SIMULATION OF WATER VAPOR CONDENSATION ON LOX DROPLET SURFACE USING LIQUID NITROGEN **c25**
Eugene A. Powell *In* Alabama Univ., Research Reports: 1988 NASA/ASEE Summer Faculty Fellowship Program Dec. 1988 26 p (For primary document see N89-21726 14-99)
Avail: NTIS HC A99/MF E03 CSCL 07D

The formation of ice or water layers on liquid oxygen (LOX) droplets in the Space Shuttle Main Engine (SSME) environment was investigated. Formulation of such ice/water layers is indicated by phase-equilibrium considerations under conditions of high partial pressure of water vapor (steam) and low LOX droplet temperature prevailing in the SSME preburner or main chamber. An experimental investigation was begun using liquid nitrogen as a LOX simulant. A monodisperse liquid nitrogen droplet generator was developed which uses an acoustic driver to force the stream of liquid emerging from a capillary tube to break up into a stream of regularly space uniformly sized spherical droplets. The atmospheric pressure liquid nitrogen in the droplet generator reservoir was cooled below its boiling point to prevent two phase flow from occurring in the capillary tube. An existing steam chamber was modified for injection of liquid nitrogen droplets into atmospheric pressure superheated steam. The droplets were imaged using a stroboscopic video system and a laser shadowgraphy system. Several tests were conducted in which liquid nitrogen droplets were injected into the steam chamber. Under conditions of periodic droplet formation, images of 600 micron diameter liquid nitrogen droplets were obtained with the stroboscopic video systems. Author

N89-21750*# Alabama Univ., Huntsville. Dept. of Mechanical Engineering.
FURTHER INVESTIGATIONS OF OBLIQUE HYPERVELOCITY IMPACT PHENOMENA **c37**
William P. Schonberg *In* Alabama Univ., Research Reports: 1988 NASA/ASEE Summer Faculty Fellowship Program Dec. 1988 45 p (For primary document see N89-21726 14-99)
Avail: NTIS HC A99/MF E03 CSCL 13I

The results of a continuing investigation of the phenomena associated with the oblique hypervelocity impact of spherical projectiles onto multi-sheet aluminum structures are described. A series of equations that quantitatively describes these phenomena is obtained through a regression of experimental data. These equations characterize observed ricoshet and penetration damage phenomena in a multi-sheet structure as functions of the geometric parameters of the structure and the diameter, obliquity, and velocity of the impacting projectile. Crater damage observed on the ricochet witness plates is used to determine the sizes and speeds of the ricochet debris particles that caused the damage. It is shown that, in general, the most damaging ricochet debris particle is approximately 0.25 cm (0.10 in) in diameter and travels at the speed of approximately 2.1 km/sec (6,890 ft/sec). The equations necessary for the design of shielding panels that will protect external systems from such ricochet debris damage are also developed. The dimensions of these shielding panels are shown to be strongly dependent on their inclination and on their circumferential distribution around the spacecraft. It is concluded that obliquity effects of high-speed impacts must be considered in the design of any structure exposed to the meteoroid and space debris environment. Author

N89-21751*# Arkansas Univ., Fayetteville. Dept. of Mechanical Engineering.
EVALUATE THE APPLICATION OF MODAL TEST AND ANALYSIS PROCESSES TO STRUCTURAL FAULT DETECTION IN MSFC-STS PROJECT ELEMENTS **c39**
William T. Springer *In* Alabama Univ., Research Reports: 1988 NASA/ASEE Summer Faculty Fellowship Program Dec. 1988 23 p (For primary document see N89-21726 14-99)
Avail: NTIS HC A99/MF E03 CSCL 20K

The Space Transportation System (STS) is a very complex and expensive flight system which is intended to carry payloads into low Earth orbit and return. A catastrophic failure of the STS (such as experienced in the 51-L incident) results in the loss of both human life as well as very expensive hardware. One impact of this incident was to reaffirm the need to do everything possible to insure the integrity and reliability of the STS is sufficient to produce a safe flight. One means of achieving this goal is to expand the number of inspection technologies available for use on the STS. The purpose was to begin to evaluate the possible use of assessing the structural integrity of STS components for which Marshall Space Flight Center (MSFC) has responsibility. This entailed reviewing the available literature and determining a low-level experimental program which could be performed by MSFC and would help establish the feasibility of using this technology for structural fault detection. Author

N89-21752*# Alabama A & M Univ., Huntsville. Dept. of Mathematics.
SSME PROPULSION PERFORMANCE RECONSTRUCTION TECHNIQUES **c20**
Enoch C. Temple *In* Alabama Univ., Research Reports: 1988 NASA/ASEE Summer Faculty Fellowship Program Dec. 1988 11 p (For primary document see N89-21726 14-99)
Avail: NTIS HC A99/MF E03 CSCL 21H

In view of the complex flight operation of the Space Shuttle propulsion system together with an expected launch rate increase, the flight performance reconstruction process needs to be performed by automated computer programs. These programs must have the capability to quickly and reliably determine the true behavior of the various components of the propulsion system. For the flight reconstruction, measured values from the solid rocket motors, liquid engines, and trajectory are appraised through the Kalman filter technique to identify the most likely flight propulsion performance. A more detailed data collection program for the single SSME engine captive test firing evaluation is scheduled for startup in September of 1988. Engine performance evaluation for the captive test firing requires a reconstruction process that is similar to the process that is used for the flight reconstruction. Analytical tools that may be used to reconstruct a propulsion system's true performance under flight and/or test conditions are described. Author

N89-21753*# Georgia Inst. of Tech., Atlanta.
DYNAMIC FATIGUE TESTING OF ZERODUR GLASS-CERAMIC **c27**
Dennis S. Tucker *In* Alabama Univ., Research Reports: 1988 NASA/ASEE Summer Faculty Fellowship Program Dec. 1988 22 p (For primary document see N89-21726 14-99)
Avail: NTIS HC A99/MF E03 CSCL 11B

The inherent brittleness of glass invariably leads to a large variability in strength data and a time dependence in strength. Leading rate plays a large role in strength values. Glass is found to be weaker when supporting loads over long periods of time as

compared to glass which undergoes rapid leading. These properties complicate the structural design allowables for the utilization of glass components in an application such as Advanced X-ray Astrophysics Facility (AXAF). The test methodology to obtain parameters which can be used to predict the reliability and life time of Zerodur glass-ceramic which is to be used for the mirrors in the AXAF is described. Author

N89-21754*# Alabama Univ., Huntsville. Dept. of Mechanical Engineering.
SOFTWARE SYSTEM SAFETY c61
James G. Uber *In* Alabama Univ., Research Reports: 1988 NASA/ASEE Summer Faculty Fellowship Program Dec. 1988 28 p (For primary document see N89-21726 14-99)
Avail: NTIS HC A99/MF E03 CSCL 09B

Software itself is not hazardous, but since software and hardware share common interfaces there is an opportunity for software to create hazards. Further, these software systems are complex, and proven methods for the design, analysis, and measurement of software safety are not yet available. Some past software failures, future NASA software trends, software engineering methods, and tools and techniques for various software safety analyses are reviewed. Recommendations to NASA are made based on this review. Author

N89-21755*# California Polytechnic State Univ., San Luis Obispo. Dept. of Metallurgy and Materials Engineering.
THE KEYHOLE REGION IN VPPA WELDS c37
Daniel W. Walsh *In* Alabama Univ., Research Reports: 1988 NASA/ASEE Summer Faculty Fellowship Program Dec. 1988 27 p (For primary document see N89-21726 14-99)
Avail: NTIS HC A99/MF E03 CSCL 13I

The morphology and properties of the Variable Polarity Plasma Arc (VPPA) weld composite zone are intimately related to the physical processes associated with the keyhole. The effects of microsegregation and transient weld stress on macrosegregation in the weld tool are examined. In addition the electrical character of straight and reverse polarity portions of the arc cycle were characterized. The results of the former study indicate that alloy 2219 is weldable because large liquid volumes are available during latter stages of weld solidification. Strains in the pool region, acting in conjunction with weld microsegregation can produce macrosegregation great enough to produce radiographic contrast effects in welds. Mechanisms of surface copper enrichment were identified. The latter study has demonstrated that increased heat is delivered to workpieces if the reverse polarity proportion of the weld cycle is increased. Current in the straight polarity portion of the welding cycle increased as the reverse cycle proportion increased. Voltage during reverse polarity segments is large. Author

N89-21756*# Alabama Univ., Huntsville. Dept. of Aerospace Engineering.
THE ROLE OF THE TURBULENT PRANDTL NUMBER IN TURBINE BLADE HEAT TRANSFER PREDICTION c34
Kevin W. Whitaker *In* Alabama Univ., Research Reports: 1988 NASA/ASEE Summer Faculty Fellowship Program Dec. 1988 20 p (For primary document see N89-21726 14-99)
Avail: NTIS HC A99/MF E03 CSCL 20D

Improvement of the prediction of external (gas-to-blade) heat transfer coefficients in gas turbine engines was undertaken. The effects of improved eddy diffusivity of heat modeling in the turbulence model was specifically investigated. A two-dimensional boundary STAN5, was selected and modified by incorporating several different turbulent Prandtl number models. Results indicated that slight effects were attributable to the modified turbulence model. Boundary layer character appeared to be much more significant. Author

N89-21757*# Alaska Univ., Fairbanks. Dept. of Computer Science.
DEVELOPMENT OF A PROTOTYPE COMMONALITY ANALYSIS TOOL FOR USE IN SPACE PROGRAMS c61
Dorian P. Yeager *In* Alabama Univ., Research Reports: 1988 NASA/ASEE Summer Faculty Fellowship Program Dec. 1988 28 p (For primary document see N89-21726 14-99)
Avail: NTIS HC A99/MF E03 CSCL 09B

A software tool to aid in performing commonality analyses, called Commonality Analysis Problem Solver (CAPS), was designed, and a prototype version (CAPS 1.0) was implemented and tested. The CAPS 1.0 runs in an MS-DOS or IBM PC-DOS environment. The CAPS is designed around a simple input language which provides a natural syntax for the description of feasibility constraints. It provides its users with the ability to load a database representing a set of design items, describe the feasibility constraints on items in that database, and do a comprehensive cost analysis to find the most economical substitution pattern. Author

N89-21758*# Alabama Univ., Huntsville. Dept. of Biological Sciences.
TECHNIQUES FOR STUDYING THE EFFECTS OF MICROGRAVITY ON MODEL PARTICLE/CELL SYSTEMS c29
Ronald B. Young *In* Alabama Univ., Research Reports: 1988 NASA/ASEE Summer Faculty Fellowship Program Dec. 1988 17 p (For primary document see N89-21726 14-99)
Avail: NTIS HC A99/MF E03 CSCL 22A

To study the direct effects of a low gravity environment on skeletal and cardiac muscle cells, experiments were initiated to determine whether skeletal and/or cardiac muscule cells would grow within the lumen of XM-80 hollow fibers (i.d. = 0.5 mm). Cells were prepared from skeletal or cardiac muscle tissue of 12 day embryos and were cultured for up to 7 days in the hollow fiber environment. Light microscopy revealed that cells proliferated to confluency over this period of time and fusion was apparent in the skeletal muscle cells. Once it was verified that cells would grow to confluency, additional XM-80 fibers containing cells were placed in a Clinostat in the horizontal position at 100 rpm. Fibers were stretched by a built-in spring mechanism to hold the fiber tightly at the center of rotation. Under these conditions, the gravity vector approaches zero and the cells are in an environment that simulates microgravity. Examination of skeletal muscle cells by electron microscopy revealed that myoblast fusion and myofibril accumulation were extensive. Although data obtained thus far are preliminary, they suggest that myofibril organization in chicken skeletal muscle cultures is somewhat more poorly defined in Clinostat rotated cultures than in controls that were not subjected to Clinostat conditions. Author

N89-21759*# Auburn Univ., AL. Dept. of Algebra, Combinatorics and Analysis.
ROTORDYNAMIC ANALYSIS OF A BEARING TESTER c37
Richard A. Zalik *In* Alabama Univ., Research Reports: 1988 NASA/ASEE Summer Faculty Fellowship Program Dec. 1988 25 p (For primary document see N89-21726 14-99)
Avail: NTIS HC A99/MF E03 CSCL 13I

The properties of the solutions of a system of four coupled nonlinear differential equations that model the behavior of the rotating shaft of a bearing tester are studied. In particular, it is shown how the bounds for the rotations of these equations can be obtained from bounds for the solutions of the linearized equations. By studying the behavior of the Fourier transforms of the solution, the approach to the stability boundary can also be predicted. These conclusions are verified by means of numerical solutions of the equations, and of power spectrum density (PSD) plots. Author

N89-21760*# Alabama Univ., Huntsville. Dept. of Computer Science.
SPACE SHUTTLE MAIN ENGINE NUMERICAL MODELING CODE MODIFICATIONS AND ANALYSIS c20
John P. Ziebarth *In* Alabama Univ., Research Reports: 1988 NASA/ASEE Summer Faculty Fellowship Program Dec. 1988 21 p (For primary document see N89-21726 14-99)
Avail: NTIS HC A99/MF E03 CSCL 21H

The user of computational fluid dynamics (CFD) codes must

be concerned with the accuracy and efficiency of the codes if they are to be used for timely design and analysis of complicated three-dimensional fluid flow configurations. A brief discussion of how accuracy and efficiency effect the CFD solution process is given. A more detailed discussion of how efficiency can be enhanced by using a few Cray Research Inc. utilities to address vectorization is presented and these utilities are applied to a three-dimensional Navier-Stokes CFD code (INS3D). Author

N89-21761*# National Aeronautics and Space Administration, Washington, DC.

RESEARCH AND TECHNOLOGY OBJECTIVES AND PLANS SUMMARY, FISCAL YEAR 1987

Jan. 1987 143 p

(NASA-TM-89241; NAS 1.15:89241) Avail: NTIS HC A07/MF A01 CSCL 05D

This publication represents the NASA research and technology program for FY87. It is a compilation of the Summary portions of each of the RTOPs (Research and Technology Objectives and Plans) used for management review and control of research currently in progress throughout NASA. The RTOP Summary is designed to facilitate communication and coordination among concerned technical personnel in government, in industry, and in universities. The first section containing citations and abstracts of the RTOPs is followed by four indexes: Subject, Technical Monitor, Responsible NASA Organization, and RTOP Number. Author

Typical Subject Index Listing

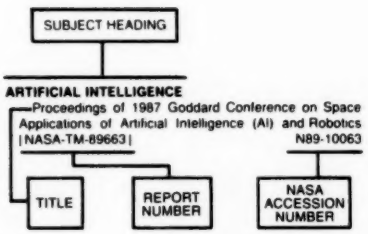

The subject heading is the key to the subject content of the document. Titles, report numbers, and accession numbers of pertinent documents are provided under each subject heading. When the title is insufficiently descriptive of the document content, a title extension has been added, separated from the title by three hyphens. The report number helps to indicate the type of document cited (e.g., NASA report, NASA translation, NASA contractor report). The NASA accession number is the number by which the document abstracts are arranged in this journal and by which the document is sold or requested. The titles, with title extensions if present, are arranged under each subject heading in ascending accession number order. The subject headings have been selected from the latest revision of the *NASA Thesaurus* (NASA SP-7064).

A

ABSORBERS (MATERIALS)
Attenuation of blast waves using foam and other materials
[AD-A203148] N89-21632

ABSORPTIVITY
Utility of a dual-lidar method to measure integrated extinction
[AD-A203145] N89-21439

ABUNDANCE
Nitrogen geochemistry of a Cretaceous-Tertiary boundary site in New Zealand N89-21320
Ion microprobe of Mg, Ca, Ti and Fe isotopic ratios and trace element abundances in hibonite-bearing inclusions from primitive meteorites N89-21719

ACCELERATION (PHYSICS)
G-induced loss of consciousness and its prevention
[AD-A202960] N89-21471

ACCELERATION TOLERANCE
G-induced loss of consciousness and its prevention
[AD-A202960] N89-21471

ACCIDENTS
Reentry response of the light weight radioisotope heater unit resulting from a Venus-Earth-Earth gravity assist maneuver accident
[DE89-005359] N89-21024
Space Propulsion Hazards Analysis Manual (SPHAM), volume 1
[AD-A203204] N89-21029

ACETYLENE
High temperature composites using Schiff's base pyropolymer matrices
[AD-A203311] N89-21043
Physical and mechanical properties of American Cyanamid's acetylene-terminated prepreg system: T-300/CATB-44
[AD-A203737] N89-21045

ACID RAIN
Biospheric traumas caused by large impacts and predicted relics in the sedimentary record N89-21371

ACOUSTIC COUPLING
Research on acoustic coupling to electromagnetic pulses in tissue
[AD-A195644] N89-21140

ACOUSTIC EMISSION
Acoustic emission source location in fibre reinforced plastic composites
[AERE-R-13039] N89-21035
On-line location of partial discharges in power transformer through acoustic emission
[DE88-757043] N89-21188
Acoustic damage to large-aperture optics: Revision 1
[DE89-008025] N89-21654

ACOUSTIC MEASUREMENT
Localizing and beamforming freely-drifting VLF (Very Low Frequency) acoustic sensors
[AD-A202638] N89-21217

ACOUSTIC MICROSCOPES
Acoustic microscopy of low ductility materials
[AERE-R-12848] N89-21101

ACOUSTIC SIMULATION
Analysis and simulation of an audio adaptive equalizer
[AD-A202569] N89-21631

ACOUSTICS
Surface acoustic wave detection of organophosphorus compounds
[AD-A202909] N89-21058
Speech recognition: Acoustic-phonetic knowledge acquisition and representation
[AD-A203081] N89-21160
Localizing and beamforming freely-drifting VLF (Very Low Frequency) acoustic sensors
[AD-A202638] N89-21217
Comparison of propeller cruise noise data taken in the NASA Lewis 8- by 6-foot wind tunnel with other tunnel and flight data
[NASA-TM-101976] N89-21628
Sounds in one-dimensional superfluid helium
[AD-A202428] N89-21629
Speech database development
[AD-A202461] N89-21699

ACOUSTO-OPTICS
A continued study of optical sound generation and amplification
[AD-A202484] N89-21630
A theoretical and experimental investigation of linear and nonlinear focussing chirped optical diffraction gratings
[AD-A203396] N89-21650

ACTIVE CONTROL
Active control technique evaluation for spacecraft (ACES)
[AD-A202475] N89-21016
Active control of a large space structure as applied to the phase 1 CETF (Critical Evaluation Task Force) space station
[AD-A203293] N89-21020

ACTIVE GALACTIC NUCLEI
The evolution of active galactic nuclei and globular clusters: Multi-component models N89-21720

ACTUATORS
Actuation constraints in multivariable flight control systems N89-20998
RCS/linear discrete actuator study
[AD-A202822] N89-21028
A magnetic bearing control approach using flux feedback
[NASA-TM-100672] N89-21135
Modeling robot dynamic performance for endpoint force control
[AD-A202881] N89-21251

ADAPTATION
A robust adaptive array structure using the soft constrained LMS algorithm
[AD-A203959] N89-21167
Adaptive optical linear algebra processors
[AD-A202996] N89-21605

ADAPTIVE CONTROL
Computer simulation of a pilot in V/STOL aircraft control loops
[NASA-CR-184815] N89-21479

ADAPTIVE FILTERS
Performance of an adaptive matched filter using the Griffiths algorithm
[AD-A202578] N89-21147
LMS adaptive filtering applied to a microwave arterial pulse monitor
[AD-A202732] N89-21465
Analysis and simulation of an audio adaptive equalizer
[AD-A202569] N89-21631

ADAPTIVE OPTICS
Bibliography of Soviet laser developments, September-October 1987
[AD-A203366] N89-21232
New techniques for high-resolution optical space surveillance
[AD-A202785] N89-21647

ADDITION
Best ordering for floating-point addition
[AD-A203990] N89-21612

ADDITIVES
High temperature evaluation of new ferroelastic toughened ceramic materials
[AD-A203197] N89-21120
Effect of TNT miscible additives on the mechanical behavior and shock sensitivity of Composition B
[AD-A203968] N89-21132

ADHESION
Adhesion in chemically hostile environments: The use of filled polymers as diffusion barriers
[AD-A203333] N89-21121

ADHESIVE BONDING
The use of primers in the adhesive bonding of carbon-fibre reinforced composites
[AD-A202542] N89-21039

ADHESIVES
The use of primers in the adhesive bonding of carbon-fibre reinforced composites
[AD-A202542] N89-21039
Adhesion in chemically hostile environments: The use of filled polymers as diffusion barriers
[AD-A203333] N89-21121

ADSORBENTS
Surface acoustic wave detection of organophosphorus compounds
[AD-A202909] N89-21058

ADVANCED VERY HIGH RESOLUTION RADIOMETER
Ice cover on Chesapeake Bay from AVHRR (Advanced Very High Resolution Radiometer) and LANDSAT imagery, winter of 1987-88
[PB89-117261] N89-21415

ADVECTION
Numerical solution of parabolic problems in high dimensions N89-21501

AERIAL PHOTOGRAPHY
Auroral photography experiment
[AD-A203623] N89-21441

AEROASSIST
Guidance for an aeroassisted orbital transfer vehicle N89-21740

AERODYNAMIC BALANCE
An experimental study of transonic buffet of a supercritical airfoil with trailing edge flap
[AD-A203189] N89-20968

AERODYNAMIC CHARACTERISTICS
Airframe/propulsion integration characteristics at transonic speeds N89-20926
A study of transonic drag reduction of a blunt cylinder by a cylinder probe
[AD-A202557] N89-20965
Volumetric rendering techniques for the display of three-dimensional aerodynamic flow field data
[AD-A202661] N89-21204

AERODYNAMIC CONFIGURATIONS
Transonic CFD applications at Boeing N89-20929
Applied transonics at Grumman N89-20931
Vector potential methods N89-20939

AERODYNAMIC DRAG
Effect of riblets upon flow separation in a subsonic diffuser
[AD-A203178] N89-20967
Numerical simulation of flow over iced airfoils
[AD-A203291] N89-20969
AERODYNAMIC FORCES
Influence of reflected shock waves on a hypersonic shaped charge jet N89-21522
AERODYNAMIC INTERFERENCE
Turbulence and modeling in transonic flow N89-20951
Wall interference assessment and corrections N89-20958
Two-measured variable method for wall interference assessment/correction N89-20959
Comparison of airfoil results from an adaptive wall test section and a porous wall test section N89-20960
Capabilities of wind tunnels with two-adaptive walls to minimize boundary interference in 3-D model testing N89-20961
AERODYNAMIC LOADS
Method to predict external store carriage loads at transonic speeds N89-20945
Integrated aerodynamic/dynamic optimization of helicopter rotor blades
[NASA-TM-101553] N89-20982
DATAMAP upgrade version 4.0
[NASA-TM-100993] N89-21541
AERODYNAMIC STABILITY
A wind tunnel and computer investigation of the low speed aerodynamic characteristics of the prone escape system (PRESS)
[AD-A202768] N89-20988
Flight controller design with nonlinear aerodynamics, large parameter uncertainty and pilot compensation
[AD-A202727] N89-21000
AERODYNAMICS
Two-dimensional Navier-Stokes solution of the flow over a thick supercritical airfoil with strong shock-induced separation
[AD-A203331] N89-20971
Icing considerations for HALE (High Altitude, Long Endurance) aircraft
[AD-A202584] N89-20975
Integrated aerodynamic/dynamic optimization of helicopter rotor blades
[NASA-TM-101553] N89-20982
Wind energy program summary. Volume 1, Overview: Fiscal year 1988
[DE89-000856] N89-21420
DATAMAP upgrade version 4.0
[NASA-TM-100993] N89-21541
AEROELASTICITY
Additional development of the XTRAN3S computer program
[NASA-CR-181743] N89-20922
Aeroelastic modeling for the FIT team F/A-18 simulation
[NASA-TM-101569] N89-20991
AERONAUTICAL ENGINEERING
Flight research and testing N89-20927
Preliminary design of a modular unmanned research vehicle. Volume 1: System design document
[AD-A202765] N89-20987
AEROSOLS
Global environmental effects of impact-generated aerosols: Results from a general circulation model N89-21306
A 3-dimensional numerical simulation of the atmospheric injection of aerosols by a hypothetical basaltic fissure eruption N89-21401
Evaluation of aerosol size distribution models
[AD-A202736] N89-21645
AEROSPACE ENGINEERING
Space technology and the Soviet/US strategic competition: A perspective and forecast using 12-year cycles
[AD-A202538] N89-21006
Research and technology objectives and plans summary, fiscal year 1987
[NASA-TM-89241] N89-21761
AEROSPACE INDUSTRY
Guide to Canadian aerospace related industries
[AD-A203738] N89-21697
AEROSPACE MEDICINE
Aerospace medicine and biology: A continuing bibliography with indexes (supplement 321)
[NASA-SP-7011(321)] N89-21475
Aerospace medicine and biology: A continuing bibliography with indexes (supplement 322)
[NASA-SP-7011(322)] N89-21476
SPH-4 US Army flight helmet performance 1983-1987
[AD-A202589] N89-21482
AEROSPACE SCIENCES
Research and technology objectives and plans summary, fiscal year 1987
[NASA-TM-89241] N89-21761
AEROSPACE SYSTEMS
A diagnostic system blending deep and shallow reasoning
[AD-A202547] N89-20979
Conjugating binary systems for spacecraft thermal control
[NASA-CR-183608] N89-21023
Strategic defense initiative: A chronology, 1983 - 1988
[AD-A203576] N89-21619
National space policy
[AD-A202644] N89-21711
AEROSPACE VEHICLES
A review of reaction rates and thermodynamic and transport properties for the 11-species air model for chemical and thermal nonequilibrium calculations to 30000 K
[NASA-TM-101528] N89-21193
AEROTHERMODYNAMICS
Experimental examination of the aerothermal performance of the T-10 test cell at NAS (Naval Air Station), Cubi Point
[AD-A203887] N89-21005
High density fuel effects
[AD-A202426] N89-21125
AGING (MATERIALS)
Effect of geometry on thermal aging behavior of Celion/LARC-160 composites
[NASA-TM-100496] N89-21047
AIR FLOW
Numerical simulation of flow over iced airfoils
[AD-A203291] N89-20969
Coherent structures in fully developed turbulent pipe flow N89-21195
Incompressible flow friction coefficients in a simulated heat pipe
[AD-A203176] N89-21207
A simple model for wind field estimation in complex terrain
[DE89-007240] N89-21457
AIR LAND INTERACTIONS
The role of radiation-dynamics interaction in regional numerical weather prediction N89-21732
AIR POLLUTION
Effects of global atmospheric perturbations on forest ecosystems: Predictions of seasonal and cumulative effects N89-21399
A simple model for wind field estimation in complex terrain
[DE89-007240] N89-21457
AIR QUALITY
Air quality and forest health issues in the 1990s
[DE89-006941] N89-21427
AIR TRAFFIC CONTROL
Microwave landing systems: Additional systems should not be procured unless benefits proven
[GAO/RCED-88-118] N89-20977
AIR WATER INTERACTIONS
Geochemistry of K/T boundaries in India and contributions of Deccan volcanism N89-21296
Abrupt climate change and extinction events N89-21308
OSRMS (Ocean Surface Roughness Measurement System): The DREP (Defence Research Establishment Pacific) near-nadir scatterometer
[AD-A202983] N89-21460
AIRCRAFT ACCIDENTS
SPH-4 US Army flight helmet performance 1983-1987
[AD-A202589] N89-21482
AIRCRAFT CONFIGURATIONS
Aerodynamic analysis of three advanced configurations using the TranAir full-potential code N89-20944
Steady and unsteady transonic small disturbance analysis of realistic aircraft configurations N89-20946
Euler/Navier-Stokes calculations of transonic flow past fixed- and rotary-wing aircraft configurations N89-20948
Preliminary design of a modular unmanned research vehicle. Volume 1: System design document
[AD-A202765] N89-20987
Tailless aircraft performance improvements with relaxed static stability
[NASA-CR-181806] N89-20999
AIRCRAFT CONSTRUCTION MATERIALS
The properties of advanced aluminium alloy systems N89-21074
AIRCRAFT CONTROL
Numerical simulation of the flow field over delta wings with leading edge blowing N89-20924
Tailless aircraft performance improvements with relaxed static stability
[NASA-CR-181806] N89-20999
Capacity of human operator using smart stick controller
[AD-A202712] N89-21483
AIRCRAFT DESIGN
Transonic Symposium: Theory, Application, and Experiment, Volume 1, Part 1
[NASA-CP-3020-VOL-1-PT-1] N89-20925
Airframe/propulsion integration characteristics at transonic speeds N89-20926
Flight research and testing N89-20927
Shock-boundary-layer interaction in flight N89-20928
Transonic CFD applications at Boeing N89-20929
The application of CFD for military aircraft design at transonic speeds N89-20930
Applied transonics at Grumman N89-20931
Transonics and fighter aircraft: Challenges and opportunities for CFD N89-20932
Computation of aircraft component flow fields at transonic Mach numbers using a three-dimensional Navier-Stokes algorithm N89-20933
Transonic aerodynamic design experience N89-20934
Wave drag due to lift for transonic airplanes N89-20938
Transonic propulsion system integration analysis at McDonnell Aircraft Company N89-20943
Performance optimization for rotors in hover and axial flight
[NASA-CR-177524] N89-20973
Hypersonic drone design: A multidisciplinary experience
[NASA-CR-184740] N89-20981
AIRCRAFT DETECTION
Aircraft tracking with dual TACAN
[AD-A202647] N89-20980
Analysis of space-based lidar for aircraft tracking
[AD-A202665] N89-21230
AIRCRAFT HAZARDS
Icing considerations for HALE (High Altitude, Long Endurance) aircraft
[AD-A202584] N89-20975
AIRCRAFT MANEUVERS
Numerical simulation of the flow field over delta wings with leading edge blowing N89-20924
AIRCRAFT NOISE
LCP-10 intelligibility of oxygen masks and microphones in aircraft noise
[AD-A202474] N89-21481
Attenuation of blast waves using foam and other materials
[AD-A203148] N89-21632
AIRCRAFT PERFORMANCE
Tailless aircraft performance improvements with relaxed static stability
[NASA-CR-181806] N89-20999
AIRCRAFT PILOTS
Saccadic eye movement during spaceflight
[NASA-TM-100475] N89-21463
The impact of the US Army's AH-64 helmet mounted display on future aviation helmet design
[AD-A202984] N89-21486
Polycarbonate ophthalmic lenses for ametropic Army aviators using night vision goggles
[AD-A203100] N89-21488
AIRCRAFT RELIABILITY
Application of the boundary element method to fatigue crack growth analysis
[AD-A202565] N89-21270
AIRCRAFT SAFETY
Aviation safety: Measuring how safely individual airlines operate
[GAO/RCED-88-61] N89-20974
A digital rate controller for the control reconfigurable combat aircraft designed using quantitative feedback theory
[AD-A203050] N89-21001
AIRFOIL PROFILES
Wall interference assessment and corrections N89-20958
Comparison of airfoil results from an adaptive wall test section and a porous wall test section N89-20960
Numerical simulation of flow over iced airfoils
[AD-A203291] N89-20969
AIRFOILS
Developments and trends in three-dimensional mesh generation N89-20940
Unsteady force calculations on circular cylinders and elliptical airfoils with circulation control
[UMAERO-87-37] N89-20962
Numerical simulation of flow over iced airfoils
[AD-A203291] N89-20969
Whole field measurements of vorticity in turbulent and unsteady flows
[AD-A203349] N89-21209

AIRGLOW
Auroral photography experiment
[AD-A203623] N89-21441
AIRLINE OPERATIONS
Aviation safety: Measuring how safely individual airlines operate
[GAO/RCED-88-61] N89-20974
AIRPORT PLANNING
Heliport system planning guidelines
[AD-A199081] N89-21003
ALGAE
Response of marine and freshwater algae to nitric acid and elevated carbon dioxide levels simulating environmental effects of bolide impact N89-21298
ALGEBRA
Image processing language, phase 2
[AD-A203994] N89-21577
An algebraic theory of program correctness in a problem domain
[DE89-008450] N89-21579
Adaptive optical linear algebra processors
[AD-A202996] N89-21605
Numerical solution of nonlinear algebraic equations in stiff ODE solving
[DE89-008284] N89-21613
ALGORITHMS
Computation of aircraft component flow fields at transonic Mach numbers using a three-dimensional Navier-Stokes algorithm N89-20933
Generation of unstructured grids and Euler solutions for complex geometries N89-20941
A digital rate controller for the control reconfigurable combat aircraft designed using quantitative feedback theory
[AD-A203050] N89-21001
Control system for maintaining stable orbits around phobos
[AD-A202776] N89-21008
Derivation and testing of computer algorithms for automatic real-time determination of space vehicle potentials in various plasma environments
[AD-A203019] N89-21019
Acoustic emission source location in fibre reinforced plastic composites
[AERE-R-13039] N89-21035
Performance of an adaptive matched filter using the Griffiths algorithm
[AD-A202578] N89-21147
Multiple model adaptive tracking of airborne targets
[AD-A202696] N89-21148
Speech recognition: Acoustic-phonetic knowledge acquisition and representation
[AD-A203081] N89-21160
A robust adaptive array structure using the soft constrained LMS algorithm
[AD-A203959] N89-21167
Soft constrained LMS algorithms: A robust procedure for signal misalignment
[AD-A203880] N89-21187
Development of a shock capturing code for use as a tool in designing high-work low aspect ratio turbines
[AD-A202706] N89-21248
Dynamic structural optimization and experiment
[PB89-111462] N89-21259
Algorithms for rational spline curves N89-21502
An algorithm for processing scanning spectrometer data N89-21506
A posteriori error estimation of adaptive finite difference schemes for hyperbolic systems N89-21513
A very simple polynomial-time algorithm for linear programming
[AD-A202502] N89-21548
Time delay estimation in stationary and non-stationary environments
[AD-A202507] N89-21549
Grasp: A graph specification language
[AD-A202524] N89-21550
Architecture and design for a laser programmable double precision floating point application specific processor
[AD-A202560] N89-21553
A vectorized hidden-surface algorithm implemented on the Cray-2 supercomputer
[AD-A202657] N89-21560
Distributed discrete-event simulation using variants of the Chandy-Misra algorithm on the intel hypercube
[AD-A202849] N89-21563
Influence diagrams: Automated analysis with dynamic programming
[AD-A203045] N89-21567
A neural network implementation of chaotic time series prediction
[AD-A203049] N89-21569
Nonprocedural implementation of mathematical programming algorithms
[AD-A203392] N89-21573
A theory of problem domains and program correctness
[DE89-008451] N89-21580
Lookahead in parallel discrete event simulation
[AD-A203902] N89-21588
Performance evaluation of parallel algorithms and architectures in concurrent multiprocessor systems
[AD-A203982] N89-21589
On random correlation matrices
[AD-A202786] N89-21603
Best ordering for floating-point addition
[AD-A203990] N89-21612
Modified backward error propagation for tactical target recognition
[AD-A202666] N89-21644
Extracting shape reflectance of Lambertian, specular, and hybrid surfaces
[AD-A203772] N89-21652
Investigation of practical applications of H infinity control theory to the design of control systems for large space structures N89-21743
ALKALI METALS
Solar-powered alkali metal vapor lasers
[NASA-CR-180480] N89-21226
ALKALINITY
Ocean alkalinity and the Cretaceous/Tertiary boundary N89-21300
ALLOYS
Hydrogen segregation to grain boundaries and external surfaces
[AD-A202892] N89-21084
ALUMINIDES
Thermodynamic analysis of chemical compatibility of several reinforcement materials with niobium aluminides
[NASA-CR-182260] N89-21036
Chemical vapor synthesis of niobium aluminides
[AD-A202591] N89-21055
ALUMINUM
Investigation of Weibull statistics in fracture analysis of cast aluminum
[NASA-TM-102000] N89-21245
Oblique hypervelocity impact response of dual-sheet structures
[NASA-TM-100358] N89-21246
ALUMINUM ALLOYS
Thermodynamic analysis of chemical compatibility of several reinforcement materials with niobium aluminides
[NASA-CR-182260] N89-21036
The properties of advanced aluminium alloy systems N89-21074
Investigation of crack growth in titanium-aluminide at elevated temperatures
[AD-A202570] N89-21081
Crack growth of a titanium-aluminide alloy under thermal-mechanical fatigue
[AD-A202767] N89-21083
Synthesis processing of high-lithium Al-Li alloys
[AD-A203401] N89-21088
The microstructural and phase characterization of RST Al-Ti-X alloys
[AD-A203734] N89-21092
Structural energy differences in Al3Ti: The role of tetragonal distortion in APB and twin energies
[DE89-007210] N89-21096
Mechanisms of fatigue crack propagation and fracture toughness behavior in advanced aluminum-lithium alloys
[DE89-008300] N89-21098
Diffusion welding of an RS/PM aluminum alloy N89-21241
Characterization of Nb-Al superconducting material
[DE89-008296] N89-21690
ALUMINUM GALLIUM ARSENIDES
Investigation of a self-aligned, strained-channel,n sup(+)-In As/Al 0.5 As/In 0.15 Ga 0.85 As Semiconductor Insulator Semiconductor FET (SISFET)
[AD-A203147] N89-21676
ALUMINUM OXIDES
Holographic investigation of solid propellant combustion
[AD-A203928] N89-21067
AMMONIUM NITRATES
Density of triethanolammonium nitrate and liquid propellant
[AD-A203767] N89-21131
AMMONIUM PERCHLORATES
Magnetic flowmeter measurement of solid propellant pressure-coupled and velocity-coupled responses
[AD-A203988] N89-21133
AMORPHOUS MATERIALS
Magnetic properties of nano-heterogeneous amorphous, thin films
[AD-A203727] N89-21680
AMPLIFIER DESIGN
Microwave power amplifier analysis and design
[AD-A203170] N89-21182
AMPLIFIERS
On the impulse response of monopulse radars
[AD-A202936] N89-21153
AMPLITUDES
Subharmonic and fundamental high amplitude excitation of an axisymmetric jet
[NASA-TM-101946] N89-20920
ANALYZERS
A source code analyzer to predict compilation time for avionics software using software science measures. Volume 1: Main report
[AD-A202737] N89-20992
ANGULAR MOMENTUM
A magnetic bearing control approach using flux feedback
[NASA-TM-100672] N89-21135
ANGULAR VELOCITY
Angular response calibration of the burst and transient source experiment N89-21745
ANILINE
Molecular jet studies of vdW (van der Waals) clusters and solvation
[AD-A203766] N89-21212
ANIMALS
Darkness after the K-T impact: Effects of soot N89-21411
ANISOTROPIC PLATES
Transverse shear considerations in anisotropic plates
[AD-A203187] N89-21283
ANISOTROPY
Deformation modeling and constitutive modeling for anisotropic superalloys
[NASA-CR-4215] N89-21258
ANNEALING
Studies of the initial oxidation of Fe-Si alloys by AES, XPS, EELS and LEED
[DE89-007610] N89-21077
Synthesis processing of high-lithium Al-Li alloys
[AD-A203401] N89-21088
ANNIHILATION REACTIONS
Electronic structure and properties of defect complexes in metals
[AD-A203657] N89-21091
ANNUAL VARIATIONS
The seasonal cycle of energetics from the GLAS/UMD climate GCM
[NASA-TM-100714] N89-21448
Upper-wind climatology for CONUS
[AD-A203961] N89-21453
Seasonal snowfall statistics for selected stations
[AD-A203965] N89-21454
ANNULAR NOZZLES
Fouling tests of AGT-1500 gas turbine fuel nozzles
[AD-A203360] N89-21253
ANNULI
A cancellation technique for reducing background noise within turbulent flow environments characterized by pipes and annuli
[AD-A202924] N89-21206
Variable wall temperature effects on multicellular natural convection in a horizontal annulus
[AD-A202762] N89-21691
ANOMALIES
Possible world-wide middle miocene iridium anomaly and its relationship to periodicity of impacts and extinctions N89-21291
Deccan volcanism at the Cretaceous-Tertiary boundary N89-21305
The Sudbury Structure (Ontario, Canada) and Vredefort Structure (South Africa): A comparison N89-21311
Iridium emissions from Hawaiian volcanoes N89-21314
ANOXIA
The end-triassic mass extinction event N89-21324
ANTARCTIC OCEAN
Evidence of volcanic ash at a K-T boundary section: Ocean drilling program hole 690 C, Maud Rise, Weddell Sea off East Antarctica N89-21410
ANTARCTIC REGIONS
Evidence of volcanic ash at a K-T boundary section: Ocean drilling program hole 690 C, Maud Rise, Weddell Sea off East Antarctica N89-21410
ANTENNA ARRAYS
Estimated satellite cluster elements in near circular orbit
[AD-A202938] N89-21011
Effect of two-body motion on radar beam quality for various distributed sparse array configurations
[AD-A202937] N89-21154
A robust adaptive array structure using the soft constrained LMS algorithm
[AD-A203959] N89-21167
Soft constrained LMS algorithms: A robust procedure for signal misalignment
[AD-A203880] N89-21187

Correction of gain and optical throughput variations in a two-dimensional imaging spectrometer
[AD-A203495] N89-21222
ANTENNA DESIGN
A comparison of reflector antenna designs for wide-angle scanning
[NASA-TM-101459] N89-21138
ANTENNA FEEDS
A comparison of reflector antenna designs for wide-angle scanning
[NASA-TM-101459] N89-21138
ANTHROPOMETRY
Measurer's handbook: US Army anthropometric survey, 1987-1988
[AD-A202721] N89-21484
ANTIBODIES
Development and characterization of a fiber optic immuno biosensor
[DE89-005062] N89-21225
Immunoassay procedures for fiber optic sensors
[AD-A203069] N89-21649
ANTIMISSILE DEFENSE
Performance evaluation of parallel algorithms and architectures in concurrent multiprocessor systems
[AD-A203982] N89-21589
SDI (Strategic Defense Initiative) and national security policy
[AD-A202730] N89-21617
Strategic defense initiative program: Better management direction and controls needed
[GAO/NSIAD-88-26] N89-21694
ANTIMISSILE MISSILES
Strategic defense initiative: A chronology, 1983 - 1988
[AD-A203576] N89-21619
APPROXIMATION
Function theory for thin elastic shells
[PB89-101943] N89-21257
Knot selection for least squares approximation using thin plate splines N89-21504
Asymptotics beyond all orders N89-21508
A very simple polynomial-time algorithm for linear programming
[AD-A202502] N89-21548
ARC SPRAYING
Plasma reaction method and apparatus
[DE89-007360] N89-21656
ARCHITECTURE (COMPUTERS)
Neural networks and the symmetric group S(sub N) N89-21529
HOP (Hardware viewed as Objects and Processes): A process model for synchronous hardware systems
[AD-A203090] N89-21535
A language comparison for scientific computing on MIMD architectures
[NASA-CR-181779] N89-21537
Architecture and design for a laser programmable double precision floating point application specific processor
[AD-A202560] N89-21553
Performance directed simulation
[AD-A203089] N89-21570
An algebraic theory of program correctness in a problem domain
[DE89-008450] N89-21579
A theory of problem domains and program correctness
[DE89-008451] N89-21580
Advanced information processing system: Local system services
[NASA-CR-181767] N89-21582
Performance evaluation of parallel algorithms and architectures in concurrent multiprocessor systems
[AD-A203982] N89-21589
Architecture studies and system demonstrations of optical parallel processor for AI (Artificial Intelligence) and NI (Neural Intelligence)
[AD-A203241] N89-21593
Nonlinear real-time optical signal processing
[AD-A202445] N89-21641
Optimization of large matrix calculations for execution on the Cray X-MP vector supercomputer N89-21742
ARGON
Theoretical studies of rare gas halide systems
[AD-A203985] N89-21068
ARGON LASERS
Laser beam coupling via optical phase conjugation in BaTiO3
[AD-A202874] N89-21231
ARMED FORCES (UNITED STATES)
Guide to Canadian aerospace related industries
[AD-A203738] N89-21697
ARRAYS
Application of a single area array detector for acquisition, tracking and point-ahead in space optical communications
[NASA-CR-183423] N89-21168
ARRIVALS
A generalized approach to direction finding
[AD-A203768] N89-21186
ARTIFICIAL INTELLIGENCE
Speech recognition: Acoustic-phonetic knowledge acquisition and representation
[AD-A203081] N89-21160
Design of a feeling-thinking machine N89-21510
Image processing language, phase 2
[AD-A203994] N89-21577
Architecture studies and system demonstrations of optical parallel processor for AI (Artificial Intelligence) and NI (Neural Intelligence)
[AD-A203241] N89-21593
A methodology for screening potential artificial intelligence applications
[AD-A203966] N89-21594
Intelligent data reduction for autonomous power systems N89-21737
ARTIFICIAL SATELLITES
The use of chaff in space as a jamming device between ground stations and satellites
[AD-A202577] N89-21146
Artificial asteroid impact on defensive satellites
[DE89-008407] N89-21620
ASCENT TRAJECTORIES
Aircraft tracking with dual TACAN
[AD-A202647] N89-20980
ASHES
Volcanic ash layers in blue ice fields (Beardmore Glacier Area, Antarctica): Iridium enrichments N89-21340
Evidence of volcanic ash at a K-T boundary section: Ocean drilling program hole 690 C, Maud Rise, Weddell Sea off East Antarctica N89-21410
ASSESSMENTS
Risk to civilization: A planetary science perspective N89-21302
ASSOCIATIVE PROCESSING (COMPUTERS)
A position, scale and rotation invariant holographic associative memory
[AD-A203289] N89-21221
Center for the Integration of Optical Computing
[AD-A203254] N89-21536
Optical information processing in a confocal Fabry-Perot resonator
[AD-A202566] N89-21556
ASTEROID BELTS
Collisions with ice-volatile objects: Geological implications N89-21409
ASTEROIDS
Implications of asteroid composition for the geochemistry of the ancient terrestrial projectile flux N89-21294
Computer modeling of large asteroid impacts into continental and oceanic sites: Atmospheric, cratering, and ejecta dynamics N89-21379
Asteroid and comet flux in the neighborhood of the earth N89-21387
The cometary and asteroidal impactor flux at the earth N89-21407
ASTRONOMICAL MAPS
The 408 MHz radio observations of a quasar sample N89-21714
ASTROPHYSICS
Astrophysical implications of periodicity N89-21361
Center for Atomic, Molecular and Optical Physics technical activities, 1988
[PB89-132302] N89-21623
Positron line radiation from halo WIMP annihilations as a dark matter signature
[NASA-CR-182918] N89-21635
ASYMPTOTIC METHODS
Asymptotic methods for internal transonic flows N89-20937
Wave drag due to lift for transonic airplanes N89-20938
Asymptotics beyond all orders N89-21508
Optimal and robust memoryless discrimination from dependent observations
[AD-A202806] N89-21604
ASYMPTOTIC PROPERTIES
Conditionally and strictly distribution-free tests for randomized block designs that are asymptotically optimal
[CWI-MS-R8802] N89-21615
ATLANTIC OCEAN
Macrofossil extinction patterns at Bay of Biscay Cretaceous-Tertiary boundary sections N89-21404
ATMOSPHERIC ATTENUATION
Utility of a dual-lidar method to measure integrated extinction
[AD-A203145] N89-21439
ATMOSPHERIC CIRCULATION
Global environmental effects of impact-generated aerosols: Results from a general circulation model N89-21306
Volcanism, global catastrophe and mass mortality N89-21316
Acute effects of a large bolide impact simulated by a global atmospheric circulation model N89-21398
Observations of neutral circulation at mid-latitudes during the Equinox Transition Study
[NASA-CR-184792] N89-21429
Enhancements to the AFGL (Air Force Geophysics Laboratory) Statistical Analysis Program (ASAP) for the global multivariate analysis of heights and winds
[AD-A202912] N89-21450
Satellite signatures of rapid cyclogenesis
[AD-A203934] N89-21452
ATMOSPHERIC COMPOSITION
Carbon dioxide catastrophes: Past and future menace N89-21293
Dynamics of exploding magma chambers: Implications for K-T volcanism and mass extinctions N89-21377
Assessment of the atmospheric impact of volcanic eruptions N89-21388
Acute effects of a large bolide impact simulated by a global atmospheric circulation model N89-21398
Air quality and forest health issues in the 1990s
[DE89-006941] N89-21427
National Climate Program
[PB89-118608] N89-21445
ATMOSPHERIC EFFECTS
Atmospheric effects on laser propagation
[DE89-008646] N89-21237
Volcanoes and global catastrophes N89-21389
Multi-year global climatic effects of atmospheric dust from large bolide impacts N89-21397
Acute effects of a large bolide impact simulated by a global atmospheric circulation model N89-21398
Operational implications of a cloud model simulation of space shuttle exhaust clouds in different atmospheric conditions
[NASA-CR-4222] N89-21425
A cloud model simulation of space shuttle exhaust clouds in different atmospheric conditions
[NASA-CR-4223] N89-21426
Guidance for an aeroassisted orbital transfer vehicle N89-21740
ATMOSPHERIC ENERGY SOURCES
The seasonal cycle of energetics from the GLAS/UMD climate GCM
[NASA-TM-100714] N89-21448
ATMOSPHERIC GENERAL CIRCULATION MODELS
Abrupt climate change and extinction events N89-21308
ATMOSPHERIC HEATING
Climatic changes resulting from mass extinctions at the K-T boundary (and other bio-events) N89-21373
ATMOSPHERIC LASERS
Analysis of space-based lidar for aircraft tracking
[AD-A202665] N89-21230
ATMOSPHERIC MODELS
Global environmental effects of impact-generated aerosols: Results from a general circulation model N89-21306
Multi-year global climatic effects of atmospheric dust from large bolide impacts N89-21397
Acute effects of a large bolide impact simulated by a global atmospheric circulation model N89-21398
A 3-dimensional numerical simulation of the atmospheric injection of aerosols by a hypothetical basaltic fissure eruption N89-21401
CCM (Community Climate Model)
[PB89-120927] N89-21446
Coupled dynamical-radiational model of stratocumulus and its applications
[PB89-104137] N89-21447
Blending of surface and rawinsonde data in mesoscale objective analysis
[AD-A203984] N89-21456
Evaluation of aerosol size distribution models
[AD-A202736] N89-21645
ATMOSPHERIC PHYSICS
Flux and sounding data from the NCAR (National Center for Atmospheric Research) King Air aircraft during HAPEX (hydrologic atmospheric pilot experiment)
[PB89-124481] N89-21433
Commentary on fast atmospheric pulsations
[AD-A203172] N89-21440
The seasonal cycle of energetics from the GLAS/UMD climate GCM
[NASA-TM-100714] N89-21448
ATMOSPHERIC PRESSURE
Enhancements to the AFGL (Air Force Geophysics Laboratory) Statistical Analysis Program (ASAP) for the global multivariate analysis of heights and winds
[AD-A202912] N89-21450
Summary of Meteorological Observations, Surface (SMOS) for Moffett Field, California
[AD-A203628] N89-21451

ATMOSPHERIC RADIATION
Coupled dynamical-radiational model of stratocumulus and its applications
[PB89-104137] N89-21447
ATMOSPHERIC REFRACTION
Infrared sea-radiance modeling using LOWTRAN 6
[AD-A202582] N89-21643
ATMOSPHERIC SOUNDING
Flux and sounding data from the NCAR (National Center for Atmospheric Research) King Air aircraft during HAPEX (hydrologic atmospheric pilot experiment)
[PB89-124481] N89-21433
ATMOSPHERIC TEMPERATURE
Enhancements to the AFGL (Air Force Geophysics Laboratory) Statistical Analysis Program (ASAP) for the global multivariate analysis of heights and winds
[AD-A202912] N89-21450
ATMOSPHERIC TURBULENCE
New techniques for high-resolution optical space surveillance
[AD-A202785] N89-21647
ATOMIC COLLISIONS
Laser enhanced chemical reactions
[DE89-008084] N89-21236
The measurement of angular differential cross sections at the SSL Atomic Scattering Facility N89-21744
Fluctuation analysis of relativistic nucleus-nucleus collisions in emulsion chambers N89-21747
ATOMIC PHYSICS
Center for Atomic, Molecular and Optical Physics technical activities, 1988
[PB89-132302] N89-21623
ATOMIC STRUCTURE
Calculation of the energetics of chemical reactions
[DE89-007262] N89-21070
Electronic structure and properties of defect complexes in metals
[AD-A203657] N89-21091
Atomistic simulations of interfaces in metals and alloys
[DE89-006521] N89-21685
ATOMIZING
Turbulence modulation and dense-spray structure
[AD-A202449] N89-21201
ATTACK AIRCRAFT
Shock-boundary-layer interaction in flight N89-20928
ATTITUDE CONTROL
Active control technique evaluation for spacecraft (ACES)
[AD-A202475] N89-21016
Active control of a large space structure as applied to the phase 1 CETF (Critical Evaluation Task Force) space station
[AD-A203293] N89-21020
ATTITUDE GYROS
Radio-controlled model gyro measurement study
[AD-A204002] N89-21223
AUDIO FREQUENCIES
Performance analysis of the fiber distributed data interface in the super cockpit audio world
[AD-A202535] N89-20985
Analysis and simulation of an audio adaptive equalizer
[AD-A202569] N89-21631
AUGER SPECTROSCOPY
Studies of the initial oxidation of Fe-Si alloys by AES, XPS, EELS and LEED
[DE89-007610] N89-21077
AURORAS
Charging potentials for two sample sets of spectra from DMSP satellites
[AD-A203694] N89-21021
Auroral photography experiment
[AD-A203623] N89-21441
AUSTENITE
Nb modification of microcomposite Fe/C/Cr/Mn steel
[DE89-008297] N89-21097
AUTOCLAVES
High temperature composites using Schiff's base pyropolymer matrices
[AD-A203311] N89-21043
AUTOMATA THEORY
Design of a feeling-thinking machine N89-21510
Deductive programming
[AD-A202489] N89-21546
AUTOMATIC CONTROL
Experiments in end-point control of manipulators with elastic drives N89-21240
Automated library systems and document tracking systems: Commercial software alternatives, volume 1
[DE89-007716] N89-21706
AUTOMATIC PILOTS
G-induced loss of consciousness and its prevention
[AD-A202960] N89-21471
AUTOMATIC TEST EQUIPMENT
A diagnostic system blending deep and shallow reasoning
[AD-A202547] N89-20979
AUTOMOBILE ENGINES
Operation of vehicle engines in cold conditions: Start up, lubrication and fuel consumption
[DE88-757111] N89-21255
AUTOMOBILE FUELS
CRC (Coordinating Research Council) hot-start and driveaway driveability program at high and intermediate temperatures using gasoline-alcohol blends
[AD-A202471] N89-21126
AVALANCHE DIODES
Optical communication with semiconductor laser diode
[NASA-CR-184817] N89-21141
AVIONICS
A source code analyzer to predict compilation time for avionics software using software science measures. Volume 1: Main report
[AD-A202737] N89-20992
Software development guidelines
[AD-A203332] N89-21572
AXISYMMETRIC FLOW
Subharmonic and fundamental high amplitude excitation of an axisymmetric jet
[NASA-TM-101946] N89-20920
Comparison of 3D computation and experiment for non-axisymmetric nozzles
[NASA-CR-182245] N89-20921

B

B STARS
An optical study of three transient X-ray sources N89-21724
BACKGROUND NOISE
A cancellation technique for reducing background noise within turbulent flow environments characterized by pipes and annuli
[AD-A202924] N89-21206
BACKGROUND RADIATION
Infrared sea-radiance modeling using LOWTRAN 6
[AD-A202582] N89-21643
BACKSCATTERING
Spectral characteristics of High Frequency (HF) backscatter for high latitude ionospheric irregularities: Preliminary analysis of statistical properties
[AD-A202998] N89-21156
Rapid backscatter simulation techniques for detailed B-spline target models
[AD-A203260] N89-21163
Utility of a dual-lidar method to measure integrated extinction
[AD-A203145] N89-21439
A rapid-backscatter simulation technique for complex B-spline target models N89-21505
BALL BEARINGS
The simulation of the alternate turbopump development high pressure oxygen and fuel turbopumps for the space shuttle main engine using the Shaberth computer program N89-21746
BARIUM COMPOUNDS
An in-situ, high-temperature study of the superconductor YBa1.67Sr0.33Cu3O(6+x)
[DE89-007375] N89-21686
BARIUM TITANATES
Laser beam coupling via optical phase conjugation in BaTiO3
[AD-A202874] N89-21231
BARRIER LAYERS
Adhesion in chemically hostile environments: The use of filled polymers as diffusion barriers
[AD-A203333] N89-21121
Investigation of Schottky barrier on GaAs and InP using a multidisciplined approach
[AD-A202953] N89-21675
BARYONS
Surface energy from order parameter profile: At the QCD phase transition
[NASA-CR-184890] N89-21633
BASALT
Flood basalts and mass extinctions N89-21360
Deccan volcanism and K-T boundary signatures N89-21362
Flood basalt eruptions, comet showers, and mass extinction events N89-21372
Some volcanologic aspects of Columbia River basalt volcanism relevant to the extinction controversy N89-21393
A 3-dimensional numerical simulation of the atmospheric injection of aerosols by a hypothetical basaltic fissure eruption N89-21401
BATHYMETERS
Localizing and beamforming freely-drifting VLF (Very Low Frequency) acoustic sensors
[AD-A202638] N89-21217
BAYS (STRUCTURAL UNITS)
Adapting Schottky diode detector technology to a space platform
[AD-A202825] N89-21219
BEAMS (RADIATION)
Optical power limiter
[AD-A203964] N89-21234
BEAMS (SUPPORTS)
Analytical and experimental investigation of constrained viscoelastic layer damping for a plate and shell model
[AD-A202698] N89-21273
BEARINGS
Vibration control in rotating machinery using variable dynamic stiffness squeeze-films
[AD-A202902] N89-21252
Rotordynamic analysis of a bearing tester N89-21759
BEHAVIOR
Satellite telemetry: A new tool for wildlife research and management
[PB88-249255] N89-21013
Behavioral effects of microwaves: Relationship of total dose and dose rate
[PB89-118640] N89-21462
Rotordynamic analysis of a bearing tester N89-21759
BENDING
Compressive properties of high performance polymeric fibers
[AD-A202947] N89-21117
Bending and vibration of variable thickness orthotropic plates N89-21264
Three dimensional effects near a crack tip in a ductile three point bend specimen. Part 2: An experimental investigation using interferometry and caustics
[AD-A202637] N89-21272
Element level elimination of nonlinear constraints in total Lagrangian finite element formulations N89-21496
BENDING MOMENTS
A triangular thin shell element for the linear analysis of stiffened composite structures
[AD-A202864] N89-21277
BENDING THEORY
Vibration and buckling characteristics of composite cylindrical panels incorporating the effects of a higher order shear theory
[AD-A202939] N89-21278
BIAS
Aircraft tracking with dual TACAN
[AD-A202647] N89-20980
BIBLIOGRAPHIES
Bibliography of Soviet laser developments, September-October 1987
[AD-A203366] N89-21232
Aerospace medicine and biology: A continuing bibliography with indexes (supplement 321)
[NASA-SP-7011(321)] N89-21475
Aerospace medicine and biology: A continuing bibliography with indexes (supplement 322)
[NASA-SP-7011(322)] N89-21476
Review and analysis of the literature in the area of human performance modeling
[DE89-006800] N89-21480
Defense technical information center's role in numeric database development
[AD-A202901] N89-21701
BINARY ALLOYS
The microstructural and phase characterization of RST Al-Ti-X alloys
[AD-A203734] N89-21092
BINARY DATA
Dimensionality of binary items
[AD-A203238] N89-21608
BINARY DIGITS
Dimensionality of binary items
[AD-A203238] N89-21608
BINARY STARS
A search for gravitational waves from coalesing binary stars using the Caltech 40 meter gravity wave detector N89-21721
BINARY SYSTEMS (MATERIALS)
Conjugating binary systems for spacecraft thermal control
[NASA-CR-183608] N89-21023
BINDERS (MATERIALS)
Synthesis of energetic binders
[AD-A203060] N89-21127
BINOCULAR VISION
Reconstruction of binocular depth across continuous surfaces
[AD-A202827] N89-21469

BIOASTRONAUTICS
Saccadic eye movement during spaceflight
[NASA-TM-100475] N89-21463
Aerospace medicine and biology: A continuing bibliography with indexes (supplement 321)
[NASA-SP-7011(321)] N89-21475
Aerospace medicine and biology: A continuing bibliography with indexes (supplement 322)
[NASA-SP-7011(322)] N89-21476
BIOGEOCHEMISTRY
Ocean alkalinity and the Cretaceous/Tertiary boundary N89-21300
BIOINSTRUMENTATION
Development and characterization of a fiber optic immuno biosensor
[DE89-005062] N89-21225
BIOLOGICAL EFFECTS
Proximal ecological effects of the 1980 eruptions of Mount St. Helens N89-21394
Behavioral effects of microwaves: Relationship of total dose and dose rate
[PB89-118640] N89-21462
Saccadic eye movement during spaceflight
[NASA-TM-100475] N89-21463
Aerospace medicine and biology: A continuing bibliography with indexes (supplement 321)
[NASA-SP-7011(321)] N89-21475
Aerospace medicine and biology: A continuing bibliography with indexes (supplement 322)
[NASA-SP-7011(322)] N89-21476
BIOLOGICAL EVOLUTION
Patterns of megafloral change across the Cretaceous-Tertiary boundary in the Northern Great Plains and Rocky Mountains N89-21336
Earth orbital variations and vertebrate bioevolution N89-21357
BIOMAGNETISM
Applications, dosimetry and biological interactions of static and time-varying magnetic fields
[DE89-006944] N89-21627
BIOMASS
The global Cretaceous-Tertiary fire: Biomass or fossil carbon N89-21321
Strangelove ocean at era boundaries, terrestrial or extraterrestrial cause N89-21332
Mass mortality and extraterrestrial impacts N89-21335
Extended period of K/T boundary mass extinction in the marine realm N89-21337
Widespread habitat change through paludification as an interactive mechanism in mass extinction events N89-21339
Impact as a general cause of extinction: A feasibility test N89-21374
Effects of global atmospheric perturbations on forest ecosystems: Predictions of seasonal and cumulative effects N89-21399
BIOSPHERE
Carbon dioxide catastrophes: Past and future menace N89-21293
Biospheric traumas caused by large impacts and predicted relics in the sedimentary record N89-21371
Effects of global atmospheric perturbations on forest ecosystems: Predictions of seasonal and cumulative effects N89-21399
BIREFRINGENCE
Optical activity and its influence on photorefractive materials
[AD-A202530] N89-21542
BLACKOUT (PHYSIOLOGY)
G-induced loss of consciousness and its prevention
[AD-A202960] N89-21471
BLOWING
Potential flow evaluation of the interference effect of strut-through-appendage-tip model mounting technique and reduction of the effect using blowing and suction
[AD-A202424] N89-21199
BLUNT BODIES
A study of transonic drag reduction of a blunt cylinder by a cylinder probe
[AD-A202557] N89-20965
Investigation of the development of laminar boundary-layer instabilities along a blunted cone
[AD-A202425] N89-21200
BODY SIZE (BIOLOGY)
Measurer's handbook: US Army anthropometric survey, 1987-1988
[AD-A202721] N89-21484
BODY TEMPERATURE
Thermal protection afforded by two anti-exposure coveralls when worn in cold water
[AD-A202865] N89-21485
BODY-WING CONFIGURATIONS
Applied transonics at Grumman N89-20931
Computation of aircraft component flow fields at transonic Mach numbers using a three-dimensional Navier-Stokes algorithm N89-20933
Transonic aerodynamic design experience N89-20934
Wave drag due to lift for transonic airplanes N89-20938
Method to predict external store carriage loads at transonic speeds N89-20945
Euler/Navier-Stokes calculations of transonic flow past fixed- and rotary-wing aircraft configurations N89-20948
BOLIDES
Late Wenlock (middle Silurian) bio-events: Caused by volatile boloid impact/s N89-21295
Sedimentological effects of tsunamis, with particular reference to impact-generated and volcanogenic waves N89-21299
Multi-year global climatic effects of atmospheric dust from large bolide impacts N89-21397
Acute effects of a large bolide impact simulated by a global atmospheric circulation model N89-21398
BOLTS
Fractographic analysis of a failed crane bolt
[AD-A202703] N89-21274
BONES
Dinosaur bone beds and mass mortality: Implications for the K-T extinction N89-21301
BOOLEAN ALGEBRA
A diagnostic system using Boolean reasoning
[AD-A202764] N89-21602
BOSONS
Experimentally verifiable Yang-Mills spin 2 gauge theory of gravity with group U(1) x SU(2) N89-21693
BOUNDARIES
Darkness after the K-T impact: Effects of soot N89-21411
BOUNDARY ELEMENT METHOD
Application of the boundary element method to fatigue crack growth analysis
[AD-A202565] N89-21270
BOUNDARY LAYER COMBUSTION
Holographic particle sizing in solid fuel ramjets
[AD-A202699] N89-20997
BOUNDARY LAYER CONTROL
Effect of riblets upon flow separation in a subsonic diffuser
[AD-A203178] N89-20967
Performance of the active sidewall boundary-layer removal system for the Langley 0.3-meter Transonic Cryogenic Tunnel
[NASA-CR-181793] N89-21004
BOUNDARY LAYER EQUATIONS
Unsteady force calculations on circular cylinders and elliptical airfoils with circulation control
[UMAERO-87-37] N89-20962
Numerical study of three viscous/inviscid interaction methods
[AD-A202575] N89-21203
Variable wall temperature effects on multicellular natural convection in a horizontal annulus
[AD-A202762] N89-21691
BOUNDARY LAYER FLOW
Turbulence and modeling in transonic flow N89-20951
Turbulent eddy viscosity modeling in transonic shock/boundary-layer interactions N89-20952
Capabilities of wind tunnels with two-adaptive walls to minimize boundary interference in 3-D model testing N89-20961
BOUNDARY LAYER SEPARATION
An LDA (Laser-Doppler Anemometry) investigation of three-dimensional normal shock wave boundary-layer interactions N89-20956
Effect of riblets upon flow separation in a subsonic diffuser
[AD-A203178] N89-20967
Numerical simulation of flow over iced airfoils
[AD-A203291] N89-20969
Two-dimensional Navier-Stokes solution of the flow over a thick supercritical airfoil with strong shock-induced separation
[AD-A203331] N89-20971
Numerical study of three viscous/inviscid interaction methods
[AD-A202575] N89-21203
BOUNDARY LAYER STABILITY
Stability of compressible boundary layers N89-20953
Secondary three-dimensional instability in compressible boundary layers N89-20954
Investigation of the development of laminar boundary-layer instabilities along a cooled-wall cone in hypersonic flows
[AD-A202587] N89-20966
Investigation of the development of laminar boundary-layer instabilities along a blunted cone
[AD-A202425] N89-21200
BOUNDARY LAYERS
Shock-boundary-layer interaction in flight N89-20928
Investigation of modeling of damage growth in composite laminates
[AD-A202433] N89-21037
The implementation of a nonreflecting boundary into the SAMSON2 code
[AD-A203394] N89-21284
Blending of surface and rawinsonde data in mesoscale objective analysis
[AD-A203984] N89-21456
BOUNDARY VALUE PROBLEMS
Dilatationally nonlinear elastic materials. Part 2: An example illustrating stress concentration reduction
[AD-A202521] N89-21111
A rapid numerical procedure for determining axisymmetric transverse electric electromagnetic fields via boundary integrals
[AD-A202959] N89-21155
Bending and vibration of variable thickness orthotropic plates N89-21264
Film elastic properties determined by the indentation test-theoretical considerations
[AD-A203997] N89-21683
Guidance for an aeroassisted orbital transfer vehicle N89-21740
BRAIN
Brain activity during tactical decision-making. Part 5: A cross-study validation of evoked potentials as indices of workload
[AD-A203763] N89-21474
Design of a feeling-thinking machine N89-21510
BRANCHING (MATHEMATICS)
Application of the Laplace-Borel transformation to the representation of analytical solutions of Duffing's equation
[NASA-TM-100058] N89-21532
BRAZING
Design, fabrication, and performance of brazed, graphite electrode, multistage depressed collectors with 500-W, continuous wave, 4.8- to 9.6-GHz traveling-wave tubes
[NASA-TP-2904] N89-21171
BREMSSTRAHLUNG
Mechanisms for the source and loss of electrons
[AD-A203066] N89-21438
BRIGHTNESS
Reconstruction of binocular depth across continuous surfaces
[AD-A202827] N89-21469
BRILLOUIN ZONES
Molecular jet studies of vdW (van der Waals) clusters and solvation
[AD-A203766] N89-21212
BRITTLE MATERIALS
Fracture toughness testing of a ceramic matrix composite at elevated temperatures
[AD-A202738] N89-21114
BRITTLENESS
The effect of mixed-mode loading on stress-driven solute segregation during high-temperature brittle intergranular fracture
[AERE-R-12897] N89-21073
BROADBAND
Thermopile temperature sensitivity calibration procedure for Eppley broadband radiometers
[PB89-104129] N89-21215
BROKEN SYMMETRY
Symmetry breaking bifurcations and the growth of chaos in a rotating fluid
[AD-A204010] N89-21213
BUCKLING
Vibration and buckling characteristics of composite cylindrical panels incorporating the effects of a higher order shear theory
[AD-A202939] N89-21278
Transverse shear considerations in anisotropic plates
[AD-A203187] N89-21283
BUFFETING
An experimental study of transonic buffet of a supercritical airfoil with trailing edge flap
[AD-A203189] N89-20968
BUOYS
Localizing and beamforming freely-drifting VLF (Very Low Frequency) acoustic sensors
[AD-A202638] N89-21217

C

CADMIUM TELLURIDES
Electron paramagnetic resonance and photoluminescence studies of impurities in CdTe
[AD-A202841] N89-21056

CALCIUM ISOTOPES
Ion microprobe of Mg, Ca, Ti and Fe isotopic ratios and trace element abundances in hibonite-bearing inclusions from primitive meteorites N89-21719
CALCULUS
Semantical paradigms: Notes for an invited lecture [AD-A202995] N89-21565
CALIBRATING
Thermopile temperature sensitivity calibration procedure for Eppley broadband radiometers [PB89-104129] N89-21215
Construction of an alternating gradient magnetometer N89-21739
Angular response calibration of the burst and transient source experiment N89-21745
CALORIMETERS
Performance of a prototype electromagnetic calorimeter [DE89-007608] N89-21216
CAMERAS
Adapting Schottky diode detector technology to a space platform [AD-A202825] N89-21219
CANADA
Guide to Canadian aerospace related industries [AD-A203738] N89-21697
CANCELLATION
A cancellation technique for reducing background noise within turbulent flow environments characterized by pipes and annuli [AD-A202924] N89-21206
CAPACITANCE
Continued development and characterization of doped layers, contacts and associated electronic devices in silicon carbide [AD-A202450] N89-21176
Calculation of carriers in depletion region of semiconductors with capacitance-voltage measurements [AD-A202529] N89-21668
CAPACITANCE-VOLTAGE CHARACTERISTICS
Calculation of carriers in depletion region of semiconductors with capacitance-voltage measurements [AD-A202529] N89-21668
CAPACITORS
Advanced double layer capacitor [AD-A203059] N89-21181
CAPILLARY FLOW
Infrared surface temperature measurements for the surface tension driven convection experiment [NASA-TM-101353] N89-21224
CARBON
Research on silicon, carbon, and silicon carbide heterostructures [AD-A202866] N89-21116
Evidence for a single impact at the Cretaceous-Tertiary boundary from trace elements N89-21319
CARBON DIOXIDE
Impact production of NO and reduced species N89-21413
National Climate Program [PB89-118608] N89-21445
CARBON DIOXIDE CONCENTRATION
Carbon dioxide catastrophes: Past and future menace N89-21293
Environmental effects of large impacts on the earth; relation to extinction mechanisms N89-21365
Dynamics of exploding magma chambers: Implications for K-T volcanism and mass extinctions N89-21377
CARBON FIBERS
The use of primers in the adhesive bonding of carbon-fibre reinforced composites [AD-A202542] N89-21039
High temperature composites using Schiff's base pyropolymer matrices [AD-A203311] N89-21043
Physical and mechanical properties of American Cyanamid's acetylene-terminated prepreg system: T-300/CATB-44 [AD-A203737] N89-21045
CARBON ISOTOPES
Strangelove ocean at era boundaries, terrestrial or extraterrestrial cause N89-21332
The Cretaceous-Tertiary boundary marine extinction and global primary productivity collapse N89-21412
CARBON MONOXIDE
Theoretical studies of potential energy storage molecules [AD-A203986] N89-21638
CARBON 13
The global Cretaceous-Tertiary fire: Biomass or fossil carbon N89-21321
CARBONACEOUS CHONDRITES
Heavy metal toxicity as a kill mechanism in impact caused mass extinctions N89-21406
CARBOXYLIC ACIDS
Synthesis of energetic binders [AD-A203060] N89-21127
CASCADE FLOW
Asymptotic methods for internal transonic flows N89-20937
CASTING
Advanced single crystal for SSME turbopumps [NASA-CR-182244] N89-21072
Investigation of Weibull statistics in fracture analysis of cast aluminum [NASA-TM-102000] N89-21245
CATALYSIS
Center for Advanced Materials [DE89-008854] N89-21033
Theoretical studies of heterogeneous reactions in silicon CVD (Silicon Vapor Deposition) catalysis [AD-A202905] N89-21057
CATALYTIC ACTIVITY
Fuel-rich catalytic combustion of Jet-A fuel-equivalence ratios 5.0 to 8.0 [NASA-TM-101975] N89-21051
CATHODIC COATINGS
Electrolytic protection against high-temperature oxidation [AD-A203890] N89-21123
CATHODOLUMINESCENCE
Cathodoluminescence of shocked quartz at the Cretaceous-Tertiary boundary N89-21369
CATIONS
A fresh look at transport in perfluorosulfonate ionomers: Ultramicroelectrode investigations of Nafion and Dow ionomers [AD-A203855] N89-21066
CAUSES
The causality horizon and parallel processing for simulations with wide geographical dispersions [DE89-008484] N89-21590
CAVITIES
A numerical study of the turbulent free convection in rectangular cavities N89-21194
CAVITY RESONATORS
Transformations of Gaussian light beams caused by reflection in FEL (Free Electron Lasers) resonators [AD-A202472] N89-21227
CEILINGS (METEOROLOGY)
ER-2 lidar observations from the October 1986 fire cirrus experiment [NASA-TM-100704] N89-21444
CELLS (BIOLOGY)
Effects of simultaneous radiofrequency radiation and chemical exposure of mammalian cells, volume 2 [AD-A202780] N89-21467
Techniques for studying the effects of microgravity on model particle/cell systems N89-21758
CENSORED DATA (MATHEMATICS)
Order statistics and robust inference [AD-A203440] N89-21616
CERAMIC FIBERS
A study of the stress wave factor technique for evaluation of composite materials [NASA-CR-4195] N89-21256
CERAMIC MATRIX COMPOSITES
The behavior of ceramic matrix, fiber composites under combined impact and tensile stresses [AD-A202518] N89-21038
Investigation of failure modes in fiber reinforced ceramic matrix composites [AD-A202705] N89-21113
Fracture toughness testing of a ceramic matrix composite at elevated temperatures [AD-A202738] N89-21114
A study of the stress wave factor technique for evaluation of composite materials [NASA-CR-4195] N89-21256
CERAMICS
Nondestructive testing techniques for metal matrix composites [AERE-R-13040] N89-21034
Static tensile and tensile creep testing of five ceramic fibers at elevated temperatures [NASA-CR-177525] N89-21046
Acoustic microscopy of low ductility materials [AERE-R-12848] N89-21101
Synthesis of ceramics at low temperatures N89-21102
Investigation of the impact performance of various glass and ceramic systems [AD-A202443] N89-21106
Surface chemistry and structural effects in the stress corrosion of glass and ceramic materials [AD-A202452] N89-21107
Ceramics [AD-A202504] N89-21109
High temperature evaluation of new ferroelastic toughened ceramic materials [AD-A203197] N89-21120
Pre-pilot synthesis of low carbon Si3N4 [DE89-007202] N89-21124
High-temperature ceramic superconductors [AD-A202867] N89-21674
Dynamic fatigue testing of Zerodur glass-ceramic N89-21753
CEREBRAL CORTEX
Psychophysical studies of visual cortical functions [AD-A202814] N89-21468
CERENKOV COUNTERS
A novel approach to gamma-ray and neutrino astro-particle physics: The GRANDE experiment [DE89-006515] N89-21725
CHAFF
The use of chaff in space as a jamming device between ground stations and satellites [AD-A202577] N89-21146
CHANNEL FLOW
Asymptotic methods for internal transonic flows N89-20937
Instabilities in shear flow of viscoelastic fluids with fading memory [AD-A203735] N89-21211
Studies of liquid metal flows and power losses in ducts with moving conducting wall, slanted magnetic field, and applied external electric potential [AD-A203981] N89-21626
CHANNEL NOISE
Analysis and simulation of a pseudonoise synchronization system [AD-A202779] N89-21149
LCP-10 intelligibility of oxygen masks and microphones in aircraft noise [AD-A202474] N89-21481
CHAOS
Symmetry breaking bifurcations and the growth of chaos in a rotating fluid [AD-A204010] N89-21213
A neural network implementation of chaotic time series prediction [AD-A203049] N89-21569
CHARACTERIZATION
In-flight lightning characterization program on a CV-580 aircraft [AD-A203954] N89-20976
Prepolymer characterization [AD-A202821] N89-21115
Two photon characterization [AD-A203355] N89-21678
CHARGE CARRIERS
Analytic distribution for charge carriers in a semiconductor dominated by equivalent intervalley scattering [AD-A202537] N89-21669
CHARGED PARTICLES
Nuclear-pumped lasers for large-scale applications [DE89-006532] N89-21235
Corona wind cooling comparisons for horizontal cylinders [AD-A202714] N89-21625
CHEMICAL ANALYSIS
Hydrogen and deuterium internal friction behavior in vanadium-niobium alloys [DE89-007616] N89-21078
Iridium emissions from Hawaiian volcanoes N89-21314
Provenance of the K/T boundary layers N89-21331
Mass mortality and extraterrestrial impacts N89-21335
Faunal and erosional events in the Eastern Tethyan Sea across the K/T boundary N89-21338
Accretion rate of extraterrestrial matter: Iridium deposited over the last 70 million years N89-21344
Seawater strontium isotopes at the Cretaceous-Tertiary boundary N89-21350
Trace element and isotope geochemistry of Cretaceous-Tertiary boundary sediments: identification of extra-terrestrial and volcanic components N89-21352
Marine and continental K-T boundary clays compared N89-21382
CHEMICAL ATTACK
Experimental results on atomic oxygen corrosion of silver N89-21738
CHEMICAL BONDS
Organic functional group reactivities at metal surfaces [AD-A203094] N89-21086
Synthesis of ceramics at low temperatures N89-21102
Diffusion welding of an RS/PM aluminum alloy N89-21241

CHEMICAL COMPOSITION
Holographic investigation of solid propellant combustion
[AD-A203928] N89-21067
Investigation of the impedance modulation of thin films with a chemically-sensitive field-effect transistor
[AD-A202766] N89-21180
Implications of asteroid composition for the geochemistry of the ancient terrestrial projectile flux N89-21294
Ocean alkalinity and the Cretaceous/Tertiary boundary N89-21300
CHEMICAL EXPLOSIONS
Dynamics of exploding magma chambers: Implications for K-T volcanism and mass extinctions N89-21377
CHEMICAL LASERS
Nuclear-pumped lasers for large-scale applications
[DE89-006532] N89-21235
CHEMICAL REACTIONS
MOPAC manual, 5th edition: A general molecular orbital package
[AD-A204003] N89-21069
Calculation of the energetics of chemical reactions
[DE89-007262] N89-21070
Fuels combustion research
[AD-A204161] N89-21071
A review of reaction rates and thermodynamic and transport properties for the 11-species air model for chemical and thermal nonequilibrium calculations to 30000 K
[NASA-TM-101528] N89-21193
Laser enhanced chemical reactions
[DE89-008084] N89-21236
Carbon dioxide catastrophes: Past and future menace N89-21293
Time and state resolved studies of molecular decomposition
[AD-A202464] N89-21836
CHEMILUMINESCENCE
Correction of gain and optical throughput variations in a two-dimensional imaging spectrometer
[AD-A203495] N89-21222
CHEMISORPTION
Topics in chemical physics. 1: Semiclassical reactive scattering theory. 2: Corrected effective medium theory
[DE89-007606] N89-21053
CHESAPEAKE BAY (US)
Ice cover on Chesapeake Bay from AVHRR (Advanced Very High Resolution Radiometer) and LANDSAT imagery, winter of 1987-88
[PB89-117261] N89-21415
CHINA
New approach to the origin of the tektite in China N89-21414
CHIPS (ELECTRONICS)
The design and performance of the rollback chip: Hardware support for time warp
[AD-A203160] N89-21571
The design and implementation of a special purpose cache for the roll back chip
[AD-A203091] N89-21583
CHIPS (MEMORY DEVICES)
The 8755 emulator design
[AD-A202649] N89-21178
CHIRON
Disruption of giant comets in the solar system and around other stars N89-21408
CHIRP
A theoretical and experimental investigation of linear and nonlinear focussing chirped optical diffraction gratings
[AD-A203396] N89-21650
CHOLESKY FACTORIZATION
A language comparison for scientific computing on MIMD architectures
[NASA-CR-181779] N89-21537
CHROMOSPHERE
Luminosity variations of stars similar to the sun
[AD-A203664] N89-21713
CHRONOLOGY
Strategic defense initiative: A chronology, 1983 - 1988
[AD-A203576] N89-21619
CIRCUITS
Performance of a prototype electromagnetic calorimeter
[DE89-007608] N89-21216
HOP (Hardware viewed as Objects and Processes): A process model for synchronous hardware systems
[AD-A203090] N89-21535
CIRCULAR CYLINDERS
Unsteady force calculations on circular cylinders and elliptical airfoils with circulation control
[UMAERO-87-37] N89-20962
Computational studies of an impulsively started viscous flow
[NASA-TM-101037] N89-21190
A simple analysis of swage autofrettage process N89-21498
CIRCULAR ORBITS
Optimal launch time for a discontinuous low thrust orbit transfer
[AD-A202693] N89-21007
Control system for maintaining stable orbits around phobos
[AD-A202776] N89-21008
Estimated satellite cluster elements in near circular orbit
[AD-A202938] N89-21011
CIRRUS CLOUDS
ER-2 lidar observations from the October 1986 fire cirrus experiment
[NASA-TM-100704] N89-21444
CLASSIFICATIONS
Dynamic analysis of feedforward neural networks using simulated and measured data
[AD-A202573] N89-21591
SESC (Space Environment Services Center) glossary of solar-terrestrial terms, 2nd edition
[PB89-120802] N89-21698
CLAYS
Shocked quartz and more: Impact signatures in K-T boundary clays and claystones N89-21297
Impact wave deposits provide new constraints on the location of the K/T boundary impact N89-21330
Faunal and erosional events in the Eastern Tethyan Sea across the K/T boundary N89-21338
Marine and continental K-T boundary clays compared N89-21382
Evidence of volcanic ash at a K-T boundary section: Ocean drilling program hole 690 C, Maud Rise, Weddell Sea off East Antarctica N89-21410
CLIMATE
Corrosion control climatology
[AD-A202477] N89-21079
An extended Cretaceous-Tertiary (K/T) stable isotope record. Implications for paleoclimate and the nature of the K/T boundary event N89-21310
Volcanism, global catastrophe and mass mortality N89-21316
Air quality and forest health issues in the 1990s
[DE89-006941] N89-21427
CCM (Community Climate Model)
[PB89-120927] N89-21446
CLIMATE CHANGE
Global Catastrophes in Earth History: An Interdisciplinary Conference on Impacts, Volcanism, and Mass Mortality
[NASA-CR-183329] N89-21287
Late Wenlock (middle Silurian) bio-events: Caused by volatile boloid impact/s N89-21295
Abrupt climate change and extinction events N89-21308
The end-triassic mass extinction event N89-21324
Patterns of megafloral change across the Cretaceous-Tertiary boundary in the Northern Great Plains and Rocky Mountains N89-21336
Catastrophic volcanism N89-21346
Mass killings and detection of impacts N89-21356
Earth orbital variations and vertebrate bioevolution N89-21357
Permo-Triassic vertebrate extinctions: A program N89-21367
Climatic changes resulting from mass extinctions at the K-T boundary (and other bio-events) N89-21373
Assessment of the atmospheric impact of volcanic eruptions N89-21388
Cretaceous-Tertiary boundary in the Antarctic: Climatic cooling precedes biotic crisis N89-21392
A regional perspective on the palynofloral response to K-T boundary event(s) with emphasis on variations imposed by the effects of sedimentary facies and latitude N89-21395
Multi-year global climatic effects of atmospheric dust from large bolide impacts N89-21397
An individual-based forest ecosystems model for projecting forest response to nutrient cycling and climate changes
[DE89-007212] N89-21428
National Climate Program
[PB89-118608] N89-21445
CLIMATOLOGY
Corrosion control climatology
[AD-A202477] N89-21079
Late Wenlock (middle Silurian) bio-events: Caused by volatile boloid impact/s N89-21295
High resolution chronology of late Cretaceous-early Tertiary events determined from 21,000 yr orbital-climatic cycles in marine sediments N89-21328
Step-wise extinctions at the Cretaceous-Tertiary boundary and their climatic implications N89-21354
Cretaceous-Tertiary boundary in the Antarctic: Climatic cooling precedes biotic crisis N89-21392
The seasonal cycle of energetics from the GLAS/UMD climate GCM
[NASA-TM-100714] N89-21448
Upper-wind climatology for CONUS
[AD-A203961] N89-21453
Seasonal snowfall statistics for selected stations
[AD-A203965] N89-21454
Global snow depth climatology
[AD-A203969] N89-21455
CLINICAL MEDICINE
Nonparamteric estimation from queues arising in staggered entry clinical trials N89-21520
CLOCKS
The design and performance of the rollback chip: Hardware support for time warp
[AD-A203160] N89-21571
CLOUD COVER
Climatic changes resulting from mass extinctions at the K-T boundary (and other bio-events) N89-21373
Summary of Meteorological Observations, Surface (SMOS) for Moffett Field, California
[AD-A203628] N89-21451
CLOUD DISPERSAL
A cloud model simulation of space shuttle exhaust clouds in different atmospheric conditions
[NASA-CR-4223] N89-21426
CLOUD HEIGHT INDICATORS
ER-2 lidar observations from the October 1986 fire cirrus experiment
[NASA-TM-100704] N89-21444
CLOUD PHYSICS
Icing considerations for HALE (High Altitude, Long Endurance) aircraft
[AD-A202584] N89-20975
A cloud model simulation of space shuttle exhaust clouds in different atmospheric conditions
[NASA-CR-4223] N89-21426
Satellite signatures of rapid cyclogenesis
[AD-A203934] N89-21452
CLOUDS (METEOROLOGY)
The use of chaff in space as a jamming device between ground stations and satellites
[AD-A202577] N89-21146
Satellite signatures of rapid cyclogenesis
[AD-A203934] N89-21452
CLUSTER ANALYSIS
Statistical machine learning for the cognitive selection of nonlinear programming algorithms in engineering design optimization N89-21493
CLUTTER
Spectral characteristics of High Frequency (HF) backscatter for high latitude ionospheric irregularities: Preliminary analysis of statistical properties
[AD-A202998] N89-21156
COALESCING
A search for gravitational waves from coalesing binary stars using the Caltech 40 meter gravity wave detector N89-21721
COASTAL CURRENTS
Computer program for calculating frequencies and modal structures of free coastal-trapped waves
[PB88-243928] N89-21459
COATINGS
Surface acoustic wave detection of organophosphorus compounds
[AD-A202909] N89-21058
Advanced tribological coatings for high specific strength alloys
[AD-A202505] N89-21110
The radar cross section of a two dimensional dielectric coated cylinder using on-surface radiation conditions
[AD-A202935] N89-21152
Plasma reaction method and apparatus
[DE89-007360] N89-21656
COCKPITS
Performance analysis of the fiber distributed data interface in the super cockpit audio world
[AD-A202535] N89-20985
F-16 speaker-independent speech recognition system using cockpit commands (70 words)
[AD-A203177] N89-21489
CODING
Optical computing research
[AD-A202963] N89-21564
COGNITION
The Rochester robot
[AD-A202633] N89-21247
Coping with novelty and human intelligence: The role of counterfactual reasoning
[AD-A203624] N89-21478
COLD CATHODE TUBES
Study of the generation of intense pulsed electron beams using glow discharges
[AD-A202438] N89-21624

COLD FLOW TESTS
Operation of vehicle engines in cold conditions: Start up, lubrication and fuel consumption
[DE88-757111] N89-21255
COLD WATER
Thermal protection afforded by two anti-exposure coveralls when worn in cold water
[AD-A202865] N89-21485
COLLIMATION
A robust adaptive array structure using the soft constrained LMS algorithm
[AD-A203959] N89-21167
COLLISION RATES
Asteroid and comet flux in the neighborhood of the earth N89-21387
COLLISIONS
Collisions with ice-volatile objects: Geological implications N89-21409
COLOR
A helmet-mounted virtual environment display system
[AD-A203055] N89-20994
Cathodoluminescence of shocked quartz at the Cretaceous-Tertiary boundary N89-21369
COLOR PHOTOGRAPHY
High resolution chronology of late Cretaceous-early Tertiary events determined from 21,000 yr orbital-climatic cycles in marine sediments N89-21328
COMBAT
Light satellites: A dilemma for the US Army
[AD-A202648] N89-21017
COMBINED STRESS
The behavior of ceramic matrix, fiber composites under combined impact and tensile stresses
[AD-A202518] N89-21038
COMBUSTIBLE FLOW
High density fuel effects
[AD-A202426] N89-21125
Advanced diagnostics for reacting flows
[AD-A202451] N89-21202
COMBUSTION
Spectral analysis of a fourth-order singular differential operator arising in combustion
[DE89-005841] N89-21052
Magnetic microspherules associated with the K/T and upper Eocene extinction events N89-21303
COMBUSTION CHAMBERS
Automatic measurement of particles from holograms taken in the combustion chamber of a rocket motor
[AD-A203955] N89-21030
The effect of platinum catalysts on propane oxidation at elevated pressure
[AD-A202999] N89-21060
High density fuel effects
[AD-A202426] N89-21125
Magnetic flowmeter measurement of solid propellant pressure-coupled and velocity-coupled responses
[AD-A203988] N89-21133
COMBUSTION CONTROL
Fuels combustion research
[AD-A204161] N89-21071
COMBUSTION EFFICIENCY
Holographic particle sizing in solid fuel ramjets
[AD-A202699] N89-20997
COMBUSTION PHYSICS
Fuels combustion research
[AD-A204161] N89-21071
COMBUSTION STABILITY
Magnetic flowmeter measurement of solid propellant pressure-coupled and velocity-coupled responses
[AD-A203988] N89-21133
COMBUSTION TEMPERATURE
Gas turbine alternative fuels combustion characteristics
[NASA-TM-101470] N89-21417
COMETS
Asteroid and comet flux in the neighborhood of the earth N89-21387
The cometary and asteroidal impactor flux at the earth N89-21407
Disruption of giant comets in the solar system and around other stars N89-21408
New approach to the origin of the tektite in China N89-21414
COMMAND AND CONTROL
Strategic defense initiative program: Better management direction and controls needed
[GAO/NSIAD-88-26] N89-21694
COMMONALITY
Development of a prototype commonality analysis tool for use in space programs N89-21757
COMMUNICATION
Estimated satellite cluster elements in near circular orbit
[AD-A202938] N89-21011
COMMUNICATION CABLES
SURVNET user's manual
[AD-A203372] N89-21164
COMMUNICATION EQUIPMENT
AH-1S communication switch integration program
[NASA-TM-101053] N89-20978
COMMUNICATION NETWORKS
Performance analysis of the fiber distributed data interface in the super cockpit audio world
[AD-A202535] N89-20985
A modeling perspective for meteor burst communication
[AD-A202562] N89-21145
Improving the survivability of a stochastic communication network
[AD-A202872] N89-21150
SURVNET user's manual
[AD-A203372] N89-21164
Performance directed simulation
[AD-A203089] N89-21570
SpringNet: A network of multiprocessors for hard real-time
[AD-A203348] N89-21587
Lookahead in parallel discrete event simulation
[AD-A203902] N89-21588
Scientific and Technical Information Network (STINET) and DOD Gateway Information System (DGIS): Reference publications bibliography
[AD-A203926] N89-21704
COMMUNICATION THEORY
Domain modeling for language analysis
[AD-A203444] N89-21574
COMPARISON
Comparison of propeller cruise noise data taken in the NASA Lewis 8- by 6-foot wind tunnel with other tunnel and flight data
[NASA-TM-101976] N89-21628
Luminosity variations of stars similar to the sun
[AD-A203864] N89-21713
COMPENSATORY TRACKING
Response equivocation analysis for the smart stick controller
[AD-A203146] N89-20989
COMPILERS
FX-87 performance measurements: Dataflow implementation
[AD-A203150] N89-21585
COMPLEX COMPOUNDS
Excited state energetics and dynamics of large molecules, complexes and clusters
[AD-A203514] N89-21065
COMPONENT RELIABILITY
Evaluate the application of modal test and analysis processes to structural fault detection in MSFC-STS project elements N89-21751
COMPONENTS
WhiteStar project engineering component selection database
[DE89-008321] N89-21709
COMPOSITE MATERIALS
Center for Advanced Materials
[DE89-008854] N89-21033
Thermodynamic analysis of chemical compatibility of several reinforcement materials with niobium aluminides
[NASA-CR-182260] N89-21036
Investigation of modeling of damage growth in composite laminates
[AD-A202433] N89-21037
The use of primers in the adhesive bonding of carbon-fibre reinforced composites
[AD-A202542] N89-21039
A study of failure characteristics in a thermoplastic composite material at high temperature
[AD-A203015] N89-21040
Microscopic aspects of failure and fracture in cross-ply fiber-reinforced composite laminates
[AD-A203202] N89-21042
An investigation of stresses and strains in an internally pressurized, composite-jacketed, steel cylinder
[AD-A202969] N89-21281
Transactions of the Fifth Army Conference on Applied Mathematics and Computing
[AD-A193384] N89-21490
Optimal design of a two-way conductor N89-21499
COMPOSITE STRUCTURES
Effects of battle damage repair on the natural frequencies and mode shapes of curved rectangular composite panels
[AD-A203179] N89-21041
Inelastic deformation and failure analysis of filament-wound composite structures
[AD-A203382] N89-21044
Physical and mechanical properties of American Cyanamid's acetylene-terminated prepreg system: T-300/CATB-44
[AD-A203737] N89-21045
Nb modification of microcomposite Fe/C/Cr/Mn steel
[DE89-008297] N89-21097
Nonlinear finite element analysis of a general composite shell
[AD-A202572] N89-21271
A triangular thin shell element for the linear analysis of stiffened composite structures
[AD-A202864] N89-21277
Vibration and buckling characteristics of composite cylindrical panels incorporating the effects of a higher order shear theory
[AD-A202939] N89-21278
Finite element analysis of composite plates including shear deformation
[AD-A202941] N89-21279
On a refined nonlinear theory of laminated composite plates N89-21500
COMPRESSIBILITY
Compressive properties of high performance polymeric fibers
[AD-A202947] N89-21117
COMPRESSIBLE BOUNDARY LAYER
Secondary three-dimensional instability in compressible boundary layers N89-20954
COMPRESSIBLE FLOW
Transverse jets in compressible crossflows N89-20923
Stability of compressible boundary layers N89-20953
Experimental examination of the aerothermal performance of the T-10 test cell at NAS (Naval Air Station), Cubi Point
[AD-A203887] N89-21005
Studies in the computation of compressible and viscous flow
[AD-A203334] N89-21208
COMPRESSION LOADS
Effect of TNT miscible additives on the mechanical behavior and shock sensitivity of Composition B
[AD-A203968] N89-21132
COMPRESSORS
Performance of the active sidewall boundary-layer removal system for the Langley 0.3-meter Transonic Cryogenic Tunnel
[NASA-CR-181793] N89-21004
COMPUTATION
Calculation of the energetics of chemical reactions
[DE89-007262] N89-21070
Calculation of the glass transition temperatures of linear polymers. Part 3: Evaluation of calculation relationships
[AD-A203357] N89-21122
A generalized approach to direction finding
[AD-A203768] N89-21186
Studies in the computation of compressible and viscous flow
[AD-A203334] N89-21208
Computational issues in goal programming resource allocation N89-21509
Spline-based finite-element method for solving a Stefan's problem in a finite domain: Formulation N89-21516
A block QR factorization scheme for loosely coupled systems of array processors N89-21519
Center for the Integration of Optical Computing
[AD-A203254] N89-21536
Critical problems in very large scale computer systems
[AD-A203299] N89-21586
COMPUTATIONAL FLUID DYNAMICS
Comparison of 3D computation and experiment for non-axisymmetric nozzles
[NASA-CR-182245] N89-20921
Transonic Symposium: Theory, Application, and Experiment, Volume 1, Part 1
[NASA-CP-3020-VOL-1-PT-1] N89-20925
Airframe/propulsion integration characteristics at transonic speeds N89-20926
Transonic CFD applications at Boeing N89-20929
The application of CFD for military aircraft design at transonic speeds N89-20930
Applied transonics at Grumman N89-20931
Transonics and fighter aircraft: Challenges and opportunities for CFD N89-20932
Computation of aircraft component flow fields at transonic Mach numbers using a three-dimensional Navier-Stokes algorithm N89-20933
Transonic aerodynamic design experience N89-20934
Euler solvers for transonic applications N89-20935
An embedded mesh procedure for leading-edge vortex flows N89-20936
Asymptotic methods for internal transonic flows N89-20937
Vector potential methods N89-20939
Developments and trends in three-dimensional mesh generation N89-20940
Generation of unstructured grids and Euler solutions for complex geometries N89-20941

Transonic Symposium: Theory, Application, and Experiment, volume 1, part 2
[NASA-CP-3020-VOL-1-PT-2] N89-20942
Thin-layer Navier-Stokes solutions for a cranked delta wing
[AD-A203292] N89-20970
Convection and chemistry effects in CVD: A 3-D analysis for silicon deposition
[NASA-TM-102001] N89-21032
Computational studies of an impulsively started viscous flow
[NASA-TM-101037] N89-21190
Volumetric rendering techniques for the display of three-dimensional aerodynamic flow field data
[AD-A202661] N89-21204
Skew grids and irrotational flow N89-21523
Adaptive optical linear algebra processors
[AD-A202996] N89-21605
Research Reports: 1988 NASA/ASEE Summer Faculty Fellowship Program
[NASA-CR-183553] N89-21726
The role of the turbulent Prandtl number in turbine blade heat transfer prediction N89-21756
Space shuttle main engine numerical modeling code modifications and analysis N89-21760

COMPUTATIONAL GRIDS
Generation of unstructured grids and Euler solutions for complex geometries N89-20941
Aerodynamic analysis of three advanced configurations using the TranAir full-potential code N89-20944
Two-dimensional Navier-Stokes solution of the flow over a thick supercritical airfoil with strong shock-induced separation
[AD-A203331] N89-20971
Condition of the finite element stiffness matrix of highly irregular triangular grids N89-21497
A posteriori error estimation of adaptive finite difference schemes for hyperbolic systems N89-21513
An adaptive overlapping local grid refinement method for two-dimensional parabolic systems N89-21514
Skew grids and irrotational flow N89-21523

COMPUTER AIDED DESIGN
Transonic propulsion system integration analysis at McDonnell Aircraft Company N89-20943
Euler/Navier-Stokes calculations of transonic flow past fixed- and rotary-wing aircraft configurations N89-20948
Navier-Stokes and viscous-inviscid interaction N89-20949
Performance optimization for rotors in hover and axial flight
[NASA-CR-177524] N89-20973
A compendium of controlled diffusion blades generated by an automated inverse design procedure
[NASA-TM-101968] N89-20996
The boundary-integral method for planar microstrip circuits
[AD-A203715] N89-21185
Comparison study of gear dynamic computer programs at NASA Lewis Research Center
[NASA-TP-2901] N89-21243
Knowledge representation and planning control in an expert system for the creative design of mechanisms N89-21492
Model-based silhouette recognition
[AD-A202540] N89-21552
Computer-aided X-ray imaging system design and evaluation
[DE89-006599] N89-21653

COMPUTER AIDED MANUFACTURING
Computer-aided fabrication system implementation
[AD-A203651] N89-21576
Migration strategies roles for data management in CIM
[DE89-008112] N89-21708

COMPUTER ASSISTED INSTRUCTION
Refining, revising, augmenting, compiling and developing computer assisted instruction K-12 aerospace materials for implementation in NASA spacelink electronic information system N89-21729

COMPUTER GRAPHICS
Graphical man-machine interface for an integrated evaluation environment
[AD-A203054] N89-21487
GRAPS (Graphical Plotting System) user's guide. A graphical plotting system for displaying scientific and engineering data
[AD-A202583] N89-21559
Influence diagrams: Automated analysis with dynamic programming
[AD-A203045] N89-21567
Time-of-flight small-angle neutron scattering data reduction and analysis at LANSCE with program SMR
[DE89-006520] N89-21578

COMPUTER NETWORKS
Nonprocedural implementation of mathematical programming algorithms
[AD-A203392] N89-21573
VAX to CRAY NASTRAN user interface
[AD-A203447] N89-21575
Advanced information processing system: Local system services
[NASA-CR-181767] N89-21582
Development of the domain name system
[AD-A203901] N89-21703

COMPUTER PROGRAM INTEGRITY
Maintenance metrics for Jovial (J73) software
[AD-A202713] N89-21561

COMPUTER PROGRAMMING
A source code analyzer to predict compilation time for avionics software using software science measures. Volume 1: Main report
[AD-A202737] N89-20992
The 8755 emulator design
[AD-A202649] N89-21178
Transactions of the Fifth Army Conference on Applied Mathematics and Computing
[AD-A193384] N89-21490
Computational issues in goal programming resource allocation N89-21509
The Environment for Application Software Integration and Execution (EASIE) version 1.0. Volume 1: Executive overview
[NASA-TM-100573] N89-21538
Parallel solution of sparse one-dimensional dynamic programming problems
[NASA-CR-181812] N89-21542
A decision-based methodology for object oriented-design
[AD-A202579] N89-21558
The design and performance of the rollback chip: Hardware support for time warp
[AD-A203160] N89-21571
Software development guidelines
[AD-A203332] N89-21572
Institute for Computational Mechanics in Propulsion (ICOMP)
[NASA-TM-101961] N89-21595
Strategic defense initiative program: Better management direction and controls needed
[GAO/NSIAD-88-26] N89-21694
Optimization of large matrix calculations for execution on the Cray X-MP vector supercomputer N89-21742

COMPUTER PROGRAMS
Additional development of the XTRAN3S computer program
[NASA-CR-181743] N89-20922
The application of CFD for military aircraft design at transonic speeds N89-20930
Applied transonics at Grumman N89-20931
Aerodynamic analysis of three advanced configurations using the TranAir full-potential code N89-20944
An analytical framework for determining life cycle cost implications of the advanced launch system
[AD-A202873] N89-21012
Derivation and testing of computer algorithms for automatic real-time determination of space vehicle potentials in various plasma environments
[AD-A203019] N89-21019
Automatic measurement of particles from holograms taken in the combustion chamber of a rocket motor
[AD-A203955] N89-21030
Convection and chemistry effects in CVD: A 3-D analysis for silicon deposition
[NASA-TM-102001] N89-21032
XRAYL: A powder diffraction profile refinement program
[PB89-127567] N89-21050
MOPAC manual, 5th edition: A general molecular orbital package
[AD-A204003] N89-21069
Computer simulation of macrosegregation in directionally solidified circular ingots
[NASA-CR-182838] N89-21134
Performance of an adaptive matched filter using the Griffiths algorithm
[AD-A202578] N89-21147
On the impulse response of monopulse radars
[AD-A202936] N89-21153
Effect of two-body motion on radar beam quality for various distributed sparse array configurations
[AD-A202937] N89-21154
The boundary-integral method for planar microstrip circuits
[AD-A203715] N89-21185
Analysis of space-based lidar for aircraft tracking
[AD-A202665] N89-21230
Advanced helium purge seals for Liquid Oxygen (LOX) turbopumps
[NASA-CR-182105] N89-21239
Comparison study of gear dynamic computer programs at NASA Lewis Research Center
[NASA-TP-2901] N89-21243
Bending and vibration of variable thickness orthotropic plates N89-21264
The implementation of a nonreflecting boundary into the SAMSON2 code
[AD-A203394] N89-21284
Computer program for calculating frequencies and modal structures of free coastal-trapped waves
[PB88-243928] N89-21459
LMS adaptive filtering applied to a microwave arterial pulse monitor
[AD-A202732] N89-21465
Accurate determination of the complex permittivity of biological tissue around 35 GHz
[AD-A202907] N89-21470
Graphical man-machine interface for an integrated evaluation environment
[AD-A203054] N89-21487
An algorithm for processing scanning spectrometer data N89-21506
Computational issues in goal programming resource allocation N89-21509
DATAMAP upgrade version 4.0
[NASA-TM-100993] N89-21541
Documentation of the finite element code VISCOT/UX for thermomechanical analyses: Version 0.01
[DE89-004719] N89-21544
Simulating rule-based systems
[AD-A202563] N89-21555
A decision-based methodology for object oriented-design
[AD-A202579] N89-21558
GRAPS (Graphical Plotting System) user's guide. A graphical plotting system for displaying scientific and engineering data
[AD-A202583] N89-21559
Maintenance metrics for Jovial (J73) software
[AD-A202713] N89-21561
Influence diagrams: Automated analysis with dynamic programming
[AD-A203045] N89-21567
Software development guidelines
[AD-A203332] N89-21572
Nonprocedural implementation of mathematical programming algorithms
[AD-A203392] N89-21573
Computer-aided fabrication system implementation
[AD-A203651] N89-21576
Time-of-flight small-angle neutron scattering data reduction and analysis at LANSCE with program SMR
[DE89-006520] N89-21578
Otter 1.0 users' guide
[DE89-008656] N89-21581
Selection of a frequency sensitive QFT (Quantitative Feedback Theory) weighting matrix using the method of specified outputs
[AD-A202692] N89-21592
The interdependencies of theory formation, revision, and experimentation
[AD-A202882] N89-21618
Nonlinear real-time optical signal processing
[AD-A202445] N89-21641
A numerical model for the computation of radiance distributions in natural waters with wind-roughened surfaces. Part 2: User's guide and code listing
[AD-A203441] N89-21651
Computer-aided X-ray imaging system design and evaluation
[DE89-006599] N89-21653
Analysis of the Federal Aviation Administration's host computer acquisition process and potential application in Department of Defense acquisitions
[AD-A202623] N89-21695
Computer codes for thermal analysis of a solid rocket motor nozzle N89-21733
The simulation of the alternate turbopump development high pressure oxygen and fuel turbopumps for the space shuttle main engine using the Shaberth computer program N89-21746
Electron mobility in mercury cadmium telluride N89-21748
Simulation of water vapor condensation on LOX droplet surface using liquid nitrogen N89-21749
The role of the turbulent Prandtl number in turbine blade heat transfer prediction N89-21756
Development of a prototype commonality analysis tool for use in space programs N89-21757
Space shuttle main engine numerical modeling code modifications and analysis N89-21760

COMPUTER STORAGE DEVICES
A block QR factorization scheme for loosely coupled systems of array processors N89-21519
The virtual time machine
[AD-A203087] N89-21533

Center for the Integration of Optical Computing
[AD-A203254] N89-21536
The design and implementation of a special purpose cache for the roll back chip
[AD-A203091] N89-21583

COMPUTER SYSTEMS DESIGN
A helmet-mounted virtual environment display system
[AD-A203055] N89-20994
Graphical man-machine interface for an integrated evaluation environment
[AD-A203054] N89-21487
SpringNet: A network of multiprocessors for hard real-time
[AD-A203348] N89-21587

COMPUTER SYSTEMS PERFORMANCE
Distributed discrete-event simulation using variants of the Chandy-Misra algorithm on the intel hypercube
[AD-A202849] N89-21563

COMPUTER SYSTEMS PROGRAMS
Real-time display of time dependent data using a head-mounted display
[AD-A203051] N89-20993
The Environment for Application Software Integration and Execution (EASIE) version 1.0. Volume 1: Executive overview
[NASA-TM-100573] N89-21538

COMPUTER TECHNIQUES
Nonlinear finite element analysis of a general composite shell
[AD-A202572] N89-21271
Computational issues in goal programming resource allocation N89-21509
Objects as closures: Abstract semantics of object oriented languages
[NASA-CR-184877] N89-21540
Parallel solution of sparse one-dimensional dynamic programming problems
[NASA-CR-181812] N89-21542
Deductive programming
[AD-A202489] N89-21546
TABLOG: The deductive tableau programming language
[AD-A202490] N89-21547
Model-based silhouette recognition
[AD-A202540] N89-21552
Computer-aided fabrication system implementation
[AD-A203651] N89-21576
Institute for Computational Mechanics in Propulsion (ICOMP)
[NASA-TM-101961] N89-21595
A diagnostic system using Boolean reasoning
[AD-A202764] N89-21602
Computer assisted analysis and modelling of structured problems
[AD-A203040] N89-21607
Research Reports: 1988 NASA/ASEE Summer Faculty Fellowship Program
[NASA-CR-183553] N89-21726

COMPUTERIZED SIMULATION
Numerical simulation of the flow field over delta wings with leading edge blowing N89-20924
Transonic aerodynamic design experience N89-20934
Vector potential methods N89-20939
Developments and trends in three-dimensional mesh generation N89-20940
Transonic Symposium: Theory, Application, and Experiment, volume 1, part 2
[NASA-CP-3020-VOL-1-PT-2] N89-20942
Simulation at Dryden Flight Research Facility from 1957 to 1982
[NASA-TM-101695] N89-20983
Performance analysis of the fiber distributed data interface in the super cockpit audio world
[AD-A202535] N89-20985
A wind tunnel and computer investigation of the low speed aerodynamic characteristics of the prone escape system (PRESS)
[AD-A202768] N89-20988
Ceramics
[AD-A202504] N89-21109
Computer simulation of macrosegregation in directionally solidified circular ingots
[NASA-CR-182838] N89-21134
A modeling perspective for meteor burst communication
[AD-A202562] N89-21145
Computer strategy for detecting line features on simulated binary arrays in support of radar feature extraction
[AD-A203257] N89-21162
Studies in the computation of compressible and viscous flow
[AD-A203334] N89-21208
Computer modeling of large asteroid impacts into continental and oceanic sites: Atmospheric, cratering, and ejecta dynamics N89-21379
Essential elements in the numerical modeling of solar cells
[DE89-008113] N89-21424
Enhancements to the AFGL (Air Force Geophysics Laboratory) Statistical Analysis Program (ASAP) for the global multivariate analysis of heights and winds
[AD-A202912] N89-21450
Computer simulation of a pilot in V/STOL aircraft control loops
[NASA-CR-184815] N89-21479
Transactions of the Fifth Army Conference on Applied Mathematics and Computing
[AD-A193384] N89-21490
Design of a feeling-thinking machine N89-21510
The numerical simulation of Richtmyer-Meshkov unstable interfaces: A conference report N89-21512
Time warp on a shared memory multiprocessor
[AD-A203088] N89-21534
HOP (Hardware viewed as Objects and Processes): A process model for synchronous hardware systems
[AD-A203090] N89-21535
Empirical demonstration of isoperformance methodology preparatory of an interactive expert computerized decision aid
[AD-A202439] N89-21545
Response surface analysis of stochastic network performance
[AD-A202561] N89-21554
Simulating rule-based systems
[AD-A202563] N89-21555
Distributed discrete-event simulation using variants of the Chandy-Misra algorithm on the intel hypercube
[AD-A202849] N89-21563
A software system to create a hierarchical, multiple level of detail terrain model
[AD-A203047] N89-21568
Performance directed simulation
[AD-A203089] N89-21570
The design and performance of the rollback chip: Hardware support for time warp
[AD-A203160] N89-21571
SpringNet: A network of multiprocessors for hard real-time
[AD-A203348] N89-21587
The causality horizon and parallel processing for simulations with wide geographical dispersions
[DE89-008484] N89-21590
Optical activity and its influence on photorefractive materials
[AD-A202530] N89-21642
A numerical model for the computation of radiance distributions in natural waters with wind-roughened surfaces. Part 2: User's guide and code listing
[AD-A203441] N89-21651
Computer-aided X-ray imaging system design and evaluation
[DE89-006599] N89-21653
Computer modeling and simulation in inertial confinement fusion
[DE89-008304] N89-21661
Distribution of boron atoms in ion implanted compound semiconductors
[AD-A203173] N89-21677
Finite element simulation of thunderstorm electrodynamics in the proximity of the storm N89-21728
Small expendable deployer system measurement analysis N89-21731
Investigation of practical applications of H infinity control theory to the design of control systems for large space structures N89-21743
Fluctuation analysis of relativistic nucleus-nucleus collisions in emulsion chambers N89-21747

COMPUTERS
Defense technical information center's role in numeric database development
[AD-A202901] N89-21701

CONCURRENT PROCESSING
The causality horizon and parallel processing for simulations with wide geographical dispersions
[DE89-008484] N89-21590

CONDENSING
Simulation of water vapor condensation on LOX droplet surface using liquid nitrogen N89-21749

CONFERENCES
Transonic Symposium: Theory, Application, and Experiment, Volume 1, Part 1
[NASA-CP-3020-VOL-1-PT-1] N89-20925
Optoelectronic workshops. Part 4: Liquid Crystals for Laser Applications
[AD-A202526] N89-21228
Global Catastrophes in Earth History: An Interdisciplinary Conference on Impacts, Volcanism, and Mass Mortality
[NASA-CR-183329] N89-21287
Transactions of the Fifth Army Conference on Applied Mathematics and Computing
[AD-A193384] N89-21490

CONFIDENCE LIMITS
Response surface methodology applied to the radar range equation
[AD-A203044] N89-21157
Confidence set inference with a prior quadratic bound
[NASA-CR-184839] N89-21435

CONFIGURATION MANAGEMENT
Software development guidelines
[AD-A203332] N89-21572

CONFINEMENT
A laser trap for neutral atoms
[AD-A202581] N89-21229

CONGRESSIONAL REPORTS
Aviation safety: Measuring how safely individual airlines operate
[GAO/RCED-88-61] N89-20974
Microwave landing systems: Additional systems should not be procured unless benefits proven
[GAO/RCED-88-118] N89-20977
Strategic defense initiative program: Better management direction and controls needed
[GAO/NSIAD-88-26] N89-21694

CONICAL BODIES
Investigation of the development of laminar boundary-layer instabilities along a cooled-wall cone in hypersonic flows
[AD-A202587] N89-20966
Investigation of the development of laminar boundary-layer instabilities along a blunted cone
[AD-A202425] N89-21200

CONICAL NOZZLES
Excited state energetics and dynamics of large molecules, complexes and clusters
[AD-A203514] N89-21065

CONJUGATION
Conjugating binary systems for spacecraft thermal control
[NASA-CR-183608] N89-21023

CONNECTORS
Characterization of structural connections using free and forced response test data
[NASA-TM-101991] N89-21266

CONSERVATION LAWS
The interaction of nonlinear hyperbolic waves: A conference report N89-21530

CONSTITUTIVE EQUATIONS
Deformation modeling and constitutive modeling for anisotropic superalloys
[NASA-CR-4215] N89-21258

CONSTRAINTS
Critical problems in very large scale computer systems
[AD-A203299] N89-21586

CONTAMINANTS
X-ray fluorescence surface contaminant analyzer: A feasibility study N89-21736

CONTAMINATION
Contamination of the exterior of a C-130E aircraft used for aerial spray, 907 TAG, Rickenbacker ANGB, OH
[AD-A202430] N89-20984
Continued development and characterization of doped layers, contacts and associated electronic devices in silicon carbide
[AD-A202450] N89-21176

CONTINENTAL SHELVES
Extended period of K/T boundary mass extinction in the marine realm N89-21337

CONTINENTS
K-T impact(s): Continental, oceanic or both N89-21386

CONTINUITY
Semanticai paradigms: Notes for an invited lecture
[AD-A202995] N89-21585

CONTINUOUS RADIATION
Design, fabrication, and performance of brazed, graphite electrode, multistage depressed collectors with 500-W, continuous wave, 4.8- to 9.6-GHz traveling-wave tubes
[NASA-TP-2904] N89-21171

CONTINUOUS WAVE RADAR
Response surface methodology applied to the radar range equation
[AD-A203044] N89-21157

CONTINUUM MECHANICS
A continuum diffusion model for viscoelastic materials
[AD-A202588] N89-21112

CONTINUUM MODELING
A continuum diffusion model for viscoelastic materials
[AD-A202588] N89-21112

CONTRACTION
Contraction of Z(sub 2) graded Lie algebras
[DE88-705356] N89-21596

CONTRACTS
Systems engineering and technical assistance
[AD-A203479] N89-21696
CONTROL MOMENT GYROSCOPES
RCS/linear discrete actuator study
[AD-A202822] N89-21028
CONTROL SIMULATION
A comparison of control variates for queueing network simulation
[AD-A202576] N89-21599
CONTROL STABILITY
Evaluation of time delay requirements for closed-loop stability using classical and modern methods
[DE89-006417] N89-21189
CONTROL STICKS
Response equivocation analysis for the smart stick controller
[AD-A203146] N89-20989
Capacity of human operator using smart stick controller
[AD-A202712] N89-21483
CONTROL SURFACES
Actuation constraints in multivariable flight control systems N89-20998
Selection of a frequency sensitive QFT (Quantitative Feedback Theory) weighting matrix using the method of specified outputs
[AD-A202692] N89-21592
CONTROL SYSTEMS DESIGN
Flight controller design with nonlinear aerodynamics, large parameter uncertainty and pilot compensation
[AD-A202727] N89-21000
A digital rate controller for the control reconfigurable combat aircraft designed using quantitative feedback theory
[AD-A203050] N89-21001
Active control technique evaluation for spacecraft (ACES)
[AD-A202475] N89-21016
Active control of a large space structure as applied to the phase 1 CETF (Critical Evaluation Task Force) space station
[AD-A203293] N89-21020
Evaluation of time delay requirements for closed-loop stability using classical and modern methods
[DE89-006417] N89-21189
Manipulator primitive level task decomposition
[PB89-133532] N89-21238
An intelligent advisor for the design manager
[NASA-TM-101558] N89-21539
Optical fiber sensors and signal processing for intelligent structure monitoring
[NASA-CR-184841] N89-21640
Research Reports: 1988 NASA/ASEE Summer Faculty Fellowship Program
[NASA-CR-183553] N89-21726
Investigation of practical applications of H infinity control theory to the design of control systems for large space structures N89-21743
Software system safety N89-21754
CONTROL THEORY
Response equivocation analysis for the smart stick controller
[AD-A203146] N89-20989
Actuation constraints in multivariable flight control systems N89-20998
A digital rate controller for the control reconfigurable combat aircraft designed using quantitative feedback theory
[AD-A203050] N89-21001
Optimal launch time for a discontinuous low thrust orbit transfer
[AD-A202693] N89-21007
Control system for maintaining stable orbits around phobos
[AD-A202776] N89-21008
Stability solution to linearized equations of motion for a symmetric spinning satellite in an elliptical orbit applied to the non-linear equations
[AD-A202934] N89-21010
Remote orbital capture using an orbital maneuvering vehicle equipped with a multibody grappling arm assembly
[AD-A202760] N89-21018
Robotic compliant motion control for aircraft refueling applications
[AD-A202710] N89-21249
Selection of a frequency sensitive QFT (Quantitative Feedback Theory) weighting matrix using the method of specified outputs
[AD-A202692] N89-21592
Investigation of practical applications of H infinity control theory to the design of control systems for large space structures N89-21743
CONTROLLERS
Response equivocation analysis for the smart stick controller
[AD-A203146] N89-20989
A digital rate controller for the control reconfigurable combat aircraft designed using quantitative feedback theory
[AD-A203050] N89-21001
Active control technique evaluation for spacecraft (ACES)
[AD-A202475] N89-21016
Active control of a large space structure as applied to the phase 1 CETF (Critical Evaluation Task Force) space station
[AD-A203293] N89-21020
CONVECTION
Infrared surface temperature measurements for the surface tension driven convection experiment
[NASA-TM-101353] N89-21224
Variable wall temperature effects on multicellular natural convection in a horizontal annulus
[AD-A202762] N89-21691
CONVECTIVE HEAT TRANSFER
A model for interface temperatures induced by convection heat transfer in porous materials
[DE89-008202] N89-21214
Corona wind cooling comparisons for horizontal cylinders
[AD-A202714] N89-21625
Transient natural convection heat and mass transfer in crystal growth N89-21741
CONVERGENCE
On some finite element error estimates for stress intensity factors in Mode 1 linear elastic fracture problems N89-21517
COOLING
Investigation of the development of laminar boundary-layer instabilities along a cooled-wall cone in hypersonic flows
[AD-A202587] N89-20966
The Manson impact structure, a possible site for a Cretaceous-Tertiary (K-T) boundary impact N89-21326
Cretaceous-Tertiary boundary in the Antarctic: Climatic cooling precedes biotic crisis N89-21392
Some volcanologic aspects of Columbia River basalt volcanism relevant to the extinction controversy N89-21393
Corona wind cooling comparisons for horizontal cylinders
[AD-A202714] N89-21625
COOLING SYSTEMS
A cryocooler for high acceleration applications
[AD-A203063] N89-21137
COORDINATE TRANSFORMATIONS
Radio-controlled model gyro measurement study
[AD-A204002] N89-21223
COORDINATES
Multiple model adaptive tracking of airborne targets
[AD-A202696] N89-21148
Spline-based finite-element method for solving a Stefan's problem in a finite domain: Formulation N89-21516
The application of modal coordinate methods to large nonlinear time-dependent problems
[AD-A203913] N89-21611
COPPER
Measurement of ground state copper density using hook spectroscopy
[DE89-005096] N89-21093
COPPER OXIDES
An in-situ, high-temperature study of the superconductor YBa1.67Sr0.33Cu3O(6+x)
[DE89-007375] N89-21686
COROTATION
Numerical studies of gas flow in spiral galaxies N89-21718
CORROSION
Center for Advanced Materials
[DE89-008854] N89-21033
CORRUGATING
Photochemistry at corrugated thin metal films: A phenomenological approach
[AD-A203070] N89-21061
COSMOLOGY
Surface energy from order parameter profile: At the QCD phase transition
[NASA-CR-184890] N89-21633
A new class of non-topological solitons
[NASA-CR-184889] N89-21634
Evolution of cosmic string networks
[NASA-CR-182836] N89-21716
COST ANALYSIS
An analytical framework for determining life cycle cost implications of the advanced launch system
[AD-A202873] N89-21012
COST REDUCTION
Reduction of M1 weld fabrication costs: The effect of weld shielding gas composition
[AD-A204001] N89-21254
COSTS
Critical problems in very large scale computer systems
[AD-A203299] N89-21586
COUETTE FLOW
Symmetry breaking bifurcations and the growth of chaos in a rotating fluid
[AD-A204010] N89-21213
COUNTER ROTATION
Comparison of propeller cruise noise data taken in the NASA Lewis 8- by 6-foot wind tunnel with other tunnel and flight data
[NASA-TM-101976] N89-21628
COUPLING COEFFICIENTS
Stability solution to linearized equations of motion for a symmetric spinning satellite in an elliptical orbit applied to the non-linear equations
[AD-A202934] N89-21010
COVERALLS
Thermal protection afforded by two anti-exposure coveralls when worn in cold water
[AD-A202865] N89-21485
CRACK CLOSURE
The effects of loading history and closure of the fatigue characteristics of heat treated Ti-6Al-2Sn-4Zr-6Mo
[AD-A202652] N89-21082
Implementation of equivalent domain integral method in the two-dimensional analysis of mixed mode problems
[NASA-CR-181813] N89-21267
CRACK INITIATION
The properties of advanced aluminium alloy systems N89-21074
Analysis of interface crack branching
[NASA-CR-182273] N89-21265
CRACK OPENING DISPLACEMENT
The effects of loading history and closure of the fatigue characteristics of heat treated Ti-6Al-2Sn-4Zr-6Mo
[AD-A202652] N89-21082
CRACK PROPAGATION
The effect of mixed-mode loading on stress-driven solute segregation during high-temperature brittle intergranular fracture
[AERE-R-12897] N89-21073
Investigation of crack growth in titanium-aluminide at elevated temperatures
[AD-A202570] N89-21081
Crack growth of a titanium-aluminide alloy under thermal-mechanical fatigue
[AD-A202767] N89-21083
Mechanisms of fatigue crack propagation and fracture toughness behavior in advanced aluminum-lithium alloys
[DE89-008300] N89-21098
Fracture characteristics of balloon films
[NASA-CR-181686] N89-21099
Surface chemistry and structural effects in the stress corrosion of glass and ceramic materials
[AD-A202452] N89-21107
Fracture toughness testing of a ceramic matrix composite at elevated temperatures
[AD-A202738] N89-21114
Global-local methodology for fracture analysis of engineering structures N89-21262
Analysis of interface crack branching
[NASA-CR-182273] N89-21265
Further studies of the HRR field of a moving crack. An experimental analysis
[AD-A202545] N89-21269
Application of the boundary element method to fatigue crack growth analysis
[AD-A202565] N89-21270
On the energy release rate for dynamic transient anti-plane shear crack propagation in a general linear viscoelastic body
[AD-A202942] N89-21280
Macrocrack-multiple defect interaction considering elastic, plastic and viscoplastic effects
[AD-A203186] N89-21282
An investigation of viscoelastic fracture near and at interfaces
[AD-A203760] N89-21285
CRACK TIPS
Further studies of the HRR field of a moving crack. An experimental analysis
[AD-A202545] N89-21269
Three dimensional effects near a crack tip in a ductile three point bend specimen. Part 2: An experimental investigation using interferometry and caustics
[AD-A202637] N89-21272
CRACKING (FRACTURING)
Investigation of crack growth in titanium-aluminide at elevated temperatures
[AD-A202570] N89-21081

Fractographic analysis of a failed crane bolt
[AD-A202703] N89-21274

CRACKS
Global-local methodology for fracture analysis of engineering structures N89-21262
Three dimensional effects near a crack tip in a ductile three point bend specimen. Part 2: An experimental investigation using interferometry and caustics
[AD-A202637] N89-21272
Macrocrack-multiple defect interaction considering elastic, plastic and viscoplastic effects
[AD-A203186] N89-21282

CRANES
Fractographic analysis of a failed crane bolt
[AD-A202703] N89-21274

CRASHES
G-induced loss of consciousness and its prevention
[AD-A202960] N89-21471

CRATERING
The cratering record in the inner solar system: Implications for earth N89-21292
Impact, and its implications for geology N89-21353
Non-random cratering flux in recent time N89-21384
Tektites: Origin as melts produced by the impact of small projectiles onto dry targets N89-21405
The cometary and asteroidal impactor flux at the earth N89-21407

CRAY COMPUTERS
A vectorized hidden-surface algorithm implemented on the Cray-2 supercomputer
[AD-A202657] N89-21560
Optimization of large matrix calculations for execution on the Cray X-MP vector supercomputer N89-21742

CREEP TESTS
Static tensile and tensile creep testing of five ceramic fibers at elevated temperatures
[NASA-CR-177525] N89-21046

CROSS FLOW
Transverse jets in compressible crossflows N89-20923
Magnetic flowmeter measurement of solid propellant pressure-coupled and velocity-coupled responses
[AD-A203988] N89-21133

CROSSINGS
Time domain wave propagation in multilayered integrated circuits
[AD-A202427] N89-21175

CROSSLINKING
Degradation and crosslinking of perfluoroalkyl polyethers under X-ray irradiation in ultrahigh vacuum
[NASA-TP-2910] N89-21103

CRUSHING
New approach to the origin of the tektite in China N89-21414

CRYOGENIC COOLING
A cryocooler for high acceleration applications
[AD-A203063] N89-21137

CRYOGENIC FLUIDS
Cryogenic fluid management in space N89-21727

CRYOGENIC WIND TUNNELS
Test techniques: A survey paper on cryogenic tunnels, adaptive wall test sections, and magnetic suspension and balance systems N89-20955
Performance of the active sidewall boundary-layer removal system for the Langley 0.3-meter Transonic Cryogenic Tunnel
[NASA-CR-181793] N89-21004

CRYOGENICS
Cryogenic reactant storage for lunar base regenerative fuel cells
[NASA-TM-101980] N89-21419
Research Reports: 1988 NASA/ASEE Summer Faculty Fellowship Program
[NASA-CR-183553] N89-21726

CRYOSTATS
A cryocooler for high acceleration applications
[AD-A203063] N89-21137

CRYSTAL DEFECTS
Theoretical studies of the chemistry and physics of oxygen in silicon
[AD-A203168] N89-21063
Two photon characterization
[AD-A203355] N89-21678

CRYSTAL GROWTH
Bibliography of Soviet laser developments, September-October 1987
[AD-A203366] N89-21232
Contributive research in compound semiconductor material and related devices
[AD-A202586] N89-21670
Center for thin film studies
[AD-A202742] N89-21673
Investigation of Schottky barrier on GaAs and InP using a multidisciplined approach
[AD-A202953] N89-21675
Research Reports: 1988 NASA/ASEE Summer Faculty Fellowship Program
[NASA-CR-183553] N89-21726
Transient natural convection heat and mass transfer in crystal growth N89-21741

CRYSTAL LATTICES
Grain boundary kinetics. 1: In-situ observations of coupled grain boundary dislocation motion, crystal translation and boundary displacement
[DE89-006790] N89-21665
Structure maps and phase stability in AlTi3 alloyed with rare-earth elements
[DE89-005106] N89-21684
Order in cold ionic systems: Dynamic effects
[DE89-007377] N89-21687

CRYSTAL STRUCTURE
Hydrogen and deuterium internal friction behavior in vanadium-niobium alloys
[DE89-007616] N89-21078
Structural energy differences in Al3Ti: The role of tetragonal distortion in APB and twin energies
[DE89-007210] N89-21096
Grain boundary kinetics. 1: In-situ observations of coupled grain boundary dislocation motion, crystal translation and boundary displacement
[DE89-006790] N89-21665
Low temperature properties of ternary magnetic rare earth transition metal germanides with the Sc5Co4Ge10-type structure
[DE89-007628] N89-21666
Central research project report on superconductivity (1988). Part 1: Materials and IR detectors
[AD-A203891] N89-21681
Structure maps and phase stability in AlTi3 alloyed with rare-earth elements
[DE89-005106] N89-21684

CRYSTAL SURFACES
Fracture toughness testing of a ceramic matrix composite at elevated temperatures
[AD-A202738] N89-21114
Evaluation of the spatial and temporal characteristics of the conducting PRIZ
[AD-A202593] N89-21671

CRYSTALLOGRAPHY
The microstructural and phase characterization of RST Al-Ti-X alloys
[AD-A203734] N89-21092
The determination of Crystallite Orientation Distribution Functions (CODF) and their use in surface texture analysis using X-ray diffraction
[AERE-R-12839] N89-21663

CRYSTALS
Theoretical studies of the chemistry and physics of oxygen in silicon
[AD-A203168] N89-21063
Optical activity and its influence on photorefractive materials
[AD-A202530] N89-21642

CULTURE TECHNIQUES
Techniques for studying the effects of microgravity on model particle/cell systems N89-21758

CURRENT DENSITY
High-temperature ceramic superconductors
[AD-A202867] N89-21674

CURRENT DISTRIBUTION
Magnetic mapping of current distributions in two-dimensional electronic devices
[AD-A203035] N89-21220

CURVED PANELS
Effects of battle damage repair on the natural frequencies and mode shapes of curved rectangular composite panels
[AD-A203179] N89-21041

CURVES
Algorithms for rational spline curves N89-21502

CYCLES
An individual-based forest ecosystems model for projecting forest response to nutrient cycling and climate changes
[DE89-007212] N89-21428

CYCLOGENESIS
Satellite signatures of rapid cyclogenesis
[AD-A203934] N89-21452

CYLINDRICAL BODIES
A study of transonic drag reduction of a blunt cylinder by a cylinder probe
[AD-A202557] N89-20965
Effects of battle damage repair on the natural frequencies and mode shapes of curved rectangular composite panels
[AD-A203179] N89-21041
Analytical model of a five degree of freedom magnetic suspension and positioning system
[NASA-TM-100671] N89-21136
An investigation of stresses and strains in an internally pressurized, composite-jacketed, steel cylinder
[AD-A202969] N89-21281
Corona wind cooling comparisons for horizontal cylinders
[AD-A202714] N89-21625

CYLINDRICAL SHELLS
Vibration and buckling characteristics of composite cylindrical panels incorporating the effects of a higher order shear theory
[AD-A202939] N89-21278

D

DAMAGE
Investigation of modeling of damage growth in composite laminates
[AD-A202433] N89-21037
Effects of battle damage repair on the natural frequencies and mode shapes of curved rectangular composite panels
[AD-A203179] N89-21041

DARK MATTER
Positron line radiation from halo WIMP annihilations as a dark matter signature
[NASA-CR-182918] N89-21635

DARKNESS
Darkness after the K-T impact: Effects of soot N89-21411

DATA ACQUISITION
Analysis of the Federal Aviation Administration's host computer acquisition process and potential application in Department of Defense acquisitions
[AD-A202623] N89-21695

DATA BASE MANAGEMENT SYSTEMS
GRAPS (Graphical Plotting System) user's guide. A graphical plotting system for displaying scientific and engineering data
[AD-A202583] N89-21559
Migration strategies roles for data management in CIM
[DE89-008112] N89-21708

DATA BASES
Upper-wind climatology for CONUS
[AD-A203961] N89-21453
Global snow depth climatology
[AD-A203969] N89-21455
Statistical machine learning for the cognitive selection of nonlinear programming algorithms in engineering design optimization N89-21493
A decision-based methodology for object oriented-design
[AD-A202579] N89-21558
Speech database development
[AD-A202461] N89-21699
Evaluation of the high temperature materials information analysis center online numeric database
[AD-A202900] N89-21700
Defense technical information center's role in numeric database development
[AD-A202901] N89-21701
Acquiring generalizations to organize human databases
[AD-A202964] N89-21702
Development of the domain name system
[AD-A203901] N89-21703
WhiteStar project engineering component selection database
[DE89-008321] N89-21709
Refining, revising, augmenting, compiling and developing computer assisted instruction K-12 aerospace materials for implementation in NASA spacelink electronic information system N89-21729

DATA LINKS
Optical communication with semiconductor laser diode
[NASA-CR-184817] N89-21141

DATA MANAGEMENT
Migration strategies roles for data management in CIM
[DE89-008112] N89-21708
SIRE: A Simple Interactive Rule Editor for NICBES N89-21730

DATA PROCESSING
The interpretation of crustal dynamics data in terms of plate motions and regional deformation near plate boundaries
[NASA-CR-180077] N89-21436
Enhancements to the AFGL (Air Force Geophysics Laboratory) Statistical Analysis Program (ASAP) for the global multivariate analysis of heights and winds
[AD-A202912] N89-21450
Transactions of the Fifth Army Conference on Applied Mathematics and Computing
[AD-A193384] N89-21490
An algorithm for processing scanning spectrometer data N89-21506

Time-of-flight small-angle neutron scattering data reduction and analysis at LANSCE with program SMR
[DE89-006520] N89-21578
Lockheed Aeronautical Systems Company technical order transfer tests
[DE89-008092] N89-21707

DATA REDUCTION
Whole field measurements of vorticity in turbulent and unsteady flows
[AD-A203349] N89-21209
Time-of-flight small-angle neutron scattering data reduction and analysis at LANSCE with program SMR
[DE89-006520] N89-21578
Intelligent data reduction for autonomous power systems N89-21737

DATA SAMPLING
Large sample theory for statistical inference in several software reliability models
[CWI-MS-R8807] N89-21543

DATA STORAGE
Simulating rule-based systems
[AD-A202563] N89-21555
A software system to create a hierarchical, multiple level of detail terrain model
[AD-A203047] N89-21568

DATA TRANSMISSION
A modeling perspective for meteor burst communication
[AD-A202562] N89-21145

DECARBOXYLATION
Synthesis of energetic binders
[AD-A203060] N89-21127

DECISION MAKING
Light satellites: A dilemma for the US Army
[AD-A202648] N89-21017
A modeling perspective for meteor burst communication
[AD-A202562] N89-21145
Brain activity during tactical decision-making. Part 5: A cross-study validation of evoked potentials as indices of workload
[AD-A203763] N89-21474
Empirical demonstration of isoperformance methodology preparatory of an interactive expert computerized decision aid
[AD-A202439] N89-21545
A decision-based methodology for object oriented-design
[AD-A202579] N89-21558
Influence diagrams: Automated analysis with dynamic programming
[AD-A203045] N89-21567
Dynamic analysis of feedforward neural networks using simulated and measured data
[AD-A202573] N89-21591
Information acquisition for model construction: An integrative, decision-theoretic perspective N89-21705

DECISION THEORY
Information acquisition for model construction: An integrative, decision-theoretic perspective N89-21705

DECODING
Optical computing research
[AD-A202963] N89-21564

DECOMPOSITION
Manipulator primitive level task decomposition
[PB89-133532] N89-21238
Time and state resolved studies of molecular decomposition
[AD-A202464] N89-21636

DEFECTS
Electronic structure and properties of defect complexes in metals
[AD-A203657] N89-21091
Macrocrack-multiple defect interaction considering elastic, plastic and viscoplastic effects
[AD-A203186] N89-21252

DEFENSE PROGRAM
Empirical demonstration of isoperformance methodology preparatory of an interactive expert computerized decision aid
[AD-A202439] N89-21545
Strategic defense initiative: A chronology, 1983 - 1988
[AD-A203576] N89-21619
Analysis of the Federal Aviation Administration's host computer acquisition process and potential application in Department of Defense acquisitions
[AD-A202623] N89-21695

DEFINITION
SESC (Space Environment Services Center) glossary of solar-terrestrial terms, 2nd edition
[PB89-120802] N89-21698

DEFLECTION
Fast acting optical beam deflection system
[AD-A203042] N89-21648

DEFORMATION
Deformation, fracture and explosive properties of reactive materials
[AD-A203083] N89-21128
Deformation modeling and constitutive modeling for anisotropic superalloys
[NASA-CR-4215] N89-21258
Large deformations near a pair of closely-spaced spherical voids in a rate-dependent solid
[AD-A202465] N89-21268
Finite element analysis of composite plates including shear deformation
[AD-A202941] N89-21279
Transverse shear considerations in anisotropic plates
[AD-A203187] N89-21283
An investigation of viscoelastic fracture near and at interfaces
[AD-A203760] N89-21285
Microdeformation in Vredefort rocks; evidence for shock metamorphism N89-21376
The interpretation of crustal dynamics data in terms of plate motions and regional deformation near plate boundaries
[NASA-CR-180077] N89-21436
Condition of the finite element stiffness matrix of highly irregular triangular grids N89-21497
A simple analysis of swage autofrettage process N89-21498
On a refined nonlinear theory of laminated composite plates N89-21500
Some issues of numerical integration and penalty relaxation in anisoparametric shell element formulation N89-21518

DELAMINATING
Strain energy release rate as a function of temperature and preloading history utilizing the edge delamination fatique test method
[NASA-CR-184966] N89-21286

DELTA WINGS
Numerical simulation of the flow field over delta wings with leading edge blowing N89-20924
An embedded mesh procedure for leading-edge vortex flows N89-20936
Thin-layer Navier-Stokes solutions for a cranked delta wing
[AD-A203292] N89-20970

DENSITY (MASS/VOLUME)
Measurement of ground state copper density using hook spectroscopy
[DE89-005098] N89-21093
High density fuel effects
[AD-A202426] N89-21125

DENSITY MEASUREMENT
Density of triethanolammonium nitrate and liquid propellant
[AD-A203767] N89-21131

DENSITY WAVE MODEL
Numerical studies of gas flow in spiral galaxies N89-21718

DEPLOYMENT
Small expendable deployer system measurement analysis N89-21731

DEPOSITION
Contamination of the exterior of a C-130E aircraft used for aerial spray, 907 TAG, Rickenbacker ANGB, OH
[AD-A202430] N89-20984
Laser-induced metal deposition on semiconductors from liquid electrolytes
[AD-A203612] N89-21089
Evidence for a single impact at the Cretaceous-Tertiary boundary from trace elements N89-21319
Acute effects of a large bolide impact simulated by a global atmospheric circulation model N89-21398
Tektites: Origin as melts produced by the impact of small projectiles onto dry targets N89-21405
Collisions with ice-volatile objects: Geological implications N89-21409

DEPOSITS
Advanced tribological coatings for high specific strength alloys
[AD-A202505] N89-21110
Geochemistry of K/T boundaries in India and contributions of Deccan volcanism N89-21296
Shocked quartz and more: Impact signatures in K-T boundary clays and claystones N89-21297
The Manson impact structure, a possible site for a Cretaceous-Tertiary (K-T) boundary impact N89-21326

DEPTH
Global snow depth climatology
[AD-A203969] N89-21455

DESIGN ANALYSIS
Global-local methodology for fracture analysis of engineering structures N89-21262
Optimal design of a two-way conductor N89-21499
The Environment for Application Software Integration and Execution (EASIE) version 1.0. Volume 1: Executive overview
[NASA-TM-100573] N89-21538
An intelligent advisor for the design manager
[NASA-TM-101558] N89-21539
The design and implementation of a special purpose cache for the roll back chip
[AD-A203091] N89-21583
Design specifications for hardware assisted rollback computation
[AD-A203092] N89-21584
WhiteStar project engineering component selection database
[DE89-008321] N89-21709

DESTRUCTION
Risk to civilization: A planetary science perspective N89-21302

DETECTION
An optimal scale for edge detection
[AD-A202747] N89-21646

DETONATION
Effect of TNT miscible additives on the mechanical behavior and shock sensitivity of Composition B
[AD-A203968] N89-21132

DETONATION WAVES
Influence of reflected shock waves on a hypersonic shaped charge jet N89-21522

DEUTERIUM
Hydrogen and deuterium internal friction behavior in vanadium-niobium alloys
[DE89-007616] N89-21078

DIAGNOSIS
A diagnostic system using Boolean reasoning
[AD-A202764] N89-21602
Computer assisted analysis and modelling of structured problems
[AD-A203040] N89-21607

DICTIONARIES
SESC (Space Environment Services Center) glossary of solar-terrestrial terms, 2nd edition
[PB89-120802] N89-21698

DIELECTRIC PROPERTIES
Accurate determination of the complex permittivity of biological tissue around 35 GHz
[AD-A202907] N89-21470

DIELECTRICS
Spectroscopic studies of fluid/solid interfaces
[AD-A202436] N89-21054
The radar cross section of a two dimensional dielectric coated cylinder using on-surface radiation conditions
[AD-A202935] N89-21152
Dielectric spectroscopy of semiconductors
[AD-A203457] N89-21679

DIESEL ENGINES
The effect of platinum catalysts on propane oxidation at elevated pressure
[AD-A202999] N89-21060

DIESEL FUELS
Fouling tests of AGT-1500 gas turbine fuel nozzles
[AD-A203360] N89-21253

DIFFERENTIAL EQUATIONS
Spectral analysis of a fourth-order singular differential operator arising in combustion
[DE89-005841] N89-21052
Conformal time domain finite difference method of solving electromagnetic wave scattering
[AD-A202434] N89-21143
Studies in the computation of compressible and viscous flow
[AD-A203334] N89-21208
A model for interface temperatures induced by convection heat transfer in porous materials
[DE89-008202] N89-21214
Asymptotics beyond all orders N89-21508
Numerical solution of nonlinear algebraic equations in stiff ODE solving
[DE89-008284] N89-21613
Rotordynamic analysis of a bearing tester N89-21759

DIFFRACTION
A theoretical and experimental investigation of linear and nonlinear focussing chirped optical diffraction gratings
[AD-A203396] N89-21650

DIFFRACTION PATTERNS
The numerical simulation of Richtmyer-Meshkov unstable interfaces: A conference report N89-21512

DIFFUSION
A compendium of controlled diffusion blades generated by an automated inverse design procedure
[NASA-TM-101968] N89-20996
A continuum diffusion model for viscoelastic materials
[AD-A202588] N89-21112
Numerical solution of parabolic problems in high dimensions N89-21501

DIFFUSION COEFFICIENT
A fresh look at transport in perfluorosulfonate ionomers: Ultramicroelectrode investigations of Nafion and Dow ionomers
[AD-A203855] N89-21066
DIFFUSION ELECTRODES
A fresh look at transport in perfluorosulfonate ionomers: Ultramicroelectrode investigations of Nafion and Dow ionomers
[AD-A203855] N89-21066
DIFFUSION FLAMES
Fuels combustion research
[AD-A204161] N89-21071
DIFFUSION THEORY
Polynominal definition of discrete field point of map of diffusion equation N89-21511
DIFFUSION WELDING
Diffusion welding of an RS/PM aluminum alloy
N89-21241
DIGITAL DATA
A software system to create a hierarchical, multiple level of detail terrain model
[AD-A203047] N89-21568
DIGITAL FILTERS
An analysis of noise reduction using back-propagation neural networks
[AD-A203057] N89-21159
Analysis and simulation of an audio adaptive equalizer
[AD-A202569] N89-21631
DIGITAL SIMULATION
A real-time simulator of a turbofan engine
[NASA-TM-100869] N89-20995
Symmetry breaking bifurcations and the growth of chaos in a rotating fluid
[AD-A204010] N89-21213
DIGITAL SYSTEMS
In-flight lightning characterization program on a CV-580 aircraft
[AD-A203954] N89-20976
A digital rate controller for the control reconfigurable combat aircraft designed using quantitative feedback theory
[AD-A203050] N89-21001
Computer strategy for detecting line features on simulated binary arrays in support of radar feature extraction
[AD-A203257] N89-21162
Implementation and testing of a new 16-PSK transmitter
[AD-A203936] N89-21166
Architecture and design for a laser programmable double precision floating point application specific processor
[AD-A202560] N89-21553
DILUENTS
A NMR (Nuclear Magnetic Resonance) study of the molecular interactions and dynamic behavior in polymer-diluent blends in the solid state
[AD-A202459] N89-21108
DIMENSIONS
Correction of gain and optical throughput variations in a two-dimensional imaging spectrometer
[AD-A203495] N89-21222
DIRECTION FINDING
A generalized approach to direction finding
[AD-A203768] N89-21186
DIRECTIONAL SOLIDIFICATION (CRYSTALS)
Computer simulation of macrosegregation in directionally solidified circular ingots
[NASA-CR-182838] N89-21134
DISASTERS
Global Catastrophes in Earth History: An Interdisciplinary Conference on Impacts, Volcanism, and Mass Mortality
[NASA-CR-183329] N89-21287
Proterozoic Bushveld-Vredefort catastrophe: Possible causes and consequences N89-21312
Volcanism, global catastrophe and mass mortality
N89-21316
Volcanoes and global catastrophes N89-21389
DISK GALAXIES
Numerical studies of gas flow in spiral galaxies
N89-21718
DISPLACEMENT
Further studies of the HRR field of a moving crack. An experimental analysis
[AD-A202545] N89-21269
Nonlinear finite element analysis of a general composite shell
[AD-A202572] N89-21271
On the energy release rate for dynamic transient anti-plane shear crack propagation in a general linear viscoelastic body
[AD-A202942] N89-21280
DISPLAY DEVICES
Implementation and testing of a new 16-PSK transmitter
[AD-A203936] N89-21166
A vectorized hidden-surface algorithm implemented on the Cray-2 supercomputer
[AD-A202657] N89-21560
DISTORTION
Structural energy differences in Al3Ti: The role of tetragonal distortion in APB and twin energies
[DE89-007210] N89-21096
DISTRIBUTED PARAMETER SYSTEMS
Development of the domain name system
[AD-A203901] N89-21703
DISTRIBUTION FUNCTIONS
Derivation and testing of computer algorithms for automatic real-time determination of space vehicle potentials in various plasma environments
[AD-A203019] N89-21019
Eigenvectors of graphs
[AD-A203317] N89-21609
The determination of Crystallite Orientation Distribution Functions (CODF) and their use in surface texture analysis using X-ray diffraction
[AERE-R-12839] N89-21663
DMSP SATELLITES
Charging potentials for two sample sets of spectra from DMSP satellites
[AD-A203694] N89-21021
Precipitating ion and electron detectors (SSJ/4) for the block 5D/Flight 8 DMSP (Defense Meteorological Satellite Program) satellite
[AD-A203999] N89-21022
DOCUMENT STORAGE
Improving the survivability of a stochastic communication network
[AD-A202872] N89-21150
DOMAINS
A theory of problem domains and program correctness
[DE89-008451] N89-21580
DOPED CRYSTALS
Continued development and characterization of doped layers, contacts and associated electronic devices in silicon carbide
[AD-A202450] N89-21176
Spectroscopy and laser performance of Ti(sup 3+) doped and Cr(sup 3+), Nd(sup 3+) co-doped crystals
[AD-A203911] N89-21682
DOPPLER EFFECT
Spectral characteristics of High Frequency (HF) backscatter for high latitude ionospheric irregularities: Preliminary analysis of statistical properties
[AD-A202998] N89-21156
DRAG
Wave drag due to lift for transonic airplanes
N89-20938
Guidance for an aeroassisted orbital transfer vehicle
N89-21740
DRAG REDUCTION
A study of transonic drag reduction of a blunt cylinder by a cylinder probe
[AD-A202557] N89-20965
DRIFT RATE
Observations of neutral circulation at mid-latitudes during the Equinox Transition Study
[NASA-CR-184792] N89-21429
DRILLING
Evidence of volcanic ash at a K-T boundary section: Ocean drilling program hole 690 C, Maud Rise, Weddell Sea off East Antarctica N89-21410
DRONE AIRCRAFT
Hypersonic drone design: A multidisciplinary experience
[NASA-CR-184740] N89-20981
DUCTED FLOW
Studies of liquid metal flows and power losses in ducts with moving conducting wall, slanted magnetic field, and applied external electric potential
[AD-A203981] N89-21626
DUCTILITY
Acoustic microscopy of low ductility materials
[AERE-R-12848] N89-21101
Large deformations near a pair of closely-spaced spherical voids in a rate-dependent solid
[AD-A202465] N89-21268
Three dimensional effects near a crack tip in a ductile three point bend specimen. Part 2: An experimental investigation using interferometry and caustics
[AD-A202637] N89-21272
DUCTS
Studies of liquid metal flows and power losses in ducts with moving conducting wall, slanted magnetic field, and applied external electric potential
[AD-A203981] N89-21626
DUFFING DIFFERENTIAL EQUATION
Application of the Laplace-Borel transformation to the representation of analytical solutions of Duffing's equation
[NASA-TM-100058] N89-21532
DUST
Multi-year global climatic effects of atmospheric dust from large bolide impacts N89-21397
Acute effects of a large bolide impact simulated by a global atmospheric circulation model N89-21398
Darkness after the K-T impact: Effects of soot
N89-21411
DYNAMIC CHARACTERISTICS
Estimated satellite cluster elements in near circular orbit
[AD-A202938] N89-21011
Theoretical studies of heterogeneous reactions in silicon CVD (Silicon Vapor Deposition) catalysis
[AD-A202905] N89-21057
Excited state energetics and dynamics of large molecules, complexes and clusters
[AD-A203514] N89-21065
A NMR (Nuclear Magnetic Resonance) study of the molecular interactions and dynamic behavior in polymer-diluent blends in the solid state
[AD-A202459] N89-21108
Structure development during converging flow of a liquid crystal dispersed two-phase fluid
[AD-A203062] N89-21119
Speech recognition using neural nets and dynamic time warping
[AD-A202528] N89-21144
Dynamic analysis of feedforward neural networks using simulated and measured data
[AD-A202573] N89-21591
DYNAMIC CONTROL
Modeling robot dynamic performance for endpoint force control
[AD-A202881] N89-21251
Vibration control in rotating machinery using variable dynamic stiffness squeeze-films
[AD-A202902] N89-21252
DYNAMIC LOADS
Investigation of modeling of damage growth in composite laminates
[AD-A202433] N89-21037
Time-discretized moments of a randomly excited uncertain linear oscillator
[DE89-008318] N89-21614
DYNAMIC MODELS
The role of radiation-dynamics interaction in regional numerical weather prediction N89-21732
DYNAMIC PROGRAMMING
F-16 speaker-independent speech recognition system using cockpit commands (70 words)
[AD-A203177] N89-21489
Influence diagrams: Automated analysis with dynamic programming
[AD-A203045] N89-21567
DYNAMIC RESPONSE
Origination, diversity, and extinction metrics essential for analysis of mass biotic crisis events: An example from cretaceous ammonoidea N89-21304
DYNAMIC STRUCTURAL ANALYSIS
Dynamic structural optimization and experiment
[PB89-111462] N89-21259
Characterization of structural connections using free and forced response test data
[NASA-TM-101991] N89-21266
DYNAMIC TESTS
Dynamic fatigue testing of Zerodur glass-ceramic
N89-21753

E

EARTH (PLANET)
Asteroid and comet flux in the neighborhood of the earth N89-21387
The cometary and asteroidal impactor flux at the earth
N89-21407
EARTH ATMOSPHERE
New approach to the origin of the tektite in China
N89-21414
Flux and sounding data from the NCAR (National Center for Atmospheric Research) King Air aircraft during HAPEX (hydrologic atmospheric pilot experiment)
[PB89-124481] N89-21433
EARTH CRUST
Finite-difference modeling of Rayleigh wave scattering and P-SV(Lg) coupling problems
[AD-A203221] N89-21161
The Manson impact structure, a possible site for a Cretaceous-Tertiary (K-T) boundary impact N89-21326
K-T impact(s): Continental, oceanic or both
N89-21386
The interpretation of crustal dynamics data in terms of plate motions and regional deformation near plate boundaries
[NASA-CR-180077] N89-21436

EARTH IONOSPHERE
The role of hydromagnetic waves in the magnetosphere and the ionosphere
[AD-A202800] N89-21437
Space plasma contractor research, 1988
[NASA-CR-182283] N89-21658

EARTH MAGNETOSPHERE
The role of hydromagnetic waves in the magnetosphere and the ionosphere
[AD-A202800] N89-21437
Commentary on fast atmospheric pulsations
[AD-A203172] N89-21440

EARTH MANTLE
The Western North American Cretaceous-Tertiary (K-T) boundary interval and its content of shock-metamorphosed minerals: Implications concerning the K-T boundary impact-extinction theory N89-21334
Flood basalts and mass extinctions N89-21360

EARTH ORBITAL ENVIRONMENTS
Excitation and diagnostics of optical contamination in the spacecraft environment
[AD-A202429] N89-21015
Simulation of the low earth orbital atomic oxygen interaction with materials by means of an oxygen ion beam
[NASA-TM-101971] N89-21104

EARTH ORBITS
Optimal launch time for a discontinuous low thrust orbit transfer
[AD-A202693] N89-21007
Earth orbital variations and vertebrate bioevolution N89-21357

EARTH PLANETARY STRUCTURE
Finite-difference modeling of Rayleigh wave scattering and P-SV(Lg) coupling problems
[AD-A203221] N89-21161

EARTH ROTATION
Relationships of earthquakes (and earthquake-associated mass movements) and polar motion as determined by Kalman filtered, Very-Long-Baseline-Interferometry
[NASA-TM-100711] N89-21430

EARTH SURFACE
Global environmental effects of impact-generated aerosols: Results from a general circulation model N89-21306
Acute effects of a large bolide impact simulated by a global atmospheric circulation modal N89-21398
Heavy metal toxicity as a kill mechanism in impact caused mass extinctions N89-21406
Propagator matrices in the solution of EMP problems N89-21515

EARTHQUAKES
Relationships of earthquakes (and earthquake-associated mass movements) and polar motion as determined by Kalman filtered, Very-Long-Baseline-Interferometry
[NASA-TM-100711] N89-21430
The interpretation of crustal dynamics data in terms of plate motions and regional deformation near plate boundaries
[NASA-CR-180077] N89-21436

ECOLOGY
Rocks, resolution, and the record at the terrestrial K/T boundary, eastern Montana and western North Dakota N89-21313
Proximal ecological effects of the 1980 eruptions of Mount St. Helens N89-21394

ECOSYSTEMS
The Cretaceous-Tertiary boundary biotic crisis in the Basque country N89-21345
Permo-Triassic vertebrate extinctions: A program N89-21367
Proximal ecological effects of the 1980 eruptions of Mount St. Helens N89-21394
Effects of global atmospheric perturbations on forest ecosystems: Predictions of seasonal and cumulative effects N89-21399
An individual-based forest ecosystems model for projecting forest response to nutrient cycling and climate changes
[DE89-007212] N89-21428

EDDY VISCOSITY
Turbulent eddy viscosity modeling in transonic shock/boundary-layer interactions N89-20952

EDGE LOADING
Strain energy release rate as a function of temperature and preloading history utilizing the edge delamination fatique test method
[NASA-CR-184966] N89-21286

EDGES
An optimal scale for edge detection
[AD-A202747] N89-21646

EDITING ROUTINES (COMPUTERS)
SIRE: A Simple Interactive Rule Editor for NICBES N89-21730

EDUCATION
An educational expert system shell integrating object-attribute-value triples and frames
[AD-A202574] N89-21557

EGGS
Diachronism between extinction time of terrestrial and marine dinosaurs N89-21325

EIGENVALUES
Actuation constraints in multivariable flight control systems N89-20998
Dimensionality of binary items
[AD-A203238] N89-21608
Eigenvectors of graphs
[AD-A203317] N89-21609

EIGENVECTORS
The radar cross section of a two dimensional dielectric coated cylinder using on-surface radiation conditions
[AD-A202935] N89-21152
Eigenvectors of graphs
[AD-A203317] N89-21609

EJECTA
Impact wave deposits provide new constraints on the location of the K/T boundary impact N89-21330
Evidence for and implications of an Early Archean terrestrial impact record N89-21348
Bio-, Magneto- and event-stratigraphy across the K-T boundary N89-21370
Computer modeling of large asteroid impacts into continental and oceanic sites: Atmospheric, cratering, and ejecta dynamics N89-21379
Oblique impacts: Catastrophic vs. protracted effects N89-21383
Non-random cratering flux in recent time N89-21384
Some volcanologic aspects of Columbia River basalt volcanism relevant to the extinction controversy N89-21393
Acute effects of a large bolide impact simulated by a global atmospheric circulation model N89-21398
Darkness after the K-T impact: Effects of soot N89-21411

EJECTION
An experimental investigation of flow mixing on thrust ejection efficiency
[AD-A202707] N89-21205

EJECTION SEATS
A wind tunnel and computer investigation of the low speed aerodynamic characteristics of the prone escape system (PRESS)
[AD-A202768] N89-20988

ELASTIC DEFORMATION
Inelastic deformation and failure analysis of filament-wound composite structures
[AD-A203382] N89-21044
Dilatationally nonlinear elastic materials. Part 2: An example illustrating stress concentration reduction
[AD-A202521] N89-21111
Dilatationally nonlinear elastic materials. (1): Some theory
[AD-A202824] N89-21276
Element level elimination of nonlinear constraints in total Lagrangian finite element formulations N89-21496

ELASTIC PROPERTIES
Global-local methodology for fracture analysis of engineering structures N89-21262
Implementation of equivalent domain integral method in the two-dimensional analysis of mixed mode problems
[NASA-CR-181813] N89-21267
Macrocrack-multiple defect interaction considering elastic, plastic and viscoplastic effects
[AD-A203186] N89-21282
On some finite element error estimates for stress intensity factors in Mode 1 linear elastic fracture problems N89-21517
Stabilization of Ziegler's pendulum by means of the method of vibrational control N89-21531

ELASTIC SHELLS
Function theory for thin elastic shells
[PB89-101943] N89-21257

ELASTODYNAMICS
Further investigations of oblique hypervelocity impact phenomena N89-21750

ELASTOMERS
Condition of the finite element stiffness matrix of highly irregular triangular grids N89-21497

ELASTOSTATICS
Dilatationally nonlinear elastic materials. Part 2: An example illustrating stress concentration reduction
[AD-A202521] N89-21111

ELECTRIC BATTERIES
Electric energy systems energy storage
[DE88-007217] N89-21418

ELECTRIC CONDUCTORS
Optimal design of a two-way conductor N89-21499

ELECTRIC CONTACTS
Studies of liquid metal flows and power losses in ducts with moving conducting wall, slanted magnetic field, and applied external electric potential
[AD-A203981] N89-21626

ELECTRIC CORONA
Corona wind cooling comparisons for horizontal cylinders
[AD-A202714] N89-21625

ELECTRIC CURRENT
Restrictive loads powered by separate or by common electrical sources
[NASA-TM-102008] N89-21174

ELECTRIC DISCHARGES
On-line location of partial discharges in power transformer through acoustic emission
[DE88-757043] N89-21188
Auroral photography experiment
[AD-A203623] N89-21441

ELECTRIC FIELDS
A rapid numerical procedure for determining axisymmetric transverse electric electromagnetic fields via boundary integrals
[AD-A202959] N89-21155
Propagator matrices in the solution of EMP problems N89-21515
Analytic distribution for charge carriers in a semiconductor dominated by equivalent intervalley scattering
[AD-A202537] N89-21669

ELECTRIC FILTERS
On the impulse response of monopulse radars
[AD-A202936] N89-21153

ELECTRIC POTENTIAL
Restrictive loads powered by separate or by common electrical sources
[NASA-TM-102008] N89-21174

ELECTRIC POWER TRANSMISSION
Electric energy systems energy storage
[DE88-007217] N89-21418

ELECTRICAL ENGINEERING
Center for Electronics and Electrical Engineering technical progress bulletin covering center programs, April to June 1988 with 1988 CEEE events calendar
[PB89-123137] N89-21170

ELECTRICAL IMPEDANCE
Investigation of the impedance modulation of thin films with a chemically-sensitive field-effect transistor
[AD-A202766] N89-21180
Advanced double layer capacitor
[AD-A203059] N89-21181

ELECTRICAL INSULATION
Investigation of a self-aligned, strained-channel,n sup(+)-In As/Al 0.5 As/In 0.15 Ga 0.85 As Semiconductor Insulator Semiconductor FET (SISFET)
[AD-A203147] N89-21676

ELECTRICAL MEASUREMENT
A fresh look at transport in perfluorosulfonate ionomers: Ultramicroelectrode investigations of Nafion and Dow ionomers
[AD-A203855] N89-21066

ELECTRICAL PROPERTIES
Electronic structure and properties of defect complexes in metals
[AD-A203657] N89-21091
Ceramics
[AD-A202504] N89-21109
Reliability/maintainability/testability design for dormancy
[AD-A202704] N89-21179

ELECTRICAL RESISTANCE
Restrictive loads powered by separate or by common electrical sources
[NASA-TM-102008] N89-21174

ELECTRICAL RESISTIVITY
High temperature oxidation and electrochemical studies related to hot corrosion
[AD-A203038] N89-21085

ELECTRICITY
Electric energy systems energy storage
[DE88-007217] N89-21418
Studies of liquid metal flows and power losses in ducts with moving conducting wall, slanted magnetic field, and applied external electric potential
[AD-A203981] N89-21626

ELECTRO-OPTICS
External electro-optic probing of millimeter-wave integrated circuits
[NASA-TM-101990] N89-21142
Optoelectronic workshops. Part 4: Liquid Crystals for Laser Applications
[AD-A202526] N89-21228
Devices and systems for nonlinear optical information processing
[AD-A203034] N89-21566

Architecture studies and system demonstrations of optical parallel processor for AI (Artificial Intelligence) and NI (Neural Intelligence)
[AD-A203241] N89-21593

ELECTROCHEMICAL CORROSION
High temperature oxidation and electrochemical studies related to hot corrosion
[AD-A203038] N89-21085

ELECTROCHEMICAL OXIDATION
High temperature oxidation and electrochemical studies related to hot corrosion
[AD-A203038] N89-21085

ELECTROCHEMISTRY
Synthesis processing of high-lithium Al-Li alloys
[AD-A203401] N89-21088
Advanced double layer capacitor
[AD-A203059] N89-21181
Electric energy systems energy storage
[DE88-007217] N89-21418

ELECTRODE MATERIALS
Design, fabrication, and performance of brazed, graphite electrode, multistage depressed collectors with 500-W, continuous wave, 4.8- to 9.6-GHz traveling-wave tubes
[NASA-TP-2904] N89-21171
Advanced double layer capacitor
[AD-A203059] N89-21181

ELECTRODEPOSITION
An in-situ grazing incidence X-ray scattering study of the initial stages of electrochemical growth of lead on silver (III)
[AD-A203385] N89-21064

ELECTRODES
An in-situ grazing incidence X-ray scattering study of the initial stages of electrochemical growth of lead on silver (III)
[AD-A203385] N89-21064
Corona wind cooling comparisons for horizontal cylinders
[AD-A202714] N89-21625

ELECTRODYNAMICS
Finite element simulation of thunderstorm electrodynamics in the proximity of the storm
N89-21726

ELECTROENCEPHALOGRAPHY
Brain activity during tactical decision-making. Part 5: A cross-study validation of evoked potentials as indices of workload
[AD-A203763] N89-21474

ELECTROLYTES
Laser-induced metal deposition on semiconductors from liquid electrolytes
[AD-A203612] N89-21089

ELECTROMAGNETIC ABSORPTION
Research on silicon, carbon, and silicon carbide heterostructures
[AD-A202866] N89-21116

ELECTROMAGNETIC FIELDS
A rapid numerical procedure for determining axisymmetric transverse electric electromagnetic fields via boundary integrals
[AD-A202959] N89-21155

ELECTROMAGNETIC NOISE
Demonstration of SQUID parametric amplifier
[AD-A203252] N89-21183

ELECTROMAGNETIC PULSES
In-flight lightning characterization program on a CV-580 aircraft
[AD-A203954] N89-20976
Research on acoustic coupling to electromagnetic pulses in tissue
[AD-A195644] N89-21140
Propagator matrices in the solution of EMP problems
N89-21515

ELECTROMAGNETIC RADIATION
Analytical and experimental procedures for determining propagation characteristics of millimeter-wave gallium arsenide microstrip lines
[NASA-TP-2899] N89-21169
Theoretical studies of the heating of toroidal plasmas with radiofrequency electromagnetic radiation
[DE89-008003] N89-21660

ELECTROMAGNETIC SCATTERING
Conformal time domain finite difference method of solving electromagnetic wave scattering
[AD-A202434] N89-21143
Rapid backscatter simulation techniques for detailed B-spline target models
[AD-A203260] N89-21163

ELECTROMAGNETIC WAVE TRANSMISSION
Research on acoustic coupling to electromagnetic pulses in tissue
[AD-A195644] N89-21140
Time domain wave propagation in multilayered integrated circuits
[AD-A202427] N89-21175

ELECTROMAGNETS
Performance of a prototype electromagnetic calorimeter
[DE89-007608] N89-21216

ELECTROMECHANICAL DEVICES
A fresh look at transport in perfluorosulfonate ionomers: Ultramicroelectrode investigations of Nafion and Dow ionomers
[AD-A203855] N89-21066

ELECTRON BEAMS
Performance of a prototype electromagnetic calorimeter
[DE89-007608] N89-21216
Study of the generation of intense pulsed electron beams using glow discharges
[AD-A202438] N89-21624

ELECTRON COUNTERS
Precipitating ion and electron detectors (SSJ/4) for the block 5D/Flight 8 DMSP (Defense Meteorological Satellite Program) satellite
[AD-A203999] N89-21022

ELECTRON DENSITY (CONCENTRATION)
Observations of neutral circulation at mid-latitudes during the Equinox Transition Study
[NASA-CR-184792] N89-21429
Mechanisms for the source and loss of electrons
[AD-A203066] N89-21438

ELECTRON DISTRIBUTION
Analytic distribution for charge carriers in a semiconductor dominated by equivalent intervalley scattering
[AD-A202537] N89-21669

ELECTRON EMISSION
Design, fabrication, and performance of brazed, graphite electrode, multistage depressed collectors with 500-W, continuous wave, 4.8- to 9.6-GHz traveling-wave tubes
[NASA-TP-2904] N89-21171

ELECTRON ENERGY
Solar-powered alkali metal vapor lasers
[NASA-CR-180480] N89-21226
Short wave electron temperature gradient driven drift wave turbulence
[DE89-008465] N89-21662

ELECTRON MICROSCOPES
Microscopic aspects of failure and fracture in cross-ply fiber-reinforced composite laminates
[AD-A203202] N89-21042

ELECTRON MICROSCOPY
Grain boundary kinetics. 1: In-situ observations of coupled grain boundary dislocation motion, crystal translation and boundary displacement
[DE89-006790] N89-21665

ELECTRON MOBILITY
Electron mobility in mercury cadmium telluride
N89-21748

ELECTRON PARAMAGNETIC RESONANCE
Electron paramagnetic resonance and photoluminescence studies of impurities in CdTe
[AD-A202841] N89-21056

ELECTRON PHONON INTERACTIONS
Analytic distribution for charge carriers in a semiconductor dominated by equivalent intervalley scattering
[AD-A202537] N89-21669

ELECTRON PRECIPITATION
Charging potentials for two sample sets of spectra from DMSP satellites
[AD-A203694] N89-21021
Precipitating ion and electron detectors (SSJ/4) for the block 5D/Flight 8 DMSP (Defense Meteorological Satellite Program) satellite
[AD-A203999] N89-21022
Mechanisms for the source and loss of electrons
[AD-A203066] N89-21438

ELECTRON SPECTROSCOPY
Studies of the initial oxidation of Fe-Si alloys by AES, XPS, EELS and LEED
[DE89-007610] N89-21077
Study of semiconductor valence plasmon line shapes via electron energy-loss spectroscopy in the transmission electron microscope
[DE89-008152] N89-21689

ELECTRON STATES
Theoretical studies of rare gas halide systems
[AD-A203985] N89-21068
Electronic structure and properties of defect complexes in metals
[AD-A203657] N89-21091
Time and state resolved studies of molecular decomposition
[AD-A202464] N89-21636

ELECTRON TUBES
Demonstration of SQUID parametric amplifier
[AD-A203252] N89-21183

ELECTRONIC EQUIPMENT
Analysis and simulation of a pseudonoise synchronization system
[AD-A202779] N89-21149
Center for Electronics and Electrical Engineering technical progress bulletin covering center programs, April to June 1988 with 1988 CEEE events calendar
[PB89-123137] N89-21170
Continued development and characterization of doped layers, contacts and associated electronic devices in silicon carbide
[AD-A202450] N89-21176
Reliability/maintainability/testability design for dormancy
[AD-A202704] N89-21179
WhiteStar project engineering component selection database
[DE89-008321] N89-21709

ELECTRONIC PACKAGING
Reliability/maintainability/testability design for dormancy
[AD-A202704] N89-21179

ELECTRONIC SPECTRA
Electronic structure and properties of defect complexes in metals
[AD-A203657] N89-21091
Solar-powered alkali metal vapor lasers
[NASA-CR-180480] N89-21226

ELECTRONIC WARFARE
Response surface methodology applied to the radar range equation
[AD-A203044] N89-21157

ELECTRONS
A fresh look at transport in perfluorosulfonate ionomers: Ultramicroelectrode investigations of Nafion and Dow ionomers
[AD-A203855] N89-21066

ELECTROPHYSIOLOGY
Gating kinetics and ion transfer in channels of nerve membrane
[AD-A202509] N89-21464

ELECTROPLATING
Diffusion welding of an RS/PM aluminum alloy
N89-21241

ELECTROSTATIC PRECIPITATORS
Commentary on fast atmospheric pulsations
[AD-A203172] N89-21440

ELECTROSTATIC PROBES
Derivation and testing of computer algorithms for automatic real-time determination of space vehicle potentials in various plasma environments
[AD-A203019] N89-21019
Precipitating ion and electron detectors (SSJ/4) for the block 5D/Flight 8 DMSP (Defense Meteorological Satellite Program) satellite
[AD-A203999] N89-21022

ELECTROSTATICS
Corona wind cooling comparisons for horizontal cylinders
[AD-A202714] N89-21625

ELECTROSTRICTION
Acoustic damage to large-aperture optics: Revision 1
[DE89-008025] N89-21654

ELLIPSOIDS
Downward continuation of the free-air gravity anomalies to the ellipsoid using the gradient solution, Poisson's integral and terrain correction-numerical comparison and computations
[AD-A203739] N89-21442

ELLIPTIC DIFFERENTIAL EQUATIONS
A rapid numerical procedure for determining axisymmetric transverse electric electromagnetic fields via boundary integrals
[AD-A202959] N89-21155

ELLIPTICAL ORBITS
Stability solution to linearized equations of motion for a symmetric spinning satellite in an elliptical orbit applied to the non-linear equations
[AD-A202934] N89-21010

ELONGATION
Shear banding in titanium with controlled elongations at 1 million/sec
[DE89-006555] N89-21094

ENDOTHERMIC REACTIONS
Effective ignition kinetics for LOVA propellant
[AD-A203149] N89-21129

ENERGY ABSORPTION
SPH-4 US Army flight helmet performance 1983-1987
[AD-A202589] N89-21482

ENERGY CONSERVATION
Fusion: A necessary component of US energy policy
[DE89-006234] N89-21659

ENERGY DISSIPATION
Study of semiconductor valence plasmon line shapes via electron energy-loss spectroscopy in the transmission electron microscope
[DE89-008152] N89-21689
ENERGY DISTRIBUTION
Electric energy systems energy storage
[DE88-007217] N89-21418
ENERGY LEVELS
Structural energy differences in Al3Ti: The role of tetragonal distortion in APB and twin energies
[DE89-007210] N89-21096
ENERGY SPECTRA
Mechanisms for the source and loss of electrons
[AD-A203066] N89-21438
ENERGY STORAGE
Theoretical studies of rare gas halide systems
[AD-A203985] N89-21068
Electric energy systems energy storage
[DE88-007217] N89-21418
Cryogenic reactant storage for lunar base regenerative fuel cells
[NASA-TM-101980] N89-21419
Theoretical studies of potential energy storage molecules
[AD-A203986] N89-21638
ENERGY TRANSFER
The spectroscopy and energy transfer kinetics of the interhalogens
[AD-A202954] N89-21059
On the energy release rate for dynamic transient anti-plane shear crack propagation in a general linear viscoelastic body
[AD-A202942] N89-21280
Time and state resolved studies of molecular decomposition
[AD-A202464] N89-21636
ENGINE DESIGN
Knowledge representation and planning control in an expert system for the creative design of mechanisms N89-21492
Research Reports: 1988 NASA/ASEE Summer Faculty Fellowship Program
[NASA-CR-183553] N89-21726
Radiation effect on rocket engine performance N89-21734
The simulation of the alternate turbopump development high pressure oxygen and fuel turbopumps for the space shuttle main engine using the Shaberth computer program N89-21746
ENGINE TESTS
A real-time simulator of a turbofan engine
[NASA-TM-100869] N89-20995
Experimental examination of the aerothermal performance of the T-10 test cell at NAS (Naval Air Station), Cubi Point
[AD-A203887] N89-21005
ENRICHMENT
Shocked quartz and more: Impact signatures in K-T boundary clays and claystones N89-21297
Evidence for a single impact at the Cretaceous-Tertiary boundary from trace elements N89-21319
Nitrogen geochemistry of a Cretaceous-Tertiary boundary site in New Zealand N89-21320
Mineralogy and phase-chemistry of the Cretaceous/Tertiary section in the Lattengebirge, Bavarian Alps N89-21323
ENTROPY
Toward a nonequilibrium thermodynamics of two phase materials with sharp interface N89-21494
ENVIRONMENT EFFECTS
Global environmental effects of impact-generated aerosols: Results from a general circulation model N89-21306
Volcanism, global catastrophe and mass mortality N89-21316
Environmental effects of large impacts on the earth; relation to extinction mechanisms N89-21365
Mass extinctions in the deep sea N89-21396
Operational implications of a cloud model simulation of space shuttle exhaust clouds in different atmospheric conditions
[NASA-CR-4222] N89-21425
ENVIRONMENTAL TESTS
Simulation of the low earth orbital atomic oxygen interaction with materials by means of an oxygen ion beam
[NASA-TM-101971] N89-21104
ENZYMES
Center for Advanced Materials
[DE89-008854] N89-21033
EPOXY COMPOUNDS
The use of primers in the adhesive bonding of carbon-fibre reinforced composites
[AD-A202542] N89-21039
EPOXY MATRIX COMPOSITES
Evaluation of atomic oxygen resistant protective coatings for fiberglass-epoxy composites in LEO
[NASA-TM-101955] N89-21100
EPOXY RESINS
Transverse shear considerations in anisotropic plates
[AD-A203187] N89-21283
EQUATIONS OF STATE
Fluids, both ionic and nonionic, over wide ranges of temperature and composition
[DE89-001265] N89-21048
Root placement with transfer function methods (full state feedback)
[AD-A203877] N89-21610
Small expendable deployer system measurement analysis N89-21731
EQUILIBRIUM FLOW
Thin-layer Navier-Stokes solutions for a cranked delta wing
[AD-A203292] N89-20970
EQUINOXES
Observations of neutral circulation at mid-latitudes during the Equinox Transition Study
[NASA-CR-184792] N89-21429
EQUIPMENT SPECIFICATIONS
Construction of an alternating gradient magnetometer N89-21739
The measurement of angular differential cross sections at the SSL Atomic Scattering Facility N89-21744
EROSION
Faunal and erosional events in the Eastern Tethyan Sea across the K/T boundary N89-21338
Atmospheric erosion by impacts: An analytic investigation N89-21403
ERROR ANALYSIS
Problem specific applications for neural networks
[AD-A203052] N89-21158
Disruption of giant comets in the solar system and around other stars N89-21408
A posteriori error estimation of adaptive finite difference schemes for hyperbolic systems N89-21513
On some finite element error estimates for stress intensity factors in Mode 1 linear elastic fracture problems N89-21517
Large sample theory for statistical inference in several software reliability models
[CWI-MS-R8807] N89-21543
Modified backward error propagation for tactical target recognition
[AD-A202666] N89-21644
ERROR CORRECTING CODES
Optical computing research
[AD-A202963] N89-21564
ERRORS
On the impulse response of monopulse radars
[AD-A202936] N89-21153
Thermopile temperature sensitivity calibration procedure for Eppley broadband radiometers
[PB89-104129] N89-21215
ESCAPE SYSTEMS
A wind tunnel and computer investigation of the low speed aerodynamic characteristics of the prone escape system (PRESS)
[AD-A202768] N89-20988
ESTIMATES
Asteroid and comet flux in the neighborhood of the earth N89-21387
The cometary and asteroidal impactor flux at the earth N89-21407
A posteriori error estimation of adaptive finite difference schemes for hyperbolic systems N89-21513
On some finite element error estimates for stress intensity factors in Mode 1 linear elastic fracture problems N89-21517
Nonparamteric estimation from queues arising in staggered entry clinical trials N89-21520
Order statistics and robust inference
[AD-A203440] N89-21616
EULER EQUATIONS OF MOTION
Computation of aircraft component flow fields at transonic Mach numbers using a three-dimensional Navier-Stokes algorithm N89-20933
Euler solvers for transonic applications N89-20935
Generation of unstructured grids and Euler solutions for complex geometries N89-20941
Euler/Navier-Stokes calculations of transonic flow past fixed- and rotary-wing aircraft configurations N89-20948
The 3-D Euler and Navier-Stokes calculations for aircraft components N89-20950
Radio-controlled model gyro measurement study
[AD-A204002] N89-21223
EUTECTICS
Effect of Te on the microstructural changes during the gray-to-white and white-to-gray transition in directional solidification of Fe-C-Si alloys
[DE89-007607] N89-21076
EVENTS
The causality horizon and parallel processing for simulations with wide geographical dispersions
[DE89-008484] N89-21590
EVOKED RESPONSE (PSYCHOPHYSIOLOGY)
Brain activity during tactical decision-making. Part 5: A cross-study validation of evoked potentials as indices of workload
[AD-A203763] N89-21474
EXCITATION
Subharmonic and fundamental high amplitude excitation of an axisymmetric jet
[NASA-TM-101946] N89-20920
Excitation and diagnostics of optical contamination in the spacecraft environment
[AD-A202429] N89-21015
Laser enhanced chemical reactions
[DE89-008084] N89-21236
Lie transforms applied to a nonlinear parametric excitation problem N89-21491
EXHAUST CLOUDS
A cloud model simulation of space shuttle exhaust clouds in different atmospheric conditions
[NASA-CR-4223] N89-21426
EXHAUST EMISSION
Gas turbine alternative fuels combustion characteristics
[NASA-TM-101470] N89-21417
EXOBIOLOGY
Aerospace medicine and biology: A continuing bibliography with indexes (supplement 321)
[NASA-SP-7011(321)] N89-21475
Aerospace medicine and biology: A continuing bibliography with indexes (supplement 322)
[NASA-SP-7011(322)] N89-21476
EXPENDABLE STAGES (SPACECRAFT)
An analytical framework for determining life cycle cost implications of the advanced launch system
[AD-A202873] N89-21012
EXPERIMENT DESIGN
Conditionally and strictly distribution-free tests for randomized block designs that are asymptotically optimal
[CWI-MS-R8802] N89-21615
Angular response calibration of the burst and transient source experiment N89-21745
EXPERIMENTATION
Nonparamteric estimation from queues arising in staggered entry clinical trials N89-21520
EXPERT SYSTEMS
A diagnostic system blending deep and shallow reasoning
[AD-A202547] N89-20979
Transactions of the Fifth Army Conference on Applied Mathematics and Computing
[AD-A193384] N89-21490
Knowledge representation and planning control in an expert system for the creative design of mechanisms N89-21492
Empirical demonstration of isoperformance methodology preparatory of an interactive expert computerized decision aid
[AD-A202439] N89-21545
Simulating rule-based systems
[AD-A202563] N89-21555
An educational expert system shell integrating object-attribute-value triples and frames
[AD-A202574] N89-21557
A methodology for screening potential artificial intelligence applications
[AD-A203966] N89-21594
SIRE: A Simple Interactive Rule Editor for NICBES N89-21730
Intelligent data reduction for autonomous power systems N89-21737
EXPLOSIONS
Explosive volcanism, shock metamorphism and the K-T boundary N89-21309
Isotopic investigations in the area of the Tunguska catastrophe in 1908 year N89-21342
Search for the Tunguska event in the Antarctic snow N89-21378
Propagator matrices in the solution of EMP problems N89-21515
EXPLOSIVES
Deformation, fracture and explosive properties of reactive materials
[AD-A203083] N89-21128
EXTERNAL STORES
Method to predict external store carriage loads at transonic speeds N89-20945

EXTINCTION
Global Catastrophes in Earth History: An Interdisciplinary Conference on Impacts, Volcanism, and Mass Mortality [NASA-CR-183329] N89-21287
The debate over the Cretaceous-Tertiary boundary N89-21288
Limitations on K-T mass extinction theories based upon the vertebrate record N89-21290
Possible world-wide middle miocene iridium anomaly and its relationship to periodicity of impacts and extinctions N89-21291
The cratering record in the inner solar system: Implications for earth N89-21292
Carbon dioxide catastrophes: Past and future menace N89-21293
Geochemistry of K/T boundaries in India and contributions of Deccan volcanism N89-21296
Response of marine and freshwater algae to nitric acid and elevated carbon dioxide levels simulating environmental effects of bolide impact N89-21298
Dinosaur bone beds and mass mortality: Implications for the K-T extinction N89-21301
Magnetic microspherules associated with the K/T and upper Eocene extinction events N89-21303
Origination, diversity, and extinction metrics essential for analysis of mass biotic crisis events: An example from cretaceous ammonoidea N89-21304
Abrupt climate change and extinction events N89-21308
Rocks, resolution, and the record at the terrestrial K/T boundary, eastern Montana and western North Dakota N89-21313
The impact of mass extinctions N89-21315
Volcanism, global catastrophe and mass mortality N89-21316
The Frasnian-Famennian mass killing event(s), methods of identification and evaluation N89-21318
Late Eocene impact events recorded in deep-sea sediments N89-21322
The end-triassic mass extinction event N89-21324
Diachronism between extinction time of terrestrial and marine dinosaurs N89-21325
High resolution chronology of late Cretaceous-early Tertiary events determined from 21,000 yr orbital-climatic cycles in marine sediments N89-21328
Selective extinction of marine plankton at the end of the Mesozoic era: The fossil and stable isotope record N89-21329
Impact wave deposits provide new constraints on the location of the K/T boundary impact N89-21330
Strangelove ocean at era boundaries, terrestrial or extraterrestrial cause N89-21332
Mass mortality and extraterrestrial impacts N89-21335
Patterns of megafloral change across the Cretaceous-Tertiary boundary in the Northern Great Plains and Rocky Mountains N89-21336
Extended period of K/T boundary mass extinction in the marine realm N89-21337
Widespread habitat change through paludification as an interactive mechanism in mass extinction events N89-21339
The Karskiy craters are the probable records of catastrophe at the Cretaceous-Tertiary boundary N89-21343
The Cretaceous-Tertiary boundary biotic crisis in the Basque country N89-21345
Catastrophic volcanism N89-21346
Magnetic reversal spurts: Rain gauges for comet showers N89-21349
Inducement of heterochronic variation in a species of planktic foraminifera by a Late Eocene impact event N89-21351
Trace element and isotope geochemistry of Cretaceous-Tertiary boundary sediments: identification of extra-terrestrial and volcanic components N89-21352
Step-wise extinctions at the Cretaceous-Tertiary boundary and their climatic implications N89-21354
Mass killings and detection of impacts N89-21356
Earth orbital variations and vertebrate bioevolution N89-21357
Flood basalts and mass extinctions N89-21360
Astrophysical implications of periodicity N89-21361
Deccan volcanism and K-T boundary signatures N89-21362
Plant microfossil record of the terminal Cretaceous event in the western United States and Canada N89-21363
Cretaceous-Tertiary findings, paradigms and problems N89-21364
Environmental effects of large impacts on the earth; relation to extinction mechanisms N89-21365
The Triassic-Jurassic boundary in eastern North America N89-21366
Permo-Triassic vertebrate extinctions: A program N89-21367
Biospheric traumas caused by large impacts and predicted relics in the sedimentary record N89-21371
Flood basalt eruptions, comet showers, and mass extinction events N89-21372
Climatic changes resulting from mass extinctions at the K-T boundary (and other bio-events) N89-21373
Impact as a general cause of extinction: A feasibility test N89-21374
Report on an international workshop on Cryptoexplosions and Catastrophes in the Geological Record, with a Special Focus on the Vredefort Structure N89-21375
Dynamics of exploding magma chambers: Implications for K-T volcanism and mass extinctions N89-21377
Late Frasnian mass extinction: Conodont event stratigraphy, global changes, and possible causes N89-21380
Crater size estimates for large-body terrestrial impact N89-21381
Oblique impacts: Catastrophic vs. protracted effects N89-21383
Periodicity of extinction: A 1988 update N89-21385
Volcanoes and global catastrophes N89-21389
Biostratigraphic case studies of six major extinctions N89-21390
Impact and extinction signatures in complete Cretaceous-Tertiary (K-T) boundary sections N89-21391
Cretaceous-Tertiary boundary in the Antarctic: Climatic cooling precedes biotic crisis N89-21392
Some volcanologic aspects of Columbia River basalt volcanism relevant to the extinction controversy N89-21393
A regional perspective on the palynofloral response to K-T boundary event(s) with emphasis on variations imposed by the effects of sedimentary facies and latitude N89-21395
Mass extinctions in the deep sea N89-21396
Macrofossil extinction patterns at Bay of Biscay Cretaceous-Tertiary boundary sections N89-21404
Heavy metal toxicity as a kill mechanism in impact caused mass extinctions N89-21406
The cometary and asteroidal impactor flux at the earth N89-21407
Darkness after the K-T impact: Effects of soot N89-21411
The Cretaceous-Tertiary boundary marine extinction and global primary productivity collapse N89-21412
Utility of a dual-lidar method to measure integrated extinction [AD-A203145] N89-21439
EXTRAPOLATION
A posteriori error estimation of adaptive finite difference schemes for hyperbolic systems N89-21513
EYE (ANATOMY)
Polycarbonate ophthalmic lenses for ametropic Army aviators using night vision goggles [AD-A203100] N89-21488

F

F REGION
Observations of neutral circulation at mid-latitudes during the Equinox Transition Study [NASA-CR-184792] N89-21429
F-16 AIRCRAFT
Incorporating five nations' operational requirements into a single aircraft: The F-16 multinational fighter program viewed from the operational side [AD-A202552] N89-20986
F-16 speaker-independent speech recognition system using cockpit commands (70 words) [AD-A203177] N89-21489
FABRICATION
Focused ion beam fabrication of graded channel Field Effect Transistors (FETs) in GaAs and Si [AD-A203365] N89-21184
Robotic tactile sensor fabricated from piezoelectric polyvinylidene fluoride films [AD-A202724] N89-21250
Reduction of M1 weld fabrication costs: The effect of weld shielding gas composition [AD-A204001] N89-21254
Computer-aided fabrication system implementation [AD-A203651] N89-21576
FABRY-PEROT INTERFEROMETERS
A search for gravitational waves from coalesing binary stars using the Caltech 40 meter gravity wave detector N89-21721
FACTOR ANALYSIS
Dimensionality of binary items [AD-A203238] N89-21608
FACTORIZATION
A block QR factorization scheme for loosely coupled systems of array processors N89-21519
FAILURE ANALYSIS
Inelastic deformation and failure analysis of filament-wound composite structures [AD-A203382] N89-21044
On the energy release rate for dynamic transient anti-plane shear crack propagation in a general linear viscoelastic body [AD-A202942] N89-21280
Computer codes for thermal analysis of a solid rocket motor nozzle N89-21733
Evaluate the application of modal test and analysis processes to structural fault detection in MSFC-STS project elements N89-21751
Software system safety N89-21754
FAILURE MODES
Investigation of failure modes in fiber reinforced ceramic matrix composites [AD-A202705] N89-21113
Fractographic analysis of a failed crane bolt [AD-A202703] N89-21274
FAR FIELDS
A comparison of reflector antenna designs for wide-angle scanning [NASA-TM-101459] N89-21138
FARM CROPS
Effects of global atmospheric perturbations on forest ecosystems: Predictions of seasonal and cumulative effects N89-21399
FAST FOURIER TRANSFORMATIONS
Superresolved imaging using the Hartley transform and a hemispherical object space [AD-A202527] N89-21551
FATIGUE (MATERIALS)
Mechanisms of fatigue crack propagation and fracture toughness behavior in advanced aluminum-lithium alloys [DE89-008300] N89-21098
Surface chemistry and structural effects in the stress corrosion of glass and ceramic materials [AD-A202452] N89-21107
Global-local methodology for fracture analysis of engineering structures N89-21262
FATIGUE TESTS
Investigation of crack growth in titanium-aluminide at elevated temperatures [AD-A202570] N89-21081
Crack growth of a titanium-aluminide alloy under thermal-mechanical fatigue [AD-A202767] N89-21083
Strain energy release rate as a function of temperature and preloading history utilizing the edge delamination fatigue test method [NASA-CR-184966] N89-21286
Dynamic fatigue testing of Zerodur glass-ceramic N89-21753
FAULT TOLERANCE
Advanced information processing system: Local system services [NASA-CR-181767] N89-21582
FEDERAL BUDGETS
An analysis of the biennial budget process [AD-A202626] N89-21710
FEEDBACK
A digital rate controller for the control reconfigurable combat aircraft designed using quantitative feedback theory [AD-A203050] N89-21001
Modeling robot dynamic performance for endpoint force control [AD-A202881] N89-21251
Selection of a frequency sensitive QFT (Quantitative Feedback Theory) weighting matrix using the method of specified outputs [AD-A202692] N89-21592
FEEDBACK CONTROL
Actuation constraints in multivariable flight control systems N89-20998
Flight controller design with nonlinear aerodynamics, large parameter uncertainty and pilot compensation [AD-A202727] N89-21000
A magnetic bearing control approach using flux feedback [NASA-TM-100672] N89-21135
Evaluation of time delay requirements for closed-loop stability using classical and modern methods [DE89-006417] N89-21189
Root placement with transfer function methods (full state feedback) [AD-A203877] N89-21610
FEEDFORWARD CONTROL
Dynamic analysis of feedforward neural networks using simulated and measured data [AD-A202573] N89-21591
FERMI LIQUIDS
Fermi liquid theory for high temperature superconductors [DE89-007982] N89-21688

FERMI SURFACES
Investigation of Schottky barrier on GaAs and InP using a multidisciplined approach
[AD-A202953] N89-21675
FIBER COMPOSITES
Acoustic emission source location in fibre reinforced plastic composites
[AERE-R-13039] N89-21035
The behavior of ceramic matrix, fiber composites under combined impact and tensile stresses
[AD-A202518] N89-21038
Microscopic aspects of failure and fracture in cross-ply fiber-reinforced composite laminates
[AD-A203202] N89-21042
High temperature composites using Schiff's base pyropolymer matrices
[AD-A203311] N89-21043
Physical and mechanical properties of American Cyanamid's acetylene-terminated prepreg system: T-300/CATB-44
[AD-A203737] N89-21045
Effect of geometry on thermal aging behavior of Celion/LARC-160 composites
[NASA-TM-100496] N89-21047
Acoustic microscopy of low ductility materials
[AERE-R-12848] N89-21101
Investigation of failure modes in fiber reinforced ceramic matrix composites
[AD-A202705] N89-21113
Fracture toughness testing of a ceramic matrix composite at elevated temperatures
[AD-A202738] N89-21114
A study of the stress wave factor technique for evaluation of composite materials
[NASA-CR-4195] N89-21256
The shear-lag model for a unidirectional composite with viscoelastic matrix N89-21495
FIBER OPTICS
Performance analysis of the fiber distributed data interface in the super cockpit audio world
[AD-A202535] N89-20985
Center for Electronics and Electrical Engineering technical progress bulletin covering center programs, April to June 1988 with 1988 CEEE events calendar
[PB89-123137] N89-21170
Development and characterization of a fiber optic immuno biosensor
[DE89-005062] N89-21225
Optical fiber sensors and signal processing for intelligent structure monitoring
[NASA-CR-184841] N89-21640
Immunoassay procedures for fiber optic sensors
[AD-A203069] N89-21649
FIBERS
Static tensile and tensile creep testing of five ceramic fibers at elevated temperatures
[NASA-CR-177525] N89-21046
Compressive properties of high performance polymeric fibers
[AD-A202947] N89-21117
FIELD EFFECT TRANSISTORS
Development of gallium arsenide high-speed, low-power serial parallel interface modules: Executive summary
[NASA-CR-182272] N89-21173
Investigation of the impedance modulation of thin films with a chemically-sensitive field-effect transistor
[AD-A202766] N89-21180
Focused ion beam fabrication of graded channel Field Effect Transistors (FETs) in GaAs and Si
[AD-A203365] N89-21184
Investigation of a self-aligned, strained-channel,n sup(+)-In As/Al 0.5 As/In 0.15 Ga 0.85 As Semiconductor Insulator Semiconductor FET (SISFET)
[AD-A203147] N89-21676
FIGHTER AIRCRAFT
Transonics and fighter aircraft: Challenges and opportunities for CFD N89-20932
Aeroelastic modeling for the FIT team F/A-18 simulation
[NASA-TM-101569] N89-20991
A digital rate controller for the control reconfigurable combat aircraft designed using quantitative feedback theory
[AD-A203050] N89-21001
Selection of a frequency sensitive QFT (Quantitative Feedback Theory) weighting matrix using the method of specified outputs
[AD-A202692] N89-21592
FILAMENT WINDING
Inelastic deformation and failure analysis of filament-wound composite structures
[AD-A203382] N89-21044
FILLERS
Adhesion in chemically hostile environments: The use of filled polymers as diffusion barriers
[AD-A203333] N89-21121
FINANCIAL MANAGEMENT
An analysis of the biennial budget process
[AD-A202626] N89-21710
FINITE DIFFERENCE THEORY
Conformal time domain finite difference method of solving electromagnetic wave scattering
[AD-A202434] N89-21143
Finite-difference modeling of Rayleigh wave scattering and P-SV(Lg) coupling problems
[AD-A203221] N89-21161
Numerical computation of shock wave-turbulent boundary layer interaction in transonic flow over an axisymmetric curved hill
[NASA-TM-101473] N89-21192
Transactions of the Fifth Army Conference on Applied Mathematics and Computing
[AD-A193384] N89-21490
Polynominal definition of discrete field point of map of diffusion equation N89-21511
A posteriori error estimation of adaptive finite difference schemes for hyperbolic systems N89-21513
Skew grids and irrotational flow N89-21523
FINITE ELEMENT METHOD
Effects of battle damage repair on the natural frequencies and mode shapes of curved rectangular composite panels
[AD-A203179] N89-21041
Conformal time domain finite difference method of solving electromagnetic wave scattering
[AD-A202434] N89-21143
Modal analysis of gear housing and mounts
[NASA-TM-101445] N89-21244
Nonlinear shell analyses of the space shuttle solid rocket boosters
[NASA-TM-101546] N89-21260
Global-local methodology for fracture analysis of engineering structures N89-21262
Application of the boundary element method to fatigue crack growth analysis
[AD-A202565] N89-21270
Nonlinear finite element analysis of a general composite shell
[AD-A202572] N89-21271
Three dimensional effects near a crack tip in a ductile three point bend specimen. Part 2: An experimental investigation using interferometry and caustics
[AD-A202637] N89-21272
Analytical and experimental investigation of constrained viscoelastic layer damping for a plate and shell model
[AD-A202698] N89-21273
Finite element analysis of composite plates including shear deformation
[AD-A202941] N89-21279
Macrocrack-multiple defect interaction considering elastic, plastic and viscoplastic effects
[AD-A203186] N89-21282
The implementation of a nonreflecting boundary into the SAMSON2 code
[AD-A203394] N89-21284
Transactions of the Fifth Army Conference on Applied Mathematics and Computing
[AD-A193384] N89-21490
Element level elimination of nonlinear constraints in total Lagrangian finite element formulations N89-21496
Condition of the finite element stiffness matrix of highly irregular triangular grids N89-21497
An adaptive overlapping local grid refinement method for two-dimensional parabolic systems N89-21514
Spline-based finite-element method for solving a Stefan's problem in a finite domain: Formulation N89-21516
On some finite element error estimates for stress intensity factors in Mode 1 linear elastic fracture problems N89-21517
Some issues of numerical integration and penalty relaxation in anisoparametric shell element formulation N89-21518
Documentation of the finite element code VISCOT/UX for thermomechanical analyses: Version 0.01
[DE89-004719] N89-21544
Adaptive optical linear algebra processors
[AD-A202996] N89-21605
The application of modal coordinate methods to large nonlinear time-dependent problems
[AD-A203913] N89-21611
Time-discretized moments of a randomly excited uncertain linear oscillator
[DE89-008318] N89-21614
Finite element simulation of thunderstorm electrodynamics in the proximity of the storm N89-21728
FIRE EXTINGUISHERS
Study of the ignition inhibiting properties of compressed air foam
[PB89-127559] N89-21049
FIRES
The global Cretaceous-Tertiary fire: Biomass or fossil carbon N89-21321
FLAMMABILITY
Study of the ignition inhibiting properties of compressed air foam
[PB89-127559] N89-21049
Modelling of the lean flammability limit in flame theory N89-21527
FLAT PLATES
Effect of riblets upon flow separation in a subsonic diffuser
[AD-A203178] N89-20967
The response of a laminar boundary layer in supersonic flow to small amplitude progressive waves
[NASA-TM-101965] N89-21197
Numerical study of three viscous/inviscid interaction methods
[AD-A202575] N89-21203
Vibration and buckling characteristics of composite cylindrical panels incorporating the effects of a higher order shear theory
[AD-A202939] N89-21278
On a refined nonlinear theory of laminated composite plates N89-21500
FLEXIBLE SPACECRAFT
Time optimal slewing of flexible spacecraft N89-21014
FLEXING
Comparison of airfoil results from an adaptive wall test section and a porous wall test section N89-20960
FLIGHT CLOTHING
SPH-4 US Army flight helmet performance 1983-1987
[AD-A202589] N89-21482
FLIGHT CONTROL
AH-1S communication switch integration program
[NASA-TM-101053] N89-20978
Preliminary design of a modular unmanned research vehicle. Volume 1: System design document
[AD-A202765] N89-20987
Flight controller design with nonlinear aerodynamics, large parameter uncertainty and pilot compensation
[AD-A202727] N89-21000
Computer simulation of a pilot in V/STOL aircraft control loops
[NASA-CR-184815] N89-21479
Capacity of human operator using smart stick controller
[AD-A202712] N89-21483
Selection of a frequency sensitive QFT (Quantitative Feedback Theory) weighting matrix using the method of specified outputs
[AD-A202692] N89-21592
FLIGHT HAZARDS
In-flight lightning characterization program on a CV-580 aircraft
[AD-A203954] N89-20976
FLIGHT SAFETY
Simulation at Dryden Flight Research Facility from 1957 to 1982
[NASA-TM-101695] N89-20983
Evaluate the application of modal test and analysis processes to structural fault detection in MSFC-STS project elements N89-21751
FLIGHT SIMULATION
Aircraft tracking with dual TACAN
[AD-A202647] N89-20980
Simulation at Dryden Flight Research Facility from 1957 to 1982
[NASA-TM-101695] N89-20983
FLIGHT TEST VEHICLES
Preliminary design of a modular unmanned research vehicle. Volume 1: System design document
[AD-A202765] N89-20987
FLIGHT TESTS
Transonic Symposium: Theory, Application, and Experiment, Volume 1, Part 1
[NASA-CP-3020-VOL-1-PT-1] N89-20925
Flight research and testing N89-20927
AH-1S communication switch integration program
[NASA-TM-101053] N89-20978
Aircraft tracking with dual TACAN
[AD-A202647] N89-20980
Contamination of the exterior of a C-130E aircraft used for aerial spray, 907 TAG, Rickenbacker ANGB, OH
[AD-A202430] N89-20984
Capacity of human operator using smart stick controller
[AD-A202712] N89-21483
Comparison of propeller cruise noise data taken in the NASA Lewis 8- by 6-foot wind tunnel with other tunnel and flight data
[NASA-TM-101976] N89-21628
FLIR DETECTORS
Multiple model adaptive tracking of airborne targets
[AD-A202696] N89-21148

Modified backward error propagation for tactical target recognition
[AD-A202666] N89-21644
Evaluation of aerosol size distribution models
[AD-A202736] N89-21645

FLOATING POINT ARITHMETIC
Architecture and design for a laser programmable double precision floating point application specific processor
[AD-A202560] N89-21553
Best ordering for floating-point addition
[AD-A203990] N89-21612

FLOATS
Localizing and beamforming freely-drifting VLF (Very Low Frequency) acoustic sensors
[AD-A202638] N89-21217

FLOOD PLAINS
Flood basalts and mass extinctions N89-21360
Deccan volcanism and K-T boundary signatures N89-21362
Flood basalt eruptions, comet showers, and mass extinction events N89-21372

FLOW CHARACTERISTICS
On the conditions for resonance interactions of instability waves in the axisymmetric jet
[NASA-TM-101477] N89-21196

FLOW COEFFICIENTS
Incompressible flow friction coefficients in a simulated heat pipe
[AD-A203176] N89-21207

FLOW DEFLECTION
An experimental study of transonic buffet of a supercritical airfoil with trailing edge flap
[AD-A203189] N89-20968

FLOW DISTRIBUTION
Additional development of the XTRAN3S computer program
[NASA-CR-181743] N89-20922
Numerical simulation of the flow field over delta wings with leading edge blowing N89-20924
Computation of aircraft component flow fields at transonic Mach numbers using a three-dimensional Navier-Stokes algorithm N89-20933
An embedded mesh procedure for leading-edge vortex flows N89-20936
Generation of unstructured grids and Euler solutions for complex geometries N89-20941
Aerodynamic analysis of three advanced configurations using the TranAir full-potential code N89-20944
Steady and unsteady transonic small disturbance analysis of realistic aircraft configurations N89-20946
Navier-Stokes and viscous-inviscid interaction N89-20949
Instrumentation advances for transonic testing N89-20957
Comparison of airfoil results from an adaptive wall test section and a porous wall test section N89-20960
A study of transonic drag reduction of a blunt cylinder by a cylinder probe
[AD-A202557] N89-20965
Numerical simulation of flow over iced airfoils
[AD-A203291] N89-20969
Flowfield measurements in the NASA Lewis Research Center 9- by 15-foot low-speed wind tunnel
[NASA-TM-100883] N89-21002
Structure development during converging flow of a liquid crystal dispersed two-phase fluid
[AD-A203062] N89-21119
Computational studies of an impulsively started viscous flow
[NASA-TM-101037] N89-21190
Potential flow evaluation of the interference effect of strut-through-appendage-tip model mounting technique and reduction of the effect using blowing and suction
[AD-A202424] N89-21199
Investigation of the development of laminar boundary-layer instabilities along a blunted cone
[AD-A202425] N89-21200
Advanced diagnostics for reacting flows
[AD-A202451] N89-21202
Volumetric rendering techniques for the display of three-dimensional aerodynamic flow field data
[AD-A202661] N89-21204
Whole field measurements of vorticity in turbulent and unsteady flows
[AD-A203349] N89-21209
Influence of reflected shock waves on a hypersonic shaped charge jet N89-21522

FLOW EQUATIONS
Numerical study of three viscous/inviscid interaction methods
[AD-A202575] N89-21203

FLOW MEASUREMENT
Flow reactor studies of elementary radical reaction rates
[AD-A203126] N89-21062
Coherent structures in fully developed turbulent pipe flow N89-21195

FLOW STABILITY
Transient natural convection heat and mass transfer in crystal growth N89-21741

FLOW VELOCITY
Flow reactor studies of elementary radical reaction rates
[AD-A203126] N89-21062
Coherent structures in fully developed turbulent pipe flow N89-21195
Instabilities in shear flow of viscoelastic fluids with fading memory
[AD-A203735] N89-21211
Computer program for calculating frequencies and modal structures of free coastal-trapped waves
[PB88-243928] N89-21459

FLOW VISUALIZATION
Coherent structures in fully developed turbulent pipe flow N89-21195

FLOWMETERS
Magnetic flowmeter measurement of solid propellant pressure-coupled and velocity-coupled responses
[AD-A203988] N89-21133

FLUENCE
Acoustic damage to large-aperture optics: Revision 1
[DE89-008025] N89-21654

FLUID DYNAMICS
Cryogenic fluid management in space N89-21727

FLUID JETS
Transverse jets in compressible crossflows N89-20923
Investigation of the impact performance of various glass and ceramic systems
[AD-A202443] N89-21106

FLUID MANAGEMENT
Cryogenic fluid management in space N89-21727

FLUID PRESSURE
A continued study of optical sound generation and amplification
[AD-A202484] N89-21630

FLUORESCENCE
Spectroscopic studies of fluid/solid interfaces
[AD-A202436] N89-21054

FLUORIDES
Robotic tactile sensor fabricated from piezoelectric polyvinylidene fluoride films
[AD-A202724] N89-21250

FLUTTER ANALYSIS
Additional development of the XTRAN3S computer program
[NASA-CR-181743] N89-20922

FOAMS
Study of the ignition inhibiting properties of compressed air foam
[PB89-127559] N89-21049
Attenuation of blast waves using foam and other materials
[AD-A203148] N89-21632

FOCUSING
A theoretical and experimental investigation of linear and nonlinear focussing chirped optical diffraction gratings
[AD-A203396] N89-21650
Order in cold ionic systems: Dynamic effects
[DE89-007377] N89-21687

FOKKER-PLANCK EQUATION
Diffusion in symplectic maps
[DE89-008083] N89-21622
The evolution of active galactic nuclei and globular clusters: Multi-component models N89-21720

FOOD CHAIN
The Cretaceous-Tertiary boundary marine extinction and global primary productivity collapse N89-21412

FORCE-FREE MAGNETIC FIELDS
Force-free magnetic fields: Is there a loss of equilibrium
[AD-A203030] N89-21717

FORECASTING
Icing considerations for HALE (High Altitude, Long Endurance) aircraft
[AD-A202584] N89-20975
An individual-based forest ecosystems model for projecting forest response to nutrient cycling and climate changes
[DE89-007212] N89-21428

FORESTS
The global Cretaceous-Tertiary fire: Biomass or fossil carbon N89-21321
Widespread habitat change through paludification as an interactive mechanism in mass extinction events N89-21339
Effects of global atmospheric perturbations on forest ecosystems: Predictions of seasonal and cumulative effects N89-21399
Air quality and forest health issues in the 1990s
[DE89-006941] N89-21427
An individual-based forest ecosystems model for projecting forest response to nutrient cycling and climate changes
[DE89-007212] N89-21428

FORMAT
GRAPS (Graphical Plotting System) user's guide. A graphical plotting system for displaying scientific and engineering data
[AD-A202583] N89-21559
A software system to create a hierarchical, multiple level of detail terrain model
[AD-A203047] N89-21568

FORTRAN
A language comparison for scientific computing on MIMD architectures
[NASA-CR-181779] N89-21537

FOSSILS
Geochemistry of K/T boundaries in India and contributions of Deccan volcanism N89-21296
An extended Cretaceous-Tertiary (K/T) stable isotope record. Implications for paleoclimate and the nature of the K/T boundary event N89-21310
Rocks, resolution, and the record at the terrestrial K/T boundary, eastern Montana and western North Dakota N89-21313
The impact of mass extinctions N89-21315
The global Cretaceous-Tertiary fire: Biomass or fossil carbon N89-21321
The end-triassic mass extinction event N89-21324
Diachronism between extinction time of terrestrial and marine dinosaurs N89-21325
How many upper Eocene microspherule layers: More than we thought N89-21327
Bio-, Magneto- and event-stratigraphy across the K-T boundary N89-21370
Late Frasnian mass extinction: Conodont event stratigraphy, global changes, and possible causes N89-21380
Periodicity of extinction: A 1988 update N89-21385
Cretaceous-Tertiary boundary in the Antarctic: Climatic cooling precedes biotic crisis N89-21392
A regional perspective on the palynofloral response to K-T boundary event(s) with emphasis on variations imposed by the effects of sedimentary facies and latitude N89-21395
Macrofossil extinction patterns at Bay of Biscay Cretaceous-Tertiary boundary sections N89-21404

FOULING
Fouling tests of AGT-1500 gas turbine fuel nozzles
[AD-A203360] N89-21253

FOURIER TRANSFORMATION
A position, scale and rotation invariant holographic associative memory
[AD-A203289] N89-21221
Downward continuation of the free-air gravity anomalies to the ellipsoid using the gradient solution, Poisson's integral and terrain correction-numerical comparison and computations
[AD-A203739] N89-21442
Hybrid calculation of invariant moments
[AD-A202594] N89-21600
Adaptive optical linear algebra processors
[AD-A202996] N89-21605
Diffusion in symplectic maps
[DE89-008083] N89-21622

FRACTIONATION
Noble metals in mid-ocean ridge volcanism: A significant fractionation of gold with respect to platinum group metals N89-21307

FRACTOGRAPHY
Microscopic observations of adiabatic shear bands in three different steels
[AD-A202522] N89-21080
Fractographic analysis of a failed crane bolt
[AD-A202703] N89-21274

FRACTURE MECHANICS
Microscopic aspects of failure and fracture in cross-ply fiber-reinforced composite laminates
[AD-A203202] N89-21042
The effect of mixed-mode loading on stress-driven solute segregation during high-temperature brittle intergranular fracture
[AERE-R-12897] N89-21073
Microscopic observations of adiabatic shear bands in three different steels
[AD-A202522] N89-21080
Crack growth of a titanium-aluminide alloy under thermal-mechanical fatigue
[AD-A202767] N89-21083
Stress-corrosion cracking of liquid-phase sintered tungsten alloys
[AD-A203201] N89-21087

Surface chemistry and structural effects in the stress corrosion of glass and ceramic materials
[AD-A202452] N89-21107
Ceramics
[AD-A202504] N89-21109
Investigation of Weibull statistics in fracture analysis of cast aluminum
[NASA-TM-102000] N89-21245
Global-local methodology for fracture analysis of engineering structures N89-21262
Stress intensity factors for bodies containing initial stress N89-21263
Analysis of interface crack branching
[NASA-CR-182273] N89-21265
Large deformations near a pair of closely-spaced spherical voids in a rate-dependent solid
[AD-A202465] N89-21268
Application of the boundary element method to fatigue crack growth analysis
[AD-A202565] N89-21270
Three dimensional effects near a crack tip in a ductile three point bend specimen. Part 2: An experimental investigation using interferometry and caustics
[AD-A202637] N89-21272
Fractographic analysis of a failed crane bolt
[AD-A202703] N89-21274

FRACTURE STRENGTH
Mechanisms of fatigue crack propagation and fracture toughness behavior in advanced aluminum-lithium alloys
[DE89-008300] N89-21098
Fracture characteristics of balloon films
[NASA-CR-181686] N89-21099
Fracture toughness testing of a ceramic matrix composite at elevated temperatures
[AD-A202738] N89-21114
High temperature evaluation of new ferroelastic toughened ceramic materials
[AD-A203197] N89-21120
Investigation of Weibull statistics in fracture analysis of cast aluminum
[NASA-TM-102000] N89-21245

FRACTURES (MATERIALS)
An investigation of viscoelastic fracture near and at interfaces
[AD-A203760] N89-21285

FRACTURING
Deformation, fracture and explosive properties of reactive materials
[AD-A203083] N89-21128
An investigation of viscoelastic fracture near and at interfaces
[AD-A203760] N89-21285
On some finite element error estimates for stress intensity factors in Mode 1 linear elastic fracture problems N89-21517

FRAGMENTS
New approach to the origin of the tektite in China N89-21414

FREE CONVECTION
A numerical study of the turbulent free convection in rectangular cavities N89-21194

FREE ELECTRON LASERS
Initiative for the 21st century: Advanced space power and propulsion based on lasers
[DE89-008034] N89-21031
Transformations of Gaussian light beams caused by reflection in FEL (Free Electron Lasers) resonators
[AD-A202472] N89-21227

FREE FLOW
The response of a laminar boundary layer in supersonic flow to small amplitude progressive waves
[NASA-TM-101965] N89-21197
Computer program for calculating frequencies and modal structures of free coastal-trapped waves
[PB88-243928] N89-21459

FREE VIBRATION
Bending and vibration of variable thickness orthotropic plates N89-21264

FREEZING
Spline-based finite-element method for solving a Stefan's problem in a finite domain: Formulation N89-21516

FUEL COMBUSTION
Fuel-rich catalytic combustion of Jet-A fuel-equivalence ratios 5.0 to 8.0
[NASA-TM-101975] N89-21051
Fuels combustion research
[AD-A204161] N89-21071
CRC (Coordinating Research Council) hot-start and driveaway driveability program at high and intermediate temperatures using gasoline-alcohol blends
[AD-A202471] N89-21126
Gas turbine alternative fuels combustion characteristics
[NASA-TM-101470] N89-21417
Modelling of the lean flammability limit in flame theory N89-21527

FUEL CONSUMPTION
Operation of vehicle engines in cold conditions: Start up, lubrication and fuel consumption
[DE88-757111] N89-21255

FUEL INJECTION
CRC (Coordinating Research Council) hot-start and driveaway driveability program at high and intermediate temperatures using gasoline-alcohol blends
[AD-A202471] N89-21126
Fouling tests of AGT-1500 gas turbine fuel nozzles
[AD-A203360] N89-21253

FUEL SYSTEMS
CRC (Coordinating Research Council) hot-start and driveaway driveability program at high and intermediate temperatures using gasoline-alcohol blends
[AD-A202471] N89-21126
Robotic compliant motion control for aircraft refueling applications
[AD-A202710] N89-21249

FUEL TESTS
Fouling tests of AGT-1500 gas turbine fuel nozzles
[AD-A203360] N89-21253

FUELS
Modelling of the lean flammability limit in flame theory N89-21527

FUNCTIONAL DESIGN SPECIFICATIONS
An intelligent advisor for the design manager
[NASA-TM-101558] N89-21539

FUNCTIONS (MATHEMATICS)
Asymptotics beyond all orders N89-21508
Devices and systems for nonlinear optical information processing
[AD-A203034] N89-21566
Bispectral inversion: The construction of a time series from its bispectrum
[AD-A202508] N89-21598

G

GALACTIC CLUSTERS
Evolution of cosmic string networks
[NASA-CR-182836] N89-21716

GALACTIC EVOLUTION
Evolution of cosmic string networks
[NASA-CR-182836] N89-21716

GALERKIN METHOD
An adaptive overlapping local grid refinement method for two-dimensional parabolic systems N89-21514

GALLIUM ARSENIDE LASERS
Optical communication with semiconductor laser diode
[NASA-CR-184817] N89-21141

GALLIUM ARSENIDES
Development of gallium arsenide high-speed, low-power serial parallel interface modules: Executive summary
[NASA-CR-182272] N89-21173
Focused ion beam fabrication of graded channel Field Effect Transistors (FETs) in GaAs and Si
[AD-A203365] N89-21184
The potential of GaAs-based mechanically stacked multijunction solar concentrator cells
[DE89-007975] N89-21423
Contributive research in compound semiconductor material and related devices
[AD-A202586] N89-21670
Investigation of Schottky barrier on GaAs and InP using a multidisciplined approach
[AD-A202953] N89-21675
Distribution of boron atoms in ion implanted compound semiconductors
[AD-A203173] N89-21677

GAMMA RAYS
A novel approach to gamma-ray and neutrino astro-particle physics: The GRANDE experiment
[DE89-006515] N89-21725

GAS COMPOSITION
Reduction of M1 weld fabrication costs: The effect of weld shielding gas composition
[AD-A204001] N89-21254

GAS DYNAMICS
Instabilities in shear flow of viscoelastic fluids with fading memory
[AD-A203735] N89-21211

GAS FLOW
Numerical studies of gas flow in spiral galaxies N89-21718

GAS JETS
Transverse jets in compressible crossflows N89-20923

GAS LASERS
Nuclear-pumped lasers for large-scale applications
[DE89-006532] N89-21235

GAS MIXTURES
Reduction of M1 weld fabrication costs: The effect of weld shielding gas composition
[AD-A204001] N89-21254

GAS TURBINE ENGINES
Fuel-rich catalytic combustion of Jet-A fuel-equivalence ratios 5.0 to 8.0
[NASA-TM-101975] N89-21051
High density fuel effects
[AD-A202426] N89-21125
Gas turbine alternative fuels combustion characteristics
[NASA-TM-101470] N89-21417

GAS TURBINES
Development of a shock capturing code for use as a tool in designing high-work low aspect ratio turbines
[AD-A202706] N89-21248
Fouling tests of AGT-1500 gas turbine fuel nozzles
[AD-A203360] N89-21253

GASES
Flow reactor studies of elementary radical reaction rates
[AD-A203126] N89-21062

GASOHOL (FUEL)
CRC (Coordinating Research Council) hot-start and driveaway driveability program at high and intermediate temperatures using gasoline-alcohol blends
[AD-A202471] N89-21126

GATES (CIRCUITS)
Investigation of the impedance modulation of thin films with a chemically-sensitive field-effect transistor
[AD-A202766] N89-21180

GAUGE INVARIANCE
Thermodynamic gauge theory of solids and quantum liquids with internal phase N89-21525
Lagrangian formulation of relativistic thermodynamics N89-21526

GAUGE THEORY
Thermodynamic gauge theory of solids and quantum liquids with internal phase N89-21525
Experimentally verifiable Yang-Mills spin 2 gauge theory of gravity with group U(1) x SU(2) N89-21693

GEARS
Comparison study of gear dynamic computer programs at NASA Lewis Research Center
[NASA-TP-2901] N89-21243
Modal analysis of gear housing and mounts
[NASA-TM-101445] N89-21244

GEOCHEMISTRY
Implications of asteroid composition for the geochemistry of the ancient terrestrial projectile flux N89-21294
Geochemistry of K/T boundaries in India and contributions of Deccan volcanism N89-21296
Shocked quartz and more: Impact signatures in K-T boundary clays and claystones N89-21297
Deccan volcanism at the Cretaceous-Tertiary boundary N89-21305
The Frasnian-Famennian mass killing event(s), methods of identification and evaluation N89-21318
Nitrogen geochemistry of a Cretaceous-Tertiary boundary site in New Zealand N89-21320
Mineralogy and phase-chemistry of the Cretaceous/Tertiary section in the Lattengsbirge, Bavarian Alps N89-21323
Strangelove ocean at era boundaries, terrestrial or extraterrestrial cause N89-21332
The Western North American Cretaceous-Tertiary (K-T) boundary interval and its content of shock-metamorphosed minerals: Implications concerning the K-T boundary impact-extinction theory N89-21334
Mass mortality and extraterrestrial impacts N89-21335
Faunal and erosional events in the Eastern Tethyan Sea across the K/T boundary N89-21338
The Kara and Ust-Kara impact structures (USSR) and their relevance to the K/T boundary event N89-21341
Isotopic investigations in the area of the Tunguska catastrophe in 1908 year N89-21342
The Karskiy craters are the probable records of catastrophe at the Cretaceous-Tertiary boundary N89-21343
Accretion rate of extraterrestrial matter: Iridium deposited over the last 70 million years N89-21344
Seawater strontium isotopes at the Cretaceous-Tertiary boundary N89-21350
Trace element and isotope geochemistry of Cretaceous-Tertiary boundary sediments: identification of extra-terrestrial and volcanic components N89-21352
Mass killings and detection of impacts N89-21356
Mineralogical and geochemical anomalous data of the K-T boundary samples N89-21359
Plant microfossil record of the terminal Cretaceous event in the western United States and Canada N89-21363
Iridium abundance measurements across bio-event horizons in the geological record N89-21368

Flood basalt eruptions, comet showers, and mass extinction events N89-21372
Dynamics of exploding magma chambers: Implications for K-T volcanism and mass extinctions N89-21377
Marine and continental K-T boundary clays compared N89-21382
K-T impact(s): Continental, oceanic or both N89-21386
Impact and extinction signatures in complete Cretaceous-Tertiary (K-T) boundary sections N89-21391
Geochemical comparison of K-T boundaries from the Northern and Southern Hemispheres N89-21400
The Cretaceous-Tertiary boundary marine extinction and global primary productivity collapse N89-21412

GEOCHRONOLOGY

Global Catastrophes in Earth History: An Interdisciplinary Conference on Impacts, Volcanism, and Mass Mortality [NASA-CR-183329] N89-21287
The debate over the Cretaceous-Tertiary boundary N89-21288
Limitations on K-T mass extinction theories based upon the vertebrate record N89-21290
Possible world-wide middle miocene iridium anomaly and its relationship to periodicity of impacts and extinctions N89-21291
The cratering record in the inner solar system: Implications for earth N89-21292
Carbon dioxide catastrophes: Past and future menace N89-21293
Implications of asteroid composition for the geochemistry of the ancient terrestrial projectile flux N89-21294
Late Wenlock (middle Silurian) bio-events: Caused by volatile boloid impact/s N89-21295
Geochemistry of K/T boundaries in India and contributions of Deccan volcanism N89-21296
Shocked quartz and more: Impact signatures in K-T boundary clays and claystones N89-21297
Response of marine and freshwater algae to nitric acid and elevated carbon dioxide levels simulating environmental effects of bolide impact N89-21298
Dinosaur bone beds and mass mortality: Implications for the K-T extinction N89-21301
Magnetic microspherules associated with the K/T and upper Eocene extinction events N89-21303
Origination, diversity, and extinction metrics essential for analysis of mass biotic crisis events: An example from cretaceous ammonoidea N89-21304
Deccan volcanism at the Cretaceous-Tertiary boundary N89-21305
Abrupt climate change and extinction events N89-21308
Explosive volcanism, shock metamorphism and the K-T boundary N89-21309
An extended Cretaceous-Tertiary (K/T) stable isotope record. Implications for paleoclimate and the nature of the K/T boundary event N89-21310
Rocks, resolution, and the record at the terrestrial K/T boundary, eastern Montana and western North Dakota N89-21313
The Frasnian-Famennian mass killing event(s), methods of identification and evaluation N89-21318
Evidence for a single impact at the Cretaceous-Tertiary boundary from trace elements N89-21319
Nitrogen geochemistry of a Cretaceous-Tertiary boundary site in New Zealand N89-21320
The global Cretaceous-Tertiary fire: Biomass or fossil carbon N89-21321
Late Eocene impact events recorded in deep-sea sediments N89-21322
Mineralogy and phase-chemistry of the Cretaceous/Tertiary section in the Lattengebirge, Bavarian Alps N89-21323
The end-triassic mass extinction event N89-21324
Diachronism between extinction time of terrestrial and marine dinosaurs N89-21325
The Manson impact structure, a possible site for a Cretaceous-Tertiary (K-T) boundary impact N89-21326
How many upper Eocene microspherule layers: More than we thought N89-21327
High resolution chronology of late Cretaceous-early Tertiary events determined from 21,000 yr orbital-climatic cycles in marine sediments N89-21328
Selective extinction of marine plankton at the end of the Mesozoic era: The fossil and stable isotope record N89-21329
Impact wave deposits provide new constraints on the location of the K/T boundary impact N89-21330
Provenance of the K/T boundary layers N89-21331
Strangelove ocean at era boundaries, terrestrial or extraterrestrial cause N89-21332
Iridium, shocked minerals, and trace elements across the Cretaceous/Tertiary boundary at Maud Rise, Wedell Sea, and Walvis Ridge, South Atlantic Ocean N89-21333
The Western North American Cretaceous-Tertiary (K-T) boundary interval and its content of shock-metamorphosed minerals: Implications concerning the K-T boundary impact-extinction theory N89-21334
Mass mortality and extraterrestrial impacts N89-21335
Patterns of megafloral change across the Cretaceous-Tertiary boundary in the Northern Great Plains and Rocky Mountains N89-21336
Extended period of K/T boundary mass extinction in the marine realm N89-21337
Faunal and erosional events in the Eastern Tethyan Sea across the K/T boundary N89-21338
Widespread habitat change through paludification as an interactive mechanism in mass extinction events N89-21339
Volcanic ash layers in blue ice fields (Beardmore Glacier Area, Antarctica): Iridium enrichments N89-21340
The Kara and Ust-Kara impact structures (USSR) and their relevance to the K/T boundary event N89-21341
Isotopic investigations in the area of the Tunguska catastrophe in 1908 year N89-21342
The Karskiy craters are the probable records of catastrophe at the Cretaceous-Tertiary boundary N89-21343
Accretion rate of extraterrestrial matter: Iridium deposited over the last 70 million years N89-21344
The Cretaceous-Tertiary boundary biotic crisis in the Basque country N89-21345
Catastrophic volcanism N89-21346
Catastrophic volcanism as a cause of shocked features found at the K/T boundary and in cryptoexplosion structures N89-21347
Evidence for and implications of an Early Archean terrestrial impact record N89-21348
Magnetic reversal spurts: Rain gauges for comet showers N89-21349
Seawater strontium isotopes at the Cretaceous-Tertiary boundary N89-21350
Inducement of heterochronic variation in a species of planktic foraminifera by a Late Eocene impact event N89-21351
Trace element and isotope geochemistry of Cretaceous-Tertiary boundary sediments: identification of extra-terrestrial and volcanic components N89-21352
Step-wise extinctions at the Cretaceous-Tertiary boundary and their climatic implications N89-21354
Shatter cones: Diagnostic impact signatures N89-21355
Earth orbital variations and vertebrate bioevolution N89-21357
Mineralogical and geochemical anomalous data of the K-T boundary samples N89-21359
Flood basalts and mass extinctions N89-21360
Astrophysical implications of periodicity N89-21361
Deccan volcanism and K-T boundary signatures N89-21362
Plant microfossil record of the terminal Cretaceous event in the western United States and Canada N89-21363
Cretaceous-Tertiary findings, paradigms and problems N89-21364
Environmental effects of large impacts on the earth; relation to extinction mechanisms N89-21365
The Triassic-Jurassic boundary in eastern North America N89-21366
Permo-Triassic vertebrate extinctions: A program N89-21367
Iridium abundance measurements across bio-event horizons in the geological record N89-21368
Cathodoluminescence of shocked quartz at the Cretaceous-Tertiary boundary N89-21369
Bio-, Magneto- and event-stratigraphy across the K-T boundary N89-21370
Biospheric traumas caused by large impacts and predicted relics in the sedimentary record N89-21371
Flood basalt eruptions, comet showers, and mass extinction events N89-21372
Climatic changes resulting from mass extinctions at the K-T boundary (and other bio-events) N89-21373
Impact as a general cause of extinction: A feasibility test N89-21374
Report on an international workshop on Cryptoexplosions and Catastrophes in the Geological Record, with a Special Focus on the Vredefort Structure N89-21375
Microdeformation in Vredefort rocks; evidence for shock metamorphism N89-21376
Dynamics of exploding magma chambers: Implications for K-T volcanism and mass extinctions N89-21377
Search for the Tunguska event in the Antarctic snow N89-21378
Late Frasnian mass extinction: Conodont event stratigraphy, global changes, and possible causes N89-21380
Marine and continental K-T boundary clays compared N89-21382
Oblique impacts: Catastrophic vs. protracted effects N89-21383
Non-random cratering flux in recent time N89-21384
Periodicity of extinction: A 1988 update N89-21385
K-T impact(s): Continental, oceanic or both N89-21386
Asteroid and comet flux in the neighborhood of the earth N89-21387
Volcanoes and global catastrophes N89-21389
Biostratigraphic case studies of six major extinctions N89-21390
Impact and extinction signatures in complete Cretaceous-Tertiary (K-T) boundary sections N89-21391
Cretaceous-Tertiary boundary in the Antarctic: Climatic cooling precedes biotic crisis N89-21392
Some volcanologic aspects of Columbia River basalt volcanism relevant to the extinction controversy N89-21393
A regional perspective on the palynofloral response to K-T boundary event(s) with emphasis on variations imposed by the effects of sedimentary facies and latitude N89-21395
Geochemical comparison of K-T boundaries from the Northern and Southern Hemispheres N89-21400
The causes for geographical variations in OS187/OS186 at the Cretaceous-Tertiary boundary N89-21402
Macrofossil extinction patterns at Bay of Biscay Cretaceous-Tertiary boundary sections N89-21404
Evidence of volcanic ash at a K-T boundary section: Ocean drilling program hole 690 C, Maud Rise, Weddell Sea off East Antarctica N89-21410
Darkness after the K-T impact: Effects of soot N89-21411
The Cretaceous-Tertiary boundary marine extinction and global primary productivity collapse N89-21412
New approach to the origin of the tektite in China N89-21414

GEODESY

Relationships of earthquakes (and earthquake-associated mass movements) and polar motion as determined by Kalman filtered, Very-Long-Baseline-Interferometry [NASA-TM-100711] N89-21430
Downward continuation of the free-air gravity anomalies to the ellipsoid using the gradient solution, Poisson's integral and terrain correction-numerical comparison and computations [AD-A203739] N89-21442

GEODYNAMICS

Deccan volcanism at the Cretaceous-Tertiary boundary N89-21305
The interpretation of crustal dynamics data in terms of plate motions and regional deformation near plate boundaries [NASA-CR-180077] N89-21436

GEOGRAPHY

Multi-year global climatic effects of atmospheric dust from large bolide impacts N89-21397

GEOLOGICAL FAULTS

Impact, and its implications for geology N89-21353
The Calvin 28 cryptoexplosive disturbance, Cass County, Michigan: Evidence for impact origin N89-21358
Neotectonics in Central Mexico from LANDSAT TM data [NASA-CR-183416] N89-21416

GEOLOGY

Rocks, resolution, and the record at the terrestrial K/T boundary, eastern Montana and western North Dakota N89-21313
Volcanism, global catastrophe and mass mortality N89-21316
Geological remote sensing signatures of terrestrial impact craters N89-21317
Impact, and its implications for geology N89-21353
Bio-, Magneto- and event-stratigraphy across the K-T boundary N89-21370
Collisions with ice-volatile objects: Geological implications N89-21409

GEOMAGNETISM

Geomagnetic field energy as a source of thrust [AD-A202567] N89-21027

GEOMETRICAL OPTICS

A rapid-backscatter simulation technique for complex B-spline target models N89-21505

GEOMORPHOLOGY

Permo-Triassic vertebrate extinctions: A program N89-21367

GEOPHYSICS

The Sudbury Structure (Ontario, Canada) and Vredefort Structure (South Africa): A comparison N89-21311
Geological remote sensing signatures of terrestrial impact craters N89-21317
The Calvin 28 cryptoexplosive disturbance, Cass County, Michigan: Evidence for impact origin N89-21358
Astrophysical implications of periodicity N89-21361

Deccan volcanism and K-T boundary signatures N89-21362
Relationships of earthquakes (and earthquake-associated mass movements) and polar motion as determined by Kalman filtered, Very-Long-Baseline-Interferometry [NASA-TM-100711] N89-21430
Solar-geophysical data number 529, September 1988. Part 1: (Prompt reports). Data for August, July 1988 and late data [PB89-121305] N89-21431
Solar-geophysical data number 529, September 1988. Part 2: (Comprehensive reports). Data for March 1988 [PB89-121313] N89-21432
Enhancements to the AFGL (Air Force Geophysics Laboratory) Statistical Analysis Program (ASAP) for the global multivariate analysis of heights and winds [AD-A202912] N89-21450
Solar-geophysical data number 528, August 1988. Part 2: (Comprehensive reports). Data for February 1988 [PB89-109912] N89-21722

GEOPOTENTIAL
Hypersurface insertion window for long term orbital stability of artificial satellites about the planet Venus [AD-A202808] N89-21009

GEOTHERMAL ENERGY CONVERSION
Geothermal energy program summary: Volume 1: Overview Fiscal Year 1988 [DE89-000864] N89-21422

GEOTHERMAL ENERGY EXTRACTION
Geothermal energy program summary: Volume 1: Overview Fiscal Year 1988 [DE89-000864] N89-21422

GEOTHERMAL RESOURCES
Geothermal energy program summary: Volume 1: Overview Fiscal Year 1988 [DE89-000864] N89-21422

GEOTHERMAL TECHNOLOGY
Geothermal energy program summary: Volume 1: Overview Fiscal Year 1988 [DE89-000864] N89-21422

GERMANIDES
Low temperature properties of ternary magnetic rare earth transition metal germanides with the Sc5Co4Ge10-type structure [DE89-007628] N89-21666

GIMBALS
Low-cost Pointing-and-Tracking System for Optical Communications (PATSOC) [AD-A202921] N89-21151

GLACIAL DRIFT
Volcanic ash layers in blue ice fields (Beardmore Glacier Area, Antarctica): Iridium enrichments N89-21340
Late Frasnian mass extinction: Conodont event stratigraphy, global changes, and possible causes N89-21380

GLASS
Investigation of the impact performance of various glass and ceramic systems [AD-A202443] N89-21106
Surface chemistry and structural effects in the stress corrosion of glass and ceramic materials [AD-A202452] N89-21107
Polycarbonate ophthalmic lenses for ametropic Army aviators using night vision goggles [AD-A203100] N89-21488
Dynamic fatigue testing of Zerodur glass-ceramic N89-21753

GLASS FIBER REINFORCED PLASTICS
Evaluation of atomic oxygen resistant protective coatings for fiberglass-epoxy composites in LEO [NASA-TM-101955] N89-21100

GLOBAL POSITIONING SYSTEM
On principles, methods and recent advances in studies towards a GPS-based control system for geodesy and geodynamics [NASA-TM-100716] N89-21434

GLOBULAR CLUSTERS
The evolution of active galactic nuclei and globular clusters: Multi-component models N89-21720

GLOW DISCHARGES
Study of the generation of intense pulsed electron beams using glow discharges [AD-A202438] N89-21624

GLUONS
Surface energy from order parameter profile: At the QCD phase transition [NASA-CR-184890] N89-21633

GOGGLES
Helicopter flights with night-vision goggles: Human factors aspects [NASA-TM-101039] N89-21477
Polycarbonate ophthalmic lenses for ametropic Army aviators using night vision goggles [AD-A203100] N89-21488

GOLD
Noble metals in mid-ocean ridge volcanism: A significant fractionation of gold with respect to platinum group metals N89-21307

GOVERNMENT PROCUREMENT
Incorporating five nations' operational requirements into a single aircraft: The F-16 multinational fighter program viewed from the operational side [AD-A202552] N89-20986

GRAIN BOUNDARIES
Hydrogen segregation to grain boundaries and external surfaces [AD-A202892] N89-21084
The microstructural and phase characterization of RST Al-Ti-X alloys [AD-A203734] N89-21092
Grain boundary kinetics. 1: In-situ observations of coupled grain boundary dislocation motion, crystal translation and boundary displacement [DE89-006790] N89-21665
Atomistic simulations of interfaces in metals and alloys [DE89-006521] N89-21685

GRAMMARS
Domain modeling for language analysis [AD-A203444] N89-21574

GRAPH THEORY
Grasp: A graph specification language [AD-A202524] N89-21550
Eigenvectors of graphs [AD-A203317] N89-21609

GRAPHIC ARTS
A decision-based methodology for object oriented-design [AD-A202579] N89-21558
Dynamic analysis of feedforward neural networks using simulated and measured data [AD-A202573] N89-21591

GRAPHITE
High temperature composites using Schiff's base pyropolymer matrices [AD-A203311] N89-21043

GRAPHITE-EPOXY COMPOSITES
Effect of geometry on thermal aging behavior of Celion/LARC-160 composites [NASA-TM-100496] N89-21047

GRATINGS (SPECTRA)
Fast acting optical beam deflection system [AD-A203042] N89-21648
A theoretical and experimental investigation of linear and nonlinear focussing chirped optical diffraction gratings [AD-A203396] N89-21650

GRAVITATION THEORY
Experimentally verifiable Yang-Mills spin 2 gauge theory of gravity with group U(1) x SU(2) N89-21693

GRAVITATIONAL EFFECTS
Techniques for studying the effects of microgravity on model particle/cell systems N89-21758

GRAVITATIONAL FIELDS
Proterozoic Bushveld-Vredefort catastrophe: Possible causes and consequences N89-21312

GRAVITATIONAL WAVES
A search for gravitational waves from coalesing binary stars using the Caltech 40 meter gravity wave detector N89-21721

GRAVITY ANOMALIES
Geological indicators for impact: The anomalous case of the Vredefort structure, South Africa N89-21289
Downward continuation of the free-air gravity anomalies to the ellipsoid using the gradient solution, Poisson's integral and terrain correction-numerical comparison and computations [AD-A203739] N89-21442

GRAZING INCIDENCE
An in-situ grazing incidence X-ray scattering study of the initial stages of electrochemical growth of lead on silver (III) [AD-A203385] N89-21064

GREEN'S FUNCTIONS
Time domain wave propagation in multilayered integrated circuits [AD-A202427] N89-21175

GREENHOUSE EFFECT
Carbon dioxide catastrophes: Past and future menace N89-21293
Air quality and forest health issues in the 1990s [DE89-006941] N89-21427
National Climate Program [PB89-118608] N89-21445

GRID GENERATION (MATHEMATICS)
Transonic Symposium: Theory, Application, and Experiment, Volume 1, Part 1 [NASA-CP-3020-VOL-1-PT-1] N89-20925
Euler solvers for transonic applications N89-20935
Developments and trends in three-dimensional mesh generation N89-20940
Generation of unstructured grids and Euler solutions for complex geometries N89-20941
Transonic Symposium: Theory, Application, and Experiment, volume 1, part 2 [NASA-CP-3020-VOL-1-PT-2] N89-20942
Transonic propulsion system integration analysis at McDonnell Aircraft Company N89-20943
Method to predict external store carriage loads at transonic speeds N89-20945

GROUND RESONANCE
Nonlinear rotorcraft analysis-experimental and analytical [AD-A203967] N89-20990

GROUND STATE
Theoretical studies of rare gas halide systems [AD-A203985] N89-21068
Measurement of ground state copper density using hook spectroscopy [DE89-005098] N89-21093

GROUND STATIONS
The use of chaff in space as a jamming device between ground stations and satellites [AD-A202577] N89-21146

GROUP THEORY
The solution of the type-problem for N less than or equal to 4 N89-21528
The GL(2n-1,R) spherical representations of SL(2n,R) [ZW-8802] N89-21621

GUN PROPELLANTS
Density of triethanolammonium nitrate and liquid propellant [AD-A203767] N89-21131

H

HABITATS
Widespread habitat change through paludification as an interactive mechanism in mass extinction events N89-21339
Effects of global atmospheric perturbations on forest ecosystems: Predictions of seasonal and cumulative effects N89-21399

HADRONS
Surface energy from order parameter profile: At the QCD phase transition [NASA-CR-184890] N89-21633

HAIL
A 3-dimensional numerical simulation of the atmospheric injection of aerosols by a hypothetical basaltic fissure eruption N89-21401

HALIDES
Theoretical studies of rare gas halide systems [AD-A203985] N89-21068

HALL EFFECT
MBE of (Hg,Cd)Te [AD-A202448] N89-21667

HALOGEN COMPOUNDS
The spectroscopy and energy transfer kinetics of the interhalogens [AD-A202954] N89-21059

HANDBOOKS
Measurer's handbook: US Army anthropometric survey, 1987-1988 [AD-A202721] N89-21484

HARMONIC OSCILLATORS
Lie transforms applied to a nonlinear parametric excitation problem N89-21491

HARMONICS
Subharmonic and fundamental high amplitude excitation of an axisymmetric jet [NASA-TM-101946] N89-20920
Microwave power amplifier analysis and design [AD-A203170] N89-21182
Downward continuation of the free-air gravity anomalies to the ellipsoid using the gradient solution, Poisson's integral and terrain correction-numerical comparison and computations [AD-A203739] N89-21442

HARRIER AIRCRAFT
Computer simulation of a pilot in V/STOL aircraft control loops [NASA-CR-184815] N89-21479

HAZARDS
AH-1S communication switch integration program [NASA-TM-101053] N89-20978
Contamination of the exterior of a C-130E aircraft used for aerial spray, 907 TAG, Rickenbacker ANGB, OH [AD-A202430] N89-20984
Space Propulsion Hazards Analysis Manual (SPHAM), volume 1 [AD-A203204] N89-21029
Risk to civilization: A planetary science perspective N89-21302

Helicopter flights with night-vision goggles: Human factors aspects
[NASA-TM-101039] N89-21477
Software system safety N89-21754
HEAD (ANATOMY)
SPH-4 US Army flight helmet performance 1983-1987
[AD-A202589] N89-21482
HEART RATE
LMS adaptive filtering applied to a microwave arterial pulse monitor
[AD-A202732] N89-21465
HEAT EXCHANGERS
Thermal and dynamic analysis of the RING (Radiatively-cooled, Inertially-driven Nuclear Generator) power system radiator
[DE89-007236] N89-21639
HEAT FLUX
A numerical study of the turbulent free convection in rectangular cavities N89-21194
HEAT PIPES
High capacity demonstration of honeycomb panel heat pipes
[NASA-CR-181776] N89-21191
Incompressible flow friction coefficients in a simulated heat pipe
[AD-A203176] N89-21207
HEAT RESISTANT ALLOYS
Advanced single crystal for SSME turbopumps
[NASA-CR-182244] N89-21072
Synthesis processing of high-lithium Al-Li alloys
[AD-A203401] N89-21088
Deformation modeling and constitutive modeling for anisotropic superalloys
[NASA-CR-4215] N89-21258
Macrocrack-multiple defect interaction considering elastic, plastic and viscoplastic effects
[AD-A203186] N89-21282
HEAT TRANSFER
Three dimensional thermal analysis of rocket thrust chambers
[NASA-TM-101973] N89-21025
A model for interface temperatures induced by convection heat transfer in porous materials
[DE89-008202] N89-21214
Thermomechanical analysis with phase transformations: A unified approach
[AD-A203383] N89-21692
The role of the turbulent Prandtl number in turbine blade heat transfer prediction N89-21756
HEAT TREATMENT
High temperature composites using Schiff's base pyropolymer matrices
[AD-A203311] N89-21043
The effects of loading history and closure of the fatigue characteristics of heat treated Ti-6Al-2Sn-4Zr-6Mo
[AD-A202652] N89-21082
Synthesis processing of high-lithium Al-Li alloys
[AD-A203401] N89-21088
Advanced tribological coatings for high specific strength alloys
[AD-A202505] N89-21110
HEATERS
Reentry response of the light weight radioisotope heater unit resulting from a Venus-Earth-Earth gravity assist maneuver accident
[DE89-005359] N89-21024
HEATING
The Manson impact structure, a possible site for a Cretaceous-Tertiary (K-T) boundary impact N89-21326
HEIGHT
Enhancements to the AFGL (Air Force Geophysics Laboratory) Statistical Analysis Program (ASAP) for the global multivariate analysis of heights and winds
[AD-A202912] N89-21450
HELICOPTER PERFORMANCE
Nonlinear rotorcraft analysis-experimental and analytical
[AD-A203967] N89-20990
HELICOPTER WAKES
Performance optimization for rotors in hover and axial flight
[NASA-CR-177524] N89-20973
HELICOPTERS
Performance optimization for rotors in hover and axial flight
[NASA-CR-177524] N89-20973
Integrated aerodynamic/dynamic optimization of helicopter rotor blades
[NASA-TM-101553] N89-20982
Heliport system planning guidelines
[AD-A199081] N89-21003
DATAMAP upgrade version 4.0
[NASA-TM-100993] N89-21541
HELIOSEISMOLOGY
New picture for the internal rotation of the sun
[PB89-113377] N89-21723
HELIPORTS
Heliport system planning guidelines
[AD-A199081] N89-21003
HELIUM
Molecular jet studies of vdW (van der Waals) clusters and solvation
[AD-A203766] N89-21212
Advanced helium purge seals for Liquid Oxygen (LOX) turbopumps
[NASA-CR-182105] N89-21239
Study of the generation of intense pulsed electron beams using glow discharges
[AD-A202438] N89-21624
HELIUM ISOTOPES
Half-solitons in superfluid (3)He-A: Novel pi/2-quanta of phase slippage
[PB89-128904] N89-21664
HELMET MOUNTED DISPLAYS
Real-time display of time dependent data using a head-mounted display
[AD-A203051] N89-20993
A helmet-mounted virtual environment display system
[AD-A203055] N89-20994
The impact of the US Army's AH-64 helmet mounted display on future aviation helmet design
[AD-A202984] N89-21486
HELMETS
SPH-4 US Army flight helmet performance 1983-1987
[AD-A202589] N89-21482
The impact of the US Army's AH-64 helmet mounted display on future aviation helmet design
[AD-A202984] N89-21486
HETERODYNING
Demonstration of SQUID parametric amplifier
[AD-A203252] N89-21183
HETEROGENEITY
Theoretical studies of heterogeneous reactions in silicon CVD (Silicon Vapor Deposition) catalysis
[AD-A202905] N89-21057
Magnetic properties of nano-heterogeneous amorphous, thin films
[AD-A203727] N89-21680
HETEROJUNCTION DEVICES
Development of gallium arsenide high-speed, low-power serial parallel interface modules: Executive summary
[NASA-CR-182272] N89-21173
HETEROJUNCTIONS
MBE of (Hg,Cd)Te
[AD-A202448] N89-21667
HIERARCHIES
A software system to create a hierarchical, multiple level of detail terrain model
[AD-A203047] N89-21568
Development of the domain name system
[AD-A203901] N89-21703
HIGH ACCELERATION
A cryocooler for high acceleration applications
[AD-A203063] N89-21137
HIGH ALTITUDE BALLOONS
Fracture characteristics of balloon films
[NASA-CR-181686] N89-21099
HIGH ALTITUDE ENVIRONMENTS
Icing considerations for HALE (High Altitude, Long Endurance) aircraft
[AD-A202584] N89-20975
HIGH ENERGY INTERACTIONS
Theoretical studies of rare gas halide systems
[AD-A203985] N89-21068
HIGH FREQUENCIES
Frequency dependent ultrasonic ray tracing: A preliminary study
[AERE-R-13119] N89-21139
HIGH POWER LASERS
A laser trap for neutral atoms
[AD-A202581] N89-21229
HIGH PRESSURE
A performance/loss evaluation of SSME HPFTP turbine N89-21735
HIGH RESOLUTION
High resolution chronology of late Cretaceous-early Tertiary events determined from 21,000 yr orbital-climatic cycles in marine sediments N89-21328
New techniques for high-resolution optical space surveillance
[AD-A202785] N89-21647
HIGH SPEED CAMERAS
A study of failure characteristics in a thermoplastic composite material at high temperature
[AD-A203015] N89-21040
HIGH STRENGTH ALLOYS
Advanced tribological coatings for high specific strength alloys
[AD-A202505] N89-21110
HIGH TEMPERATURE
Improved high-temperature resistant matrix resins
[NASA-CR-180826] N89-21105
HIGH TEMPERATURE FLUIDS
Fuel-rich catalytic combustion of Jet-A fuel-equivalence ratios 5.0 to 8.0
[NASA-TM-101975] N89-21051
HIGH TEMPERATURE PROPELLANTS
Effective ignition kinetics for LOVA propellant
[AD-A203149] N89-21129
HIGH TEMPERATURE SUPERCONDUCTORS
High-temperature ceramic superconductors
[AD-A202867] N89-21674
Central research project report on superconductivity (1988). Part 1: Materials and IR detectors
[AD-A203891] N89-21681
An in-situ, high-temperature study of the superconductor YBa1.67Sr0.33Cu3O(6+x)
[DE89-007375] N89-21686
Fermi liquid theory for high temperature superconductors
[DE89-007982] N89-21688
HIGH TEMPERATURE TESTS
Static tensile and tensile creep testing of five ceramic fibers at elevated temperatures
[NASA-CR-177525] N89-21046
HILBERT SPACE
The GL(2n-1,R) spherical representations of SL(2n,R)
[ZW-8802] N89-21621
HINGES
Stabilization of Ziegler's pendulum by means of the method of vibrational control N89-21531
HISTORIES
Strategic defense initiative: A chronology, 1983 - 1988
[AD-A203576] N89-21619
HOLLOW CATHODES
Space plasma contractor research, 1988
[NASA-CR-182283] N89-21658
HOLOGRAPHIC INTERFEROMETRY
Effects of battle damage repair on the natural frequencies and mode shapes of curved rectangular composite panels
[AD-A203179] N89-21041
HOLOGRAPHY
Holographic particle sizing in solid fuel ramjets
[AD-A202699] N89-20997
Automatic measurement of particles from holograms taken in the combustion chamber of a rocket motor
[AD-A203955] N89-21030
Holographic investigation of solid propellant combustion
[AD-A203928] N89-21067
A position, scale and rotation invariant holographic associative memory
[AD-A203289] N89-21221
HONEYCOMB STRUCTURES
High capacity demonstration of honeycomb panel heat pipes
[NASA-CR-181776] N89-21191
HOT CORROSION
High temperature oxidation and electrochemical studies related to hot corrosion
[AD-A203038] N89-21085
HOVERING
Performance optimization for rotors in hover and axial flight
[NASA-CR-177524] N89-20973
HUBS
Integrated aerodynamic/dynamic optimization of helicopter rotor blades
[NASA-TM-101553] N89-20982
HUMAN BEINGS
Seeing Ghost solutions in stereo vision
[AD-A203581] N89-21473
Acquiring generalizations to organize human databases
[AD-A202964] N89-21702
HUMAN FACTORS ENGINEERING
Helicopter flights with night-vision goggles: Human factors aspects
[NASA-TM-101039] N89-21477
Capacity of human operator using smart stick controller
[AD-A202712] N89-21483
Measurer's handbook: US Army anthropometric survey, 1987-1988
[AD-A202721] N89-21484
The impact of the US Army's AH-64 helmet mounted display on future aviation helmet design
[AD-A202984] N89-21486
Empirical demonstration of isoperformance methodology preparatory of an interactive expert computerized decision aid
[AD-A202439] N89-21545
HUMAN PERFORMANCE
Review and analysis of the literature in the area of human performance modeling
[DE89-006800] N89-21480

HUMIDITY
Corrosion control climatology
[AD-A202477] N89-21079
HYDRAULIC EQUIPMENT
A simple analysis of swage autofrettage process N89-21498
HYDROCARBON FUELS
CRC (Coordinating Research Council) hot-start and driveaway driveability program at high and intermediate temperatures using gasoline-alcohol blends
[AD-A202471] N89-21126
HYDROCARBONS
Fluids, both ionic and nonionic, over wide ranges of temperature and composition
[DE89-001265] N89-21048
Gas turbine alternative fuels combustion characteristics
[NASA-TM-101470] N89-21417
HYDRODYNAMIC EQUATIONS
Sounds in one-dimensional superfluid helium
[AD-A202428] N89-21629
HYDRODYNAMICS
Imaging of ocean waves by SAR
[AD-A203604] N89-21165
Computer modeling and simulation in inertial confinement fusion
[DE89-008304] N89-21661
HYDROGEN
Nuclear magnetic resonance study of hydrogen in niobium-vanadium alloys
[DE89-007578] N89-21075
Hydrogen and deuterium internal friction behavior in vanadium-niobium alloys
[DE89-007616] N89-21078
Hydrogen segregation to grain boundaries and external surfaces
[AD-A202892] N89-21084
HYDROGEN ISOTOPES
Hydrogen segregation to grain boundaries and external surfaces
[AD-A202892] N89-21084
HYDROGEN OXYGEN FUEL CELLS
Cryogenic reactant storage for lunar base regenerative fuel cells
[NASA-TM-101980] N89-21419
HYDROLOGICAL CYCLE
Flux and sounding data from the NCAR (National Center for Atmospheric Research) King Air aircraft during HAPEX (hydrologic atmospheric pilot experiment)
[PB89-124481] N89-21433
HYPERCUBE MULTIPROCESSORS
Distributed discrete-event simulation using variants of the Chandy-Misra algorithm on the intel hypercube
[AD-A202849] N89-21563
HYPERSONIC BOUNDARY LAYER
Investigation of the development of laminar boundary-layer instabilities along a cooled-wall cone in hypersonic flows
[AD-A202587] N89-20966
Investigation of the development of laminar boundary-layer instabilities along a blunted cone
[AD-A202425] N89-21200
HYPERSONIC FLOW
A review of reaction rates and thermodynamic and transport properties for the 11-species air model for chemical and thermal nonequilibrium calculations to 30000 K
[NASA-TM-101528] N89-21193
Influence of reflected shock waves on a hypersonic shaped charge jet N89-21522
HYPERSONIC VEHICLES
Hypersonic drone design: A multidisciplinary experience
[NASA-CR-184740] N89-20981
HYPERVELOCITY PROJECTILES
Oblique hypervelocity impact response of dual-sheet structures
[NASA-TM-100358] N89-21246
Further investigations of oblique hypervelocity impact phenomena N89-21750
HYPOTHESES
Optimal and robust memoryless discrimination from dependent observations
[AD-A202806] N89-21604
The interdependencies of theory formation, revision, and experimentation
[AD-A202882] N89-21618

I

ICE
Numerical simulation of flow over iced airfoils
[AD-A203291] N89-20969
Volcanic ash layers in blue ice fields (Beardmore Glacier Area, Antarctica): Iridium enrichments N89-21340
Collisions with ice-volatile objects: Geological implications N89-21409
Ice cover on Chesapeake Bay from AVHRR (Advanced Very High Resolution Radiometer) and LANDSAT imagery, winter of 1987-88
[PB89-117261] N89-21415
ICE FORMATION
Icing considerations for HALE (High Altitude, Long Endurance) aircraft
[AD-A202584] N89-20975
Ice cover on Chesapeake Bay from AVHRR (Advanced Very High Resolution Radiometer) and LANDSAT imagery, winter of 1987-88
[PB89-117261] N89-21415
Simulation of water vapor condensation on LOX droplet surface using liquid nitrogen N89-21749
ICE MAPPING
Ice cover on Chesapeake Bay from AVHRR (Advanced Very High Resolution Radiometer) and LANDSAT imagery, winter of 1987-88
[PB89-117261] N89-21415
IDENTIFYING
Modern multiple-pulse, high field NMR studies of high density jet fuels
[AD-A203320] N89-21130
Seeing Ghost solutions in stereo vision
[AD-A203581] N89-21473
IGNITION
The effect of platinum catalysts on propane oxidation at elevated pressure
[AD-A202999] N89-21060
Deformation, fracture and explosive properties of reactive materials
[AD-A203083] N89-21128
Effect of TNT miscible additives on the mechanical behavior and shock sensitivity of Composition B
[AD-A203968] N89-21132
IMAGE CORRELATORS
Multiple model adaptive tracking of airborne targets
[AD-A202696] N89-21148
IMAGE FILTERS
Multiple model adaptive tracking of airborne targets
[AD-A202696] N89-21148
Dynamic analysis of feedforward neural networks using simulated and measured data
[AD-A202573] N89-21591
An optimal scale for edge detection
[AD-A202747] N89-21646
IMAGE PROCESSING
Computer strategy for detecting line features on simulated binary arrays in support of radar feature extraction
[AD-A203257] N89-21162
Whole field measurements of vorticity in turbulent and unsteady flows
[AD-A203349] N89-21209
Correction of gain and optical throughput variations in a two-dimensional imaging spectrometer
[AD-A203495] N89-21222
Model-based silhouette recognition
[AD-A202540] N89-21552
A vectorized hidden-surface algorithm implemented on the Cray-2 supercomputer
[AD-A202657] N89-21560
Image processing language, phase 2
[AD-A203994] N89-21577
An optimal scale for edge detection
[AD-A202747] N89-21646
New techniques for high-resolution optical space surveillance
[AD-A202785] N89-21647
Computer-aided X-ray imaging system design and evaluation
[DE89-006599] N89-21653
IMAGE RESOLUTION
Holographic particle sizing in solid fuel ramjets
[AD-A202699] N89-20997
Superresolved imaging using the Hartley transform and a hemispherical object space
[AD-A202527] N89-21551
Model-based silhouette recognition
[AD-A202540] N89-21552
IMAGERY
Geological remote sensing signatures of terrestrial impact craters N89-21317
IMAGES
Volumetric rendering techniques for the display of three-dimensional aerodynamic flow field data
[AD-A202661] N89-21204
Correction of gain and optical throughput variations in a two-dimensional imaging spectrometer
[AD-A203495] N89-21222
Psychophysical studies of visual cortical functions
[AD-A202814] N89-21468
A vectorized hidden-surface algorithm implemented on the Cray-2 supercomputer
[AD-A202657] N89-21560
Optical activity and its influence on photorefractive materials
[AD-A202530] N89-21642
IMAGING SPECTROMETERS
Correction of gain and optical throughput variations in a two-dimensional imaging spectrometer
[AD-A203495] N89-21222
IMAGING TECHNIQUES
Acoustic microscopy of low ductility materials
[AERE-R-12848] N89-21101
Imaging of ocean waves by SAR
[AD-A203604] N89-21165
Adapting Schottky diode detector technology to a space platform
[AD-A202825] N89-21219
Superresolved imaging using the Hartley transform and a hemispherical object space
[AD-A202527] N89-21551
Extracting shape reflectance of Lambertian, specular, and hybrid surfaces
[AD-A203772] N89-21652
IMMUNOASSAY
Development and characterization of a fiber optic immuno biosensor
[DE89-005062] N89-21225
Immunoassay procedures for fiber optic sensors
[AD-A203069] N89-21649
IMPACT
Multi-year global climatic effects of atmospheric dust from large bolide impacts N89-21397
IMPACT DAMAGE
Further investigations of oblique hypervelocity impact phenomena N89-21750
IMPACT LOADS
The behavior of ceramic matrix, fiber composites under combined impact and tensile stresses
[AD-A202518] N89-21038
Deformation, fracture and explosive properties of reactive materials
[AD-A203083] N89-21128
IMPACT MELTS
The Kara and Ust-Kara impact structures (USSR) and their relevance to the K/T boundary event N89-21341
IMPACT PREDICTION
Artificial asteroid impact on defensive satellites
[DE89-008407] N89-21620
IMPACT TESTS
The behavior of ceramic matrix, fiber composites under combined impact and tensile stresses
[AD-A202518] N89-21038
Investigation of the impact performance of various glass and ceramic systems
[AD-A202443] N89-21106
IMPACTORS
Acute effects of a large bolide impact simulated by a global atmospheric circulation model N89-21398
IMPURITIES
Electron paramagnetic resonance and photoluminescence studies of impurities in CdTe
[AD-A202841] N89-21056
IN-FLIGHT MONITORING
In-flight lightning characterization program on a CV-580 aircraft
[AD-A203954] N89-20976
INCOHERENT SCATTERING
Evaluation of the spatial and temporal characteristics of the conducting PRIZ
[AD-A202593] N89-21671
INCOMPRESSIBLE FLOW
Incompressible flow friction coefficients in a simulated heat pipe
[AD-A203176] N89-21207
Skew grids and irrotational flow N89-21523
INDENTATION
Film elastic properties determined by the indentation test-theoretical considerations
[AD-A203997] N89-21683
INDEXES (DOCUMENTATION)
Aerospace medicine and biology: A continuing bibliography with indexes (supplement 321)
[NASA-SP-7011(321)] N89-21475
Aerospace medicine and biology: A continuing bibliography with indexes (supplement 322)
[NASA-SP-7011(322)] N89-21476
INDIUM ANTIMONIDES
An analysis of platinum silicide and indium antimonide for remote sensors in the 3 to 5 micrometer wavelength band
[AD-A202663] N89-21218
The response of single element HgCdTe and InSb solid state infrared detectors to millimeter wave electromagnetic energy
[AD-A202667] N89-21672

INDIUM ARSENIDES
Investigation of a self-aligned, strained-channel,n sup(+)-In As/Al 0.5 As/In 0.15 Ga 0.85 As Semiconductor Insulator Semiconductor FET (SISFET)
[AD-A203147] N89-21676
INDIUM PHOSPHIDES
Investigation of Schottky barrier on GaAs and InP using a multidisciplined approach
[AD-A202953] N89-21675
INERTIAL CONFINEMENT FUSION
Computer modeling and simulation in inertial confinement fusion
[DE89-008304] N89-21661
INERTIAL NAVIGATION
A diagnostic system blending deep and shallow reasoning
[AD-A202547] N89-20979
Aircraft tracking with dual TACAN
[AD-A202647] N89-20980
INFERENCE
Confidence set inference with a prior quadratic bound
[NASA-CR-184839] N89-21435
Order statistics and robust inference
[AD-A203440] N89-21616
INFORMATION FLOW
Lockheed Aeronautical Systems Company technical order transfer tests
[DE89-008092] N89-21707
INFORMATION MANAGEMENT
Automated library systems and document tracking systems: Commercial software alternatives, volume 1
[DE89-007716] N89-21706
INFORMATION RETRIEVAL
Defense technical information center's role in numeric database development
[AD-A202901] N89-21701
Automated library systems and document tracking systems: Commercial software alternatives, volume 1
[DE89-007716] N89-21706
INFORMATION SYSTEMS
Advanced information processing system: Local system services
[NASA-CR-181767] N89-21582
Evaluation of the high temperature materials information analysis center online numeric database
[AD-A202900] N89-21700
Development of the domain name system
[AD-A203901] N89-21703
Scientific and Technical Information Network (STINET) and DOD Gateway Information System (DGIS): Reference publications bibliography
[AD-A203926] N89-21704
Automated library systems and document tracking systems: Commercial software alternatives, volume 1
[DE89-007716] N89-21706
Lockheed Aeronautical Systems Company technical order transfer tests
[DE89-008092] N89-21707
Refining, revising, augmenting, compiling and developing computer assisted instruction K-12 aerospace materials for implementation in NASA spacelink electronic information system N89-21729
INFORMATION THEORY
Response equivocation analysis for the smart stick controller
[AD-A203146] N89-20989
Information acquisition for model construction: An integrative, decision-theoretic perspective N89-21705
INFORMATION TRANSFER
Lockheed Aeronautical Systems Company technical order transfer tests
[DE89-008092] N89-21707
INFRARED DETECTORS
The response of single element HgCdTe and InSb solid state infrared detectors to millimeter wave electromagnetic energy
[AD-A202667] N89-21672
Central research project report on superconductivity (1988). Part 1: Materials and IR detectors
[AD-A203891] N89-21681
INFRARED IMAGERY
Infrared surface temperature measurements for the surface tension driven convection experiment
[NASA-TM-101353] N89-21224
Satellite signatures of rapid cyclogenesis
[AD-A203934] N89-21452
Infrared sea-radiance modeling using LOWTRAN 6
[AD-A202582] N89-21643
Modified backward error propagation for tactical target recognition
[AD-A202666] N89-21644
INFRARED SIGNATURES
Satellite signatures of rapid cyclogenesis
[AD-A203934] N89-21452
INGOTS
Computer simulation of macrosegregation in directionally solidified circular ingots
[NASA-CR-182838] N89-21134
INJECTION
A 3-dimensional numerical simulation of the atmospheric injection of aerosols by a hypothetical basaltic fissure eruption N89-21401
INPUT/OUTPUT ROUTINES
Thin-layer Navier-Stokes solutions for a cranked delta wing
[AD-A203292] N89-20970
Maintenance metrics for Jovial (J73) software
[AD-A202713] N89-21561
INSPECTION
Aviation safety: Measuring how safely individual airlines operate
[GAO/RCED-88-61] N89-20974
Nondestructive testing techniques for metal matrix composites
[AERE-R-13040] N89-21034
INSTRUCTORS
Refining, revising, augmenting, compiling and developing computer assisted instruction K-12 aerospace materials for implementation in NASA spacelink electronic information system N89-21729
INTEGRAL EQUATIONS
Time domain wave propagation in multilayered integrated circuits
[AD-A202427] N89-21175
Numerical study of three viscous/inviscid interaction methods
[AD-A202575] N89-21203
INTEGRALS
A rapid numerical procedure for determining axisymmetric transverse electric electromagnetic fields via boundary integrals
[AD-A202959] N89-21155
INTEGRATED CIRCUITS
External electro-optic probing of millimeter-wave integrated circuits
[NASA-TM-101990] N89-21142
Time domain wave propagation in multilayered integrated circuits
[AD-A202427] N89-21175
A multiple-valued logic system for circuit extraction to VHDL 1076-1987
[AD-A202646] N89-21177
Computer-aided fabrication system implementation
[AD-A203651] N89-21576
A diagnostic system using Boolean reasoning
[AD-A202764] N89-21602
INTELLECT
Coping with novelty and human intelligence: The role of counterfactual reasoning
[AD-A203624] N89-21478
INTELLIGENCE
Coping with novelty and human intelligence: The role of counterfactual reasoning
[AD-A203624] N89-21478
INTERACTIONAL AERODYNAMICS
Transonic Symposium: Theory, Application, and Experiment, volume 1, part 2
[NASA-CP-3020-VOL-1-PT-2] N89-20942
Inverse wing design in transonic flow including viscous interaction N89-20947
Navier-Stokes and viscous-inviscid interaction N89-20949
Turbulent eddy viscosity modeling in transonic shock/boundary-layer interactions N89-20952
An LDA (Laser-Doppler Anemometry) investigation of three-dimensional normal shock wave boundary-layer interactions N89-20956
INTERCEPTION
Remote orbital capture using an orbital maneuvering vehicle equipped with a multibody grappling arm assembly
[AD-A202760] N89-21018
INTERFACES
Performance analysis of the fiber distributed data interface in the super cockpit audio world
[AD-A202535] N89-20985
An investigation of viscoelastic fracture near and at interfaces
[AD-A203760] N89-21285
VAX to CRAY NASTRAN user interface
[AD-A203447] N89-21575
Atomistic simulations of interfaces in metals and alloys
[DE89-006521] N89-21685
SIRE: A Simple Interactive Rule Editor for NICBES N89-21730
INTERFACIAL TENSION
Infrared surface temperature measurements for the surface tension driven convection experiment
[NASA-TM-101353] N89-21224
INTERFERENCE GRATING
Peripheral limitations on spatial vision
[AD-A203388] N89-21472
Fast acting optical beam deflection system
[AD-A203042] N89-21648
INTERFEROMETRY
Three dimensional effects near a crack tip in a ductile three point bend specimen. Part 2: An experimental investigation using interferometry and caustics
[AD-A202637] N89-21272
INTERMETALLICS
Investigation of crack growth in titanium-aluminide at elevated temperatures
[AD-A202570] N89-21081
Shock-induced chemical synthesis of intermetallic compounds
[DE89-007035] N89-21095
INTERNAL COMBUSTION ENGINES
Knowledge representation and planning control in an expert system for the creative design of mechanisms N89-21492
INTERNAL FRICTION
Hydrogen and deuterium internal friction behavior in vanadium-niobium alloys
[DE89-007616] N89-21078
INTERNAL WAVES
OSRMS (Ocean Surface Roughness Measurement System): The DREP (Defence Research Establishment Pacific) near-nadir scatterometer
[AD-A202983] N89-21460
INTERPOLATION
Enhancements to the AFGL (Air Force Geophysics Laboratory) Statistical Analysis Program (ASAP) for the global multivariate analysis of heights and winds
[AD-A202912] N89-21450
Seeing Ghost solutions in stereo vision
[AD-A203581] N89-21473
Transactions of the Fifth Army Conference on Applied Mathematics and Computing
[AD-A193384] N89-21490
Algorithms for rational spline curves N89-21502
Convexity-preserving quasi-interpolation and interpolation by box spline surfaces N89-21503
INTERPROCESSOR COMMUNICATION
VAX to CRAY NASTRAN user interface
[AD-A203447] N89-21575
INVARIANCE
The interaction of nonlinear hyperbolic waves: A conference report N89-21530
Hybrid calculation of invariant moments
[AD-A202594] N89-21600
INVISCID FLOW
Vector potential methods N89-20939
Navier-Stokes and viscous-inviscid interaction N89-20949
Numerical study of three viscous/inviscid interaction methods
[AD-A202575] N89-21203
ION BEAMS
Simulation of the low earth orbital atomic oxygen interaction with materials by means of an oxygen ion beam
[NASA-TM-101971] N89-21104
Focused ion beam fabrication of graded channel Field Effect Transistors (FETs) in GaAs and Si
[AD-A203365] N89-21184
Order in cold ionic systems: Dynamic effects
[DE89-007377] N89-21687
ION CONCENTRATION
Ocean alkalinity and the Cretaceous/Tertiary boundary N89-21300
ION CURRENTS
Gating kinetics and ion transfer in channels of nerve membrane
[AD-A202509] N89-21464
ION DENSITY (CONCENTRATION)
Charging potentials for two sample sets of spectra from DMSP satellites
[AD-A203694] N89-21021
ION DISTRIBUTION
Precipitating ion and electron detectors (SSJ/4) for the block 5D/Flight 8 DMSP (Defense Meteorological Satellite Program) satellite
[AD-A203999] N89-21022
Distribution of boron atoms in ion implanted compound semiconductors
[AD-A203173] N89-21677
ION EXCHANGING
A fresh look at transport in perfluorosulfonate ionomers: Ultramicroelectrode investigations of Nafion and Dow ionomers
[AD-A203855] N89-21066

ION IMPLANTATION
Continued development and characterization of doped layers, contacts and associated electronic devices in silicon carbide
[AD-A202450] N89-21176
Investigation of a self-aligned, strained-channel,n sup(+)-In As/Al 0.5 As/In 0.15 Ga 0.85 As Semiconductor Insulator Semiconductor FET (SISFET)
[AD-A203147] N89-21676
Distribution of boron atoms in ion implanted compound semiconductors
[AD-A203173] N89-21677
ION IRRADIATION
Study of the generation of intense pulsed electron beams using glow discharges
[AD-A202438] N89-21624
Basic studies of ion mixing
[AD-A203093] N89-21637
IONIZATION POTENTIALS
Derivation and testing of computer algorithms for automatic real-time determination of space vehicle potentials in various plasma environments
[AD-A203019] N89-21019
IONOSPHERIC DISTURBANCES
Spectral characteristics of High Frequency (HF) backscatter for high latitude ionospheric irregularities: Preliminary analysis of statistical properties
[AD-A202998] N89-21156
Commentary on fast atmospheric pulsations
[AD-A203172] N89-21440
IONS
Observations of neutral circulation at mid-latitudes during the Equinox Transition Study
[NASA-CR-184792] N89-21429
Basic studies of ion mixing
[AD-A203093] N89-21637
IRIDIUM
Possible world-wide middle miocene iridium anomaly and its relationship to periodicity of impacts and extinctions N89-21291
Iridium, shocked minerals, and trace elements across the Cretaceous/Tertiary boundary at Maud Rise, Wedell Sea, and Walvis Ridge, South Atlantic Ocean N89-21333
Accretion rate of extraterrestrial matter: Iridium deposited over the last 70 million years N89-21344
Iridium abundance measurements across bio-event horizons in the geological record N89-21368
Search for the Tunguska event in the Antarctic snow N89-21378
IRIDIUM ISOTOPES
Selective extinction of marine plankton at the end of the Mesozoic era: The fossil and stable isotope record N89-21329
Volcanic ash layers in blue ice fields (Beardmore Glacier Area, Antarctica): Iridium enrichments N89-21340
IRON
Effect of Te on the microstructural changes during the gray-to-white and white-to-gray transition in directional solidification of Fe-C-Si alloys
[DE89-007607] N89-21076
IRREVERSIBLE PROCESSES
A continuum diffusion model for viscoelastic materials
[AD-A202588] N89-21112
ISOTOPE SEPARATION
Ion microprobe of Mg, Ca, Ti and Fe isotopic ratios and trace element abundances in hibonite-bearing inclusions from primitive meteorites N89-21719
ISOTOPES
Nitrogen geochemistry of a Cretaceous-Tertiary boundary site in New Zealand N89-21320
The causes for geographical variations in OS187/OS186 at the Cretaceous-Tertiary boundary N89-21402
Sample introduction techniques for inductively coupled plasma mass spectrometry
[DE89-005724] N89-21655
ISOTOPIC LABELING
Selective extinction of marine plankton at the end of the Mesozoic era: The fossil and stable isotope record N89-21329
Provenance of the K/T boundary layers N89-21331
Volcanic ash layers in blue ice fields (Beardmore Glacier Area, Antarctica): Iridium enrichments N89-21340
Isotopic investigations in the area of the Tunguska catastrophe in 1908 year N89-21342
Sample introduction techniques for inductively coupled plasma mass spectrometry
[DE89-005724] N89-21655
ITERATION
Optical information processing in a confocal Fabry-Perot resonator
[AD-A202566] N89-21556
Adaptive optical linear algebra processors
[AD-A202996] N89-21605
ITERATIVE SOLUTION
Two-measured variable method for wall interference assessment/correction N89-20959
Dynamic structural optimization and experiment
[PB89-111462] N89-21259
The application of modal coordinate methods to large nonlinear time-dependent problems
[AD-A203913] N89-21611

J

J INTEGRAL
Implementation of equivalent domain integral method in the two-dimensional analysis of mixed mode problems
[NASA-CR-181813] N89-21267
Three dimensional effects near a crack tip in a ductile three point bend specimen. Part 2: An experimental investigation using interferometry and caustics
[AD-A202637] N89-21272
JAMMING
A modeling perspective for meteor burst communication
[AD-A202562] N89-21145
The use of chaff in space as a jamming device between ground stations and satellites
[AD-A202577] N89-21146
Performance of an adaptive matched filter using the Griffiths algorithm
[AD-A202578] N89-21147
JET ENGINE FUELS
Holographic particle sizing in solid fuel ramjets
[AD-A202699] N89-20997
Fuel-rich catalytic combustion of Jet-A fuel-equivalence ratios 5.0 to 8.0
[NASA-TM-101975] N89-21051
Fuels combustion research
[AD-A204161] N89-21071
Modern multiple-pulse, high field NMR studies of high density jet fuels
[AD-A203320] N89-21130
JET ENGINES
Experimental examination of the aerothermal performance of the T-10 test cell at NAS (Naval Air Station), Cubi Point
[AD-A203887] N89-21005
JET EXHAUST
Experimental examination of the aerothermal performance of the T-10 test cell at NAS (Naval Air Station), Cubi Point
[AD-A203887] N89-21005
JET FLOW
Subharmonic and fundamental high amplitude excitation of an axisymmetric jet
[NASA-TM-101946] N89-20920
On the conditions for resonance interactions of instability waves in the axisymmetric jet
[NASA-TM-101477] N89-21196
Influence of reflected shock waves on a hypersonic shaped charge jet N89-21522
JET STREAMS (METEOROLOGY)
Combined VHF Dopplar radar and airborne (CV-990) measurements of atmospheric winds on the mesoscale
[NASA-CR-184953] N89-21449
JOINTS (JUNCTIONS)
The use of primers in the adhesive bonding of carbon-fibre reinforced composites
[AD-A202542] N89-21039
JOSEPHSON JUNCTIONS
Demonstration of SQUID parametric amplifier
[AD-A203252] N89-21183
JOURNAL BEARINGS
Vibration control in rotating machinery using variable dynamic stiffness squeeze-films
[AD-A202902] N89-21252
JP-4 JET FUEL
High density fuel effects
[AD-A202426] N89-21125

K

K-EPSILON TURBULENCE MODEL
A numerical study of the turbulent free convection in rectangular cavities N89-21194
KALMAN FILTERS
Estimated satellite cluster elements in near circular orbit
[AD-A202938] N89-21011
Multiple model adaptive tracking of airborne targets
[AD-A202696] N89-21148
SSME propulsion performance reconstruction techniques N89-21752
KINETIC ENERGY
Time and state resolved studies of molecular decomposition
[AD-A202464] N89-21636
KINETICS
The spectroscopy and energy transfer kinetics of the interhalogens
[AD-A202954] N89-21059
Effect of Te on the microstructural changes during the gray-to-white and white-to-gray transition in directional solidification of Fe-C-Si alloys
[DE89-007607] N89-21076
Dilatationally nonlinear elastic materials. Part 2: An example illustrating stress concentration reduction
[AD-A202521] N89-21111
Dilatationally nonlinear elastic materials. (1): Some theory
[AD-A202824] N89-21276
Gating kinetics and ion transfer in channels of nerve membrane
[AD-A202509] N89-21464
Grain boundary kinetics. 1: In-situ observations of coupled grain boundary dislocation motion, crystal translation and boundary displacement
[DE89-006790] N89-21665
KNOWLEDGE BASES (ARTIFICIAL INTELLIGENCE)
SIRE: A Simple Interactive Rule Editor for NICBES N89-21730
Intelligent data reduction for autonomous power systems N89-21737
KNOWLEDGE REPRESENTATION
Simulating rule-based systems
[AD-A202563] N89-21555

L

LAMBERT SURFACE
Extracting shape reflectance of Lambertian, specular, and hybrid surfaces
[AD-A203772] N89-21652
LAMINAR BOUNDARY LAYER
Investigation of the development of laminar boundary-layer instabilities along a cooled-wall cone in hypersonic flows
[AD-A202587] N89-20966
The response of a laminar boundary layer in supersonic flow to small amplitude progressive waves
[NASA-TM-101965] N89-21197
Investigation of the development of laminar boundary-layer instabilities along a blunted cone
[AD-A202425] N89-21200
LAMINAR FLOW
A numerical study of the turbulent free convection in rectangular cavities N89-21194
Incompressible flow friction coefficients in a simulated heat pipe
[AD-A203176] N89-21207
LAMINATES
High temperature composites using Schiff's base pyropolymer matrices
[AD-A203311] N89-21043
Transverse shear considerations in anisotropic plates
[AD-A203187] N89-21283
On a refined nonlinear theory of laminated composite plates N89-21500
MBE of (Hg,Cd)Te
[AD-A202448] N89-21667
LANGUAGES
Domain modeling for language analysis
[AD-A203444] N89-21574
LAPLACE TRANSFORMATION
Application of the Laplace-Borel transformation to the representation of analytical solutions of Duffing's equation
[NASA-TM-100058] N89-21532
LARGE SPACE STRUCTURES
Active control technique evaluation for spacecraft (ACES)
[AD-A202475] N89-21016
Active control of a large space structure as applied to the phase 1 CETF (Critical Evaluation Task Force) space station
[AD-A203293] N89-21020
Investigation of practical applications of H infinity control theory to the design of control systems for large space structures N89-21743
LASER ANEMOMETERS
An LDA (Laser-Doppler Anemometry) investigation of three-dimensional normal shock wave boundary-layer interactions N89-20956
Whole field measurements of vorticity in turbulent and unsteady flows
[AD-A203349] N89-21209

Rotationally sampled wind characteristics for several rotor sizes using laser anemometer measurements
[DE89-007942] N89-21458

LASER APPLICATIONS
Laser-induced metal deposition on semiconductors from liquid electrolytes
[AD-A203612] N89-21089
Application of a single area array detector for acquistion, tracking and point-ahead in space optical communications
[NASA-CR-183423] N89-21168
A laser trap for neutral atoms
[AD-A202581] N89-21229
Bibliography of Soviet laser developments, September-October 1987
[AD-A203366] N89-21232
Architecture and design for a laser programmable double precision floating point application specific processor
[AD-A202560] N89-21553

LASER BEAMS
Laser beam coupling via optical phase conjugation in BaTiO3
[AD-A202874] N89-21231
Acoustic damage to large-aperture optics: Revision 1
[DE89-008025] N89-21654

LASER DAMAGE
People's Republic of China laser radiation safety standard
[AD-A203777] N89-21233
Acoustic damage to large-aperture optics: Revision 1
[DE89-008025] N89-21654

LASER DOPPLER VELOCIMETERS
An LDA (Laser-Doppler Anemometry) investigation of three-dimensional normal shock wave boundary-layer interactions N89-20956

LASER INDUCED FLUORESCENCE
Flow reactor studies of elementary radical reaction rates
[AD-A203126] N89-21062
Advanced diagnostics for reacting flows
[AD-A202451] N89-21202

LASER MATERIALS
Bibliography of Soviet laser developments, September-October 1987
[AD-A203366] N89-21232
Spectroscopy and laser performance of Ti(sup 3+) doped and Cr(sup 3+), Nd(sup 3+) co-doped crystals
[AD-A203911] N89-21682

LASER OUTPUTS
Laser beam coupling via optical phase conjugation in BaTiO3
[AD-A202874] N89-21231
Bibliography of Soviet laser developments, September-October 1987
[AD-A203366] N89-21232
People's Republic of China laser radiation safety standard
[AD-A203777] N89-21233
Atmospheric effects on laser propagation
[DE89-008646] N89-21237
A continued study of optical sound generation and amplification
[AD-A202484] N89-21630

LASER SPECTROSCOPY
The spectroscopy and energy transfer kinetics of the interhalogens
[AD-A202954] N89-21059
Measurement of ground state copper density using hook spectroscopy
[DE89-005098] N89-21093
Solar-powered alkali metal vapor lasers
[NASA-CR-180480] N89-21226
Bibliography of Soviet laser developments, September-October 1987
[AD-A203366] N89-21232
Spectroscopy and laser performance of Ti(sup 3+) doped and Cr(sup 3+), Nd(sup 3+) co-doped crystals
[AD-A203911] N89-21682

LASERS
Low-cost Pointing-and-Tracking System for Optical Communications (PATSOC)
[AD-A202921] N89-21151
A laser trap for neutral atoms
[AD-A202581] N89-21229

LATITUDE
Observations of neutral circulation at mid-latitudes during the Equinox Transition Study
[NASA-CR-184792] N89-21429

LAUNCH VEHICLES
Space Propulsion Hazards Analysis Manual (SPHAM), volume 1
[AD-A203204] N89-21029

LAUNCH WINDOWS
Optimal launch time for a discontinuous low thrust orbit transfer
[AD-A202693] N89-21007

LAUNCHING
An analytical framework for determining life cycle cost implications of the advanced launch system
[AD-A202873] N89-21012

LAVA
Some volcanologic aspects of Columbia River basalt volcanism relevant to the extinction controversy N89-21393
A 3-dimensional numerical simulation of the atmospheric injection of aerosols by a hypothetical basaltic fissure eruption N89-21401

LEAD (METAL)
An in-situ grazing incidence X-ray scattering study of the initial stages of electrochemical growth of lead on silver (III)
[AD-A203385] N89-21064

LEADING EDGES
Numerical simulation of the flow field over delta wings with leading edge blowing N89-20924
An embedded mesh procedure for leading-edge vortex flows N89-20936
Thin-layer Navier-Stokes solutions for a cranked delta wing
[AD-A203292] N89-20970

LEARNING
Acquiring generalizations to organize human databases
[AD-A202964] N89-21702

LEAST SQUARES METHOD
XRAYL: A powder diffraction profile refinement program
[PB89-127567] N89-21050
Transactions of the Fifth Army Conference on Applied Mathematics and Computing
[AD-A193384] N89-21490
Knot selection for least squares approximation using thin plate splines N89-21504
A comparison of variable selection criteria for multiple linear regression: A simulation study
[AD-A202708] N89-21601

LENSES
Polycarbonate ophthalmic lenses for ametropic Army aviators using night vision goggles
[AD-A203100] N89-21488
A theoretical and experimental investigation of linear and nonlinear focussing chirped optical diffraction gratings
[AD-A203396] N89-21650

LIBRARIES
Systems engineering and technical assistance
[AD-A203479] N89-21696
Automated library systems and document tracking systems: Commercial software alternatives, volume 1
[DE89-007716] N89-21706

LIE GROUPS
Transactions of the Fifth Army Conference on Applied Mathematics and Computing
[AD-A193384] N89-21490
Lie transforms applied to a nonlinear parametric excitation problem N89-21491
Contraction of Z(sub 2) graded Lie algebras
[DE88-705356] N89-21596

LIFE (DURABILITY)
Reliability/maintainability/testability design for dormancy
[AD-A202704] N89-21179
Maintenance metrics for Jovial (J73) software
[AD-A202713] N89-21561

LIFE CYCLE COSTS
An analytical framework for determining life cycle cost implications of the advanced launch system
[AD-A202873] N89-21012

LIFT
Wave drag due to lift for transonic airplanes N89-20938
Investigation of a free-tip rotor configuration for research on spanwise life distributions and wake velocity surveys of a semi-span wing with a discontinuous twist
[NASA-CR-184948] N89-20963
Numerical simulation of flow over iced airfoils
[AD-A203291] N89-20969
Thin-layer Navier-Stokes solutions for a cranked delta wing
[AD-A203292] N89-20970
Methodology for using steady experimental aerodynamic data to improve steady and unsteady aerodynamic analysis N89-20972

LIGHT BEAMS
Transformations of Gaussian light beams caused by reflection in FEL (Free Electron Lasers) resonators
[AD-A202472] N89-21227
Fast acting optical beam deflection system
[AD-A203042] N89-21648

LIGHT CURVE
Supernova 1987A: 18 months later
[NASA-CR-184891] N89-21715

LIGHT MODULATION
Center for the Integration of Optical Computing
[AD-A203254] N89-21536
Devices and systems for nonlinear optical information processing
[AD-A203034] N89-21566

LIGHT SCATTERING
Advanced diagnostics for reacting flows
[AD-A202451] N89-21202
Molecular jet studies of vdW (van der Waals) clusters and solvation
[AD-A203766] N89-21212

LIGHTNING
In-flight lightning characterization program on a CV-580 aircraft
[AD-A203954] N89-20976

LIMESTONE
Faunal and erosional events in the Eastern Tethyan Sea across the K/T boundary N89-21338

LINE SPECTRA
An algorithm for processing scanning spectrometer data N89-21506
Positron line radiation from halo WIMP annihilations as a dark matter signature
[NASA-CR-182918] N89-21635

LINEAR EQUATIONS
Response surface methodology applied to the radar range equation
[AD-A203044] N89-21157
Adaptive optical linear algebra processors
[AD-A202996] N89-21605

LINEAR PROGRAMMING
Improving the survivability of a stochastic communication network
[AD-A202872] N89-21150
A very simple polynomial-time algorithm for linear programming
[AD-A202502] N89-21548
Triangularity of the basis in linear programs for material requirements planning, revision
[AD-A203039] N89-21606

LINEAR QUADRATIC GAUSSIAN CONTROL
Experiments in end-point control of manipulators with elastic drives N89-21240

LINEAR SYSTEMS
Root placement with transfer function methods (full state feedback)
[AD-A203877] N89-21610

LINEAR VIBRATION
Optical information processing in a confocal Fabry-Perot resonator
[AD-A202566] N89-21556

LINEARITY
A comparison of variable selection criteria for multiple linear regression: A simulation study
[AD-A202708] N89-21601

LINGUISTICS
Domain modeling for language analysis
[AD-A203444] N89-21574

LININGS
X-ray fluorescence surface contaminant analyzer: A feasibility study N89-21736

LINKAGES
Vibration control in rotating machinery using variable dynamic stiffness squeeze-films
[AD-A202902] N89-21252

LIQUID CRYSTALS
A helmet-mounted virtual environment display system
[AD-A203055] N89-20994
Structure development during converging flow of a liquid crystal dispersed two-phase fluid
[AD-A203062] N89-21119
Optoelectronic workshops. Part 4: Liquid Crystals for Laser Applications
[AD-A202526] N89-21228

LIQUID FUELS
Density of triethanolammonium nitrate and liquid propellant
[AD-A203767] N89-21131

LIQUID HELIUM
Half-solitons in superfluid (3)He-A: Novel pi/2-quanta of phase slippage
[PB89-128904] N89-21664

LIQUID HELIUM 2
Sounds in one-dimensional superfluid helium
[AD-A202428] N89-21629

LIQUID METALS
Studies of liquid metal flows and power losses in ducts with moving conducting wall, slanted magnetic field, and applied external electric potential
[AD-A203981] N89-21626

LIQUID OXYGEN
Simulation of water vapor condensation on LOX droplet surface using liquid nitrogen N89-21749

LIQUID PHASES
Stress-corrosion cracking of liquid-phase sintered tungsten alloys
[AD-A203201] N89-21087
Turbulence modulation and dense-spray structure
[AD-A202449] N89-21201
LIQUID SURFACES
Spectroscopic studies of fluid/solid interfaces
[AD-A202436] N89-21054
LIQUID-SOLID INTERFACES
Spectroscopic studies of fluid/solid interfaces
[AD-A202436] N89-21054
LIQUID-VAPOR INTERFACES
Computational techniques for shock wave diffraction problems
[AD-A203439] N89-21210
LIQUIDS
Fluids, both ionic and nonionic, over wide ranges of temperature and composition
[DE89-001265] N89-21048
Laser-induced metal deposition on semiconductors from liquid electrolytes
[AD-A203612] N89-21089
LITHIUM ALLOYS
Synthesis processing of high-lithium Al-Li alloys
[AD-A203401] N89-21088
Mechanisms of fatigue crack propagation and fracture toughness behavior in advanced aluminum-lithium alloys
[DE89-008300] N89-21098
LITHOLOGY
K-T impact(s): Continental, oceanic or both
N89-21386
Impact and extinction signatures in complete Cretaceous-Tertiary (K-T) boundary sections
N89-21391
Cretaceous-Tertiary boundary in the Antarctic: Climatic cooling precedes biotic crisis N89-21392
LOAD DISTRIBUTION (FORCES)
Investigation of a free-tip rotor configuration for research on spanwise life distributions and wake velocity surveys of a semi-span wing with a discontinuous twist
[NASA-CR-184948] N89-20963
LOADS (FORCES)
Unsteady force calculations on circular cylinders and elliptical airfoils with circulation control
[UMAERO-87-37] N89-20962
The effect of mixed-mode loading on stress-driven solute segregation during high-temperature brittle intergranular fracture
[AERE-R-12897] N89-21073
A new model for the forced response of a mistuned disk
[AD-A202769] N89-21275
LOCAL AREA NETWORKS
SURVNET user's manual
[AD-A203372] N89-21164
LOGARITHMS
A very simple polynomial-time algorithm for linear programming
[AD-A202502] N89-21548
LOGIC CIRCUITS
A multiple-valued logic system for circuit extraction to VHDL 1076-1987
[AD-A202646] N89-21177
LOGIC PROGRAMMING
Deductive programming
[AD-A202489] N89-21546
TABLOG: The deductive tableau programming language
[AD-A202490] N89-21547
Semantical paradigms: Notes for an invited lecture
[AD-A202995] N89-21565
LOGICAL ELEMENTS
Optical computing research
[AD-A202963] N89-21564
Nonlinear real-time optical signal processing
[AD-A202445] N89-21641
LOGISTICS
A decision-based methodology for object oriented-design
[AD-A202579] N89-21558
An analysis of the biennial budget process
[AD-A202626] N89-21710
LOOPS
The solution of the type-problem for N less than or equal to 4 N89-21528
LOSSES
The radar cross section of a two dimensional dielectric coated cylinder using on-surface radiation conditions
[AD-A202935] N89-21152
A performance/loss evaluation of SSME HPFTP turbine N89-21735
LOW ASPECT RATIO
Development of a shock capturing code for use as a tool in designing high-work low aspect ratio turbines
[AD-A202706] N89-21248
LOW DENSITY MATERIALS
Study of the ignition inhibiting properties of compressed air foam
[PB89-127559] N89-21049
LOW SPEED WIND TUNNELS
Flowfield measurements in the NASA Lewis Research Center 9- by 15-foot low-speed wind tunnel
[NASA-TM-100883] N89-21002
LOW TEMPERATURE
Synthesis of ceramics at low temperatures
N89-21102
Low temperature properties of ternary magnetic rare earth transition metal germanides with the Sc5Co4Ge10-type structure
[DE89-007628] N89-21666
LOW TEMPERATURE TESTS
Investigation of the development of laminar boundary-layer instabilities along a cooled-wall cone in hypersonic flows
[AD-A202587] N89-20966
LOW THRUST
Optimal launch time for a discontinuous low thrust orbit transfer
[AD-A202693] N89-21007
LUBRICATING OILS
Operation of vehicle engines in cold conditions: Start up, lubrication and fuel consumption
[DE88-757111] N89-21255
LUBRICATION
Mild wear in dry and lubricated sliding systems
N89-21242
LUMINANCE
Evaluation of the spatial and temporal characteristics of the conducting PRIZ
[AD-A202593] N89-21671

M

MACHINE LEARNING
Statistical machine learning for the cognitive selection of nonlinear programming algorithms in engineering design optimization N89-21493
MAGELLANIC CLOUDS
Supernova 1987A: 18 months later
[NASA-CR-184891] N89-21715
MAGMA
Dynamics of exploding magma chambers: Implications for K-T volcanism and mass extinctions N89-21377
MAGNETIC ANOMALIES
Geological indicators for impact: The anomalous case of the Vredefort structure, South Africa N89-21289
MAGNETIC BEARINGS
A magnetic bearing control approach using flux feedback
[NASA-TM-100672] N89-21135
MAGNETIC CONTROL
A magnetic bearing control approach using flux feedback
[NASA-TM-100672] N89-21135
MAGNETIC DIPOLES
Geomagnetic field energy as a source of thrust
[AD-A202567] N89-21027
MAGNETIC FIELD CONFIGURATIONS
Force-free magnetic fields: Is there a loss of equilibrium
[AD-A203030] N89-21717
MAGNETIC FIELD INVERSIONS
Magnetic reversal spurts: Rain gauges for comet showers N89-21349
MAGNETIC FIELDS
Geomagnetic field energy as a source of thrust
[AD-A202567] N89-21027
Magnetic mapping of current distributions in two-dimensional electronic devices
[AD-A203035] N89-21220
Solar-geophysical data number 529, September 1988. Part 1: (Prompt reports). Data for August, July 1988 and late data
[PB89-121305] N89-21431
Propagator matrices in the solution of EMP problems
N89-21515
Studies of liquid metal flows and power losses in ducts with moving conducting wall, slanted magnetic field, and applied external electric potential
[AD-A203981] N89-21626
Applications, dosimetry and biological interactions of static and time-varying magnetic fields
[DE89-006944] N89-21627
MAGNETIC FLUX
A magnetic bearing control approach using flux feedback
[NASA-TM-100672] N89-21135
MAGNETIC MATERIALS
Low temperature properties of ternary magnetic rare earth transition metal germanides with the Sc5Co4Ge10-type structure
[DE89-007628] N89-21666
MAGNETIC MEASUREMENT
Magnetic flowmeter measurement of solid propellant pressure-coupled and velocity-coupled responses
[AD-A203988] N89-21133
MAGNETIC PROPERTIES
Electronic structure and properties of defect complexes in metals
[AD-A203657] N89-21091
Low temperature properties of ternary magnetic rare earth transition metal germanides with the Sc5Co4Ge10-type structure
[DE89-007628] N89-21666
Magnetic properties of nano-heterogeneous amorphous, thin films
[AD-A203727] N89-21680
MAGNETIC SHIELDING
High-temperature ceramic superconductors
[AD-A202867] N89-21674
MAGNETIC STORMS
Commentary on fast atmospheric pulsations
[AD-A203172] N89-21440
MAGNETIC SUSPENSION
Test techniques: A survey paper on cryogenic tunnels, adaptive wall test sections, and magnetic suspension and balance systems N89-20955
Analytical model of a five degree of freedom magnetic suspension and positioning system
[NASA-TM-100671] N89-21136
MAGNETO-OPTICS
Two photon characterization
[AD-A203355] N89-21678
Magnetic properties of nano-heterogeneous amorphous, thin films
[AD-A203727] N89-21680
MAGNETOHYDRODYNAMIC FLOW
Advanced diagnostics for reacting flows
[AD-A202451] N89-21202
Studies of liquid metal flows and power losses in ducts with moving conducting wall, slanted magnetic field, and applied external electric potential
[AD-A203981] N89-21626
MAGNETOHYDRODYNAMIC STABILITY
The role of hydromagnetic waves in the magnetosphere and the ionosphere
[AD-A202800] N89-21437
Studies of liquid metal flows and power losses in ducts with moving conducting wall, slanted magnetic field, and applied external electric potential
[AD-A203981] N89-21626
MAGNETOHYDRODYNAMIC WAVES
The role of hydromagnetic waves in the magnetosphere and the ionosphere
[AD-A202800] N89-21437
MAGNETOMETERS
Magnetic mapping of current distributions in two-dimensional electronic devices
[AD-A203035] N89-21220
Construction of an alternating gradient magnetometer
N89-21739
MAINTAINABILITY
Reliability/maintainability/testability design for dormancy
[AD-A202704] N89-21179
Maintenance metrics for Jovial (J73) software
[AD-A202713] N89-21561
MAINTENANCE
A diagnostic system blending deep and shallow reasoning
[AD-A202547] N89-20979
Contamination of the exterior of a C-130E aircraft used for aerial spray, 907 TAG, Rickenbacker ANGB, OH
[AD-A202430] N89-20984
MAMMALS
Effects of simultaneous radiofrequency radiation and chemical exposure of mammalian cells, volume 2
[AD-A202780] N89-21467
Design of a feeling-thinking machine N89-21510
MAN MACHINE SYSTEMS
Flight controller design with nonlinear aerodynamics, large parameter uncertainty and pilot compensation
[AD-A202727] N89-21000
MAN-COMPUTER INTERFACE
Graphical man-machine interface for an integrated evaluation environment
[AD-A203054] N89-21487
MANAGEMENT METHODS
Satellite telemetry: A new tool for wildlife research and management
[PB88-249255] N89-21013

Automated library systems and document tracking systems: Commercial software alternatives, volume 1
[DE89-007716] N89-21706

MANAGEMENT PLANNING
Systems engineering and technical assistance
[AD-A203479] N89-21696

MANIPULATORS
Manipulator primitive level task decomposition
[PB89-133532] N89-21238
Experiments in end-point control of manipulators with elastic drives N89-21240
The Rochester robot
[AD-A202633] N89-21247
Robotic compliant motion control for aircraft refueling applications
[AD-A202710] N89-21249

MANNED SPACE FLIGHT
NASA directions in space propulsion for 2000 and beyond
[NASA-TM-102281] N89-21026
Saccadic eye movement during spaceflight
[NASA-TM-100475] N89-21463

MANPOWER
Empirical demonstration of isoperformance methodology preparatory of an interactive expert computerized decision aid
[AD-A202439] N89-21545

MANUAL CONTROL
Capacity of human operator using smart stick controller
[AD-A202712] N89-21483

MAPPING
Magnetic mapping of current distributions in two-dimensional electronic devices
[AD-A203035] N89-21220
Diffusion in symplectic maps
[DE89-008083] N89-21622

MAPS
Column movement model used to support AMM N89-21521

MARINE BIOLOGY
Response of marine and freshwater algae to nitric acid and elevated carbon dioxide levels simulating environmental effects of bolide impact N89-21298
High resolution chronology of late Cretaceous-early Tertiary events determined from 21,000 yr orbital-climatic cycles in marine sediments N89-21328
Trace element and isotope geochemistry of Cretaceous-Tertiary boundary sediments: identification of extra-terrestrial and volcanic components N89-21352
Cretaceous-Tertiary findings, paradigms and problems N89-21364

MARINE CHEMISTRY
Ocean alkalinity and the Cretaceous/Tertiary boundary N89-21300

MARINE ENVIRONMENTS
Global Catastrophes in Earth History: An Interdisciplinary Conference on Impacts, Volcanism, and Mass Mortality
[NASA-CR-183329] N89-21287
Response of marine and freshwater algae to nitric acid and elevated carbon dioxide levels simulating environmental effects of bolide impact N89-21298
Proterozoic Bushveld-Vredefort catastrophe: Possible causes and consequences N89-21312
The end-triassic mass extinction event N89-21324
Diachronism between extinction time of terrestrial and marine dinosaurs N89-21325
How many upper Eocene microspherule layers: More than we thought N89-21327
Selective extinction of marine plankton at the end of the Mesozoic era: The fossil and stable isotope record N89-21329
Extended period of K/T boundary mass extinction in the marine realm N89-21337
Marine and continental K-T boundary clays compared N89-21382
Mass extinctions in the deep sea N89-21396
The causes for geographical variations in OS187/OS186 at the Cretaceous-Tertiary boundary N89-21402
Macrofossil extinction patterns at Bay of Biscay Cretaceous-Tertiary boundary sections N89-21404
Infrared sea-radiance modeling using LOWTRAN 6
[AD-A202582] N89-21643
Evaluation of aerosol size distribution models
[AD-A202736] N89-21645

MARINE METEOROLOGY
Geochemistry of K/T boundaries in India and contributions of Deccan volcanism N89-21296

MARKOV CHAINS
Rootfinding for Markov chains with quasi-triangular transition matrices
[AD-A202468] N89-21597

MARKOV PROCESSES
Finite-difference modeling of Rayleigh wave scattering and P-SV(Lg) coupling problems
[AD-A203221] N89-21161

MARTENSITE
Martensitic phase transitions in nanocrystalline materials
[AD-A203636] N89-21090
Nb modification of microcomposite Fe/C/Cr/Mn steel
[DE89-008297] N89-21097

MASS DISTRIBUTION
The cometary and asteroidal impactor flux at the earth N89-21407
Disruption of giant comets in the solar system and around other stars N89-21408

MASS FLOW
Performance of the active sidewall boundary-layer removal system for the Langley 0.3-meter Transonic Cryogenic Tunnel
[NASA-CR-181793] N89-21004
Magnetic flowmeter measurement of solid propellant pressure-coupled and velocity-coupled responses
[AD-A203988] N89-21133

MASS SPECTROMETERS
Sample introduction techniques for inductively coupled plasma mass spectrometry
[DE89-005724] N89-21655

MASS SPECTROSCOPY
Flow reactor studies of elementary radical reaction rates
[AD-A203126] N89-21062
Surface chemistry and structural effects in the stress corrosion of glass and ceramic materials
[AD-A202452] N89-21107

MASS TRANSFER
Computer program for calculating frequencies and modal structures of free coastal-trapped waves
[PB88-243928] N89-21459
Transient natural convection heat and mass transfer in crystal growth N89-21741

MATCHED FILTERS
Performance of an adaptive matched filter using the Griffiths algorithm
[AD-A202578] N89-21147
Analysis and simulation of a pseudonoise synchronization system
[AD-A202779] N89-21149
A theoretical and experimental investigation of linear and nonlinear focussing chirped optical diffraction gratings
[AD-A203396] N89-21650

MATERIAL ABSORPTION
Optical power limiter
[AD-A203964] N89-21234

MATHEMATICAL LOGIC
Otter 1.0 users' guide
[DE89-008656] N89-21581

MATHEMATICAL MODELS
Transverse jets in compressible crossflows N89-20923
Performance analysis of the fiber distributed data interface in the super cockpit audio world
[AD-A202535] N89-20985
Aeroelastic modeling for the FIT team F/A-18 simulation
[NASA-TM-101569] N89-20991
A source code analyzer to predict compilation time for avionics software using software science measures. Volume 1: Main report
[AD-A202737] N89-20992
An analytical framework for determining life cycle cost implications of the advanced launch system
[AD-A202873] N89-21012
Light satellites: A dilemma for the US Army
[AD-A202648] N89-21017
Space Propulsion Hazards Analysis Manual (SPHAM), volume 1
[AD-A203204] N89-21029
Investigation of modeling of damage growth in composite laminates
[AD-A202433] N89-21037
Spectral analysis of a fourth-order singular differential operator arising in combustion
[DE89-005841] N89-21052
Computer simulation of macrosegregation in directionally solidified circular ingots
[NASA-CR-182838] N89-21134
Analytical model of a five degree of freedom magnetic suspension and positioning system
[NASA-TM-100671] N89-21136
Frequency dependent ultrasonic ray tracing: A preliminary study
[AERE-R-13119] N89-21139
A modeling perspective for meteor burst communication
[AD-A202562] N89-21145
On the impulse response of monopulse radars
[AD-A202936] N89-21153
Effect of two-body motion on radar beam quality for various distributed sparse array configurations
[AD-A202937] N89-21154
Numerical study of three viscous/inviscid interaction methods
[AD-A202575] N89-21203
Computational techniques for shock wave diffraction problems
[AD-A203439] N89-21210
Mild wear in dry and lubricated sliding systems N89-21242
Function theory for thin elastic shells
[PB89-101943] N89-21257
Deformation modeling and constitutive modeling for anisotropic superalloys
[NASA-CR-4215] N89-21258
Characterization of structural connections using free and forced response test data
[NASA-TM-101991] N89-21266
Implementation of equivalent domain integral method in the two-dimensional analysis of mixed mode problems
[NASA-CR-181813] N89-21267
Nonlinear finite element analysis of a general composite shell
[AD-A202572] N89-21271
Essential elements in the numerical modeling of solar cells
[DE89-008113] N89-21424
CCM (Community Climate Model)
[PB89-120927] N89-21446
A simple model for wind field estimation in complex terrain
[DE89-007240] N89-21457
A study of motion sickness: Mathematical modeling and data analysis
[AD-A202770] N89-21466
Modelling of the lean flammability limit in flame theory N89-21527
HOP (Hardware viewed as Objects and Processes): A process model for synchronous hardware systems
[AD-A203090] N89-21535
Documentation of the finite element code VISCOT/UX for thermomechanical analyses: Version 0.01
[DE89-004719] N89-21544
Optical information processing in a confocal Fabry-Perot resonator
[AD-A202566] N89-21556
Computer-aided fabrication system implementation
[AD-A203651] N89-21576
An algebraic theory of program correctness in a problem domain
[DE89-008450] N89-21579
A theory of problem domains and program correctness
[DE89-008451] N89-21580
Computer assisted analysis and modelling of structured problems
[AD-A203040] N89-21607
The application of modal coordinate methods to large nonlinear time-dependent problems
[AD-A203913] N89-21611
Best ordering for floating-point addition
[AD-A203990] N89-21612
Time-discretized moments of a randomly excited uncertain linear oscillator
[DE89-008318] N89-21614
Artificial asteroid impact on defensive satellites
[DE89-008407] N89-21620
Infrared sea-radiance modeling using LOWTRAN 6
[AD-A202582] N89-21643
A numerical model for the computation of radiance distributions in natural waters with wind-roughened surfaces. Part 2: User's guide and code listing
[AD-A203441] N89-21651
Numerical modeling of narrow band soft X-ray sources
[AD-A203368] N89-21657
Computer modeling and simulation in inertial confinement fusion
[DE89-008304] N89-21661
Short wave electron temperature gradient driven drift wave turbulence
[DE89-008465] N89-21662
Order in cold ionic systems: Dynamic effects
[DE89-007377] N89-21687
Information acquisition for model construction: An integrative, decision-theoretic perspective N89-21705
Evolution of cosmic string networks
[NASA-CR-182836] N89-21716
The evolution of active galactic nuclei and globular clusters: Multi-component models N89-21720
Finite element simulation of thunderstorm electrodynamics in the proximity of the storm N89-21728
Small expendable deployer system measurement analysis N89-21731

Radiation effect on rocket engine performance N89-21734
The simulation of the alternate turbopump development high pressure oxygen and fuel turbopumps for the space shuttle main engine using the Shaberth computer program N89-21746
SSME propulsion performance reconstruction techniques N89-21752
Rotordynamic analysis of a bearing tester N89-21759
Space shuttle main engine numerical modeling code modifications and analysis N89-21760

MATHEMATICAL PROGRAMMING
Improving the survivability of a stochastic communication network
[AD-A202872] N89-21150
Nonprocedural implementation of mathematical programming algorithms
[AD-A203392] N89-21573
Computer assisted analysis and modelling of structured problems
[AD-A203040] N89-21607

MATRICES (MATHEMATICS)
A block QR factorization scheme for loosely coupled systems of array processors N89-21519
Objects as closures: Abstract semantics of object oriented languages
[NASA-CR-184877] N89-21540
Selection of a frequency sensitive QFT (Quantitative Feedback Theory) weighting matrix using the method of specified outputs
[AD-A202692] N89-21592
Rootfinding for Markov chains with quasi-triangular transition matrices
[AD-A202468] N89-21597
On random correlation matrices
[AD-A202786] N89-21603
Optimization of large matrix calculations for execution on the Cray X-MP vector supercomputer N89-21742

MATRIX MATERIALS
High temperature composites using Schiff's base pyropolymer matrices
[AD-A203311] N89-21043
Fracture toughness testing of a ceramic matrix composite at elevated temperatures
[AD-A202738] N89-21114
The shear-lag model for a unidirectional composite with viscoelastic matrix N89-21495

MATRIX METHODS
Selection of a frequency sensitive QFT (Quantitative Feedback Theory) weighting matrix using the method of specified outputs
[AD-A202692] N89-21592

MATRIX THEORY
Root placement with transfer function methods (full state feedback)
[AD-A203877] N89-21610

MATTER (PHYSICS)
Thermodynamic gauge theory of solids and quantum liquids with internal phase N89-21525
Lagrangian formulation of relativistic thermodynamics N89-21526

MAXIMUM LIKELIHOOD ESTIMATES
Time delay estimation in stationary and non-stationary environments
[AD-A202507] N89-21549

MEASURING INSTRUMENTS
Application of a single area array detector for acquistion, tracking and point-ahead in space optical communications
[NASA-CR-183423] N89-21168
On-line location of partial discharges in power transformer through acoustic emission
[DE88-757043] N89-21188
Robotic tactile sensor fabricated from piezoelectric polyvinylidene fluoride films
[AD-A202724] N89-21250
Angular response calibration of the burst and transient source experiment N89-21745

MECHANICAL DRIVES
Comparison study of gear dynamic computer programs at NASA Lewis Research Center
[NASA-TP-2901] N89-21243
Modal analysis of gear housing and mounts
[NASA-TM-101445] N89-21244

MECHANICAL PROPERTIES
Mechanisms of fatigue crack propagation and fracture toughness behavior in advanced aluminum-lithium alloys
[DE89-008300] N89-21098
Investigation of the impact performance of various glass and ceramic systems
[AD-A202443] N89-21106
Ceramics
[AD-A202504] N89-21109
Investigation of failure modes in fiber reinforced ceramic matrix composites
[AD-A202705] N89-21113
Deformation modeling and constitutive modeling for anisotropic superalloys
[NASA-CR-4215] N89-21258
Optical information processing in a confocal Fabry-Perot resonator
[AD-A202566] N89-21556
Extracting shape reflectance of Lambertian, specular, and hybrid surfaces
[AD-A203772] N89-21652
Center for thin film studies
[AD-A202742] N89-21673
Atomistic simulations of interfaces in metals and alloys
[DE89-006521] N89-21685
Dynamic fatigue testing of Zerodur glass-ceramic N89-21753

MELTING
Toward a nonequilibrium thermodynamics of two phase materials with sharp interface N89-21494

MEMBRANE STRUCTURES
A triangular thin shell element for the linear analysis of stiffened composite structures
[AD-A202864] N89-21277

MEMBRANES
Gating kinetics and ion transfer in channels of nerve membrane
[AD-A202509] N89-21464

MEMORY
Acquiring generalizations to organize human databases
[AD-A202964] N89-21702

MEMORY (COMPUTERS)
A position, scale and rotation invariant holographic associative memory
[AD-A203289] N89-21221
Time warp on a shared memory multiprocessor
[AD-A203088] N89-21534

MENTAL PERFORMANCE
Coping with novelty and human intelligence: The role of counterfactual reasoning
[AD-A203624] N89-21478

MERCURY CADMIUM TELLURIDES
MBE of (Hg,Cd)Te
[AD-A202448] N89-21667
The response of single element HgCdTe and InSb solid state infrared detectors to millimeter wave electromagnetic energy
[AD-A202667] N89-21672
Distribution of boron atoms in ion implanted compound semiconductors
[AD-A203173] N89-21677
Two photon characterization
[AD-A203355] N89-21678
Electron mobility in mercury cadmium telluride N89-21748

MESOSCALE PHENOMENA
Blending of surface and rawinsonde data in mesoscale objective analysis
[AD-A203984] N89-21456
The role of radiation-dynamics interaction in regional numerical weather prediction N89-21732

MESSAGE PROCESSING
A modeling perspective for meteor burst communication
[AD-A202562] N89-21145
Software development guidelines
[AD-A203332] N89-21572

METAL BONDING
Adhesion in chemically hostile environments: The use of filled polymers as diffusion barriers
[AD-A203333] N89-21121

METAL FATIGUE
The properties of advanced aluminium alloy systems N89-21074
The effects of loading history and closure of the fatigue characteristics of heat treated Ti-6Al-2Sn-4Zr-6Mo
[AD-A202652] N89-21082
Crack growth of a titanium-aluminide alloy under thermal-mechanical fatigue
[AD-A202767] N89-21083

METAL FILMS
Photochemistry at corrugated thin metal films: A phenomenological approach
[AD-A203070] N89-21061

METAL MATRIX COMPOSITES
Nondestructive testing techniques for metal matrix composites
[AERE-R-13040] N89-21034
The properties of advanced aluminium alloy systems N89-21074

METAL OXIDE SEMICONDUCTORS
A multiple-valued logic system for circuit extraction to VHDL 1076-1987
[AD-A202646] N89-21177
HOP (Hardware viewed as Objects and Processes): A process model for synchronous hardware systems
[AD-A203090] N89-21535

METAL POWDER
Shock-induced chemical synthesis of intermetallic compounds
[DE89-007035] N89-21095

METAL PROPELLANTS
Effective ignition kinetics for LOVA propellant
[AD-A203149] N89-21129

METAL SHEETS
Oblique hypervelocity impact response of dual-sheet structures
[NASA-TM-100358] N89-21246

METAL SURFACES
Organic functional group reactivities at metal surfaces
[AD-A203094] N89-21086

METAL VAPORS
Solar-powered alkali metal vapor lasers
[NASA-CR-180480] N89-21226

METAL-GAS SYSTEMS
Hydrogen and deuterium internal friction behavior in vanadium-niobium alloys
[DE89-007616] N89-21078

METALLOIDS
Electronic structure and properties of defect complexes in metals
[AD-A203657] N89-21091

METALS
Laser-induced metal deposition on semiconductors from liquid electrolytes
[AD-A203612] N89-21089
Heavy metal toxicity as a kill mechanism in impact caused mass extinctions N89-21406

METAMORPHISM (GEOLOGY)
Geological indicators for impact: The anomalous case of the Vredefort structure, South Africa N89-21289
Shocked quartz and more: Impact signatures in K-T boundary clays and claystones N89-21297
Magnetic microspherules associated with the K/T and upper Eocene extinction events N89-21303
Explosive volcanism, shock metamorphism and the K-T boundary N89-21309
The Western North American Cretaceous-Tertiary (K-T) boundary interval and its content of shock-metamorphosed minerals: Implications concerning the K-T boundary impact-extinction theory N89-21334
The Kara and Ust-Kara impact structures (USSR) and their relevance to the K/T boundary event N89-21341
Inducement of heterochronic variation in a species of planktic foraminifera by a Late Eocene impact event N89-21351
The Calvin 28 cryptoexplosive disturbance, Cass County, Michigan: Evidence for impact origin N89-21358
Cathodoluminescence of shocked quartz at the Cretaceous-Tertiary boundary N89-21369
Microdeformation in Vredefort rocks; evidence for shock metamorphism N89-21376

METASTABLE STATE
The spectroscopy and energy transfer kinetics of the interhalogens
[AD-A202954] N89-21059

METEORITE COLLISIONS
Global Catastrophes in Earth History: An Interdisciplinary Conference on Impacts, Volcanism, and Mass Mortality
[NASA-CR-183329] N89-21287
The debate over the Cretaceous-Tertiary boundary N89-21288
Geological indicators for impact: The anomalous case of the Vredefort structure, South Africa N89-21289
Possible world-wide middle miocene iridium anomaly and its relationship to periodicity of impacts and extinctions N89-21291
The cratering record in the inner solar system: Implications for earth N89-21292
Late Wenlock (middle Silurian) bio-events: Caused by volatile boloid impact/s N89-21295
Shocked quartz and more: Impact signatures in K-T boundary clays and claystones N89-21297
Response of marine and freshwater algae to nitric acid and elevated carbon dioxide levels simulating environmental effects of bolide impact N89-21298
Sedimentological effects of tsunamis, with particular reference to impact-generated and volcanogenic waves N89-21299
Dinosaur bone beds and mass mortality: Implications for the K-T extinction N89-21301
Risk to civilization: A planetary science perspective N89-21302
Magnetic microspherules associated with the K/T and upper Eocene extinction events N89-21303

Global environmental effects of impact-generated aerosols: Results from a general circulation model N89-21306
The Sudbury Structure (Ontario, Canada) and Vredefort Structure (South Africa): A comparison N89-21311
Proterozoic Bushveld-Vredefort catastrophe: Possible causes and consequences N89-21312
Geological remote sensing signatures of terrestrial impact craters N89-21317
Evidence for a single impact at the Cretaceous-Tertiary boundary from trace elements N89-21319
Nitrogen geochemistry of a Cretaceous-Tertiary boundary site in New Zealand N89-21320
The global Cretaceous-Tertiary fire: Biomass or fossil carbon N89-21321
Late Eocene impact events recorded in deep-sea sediments N89-21322
Mineralogy and phase-chemistry of the Cretaceous/Tertiary section in the Lattengebirge, Bavarian Alps N89-21323
The Manson impact structure, a possible site for a Cretaceous-Tertiary (K-T) boundary impact N89-21326
Impact wave deposits provide new constraints on the location of the K/T boundary impact N89-21330
Provenance of the K/T boundary layers N89-21331
Strangelove ocean at era boundaries, terrestrial or extraterrestrial cause N89-21332
Iridium, shocked minerals, and trace elements across the Cretaceous/Tertiary boundary at Maud Rise, Wedell Sea, and Walvis Ridge, South Atlantic Ocean N89-21333
The Western North American Cretaceous-Tertiary (K-T) boundary interval and its content of shock-metamorphosed minerals: Implications concerning the K-T boundary impact-extinction theory N89-21334
Mass mortality and extraterrestrial impacts N89-21335
Patterns of megafloral change across the Cretaceous-Tertiary boundary in the Northern Great Plains and Rocky Mountains N89-21336
The Kara and Ust-Kara impact structures (USSR) and their relevance to the K/T boundary event N89-21341
The Karskiy craters are the probable records of catastrophe at the Cretaceous-Tertiary boundary N89-21343
Catastrophic volcanism N89-21346
Catastrophic volcanism as a cause of shocked features found at the K/T boundary and in cryptoexplosion structures N89-21347
Evidence for and implications of an Early Archean terrestrial impact record N89-21348
Magnetic reversal spurts: Rain gauges for comet showers N89-21349
Inducement of heterochronic variation in a species of planktic foraminifera by a Late Eocene impact event N89-21351
Impact, and its implications for geology N89-21353
Shatter cones: Diagnostic impact signatures N89-21355
Mass killings and detection of impacts N89-21356
The Calvin 28 cryptoexplosive disturbance, Cass County, Michigan: Evidence for impact origin N89-21358
Mineralogical and geochemical anomalous data of the K-T boundary samples N89-21359
Astrophysical implications of periodicity N89-21361
Plant microfossil record of the terminal Cretaceous event in the western United States and Canada N89-21363
Cretaceous-Tertiary findings, paradigms and problems N89-21364
Environmental effects of large impacts on the earth; relation to extinction mechanisms N89-21365
Permo-Triassic vertebrate extinctions: A program N89-21367
Biospheric traumas caused by large impacts and predicted relics in the sedimentary record N89-21371
Flood basalt eruptions, comet showers, and mass extinction events N89-21372
Impact as a general cause of extinction: A feasibility test N89-21374
Report on an international workshop on Cryptoexplosions and Catastrophes in the Geological Record, with a Special Focus on the Vredefort Structure N89-21375
Search for the Tunguska event in the Antarctic snow N89-21378
Computer modeling of large asteroid impacts into continental and oceanic sites: Atmospheric, cratering, and ejecta dynamics N89-21379
Crater size estimates for large-body terrestrial impact N89-21381
Oblique impacts: Catastrophic vs. protracted effects N89-21383
Non-random cratering flux in recent time N89-21384
Periodicity of extinction: A 1988 update N89-21385
K-T impact(s): Continental, oceanic or both N89-21386
Assessment of the atmospheric impact of volcanic eruptions N89-21388
Impact and extinction signatures in complete Cretaceous-Tertiary (K-T) boundary sections N89-21391
Mass extinctions in the deep sea N89-21396
Acute effects of a large bolide impact simulated by a global atmospheric circulation model N89-21398
Geochemical comparison of K-T boundaries from the Northern and Southern Hemispheres N89-21400
The causes for geographical variations in OS187/OS186 at the Cretaceous-Tertiary boundary N89-21402
Atmospheric erosion by impacts: An analytic investigation N89-21403
Tektites: Origin as melts produced by the impact of small projectiles onto dry targets N89-21405
Heavy metal toxicity as a kill mechanism in impact caused mass extinctions N89-21406
Darkness after the K-T impact: Effects of soot N89-21411
Impact production of NO and reduced species N89-21413

METEORITE CRATERS
The cratering record in the inner solar system: Implications for earth N89-21292
Implications of asteroid composition for the geochemistry of the ancient terrestrial projectile flux N89-21294
Shocked quartz and more: Impact signatures in K-T boundary clays and claystones N89-21297
Geological remote sensing signatures of terrestrial impact craters N89-21317
Late Eocene impact events recorded in deep-sea sediments N89-21322
The Manson impact structure, a possible site for a Cretaceous-Tertiary (K-T) boundary impact N89-21326
The Karskiy craters are the probable records of catastrophe at the Cretaceous-Tertiary boundary N89-21343
Magnetic reversal spurts: Rain gauges for comet showers N89-21349
Mineralogical and geochemical anomalous data of the K-T boundary samples N89-21359
Flood basalt eruptions, comet showers, and mass extinction events N89-21372
Report on an international workshop on Cryptoexplosions and Catastrophes in the Geological Record, with a Special Focus on the Vredefort Structure N89-21375
Microdeformation in Vredefort rocks; evidence for shock metamorphism N89-21376
Computer modeling of large asteroid impacts into continental and oceanic sites: Atmospheric, cratering, and ejecta dynamics N89-21379
Crater size estimates for large-body terrestrial impact N89-21381
Non-random cratering flux in recent time N89-21384
K-T impact(s): Continental, oceanic or both N89-21386
Tektites: Origin as melts produced by the impact of small projectiles onto dry targets N89-21405
The cometary and asteroidal impactor flux at the earth N89-21407

METEORITES
Implications of asteroid composition for the geochemistry of the ancient terrestrial projectile flux N89-21294
Volcanic ash layers in blue ice fields (Beardmore Glacier Area, Antarctica): Iridium enrichments N89-21340
The causes for geographical variations in OS187/OS186 at the Cretaceous-Tertiary boundary N89-21402
Ion microprobe of Mg, Ca, Ti and Fe isotopic ratios and trace element abundances in hibonite-bearing inclusions from primitive meteorites N89-21719

METEORITIC COMPOSITION
Impact, and its implications for geology N89-21353

METEORITIC DAMAGE
Oblique hypervelocity impact response of dual-sheet structures [NASA-TM-100358] N89-21246

METEOROID CONCENTRATION
Search for the Tunguska event in the Antarctic snow N89-21378

METEOROID PROTECTION
Oblique hypervelocity impact response of dual-sheet structures [NASA-TM-100358] N89-21246

METEOROID SHOWERS
Isotopic investigations in the area of the Tunguska catastrophe in 1908 year N89-21342
Evidence for and implications of an Early Archean terrestrial impact record N89-21348
Magnetic reversal spurts: Rain gauges for comet showers N89-21349

METEOROLOGICAL PARAMETERS
CCM (Community Climate Model) [PB89-120927] N89-21446
Summary of Meteorological Observations, Surface (SMOS) for Moffett Field, California [AD-A203628] N89-21451

METEOROLOGICAL SATELLITES
Enhancements to the AFGL (Air Force Geophysics Laboratory) Statistical Analysis Program (ASAP) for the global multivariate analysis of heights and winds [AD-A202912] N89-21450

METHYL COMPOUNDS
Surface acoustic wave detection of organophosphorus compounds [AD-A202909] N89-21058

METROLOGY
Center for Electronics and Electrical Engineering technical progress bulletin covering center programs, April to June 1988 with 1988 CEEE events calendar [PB89-123137] N89-21170
Center for Atomic, Molecular and Optical Physics technical activities, 1988 [PB89-132302] N89-21623

MICROCOMPUTERS
The 8755 emulator design [AD-A202649] N89-21178

MICROCRACKS
Microscopic observations of adiabatic shear bands in three different steels [AD-A202522] N89-21080

MICROELECTRONICS
A fresh look at transport in perfluorosulfonate ionomers: Ultramicroelectrode investigations of Nafion and Dow ionomers [AD-A203855] N89-21066
The 8755 emulator design [AD-A202649] N89-21178

MICROMETEOROIDS
Search for the Tunguska event in the Antarctic snow N89-21378

MICROPHONES
LCP-10 intelligibility of oxygen masks and microphones in aircraft noise [AD-A202474] N89-21481

MICROSCOPY
Microscopic observations of adiabatic shear bands in three different steels [AD-A202522] N89-21080

MICROSTRIP TRANSMISSION LINES
Analytical and experimental procedures for determining propagation characteristics of millimeter-wave gallium arsenide microstrip lines [NASA-TP-2899] N89-21169

MICROSTRUCTURE
Effect of Te on the microstructural changes during the gray-to-white and white-to-gray transition in directional solidification of Fe-C-Si alloys [DE89-007607] N89-21076
The microstructural and phase characterization of RST Al-Ti-X alloys [AD-A203734] N89-21092
Nb modification of microcomposite Fe/C/Cr/Mn steel [DE89-008297] N89-21097
Mechanisms of fatigue crack propagation and fracture toughness behavior in advanced aluminum-lithium alloys [DE89-008300] N89-21098
Acoustic microscopy of low ductility materials [AERE-R-12848] N89-21101
Pre-pilot synthesis of low carbon Si3N4 [DE89-007202] N89-21124
Diffusion welding of an RS/PM aluminum alloy N89-21241
Deformation modeling and constitutive modeling for anisotropic superalloys [NASA-CR-4215] N89-21258
Structure maps and phase stability in AlTi3 alloyed with rare-earth elements [DE89-005106] N89-21684
Characterization of Nb-Al superconducting material [DE89-008296] N89-21690

MICROWAVE AMPLIFIERS
Demonstration of SQUID parametric amplifier [AD-A203252] N89-21183

MICROWAVE EQUIPMENT
A rapid numerical procedure for determining axisymmetric transverse electric electromagnetic fields via boundary integrals [AD-A202959] N89-21155

MICROWAVE LANDING SYSTEMS
Microwave landing systems: Additional systems should not be procured unless benefits proven [GAO/RCED-88-118] N89-20977

MICROWAVE SPECTRA
The response of single element HgCdTe and InSb solid state infrared detectors to millimeter wave electromagnetic energy
[AD-A202667] N89-21672
MICROWAVE TRANSMISSION
Analytical and experimental procedures for determining propagation characteristics of millimeter-wave gallium arsenide microstrip lines
[NASA-TP-2899] N89-21169
Channelized coplanar waveguide: Discontinuities, junctions, and propagation characteristics
[NASA-TM-101483] N89-21172
MICROWAVES
An analysis of platinum silicide and indium antimonide for remote sensors in the 3 to 5 micrometer wavelength band
[AD-A202663] N89-21218
Behavioral effects of microwaves: Relationship of total dose and dose rate
[PB89-118640] N89-21462
LMS adaptive filtering applied to a microwave arterial pulse monitor
[AD-A202732] N89-21465
MIE SCATTERING
Advanced diagnostics for reacting flows
[AD-A202451] N89-21202
MIGRATION
The effect of mixed-mode loading on stress-driven solute segregation during high-temperature brittle intergranular fracture
[AERE-R-12897] N89-21073
MILITARY AIRCRAFT
The application of CFD for military aircraft design at transonic speeds N89-20930
MILITARY HELICOPTERS
The impact of the US Army's AH-64 helmet mounted display on future aviation helmet design
[AD-A202984] N89-21486
MILITARY OPERATIONS
Optoelectronic workshops. Part 4: Liquid Crystals for Laser Applications
[AD-A202526] N89-21228
Strategic defense initiative: A chronology, 1983 - 1988
[AD-A203576] N89-21619
MILITARY TECHNOLOGY
A modeling perspective for meteor burst communication
[AD-A202562] N89-21145
MILLIMETER WAVES
External electro-optic probing of millimeter-wave integrated circuits
[NASA-TM-101990] N89-21142
Demonstration of SQUID parametric amplifier
[AD-A203252] N89-21183
The response of single element HgCdTe and InSb solid state infrared detectors to millimeter wave electromagnetic energy
[AD-A202667] N89-21672
MINERALOGY
Geological indicators for impact: The anomalous case of the Vredefort structure, South Africa N89-21289
Implications of asteroid composition for the geochemistry of the ancient terrestrial projectile flux N89-21294
Shocked quartz and more: Impact signatures in K-T boundary clays and claystones N89-21297
The Sudbury Structure (Ontario, Canada) and Vredefort Structure (South Africa): A comparison N89-21311
Proterozoic Bushveld-Vredefort catastrophe: Possible causes and consequences N89-21312
Mineralogy and phase-chemistry of the Cretaceous/Tertiary section in the Lattengebirge, Bavarian Alps N89-21323
Mineralogical and geochemical anomalous data of the K-T boundary samples N89-21359
Marine and continental K-T boundary clays compared N89-21382
K-T impact(s): Continental, oceanic or both N89-21386
Impact and extinction signatures in complete Cretaceous-Tertiary (K-T) boundary sections N89-21391
MINERALS
Magnetic microspherules associated with the K/T and upper Eocene extinction events N89-21303
Deccan volcanism at the Cretaceous-Tertiary boundary N89-21305
Mineralogy and phase-chemistry of the Cretaceous/Tertiary section in the Lattengebirge, Bavarian Alps N89-21323
MINIMAX TECHNIQUE
Optimal and robust memoryless discrimination from dependent observations
[AD-A202806] N89-21604
Conditionally and strictly distribution-free tests for randomized block designs that are asymptotically optimal
[CWI-MS-R8802] N89-21615
MIRRORS
Transformations of Gaussian light beams caused by reflection in FEL (Free Electron Lasers) resonators
[AD-A202472] N89-21227
Dynamic fatigue testing of Zerodur glass-ceramic N89-21753
MISALIGNMENT
A robust adaptive array structure using the soft constrained LMS algorithm
[AD-A203959] N89-21167
MIXING
An experimental investigation of flow mixing on thrust ejection efficiency
[AD-A202707] N89-21205
Basic studies of ion mixing
[AD-A203093] N89-21637
MIXTURES
Modelling of the lean flammability limit in flame theory N89-21527
MODELS
Investigation of the development of laminar boundary-layer instabilities along a cooled-wall cone in hypersonic flows
[AD-A202587] N89-20966
Holographic particle sizing in solid fuel ramjets
[AD-A202699] N89-20997
Chemical vapor synthesis of niobium aluminides
[AD-A202591] N89-21055
Investigation of crack growth in titanium-aluminide at elevated temperatures
[AD-A202570] N89-21081
Effective ignition kinetics for LOVA propellant
[AD-A203149] N89-21129
Microwave power amplifier analysis and design
[AD-A203170] N89-21182
A new model for the forced response of a mistuned disk
[AD-A202769] N89-21275
Downward continuation of the free-air gravity anomalies to the ellipsoid using the gradient solution, Poisson's integral and terrain correction-numerical comparison and computations
[AD-A203739] N89-21442
A software system to create a hierarchical, multiple level of detail terrain model
[AD-A203047] N89-21568
Dimensionality of binary items
[AD-A203238] N89-21608
The interdependencies of theory formation, revision, and experimentation
[AD-A202882] N89-21618
Extracting shape reflectance of Lambertian, specular, and hybrid surfaces
[AD-A203772] N89-21652
MODULATION
Investigation of the impedance modulation of thin films with a chemically-sensitive field-effect transistor
[AD-A202766] N89-21180
Turbulence modulation and dense-spray structure
[AD-A202449] N89-21201
MODULES
Preliminary design of a modular unmanned research vehicle. Volume 1: System design document
[AD-A202765] N89-20987
MODULUS OF ELASTICITY
Film elastic properties determined by the indentation test-theoretical considerations
[AD-A203997] N89-21683
MOIRE INTERFEROMETRY
Further studies of the HRR field of a moving crack. An experimental analysis
[AD-A202545] N89-21269
MOLECULAR BEAM EPITAXY
MBE of (Hg,Cd)Te
[AD-A202448] N89-21667
Center for thin film studies
[AD-A202742] N89-21673
MOLECULAR COLLISIONS
Laser enhanced chemical reactions
[DE89-008084] N89-21236
MOLECULAR DIFFUSION
Adhesion in chemically hostile environments: The use of filled polymers as diffusion barriers
[AD-A203333] N89-21121
MOLECULAR ENERGY LEVELS
Excited state energetics and dynamics of large molecules, complexes and clusters
[AD-A203514] N89-21065
MOLECULAR EXCITATION
Excited state energetics and dynamics of large molecules, complexes and clusters
[AD-A203514] N89-21065
MOPAC manual, 5th edition: A general molecular orbital package
[AD-A204003] N89-21069
Time and state resolved studies of molecular decomposition
[AD-A202464] N89-21636
MOLECULAR INTERACTIONS
A NMR (Nuclear Magnetic Resonance) study of the molecular interactions and dynamic behavior in polymer-diluent blends in the solid state
[AD-A202459] N89-21108
MOLECULAR RELAXATION
Atomistic simulations of interfaces in metals and alloys
[DE89-006521] N89-21685
MOLECULAR STRUCTURE
Spectroscopic studies of fluid/solid interfaces
[AD-A202436] N89-21054
Excited state energetics and dynamics of large molecules, complexes and clusters
[AD-A203514] N89-21065
Time and state resolved studies of molecular decomposition
[AD-A202464] N89-21636
MOLECULAR WEIGHT
Prepolymer characterization
[AD-A202821] N89-21115
MOLECULES
MOPAC manual, 5th edition: A general molecular orbital package
[AD-A204003] N89-21069
A NMR (Nuclear Magnetic Resonance) study of the molecular interactions and dynamic behavior in polymer-diluent blends in the solid state
[AD-A202459] N89-21108
Theoretical studies of potential energy storage molecules
[AD-A203986] N89-21638
MONITORS
LMS adaptive filtering applied to a microwave arterial pulse monitor
[AD-A202732] N89-21465
Intelligent data reduction for autonomous power systems N89-21737
MONOMERS
Synthesis of energetic binders
[AD-A203060] N89-21127
MONOPULSE RADAR
On the impulse response of monopulse radars
[AD-A202936] N89-21153
MONTE CARLO METHOD
Response surface analysis of stochastic network performance
[AD-A202561] N89-21554
Distribution of boron atoms in ion implanted compound semiconductors
[AD-A203173] N89-21677
Fluctuation analysis of relativistic nucleus-nucleus collisions in emulsion chambers N89-21747
MORPHOLOGY
Shock-induced chemical synthesis of intermetallic compounds
[DE89-007035] N89-21095
Geological remote sensing signatures of terrestrial impact craters N89-21317
The keyhole region in VPPA welds N89-21755
MORTALITY
Late Wenlock (middle Silurian) bio-events: Caused by volatile boloid impact/s N89-21295
Response of marine and freshwater algae to nitric acid and elevated carbon dioxide levels simulating environmental effects of bolide impact N89-21298
Dinosaur bone beds and mass mortality: Implications for the K-T extinction N89-21301
Mass mortality and extraterrestrial impacts N89-21335
Impact as a general cause of extinction: A feasibility test N89-21374
Volcanoes and global catastrophes N89-21389
MOSSBAUER EFFECT
Martensitic phase transitions in nanocrystalline materials
[AD-A203636] N89-21090
MOTION SICKNESS
A study of motion sickness: Mathematical modeling and data analysis
[AD-A202770] N89-21466
MOTION SICKNESS DRUGS
A study of motion sickness: Mathematical modeling and data analysis
[AD-A202770] N89-21466
MOTOR VEHICLES
Column movement model used to support AMM N89-21521

MOUNTING
Potential flow evaluation of the interference effect of strut-through-appendage-tip model mounting technique and reduction of the effect using blowing and suction
[AD-A202424] N89-21199
MULTIPHASE FLOW
Turbulence modulation and dense-spray structure
[AD-A202449] N89-21201
MULTIPROCESSING (COMPUTERS)
The virtual time machine
[AD-A203087] N89-21533
Time warp on a shared memory multiprocessor
[AD-A203088] N89-21534
A language comparison for scientific computing on MIMD architectures
[NASA-CR-181779] N89-21537
Parallel solution of sparse one-dimensional dynamic programming problems
[NASA-CR-181812] N89-21542
Distributed discrete-event simulation using variants of the Chandy-Misra algorithm on the intel hypercube
[AD-A202849] N89-21563
Advanced information processing system: Local system services
[NASA-CR-181767] N89-21582
FX-87 performance measurements: Dataflow implementation
[AD-A203150] N89-21585
SpringNet: A network of multiprocessors for hard real-time
[AD-A203348] N89-21587
Performance evaluation of parallel algorithms and architectures in concurrent multiprocessor systems
[AD-A203982] N89-21589
Architecture studies and system demonstrations of optical parallel processor for AI (Artificial Intelligence) and NI (Neural Intelligence)
[AD-A203241] N89-21593
MULTISPECTRAL BAND SCANNERS
Ice cover on Chesapeake Bay from AVHRR (Advanced Very High Resolution Radiometer) and LANDSAT imagery, winter of 1987-88
[PB89-117261] N89-21415
MULTIVARIATE STATISTICAL ANALYSIS
A digital rate controller for the control reconfigurable combat aircraft designed using quantitative feedback theory
[AD-A203050] N89-21001
Enhancements to the AFGL (Air Force Geophysics Laboratory) Statistical Analysis Program (ASAP) for the global multivariate analysis of heights and winds
[AD-A202912] N89-21450
MUSCLES
Techniques for studying the effects of microgravity on model particle/cell systems N89-21758
MUSHY ZONES
Computer simulation of macrosegregation in directionally solidified circular ingots
[NASA-CR-182838] N89-21134
MUTATIONS
Effects of simultaneous radiofrequency radiation and chemical exposure of mammalian cells, volume 2
[AD-A202780] N89-21467

N

N-TYPE SEMICONDUCTORS
Laser-induced metal deposition on semiconductors from liquid electrolytes
[AD-A203612] N89-21089
NAMING
Development of the domain name system
[AD-A203901] N89-21703
NAP-OF-THE-EARTH NAVIGATION
AH-1S communication switch integration program
[NASA-TM-101053] N89-20978
NASA PROGRAMS
NASA directions in space propulsion for 2000 and beyond
[NASA-TM-102281] N89-21026
Research and technology objectives and plans summary, fiscal year 1987
[NASA-TM-89241] N89-21761
NASTRAN
VAX to CRAY NASTRAN user interface
[AD-A203447] N89-21575
NATIONAL AIRSPACE SYSTEM
Microwave landing systems: Additional systems should not be procured unless benefits proven
[GAO/RCED-88-118] N89-20977
NAVIER-STOKES EQUATION
Comparison of 3D computation and experiment for non-axisymmetric nozzles
[NASA-CR-182245] N89-20921
Computation of aircraft component flow fields at transonic Mach numbers using a three-dimensional Navier-Stokes algorithm N89-20933
Euler solvers for transonic applications N89-20935
Euler/Navier-Stokes calculations of transonic flow past fixed- and rotary-wing aircraft configurations N89-20948
Navier-Stokes and viscous-inviscid interaction N89-20949
The 3-D Euler and Navier-Stokes calculations for aircraft components N89-20950
Three-dimensional singular points in aerodynamics
[NASA-TM-100045] N89-20964
Thin-layer Navier-Stokes solutions for a cranked delta wing
[AD-A203292] N89-20970
Two-dimensional Navier-Stokes solution of the flow over a thick supercritical airfoil with strong shock-induced separation
[AD-A203331] N89-20971
Computational studies of an impulsively started viscous flow
[NASA-TM-101037] N89-21190
Volumetric rendering techniques for the display of three-dimensional aerodynamic flow field data
[AD-A202661] N89-21204
Whole field measurements of vorticity in turbulent and unsteady flows
[AD-A203349] N89-21209
Numerical solution of parabolic problems in high dimensions N89-21501
Space shuttle main engine numerical modeling code modifications and analysis N89-21760
NERVES
Gating kinetics and ion transfer in channels of nerve membrane
[AD-A202509] N89-21464
NETWORK ANALYSIS
The 8755 emulator design
[AD-A202649] N89-21178
A neural network implementation of chaotic time series prediction
[AD-A203049] N89-21569
Lookahead in parallel discrete event simulation
[AD-A203902] N89-21588
NETWORK CONTROL
A comparison of control variates for queueing network simulation
[AD-A202576] N89-21599
NEURAL NETS
Speech recognition using neural nets and dynamic time warping
[AD-A202528] N89-21144
Problem specific applications for neural networks
[AD-A203052] N89-21158
An analysis of noise reduction using back-propagation neural networks
[AD-A203057] N89-21159
Speech recognition: Acoustic-phonetic knowledge acquisition and representation
[AD-A203081] N89-21160
The Rochester robot
[AD-A202633] N89-21247
Neural networks and the symmetric group S(sub N) N89-21529
Center for the Integration of Optical Computing
[AD-A203254] N89-21536
Optical computing research
[AD-A202963] N89-21564
A neural network implementation of chaotic time series prediction
[AD-A203049] N89-21569
Dynamic analysis of feedforward neural networks using simulated and measured data
[AD-A202573] N89-21591
Modified backward error propagation for tactical target recognition
[AD-A202666] N89-21644
NEUROMUSCULAR TRANSMISSION
Gating kinetics and ion transfer in channels of nerve membrane
[AD-A202509] N89-21464
NEUTRAL ATOMS
A laser trap for neutral atoms
[AD-A202581] N89-21229
NEUTRINOS
Positron line radiation from halo WIMP annihilations as a dark matter signature
[NASA-CR-182918] N89-21635
Supernova 1987A: 18 months later
[NASA-CR-184891] N89-21715
A novel approach to gamma-ray and neutrino astro-particle physics: The GRANDE experiment
[DE89-006515] N89-21725
NEUTRON ACTIVATION ANALYSIS
Isotopic investigations in the area of the Tunguska catastrophe in 1908 year N89-21342
NEUTRON BEAMS
Nuclear-pumped lasers for large-scale applications
[DE89-006532] N89-21235
NEUTRON DIFFRACTION
An in-situ, high-temperature study of the superconductor YBa1.67Sr0.33Cu3O(6+x)
[DE89-007375] N89-21686
NEUTRON SCATTERING
Time-of-flight small-angle neutron scattering data reduction and analysis at LANSCE with program SMR
[DE89-006520] N89-21578
NEUTRON STARS
An optical study of three transient X-ray sources N89-21724
NEUTRONS
Nuclear-pumped lasers for large-scale applications
[DE89-006532] N89-21235
NICKEL ALLOYS
Advanced single crystal for SSME turbopumps
[NASA-CR-182244] N89-21072
NIGHT FLIGHTS (AIRCRAFT)
Helicopter flights with night-vision goggles: Human factors aspects
[NASA-TM-101039] N89-21477
NIGHT VISION
Helicopter flights with night-vision goggles: Human factors aspects
[NASA-TM-101039] N89-21477
Polycarbonate ophthalmic lenses for ametropic Army aviators using night vision goggles
[AD-A203100] N89-21488
NIOBIUM
Chemical vapor synthesis of niobium aluminides
[AD-A202591] N89-21055
Nb modification of microcomposite Fe/C/Cr/Mn steel
[DE89-008297] N89-21097
NIOBIUM ALLOYS
Thermodynamic analysis of chemical compatibility of several reinforcement materials with niobium aluminides
[NASA-CR-182260] N89-21036
Nuclear magnetic resonance study of hydrogen in niobium-vanadium alloys
[DE89-007578] N89-21075
Characterization of Nb-Al superconducting material
[DE89-008296] N89-21690
NITRAMINE PROPELLANTS
Effective ignition kinetics for LOVA propellant
[AD-A203149] N89-21129
NITRIC ACID
Biospheric traumas caused by large impacts and predicted relics in the sedimentary record N89-21371
NITROGEN
Nitrogen geochemistry of a Cretaceous-Tertiary boundary site in New Zealand N89-21320
NITROGEN POLYMERS
MOPAC manual, 5th edition: A general molecular orbital package
[AD-A204003] N89-21069
NITROGEN 15
Nitrogen geochemistry of a Cretaceous-Tertiary boundary site in New Zealand N89-21320
NITROUS OXIDES
Impact production of NO and reduced species N89-21413
NOBLE METALS
Noble metals in mid-ocean ridge volcanism: A significant fractionation of gold with respect to platinum group metals N89-21307
NOISE (SOUND)
Comparison of propeller cruise noise data taken in the NASA Lewis 8- by 6-foot wind tunnel with other tunnel and flight data
[NASA-TM-101976] N89-21628
NOISE REDUCTION
An analysis of noise reduction using back-propagation neural networks
[AD-A203057] N89-21159
A cancellation technique for reducing background noise within turbulent flow environments characterized by pipes and annuli
[AD-A202924] N89-21206
LMS adaptive filtering applied to a microwave arterial pulse monitor
[AD-A202732] N89-21465
LCP-10 intelligibility of oxygen masks and microphones in aircraft noise
[AD-A202474] N89-21481
Attenuation of blast waves using foam and other materials
[AD-A203148] N89-21632

NOISE SPECTRA
An analysis of noise reduction using back-propagation neural networks
[AD-A203057] N89-21159
NONDESTRUCTIVE TESTS
Nondestructive testing techniques for metal matrix composites
[AERE-R-13040] N89-21034
Magnetic mapping of current distributions in two-dimensional electronic devices
[AD-A203035] N89-21220
A study of the stress wave factor technique for evaluation of composite materials
[NASA-CR-4195] N89-21256
Distribution of boron atoms in ion implanted compound semiconductors
[AD-A203173] N89-21677
Evaluate the application of modal test and analysis processes to structural fault detection in MSFC-STS project elements N89-21751
NONEQUILIBRIUM FLOW
A continued study of optical sound generation and amplification
[AD-A202484] N89-21630
NONLINEAR EQUATIONS
The KP equation: A comparison to laboratory generated biperiodic waves N89-21507
Adaptive optical linear algebra processors
[AD-A202996] N89-21605
Numerical solution of nonlinear algebraic equations in stiff ODE solving
[DE89-008264] N89-21613
NONLINEAR FEEDBACK
Flight controller design with nonlinear aerodynamics, large parameter uncertainty and pilot compensation
[AD-A202727] N89-21000
Remote orbital capture using an orbital maneuvering vehicle equipped with a multibody grappling arm assembly
[AD-A202760] N89-21018
NONLINEAR OPTICS
A position, scale and rotation invariant holographic associative memory
[AD-A203289] N89-21221
NONLINEAR PROGRAMMING
Statistical machine learning for the cognitive selection of nonlinear programming algorithms in engineering design optimization N89-21493
NONLINEAR SYSTEMS
Dilatationally nonlinear elastic materials. Part 2: An example illustrating stress concentration reduction
[AD-A202521] N89-21111
Optical power limiter
[AD-A203964] N89-21234
Nonlinear finite element analysis of a general composite shell
[AD-A202572] N89-21271
Dilatationally nonlinear elastic materials. (1): Some theory
[AD-A202824] N89-21276
Application of the Laplace-Borel transformation to the representation of analytical solutions of Duffing's equation
[NASA-TM-100058] N89-21532
Optical information processing in a confocal Fabry-Perot resonator
[AD-A202566] N89-21556
The application of modal coordinate methods to large nonlinear time-dependent problems
[AD-A203913] N89-21611
A continued study of optical sound generation and amplification
[AD-A202484] N89-21630
NONLINEARITY
Dilatationally nonlinear elastic materials. (1): Some theory
[AD-A202824] N89-21276
Lie transforms applied to a nonlinear parametric excitation problem N89-21491
Element level elimination of nonlinear constraints in total Lagrangian finite element formulations N89-21496
On a refined nonlinear theory of laminated composite plates N89-21500
The KP equation: A comparison to laboratory generated biperiodic waves N89-21507
The interaction of nonlinear hyperbolic waves: A conference report N89-21530
NONPARAMETRIC STATISTICS
Order statistics and robust inference
[AD-A203440] N89-21616
NORMAL SHOCK WAVES
An LDA (Laser-Doppler Anemometry) investigation of three-dimensional normal shock wave boundary-layer interactions N89-20956
NORTHERN HEMISPHERE
Geochemical comparison of K-T boundaries from the Northern and Southern Hemispheres N89-21400
Commentary on fast atmospheric pulsations
[AD-A203172] N89-21440
NOTCH SENSITIVITY
Fracture characteristics of balloon films
[NASA-CR-181686] N89-21099
NOZZLE DESIGN
Comparison of 3D computation and experiment for non-axisymmetric nozzles
[NASA-CR-182245] N89-20921
Effect of riblets upon flow separation in a subsonic diffuser
[AD-A203178] N89-20967
Computer codes for thermal analysis of a solid rocket motor nozzle N89-21733
NOZZLE FLOW
An experimental investigation of flow mixing on thrust ejection efficiency
[AD-A202707] N89-21205
NOZZLE GEOMETRY
An experimental investigation of flow mixing on thrust ejection efficiency
[AD-A202707] N89-21205
NUCLEAR BINDING ENERGY
Theoretical studies of potential energy storage molecules
[AD-A203986] N89-21638
NUCLEAR EMULSIONS
Fluctuation analysis of relativistic nucleus-nucleus collisions in emulsion chambers N89-21747
NUCLEAR EXPLOSION EFFECT
Acute effects of a large bolide impact simulated by a global atmospheric circulation model N89-21398
NUCLEAR EXPLOSIONS
Effects of global atmospheric perturbations on forest ecosystems: Predictions of seasonal and cumulative effects N89-21399
NUCLEAR FUSION
Diffusion in symplectic maps
[DE89-008083] N89-21622
Surface energy from order parameter profile: At the QCD phase transition
[NASA-CR-184890] N89-21633
Supernova 1987A: 18 months later
[NASA-CR-184891] N89-21715
NUCLEAR MAGNETIC RESONANCE
Nuclear magnetic resonance study of hydrogen in niobium-vanadium alloys
[DE89-007578] N89-21075
A NMR (Nuclear Magnetic Resonance) study of the molecular interactions and dynamic behavior in polymer-diluent blends in the solid state
[AD-A202459] N89-21108
Modern multiple-pulse, high field NMR studies of high density jet fuels
[AD-A203320] N89-21130
Applications, dosimetry and biological interactions of static and time-varying magnetic fields
[DE89-006944] N89-21627
NUCLEAR PUMPING
Nuclear-pumped lasers for large-scale applications
[DE89-006532] N89-21235
NUCLEAR REACTIONS
Nuclear-pumped lasers for large-scale applications
[DE89-006532] N89-21235
NUCLEAR WARFARE
SDI (Strategic Defense Initiative) and national security policy
[AD-A202730] N89-21617
NUMERICAL ANALYSIS
Wave drag due to lift for transonic airplanes N89-20938
A rapid numerical procedure for determining axisymmetric transverse electric electromagnetic fields via boundary integrals
[AD-A202959] N89-21155
A numerical study of the turbulent free convection in rectangular cavities N89-21194
Instabilities in shear flow of viscoelastic fluids with fading memory
[AD-A203735] N89-21211
Stress intensity factors for bodies containing initial stress N89-21263
Implementation of equivalent domain integral method in the two-dimensional analysis of mixed mode problems
[NASA-CR-181813] N89-21267
Application of the boundary element method to fatigue crack growth analysis
[AD-A202565] N89-21270
Downward continuation of the free-air gravity anomalies to the ellipsoid using the gradient solution, Poisson's integral and terrain correction-numerical comparison and computations
[AD-A203739] N89-21442
Best ordering for floating-point addition
[AD-A203990] N89-21612
An optimal scale for edge detection
[AD-A202747] N89-21646
The determination of Crystallite Orientation Distribution Functions (CODF) and their use in surface texture analysis using X-ray diffraction
[AERE-R-12839] N89-21663
Variable wall temperature effects on multicellular natural convection in a horizontal annulus
[AD-A202762] N89-21691
Numerical studies of gas flow in spiral galaxies N89-21718
Transient natural convection heat and mass transfer in crystal growth N89-21741
Investigation of practical applications of H infinity control theory to the design of control systems for large space structures N89-21743
Electron mobility in mercury cadmium telluride N89-21748
NUMERICAL INTEGRATION
Computational studies of an impulsively started viscous flow
[NASA-TM-101037] N89-21190
Some issues of numerical integration and penalty relaxation in anisoparametric shell element formulation N89-21518
NUMERICAL WEATHER FORECASTING
The role of radiation-dynamics interaction in regional numerical weather prediction N89-21732

O

OBLIQUENESS
Oblique impacts: Catastrophic vs. protracted effects N89-21383
OCEAN BOTTOM
Possible world-wide middle miocene iridium anomaly and its relationship to periodicity of impacts and extinctions N89-21291
Magnetic microspherules associated with the K/T and upper Eocene extinction events N89-21303
An extended Cretaceous-Tertiary (K/T) stable isotope record. Implications for paleoclimate and the nature of the K/T boundary event N89-21310
Late Eocene impact events recorded in deep-sea sediments N89-21322
Seawater strontium isotopes at the Cretaceous-Tertiary boundary N89-21350
K-T impact(s): Continental, oceanic or both N89-21386
Mass extinctions in the deep sea N89-21396
Macrofossil extinction patterns at Bay of Biscay Cretaceous-Tertiary boundary sections N89-21404
The Cretaceous-Tertiary boundary marine extinction and global primary productivity collapse N89-21412
OCEAN CURRENTS
Ocean energy program summary. Volume 1, Overview: Fiscal year 1988
[DE89-000858] N89-21421
OCEAN DYNAMICS
Volcanism, global catastrophe and mass mortality N89-21316
Cretaceous-Tertiary boundary in the Antarctic: Climatic cooling precedes biotic crisis N89-21392
OCEAN MODELS
Ocean alkalinity and the Cretaceous/Tertiary boundary N89-21300
Abrupt climate change and extinction events N89-21308
OCEAN SURFACE
Imaging of ocean waves by SAR
[AD-A203604] N89-21165
OSRMS (Ocean Surface Roughness Measurement System): The DREP (Defence Research Establishment Pacific) near-nadir scatterometer
[AD-A202983] N89-21460
OCEAN THERMAL ENERGY CONVERSION
Ocean energy program summary. Volume 1, Overview: Fiscal year 1988
[DE89-000858] N89-21421
OCEANS
Localizing and beamforming freely-drifting VLF (Very Low Frequency) acoustic sensors
[AD-A202638] N89-21217
Infrared sea-radiance modeling using LOWTRAN 6
[AD-A202582] N89-21643
ON-LINE SYSTEMS
Evaluation of the high temperature materials information analysis center online numeric database
[AD-A202900] N89-21700

OPERATIONAL CALCULUS
Application of the Laplace-Borel transformation to the representation of analytical solutions of Duffing's equation
[NASA-TM-100058] N89-21532
OPERATIONS RESEARCH
Light satellites: A dilemma for the US Army
[AD-A202648] N89-21017
Computational issues in goal programming resource allocation N89-21509
Triangularity of the basis in linear programs for material requirements planning, revision
[AD-A203039] N89-21606
Computer assisted analysis and modelling of structured problems
[AD-A203040] N89-21607
OPERATORS (MATHEMATICS)
Spectral analysis of a fourth-order singular differential operator arising in combustion
[DE89-005841] N89-21052
OPHTHALMOLOGY
Polycarbonate ophthalmic lenses for ametropic Army aviators using night vision goggles
[AD-A203100] N89-21488
OPTICAL ACTIVITY
Optical activity and its influence on photorefractive materials
[AD-A202530] N89-21642
OPTICAL COMMUNICATION
Optical communication with semiconductor laser diode
[NASA-CR-184817] N89-21141
Low-cost Pointing-and-Tracking System for Optical Communications (PATSOC)
[AD-A202921] N89-21151
Application of a single area array detector for acquistion, tracking and point-ahead in space optical communications
[NASA-CR-183423] N89-21168
OPTICAL COMPUTERS
Center for the Integration of Optical Computing
[AD-A203254] N89-21536
Optical computing research
[AD-A202963] N89-21564
Architecture studies and system demonstrations of optical parallel processor for AI (Artificial Intelligence) and NI (Neural Intelligence)
[AD-A203241] N89-21593
Adaptive optical linear algebra processors
[AD-A202996] N89-21605
OPTICAL COUPLING
Laser beam coupling via optical phase conjugation in BaTiO3
[AD-A202874] N89-21231
OPTICAL DATA PROCESSING
Center for the Integration of Optical Computing
[AD-A203254] N89-21536
Optical information processing in a confocal Fabry-Perot resonator
[AD-A202566] N89-21556
Optical computing research
[AD-A202963] N89-21564
Devices and systems for nonlinear optical information processing
[AD-A203034] N89-21566
Nonlinear real-time optical signal processing
[AD-A202445] N89-21641
OPTICAL EQUIPMENT
Low-cost Pointing-and-Tracking System for Optical Communications (PATSOC)
[AD-A202921] N89-21151
Superresolved imaging using the Hartley transform and a hemispherical object space
[AD-A202527] N89-21551
Devices and systems for nonlinear optical information processing
[AD-A203034] N89-21566
Nonlinear real-time optical signal processing
[AD-A202445] N89-21641
NASA Marshall Space Flight Center solar observatory report, January - December 1987
[NASA-TM-100360] N89-21712
OPTICAL FIBERS
Immunoassay procedures for fiber optic sensors
[AD-A203069] N89-21649
OPTICAL MEASURING INSTRUMENTS
Immunoassay procedures for fiber optic sensors
[AD-A203069] N89-21649
OPTICAL MEMORY (DATA STORAGE)
Center for the Integration of Optical Computing
[AD-A203254] N89-21536
Optical information processing in a confocal Fabry-Perot resonator
[AD-A202566] N89-21556
OPTICAL PROPERTIES
Adapting Schottky diode detector technology to a space platform
[AD-A202825] N89-21219
Optical power limiter
[AD-A203964] N89-21234
Three dimensional effects near a crack tip in a ductile three point bend specimen. Part 2: An experimental investigation using interferometry and caustics
[AD-A202637] N89-21272
Optical activity and its influence on photorefractive materials
[AD-A202530] N89-21642
Two photon characterization
[AD-A203355] N89-21678
An optical study of three transient X-ray sources N89-21724
OPTICAL RADAR
Analysis of space-based lidar for aircraft tracking
[AD-A202665] N89-21230
Utility of a dual-lidar method to measure integrated extinction
[AD-A203145] N89-21439
ER-2 lidar observations from the October 1986 fire cirrus experiment
[NASA-TM-100704] N89-21444
OPTICAL REFLECTION
Transformations of Gaussian light beams caused by reflection in FEL (Free Electron Lasers) resonators
[AD-A202472] N89-21227
OPTICAL TRACKING
Low-cost Pointing-and-Tracking System for Optical Communications (PATSOC)
[AD-A202921] N89-21151
OPTIMAL CONTROL
Computer simulation of a pilot in V/STOL aircraft control loops
[NASA-CR-184815] N89-21479
Numerical solution of parabolic problems in high dimensions N89-21501
OPTIMIZATION
Performance optimization for rotors in hover and axial flight
[NASA-CR-177524] N89-20973
Integrated aerodynamic/dynamic optimization of helicopter rotor blades
[NASA-TM-101553] N89-20982
Time optimal slewing of flexible spacecraft N89-21014
The 8755 emulator design
[AD-A202649] N89-21178
Diffusion welding of an RS/PM aluminum alloy N89-21241
Dynamic structural optimization and experiment
[PB89-111462] N89-21259
Optimal design of a two-way conductor N89-21499
Optimal and robust memoryless discrimination from dependent observations
[AD-A202806] N89-21604
Optimization of large matrix calculations for execution on the Cray X-MP vector supercomputer N89-21742
ORBIT PERTURBATION
Control system for maintaining stable orbits around phobos
[AD-A202776] N89-21008
Hypersurface insertion window for long term orbital stability of artificial satellites about the planet Venus
[AD-A202808] N89-21009
Earth orbital variations and vertebrate bioevolution N89-21357
ORBIT TRANSFER VEHICLES
Optimal launch time for a discontinuous low thrust orbit transfer
[AD-A202693] N89-21007
Guidance for an aeroassisted orbital transfer vehicle N89-21740
ORBITAL MANEUVERING VEHICLES
Remote orbital capture using an orbital maneuvering vehicle equipped with a multibody grappling arm assembly
[AD-A202760] N89-21018
ORBITAL MECHANICS
Stability solution to linearized equations of motion for a symmetric spinning satellite in an elliptical orbit applied to the non-linear equations
[AD-A202934] N89-21010
Analysis of space-based lidar for aircraft tracking
[AD-A202665] N89-21230
Guidance for an aeroassisted orbital transfer vehicle N89-21740
ORBITAL POSITION ESTIMATION
Estimated satellite cluster elements in near circular orbit
[AD-A202938] N89-21011
ORDER-DISORDER TRANSFORMATIONS
Electronic structure and properties of defect complexes in metals
[AD-A203657] N89-21091
ORGANIC CHEMISTRY
Organic chemistry in two dimensions: Surface-functionalized polymers and self-assembled monolayer films
[AD-A202955] N89-21118
ORGANIC PHOSPHORUS COMPOUNDS
Surface acoustic wave detection of organophosphorus compounds
[AD-A202909] N89-21058
ORGANISMS
Limitations on K-T mass extinction theories based upon the vertebrate record N89-21290
The Triassic-Jurassic boundary in eastern North America N89-21366
Mass extinctions in the deep sea N89-21396
ORTHOTROPIC PLATES
Bending and vibration of variable thickness orthotropic plates N89-21264
OSCILLATORS
Time-discretized moments of a randomly excited uncertain linear oscillator
[DE89-008318] N89-21614
OSMIUM
The causes for geographical variations in OS187/OS186 at the Cretaceous-Tertiary boundary N89-21402
OSMIUM ISOTOPES
Provenance of the K/T boundary layers N89-21331
OVERPRESSURE
Explosive volcanism, shock metamorphism and the K-T boundary N89-21309
OXIDATION
Studies of the initial oxidation of Fe-Si alloys by AES, XPS, EELS and LEED
[DE89-007610] N89-21077
Experimental results on atomic oxygen corrosion of silver N89-21738
OXIDATION RESISTANCE
Evaluation of atomic oxygen resistant protective coatings for fiberglass-epoxy composites in LEO
[NASA-TM-101955] N89-21100
Electrolytic protection against high-temperature oxidation
[AD-A203890] N89-21123
OXYGEN
Theoretical studies of the chemistry and physics of oxygen in silicon
[AD-A203168] N89-21063
OXYGEN ATOMS
Evaluation of atomic oxygen resistant protective coatings for fiberglass-epoxy composites in LEO
[NASA-TM-101955] N89-21100
Experimental results on atomic oxygen corrosion of silver N89-21738
The measurement of angular differential cross sections at the SSL Atomic Scattering Facility N89-21744
OXYGEN IONS
Simulation of the low earth orbital atomic oxygen interaction with materials by means of an oxygen ion beam
[NASA-TM-101971] N89-21104
OZONE
Air quality and forest health issues in the 1990s
[DE89-006941] N89-21427
Pulmonary function studies in the rat addressing concentration versus time relationships of ozone (O3)
[PB89-129050] N89-21461
OZONE DEPLETION
Assessment of the atmospheric impact of volcanic eruptions N89-21388

P

P-N JUNCTIONS
Laser-induced metal deposition on semiconductors from liquid electrolytes
[AD-A203612] N89-21089
P-TYPE SEMICONDUCTORS
Laser-induced metal deposition on semiconductors from liquid electrolytes
[AD-A203612] N89-21089
Continued development and characterization of doped layers, contacts and associated electronic devices in silicon carbide
[AD-A202450] N89-21176
PALEOBIOLOGY
Origination, diversity, and extinction metrics essential for analysis of mass biotic crisis events: An example from cretaceous ammonoidea N89-21304
PALEOCLIMATOLOGY
Plant microfossil record of the terminal Cretaceous event in the western United States and Canada N89-21363

Climatic changes resulting from mass extinctions at the K-T boundary (and other bio-events) N89-21373

PALEOMAGNETISM

Deccan volcanism at the Cretaceous-Tertiary boundary N89-21305

Diachronism between extinction time of terrestrial and marine dinosaurs N89-21325

High resolution chronology of late Cretaceous-early Tertiary events determined from 21,000 yr orbital-climatic cycles in marine sediments N89-21328

PALEONTOLOGY

Deccan volcanism at the Cretaceous-Tertiary boundary N89-21305

An extended Cretaceous-Tertiary (K/T) stable isotope record. Implications for paleoclimate and the nature of the K/T boundary event N89-21310

The impact of mass extinctions N89-21315

Volcanism, global catastrophe and mass mortality N89-21316

The Frasnian-Famennian mass killing event(s), methods of identification and evaluation N89-21318

The Western North American Cretaceous-Tertiary (K-T) boundary interval and its content of shock-metamorphosed minerals: Implications concerning the K-T boundary impact-extinction theory N89-21334

Cretaceous-Tertiary findings, paradigms and problems N89-21364

The Triassic-Jurassic boundary in eastern North America N89-21366

A regional perspective on the palynofloral response to K-T boundary event(s) with emphasis on variations imposed by the effects of sedimentary facies and latitude N89-21395

PANEL METHOD (FLUID DYNAMICS)

Investigation of a free-tip rotor configuration for research on spanwise life distributions and wake velocity surveys of a semi-span wing with a discontinuous twist [NASA-CR-184948] N89-20963

PANELS

Physical and mechanical properties of American Cyanamid's acetylene-terminated prepreg system: T-300/CATB-44 [AD-A203737] N89-21045

Vibration and buckling characteristics of composite cylindrical panels incorporating the effects of a higher order shear theory [AD-A202939] N89-21278

PARABOLIC DIFFERENTIAL EQUATIONS

Numerical solution of parabolic problems in high dimensions N89-21501

An adaptive overlapping local grid refinement method for two-dimensional parabolic systems N89-21514

A language comparison for scientific computing on MIMD architectures [NASA-CR-181779] N89-21537

PARALLEL COMPUTERS

The virtual time machine [AD-A203087] N89-21533

PARALLEL PROCESSING (COMPUTERS)

A block QR factorization scheme for loosely coupled systems of array processors N89-21519

Lookahead in parallel discrete event simulation [AD-A203902] N89-21588

The causality horizon and parallel processing for simulations with wide geographical dispersions [DE89-006484] N89-21590

Architecture studies and system demonstrations of optical parallel processor for AI (Artificial Intelligence) and NI (Neural Intelligence) [AD-A203241] N89-21593

Triangularity of the basis in linear programs for material requirements planning, revision [AD-A203039] N89-21606

PARALLEL PROGRAMMING

The virtual time machine [AD-A203087] N89-21533

A language comparison for scientific computing on MIMD architectures [NASA-CR-181779] N89-21537

Parallel solution of sparse one-dimensional dynamic programming problems [NASA-CR-181812] N89-21542

Nonprocedural implementation of mathematical programming algorithms [AD-A203392] N89-21573

FX-87 performance measurements: Dataflow implementation [AD-A203150] N89-21585

Performance evaluation of parallel algorithms and architectures in concurrent multiprocessor systems [AD-A203982] N89-21589

Architecture studies and system demonstrations of optical parallel processor for AI (Artificial Intelligence) and NI (Neural Intelligence) [AD-A203241] N89-21593

PARAMETER IDENTIFICATION

Calculation of the glass transition temperatures of linear polymers. Part 3: Evaluation of calculation relationships [AD-A203357] N89-21122

Characterization of structural connections using free and forced response test data [NASA-TM-101991] N89-21266

PARAMETERIZATION

Relationships of earthquakes (and earthquake-associated mass movements) and polar motion as determined by Kalman filtered, Very-Long-Baseline-Interferometry [NASA-TM-100711] N89-21430

Algorithms for rational spline curves N89-21502

PARAMETRIC AMPLIFIERS

Demonstration of SQUID parametric amplifier [AD-A203252] N89-21183

PARTIAL DIFFERENTIAL EQUATIONS

A numerical study of the turbulent free convection in rectangular cavities N89-21194

Polynominal definition of discrete field point of map of diffusion equation N89-21511

Adaptive optical linear algebra processors [AD-A202996] N89-21605

PARTICLE EMISSION

Mechanisms for the source and loss of electrons [AD-A203066] N89-21438

PARTICLE ENERGY

Optical power limiter [AD-A203964] N89-21234

PARTICLE INTERACTIONS

Basic studies of ion mixing [AD-A203093] N89-21637

PARTICLE SIZE DISTRIBUTION

Holographic particle sizing in solid fuel ramjets [AD-A202699] N89-20997

Automatic measurement of particles from holograms taken in the combustion chamber of a rocket motor [AD-A203955] N89-21030

Holographic investigation of solid propellant combustion [AD-A203928] N89-21067

Evaluation of aerosol size distribution models [AD-A202736] N89-21645

PARTICULATES

Iridium emissions from Hawaiian volcanoes N89-21314

PASCAL (PROGRAMMING LANGUAGE)

Image processing language, phase 2 [AD-A203994] N89-21577

PATTERN RECOGNITION

Modern multiple-pulse, high field NMR studies of high density jet fuels [AD-A203320] N89-21130

Computer strategy for detecting line features on simulated binary arrays in support of radar feature extraction [AD-A203257] N89-21162

Statistical machine learning for the cognitive selection of nonlinear programming algorithms in engineering design optimization N89-21493

Model-based silhouette recognition [AD-A202540] N89-21552

Image processing language, phase 2 [AD-A203994] N89-21577

Dynamic analysis of feedforward neural networks using simulated and measured data [AD-A202573] N89-21591

Hybrid calculation of invariant moments [AD-A202594] N89-21600

Nonlinear real-time optical signal processing [AD-A202445] N89-21641

PATTERSON MAP

Structure maps and phase stability in AlTi3 alloyed with rare-earth elements [DE89-005106] N89-21684

PEEK

A study of failure characteristics in a thermoplastic composite material at high temperature [AD-A203015] N89-21040

PENCIL BEAMS

A generalized approach to direction finding [AD-A203768] N89-21166

PENDULUMS

Stabilization of Ziegler's pendulum by means of the method of vibrational control N89-21531

PENETRATION

Condition of the finite element stiffness matrix of highly irregular triangular grids N89-21497

A simple analysis of swage autofrettage process N89-21498

PERCEPTUAL ERRORS

Problem specific applications for neural networks [AD-A203052] N89-21158

PERFORMANCE PREDICTION

Performance optimization for rotors in hover and axial flight [NASA-CR-177524] N89-20973

Nonlinear rotorcraft analysis-experimental and analytical [AD-A203967] N89-20990

High capacity demonstration of honeycomb panel heat pipes [NASA-CR-181776] N89-21191

Modeling robot dynamic performance for endpoint force control [AD-A202881] N89-21251

Review and analysis of the literature in the area of human performance modeling [DE89-006800] N89-21480

Column movement model used to support AMM N89-21521

Performance directed simulation [AD-A203089] N89-21570

A performance/loss evaluation of SSME HPFTP turbine N89-21735

Simulation of water vapor condensation on LOX droplet surface using liquid nitrogen N89-21749

SSME propulsion performance reconstruction techniques N89-21752

Rotordynamic analysis of a bearing tester N89-21759

PERFORMANCE TESTS

A study of transonic drag reduction of a blunt cylinder by a cylinder probe [AD-A202557] N89-20965

High density fuel effects [AD-A202426] N89-21125

A comparison of reflector antenna designs for wide-angle scanning [NASA-TM-101459] N89-21138

Fouling tests of AGT-1500 gas turbine fuel nozzles [AD-A203360] N89-21253

Corona wind cooling comparisons for horizontal cylinders [AD-A202714] N89-21625

A performance/loss evaluation of SSME HPFTP turbine N89-21735

SSME propulsion performance reconstruction techniques N89-21752

Rotordynamic analysis of a bearing tester N89-21759

PERIODIC VARIATIONS

Possible world-wide middle miocene iridium anomaly and its relationship to periodicity of impacts and extinctions N89-21291

Astrophysical implications of periodicity N89-21361

Periodicity of extinction: A 1988 update N89-21385

PERIPHERAL VISION

Peripheral limitations on spatial vision [AD-A203388] N89-21472

PERMITTIVITY

Accurate determination of the complex permittivity of biological tissue around 35 GHz [AD-A202907] N89-21470

PERSONAL COMPUTERS

GRAPS (Graphical Plotting System) user's guide. A graphical plotting system for displaying scientific and engineering data [AD-A202583] N89-21559

PERSONNEL

Measurer's handbook: US Army anthropometric survey, 1987-1988 [AD-A202721] N89-21484

Empirical demonstration of isoperformance methodology preparatory of an interactive expert computerized decision aid [AD-A202439] N89-21545

PERTURBATION

Time optimal slewing of flexible spacecraft N89-21014

The response of a laminar boundary layer in supersonic flow to small amplitude progressive waves [NASA-TM-101965] N89-21197

Lie transforms applied to a nonlinear parametric excitation problem N89-21491

The numerical simulation of Richtmyer-Meshkov unstable interfaces: A conference report N89-21512

PERTURBATION THEORY

Variable wall temperature effects on multicellular natural convection in a horizontal annulus [AD-A202762] N89-21691

PESTICIDES

Development and characterization of a fiber optic immuno biosensor [DE89-005062] N89-21225

PETROGRAPHY

Explosive volcanism, shock metamorphism and the K-T boundary N89-21309

PHASE CHANGE MATERIALS
Conjugating binary systems for spacecraft thermal control
[NASA-CR-183608] N89-21023
Thermomechanical analysis with phase transformations: A unified approach
[AD-A203383] N89-21692
PHASE CONJUGATION
Laser beam coupling via optical phase conjugation in BaTiO3
[AD-A202874] N89-21231
PHASE TRANSFORMATIONS
Effect of Te on the microstructural changes during the gray-to-white and white-to-gray transition in directional solidification of Fe-C-Si alloys
[DE89-007607] N89-21076
Martensitic phase transitions in nanocrystalline materials
[AD-A203636] N89-21090
Structural energy differences in Al3Ti: The role of tetragonal distortion in APB and twin energies
[DE89-007210] N89-21096
Molecular jet studies of vdW (van der Waals) clusters and solvation
[AD-A203766] N89-21212
A new class of non-topological solitons
[NASA-CR-184889] N89-21634
Thermomechanical analysis with phase transformations: A unified approach
[AD-A203383] N89-21692
PHASE VELOCITY
Turbulence modulation and dense-spray structure
[AD-A202449] N89-21201
PHASED ARRAYS
Effect of two-body motion on radar beam quality for various distributed sparse array configurations
[AD-A202937] N89-21154
PHONEMES
Speech database development
[AD-A202461] N89-21699
PHONETICS
Speech recognition: Acoustic-phonetic knowledge acquisition and representation
[AD-A203081] N89-21160
Speech database development
[AD-A202461] N89-21699
PHOTOCHEMICAL REACTIONS
Photochemistry at corrugated thin metal films: A phenomenological approach
[AD-A203070] N89-21061
PHOTODIODES
Optical communication with semiconductor laser diode
[NASA-CR-184817] N89-21141
PHOTODISSOCIATION
Time and state resolved studies of molecular decomposition
[AD-A202464] N89-21636
PHOTOELECTRON SPECTROSCOPY
Degradation and crosslinking of perfluoroalkyl polyethers under X-ray irradiation in ultrahigh vacuum
[NASA-TP-2910] N89-21103
PHOTOIONIZATION
A laser trap for neutral atoms
[AD-A202581] N89-21229
PHOTOLUMINESCENCE
Electron paramagnetic resonance and photoluminescence studies of impurities in CdTe
[AD-A202841] N89-21056
PHOTOMETRY
Luminosity variations of stars similar to the sun
[AD-A203864] N89-21713
PHOTORECEPTORS
Peripheral limitations on spatial vision
[AD-A203388] N89-21472
PHOTOSPHERE
Force-free magnetic fields: Is there a loss of equilibrium
[AD-A203030] N89-21717
PHYSICAL CHEMISTRY
Topics in chemical physics. 1: Semiclassical reactive scattering theory. 2: Corrected effective medium theory
[DE89-007606] N89-21053
PHYSIOLOGICAL EFFECTS
Pulmonary function studies in the rat addressing concentration versus time relationships of ozone (O3)
[PB89-129050] N89-21461
PHYSIOLOGICAL RESPONSES
Proximal ecological effects of the 1980 eruptions of Mount St. Helens N89-21394
PHYTOPLANKTON
Selective extinction of marine plankton at the end of the Mesozoic era: The fossil and stable isotope record N89-21329
PIEZOELECTRICITY
Robotic tactile sensor fabricated from piezoelectric polyvinylidene fluoride films
[AD-A202724] N89-21250
PILOT PERFORMANCE
AH-1S communication switch integration program
[NASA-TM-101053] N89-20978
Response equivocation analysis for the smart stick controller
[AD-A203146] N89-20989
Helicopter flights with night-vision goggles: Human factors aspects
[NASA-TM-101039] N89-21477
Computer simulation of a pilot in V/STOL aircraft control loops
[NASA-CR-184815] N89-21479
Capacity of human operator using smart stick controller
[AD-A202712] N89-21483
PINS
Mild wear in dry and lubricated sliding systems N89-21242
PIPE FLOW
Coherent structures in fully developed turbulent pipe flow N89-21195
A cancellation technique for reducing background noise within turbulent flow environments characterized by pipes and annuli
[AD-A202924] N89-21206
PIPES (TUBES)
A cancellation technique for reducing background noise within turbulent flow environments characterized by pipes and annuli
[AD-A202924] N89-21206
Incompressible flow friction coefficients in a simulated heat pipe
[AD-A203176] N89-21207
PLANAR STRUCTURES
Research on acoustic coupling to electromagnetic pulses in tissue
[AD-A195644] N89-21140
The boundary-integral method for planar microstrip circuits
[AD-A203715] N89-21185
PLANETARY WAVES
Symmetry breaking bifurcations and the growth of chaos in a rotating fluid
[AD-A204010] N89-21213
PLANETS
Risk to civilization: A planetary science perspective N89-21302
PLANKTON
Extended period of K/T boundary mass extinction in the marine realm N89-21337
The Cretaceous-Tertiary boundary biotic crisis in the Basque country N89-21345
The Cretaceous-Tertiary boundary marine extinction and global primary productivity collapse N89-21412
PLANNING
Defense technical information center's role in numeric database development
[AD-A202901] N89-21701
PLASMA ARC WELDING
The keyhole region in VPPA welds N89-21755
PLASMA CONTROL
Short wave electron temperature gradient driven drift wave turbulence
[DE89-008465] N89-21662
PLASMA DIAGNOSTICS
Advanced diagnostics for reacting flows
[AD-A202451] N89-21202
PLASMA GENERATORS
Plasma reaction method and apparatus
[DE89-007360] N89-21656
PLASMA GUNS
Initiative for the 21st century: Advanced space power and propulsion based on lasers
[DE89-008034] N89-21031
PLASMA HEATING
Theoretical studies of the heating of toroidal plasmas with radiofrequency electromagnetic radiation
[DE89-008003] N89-21660
PLASMA JETS
Plasma reaction method and apparatus
[DE89-007360] N89-21656
PLASMA PHYSICS
Center for Atomic, Molecular and Optical Physics technical activities, 1988
[PB89-132302] N89-21623
Surface energy from order parameter profile: At the QCD phase transition
[NASA-CR-184890] N89-21633
Space plasma contractor research, 1988
[NASA-CR-182283] N89-21658
PLASMA WAVES
Short wave electron temperature gradient driven drift wave turbulence
[DE89-008465] N89-21662
PLASMAS (PHYSICS)
Derivation and testing of computer algorithms for automatic real-time determination of space vehicle potentials in various plasma environments
[AD-A203019] N89-21019
Surface energy from order parameter profile: At the QCD phase transition
[NASA-CR-184890] N89-21633
Sample introduction techniques for inductively coupled plasma mass spectrometry
[DE89-005724] N89-21655
Numerical modeling of narrow band soft X-ray sources
[AD-A203368] N89-21657
PLASMONS
Study of semiconductor valence plasmon line shapes via electron energy-loss spectroscopy in the transmission electron microscope
[DE89-008152] N89-21689
PLASTIC DEFORMATION
A simple analysis of swage autofrettage process N89-21498
Documentation of the finite element code VISCOT/UX for thermomechanical analyses: Version 0.01
[DE89-004719] N89-21544
Thermomechanical analysis with phase transformations: A unified approach
[AD-A203383] N89-21692
PLASTICIZERS
A NMR (Nuclear Magnetic Resonance) study of the molecular interactions and dynamic behavior in polymer-diluent blends in the solid state
[AD-A202459] N89-21108
PLASTICS
Calculation of the glass transition temperatures of linear polymers. Part 3: Evaluation of calculation relationships
[AD-A203357] N89-21122
PLATES (STRUCTURAL MEMBERS)
Analytical and experimental investigation of constrained viscoelastic layer damping for a plate and shell model
[AD-A202698] N89-21273
PLATES (TECTONICS)
The interpretation of crustal dynamics data in terms of plate motions and regional deformation near plate boundaries
[NASA-CR-180077] N89-21436
A comprehensive study of the seismotectonics of the eastern Aleutian arc and associated volcanic systems
[DE89-007357] N89-21443
PLATINUM
Noble metals in mid-ocean ridge volcanism: A significant fractionation of gold with respect to platinum group metals N89-21307
PLATINUM COMPOUNDS
An analysis of platinum silicide and indium antimonide for remote sensors in the 3 to 5 micrometer wavelength band
[AD-A202663] N89-21218
PLOTTING
GRAPS (Graphical Plotting System) user's guide. A graphical plotting system for displaying scientific and engineering data
[AD-A202583] N89-21559
PLY ORIENTATION
Effect of geometry on thermal aging behavior of Celion/LARC-160 composites
[NASA-TM-100496] N89-21047
POINT DEFECTS
The effect of mixed-mode loading on stress-driven solute segregation during high-temperature brittle intergranular fracture
[AERE-R-12897] N89-21073
POINTING CONTROL SYSTEMS
RCS/linear discrete actuator study
[AD-A202822] N89-21028
Analytical model of a five degree of freedom magnetic suspension and positioning system
[NASA-TM-100671] N89-21136
Application of a single area array detector for acquistion, tracking and point-ahead in space optical communications
[NASA-CR-183423] N89-21168
POISSON RATIO
The implementation of a nonreflecting boundary into the SAMSON2 code
[AD-A203394] N89-21284
POLAR REGIONS
Derivation and testing of computer algorithms for automatic real-time determination of space vehicle potentials in various plasma environments
[AD-A203019] N89-21019
POLARITY
The keyhole region in VPPA welds N89-21755

POLARIZED ELECTROMAGNETIC RADIATION
The response of single element HgCdTe and InSb solid state infrared detectors to millimeter wave electromagnetic energy
[AD-A202667] N89-21672
POLICIES
NASA directions in space propulsion for 2000 and beyond
[NASA-TM-102281] N89-21026
SDI (Strategic Defense Initiative) and national security policy
[AD-A202730] N89-21617
Strategic defense initiative: A chronology, 1983 - 1988
[AD-A203576] N89-21619
Fusion: A necessary component of US energy policy
[DE89-006234] N89-21659
National space policy
[AD-A202644] N89-21711
POLYATOMIC MOLECULES
Laser enhanced chemical reactions
[DE89-008084] N89-21236
POLYBUTADIENE
Prepolymer characterization
[AD-A202821] N89-21115
POLYCARBONATES
A NMR (Nuclear Magnetic Resonance) study of the molecular interactions and dynamic behavior in polymer-diluent blends in the solid state
[AD-A202459] N89-21108
Polycarbonate ophthalmic lenses for ametropic Army aviators using night vision goggles
[AD-A203100] N89-21488
POLYESTER RESINS
Nonlinear finite element analysis of a general composite shell
[AD-A202572] N89-21271
POLYETHER RESINS
Degradation and crosslinking of perfluoroalkyl polyethers under X-ray irradiation in ultrahigh vacuum
[NASA-TP-2910] N89-21103
POLYETHYLENES
Fracture characteristics of balloon films
[NASA-CR-181686] N89-21099
POLYIMIDE RESINS
High temperature composites using Schiff's base pyropolymer matrices
[AD-A203311] N89-21043
POLYMERIC FILMS
Fracture characteristics of balloon films
[NASA-CR-181686] N89-21099
POLYMERIZATION
Compressive properties of high performance polymeric fibers
[AD-A202947] N89-21117
POLYNOMIALS
Algorithms for rational spline curves N89-21502
Polynominal definition of discrete field point of map of diffusion equation N89-21511
A very simple polynomial-time algorithm for linear programming
[AD-A202502] N89-21548
POLYSTYRENE
A NMR (Nuclear Magnetic Resonance) study of the molecular interactions and dynamic behavior in polymer-diluent blends in the solid state
[AD-A202459] N89-21108
Prepolymer characterization
[AD-A202821] N89-21115
POLYURETHANE RESINS
Adhesion in chemically hostile environments: The use of filled polymers as diffusion barriers
[AD-A203333] N89-21121
POPULATION THEORY
Dimensionality of binary items
[AD-A203238] N89-21608
POPULATIONS
The impact of mass extinctions N89-21315
The Frasnian-Famennian mass killing event(s), methods of identification and evaluation N89-21318
Late Eocene impact events recorded in deep-sea sediments N89-21322
POROSITY
Comparison of airfoil results from an adaptive wall test section and a porous wall test section N89-20960
POROUS MATERIALS
A model for interface temperatures induced by convection heat transfer in porous materials
[DE89-006202] N89-21214
POSITION (LOCATION)
Acoustic emission source location in fibre reinforced plastic composites
[AERE-R-13039] N89-21035
Analytical model of a five degree of freedom magnetic suspension and positioning system
[NASA-TM-100671] N89-21136
POSITION SENSING
Experiments in end-point control of manipulators with elastic drives N89-21240
POSITRON ANNIHILATION
Positron line radiation from halo WIMP annihilations as a dark matter signature
[NASA-CR-182918] N89-21635
POTASSIUM
A laser trap for neutral atoms
[AD-A202581] N89-21229
POTENTIAL ENERGY
Element level elimination of nonlinear constraints in total Lagrangian finite element formulations N89-21496
Theoretical studies of potential energy storage molecules
[AD-A203986] N89-21638
POTENTIAL FLOW
Potential flow evaluation of the interference effect of strut-through-appendage-tip model mounting technique and reduction of the effect using blowing and suction
[AD-A202424] N89-21199
POTENTIAL THEORY
Vector potential methods N89-20939
POWDER (PARTICLES)
XRAYL: A powder diffraction profile refinement program
[PB89-127567] N89-21050
Martensitic phase transitions in nanocrystalline materials
[AD-A203636] N89-21090
POWDER METALLURGY
The properties of advanced aluminium alloy systems N89-21074
The microstructural and phase characterization of RST Al-Ti-X alloys
[AD-A203734] N89-21092
POWER AMPLIFIERS
Microwave power amplifier analysis and design
[AD-A203170] N89-21182
POWER LIMITERS
Channelized coplanar waveguide: Discontinuities, junctions, and propagation characteristics
[NASA-TM-101483] N89-21172
Optical power limiter
[AD-A203964] N89-21234
PRANDTL NUMBER
The role of the turbulent Prandtl number in turbine blade heat transfer prediction N89-21756
PREAMPLIFIERS
Demonstration of SQUID parametric amplifier
[AD-A203252] N89-21183
PRECAMBRIAN PERIOD
Geological indicators for impact: The anomalous case of the Vredefort structure, South Africa N89-21289
Proterozoic Bushveld-Vredefort catastrophe: Possible causes and consequences N89-21312
The Manson impact structure, a possible site for a Cretaceous-Tertiary (K-T) boundary impact N89-21326
PRECIPITATION (METEOROLOGY)
Summary of Meteorological Observations, Surface (SMOS) for Moffett Field, California
[AD-A203628] N89-21451
PRECIPITATION PARTICLE MEASUREMENT
Precipitating ion and electron detectors (SSJ/4) for the block 5D/Flight 8 DMSP (Defense Meteorological Satellite Program) satellite
[AD-A203999] N89-21022
Mechanisms for the source and loss of electrons
[AD-A203066] N89-21438
PREDICTION ANALYSIS TECHNIQUES
Investigation of a free-tip rotor configuration for research on spanwise life distributions and wake velocity surveys of a semi-span wing with a discontinuous twist
[NASA-CR-184948] N89-20963
Two-dimensional Navier-Stokes solution of the flow over a thick supercritical airfoil with strong shock-induced separation
[AD-A203331] N89-20971
Frequency dependent ultrasonic ray tracing: A preliminary study
[AERE-R-13119] N89-21139
Imaging of ocean waves by SAR
[AD-A203604] N89-21165
Studies in the computation of compressible and viscous flow
[AD-A203334] N89-21208
Enhancements to the AFGL (Air Force Geophysics Laboratory) Statistical Analysis Program (ASAP) for the global multivariate analysis of heights and winds
[AD-A202912] N89-21450
Blending of surface and rawinsonde data in mesoscale objective analysis
[AD-A203984] N89-21456
A neural network implementation of chaotic time series prediction
[AD-A203049] N89-21569
Dynamic fatigue testing of Zerodur glass-ceramic N89-21753
The role of the turbulent Prandtl number in turbine blade heat transfer prediction N89-21756
PREDICTIONS
Proximal ecological effects of the 1980 eruptions of Mount St. Helens N89-21394
The KP equation: A comparison to laboratory generated biperiodic waves N89-21507
PREPOLYMERS
Prepolymer characterization
[AD-A202821] N89-21115
PREPREGS
Physical and mechanical properties of American Cyanamid's acetylene-terminated prepreg system: T-300/CATB-44
[AD-A203737] N89-21045
PRESSURE BREATHING
G-induced loss of consciousness and its prevention
[AD-A202960] N89-21471
PRESSURE DISTRIBUTION
Inverse wing design in transonic flow including viscous interaction N89-20947
Methodology for using steady experimental aerodynamic data to improve steady and unsteady aerodynamic analysis N89-20972
A cancellation technique for reducing background noise within turbulent flow environments characterized by pipes and annuli
[AD-A202924] N89-21206
Computer program for calculating frequencies and modal structures of free coastal-trapped waves
[PB88-243928] N89-21459
PRESSURE GRADIENTS
Stability of compressible boundary layers N89-20953
Incompressible flow friction coefficients in a simulated heat pipe
[AD-A203176] N89-21207
PRESSURE MEASUREMENT
A cancellation technique for reducing background noise within turbulent flow environments characterized by pipes and annuli
[AD-A202924] N89-21206
PRESSURE PULSES
Implications of pressure diffusion for shock waves
[NASA-CR-184858] N89-21198
A continued study of optical sound generation and amplification
[AD-A202484] N89-21630
PRESSURE VESSELS
Investigation of Weibull statistics in fracture analysis of cast aluminum
[NASA-TM-102000] N89-21245
An investigation of stresses and strains in an internally pressurized, composite-jacketed, steel cylinder
[AD-A202969] N89-21281
PRIMITIVE EARTH ATMOSPHERE
New approach to the origin of the tektite in China N89-21414
PROBABILITY DISTRIBUTION FUNCTIONS
Time delay estimation in stationary and non-stationary environments
[AD-A202507] N89-21549
Rootfinding for Markov chains with quasi-triangular transition matrices
[AD-A202468] N89-21597
PROBABILITY THEORY
Icing considerations for HALE (High Altitude, Long Endurance) aircraft
[AD-A202584] N89-20975
Space Propulsion Hazards Analysis Manual (SPHAM), volume 1
[AD-A203204] N89-21029
Risk to civilization: A planetary science perspective N89-21302
PROBLEM SOLVING
Hypersonic drone design: A multidisciplinary experience
[NASA-CR-184740] N89-20981
Confidence set inference with a prior quadratic bound
[NASA-CR-184839] N89-21435
Numerical solution of parabolic problems in high dimensions N89-21501
A language comparison for scientific computing on MIMD architectures
[NASA-CR-181779] N89-21537
Architecture and design for a laser programmable double precision floating point application specific processor
[AD-A202560] N89-21553
Development of a prototype commonality analysis tool for use in space programs N89-21757
PROCUREMENT
Empirical demonstration of isoperformance methodology preparatory of an interactive expert computerized decision aid
[AD-A202439] N89-21545

PRODUCTION ENGINEERING
Incorporating five nations' operational requirements into a single aircraft: The F-16 multinational fighter program viewed from the operational side
[AD-A202552] N89-20986
PRODUCTION PLANNING
Triangularity of the basis in linear programs for material requirements planning, revision
[AD-A203039] N89-21606
PRODUCTIVITY
Ocean alkalinity and the Cretaceous/Tertiary boundary N89-21300
An extended Cretaceous-Tertiary (K/T) stable isotope record. Implications for paleoclimate and the nature of the K/T boundary event N89-21310
The Cretaceous-Tertiary boundary marine extinction and global primary productivity collapse N89-21412
PROGRAM VERIFICATION (COMPUTERS)
Transonics and fighter aircraft: Challenges and opportunities for CFD N89-20932
A source code analyzer to predict compilation time for avionics software using software science measures. Volume 1: Main report
[AD-A202737] N89-20992
Design of a syntax validation tool for requirements analysis using Structured Analysis and Design Technique (SADT)
[AD-A202725] N89-21562
A theory of problem domains and program correctness
[DE89-008451] N89-21580
PROGRAMMING LANGUAGES
HOP (Hardware viewed as Objects and Processes): A process model for synchronous hardware systems
[AD-A203090] N89-21535
Objects as closures: Abstract semantics of object oriented languages
[NASA-CR-184877] N89-21540
Deductive programming
[AD-A202489] N89-21546
TABLOG: The deductive tableau programming language
[AD-A202490] N89-21547
Grasp: A graph specification language
[AD-A202524] N89-21550
Semantical paradigms: Notes for an invited lecture
[AD-A202995] N89-21565
A software system to create a hierarchical, multiple level of detail terrain model
[AD-A203047] N89-21568
FX-87 performance measurements: Dataflow implementation
[AD-A203150] N89-21585
PROJECT MANAGEMENT
Institute for Computational Mechanics in Propulsion (ICOMP)
[NASA-TM-101961] N89-21595
Analysis of the Federal Aviation Administration's host computer acquisition process and potential application in Department of Defense acquisitions
[AD-A202623] N89-21695
PROPAGATION MODES
An analysis of noise reduction using back-propagation neural networks
[AD-A203057] N89-21159
Implications of pressure diffusion for shock waves
[NASA-CR-184858] N89-21198
PROPANE
The effect of platinum catalysts on propane oxidation at elevated pressure
[AD-A202999] N89-21060
PROPELLANT COMBUSTION
Magnetic flowmeter measurement of solid propellant pressure-coupled and velocity-coupled responses
[AD-A203988] N89-21133
PROPELLANT TRANSFER
Robotic compliant motion control for aircraft refueling applications
[AD-A202710] N89-21249
PROPELLANTS
Prepolymer characterization
[AD-A202821] N89-21115
PROPELLERS
Comparison of propeller cruise noise data taken in the NASA Lewis 8- by 6-foot wind tunnel with other tunnel and flight data
[NASA-TM-101976] N89-21628
PROPULSION SYSTEM CONFIGURATIONS
Institute for Computational Mechanics in Propulsion (ICOMP)
[NASA-TM-101961] N89-21595
PROPULSION SYSTEM PERFORMANCE
Transonic propulsion system integration analysis at McDonnell Aircraft Company N89-20943
Initiative for the 21st century: Advanced space power and propulsion based on lasers
[DE89-008034] N89-21031
PROTECTIVE CLOTHING
Thermal protection afforded by two anti-exposure coveralls when worn in cold water
[AD-A202865] N89-21485
PROTECTIVE COATINGS
Evaluation of atomic oxygen resistant protective coatings for fiberglass-epoxy composites in LEO
[NASA-TM-101955] N89-21100
Electrolytic protection against high-temperature oxidation
[AD-A203890] N89-21123
PROTOCOL (COMPUTERS)
The interdependencies of theory formation, revision, and experimentation
[AD-A202882] N89-21618
PROTOPLANETS
Atmospheric erosion by impacts: An analytic investigation N89-21403
PROTOTYPES
Critical problems in very large scale computer systems
[AD-A203299] N89-21586
Development of a prototype commonality analysis tool for use in space programs N89-21757
PSEUDONOISE
Analysis and simulation of a pseudonoise synchronization system
[AD-A202779] N89-21149
PSYCHOLOGICAL FACTORS
Risk to civilization: A planetary science perspective N89-21302
PSYCHOLOGY
Coping with novelty and human intelligence: The role of counterfactual reasoning
[AD-A203624] N89-21478
PSYCHOMOTOR PERFORMANCE
Coping with novelty and human intelligence: The role of counterfactual reasoning
[AD-A203624] N89-21478
PSYCHOPHYSICS
Psychophysical studies of visual cortical functions
[AD-A202814] N89-21468
Peripheral limitations on spatial vision
[AD-A203388] N89-21472
PULMONARY FUNCTIONS
Pulmonary function studies in the rat addressing concentration versus time relationships of ozone (O3)
[PB89-129050] N89-21461
PULSE COMMUNICATION
Optical communication with semiconductor laser diode
[NASA-CR-184817] N89-21141
PULSE POSITION MODULATION
Optical communication with semiconductor laser diode
[NASA-CR-184817] N89-21141
PULSE RATE
LMS adaptive filtering applied to a microwave arterial pulse monitor
[AD-A202732] N89-21465
PULSES
Study of the generation of intense pulsed electron beams using glow discharges
[AD-A202438] N89-21624
Analysis and simulation of an audio adaptive equalizer
[AD-A202569] N89-21631
PUMP SEALS
Advanced helium purge seals for Liquid Oxygen (LOX) turbopumps
[NASA-CR-182105] N89-21239
PYRANOMETERS
Thermopile temperature sensitivity calibration procedure for Eppley broadband radiometers
[PB89-104129] N89-21215
PYROLYSIS
The global Cretaceous-Tertiary fire: Biomass or fossil carbon N89-21321

Q

QUADRATIC EQUATIONS
Performance of an adaptive matched filter using the Griffiths algorithm
[AD-A202578] N89-21147
A very simple polynomial-time algorithm for linear programming
[AD-A202502] N89-21548
QUALITATIVE ANALYSIS
Hydrogen segregation to grain boundaries and external surfaces
[AD-A202892] N89-21084
QUALITY CONTROL
Prepolymer characterization
[AD-A202821] N89-21115
QUANTUM CHEMISTRY
Excited state energetics and dynamics of large molecules, complexes and clusters
[AD-A203514] N89-21065
QUANTUM CHROMODYNAMICS
Surface energy from order parameter profile: At the QCD phase transition
[NASA-CR-184890] N89-21633
Fluctuation analysis of relativistic nucleus-nucleus collisions in emulsion chambers N89-21747
QUANTUM EFFICIENCY
An analysis of platinum silicide and indium antimonide for remote sensors in the 3 to 5 micrometer wavelength band
[AD-A202663] N89-21218
QUANTUM THEORY
Lagrangian formulation of relativistic thermodynamics N89-21526
MBE of (Hg,Cd)Te
[AD-A202448] N89-21667
QUARKS
Surface energy from order parameter profile: At the QCD phase transition
[NASA-CR-184890] N89-21633
QUARTZ
Shocked quartz and more: Impact signatures in K-T boundary clays and claystones N89-21297
Explosive volcanism, shock metamorphism and the K-T boundary N89-21309
Cathodoluminescence of shocked quartz at the Cretaceous-Tertiary boundary N89-21369
Microdeformation in Vredefort rocks; evidence for shock metamorphism N89-21376
QUARTZ CRYSTALS
Martensitic phase transitions in nanocrystalline materials
[AD-A203636] N89-21090
QUASARS
The 408 MHz radio observations of a quasar sample N89-21714
QUEUEING THEORY
Nonparamteric estimation from queues arising in staggered entry clinical trials N89-21520
A comparison of control variates for queueing network simulation
[AD-A202576] N89-21599

R

RADAR
A theoretical and experimental investigation of linear and nonlinear focussing chirped optical diffraction gratings
[AD-A203396] N89-21650
RADAR BEAMS
Effect of two-body motion on radar beam quality for various distributed sparse array configurations
[AD-A202937] N89-21154
RADAR CROSS SECTIONS
The radar cross section of a two dimensional dielectric coated cylinder using on-surface radiation conditions
[AD-A202935] N89-21152
RADAR DETECTION
Spectral characteristics of High Frequency (HF) backscatter for high latitude ionospheric irregularities: Preliminary analysis of statistical properties
[AD-A202998] N89-21156
RADAR EQUIPMENT
On the impulse response of monopulse radars
[AD-A202936] N89-21153
RADAR IMAGERY
Computer strategy for detecting line features on simulated binary arrays in support of radar feature extraction
[AD-A203257] N89-21162
Imaging of ocean waves by SAR
[AD-A203604] N89-21165
RADAR MEASUREMENT
Combined VHF Doppler radar and airborne (CV-990) measurements of atmospheric winds on the mesoscale
[NASA-CR-184953] N89-21449
RADAR RANGE
Response surface methodology applied to the radar range equation
[AD-A203044] N89-21157
RADAR RECEIVERS
A rapid-backscatter simulation technique for complex B-spline target models N89-21505
RADAR SIGNATURES
Rapid backscatter simulation techniques for detailed B-spline target models
[AD-A203260] N89-21163
A rapid-backscatter simulation technique for complex B-spline target models N89-21505

RADAR TARGETS
A rapid-backscatter simulation technique for complex B-spline target models N89-21505
RADAR TRACKING
Rapid backscatter simulation techniques for detailed B-spline target models
[AD-A203260] N89-21163
ER-2 lidar observations from the October 1986 fire cirrus experiment
[NASA-TM-100704] N89-21444
A rapid-backscatter simulation technique for complex B-spline target models N89-21505
RADIANCE
Excitation and diagnostics of optical contamination in the spacecraft environment
[AD-A202429] N89-21015
Infrared sea-radiance modeling using LOWTRAN 6
[AD-A202582] N89-21643
A numerical model for the computation of radiance distributions in natural waters with wind-roughened surfaces. Part 2: User's guide and code listing
[AD-A203441] N89-21651
RADIATION DAMAGE
Applications, dosimetry and biological interactions of static and time-varying magnetic fields
[DE89-006944] N89-21627
Fast acting optical beam deflection system
[AD-A203042] N89-21648
RADIATION DETECTORS
A novel approach to gamma-ray and neutrino astro-particle physics: The GRANDE experiment
[DE89-006515] N89-21725
RADIATION DOSAGE
Behavioral effects of microwaves: Relationship of total dose and dose rate
[PB89-118640] N89-21462
Effects of simultaneous radiofrequency radiation and chemical exposure of mammalian cells, volume 2
[AD-A202780] N89-21467
Applications, dosimetry and biological interactions of static and time-varying magnetic fields
[DE89-006944] N89-21627
RADIATION EFFECTS
Reentry response of the light weight radioisotope heater unit resulting from a Venus-Earth-Earth gravity assist maneuver accident
[DE89-005359] N89-21024
Evaluation of atomic oxygen resistant protective coatings for fiberglass-epoxy composites in LEO
[NASA-TM-101955] N89-21100
Degradation and crosslinking of perfluoroalkyl polyethers under X-ray irradiation in ultrahigh vacuum
[NASA-TP-2910] N89-21103
Behavioral effects of microwaves: Relationship of total dose and dose rate
[PB89-118640] N89-21462
Effects of simultaneous radiofrequency radiation and chemical exposure of mammalian cells, volume 2
[AD-A202780] N89-21467
Radiation effect on rocket engine performance N89-21734
RADIATION PROTECTION
People's Republic of China laser radiation safety standard
[AD-A203777] N89-21233
RADIATION SPECTRA
The spectroscopy and energy transfer kinetics of the interhalogens
[AD-A202954] N89-21059
RADIATION TOLERANCE
Effects of simultaneous radiofrequency radiation and chemical exposure of mammalian cells, volume 2
[AD-A202780] N89-21467
RADICALS
Flow reactor studies of elementary radical reaction rates
[AD-A203126] N89-21062
RADIO COMMUNICATION
A modeling perspective for meteor burst communication
[AD-A202562] N89-21145
RADIO FREQUENCY HEATING
Theoretical studies of the heating of toroidal plasmas with radiofrequency electromagnetic radiation
[DE89-008003] N89-21660
RADIO JETS (ASTRONOMY)
The 408 MHz radio observations of a quasar sample N89-21714
RADIO WAVES
Effects of simultaneous radiofrequency radiation and chemical exposure of mammalian cells, volume 2
[AD-A202780] N89-21467
RADIOACTIVE ISOTOPES
Reentry response of the light weight radioisotope heater unit resulting from a Venus-Earth-Earth gravity assist maneuver accident
[DE89-005359] N89-21024
RADIOACTIVITY
Isotopic investigations in the area of the Tunguska catastrophe in 1908 year N89-21342
RADIOCHEMICAL SEPARATION
Iridium abundance measurements across bio-event horizons in the geological record N89-21368
RADIOCHEMISTRY
Noble metals in mid-ocean ridge volcanism: A significant fractionation of gold with respect to platinum group metals N89-21307
RADIOMETERS
Thermopile temperature sensitivity calibration procedure for Eppley broadband radiometers
[PB89-104129] N89-21215
RAIN
A 3-dimensional numerical simulation of the atmospheric injection of aerosols by a hypothetical basaltic fissure eruption N89-21401
RANDOM PROCESSES
A randomness property of m-sequences N89-21524
RANDOM VARIABLES
Conditionally and strictly distribution-free tests for randomized block designs that are asymptotically optimal
[CWI-MS-R8802] N89-21615
RANKING
Computational issues in goal programming resource allocation N89-21509
RARE EARTH ALLOYS
Low temperature properties of ternary magnetic rare earth transition metal germanides with the Sc5Co4Ge10-type structure
[DE89-007628] N89-21666
RAWINSONDES
Blending of surface and rawinsonde data in mesoscale objective analysis
[AD-A203984] N89-21456
RAY TRACING
Frequency dependent ultrasonic ray tracing: A preliminary study
[AERE-R-13119] N89-21139
RAYLEIGH SCATTERING
Finite-difference modeling of Rayleigh wave scattering and P-SV(Lg) coupling problems
[AD-A203221] N89-21161
RDX
Effect of TNT miscible additives on the mechanical behavior and shock sensitivity of Composition B
[AD-A203968] N89-21132
REACTION KINETICS
Excitation and diagnostics of optical contamination in the spacecraft environment
[AD-A202429] N89-21015
Fluids, both ionic and nonionic, over wide ranges of temperature and composition
[DE89-001265] N89-21048
Theoretical studies of heterogeneous reactions in silicon CVD (Silicon Vapor Deposition) catalysis
[AD-A202905] N89-21057
Flow reactor studies of elementary radical reaction rates
[AD-A203126] N89-21062
Calculation of the energetics of chemical reactions
[DE89-007262] N89-21070
Fuels combustion research
[AD-A204161] N89-21071
Organic functional group reactivities at metal surfaces
[AD-A203094] N89-21086
Effect of TNT miscible additives on the mechanical behavior and shock sensitivity of Composition B
[AD-A203968] N89-21132
Nuclear-pumped lasers for large-scale applications
[DE89-006532] N89-21235
Explosive volcanism, shock metamorphism and the K-T boundary N89-21309
Experimental results on atomic oxygen corrosion of silver N89-21738
REACTIVITY
Research on silicon, carbon, and silicon carbide heterostructures
[AD-A202866] N89-21116
Deformation, fracture and explosive properties of reactive materials
[AD-A203083] N89-21128
REACTOR TECHNOLOGY
Fusion: A necessary component of US energy policy
[DE89-006234] N89-21659
REAL TIME OPERATION
Real-time display of time dependent data using a head-mounted display
[AD-A203051] N89-20993
A vectorized hidden-surface algorithm implemented on the Cray-2 supercomputer
[AD-A202657] N89-21560
SpringNet: A network of multiprocessors for hard real-time
[AD-A203348] N89-21587
RECEIVERS
Low-cost Pointing-and-Tracking System for Optical Communications (PATSOC)
[AD-A202921] N89-21151
Demonstration of SQUID parametric amplifier
[AD-A203252] N89-21183
Time delay estimation in stationary and non-stationary environments
[AD-A202507] N89-21549
RECONNAISSANCE SPACECRAFT
Light satellites: A dilemma for the US Army
[AD-A202648] N89-21017
RECORDING
Adapting Schottky diode detector technology to a space platform
[AD-A202825] N89-21219
RECTANGULAR PANELS
Effects of battle damage repair on the natural frequencies and mode shapes of curved rectangular composite panels
[AD-A203179] N89-21041
RECTANGULAR PLATES
Finite element analysis of composite plates including shear deformation
[AD-A202941] N89-21279
REDUCED GRAVITY
Convection and chemistry effects in CVD: A 3-D analysis for silicon deposition
[NASA-TM-102001] N89-21032
Cryogenic fluid management in space N89-21727
Techniques for studying the effects of microgravity on model particle/cell systems N89-21758
REDUNDANCY
Advanced information processing system: Local system services
[NASA-CR-181767] N89-21582
REENTRY VEHICLES
Reentry response of the light weight radioisotope heater unit resulting from a Venus-Earth-Earth gravity assist maneuver accident
[DE89-005359] N89-21024
REFLECTANCE
Analytical and experimental procedures for determining propagation characteristics of millimeter-wave gallium arsenide microstrip lines
[NASA-TP-2899] N89-21169
Infrared sea-radiance modeling using LOWTRAN 6
[AD-A202582] N89-21643
Extracting shape reflectance of Lambertian, specular, and hybrid surfaces
[AD-A203772] N89-21652
REFLECTED WAVES
Transformations of Gaussian light beams caused by reflection in FEL (Free Electron Lasers) resonators
[AD-A202472] N89-21227
REFLECTOR ANTENNAS
A comparison of reflector antenna designs for wide-angle scanning
[NASA-TM-101459] N89-21138
REFRACTORY MATERIALS
High temperature evaluation of new ferroelastic toughened ceramic materials
[AD-A203197] N89-21120
Evaluation of the high temperature materials information analysis center online numeric database
[AD-A202900] N89-21700
REFUELING
Robotic compliant motion control for aircraft refueling applications
[AD-A202710] N89-21249
REGENERATIVE FUEL CELLS
Cryogenic reactant storage for lunar base regenerative fuel cells
[NASA-TM-101980] N89-21419
REGRESSION ANALYSIS
Holographic particle sizing in solid fuel ramjets
[AD-A202699] N89-20997
A comparison of variable selection criteria for multiple linear regression: A simulation study
[AD-A202708] N89-21601
REGULATIONS
Aviation safety: Measuring how safely individual airlines operate
[GAO/RCED-88-61] N89-20974
REINFORCED PLASTICS
Effect of geometry on thermal aging behavior of Celion/LARC-160 composites
[NASA-TM-100496] N89-21047

REINFORCING FIBERS
High temperature composites using Schiff's base pyropolymer matrices
[AD-A203311] N89-21043
Investigation of failure modes in fiber reinforced ceramic matrix composites
[AD-A202705] N89-21113
The shear-lag model for a unidirectional composite with viscoelastic matrix N89-21495
RELATIVISTIC EFFECTS
Time warp on a shared memory multiprocessor
[AD-A203088] N89-21534
Fluctuation analysis of relativistic nucleus-nucleus collisions in emulsion chambers N89-21747
RELAXATION (MECHANICS)
The interpretation of crustal dynamics data in terms of plate motions and regional deformation near plate boundaries
[NASA-CR-180077] N89-21436
RELAXATION METHOD (MATHEMATICS)
Dynamic structural optimization and experiment
[PB89-111462] N89-21259
RELIABILITY
Reliability/maintainability/testability design for dormancy
[AD-A202704] N89-21179
RELIABILITY ANALYSIS
Large sample theory for statistical inference in several software reliability models
[CWI-MS-R8807] N89-21543
REMOTE SENSING
Geological remote sensing signatures of terrestrial impact craters N89-21317
The Frasnian-Famennian mass killing event(s), methods of identification and evaluation N89-21318
REMOTE SENSORS
An analysis of platinum silicide and indium antimonide for remote sensors in the 3 to 5 micrometer wavelength band
[AD-A202663] N89-21218
REMOTELY PILOTED VEHICLES
Tailless aircraft performance improvements with relaxed static stability
[NASA-CR-181806] N89-20999
REMOVAL
Performance of the active sidewall boundary-layer removal system for the Langley 0.3-meter Transonic Cryogenic Tunnel
[NASA-CR-181793] N89-21004
REPRESENTATIONS
The GL(2n-1,R) spherical representations of SL(2n,R)
[ZW-8802] N89-21621
REPTILES
Diachronism between extinction time of terrestrial and marine dinosaurs N89-21325
REPUBLIC OF SOUTH AFRICA
Geological indicators for impact: The anomalous case of the Vredefort structure, South Africa N89-21289
REQUIREMENTS
Incorporating five nations' operational requirements into a single aircraft: The F-16 multinational fighter program viewed from the operational side
[AD-A202552] N89-20986
Optoelectronic workshops. Part 4: Liquid Crystals for Laser Applications
[AD-A202526] N89-21228
Design of a syntax validation tool for requirements analysis using Structured Analysis and Design Technique (SADT)
[AD-A202725] N89-21562
An analysis of the biennial budget process
[AD-A202626] N89-21710
RESEARCH
Attenuation of blast waves using foam and other materials
[AD-A203148] N89-21632
RESEARCH AIRCRAFT
Simulation at Dryden Flight Research Facility from 1957 to 1982
[NASA-TM-101695] N89-20983
Preliminary design of a modular unmanned research vehicle. Volume 1: System design document
[AD-A202765] N89-20987
RESEARCH AND DEVELOPMENT
Electric energy systems energy storage
[DE88-007217] N89-21418
Center for Atomic, Molecular and Optical Physics technical activities, 1988
[PB89-132302] N89-21623
Research and technology objectives and plans summary, fiscal year 1987
[NASA-TM-89241] N89-21761
RESEARCH FACILITIES
Institute for Computational Mechanics in Propulsion (ICOMP)
[NASA-TM-101961] N89-21595
NASA Marshall Space Flight Center solar observatory report, January - December 1987
[NASA-TM-100360] N89-21712
The measurement of angular differential cross sections at the SSL Atomic Scattering Facility N89-21744
RESEARCH MANAGEMENT
Flight research and testing N89-20927
Contributive research in compound semiconductor material and related devices
[AD-A202586] N89-21670
Research and technology objectives and plans summary, fiscal year 1987
[NASA-TM-89241] N89-21761
RESEARCH VEHICLES
Preliminary design of a modular unmanned research vehicle. Volume 1: System design document
[AD-A202765] N89-20987
RESIDUAL STRESS
Stress-corrosion cracking of liquid-phase sintered tungsten alloys
[AD-A203201] N89-21087
A simple analysis of swage autofrettage process N89-21498
RESIN MATRIX COMPOSITES
Improved high-temperature resistant matrix resins
[NASA-CR-180826] N89-21105
RESONANCE
Accurate determination of the complex permittivity of biological tissue around 35 GHz
[AD-A202907] N89-21470
RESONANCE FLUORESCENCE
Flow reactor studies of elementary radical reaction rates
[AD-A203126] N89-21062
RESONANT FREQUENCIES
Effects of battle damage repair on the natural frequencies and mode shapes of curved rectangular composite panels
[AD-A203179] N89-21041
On the conditions for resonance interactions of instability waves in the axisymmetric jet
[NASA-TM-101477] N89-21196
Lie transforms applied to a nonlinear parametric excitation problem N89-21491
RESONANT VIBRATION
A new model for the forced response of a mistuned disk
[AD-A202769] N89-21275
RESONATORS
Optical information processing in a confocal Fabry-Perot resonator
[AD-A202566] N89-21556
RESPIRATORY SYSTEM
Pulmonary function studies in the rat addressing concentration versus time relationships of ozone (O3)
[PB89-129050] N89-21461
RESPONSES
Response surface analysis of stochastic network performance
[AD-A202561] N89-21554
REUSABLE LAUNCH VEHICLES
An analytical framework for determining life cycle cost implications of the advanced launch system
[AD-A202873] N89-21012
RIBLETS
Effect of riblets upon flow separation in a subsonic diffuser
[AD-A203178] N89-20967
RIGID ROTORS
Nonlinear rotorcraft analysis-experimental and analytical
[AD-A203967] N89-20990
RIGID STRUCTURES
A triangular thin shell element for the linear analysis of stiffened composite structures
[AD-A202864] N89-21277
RISK
Space Propulsion Hazards Analysis Manual (SPHAM), volume 1
[AD-A203204] N89-21029
Risk to civilization: A planetary science perspective N89-21302
A methodology for screening potential artificial intelligence applications
[AD-A203966] N89-21594
ROBOTICS
Experiments in end-point control of manipulators with elastic drives N89-21240
Robotic compliant motion control for aircraft refueling applications
[AD-A202710] N89-21249
Robotic tactile sensor fabricated from piezoelectric polyvinylidene fluoride films
[AD-A202724] N89-21250
ROBOTS
The Rochester robot
[AD-A202633] N89-21247
Robotic compliant motion control for aircraft refueling applications
[AD-A202710] N89-21249
Modeling robot dynamic performance for endpoint force control
[AD-A202881] N89-21251
ROBUSTNESS (MATHEMATICS)
Actuation constraints in multivariable flight control systems N89-20998
Soft constrained LMS algorithms: A robust procedure for signal misalignment
[AD-A203880] N89-21187
Optimal and robust memoryless discrimination from dependent observations
[AD-A202806] N89-21604
Order statistics and robust inference
[AD-A203440] N89-21616
ROCKET ENGINE CASES
Three dimensional thermal analysis of rocket thrust chambers
[NASA-TM-101973] N89-21025
X-ray fluorescence surface contaminant analyzer: A feasibility study N89-21736
ROCKET EXHAUST
Operational implications of a cloud model simulation of space shuttle exhaust clouds in different atmospheric conditions
[NASA-CR-4222] N89-21425
ROCKS
The Triassic-Jurassic boundary in eastern North America N89-21366
ROOTS OF EQUATIONS
Rootfinding for Markov chains with quasi-triangular transition matrices
[AD-A202468] N89-21597
ROSSBY REGIMES
Symmetry breaking bifurcations and the growth of chaos in a rotating fluid
[AD-A204010] N89-21213
ROTARY WING AIRCRAFT
Nonlinear rotorcraft analysis-experimental and analytical
[AD-A203967] N89-20990
ROTARY WINGS
Integrated aerodynamic/dynamic optimization of helicopter rotor blades
[NASA-TM-101553] N89-20982
ROTATING ENVIRONMENTS
A study of motion sickness: Mathematical modeling and data analysis
[AD-A202770] N89-21466
ROTATING FLUIDS
Symmetry breaking bifurcations and the growth of chaos in a rotating fluid
[AD-A204010] N89-21213
ROTATING MIRRORS
A position, scale and rotation invariant holographic associative memory
[AD-A203289] N89-21221
ROTATING SHAFTS
Rotordynamic analysis of a bearing tester N89-21759
ROTATION
Time optimal slewing of flexible spacecraft N89-21014
A position, scale and rotation invariant holographic associative memory
[AD-A203289] N89-21221
Vibration control in rotating machinery using variable dynamic stiffness squeeze-films
[AD-A202902] N89-21252
ROTOR AERODYNAMICS
Rotordynamic analysis of a bearing tester N89-21759
ROTORS
Performance optimization for rotors in hover and axial flight
[NASA-CR-177524] N89-20973
RUNGE-KUTTA METHOD
The 3-D Euler and Navier-Stokes calculations for aircraft components N89-20950

S

SACCADIC EYE MOVEMENTS
Saccadic eye movement during spaceflight
[NASA-TM-100475] N89-21463
Psychophysical studies of visual cortical functions
[AD-A202814] N89-21468
SADDLE POINTS
Three-dimensional singular points in aerodynamics
[NASA-TM-100045] N89-20964

SAFETY
Nonlinear rotorcraft analysis-experimental and analytical
[AD-A203967] N89-20990
Fusion: A necessary component of US energy policy
[DE89-006234] N89-21659
Software system safety N89-21754
SALINITY
Ocean energy program summary. Volume 1, Overview: Fiscal year 1988
[DE89-000858] N89-21421
SAMPLING
In-flight lightning characterization program on a CV-580 aircraft
[AD-A203954] N89-20976
Iridium emissions from Hawaiian volcanoes N89-21314
A regional perspective on the palynofloral response to K-T boundary event(s) with emphasis on variations imposed by the effects of sedimentary facies and latitude N89-21395
SAPPHIRE
Spectroscopy and laser performance of Ti(sup 3+) doped and Cr(sup 3+), Nd(sup 3+) co-doped crystals
[AD-A203911] N89-21682
SATELLITE ATTITUDE CONTROL
Stability solution to linearized equations of motion for a symmetric spinning satellite in an elliptical orbit applied to the non-linear equations
[AD-A202934] N89-21010
SATELLITE LIFETIME
Hypersurface insertion window for long term orbital stability of artificial satellites about the planet Venus
[AD-A202808] N89-21009
SATELLITE NAVIGATION SYSTEMS
On principles, methods and recent advances in studies towards a GPS-based control system for geodesy and geodynamics
[NASA-TM-100716] N89-21434
SATELLITE OBSERVATION
ER-2 lidar observations from the October 1986 fire cirrus experiment
[NASA-TM-100704] N89-21444
SATELLITE ORBITS
Control system for maintaining stable orbits around phobos
[AD-A202776] N89-21006
Estimated satellite cluster elements in near circular orbit
[AD-A202938] N89-21011
SATELLITE PERTURBATION
Stability solution to linearized equations of motion for a symmetric spinning satellite in an elliptical orbit applied to the non-linear equations
[AD-A202934] N89-21010
SCALARS
Control system for maintaining stable orbits around phobos
[AD-A202776] N89-21006
A new class of non-topological solitons
[NASA-CR-184889] N89-21634
SCALING LAWS
Crater size estimates for large-body terrestrial impact N89-21381
SCANNERS
An algorithm for processing scanning spectrometer data N89-21506
SCATTERING
Topics in chemical physics. 1: Semiclassical reactive scattering theory. 2: Corrected effective medium theory
[DE89-007606] N89-21053
Analytic distribution for charge carriers in a semiconductor dominated by equivalent intervalley scattering
[AD-A202537] N89-21669
SCATTERING COEFFICIENTS
Utility of a dual-lidar method to measure integrated extinction
[AD-A203145] N89-21439
SCATTERING CROSS SECTIONS
The measurement of angular differential cross sections at the SSL Atomic Scattering Facility N89-21744
SCATTEROMETERS
OSRMS (Ocean Surface Roughness Measurement System): The DREP (Defence Research Establishment Pacific) near-nadir scatterometer
[AD-A202983] N89-21460
SCHEDULING
FX-87 performance measurements: Dataflow implementation
[AD-A203150] N89-21585
SpringNet: A network of multiprocessors for hard real-time
[AD-A203348] N89-21587
SCHOTTKY DIODES
Adapting Schottky diode detector technology to a space platform
[AD-A202825] N89-21219
Investigation of Schottky barrier on GaAs and InP using a multidisciplined approach
[AD-A202953] N89-21675
SCHROEDINGER EQUATION
Calculation of the energetics of chemical reactions
[DE89-007262] N89-21070
SEA WATER
Noble metals in mid-ocean ridge volcanism: A significant fractionation of gold with respect to platinum group metals N89-21307
Impact production of NO and reduced species N89-21413
SEALING
Advanced helium purge seals for Liquid Oxygen (LOX) turbopumps
[NASA-CR-182105] N89-21239
SEAS
Possible world-wide middle miocene iridium anomaly and its relationship to periodicity of impacts and extinctions N89-21291
SEASONS
Observations of neutral circulation at mid-latitudes during the Equinox Transition Study
[NASA-CR-184792] N89-21429
SECONDARY EMISSION
Charging potentials for two sample sets of spectra from DMSP satellites
[AD-A203694] N89-21021
SECONDARY FLOW
Secondary three-dimensional instability in compressible boundary layers N89-20954
SEDIMENTARY ROCKS
The Western North American Cretaceous-Tertiary (K-T) boundary interval and its content of shock-metamorphosed minerals: Implications concerning the K-T boundary impact-extinction theory N89-21334
SEDIMENTS
Possible world-wide middle miocene iridium anomaly and its relationship to periodicity of impacts and extinctions N89-21291
Sedimentological effects of tsunamis, with particular reference to impact-generated and volcanogenic waves N89-21299
Noble metals in mid-ocean ridge volcanism: A significant fractionation of gold with respect to platinum group metals N89-21307
Step-wise extinctions at the Cretaceous-Tertiary boundary and their climatic implications N89-21354
Mass killings and detection of impacts N89-21356
Deccan volcanism and K-T boundary signatures N89-21362
Environmental effects of large impacts on the earth; relation to extinction mechanisms N89-21365
Marine and continental K-T boundary clays compared N89-21382
Biostratigraphic case studies of six major extinctions N89-21390
The causes for geographical variations in OS187/OS186 at the Cretaceous-Tertiary boundary N89-21402
Tektites: Origin as melts produced by the impact of small projectiles onto dry targets N89-21405
The Cretaceous-Tertiary boundary marine extinction and global primary productivity collapse N89-21412
New approach to the origin of the tektite in China N89-21414
SEISMIC WAVES
Finite-difference modeling of Rayleigh wave scattering and P-SV(Lg) coupling problems
[AD-A203221] N89-21161
SEISMOLOGY
The Calvin 28 cryptoexplosive disturbance, Cass County, Michigan: Evidence for impact origin N89-21358
Relationships of earthquakes (and earthquake-associated mass movements) and polar motion as determined by Kalman filtered, Very-Long-Baseline-Interferometry
[NASA-TM-100711] N89-21430
The interpretation of crustal dynamics data in terms of plate motions and regional deformation near plate boundaries
[NASA-CR-180077] N89-21436
A comprehensive study of the seismotectonics of the eastern Aleutian arc and associated volcanic systems
[DE89-007357] N89-21443
SELF ORGANIZING SYSTEMS
Problem specific applications for neural networks
[AD-A203052] N89-21158
SEMANTICS
HOP (Hardware viewed as Objects and Processes): A process model for synchronous hardware systems
[AD-A203090] N89-21535
Objects as closures: Abstract semantics of object oriented languages
[NASA-CR-184877] N89-21540
Semantical paradigms: Notes for an invited lecture
[AD-A202995] N89-21565
SEMICONDUCTING FILMS
Film elastic properties determined by the indentation test-theoretical considerations
[AD-A203997] N89-21683
SEMICONDUCTOR DEVICES
Contributive research in compound semiconductor material and related devices
[AD-A202586] N89-21670
SEMICONDUCTOR JUNCTIONS
The potential of GaAs-based mechanically stacked multijunction solar concentrator cells
[DE89-007975] N89-21423
SEMICONDUCTORS (MATERIALS)
Electron paramagnetic resonance and photoluminescence studies of impurities in CdTe
[AD-A202841] N89-21056
Theoretical studies of the chemistry and physics of oxygen in silicon
[AD-A203168] N89-21063
Laser-induced metal deposition on semiconductors from liquid electrolytes
[AD-A203612] N89-21089
Optical power limiter
[AD-A203964] N89-21234
Calculation of carriers in depletion region of semiconductors with capacitance-voltage measurements
[AD-A202529] N89-21668
Analytic distribution for charge carriers in a semiconductor dominated by equivalent intervalley scattering
[AD-A202537] N89-21669
Contributive research in compound semiconductor material and related devices
[AD-A202586] N89-21670
Investigation of a self-aligned, strained-channel,n sup(+)-In As/Al 0.5 As/In 0.15 Ga 0.85 As Semiconductor Insulator Semiconductor FET (SISFET)
[AD-A203147] N89-21676
Distribution of boron atoms in ion implanted compound semiconductors
[AD-A203173] N89-21677
Two photon characterization
[AD-A203355] N89-21678
Dielectric spectroscopy of semiconductors
[AD-A203457] N89-21679
Study of semiconductor valence plasmon line shapes via electron energy-loss spectroscopy in the transmission electron microscope
[DE89-008152] N89-21689
SENSORY PERCEPTION
Psychophysical studies of visual cortical functions
[AD-A202814] N89-21468
SEPARATED FLOW
Three-dimensional singular points in aerodynamics
[NASA-TM-100045] N89-20964
Effect of riblets upon flow separation in a subsonic diffuser
[AD-A203178] N89-20967
Numerical simulation of flow over iced airfoils
[AD-A203291] N89-20969
Two-dimensional Navier-Stokes solution of the flow over a thick supercritical airfoil with strong shock-induced separation
[AD-A203331] N89-20971
Numerical study of three viscous/inviscid interaction methods
[AD-A202575] N89-21203
SEQUENCING
FX-87 performance measurements: Dataflow implementation
[AD-A203150] N89-21585
SERIES EXPANSION
Asymptotics beyond all orders N89-21508
SERVOMECHANISMS
Modeling robot dynamic performance for endpoint force control
[AD-A202881] N89-21251
SET THEORY
Confidence set inference with a prior quadratic bound
[NASA-CR-184839] N89-21435
SHAFTS (MACHINE ELEMENTS)
Modal analysis of gear housing and mounts
[NASA-TM-101445] N89-21244
SHALLOW WATER
The KP equation: A comparison to laboratory generated biperiodic waves N89-21507
SHAPED CHARGES
Influence of reflected shock waves on a hypersonic shaped charge jet N89-21522

SHAPES
Model-based silhouette recognition
[AD-A202540] N89-21552
Extracting shape reflectance of Lambertian, specular, and hybrid surfaces
[AD-A203772] N89-21652
SHATTER CONES
Shatter cones: Diagnostic impact signatures
N89-21355
SHEAR FLOW
Structure development during converging flow of a liquid crystal dispersed two-phase fluid
[AD-A203062] N89-21119
Instabilities in shear flow of viscoelastic fluids with fading memory
[AD-A203735] N89-21211
SHEAR LAYERS
Subharmonic and fundamental high amplitude excitation of an axisymmetric jet
[NASA-TM-101946] N89-20920
SHEAR PROPERTIES
Integrated aerodynamic/dynamic optimization of helicopter rotor blades
[NASA-TM-101553] N89-20982
Microscopic observations of adiabatic shear bands in three different steels
[AD-A202522] N89-21080
Shear banding in titanium with controlled elongations at 1 million/sec
[DE89-006555] N89-21094
Symmetry breaking bifurcations and the growth of chaos in a rotating fluid
[AD-A204010] N89-21213
Vibration and buckling characteristics of composite cylindrical panels incorporating the effects of a higher order shear theory
[AD-A202939] N89-21278
Finite element analysis of composite plates including shear deformation
[AD-A202941] N89-21279
On a refined nonlinear theory of laminated composite plates N89-21500
Some issues of numerical integration and penalty relaxation in anisoparametric shell element formulation
N89-21518
SHEAR STRESS
A numerical study of the turbulent free convection in rectangular cavities N89-21194
Instabilities in shear flow of viscoelastic fluids with fading memory
[AD-A203735] N89-21211
Transverse shear considerations in anisotropic plates
[AD-A203187] N89-21283
Sedimentological effects of tsunamis, with particular reference to impact-generated and volcanogenic waves
N89-21299
SHELL STABILITY
Nonlinear shell analyses of the space shuttle solid rocket boosters
[NASA-TM-101546] N89-21260
SHELL THEORY
Function theory for thin elastic shells
[PB89-101943] N89-21257
SHELLFISH
Macrofossil extinction patterns at Bay of Biscay Cretaceous-Tertiary boundary sections N89-21404
SHELLS (STRUCTURAL FORMS)
Nonlinear finite element analysis of a general composite shell
[AD-A202572] N89-21271
Some issues of numerical integration and penalty relaxation in anisoparametric shell element formulation
N89-21518
An educational expert system shell integrating object-attribute-value triples and frames
[AD-A202574] N89-21557
SHIELDING
Reduction of M1 weld fabrication costs: The effect of weld shielding gas composition
[AD-A204001] N89-21254
Further investigations of oblique hypervelocity impact phenomena N89-21750
SHIFT REGISTERS
Implementation and testing of a new 16-PSK transmitter
[AD-A203936] N89-21166
A randomness property of m-sequences N89-21524
SHIPS
Low-cost Pointing-and-Tracking System for Optical Communications (PATSOC)
[AD-A202921] N89-21151
SHOCK FRONTS
Computational techniques for shock wave diffraction problems
[AD-A203439] N89-21210
Shatter cones: Diagnostic impact signatures
N89-21355
SHOCK LAYERS
Shock-boundary-layer interaction in flight N89-20928
SHOCK LOADS
Effect of TNT miscible additives on the mechanical behavior and shock sensitivity of Composition B
[AD-A203968] N89-21132
Development of a shock capturing code for use as a tool in designing high-work low aspect ratio turbines
[AD-A202706] N89-21248
The Western North American Cretaceous-Tertiary (K-T) boundary interval and its content of shock-metamorphosed minerals: Implications concerning the K-T boundary impact-extinction theory N89-21334
Catastrophic volcanism as a cause of shocked features found at the K/T boundary and in cryptoexplosion structures N89-21347
Microdeformation in Vredefort rocks; evidence for shock metamorphism N89-21376
SHOCK WAVE INTERACTION
Turbulent eddy viscosity modeling in transonic shock/boundary-layer interactions N89-20952
An LDA (Laser-Doppler Anemometry) investigation of three-dimensional normal shock wave boundary-layer interactions N89-20956
Computational techniques for shock wave diffraction problems
[AD-A203439] N89-21210
SHOCK WAVE PROFILES
Implications of pressure diffusion for shock waves
[NASA-CR-184858] N89-21198
SHOCK WAVE PROPAGATION
Implications of pressure diffusion for shock waves
[NASA-CR-184858] N89-21198
SHOCK WAVES
Numerical computation of shock wave-turbulent boundary layer interaction in transonic flow over an axisymmetric curved hill
[NASA-TM-101473] N89-21192
Iridium, shocked minerals, and trace elements across the Cretaceous/Tertiary boundary at Maud Rise, Wedell Sea, and Walvis Ridge, South Atlantic Ocean
N89-21333
Shatter cones: Diagnostic impact signatures
N89-21355
Computer modeling of large asteroid impacts into continental and oceanic sites: Atmospheric, cratering, and ejecta dynamics N89-21379
The numerical simulation of Richtmyer-Meshkov unstable interfaces: A conference report N89-21512
The interaction of nonlinear hyperbolic waves: A conference report N89-21530
SIDELOBES
Soft constrained LMS algorithms: A robust procedure for signal misalignment
[AD-A203880] N89-21187
SIGNAL ANALYSIS
External electro-optic probing of millimeter-wave integrated circuits
[NASA-TM-101990] N89-21142
SIGNAL ANALYZERS
Performance of an adaptive matched filter using the Griffiths algorithm
[AD-A202578] N89-21147
SIGNAL DETECTION
Implementation and testing of a new 16-PSK transmitter
[AD-A203936] N89-21166
Optimal and robust memoryless discrimination from dependent observations
[AD-A202806] N89-21604
SIGNAL DETECTORS
Localizing and beamforming freely-drifting VLF (Very Low Frequency) acoustic sensors
[AD-A202638] N89-21217
SIGNAL DISTORTION
Analysis and simulation of an audio adaptive equalizer
[AD-A202569] N89-21631
SIGNAL FADING
The use of chaff in space as a jamming device between ground stations and satellites
[AD-A202577] N89-21146
SIGNAL MEASUREMENT
Microwave power amplifier analysis and design
[AD-A203170] N89-21182
SIGNAL PROCESSING
On the impulse response of monopulse radars
[AD-A202936] N89-21153
Spectral characteristics of High Frequency (HF) backscatter for high latitude ionospheric irregularities: Preliminary analysis of statistical properties
[AD-A202998] N89-21156
A robust adaptive array structure using the soft constrained LMS algorithm
[AD-A203959] N89-21167
Blending of surface and rawinsonde data in mesoscale objective analysis
[AD-A203984] N89-21456
LMS adaptive filtering applied to a microwave arterial pulse monitor
[AD-A202732] N89-21465
Image processing language, phase 2
[AD-A203994] N89-21577
On random correlation matrices
[AD-A202786] N89-21603
Optical fiber sensors and signal processing for intelligent structure monitoring
[NASA-CR-184841] N89-21640
SIGNAL RECEPTION
Soft constrained LMS algorithms: A robust procedure for signal misalignment
[AD-A203880] N89-21187
SIGNAL TO NOISE RATIOS
Analysis and simulation of a pseudonoise synchronization system
[AD-A202779] N89-21149
SIGNATURES
Implications of asteroid composition for the geochemistry of the ancient terrestrial projectile flux
N89-21294
Deccan volcanism at the Cretaceous-Tertiary boundary N89-21305
Geological remote sensing signatures of terrestrial impact craters N89-21317
Impact and extinction signatures in complete Cretaceous-Tertiary (K-T) boundary sections
N89-21391
SILICIDES
An analysis of platinum silicide and indium antimonide for remote sensors in the 3 to 5 micrometer wavelength band
[AD-A202663] N89-21218
SILICON
Theoretical studies of heterogeneous reactions in silicon CVD (Silicon Vapor Deposition) catalysis
[AD-A202905] N89-21057
Theoretical studies of the chemistry and physics of oxygen in silicon
[AD-A203168] N89-21063
Research on silicon, carbon, and silicon carbide heterostructures
[AD-A202866] N89-21116
SILICON ALLOYS
Studies of the initial oxidation of Fe-Si alloys by AES, XPS, EELS and LEED
[DE89-007610] N89-21077
SILICON CARBIDES
Research on silicon, carbon, and silicon carbide heterostructures
[AD-A202866] N89-21116
Continued development and characterization of doped layers, contacts and associated electronic devices in silicon carbide
[AD-A202450] N89-21176
SILICON FILMS
Convection and chemistry effects in CVD: A 3-D analysis for silicon deposition
[NASA-TM-102001] N89-21032
SILICON NITRIDES
Pre-pilot synthesis of low carbon Si3N4
[DE89-007202] N89-21124
SILVER
An in-situ grazing incidence X-ray scattering study of the initial stages of electrochemical growth of lead on silver (III)
[AD-A203385] N89-21064
Experimental results on atomic oxygen corrosion of silver N89-21738
SIMULATION
Incompressible flow friction coefficients in a simulated heat pipe
[AD-A203176] N89-21207
A 3-dimensional numerical simulation of the atmospheric injection of aerosols by a hypothetical basaltic fissure eruption N89-21401
Brain activity during tactical decision-making. Part 5: A cross-study validation of evoked potentials as indices of workload
[AD-A203763] N89-21474
A rapid-backscatter simulation technique for complex B-spline target models N89-21505
Lookahead in parallel discrete event simulation
[AD-A203902] N89-21588
A comparison of variable selection criteria for multiple linear regression: A simulation study
[AD-A202708] N89-21601
Atomistic simulations of interfaces in metals and alloys
[DE89-006521] N89-21685
Guidance for an aeroassisted orbital transfer vehicle
N89-21740

SIMULATORS
A real-time simulator of a turbofan engine
[NASA-TM-100869] N89-20995
SIMULTANEOUS EQUATIONS
Spline-based finite-element method for solving a Stefan's problem in a finite domain: Formulation
N89-21516
SINGLE CRYSTALS
Advanced single crystal for SSME turbopumps
[NASA-CR-182244] N89-21072
Transient natural convection heat and mass transfer in crystal growth N89-21741
SINGULARITY (MATHEMATICS)
Three-dimensional singular points in aerodynamics
[NASA-TM-100045] N89-20964
Spectral analysis of a fourth-order singular differential operator arising in combustion
[DE89-005841] N89-21052
SINTERING
Stress-corrosion cracking of liquid-phase sintered tungsten alloys
[AD-A203201] N89-21087
Pre-pilot synthesis of low carbon Si3N4
[DE89-007202] N89-21124
SLEWING
Time optimal slewing of flexible spacecraft
N89-21014
SLIDING FRICTION
Mild wear in dry and lubricated sliding systems
N89-21242
SMALL PERTURBATION FLOW
Steady and unsteady transonic small disturbance analysis of realistic aircraft configurations N89-20946
SMOKE
A 3-dimensional numerical simulation of the atmospheric injection of aerosols by a hypothetical basaltic fissure eruption N89-21401
SNOW
Search for the Tunguska event in the Antarctic snow
N89-21378
Seasonal snowfall statistics for selected stations
[AD-A203965] N89-21454
Global snow depth climatology
[AD-A203969] N89-21455
SODIUM SULFATES
High temperature oxidation and electrochemical studies related to hot corrosion
[AD-A203038] N89-21085
SODIUM VAPOR
Solar-powered alkali metal vapor lasers
[NASA-CR-180480] N89-21226
SOFTWARE ENGINEERING
Large sample theory for statistical inference in several software reliability models
[CWI-MS-R8807] N89-21543
Software development guidelines
[AD-A203332] N89-21572
Optimization of large matrix calculations for execution on the Cray X-MP vector supercomputer N89-21742
Software system safety N89-21754
SOFTWARE TOOLS
HOP (Hardware viewed as Objects and Processes): A process model for synchronous hardware systems
[AD-A203090] N89-21535
The Environment for Application Software Integration and Execution (EASIE) version 1.0. Volume 1: Executive overview
[NASA-TM-100573] N89-21538
Maintenance metrics for Jovial (J73) software
[AD-A202713] N89-21561
Design of a syntax validation tool for requirements analysis using Structured Analysis and Design Technique (SADT)
[AD-A202725] N89-21562
Influence diagrams: Automated analysis with dynamic programming
[AD-A203045] N89-21567
A theory of problem domains and program correctness
[DE89-008451] N89-21580
Software system safety N89-21754
Development of a prototype commonality analysis tool for use in space programs N89-21757
SOILS
An individual-based forest ecosystems model for projecting forest response to nutrient cycling and climate changes
[DE89-007212] N89-21428
SOLAR ACTIVITY
Solar-geophysical data number 529, September 1988. Part 1: (Prompt reports). Data for August, July 1988 and late data
[PB89-121305] N89-21431
Force-free magnetic fields: Is there a loss of equilibrium
[AD-A203030] N89-21717
SOLAR CELLS
Theoretical studies of heterogeneous reactions in silicon CVD (Silicon Vapor Deposition) catalysis
[AD-A202905] N89-21057
Restrictive loads powered by separate or by common electrical sources
[NASA-TM-102008] N89-21174
The potential of GaAs-based mechanically stacked multijunction solar concentrator cells
[DE89-007975] N89-21423
Essential elements in the numerical modeling of solar cells
[DE89-008113] N89-21424
SOLAR COLLECTORS
The potential of GaAs-based mechanically stacked multijunction solar concentrator cells
[DE89-007975] N89-21423
SOLAR ELECTRIC PROPULSION
Optimal launch time for a discontinuous low thrust orbit transfer
[AD-A202693] N89-21007
SOLAR FLARES
Solar-geophysical data number 529, September 1988. Part 2: (Comprehensive reports). Data for March 1988
[PB89-121313] N89-21432
Solar-geophysical data number 528, August 1988. Part 2: (Comprehensive reports). Data for February 1988
[PB89-109912] N89-21722
SOLAR INTERIOR
New picture for the internal rotation of the sun
[PB89-113377] N89-21723
SOLAR MAGNETIC FIELD
Force-free magnetic fields: Is there a loss of equilibrium
[AD-A203030] N89-21717
SOLAR OBSERVATORIES
NASA Marshall Space Flight Center solar observatory report, January - December 1987
[NASA-TM-100360] N89-21712
SOLAR PHYSICS
Solar-geophysical data number 529, September 1988. Part 1: (Prompt reports). Data for August, July 1988 and late data
[PB89-121305] N89-21431
Solar-geophysical data number 529, September 1988. Part 2: (Comprehensive reports). Data for March 1988
[PB89-121313] N89-21432
Solar-geophysical data number 528, August 1988. Part 2: (Comprehensive reports). Data for February 1988
[PB89-109912] N89-21722
New picture for the internal rotation of the sun
[PB89-113377] N89-21723
SOLAR PROMINENCES
Solar-geophysical data number 529, September 1988. Part 2: (Comprehensive reports). Data for March 1988
[PB89-121313] N89-21432
Solar-geophysical data number 528, August 1988. Part 2: (Comprehensive reports). Data for February 1988
[PB89-109912] N89-21722
SOLAR RADIO BURSTS
Solar-geophysical data number 529, September 1988. Part 2: (Comprehensive reports). Data for March 1988
[PB89-121313] N89-21432
Solar-geophysical data number 528, August 1988. Part 2: (Comprehensive reports). Data for February 1988
[PB89-109912] N89-21722
SOLAR RADIO EMISSION
Solar-geophysical data number 529, September 1988. Part 1: (Prompt reports). Data for August, July 1988 and late data
[PB89-121305] N89-21431
SOLAR ROTATION
New picture for the internal rotation of the sun
[PB89-113377] N89-21723
SOLAR SYSTEM
Disruption of giant comets in the solar system and around other stars N89-21408
SOLAR TERRESTRIAL INTERACTIONS
SESC (Space Environment Services Center) glossary of solar-terrestrial terms, 2nd edition
[PB89-120802] N89-21698
SOLAR WIND
Geomagnetic field energy as a source of thrust
[AD-A202567] N89-21027
SOLAR X-RAYS
Solar-geophysical data number 529, September 1988. Part 2: (Comprehensive reports). Data for March 1988
[PB89-121313] N89-21432
Solar-geophysical data number 528, August 1988. Part 2: (Comprehensive reports). Data for February 1988
[PB89-109912] N89-21722
SOLID ELECTRODES
Design, fabrication, and performance of brazed, graphite electrode, multistage depressed collectors with 500-W, continuous wave, 4.8- to 9.6-GHz traveling-wave tubes
[NASA-TP-2904] N89-21171
SOLID ELECTROLYTES
Electrolytic protection against high-temperature oxidation
[AD-A203890] N89-21123
Advanced double layer capacitor
[AD-A203059] N89-21181
SOLID PROPELLANT COMBUSTION
Holographic investigation of solid propellant combustion
[AD-A203928] N89-21067
SOLID PROPELLANT IGNITION
Effective ignition kinetics for LOVA propellant
[AD-A203149] N89-21129
SOLID PROPELLANT ROCKET ENGINES
Automatic measurement of particles from holograms taken in the combustion chamber of a rocket motor
[AD-A203955] N89-21030
Holographic investigation of solid propellant combustion
[AD-A203928] N89-21067
Computer codes for thermal analysis of a solid rocket motor nozzle N89-21733
X-ray fluorescence surface contaminant analyzer: A feasibility study N89-21736
SOLID ROCKET PROPELLANTS
Magnetic flowmeter measurement of solid propellant pressure-coupled and velocity-coupled responses
[AD-A203988] N89-21133
SOLID STATE
A NMR (Nuclear Magnetic Resonance) study of the molecular interactions and dynamic behavior in polymer-diluent blends in the solid state
[AD-A202459] N89-21108
SOLID STATE DEVICES
Development of gallium arsenide high-speed, low-power serial parallel interface modules: Executive summary
[NASA-CR-182272] N89-21173
Correction of gain and optical throughput variations in a two-dimensional imaging spectrometer
[AD-A203495] N89-21222
SOLID STATE LASERS
Spectroscopy and laser performance of Ti(sup 3+) doped and Cr(sup 3+), Nd(sup 3+) co-doped crystals
[AD-A203911] N89-21682
SOLIDIFICATION
Effect of Te on the microstructural changes during the gray-to-white and white-to-gray transition in directional solidification of Fe-C-Si alloys
[DE89-007607] N89-21076
Synthesis processing of high-lithium Al-Li alloys
[AD-A203401] N89-21088
The microstructural and phase characterization of RST Al-Ti-X alloys
[AD-A203734] N89-21092
Toward a nonequilibrium thermodynamics of two phase materials with sharp interface N89-21494
SOLIDS
Large deformations near a pair of closely-spaced spherical voids in a rate-dependent solid
[AD-A202465] N89-21268
SOLITARY WAVES
A new class of non-topological solitons
[NASA-CR-184889] N89-21634
Half-solitons in superfluid (3)He-A: Novel pi/2-quanta of phase slippage
[PB89-128904] N89-21664
SOLUBILITY
Fluids, both ionic and nonionic, over wide ranges of temperature and composition
[DE89-001265] N89-21048
SOLUTES
The effect of mixed-mode loading on stress-driven solute segregation during high-temperature brittle intergranular fracture
[AERE-R-12897] N89-21073
SOLVATION
Molecular jet studies of vdW (van der Waals) clusters and solvation
[AD-A203766] N89-21212
SOOT
Fuels combustion research
[AD-A204161] N89-21071
SOUND GENERATORS
A continued study of optical sound generation and amplification
[AD-A202484] N89-21630
SOUND TRANSMISSION
A cancellation technique for reducing background noise within turbulent flow environments characterized by pipes and annuli
[AD-A202924] N89-21206
A continued study of optical sound generation and amplification
[AD-A202484] N89-21630

SOUND WAVES
Surface acoustic wave detection of organophosphorus compounds
[AD-A202909] N89-21058
Time delay estimation in stationary and non-stationary environments
[AD-A202507] N89-21549
SOUTHERN HEMISPHERE
Geochemical comparison of K-T boundaries from the Northern and Southern Hemispheres N89-21400
Commentary on fast atmospheric pulsations
[AD-A203172] N89-21440
SPACE ADAPTATION SYNDROME
Techniques for studying the effects of microgravity on model particle/cell systems N89-21758
SPACE BASED RADAR
Estimated satellite cluster elements in near circular orbit
[AD-A202938] N89-21011
SPACE CHARGE
Space plasma contractor research, 1988
[NASA-CR-182283] N89-21658
Order in cold ionic systems: Dynamic effects
[DE89-007377] N89-21687
SPACE DEBRIS
Further investigations of oblique hypervelocity impact phenomena N89-21750
SPACE EXPLORATION
NASA directions in space propulsion for 2000 and beyond
[NASA-TM-102281] N89-21026
SPACE FLIGHT
Space Propulsion Hazards Analysis Manual (SPHAM), volume 1
[AD-A203204] N89-21029
SPACE LAW
National space policy
[AD-A202644] N89-21711
SPACE MISSIONS
National space policy
[AD-A202644] N89-21711
SPACE NAVIGATION
On principles, methods and recent advances in studies towards a GPS-based control system for geodesy and geodynamics
[NASA-TM-100716] N89-21434
SPACE OBSERVATIONS (FROM EARTH)
New techniques for high-resolution optical space surveillance
[AD-A202785] N89-21647
SPACE PERCEPTION
Reconstruction of binocular depth across continuous surfaces
[AD-A202827] N89-21469
Peripheral limitations on spatial vision
[AD-A203388] N89-21472
Seeing Ghost solutions in stereo vision
[AD-A203581] N89-21473
SPACE PLASMAS
Space plasma contractor research, 1988
[NASA-CR-182283] N89-21658
SPACE PROGRAMS
Development of a prototype commonality analysis tool for use in space programs N89-21757
SPACE SHUTTLE BOOSTERS
Nonlinear shell analyses of the space shuttle solid rocket boosters
[NASA-TM-101546] N89-21260
SPACE SHUTTLE MAIN ENGINE
Advanced single crystal for SSME turbopumps
[NASA-CR-182244] N89-21072
Radiation effect on rocket engine performance N89-21734
A performance/loss evaluation of SSME HPFTP turbine N89-21735
The simulation of the alternate turbopump development high pressure oxygen and fuel turbopumps for the space shuttle main engine using the Shaberth computer program N89-21746
Simulation of water vapor condensation on LOX droplet surface using liquid nitrogen N89-21749
SSME propulsion performance reconstruction techniques N89-21752
Space shuttle main engine numerical modeling code modifications and analysis N89-21760
SPACE SHUTTLES
Excitation and diagnostics of optical contamination in the spacecraft environment
[AD-A202429] N89-21015
Adapting Schottky diode detector technology to a space platform
[AD-A202825] N89-21219
Operational implications of a cloud model simulation of space shuttle exhaust clouds in different atmospheric conditions
[NASA-CR-4222] N89-21425
A cloud model simulation of space shuttle exhaust clouds in different atmospheric conditions
[NASA-CR-4223] N89-21426
Saccadic eye movement during spaceflight
[NASA-TM-100475] N89-21463
SPACE STATIONS
Active control of a large space structure as applied to the phase 1 CETF (Critical Evaluation Task Force) space station
[AD-A203293] N89-21020
SPACE TRANSPORTATION SYSTEM
Evaluate the application of modal test and analysis processes to structural fault detection in MSFC-STS project elements N89-21751
SPACE WEAPONS
SDI (Strategic Defense Initiative) and national security policy
[AD-A202730] N89-21617
Artificial asteroid impact on defensive satellites
[DE89-008407] N89-21620
WhiteStar project engineering component selection database
[DE89-008321] N89-21709
SPACEBORNE EXPERIMENTS
Infrared surface temperature measurements for the surface tension driven convection experiment
[NASA-TM-101353] N89-21224
Angular response calibration of the burst and transient source experiment N89-21745
SPACECRAFT CHARGING
Charging potentials for two sample sets of spectra from DMSP satellites
[AD-A203694] N89-21021
SPACECRAFT CONTAMINATION
Excitation and diagnostics of optical contamination in the spacecraft environment
[AD-A202429] N89-21015
SPACECRAFT CONTROL
Active control technique evaluation for spacecraft (ACES)
[AD-A202475] N89-21016
Active control of a large space structure as applied to the phase 1 CETF (Critical Evaluation Task Force) space station
[AD-A203293] N89-21020
SPACECRAFT GLOW
Excitation and diagnostics of optical contamination in the spacecraft environment
[AD-A202429] N89-21015
SPACECRAFT GUIDANCE
Guidance for an aeroassisted orbital transfer vehicle N89-21740
SPACECRAFT LAUNCHING
Optimal launch time for a discontinuous low thrust orbit transfer
[AD-A202693] N89-21007
SPACECRAFT MANEUVERS
Time optimal slewing of flexible spacecraft N89-21014
SPACECRAFT MOTION
Active control of a large space structure as applied to the phase 1 CETF (Critical Evaluation Task Force) space station
[AD-A203293] N89-21020
SPACECRAFT POWER SUPPLIES
Conjugating binary systems for spacecraft thermal control
[NASA-CR-183608] N89-21023
Initiative for the 21st century: Advanced space power and propulsion based on lasers
[DE89-008034] N89-21031
Thermal and dynamic analysis of the RING (Radiatively-cooled, Inertially-driven Nuclear Generator) power system radiator
[DE89-007236] N89-21639
Intelligent data reduction for autonomous power systems N89-21737
SPACECRAFT PROPULSION
NASA directions in space propulsion for 2000 and beyond
[NASA-TM-102281] N89-21026
Geomagnetic field energy as a source of thrust
[AD-A202567] N89-21027
Space Propulsion Hazards Analysis Manual (SPHAM), volume 1
[AD-A203204] N89-21029
Initiative for the 21st century: Advanced space power and propulsion based on lasers
[DE89-008034] N89-21031
SPACECRAFT RADIATORS
High capacity demonstration of honeycomb panel heat pipes
[NASA-CR-181776] N89-21191
SPACECRAFT SHIELDING
Oblique hypervelocity impact response of dual-sheet structures
[NASA-TM-100358] N89-21246
SPACECRAFT STRUCTURES
Active control of a large space structure as applied to the phase 1 CETF (Critical Evaluation Task Force) space station
[AD-A203293] N89-21020
Simulation of the low earth orbital atomic oxygen interaction with materials by means of an oxygen ion beam
[NASA-TM-101971] N89-21104
Further investigations of oblique hypervelocity impact phenomena N89-21750
SPACECRAFT TRAJECTORIES
Optimal launch time for a discontinuous low thrust orbit transfer
[AD-A202693] N89-21007
SPATIAL DISTRIBUTION
Non-random cratering flux in recent time N89-21384
Devices and systems for nonlinear optical information processing
[AD-A203034] N89-21566
SPATIAL RESOLUTION
External electro-optic probing of millimeter-wave integrated circuits
[NASA-TM-101990] N89-21142
Peripheral limitations on spatial vision
[AD-A203388] N89-21472
Evaluation of the spatial and temporal characteristics of the conducting PRIZ
[AD-A202593] N89-21671
SPECIFICATIONS
Grasp: A graph specification language
[AD-A202524] N89-21550
Design specifications for hardware assisted rollback computation
[AD-A203092] N89-21584
Lockheed Aeronautical Systems Company technical order transfer tests
[DE89-008092] N89-21707
SPECKLE PATTERNS
New techniques for high-resolution optical space surveillance
[AD-A202785] N89-21647
SPECTRA
Charging potentials for two sample sets of spectra from DMSP satellites
[AD-A203694] N89-21021
Spectroscopic studies of fluid/solid interfaces
[AD-A202436] N89-21054
Time delay estimation in stationary and non-stationary environments
[AD-A202507] N89-21549
Study of semiconductor valence plasmon line shapes via electron energy-loss spectroscopy in the transmission electron microscope
[DE89-008152] N89-21689
SPECTRAL ENERGY DISTRIBUTION
Fast acting optical beam deflection system
[AD-A203042] N89-21648
The 408 MHz radio observations of a quasar sample N89-21714
SPECTROMETERS
An algorithm for processing scanning spectrometer data N89-21506
SPECTROSCOPY
Spectroscopic studies of fluid/solid interfaces
[AD-A202436] N89-21054
The spectroscopy and energy transfer kinetics of the interhalogens
[AD-A202954] N89-21059
Modern multiple-pulse, high field NMR studies of high density jet fuels
[AD-A203320] N89-21130
Two photon characterization
[AD-A203355] N89-21678
Dielectric spectroscopy of semiconductors
[AD-A203457] N89-21679
SPECTRUM ANALYSIS
Spectral analysis of a fourth-order singular differential operator arising in combustion
[DE89-005841] N89-21052
High resolution chronology of late Cretaceous-early Tertiary events determined from 21,000 yr orbital-climatic cycles in marine sediments N89-21328
SPECULAR REFLECTION
Rapid backscatter simulation techniques for detailed B-spline target models
[AD-A203260] N89-21163
SPEECH
F-16 speaker-independent speech recognition system using cockpit commands (70 words)
[AD-A203177] N89-21489

SPEECH RECOGNITION
Speech recognition using neural nets and dynamic time warping
[AD-A202528] N89-21144
Speech recognition: Acoustic-phonetic knowledge acquisition and representation
[AD-A203081] N89-21160
F-16 speaker-independent speech recognition system using cockpit commands (70 words)
[AD-A203177] N89-21489
Speech database development
[AD-A202461] N89-21699

SPHERES
Large deformations near a pair of closely-spaced spherical voids in a rate-dependent solid
[AD-A202465] N89-21268

SPIN DYNAMICS
Remote orbital capture using an orbital maneuvering vehicle equipped with a multibody grappling arm assembly
[AD-A202760] N89-21018

SPIN STABILIZATION
Stability solution to linearized equations of motion for a symmetric spinning satellite in an elliptical orbit applied to the non-linear equations
[AD-A202934] N89-21010
Remote orbital capture using an orbital maneuvering vehicle equipped with a multibody grappling arm assembly
[AD-A202760] N89-21018

SPIN-LATTICE RELAXATION
Nuclear magnetic resonance study of hydrogen in niobium-vanadium alloys
[DE89-007578] N89-21075

SPIN-SPIN COUPLING
Stability solution to linearized equations of motion for a symmetric spinning satellite in an elliptical orbit applied to the non-linear equations
[AD-A202934] N89-21010

SPIRAL GALAXIES
Numerical studies of gas flow in spiral galaxies
N89-21718

SPLINE FUNCTIONS
Rapid backscatter simulation techniques for detailed B-spline target models
[AD-A203260] N89-21163
Transactions of the Fifth Army Conference on Applied Mathematics and Computing
[AD-A193384] N89-21490
Algorithms for rational spline curves N89-21502
Convexity-preserving quasi-interpolation and interpolation by box spline surfaces N89-21503
Knot selection for least squares approximation using thin plate splines N89-21504
A rapid-backscatter simulation technique for complex B-spline target models N89-21505
Spline-based finite-element method for solving a Stefan's problem in a finite domain: Formulation
N89-21516

SPORES
A regional perspective on the palynofloral response to K-T boundary event(s) with emphasis on variations imposed by the effects of sedimentary facies and latitude N89-21395

SPRAYERS
Contamination of the exterior of a C-130E aircraft used for aerial spray, 907 TAG, Rickenbacker ANGB, OH
[AD-A202430] N89-20984
Turbulence modulation and dense-spray structure
[AD-A202449] N89-21201

SPREAD SPECTRUM TRANSMISSION
A randomness property of m-sequences N89-21524

SQUID (DETECTORS)
Magnetic mapping of current distributions in two-dimensional electronic devices
[AD-A203035] N89-21220

STABILITY
Actuation constraints in multivariable flight control systems N89-20998
Abrupt climate change and extinction events
N89-21308
Stabilization of Ziegler's pendulum by means of the method of vibrational control N89-21531
Structure maps and phase stability in AlTi3 alloyed with rare-earth elements
[DE89-005106] N89-21684

STABILITY DERIVATIVES
Methodology for using steady experimental aerodynamic data to improve steady and unsteady aerodynamic analysis N89-20972
Aeroelastic modeling for the FIT team F/A-18 simulation
[NASA-TM-101569] N89-20991

STABILITY TESTS
Investigation of the development of laminar boundary-layer instabilities along a cooled-wall cone in hypersonic flows
[AD-A202587] N89-20966

STAGNATION FLOW
Turbulence modulation and dense-spray structure
[AD-A202449] N89-21201

STANDARD DEVIATION
Seasonal snowfall statistics for selected stations
[AD-A203965] N89-21454

STANDARDIZATION
Evaluation of the spatial and temporal characteristics of the conducting PRIZ
[AD-A202593] N89-21671
WhiteStar project engineering component selection database
[DE89-008321] N89-21709

STANDARDS
Hydrogen segregation to grain boundaries and external surfaces
[AD-A202892] N89-21084
Center for Electronics and Electrical Engineering technical progress bulletin covering center programs, April to June 1988 with 1988 CEEE events calendar
[PB89-123137] N89-21170
People's Republic of China laser radiation safety standard
[AD-A203777] N89-21233
Lockheed Aeronautical Systems Company technical order transfer tests
[DE89-008092] N89-21707

STATIC LOADS
Finite element analysis of composite plates including shear deformation
[AD-A202941] N89-21279

STATIC PRESSURE
Flowfield measurements in the NASA Lewis Research Center 9- by 15-foot low-speed wind tunnel
[NASA-TM-100883] N89-21002

STATIC STABILITY
A wind tunnel and computer investigation of the low speed aerodynamic characteristics of the prone escape system (PRESS)
[AD-A202768] N89-20988
Tailless aircraft performance improvements with relaxed static stability
[NASA-CR-181806] N89-20999

STATIC TESTS
Static tensile and tensile creep testing of five ceramic fibers at elevated temperatures
[NASA-CR-177525] N89-21046

STATIONKEEPING
Hypersurface insertion window for long term orbital stability of artificial satellites about the planet Venus
[AD-A202808] N89-21009

STATISTICAL ANALYSIS
Operational implications of a cloud model simulation of space shuttle exhaust clouds in different atmospheric conditions
[NASA-CR-4222] N89-21425
Behavioral effects of microwaves: Relationship of total dose and dose rate
[PB89-118640] N89-21462
Statistical machine learning for the cognitive selection of nonlinear programming algorithms in engineering design optimization N89-21493
Nonparamteric estimation from queues arising in staggered entry clinical trials N89-21520
Response surface analysis of stochastic network performance
[AD-A202561] N89-21554
Best ordering for floating-point addition
[AD-A203990] N89-21612

STATISTICAL CORRELATION
On random correlation matrices
[AD-A202786] N89-21603

STATISTICAL DISTRIBUTIONS
The cratering record in the inner solar system: Implications for earth N89-21292
Origination, diversity, and extinction metrics essential for analysis of mass biotic crisis events: An example from cretaceous ammonoidea N89-21304
Conditionally and strictly distribution-free tests for randomized block designs that are asymptotically optimal
[CWI-MS-R8802] N89-21615

STATISTICAL MECHANICS
The use of chaff in space as a jamming device between ground stations and satellites
[AD-A202577] N89-21146
Evolution of cosmic string networks
[NASA-CR-182836] N89-21716

STATISTICAL TESTS
A comparison of variable selection criteria for multiple linear regression: A simulation study
[AD-A202708] N89-21601

STEADY FLOW
Steady and unsteady transonic small disturbance analysis of realistic aircraft configurations N89-20946
Methodology for using steady experimental aerodynamic data to improve steady and unsteady aerodynamic analysis N89-20972

STEADY STATE
Root placement with transfer function methods (full state feedback)
[AD-A203877] N89-21610

STEAM
Simulation of water vapor condensation on LOX droplet surface using liquid nitrogen N89-21749

STEEL STRUCTURES
Numerical and experimental determination of strain (stress) concentration factors of welded joints between square hollow sections
[PB89-131734] N89-21261

STEELS
Microscopic observations of adiabatic shear bands in three different steels
[AD-A202522] N89-21080
Nb modification of microcomposite Fe/C/Cr/Mn steel
[DE89-008297] N89-21097
An investigation of stresses and strains in an internally pressurized, composite-jacketed, steel cylinder
[AD-A202969] N89-21281

STEEPEST DESCENT METHOD
Modified backward error propagation for tactical target recognition
[AD-A202666] N89-21644

STELLAR EVOLUTION
The evolution of active galactic nuclei and globular clusters: Multi-component models N89-21720

STELLAR LUMINOSITY
Luminosity variations of stars similar to the sun
[AD-A203864] N89-21713

STELLAR MASS
A search for gravitational waves from coalesing binary stars using the Caltech 40 meter gravity wave detector
N89-21721

STELLAR MASS EJECTION
Solar-geophysical data number 529, September 1988. Part 2: (Comprehensive reports). Data for March 1988
[PB89-121313] N89-21432
Solar-geophysical data number 528, August 1988. Part 2: (Comprehensive reports). Data for February 1988
[PB89-109912] N89-21722

STELLAR PHYSICS
Supernova 1987A: 18 months later
[NASA-CR-184891] N89-21715
A search for gravitational waves from coalesing binary stars using the Caltech 40 meter gravity wave detector
N89-21721

STEREOSCOPIC VISION
Seeing Ghost solutions in stereo vision
[AD-A203581] N89-21473

STEREOSCOPY
Reconstruction of binocular depth across continuous surfaces
[AD-A202827] N89-21469
Seeing Ghost solutions in stereo vision
[AD-A203581] N89-21473

STERILIZATION
Hypersurface insertion window for long term orbital stability of artificial satellites about the planet Venus
[AD-A202808] N89-21009

STIFFNESS
Vibration control in rotating machinery using variable dynamic stiffness squeeze-films
[AD-A202902] N89-21252
Condition of the finite element stiffness matrix of highly irregular triangular grids N89-21497

STOCHASTIC PROCESSES
Improving the survivability of a stochastic communication network
[AD-A202872] N89-21150
Coherent structures in fully developed turbulent pipe flow N89-21195
Turbulence modulation and dense-spray structure
[AD-A202449] N89-21201
Time delay estimation in stationary and non-stationary environments
[AD-A202507] N89-21549
Response surface analysis of stochastic network performance
[AD-A202561] N89-21554
Bispectral inversion: The construction of a time series from its bispectrum
[AD-A202508] N89-21598
Speech database development
[AD-A202461] N89-21699

STORAGE BATTERIES
Cryogenic reactant storage for lunar base regenerative fuel cells
[NASA-TM-101980] N89-21419
STORMS (METEOROLOGY)
The role of radiation-dynamics interaction in regional numerical weather prediction N89-21732
STRAIN DISTRIBUTION
Numerical and experimental determination of strain (stress) concentration factors of welded joints between square hollow sections
[PB89-131734] N89-21261
STRAIN ENERGY RELEASE RATE
Analysis of interface crack branching
[NASA-CR-182273] N89-21265
Strain energy release rate as a function of temperature and preloading history utilizing the edge delamination fatique test method
[NASA-CR-184966] N89-21286
STRAIN GAGES
Optical fiber sensors and signal processing for intelligent structure monitoring
[NASA-CR-184841] N89-21640
STRAIN RATE
Shear banding in titanium with controlled elongations at 1 million/sec
[DE89-006555] N89-21094
STRATA
The Sudbury Structure (Ontario, Canada) and Vredefort Structure (South Africa): A comparison N89-21311
STRATEGY
A source code analyzer to predict compilation time for avionics software using software science measures. Volume 1: Main report
[AD-A202737] N89-20992
Computer strategy for detecting line features on simulated binary arrays in support of radar feature extraction
[AD-A203257] N89-21162
SDI (Strategic Defense Initiative) and national security policy
[AD-A202730] N89-21617
Strategic defense initiative: A chronology, 1983 - 1988
[AD-A203576] N89-21619
Strategic defense initiative program: Better management direction and controls needed
[GAO/NSIAD-88-26] N89-21694
Analysis of the Federal Aviation Administration's host computer acquisition process and potential application in Department of Defense acquisitions
[AD-A202623] N89-21695
STRATIGRAPHY
Global Catastrophes in Earth History: An Interdisciplinary Conference on Impacts, Volcanism, and Mass Mortality
[NASA-CR-183329] N89-21287
The debate over the Cretaceous-Tertiary boundary N89-21288
Geochemistry of K/T boundaries in India and contributions of Deccan volcanism N89-21296
The impact of mass extinctions N89-21315
The end-triassic mass extinction event N89-21324
How many upper Eocene microspherule layers: More than we thought N89-21327
The Calvin 28 cryptoexplosive disturbance, Cass County, Michigan: Evidence for impact origin N89-21358
The Triassic-Jurassic boundary in eastern North America N89-21366
Iridium abundance measurements across bio-event horizons in the geological record N89-21368
Bio-, Magneto- and event-stratigraphy across the K-T boundary N89-21370
Late Frasnian mass extinction: Conodont event stratigraphy, global changes, and possible causes N89-21380
Oblique impacts: Catastrophic vs. protracted effects N89-21383
Biostratigraphic case studies of six major extinctions N89-21390
Impact and extinction signatures in complete Cretaceous-Tertiary (K-T) boundary sections N89-21391
STRATOCUMULUS CLOUDS
Coupled dynamical-radiational model of stratocumulus and its applications
[PB89-104137] N89-21447
STRESS ANALYSIS
High temperature evaluation of new ferroelastic toughened ceramic materials
[AD-A203197] N89-21120
Modal analysis of gear housing and mounts
[NASA-TM-101445] N89-21244
Investigation of Weibull statistics in fracture analysis of cast aluminum
[NASA-TM-102000] N89-21245
Condition of the finite element stiffness matrix of highly irregular triangular grids N89-21497
STRESS CONCENTRATION
Investigation of modeling of damage growth in composite laminates
[AD-A202433] N89-21037
Dilatationally nonlinear elastic materials. Part 2: An example illustrating stress concentration reduction
[AD-A202521] N89-21111
Compressive properties of high performance polymeric fibers
[AD-A202947] N89-21117
Numerical and experimental determination of strain (stress) concentration factors of welded joints between square hollow sections
[PB89-131734] N89-21261
STRESS CORROSION
Surface chemistry and structural effects in the stress corrosion of glass and ceramic materials
[AD-A202452] N89-21107
STRESS CORROSION CRACKING
Stress-corrosion cracking of liquid-phase sintered tungsten alloys
[AD-A203201] N89-21087
STRESS DISTRIBUTION
Analysis of interface crack branching
[NASA-CR-182273] N89-21265
A simple analysis of swage autofrettage process N89-21498
STRESS INTENSITY FACTORS
Stress intensity factors for bodies containing initial stress N89-21263
On the energy release rate for dynamic transient anti-plane shear crack propagation in a general linear viscoelastic body
[AD-A202942] N89-21280
On some finite element error estimates for stress intensity factors in Mode 1 linear elastic fracture problems N89-21517
STRESS WAVES
A study of the stress wave factor technique for evaluation of composite materials
[NASA-CR-4195] N89-21256
STRESS-STRAIN RELATIONSHIPS
A study of failure characteristics in a thermoplastic composite material at high temperature
[AD-A203015] N89-21040
Numerical and experimental determination of strain (stress) concentration factors of welded joints between square hollow sections
[PB89-131734] N89-21261
Macrocrack-multiple defect interaction considering elastic, plastic and viscoplastic effects
[AD-A203186] N89-21282
STRESSES
Investigation of the impact performance of various glass and ceramic systems
[AD-A202443] N89-21106
Global-local methodology for fracture analysis of engineering structures N89-21262
An investigation of stresses and strains in an internally pressurized, composite-jacketed, steel cylinder
[AD-A202969] N89-21281
The interpretation of crustal dynamics data in terms of plate motions and regional deformation near plate boundaries
[NASA-CR-180077] N89-21436
STRING THEORY
A new class of non-topological solitons
[NASA-CR-184889] N89-21634
Evolution of cosmic string networks
[NASA-CR-182836] N89-21716
STRIP TRANSMISSION LINES
Time domain wave propagation in multilayered integrated circuits
[AD-A202427] N89-21175
The boundary-integral method for planar microstrip circuits
[AD-A203715] N89-21185
STRONTIUM
Impact production of NO and reduced species N89-21413
STRONTIUM COMPOUNDS
An in-situ, high-temperature study of the superconductor YBa1.67Sr0.33Cu3O(6+x)
[DE89-007375] N89-21686
STRONTIUM ISOTOPES
Seawater strontium isotopes at the Cretaceous-Tertiary boundary N89-21350
STRUCTURAL ANALYSIS
Reentry response of the light weight radioisotope heater unit resulting from a Venus-Earth-Earth gravity assist maneuver accident
[DE89-005359] N89-21024
Inelastic deformation and failure analysis of filament-wound composite structures
[AD-A203382] N89-21044
Synthesis processing of high-lithium Al-Li alloys
[AD-A203401] N89-21088
Nonlinear shell analyses of the space shuttle solid rocket boosters
[NASA-TM-101546] N89-21260
A triangular thin shell element for the linear analysis of stiffened composite structures
[AD-A202864] N89-21277
Design of a syntax validation tool for requirements analysis using Structured Analysis and Design Technique (SADT)
[AD-A202725] N89-21562
VAX to CRAY NASTRAN user interface
[AD-A203447] N89-21575
Evaluate the application of modal test and analysis processes to structural fault detection in MSFC-STS project elements N89-21751
STRUCTURAL DESIGN
A robust adaptive array structure using the soft constrained LMS algorithm
[AD-A203959] N89-21167
Manipulator primitive level task decomposition
[PB89-133532] N89-21238
Stress intensity factors for bodies containing initial stress N89-21263
Design of a syntax validation tool for requirements analysis using Structured Analysis and Design Technique (SADT)
[AD-A202725] N89-21562
STRUCTURAL ENGINEERING
Global-local methodology for fracture analysis of engineering structures N89-21262
VAX to CRAY NASTRAN user interface
[AD-A203447] N89-21575
STRUCTURAL FAILURE
Nonlinear shell analyses of the space shuttle solid rocket boosters
[NASA-TM-101546] N89-21260
STRUCTURAL PROPERTIES (GEOLOGY)
Geological indicators for impact: The anomalous case of the Vredefort structure, South Africa N89-21289
The Sudbury Structure (Ontario, Canada) and Vredefort Structure (South Africa): A comparison N89-21311
The Frasnian-Famennian mass killing event(s), methods of identification and evaluation N89-21318
Mineralogy and phase-chemistry of the Cretaceous/Tertiary section in the Lattengebirge, Bavarian Alps N89-21323
STRUCTURAL RELIABILITY
Stress-corrosion cracking of liquid-phase sintered tungsten alloys
[AD-A203201] N89-21087
STRUCTURAL VIBRATION
Analytical and experimental investigation of constrained viscoelastic layer damping for a plate and shell model
[AD-A202698] N89-21273
SUBDUCTION (GEOLOGY)
Assessment of the atmospheric impact of volcanic eruptions N89-21388
A comprehensive study of the seismotectonics of the eastern Aleutian arc and associated volcanic systems
[DE89-007357] N89-21443
SUBSONIC FLOW
Effect of riblets upon flow separation in a subsonic diffuser
[AD-A203178] N89-20967
Numerical simulation of flow over iced airfoils
[AD-A203291] N89-20969
SUBSTRATES
Advanced tribological coatings for high specific strength alloys
[AD-A202505] N89-21110
Center for thin film studies
[AD-A202742] N89-21673
SUCTION
Potential flow evaluation of the interference effect of strut-through-appendage-tip model mounting technique and reduction of the effect using blowing and suction
[AD-A202424] N89-21199
SUN
Luminosity variations of stars similar to the sun
[AD-A203864] N89-21713
New picture for the internal rotation of the sun
[PB89-113377] N89-21723
SUNLIGHT
Darkness after the K-T impact: Effects of soot N89-21411
SUPERCOMPUTERS
Design specifications for hardware assisted rollback computation
[AD-A203092] N89-21584
Critical problems in very large scale computer systems
[AD-A203299] N89-21586
SUPERCONDUCTING MAGNETS
High-temperature ceramic superconductors
[AD-A202867] N89-21674

SUPERCONDUCTIVITY
Central research project report on superconductivity (1988). Part 1: Materials and IR detectors
[AD-A203891] N89-21681
Fermi liquid theory for high temperature superconductors
[DE89-007982] N89-21688
SUPERCONDUCTORS
Center for Electronics and Electrical Engineering technical progress bulletin covering center programs, April to June 1988 with 1988 CEEE events calendar
[PB89-123137] N89-21170
Characterization of Nb-Al superconducting material
[DE89-008296] N89-21690
Construction of an alternating gradient magnetometer N89-21739
SUPERCRITICAL AIRFOILS
An experimental study of transonic buffet of a supercritical airfoil with trailing edge flap
[AD-A203189] N89-20968
Two-dimensional Navier-Stokes solution of the flow over a thick supercritical airfoil with strong shock-induced separation
[AD-A203331] N89-20971
SUPERCRITICAL FLOW
Spectroscopic studies of fluid/solid interfaces
[AD-A202436] N89-21054
SUPERFLUIDITY
Sounds in one-dimensional superfluid helium
[AD-A202428] N89-21629
Half-solitons in superfluid (3)He-A: Novel pi/2-quanta of phase slippage
[PB89-128904] N89-21664
SUPERNOVA 1987A
Supernova 1987A: 18 months later
[NASA-CR-184891] N89-21715
SUPERSONIC FLOW
Comparison of 3D computation and experiment for non-axisymmetric nozzles
[NASA-CR-182245] N89-20921
Transverse jets in compressible crossflows N89-20923
The response of a laminar boundary layer in supersonic flow to small amplitude progressive waves
[NASA-TM-101965] N89-21197
SUPERSONIC WIND TUNNELS
A study of transonic drag reduction of a blunt cylinder by a cylinder probe
[AD-A202557] N89-20965
SUPPORT INTERFERENCE
Test techniques: A survey paper on cryogenic tunnels, adaptive wall test sections, and magnetic suspension and balance systems N89-20955
Potential flow evaluation of the interference effect of strut-through-appendage-tip model mounting technique and reduction of the effect using blowing and suction
[AD-A202424] N89-21199
SUPPRESSORS
RCS/linear discrete actuator study
[AD-A202822] N89-21028
SURFACE ACOUSTIC WAVE DEVICES
Surface acoustic wave detection of organophosphorus compounds
[AD-A202909] N89-21058
SURFACE COOLING
Global environmental effects of impact-generated aerosols: Results from a general circulation model N89-21306
SURFACE ENERGY
Surface energy from order parameter profile: At the QCD phase transition
[NASA-CR-184890] N89-21633
SURFACE LAYERS
Calculation of carriers in depletion region of semiconductors with capacitance-voltage measurements
[AD-A202529] N89-21668
Evaluation of the spatial and temporal characteristics of the conducting PRIZ
[AD-A202593] N89-21671
SURFACE PROPERTIES
Organic functional group reactivities at metal surfaces
[AD-A203094] N89-21086
Response surface analysis of stochastic network performance
[AD-A202561] N89-21554
Extracting shape reflectance of Lambertian, specular, and hybrid surfaces
[AD-A203772] N89-21652
The determination of Crystallite Orientation Distribution Functions (CODF) and their use in surface texture analysis using X-ray diffraction
[AERE-R-12839] N89-21663
X-ray fluorescence surface contaminant analyzer: A feasibility study N89-21736
SURFACE REACTIONS
Excitation and diagnostics of optical contamination in the spacecraft environment
[AD-A202429] N89-21015
Surface chemistry and structural effects in the stress corrosion of glass and ceramic materials
[AD-A202452] N89-21107
Organic chemistry in two dimensions: Surface-functionalized polymers and self-assembled monolayer films
[AD-A202955] N89-21118
Atomistic simulations of interfaces in metals and alloys
[DE89-006521] N89-21685
SURFACE ROUGHNESS
OSRMS (Ocean Surface Roughness Measurement System): The DREP (Defence Research Establishment Pacific) near-nadir scatterometer
[AD-A202983] N89-21460
SURFACE TEMPERATURE
Infrared surface temperature measurements for the surface tension driven convection experiment
[NASA-TM-101353] N89-21224
Ice cover on Chesapeake Bay from AVHRR (Advanced Very High Resolution Radiometer) and LANDSAT imagery, winter of 1987-88
[PB89-117261] N89-21415
SURFACE WAVES
A theoretical and experimental investigation of linear and nonlinear focussing chirped optical diffraction gratings
[AD-A203396] N89-21650
SURFACES
The numerical simulation of Richtmyer-Meshkov unstable interfaces: A conference report N89-21512
SURVEILLANCE
Light satellites: A dilemma for the US Army
[AD-A202648] N89-21017
SURVEYS
Asteroid and comet flux in the neighborhood of the earth N89-21387
Measurer's handbook: US Army anthropometric survey, 1987-1988
[AD-A202721] N89-21484
SURVIVAL
Limitations on K-T mass extinction theories based upon the vertebrate record N89-21290
Nonparamteric estimation from queues arising in staggered entry clinical trials N89-21520
SWITCHES
AH-1S communication switch integration program
[NASA-TM-101053] N89-20978
SYNCHRONISM
Analysis and simulation of a pseudonoise synchronization system
[AD-A202779] N89-21149
The design and performance of the rollback chip: Hardware support for time warp
[AD-A203160] N89-21571
SYNTAX
Design of a syntax validation tool for requirements analysis using Structured Analysis and Design Technique (SADT)
[AD-A202725] N89-21562
Semantical paradigms: Notes for an invited lecture
[AD-A202995] N89-21565
SYNTHESIS (CHEMISTRY)
Chemical vapor synthesis of niobium aluminides
[AD-A202591] N89-21055
Shock-induced chemical synthesis of intermetallic compounds
[DE89-007035] N89-21095
Synthesis of ceramics at low temperatures N89-21102
Synthesis of energetic binders
[AD-A203060] N89-21127
SYNTHETIC APERTURE RADAR
Imaging of ocean waves by SAR
[AD-A203604] N89-21165
SYNTHETIC FUELS
Gas turbine alternative fuels combustion characteristics
[NASA-TM-101470] N89-21417
SYSTEMS ANALYSIS
Optical fiber sensors and signal processing for intelligent structure monitoring
[NASA-CR-184841] N89-21640
Small expendable deployer system measurement analysis N89-21731
SYSTEMS ENGINEERING
Application of a single area array detector for acquistion, tracking and point-ahead in space optical communications
[NASA-CR-183423] N89-21168
Reliability/maintainability/testability design for dormancy
[AD-A202704] N89-21179
Cryogenic reactant storage for lunar base regenerative fuel cells
[NASA-TM-101980] N89-21419
An intelligent advisor for the design manager
[NASA-TM-101558] N89-21539
Architecture and design for a laser programmable double precision floating point application specific processor
[AD-A202560] N89-21553
An educational expert system shell integrating object-attribute-value triples and frames
[AD-A202574] N89-21557
A decision-based methodology for object oriented-design
[AD-A202579] N89-21558
A methodology for screening potential artificial intelligence applications
[AD-A203966] N89-21594
Evaluation of aerosol size distribution models
[AD-A202736] N89-21645
Systems engineering and technical assistance
[AD-A203479] N89-21696
SYSTEMS INTEGRATION
Transonic propulsion system integration analysis at McDonnell Aircraft Company N89-20943
Aeroelastic modeling for the FIT team F/A-18 simulation
[NASA-TM-101569] N89-20991
Software development guidelines
[AD-A203332] N89-21572
SYSTEMS MANAGEMENT
Analysis of the Federal Aviation Administration's host computer acquisition process and potential application in Department of Defense acquisitions
[AD-A202623] N89-21695

T

TABLES (DATA)
Corrosion control climatology
[AD-A202477] N89-21079
TACAN
Aircraft tracking with dual TACAN
[AD-A202647] N89-20980
TAIL ASSEMBLIES
Tailless aircraft performance improvements with relaxed static stability
[NASA-CR-181806] N89-20999
TARGET ACQUISITION
Light satellites: A dilemma for the US Army
[AD-A202648] N89-21017
TARGET RECOGNITION
Seeing Ghost solutions in stereo vision
[AD-A203581] N89-21473
Modified backward error propagation for tactical target recognition
[AD-A202666] N89-21644
TARGETS
Multiple model adaptive tracking of airborne targets
[AD-A202696] N89-21148
Numerical modeling of narrow band soft X-ray sources
[AD-A203368] N89-21657
TASKS
Manipulator primitive level task decomposition
[PB89-133532] N89-21238
TAXONOMY
Limitations on K-T mass extinction theories based upon the vertebrate record N89-21290
The Triassic-Jurassic boundary in eastern North America N89-21366
TECHNOLOGY ASSESSMENT
Wind energy program summary. Volume 1, Overview: Fiscal year 1988
[DE89-000856] N89-21420
Ocean energy program summary. Volume 1, Overview: Fiscal year 1988
[DE89-000858] N89-21421
Fusion: A necessary component of US energy policy
[DE89-006234] N89-21659
TECHNOLOGY UTILIZATION
Geothermal energy program summary: Volume 1: Overview Fiscal Year 1988
[DE89-000864] N89-21422
TECTONICS
The cratering record in the inner solar system: Implications for earth N89-21292
The Sudbury Structure (Ontario, Canada) and Vredefort Structure (South Africa): A comparison N89-21311
Evidence of volcanic ash at a K-T boundary section: Ocean drilling program hole 690 C, Maud Rise, Weddell Sea off East Antarctica N89-21410

Neotectonics in Central Mexico from LANDSAT TM data
[NASA-CR-183416] N89-21416
A comprehensive study of the seismotectonics of the eastern Aleutian arc and associated volcanic systems
[DE89-007357] N89-21443

TEKTITES
Magnetic microspherules associated with the K/T and upper Eocene extinction events N89-21303
Tektites: Origin as melts produced by the impact of small projectiles onto dry targets N89-21405
New approach to the origin of the tektite in China N89-21414

TELEMETRY
Satellite telemetry: A new tool for wildlife research and management
[PB88-249255] N89-21013
Satellite signatures of rapid cyclogenesis
[AD-A203934] N89-21452
Evaluation of aerosol size distribution models
[AD-A202736] N89-21645
Small expendable deployer system measurement analysis N89-21731

TELESCOPES
NASA Marshall Space Flight Center solar observatory report, January - December 1987
[NASA-TM-100360] N89-21712

TEMPERATURE CONTROL
Conjugating binary systems for spacecraft thermal control
[NASA-CR-183608] N89-21023
High capacity demonstration of honeycomb panel heat pipes
[NASA-CR-181776] N89-21191

TEMPERATURE DISTRIBUTION
Spline-based finite-element method for solving a Stefan's problem in a finite domain: Formulation N89-21516

TEMPERATURE EFFECTS
Effect of geometry on thermal aging behavior of Celion/LARC-160 composites
[NASA-TM-100496] N89-21047
Operation of vehicle engines in cold conditions: Start up, lubrication and fuel consumption
[DE88-757111] N89-21255
Strain energy release rate as a function of temperature and preloading history utilizing the edge delamination fatique test method
[NASA-CR-184966] N89-21286

TEMPERATURE MEASUREMENT
Thermopile temperature sensitivity calibration procedure for Eppley broadband radiometers
[PB89-104129] N89-21215
Infrared surface temperature measurements for the surface tension driven convection experiment
[NASA-TM-101353] N89-21224

TEMPERATURE RATIO
Sounds in one-dimensional superfluid helium
[AD-A202428] N89-21629

TEMPERING
Advanced tribological coatings for high specific strength alloys
[AD-A202505] N89-21110

TENSILE PROPERTIES
Microscopic aspects of failure and fracture in cross-ply fiber-reinforced composite laminates
[AD-A203202] N89-21042
Investigation of failure modes in fiber reinforced ceramic matrix composites
[AD-A202705] N89-21113

TENSILE STRENGTH
A study of failure characteristics in a thermoplastic composite material at high temperature
[AD-A203015] N89-21040

TENSILE STRESS
The behavior of ceramic matrix, fiber composites under combined impact and tensile stresses
[AD-A202518] N89-21038

TENSILE TESTS
Static tensile and tensile creep testing of five ceramic fibers at elevated temperatures
[NASA-CR-177525] N89-21046

TENSORS
Diffusion in symplectic maps
[DE89-008083] N89-21622

TERMS
SESC (Space Environment Services Center) glossary of solar-terrestrial terms, 2nd edition
[PB89-120802] N89-21698

TERNARY ALLOYS
Low temperature properties of ternary magnetic rare earth transition metal germanides with the Sc5Co4Ge10-type structure
[DE89-007628] N89-21666

TERRAIN
Proximal ecological effects of the 1980 eruptions of Mount St. Helens N89-21394
Downward continuation of the free-air gravity anomalies to the ellipsoid using the gradient solution, Poisson's integral and terrain correction-numerical comparison and computations
[AD-A203739] N89-21442
A simple model for wind field estimation in complex terrain
[DE89-007240] N89-21457
Column movement model used to support AMM N89-21521
A software system to create a hierarchical, multiple level of detail terrain model
[AD-A203047] N89-21568

TERRAIN ANALYSIS
Computer strategy for detecting line features on simulated binary arrays in support of radar feature extraction
[AD-A203257] N89-21162
A software system to create a hierarchical, multiple level of detail terrain model
[AD-A203047] N89-21568

TERRESTRIAL PLANETS
Atmospheric erosion by impacts: An analytic investigation N89-21403

TEST FACILITIES
Simulation at Dryden Flight Research Facility from 1957 to 1982
[NASA-TM-101695] N89-20983
A real-time simulator of a turbofan engine
[NASA-TM-100869] N89-20995

TEST FIRING
Dynamic analysis of feedforward neural networks using simulated and measured data
[AD-A202573] N89-21591
SSME propulsion performance reconstruction techniques N89-21752

TEXTURES
The determination of Crystallite Orientation Distribution Functions (CODF) and their use in surface texture analysis using X-ray diffraction
[AERE-R-12839] N89-21663

THALLIUM COMPOUNDS
Central research project report on superconductivity (1988). Part 1: Materials and IR detectors
[AD-A203891] N89-21681

THEMATIC MAPPERS (LANDSAT)
Neotectonics in Central Mexico from LANDSAT TM data
[NASA-CR-183416] N89-21416

THEMATIC MAPPING
Neotectonics in Central Mexico from LANDSAT TM data
[NASA-CR-183416] N89-21416

THEORETICAL PHYSICS
Theoretical studies of the chemistry and physics of oxygen in silicon
[AD-A203168] N89-21063
Center for Atomic, Molecular and Optical Physics technical activities, 1988
[PB89-132302] N89-21623

THEORIES
The interdependencies of theory formation, revision, and experimentation
[AD-A202882] N89-21618

THERMAL ANALYSIS
Three dimensional thermal analysis of rocket thrust chambers
[NASA-TM-101973] N89-21025
Thermal and dynamic analysis of the RING (Radiatively-cooled, Inertially-driven Nuclear Generator) power system radiator
[DE89-007236] N89-21639
Computer codes for thermal analysis of a solid rocket motor nozzle N89-21733

THERMAL BLOOMING
Atmospheric effects on laser propagation
[DE89-008646] N89-21237

THERMAL CONDUCTIVITY
A numerical study of the turbulent free convection in rectangular cavities N89-21194
A model for interface temperatures induced by convection heat transfer in porous materials
[DE89-008202] N89-21214

THERMAL FATIGUE
Crack growth of a titanium-aluminide alloy under thermal-mechanical fatigue
[AD-A202767] N89-21083

THERMAL PROTECTION
Thermal protection afforded by two anti-exposure coveralls when worn in cold water
[AD-A202865] N89-21485

THERMIONIC EMISSION
Optical power limiter
[AD-A203964] N89-21234

THERMODYNAMIC PROPERTIES
Thermodynamic analysis of chemical compatibility of several reinforcement materials with niobium aluminides
[NASA-CR-182260] N89-21036
Improved high-temperature resistant matrix resins
[NASA-CR-180826] N89-21105
A review of reaction rates and thermodynamic and transport properties for the 11-species air model for chemical and thermal nonequilibrium calculations to 30000 K
[NASA-TM-101528] N89-21193
Basic studies of ion mixing
[AD-A203093] N89-21637
The role of the turbulent Prandtl number in turbine blade heat transfer prediction N89-21756

THERMODYNAMICS
Fluids, both ionic and nonionic, over wide ranges of temperature and composition
[DE89-001265] N89-21048
A continuum diffusion model for viscoelastic materials
[AD-A202588] N89-21112
Transactions of the Fifth Army Conference on Applied Mathematics and Computing
[AD-A193384] N89-21490
Toward a nonequilibrium thermodynamics of two phase materials with sharp interface N89-21494
Thermodynamic gauge theory of solids and quantum liquids with internal phase N89-21525
Lagrangian formulation of relativistic thermodynamics N89-21526
Documentation of the finite element code VISCOT/UX for thermomechanical analyses: Version 0.01
[DE89-004719] N89-21544
Thermomechanical analysis with phase transformations: A unified approach
[AD-A203383] N89-21692
Cryogenic fluid management in space N89-21727
The role of radiation-dynamics interaction in regional numerical weather prediction N89-21732

THERMONUCLEAR REACTIONS
Computer modeling and simulation in inertial confinement fusion
[DE89-008304] N89-21661

THERMOPLASTIC RESINS
A study of failure characteristics in a thermoplastic composite material at high temperature
[AD-A203015] N89-21040

THERMOSETTING RESINS
The shear-lag model for a unidirectional composite with viscoelastic matrix N89-21495

THICK PLATES
Transverse shear considerations in anisotropic plates
[AD-A203187] N89-21283

THIN FILMS
Chemical vapor synthesis of niobium aluminides
[AD-A202591] N89-21055
Photochemistry at corrugated thin metal films: A phenomenological approach
[AD-A203070] N89-21061
Research on silicon, carbon, and silicon carbide heterostructures
[AD-A202866] N89-21116
Organic chemistry in two dimensions: Surface-functionalized polymers and self-assembled monolayer films
[AD-A202955] N89-21118
Investigation of the impedance modulation of thin films with a chemically-sensitive field-effect transistor
[AD-A202766] N89-21180
Center for thin film studies
[AD-A202742] N89-21673
Magnetic properties of nano-heterogeneous amorphous, thin films
[AD-A203727] N89-21680
Film elastic properties determined by the indentation test-theoretical considerations
[AD-A203997] N89-21683

THIN WALLED SHELLS
Function theory for thin elastic shells
[PB89-101943] N89-21257
A triangular thin shell element for the linear analysis of stiffened composite structures
[AD-A202864] N89-21277

THREE DIMENSIONAL BOUNDARY LAYER
Transonic CFD applications at Boeing N89-20929
Secondary three-dimensional instability in compressible boundary layers N89-20954

THREE DIMENSIONAL FLOW
The 3-D Euler and Navier-Stokes calculations for aircraft components N89-20950
Stability of compressible boundary layers N89-20953
The KP equation: A comparison to laboratory generated biperiodic waves N89-21507

Space shuttle main engine numerical modeling code modifications and analysis N89-21760

THREE DIMENSIONAL MODELS

Comparison of 3D computation and experiment for non-axisymmetric nozzles
[NASA-CR-182245] N89-20921

Capabilities of wind tunnels with two-adaptive walls to minimize boundary interference in 3-D model testing N89-20961

Three-dimensional singular points in aerodynamics
[NASA-TM-100045] N89-20964

A 3-dimensional numerical simulation of the atmospheric injection of aerosols by a hypothetical basaltic fissure eruption N89-21401

Operational implications of a cloud model simulation of space shuttle exhaust clouds in different atmospheric conditions
[NASA-CR-4222] N89-21425

THREE DIMENSIONAL MOTION

Effect of two-body motion on radar beam quality for various distributed sparse array configurations
[AD-A202937] N89-21154

THRUST

Geomagnetic field energy as a source of thrust
[AD-A202567] N89-21027

THRUST AUGMENTATION

An experimental investigation of flow mixing on thrust ejection efficiency
[AD-A202707] N89-21205

THRUST CHAMBERS

Three dimensional thermal analysis of rocket thrust chambers
[NASA-TM-101973] N89-21025

THUNDERSTORMS

Corrosion control climatology
[AD-A202477] N89-21079

Finite element simulation of thunderstorm electrodynamics in the proximity of the storm N89-21728

TIME

A source code analyzer to predict compilation time for avionics software using software science measures. Volume 1: Main report
[AD-A202737] N89-20992

Speech recognition using neural nets and dynamic time warping
[AD-A202528] N89-21144

A very simple polynomial-time algorithm for linear programming
[AD-A202502] N89-21548

Distributed discrete-event simulation using variants of the Chandy-Misra algorithm on the intel hypercube
[AD-A202849] N89-21563

TIME DEPENDENCE

Real-time display of time dependent data using a head-mounted display
[AD-A203051] N89-20993

The application of modal coordinate methods to large nonlinear time-dependent problems
[AD-A203913] N89-21611

TIME LAG

Evaluation of time delay requirements for closed-loop stability using classical and modern methods
[DE89-006417] N89-21189

The shear-lag model for a unidirectional composite with viscoelastic matrix N89-21495

Time delay estimation in stationary and non-stationary environments
[AD-A202507] N89-21549

TIME MARCHING

Euler solvers for transonic applications N89-20935

TIME MEASUREMENT

Biostratigraphic case studies of six major extinctions N89-21390

TIME OPTIMAL CONTROL

Time optimal slewing of flexible spacecraft N89-21014

TIME SERIES ANALYSIS

High resolution chronology of late Cretaceous-early Tertiary events determined from 21,000 yr orbital-climatic cycles in marine sediments N89-21328

Periodicity of extinction: A 1988 update N89-21385

A neural network implementation of chaotic time series prediction
[AD-A203049] N89-21569

Bispectral inversion: The construction of a time series from its bispectrum
[AD-A202508] N89-21598

TIME SHARING

Time warp on a shared memory multiprocessor
[AD-A203088] N89-21534

TISSUES (BIOLOGY)

Research on acoustic coupling to electromagnetic pulses in tissue
[AD-A195644] N89-21140

Gating kinetics and ion transfer in channels of nerve membrane
[AD-A202509] N89-21464

Accurate determination of the complex permittivity of biological tissue around 35 GHz
[AD-A202907] N89-21470

TITANIUM

Shear banding in titanium with controlled elongations at 1 million/sec
[DE89-006555] N89-21094

Spectroscopy and laser performance of Ti(sup 3+) doped and Cr(sup 3+), Nd(sup 3+) co-doped crystals
[AD-A203911] N89-21682

TITANIUM ALLOYS

Investigation of crack growth in titanium-aluminide at elevated temperatures
[AD-A202570] N89-21081

The effects of loading history and closure of the fatigue characteristics of heat treated Ti-6Al-2Sn-4Zr-6Mo
[AD-A202652] N89-21082

Crack growth of a titanium-aluminide alloy under thermal-mechanical fatigue
[AD-A202767] N89-21083

The microstructural and phase characterization of RST Al-Ti-X alloys
[AD-A203734] N89-21092

Structural energy differences in Al3Ti: The role of tetragonal distortion in APB and twin energies
[DE89-007210] N89-21096

TITANIUM ISOTOPES

Ion microprobe of Mg, Ca, Ti and Fe isotopic ratios and trace element abundances in hibonite-bearing inclusions from primitive meteorites- N89-21719

TOKAMAK DEVICES

Short wave electron temperature gradient driven drift wave turbulence
[DE89-008465] N89-21662

TOLERANCES (PHYSIOLOGY)

A study of motion sickness: Mathematical modeling and data analysis
[AD-A202770] N89-21466

TOMOGRAPHY

Correction of gain and optical throughput variations in a two-dimensional imaging spectrometer
[AD-A203495] N89-21222

TOPOGRAPHY

Proximal ecological effects of the 1980 eruptions of Mount St. Helens N89-21394

TOROIDAL PLASMAS

Theoretical studies of the heating of toroidal plasmas with radiofrequency electromagnetic radiation
[DE89-008003] N89-21660

TORSIONAL VIBRATION

A new model for the forced response of a mistuned disk
[AD-A202769] N89-21275

TOUCH

Robotic tactile sensor fabricated from piezoelectric polyvinylidene fluoride films
[AD-A202724] N89-21250

TOUGHNESS

Investigation of the impact performance of various glass and ceramic systems
[AD-A202443] N89-21106

TOXICITY

Heavy metal toxicity as a kill mechanism in impact caused mass extinctions N89-21406

TRACE ELEMENTS

Evidence for a single impact at the Cretaceous-Tertiary boundary from trace elements N89-21319

Iridium, shocked minerals, and trace elements across the Cretaceous/Tertiary boundary at Maud Rise, Wedell Sea, and Walvis Ridge, South Atlantic Ocean N89-21333

Trace element and isotope geochemistry of Cretaceous-Tertiary boundary sediments: identification of extra-terrestrial and volcanic components N89-21352

Ion microprobe of Mg, Ca, Ti and Fe isotopic ratios and trace element abundances in hibonite-bearing inclusions from primitive meteorites N89-21719

TRACKING (POSITION)

Aircraft tracking with dual TACAN
[AD-A202647] N89-20980

Satellite telemetry: A new tool for wildlife research and management
[PB88-249255] N89-21013

Multiple model adaptive tracking of airborne targets
[AD-A202696] N89-21148

Application of a single area array detector for acquistion, tracking and point-ahead in space optical communications
[NASA-CR-183423] N89-21168

Localizing and beamforming freely-drifting VLF (Very Low Frequency) acoustic sensors
[AD-A202638] N89-21217

Analysis of space-based lidar for aircraft tracking
[AD-A202665] N89-21230

The Rochester robot
[AD-A202633] N89-21247

The numerical simulation of Richtmyer-Meshkov unstable interfaces: A conference report N89-21512

TRAILING EDGE FLAPS

An experimental study of transonic buffet of a supercritical airfoil with trailing edge flap
[AD-A203189] N89-20968

TRAINING DEVICES

Real-time display of time dependent data using a head-mounted display
[AD-A203051] N89-20993

TRAJECTORIES

Stability solution to linearized equations of motion for a symmetric spinning satellite in an elliptical orbit applied to the non-linear equations
[AD-A202934] N89-21010

TRAJECTORY ANALYSIS

A rapid-backscatter simulation technique for complex B-spline target models N89-21505

TRANSFER FUNCTIONS

Root placement with transfer function methods (full state feedback)
[AD-A203877] N89-21610

TRANSFERRING

Lockheed Aeronautical Systems Company technical order transfer tests
[DE89-008092] N89-21707

TRANSFORMATIONS (MATHEMATICS)

Lie transforms applied to a nonlinear parametric excitation problem N89-21491

TRANSFORMERS

On-line location of partial discharges in power transformer through acoustic emission
[DE88-757043] N89-21188

TRANSIENT RESPONSE

Characterization of structural connections using free and forced response test data
[NASA-TM-101991] N89-21266

TRANSISTOR CIRCUITS

A multiple-valued logic system for circuit extraction to VHDL 1076-1987
[AD-A202646] N89-21177

TRANSISTOR LOGIC

A multiple-valued logic system for circuit extraction to VHDL 1076-1987
[AD-A202646] N89-21177

TRANSITION FLOW

A study of transonic drag reduction of a blunt cylinder by a cylinder probe
[AD-A202557] N89-20965

TRANSITION METALS

Organic functional group reactivities at metal surfaces
[AD-A203094] N89-21086

Low temperature properties of ternary magnetic rare earth transition metal germanides with the Sc5Co4Ge10-type structure
[DE89-007628] N89-21666

TRANSITION TEMPERATURE

Calculation of the glass transition temperatures of linear polymers. Part 3: Evaluation of calculation relationships
[AD-A203357] N89-21122

TRANSLATING

Domain modeling for language analysis
[AD-A203444] N89-21574

TRANSMISSION LINES

Channelized coplanar waveguide: Discontinuities, junctions, and propagation characteristics
[NASA-TM-101483] N89-21172

LCP-10 intelligibility of oxygen masks and microphones in aircraft noise
[AD-A202474] N89-21481

TRANSMITTANCE

Hybrid calculation of invariant moments
[AD-A202594] N89-21600

TRANSMITTERS

Satellite telemetry: A new tool for wildlife research and management
[PB88-249255] N89-21013

Implementation and testing of a new 16-PSK transmitter
[AD-A203936] N89-21166

TRANSONIC FLOW

Additional development of the XTRAN3S computer program
[NASA-CR-181743] N89-20922

Airframe/propulsion integration characteristics at transonic speeds N89-20926

Shock-boundary-layer interaction in flight N89-20928

Transonic CFD applications at Boeing N89-20929

Transonics and fighter aircraft: Challenges and opportunities for CFD N89-20932

Transonic aerodynamic design experience N89-20934

Euler solvers for transonic applications N89-20935
Asymptotic methods for internal transonic flows N89-20937
Wave drag due to lift for transonic airplanes N89-20938
Developments and trends in three-dimensional mesh generation N89-20940
Transonic Symposium: Theory, Application, and Experiment, volume 1, part 2 [NASA-CP-3020-VOL-1-PT-2] N89-20942
Transonic propulsion system integration analysis at McDonnell Aircraft Company N89-20943
Aerodynamic analysis of three advanced configurations using the TranAir full-potential code N89-20944
Steady and unsteady transonic small disturbance analysis of realistic aircraft configurations N89-20946
Inverse wing design in transonic flow including viscous interaction N89-20947
Euler/Navier-Stokes calculations of transonic flow past fixed- and rotary-wing aircraft configurations N89-20948
The 3-D Euler and Navier-Stokes calculations for aircraft components N89-20950
Turbulence and modeling in transonic flow N89-20951
Turbulent eddy viscosity modeling in transonic shock/boundary-layer interactions N89-20952
Wall interference assessment and corrections N89-20958
Two-measured variable method for wall interference assessment/correction N89-20959
A study of transonic drag reduction of a blunt cylinder by a cylinder probe [AD-A202557] N89-20965
An experimental study of transonic buffet of a supercritical airfoil with trailing edge flap [AD-A203189] N89-20968
Two-dimensional Navier-Stokes solution of the flow over a thick supercritical airfoil with strong shock-induced separation [AD-A203331] N89-20971
Numerical computation of shock wave-turbulent boundary layer interaction in transonic flow over an axisymmetric curved hill [NASA-TM-101473] N89-21192
Development of a shock capturing code for use as a tool in designing high-work low aspect ratio turbines [AD-A202706] N89-21248

TRANSONIC SPEED
The application of CFD for military aircraft design at transonic speeds N89-20930
Method to predict external store carriage loads at transonic speeds N89-20945
Two-measured variable method for wall interference assessment/correction N89-20959

TRANSONIC WIND TUNNELS
Instrumentation advances for transonic testing N89-20957
Performance of the active sidewall boundary-layer removal system for the Langley 0.3-meter Transonic Cryogenic Tunnel [NASA-CR-181793] N89-21004

TRANSPORT PROPERTIES
A review of reaction rates and thermodynamic and transport properties for the 11-species air model for chemical and thermal nonequilibrium calculations to 30000 K [NASA-TM-101528] N89-21193
Electron mobility in mercury cadmium telluride N89-21748

TRAPPED PARTICLES
Order in cold ionic systems: Dynamic effects [DE89-007377] N89-21687

TRAPS
A laser trap for neutral atoms [AD-A202581] N89-21229

TRAVELING WAVE TUBES
Design, fabrication, and performance of brazed, graphite electrode, multistage depressed collectors with 500-W, continuous wave, 4.8- to 9.6-GHz traveling-wave tubes [NASA-TP-2904] N89-21171

TREND ANALYSIS
Limitations on K-T mass extinction theories based upon the vertebrate record N89-21290
Rocks, resolution, and the record at the terrestrial K/T boundary, eastern Montana and western North Dakota N89-21313
The impact of mass extinctions N89-21315
A study of motion sickness: Mathematical modeling and data analysis [AD-A202770] N89-21466

TRENDS
Abrupt climate change and extinction events N89-21308
Geochemical comparison of K-T boundaries from the Northern and Southern Hemispheres N89-21400
Software system safety N89-21754

TRIANGULATION
Rootfinding for Markov chains with quasi-triangular transition matrices [AD-A202468] N89-21597
Triangularity of the basis in linear programs for material requirements planning, revision [AD-A203039] N89-21606

TRIBOLOGY
Advanced tribological coatings for high specific strength alloys [AD-A202505] N89-21110

TRINITROTOLUENE
Effect of TNT miscible additives on the mechanical behavior and shock sensitivity of Composition B [AD-A203968] N89-21132

TRUNCATION ERRORS
Studies in the computation of compressible and viscous flow [AD-A203334] N89-21208

TSUNAMI WAVES
Sedimentological effects of tsunamis, with particular reference to impact-generated and volcanogenic waves N89-21299

TUNGSTEN ALLOYS
Stress-corrosion cracking of liquid-phase sintered tungsten alloys [AD-A203201] N89-21087

TURBINE BLADES
A compendium of controlled diffusion blades generated by an automated inverse design procedure [NASA-TM-101968] N89-20996
The role of the turbulent Prandtl number in turbine blade heat transfer prediction N89-21756

TURBINE PUMPS
Advanced single crystal for SSME turbopumps [NASA-CR-182244] N89-21072
Advanced helium purge seals for Liquid Oxygen (LOX) turbopumps [NASA-CR-182105] N89-21239
A performance/loss evaluation of SSME HPFTP turbine N89-21735
The simulation of the alternate turbopump development high pressure oxygen and fuel turbopumps for the space shuttle main engine using the Shaberth computer program N89-21746

TURBINE WHEELS
A new model for the forced response of a mistuned disk [AD-A202769] N89-21275

TURBOFAN ENGINES
A real-time simulator of a turbofan engine [NASA-TM-100869] N89-20995

TURBULENCE
Rotationally sampled wind characteristics for several rotor sizes using laser anemometer measurements [DE89-007942] N89-21458
Short wave electron temperature gradient driven drift wave turbulence [DE89-008465] N89-21662
A performance/loss evaluation of SSME HPFTP turbine N89-21735

TURBULENCE MODELS
Turbulence and modeling in transonic flow N89-20951
The role of the turbulent Prandtl number in turbine blade heat transfer prediction N89-21756

TURBULENT BOUNDARY LAYER
A cancellation technique for reducing background noise within turbulent flow environments characterized by pipes and annuli [AD-A202924] N89-21206
Whole field measurements of vorticity in turbulent and unsteady flows [AD-A203349] N89-21209

TURBULENT DIFFUSION
Diffusion in symplectic maps [DE89-008083] N89-21622

TURBULENT FLOW
Turbulent eddy viscosity modeling in transonic shock/boundary-layer interactions N89-20952
Effect of riblets upon flow separation in a subsonic diffuser [AD-A203178] N89-20967
Numerical computation of shock wave-turbulent boundary layer interaction in transonic flow over an axisymmetric curved hill [NASA-TM-101473] N89-21192
A numerical study of the turbulent free convection in rectangular cavities N89-21194
Coherent structures in fully developed turbulent pipe flow N89-21195
On the conditions for resonance interactions of instability waves in the axisymmetric jet [NASA-TM-101477] N89-21196
A cancellation technique for reducing background noise within turbulent flow environments characterized by pipes and annuli [AD-A202924] N89-21206
Whole field measurements of vorticity in turbulent and unsteady flows [AD-A203349] N89-21209

TURBULENT JETS
Experimental examination of the aerothermal performance of the T-10 test cell at NAS (Naval Air Station), Cubi Point [AD-A203887] N89-21005

TURBULENT MIXING
Computational techniques for shock wave diffraction problems [AD-A203439] N89-21210

TURBULENT WAKES
Turbulence modulation and dense-spray structure [AD-A202449] N89-21201

TWINNING
Structural energy differences in Al3Ti: The role of tetragonal distortion in APB and twin energies [DE89-007210] N89-21096

TWO DIMENSIONAL FLOW
Asymptotic methods for internal transonic flows N89-20937
Stability of compressible boundary layers N89-20953
Two-dimensional Navier-Stokes solution of the flow over a thick supercritical airfoil with strong shock-induced separation [AD-A203331] N89-20971

TWO DIMENSIONAL MODELS
A numerical study of the turbulent free convection in rectangular cavities N89-21194

TWO PHASE FLOW
Structure development during converging flow of a liquid crystal dispersed two-phase fluid [AD-A203062] N89-21119

U

U.S.S.R. SPACE PROGRAM
Space technology and the Soviet/US strategic competition: A perspective and forecast using 12-year cycles [AD-A202538] N89-21006

ULTRAHIGH VACUUM
Research on silicon, carbon, and silicon carbide heterostructures [AD-A202866] N89-21116

ULTRASONIC TESTS
A study of the stress wave factor technique for evaluation of composite materials [NASA-CR-4195] N89-21256

ULTRASONICS
Frequency dependent ultrasonic ray tracing: A preliminary study [AERE-R-13119] N89-21139

UNIQUENESS
Confidence set inference with a prior quadratic bound [NASA-CR-184839] N89-21435

UNITED STATES
Space technology and the Soviet/US strategic competition: A perspective and forecast using 12-year cycles [AD-A202538] N89-21006

UNIVERSE
Surface energy from order parameter profile: At the QCD phase transition [NASA-CR-184890] N89-21633
A new class of non-topological solitons [NASA-CR-184889] N89-21634

UNSTEADY AERODYNAMICS
Additional development of the XTRAN3S computer program [NASA-CR-181743] N89-20922
Unsteady force calculations on circular cylinders and elliptical airfoils with circulation control [UMAERO-87-37] N89-20962
Methodology for using steady experimental aerodynamic data to improve steady and unsteady aerodynamic analysis N89-20972
Aeroelastic modeling for the FIT team F/A-18 simulation [NASA-TM-101569] N89-20991

UNSTEADY FLOW
Steady and unsteady transonic small disturbance analysis of realistic aircraft configurations N89-20946
Whole field measurements of vorticity in turbulent and unsteady flows [AD-A203349] N89-21209
A performance/loss evaluation of SSME HPFTP turbine N89-21735

USER MANUALS (COMPUTER PROGRAMS)
MOPAC manual, 5th edition: A general molecular orbital package
[AD-A204003] N89-21069
SURVNET user's manual
[AD-A203372] N89-21164
Otter 1.0 users' guide
[DE89-008656] N89-21581
USER REQUIREMENTS
Microwave landing systems: Additional systems should not be procured unless benefits proven
[GAO/RCED-88-118] N89-20977

V

VALENCE
Study of semiconductor valence plasmon line shapes via electron energy-loss spectroscopy in the transmission electron microscope
[DE89-008152] N89-21689
VAN DER WAAL FORCES
Molecular jet studies of vdW (van der Waals) clusters and solvation
[AD-A203766] N89-21212
VANADIUM ALLOYS
Nuclear magnetic resonance study of hydrogen in niobium-vanadium alloys
[DE89-007578] N89-21075
VAPOR DEPOSITION
Convection and chemistry effects in CVD: A 3-D analysis for silicon deposition
[NASA-TM-102001] N89-21032
Chemical vapor synthesis of niobium aluminides
[AD-A202591] N89-21055
Theoretical studies of heterogeneous reactions in silicon CVD (Silicon Vapor Deposition) catalysis
[AD-A202905] N89-21057
Research on silicon, carbon, and silicon carbide heterostructures
[AD-A202866] N89-21116
VAPOR PHASES
Iridium emissions from Hawaiian volcanoes N89-21314
VARIABILITY
The causes for geographical variations in OS187/OS186 at the Cretaceous-Tertiary boundary N89-21402
VARIABLE THRUST
Radiation effect on rocket engine performance N89-21734
VARIATIONS
A comparison of control variates for queueing network simulation
[AD-A202576] N89-21599
VECTOR ANALYSIS
Radio-controlled model gyro measurement study
[AD-A204002] N89-21223
VECTORS (MATHEMATICS)
Vector potential methods N89-20939
Three-dimensional singular points in aerodynamics
[NASA-TM-100045] N89-20964
An adaptive overlapping local grid refinement method for two-dimensional parabolic systems N89-21514
A vectorized hidden-surface algorithm implemented on the Cray-2 supercomputer
[AD-A202657] N89-21560
Half-solitons in superfluid (3)He-A: Novel pi/2-quanta of phase slippage
[PB89-128904] N89-21664
Optimization of large matrix calculations for execution on the Cray X-MP vector supercomputer N89-21742
VEGETATION
Patterns of megafloral change across the Cretaceous-Tertiary boundary in the Northern Great Plains and Rocky Mountains N89-21336
Widespread habitat change through paludification as an interactive mechanism in mass extinction events N89-21339
A regional perspective on the palynofloral response to K-T boundary event(s) with emphasis on variations imposed by the effects of sedimentary facies and latitude N89-21395
VELOCITY
Column movement model used to support AMM N89-21521
VELOCITY DISTRIBUTION
A simple model for wind field estimation in complex terrain
[DE89-007240] N89-21457
VELOCITY MEASUREMENT
Acoustic emission source location in fibre reinforced plastic composites
[AERE-R-13039] N89-21035
Coherent structures in fully developed turbulent pipe flow N89-21195
VENUS ATMOSPHERE
Hypersurface insertion window for long term orbital stability of artificial satellites about the planet Venus
[AD-A202808] N89-21009
VERTEBRATES
Limitations on K-T mass extinction theories based upon the vertebrate record N89-21290
Dinosaur bone beds and mass mortality: Implications for the K-T extinction N89-21301
Permo-Triassic vertebrate extinctions: A program N89-21367
VERY LARGE SCALE INTEGRATION
Architecture and design for a laser programmable double precision floating point application specific processor
[AD-A202560] N89-21553
The design and implementation of a special purpose cache for the roll back chip
[AD-A203091] N89-21583
VERY LONG BASE INTERFEROMETRY
On principles, methods and recent advances in studies towards a GPS-based control system for geodesy and geodynamics
[NASA-TM-100716] N89-21434
VERY LOW FREQUENCIES
Localizing and beamforming freely-drifting VLF (Very Low Frequency) acoustic sensors
[AD-A202638] N89-21217
VIBRATION DAMPING
Experiments in end-point control of manipulators with elastic drives N89-21240
Vibration control in rotating machinery using variable dynamic stiffness squeeze-films
[AD-A202902] N89-21252
Stabilization of Ziegler's pendulum by means of the method of vibrational control N89-21531
VIBRATION EFFECTS
Vibration and buckling characteristics of composite cylindrical panels incorporating the effects of a higher order shear theory
[AD-A202939] N89-21278
VIBRATION MODE
Effects of battle damage repair on the natural frequencies and mode shapes of curved rectangular composite panels
[AD-A203179] N89-21041
VIBRATION SIMULATORS
RCS/linear discrete actuator study
[AD-A202822] N89-21028
VIBRATIONAL SPECTRA
MOPAC manual, 5th edition: A general molecular orbital package
[AD-A204003] N89-21069
VINYL POLYMERS
Robotic tactile sensor fabricated from piezoelectric polyvinylidene fluoride films
[AD-A202724] N89-21250
VIRTUAL MEMORY SYSTEMS
A helmet-mounted virtual environment display system
[AD-A203055] N89-20994
The virtual time machine
[AD-A203087] N89-21533
VISCOELASTIC DAMPING
Analytical and experimental investigation of constrained viscoelastic layer damping for a plate and shell model
[AD-A202698] N89-21273
VISCOELASTICITY
A continuum diffusion model for viscoelastic materials
[AD-A202588] N89-21112
Instabilities in shear flow of viscoelastic fluids with fading memory
[AD-A203735] N89-21211
On the energy release rate for dynamic transient anti-plane shear crack propagation in a general linear viscoelastic body
[AD-A202942] N89-21280
An investigation of viscoelastic fracture near and at interfaces
[AD-A203760] N89-21285
The shear-lag model for a unidirectional composite with viscoelastic matrix N89-21495
VISCOPLASTICITY
Macrocrack-multiple defect interaction considering elastic, plastic and viscoplastic effects
[AD-A203186] N89-21282
VISCOSITY
Structure development during converging flow of a liquid crystal dispersed two-phase fluid
[AD-A203062] N89-21119
VISCOUS FLOW
Vector potential methods N89-20939
Inverse wing design in transonic flow including viscous interaction N89-20947
Navier-Stokes and viscous-inviscid interaction N89-20949
Numerical study of three viscous/inviscid interaction methods
[AD-A202575] N89-21203
Studies in the computation of compressible and viscous flow
[AD-A203334] N89-21208
The implementation of a nonreflecting boundary into the SAMSON2 code
[AD-A203394] N89-21284
VISCOUS FLUIDS
Instabilities in shear flow of viscoelastic fluids with fading memory
[AD-A203735] N89-21211
VISION
The Rochester robot
[AD-A202633] N89-21247
Psychophysical studies of visual cortical functions
[AD-A202814] N89-21468
VISUAL ACUITY
Peripheral limitations on spatial vision
[AD-A203388] N89-21472
VISUAL STIMULI
Reconstruction of binocular depth across continuous surfaces
[AD-A202827] N89-21469
VOICE COMMUNICATION
LCP-10 intelligibility of oxygen masks and microphones in aircraft noise
[AD-A202474] N89-21481
Speech database development
[AD-A202461] N89-21699
VOICE DATA PROCESSING
F-16 speaker-independent speech recognition system using cockpit commands (70 words)
[AD-A203177] N89-21489
VOIDS
Large deformations near a pair of closely-spaced spherical voids in a rate-dependent solid
[AD-A202465] N89-21268
VOLCANOES
The cratering record in the inner solar system: Implications for earth N89-21292
Iridium emissions from Hawaiian volcanoes N89-21314
Impact wave deposits provide new constraints on the location of the K/T boundary impact N89-21330
Iridium, shocked minerals, and trace elements across the Cretaceous/Tertiary boundary at Maud Rise, Wedell Sea, and Walvis Ridge, South Atlantic Ocean N89-21333
Volcanic ash layers in blue ice fields (Beardmore Glacier Area, Antarctica): Iridium enrichments N89-21340
Mass killings and detection of impacts N89-21356
Report on an international workshop on Cryptoexplosions and Catastrophes in the Geological Record, with a Special Focus on the Vredefort Structure N89-21375
Assessment of the atmospheric impact of volcanic eruptions N89-21388
Volcanoes and global catastrophes N89-21389
Some volcanologic aspects of Columbia River basalt volcanism relevant to the extinction controversy N89-21393
Proximal ecological effects of the 1980 eruptions of Mount St. Helens N89-21394
Evidence of volcanic ash at a K-T boundary section: Ocean drilling program hole 690 C, Maud Rise, Weddell Sea off East Antarctica N89-21410
A comprehensive study of the seismotectonics of the eastern Aleutian arc and associated volcanic systems
[DE89-007357] N89-21443
VOLCANOLOGY
Global Catastrophes in Earth History: An Interdisciplinary Conference on Impacts, Volcanism, and Mass Mortality
[NASA-CR-183329] N89-21287
Shocked quartz and more: Impact signatures in K-T boundary clays and claystones N89-21297
Sedimentological effects of tsunamis, with particular reference to impact-generated and volcanogenic waves N89-21299
Deccan volcanism at the Cretaceous-Tertiary boundary N89-21305
Noble metals in mid-ocean ridge volcanism: A significant fractionation of gold with respect to platinum group metals N89-21307
Explosive volcanism, shock metamorphism and the K-T boundary N89-21309
The Sudbury Structure (Ontario, Canada) and Vredefort Structure (South Africa): A comparison N89-21311
Volcanism, global catastrophe and mass mortality N89-21316
Catastrophic volcanism N89-21346
Catastrophic volcanism as a cause of shocked features found at the K/T boundary and in cryptoexplosion structures N89-21347

Step-wise extinctions at the Cretaceous-Tertiary boundary and their climatic implications N89-21354
Flood basalts and mass extinctions N89-21360
Deccan volcanism and K-T boundary signatures N89-21362
Cretaceous-Tertiary findings, paradigms and problems N89-21364
Environmental effects of large impacts on the earth; relation to extinction mechanisms N89-21365
Permo-Triassic vertebrate extinctions: A program N89-21367
Dynamics of exploding magma chambers: Implications for K-T volcanism and mass extinctions N89-21377
Computer modeling of large asteroid impacts into continental and oceanic sites: Atmospheric, cratering, and ejecta dynamics N89-21379
Assessment of the atmospheric impact of volcanic eruptions N89-21388
Volcanoes and global catastrophes N89-21389
Biostratigraphic case studies of six major extinctions N89-21390
Some volcanologic aspects of Columbia River basalt volcanism relevant to the extinction controversy N89-21393
Geochemical comparison of K-T boundaries from the Northern and Southern Hemispheres N89-21400
A 3-dimensional numerical simulation of the atmospheric injection of aerosols by a hypothetical basaltic fissure eruption N89-21401
Evidence of volcanic ash at a K-T boundary section: Ocean drilling program hole 690 C, Maud Rise, Weddell Sea off East Antarctica N89-21410
Neotectonics in Central Mexico from LANDSAT TM data
[NASA-CR-183416] N89-21416

VORTEX BREAKDOWN
Numerical simulation of the flow field over delta wings with leading edge blowing N89-20924

VORTEX RINGS
Whole field measurements of vorticity in turbulent and unsteady flows
[AD-A203349] N89-21209

VORTEX SHEETS
Computational studies of an impulsively started viscous flow
[NASA-TM-101037] N89-21190

VORTICES
Numerical simulation of the flow field over delta wings with leading edge blowing N89-20924
An embedded mesh procedure for leading-edge vortex flows N89-20936
Thin-layer Navier-Stokes solutions for a cranked delta wing
[AD-A203292] N89-20970

VORTICITY
Whole field measurements of vorticity in turbulent and unsteady flows
[AD-A203349] N89-21209

VULNERABILITY
Improving the survivability of a stochastic communication network
[AD-A202872] N89-21150

W

WAFERS
Experimental results on atomic oxygen corrosion of silver N89-21738

WALL PRESSURE
Wall interference assessment and corrections N89-20958
A cancellation technique for reducing background noise within turbulent flow environments characterized by pipes and annuli
[AD-A202924] N89-21206

WALLS
Studies of liquid metal flows and power losses in ducts with moving conducting wall, slanted magnetic field, and applied external electric potential
[AD-A203981] N89-21626

WARFARE
The causality horizon and parallel processing for simulations with wide geographical dispersions
[DE89-008484] N89-21590
Strategic defense initiative: A chronology, 1983 - 1988
[AD-A203576] N89-21619

WARNING SYSTEMS
G-induced loss of consciousness and its prevention
[AD-A202960] N89-21471

WATER
Spline-based finite-element method for solving a Stefan's problem in a finite domain: Formulation N89-21516
A numerical model for the computation of radiance distributions in natural waters with wind-roughened surfaces. Part 2: User's guide and code listing
[AD-A203441] N89-21651

WATER WAVES
Imaging of ocean waves by SAR
[AD-A203604] N89-21165
The KP equation: A comparison to laboratory generated biperiodic waves N89-21507

WAVE DIFFRACTION
Computational techniques for shock wave diffraction problems
[AD-A203439] N89-21210

WAVE DISPERSION
Atmospheric effects on laser propagation
[DE89-008646] N89-21237

WAVE EQUATIONS
The role of hydromagnetic waves in the magnetosphere and the ionosphere
[AD-A202800] N89-21437
The interaction of nonlinear hyperbolic waves: A conference report N89-21530

WAVE FRONTS
The interaction of nonlinear hyperbolic waves: A conference report N89-21530

WAVE FUNCTIONS
Topics in chemical physics. 1: Semiclassical reactive scattering theory. 2: Corrected effective medium theory
[DE89-007606] N89-21053
Calculation of the energetics of chemical reactions
[DE89-007262] N89-21070

WAVE INTERACTION
On the conditions for resonance interactions of instability waves in the axisymmetric jet
[NASA-TM-101477] N89-21196
The role of hydromagnetic waves in the magnetosphere and the ionosphere
[AD-A202800] N89-21437
The numerical simulation of Richtmyer-Meshkov unstable interfaces: A conference report N89-21512
The interaction of nonlinear hyperbolic waves: A conference report N89-21530

WAVE PACKETS
Topics in chemical physics. 1: Semiclassical reactive scattering theory. 2: Corrected effective medium theory
[DE89-007606] N89-21053

WAVE PROPAGATION
Time domain wave propagation in multilayered integrated circuits
[AD-A202427] N89-21175
On the conditions for resonance interactions of instability waves in the axisymmetric jet
[NASA-TM-101477] N89-21196
Atmospheric effects on laser propagation
[DE89-008646] N89-21237
The KP equation: A comparison to laboratory generated biperiodic waves N89-21507
Propagator matrices in the solution of EMP problems N89-21515
Lagrangian formulation of relativistic thermodynamics N89-21526

WAVE REFLECTION
Finite-difference modeling of Rayleigh wave scattering and P-SV(Lg) coupling problems
[AD-A203221] N89-21161
Influence of reflected shock waves on a hypersonic shaped charge jet N89-21522

WAVEGUIDES
Channelized coplanar waveguide: Discontinuities, junctions, and propagation characteristics
[NASA-TM-101483] N89-21172

WEAR
Mild wear in dry and lubricated sliding systems N89-21242
The simulation of the alternate turbopump development high pressure oxygen and fuel turbopumps for the space shuttle main engine using the Shaberth computer program N89-21746

WEATHER
CCM (Community Climate Model)
[PB89-120927] N89-21446
Summary of Meteorological Observations, Surface (SMOS) for Moffett Field, California
[AD-A203628] N89-21451

WEATHER FORECASTING
Blending of surface and rawinsonde data in mesoscale objective analysis
[AD-A203984] N89-21456
Research Reports: 1988 NASA/ASEE Summer Faculty Fellowship Program
[NASA-CR-183553] N89-21726

WEATHERING
Ocean alkalinity and the Cretaceous/Tertiary boundary N89-21300
Dinosaur bone beds and mass mortality: Implications for the K-T extinction N89-21301

WEIBULL DENSITY FUNCTIONS
Investigation of Weibull statistics in fracture analysis of cast aluminum
[NASA-TM-102000] N89-21245

WEIGHT REDUCTION
Integrated aerodynamic/dynamic optimization of helicopter rotor blades
[NASA-TM-101553] N89-20982
Thermal and dynamic analysis of the RING (Radiatively-cooled, Inertially-driven Nuclear Generator) power system radiator
[DE89-007236] N89-21639

WEIGHTING FUNCTIONS
Selection of a frequency sensitive QFT (Quantitative Feedback Theory) weighting matrix using the method of specified outputs
[AD-A202692] N89-21592

WELDABILITY
The keyhole region in VPPA welds N89-21755

WELDED JOINTS
Numerical and experimental determination of strain (stress) concentration factors of welded joints between square hollow sections
[PB89-131734] N89-21261

WELDED STRUCTURES
The keyhole region in VPPA welds N89-21755

WELDING
Frequency dependent ultrasonic ray tracing: A preliminary study
[AERE-R-13119] N89-21139
Reduction of M1 weld fabrication costs: The effect of weld shielding gas composition
[AD-A204001] N89-21254

WHITE NOISE
Time-discretized moments of a randomly excited uncertain linear oscillator
[DE89-008318] N89-21614

WILDLIFE
Satellite telemetry: A new tool for wildlife research and management
[PB88-249255] N89-21013

WIND (METEOROLOGY)
Observations of neutral circulation at mid-latitudes during the Equinox Transition Study
[NASA-CR-184792] N89-21429
Upper-wind climatology for CONUS
[AD-A203961] N89-21453
A simple model for wind field estimation in complex terrain
[DE89-007240] N89-21457

WIND DIRECTION
Combined VHF Dopplar radar and airborne (CV-990) measurements of atmospheric winds on the mesoscale
[NASA-CR-184953] N89-21449

WIND EFFECTS
A numerical model for the computation of radiance distributions in natural waters with wind-roughened surfaces. Part 2: User's guide and code listing
[AD-A203441] N89-21651

WIND MEASUREMENT
Combined VHF Dopplar radar and airborne (CV-990) measurements of atmospheric winds on the mesoscale
[NASA-CR-184953] N89-21449
Rotationally sampled wind characteristics for several rotor sizes using laser anemometer measurements
[DE89-007942] N89-21458

WIND PROFILES
Enhancements to the AFGL (Air Force Geophysics Laboratory) Statistical Analysis Program (ASAP) for the global multivariate analysis of heights and winds
[AD-A202912] N89-21450

WIND SHEAR
Combined VHF Dopplar radar and airborne (CV-990) measurements of atmospheric winds on the mesoscale
[NASA-CR-184953] N89-21449

WIND TUNNEL APPARATUS
Instrumentation advances for transonic testing N89-20957

WIND TUNNEL CALIBRATION
Flowfield measurements in the NASA Lewis Research Center 9- by 15-foot low-speed wind tunnel
[NASA-TM-100883] N89-21002

WIND TUNNEL MODELS
Capabilities of wind tunnels with two-adaptive walls to minimize boundary interference in 3-D model testing N89-20961

WIND TUNNEL TESTS
Transonic Symposium: Theory, Application, and Experiment, Volume 1, Part 1
[NASA-CP-3020-VOL-1-PT-1] N89-20925
Airframe/propulsion integration characteristics at transonic speeds N89-20926
Transonic Symposium: Theory, Application, and Experiment, volume 1, part 2
[NASA-CP-3020-VOL-1-PT-2] N89-20942

Test techniques: A survey paper on cryogenic tunnels, adaptive wall test sections, and magnetic suspension and balance systems N89-20955
An LDA (Laser-Doppler Anemometry) investigation of three-dimensional normal shock wave boundary-layer interactions N89-20956
Instrumentation advances for transonic testing N89-20957
Wall interference assessment and corrections N89-20958
Comparison of airfoil results from an adaptive wall test section and a porous wall test section N89-20960
Capabilities of wind tunnels with two-adaptive walls to minimize boundary interference in 3-D model testing N89-20961
Investigation of a free-tip rotor configuration for research on spanwise life distributions and wake velocity surveys of a semi-span wing with a discontinuous twist
[NASA-CR-184948] N89-20963
A wind tunnel and computer investigation of the low speed aerodynamic characteristics of the prone escape system (PRESS)
[AD-A202788] N89-20988
Flowfield measurements in the NASA Lewis Research Center 9- by 15-foot low-speed wind tunnel
[NASA-TM-100883] N89-21002
Comparison of propeller cruise noise data taken in the NASA Lewis 8- by 6-foot wind tunnel with other tunnel and flight data
[NASA-TM-101976] N89-21628

WIND TUNNEL WALLS
Test techniques: A survey paper on cryogenic tunnels, adaptive wall test sections, and magnetic suspension and balance systems N89-20955
Wall interference assessment and corrections N89-20958
Two-measured variable method for wall interference assessment/correction N89-20959
Comparison of airfoil results from an adaptive wall test section and a porous wall test section N89-20960
Capabilities of wind tunnels with two-adaptive walls to minimize boundary interference in 3-D model testing N89-20961
Performance of the active sidewall boundary-layer removal system for the Langley 0.3-meter Transonic Cryogenic Tunnel
[NASA-CR-181793] N89-21004

WIND TURBINES
Wind energy program summary. Volume 1, Overview: Fiscal year 1988
[DE89-000856] N89-21420
Rotationally sampled wind characteristics for several rotor sizes using laser anemometer measurements
[DE89-007942] N89-21458

WIND VARIATIONS
Upper-wind climatology for CONUS
[AD-A203961] N89-21453

WIND VELOCITY
Observations of neutral circulation at mid-latitudes during the Equinox Transition Study
[NASA-CR-184792] N89-21429
Combined VHF Dopplar radar and airborne (CV-990) measurements of atmospheric winds on the mesoscale
[NASA-CR-184953] N89-21449
A simple model for wind field estimation in complex terrain
[DE89-007240] N89-21457
Rotationally sampled wind characteristics for several rotor sizes using laser anemometer measurements
[DE89-007942] N89-21458

WINDPOWER UTILIZATION
Wind energy program summary. Volume 1, Overview: Fiscal year 1988
[DE89-000856] N89-21420

WING NACELLE CONFIGURATIONS
The 3-D Euler and Navier-Stokes calculations for aircraft components N89-20950

WING PROFILES
Additional development of the XTRAN3S computer program
[NASA-CR-181743] N89-20922
Inverse wing design in transonic flow including viscous interaction N89-20947
Turbulence and modeling in transonic flow N89-20951

WINGS
Investigation of a free-tip rotor configuration for research on spanwise life distributions and wake velocity surveys of a semi-span wing with a discontinuous twist
[NASA-CR-184948] N89-20963

WIRE
Characterization of Nb-Al superconducting material
[DE89-008296] N89-21690

WORDS (LANGUAGE)
F-16 speaker-independent speech recognition system using cockpit commands (70 words)
[AD-A203177] N89-21489

WORKLOADS (PSYCHOPHYSIOLOGY)
Brain activity during tactical decision-making. Part 5: A cross-study validation of evoked potentials as indices of workload
[AD-A203763] N89-21474

X

X RAY ANALYSIS
Mechanisms for the source and loss of electrons
[AD-A203066] N89-21438

X RAY BINARIES
An optical study of three transient X-ray sources N89-21724

X RAY DIFFRACTION
XRAYL: A powder diffraction profile refinement program
[PB89-127567] N89-21050
The determination of Crystallite Orientation Distribution Functions (CODF) and their use in surface texture analysis using X-ray diffraction
[AERE-R-12839] N89-21663

X RAY FLUORESCENCE
X-ray fluorescence surface contaminant analyzer: A feasibility study N89-21736

X RAY IMAGERY
Computer-aided X-ray imaging system design and evaluation
[DE89-006599] N89-21653

X RAY SCATTERING
An in-situ grazing incidence X-ray scattering study of the initial stages of electrochemical growth of lead on silver (III)
[AD-A203385] N89-21064

X RAY SOURCES
Numerical modeling of narrow band soft X-ray sources
[AD-A203368] N89-21657
An optical study of three transient X-ray sources N89-21724

Y

YANG-MILLS THEORY
Experimentally verifiable Yang-Mills spin 2 gauge theory of gravity with group U(1) x SU(2) N89-21693

YTTRIUM COMPOUNDS
An in-situ, high-temperature study of the superconductor YBa1.67Sr0.33Cu3O(6+x)
[DE89-007375] N89-21686

Z

ZINC TELLURIDES
MBE of (Hg,Cd)Te
[AD-A202448] N89-21667

ZIRCONIUM OXIDES
High temperature evaluation of new ferroelastic toughened ceramic materials
[AD-A203197] N89-21120

ZODIACAL DUST
Disruption of giant comets in the solar system and around other stars N89-21408

ZOOPLANKTON
Selective extinction of marine plankton at the end of the Mesozoic era: The fossil and stable isotope record N89-21329

Typical Personal Author Index Listing

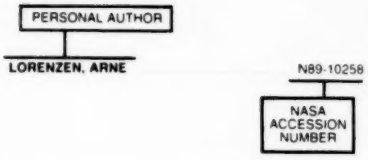

Listings in this index are arranged alphabetically by personal author. The NASA accession number denotes the number by which the citation is identified.

A

ABEDIN, FARIA N89-21223
ABEYARATNE, ROHAN N89-21111
N89-21276
ABROUS, ABDELOUAHAB N89-21194
ACOSTA, R. N89-21136
ADAMS, A. N89-21725
ADAMS, DONALD F. N89-21046
N89-21286
ADAMSON, T. C., JR. N89-20937
AGARWAL, ANANT N89-21586
AGARWAL, R. K. N89-20948
AHRENS, THOMAS J. N89-21365
ALBRECHT, ANDREAS N89-21716
ALDERMAN, DONALD W. N89-21130
ALGER, LINDA N89-21582
ALLISON, PETER S. N89-21598
ALVAREZ, L. W. N89-21288
N89-21291
ALVAREZ, W. N89-21288
N89-21291
AMMAR, H. H. N89-21589
AMSTRUP, STEVEN E. N89-21013
ANANTHANARAYANAN, V. N89-21241
ANDERS, EDWARD N89-21319
N89-21411
ANDERS, MARK H. N89-21291
N89-21369
ANDERSON, G. L. N89-21531
ANDERSON, MARK RONALD N89-20998
ANDERSON, R. E. N89-21235
ANDERSON, R. R. N89-21326
ANDREOLI, M. A. G. N89-21376
ANDREWS, G. L. N89-21457
ANTAR, BASIL N. N89-21727
ANTOINE, L. A. G. N89-21289
ANTOLOVICH, STEPHEN D. N89-21258
APLEY, WALTER J. N89-21639
APPELBAUM, J. N89-21174
ARCHIBALD, J. DAVID N89-21290
ARMSTRONG, E. S. N89-21025
ARNEY, DAVID C. N89-21513
ARSENAULT, R. J. N89-21109
ARTHUS, M. A. N89-21412
ASARO, F. N89-21288
N89-21291
ASHKENAS, IRVING L. N89-20999
ATANGAN, JOSE F. H. N89-21452
ATES, MEHMET N89-21610
ATTREP, M., JR. N89-21368
AVELLINI, BARBARA A. N89-21485
AYERS, THEODORE G. N89-20927

B

BABB, ALBERT L. N89-21639
BABCOCK, S. E. N89-21665
BACKUS, GEORGE E. N89-21435
BADJUKOV, D. D. N89-21343
BAER, M. R. N89-21214
BAGINSKI, MICHAEL EDWARD N89-21728
BAILEY, J. M. N89-21189
BAILEY, THOMAS N89-21028
BAILEY, THOMAS GLENN N89-21554
BAKER, K. B. N89-21156
BAKER, TIMOTHY J. N89-20940
BAKIS, C. E. N89-21037
BALAKRISHNA, S. N89-21004
BALLARINI, R. N89-21265
BALLUFFI, R. W. N89-21665
BALTZLEY, DENNIS R. N89-21545
BANDYOPADHYAY, S. N89-21042
BANKS, BRUCE A. N89-21104
BANKS, WILLIAM W. N89-21480
BANNING, DOUGLAS W. N89-21029
BARI, MOHAMMAD A. N89-21679
BARKER, P. F. N89-21410
BARKER, ROBERT J. N89-21657
BARKER, T. G. N89-21021
BARLOW, N. G. N89-21292
BARMORE, GARY DEAN N89-21144
BARNES, PATRICK DENIS N89-21558
BARON, CHRISTOPHER THOMAS N89-21567
BARRETT, J. L. N89-21015
BASORE, PAUL A. N89-21424
BASS, HENRY E. N89-21630
BATINA, JOHN T. N89-20946
BAUR, MARIO E. N89-21293
BEDELL, KEVIN S. N89-21688
BEKKI, N. N89-21662
BELL, JEFFREY F. N89-21294
BEN-ASHER, JOSEPH ZALMAN N89-21014
BENJAMINI, C. N89-21338
BENNETT, DAVID L. N89-21691
BENNETT, ROBERT M. N89-20946
BERGGREN, R. R. N89-21235
BERGHAGE, THOMAS E. N89-21480
BERNARD, ROBERT S. N89-21523
BERNSTEIN, ELLIOT R. N89-21212
BERNSTEIN, IRA B. N89-21155
BERRIER, BOBBY L. N89-20926
BERRY, W. B. N. N89-21295
N89-21409
BERTELRUD, ARILD N89-20928
BESSE, J. N89-21305
BHANDARI, N. N89-21296
BHASIN, K. B. N89-21142
BHATELEY, I. C. N89-20930
BHATIA, NAM P. N89-21526
BHATTACHARYA, S. K. N89-21329
BICK, FRANK J. N89-20978
BIRNBAUM, H. K. N89-21084
BISHOP, F. JOSEPH N89-21018
BISWAS, RUPAK N89-21513
BLAKE, JEAN A. N89-21729
BLAND, SAMUEL R. N89-20946
BLANKENSHIP, MARK H. N89-21474
BLISS, D. B. N89-20973
BLOUNT, CHARLES E. N89-21226
BLUM, LESSER N89-21064
BLUME, JANET A. N89-21268
BOBBITT, PERCY J. N89-20957
BOHOR, BRUCE F. N89-21297
BOND, R. N89-21725
BONNER, E. N89-20934
BONTE, PH. N89-21378
BOOTH, L. N89-21724
BORGES, G. L. N89-21064
BORLAND, C. J. N89-20922
BOSTON, P. J. N89-21298
BOURGEOIS, JOANNE N89-21299
BOWER, GORDON H. N89-21702
BOWMAN, R. C., JR. N89-21056
N89-21677
BOYD, STUART R. N89-21320
BOYD, T. N89-21443
BOYNTON, W. V. N89-21330
N89-21331
BRABBS, THEODORE A. N89-21051
BRADTMILLER, BRUCE N89-21484
BRADY, JOYCE A. N89-21100
BRANSTETTER, LINDA JEAN N89-21614
BRATTON, C. B. N89-21725
BRAY, OLIN H. N89-21708
BRAYMEN, W. W. N89-20930
BRETZLAFF, ROBERT S. N89-21121
BRICKNER, MICHAEL S. N89-21477
BRIDGES, DAVID H. N89-20965
BRIDGES, DAVID J. N89-21204
BRIGGS, G. A. D. N89-21101
BRITCHER, COLIN P. N89-20955
BROCK, GEORGE S. N89-21166
BROOK, M. R. N89-21089
BROOKES, ALLEN N89-21469
BROWN, A. E. N89-21654
BROWN, CHRISTOPHER M. N89-21247
BROWN, SAMUEL H. N89-21626
BROWNRIGG, T. E. N89-21015
BRUCK, JEHOSUA N89-21564
BRYANT, LAURIE J. N89-21290
BRYANT, W. R. N89-21410
BUCKLEY, LEONARDI J. N89-21043
BULLOUGH, R. N89-21073
BUNKIN, F. V. N89-21089
BUONSANTO, M. J. N89-21429
BURCH, I. A. N89-21087
BURCKLE, L. H. N89-21410
BURGESS, DAVID G. N89-21083
BURKE, K. N89-21316
N89-21341
N89-21386
BURKET, HAROLD D. N89-20976
BURKHARDT, LAURA N89-21582
BURNSIDE, R. G. N89-21429
BURTON, HILARY D. N89-21480
BUTLER, ALBERT GEORGE N89-21067
BUTLER, JAMIE L. N89-21380
BUTLER, JANICE N89-21480
BUTTLE, D. J. N89-21035
BYERLY, GARY R. N89-21348
BYKAT, ALEX N89-21730

C

CALDEIRA, K. G. N89-21300
CAMPBELL, RICHARD L. N89-20947
CANAVAN, GREGORY H. N89-21620
CANTIN, GILLES N89-21277
CARLSON, LELAND A. N89-20947
CARMICHAEL, R. L. N89-20944
CARPENTER, KENNETH N89-21301
CARRIER, DENIS JOSEPH GASTON N89-21030
CARRINGTON, CONNIE K. N89-21731
CARTER, NEVILLE L. N89-21333
CASASENT, DAVID N89-21605
CATALANO, JAMES E. N89-21254
CHAIT, A. N89-21032
CHALOUPKA, V. N89-21725
CHANG, CHIA-BO N89-21732
CHANG, G. E. N89-21105
CHANG, SANCHI S. N89-21185
CHAPMAN, CLARK R. N89-21302
CHAPMAN, R. O. N89-21580
CHAPPELL, CHARLES R. N89-21726
CHATTOPADHYAY, ADITI N89-20982
CHAUDHRI, M. M. N89-21128
CHAUHAN, RAJINDER SINGH N89-21733
CHEN, C. N89-21426
CHEN, JIFENG N89-21259
CHEN, K. C. N89-21674
CHEN, PETER C. T. N89-21498
CHEN, S. P. N89-21685
CHERRY, M. N89-21725
CHI, Y. C. N89-21080
CHIANG, C. J. N89-21423
CHIENG, WEI-HUA N89-21492
N89-21493
CHIU, HUEI-HUANG N89-21734
CHO, K. N89-21080
CHOYKE, W. J. N89-21116
CHRISS, R. M. N89-20956
CHU, C. C. N89-21209
CHUI, CHARLES K. N89-21503
CHUNG, I. N89-21133
CHYU, MINGKING K. N89-21735

CIARAVINO, VICTOR N89-21467
CIARCIA, C. A. N89-21653
CISOWSKI, STANLEY M. N89-21303
CLAPPER, JOHN N89-21702
CLARK, D. L. N89-21168
CLARK, EDDY G. N89-21557
CLAUS, R. O. N89-21640
CLAUSER, CHARLES N89-21484
CODER, DAVID W. N89-21199
COFFEY, HELEN E. N89-21431
N89-21432
N89-21722
COHEN, A. N89-21129
COHEN, BARBARA J. N89-21695
COLE, JULIAN D. N89-20938
COLEMAN, L. N89-21725
COLEMAN, LARRY A. N89-20969
COLLOM, CHRISTOPHER J. N89-21304
COLOZZA, A. N89-21133
COMET, B. N89-21356
COMTOIS, JOHN HENRY N89-21553
CONNELL, J. R. N89-21458
COOPER, D. E. N89-21056
COOPER, E. E. N89-21005
COPE, DALE A. N89-21020
CORBETT, JAMES W. N89-21063
CORRELL, DONALD L., JR. N89-21659
COSGROVE, M. N89-21168
COSMADAKIS, STAVROS S. N89-21565
COSNER, RAYMOND R. N89-20943
COSTA, D. L. N89-21461
COTHRAN, ERNESTINE K. N89-21726
COURTILLOT, V. N89-21305
COVEY, C. N89-21306
COX, DAVE N89-21640
COX, KEVIN S. N89-21159
COX, STEPHEN K. N89-21215
COZZONE, ADOLPHO N89-21483
CRIM, F. FLEMING N89-21636
CRISS, GEORGE W., III N89-21006
CROCKET, JAMES H. N89-21307
N89-21333
CROSBIE, G. M. N89-21124
CROSLEY, JOHN K. N89-21488
CROSS, STEPHEN E. N89-21594
CROWLEY, THOMAS J. N89-21308
CRUTZEN, P. J. N89-21398
CULVER, RICHARD L. N89-21217
CUNNINGHAM, HERBERT J. N89-20946
CURBY, CATHERINE H. N89-21013
CURLISS, D. B. N89-21045
CURTIS, JANET C. N89-21130

D

DADKHAH, MAHYAR S. N89-21269
DALLY, WILLIAM J. N89-21586
DANBERG, J. E. N89-21522
DAO-YI, XU N89-21414
DAS-GUPTA, D. K. N89-21648
DATLOWE, D. W. N89-21438
DAVENPORT, S. A. N89-21406
DAVID, ROBERT A. N89-21616
DAVIDSON, FREDERIC N89-21141
DAVIS, DENNIS M. N89-21058
DAVIS, JOHN S. N89-21538
DAVIS, R. F. N89-21176
DAVIS, RICHARD W. N89-21617
DAVIS, SANFORD S. N89-21190
DAVIS, W. H. N89-20931
DAVY, ROBERT D. N89-21455
DAWSON, DAVID M. N89-21038
DEAN, EDWARD N89-21501
DEAN, W. E. N89-21412
DEAN, WILLIAM G. N89-21023
DEANGELIS, M. N89-21378
DEESE, J. E. N89-20948
DEJONGE, R. N89-21391
DEJPOUR, SHABOB R. N89-21541
DEKONING, C. H. M. N89-21261
DELAAT, JOHN C. N89-20995
DELIKARAOGLOU, DEMITRIS N89-21434
DESILVA, S. L. N89-21309
DEWIT, C. B. N89-21400
DHONDT, STEVEN N89-21310
N89-21328
DIAMOND, HARVEY N89-21503
DIETZ, R. S. N89-21355
DILLON, LONNIE R. N89-20988
DINGUS, MICHAEL L. N89-21137
DITTMAR, JAMES H. N89-21628
DOCLET, D. N89-21378
DODGE, LEE G. N89-21253
DOEHNE, E. F. N89-21352
DONALDSON, J. C. N89-20966
N89-21200
DONEHOWER, ROY N89-21560
DONOVAN, WILLIAM F. N89-21511
DOUGHERTY, DANIEL P. N89-21262
DOUGHERTY, EDWARD R. N89-21577
DOUGLAS, DAVID C. N89-21013
DOWGIALLO, MICHAEL J. N89-21415
DOWNEY, J. W. N89-21686
DOWNING, R. G. N89-21677
DRAKE, C. L. N89-21364
DREESEN, ROLAND N89-21380
DRESS, DAVID A. N89-20955
DRESSLER, B. O. N89-21311
DRIVER, MARK A. N89-21248
DRYER, FREDERICK L. N89-21071
DUCK, PETER W. N89-21197
DUDLEY, ROBERT L., JR. N89-21009
DUESBERY, M. N89-21109
DUFFY, J. N89-21080
DUKE, J. C., JR. N89-21256
DUKES, MICHAEL A. N89-21177
DUNLAP, KEVIN J. N89-21703
DUNNING, T. H., JR. N89-21070
DUVALL, DAVID J. N89-21249

E

EAGAN, PHYLLIS N89-21467
EBIHARA, BEN N89-21171
EDGAR, BRUCE KEVIN N89-21718
EGAN, GREGORY S. N89-21271
EGEBERG, P. K. N89-21410
EGERLAND, WALTER O. N89-21528
EHRLICH, R. B. N89-21654
EL-HADY, NABIL M. N89-20954
ELDRIDGE, HUDSON B. N89-21736
ELLSWORTH, R. N89-21725
ELSTON, W. E. N89-21312
ENGLE, R. B. N89-21654
EPPINGER, STEVEN D. N89-21251
ERDAHL, DAVID C. N89-21029
ERONEN, HEIKKI N89-21188
ESSER, B. K. N89-21402
ESSNER, SADIK C. N89-21593
ESTABROOK, C. N89-21443
ETZL, JULIUS M. N89-21179
EVEN, UZI N89-21065

F

FABER, JOHN, JR. N89-21686
FAETH, G. M. N89-21201
FAHEY, ALBERT JOSEPH N89-21719
FAIRALL, CHRISTOPHER W. N89-21449
FALCO, R. E. N89-21209
FALKENHAINER, BRIAN N89-21618
FANCY, STEVE G. N89-21013
FASTOVSKY, D. E. N89-21313
FATKIN, D. G. P. N89-21101
FAWAZ, SCOTT A. N89-21117
FAWZY, WAFAA M. N89-21059
FEGLEY, B., JR. N89-21371
FERGUSON, GREGORY S. N89-21118
FIELD, J. E. N89-21106
N89-21128
FIELDING, KENNETH H. N89-21221
FINNEGAN, D. L. N89-21314
FISHER, JAMES M. N89-21040
FISHMAN, HARVEY M. N89-21464
FITZMAURICE, M. N89-21168
FLAHERTY, JOSEPH E. N89-21513
N89-21514
FLEMING, R. F. N89-21363
FLESSA, KARL W. N89-21315
FLOYD, STEPHEN A. N89-21737
FLYNN, G. W. N89-21236
FONG, Y. S. N89-21589
FORLANDA, JUANCHO E. N89-20985
FORTIN, PAUL N89-20963
FOSTER, DUDLEY F., JR. N89-21455
FOUGHNER, JEROME T., JR. N89-20925
N89-20942
FRANCIS, P. W. N89-21316
FRANKE, RICHARD N89-21504
FRAZIER, WILLIAM E. N89-21092
FREDRICKSEN, HAROLD N89-21524
FREEMAN, L. MICHAEL N89-21726
FREI, Z. N89-21633
FRIED, I. N89-21497
FRIEMAN, JOSHUA A. N89-21634
FRITZEMEIER, L. G. N89-21072
FROMHOLD, ALBERT T. N89-21738
FUJIMOTO, RICHARD M. N89-21533
N89-21534
N89-21535
N89-21570
N89-21588
FUNG, K-Y. N89-21208
FUTTERER, D. K. N89-21410

G

GABRIEL, J. R. N89-21579
N89-21580
GAIDOS, J. N89-21725
GALLY, THOMAS A. N89-20947
GARDNER, PATRICK J. N89-21671
GARLAND, MICHAEL M. N89-21739
GARNER, GERALD W. N89-21013
GARRIZ, J. A. N89-20958
GARVIN, J. B. N89-21317
GEBBIE, KATHARINE N89-21623
GEBHART, B. D. N89-21222
GEDEON, STEVEN A. N89-21254
GEE, J. M. N89-21423
GEIGER, DAVI N89-21646
GELDSETZER, H. H. J. N89-21318
GELLERT, E. P. N89-21042
GENDRICH, C. P. N89-21209
GEOPPER, ERIC R. N89-20992
GEORGE, THOMAS F. N89-21061
N89-21089
GEURTS, W. A. J. N89-21543
GHAN, S. J. N89-21306
GIARDINA, CHARLES R. N89-21577
GIBSON, URSULA J. N89-21673
GIFFORD, DAVID K. N89-21585
GILBERT, ROBERT P. N89-21257
GILLIAN, RONNIE E. N89-21260
GILMOUR, IAIN N89-21319
N89-21320
N89-21321
GLASS, B. P. N89-21322
GLASSER, LANCE A. N89-21586
GLASSMAN, IRVIN N89-21071
GLEITER, H. N89-21090
GLIMM, JAMES N89-21210
N89-21530
GLOVER, VINCE N89-21215
GLOWINSKI, ROLAND N89-21501
GOKOGLU, S. A. N89-21032
GOLDE, MICHAEL F. N89-21062
GOLDING, T. D. N89-21667
GOODMAN, J. N89-21725
GOODMAN, JOSEPH W. N89-21564
GOODSELL, G. N89-21517
GOODWIN, M. J. N89-21252
GOODWIN, WILLIAM P. N89-21041
GOPALAKRISHNAN, GANESH C. N89-21535
GORDON, CLAIRE N89-21484
GRACIA-SALCEDO, CARMEN M. N89-21051
GRADSTEIN, F. M. N89-21335
GRAHAM, ROBERT A. N89-21095
GRAHAM, STEPHEN MURPHY N89-21263
GRANT, DAVID M. N89-21130
GRANT, L. B. N89-21379
GRAUP, G. N89-21323
GRAY, ALTON J. N89-21094
GREEN, AL N89-21675
GREEN, H. E. N89-21105
GREENWALD, R. A. N89-21156
GRIEVE, R. A. F. N89-21317
GRIFFITHS, S. K. N89-21632
GRISHMAN, RALPH N89-21574
GRODZKA, PHILOMENA G. N89-21023
GROOM, NELSON J. N89-21135
N89-21136
GROOT, H. N89-21391
GROSS, TODD A. N89-21550
GROSSKOPF, P. P. N89-21256
GROVE, JOHN N89-21210
N89-21512
GRUZEN, ALEXANDER N89-21028
GUENTHER, FRANK N89-21321
GUPTA, M. N89-21296
GUPTA, ROOP N. N89-21193
GURTIN, MORTON E. N89-21494

H

HADDLETON, FRANK LESLIE N89-21074
HAFEZ, M. N89-20939
HAGAN, JAMES C. N89-21024
HAINES, T. N89-21725
HALL, CHRISTOPHER D. N89-20987
HALL, KENNETH R. N89-21740
HALLAM, A. N89-21324
HALLER, HUDDY B. N89-21700
N89-21701
HAMILTON, N. N89-21410

HAMMEL, R. T. N89-21585
HAMMETTER, WILLIAM F. N89-21095
HAN, SAMUEL S. N89-21741
HANDLER, R. A. N89-21206
HANSEN, H. J. N89-21325
HANSEN, ROSS J. N89-21601
HANSON, ERIC N. N89-21594
HANSON, J. D. N89-21660
HANSON, R. K. N89-21202
HARDING, L. B. N89-21070
HARDY, D. A. N89-21022
HARRIS, CARL M. N89-21597
HARRIS, JOEL M. N89-21054
HARRISON, CHRISTOPHER G. A. N89-21416
HARRISON, R. J. N89-21070
HARRISON, T. M. N89-21341
HART, R. J. N89-21376
N89-21400
HART, W. D. N89-21444
HARTLEY, D. S., III N89-21590
HARTUNG, J. B. N89-21326
HASSELAAR, M. M. A. N89-21543
HASSIG, P. J. N89-21379
HATCH, G. E. N89-21461
HATCHER, M. G. N89-20966
HATKE, GARY F. N89-21167
N89-21187
HAVERSON, B. L. N89-21284
HAWORTH, LORAN N89-20978
HAZEL, JOSEPH E. N89-21327
HEALY, BRIAN C. N89-21145
HEATON, K. C. N89-21515
HEAVEN, MICHAEL C. N89-21059
HEBERLEIN, J. V. R. N89-21116
HEISTER, STEPHEN DOUGLAS N89-20923
HENDERSON, WILLIAM P. N89-20926
HENDRICKS, E. W. N89-21208
HENNEKE, E. G., II N89-21256
HENYEY, F. S. N89-21165
HERBERT, TIMOTHY D. N89-21328
HERMAN, Y. N89-21329
HERRMANN, J. M. N89-21280
HERRMANN, LEONARD R. N89-21611
HEVESI, I. N89-21089
HICKEY, LEO J. N89-21336
HIEFTJE, GARY M. N89-21222
HIGHFILL, J. N89-21461
HILDEBRAND, A. R. N89-21330
N89-21331
HILDEBRAND, PETER H. N89-21433
HILDENBRANDT, STEPHEN R. N89-21027
HINDS, W. TED N89-21427
HINGST, W. R. N89-20956
HIPPSLEY, C. A. N89-21073
HITTERMAN, R. L. N89-21686
HJELM, REX P., JR. N89-21578
HLAVKA, D. L. N89-21444
HO, JAMES K. N89-21573
N89-21606
HODGE, PAMELA R. N89-21625
HODGSON, STUART GREGORY N89-21242
HOELTZEL, DAVID A. N89-21492
N89-21493
HOFFMAN, ROSS N. N89-21450
HOLLAND, FREDERIC A., JR. N89-21245
HOLLARS, MICHAEL GRANT N89-21240
HOLLIG, KLAUS N89-21502
HOLMES, H. E. N89-21129
HOLMES, RANDALL ROBERT N89-21216
HOLMES, ROBERT B. N89-21603
HONG, B. G. N89-21662
HONG, S. K. N89-21629
HONG, WILLIAM S. N89-21681
HORNE, M. P. N89-21206
HORNFECK, WILLIAM A. N89-21742
HORTON, J. A. N89-21684
HORTON, W. N89-21662
HOUSEN, KEVIN R. N89-21381
HOUSHMAND, B. N89-21138
HOVE, JOHN E. N89-21681
HSUE, KENNETH J. N89-21332
HUBBARD, C. R. N89-21050
HUBER, A. N89-21022
HUCKELBRIDGE, ARTHUR A. N89-21266
HUFFMAN, ALAN R. N89-21333
HUGHES, B. A. N89-21460
HUGHES, CHRISTOPHER E. N89-21002
HUGHES, S. J. N89-21460
HUI, CHUNG-YUEN N89-21495
HUMPHREYS, LLOYD G. N89-21608
HUNTLEY, J. N. N89-21128
HUPPI, RONALD N89-21219

I

IKEUCHI, KATSUSHI N89-21652
IM, YOONSOON N89-21690
IMAI, M. N89-21359
IMHOF, W. L. N89-21438
INGER, G. R. N89-20952
INGLEFIELD, PAUL T. N89-21108
IRWIN, R. D. N89-21016
IRWIN, R. DENNIS N89-21743
ITOH, TATSUO N89-21185
IZETT, G. A. N89-21334

J

JACKSON, ARTHUR J. N89-21456
JACKSON, T. A. N89-21142
JACOB, K. H. N89-21443
JACOBS, DENICE S. N89-21572
JACOBS, STEPHEN N89-21228
JAENICKE, R. A. N89-21552
JAMES, M. R. N89-21575
JANSA, L. F. N89-21335
JEHANNO, C. N89-21378
JELSKI, DANIEL A. N89-21089
JENA, PURUSOTTAM N89-21091
JENKINS, B. K. N89-21641
JIAN, YIGAO N89-21233
JIANG, GUO-HUA N89-21111
N89-21276
JIANG, SHIUH-JEN N89-21655
JIH, RONG-SONG N89-21161
JOHNSON, A. R. N89-21496
N89-21497
JOHNSON, CHRISTOPHER A. N89-21416
JOHNSON, JOHN L. N89-21529
JOHNSON, KIRK R. N89-21336
JOHNSON, MARK N89-21510
JOHNSON, RICHARD L. N89-20987
JONES, A. M. N89-21663
JONES, ALAN A. N89-21108
JONES, D. D. N89-21406
JONES, MARK T. N89-21537
JONES, MARSHALL B. N89-21545
JONES, VICTORIA N89-21016
JONG, KIM HYUN N89-21668
JONSCHER, ANDREW K. N89-21679
JORTNER, JOSHUA N89-21065
JOYCE, K. A. N89-21151
JUNG, DONG H. N89-21562

K

KAHNG, W. H. N89-21629
KAINEC, JAMES J. N89-21602
KANADE, TAKEO N89-21652
KANSKI, JERRY J. N89-21487
KAPER, HANS G. N89-21052
KAPUSTA, A. A. N89-21274
KARR, GERALD R. N89-21726
KARR, T. J. N89-21237
KARU, ZAIN S. N89-21023
KASTING, J. N89-21413
KAUFMAN, A. E. N89-20973
KEARNS, THOMAS F. N89-21123
KEITH, T. G., JR. N89-20956
KELLER, G. N89-21337
N89-21338
KELLEY, TIMOTHY C. N89-21270
KELLY, SHAWN L. N89-21551
KEMP, W. B., JR. N89-20958
KENNEDY, ROBERT S. N89-21545
KENNETT, JAMES P. N89-21291
N89-21392
N89-21410
KERBACHER, JAMES J. N89-21467
KHAN, M. Z. SHAH N89-21087
KIERNAN, M. T. N89-21256
KILGORE, ROBERT A. N89-20955
KILGORE, W. ALLEN N89-21004
KIM, D-H. N89-21085
KIM, JONGKEUN N89-21097
KIM, PETER Y. N89-21489
KIM, S.-W. N89-21192
KIM, SEON JIN N89-21078
KIM, Y. S. N89-21061
KING, D. L. N89-21423
KINSEY, DON W. N89-20971
KISSMEYER, KIRSTEN Y. N89-21164
KITCHELL, J. A. N89-21351
KLIMCHUK, JAMES A. N89-21717
KLINE, L. E. N89-21116
KLINGER, L. F. N89-21339
KLYDE, DAVID H. N89-20999
KNAUSS, WOLFGANG G. N89-21285
KNIGHT, NORMAN F., JR. N89-21260
KNIGHT, THOMAS F., JR. N89-21586
KNUDSEN, J. F. N89-21677
KOBAYASHI, ALBERT S. N89-21269
KOBYLARZ, THOMAS J. N89-21000
KODRES, C. A. N89-21005
KOEBERL, CHRISTIAN N89-21340
N89-21341
KOFSKY, I. L. N89-21015
KOHN, ROBERT N89-21499
KOHOUT, LISA L. N89-21419
KOICHI, YOKOYAMA N89-21656
KOLESNIKOV, E. M. N89-21342
N89-21343
KONG, JIN A. N89-21175
KONOWALOW, DANIEL D. N89-21638
KOOK, HYUNG-TAE N89-21622
KORTRIGHT, J. B. N89-21064
KOSCHNY, DETLEF N89-21365
KOTLAR, A. J. N89-21129
KRAHN, GARY N89-21524
KREMER, R. E. N89-21677
KRESS, JOEL DAVID N89-21053
KREYENHAGEN, K. N. N89-21379
KRIER, HERMAN N89-21632
KRISTL, JOSEPH N89-21219
KUCUK, SENOL N89-21479
KUCZMARSKI, M. A. N89-21032
KUHN, ALLAN D. N89-21704
KUMAGAI, HIROYUKI N89-20963
KUMAR, B. V. N89-21605
KUNDMANN, MICHAEL K. N89-21689
KUNK, M. J. N89-21326
KUO, S. P. N89-21437
KUSHNER, L. J. N89-21182
KVALE, THOMAS J. N89-21744
KYRAZIS, D. T. N89-21654
KYTE, FRANK T. N89-21344
KYTOE, MATTI N89-21255

L

LACONTI, ANTHONY B. N89-21181
LADNA, B. N89-21084
LAGOUDAS, DIMITRIS C. N89-21495
LAI, H. N89-20921
LAMATSCH, PETER J. N89-20987
LAMOLDA, M. A. N89-21345
LANOUE, BERNARD N89-21482
LAUB, RICHARD J. N89-21115
LAURIKKO, JUHANI N89-21255
LAW, K. S. N89-21212
LAWRENCE, CHARLES N89-21266
LAWRENCE, S. N89-21109
LEE, B. H. N89-20968
LEE, CHESTER C. N89-21239
LEE, EDWIN E., JR. N89-20961
LEE, RICHARD J. N89-21038
LEE, S. W. N89-21138
LEE, SING H. N89-21593
LEE, W. A. N89-21122
LEE, WANNAM N89-21060
LEE, YOUNG PAK N89-21077
LEIGHTON, F. THOMSON N89-21586
LEISERSON, CHARLES E. N89-21586
LEKAKIS, IOANNIS CONSTANTINOS N89-21195
LEN, JONATHAN L. N89-21491
LEONARD, E. M. N89-21235
LESSNER, PHILIP N89-21181
LESTRADE, JOHN PATRICK N89-21745
LEUNG, P. T. N89-21061
LEWIS, GREGORY W. N89-21474
LEWIS, M. F. N89-21650
LI, CHIN-HSIEN N89-21501
LIBOFF, RICHARD L. N89-21669
LICHTY, LYLE RAYMOND N89-21075
LIGLER, FRANCES S. N89-21649
LILLIE, THOMAS H. N89-20984
LIM, TEIK C. N89-21244
LINDER, BARRY J. N89-21463
LINDNER, D. K. N89-21640
LINDNER, E. N. N89-21544
LINNEMANN, PETER E. N89-21278
LIPMAN, PETER W. N89-21346
LITT, JONATHAN S. N89-20995
LITZINGER, THOMAS A. N89-21060
LIU, C. T. N89-21684
LIU, WEI-CHEUN N89-21264
LO, C. F. N89-20959
LOCKWOOD, G. W. N89-21713
LOEHNER, RAINALD N89-20941
LOGAN, B. G. N89-21031
LOGAN, JAMES C. N89-21559

LONDENBERG, W. K. N89-20930
LOPER, D. E. N89-21347
LORIMOR, GARY K. N89-20993
LOUAT, N. N89-21109
LOWE, DONALD R. N89-21348
LUCAS, CORMAC N89-21607
LUDFORD, G. S. S. N89-21527
LUKYANCHUK, B. S. N89-21089
LUTEY, MARK K. N89-21158
LUTZ, T. M. N89-21349
LYNN, BRYAN W. N89-21634

M

MACDOUGALL, J. D. N89-21350
MACLEOD, KENNETH N89-21404
MACLEOD, N. N89-21351
MACLER, MICHEL N89-21059
MADDEN, PAUL N89-21028
MADRZYKOWSKI, DANIEL N89-21049
MADSON, M. D. N89-20944
MAHABA, NIZAR MAHMOUD N89-21555
MALMUTH, NORMAN D. N89-20938
MANI, NARAYANA S. N89-21583
MANKBADI, REDA R. N89-21196
MANLEY, DAVID A. N89-21207
MANNA, ZOHAR N89-21546
N89-21547
MANNIX, DAVID L. N89-21563
MANSER, G. E. N89-21127
MANTHA, SURYA N89-21583
MARBACH, HOWARD W., JR. N89-21253
MARGOLIS, S. V. N89-21352
MARTENS, NATHAN W. N89-20967
MARTIN, CHARLES R. N89-21066
MARTIN, E. N89-21350
MARTIN, JOHN S. N89-21486
MARTZAKLIS, KONSTANTINOS S. N89-21172
MARVIN, URSULA B. N89-21353
MATESE, J. J. N89-21408
MATSUMOTO, ROGER N89-21120
MAURITSCH, H. J. N89-21370
MAURRASSE, FLORENTIN J-M. R. N89-21354
MAYHEW, ROBERT J. N89-21120
MAYNE, CHARLES L. N89-21130
MAZDIYASNI, K. S. N89-21674
MCCABE, DOUGLAS A. N89-20987
MCCANN, JEFFREY M. N89-21007
MCCARTNEY, K. N89-21347
MCCONVILLE, JOHN N89-21484
MCCORMACK, CHRISTOPHER J. N89-20980
MCCRORY, R. L. N89-21661
MCCUNE, WILLIAM W. N89-21581
MCDONALD, GARY H. N89-21746
MCGARITY, J. N89-21022
MCGUIRE, STEPHEN C. N89-21747
MCHONE, J. F. N89-21355
MCKENNY, WILLIAM A. N89-21606
MCKINLEY, GEORGE B. N89-21521
MCKINLEY, RICHARD L. N89-21481
MCKINNON, JOHN A. N89-21431
N89-21432
N89-21722
MCLAREN, DIGBY J. N89-21356
MCLAUGHLIN, KEITH L. N89-21161
MCLEAN, DEWEY M. N89-21357
MCMAHON, JOHN R. N89-21504
MCNICHOLL, P. N. N89-21015
MEDLER, LEON N89-21509
MEI, KENNETH K. N89-21143
MEISS, JAMES D. N89-21622
MELLISH, ROBERT W. N89-21199
MELNGAILIS, JOHN N89-21184
MELOSH, H. J. N89-21403
MELROY, O. R. N89-21064
MELTZ, MARTIN L. N89-21467
MENAPACE, J. A. N89-21212
MENDE, STEPHEN B. N89-21441
MENDOZA, J. P. N89-20944
MERRILL, WALTER C. N89-20995
MESSITER, A. F. N89-20937
MEYER, ALBERT R. N89-21565
MEYER, H. W. N89-21522
MEYERS, MARC A. N89-21095
MICCI, M. M. N89-21133
MICHEL, H. V. N89-21288
N89-21291
MICKELSON, MARK N89-21450
MICKLE, MARLIN H. N89-21479
MILLER, G. R. N89-21265
MILLER, K. L. N89-21429
MILLER, M. S. N89-21129
MILLER, RAYMOND E. N89-21058
MILLER, T. M. N89-21314
MILLIGAN, WALTER W. N89-21258
MILSTEIN, RANDALL L. N89-21358
MINECK, RAYMOND E. N89-20960
MIRANDA, LUIS R. N89-20932
MISH, KYRAN D. N89-21611
MISRA, AJAY K. N89-21036
MITCHELL, R. R. N89-21116
MITRA, GAUTAM N89-21607
MIURA, Y. N89-21359
MOBILIA, J. N89-21438
MOBLEY, CURTIS D. N89-21651
MOCKAPETRIS, PAUL V. N89-21703
MOL, JOHN H. N89-21114
MOLANDER, WILLIAM A. N89-21093
MONGIA, H. C. N89-21125
MONNING, C. A. N89-21222
MONTANARI, A. N89-21291
MOORE, PETER K. N89-21514
MOORE, THOMAS D. N89-21672
MOORE, THOMAS P. N89-21463
MORALES, WILFREDO N89-21103
MORAN, S. N89-21022
MORFITT, DONALD J., JR. N89-21205
MORGAN, FERNANDO A. N89-21149
MORGAN, W. JASON N89-21360
MORI, SHIGEYUKI N89-21103
MOROSIN, B. N89-21050
MORRIS, V. R. N89-21458
MORRISON, DAVID N89-21302
MORROW, CHERILYNN ANN N89-21723
MOSCHLER, JOSEPH W., JR. N89-21113
MOSES, HARRY E. N89-21140
MOUROU, G. A. N89-21142
MUELLER, PAUL J., III N89-20987
MUKAI, D. J. N89-21265
MUKUNDAN, R. N89-21589
MULLER, RICHARD A. N89-21361
MURALI, A. V. N89-21341
N89-21362
N89-21386
MURMAN, EARLL M. N89-20936
MURPHY, BRIAN WILLIAM N89-21720
MURPHY, G. V. N89-21189
MURRAY, J. F. N89-21654
MURTHY, A. V. N89-21004

N

NAKAYAMA, KEN N89-21468
NANAI, L. N89-21089
NARAGHI, M. H. N. N89-21025
NAULT, JAMES R. N89-21273
NAYAR, SHREE K. N89-21652
NAYFEH, ALI H. N89-20953
NAZAROV, M. A. N89-21341
N89-21343
NEHRKORN, THOMAS N89-21450
NELSON, E. N89-20921
NELSON, JAMES B. N89-21047
NEMETH, MICHAEL P. N89-21260
NEUMANN, KURT NYLE N89-21001
NEWMAN, NATHAN N89-21675
NEWMAN, P. A. N89-20958
NICHOLS, D. J. N89-21363
NICHOLSON, D. M. N89-21096
NICHOLSON, J. M. N89-21124
NICOL, DAVID M. N89-21542
NICOLET, M.-A. N89-21637
NIGON, RICHARD N89-21223
NILES, JOHN R. N89-21697
NIXON, CHARLES W. N89-21481
NORMAN, J. H. N89-21055
NORTHRUP, M. ALLEN N89-21225
NORTON, JOHN E. N89-21148
NOWICKI, L. J. N89-21686
NYLUND, NILS-OLOF N89-21255

O

OCONNELL, S. N89-21410
OCONNOR, MARY ELLEN N89-21462
OECHSIE, V. L. N89-21125
OETTING, WILLIAM D. N89-21152
OFFICER, C. B. N89-21364
OGILVY, J. A. N89-21139
OH, H. G. N89-21629
OKEEFE, JOHN D. N89-21365
OLIVER, W. L. N89-21429
OLSEN, P. E. N89-21366
OLSON, E. C. N89-21367
ORELL, M. K. N89-21105
ORTH, C. J. N89-21368
ORTH, CHARLES J. N89-21411
OUIBRAHIM, HAMZA N89-21186
OWEN, MICHAEL R. N89-21369
OWENS, MICHAEL E. N89-21279

P

PADDEN, RICHARD J. N89-21642
PADULA, SHARON L. N89-21539
PAKATH, RAMAKRISHNAN N89-21705
PANCZAK, TIMOTHY D. N89-21632
PANDEY, J. N89-21296
PANK, LARRY F. N89-21013
PANTANO, CARLO G. N89-21107
PANTAZIS, J. N89-21022
PAREKH, P. P. N89-21362
PARENGKUAN, CHANSON N89-21666
PARIKH, PARESH N89-20941
PARK, H. N89-21168
PARK, JANG-SIK N89-21076
PARK, NICHOLAS N89-21038
PARKER, B. M. N89-21039
PARRY, M. P. N89-21128
PARSONS, JOHN A. N89-21058
PARTHASARATHY, R. N. N89-21201
PARTLOW, W. D. N89-21116
PASKO, PETER D. N89-21147
PASTOR, JOHN N89-21428
PATKOS, A. N89-21633
PATRA, M. K. N89-21596
PATRICK, MERRELL L. N89-21537
PATTERSON, JAMES D. N89-21748
PATY, ROBERT P. N89-20997
PAUL, MICHAEL E. N89-20987
PAULIKAS, A. P. N89-21686
PAULSEN, PHILLIP E. N89-21100
N89-21104
PAULSON, M. R. N89-21439
PEARSON, DONALD J. N89-21697
PEIRCE, DANIEL C. N89-21692
PEISEN, DEBORAH N89-21003
PEMPEL, L. C. N89-21460
PENFIELD, PAUL, JR. N89-21576
N89-21586
PENG, HUEI N89-21693
PEPPER, M. N89-21667
PERCH-NIELSEN, K. N89-21400
PEREIRA, C. M. N89-21128
PEREZ, JERARDO A. N89-21082
PETTIFOR, D. G. N89-21096
N89-21684
PHELAN, MICHAEL J. N89-21520
PHILLIPS, D. CLIVE N89-21038
PHILLIPS, J. T. N89-21706
PHILLIPS, WILLIAM D. N89-21592
PHOENIX, S. LEIGH N89-21495
PIAZZA, CHARLES C. N89-21644
PIERRE-AUBRY, M. N89-21335
PIERSON, JAMES R. N89-21017
PIMENTAL, NANCY A. N89-21485
PITZER, KENNETH S. N89-21048
PLINE, ALEXANDER D. N89-21224
PLOHR, BRADLEY J. N89-21211
POEL, M. N89-21621
POGGIO, TOMASO N89-21646
POHL, LETITIA M. N89-20987
POHLMANN, JUERGEN N89-21228
POIRIER, D. R. N89-21134
POMALAZA-RAEZ, C. A. N89-21589
PONCHAK, GEORGE E. N89-21172
POOL, SAM L. N89-21463
PORTANOVA, MARC A. N89-21099
POSPICHAL, J. N89-21410
POST, WILFRED M. N89-21428
POWELL, EUGENE A. N89-21749
POWELL, KENNETH G. N89-20936
POWERS, DAVID N89-21609
POWERS, JOSEPH M. N89-21632
PRABHU, N. U. N89-21520
PRACHER, JOHN M. N89-20989
PREDMESKY, R. L. N89-21124
PREDOEHL, MARTIN C. N89-21415
PREISIG, JOSEPH RICHARD MARK N89-21430
PREISINGER, A. N89-21370
PRESTON, ROY F. N89-21038
PRINN, R. G. N89-21371
PRITTS, DOUGLAS N89-21482
PUCKETT, D. L. N89-21129
PUGMIRE, RONALD J. N89-21130
PURNELL, ARTHUR W. N89-21179
PUTHLI, R. S. N89-21261
PUTNAM, TERRILL W. N89-20927

Q

QIN-WEN, ZHANG N89-21414
QUACKENBUSH, T. R. N89-20973

QUIGLEY, C. J. N89-21496
QUINBY-HUNT, M. S. N89-21409

R

RAFF, LIONEL M. N89-21057
RAGHAVAN, VENKATRAMAN N89-20962
RAHMAT-SAMII, Y. N89-21138
RAJAMONEY, SHANKAR N89-21618
RAJU, I. S. N89-21267
RAM, RAM BACHAN N89-21198
RAMAMRITHAM, KRITHI N89-21587
RAMAN, GANESH N89-20920
N89-21196
RAMINS, PETER N89-21171
RAMPINO, MICHAEL R. N89-21300
N89-21372
N89-21373
RAND, RICHARD H. N89-21491
RAPHAEL, LOUISE A. N89-21503
RAPP, DAVID W. N89-21676
RASH, CLARENCE E. N89-21486
RASPET, RICHARD N89-21632
RATCLIFF, ROBERT R. N89-20947
RATH, B. B. N89-21683
RAUH, H. N89-21073
RAUP, DAVID M. N89-21374
RAVIZZA, G. E. N89-21402
REAMS, RICHARD H. N89-21283
REAZER, JEAN S. N89-20976
REBO, ROBERT KEITH N89-20994
REBSTOCK, RAINER N89-20961
RECK, GREGORY M. N89-21026
REDDY, J. N. N89-21500
REDDY, UDAY S. N89-21540
REGELIN, WAYNE L. N89-21013
REID, ALLISON N89-21714
REIDY, R. F. N89-21085
REIFSNIDER, K. N89-21037
REIMOLD, W. U. N89-21289
N89-21311
N89-21375
N89-21376
REINIG, KARL D. N89-21163
N89-21505
RESTON, ROCKY R. N89-21250
REYES-SAUTER, SUSAN N89-21453
REYNOLDS, G. H. N89-21055
REYNOLDS, W. N. N89-21034
RICE, A. R. N89-21377
RICE, EDWARD J. N89-20920
N89-21196
RICE, SALLY C. N89-21016
RICHARDS, P. G. N89-21429
RILEY, MICHAEL F. N89-20982
RIYOPOULOS, S. N89-21227
RIZK, N. K. N89-21125
ROACH, M. P. N89-21252
ROBERTAZZI, T. G. N89-21612
ROBERTS, LEEANNE N89-21568
ROBIN, E. N89-21378
ROBINSON, VICKY LYNN N89-21600
ROCCA, JORGE J. N89-21624
ROCCHIA, R. N89-21378
RODDY, D. J. N89-21379
N89-21399
ROGERS, JAMES L. N89-21539
ROGOWSKI, ROBERT N89-21640
ROHDE, FREDERICK W. N89-21162
ROKHLIN, V. N89-21155
ROLLBUHLER, R. JAMES N89-21417
ROMANOFSKY, ROBERT R. N89-21142
N89-21169
N89-21172
ROSAKIS, ARES J. N89-21272
ROSATI, RUTH N89-21696
ROSEN, BRUCE S. N89-20945
ROSENBLATT, M. N89-21379
ROSENKRANTZ, MARCY N89-21068
ROSS, P. N89-21064
ROSS, P. T. N89-21125
ROUNTREE, SUZANNE L. K. N89-21709
ROWELL, LAWRENCE F. N89-21538
ROZNOWSKI, MARY A. N89-21608
RUAN, JUAI N89-21116
RUBESIN, MORRIS W. N89-20951
RUFF, G. A. N89-21201
RUPP, T. D. N89-21653
RUTLEDGE, SHARON K. N89-21100
N89-21104
RYDER, G. N89-21386
RYUJI, KURUMAJI N89-21656

S

SAITO, S. N89-21359
SALAH, J. E. N89-21429
SALAS, MANUEL D. N89-20941
SALOMAA, M. M. N89-21664
SAMANT, M. G. N89-21064
SANDAY, S. C. N89-21683
SANDBERG, CHARLES A. N89-21380
SANTAVICCA, DOMENIC A. N89-21060
SANZ, JOSE M. N89-20996
SASSE, RONALD A. N89-21131
SAUDER, DOUGLAS W. N89-21604
SAWCHUK, A. A. N89-21536
N89-21641
SCANLON, RAY N89-21510
SCAVULLO, M. A. N89-21281
SCHAUER, MARK N89-21212
SCHEFFNER, NORMAN W. N89-21507
SCHENTER, GREGORY K. N89-21669
SCHEPLER, K. L. N89-21682
SCHIFFER, JOHN P. N89-21687
SCHILLING, LAWRENCE J. N89-20983
SCHMIDT, ROBERT M. N89-21381
SCHMITZ, B. N89-21382
SCHNETZLER, C. N89-21317
SCHONBERG, WILLIAM P. N89-21246
N89-21750
SCHOON, NEIL F. N89-21218
SCHRAMM, DAVID N. N89-21715
SCHULT, R. L. N89-21165
SCHULTZ, P. H. N89-21383
N89-21384
SCHULTZE, BERND N89-21052
SCHUMAKER, T. L. N89-21022
SCHURAYTZ, B. C. N89-21362
N89-21386
SCHUSTER, DAVID M. N89-20933
SCHUSTER, S. H. N89-21379
SCHWARTZ, STUART C. N89-21167
N89-21187
N89-21612
SCOTT, MARK F. N89-21466
SCRUBY, C. B. N89-21035
N89-21101
SEEGER, PHILIP A. N89-21578
SEGAL, MORDECHAI N89-21549
SEGUR, HARVEY N89-21508
SEIDEL, DAVID A. N89-20946
SEILER, DAVID G. N89-21678
SELLSCHOP, J. P. F. N89-21400
SELTZER, SHERMAN M. N89-21016
SEMAN, ROBERT M. N89-21179
SEPKOWSKI, J. JOHN, JR. N89-21385
SERRANO, ARTURO V. N89-20976
SHAFEEV, G. A. N89-21089
SHAKED, H. N89-21686
SHALEV, DORON N89-21037
SHANNON, ROBERT R. N89-21673
SHAPIRO, WILBUR N89-21239
SHARPTON, V. L. N89-21309
N89-21341
N89-21386
SHEA, R. E. N89-21235
SHELL, DALE E. N89-21010
SHEPARD, R. L. N89-21070
SHEPPARD, RODNEY J. N89-21470
SHIBYA, G. N89-21359
SHIELDS, F. DOUGLAS N89-21630
SHIVAKUMAR, K. N. N89-21267
SHIVELY, ROBERT N89-20978
SHOEMAKER, CAROLYN S. N89-21387
SHOEMAKER, EUGENE M. N89-21387
SHREWSBURY, GEORGE D. N89-20933
SHUKLA, J. N89-21448
SHUKLA, P. N. N89-21296
SHUKOLYUKOV, YU. A. N89-21343
SHUMAN, LUVENIA M. N89-21710
SICKLES, W. L. N89-20959
SIGURDSSON, H. N89-21388
SILSBEE, MICHAEL RAY N89-21102
SILVA, V. M. N89-21042
SIMES, BRIAN J. N89-21465
SIMKIN, TOM N89-21389
SIMKOVICH, G. N89-21085
SIMMONSA, SCOTT P. N89-21230
SIMON, ELVIS D. N89-21029
SIMONS, RAINEE N. N89-21172
SIMONS, S. A. N89-21200
SINGH, RAJ. N89-21244
SIROIS, E. N89-21084
SISK, LORI A. N89-21023
SKIFF, B. A. N89-21713
SKINNER, JAMES M. N89-20979
SKYLLINGSTAD, E. D. N89-21457
SLEEP, N. N89-21413
SLOAN, R. E. N89-21390
SMEDSVIG, EINAR N89-20986
SMIT, J. N89-21391
SMIT, P. N89-21391
SMITH, ALLEN N89-21594
SMITH, C. B. N89-21400
SMITH, C. W. N89-20930
SMITH, FRANCIS R. N89-20970
SMITH, J. R. N89-21654
SMITH, JAMES E. N89-21712
SMITH, JOHN P. N89-20983
SMITH, LEROY K. N89-21282
SMITH, MARILYN J. N89-20933
SMITH, SHERYL LEIGH N89-21721
SMITH, W. L., JR. N89-21215
SNYDER, LAWRENCE C. N89-21063
SOILEAU, M. J. N89-21234
SOLOMON, MARY K. N89-21008
SOLOMON, SEAN C. N89-21436
SONDERGAARD, NEAL A. N89-21626
SORENSEN, H. C. N89-21284
SPANN, R. N89-21109
SPENCER, MICHAEL G. N89-21154
SPICER, WILLIAM E. N89-21675
SPIEGEL, STANLEY L. N89-21019
SPINHIRNE, J. D. N89-21444
SPIRIDIGLIOZZI, LUCIANO N89-21518
SPRANGLE, P. N89-21227
SPRINGER, WILLIAM T. N89-21751
ST.JOHN, CHRISTOPHER N89-21544
STANKER, LARRY H. N89-21225
STANKOVIC, JOHN A. N89-21587
STASIOWSKI, PETER N89-21582
STAUBS, ERNEST A. N89-21081
STAUDHAMMER, KARL P. N89-21094
STAVINOHA, LEO L. N89-21253
STEGER, JOSEPH L. N89-20949
STEIER, W. H. N89-21536
STERNBERG, ROBERT J. N89-21478
STERNE, P. N89-21096
STERNS, ALAN R. N89-21146
STEUBER, THOMAS J. N89-21104
STEVENS, KENT A. N89-21469
STEVENS, M. A. N89-21461
STEWART, J. M. N89-21050
STEWART, JAMES J. P. N89-21069
STILES, E. D. N89-21124
STINCHCOMB, W. W. N89-21037
STOCKMAN, WILLIAM K. N89-21012
STOCKS, G. M. N89-21096
STONE, P. L. N89-21005
STONER, DEBRA L. N89-21079
STOTHERS, RICHARD B. N89-21372
STOTT, LOWELL D. N89-21392
STRADNER, H. N89-21370
STRANG, GILBERT N89-21499
STRASBURGER, JOHN R. N89-21631
STRATTAN, ROBERT N89-21462
STRAUCH, JOHN N89-21559
STRAUS, DAVID M. N89-21448
STRAZISAR, A. J. N89-20956
STRIGHT, JAMES R. N89-21569
STUMPF, RICHARD P. N89-21415
STURROCK, PETER A. N89-21717
STWALLEY, WILLIAM C. N89-21229
SUGIHARA, RICHARD Y. N89-21121
SUN, XIAOLI N89-21141
SUTTON, ERNEST B. N89-21711
SWANSON, D. G. N89-21660
SWANSON, DONALD A. N89-21393
SWANSON, F. J. N89-21394
SWEET, A. R. N89-21395
SWINNEY, HARRY L. N89-21213
SZOBOSZLAY, ZOLTAN N89-20978

T

TABER, J. N89-21443
TACKETT, DENNIS L. N89-21153
TADJBAKHSH, I. G. N89-21531
TAJIMA, T. N89-21662
TAKAGI, SHUNSUKA N89-21516
TAKAOKA, N. N89-21359
TAM, RICHARD Y. N89-21527
TANG, C. M. N89-21227
TANG, F. C. N89-20968
TANGUAY, ARMAND R., JR. N89-21566
TANZER, H. J. N89-21191
TARDIF, S. N89-21615
TARR, GREGORY L. N89-21591
TARRANT, P. M. N89-21706
TAYLOR, MARK S. N89-21681
TAYLOR, R. D. N89-21133
TAYLOR, ROY A. N89-21246

TEBBETTS, ILSE N89-21484
TEMMERMAN, W. M. N89-21096
TEMPLE, ENOCH C. N89-21752
TENFORDE, T. S. N89-21627
TEPPER, J. S. N89-21461
TESSLER, ALEXANDER N89-21518
THADHANI, NARESH N. N89-21095
THOMAN, STEVEN J. N89-21043
THOMAS, DANIEL N89-21640
THOMAS, E. N89-21396
THOMPSON, C. E. N89-21654
THOMPSON, DONALD L. N89-21057
THOMPSON, JAMES J. N89-21092
THOMPSON, RICHARD A. N89-21193
THOMPSON, STARLEY L. N89-21397
N89-21398
N89-21401
THOMSON, DENNIS W. N89-21449
THOMSON, RICHARD N89-21584
THORNTON, WILLIAM E. N89-21463
TINDELL, DOUGLAS R. N89-21561
TINOCO, E. N. N89-20929
TINUS, R. W. N89-21399
TOBAK, M. N89-21532
TOLLISON, DANNY K. N89-21016
TOMICK, JOHN J. N89-21599
TONEY, M. F. N89-21064
TONGUE, BENSON H. N89-20990
TRAN, N. H. N89-21015
TREDOUS, M. N89-21400
TREJO, LEONARD J. N89-21474
TRIPATHY, K. C. N89-21596
TRIPOLI, GREGORY J. N89-21401
TROMP, JEFFREY C. N89-21203
TROUNG, K. N89-21129
TRUE, WESLEY D., JR. N89-21157
TRUONG, K. V. N89-21532
TSAI, JYA-JANG N89-21571
TSENG, PAUL N89-21548
TSUI, P. N89-21032
TUCKER, DENNIS S. N89-21753
TUCKER, LEDYARD R. N89-21608
TURCOTTE, JEFFREY S. N89-21275
TUREKIAN, K. K. N89-21402
TURKEL, ELI N89-20950
TURNER, MICHAEL S. N89-21635
TUROK, NEIL N89-21716
TWIST, D. N89-21312
TWIST, JAMES R. N89-21670

U

UBER, JAMES G. N89-21754
UEDA, K. N89-21105
UM, C. I. N89-21629
UNAL, AYNUR N89-20964
N89-21532
UNDERWOOD, J. H. N89-21042
N89-21087
URI, JOHN J. N89-21463

V

VADYAK, JOSEPH N89-20933
VALDMANIS, J. A. N89-21142
VAMPOLA, A. L. N89-21440
VANDALSEM, WILLIAM R. N89-20949
VANDAMME, D. N89-21305
VANDERLAAN, MARTIN N89-21225
VANDIJK, G. N89-21621
VANDOOREN, F. J. N89-21261
VANHOVE, P. L. N89-21552
VANLEER, BRAM N89-20935
VANLOAN, CHARLES N89-21519
VANSTRYLAND, ERIC W. N89-21234
VANVRANKEN, R. N89-21168
VANWINGERDE, A. M. N89-21261
VATSA, VEER N. N89-20950
VEAL, B. W. N89-21686
VELICKY, RODOLF W. N89-21132
VENKATESWARARAO, KONDAPAVULURU TIRUMALA
N89-21098
VENTURINI, E. L. N89-21050
VERDON, C. P. N89-21661
VERHAGEN, B. TH. N89-21400
VERHAGEN, J. H. N89-21543
VICKERY, A. M. N89-21403
VIEGAS, JOHN R. N89-20951
VILLIAN, J. P. N89-21156
VOGEL, GERARD N. N89-20975
VOGT, WILLIAM G. N89-21479
VOIGT, ROBERT G. N89-21537
VOLK, TYLER N89-21373
VOLOVIK, G. E. N89-21664
VOSS, H. D. N89-21438
VYRNWY-JONES, PETER N89-21482

W

WACHSPRESS, D. A. N89-20973
WAGNER, CHARLES A. N89-20983
WALKER, HOMER F. N89-21613
WALKER, JOHN S. N89-21626
WALKO, LAWRENCE C. N89-20976
WALLACE, TIMOTHY P. N89-21647
WALSER, ROGERS M. N89-21680
WALSH, DANIEL W. N89-21755
WALSH, JOANNE L. N89-20982
WALTERS, E. JANE N89-21170
WALTON, J. R. N89-21280
WANG, YAN MING N89-21442
WANNA, J. N89-21212
WARD, MICHAEL L. N89-21011
WARD, PETER D. N89-21404
WARDENIER, J. N89-21261
WASSON, JOHN T. N89-21405
WATKINS, BRUCE E. N89-21225
WATTS, MICHAEL E. N89-21541
WAVERING, ALBERT J. N89-21238
WDOWIAK, P. N89-21406
WDOWIAK, T. J. N89-21406
WEDAN, BRUCE W. N89-20950
WEILAND, T. L. N89-21654
WEINER, DONALD N89-21186
WEINSHALL, DAPHNA N89-21473
WEINSTEIN, EHUD N89-21549
WEISS, R. A. N89-21119
WEISS, RICHARD A. N89-21525
N89-21526
WEISSMAN, PAUL R. N89-21306
N89-21407
WEITSMAN, Y. N89-21112
WEMPNER, GERALD N89-21044
WERSINGER, J. M. N89-21660
WERT, JOHN N89-21088
WEST, C. L. N89-21650
WHANG, M. H. N89-21629
WHITAKER, J. F. N89-21142
WHITAKER, KEVIN W. N89-21756
WHITE, JACOB K. N89-21586
WHITELY, LISA D. N89-21066
WHITEMAN, J. R. N89-21517
WHITESIDES, GEORGE M. N89-21118
WHITMIRE, D. P. N89-21408
WHITTREDGE, ROY N89-21582
WIBERG, PATRICIA L. N89-21299
WIESEMAN, CAROL D. N89-20991
WIESEMAN, CAROL DANIELLE N89-20972
WIKSWO, JOHN P., JR. N89-21220
WILBUR, PAUL J. N89-21658
WILCOX, R. B. N89-21654
WILCZEK, FRANK N89-21635
WILDE, P. N89-21295
N89-21409
WILKIN, JOHN L. N89-21459
WILLIAMS, DAVID R. N89-21472
WILLIAMS, FORMAN A. N89-21071
WILLIAMS, JOHN D. N89-21658
WILLIAMSON, DAVID L. N89-21446
WILSON, EDWARD N89-21277
WILSON, JEFFERY A. N89-21556
WING, S. N89-21156
WINK, KAREN A. N89-21231
WISE, S. W. N89-21410
WISEMAN, JOHN M. N89-21180
WITHERELL, M. D. N89-21281
WOLBACH, WENDY S. N89-21411
WOLF, STEPHEN W. D. N89-20955
WOLFE, RUTH F. N89-21387
WOLLENWEBER, F. G. N89-21643
WOOD, EARL H. N89-21471
WOODS, JOHN L. N89-21178
WORK, STEVE J. N89-21095
WRIGHT, J. A. N89-21165
WRIGHT, W. F. N89-21105
WU, Z. C. N89-21089
WYATT, JOHN L., JR. N89-21586

X

XU, YONGZGHI N89-21257

Y

YANISKO, P. J. N89-21119
YATES, JOHN T., JR. N89-21086
N89-21116
YE, WEIZUO N89-21447
YEAGER, DORIAN P. N89-21757
YEE, SAMUEL Y. K. N89-21456
YEH, DAVID T. N89-20924
YEUM, K. S. N89-21134
YIH, H. R. N89-21037
YIM, EUGENE N89-21150
YIN, WAN-LEE N89-21044
YOS, JERROLD M. N89-21193
YOUNG, RONALD B. N89-21758
YU, H. Y. N89-21683
YU, LI-HSING N89-21095

Z

ZACHOS, J. C. N89-21412
ZAHNLE, K. N89-21413
ZAK, J. A. N89-21425
N89-21426
ZAKRAJESEK, JAMES J. N89-21243
ZAKRAJSEK, JAMES J. N89-21244
ZALIK, RICHARD A. N89-21759
ZARETSKY, ERWIN V. N89-21245
ZEHNDER, ALAN T. N89-21272
ZEILER, THOMAS A. N89-20991
ZHANG, Y. N89-21050
ZHENG, YAN N89-21414
ZIEBARTH, JOHN P. N89-21760
ZIEGLER, WILLI N89-21380
ZIMMERMAN, M. N89-21138
ZIMMERMAN, RICHARD S. N89-21046
N89-21286
ZIPF, MARK E. N89-21479
ZISSIMIDES, JOHN N89-21492
ZOLLER, W. H. N89-21314
ZUE, VICTOR W. N89-21160
N89-21699
ZURLINDEN, JOSEPH E. N89-21506

Typical Corporate Source Index Listing

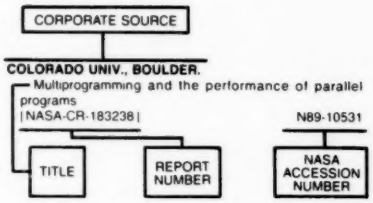

Listings in this index are arranged alphabetically by corporate source. The title of the document provides the user with a brief description of the subject matter. The report number helps to indicate the type of document cited (e.g., NASA report, translation, NASA contractor report). The NASA accession number denotes the number by which the citation is identified. The titles are arranged under each corporate source in ascending accession number order.

A

ACADEMIA SINICA, BEIJING (CHINA).
New approach to the origin of the tektite in China N89-21414

ACADEMY OF SCIENCES (USSR), MOSCOW.
The Kara and Ust-Kara impact structures (USSR) and their relevance to the K/T boundary event N89-21341
The Karskiy craters are the probable records of catastrophe at the Cretaceous-Tertiary boundary N89-21343

AEROJET SOLID PROPULSION CO., SACRAMENTO, CA.
Synthesis of energetic binders
[AD-A203060] N89-21127

AEROSPACE CORP., EL SEGUNDO, CA.
Electron paramagnetic resonance and photoluminescence studies of impurities in CdTe
[AD-A202841] N89-21056
Adhesion in chemically hostile environments: The use of filled polymers as diffusion barriers
[AD-A203333] N89-21121
Commentary on fast atmospheric pulsations
[AD-A203172] N89-21440
Distribution of boron atoms in ion implanted compound semiconductors
[AD-A203173] N89-21677

AEROSPACE MEDICAL RESEARCH LABS., WRIGHT-PATTERSON AFB, OH.
LCP-10 intelligibility of oxygen masks and microphones in aircraft noise
[AD-A202474] N89-21481

AIR FORCE ACADEMY, CO.
MOPAC manual, 5th edition: A general molecular orbital package
[AD-A204003] N89-21069

AIR FORCE ARMAMENT LAB., EGLIN AFB, FL.
A study of transonic drag reduction of a blunt cylinder by a cylinder probe
[AD-A202557] N89-20965

AIR FORCE AVIONICS LAB., WRIGHT-PATTERSON AFB, OH.
Software development guidelines
[AD-A203332] N89-21572
A methodology for screening potential artificial intelligence applications
[AD-A203966] N89-21594

AIR FORCE ENVIRONMENTAL TECHNICAL APPLICATIONS CENTER, SCOTT AFB, IL.
Corrosion control climatology
[AD-A202477] N89-21079
Upper-wind climatology for CONUS
[AD-A203961] N89-21453
Seasonal snowfall statistics for selected stations
[AD-A203965] N89-21454
Global snow depth climatology
[AD-A203969] N89-21455

AIR FORCE FLIGHT DYNAMICS LAB., WRIGHT-PATTERSON AFB, OH.
In-flight lightning characterization program on a CV-580 aircraft
[AD-A203954] N89-20976

AIR FORCE GEOPHYSICS LAB., HANSCOM AFB, MA.
Precipitating ion and electron detectors (SSJ/4) for the block 5D/Flight 8 DMSP (Defense Meteorological Satellite Program) satellite
[AD-A203999] N89-21022
Blending of surface and rawinsonde data in mesoscale objective analysis
[AD-A203984] N89-21456

AIR FORCE INST. OF TECH., WRIGHT-PATTERSON AFB, OH.
Effect of riblets upon flow separation in a subsonic diffuser
[AD-A203178] N89-20967
Numerical simulation of flow over iced airfoils
[AD-A203291] N89-20969
Thin-layer Navier-Stokes solutions for a cranked delta wing
[AD-A203292] N89-20970
Two-dimensional Navier-Stokes solution of the flow over a thick supercritical airfoil with strong shock-induced separation
[AD-A203331] N89-20971
A diagnostic system blending deep and shallow reasoning
[AD-A202547] N89-20979
Aircraft tracking with dual TACAN
[AD-A202647] N89-20980
Performance analysis of the fiber distributed data interface in the super cockpit audio world
[AD-A202535] N89-20985
Preliminary design of a modular unmanned research vehicle. Volume 1: System design document
[AD-A202765] N89-20987
A wind tunnel and computer investigation of the low speed aerodynamic characteristics of the prone escape system (PRESS)
[AD-A202768] N89-20988
Response equivocation analysis for the smart stick controller
[AD-A203146] N89-20989
A source code analyzer to predict compilation time for avionics software using software science measures. Volume 1: Main report
[AD-A202737] N89-20992
Real-time display of time dependent data using a head-mounted display
[AD-A203051] N89-20993
A helmet-mounted virtual environment display system
[AD-A203055] N89-20994
Flight controller design with nonlinear aerodynamics, large parameter uncertainty and pilot compensation
[AD-A202727] N89-21000
A digital rate controller for the control reconfigurable combat aircraft designed using quantitative feedback theory
[AD-A203050] N89-21001
Optimal launch time for a discontinuous low thrust orbit transfer
[AD-A202693] N89-21007
Control system for maintaining stable orbits around phobos
[AD-A202776] N89-21008
Hypersurface insertion window for long term orbital stability of artificial satellites about the planet Venus
[AD-A202808] N89-21009
Stability solution to linearized equations of motion for a symmetric spinning satellite in an elliptical orbit applied to the non-linear equations
[AD-A202934] N89-21010
Estimated satellite cluster elements in near circular orbit
[AD-A202938] N89-21011
An analytical framework for determining life cycle cost implications of the advanced launch system
[AD-A202873] N89-21012
Light satellites: A dilemma for the US Army
[AD-A202648] N89-21017
Remote orbital capture using an orbital maneuvering vehicle equipped with a multibody grappling arm assembly
[AD-A202760] N89-21018
Active control of a large space structure as applied to the phase 1 CETF (Critical Evaluation Task Force) space station
[AD-A203293] N89-21020
Geomagnetic field energy as a source of thrust
[AD-A202567] N89-21027
A study of failure characteristics in a thermoplastic composite material at high temperature
[AD-A203015] N89-21040
Effects of battle damage repair on the natural frequencies and mode shapes of curved rectangular composite panels
[AD-A203179] N89-21041
Investigation of crack growth in titanium-aluminide at elevated temperatures
[AD-A202570] N89-21081
The effects of loading history and closure of the fatigue characteristics of heat treated Ti-6Al-2Sn-4Zr-6Mo
[AD-A202652] N89-21082
Crack growth of a titanium-aluminide alloy under thermal-mechanical fatigue
[AD-A202767] N89-21083
Investigation of failure modes in fiber reinforced ceramic matrix composites
[AD-A202705] N89-21113
Fracture toughness testing of a ceramic matrix composite at elevated temperatures
[AD-A202738] N89-21114
Compressive properties of high performance polymeric fibers
[AD-A202947] N89-21117
Speech recognition using neural nets and dynamic time warping
[AD-A202528] N89-21144
A modeling perspective for meteor burst communication
[AD-A202562] N89-21145
The use of chaff in space as a jamming device between ground stations and satellites
[AD-A202577] N89-21146
Performance of an adaptive matched filter using the Griffiths algorithm
[AD-A202578] N89-21147
Multiple model adaptive tracking of airborne targets
[AD-A202696] N89-21148
Analysis and simulation of a pseudonoise synchronization system
[AD-A202779] N89-21149
Improving the survivability of a stochastic communication network
[AD-A202872] N89-21150
The radar cross section of a two dimensional dielectric coated cylinder using on-surface radiation conditions
[AD-A202935] N89-21152
On the impulse response of monopulse radars
[AD-A202936] N89-21153
Effect of two-body motion on radar beam quality for various distributed sparse array configurations
[AD-A202937] N89-21154
Response surface methodology applied to the radar range equation
[AD-A203044] N89-21157
Problem specific applications for neural networks
[AD-A203052] N89-21158
An analysis of noise reduction using back-propagation neural networks
[AD-A203057] N89-21159
A multiple-valued logic system for circuit extraction to VHDL 1076-1987
[AD-A202646] N89-21177
The 8755 emulator design
[AD-A202649] N89-21178
Investigation of the impedance modulation of thin films with a chemically-sensitive field-effect transistor
[AD-A202766] N89-21180

Numerical study of three viscous/inviscid interaction methods
[AD-A202575] N89-21203
Volumetric rendering techniques for the display of three-dimensional aerodynamic flow field data
[AD-A202661] N89-21204
An experimental investigation of flow mixing on thrust ejection efficiency
[AD-A202707] N89-21205
Incompressible flow friction coefficients in a simulated heat pipe
[AD-A203176] N89-21207
An analysis of platinum silicide and indium antimonide for remote sensors in the 3 to 5 micrometer wavelength band
[AD-A202663] N89-21218
A position, scale and rotation invariant holographic associative memory
[AD-A203289] N89-21221
Analysis of space-based lidar for aircraft tracking
[AD-A202665] N89-21230
Laser beam coupling via optical phase conjugation in BaTiO3
[AD-A202874] N89-21231
Development of a shock capturing code for use as a tool in designing high-work low aspect ratio turbines
[AD-A202706] N89-21248
Robotic compliant motion control for aircraft refueling applications
[AD-A202710] N89-21249
Robotic tactile sensor fabricated from piezoelectric polyvinylidene fluoride films
[AD-A202724] N89-21250
Application of the boundary element method to fatigue crack growth analysis
[AD-A202565] N89-21270
Nonlinear finite element analysis of a general composite shell
[AD-A202572] N89-21271
A new model for the forced response of a mistuned disk
[AD-A202769] N89-21275
Vibration and buckling characteristics of composite cylindrical panels incorporating the effects of a higher order shear theory
[AD-A202939] N89-21278
Finite element analysis of composite plates including shear deformation
[AD-A202941] N89-21279
Macrocrack-multiple defect interaction considering elastic, plastic and viscoplastic effects
[AD-A203186] N89-21282
Transverse shear considerations in anisotropic plates
[AD-A203187] N89-21283
LMS adaptive filtering applied to a microwave arterial pulse monitor
[AD-A202732] N89-21465
A study of motion sickness: Mathematical modeling and data analysis
[AD-A202770] N89-21466
Capacity of human operator using smart stick controller
[AD-A202712] N89-21483
Graphical man-machine interface for an integrated evaluation environment
[AD-A203054] N89-21487
F-16 speaker-independent speech recognition system using cockpit commands (70 words)
[AD-A203177] N89-21489
Superresolved imaging using the Hartley transform and a hemispherical object space
[AD-A202527] N89-21551
Architecture and design for a laser programmable double precision floating point application specific processor
[AD-A202560] N89-21553
Response surface analysis of stochastic network performance
[AD-A202561] N89-21554
Simulating rule-based systems
[AD-A202563] N89-21555
Optical information processing in a confocal Fabry-Perot resonator
[AD-A202566] N89-21556
An educational expert system shell integrating object-attribute-value triples and frames
[AD-A202574] N89-21557
A decision-based methodology for object oriented-design
[AD-A202579] N89-21558
A vectorized hidden-surface algorithm implemented on the Cray-2 supercomputer
[AD-A202657] N89-21560
Maintenance metrics for Jovial (J73) software
[AD-A202713] N89-21561
Design of a syntax validation tool for requirements analysis using Structured Analysis and Design Technique (SADT)
[AD-A202725] N89-21562
Distributed discrete-event simulation using variants of the Chandy-Misra algorithm on the intel hypercube
[AD-A202849] N89-21563
Influence diagrams: Automated analysis with dynamic programming
[AD-A203045] N89-21567
A software system to create a hierarchical, multiple level of detail terrain model
[AD-A203047] N89-21568
A neural network implementation of chaotic time series prediction
[AD-A203049] N89-21569
Dynamic analysis of feedforward neural networks using simulated and measured data
[AD-A202573] N89-21591
Selection of a frequency sensitive QFT (Quantitative Feedback Theory) weighting matrix using the method of specified outputs
[AD-A202692] N89-21592
A comparison of control variates for queueing network simulation
[AD-A202576] N89-21599
Hybrid calculation of invariant moments
[AD-A202594] N89-21600
A comparison of variable selection criteria for multiple linear regression: A simulation study
[AD-A202708] N89-21601
A diagnostic system using Boolean reasoning
[AD-A202764] N89-21602
Corona wind cooling comparisons for horizontal cylinders
[AD-A202714] N89-21625
Analysis and simulation of an audio adaptive equalizer
[AD-A202569] N89-21631
Optical activity and its influence on photorefractive materials
[AD-A202530] N89-21642
Modified backward error propagation for tactical target recognition
[AD-A202666] N89-21644
Calculation of carriers in depletion region of semiconductors with capacitance-voltage measurements
[AD-A202529] N89-21668
Evaluation of the spatial and temporal characteristics of the conducting PRIZ
[AD-A202593] N89-21671
The response of single element HgCdTe and InSb solid state infrared detectors to millimeter wave electromagnetic energy
[AD-A202667] N89-21672
Investigation of a self-aligned, strained-channel,n sup(+)-In As/Al 0.5 As/In 0.15 Ga 0.85 As Semiconductor Insulator Semiconductor FET (SISFET)
[AD-A203147] N89-21676
Variable wall temperature effects on multicellular natural convection in a horizontal annulus
[AD-A202762] N89-21691
Analysis of the Federal Aviation Administration's host computer acquisition process and potential application in Department of Defense acquisitions
[AD-A202623] N89-21695
An analysis of the biennial budget process
[AD-A202626] N89-21710

AIR FORCE LOGISTICS COMMAND, WRIGHT-PATTERSON AFB, OH.
Lockheed Aeronautical Systems Company technical order transfer tests
[DE89-008092] N89-21707

AIR FORCE MATERIALS LAB., WRIGHT-PATTERSON AFB, OH.
Physical and mechanical properties of American Cyanamid's acetylene-terminated prepreg system: T-300/CATB-44
[AD-A203737] N89-21045

AIR FORCE OCCUPATIONAL AND ENVIRONMENTAL HEALTH LAB., BROOKS AFB, TX.
Contamination of the exterior of a C-130E aircraft used for aerial spray, 907 TAG, Rickenbacker ANGB, OH
[AD-A202430] N89-20984

AIR FORCE SYSTEMS COMMAND, WRIGHT-PATTERSON AFB, OH.
People's Republic of China laser radiation safety standard
[AD-A203777] N89-21233

AIR FORCE SYSTEMS COMMAND LIASON OFFICE, OTTAWA (ONTARIO).
Guide to Canadian aerospace related industries
[AD-A203738] N89-21697

AIR FORCE WRIGHT AERONAUTICAL LABS., WRIGHT-PATTERSON AFB, OH.
Spectroscopy and laser performance of Ti(sup 3+) doped and Cr(sup 3+), Nd(sup 3+) co-doped crystals
[AD-A203911] N89-21682

AIR WAR COLL., MAXWELL AFB, AL.
Incorporating five nations' operational requirements into a single aircraft: The F-16 multinational fighter program viewed from the operational side
[AD-A202552] N89-20986
Space technology and the Soviet/US strategic competition: A perspective and forecast using 12-year cycles
[AD-A202538] N89-21006
SDI (Strategic Defense Initiative) and national security policy
[AD-A202730] N89-21617
National space policy
[AD-A202644] N89-21711

AKRON UNIV., OH.
Global-local methodology for fracture analysis of engineering structures N89-21262

ALABAMA A & M UNIV., HUNTSVILLE.
Refining, revising, augmenting, compiling and developing computer assisted instruction K-12 aerospace materials for implementation in NASA spacelink electronic information system N89-21729
Fluctuation analysis of relativistic nucleus-nucleus collisions in emulsion chambers N89-21747
SSME propulsion performance reconstruction techniques N89-21752

ALABAMA CRYOGENIC ENGINEERING, INC., HUNTSVILLE.
A cryocooler for high acceleration applications
[AD-A203063] N89-21137

ALABAMA UNIV., BIRMINGHAM.
Heavy metal toxicity as a kill mechanism in impact caused mass extinctions N89-21406

ALABAMA UNIV., HUNTSVILLE.
Experimentally verifiable Yang-Mills spin 2 gauge theory of gravity with group U(1) x SU(2) N89-21693
Research Reports: 1988 NASA/ASEE Summer Faculty Fellowship Program
[NASA-CR-183553] N89-21726
Intelligent data reduction for autonomous power systems N89-21737
Further investigations of oblique hypervelocity impact phenomena N89-21750
Software system safety N89-21754
The role of the turbulent Prandtl number in turbine blade heat transfer prediction N89-21756
Techniques for studying the effects of microgravity on model particle/cell systems N89-21758
Space shuttle main engine numerical modeling code modifications and analysis N89-21760

ALABAMA UNIV., TUSCALOOSA.
Research Reports: 1988 NASA/ASEE Summer Faculty Fellowship Program
[NASA-CR-183553] N89-21726

ALASKA UNIV., FAIRBANKS.
Development of a prototype commonality analysis tool for use in space programs N89-21757

AMES LAB., IA.
Topics in chemical physics. 1: Semiclassical reactive scattering theory. 2: Corrected effective medium theory
[DE89-007606] N89-21053
Nuclear magnetic resonance study of hydrogen in niobium-vanadium alloys
[DE89-007578] N89-21075
Effect of Te on the microstructural changes during the gray-to-white and white-to-gray transition in directional solidification of Fe-C-Si alloys
[DE89-007607] N89-21076
Studies of the initial oxidation of Fe-Si alloys by AES, XPS, EELS and LEED
[DE89-007610] N89-21077
Hydrogen and deuterium internal friction behavior in vanadium-niobium alloys
[DE89-007616] N89-21078
Performance of a prototype electromagnetic calorimeter
[DE89-007608] N89-21216
Sample introduction techniques for inductively coupled plasma mass spectrometry
[DE89-005724] N89-21655
Low temperature properties of ternary magnetic rare earth transition metal germanides with the Sc5Co4Ge10-type structure
[DE89-007628] N89-21656

ANALYTICAL SERVICES AND MATERIALS, INC., HAMPTON, VA.
Implementation of equivalent domain integral method in the two-dimensional analysis of mixed mode problems
[NASA-CR-181813] N89-21267

ANTHROPOLOGY RESEARCH PROJECT, YELLOW SPRINGS, OH.
Measurer's handbook: US Army anthropometric survey, 1987-1988
[AD-A202721] N89-21484
APPLIED RESEARCH CORP., COLLEGE STATION, TX.
Abrupt climate change and extinction events N89-21308
APPLIED TECHNOLOGY ASSOCIATES, INC., ALBUQUERQUE, NM.
Low-cost Pointing-and-Tracking System for Optical Communications (PATSOC)
[AD-A202921] N89-21151
VAX to CRAY NASTRAN user interface
[AD-A203447] N89-21575
ARGONNE NATIONAL LAB., IL.
Spectral analysis of a fourth-order singular differential operator arising in combustion
[DE89-005841] N89-21052
Calculation of the energetics of chemical reactions
[DE89-007262] N89-21070
An algebraic theory of program correctness in a problem domain
[DE89-008450] N89-21579
A theory of problem domains and program correctness
[DE89-008451] N89-21580
Otter 1.0 users' guide
[DE89-008656] N89-21581
An in-situ, high-temperature study of the superconductor YBa1.67Sr0.33Cu3O(6+x)
[DE89-007375] N89-21686
Order in cold ionic systems: Dynamic effects
[DE89-007377] N89-21687
ARIZONA STATE UNIV., TEMPE.
Bending and vibration of variable thickness orthotropic plates N89-21264
Shatter cones: Diagnostic impact signatures N89-21355
Non-random cratering flux in recent time N89-21384
ARIZONA UNIV., TUCSON.
Computer simulation of macrosegregation in directionally solidified circular ingots
[NASA-CR-182838] N89-21134
Studies in the computation of compressible and viscous flow
[AD-A203334] N89-21208
Risk to civilization: A planetary science perspective N89-21302
The impact of mass extinctions N89-21315
Impact wave deposits provide new constraints on the location of the K/T boundary impact N89-21330
Provenance of the K/T boundary layers N89-21331
Atmospheric erosion by impacts: An analytic investigation N89-21403
Numerical modeling of narrow band soft X-ray sources
[AD-A203368] N89-21657
Center for thin film studies
[AD-A202742] N89-21673
ARKANSAS UNIV., FAYETTEVILLE.
Evaluate the application of modal test and analysis processes to structural fault detection in MSFC-STS project elements N89-21751
ARKANSAS UNIV., LITTLE ROCK.
A novel approach to gamma-ray and neutrino astro-particle physics: The GRANDE experiment
[DE89-006515] N89-21725
ARMS CONTROL AND DISARMAMENT AGENCY, WASHINGTON, DC.
Strategic defense initiative: A chronology, 1983 - 1988
[AD-A203576] N89-21619
ARMY AEROMEDICAL RESEARCH LAB., FORT RUCKER, AL.
The impact of the US Army's AH-64 helmet mounted display on future aviation helmet design
[AD-A202984] N89-21486
ARMY AEROMEDICAL RESEARCH UNIT, FORT RUCKER, AL.
SPH-4 US Army flight helmet performance 1983-1987
[AD-A202589] N89-21482
Polycarbonate ophthalmic lenses for ametropic Army aviators using night vision goggles
[AD-A203100] N89-21488
ARMY ARMAMENT MUNITIONS AND CHEMICAL COMMAND, WATERVLIET, NY.
A posteriori error estimation of adaptive finite difference schemes for hyperbolic systems N89-21513
An adaptive overlapping local grid refinement method for two-dimensional parabolic systems N89-21514
ARMY ARMAMENT RESEARCH, DEVELOPMENT AND ENGINEERING CENTER, PICATINNY ARSENAL, NJ.
Effect of TNT miscible additives on the mechanical behavior and shock sensitivity of Composition B
[AD-A203968] N89-21132
ARMY ARMAMENT RESEARCH, DEVELOPMENT AND ENGINEERING CENTER, WATERVLIET, NY.
Microscopic aspects of failure and fracture in cross-ply fiber-reinforced composite laminates
[AD-A203202] N89-21042
Stress-corrosion cracking of liquid-phase sintered tungsten alloys
[AD-A203201] N89-21087
Fractographic analysis of a failed crane bolt
[AD-A202703] N89-21274
An investigation of stresses and strains in an internally pressurized, composite-jacketed, steel cylinder
[AD-A202969] N89-21281
A simple analysis of swage autofrettage process N89-21498
Design of a feeling-thinking machine N89-21510
ARMY AVIATION RESEARCH AND DEVELOPMENT COMMAND, CLEVELAND, OH.
Comparison study of gear dynamic computer programs at NASA Lewis Research Center
[NASA-TP-2901] N89-21243
ARMY AVIATION SYSTEMS COMMAND, CLEVELAND, OH.
Modal analysis of gear housing and mounts
[NASA-TM-101445] N89-21244
ARMY AVIATION SYSTEMS COMMAND, SAINT LOUIS, MO.
Three-dimensional singular points in aerodynamics
[NASA-TM-100045] N89-20964
ARMY COLD REGIONS RESEARCH AND ENGINEERING LAB., HANOVER, NH.
Spline-based finite-element method for solving a Stefan's problem in a finite domain: Formulation N89-21516
ARMY CONSTRUCTION ENGINEERING RESEARCH LAB., CHAMPAIGN, IL.
Attenuation of blast waves using foam and other materials
[AD-A203148] N89-21632
ARMY ENGINEER TOPOGRAPHIC LABS., FORT BELVOIR, VA.
Computer strategy for detecting line features on simulated binary arrays in support of radar feature extraction
[AD-A203257] N89-21162
ARMY ENGINEER WATERWAYS EXPERIMENT STATION, VICKSBURG, MS.
The KP equation: A comparison to laboratory generated biperiodic waves N89-21507
Column movement model used to support AMM N89-21521
Skew grids and irrotational flow N89-21523
Thermodynamic gauge theory of solids and quantum liquids with internal phase N89-21525
Lagrangian formulation of relativistic thermodynamics N89-21526
ARMY LAB. COMMAND, WATERTOWN, MA.
Reduction of M1 weld fabrication costs: The effect of weld shielding gas composition
[AD-A204001] N89-21254
ARMY MATERIALS TECHNOLOGY LAB., WATERTOWN, MA.
Element level elimination of nonlinear constraints in total Lagrangian finite element formulations N89-21496
Some issues of numerical integration and penalty relaxation in anisoparametric shell element formulation N89-21518
ARMY MISSILE COMMAND, REDSTONE ARSENAL, AL.
Neural networks and the symmetric group S(sub N) N89-21529
ARMY MISSILE TEST AND EVALUATION DIRECTORATE, WHITE SANDS MISSILE RANGE, NM.
An algorithm for processing scanning spectrometer data N89-21506
ARMY RESEARCH OFFICE, RESEARCH TRIANGLE PARK, NC.
Transactions of the Fifth Army Conference on Applied Mathematics and Computing
[AD-A193384] N89-21490
Stabilization of Ziegler's pendulum by means of the method of vibrational control N89-21531
ARMY TROOP SUPPORT COMMAND, FORT BELVOIR, VA.
Computational issues in goal programming resource allocation N89-21509
ARNOLD ENGINEERING DEVELOPMENT CENTER, ARNOLD AIR FORCE STATION, TN.
Investigation of the development of laminar boundary-layer instabilities along a cooled-wall cone in hypersonic flows
[AD-A202587] N89-20966
Investigation of the development of laminar boundary-layer instabilities along a blunted cone
[AD-A202425] N89-21200
ASTON UNIV., BIRMINGHAM (ENGLAND).
The properties of advanced aluminium alloy systems N89-21074
Mild wear in dry and lubricated sliding systems N89-21242
ATMOSPHERIC AND ENVIRONMENTAL RESEARCH, INC., CAMBRIDGE, MA.
Enhancements to the AFGL (Air Force Geophysics Laboratory) Statistical Analysis Program (ASAP) for the global multivariate analysis of heights and winds
[AD-A202912] N89-21450
ATOMIC ENERGY RESEARCH ESTABLISHMENT, HARWELL (ENGLAND).
Nondestructive testing techniques for metal matrix composites
[AERE-R-13040] N89-21034
Acoustic emission source location in fibre reinforced plastic composites
[AERE-R-13039] N89-21035
The behavior of ceramic matrix, fiber composites under combined impact and tensile stresses
[AD-A202518] N89-21038
The effect of mixed-mode loading on stress-driven solute segregation during high-temperature brittle intergranular fracture
[AERE-R-12897] N89-21073
Acoustic microscopy of low ductility materials
[AERE-R-12848] N89-21101
Frequency dependent ultrasonic ray tracing: A preliminary study
[AERE-R-13119] N89-21139
The determination of Crystallite Orientation Distribution Functions (CODF) and their use in surface texture analysis using X-ray diffraction
[AERE-R-12839] N89-21663
AUBURN UNIV., AL.
Theoretical studies of the heating of toroidal plasmas with radiofrequency electromagnetic radiation
[DE89-008003] N89-21660
Finite element simulation of thunderstorm electrodynamics in the proximity of the storm N89-21728
Experimental results on atomic oxygen corrosion of silver N89-21738
Rotordynamic analysis of a bearing tester N89-21759

B

BABCOCK HITACHI K.K., TOKYO (JAPAN).
Plasma reaction method and apparatus
[DE89-007360] N89-21656
BALLISTIC RESEARCH LABS., ABERDEEN PROVING GROUND, MD.
Effective ignition kinetics for LOVA propellant
[AD-A203149] N89-21129
Density of triethanolammonium nitrate and liquid propellant
[AD-A203767] N89-21131
Polynominal definition of discrete field point of map of diffusion equation N89-21511
Influence of reflected shock waves on a hypersonic shaped charge jet N89-21522
BASQUE UNIV., LEJONA (SPAIN).
The Cretaceous-Tertiary boundary biotic crisis in the Basque country N89-21345
BATTELLE MEMORIAL INST., RICHLAND, WA.
Air quality and forest health issues in the 1990s
[DE89-006941] N89-21427
BATTELLE MEMORIAL INST., WILLOWBROOK, IL.
Documentation of the finite element code VISCOT/UX for thermomechanical analyses: Version 0.01
[DE89-004719] N89-21544
BEDFORD INST. OF OCEANOGRAPHY, DARTMOUTH (NOVA SCOTIA).
Mass mortality and extraterrestrial impacts N89-21335
BEN GURION UNIV. OF THE NEGEV, BEERSHEVA (ISRAEL).
Faunal and erosional events in the Eastern Tethyan Sea across the K/T boundary N89-21338
BIRMINGHAM UNIV. (ENGLAND).
The end-triassic mass extinction event N89-21324
BOEING ADVANCED SYSTEMS CO., SEATTLE, WA.
Additional development of the XTRAN3S computer program
[NASA-CR-181743] N89-20922
BOEING AEROSPACE CO., SEATTLE, WA.
Crater size estimates for large-body terrestrial impact N89-21381
BOEING COMMERCIAL AIRPLANE CO., SEATTLE, WA.
Transonic CFD applications at Boeing N89-20929
BOSTON UNIV., MA.
Condition of the finite element stiffness matrix of highly irregular triangular grids N89-21497

BROWN UNIV., PROVIDENCE, RI.
Microscopic observations of adiabatic shear bands in three different steels
[AD-A202522] N89-21080
Large deformations near a pair of closely-spaced spherical voids in a rate-dependent solid
[AD-A202465] N89-21268
Oblique impacts: Catastrophic vs. protracted effects N89-21383
Non-random cratering flux in recent time N89-21384
BRUNEL UNIV., UXBRIDGE (ENGLAND).
On some finite element error estimates for stress intensity factors in Mode 1 linear elastic fracture problems N89-21517
Computer assisted analysis and modelling of structured problems
[AD-A203040] N89-21607

C

CAIRO UNIV. (EGYPT).
On the conditions for resonance interactions of instability waves in the axisymmetric jet
[NASA-TM-101477] N89-21196
CALIFORNIA INST. OF TECH., PASADENA.
Three dimensional effects near a crack tip in a ductile three point bend specimen. Part 2: An experimental investigation using interferometry and caustics
[AD-A202637] N89-21272
An investigation of viscoelastic fracture near and at interfaces
[AD-A203760] N89-21285
Environmental effects of large impacts on the earth; relation to extinction mechanisms N89-21365
Basic studies of ion mixing
[AD-A203093] N89-21637
A search for gravitational waves from coalesing binary stars using the Caltech 40 meter gravity wave detector N89-21721
CALIFORNIA POLYTECHNIC STATE UNIV., SAN LUIS OBISPO.
The keyhole region in VPPA welds N89-21755
CALIFORNIA RESEARCH AND TECHNOLOGY, INC., CHATSWORTH.
Computer modeling of large asteroid impacts into continental and oceanic sites: Atmospheric, cratering, and ejecta dynamics N89-21379
CALIFORNIA UNIV., BERKELEY.
Conformal time domain finite difference method of solving electromagnetic wave scattering
[AD-A202434] N89-21143
The debate over the Cretaceous-Tertiary boundary N89-21288
Limitations on K-T mass extinction theories based upon the vertebrate record N89-21290
Possible world-wide middle miocene iridium anomaly and its relationship to periodicity of impacts and extinctions N89-21291
Late Wenlock (middle Silurian) bio-events: Caused by volatile boloid impact/s N89-21295
Astrophysical implications of periodicity N89-21361
Cathodoluminescence of shocked quartz at the Cretaceous-Tertiary boundary N89-21369
Collisions with ice-volatile objects: Geological implications N89-21409
Study of semiconductor valence plasmon line shapes via electron energy-loss spectroscopy in the transmission electron microscope
[DE89-008152] N89-21689
CALIFORNIA UNIV., BERKELEY. LAWRENCE BERKELEY LAB.
Center for Advanced Materials
[DE89-008854] N89-21033
Fluids, both ionic and nonionic, over wide ranges of temperature and composition
[DE89-001265] N89-21048
Nb modification of microcomposite Fe/C/Cr/Mn steel
[DE89-008297] N89-21097
Mechanisms of fatigue crack propagation and fracture toughness behavior in advanced aluminum-lithium alloys
[DE89-008300] N89-21098
The debate over the Cretaceous-Tertiary boundary N89-21288
Possible world-wide middle miocene iridium anomaly and its relationship to periodicity of impacts and extinctions N89-21291
Astrophysical implications of periodicity N89-21361
Marine and continental K-T boundary clays compared N89-21382
Study of semiconductor valence plasmon line shapes via electron energy-loss spectroscopy in the transmission electron microscope
[DE89-008152] N89-21689
Characterization of Nb-Al superconducting material
[DE89-008296] N89-21690
CALIFORNIA UNIV., DAVIS.
Vector potential methods N89-20939
Trace element and isotope geochemistry of Cretaceous-Tertiary boundary sediments: identification of extra-terrestrial and volcanic components N89-21352
The application of modal coordinate methods to large nonlinear time-dependent problems
[AD-A203913] N89-21611
CALIFORNIA UNIV., IRVINE.
A novel approach to gamma-ray and neutrino astro-particle physics: The GRANDE experiment
[DE89-006515] N89-21725
CALIFORNIA UNIV., LOS ANGELES.
Transverse jets in compressible crossflows N89-20923
Hypersonic drone design: A multidisciplinary experience
[NASA-CR-184740] N89-20981
Accretion rate of extraterrestrial matter: Iridium deposited over the last 70 million years N89-21344
Permo-Triassic vertebrate extinctions: A program N89-21367
Tektites: Origin as melts produced by the impact of small projectiles onto dry targets N89-21405
CALIFORNIA UNIV., SAN DIEGO.
Limitations on K-T mass extinction theories based upon the vertebrate record N89-21290
CALIFORNIA UNIV., SAN DIEGO, LA JOLLA.
Architecture studies and system demonstrations of optical parallel processor for AI (Artificial Intelligence) and NI (Neural Intelligence)
[AD-A203241] N89-21593
CALIFORNIA UNIV., SANTA BARBARA.
Possible world-wide middle miocene iridium anomaly and its relationship to periodicity of impacts and extinctions N89-21291
Magnetic microspherules associated with the K/T and upper Eocene extinction events N89-21303
Cretaceous-Tertiary boundary in the Antarctic: Climatic cooling precedes biotic crisis N89-21392
A new class of non-topological solitons
[NASA-CR-184889] N89-21634
CALSPAN FIELD SERVICES, INC., ARNOLD AFS, TN.
Two-measured variable method for wall interference assessment/correction N89-20959
Investigation of the development of laminar boundary-layer instabilities along a cooled-wall cone in hypersonic flows
[AD-A202587] N89-20966
Investigation of the development of laminar boundary-layer instabilities along a blunted cone
[AD-A202425] N89-21200
CAMBRIDGE UNIV. (ENGLAND).
Investigation of the impact performance of various glass and ceramic systems
[AD-A202443] N89-21106
Deformation, fracture and explosive properties of reactive materials
[AD-A203083] N89-21128
MBE of (Hg,Cd)Te
[AD-A202448] N89-21667
CARNEGIE-MELLON UNIV., PITTSBURGH, PA.
Toward a nonequilibrium thermodynamics of two phase materials with sharp interface N89-21494
Adaptive optical linear algebra processors
[AD-A202996] N89-21605
Extracting shape reflectance of Lambertian, specular, and hybrid surfaces
[AD-A203772] N89-21652
A performance/loss evaluation of SSME HPFTP turbine N89-21735
CARPENTER (KENNETH), PHILADELPHIA, PA.
Dinosaur bone beds and mass mortality: Implications for the K-T extinction N89-21301
CASE WESTERN RESERVE UNIV., CLEVELAND, OH.
Analysis of interface crack branching
[NASA-CR-182273] N89-21265
CENTER FOR MATHEMATICS AND COMPUTER SCIENCE, AMSTERDAM (NETHERLANDS).
Large sample theory for statistical inference in several software reliability models
[CWI-MS-R8807] N89-21543
Conditionally and strictly distribution-free tests for randomized block designs that are asymptotically optimal
[CWI-MS-R8802] N89-21615
CENTRE NATIONAL DE LA RECHERCHE SCIENTIFIQUE, GIF-SUR-YVETTE (FRANCE).
Search for the Tunguska event in the Antarctic snow N89-21378
CERAMATEC, INC., SALT LAKE CITY, UT.
High temperature evaluation of new ferroelastic toughened ceramic materials
[AD-A203197] N89-21120
CHEMICAL RESEARCH AND DEVELOPMENT CENTER, ABERDEEN PROVING GROUND, MD.
Surface acoustic wave detection of organophosphorus compounds
[AD-A202909] N89-21058
CHICAGO UNIV., IL.
Evidence for a single impact at the Cretaceous-Tertiary boundary from trace elements N89-21319
Nitrogen geochemistry of a Cretaceous-Tertiary boundary site in New Zealand N89-21320
The global Cretaceous-Tertiary fire: Biomass or fossil carbon N89-21321
Impact as a general cause of extinction: A feasibility test N89-21374
Periodicity of extinction: A 1988 update N89-21385
Darkness after the K-T impact: Effects of soot N89-21411
Positron line radiation from halo WIMP annihilations as a dark matter signature
[NASA-CR-182918] N89-21635
Supernova 1987A: 18 months later
[NASA-CR-184891] N89-21715
CLARK UNIV., WORCESTER, MA.
A NMR (Nuclear Magnetic Resonance) study of the molecular interactions and dynamic behavior in polymer-diluent blends in the solid state
[AD-A202459] N89-21108
CLARKSON UNIV., POTSDAM, NY.
Performance evaluation of parallel algorithms and architectures in concurrent multiprocessor systems
[AD-A203982] N89-21589
Eigenvectors of graphs
[AD-A203317] N89-21609
COLORADO STATE UNIV., FORT COLLINS.
Molecular jet studies of vdW (van der Waals) clusters and solvation
[AD-A203766] N89-21212
Study of the generation of intense pulsed electron beams using glow discharges
[AD-A202438] N89-21624
Space plasma contractor research, 1988
[NASA-CR-182283] N89-21658
COLORADO UNIV., BOULDER.
Response of marine and freshwater algae to nitric acid and elevated carbon dioxide levels simulating environmental effects of bolide impact N89-21298
Origination, diversity, and extinction metrics essential for analysis of mass biotic crisis events: An example from cretaceous ammonoidea N89-21304
Dynamics of exploding magma chambers: Implications for K-T volcanism and mass extinctions N89-21377
COLUMBIA UNIV., NEW YORK, NY.
Laser enhanced chemical reactions
[DE89-008084] N89-21236
Knowledge representation and planning control in an expert system for the creative design of mechanisms N89-21492
Statistical machine learning for the cognitive selection of nonlinear programming algorithms in engineering design optimization N89-21493
A novel approach to gamma-ray and neutrino astro-particle physics: The GRANDE experiment
[DE89-006515] N89-21725
COMMISSARIAT A L'ENERGIE ATOMIQUE, SACLAY (FRANCE).
Search for the Tunguska event in the Antarctic snow N89-21378
CONNECTICUT UNIV., STORRS.
Structure development during converging flow of a liquid crystal dispersed two-phase fluid
[AD-A203062] N89-21119
CONTINUUM DYNAMICS, INC., PRINCETON, NJ.
Performance optimization for rotors in hover and axial flight
[NASA-CR-177524] N89-20973
CONTROL DYNAMICS CO., HUNTSVILLE, AL.
Active control technique evaluation for spacecraft (ACES)
[AD-A202475] N89-21016
COORDINATING RESEARCH COUNCIL, INC., ATLANTA, GA.
CRC (Coordinating Research Council) hot-start and driveaway driveability program at high and intermediate temperatures using gasoline-alcohol blends
[AD-A202471] N89-21126
CORNELL UNIV., ITHACA, NY.
Lie transforms applied to a nonlinear parametric excitation problem N89-21491
The shear-lag model for a unidirectional composite with viscoelastic matrix N89-21495
A block QR factorization scheme for loosely coupled systems of array processors N89-21519
Nonparamteric estimation from queues arising in staggered entry clinical trials N89-21520

Analytic distribution for charge carriers in a semiconductor dominated by equivalent intervalley scattering
[AD-A202537] N89-21669

CRYSTAL GROWTH AND MATERIALS TESTING ASSOCIATES, LANHAM, MD.
Ceramics
[AD-A202504] N89-21109

D

DARTMOUTH COLL., HANOVER, NH.
Cretaceous-Tertiary findings, paradigms and problems N89-21364

DAYTON UNIV., OH.
Theoretical studies of rare gas halide systems
[AD-A203985] N89-21068
Theoretical studies of potential energy storage molecules
[AD-A203986] N89-21638

DEFENCE RESEARCH ESTABLISHMENT PACIFIC, VICTORIA (BRITISH COLUMBIA).
OSRMS (Ocean Surface Roughness Measurement System): The DREP (Defence Research Establishment Pacific) near-nadir scatterometer
[AD-A202983] N89-21460

DEFENCE RESEARCH ESTABLISHMENT VALCARTIER (QUEBEC).
Propagator matrices in the solution of EMP problems N89-21515

DEFENSE APPLIED INFORMATION TECHNOLOGY CENTER, ALEXANDRIA, VA.
Scientific and Technical Information Network (STINET) and DOD Gateway Information System (DGIS): Reference publications bibliography
[AD-A203926] N89-21704

DEFENSE INTELLIGENCE AGENCY, WASHINGTON, DC.
Bibliography of Soviet laser developments, September-October 1987
[AD-A203366] N89-21232

DEFENSE TECHNICAL INFORMATION CENTER, ALEXANDRIA, VA.
Evaluation of the high temperature materials information analysis center online numeric database
[AD-A202900] N89-21700
Defense technical information center's role in numeric database development
[AD-A202901] N89-21701

DELAWARE UNIV., NEWARK.
Function theory for thin elastic shells
[PB89-101943] N89-21257
Late Eocene impact events recorded in deep-sea sediments N89-21322

DEPARTMENT OF ENERGY, WASHINGTON, DC.
Electric energy systems energy storage
[DE88-007217] N89-21418
Ocean energy program summary. Volume 1, Overview: Fiscal year 1988
[DE89-000858] N89-21421
Geothermal energy program summary: Volume 1: Overview Fiscal Year 1988
[DE89-000864] N89-21422

DETROIT DIESEL ALLISON, INDIANAPOLIS, IN.
High density fuel effects
[AD-A202426] N89-21125

DRAPER (CHARLES STARK) LAB., INC., CAMBRIDGE, MA.
RCS/linear discrete actuator study
[AD-A202822] N89-21028
Advanced information processing system: Local system services
[NASA-CR-181767] N89-21582

E

EASTMAN KODAK CO., ROCHESTER, NY.
Application of a single area array detector for acquistion, tracking and point-ahead in space optical communications
[NASA-CR-183423] N89-21168

EG AND G ENERGY MEASUREMENTS, INC., LOS ALAMOS, NM.
Computer-aided X-ray imaging system design and evaluation
[DE89-006599] N89-21653

EIDGENOESSISCHE TECHNISCHE HOCHSCHULE, ZURICH (SWITZERLAND).
An extended Cretaceous-Tertiary (K/T) stable isotope record. Implications for paleoclimate and the nature of the K/T boundary event N89-21310
Strangelove ocean at era boundaries, terrestrial or extraterrestrial cause N89-21332

EMORY UNIV., ATLANTA, GA.
The spectroscopy and energy transfer kinetics of the interhalogens
[AD-A202954] N89-21059

EOETVOES LORAND UNIV., BUDAPEST (HUNGARY).
Surface energy from order parameter profile: At the QCD phase transition
[NASA-CR-184890] N89-21633

ESSEX CORP., ORLANDO, FL.
Empirical demonstration of isoperformance methodology preparatory of an interactive expert computerized decision aid
[AD-A202439] N89-21545

F

FERMI NATIONAL ACCELERATOR LAB., BATAVIA, IL.
A new class of non-topological solitons
[NASA-CR-184889] N89-21634
Positron line radiation from halo WIMP annihilations as a dark matter signature
[NASA-CR-182918] N89-21635
Supernova 1987A: 18 months later
[NASA-CR-184891] N89-21715
Evolution of cosmic string networks
[NASA-CR-182836] N89-21716

FISH AND WILDLIFE SERVICE, FAIRBANKS, AK.
Satellite telemetry: A new tool for wildlife research and management
[PB88-249255] N89-21013

FLORIDA INST. OF TECH., MELBOURNE.
Electron mobility in mercury cadmium telluride N89-21748

FLORIDA INTERNATIONAL UNIV., MIAMI.
Step-wise extinctions at the Cretaceous-Tertiary boundary and their climatic implications N89-21354

FLORIDA STATE UNIV., TALLAHASSEE.
Catastrophic volcanism as a cause of shocked features found at the K/T boundary and in cryptoexplosion structures N89-21347
Evidence of volcanic ash at a K-T boundary section: Ocean drilling program hole 690 C, Maud Rise, Weddell Sea off East Antarctica N89-21410

FORD MOTOR CO., DEARBORN, MI.
Pre-pilot synthesis of low carbon Si3N4
[DE89-007202] N89-21124

FOREST SERVICE, CORVALLIS, OR.
Proximal ecological effects of the 1980 eruptions of Mount St. Helens N89-21394

FOREST SERVICE, FLAGSTAFF, AZ.
Effects of global atmospheric perturbations on forest ecosystems: Predictions of seasonal and cumulative effects N89-21399

G

GENERAL ACCOUNTING OFFICE, WASHINGTON, DC.
Aviation safety: Measuring how safely individual airlines operate
[GAO/RCED-88-61] N89-20974
Microwave landing systems: Additional systems should not be procured unless benefits proven
[GAO/RCED-88-118] N89-20977
Strategic defense initiative program: Better management direction and controls needed
[GAO/NSIAD-88-26] N89-21694

GENERAL ATOMIC CO., SAN DIEGO, CA.
High-temperature ceramic superconductors
[AD-A202867] N89-21674

GENERAL DYNAMICS CORP., FORT WORTH, TX.
The application of CFD for military aircraft design at transonic speeds N89-20930

GENERAL ELECTRIC CO., PHILADELPHIA, PA.
Development of the domain name system
[AD-A203901] N89-21703

GEO-CENTERS, INC., FORT WASHINGTON, MD.
Surface acoustic wave detection of organophosphorus compounds
[AD-A202909] N89-21058

GEOLOGICAL INST., OSTER VOLDGADE (DENMARK).
Diachronism between extinction time of terrestrial and marine dinosaurs N89-21325

GEOLOGICAL SURVEY, DENVER, CO.
Shocked quartz and more: Impact signatures in K-T boundary clays and claystones N89-21297
The Western North American Cretaceous-Tertiary (K-T) boundary interval and its content of shock-metamorphosed minerals: Implications concerning the K-T boundary impact-extinction theory N89-21334
Catastrophic volcanism N89-21346
Plant microfossil record of the terminal Cretaceous event in the western United States and Canada N89-21363
Late Frasnian mass extinction: Conodont event stratigraphy, global changes, and possible causes N89-21380
The Cretaceous-Tertiary boundary marine extinction and global primary productivity collapse N89-21412

GEOLOGICAL SURVEY, FLAGSTAFF, AZ.
Computer modeling of large asteroid impacts into continental and oceanic sites: Atmospheric, cratering, and ejecta dynamics N89-21379
Asteroid and comet flux in the neighborhood of the earth N89-21387

GEOLOGICAL SURVEY, LANSING, MI.
The Calvin 28 cryptoexplosive disturbance, Cass County, Michigan: Evidence for impact origin N89-21358

GEOLOGICAL SURVEY, VANCOUVER, WA.
Some volcanologic aspects of Columbia River basalt volcanism relevant to the extinction controversy N89-21393

GEOLOGICAL SURVEY OF CANADA, CALGARY (ALBERTA).
A regional perspective on the palynofloral response to K-T boundary event(s) with emphasis on variations imposed by the effects of sedimentary facies and latitude N89-21395

GEOLOGICAL SURVEY OF CANADA, TORONTO (ONTARIO).
The Sudbury Structure (Ontario, Canada) and Vredefort Structure (South Africa): A comparison N89-21311
Geological remote sensing signatures of terrestrial impact craters N89-21317
The Frasnian-Famennian mass killing event(s), methods of identification and evaluation N89-21318

GEORGE MASON UNIV., FAIRFAX, VA.
Rootfinding for Markov chains with quasi-triangular transition matrices
[AD-A202468] N89-21597
A novel approach to gamma-ray and neutrino astro-particle physics: The GRANDE experiment
[DE89-006515] N89-21725

GEORGE WASHINGTON UNIV., WASHINGTON, DC.
Methodology for using steady experimental aerodynamic data to improve steady and unsteady aerodynamic analysis N89-20972

GEORGIA INST. OF TECH., ATLANTA.
Nonlinear rotorcraft analysis-experimental and analytical
[AD-A203967] N89-20990
Inelastic deformation and failure analysis of filament-wound composite structures
[AD-A203382] N89-21044
Deformation modeling and constitutive modeling for anisotropic superalloys
[NASA-CR-4215] N89-21258
Simulation of water vapor condensation on LOX droplet surface using liquid nitrogen N89-21749
Dynamic fatigue testing of Zerodur glass-ceramic N89-21753

GINER, INC., WALTHAM, MA.
Advanced double layer capacitor
[AD-A203059] N89-21181

GRONINGEN RIJKSUNIVERSITEIT (NETHERLANDS).
The GL(2n-1,R) spherical representations of SL(2n,R)
[ZW-8802] N89-21621

GRUMMAN AEROSPACE CORP., BETHPAGE, NY.
Applied transonics at Grumman N89-20931
Method to predict external store carriage loads at transonic speeds N89-20945

H

HAMPTON INST., VA.
Implications of pressure diffusion for shock waves
[NASA-CR-184858] N89-21198

HARRY DIAMOND LABS., ADELPHI, MD.
Rapid backscatter simulation techniques for detailed B-spline target models
[AD-A203260] N89-21163
A rapid-backscatter simulation technique for complex B-spline target models N89-21505

HARVARD-SMITHSONIAN CENTER FOR ASTROPHYSICS, CAMBRIDGE, MA.
Impact, and its implications for geology N89-21353

HARVARD UNIV., CAMBRIDGE, MA.
Organic chemistry in two dimensions: Surface-functionalized polymers and self-assembled monolayer films
[AD-A202955] N89-21118

HAWAII UNIV., HONOLULU.
Implications of asteroid composition for the geochemistry of the ancient terrestrial projectile flux N89-21294
Risk to civilization: A planetary science perspective N89-21302

A novel approach to gamma-ray and neutrino astro-particle physics: The GRANDE experiment
[DE89-006515] N89-21725

HEALTH EFFECTS RESEARCH LAB., RESEARCH TRIANGLE PARK, NC.
Pulmonary function studies in the rat addressing concentration versus time relationships of ozone (O3)
[PB89-129050] N89-21461

HELSINKI UNIV. OF TECHNOLOGY, ESPOO (FINLAND).
Half-solitons in superfluid (3)He-A: Novel pi/2-quanta of phase slippage
[PB89-128904] N89-21664

HIGH TECHNOLOGY CORP., HAMPTON, VA.
Shock-boundary-layer interaction in flight N89-20928

HONEYWELL, INC., BLOOMINGTON, MN.
Development of gallium arsenide high-speed, low-power serial parallel interface modules: Executive summary
[NASA-CR-182272] N89-21173

HOUSTON UNIV., TX.
Numerical solution of parabolic problems in high dimensions N89-21501

HUGHES AIRCRAFT CO., TORRANCE, CA.
High capacity demonstration of honeycomb panel heat pipes
[NASA-CR-181776] N89-21191

I

IBM RESEARCH LAB., SAN JOSE, CA.
An in-situ grazing incidence X-ray scattering study of the initial stages of electrochemical growth of lead on silver (III)
[AD-A203385] N89-21064

IBM WATSON RESEARCH CENTER, YORKTOWN HEIGHTS, NY.
Semantical paradigms: Notes for an invited lecture
[AD-A202995] N89-21565

ILLINOIS UNIV., CHICAGO.
Radiation effect on rocket engine performance N89-21734

ILLINOIS UNIV., URBANA.
Hydrogen segregation to grain boundaries and external surfaces
[AD-A202892] N89-21084
Dimensionality of binary items
[AD-A203238] N89-21608
The interdependencies of theory formation, revision, and experimentation
[AD-A202882] N89-21618
Studies of liquid metal flows and power losses in ducts with moving conducting wall, slanted magnetic field, and applied external electric potential
[AD-A203981] N89-21626

ILLINOIS UNIV., URBANA-CHAMPAIGN.
A comparison of reflector antenna designs for wide-angle scanning
[NASA-TM-101459] N89-21138
Coherent structures in fully developed turbulent pipe flow N89-21195
Objects as closures: Abstract semantics of object oriented languages
[NASA-CR-184877] N89-21540
Half-solitons in superfluid (3)He-A: Novel pi/2-quanta of phase slippage
[PB89-128904] N89-21664

IMATRAN VOIMA OY, HELSINKI (FINLAND).
On-line location of partial discharges in power transformer through acoustic emission
[DE88-757043] N89-21188

INDIANA UNIV., BLOOMINGTON.
Correction of gain and optical throughput variations in a two-dimensional imaging spectrometer
[AD-A203495] N89-21222
The evolution of active galactic nuclei and globular clusters: Multi-component models N89-21720

INSTITUTE FOR COMPUTER APPLICATIONS IN SCIENCE AND ENGINEERING, HAMPTON, VA.
A language comparison for scientific computing on MIMD architectures
[NASA-CR-181779] N89-21537
Parallel solution of sparse one-dimensional dynamic programming problems
[NASA-CR-181812] N89-21542

INSTITUTE FOR DEFENSE ANALYSES, ALEXANDRIA, VA.
Electrolytic protection against high-temperature oxidation
[AD-A203890] N89-21123
Central research project report on superconductivity (1988). Part 1: Materials and IR detectors
[AD-A203891] N89-21681

INSTITUUT TNO VOOR BOUWMATERIALEN EN BOUWCONSTRUCTIES, DELFT (NETHERLANDS).
Numerical and experimental determination of strain (stress) concentration factors of welded joints between square hollow sections
[PB89-131734] N89-21261

INTERNATIONAL CENTRE FOR THEORETICAL PHYSICS, TRIESTE (ITALY).
Contraction of Z(sub 2) graded Lie algebras
[DE88-705356] N89-21596

IOWA STATE UNIV. OF SCIENCE AND TECHNOLOGY, AMES.
Turbulent eddy viscosity modeling in transonic shock/boundary-layer interactions N89-20952
Order statistics and robust inference
[AD-A203440] N89-21616

IOWA UNIV., IOWA CITY.
A laser trap for neutral atoms
[AD-A202581] N89-21229

IWATE UNIV., MORIOKA (JAPAN).
Degradation and crosslinking of perfluoroalkyl polyethers under X-ray irradiation in ultrahigh vacuum
[NASA-TP-2910] N89-21103

J

JET PROPULSION LAB., CALIFORNIA INST. OF TECH., PASADENA.
A comparison of reflector antenna designs for wide-angle scanning
[NASA-TM-101459] N89-21138
Global environmental effects of impact-generated aerosols: Results from a general circulation model N89-21306
The cometary and asteroidal impactor flux at the earth N89-21407

JOHNS HOPKINS UNIV., BALTIMORE, MD.
Optical communication with semiconductor laser diode
[NASA-CR-184817] N89-21141

JOHNS HOPKINS UNIV., LAUREL, MD.
Reentry response of the light weight radioisotope heater unit resulting from a Venus-Earth-Earth gravity assist maneuver accident
[DE89-005359] N89-21024
Spectral characteristics of High Frequency (HF) backscatter for high latitude ionospheric irregularities: Preliminary analysis of statistical properties
[AD-A202998] N89-21156

K

KANSAS UNIV. CENTER FOR RESEARCH, INC., LAWRENCE.
Investigation of a free-tip rotor configuration for research on spanwise life distributions and wake velocity surveys of a semi-span wing with a discontinuous twist
[NASA-CR-184948] N89-20963

KINGS COLL., LONDON (ENGLAND).
Accurate determination of the complex permittivity of biological tissue around 35 GHz
[AD-A202907] N89-21470

KOREA UNIV., SEOUL (SOUTH KOREA).
Sounds in one-dimensional superfluid helium
[AD-A202428] N89-21629

L

LA JOLLA INST., CA.
Imaging of ocean waves by SAR
[AD-A203604] N89-21165

LAMONT-DOHERTY GEOLOGICAL OBSERVATORY, PALISADES, NY.
The Triassic-Jurassic boundary in eastern North America N89-21366
A comprehensive study of the seismotectonics of the eastern Aleutian arc and associated volcanic systems
[DE89-007357] N89-21443

LAWRENCE LIVERMORE NATIONAL LAB., CA.
Initiative for the 21st century: Advanced space power and propulsion based on lasers
[DE89-008034] N89-21031
Measurement of ground state copper density using hook spectroscopy
[DE89-005098] N89-21093
Development and characterization of a fiber optic immuno biosensor
[DE89-005062] N89-21225
Atmospheric effects on laser propagation
[DE89-008645] N89-21237
Global environmental effects of impact-generated aerosols: Results from a general circulation model N89-21306
Review and analysis of the literature in the area of human performance modeling
[DE89-006800] N89-21480
Acoustic damage to large-aperture optics: Revision 1
[DE89-008025] N89-21654
Fusion: A necessary component of US energy policy
[DE89-006234] N89-21659
Lockheed Aeronautical Systems Company technical order transfer tests
[DE89-008092] N89-21707

LITTLE (ARTHUR D.), INC., CAMBRIDGE, MA.
Thermomechanical analysis with phase transformations: A unified approach
[AD-A203383] N89-21692

LOCKHEED AERONAUTICAL SYSTEMS CO., BURBANK, CA.
Transonics and fighter aircraft: Challenges and opportunities for CFD N89-20932

LOCKHEED AERONAUTICAL SYSTEMS CO., MARIETTA, GA.
Computation of aircraft component flow fields at transonic Mach numbers using a three-dimensional Navier-Stokes algorithm N89-20933
Lockheed Aeronautical Systems Company technical order transfer tests
[DE89-008092] N89-21707

LOCKHEED ELECTRONICS CO., PLAINFIELD, NJ.
Reliability/maintainability/testability design for dormancy
[AD-A202704] N89-21179

LOCKHEED MISSILES AND SPACE CO., HUNTSVILLE, AL.
Conjugating binary systems for spacecraft thermal control
[NASA-CR-183608] N89-21023

LOCKHEED MISSILES AND SPACE CO., PALO ALTO, CA.
Mechanisms for the source and loss of electrons
[AD-A203066] N89-21438
Auroral photography experiment
[AD-A203623] N89-21441

LOS ALAMOS NATIONAL LAB., NM.
Shear banding in titanium with controlled elongations at 1 million/sec
[DE89-006555] N89-21094
Nuclear-pumped lasers for large-scale applications
[DE89-006532] N89-21235
Iridium emissions from Hawaiian volcanoes N89-21314
Iridium abundance measurements across bio-event horizons in the geological record N89-21368
Darkness after the K-T impact: Effects of soot N89-21411
Time-of-flight small-angle neutron scattering data reduction and analysis at LANSCE with program SMR
[DE89-006520] N89-21578
Artificial asteroid impact on defensive satellites
[DE89-008407] N89-21620
Atomistic simulations of interfaces in metals and alloys
[DE89-006521] N89-21685
Fermi liquid theory for high temperature superconductors
[DE89-007982] N89-21688
A novel approach to gamma-ray and neutrino astro-particle physics: The GRANDE experiment
[DE89-006515] N89-21725

LOUISIANA STATE UNIV., BATON ROUGE.
How many upper Eocene microspherule layers: More than we thought N89-21327
Evidence for and implications of an Early Archean terrestrial impact record N89-21348
A novel approach to gamma-ray and neutrino astro-particle physics: The GRANDE experiment
[DE89-006515] N89-21725

LOWELL OBSERVATORY, FLAGSTAFF, AZ.
Luminosity variations of stars similar to the sun
[AD-A203864] N89-21713

LOWELL UNIV., MA.
Derivation and testing of computer algorithms for automatic real-time determination of space vehicle potentials in various plasma environments
[AD-A203019] N89-21019
Research on acoustic coupling to electromagnetic pulses in tissue
[AD-A195644] N89-21140

LUNAR AND PLANETARY INST., HOUSTON, TX.
Global Catastrophes in Earth History: An Interdisciplinary Conference on Impacts, Volcanism, and Mass Mortality
[NASA-CR-183329] N89-21287
The cratering record in the inner solar system: Implications for earth N89-21292
Explosive volcanism, shock metamorphism and the K-T boundary N89-21309
Volcanism, global catastrophe and mass mortality N89-21316

Volcanic ash layers in blue ice fields (Beardmore Glacier Area, Antarctica): Iridium enrichments N89-21340
The Kara and Ust-Kara impact structures (USSR) and their relevance to the K/T boundary event N89-21341
Deccan volcanism and K-T boundary signatures N89-21362
K-T impact(s): Continental, oceanic or both N89-21386

M

MANCHESTER UNIV. (ENGLAND).
The 408 MHz radio observations of a quasar sample N89-21714
MARTIN MARIETTA AEROSPACE, DENVER, CO.
Space Propulsion Hazards Analysis Manual (SPHAM), volume 1 [AD-A203204] N89-21029
MARYLAND UNIV., COLLEGE PARK.
Unsteady force calculations on circular cylinders and elliptical airfoils with circulation control [UMAERO-87-37] N89-20962
Stress intensity factors for bodies containing initial stress N89-21263
Optimal and robust memoryless discrimination from dependent observations [AD-A202806] N89-21604
MARYLAND UNIV. BALTIMORE COUNTY, CATONSVILLE.
The solution of the type-problem for N less than or equal to 4 N89-21528
MASSACHUSETTS INST. OF TECH., CAMBRIDGE.
Dilatationally nonlinear elastic materials. Part 2: An example illustrating stress concentration reduction [AD-A202521] N89-21111
Speech recognition: Acoustic-phonetic knowledge acquisition and representation [AD-A203081] N89-21160
Time domain wave propagation in multilayered integrated circuits [AD-A202427] N89-21175
Focused ion beam fabrication of graded channel Field Effect Transistors (FETs) in GaAs and Si [AD-A203365] N89-21184
Modeling robot dynamic performance for endpoint force control [AD-A202881] N89-21251
Dilatationally nonlinear elastic materials. (1): Some theory [AD-A202824] N89-21276
Biospheric traumas caused by large impacts and predicted relics in the sedimentary record N89-21371
The interpretation of crustal dynamics data in terms of plate motions and regional deformation near plate boundaries [NASA-CR-180077] N89-21436
Seeing Ghost solutions in stereo vision [AD-A203581] N89-21473
Optimal design of a two-way conductor N89-21499
A very simple polynomial-time algorithm for linear programming [AD-A202502] N89-21548
Semantical paradigms: Notes for an invited lecture [AD-A202995] N89-21565
Computer-aided fabrication system implementation [AD-A203651] N89-21576
FX-87 performance measurements: Dataflow implementation [AD-A203150] N89-21585
Critical problems in very large scale computer systems [AD-A203299] N89-21586
On random correlation matrices [AD-A202786] N89-21603
An optimal scale for edge detection [AD-A202747] N89-21646
New techniques for high-resolution optical space surveillance [AD-A202785] N89-21647
Grain boundary kinetics. 1: In-situ observations of coupled grain boundary dislocation motion, crystal translation and boundary displacement [DE89-006790] N89-21665
Speech database development [AD-A202461] N89-21699
MASSACHUSETTS INST. OF TECH., LEXINGTON.
Microwave power amplifier analysis and design [AD-A203170] N89-21182
Model-based silhouette recognition [AD-A202540] N89-21552
MASSACHUSETTS UNIV., AMHERST.
SpringNet: A network of multiprocessors for hard real-time [AD-A203348] N89-21587
MAX-PLANCK-INST. FUER CHEMIE, MAINZ (GERMANY, F.R.).
Mineralogy and phase-chemistry of the Cretaceous/Tertiary section in the Lattengebirge, Bavarian Alps N89-21323
Acute effects of a large bolide impact simulated by a global atmospheric circulation model N89-21398
MAYO CLINIC, ROCHESTER, MN.
G-induced loss of consciousness and its prevention [AD-A202960] N89-21471
MCDONNELL AIRCRAFT CO., SAINT LOUIS, MO.
Transonic propulsion system integration analysis at McDonnell Aircraft Company N89-20943
MCDONNELL-DOUGLAS RESEARCH LABS., SAINT LOUIS, MO.
Euler/Navier-Stokes calculations of transonic flow past fixed- and rotary-wing aircraft configurations N89-20948
MCMASTER UNIV., HAMILTON (ONTARIO).
Noble metals in mid-ocean ridge volcanism: A significant fractionation of gold with respect to platinum group metals N89-21307
Iridium, shocked minerals, and trace elements across the Cretaceous/Tertiary boundary at Maud Rise, Wedell Sea, and Walvis Ridge, South Atlantic Ocean N89-21333
MECHANICAL TECHNOLOGY, INC., LATHAM, NY.
Advanced helium purge seals for Liquid Oxygen (LOX) turbopumps [NASA-CR-182105] N89-21239
MEMPHIS STATE UNIV., TN.
Construction of an alternating gradient magnetometer N89-21739
MESOSCALE ENVIRONMENTAL SIMULATIONS, INC., HAMPTON, VA.
Operational implications of a cloud model simulation of space shuttle exhaust clouds in different atmospheric conditions [NASA-CR-4222] N89-21425
A cloud model simulation of space shuttle exhaust clouds in different atmospheric conditions [NASA-CR-4223] N89-21426
MIAMI UNIV., FL.
Neotectonics in Central Mexico from LANDSAT TM data [NASA-CR-183416] N89-21416
MICHIGAN STATE UNIV., EAST LANSING.
Whole field measurements of vorticity in turbulent and unsteady flows [AD-A203349] N89-21209
MICHIGAN UNIV., ANN ARBOR.
Euler solvers for transonic applications N89-20935
An embedded mesh procedure for leading-edge vortex flows N89-20936
Asymptotic methods for internal transonic flows N89-20937
Turbulence modulation and dense-spray structure [AD-A202449] N89-21201
Inducement of heterochronic variation in a species of planktic foraminifera by a Late Eocene impact event N89-21351
MIDWEST RESEARCH INST., GOLDEN, CO.
Wind energy program summary. Volume 1, Overview: Fiscal year 1988 [DE89-000856] N89-21420
MILITARY ACADEMY, WEST POINT, NY.
Knot selection for least squares approximation using thin plate splines N89-21504
A posteriori error estimation of adaptive finite difference schemes for hyperbolic systems N89-21513
MINNESOTA UNIV., MINNEAPOLIS.
Biostratigraphic case studies of six major extinctions N89-21390
Numerical studies of gas flow in spiral galaxies N89-21718
MISSISSIPPI STATE UNIV., MISSISSIPPI STATE.
Guidance for an aeroassisted orbital transfer vehicle N89-21740
Optimization of large matrix calculations for execution on the Cray X-MP vector supercomputer N89-21742
Angular response calibration of the burst and transient source experiment N89-21745
MISSISSIPPI UNIV., UNIVERSITY.
A continued study of optical sound generation and amplification [AD-A202484] N89-21630
MITRE CORP., BEDFORD, MA.
SURVNET user's manual [AD-A203372] N89-21164
MOSCOW STATE UNIV. (USSR).
Isotopic investigations in the area of the Tunguska catastrophe in 1908 year N89-21342
The Karskiy craters are the probable records of catastrophe at the Cretaceous-Tertiary boundary N89-21343
MSNW, INC., SAN MARCOS, CA.
Chemical vapor synthesis of niobium aluminides [AD-A202591] N89-21055
MURPHYS CENTER OF PLANETOLOGY, CA.
Oblique impacts: Catastrophic vs. protracted effects N89-21383

N

NATIONAL AERONAUTICAL ESTABLISHMENT, OTTAWA (ONTARIO).
An experimental study of transonic buffet of a supercritical airfoil with trailing edge flap [AD-A203189] N89-20968
NATIONAL AERONAUTICS AND SPACE ADMINISTRATION, WASHINGTON, DC.
NASA directions in space propulsion for 2000 and beyond [NASA-TM-102281] N89-21026
Aerospace medicine and biology: A continuing bibliography with indexes (supplement 321) [NASA-SP-7011(321)] N89-21475
Aerospace medicine and biology: A continuing bibliography with indexes (supplement 322) [NASA-SP-7011(322)] N89-21476
Research and technology objectives and plans summary, fiscal year 1987 [NASA-TM-89241] N89-21761
NATIONAL AERONAUTICS AND SPACE ADMINISTRATION. AMES RESEARCH CENTER, MOFFETT FIELD, CA.
Aerodynamic analysis of three advanced configurations using the TranAir full-potential code N89-20944
Navier-Stokes and viscous-inviscid interaction N89-20949
Turbulence and modeling in transonic flow N89-20951
Three-dimensional singular points in aerodynamics [NASA-TM-100045] N89-20964
AH-1S communication switch integration program [NASA-TM-101053] N89-20978
Simulation at Dryden Flight Research Facility from 1957 to 1982 [NASA-TM-101695] N89-20983
Computational studies of an impulsively started viscous flow [NASA-TM-101037] N89-21190
Impact production of NO and reduced species N89-21413
Helicopter flights with night-vision goggles: Human factors aspects [NASA-TM-101039] N89-21477
Application of the Laplace-Borel transformation to the representation of analytical solutions of Duffing's equation [NASA-TM-100058] N89-21532
DATAMAP upgrade version 4.0 [NASA-TM-100993] N89-21541
NATIONAL AERONAUTICS AND SPACE ADMINISTRATION. GODDARD SPACE FLIGHT CENTER, GREENBELT, MD.
Geological remote sensing signatures of terrestrial impact craters N89-21317
Flood basalt eruptions, comet showers, and mass extinction events N89-21372
Relationships of earthquakes (and earthquake-associated mass movements) and polar motion as determined by Kalman filtered, Very-Long-Baseline-Interferometry [NASA-TM-100711] N89-21430
On principles, methods and recent advances in studies towards a GPS-based control system for geodesy and geodynamics [NASA-TM-100716] N89-21434
ER-2 lidar observations from the October 1986 fire cirrus experiment [NASA-TM-100704] N89-21444
The seasonal cycle of energetics from the GLAS/UMD climate GCM [NASA-TM-100714] N89-21448
NATIONAL AERONAUTICS AND SPACE ADMINISTRATION. HUGH L. DRYDEN FLIGHT RESEARCH FACILITY, EDWARDS, CA.
Flight research and testing N89-20927
NATIONAL AERONAUTICS AND SPACE ADMINISTRATION. LYNDON B. JOHNSON SPACE CENTER, HOUSTON, TX.
Saccadic eye movement during spaceflight [NASA-TM-100475] N89-21463
NATIONAL AERONAUTICS AND SPACE ADMINISTRATION. LANGLEY RESEARCH CENTER, HAMPTON, VA.
Transonic Symposium: Theory, Application, and Experiment, Volume 1, Part 1 [NASA-CP-3020-VOL-1-PT-1] N89-20925

Airframe/propulsion integration characteristics at transonic speeds N89-20926
Generation of unstructured grids and Euler solutions for complex geometries N89-20941
Transonic Symposium: Theory, Application, and Experiment, volume 1, part 2
[NASA-CP-3020-VOL-1-PT-2] N89-20942
Steady and unsteady transonic small disturbance analysis of realistic aircraft configurations N89-20946
Inverse wing design in transonic flow including viscous interaction N89-20947
The 3-D Euler and Navier-Stokes calculations for aircraft components N89-20950
Test techniques: A survey paper on cryogenic tunnels, adaptive wall test sections, and magnetic suspension and balance systems N89-20955
Instrumentation advances for transonic testing N89-20957
Wall interference assessment and corrections N89-20958
Comparison of airfoil results from an adaptive wall test section and a porous wall test section N89-20960
Capabilities of wind tunnels with two-adaptive walls to minimize boundary interference in 3-D model testing N89-20961
Integrated aerodynamic/dynamic optimization of helicopter rotor blades
[NASA-TM-101553] N89-20982
Aeroelastic modeling for the FIT team F/A-18 simulation
[NASA-TM-101569] N89-20991
Effect of geometry on thermal aging behavior of Celion/LARC-160 composites
[NASA-TM-100496] N89-21047
A magnetic bearing control approach using flux feedback
[NASA-TM-100672] N89-21135
Analytical model of a five degree of freedom magnetic suspension and positioning system
[NASA-TM-100671] N89-21136
A review of reaction rates and thermodynamic and transport properties for the 11-species air model for chemical and thermal nonequilibrium calculations to 30000 K
[NASA-TM-101528] N89-21193
Nonlinear shell analyses of the space shuttle solid rocket boosters
[NASA-TM-101546] N89-21260
The Environment for Application Software Integration and Execution (EASIE) version 1.0. Volume 1: Executive overview
[NASA-TM-100573] N89-21538
An intelligent advisor for the design manager
[NASA-TM-101558] N89-21539
Optical fiber sensors and signal processing for intelligent structure monitoring
[NASA-CR-184841] N89-21640

NATIONAL AERONAUTICS AND SPACE ADMINISTRATION. LEWIS RESEARCH CENTER, CLEVELAND, OH.

An LDA (Laser-Doppler Anemometry) investigation of three-dimensional normal shock wave boundary-layer interactions N89-20958
A real-time simulator of a turbofan engine
[NASA-TM-100669] N89-20995
A compendium of controlled diffusion blades generated by an automated inverse design procedure
[NASA-TM-101968] N89-20996
Flowfield measurements in the NASA Lewis Research Center 9- by 15-foot low-speed wind tunnel
[NASA-TM-100883] N89-21002
Three dimensional thermal analysis of rocket thrust chambers
[NASA-TM-101973] N89-21025
Convection and chemistry effects in CVD: A 3-D analysis for silicon deposition
[NASA-TM-102001] N89-21032
Fuel-rich catalytic combustion of Jet-A fuel-equivalence ratios 5.0 to 8.0
[NASA-TM-101975] N89-21051
Evaluation of atomic oxygen resistant protective coatings for fiberglass-epoxy composites in LEO
[NASA-TM-101955] N89-21100
Degradation and crosslinking of perfluoroalkyl polyethers under X-ray irradiation in ultrahigh vacuum
[NASA-TP-2910] N89-21103
Simulation of the low earth orbital atomic oxygen interaction with materials by means of an oxygen ion beam
[NASA-TM-101971] N89-21104
A comparison of reflector antenna designs for wide-angle scanning
[NASA-TM-101459] N89-21138
External electro-optic probing of millimeter-wave integrated circuits
[NASA-TM-101990] N89-21142
Analytical and experimental procedures for determining propagation characteristics of millimeter-wave gallium arsenide microstrip lines
[NASA-TP-2899] N89-21169
Design, fabrication, and performance of brazed, graphite electrode, multistage depressed collectors with 500-W, continuous wave, 4.8- to 9.6-GHz traveling-wave tubes
[NASA-TP-2904] N89-21171
Channelized coplanar waveguide: Discontinuities, junctions, and propagation characteristics
[NASA-TM-101483] N89-21172
Restrictive loads powered by separate or by common electrical sources
[NASA-TM-102008] N89-21174
Numerical computation of shock wave-turbulent boundary layer interaction in transonic flow over an axisymmetric curved hill
[NASA-TM-101473] N89-21192
On the conditions for resonance interactions of instability waves in the axisymmetric jet
[NASA-TM-101477] N89-21196
The response of a laminar boundary layer in supersonic flow to small amplitude progressive waves
[NASA-TM-101965] N89-21197
Infrared surface temperature measurements for the surface tension driven convection experiment
[NASA-TM-101353] N89-21224
Comparison study of gear dynamic computer programs at NASA Lewis Research Center
[NASA-TP-2901] N89-21243
Modal analysis of gear housing and mounts
[NASA-TM-101445] N89-21244
Investigation of Weibull statistics in fracture analysis of cast aluminum
[NASA-TM-102000] N89-21245
Characterization of structural connections using free and forced response test data
[NASA-TM-101991] N89-21266
Gas turbine alternative fuels combustion characteristics
[NASA-TM-101470] N89-21417
Cryogenic reactant storage for lunar base regenerative fuel cells
[NASA-TM-101980] N89-21419
Institute for Computational Mechanics in Propulsion (ICOMP)
[NASA-TM-101961] N89-21595
Comparison of propeller cruise noise data taken in the NASA Lewis 8- by 6-foot wind tunnel with other tunnel and flight data
[NASA-TM-101976] N89-21628

NATIONAL AERONAUTICS AND SPACE ADMINISTRATION. MARSHALL SPACE FLIGHT CENTER, HUNTSVILLE, AL.

Oblique hypervelocity impact response of dual-sheet structures
[NASA-TM-100358] N89-21246
NASA Marshall Space Flight Center solar observatory report, January - December 1987
[NASA-TM-100360] N89-21712

NATIONAL BUREAU OF STANDARDS, GAITHERSBURG, MD.

The global Cretaceous-Tertiary fire: Biomass or fossil carbon N89-21321

NATIONAL CENTER FOR ATMOSPHERIC RESEARCH, BOULDER, CO.

Thermopile temperature sensitivity calibration procedure for Eppley broadband radiometers
[PB89-104129] N89-21215
Response of marine and freshwater algae to nitric acid and elevated carbon dioxide levels simulating environmental effects of bolide impact N89-21298
Widespread habitat change through paludification as an interactive mechanism in mass extinction events N89-21339
Multi-year global climatic effects of atmospheric dust from large bolide impacts N89-21397
Acute effects of a large bolide impact simulated by a global atmospheric circulation model N89-21398
A 3-dimensional numerical simulation of the atmospheric injection of aerosols by a hypothetical basaltic fissure eruption N89-21401
Flux and sounding data from the NCAR (National Center for Atmospheric Research) King Air aircraft during HAPEX (hydrologic atmospheric pilot experiment)
[PB89-124481] N89-21433
CCM (Community Climate Model)
[PB89-120927] N89-21446
Coupled dynamical-radiational model of stratocumulus and its applications
[PB89-104137] N89-21447
New picture for the internal rotation of the sun
[PB89-113377] N89-21723

NATIONAL CLIMATE PROGRAM OFFICE, ROCKVILLE, MD.

National Climate Program
[PB89-118608] N89-21445

NATIONAL GEOPHYSICAL DATA CENTER, BOULDER, CO.

Solar-geophysical data number 529, September 1988. Part 1: (Prompt reports). Data for August, July 1988 and late data
[PB89-121305] N89-21431
Solar-geophysical data number 529, September 1988. Part 2: (Comprehensive reports). Data for March 1988
[PB89-121313] N89-21432
Solar-geophysical data number 528, August 1988. Part 2: (Comprehensive reports). Data for February 1988
[PB89-109912] N89-21722

NATIONAL INST. OF STANDARDS AND TECHNOLOGY, GAITHERSBURG, MD.

Study of the ignition inhibiting properties of compressed air foam
[PB89-127559] N89-21049
XRAYL: A powder diffraction profile refinement program
[PB89-127567] N89-21050
Center for Electronics and Electrical Engineering technical progress bulletin covering center programs, April to June 1988 with 1988 CEEE events calendar
[PB89-123137] N89-21170
Manipulator primitive level task decomposition
[PB89-133532] N89-21238
Center for Atomic, Molecular and Optical Physics technical activities, 1988
[PB89-132302] N89-21623

NATIONAL OCEANIC AND ATMOSPHERIC ADMINISTRATION, WASHINGTON, DC.

Ice cover on Chesapeake Bay from AVHRR (Advanced Very High Resolution Radiometer) and LANDSAT imagery, winter of 1987-88
[PB89-117261] N89-21415

NATIONAL SCIENCE FOUNDATION, WASHINGTON, DC.

The impact of mass extinctions N89-21315

NAVAL AIR DEVELOPMENT CENTER, WARMINSTER, PA.

High temperature composites using Schiff's base pyropolymer matrices
[AD-A203311] N89-21043
The microstructural and phase characterization of RST Al-Ti-X alloys
[AD-A203734] N89-21092

NAVAL CIVIL ENGINEERING LAB., PORT HUENEME, CA.

Experimental examination of the aerothermal performance of the T-10 test cell at NAS (Naval Air Station), Cubi Point
[AD-A203887] N89-21005

NAVAL ENVIRONMENTAL PREDICTION RESEARCH FACILITY, MONTEREY, CA.

Icing considerations for HALE (High Altitude, Long Endurance) aircraft
[AD-A202584] N89-20975

NAVAL OCEAN SYSTEMS CENTER, SAN DIEGO, CA.

Utility of a dual-lidar method to measure integrated extinction
[AD-A203145] N89-21439
GRAPS (Graphical Plotting System) user's guide. A graphical plotting system for displaying scientific and engineering data
[AD-A202583] N89-21559
Infrared sea-radiance modeling using LOWTRAN 6
[AD-A202582] N89-21643

NAVAL OCEANOGRAPHY COMMAND DETACHMENT, ASHEVILLE, NC.

Summary of Meteorological Observations, Surface (SMOS) for Moffett Field, California
[AD-A203628] N89-21451

NAVAL POSTGRADUATE SCHOOL, MONTEREY, CA.

Holographic particle sizing in solid fuel ramjets
[AD-A202699] N89-20997
Automatic measurement of particles from holograms taken in the combustion chamber of a rocket motor
[AD-A203955] N89-21030
Holographic investigation of solid propellant combustion
[AD-A203928] N89-21067
Implementation and testing of a new 16-PSK transmitter
[AD-A203936] N89-21166
Analytical and experimental investigation of constrained viscoelastic layer damping for a plate and shell model
[AD-A202698] N89-21273
A triangular thin shell element for the linear analysis of stiffened composite structures
[AD-A202864] N89-21277
Satellite signatures of rapid cyclogenesis
[AD-A203934] N89-21452

A randomness property of m-sequences N89-21524
Root placement with transfer function methods (full state feedback)
[AD-A203877] N89-21610

NAVAL RESEARCH LAB., WASHINGTON, DC.
Generation of unstructured grids and Euler solutions for complex geometries N89-20941
A cancellation technique for reducing background noise within turbulent flow environments characterized by pipes and annuli
[AD-A202924] N89-21206
Transformations of Gaussian light beams caused by reflection in FEL (Free Electron Lasers) resonators
[AD-A202472] N89-21227
Immunoassay procedures for fiber optic sensors
[AD-A203069] N89-21649
Film elastic properties determined by the indentation test-theoretical considerations
[AD-A203997] N89-21683

NAVAL SHIP RESEARCH AND DEVELOPMENT CENTER, BETHESDA, MD.
Potential flow evaluation of the interference effect of strut-through-appendage-tip model mounting technique and reduction of the effect using blowing and suction
[AD-A202424] N89-21199
Radio-controlled model gyro measurement study
[AD-A204002] N89-21223
Studies of liquid metal flows and power losses in ducts with moving conducting wall, slanted magnetic field, and applied external electric potential
[AD-A203981] N89-21626

NAVY CLOTHING AND TEXTILE RESEARCH FACILITY, NATICK, MA.
Thermal protection afforded by two anti-exposure coveralls when worn in cold water
[AD-A202865] N89-21485

NAVY PERSONNEL RESEARCH AND DEVELOPMENT CENTER, SAN DIEGO, CA.
Brain activity during tactical decision-making. Part 5: A cross-study validation of evoked potentials as indices of workload
[AD-A203763] N89-21474

NEVADA UNIV., LAS VEGAS.
Grasp: A graph specification language
[AD-A202524] N89-21550

NEW MEXICO UNIV., ALBUQUERQUE.
Proterozoic Bushveld-Vredefort catastrophe: Possible causes and consequences N89-21312

NEW YORK STATE DEPT. OF HEALTH, ALBANY.
Deccan volcanism and K-T boundary signatures N89-21362

NEW YORK UNIV., NEW YORK.
Computational techniques for shock wave diffraction problems
[AD-A203439] N89-21210
Ocean alkalinity and the Cretaceous/Tertiary boundary N89-21300
Flood basalt eruptions, comet showers, and mass extinction events N89-21372
Climatic changes resulting from mass extinctions at the K-T boundary (and other bio-events) N89-21373
The numerical simulation of Richtmyer-Meshkov unstable interfaces: A conference report N89-21512
The interaction of nonlinear hyperbolic waves: A conference report N89-21530
Domain modeling for language analysis
[AD-A203444] N89-21574

NORDISK INST. FOR TEORETISK ATOMFYSIK, COPENHAGEN (DENMARK).
Half-solitons in superfluid (3)He-A: Novel pi/2-quanta of phase slippage
[PB89-128904] N89-21664

NORTH CAROLINA AGRICULTURAL AND TECHNICAL STATE UNIV., GREENSBORO.
Computer codes for thermal analysis of a solid rocket motor nozzle N89-21733

NORTH CAROLINA STATE UNIV., RALEIGH.
Continued development and characterization of doped layers, contacts and associated electronic devices in silicon carbide
[AD-A202450] N89-21176

NORTH STAFFORDSHIRE POLYTECHNIC, STAFFORD (ENGLAND).
Vibration control in rotating machinery using variable dynamic stiffness squeeze-films
[AD-A202902] N89-21252

NORTH TEXAS STATE UNIV., DENTON.
Two photon characterization
[AD-A203355] N89-21678

NORTHEAST RADIO OBSERVATORY CORP., WESTFORD, MASS. HAYSTACK OBSERVATORY.
Observations of neutral circulation at mid-latitudes during the Equinox Transition Study
[NASA-CR-184792] N89-21429

NORTHROP SERVICES, INC., RESEARCH TRIANGLE PARK, NC.
Pulmonary function studies in the rat addressing concentration versus time relationships of ozone (O3)
[PB89-129050] N89-21461

NORTHWESTERN POLYTECHNICAL UNIV., XIAN (CHINA).
Dynamic structural optimization and experiment
[PB89-111462] N89-21259

O

OAK RIDGE GASEOUS DIFFUSION PLANT, TN.
The causality horizon and parallel processing for simulations with wide geographical dispersions
[DE89-008484] N89-21590

OAK RIDGE NATIONAL LAB., TN.
Structural energy differences in Al3Ti: The role of tetragonal distortion in APB and twin energies
[DE89-007210] N89-21096
Evaluation of time delay requirements for closed-loop stability using classical and modern methods
[DE89-006417] N89-21189
An individual-based forest ecosystems model for projecting forest response to nutrient cycling and climate changes
[DE89-007212] N89-21428
Structure maps and phase stability in AlTi3 alloyed with rare-earth elements
[DE89-005106] N89-21684
Automated library systems and document tracking systems: Commercial software alternatives, volume 1
[DE89-007716] N89-21706

OHIO STATE UNIV., COLUMBUS.
Diffusion welding of an RS/PM aluminum alloy N89-21241
Downward continuation of the free-air gravity anomalies to the ellipsoid using the gradient solution, Poisson's integral and terrain correction-numerical comparison and computations
[AD-A203739] N89-21442

OHIO UNIV., ATHENS.
Investigation of practical applications of H infinity control theory to the design of control systems for large space structures N89-21743

OKLAHOMA STATE UNIV., STILLWATER.
Theoretical studies of heterogeneous reactions in silicon CVD (Silicon Vapor Deposition) catalysis
[AD-A202905] N89-21057

OLD DOMINION UNIV., NORFOLK, VA.
Secondary three-dimensional instability in compressible boundary layers N89-20954

OPEN UNIV., MILTON (ENGLAND).
Nitrogen geochemistry of a Cretaceous-Tertiary boundary site in New Zealand N89-21320

OREGON UNIV., EUGENE.
Reconstruction of binocular depth across continuous surfaces
[AD-A202827] N89-21469

OTTAWA UNIV. (ONTARIO).
Mass killings and detection of impacts N89-21356

OXFORD UNIV. (ENGLAND).
An optical study of three transient X-ray sources N89-21724

P

PACIFIC NORTHWEST LABS., RICHLAND, WA.
Air quality and forest health issues in the 1990s
[DE89-006941] N89-21427
A simple model for wind field estimation in complex terrain
[DE89-007240] N89-21457
Rotationally sampled wind characteristics for several rotor sizes using laser anemometer measurements
[DE89-007942] N89-21458
Applications, dosimetry and biological interactions of static and time-varying magnetic fields
[DE89-006944] N89-21627
Thermal and dynamic analysis of the RING (Radiatively-cooled, Inertially-driven Nuclear Generator) power system radiator
[DE89-007236] N89-21639

PARIS VI UNIV. (FRANCE).
Deccan volcanism at the Cretaceous-Tertiary boundary N89-21305

PENNSYLVANIA STATE UNIV., UNIVERSITY PARK.
The effect of platinum catalysts on propane oxidation at elevated pressure
[AD-A202999] N89-21060
High temperature oxidation and electrochemical studies related to hot corrosion
[AD-A203038] N89-21085
Synthesis of ceramics at low temperatures N89-21102
Surface chemistry and structural effects in the stress corrosion of glass and ceramic materials
[AD-A202452] N89-21107
Magnetic flowmeter measurement of solid propellant pressure-coupled and velocity-coupled responses
[AD-A203988] N89-21133
Combined VHF Dopplar radar and airborne (CV-990) measurements of atmospheric winds on the mesoscale
[NASA-CR-184953] N89-21449

PENNSYLVANIA UNIV., PHILADELPHIA.
Magnetic reversal spurts: Rain gauges for comet showers N89-21349

PHOTOMETRICS, INC., WOBURN, MA.
Excitation and diagnostics of optical contamination in the spacecraft environment
[AD-A202429] N89-21015

PHYSICAL RESEARCH LAB., AHMEDABAD (INDIA).
Geochemistry of K/T boundaries in India and contributions of Deccan volcanism N89-21296
Selective extinction of marine plankton at the end of the Mesozoic era: The fossil and stable isotope record N89-21329

PITTSBURGH UNIV., PA.
Flow reactor studies of elementary radical reaction rates
[AD-A203126] N89-21062
Organic functional group reactivities at metal surfaces
[AD-A203094] N89-21086
Computer simulation of a pilot in V/STOL aircraft control loops
[NASA-CR-184815] N89-21479

POLYTECHNIC UNIV., FARMINGDALE, NY.
The role of hydromagnetic waves in the magnetosphere and the ionosphere
[AD-A202800] N89-21437

PRC KENTRON, INC., HAMPTON, VA.
Fracture characteristics of balloon films
[NASA-CR-181686] N89-21099

PRETORIA UNIV. (SOUTH AFRICA).
Proterozoic Bushveld-Vredefort catastrophe: Possible causes and consequences N89-21312

PRINCETON UNIV., NJ.
Developments and trends in three-dimensional mesh generation N89-20940
Fuels combustion research
[AD-A204161] N89-21071
A robust adaptive array structure using the soft constrained LMS algorithm
[AD-A203959] N89-21167
Soft constrained LMS algorithms: A robust procedure for signal misalignment
[AD-A203880] N89-21187
An extended Cretaceous-Tertiary (K/T) stable isotope record. Implications for paleoclimate and the nature of the K/T boundary event N89-21310
High resolution chronology of late Cretaceous-early Tertiary events determined from 21,000 yr orbital-climatic cycles in marine sediments N89-21328
Extended period of K/T boundary mass extinction in the marine realm N89-21337
Faunal and erosional events in the Eastern Tethyan Sea across the K/T boundary N89-21338
Flood basalts and mass extinctions N89-21360

PURDUE UNIV., INDIANAPOLIS, IN.
Modelling of the lean flammability limit in flame theory N89-21527

PURDUE UNIV., WEST LAFAYETTE, IN.
Actuation constraints in multivariable flight control systems N89-20998
Information acquisition for model construction: An integrative, decision-theoretic perspective N89-21705
A novel approach to gamma-ray and neutrino astro-particle physics: The GRANDE experiment
[DE89-006515] N89-21725

R

RENSSELAER POLYTECHNIC INST., TROY, NY.
Wave drag due to lift for transonic airplanes N89-20938
An adaptive overlapping local grid refinement method for two-dimensional parabolic systems N89-21514

RHODE ISLAND UNIV., KINGSTON.
Rocks, resolution, and the record at the terrestrial K/T boundary, eastern Montana and western North Dakota N89-21313
Assessment of the atmospheric impact of volcanic eruptions N89-21388

RHODE ISLAND UNIV., NARRAGANSETT.
The Cretaceous-Tertiary boundary marine extinction and global primary productivity collapse N89-21412

ROCHESTER UNIV., NY.
Optoelectronic workshops. Part 4: Liquid Crystals for Laser Applications
[AD-A202526] N89-21228
The Rochester robot
[AD-A202633] N89-21247
Peripheral limitations on spatial vision
[AD-A203388] N89-21472
Computer modeling and simulation in inertial confinement fusion
[DE89-008304] N89-21681
ROCKWELL INTERNATIONAL CORP., CANOGA PARK, CA.
Advanced single crystal for SSME turbopumps
[NASA-CR-182244] N89-21072
ROCKWELL INTERNATIONAL CORP., LOS ANGELES, CA.
Transonic aerodynamic design experience N89-20934
ROCKWELL INTERNATIONAL SCIENCE CENTER, THOUSAND OAKS, CA.
Electron paramagnetic resonance and photoluminescence studies of impurities in CdTe
[AD-A202841] N89-21056
Further studies of the HRR field of a moving crack. An experimental analysis
[AD-A202545] N89-21269
ROYAL AIRCRAFT ESTABLISHMENT, FARNBOROUGH (ENGLAND).
The use of primers in the adhesive bonding of carbon-fibre reinforced composites
[AD-A202542] N89-21039
Calculation of the glass transition temperatures of linear polymers. Part 3: Evaluation of calculation relationships
[AD-A203357] N89-21122
ROYAL HOLLOWAY AND BEDFORD NEW COLL., EGHAM (ENGLAND).
Dielectric spectroscopy of semiconductors
[AD-A203457] N89-21679
ROYAL SIGNALS AND RADAR ESTABLISHMENT, MALVERN (ENGLAND).
A theoretical and experimental investigation of linear and nonlinear focussing chirped optical diffraction gratings
[AD-A203396] N89-21650

S

SAARLAND UNIV., SAARBRUCKEN (GERMANY, F.R.).
Martensitic phase transitions in nanocrystalline materials
[AD-A203636] N89-21090
SAINT LAWRENCE UNIV., CANTON, NY.
Cathodoluminescence of shocked quartz at the Cretaceous-Tertiary boundary N89-21369
SAN DIEGO STATE UNIV., CA.
Prepolymer characterization
[AD-A202821] N89-21115
SANDIA NATIONAL LABS., ALBUQUERQUE, NM.
Shock-induced chemical synthesis of intermetallic compounds
[DE89-007035] N89-21095
A model for interface temperatures induced by convection heat transfer in porous materials
[DE89-008202] N89-21214
The potential of GaAs-based mechanically stacked multijunction solar concentrator cells
[DE89-007975] N89-21423
Essential elements in the numerical modeling of solar cells
[DE89-008113] N89-21424
Time-discretized moments of a randomly excited uncertain linear oscillator
[DE89-008318] N89-21614
Migration strategies roles for data management in CIM
[DE89-008112] N89-21708
WhiteStar project engineering component selection database
[DE89-008321] N89-21709
SCIENCE APPLICATIONS INTERNATIONAL CORP., SAN DIEGO, CA.
Evaluation of aerosol size distribution models
[AD-A202736] N89-21645
SCRIPPS INSTITUTION OF OCEANOGRAPHY, LA JOLLA, CA.
Localizing and beamforming freely-drifting VLF (Very Low Frequency) acoustic sensors
[AD-A202638] N89-21217
Seawater strontium isotopes at the Cretaceous-Tertiary boundary N89-21350
SCRIPPS INSTITUTION OF OCEANOGRAPHY, SAN DIEGO, CA.
Confidence set inference with a prior quadratic bound
[NASA-CR-184839] N89-21435
SINGER CO., WAYNE, NJ.
Image processing language, phase 2
[AD-A203994] N89-21577
SMITH-KETTLEWELL INST. OF VISUAL SCIENCES, SAN FRANCISCO, CA.
Psychophysical studies of visual cortical functions
[AD-A202814] N89-21468
SMITHSONIAN INSTITUTION, WASHINGTON, DC.
Volcanoes and global catastrophes N89-21389
SOLAR SYSTEM ASSOCIATES, DES MOINES, IA.
The Manson impact structure, a possible site for a Cretaceous-Tertiary (K-T) boundary impact N89-21326
SOUTH CAROLINA UNIV., COLUMBIA.
Small expendable deployer system measurement analysis N89-21731
SOUTHAMPTON UNIV. (ENGLAND).
Evidence of volcanic ash at a K-T boundary section: Ocean drilling program hole 690 C, Maud Rise, Weddell Sea off East Antarctica N89-21410
SOUTHWEST RESEARCH INST., SAN ANTONIO, TX.
Fouling tests of AGT-1500 gas turbine fuel nozzles
[AD-A203360] N89-21253
SPACE ENVIRONMENT SERVICES CENTER, BOULDER, CO.
SESC (Space Environment Services Center) glossary of solar-terrestrial terms, 2nd edition
[PB89-120802] N89-21698
ST SYSTEMS CORP., HAMPTON, VA.
Operational implications of a cloud model simulation of space shuttle exhaust clouds in different atmospheric conditions
[NASA-CR-4222] N89-21425
A cloud model simulation of space shuttle exhaust clouds in different atmospheric conditions
[NASA-CR-4223] N89-21426
STANFORD LINEAR ACCELERATOR CENTER, CA.
A new class of non-topological solitons
[NASA-CR-184889] N89-21634
STANFORD UNIV., CA.
Numerical simulation of the flow field over delta wings with leading edge blowing N89-20924
Advanced diagnostics for reacting flows
[AD-A202451] N89-21202
Experiments in end-point control of manipulators with elastic drives N89-21240
Evidence for and implications of an Early Archean terrestrial impact record N89-21348
Impact production of NO and reduced species N89-21413
Deductive programming
[AD-A202489] N89-21546
TABLOG: The deductive tableau programming language
[AD-A202490] N89-21547
Optical computing research
[AD-A202963] N89-21564
A new class of non-topological solitons
[NASA-CR-184889] N89-21634
Investigation of Schottky barrier on GaAs and InP using a multidisciplined approach
[AD-A202953] N89-21675
Acquiring generalizations to organize human databases
[AD-A202964] N89-21702
Force-free magnetic fields: Is there a loss of equilibrium
[AD-A203030] N89-21717
STATE SEISMOLOGICAL BUREAU OF CHINA, BEIJING.
New approach to the origin of the tektite in China N89-21414
STATE UNIV. OF NEW YORK, ALBANY.
Theoretical studies of the chemistry and physics of oxygen in silicon
[AD-A203168] N89-21063
The Kara and Ust-Kara impact structures (USSR) and their relevance to the K/T boundary event N89-21341
STATE UNIV. OF NEW YORK, BUFFALO.
Photochemistry at corrugated thin metal films: A phenomenological approach
[AD-A203070] N89-21061
Laser-induced metal deposition on semiconductors from liquid electrolytes
[AD-A203612] N89-21089
Asymptotics beyond all orders N89-21508
Sounds in one-dimensional superfluid helium
[AD-A202428] N89-21629
STATE UNIV. OF NEW YORK, STONY BROOK.
Best ordering for floating-point addition
[AD-A203990] N89-21612
SVERDRUP TECHNOLOGY, INC., CLEVELAND, OH.
Subharmonic and fundamental high amplitude excitation of an axisymmetric jet
[NASA-TM-101946] N89-20920
Comparison of 3D computation and experiment for non-axisymmetric nozzles
[NASA-CR-182245] N89-20921
Thermodynamic analysis of chemical compatibility of several reinforcement materials with niobium aluminides
[NASA-CR-182260] N89-21036
SYRACUSE UNIV., NY.
A generalized approach to direction finding
[AD-A203768] N89-21186
SYSCON CORP., SAN DIEGO, CA.
Lockheed Aeronautical Systems Company technical order transfer tests
[DE89-008092] N89-21707
SYSTEM PLANNING CORP., ARLINGTON, VA.
Systems engineering and technical assistance
[AD-A203479] N89-21696
SYSTEMS CONTROL TECHNOLOGY, INC., ARLINGTON, VA.
Heliport system planning guideiines
[AD-A199081] N89-21003
SYSTEMS SCIENCE AND SOFTWARE, LA JOLLA, CA.
Charging potentials for two sample sets of spectra from DMSP satellites
[AD-A203694] N89-21021
SYSTEMS TECHNOLOGY, INC., HAWTHORNE, CA.
Tailless aircraft performance improvements with relaxed static stability
[NASA-CR-181806] N89-20999

T

TECHNICAL RESEARCH CENTRE OF FINLAND, ESPOO.
Operation of vehicle engines in cold conditions: Start up, lubrication and fuel consumption
[DE88-757111] N89-21255
TECHNISCHE HOGESCHOOL, DELFT (NETHERLANDS).
Numerical and experimental determination of strain (stress) concentration factors of welded joints between square hollow sections
[PB89-131734] N89-21261
TECHNISCHE UNIV., VIENNA (AUSTRIA).
Volcanic ash layers in blue ice fields (Beardmore Glacier Area, Antarctica): Iridium enrichments N89-21340
The Kara and Ust-Kara impact structures (USSR) and their relevance to the K/T boundary event N89-21341
Bio-, Magneto- and event-stratigraphy across the K-T boundary N89-21370
TEL-AVIV UNIV. (ISRAEL).
Excited state energetics and dynamics of large molecules, complexes and clusters
[AD-A203514] N89-21065
TELEDYNE GEOTECHNICAL, ALEXANDRIA, VA.
Finite-difference modeling of Rayleigh wave scattering and P-SV(Lg) coupling problems
[AD-A203221] N89-21161
TENNESSEE TECHNOLOGICAL UNIV., COOKEVILLE.
Transient natural convection heat and mass transfer in crystal growth N89-21741
TENNESSEE UNIV., CHATTANOOGA.
SIRE: A Simple Interactive Rule Editor for NICBES N89-21730
The simulation of the alternate turbopump development high pressure oxygen and fuel turbopumps for the space shuttle main engine using the Shaberth computer program N89-21748
TENNESSEE UNIV., KNOXVILLE.
Evaluation of time delay requirements for closed-loop stability using classical and modern methods
[DE89-006417] N89-21189
Nonprocedural implementation of mathematical programming algorithms
[AD-A203392] N89-21573
Triangularity of the basis in linear programs for material requirements planning, revision
[AD-A203039] N89-21606
Automated library systems and document tracking systems: Commercial software alternatives, volume 1
[DE89-007716] N89-21706
TENNESSEE UNIV., TULLAHOMA.
Cryogenic fluid management in space N89-21727
TEXAS A&M UNIV., COLLEGE STATION.
A fresh look at transport in perfluorosulfonate ionomers: Ultramicroelectrode investigations of Nafion and Dow ionomers
[AD-A203855] N89-21066
A continuum diffusion model for viscoelastic materials
[AD-A202588] N89-21112
On the energy release rate for dynamic transient anti-plane shear crack propagation in a general linear viscoelastic body
[AD-A202942] N89-21280
Iridium, shocked minerals, and trace elements across the Cretaceous/Tertiary boundary at Maud Rise, Wedell Sea, and Walvis Ridge, South Atlantic Ocean N89-21333
Convexity-preserving quasi-interpolation and interpolation by box spline surfaces N89-21503

TEXAS CHRISTIAN UNIV., FORT WORTH.
Solar-powered alkali metal vapor lasers
[NASA-CR-180480] N89-21226
TEXAS TECHNOLOGICAL UNIV., LUBBOCK.
The role of radiation-dynamics interaction in regional numerical weather prediction N89-21732
TEXAS UNIV., AUSTIN.
The boundary-integral method for planar microstrip circuits
[AD-A203715] N89-21185
Symmetry breaking bifurcations and the growth of chaos in a rotating fluid
[AD-A204010] N89-21213
Bispectral inversion: The construction of a time series from its bispectrum
[AD-A202508] N89-21598
Diffusion in symplectic maps
[DE89-008083] N89-21622
Short wave electron temperature gradient driven drift wave turbulence
[DE89-008465] N89-21662
Magnetic properties of nano-heterogeneous amorphous, thin films
[AD-A203727] N89-21680
TEXAS UNIV., GALVESTON.
Gating kinetics and ion transfer in channels of nerve membrane
[AD-A202509] N89-21464
TEXAS UNIV. HEALTH SCIENCE CENTER, SAN ANTONIO.
Effects of simultaneous radiofrequency radiation and chemical exposure of mammalian cells, volume 2
[AD-A202780] N89-21467
TITAN SYSTEMS, INC., PRINCETON, NJ.
Asymptotics beyond all orders N89-21508
TOLEDO UNIV., OH.
The measurement of angular differential cross sections at the SSL Atomic Scattering Facility N89-21744
TRW SPACE TECHNOLOGY LABS., REDONDO BEACH, CA.
Improved high-temperature resistant matrix resins
[NASA-CR-180826] N89-21105
Demonstration of SQUID parametric amplifier
[AD-A203252] N89-21183
TULSA UNIV., OK.
Behavioral effects of microwaves: Relationship of total dose and dose rate
[PB89-118640] N89-21462

U

UNITED KINGDOM ATOMIC ENERGY AUTHORITY, RISLEY (ENGLAND).
Advanced tribological coatings for high specific strength alloys
[AD-A202505] N89-21110
UNIVERSAL ENERGY SYSTEMS, INC., DAYTON, OH.
Contributive research in compound semiconductor material and related devices
[AD-A202586] N89-21670
UNIVERSITY COLL. OF NORTH WALES, BANGOR.
Fast acting optical beam deflection system
[AD-A203042] N89-21648
UNIVERSITY OF CENTRAL ARKANSAS, CONWAY.
X-ray fluorescence surface contaminant analyzer: A feasibility study N89-21736
UNIVERSITY OF CENTRAL FLORIDA, ORLANDO.
Optical power limiter
[AD-A203964] N89-21234
UNIVERSITY OF SOUTHERN CALIFORNIA, LOS ANGELES.
Carbon dioxide catastrophes: Past and future menace N89-21293
Center for the Integration of Optical Computing
[AD-A203254] N89-21536
Devices and systems for nonlinear optical information processing
[AD-A203034] N89-21566
Design specifications for hardware assisted rollback computation
[AD-A203092] N89-21584
Nonlinear real-time optical signal processing
[AD-A202445] N89-21641
UNIVERSITY OF SOUTHWESTERN LOUISIANA, LAFAYETTE.
Disruption of giant comets in the solar system and around other stars N89-21408
UNIVERSITY OF WESTERN WASHINGTON, BELLINGHAM.
Sedimentological effects of tsunamis, with particular reference to impact-generated and volcanogenic waves N89-21299
UTAH STATE UNIV., BEDFORD, MA.
Adapting Schottky diode detector technology to a space platform
[AD-A202825] N89-21219
UTAH STATE UNIV., LOGAN.
Numerical solution of nonlinear algebraic equations in stiff ODE solving
[DE89-008284] N89-21613
UTAH UNIV., SALT LAKE CITY.
Spectroscopic studies of fluid/solid interfaces
[AD-A202436] N89-21054
Modern multiple-pulse, high field NMR studies of high density jet fuels
[AD-A203320] N89-21130
The virtual time machine
[AD-A203087] N89-21533
Time warp on a shared memory multiprocessor
[AD-A203088] N89-21534
HOP (Hardware viewed as Objects and Processes): A process model for synchronous hardware systems
[AD-A203090] N89-21535
Performance directed simulation
[AD-A203089] N89-21570
The design and performance of the rollback chip: Hardware support for time warp
[AD-A203160] N89-21571
The design and implementation of a special purpose cache for the roll back chip
[AD-A203091] N89-21583
Lookahead in parallel discrete event simulation
[AD-A203902] N89-21588

V

VANDERBILT UNIV., NASHVILLE, TN.
Magnetic mapping of current distributions in two-dimensional electronic devices
[AD-A203035] N89-21220
VIGYAN RESEARCH ASSOCIATES, INC., HAMPTON, VA.
Performance of the active sidewall boundary-layer removal system for the Langley 0.3-meter Transonic Cryogenic Tunnel
[NASA-CR-181793] N89-21004
VIRGINIA COMMONWEALTH UNIV., RICHMOND.
Electronic structure and properties of defect complexes in metals
[AD-A203657] N89-21091
VIRGINIA POLYTECHNIC INST. AND STATE UNIV., BLACKSBURG.
Stability of compressible boundary layers N89-20953
Time optimal slewing of flexible spacecraft N89-21014
Investigation of modeling of damage growth in composite laminates
[AD-A202433] N89-21037
A study of the stress wave factor technique for evaluation of composite materials
[NASA-CR-4195] N89-21256
Earth orbital variations and vertebrate bioevolution N89-21357
On a refined nonlinear theory of laminated composite plates N89-21500
Optical fiber sensors and signal processing for intelligent structure monitoring
[NASA-CR-184841] N89-21640
VIRGINIA UNIV., CHARLOTTESVILLE.
Synthesis processing of high-lithium Al-Li alloys
[AD-A203401] N89-21088
VRIJE UNIV., AMSTERDAM (NETHERLANDS).
Impact and extinction signatures in complete Cretaceous-Tertiary (K-T) boundary sections N89-21391

W

WARSAW UNIV. (POLAND).
A novel approach to gamma-ray and neutrino astro-particle physics: The GRANDE experiment
[DE89-006515] N89-21725
WASHINGTON STATE UNIV., PULLMAN.
The implementation of a nonreflecting boundary into the SAMSON2 code
[AD-A203394] N89-21284
Selective extinction of marine plankton at the end of the Mesozoic era: The fossil and stable isotope record N89-21329
WASHINGTON UNIV., SEATTLE.
A numerical study of the turbulent free convection in rectangular cavities N89-21194
Sedimentological effects of tsunamis, with particular reference to impact-generated and volcanogenic waves N89-21299

Macrofossil extinction patterns at Bay of Biscay Cretaceous-Tertiary boundary sections N89-21404
A numerical model for the computation of radiance distributions in natural waters with wind-roughened surfaces. Part 2: User's guide and code listing
[AD-A203441] N89-21651
WASHINGTON UNIV., SAINT LOUIS, MO.
Ion microprobe of Mg, Ca, Ti and Fe isotopic ratios and trace element abundances in hibonite-bearing inclusions from primitive meteorites N89-21719
WESLEYAN UNIV., MIDDLETOWN, CT.
Mass extinctions in the deep sea N89-21396
WESTINGHOUSE RESEARCH AND DEVELOPMENT CENTER, PITTSBURGH, PA.
Research on silicon, carbon, and silicon carbide heterostructures
[AD-A202866] N89-21116
WHITAKER COLL., MA.
Seeing Ghost solutions in stereo vision
[AD-A203581] N89-21473
WISCONSIN UNIV., MADISON.
Instabilities in shear flow of viscoelastic fluids with fading memory
[AD-A203735] N89-21211
A 3-dimensional numerical simulation of the atmospheric injection of aerosols by a hypothetical basaltic fissure eruption N89-21401
Algorithms for rational spline curves N89-21502
Time and state resolved studies of molecular decomposition
[AD-A202464] N89-21636
A novel approach to gamma-ray and neutrino astro-particle physics: The GRANDE experiment
[DE89-006515] N89-21725
WITWATERSRAND UNIV., JOHANNESBURG (SOUTH AFRICA).
Geological indicators for impact: The anomalous case of the Vredefort structure, South Africa N89-21289
The Sudbury Structure (Ontario, Canada) and Vredefort Structure (South Africa): A comparison N89-21311
Report on an international workshop on Cryptoexplosions and Catastrophes in the Geological Record, with a Special Focus on the Vredefort Structure N89-21375
Microdeformation in Vredefort rocks; evidence for shock metamorphism N89-21376
Geochemical comparison of K-T boundaries from the Northern and Southern Hemispheres N89-21400
WOODS HOLE OCEANOGRAPHIC INSTITUTION, MA.
Mass mortality and extraterrestrial impacts N89-21335
Computer program for calculating frequencies and modal structures of free coastal-trapped waves
[PB88-243928] N89-21459
Time delay estimation in stationary and non-stationary environments
[AD-A202507] N89-21549
WYOMING UNIV., LARAMIE.
Static tensile and tensile creep testing of five ceramic fibers at elevated temperatures
[NASA-CR-177525] N89-21046
Strain energy release rate as a function of temperature and preloading history utilizing the edge delamination fatique test method
[NASA-CR-184966] N89-21286

Y

YALE UNIV., NEW HAVEN, CT.
A rapid numerical procedure for determining axisymmetric transverse electric electromagnetic fields via boundary integrals
[AD-A202959] N89-21155
Patterns of megafloral change across the Cretaceous-Tertiary boundary in the Northern Great Plains and Rocky Mountains N89-21336
The causes for geographical variations in OS187/OS186 at the Cretaceous-Tertiary boundary N89-21402
Coping with novelty and human intelligence: The role of counterfactual reasoning
[AD-A203624] N89-21478
YAMAGATA UNIV. (JAPAN).
Mineralogical and geochemical anomalous data of the K-T boundary samples N89-21359
YAMAGUCHI UNIV. (JAPAN).
Mineralogical and geochemical anomalous data of the K-T boundary samples N89-21359

Typical Contract Number Index Listing

Listings in this index are arranged alphanumerically by contract number. Under each contract number the NASA accession numbers denoting documents that have been produced as a result of research done under that contract are arranged in ascending order. The NASA accession number denotes the number by which the citation is identified.

AF PROJ. 2301 ..... N89-21624
N89-21657
AF PROJ. 2302 ..... N89-21037
N89-21252
AF PROJ. 2303 ..... N89-21057
N89-21059
AF PROJ. 2304 ..... N89-21140
AF PROJ. 2305 ..... N89-21564
N89-21566
N89-21605
N89-21641
AF PROJ. 2306 ..... N89-21220
N89-21675
AF PROJ. 2307 ..... N89-21208
N89-21209
AF PROJ. 2308 ..... N89-21201
N89-21202
AF PROJ. 2311 ..... N89-21019
N89-21437
AF PROJ. 2312 ..... N89-21470
AF PROJ. 2313 ..... N89-21468
N89-21472
N89-21702
AF PROJ. 4600 ..... N89-21156
AF PROJ. 7930 ..... N89-21471
AF-AFOSR-0015-85 ..... N89-21019
AF-AFOSR-0019-85 ..... N89-21472
AF-AFOSR-0022-88 ..... N89-21593
AF-AFOSR-0024-88 ..... N89-21564
AF-AFOSR-0037-88 ..... N89-20938
AF-AFOSR-0041-84 ..... N89-21657
AF-AFOSR-0043-86 ..... N89-21057
AF-AFOSR-0057-87 ..... N89-21202
AF-AFOSR-0071-83 ..... N89-21208
AF-AFOSR-0087-85 ..... N89-21037
AF-AFOSR-0096-86 ..... N89-21624
AF-AFOSR-0097-84 ..... N89-21470
AF-AFOSR-0133-85 ..... N89-21437
AF-AFOSR-0151-87 ..... N89-21140
AF-AFOSR-0181-84 ..... N89-21641
AF-AFOSR-0185-83 ..... N89-21566
AF-AFOSR-0197-87 ..... N89-21059
AF-AFOSR-0239-84 ..... N89-21605
AF-AFOSR-0242-86 ..... N89-21209
AF-AFOSR-0244-85 ..... N89-21201
AF-AFOSR-0263-86 ..... N89-21675
AF-AFOSR-0282-87 ..... N89-21702
AF-AFOSR-0320-83 ..... N89-21468
AF-AFOSR-0337-87 ..... N89-21220
AF-AFOSR-0368-84 ..... N89-21252
ARPA ORDER 7272 ..... N89-21696
ARPA ORDER 9526 ..... N89-21181
CAN-NSEC-A4029 ..... N89-21615
DA PROJ. 1L1-61102-A-31-B N89-21678
DA PROJ. 1L1-61102-BH-57 ..... N89-21607
DA PROJ. 1L1-61103-BH-57 ..... N89-21065
N89-21106
N89-21128
N89-21667
DA PROJ. 1L1-62209-A-47-A N89-21244
DA PROJ. 1L1-62209-AH-76 ..... N89-21243
DA PROJ. 1L7-62786-AH-20 ..... N89-21253
DA PROJ. 2Q6-65502-M-770 ..... N89-21545
DA PROJ. 3E1-62777-A-879 ..... N89-21669
DAAB07-87-C-F094 ..... N89-21678
DAAG29-80-C-0041 ..... N89-21502
DAAG29-83-K-0188 ..... N89-21210
DAAG29-84-K-0093 ..... N89-21669
DAAG29-84-K-0130 ..... N89-21512
DAAG29-85-K-0041 ..... N89-21062
DAAG29-85-K-0043 ..... N89-21060
DAAG29-85-K-0097 ..... N89-21063
DAAG29-85-K-0122 ..... N89-21636
DAAG29-85-K-0126 ..... N89-21108
DAAG29-85-K-0188 ..... N89-21530
DAAG29-85-K-0189 ..... N89-21616
DAAG29-85-K-0207 ..... N89-20990
DAAG29-85-K-0244 ..... N89-21091
DAAG29-85-K-00017 ..... N89-21500
DAAK20-83-C-0164 ..... N89-21234
DAAK60-86-C-0128 ..... N89-21484
DAAK70-85-C-0007 ..... N89-21253
DAAK70-86-C-0011 ..... N89-21126
DAAK70-87-C-0043 ..... N89-21253
DAAL03-86-C-0001 ..... N89-21692
DAAL03-86-K-0005 ..... N89-21086
DAAL03-86-K-0112 ..... N89-21514
DAAL03-86-K-0138 ..... N89-21501
DAAL03-86-K-0171 ..... N89-21499
N89-21548
DAAL03-86-K-0173 ..... N89-21228
DAAL03-86-6-0116 ..... N89-21493
DAAL03-87-G-0004 ..... N89-21550
DAAL03-87-K-0036 ..... N89-21211
DAAL03-88-K-0005 ..... N89-21185
DAAL03-88-K-0015 ..... N89-21080
N89-21268
DAAL03-88-K-0071 ..... N89-21044
DAAL04-87-C-0058A N89-21120
DACA76-85-C-0001 ..... N89-21247
DACA76-85-C-0010 ..... N89-21473
DAJA45-85-C-0008 ..... N89-21065
DAJA45-85-C-0021 ..... N89-21106
DAJA45-85-C-0052 ..... N89-21128
DAJA45-87-C-0003 ..... N89-21607
DAJA45-87-C-0008 ..... N89-21090
DAJA45-87-C-0011 ..... N89-21679
DAJA45-87-C-0033 ..... N89-21667
DAJA45-87-C-0044 ..... N89-21110
DAJA45-88-C-0019 ..... N89-21648
DARPA ORDER 6150 ..... N89-21593
DE-AC02-76ER-03077 ..... N89-21530
DE-AC02-83CH-10093 ..... N89-21420
N89-21421
N89-21422
DE-AC02-83CH-10139 ..... N89-21544
DE-AC03-76SF-00098 ..... N89-21033
N89-21048
N89-21097
N89-21098
N89-21689
N89-21690
DE-AC04-76DP-00789 ..... N89-21095
N89-21214
N89-21423
N89-21424
N89-21614
N89-21708
N89-21709
DE-AC05-84OR-21400 ..... N89-21096
N89-21124
N89-21189
N89-21428
N89-21684
DE-AC05-84OT-21400 ..... N89-21590
N89-21656
N89-21706
DE-AC06-76RL-01830 ..... N89-21427
N89-21457
N89-21458
N89-21627
N89-21639
DE-AC08-88NV-10617 ..... N89-21653
DE-AI01-85CE-50111 ..... N89-21417
DE-AI01-88NE-32140 ..... N89-21024
DE-FC03-85DP-40200 ..... N89-21661
DE-FG02-84ER-13221 ..... N89-21443
DE-FG02-86ER-25018 ..... N89-21613
DE-FG02-87ER-45310 ..... N89-21665
DE-FG02-88ER-13937 ..... N89-21236
DE-FG05-80ET-53088 ..... N89-21622
N89-21662
DE-FG05-85ER-53206 ..... N89-21660
DTFA01-87-C-00014 ..... N89-21003
EPA-68-02-4120 ..... N89-21462
EQ540 ..... N89-21615
F04611-82-X-0063 ..... N89-21133
F04611-83-C-0046 ..... N89-21068
N89-21638
F04611-84-C-0003 ..... N89-21029
F04611-84-K-0016 ..... N89-21115
F04611-85-K-0051 ..... N89-21028
F04611-85-K-0106 ..... N89-21285
F04701-85-C-0086 ..... N89-21056
N89-21121
N89-21440
N89-21677
F08635-84-C-0296 ..... N89-21577
F19628-84-K-0013 ..... N89-21713
F19628-85-C-0002 ..... N89-21182
N89-21552
N89-21603
N89-21647
F19628-85-C-0148 ..... N89-21015
F19628-86-C-0001 ..... N89-21164
F19628-86-C-0054 ..... N89-21161
F19628-86-C-0056 ..... N89-21021
F19628-86-C-0141 ..... N89-21450
F19628-86-K-0016 ..... N89-21442
F19628-86-K-0035 ..... N89-21219
F19628-87-C-0097 ..... N89-21441
F29601-85-K-0050 ..... N89-21284
F29601-86-C-0252 ..... N89-21575
F30602-81-C-0169 ..... N89-21186
N89-21589
F30602-85-C-0040 ..... N89-21179
F33615-82-C-1716 ..... N89-21670
F33615-84-C-0604 ..... N89-21467
F33615-86-C-2604 ..... N89-21125
F33615-86-C-2643 ..... N89-21130
F33615-86-C-3225 ..... N89-21016
F33615-86-C-5144 ..... N89-21038
F33615-87-C-1499 ..... N89-21652
F33615-87-C-5274 ..... N89-21055
F49620-86-C-0006 ..... N89-21071
F49620-86-C-0123 ..... N89-21673
F49620-86-K-0005 ..... N89-21107
F49620-87-C-0007 ..... N89-21536
F49620-87-C-0067 ..... N89-21680
F49620-87-C-0101 ..... N89-21116
GR/E/40538 ..... N89-21280
MDA903-84-C-0031 ..... N89-21123
MDA903-85-C-0215 ..... N89-21184
MDA903-87-C-0603 ..... N89-21545
MDA903-87-C-0719 ..... N89-21703
MDA972-88-C-0004 ..... N89-21696
MIPR-00039-87-C-5301 ..... N89-21156
NAGW-996 ..... N89-21429
NAGW-1340 ..... N89-21633
N89-21634
N89-21635
N89-21715
N89-21716
NAG1-466 ..... N89-21537
NAG1-613 ..... N89-21540
NAG1-674 ..... N89-21286
NAG1-691 ..... N89-21226
NAG1-895 ..... N89-21640
NAG1-904 ..... N89-21198
NAG3-172 ..... N89-21256
NAG3-503 ..... N89-21258
NAG3-723 ..... N89-21134
NAG3-729 ..... N89-21479
NAG3-776 ..... N89-21658
NAG3-856 ..... N89-21265
NAG5-356 ..... N89-21141
NAG5-814 ..... N89-21436

NAG5-818 ..... N89-21435
NAG8-050 ..... N89-21449
NAG9-52 ..... N89-21319
NAG9-108 ..... N89-21371
NASA ORDER A-39603-C N89-21046
NASA ORDER C-99066-G N89-21192
N89-21196
N89-21197
N89-21595
NASA ORDER W-30851 ..... N89-21191
NASW-4066 ..... N89-21287
NAS1-17674 ..... N89-21191
NAS1-17864 ..... N89-20922
NAS1-17919 ..... N89-21004
NAS1-18000 ..... N89-21099
NAS1-18061 ..... N89-21582
NAS1-18105 ..... N89-20945
NAS1-18107 ..... N89-21537
NAS1-18524 ..... N89-20999
NAS1-18599 ..... N89-21267
NAS1-18605 ..... N89-21537
N89-21542
NAS2-12789 ..... N89-20973
NAS3-23933 ..... N89-21105
NAS3-24105 ..... N89-20921
NAS3-24645 ..... N89-21239
NAS3-24646 ..... N89-21072
NAS3-24678 ..... N89-21173
NAS3-25266 ..... N89-20921
N89-21036
NAS5-28745 ..... N89-21416
NAS5-30158 ..... N89-21168
NAS8-36199 ..... N89-21023
NAS8-36715 ..... N89-21425
N89-21426
NCC2-175 ..... N89-20963
NGT-01-002-099 ..... N89-21726
NGT-21-002-080 ..... N89-20981
NR PROJ. 356856 ..... N89-21118
NR PROJ. 627838 ..... N89-21066
NSF ATM-87-09659 ..... N89-21215
N89-21433
N89-21446
N89-21447
N89-21723
NSF ATM-87-10102 ..... N89-21371
NSF ATM-87-15367 ..... N89-21429
NSF ATM-87-16036 ..... N89-21429
NSF ATM-88-08137 ..... N89-21429
NSF CCR-86-02310 ..... N89-21519
NSF CCR-87-00988 ..... N89-21540
NSF DCR-85-01843 ..... N89-21574
NSF DCR-85-04826 ..... N89-21533
N89-21534
N89-21588
NSF DCR-85-11190 ..... N89-21565
NSF DMS-83-51187 ..... N89-21502
NSF DMS-87-112058 ..... N89-21211
NSF DNS-86-01318 ..... N89-21257
NSF EAR-86-09218 ..... N89-21319
NSF EAR-88-95268 ..... N89-21327
NSF ECS-85-19058 ..... N89-21548
NSF OCE-85-21837 ..... N89-21459
NSG-1619 ..... N89-20947
N00014-79-C-0647 ..... N89-21212
N00014-81-C-0776 ..... N89-21064
N00014-81-C-2495 ..... N89-21183
N00014-81-K-0146 ..... N89-21612
N00014-82-K-0147 ..... N89-21217
N00014-82-K-0562 ..... N89-21112
N00014-82-K-0612 ..... N89-21066
N00014-82-K-0727 ..... N89-21160
N00014-83-K-0125 ..... N89-21565
N89-21585
N00014-83-K-0536 ..... N89-21499
N00014-83-K-0610 ..... N89-21155
N00014-83-K-0640 ..... N89-21519
N00014-83-K-0646 ..... N89-21229
N00014-83-K-0968 ..... N89-21084
N00014-84-C-0193 ..... N89-21630
N00014-84-K-0186 ..... N89-21608
N00014-84-K-0272 ..... N89-21143
N00014-84-K-0275 ..... N89-21637
N00014-85-G-0213 ..... N89-21604
N00014-85-K-0111 ..... N89-21717
N00014-85-K-0124 ..... N89-21251
N89-21473
N00014-85-K-0163 ..... N89-21574
N00014-85-K-0187 ..... N89-21269
N00014-85-K-0213 ..... N89-21576
N00014-85-K-0214 ..... N89-21645
N00014-85-K-0272 ..... N89-21549
N00014-85-K-0497 ..... N89-21609
N00014-85-K-0559 ..... N89-21618
N00014-85-K-0589 ..... N89-21478
N00014-85-K-0596 ..... N89-21272
N00014-85-K-0712 ..... N89-21054
N00014-85-K-0898 ..... N89-21118
N00014-86-C-0164 ..... N89-21127
N00014-86-C-2180 ..... N89-21109
N00014-86-F-0049 ..... N89-21431
N89-21432
N89-21722
N00014-86-K-0029 ..... N89-21597
N00014-86-K-0043 ..... N89-21061
N89-21089
N89-21629
N00014-86-K-0133 ..... N89-21085
N00014-86-K-0298 ..... N89-21280
N00014-86-K-0310 ..... N89-21155
N00014-86-K-0366 ..... N89-21222
N00014-86-K-0385 ..... N89-21213
N00014-86-K-0533 ..... N89-21175
N00014-86-K-0685 ..... N89-21251
N00014-86-K-0772 ..... N89-21119
N00014-87-C-0687 ..... N89-21165
N00014-87-G-0260 ..... N89-21587
N00014-87-K-0010 ..... N89-21217
N00014-87-K-0055 ..... N89-21464
N00014-87-K-0117 ..... N89-21111
N89-21276
N00014-87-K-0163 ..... N89-21573
N89-21606
N00014-87-K-0184 ..... N89-21533
N89-21534
N89-21570
N89-21588
N00014-87-K-0321 ..... N89-21469
N00014-87-K-0525 ..... N89-21651
N00014-87-K-0825 ..... N89-21586
N00014-88-C-0033 ..... N89-21438
N00014-88-C-0391 ..... N89-21181
N00014-88-C-0571 ..... N89-21137
N00014-88-C-0714 ..... N89-21674
N00014-88-K-0162 ..... N89-21167
N89-21187
N89-21176
N00014-88-K-0341 ..... N89-21546
N00039-84-C-0211 ..... N89-21547
N00039-85-C-0341 ..... N89-21699
N62583-87-M-T227 ..... N89-21611
N66001-87-C-0079 ..... N89-21471
N66001-87-C-0170 ..... N89-21645
N66001-88-C-0004 ..... N89-21151
P-86112 ..... N89-21579
PROJ. BR033-02-WH N89-21504
RR042 ..... N89-21469
RR01103 ..... N89-21229
RR04108 ..... N89-21464
RR04204 ..... N89-21608
RR04206 ..... N89-21618
W-31-109-ENG-38 ..... N89-21052
N89-21070
N89-21579
N89-21580
N89-21581
N89-21686
N89-21687
W-7405-ENG-36 ..... N89-21094
N89-21235
N89-21578
N89-21620
N89-21685
N89-21688
N89-21725
W-7405-ENG-48 ..... N89-21031
N89-21093
N89-21225
N89-21237
N89-21480
N89-21654
N89-21659
N89-21707
W-7405-ENG-82 ..... N89-21053
N89-21075
N89-21076
N89-21077
N89-21078
N89-21216
N89-21655
N89-21666
474-46-10 ..... N89-21100
505-01-01 ..... N89-21036
505-44-2C N89-21142
505-60-11-01 ..... N89-20925
N89-20942
505-60-31 ..... N89-21190
505-61-01-09 ..... N89-21004
505-61-51 ..... N89-20973
N89-20978
N89-21541
505-61-51-10 ..... N89-20982
505-61-71 ..... N89-21532
505-62-01 ..... N89-20995
505-62-21 ..... N89-20920
N89-20921
N89-20996
N89-21051
N89-21192
N89-21196
N89-21595
505-62-27 ..... N89-21197
505-63-1A N89-21032
N89-21103
505-63-1B N89-21258
N89-21266
505-63-1D N89-21245
505-63-01-01 ..... N89-21047
505-63-01-05 ..... N89-21099
N89-21267
505-63-01-07 ..... N89-21539
505-63-01-10 ..... N89-21260
505-63-21-01 ..... N89-20922
505-63-21-04 ..... N89-20991
505-63-31 ..... N89-21265
505-63-51 ..... N89-21243
N89-21244
505-66-01-02 ..... N89-20999
505-67-11 ..... N89-21477
505-68-27 ..... N89-20983
505-90-01 ..... N89-21256
505-90-21-01 ..... N89-21537
N89-21542
506-41-11 ..... N89-21174
506-43-11 ..... N89-21104
506-43-31 ..... N89-21046
506-44-2C N89-21169
N89-21172
506-44-21 ..... N89-21171
506-46-21-05 ..... N89-21582
506-49-31-01 ..... N89-21538
535-03-01 ..... N89-21002
N89-21628
582-01-11 ..... N89-21025
585-01-61-08 ..... N89-21135
N89-21136
586-01-11 ..... N89-21419
650-60-20 ..... N89-21138
650-60-21 ..... N89-21173
694-03-03 ..... N89-21224
763-01-31-19 ..... N89-21193
778-32-11 ..... N89-21417
992-21-01 ..... N89-20964

Typical Report Number Index Listing

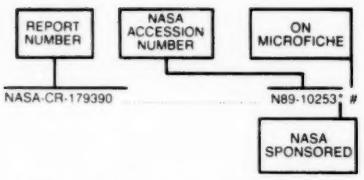

Listings in this index are arranged alphanumerically by report number. The NASA accession number denotes the number by which the citation is identified. An asterisk (*) indicates that the item is a NASA report. A pound sign (#) indicates that the item is available on microfiche.

A-88029 ..... N89-20964* #
A-88065 ..... N89-21532* #
A-88164 ..... N89-21541* #
A-88295 ..... N89-21190* #
A-88305 ..... N89-21477* #
A-89005 ..... N89-20978* #

AAMRL-TR-88-048 ..... N89-21481 #

AD-A193384 ..... N89-21490 #
AD-A195644 ..... N89-21140 #
AD-A197978 ..... N89-20964* #
AD-A199081 ..... N89-21003 #
AD-A202424 ..... N89-21199 #
AD-A202425 ..... N89-21200 #
AD-A202426 ..... N89-21125 #
AD-A202427 ..... N89-21175 #
AD-A202428 ..... N89-21629 #
AD-A202429 ..... N89-21015 #
AD-A202430 ..... N89-20984 #
AD-A202433 ..... N89-21037 #
AD-A202434 ..... N89-21143 #
AD-A202436 ..... N89-21054 #
AD-A202438 ..... N89-21624 #
AD-A202439 ..... N89-21545 #
AD-A202443 ..... N89-21106 #
AD-A202445 ..... N89-21641 #
AD-A202448 ..... N89-21667 #
AD-A202449 ..... N89-21201 #
AD-A202450 ..... N89-21176 #
AD-A202451 ..... N89-21202 #
AD-A202452 ..... N89-21107 #
AD-A202459 ..... N89-21108 #
AD-A202461 ..... N89-21699 #
AD-A202464 ..... N89-21636 #
AD-A202465 ..... N89-21268 #
AD-A202468 ..... N89-21597 #
AD-A202471 ..... N89-21126 #
AD-A202472 ..... N89-21227 #
AD-A202474 ..... N89-21481 #
AD-A202475 ..... N89-21016 #
AD-A202477 ..... N89-21079 #
AD-A202484 ..... N89-21630 #
AD-A202489 ..... N89-21546 #
AD-A202490 ..... N89-21547 #
AD-A202502 ..... N89-21548 #
AD-A202504 ..... N89-21109 #
AD-A202505 ..... N89-21110 #
AD-A202507 ..... N89-21549 #
AD-A202508 ..... N89-21598 #
AD-A202509 ..... N89-21464 #
AD-A202518 ..... N89-21038 #
AD-A202521 ..... N89-21111 #
AD-A202522 ..... N89-21080 #
AD-A202524 ..... N89-21550 #
AD-A202526 ..... N89-21228 #
AD-A202527 ..... N89-21551 #
AD-A202528 ..... N89-21144 #
AD-A202529 ..... N89-21668 #
AD-A202530 ..... N89-21642 #
AD-A202535 ..... N89-20985 #
AD-A202537 ..... N89-21669 #
AD-A202538 ..... N89-21006 #
AD-A202540 ..... N89-21552 #
AD-A202542 ..... N89-21039 #
AD-A202545 ..... N89-21269 #
AD-A202547 ..... N89-20979 #
AD-A202552 ..... N89-20986 #
AD-A202557 ..... N89-20985 #
AD-A202560 ..... N89-21553 #
AD-A202561 ..... N89-21554 #
AD-A202562 ..... N89-21145 #
AD-A202563 ..... N89-21555 #
AD-A202565 ..... N89-21270 #
AD-A202566 ..... N89-21556 #
AD-A202567 ..... N89-21027 #
AD-A202569 ..... N89-21631 #
AD-A202570 ..... N89-21081 #
AD-A202572 ..... N89-21271 #
AD-A202573 ..... N89-21591 #
AD-A202574 ..... N89-21557 #
AD-A202575 ..... N89-21203 #
AD-A202576 ..... N89-21599 #
AD-A202577 ..... N89-21146 #
AD-A202578 ..... N89-21147 #
AD-A202579 ..... N89-21558 #
AD-A202581 ..... N89-21229 #
AD-A202582 ..... N89-21643 #
AD-A202583 ..... N89-21559 #
AD-A202584 ..... N89-20975 #
AD-A202586 ..... N89-21670 #
AD-A202587 ..... N89-20966 #
AD-A202588 ..... N89-21112 #
AD-A202589 ..... N89-21482 #
AD-A202591 ..... N89-21055 #
AD-A202593 ..... N89-21671 #
AD-A202594 ..... N89-21600 #
AD-A202623 ..... N89-21695 #
AD-A202626 ..... N89-21710 #
AD-A202633 ..... N89-21247 #
AD-A202637 ..... N89-21272 #
AD-A202638 ..... N89-21217 #
AD-A202644 ..... N89-21711 #
AD-A202646 ..... N89-21177 #
AD-A202647 ..... N89-20980 #
AD-A202648 ..... N89-21017 #
AD-A202649 ..... N89-21178 #
AD-A202652 ..... N89-21082 #
AD-A202657 ..... N89-21560 #
AD-A202661 ..... N89-21204 #
AD-A202663 ..... N89-21218 #
AD-A202665 ..... N89-21230 #
AD-A202666 ..... N89-21644 #
AD-A202667 ..... N89-21672 #
AD-A202692 ..... N89-21592 #
AD-A202693 ..... N89-21007 #
AD-A202696 ..... N89-21148 #
AD-A202698 ..... N89-21273 #
AD-A202699 ..... N89-20997 #
AD-A202703 ..... N89-21274 #
AD-A202704 ..... N89-21179 #
AD-A202705 ..... N89-21113 #
AD-A202706 ..... N89-21248 #
AD-A202707 ..... N89-21205 #
AD-A202708 ..... N89-21601 #
AD-A202710 ..... N89-21249 #
AD-A202712 ..... N89-21483 #
AD-A202713 ..... N89-21561 #
AD-A202714 ..... N89-21625 #
AD-A202721 ..... N89-21484 #
AD-A202724 ..... N89-21250 #
AD-A202725 ..... N89-21562 #
AD-A202727 ..... N89-21000 #
AD-A202730 ..... N89-21617 #
AD-A202732 ..... N89-21465 #
AD-A202736 ..... N89-21645 #
AD-A202737 ..... N89-20992 #
AD-A202738 ..... N89-21114 #
AD-A202742 ..... N89-21673 #
AD-A202747 ..... N89-21646 #
AD-A202760 ..... N89-21018 #
AD-A202762 ..... N89-21691 #
AD-A202764 ..... N89-21602 #
AD-A202765 ..... N89-20987 #
AD-A202766 ..... N89-21180 #
AD-A202767 ..... N89-21083 #
AD-A202768 ..... N89-20988 #
AD-A202769 ..... N89-21275 #
AD-A202770 ..... N89-21466 #
AD-A202776 ..... N89-21008 #
AD-A202779 ..... N89-21149 #
AD-A202780 ..... N89-21467 #
AD-A202785 ..... N89-21647 #
AD-A202786 ..... N89-21603 #
AD-A202800 ..... N89-21437 #
AD-A202806 ..... N89-21604 #
AD-A202808 ..... N89-21009 #
AD-A202814 ..... N89-21468 #
AD-A202821 ..... N89-21115 #
AD-A202822 ..... N89-21028 #
AD-A202824 ..... N89-21276 #
AD-A202825 ..... N89-21219 #
AD-A202827 ..... N89-21469 #
AD-A202841 ..... N89-21056 #
AD-A202849 ..... N89-21563 #
AD-A202864 ..... N89-21277 #
AD-A202865 ..... N89-21485 #
AD-A202866 ..... N89-21116 #
AD-A202867 ..... N89-21674 #
AD-A202872 ..... N89-21150 #
AD-A202873 ..... N89-21012 #
AD-A202874 ..... N89-21231 #
AD-A202881 ..... N89-21251 #
AD-A202882 ..... N89-21618 #
AD-A202892 ..... N89-21084 #
AD-A202900 ..... N89-21700 #
AD-A202901 ..... N89-21701 #
AD-A202902 ..... N89-21252 #
AD-A202905 ..... N89-21057 #
AD-A202907 ..... N89-21470 #
AD-A202909 ..... N89-21058 #
AD-A202912 ..... N89-21450 #
AD-A202921 ..... N89-21151 #
AD-A202924 ..... N89-21206 #
AD-A202934 ..... N89-21010 #
AD-A202935 ..... N89-21152 #
AD-A202936 ..... N89-21153 #
AD-A202937 ..... N89-21154 #
AD-A202938 ..... N89-21011 #
AD-A202939 ..... N89-21278 #
AD-A202941 ..... N89-21279 #
AD-A202942 ..... N89-21280 #
AD-A202947 ..... N89-21117 #
AD-A202953 ..... N89-21675 #
AD-A202954 ..... N89-21059 #
AD-A202955 ..... N89-21118 #
AD-A202959 ..... N89-21155 #
AD-A202960 ..... N89-21471 #
AD-A202963 ..... N89-21564 #
AD-A202964 ..... N89-21702 #
AD-A202969 ..... N89-21281 #
AD-A202983 ..... N89-21460 #
AD-A202984 ..... N89-21486 #
AD-A202995 ..... N89-21565 #
AD-A202996 ..... N89-21605 #
AD-A202998 ..... N89-21156 #
AD-A202999 ..... N89-21060 #
AD-A203015 ..... N89-21040 #
AD-A203019 ..... N89-21019 #
AD-A203030 ..... N89-21717 #
AD-A203034 ..... N89-21566 #
AD-A203035 ..... N89-21220 #
AD-A203038 ..... N89-21085 #
AD-A203039 ..... N89-21606 #
AD-A203040 ..... N89-21607 #
AD-A203042 ..... N89-21648 #
AD-A203044 ..... N89-21157 #
AD-A203045 ..... N89-21567 #
AD-A203047 ..... N89-21568 #
AD-A203049 ..... N89-21569 #
AD-A203050 ..... N89-21001 #
AD-A203051 ..... N89-20993 #
AD-A203052 ..... N89-21158 #
AD-A203054 ..... N89-21487 #
AD-A203055 ..... N89-20994 #
AD-A203057 ..... N89-21159 #
AD-A203059 ..... N89-21181 #

AD-A203060 N89-21127 #
AD-A203062 N89-21119 #
AD-A203063 N89-21137 #
AD-A203066 N89-21438 #
AD-A203069 N89-21649 #
AD-A203070 N89-21061 #
AD-A203081 N89-21160 #
AD-A203083 N89-21128 #
AD-A203087 N89-21533 #
AD-A203088 N89-21534 #
AD-A203089 N89-21570 #
AD-A203090 N89-21535 #
AD-A203091 N89-21583 #
AD-A203092 N89-21584 #
AD-A203093 N89-21637 #
AD-A203094 N89-21086 #
AD-A203100 N89-21488 #
AD-A203126 N89-21062 #
AD-A203145 N89-21439 #
AD-A203146 N89-20989 #
AD-A203147 N89-21676 #
AD-A203148 N89-21632 #
AD-A203149 N89-21129 #
AD-A203150 N89-21585 #
AD-A203160 N89-21571 #
AD-A203168 N89-21063 #
AD-A203170 N89-21182 #
AD-A203172 N89-21440 #
AD-A203173 N89-21677 #
AD-A203176 N89-21207 #
AD-A203177 N89-21489 #
AD-A203178 N89-20967 #
AD-A203179 N89-21041 #
AD-A203186 N89-21282 #
AD-A203187 N89-21283 #
AD-A203189 N89-20968 #
AD-A203197 N89-21120 #
AD-A203201 N89-21087 #
AD-A203202 N89-21042 #
AD-A203204 N89-21029 #
AD-A203221 N89-21161 #
AD-A203238 N89-21608 #
AD-A203241 N89-21593 #
AD-A203252 N89-21183 #
AD-A203254 N89-21536 #
AD-A203257 N89-21162 #
AD-A203260 N89-21163 #
AD-A203289 N89-21221 #
AD-A203291 N89-20969 #
AD-A203292 N89-20970 #
AD-A203293 N89-21020 #
AD-A203299 N89-21586 #
AD-A203311 N89-21043 #
AD-A203317 N89-21609 #
AD-A203320 N89-21130 #
AD-A203331 N89-20971 #
AD-A203332 N89-21572 #
AD-A203333 N89-21121 #
AD-A203334 N89-21208 #
AD-A203348 N89-21587 #
AD-A203349 N89-21209 #
AD-A203355 N89-21678 #
AD-A203357 N89-21122 #
AD-A203360 N89-21253 #
AD-A203365 N89-21184 #
AD-A203366 N89-21232 #
AD-A203368 N89-21657 #
AD-A203372 N89-21164 #
AD-A203382 N89-21044 #
AD-A203383 N89-21692 #
AD-A203385 N89-21064 #
AD-A203388 N89-21472 #
AD-A203392 N89-21573 #
AD-A203394 N89-21284 #
AD-A203396 N89-21650 #
AD-A203401 N89-21088 #
AD-A203439 N89-21210 #
AD-A203440 N89-21616 #
AD-A203441 N89-21651 #
AD-A203444 N89-21574 #
AD-A203447 N89-21575 #
AD-A203457 N89-21679 #
AD-A203479 N89-21696 #
AD-A203495 N89-21222 #
AD-A203514 N89-21065 #
AD-A203576 N89-21619 #
AD-A203581 N89-21473 #
AD-A203604 N89-21165 #
AD-A203612 N89-21089 #
AD-A203623 N89-21441 #
AD-A203624 N89-21478 #
AD-A203628 N89-21451 #
AD-A203636 N89-21090 #
AD-A203651 N89-21576 #
AD-A203657 N89-21091 #
AD-A203694 N89-21021 #

AD-A203715 N89-21185 #
AD-A203727 N89-21680 #
AD-A203734 N89-21092 #
AD-A203735 N89-21211 #
AD-A203737 N89-21045 #
AD-A203738 N89-21697 #
AD-A203739 N89-21442 #
AD-A203760 N89-21285 #
AD-A203763 N89-21474 #
AD-A203766 N89-21212 #
AD-A203767 N89-21131 #
AD-A203768 N89-21186 #
AD-A203772 N89-21652 #
AD-A203777 N89-21233 #
AD-A203855 N89-21066 #
AD-A203864 N89-21713 #
AD-A203877 N89-21610 #
AD-A203880 N89-21187 #
AD-A203887 N89-21005 #
AD-A203890 N89-21123 #
AD-A203891 N89-21681 #
AD-A203901 N89-21703 #
AD-A203902 N89-21588 #
AD-A203911 N89-21682 #
AD-A203913 N89-21611 #
AD-A203926 N89-21704 #
AD-A203928 N89-21067 #
AD-A203934 N89-21452 #
AD-A203936 N89-21166 #
AD-A203954 N89-20976 #
AD-A203955 N89-21030 #
AD-A203959 N89-21167 #
AD-A203961 N89-21453 #
AD-A203964 N89-21234 #
AD-A203965 N89-21454 #
AD-A203966 N89-21594 #
AD-A203967 N89-20990 #
AD-A203968 N89-21132 #
AD-A203969 N89-21455 #
AD-A203981 N89-21626 #
AD-A203982 N89-21589 #
AD-A203984 N89-21456 #
AD-A203985 N89-21068 #
AD-A203986 N89-21638 #
AD-A203988 N89-21133 #
AD-A203990 N89-21612 #
AD-A203994 N89-21577 #
AD-A203997 N89-21683 #
AD-A203999 N89-21022 #
AD-A204001 N89-21254 #
AD-A204002 N89-21223 #
AD-A204003 N89-21069 #
AD-A204010 N89-21213 #
AD-A204161 N89-21071 #

AD-E501064 N89-21123 #
AD-E501065 N89-21681 #
AD-E801833 N89-21577 #
AD-E900870 N89-20980 #
AD-E900870 N89-21017 #
AD-E900870 N89-21082 #
AD-E900870 N89-21177 #
AD-E900870 N89-21178 #
AD-E900870 N89-21217 #
AD-E900870 N89-21247 #
AD-E900870 N89-21272 #
AD-E900870 N89-21560 #
AD-E900870 N89-21600 #
AD-E900870 N89-21671 #
AD-E900870 N89-21695 #
AD-E900870 N89-21710 #
AD-E900870 N89-21711 #
AD-E951302 N89-21067 #

AEDC-TSR-86-V46 N89-21200 #
AEDC-TSR-88-V32 N89-20966 #

AERE-R-12639 N89-21663 #
AERE-R-12848 N89-21101 #
AERE-R-12897 N89-21073 #
AERE-R-12941 N89-21038 #
AERE-R-13039 N89-21035 #
AERE-R-13040 N89-21034 #
AERE-R-13119 N89-21139 #

AFAL-TR-88-013 N89-21068 #
AFAL-TR-88-039 N89-21028 #
AFAL-TR-88-068 N89-21115 #
AFAL-TR-88-069 N89-21638 #
AFAL-TR-88-075 N89-21133 #
AFAL-TR-88-083 N89-21285 #
AFAL-TR-88-096-VOL-1 N89-21029 #

AFATL-TR-88-12 N89-21577 #
AFATL-TR-88-95 N89-20965 #

AFGL-ERP-1005 N89-21456 #

AFGL-IP-335 N89-21022 #

AFGL-TR-87-0234 N89-21219 #
AFGL-TR-88-0027 N89-21441 #
AFGL-TR-88-0030 N89-21022 #
AFGL-TR-88-0057 N89-21021 #
AFGL-TR-88-0093 N89-21161 #
AFGL-TR-88-0144 N89-21456 #
AFGL-TR-88-0199 N89-21442 #
AFGL-TR-88-0221 N89-21713 #
AFGL-TR-88-0279 N89-21450 #
AFGL-TR-88-0293 N89-21015 #

AFIT/GA/AA/88D-7 N89-21007 #
AFIT/GA/AA/88D-02 N89-21018 #
AFIT/GA/AA/88D-03 N89-21009 #
AFIT/GA/AA/88D-06 N89-21278 #
AFIT/GA/AA/88D-09 N89-21010 #
AFIT/GA/AA/88D-10 N89-21008 #
AFIT/GA/AA/88D-11 N89-21154 #
AFIT/GA/AA/88D-13 N89-21011 #
AFIT/GA/AA/88S-1 N89-21203 #

AFIT/GA/ENG/88D-1 N89-21249 #
AFIT/GA/ENG/88D-2 N89-21148 #

AFIT/GAE/AA/88D-3 N89-21083 #
AFIT/GAE/AA/88D-4 N89-20969 #
AFIT/GAE/AA/88D-5 N89-21020 #
AFIT/GAE/AA/88D-01 N89-21691 #
AFIT/GAE/AA/88D-09 N89-20988 #
AFIT/GAE/AA/88D-10 N89-21248 #
AFIT/GAE/AA/88D-12 N89-21271 #
AFIT/GAE/AA/88D-13 N89-21117 #
AFIT/GAE/AA/88D-15 N89-21040 #
AFIT/GAE/AA/88D-18 N89-21041 #
AFIT/GAE/AA/88D-22 N89-21207 #
AFIT/GAE/AA/88D-23 N89-20967 #
AFIT/GAE/AA/88D-26 N89-21114 #
AFIT/GAE/AA/88D-27 N89-21205 #
AFIT/GAE/AA/88D-28 N89-21113 #
AFIT/GAE/AA/88D-29 N89-21279 #
AFIT/GAE/AA/88D-30 N89-21082 #
AFIT/GAE/AA/88D-32 N89-21283 #
AFIT/GAE/AA/88D-34 N89-20970 #
AFIT/GAE/AA/88D-35 N89-21282 #
AFIT/GAE/AA/88D-36 N89-21081 #
AFIT/GAE/AA/88D-38 N89-21275 #
AFIT/GAE/AA/88S-1 N89-21270 #

AFIT/GAE/ENG/88D-01 N89-21592 #

AFIT/GCE/ENG/88D-2 N89-21557 #
AFIT/GCE/ENG/88D-3 N89-21159 #
AFIT/GCE/ENG/88D-5 N89-20979 #

AFIT/GCS/ENG/88D-1 N89-21558 #
AFIT/GCS/ENG/88D-2 N89-21204 #
AFIT/GCS/ENG/88D-3 N89-21560 #
AFIT/GCS/ENG/88D-6 N89-20985 #
AFIT/GCS/ENG/88D-7 N89-20992 #
AFIT/GCS/ENG/88D-8 N89-21145 #
AFIT/GCS/ENG/88D-14 N89-21563 #
AFIT/GCS/ENG/88D-17 N89-20994 #
AFIT/GCS/ENG/88D-18 N89-21568 #
AFIT/GCS/ENG/88S-1 N89-21562 #

AFIT/GE/AA/86J-1 N89-21625 #

AFIT/GE/ENG/ENP/88D-1 N89-21672 #

AFIT/GE/ENG/88-5 N89-21553 #
AFIT/GE/ENG/88D-7 N89-21483 #
AFIT/GE/ENG/88D-16 N89-21602 #
AFIT/GE/ENG/88D-17 N89-21487 #
AFIT/GE/ENG/88D-18 N89-21489 #
AFIT/GE/ENG/88D-19 N89-21000 #
AFIT/GE/ENG/88D-22 N89-20993 #
AFIT/GE/ENG/88D-23 N89-21158 #
AFIT/GE/ENG/88D-28 N89-20980 #
AFIT/GE/ENG/88D-31 N89-21149 #
AFIT/GE/ENG/88D-33 N89-21001 #
AFIT/GE/ENG/88D-35 N89-21147 #
AFIT/GE/ENG/88D-36 N89-21644 #
AFIT/GE/ENG/88D-38 N89-20989 #
AFIT/GE/ENG/88D-40 N89-21676 #
AFIT/GE/ENG/88D-41 N89-21250 #
AFIT/GE/ENG/88D-45 N89-21465 #
AFIT/GE/ENG/88D-49 N89-21631 #
AFIT/GE/ENG/88D-50 N89-21569 #
AFIT/GE/ENG/88D-52 N89-21153 #
AFIT/GE/ENG/88D-54 N89-21591 #
AFIT/GE/ENG/88D-57 N89-21561 #
AFIT/GE/ENG/88D-61 N89-21180 #

AFIT/GE/ENG/88D-63 ..... N89-21178 #
AFIT/GE/ENG/88S-1 ..... N89-21177 #

AFIT/GEO/ENG/88D-1 ..... N89-21144 #
AFIT/GEO/ENG/88D-2 ..... N89-21221 #
AFIT/GEO/ENG/88D-3 ..... N89-21600 #
AFIT/GEO/ENG/88D-4 ..... N89-21466 #
AFIT/GEO/ENG/88D-5 ..... N89-21556 #

AFIT/GEO/ENP/88D-3 ..... N89-21671 #
AFIT/GEO/ENP/88D-4 ..... N89-21642 #
AFIT/GEO/ENP/88D-8 ..... N89-21668 #

AFIT/GEP/ENP/88D-3 ..... N89-21551 #
AFIT/GEP/ENP/88D-7 ..... N89-21231 #

AFIT/GLM/LSY/88S-11 ..... N89-21695 #
AFIT/GLM/LSY/88S-66 ..... N89-21710 #

AFIT/GOR/ENS/88D-01 ..... N89-21554 #
AFIT/GOR/ENS/88D-12 ..... N89-21555 #
AFIT/GOR/ENS/88D-19 ..... N89-21012 #
AFIT/GOR/ENS/88D-22 ..... N89-21599 #
AFIT/GOR/ENS/88D-23 ..... N89-21157 #
AFIT/GOR/ENS/88D-25 ..... N89-21150 #

AFIT/GOR/MA/88D-1 ..... N89-21567 #
AFIT/GOR/MA/88D-3 ..... N89-21601 #

AFIT/GSE/AA/88D-2-VOL-1 ..... N89-20987 #

AFIT/GSO/ENP/88D-3 ..... N89-21027 #
AFIT/GSO/ENP/88D-4 ..... N89-21218 #
AFIT/GSO/ENP/88D-5 ..... N89-21230 #
AFIT/GSO/ENP/88D-6 ..... N89-21146 #

AFIT/GSO/MA/88D-2 ..... N89-21017 #

AFIT/MA/GE/88D-2 ..... N89-21152 #

AFOSR-88-0635TR ..... N89-21140 #
AFOSR-88-1006TR ..... N89-21624 #
AFOSR-88-1206TR ..... N89-21702 #
AFOSR-88-1211TR ..... N89-21107 #
AFOSR-88-1217TR ..... N89-21201 #
AFOSR-88-1218TR ..... N89-21202 #
AFOSR-88-1221TR ..... N89-21116 #
AFOSR-88-1226TR ..... N89-21468 #
AFOSR-88-1248TR ..... N89-21605 #
AFOSR-88-1250TR ..... N89-21566 #
AFOSR-88-1251TR ..... N89-21437 #
AFOSR-88-1253TR ..... N89-21037 #
AFOSR-88-1254TR ..... N89-21019 #
AFOSR-88-1255TR ..... N89-21059 #
AFOSR-88-1269TR ..... N89-21057 #
AFOSR-88-1270TR ..... N89-21657 #
AFOSR-88-1273TR ..... N89-21673 #
AFOSR-88-1279TR ..... N89-21220 #
AFOSR-88-1281TR ..... N89-21536 #
AFOSR-88-1282TR ..... N89-21564 #
AFOSR-88-1283TR ..... N89-21641 #
AFOSR-88-1288TR ..... N89-21593 #
AFOSR-88-1290TR ..... N89-21252 #
AFOSR-88-1291TR ..... N89-21208 #
AFOSR-88-1320TR ..... N89-21209 #
AFOSR-88-1328TR ..... N89-21675 #
AFOSR-88-1335TR ..... N89-21472 #
AFOSR-89-0064TR ..... N89-21680 #
AFOSR-89-0087TR ..... N89-21071 #

AFSC-TR-88-06 ..... N89-21697 #

AFWAL-TR-88-1037 ..... N89-21670 #
AFWAL-TR-88-1083 ..... N89-21594 #
AFWAL-TR-88-1125 ..... N89-21682 #
AFWAL-TR-88-1142 ..... N89-21572 #
AFWAL-TR-88-2046 ..... N89-21125 #
AFWAL-TR-88-2049 ..... N89-21130 #
AFWAL-TR-88-3024 ..... N89-20976 #
AFWAL-TR-88-3038 ..... N89-21016 #
AFWAL-TR-88-3085 ..... N89-20971 #
AFWAL-TR-88-4016 ..... N89-21038 #
AFWAL-TR-88-4166 ..... N89-21055 #
AFWAL-TR-88-4243 ..... N89-21045 #

AFWL-TR-87-93 ..... N89-21575 #
AFWL-TR-88-102 ..... N89-21284 #

AI-M-1073 ..... N89-21473 #
AI-M-1078 ..... N89-21646 #

AI-TR-1072 ..... N89-21251 #

AIAA-89-0007 ..... N89-20921* #
AIAA-89-0993 ..... N89-20920* #
AIAA-89-1059 ..... N89-21628* #
AIAA-89-1269 ..... N89-20982* #

AITI-88-001 ..... N89-21707 #

ANL-88-44 ..... N89-21581 #

ANL/PPRNT-89-155 ..... N89-21580 #
ANL/PPRNT-89-156 ..... N89-21579 #

ANSP-M-19 ..... N89-21024 #

ARAED-TR-88031 ..... N89-21132 #

ARCCB-TR-88039 ..... N89-21087 #
ARCCB-TR-88040 ..... N89-21042 #
ARCCB-TR-88041 ..... N89-21274 #
ARCCB-TR-88042 ..... N89-21281 #

ARI-RN-88-93 ..... N89-21545 #

ARL-TR-88-19 ..... N89-21598 #

ARO-88-1 ..... N89-21490 #
ARO-20850.3-EL ..... N89-21669 #
ARO-21623.26-PH ..... N89-21063 #
ARO-21763.2-EG ..... N89-21060 #
ARO-22413.5-CH ..... N89-21062 #
ARO-22533.12-CH ..... N89-21108 #
ARO-22557.5-EG ..... N89-20990 #
ARO-22578.2-EG ..... N89-21692 #
ARO-22604.19-MA ..... N89-21616 #
ARO-22655.19-PH ..... N89-21091 #
ARO-22770.15-MA ..... N89-21210 #
ARO-22929.3-CH ..... N89-21636 #
ARO-22997.24-CH ..... N89-21086 #
ARO-24626.52-PH-UIR ..... N89-21228 #
ARO-24635.96-MA-VIR ..... N89-21548 #
ARO-24960.27-MA ..... N89-21550 #
ARO-25045.11-EL ..... N89-21185 #
ARO-25400.1-EG ..... N89-21044 #
ARO-25544.4-EG ..... N89-21080 #
ARO-25544.5-EG ..... N89-21268 #

ATA-M-SBIR-025 ..... N89-21151 #

AVSCOM-TR-88-C-010 ..... N89-21243* #
AVSCOM-TR-88-C-041 ..... N89-21244* #
AVSCOM-TR-89-C-001 ..... N89-20995* #
AVSCOM-TR-89-C-001 ..... N89-21051* #

BFLRF-258 ..... N89-21253 #

BMI/OWTD-1 ..... N89-21544 #

BRL-MR-3724 ..... N89-21129 #
BRL-MR-3728 ..... N89-21131 #

B8827729 ..... N89-21615 #
B8827734 ..... N89-21543 #

CADCAM-067 ..... N89-21709 #

CBIP-33 ..... N89-21473 #

CERL-TM-N-89/01 ..... N89-21632 #

CMS-TSR-89-13 ..... N89-21211 #

CMU-RI-TR-88-14 ..... N89-21652 #

CONF-880810-1 ..... N89-21048 #
CONF-881155-45 ..... N89-21685 #
CONF-881155-47 ..... N89-21096 #
CONF-881244-7 ..... N89-21235 #
CONF-881268-1 ..... N89-21725 #
CONF-890103-8 ..... N89-21639 #
CONF-890133-6 ..... N89-21457 #
CONF-890145-17 ..... N89-21093 #
CONF-890145-18-REV-1 ..... N89-21654 #
CONF-890182-1 ..... N89-21659 #
CONF-890211-4 ..... N89-21424 #
CONF-890211-5 ..... N89-21423 #
CONF-890324-3 ..... N89-21094 #
CONF-890361-1 ..... N89-21189 #
CONF-890366-2 ..... N89-21708 #
CONF-8803184-1 ..... N89-21052 #
CONF-8804249-1 ..... N89-21031 #
CONF-8806105 ..... N89-21596 #
CONF-8808192-1 ..... N89-21627 #
CONF-8809117-2 ..... N89-21070 #
CONF-8810182-13 ..... N89-21578 #
CONF-8810195-5 ..... N89-21686 #
CONF-8810203-2 ..... N89-21095 #
CONF-8810292-1 ..... N89-21124 #
CONF-8810299-3 ..... N89-21688 #
CONF-8810301-1 ..... N89-21427 #
CONF-8810316-1 ..... N89-21653 #
CONF-8810321-1 ..... N89-21687 #
CONF-8811161-2 ..... N89-21684 #
CONF-8811163-1 ..... N89-21225 #
CONF-8811173-1 ..... N89-21428 #

CONTRIB-44-PT-2 ..... N89-21651 #

CRC-555 ..... N89-21126 #

CRDEC-TR-88101 ..... N89-21058 #

CSDL-R-2075 ..... N89-21028 #

CSR-88-10 ..... N89-21550 #

CWI-MS-R8802 ..... N89-21615 #
CWI-MS-R8807 ..... N89-21543 #

C87A-25-2 ..... N89-21181 #

DAITC/TR-88/011 ..... N89-21704 #

DDA-EDR-13471 ..... N89-21125 #

DEL-SG-16-88 ..... N89-21257 #

DE88-007217 ..... N89-21418 #
DE88-705356 ..... N89-21596 #
DE88-757043 ..... N89-21188 #
DE88-757111 ..... N89-21255 #
DE89-000856 ..... N89-21420 #
DE89-000858 ..... N89-21421 #
DE89-000864 ..... N89-21422 #
DE89-001265 ..... N89-21048 #
DE89-004719 ..... N89-21544 #
DE89-005062 ..... N89-21225 #
DE89-005098 ..... N89-21093 #
DE89-005106 ..... N89-21684 #
DE89-005359 ..... N89-21024 #
DE89-005724 ..... N89-21655 #
DE89-005841 ..... N89-21052 #
DE89-006234 ..... N89-21659 #
DE89-006417 ..... N89-21189 #
DE89-006515 ..... N89-21725 #
DE89-006520 ..... N89-21578 #
DE89-006521 ..... N89-21685 #
DE89-006532 ..... N89-21235 #
DE89-006555 ..... N89-21094 #
DE89-006599 ..... N89-21653 #
DE89-006790 ..... N89-21665 #
DE89-006800 ..... N89-21480 #
DE89-006941 ..... N89-21427 #
DE89-006944 ..... N89-21627 #
DE89-007035 ..... N89-21095 #
DE89-007202 ..... N89-21124 #
DE89-007210 ..... N89-21096 #
DE89-007212 ..... N89-21428 #
DE89-007236 ..... N89-21639 #
DE89-007240 ..... N89-21457 #
DE89-007262 ..... N89-21070 #
DE89-007357 ..... N89-21443 #
DE89-007360 ..... N89-21656 #
DE89-007375 ..... N89-21686 #
DE89-007377 ..... N89-21687 #
DE89-007578 ..... N89-21075 #
DE89-007606 ..... N89-21053 #
DE89-007607 ..... N89-21076 #
DE89-007608 ..... N89-21216 #
DE89-007610 ..... N89-21077 #
DE89-007616 ..... N89-21078 #
DE89-007628 ..... N89-21666 #
DE89-007716 ..... N89-21706 #
DE89-007942 ..... N89-21458 #
DE89-007975 ..... N89-21423 #
DE89-007982 ..... N89-21688 #
DE89-008003 ..... N89-21660 #
DE89-008025 ..... N89-21654 #
DE89-008034 ..... N89-21031 #
DE89-008083 ..... N89-21622 #
DE89-008084 ..... N89-21236 #
DE89-008092 ..... N89-21707 #
DE89-008112 ..... N89-21708 #
DE89-008113 ..... N89-21424 #
DE89-008152 ..... N89-21689 #
DE89-008202 ..... N89-21214 #
DE89-008284 ..... N89-21613 #
DE89-008296 ..... N89-21690 #
DE89-008297 ..... N89-21097 #
DE89-008300 ..... N89-21098 #
DE89-008304 ..... N89-21661 #
DE89-008318 ..... N89-21614 #
DE89-008321 ..... N89-21709 #
DE89-008407 ..... N89-21620 #
DE89-008450 ..... N89-21579 #
DE89-008451 ..... N89-21580 #

DE89-008465 ..... N89-21662 #
DE89-008484 ..... N89-21590 #
DE89-008646 ..... N89-21237 #
DE89-008656 ..... N89-21581 #
DE89-008854 ..... N89-21033 #

DOE/CE-30844/T1 ..... N89-21418 #

DOE/CH-10093/41 ..... N89-21420 #
DOE/CH-10093/43 ..... N89-21421 #
DOE/CH-10093/49 ..... N89-21422 #

DOE/DP-40200/85 ..... N89-21661 #

DOE/ER-13221/T4 ..... N89-21443 #
DOE/ER-13937/1 ..... N89-21236 #
DOE/ER-25018/T1 ..... N89-21613 #
DOE/ER-45310/15-PT-1 ..... N89-21665 #
DOE/ER-53206/11 ..... N89-21660 #

DOE/ET-53088/363 ..... N89-21622 #
DOE/ET-53088/364 ..... N89-21662 #

DOE/NASA/50111-3 ..... N89-21417* #

DOE/OSA-32087-19 ..... N89-21024 #

DOT/FAA/PM-87/33 ..... N89-21003 #

DOT/FAA/PP-86/3 ..... N89-21003 #

DREP-TM-88-15 ..... N89-21460 #

DRIC-BR-108037 ..... N89-21650 #
DRIC-BR-108121 ..... N89-21122 #
DRIC-BR-108255 ..... N89-21039 #

DST-2700Z-005-88 ..... N89-21232 #

DTIC/TR-88/13 ..... N89-21700 #
DTIC/TR-88/14 ..... N89-21701 #
DTIC/TR-89/6 ..... N89-21704 #

DTRC-SHD-1229-01 ..... N89-21199 #

DTRC-88/024 ..... N89-21223 #
DTRC-88/040 ..... N89-21626 #

E-4116 ..... N89-21002* #
E-4144 ..... N89-21243* #
E-4273 ..... N89-21169* #
E-4361 ..... N89-21171* #
E-4383 ..... N89-21224* #
E-4385 ..... N89-21256* #
E-4452 ..... N89-21245* #
E-4500 ..... N89-21103* #
E-4543 ..... N89-21258* #
E-4551 ..... N89-21244* #
E-4569 ..... N89-21138* #
E-4574 ..... N89-20921* #
E-4578 ..... N89-20995* #
E-4584 ..... N89-21417* #
E-4589 ..... N89-21192* #
E-4594 ..... N89-21174* #
E-4595 ..... N89-20920* #
E-4598 ..... N89-21196* #
E-4616 ..... N89-21172* #
E-4648 ..... N89-21036* #
E-4649 ..... N89-21100* #
E-4656 ..... N89-21595* #
E-4663 ..... N89-21197* #
E-4665 ..... N89-20996* #
E-4671 ..... N89-21104* #
E-4673 ..... N89-21025* #
E-4675 ..... N89-21051* #
E-4676 ..... N89-21628* #
E-4679 ..... N89-21419* #
E-4693 ..... N89-21142* #
E-4695 ..... N89-21266* #
E-4702 ..... N89-21032* #

EPA/600/D-88/256 ..... N89-21461 #
EPA/600/1-88/005 ..... N89-21462 #

ESD-TR-88-156 ..... N89-21603 #
ESD-TR-88-181 ..... N89-21182 #
ESD-TR-88-194 ..... N89-21552 #
ESD-TR-88-221 ..... N89-21647 #
ESD-TR-88-268 ..... N89-21164 #

ETL-0478 ..... N89-21162 #

ETN-89-94165 ..... N89-21621 #
ETN-89-94185 ..... N89-21615 #
ETN-89-94189 ..... N89-21543 #

FERMILAB-CONF-89/27-A ..... N89-21715* #

FERMILAB-PUB-89/31-A ..... N89-21634* #
FERMILAB-PUB-89/42-A ..... N89-21716* #
FERMILAB-PUB-89/44-A ..... N89-21635* #
FERMILAB-PUB-89/47-A ..... N89-21633* #

FJSRL-TR-88-0007 ..... N89-21069 #

FTD-ID(RS)T-0604-88 ..... N89-21233 #

GA-C19465 ..... N89-21674 #

GALCIT-SM-88-7-PT-2 ..... N89-21272 #

GAO/NSIAD-88-26 ..... N89-21694 #

GAO/RCED-88-61 ..... N89-20974 #
GAO/RCED-88-118 ..... N89-20977 #

GMU/22472/105 ..... N89-21597 #

H-1530 ..... N89-20983* #

HDL-TR-2139 ..... N89-21163 #

HL88/1061 ..... N89-21663 #
HL88/1097 ..... N89-21073 #
HL88/1135 ..... N89-21101 #
HL88/1219 ..... N89-21139 #
HL88/1238 ..... N89-21035 #
HL88/1250 ..... N89-21034 #

IATRAP-88-1 ..... N89-21229 #

IC-88/234 ..... N89-21596 #

ICASE-89-6 ..... N89-21537* #
ICASE-89-17 ..... N89-21542* #

ICOMP-89-1 ..... N89-21595* #
ICOMP-89-3 ..... N89-21192* #
ICOMP-89-4 ..... N89-21196* #
ICOMP-89-6 ..... N89-21197* #

IDA-M-548-PT-1 ..... N89-21681 #

IDA-P-2093 ..... N89-21123 #

IDA/HQ-88-33190 ..... N89-21123 #
IDA/HQ-88-34008 ..... N89-21681 #

IFSR-363 ..... N89-21622 #
IFSR-364 ..... N89-21662 #

INDU/DC/GMH-TR-47 ..... N89-21222 #

IS-T-1296 ..... N89-21078 #
IS-T-1343 ..... N89-21077 #
IS-T-1345 ..... N89-21075 #
IS-T-1350 ..... N89-21216 #
IS-T-1357 ..... N89-21655 #
IS-T-1385 ..... N89-21053 #
IS-T-1386 ..... N89-21666 #
IS-T-1387 ..... N89-21076 #

ISBN-951-754-600-9 ..... N89-21664 #
ISBN-951-9100-89-X ..... N89-21188 #

ISI/RS-88-219 ..... N89-21703 #

ISSN-0038-0911 ..... N89-21431 #
ISSN-0038-0911 ..... N89-21432 #
ISSN-0038-0911 ..... N89-21722 #
ISSN-0148-7191 ..... N89-21060 #
ISSN-0782-7415 ..... N89-21188 #

ISTIC-TR-C-000195 ..... N89-21259 #

IVO-A-04/88 ..... N89-21188 #

K/DSRD-55-VOL-1 ..... N89-21706 #
K/DSRD-59 ..... N89-21590 #

L-16501-VOL-1-PT-1 ..... N89-20925* #
L-16501-VOL-1-PT-2 ..... N89-20942* #

LA-UR-89-115 ..... N89-21685 #
LA-UR-89-119 ..... N89-21578 #
LA-UR-89-151 ..... N89-21235 #
LA-UR-89-249 ..... N89-21094 #
LA-UR-89-280 ..... N89-21725 #
LA-UR-89-501 ..... N89-21688 #

LA-11418-MS ..... N89-21620 #

LBL-25859 ..... N89-21048 #
LBL-25912 ..... N89-21033 #
LBL-26145 ..... N89-21097 #
LBL-26381 ..... N89-21690 #
LBL-26449 ..... N89-21098 #
LBL-26617 ..... N89-21689 #

LC-79-640374 ..... N89-21432 #
LC-79-640375 ..... N89-21431 #
LC-79-640375 ..... N89-21722 #
LC-88-600161 ..... N89-21013 #

LIDS-P-1818 ..... N89-21548 #

LJI-87-P-467 ..... N89-21165 #

LMSC-HEC-TR-F226066 ..... N89-21023* #

LMSC/F247028 ..... N89-21438 #

LPI-CONTRIB-673 ..... N89-21287* #

MCR-88-590-VOL-1 ..... N89-21029 #

MIT/LCS/TR-421 ..... N89-21585 #

MM-4762-88-17 ..... N89-21112 #
MM-5488-88-14 ..... N89-21280 #

MPL-U-23/88 ..... N89-21217 #

MSP-87-3-REV ..... N89-21606 #
MSP-88-1 ..... N89-21573 #

MTI-87TR72 ..... N89-21239* #

MTL-TR-88-49 ..... N89-21254 #

MTR-10295 ..... N89-21164 #

MW-88-P-5 ..... N89-21185 #

NADC-88007-60 ..... N89-21092 #
NADC-88078-60 ..... N89-21088 #
NADC-88096-60 ..... N89-21043 #

NAE-AN-54 ..... N89-20968 #

NAS 1.15:89241 ..... N89-21761* #
NAS 1.15:100045 ..... N89-20964* #
NAS 1.15:100058 ..... N89-21532* #
NAS 1.15:100358 ..... N89-21246* #
NAS 1.15:100360 ..... N89-21712* #
NAS 1.15:100475 ..... N89-21463* #
NAS 1.15:100496 ..... N89-21047* #
NAS 1.15:100573 ..... N89-21538* #
NAS 1.15:100671 ..... N89-21136* #
NAS 1.15:100672 ..... N89-21135* #
NAS 1.15:100704 ..... N89-21444* #
NAS 1.15:100711 ..... N89-21430* #
NAS 1.15:100714 ..... N89-21448* #
NAS 1.15:100716 ..... N89-21434* #
NAS 1.15:100869 ..... N89-20995* #
NAS 1.15:100883 ..... N89-21002* #
NAS 1.15:100993 ..... N89-21541* #
NAS 1.15:101037 ..... N89-21190* #
NAS 1.15:101039 ..... N89-21477* #
NAS 1.15:101053 ..... N89-20978* #
NAS 1.15:101353 ..... N89-21224* #
NAS 1.15:101445 ..... N89-21244* #
NAS 1.15:101459 ..... N89-21138* #
NAS 1.15:101470 ..... N89-21417* #
NAS 1.15:101473 ..... N89-21192* #
NAS 1.15:101477 ..... N89-21196* #
NAS 1.15:101483 ..... N89-21172* #
NAS 1.15:101528 ..... N89-21193* #
NAS 1.15:101546 ..... N89-21260* #
NAS 1.15:101553 ..... N89-20982* #
NAS 1.15:101558 ..... N89-21539* #
NAS 1.15:101569 ..... N89-20991* #
NAS 1.15:101695 ..... N89-20983* #
NAS 1.15:101946 ..... N89-20920* #
NAS 1.15:101955 ..... N89-21100* #
NAS 1.15:101961 ..... N89-21595* #
NAS 1.15:101965 ..... N89-21197* #
NAS 1.15:101968 ..... N89-20996* #
NAS 1.15:101971 ..... N89-21104* #
NAS 1.15:101973 ..... N89-21025* #
NAS 1.15:101975 ..... N89-21051* #
NAS 1.15:101976 ..... N89-21628* #
NAS 1.15:101980 ..... N89-21419* #
NAS 1.15:101990 ..... N89-21142* #
NAS 1.15:101991 ..... N89-21266* #
NAS 1.15:102000 ..... N89-21245* #
NAS 1.15:102001 ..... N89-21032* #
NAS 1.15:102008 ..... N89-21174* #

NAS 1.15:102281 ..... N89-21026* #
NAS 1.21:7011(321) N89-21475*
NAS 1.21:7011(322) N89-21476*
NAS 1.26:4195 ..... N89-21256* #
NAS 1.26:4215 ..... N89-21258* #
NAS 1.26:4222 ..... N89-21425* #
NAS 1.26:4223 ..... N89-21426* #
NAS 1.26:177524 ..... N89-20973* #
NAS 1.26:177525 ..... N89-21046* #
NAS 1.26:180077 ..... N89-21436* #
NAS 1.26:180480 ..... N89-21226* #
NAS 1.26:180826 ..... N89-21105* #
NAS 1.26:181686 ..... N89-21099* #
NAS 1.26:181743 ..... N89-20922* #
NAS 1.26:181767 ..... N89-21582* #
NAS 1.26:181776 ..... N89-21191* #
NAS 1.26:181779 ..... N89-21537* #
NAS 1.26:181793 ..... N89-21004* #
NAS 1.26:181806 ..... N89-20999* #
NAS 1.26:181812 ..... N89-21542* #
NAS 1.26:181813 ..... N89-21267* #
NAS 1.26:182105 ..... N89-21239* #
NAS 1.26:182244 ..... N89-21072* #
NAS 1.26:182245 ..... N89-20921* #
NAS 1.26:182260 ..... N89-21036* #
NAS 1.26:182272 ..... N89-21173* #
NAS 1.26:182273 ..... N89-21265* #
NAS 1.26:182283 ..... N89-21658* #
NAS 1.26:182836 ..... N89-21716* #
NAS 1.26:182838 ..... N89-21134* #
NAS 1.26:182918 ..... N89-21635* #
NAS 1.26:183329 ..... N89-21287* #
NAS 1.26:183416 ..... N89-21416*
NAS 1.26:183423 ..... N89-21168* #
NAS 1.26:183553 ..... N89-21726* #
NAS 1.26:183608 ..... N89-21023* #
NAS 1.26:184740 ..... N89-20981* #
NAS 1.26:184792 ..... N89-21429* #
NAS 1.26:184815 ..... N89-21479* #
NAS 1.26:184817 ..... N89-21141* #
NAS 1.26:184839 ..... N89-21435* #
NAS 1.26:184841 ..... N89-21640* #
NAS 1.26:184858 ..... N89-21198* #
NAS 1.26:184877 ..... N89-21540* #
NAS 1.26:184889 ..... N89-21634* #
NAS 1.26:184890 ..... N89-21633* #
NAS 1.26:184891 ..... N89-21715* #
NAS 1.26:184948 ..... N89-20963* #
NAS 1.26:184953 ..... N89-21449* #
NAS 1.26:184966 ..... N89-21286* #
NAS 1.55:3020-VOL-1-PT-1 ..... N89-20925* #
NAS 1.55:3020-VOL-1-PT-2 ..... N89-20942* #
NAS 1.60:2899 ..... N89-21169* #
NAS 1.60:2901 ..... N89-21243* #
NAS 1.60:2904 ..... N89-21171* #
NAS 1.60:2910 ..... N89-21103* #

NASA-CP-3020-VOL-1-PT-1 ..... N89-20925* #
NASA-CP-3020-VOL-1-PT-2 ..... N89-20942* #

NASA-CR-4195 ..... N89-21256* #
NASA-CR-4215 ..... N89-21258* #
NASA-CR-4222 ..... N89-21425* #
NASA-CR-4223 ..... N89-21426* #
NASA-CR-177524 ..... N89-20973* #
NASA-CR-177525 ..... N89-21046* #
NASA-CR-180077 ..... N89-21436* #
NASA-CR-180480 ..... N89-21226* #
NASA-CR-180826 ..... N89-21105* #
NASA-CR-181686 ..... N89-21099* #
NASA-CR-181743 ..... N89-20922* #
NASA-CR-181767 ..... N89-21582* #
NASA-CR-181776 ..... N89-21191* #
NASA-CR-181779 ..... N89-21537* #
NASA-CR-181793 ..... N89-21004* #
NASA-CR-181806 ..... N89-20999* #
NASA-CR-181812 ..... N89-21542* #
NASA-CR-181813 ..... N89-21267* #
NASA-CR-182105 ..... N89-21239* #
NASA-CR-182244 ..... N89-21072* #
NASA-CR-182245 ..... N89-20921* #
NASA-CR-182260 ..... N89-21036* #
NASA-CR-182272 ..... N89-21173* #
NASA-CR-182273 ..... N89-21265* #
NASA-CR-182283 ..... N89-21658* #
NASA-CR-182836 ..... N89-21716* #
NASA-CR-182838 ..... N89-21134* #
NASA-CR-182918 ..... N89-21635* #
NASA-CR-183320 ..... N89-21287* #
NASA-CR-183416 ..... N89-21416*
NASA-CR-183423 ..... N89-21168* #
NASA-CR-183553 ..... N89-21726* #
NASA-CR-183608 ..... N89-21023* #
NASA-CR-184740 ..... N89-20981* #
NASA-CR-184792 ..... N89-21429* #
NASA-CR-184815 ..... N89-21479* #
NASA-CR-184817 ..... N89-21141* #
NASA-CR-184839 ..... N89-21435* #
NASA-CR-184841 ..... N89-21640* #
NASA-CR-184858 ..... N89-21198* #
NASA-CR-184877 ..... N89-21540* #
NASA-CR-184889 ..... N89-21634* #
NASA-CR-184890 ..... N89-21633* #
NASA-CR-184891 ..... N89-21715* #
NASA-CR-184948 ..... N89-20963* #
NASA-CR-184953 ..... N89-21449* #
NASA-CR-184966 ..... N89-21286* #

NASA-SP-7011(321) N89-21475*
NASA-SP-7011(322) N89-21476*

NASA-TM-89241 ..... N89-21761* #
NASA-TM-100045 ..... N89-20964* #
NASA-TM-100058 ..... N89-21532* #
NASA-TM-100358 ..... N89-21246* #
NASA-TM-100360 ..... N89-21712* #
NASA-TM-100475 ..... N89-21463* #
NASA-TM-100496 ..... N89-21047* #
NASA-TM-100573 ..... N89-21538* #
NASA-TM-100671 ..... N89-21136* #
NASA-TM-100672 ..... N89-21135* #
NASA-TM-100704 ..... N89-21444* #
NASA-TM-100711 ..... N89-21430* #
NASA-TM-100714 ..... N89-21448* #
NASA-TM-100716 ..... N89-21434* #
NASA-TM-100869 ..... N89-20995* #
NASA-TM-100883 ..... N89-21002* #
NASA-TM-100993 ..... N89-21541* #
NASA-TM-101037 ..... N89-21190* #
NASA-TM-101039 ..... N89-21477* #
NASA-TM-101053 ..... N89-20978* #
NASA-TM-101353 ..... N89-21224* #
NASA-TM-101445 ..... N89-21244* #
NASA-TM-101459 ..... N89-21138* #
NASA-TM-101470 ..... N89-21417* #
NASA-TM-101473 ..... N89-21192* #
NASA-TM-101477 ..... N89-21196* #
NASA-TM-101483 ..... N89-21172* #
NASA-TM-101528 ..... N89-21193* #
NASA-TM-101546 ..... N89-21260* #
NASA-TM-101553 ..... N89-20982* #
NASA-TM-101558 ..... N89-21539* #
NASA-TM-101569 ..... N89-20991* #
NASA-TM-101695 ..... N89-20983* #
NASA-TM-101946 ..... N89-20920* #
NASA-TM-101955 ..... N89-21100* #
NASA-TM-101961 ..... N89-21595* #
NASA-TM-101965 ..... N89-21197* #
NASA-TM-101968 ..... N89-20996* #
NASA-TM-101971 ..... N89-21104* #
NASA-TM-101973 ..... N89-21025* #
NASA-TM-101975 ..... N89-21051* #
NASA-TM-101976 ..... N89-21628* #
NASA-TM-101980 ..... N89-21419* #
NASA-TM-101990 ..... N89-21142* #
NASA-TM-101991 ..... N89-21266* #
NASA-TM-102000 ..... N89-21245* #
NASA-TM-102001 ..... N89-21032* #
NASA-TM-102008 ..... N89-21174* #
NASA-TM-102281 ..... N89-21026* #

NASA-TP-2899 ..... N89-21169* #
NASA-TP-2901 ..... N89-21243* #
NASA-TP-2904 ..... N89-21171* #
NASA-TP-2910 ..... N89-21103* #

NATICK-TR-88/043 ..... N89-21484 #

NCAR/CT-115 ..... N89-21447 #
NCAR/CT-116 ..... N89-21723 #

NCAR/TN-319-STR ..... N89-21433 #
NCAR/TN-320-STR ..... N89-21215 #
NCAR/TN-324-PPR ..... N89-21446 #

NCEL-CR-89.002 ..... N89-21611 #

NCEL-TN-1788 ..... N89-21005 #

NCS-MAT/E-001 ..... N89-21176 #

NCTRF-172 ..... N89-21485 #

NEPRF-TR-88-11 ..... N89-20975 #

NIST/TN-1256 ..... N89-21238 #

NISTIR-88/3850 ..... N89-21050 #
NISTIR-88/3866 ..... N89-21170 #
NISTIR-88/3880 ..... N89-21049 #
NISTIR-88/3881 ..... N89-21623 #

NIT/LCS/TM-353 ..... N89-21565 #

NOAA-TM-NESDIS-AISC-14 ..... N89-21415 #

NOAA/PMEL-CONTRIB-1047-PT-2 ..... N89-21651 #

NOAA/PMEL-ERL-81-PT-2 ..... N89-21651 #

NOSC/TD-1287 ..... N89-21151 #
NOSC/TD-1326 ..... N89-21559 #
NOSC/TD-1355 ..... N89-21643 #
NOSC/TD-1361 ..... N89-21645 #
NOSC/TD-1375 ..... N89-21439 #

NPRDC-TN-89-7 ..... N89-21474 #

NPS69-88-003 ..... N89-21277 #

NRL-MR-6340 ..... N89-21604 #
NRL-MR-6347 ..... N89-21227 #
NRL-MR-6384 ..... N89-21206 #

NRL-9168 ..... N89-21683 #

OSU/DGSS-393 ..... N89-21442 #

PARGUM-88-02 ..... N89-21630 #

PB88-243928 ..... N89-21459 #
PB88-249255 ..... N89-21013 #
PB89-101943 ..... N89-21257 #
PB89-104129 ..... N89-21215 #
PB89-104137 ..... N89-21447 #
PB89-109912 ..... N89-21722 #
PB89-111462 ..... N89-21259 #
PB89-113377 ..... N89-21723 #
PB89-117261 ..... N89-21415 #
PB89-118608 ..... N89-21445 #
PB89-118640 ..... N89-21462 #
PB89-120802 ..... N89-21698 #
PB89-120927 ..... N89-21446 #
PB89-121305 ..... N89-21431 #
PB89-121313 ..... N89-21432 #
PB89-123137 ..... N89-21170 #
PB89-124481 ..... N89-21433 #
PB89-127559 ..... N89-21049 #
PB89-127567 ..... N89-21050 #
PB89-128904 ..... N89-21664 #
PB89-129050 ..... N89-21461 #
PB89-131734 ..... N89-21261 #
PB89-132302 ..... N89-21623 #
PB89-133532 ..... N89-21238 #

PHM-88-06 ..... N89-21015 #

PNL-SA-15971 ..... N89-21639 #
PNL-SA-16146 ..... N89-21627 #
PNL-SA-16315 ..... N89-21457 #
PNL-SA-16628 ..... N89-21427 #

PNL-6811 ..... N89-21458 #

PO-2193303 ..... N89-21707 #

POLY-WRI-1537-88 ..... N89-21437 #

PR-62234N/RS34A57-1-ZP180 ..... N89-21088 #

PROTEUS-M-14 ..... N89-21574 #

PUPT-89-1119 ..... N89-21716* #

R/D-4380A-R-AN ..... N89-21128 #
R/D-4759-CH-01 ..... N89-21065 #
R/D-5087-MS-01-F ..... N89-21106 #
R/D-5119-EE-01-04 ..... N89-21679 #
R/D-5338-CC-03 ..... N89-21607 #
R/D-5647-MS-01.4 ..... N89-21090 #
R/D-5821-MS-01-1/2 ..... N89-21648 #
R/D-5841-EE-01-F ..... N89-21667 #
R/D-5876-MS-01-3 ..... N89-21110 #

RADC-TR-87-284 ..... N89-21156 #
RADC-TR-88-110 ..... N89-21179 #
RADC-TR-88-176 ..... N89-21186 #
RADC-TR-88-190 ..... N89-21589 #

RAE-TR-88044 ..... N89-21122 #
RAE-TR-88048 ..... N89-21039 #

REPT-3 ..... N89-21080 #
REPT-88-1 ..... N89-21213 #
REPT-88-9S31-HETRO-R1 ..... N89-21116 #
REPT-88B0254 ..... N89-21430* #
REPT-89B00058 ..... N89-21434* #
REPT-89B00067 ..... N89-21448* #

REPT-199 ..... N89-21661 #

RESOURCE-PUB-172 ..... N89-21013 #

RI/RD-88-273 ..... N89-21072* #

RSRE-MEMO-4129 ..... N89-21650 #

S-592 ..... N89-21463* #

SAND-88-1073 ..... N89-21214 #
SAND-88-1558C ..... N89-21095 #
SAND-88-1884 ..... N89-21614 #
SAND-88-2577C ..... N89-21423 #
SAND-88-3109C ..... N89-21424 #
SAND-88-3328 ..... N89-21709 #
SAND-89-0532C ..... N89-21708 #

SD-TR-88-98 ..... N89-21121 #
SD-TR-88-100 ..... N89-21056 #
SD-TR-88-102 ..... N89-21677 #
SD-TR-88-106 ..... N89-21440 #

SGD-528-PT-2 ..... N89-21722 #
SGD-529-PT-1 ..... N89-21431 #
SGD-529-PT-2 ..... N89-21432 #

SIO-REF-88-16 ..... N89-21217 #

SPC-88-2949 ..... N89-21696 #

SR-4 ..... N89-21442 #

SSS-R-88-9339 ..... N89-21021 #

STI-TR-1252-1 ..... N89-20999* #

TGAL-88-02 ..... N89-21161 #

TKK-F-A630 ..... N89-21664 #

TR-5 ..... N89-21276 #
TR-6 ..... N89-21111 #
TR-31 ..... N89-21066 #
TR-31 ..... N89-21119 #
TR-35 ..... N89-21064 #
TR-90 ..... N89-21089 #
TR-257 ..... N89-21247 #
TR-803 ..... N89-21603 #
TR-812 ..... N89-21182 #
TR-817 ..... N89-21552 #
TR-819 ..... N89-21647 #
TR-0088(3935-03)-1 ..... N89-21121 #
TR-0088(3940-05)-6 ..... N89-21440 #
TR-0088(3945-07)-4 ..... N89-21056 #
TR-0088(3945-07)-5 ..... N89-21677 #

TR/11/88 ..... N89-21607 #

TSL-88-5 ..... N89-21209 #

UBUFFALO/DC/88/TR-88 ..... N89-21629 #
UBUFFALO/DC/88/TR-89 ..... N89-21061 #

UCID-21558 ..... N89-21480 #
UCID-21578 ..... N89-21237 #

UCRL-21177 ..... N89-21707 #
UCRL-98520 ..... N89-21031 #
UCRL-99003 ..... N89-21093 #
UCRL-99316-REV-1 ..... N89-21654 #
UCRL-100110 ..... N89-21225 #
UCRL-100194 ..... N89-21659 #

UDR-TR-88-56 ..... N89-21068 #
UDR-TR-88-60 ..... N89-21638 #

UILU-ENG-88-1744 ..... N89-21618 #

UIUCDCS-R-88-1439 ..... N89-21618 #

UMAERO-87-37 ..... N89-20962 #

USAARL-88-12 ..... N89-21488 #
USAARL-88-13 ..... N89-21486 #
USAARL-88-15 ..... N89-21482 #

USAAVSCOM-TR-87-A-14 ..... N89-20964* #
USAAVSCOM-TR-88-A-009 ..... N89-20978* #

USAFETAC/PR-88/002 ..... N89-21079 #
USAFETAC/PR-88/003 ..... N89-21453 #

USAFETAC/TN-88/005 ..... N89-21454 #
USAFETAC/TN-88/006 ..... N89-21455 #

USAFOEHL-88-137EQ0110JEF ..... N89-20984 #

USAFSAM-TR-87-13 ..... N89-21470 #
USAFSAM-TR-87-32-VOL-2 ..... N89-21467 #
USAFSAM-TR-87-41 ..... N89-21471 #

USC-88-014 ..... N89-21584 #

USC/OMDL-1501 ..... N89-21566 #

UUCS-88-003 ..... N89-21535 #
UUCS-88-019 ..... N89-21533 #
UUCS-88-021A ..... N89-21534 #

UW-CMRG-R-89-106 ..... N89-21286* #

UWA/DME/TR-88/61 ..... N89-21269 #

VTT-TIED-907 ..... N89-21255 #

W/O-11304 ..... N89-21021 #

WHOI-87-53 ..... N89-21459 #
WHOI-88-29 ..... N89-21549 #

Y/TR-89/2 ..... N89-21656 #

YALEU/DCS/RR-652 ..... N89-21155 #

ZW-8802 ..... N89-21621 #

☆ U.S. GOVERNMENT PRINTING OFFICE: 1989—241-445/00115

FEDERAL REGIONAL DEPOSITORY LIBRARIES

ALABAMA

AUBURN UNIV. AT MONTGOMERY LIBRARY
Documents Department
Montgomery, AL 36193
(205) 271-9650

UNIV. OF ALABAMA LIBRARY
Documents Dept.-Box S
University, AL 35486
(205) 348-6046

ARIZONA

DEPT. OF LIBRARY, ARCHIVES AND PUBLIC RECORDS
Third Floor—State Cap.
1700 West Washington
Phoenix, AZ 85007
(602) 255-4121

UNIVERSITY OF ARIZONA LIB.
Government Documents Dept.
Tucson, AZ 85721
(602) 621-6433

ARKANSAS

ARKANSAS STATE LIBRARY
One Capitol Mall
Little Rock, AR 72201
(501) 371-2326

CALIFORNIA

CALIFORNIA STATE LIBRARY
Govt. Publications Section
P.O. Box 2037
Sacramento, CA 95809
(916) 324-4863

COLORADO

UNIV OF COLORADO LIB.
Government Pub. Division
Campus Box 184
Boulder, CO 80309
(303) 492-8834

DENVER PUBLIC LIBRARY
Govt. Pub. Department
1357 Broadway
Denver, CO 80203
(303) 571-2131

CONNECTICUT

CONNECTICUT STATE LIBRARY
Government Documents Unit
231 Capitol Avenue
Hartford, CT 06106
(203) 566-7029

FLORIDA

UNIV. OF FLORIDA LIBRARIES
Library West
Documents Department
Gainesville, FL 32611
(904) 392-0367

GEORGIA

UNIV. OF GEORGIA LIBRARIES
Government Reference Dept.
Athens, GA 30602
(404) 542-8949

HAWAII

UNIV. OF HAWAII LIBRARY
Govt. Documents Collection
2550 The Mall
Honolulu, HI 96822
(808) 948-8230

IDAHO

UNIV. OF IDAHO LIBRARY
Documents Section
Moscow, ID 83843
(208) 885-6344

ILLINOIS

ILLINOIS STATE LIBRARY
Information Services Branch
Centennial Building
Springfield, IL 62756
(217) 782-5185

INDIANA

INDIANA STATE LIBRARY
Serials Documents Section
140 North Senate Avenue
Indianapolis, IN 46204
(317) 232-3686

IOWA

UNIV. OF IOWA LIBRARIES
Govt. Documents Department
Iowa City, IA 52242
(319) 353-3318

KANSAS

UNIVERSITY OF KANSAS
Doc. Collect—Spencer Lib.
Lawrence, KS 66045-2800
(913) 864-4662

KENTUCKY

UNIV. OF KENTUCKY LIBRARIES
Govt. Pub. Department
Lexington, KY 40506-0039
(606) 257-3139

LOUISIANA

LOUISIANA STATE UNIVERSITY
Middleton Library
Govt. Docs. Dept.
Baton Rouge, LA 70803
(504) 388-2570

LOUISIANA TECHNICAL UNIV. LIBRARY
Documents Department
Ruston, LA 71272-0046
(318) 257-4962

MAINE

UNIVERSITY OF MAINE
Raymond H. Fogler Library
Tri-State Regional Documents Depository
Orono, ME 04469
(207) 581-1680

MARYLAND

UNIVERSITY OF MARYLAND
McKeldin Lib.—Doc. Div.
College Park, MD 20742
(301) 454-3034

MASSACHUSETTS

BOSTON PUBLIC LIBRARY
Government Docs. Dept.
Boston, MA 02117
(617) 536-5400 ext.226

MICHIGAN

DETROIT PUBLIC LIBRARY
Sociology Department
5201 Woodward Avenue
Detroit, MI 48202-4093
(313) 833-1409

MICHIGAN STATE LIBRARY
P.O. Box 30007
Lansing, MI 48909
(517) 373-1593

MINNESOTA

UNIVERSITY OF MINNESOTA
Government Pubs. Division
409 Wilson Library
309 19th Avenue South
Minneapolis, MN 55455
(612) 373-7870

MISSISSIPPI

UNIV. OF MISSISSIPPI LIB.
Documents Department
University, MS 38677
(601) 232-5857

MONTANA

UNIV. OF MONTANA
Mansfield Library
Documents Division
Missoula, MT 59812
(406) 243-6700

NEBRASKA

UNIVERSITY OF NEBRASKA - LINCOLN
Love Library
Documents Department
Lincoln, NE 68588-0410
(402) 472-2562

NEVADA

UNIVERSITY OF NEVADA LIB.
Govt. Pub. Department
Reno, NV 89557-0044
(702) 784-6579

NEW JERSEY

NEWARK PUBLIC LIBRARY
5 Washington Street
Newark, NJ 07101-0630
(201) 733-7812

NEW MEXICO

UNIVERSITY OF NEW MEXICO
Zimmerman Library
Government Pub. Dept.
Albuquerque, NM 87131
(505) 277-5441

NEW MEXICO STATE LIBRARY
Reference Department
325 Don Gaspar Avenue
Santa Fe, NM 87503
(505) 827-3826

NEW YORK

NEW YORK STATE LIBRARY
Empire State Plaza
Albany, NY 12230
(518) 474-5563

NORTH CAROLINA

UNIVERSITY OF NORTH CAROLINA AT CHAPEL HILL
Davis Library
BA/SS Documents Division
Chapel Hill, NC 27515
(919) 962-1151

NORTH DAKOTA

UNIVERSITY OF NORTH DAKOTA
Chester Fritz Library
Documents Department
Grand Forks, ND 58202
(701) 777-4629
In cooperation with North Dakota State Univ. Library

OHIO

STATE LIBRARY OF OHIO
Documents Department
65 South Front Street
Columbus, OH 43266-0334
(614) 462-7051

OKLAHOMA

OKLAHOMA DEPT. OF LIB.
Government Documents
200 NE 18th Street
Oklahoma City, OK 73105
(405) 521-2502, ext. 252

OKLAHOMA STATE UNIV. LIB.
Documents Department
Stillwater, OK 74078
(405) 624-6546

OREGON

PORTLAND STATE UNIV. LIB.
Documents Department
P.O. Box 1151
Portland, OR 97207
(503) 229-3673

PENNSYLVANIA

STATE LIBRARY OF PENN.
Government Pub. Section
P.O. Box 1601
Harrisburg, PA 17105
(717) 787-3752

TEXAS

TEXAS STATE LIBRARY
Public Services Department
P.O. Box 12927—Cap. Sta.
Austin, TX 78711
(512) 475-2996

TEXAS TECH. UNIV. LIBRARY
Govt. Documents Department
Lubbock, TX 79409
(806) 742-2268

UTAH

UTAH STATE UNIVERSITY
Merrill Library, U.M.C. 30
Logan, UT 84322
(801) 750-2682

VIRGINIA

UNIVERSITY OF VIRGINIA
Alderman Lib.—Public Doc.
Charlottesville, VA 22903-2498
(804) 924-3133

WASHINGTON

WASHINGTON STATE LIBRARY
Documents Section
Olympia, WA 98504
(206) 753-4027

WEST VIRGINIA

WEST VIRGINIA UNIV. LIB.
Documents Department
Morgantown, WV 26506-6069
(304) 293-3640

WISCONSIN

MILWAUKEE PUBLIC LIBRARY
814 West Wisconsin Avenue
Milwaukee, WI 53233
(414) 278-3065

ST. HIST LIB. OF WISCONSIN
Government Pub. Section
816 State Street
Madison, WI 53706
(608) 262-4347

WYOMING

WYOMING STATE LIBRARY
Supreme Ct. & Library Bld.
Cheyenne, WY 82002
(307) 777-5919

National Aeronautics and
Space Administration
Code NTT-4
Washington, D.C.
20546

Official Business

Penalty for Private Use, $300

SPECIAL FOURTH-CLASS RATE
POSTAGE & FEES PAID
NASA
PERMIT No G-27

NASA

POSTMASTER: If Undeliverable (Section 158
Postal Manual) Do Not Return